Energy Research and Development Division
FINAL PROJECT REPORT

PILOTING THE INTEGRATION AND USE OF RENEWABLES TO ACHIEVE A FLEXIBLE AND SECURE ENERGY INFRASTRUCTURE

Prepared for: California Energy Commission
Prepared by: Advanced Power and Energy Program
University of California, Irvine

MARCH 2014
CEC-500-2015-075

Prepared by:

Primary Author(s):
Scott Samuelsen
Fabian Mueller
Josh Eichman
Brian Tarroja

Advanced Power and Energy Program
University of California, Irvine
114 Engineering Lab Facility, Bldg. 323
Irvine, CA 92697-3550
949-824-7302
www.apep.uci.edu

Contract Number: PIR-08-033

Prepared for:

California Energy Commission

Prab Sethi
Contract Manager

Prab Sethi
Project Manager

Aleecia Gutierrez
Office Manager
Energy Generation Research Office

Laurie ten Hope
Deputy Director
Energy Research and Development Division

Robert Oglesby
Executive Director

DISCLAIMER

This report was prepared as the result of work sponsored by the California Energy Commission. It does not necessarily represent the views of the Energy Commission, its employees or the State of California. The Energy Commission, the State of California, its employees, contractors and subcontractors make no warranty, express or implied, and assume no legal liability for the information in this report; nor does any party represent that the uses of this information will not infringe upon privately owned rights. This report has not been approved or disapproved by the California Energy Commission nor has the California Energy Commission passed upon the accuracy or adequacy of the information in this report.

ACKNOWLEDGEMENTS

The Primary Authors of the report would like to acknowledge the many people that have contributed to the research program so far.

- Project Administrator: Jeff Wojciechowski
- Lead Economic Analyses: Dr. Lori Schell (Empowered Energy)
- Campus Building End-Use Modeling, EE and DR Assessment and Modeling
  Jim Meacham and Brandyn Carlson (Cadmus Group Inc.)
- Renewable Resource Monitoring and Modeling – Graduate Student: Brian Tarroja
- Grid Interaction and Optimization – Graduate Student: Josh Eichman
- Building Modeling and Demand Response – Graduate Student: Hong-Hoa Do
- Electric Vehicle Modeling – Graduate Student: Li Zhang
- Solar Thermal Power Plant and Water Heater Modeling – Research Staff: Brendan Schaffer
- Project Support – Research Staff: Tim Brown
- Task 3 – Undergraduate Researcher: Ryan Ma
- Task 4 – Undergraduate Researcher: Parth Desai
- Task 5 – Undergraduate Researcher: Kersey Manliclic
- Task 5 – Undergraduate Researcher: Martin Chang
- Task 6 – Undergraduate Researcher: Tuan A. Tu
- Task 6 – Undergraduate Researcher: Boyan Kartolov

PREFACE

The California Energy Commission Energy Research and Development Division supports public interest energy research and development that will help improve the quality of life in California by bringing environmentally safe, affordable, and reliable energy services and products to the marketplace.

The Energy Research and Development Division conducts public interest research, development, and demonstration (RD&D) projects to benefit California.

The Energy Research and Development Division strives to conduct the most promising public interest energy research by partnering with RD&D entities, including individuals, businesses, utilities, and public or private research institutions.

Energy Research and Development Division funding efforts are focused on the following RD&D program areas:

- Buildings End-Use Energy Efficiency
- Energy Innovations Small Grants
- Energy-Related Environmental Research
- Energy Systems Integration
- Environmentally Preferred Advanced Generation
- Industrial/Agricultural/Water End-Use Energy Efficiency
- Renewable Energy Technologies
- Transportation

Piloting the Integration and Use of Renewables To Achieve a Flexible and Secure Energy Infrastructure is the final report for the Renewable-Based Energy Secure Communities (RESCOs) project (contract number PIR-08-033) conducted by the Advanced Power and Energy Program. The information from this project contributes to Energy Research and Development Division's Renewable Energy Technologies Program.

For more information about the Energy Research and Development Division, please visit the Energy Commission's website at www.energy.ca.gov/research/ or contact the Energy Commission at 916-327-1551.

ABSTRACT

The challenges and opportunities associated with developing Renewable-based Energy Secure Communities (RESCOs) is explored using the collection of energy resources and pilot projects at the University of California, Irvine (UCI) campus. A variety of renewable, conventional, and complementary technologies are assessed for their contribution to satisfying reliability criteria, enhancing and sustaining power quality, and minimizing the levelized cost-of-electricity.

Results from this work include an in-depth analysis of the pilot projects and the operation of UCI campus resources, as well as preferred operation for communities aspiring to become RESCOs. Pilot projects supporting UCI include a campus co-generation plant, a large thermal energy storage tank, rooftop and high-concentration solar photovoltaics, electric and alternative fueled transportation and a biogas combined heat and power plant with hydrogen co-production.

The Holistic Grid Resource Integration and Deployment (HiGRID) tool was developed to perform the analyses. This tool integrates an array of technologies including renewable and non-renewable generation plus energy efficiency, demand response, energy storage and electric transportation. All of these technologies are used to support the electric, heating and cooling requirements of campus or a generic community. Results from HiGRID are used to develop a roadmap describing how the UCI community can become a RESCO as well as a roadmap for aspiring communities wanting to become RESCOs.

Recommendations are developed for policy makers and industry leaders that support the findings in the RESCO roadmap. They provide information to advise legislation, policy and incentives that can support the RESCO goals throughout California.

Keywords: renewable integration, community, intermittent renewables, energy system modeling, high penetration, cost-of-electricity, energy efficiency, demand response, energy storage, electric transportation

Please use the following citation for this report:

Samuelsen, Scott, Mueller, Fabian, Eichman, Josh. Advanced Power and Energy Program. 2013. ***Piloting the Integration and Use of Renewables to Achieve a Flexible and Secure Energy Infrastructure.*** California Energy Commission. Publication number: CEC-500-2015-075.

TABLE OF CONTENTS

Acknowledgements i

PREFACE ii

ABSTRACT iii

TABLE OF CONTENTS iv

LIST OF FIGURES v

LIST OF TABLES vi

EXECUTIVE SUMMARY 1

Introduction 1

Project Purpose 1

Project Process 1

Project Results 2

CHAPTER 1: Introduction 5

CHAPTER 2: Scope-of-Work 6

2.1. Goal 6

2.2. Approach 7

2.3. Research Motivation 10

2.4. UCI Community and Pilot Projects 11

CHAPTER 3: University of California, Irvine Roadmap 20

3.1. Renewable Penetration Potential 23

3.2. Integration with UCI Central Plant 24

3.3. Role of Complementary Technologies 25

3.3.1. Energy Efficiency 25

3.3.2. Demand Response 26

3.3.3. Energy Storage 26

3.3.4. Electric Transportation 27

3.4. Public Transportation and Land-Use design 27

3.5. Community Role in Supporting the Grid 28

CHAPTER 4: Roadmap for Aspiring Communities **29**
4.1. Renewable Penetration Potential 31
4.2. Design Decisions 33
4.3. Role of Complementary Technologies 34
4.3.1. Energy Efficiency 34
4.3.2. Demand Response 34
4.3.3. Energy Storage 35
4.3.4. Electric Transportation 35
CHAPTER 5: Issues for Policy Makers and Industry Leaders **38**
CHAPTER 6: Conclusions and Recommendations **47**
6.1. Conclusions 47
6.2. Recommendations 49
6.3. BENEFITS TO CALIFORNIA 50
GLOSSARY **51**
REFERENCES **53**
APPENDIX A: Task 2: Substation and distribution circuit infrastructure **A-1**
Appendix B:Task 3: Distributed Energy Resource Management **B-1**
Appendix C:Task 4: Renewable Generation Deployment **C-1**
Appendix D:Task 5: Land-Use Design and Mobility **D-1**
Appendix E:Task 6: Building Design and Operation **E-1**
Appendix F:Task 7: Holistic Energy Integration and Management **F-1**
Appendix G:Task 8: Public Outreach, Education and Technology Transfer **G-1**
Appendix H:Task 9: Production Readiness Plan **H-1**

LIST OF FIGURES

Figure 1: Nexus between pilot projects and energy management modeling used to develop a roadmap for UCI RESCO implementation 8

Figure 2: Interactions between RESCO pilot projects and models within each of the project tasks 9

Figure 3: Existing UCI Infrastructure 12

Figure 4: UC Irvine Central Plant 14

Figure 5: UCI Community renewable power 14

Figure 6: Gas turbine responding to solar output 15

Figure 7: UCI Community electric vehicle charging 16

Figure 8: UCI hydrogen fueling station 17

Figure 9: UCI advanced building level CCHP system using a high temperature fuel cell, absorption chiller, and thermal energy storage tank 18

Figure 10: Integration of community distributed energy resources with regional renewable resources 21

Figure 11: UCI Roadmap for Achieving High Renewable Penetration 22

Figure 12: Roadmap for Achieving High Renewable Penetration 30

LIST OF TABLES

Table 1: Field Pilot Projects 10

Table 2: UCI Community Attributes 19

EXECUTIVE SUMMARY

Introduction

The advent of climate change is accelerating the development and deployment of alternatives to traditional combustion cycles for the generation of electricity. While wind and solar resources are evolving to play a major role, the variable and intermittent nature of these resources creates challenges to grid stability and reliability. The California Energy Commission "Renewable Based Energy Secure Community (RESCO)" initiative was promulgated to address the extent to which the design and operation of energy infrastructure in communities can, in the future, facilitate a high-penetration of intermittent renewable wind and solar. To address this important issue, the Advanced Power and Energy Program (APEP) at the University of California, Irvine (UCI) teamed with key partners to (1) adopt the UCI campus as a model community; (2) develop, with a portfolio of pilot projects, a roadmap to enable an increased penetration of renewable energy resources for the model community, and (3) develop a roadmap to make the RESCO vision a reality for communities in general.

Project Purpose

The University of California, Irvine (UCI) Advanced Power and Energy Program RESCO project used pilot demonstrations to explore potential technology development and deployment. Employing a blend of campus features, existing and new pilot studies, and modeling capabilities, the research program established:

1. An energy infrastructure (electric power , transportation, waste, buildings) roadmap for the UCI community that will maximize deployment and use of renewable energy resources while satisfying reliability criteria, enhancing and sustaining power quality, and minimizing the levelized cost-of-electricity.

2. A roadmap for communities that aspire to develop energy infrastructures to maximize deploying and using renewable energy resources while satisfying reliability criteria, enhancing and sustaining power quality, and minimizing the levelized cost of electricity.

3. A report of the issues for policy makers and industry leaders that must be addressed to facilitate renewable-based energy secure communities throughout California.

Project Process

The Holistic Grid Resource Integration and Deployment (HiGRID) tool was developed to perform the analyses. This tool integrates an array of technologies including renewable and non-renewable generation plus energy efficiency, demand response, energy storage and electric transportation. All of these technologies are used to support the electric, heating and cooling requirements of campus or a generic community. Results from HiGRID are used to develop a roadmap describing how the UCI community can become a RESCO and serve as a roadmap for communities wanting to become RESCOs. This culminated in community and generic roadmaps to achieve 100 percent secure energy for the UC Irvine campus without having to rely on non-renewable resources for load management. The pilot projects included: 1) evaluating the UCI 12 kV distribution system to determine opportunities that could sponsor a RESCO, 2)

investigating UCI cooling loads as dispatchable resources to support renewable deployments, 3) collecting data and demonstrating a 1 MW rooftop fixed photovoltaic and 113 kW dual axis tracking concentrated photovoltaic, 4) collecting data and demonstrating electric vehicle charging the uses dynamic price signals to help manage energy balance, and 5) data collection and demonstrating building demand response to support renewables.

Project Results

The HiGRID model examined various technology deployment scenarios in their effectiveness at establishing RESCOs to guide the roadmap development. The statewide modeling capabilities of the HiGRID tool makes it possible to evaluate RESCOs in an integrated context and the researchers concluded that these interactions between a community and the grid providing electricity to that community are critical to successfully installing and operating increased levels of renewables.

The HiGRID tool resulted nine major findings of the UCI RESCO program:

1. Communities must contribute to, communicate and coordinate with other utilities and the grid system operator or other communities to achieve a high-penetration of renewables.
2. New economic mechanisms such as dynamic rate structures must be developed to incentivize dispatch of community resources in response to the behavior of the larger electric grid.
3. Integrating electricity generation and transportation load provides synergistic benefits at both the community and regional level through:
    - Plug-in Electric Vehicle charging
    - H_2 production for Hydrogen Fuel Cell Electric Vehicles.
4. Reducing the capacity of carbon-fueled inflexible (base load) generation must be prioritized for meeting renewable energy goals.
5. Avoiding renewable generation curtailment is critical for reaching renewable energy goals in a cost-effective manner.
6. Complementary technologies such as energy storage and demand response are required to meet renewable use goals, but their preferred operation will change with the levels of renewable energy.
7. Significant cost, energy, and greenhouse gas savings are available through the widespread implementation of energy efficiency measures, but their impact on demand response potential must be considered.
8. To support and complement the planning roadmap, a pragmatic planning and design tool is required for community planners and policy makers.

9. A planning roadmap is desirable for community planners to determine the options for their specific community to qualify as a RESCO.

The Project Technical Goals are presented immediately below with a description of what was actually achieved and succinct comments.

Project Technical Goals	Actual Achieved	Comments
A community roadmap to achieve 100% renewable secure energy for the UC Irvine campus without having to rely on non-renewable resources for load management	A roadmap was established specific to the UC Irvine campus community as an example of a California community contributing to the State goals for a high level deployment of renewable resources.	A community alone cannot in general achieve 100% renewable security in the absence of collaboration with adjacent communities.
A generic roadmap for communities in general to achieve 100% renewable secure energy for the campus without having to rely on non-renewable resources for load management	A generic roadmap was established for California communities in general for contributing to the State goals for a high level deployment of renewable resources.	Communities cannot achieve the State goals in the absence of the grid as a whole. A comprehensive holistic energy integration and management methodology is required.
A Holistic Energy Integration and Management methodology	A Holistic Grid Resource Integration and Deployment (HiGRID) Tool was developed for the California Grid and applied to evaluate and characterize communities in general and the grid as a whole in an infrastructure with a high penetration of renewable resources.	J. Eichman, F. Mueller, B. Tarroja, L. Schell, and G.S. Samuelsen, "Exploration of the Integration of Renewable Resources Into California's Electric System Using the Holistic Grid Resource Integration and Deployment (HiGRID) Tool," Energy, 2013.
Demonstrate the Deployment and Integration of:		
• 1 MW of PV	890 kW of fixed PV; 113 kW of dual-axis Concentrated PV	A collaboration between UC Irvine, and the CPUC California Solar Initiative.
• 24/7 production of renewable hydrogen and 300kW of electricity for sustainable transportation	The deployment of a 120 kg per day hydrogen tri-generation 300kW high-temperature molten carbonate fuel cell with dispensing of bio-hydrogen for public consumption.	A collaboration between Air Products, FuelCell Energy, the Air Resources Board, the U.S. Department of Energy, the South Coast Air Quality Management District, and Southern California Gas Company.
• Electric vehicles (plug-in electric and all electric)	The deployment of 20 plug-in hybrid electric vehicles and 38 all battery electric vehicles in applications from business and personal use to a shared-use, station-vehicle program.	A collaboration with the Toyota Corporation, Southern California Edison, The City of Irvine, and Zipcar.
• Battery electric vehicle charging that utilizes dynamic price signals to incentivize the charging	The development of a methodology and model to control and characterize the use of dynamic price signals.	The model is an integral component of HiGRID.

of EVs to help manage the energy balance • Energy storage that will be required to achieve a RESCO	The modeling and utilization of an operational 4,500,000 gallon, 53,000 ton/hour thermal energy storage resource.	A collaboration between UC Irvine, Siemens Corporate Research, the U.S. DOE, and the Energy Commission.

CHAPTER 1: Introduction

Improving energy efficiency and harvesting renewable energy supplies is becoming increasingly important to California. Specifically, climate change is threatening California's water resources, coast lines, and agriculture. Even though no one knows exactly when and to what extent climate change will impact California, the impact of climate change will likely be costly and potentially devastating. Consequently, the state has been aggressively pursuing greenhouse gas (GHG) emission reductions through policy and incentives.

A major contribution to climate change is the emission of carbon dioxide that is associated with the conversion of carbon-based fossil fuels for transportation, electricity and heat. As a result, a challenge of reducing GHG emissions is reducing the dependence on fossil fuel resources. With more than a century of engineering, carbon-based fossil fuel resources can be converted to effectively provide heat, personal transportation, mobility and electricity cheaply and on demand. Consequently, California's infrastructure has been deployed and structured based on an abundant supply of cheap fossil fuel resources. Consider:

Transportation: Most Californians own and drive around in heavy automobiles powered by fossil fuels. Most commute alone in personal vehicles to work, to run errands, and to travel to destinations (e.g., sports events, resorts, meetings with clients). This driving habit is supported by an immense roadway network that enables people to use their personal vehicles without reliance on others.

Urban Layout: Cities are designed with limited public transportation based on the understanding that personal transportation will get Californians where they need to go.

Electricity: In addition to hydroelectric and nuclear power generation, the availability, reliability, and cost of electricity are managed through fossil fuel power generation. More than 50% of electricity in California is generated from fossil fuel resources.

Buildings: Buildings are designed in the simplest fashion to last as long as possible, with little design effort for efficiency (even though this is slowly improving). Fossil fuels provide electricity and heat – cheaply as needed.

Heating: Building heating and air systems are as simple and robust as possible, primarily relying on fossil fuel or electricity to provide energy for heat and air conditioning on demand.

Reductions in GHG emissions and Californians dependence on fossil fuel resources will require changes in almost every aspect of infrastructure and energy deployment, and require a change in energy use, community and infrastructure design, best available energy technologies, policy, and infrastructure operational practices.

CHAPTER 2:
Scope-of-Work

UCI's current energy infrastructure has been built to provide affordable and reliable electricity, relying predominantly on fossil fuel resources to provide energy on demand. To dramatically reduce GHG emissions, we will need to reduce our dependence on fossil fuel resources. This will require UCI to adapt and retrofit community designs, buildings, electric infrastructure, and transportation infrastructure as well as to change our societal philosophy on the consumption of energy.

This chapter identifies the project's major goals, the approach to achieve these project goals, and the motivation behind these project goals. The project's major goals were to develop roadmaps for the UCI community and communities in general to become renewable-based energy secure communities while also determining those policy issues that could facilitate or limit renewable-based energy secure communities. These goals were accomplished using field data collected from pilot projects and various modeling tools to assess technology portfolios. This chapter also provides a short history of the UCI resources and the campus' previous efforts to reduce their carbon footprint and energy costs.

2.1. Goal

The goals of the research program were to establish:

1. An energy infrastructure (electric power , transportation, waste, buildings) roadmap for the UCI community that will maximize the deployment and utilization of renewable energy resources while satisfying reliability criteria, enhancing and sustaining power quality, and minimizing the levelized cost-of-electricity (LCOE)
2. A roadmap for communities who aspire to develop energy infrastructures that maximize the deployment and utilization of renewable energy resources while satisfying reliability criteria, enhancing and sustaining power quality, and minimizing the LCOE.
3. The issues for policy makers and industry leaders that must be addressed to facilitate the implementation of renewable-based energy secure communities throughout the State

Quantitative goals of this research program were:

1. A holistic Energy Integration and Management methodology
2. In addition, the project will demonstrate the deployment and integration of:
    a. 1 MW of PV
    b. 24/7 production of renewable hydrogen and 300kW of electricity using a high temperature fuel cell for sustainable transportation

c. Electric vehicles (plug-in electric and all electric)

d. Battery electric vehicle charging that utilizes dynamic price signals to incentivize the charging of EVs to help manage the energy balance

e. Energy storage that will be required to achieve a RESCO

2.2. Approach

The Advanced Power and Energy Program (APEP) Renewable-based Energy Secure Community (RESCO) project roadmap was developed to suggest technology development and deployment that will minimize the LCOE while ensuring capacity is available and flexible enough to meet electricity demand 100% of the time, accounting for uncertainty in intermittent renewable generation. The various pilot demonstrations informed the modeling activities that allowed analysis of the RESCO capability of many technology deployment scenarios at communities, which then enabled the development of the roadmap. Over the course of this project, it has become clear that the interactions between a community and the grid providing electricity to that community are critical to the successful installation and operation of increased levels of renewables. The research also provides technical and feasibility feedback for state policy.

The research concept for the development of the RESCO project roadmap was to leverage knowledge gained from (a) UCI and APEP pilot projects, (b) UCI as a community platform to evaluate deployment, and (c) modeling of the integration and interaction between grid load balancing, efficient "smart" buildings and the distribution system.

The general approach was to:

1. Utilize installed pilot projects to provide experience and data on both mature and emerging generating and complementary technologies
2. Develop a roadmap for technology deployment
3. Evaluate the deployment of the roadmap for the UCI campus
4. Evaluate the interaction and impact of the roadmap for the state of California.

The observed operational features of various communities and field data obtained enabled the development and application of the Holistic Grid Resource Integration and Deployment (HiGRID) model that was instrumental to developing a roadmap on how to increase the renewables (Figure 1). This model facilitated the investigation of many different technology deployment scenarios at several different community types that provided insights that extended those insights from the pilot demonstrations themselves and lead to important conclusions about renewable integration in general communities. HiGRID simulates technology as well as community, load, transportation, and thermal demands. Using the developed modeling methodology, it is now possible to evaluate preferred energy strategies and sensitivities through parametric analysis of the modeled systems. With HiGRID, preferred integration of state-level renewables (e.g., wind and solar photovoltaic power), regional-level

renewables (e.g., biomass), and community-level renewables (e.g., distributed solar photovoltaic and solar heating) can be evaluated along with potential benefits in community planning and management of distributed energy resources.

Combining the results from more localized pilot projects with the statewide modeling capabilities of the HiGRID tool makes it possible to evaluate RESCOs in an integrated context. The optimal holistic renewable energy solution is site specific and will change as new concepts and technologies are developed. This analysis is used to develop the roadmap for the UCI campus community presented in Chapter 3. Further, by identifying cost-effective technologies and establishing infrastructure guidelines and strategies, a second roadmap for communities throughout California that desire to develop their own RESCOs is presented in Chapter 4.

Figure 1: Nexus between pilot projects and energy management modeling used to develop a roadmap for UCI RESCO implementation

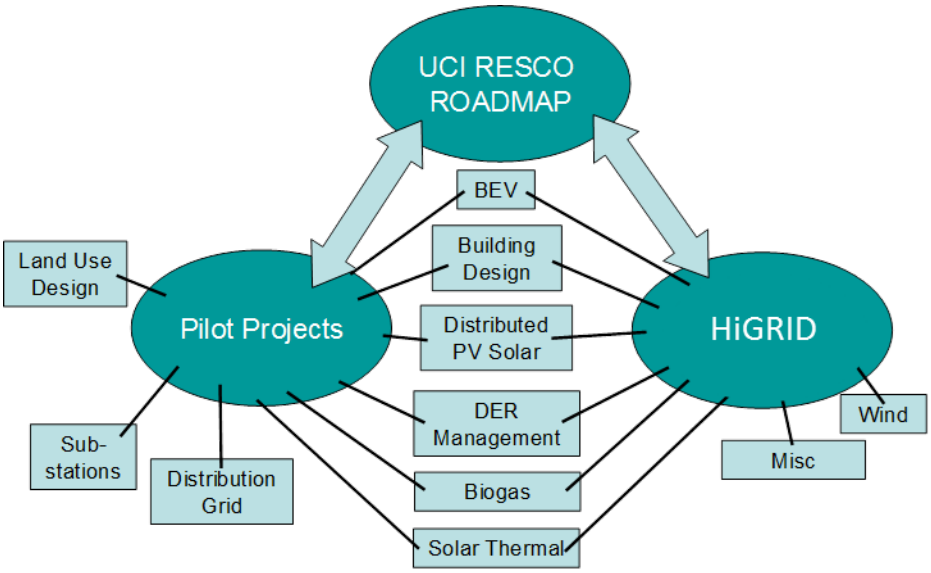

The research program consisted of the field projects listed in Table 1 (below), in addition to other available data and resources that had not heretofore been integrated into a holistic study. While the field data provide valuable insights and actual performance data to verify models, the evolution of the deployment and operation of various technologies was evaluated and optimized using specifically developed models. Specifically six levels of models were developed to construct the roadmaps, with the goal being to maximize renewable penetration at the minimum cost:

- Building models (Appendix E:Task 6:)
- Campus energy management models (Appendix B:Task 3: and Appendix C:Task 4:)
- Campus 'micro' grid models
- Vehicle models (Task 3.3)

- Wind and Solar power generation models (Appendix F:Task 7:)
- Local and Regional Holistic Grid Resource Integration and Deployment (HiGRID) model (Appendix F:Task 7:)

The interactions between the various models and pilot projects are represented in Figure 2 and are separated into the appropriate project tasks. The first technical task (Task 2) investigated the electrical engineering aspects relating to a RESCO. The characteristics of electricity transmission and distribution observed in this task were accounted for as the HiGRID tool was developed. Task 3 investigated the dispatchability of cooling loads and how they might be dispatched in such a way to support high penetrations of renewables in a RESCO. The models developed in Task 3 were integrated into the HiGRID tool. Task 4 then collected data from the various solar pilot demonstrations which informed solar model development. Information related to the electrical engineering aspects of solar overlapped with some tasks in Task 2. These Task 4 models were prepared for integration into HiGRID in Task 7. Task 5 examined the transportation aspects related to RESCOs and developed vehicle operation models for integration into HiGRID in Task 7. Task 6 gathered building operation data and performed pilot demonstrations of demand response to inform model development for integration into HiGRID in Task 7 which would enable analysis on the effectiveness of dispatchable building loads in supporting renewables. Task 7 integrated the models developed in all prior tasks into a community modeling tool – HiGRID. HiGRID was then exercised to examine various technology deployment scenarios in their effectiveness at establishing RESCOs to inform the roadmap development – this effort's primary goal.

Figure 2: Interactions between RESCO pilot projects and models within each of the project tasks

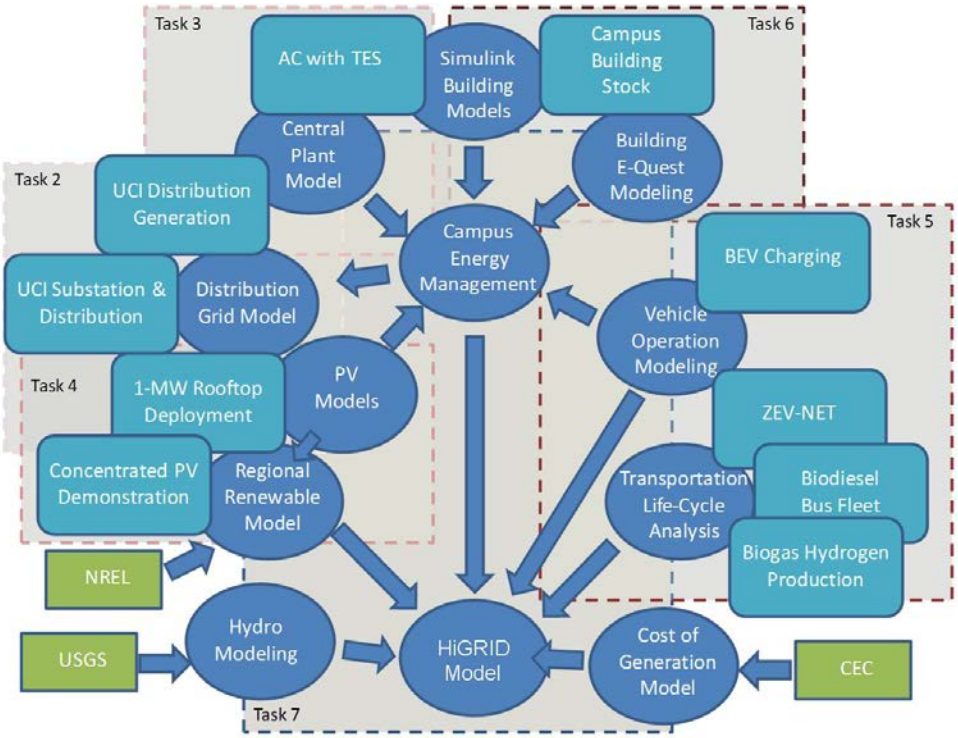

Table 1: Field Pilot Projects

Field Pilot	Implemented under RESCO	Description	Task
UCI Substation and Distribution Grid	√	Model and evaluate UCI circuit to enable the interconnection of distributed energy resources on the UCI micro-grid.	2.0
UCI Distributed Generation (13.5 MW combustion turbine + 4.5 MW steam turbine)	√	Model and evaluate the operation of UCI distributed generation equipment.	3.0
UCI Central Air Conditioners with TES	√	Model and evaluate how dispatchable air conditioning system can help manage intermittent renewable generation.	
BEV Charging	√	Monitor BEV charging and use. Provide insight to develop a BEV charger that will minimize vehicle charge cost given a price signal and charge time.	
MW Solar PV System		Monitor MW of PV generation on the UCI campus.	4.0
Concentrated PV Demonstration	√	Pilot the installation of concentrated PV systems.	
Biogas CHP Plant with H2 Co-Production		Quantify the value of a CHP and hydrogen co-production energy station operating on biogas.	
Zero Emission Vehicle – Network Enabled Transportation (ZEV-NET)		Evaluate the carbon and energy footprint of student and faculty utilization of public and alternative vehicle transportation.	5.0
Operation of Bus Fleet on Biodiesel		Evaluate the carbon and energy footprint of students, staff, and faculty that utilize public transportation.	
Campus Building Stock	√	Monitor and model building design and operational criteria to aid renewable penetration.	6.0

2.3. Research Motivation

It is essential that electric and transportation energy provisions continue to be provided, whether or not community supplies of electricity are secured from renewable or fossil-free sources of energy:

- Reliably
- Economically
- Securely and
- Transparently to the end-user,

To secure communities' energy Reliably, Economically, Securely, and Transparently (REST) with renewables requires unified and coordinated policy and investment among the community, city-government, state-government, utilities, and energy industry.

A shift in the paradigm for the provision of energy from fossil-fuel to renewable energy resources is resulting in increased interaction and dependence among electric power generators, electric distribution and transmission, electric transportation solutions, and building distributed energy resources. To achieve a fossil-free community: (a) the independent system operators (ISOs) will have to manage increasingly more dynamics and fluctuations with increasingly less dispatchable generation resources; (b) the electric utilities will have to interconnect regional renewable resources and provide an electric infrastructure that supports an increasing amount of electric vehicle charging and advanced technologies like energy storage and demand response; (c) building owners will have to more efficiently use electricity and participate in demand side management programs when possible; (d) city governments will have to site new distributed energy resources responsibly and strategically; (e) state and federal governments will have to establish increasingly aggressive policies and energy efficiency standards; and (f) companies will have to develop affordable, more flexible and more efficient products to support energy advancements.

2.4. UCI Community and Pilot Projects

UCI has been aggressively pursuing energy innovations and alternatives to minimize its carbon and environmental footprint with a unique combination of business operations, academic research, and flexible energy infrastructure (Figure 3). The strategy encompasses electric power generation, transportation, building design and operations, and modeling.

This research program has utilized these pilot projects and campus resources in concert with the HiGRID model (Task 7.1) to develop a roadmap, which minimizes the cost of energy accounting for reliability and system performance requirements.

UCI Campus. As a cornerstone of one of the youngest, largest, and most prestigious planned communities in the country (the City of Irvine), UCI was established on sprawling undeveloped acreage on the bluffs bounding the Pacific Ocean. This allowed the campus to be methodically and systematically designed from scratch with a large, circular central park encircled by a one-mile underground utility tunnel loop connected to central energy and information infrastructure. The UCI Community was integral to this modern design along with a modern district heating and cooling system. Today, the UCI Community serves more than 30,000 people and encompasses a wide array of building types (residential, office, research, classroom), transportation options (automobiles, buses, shared-cars, bicycles), and a wide array of distributed energy resources. Through an array of prior and current research programs, the UCI Advanced Power and Energy Program (APEP) has teamed and worked with the UCI Administration and Facilities Management (FM) to integrate key microgrid hardware, software, and simulation assets into the UCI Community.

Figure 3: Existing UCI Infrastructure

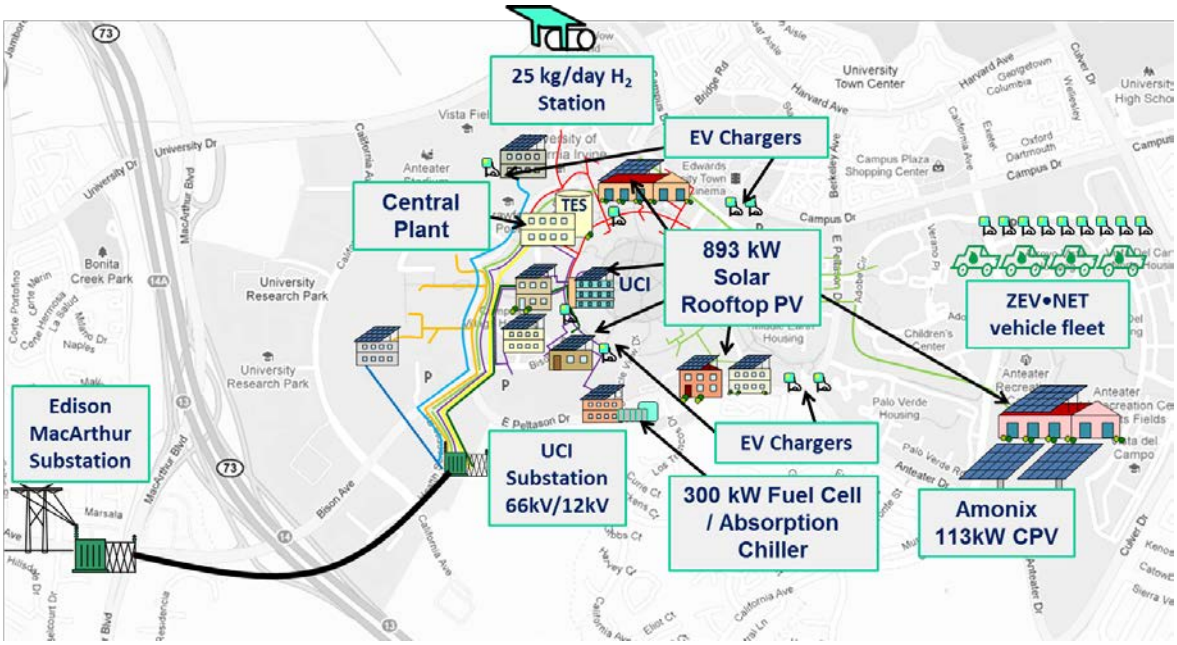

Substation and Campus Circuits

The electric service for the UCI campus has already experienced a history of change and steady growth that defines its present characteristics. The early campus was served directly from two SCE 12 kV circuits that entered the UCI central plant. Each of these two circuits separated into sub-circuits that fed the portion of campus around the central plant. A third SCE 12 kV circuit fed the East Substation, which was located on the opposite side of campus. This third line also connected to a bus bar that energized more sub-circuits to serve the east side of campus.

In 1990, the UCI Substation was built to accept a SCE 66 kV service directly and step the voltage down to 12 kV locally and thereby displace three legacy circuits. Most buildings in the main UCI campus are still served by infrastructure derivative of these three main circuits. The primary feed for the UCI Substation is an SCE 66 kV line with a single billing meter. The two UCI Substation transformers, which cannot be paralleled, each serve 5 circuits and a capacitor bank. The 12 kV side of the two transformers are connected with a tie-line switch. At present, the two capacitor banks at the UCI Substation are disconnected due to a resonance issue that occurred when the 19MW combined cycle plant was installed. The turbines associated with the plant generate reactive power to augment this need.

The history and vision of the UCI electric service have already led to a power system that is flexible for modifications. The emphasis on reliability for campus buildings has led most building transformers to have two circuit sources that can easily shift load. The circuits themselves are reconfigurable through existing switches that were installed to meet various stages of the campus growth. In addition, the utility tunnel provides convenient access to re-conductor critical circuits for increased capacity or to use high speed hard-wired fiber optic

communications strategies in the future. At present, most 12 kV circuit feeders have available capacity. There are also no exportation limitations for UCI Substation transformers, which would significantly increase the local capacity constraints on any distributed energy resources on the campus. The flexibility elsewhere in the system may improve capacity challenges on the distribution and substation transformers, but these locations are not inherently suited to direct modification.

More details on the UCI electric grid are provided in Appendix A.

Central Plant

The UC Irvine Central Plant consists of 8 electric chillers, a steam turbine chiller, a thermal energy storage tank, boilers (used only for backup), a 13.5 MW gas turbine, a heat recovery steam generator (HRSG), a duct burner, and a 5.5 MW steam turbine (Figure 2). The central plant serves all the campus heating and cooling loads as well as the majority of the campus electric loads. The 8 electric chillers are capable of supplying 14,500 tons, and the steam driven chiller is capable of an additional 2,000 tons. The campus cooling load averages 3,100 tons (74,400 ton-hours per day) with a peak annual demand of 13,900 tons. The thermal energy storage tank uses a thermocline to minimize mixing. The chillers operate to facilitate this thermocline while also increasing efficiency by recirculating water exiting the chiller back to the chiller inlet until 39 F is maintained at the chilled water exit. The thermal energy storage tank is able to shift, on average, 65% of the chilling load during the day to the night when electricity prices are lower and temperatures are cooler, which results in more efficient chiller operation via better heat rejection through the cooling towers. The campus heating load averages 44 MMBtu/hr with a peak annual demand of 100 MMBtu/hr. The heating load is served entirely through recovered heat from the gas turbine and use of the duct burner. The HRSG can supply 52,000 lbs/hr steam without duct fire and 120,000 lb/hr with duct fire. The campus electric load averages 13.4 MW with a peak annual demand of 18.6 MW (note: this is the electric load separated from the electricity used to serve the campus cooling loads). The gas turbine and steam turbine supply about 85% of the electrical needs on the campus with the balance being served by solar resources (1%) and utility import (14%).

UCI has 893 kW of fixed panel solar photovoltaic installed on the rooftops of 12 buildings (Figure 3). This system is owned and operated by a third party provider with the electricity purchased by UCI through a power purchase agreement. The capacity factor for these panels, in operation since 2008, was 0.187 in 2012, which is reasonable given the coastal climate. The system provides 1% of the campus electrical needs. An additional 2.8MW of fixed solar PV is scheduled for installation.

An additional 113 kW of concentrated solar photovoltaic with two-axis tracking was installed in 2012. Although the campus solar resources are still at a low penetration (1%), these resources are already causing the gas turbine to be turned down at times of low electric demand and high solar irradiation. Figure 6 shows UCI Community data at 15 minute resolution for a weekend in May 2012. The gas turbine can be seen having to respond to changes in solar output. These

observations have led to the HiGRID model being used to inform campus operations on how to deal with further future solar installations.

Figure 4: UC Irvine Central Plant

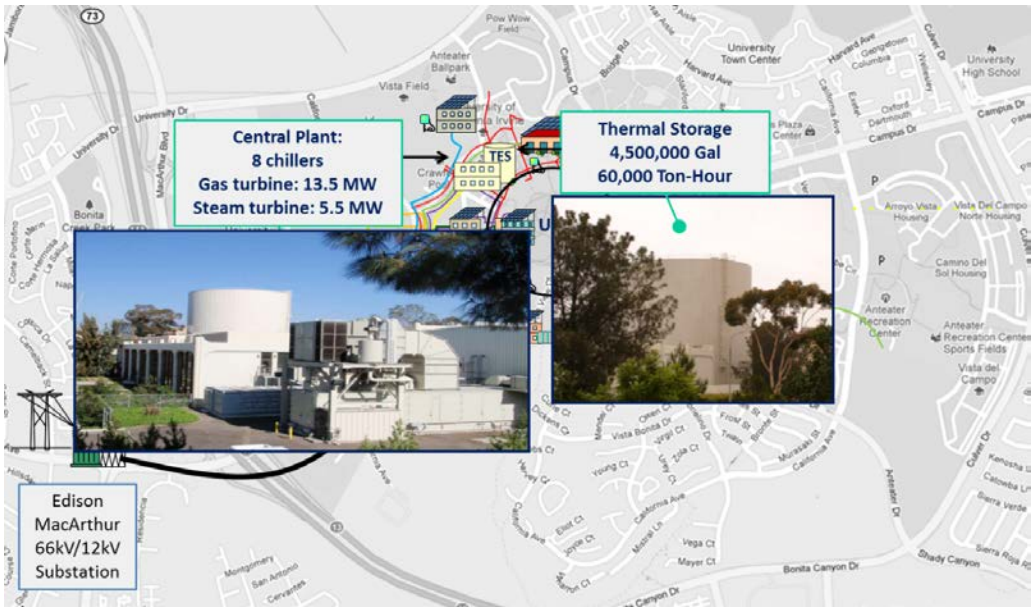

Renewable Power

Figure 5: UCI Community renewable power

Figure 6: Gas turbine responding to solar output

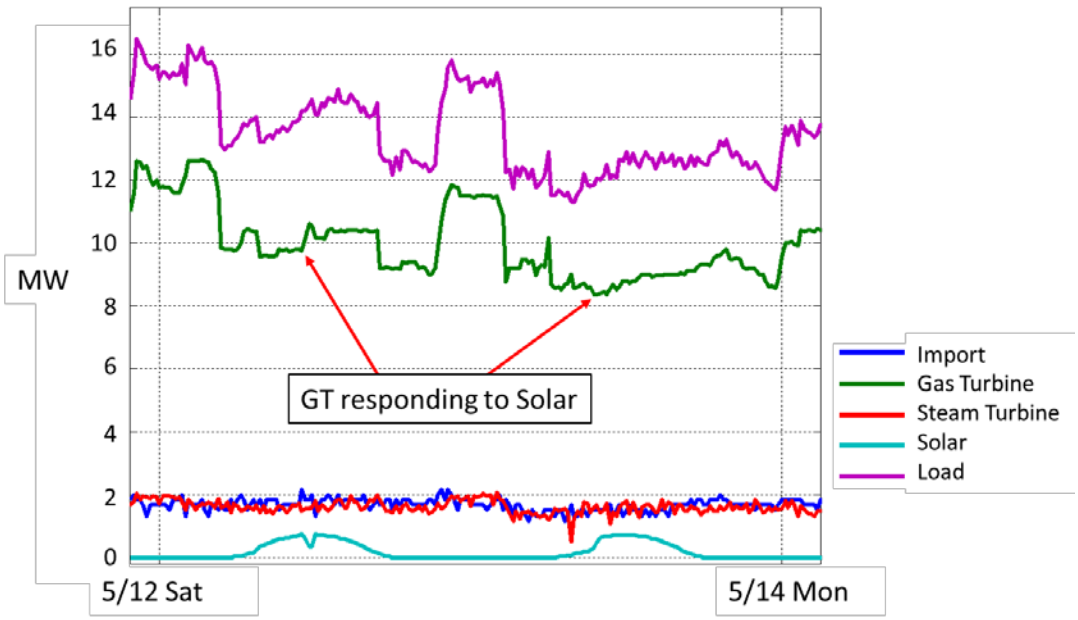

Enterprise Energy Management System

The RESCO project activities initiated a partnership between MelRoK, LLC and APEP/UCI campus operations to provide an enterprise energy management solution capable of informing the HiGRID model of the UCI Community. This solution will consist of installing 100 advanced meters capable of delivering high resolution data as well as sub-metering building loads. The locations of these meters have been chosen based on a visibility study. This solution will also incorporate existing meters already installed throughout the campus. The data from these meters will be presented to the UCI Facilities Management through MelRoK's EnergiStream software. MelRoK's system is equipped with Demand Response capabilities including Auto-Demand Response. MelRoK's system, in conjunction with the HiGRID model, will provide the UCI Facilities Management team with information necessary to make decisions as more intermittent renewables are installed in the UCI Community in addition to allowing the UCI Community to operate as a smart power and demand response asset for the California Independent System Operator.

Electric Vehicle Charging

The campus has installed 8 Coulomb Technologies level 2 chargers that are open for public use. The APEP also administers the Zero Emission Vehicle•Network Enabled Transport (ZEV•NET) program (Figure 5). This program currently involves a fleet of 77 advanced vehicles. The vehicles include battery electric vehicles (Scion iQ, Toyota Rav4), plug-in hybrid vehicles (Toyota Prius Plug In), and fuel cell hybrid vehicles (Toyota fuel cell vehicles). Some of the

vehicles in the program are used for research purposes only while others are used in a corporate ride-share program.

Figure 7: UCI Community electric vehicle charging

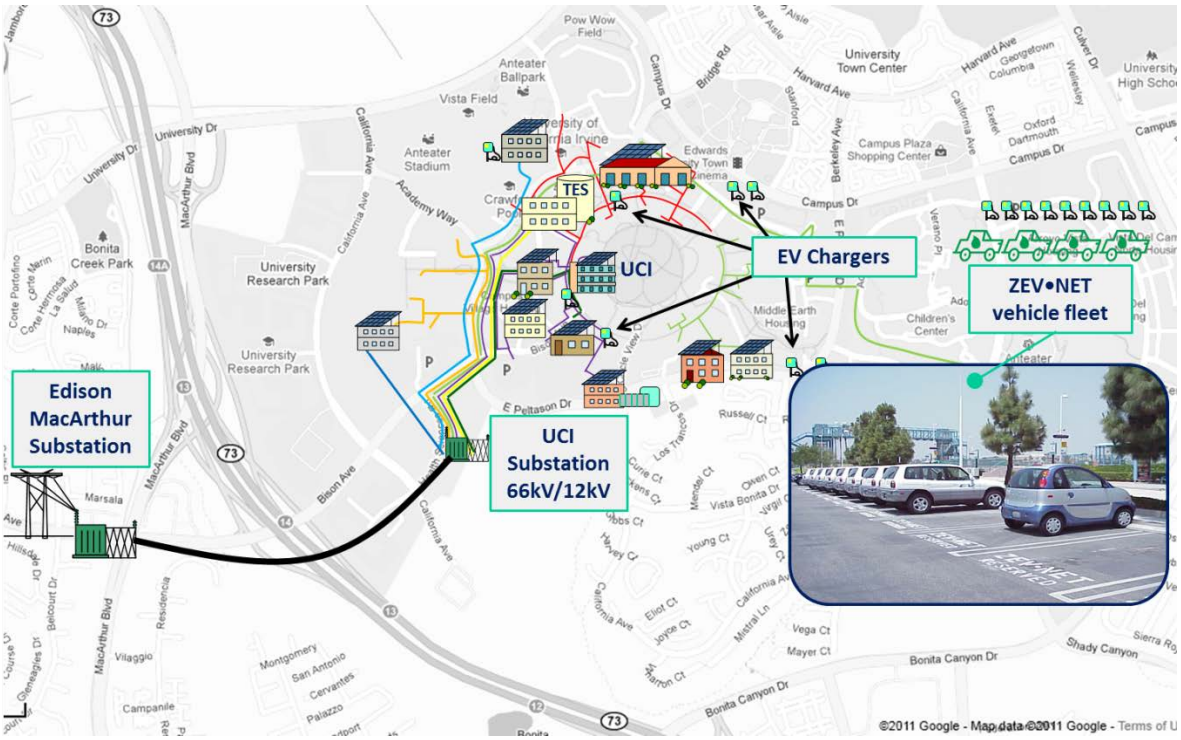

Hydrogen Fueling Station

The UCI Hydrogen Fueling Station serves the fueling needs of fuel cell vehicles for several major car manufacturers (Toyota, Honda, GM, Mercedes, Hyundai). The station is administered by APEP and is capable of delivering fills at 35MPa and 70 MPa (Figure 6). The hydrogen is delivered as a liquid and stored onsite as a liquid in a 1500 gallon insulated vessel. In 2011, the station provided over 2,500 fills with an average daily delivery of 22.4 kg. The station began operation in 2003 with a capacity of several kg per day. In 2005, the station was upgraded to a capacity of 25kg/day. Funding has been awarded to further increase the capacity of the station to 180kg/day by the end of the current calendar year.

The campus, with the support of APEP, also plans to install a 300kW molten carbonate fuel cell (MCFC) manufactured by FuelCell Energy to provide electricity to the Multi-Purpose Science and Technology building (Figure 7). The fuel cell will also be integrated with an absorption chiller (AC) and heat recovery unit to supply cooling and heating to the building as well. A thermal energy storage (TES) tank will also be used to store chilled water for later use when the absorption chiller is providing more cooling than needed by the building (e.g., at night). This installation will also have a control room where interested parties can observe system operation.

This will serve to educate the building industry, government agencies, and others on the benefits of advanced combined cooling heating and power systems.

Figure 8: UCI hydrogen fueling station

Advanced Building Level Combined Cooling Heating and Power

As with most university communities, UCI is populated with a variety of building types. Since the dedication of the campus 45 years ago, UCI has proactively pursued high levels of energy efficiency in the design of buildings, building operations, and infrastructure design. Today, the campus is aggressively designing new buildings to meet LEED standards and deploying extensive instrumentation and control systems for efficient operation. UCI currently participates in the Better Buildings Challenge through the Office of Energy Efficiency and Renewable Energy in the Department of Energy. The program was launched in December 2011 by President Obama. The challenge is to reduce the energy consumed across the campus by 20% by 2020. The program works to match participants with solution providers to enable this challenge to be met. Thus far, UCI has not only met targets but reduced energy use by 10% despite adding one million square feet. The Natural Sciences II building has also served as a showcase for the Better Buildings Challenge as a result of the Smart Labs Initiative instituted there. UCI also participates in demand response programs through, EnerNOC, a registered demand response provider for Southern California Edison. The campus has nominated 700kW of demand response so far. This is achieved in various ways involving the steam turbine, HRSG, chiller

plant, and thermal energy storage tank. UCI also has plans to implement demand response at the building level using MelRoK's technology. For more information refer to Appendix E.

Figure 9: UCI advanced building level CCHP system using a high temperature fuel cell, absorption chiller, and thermal energy storage tank

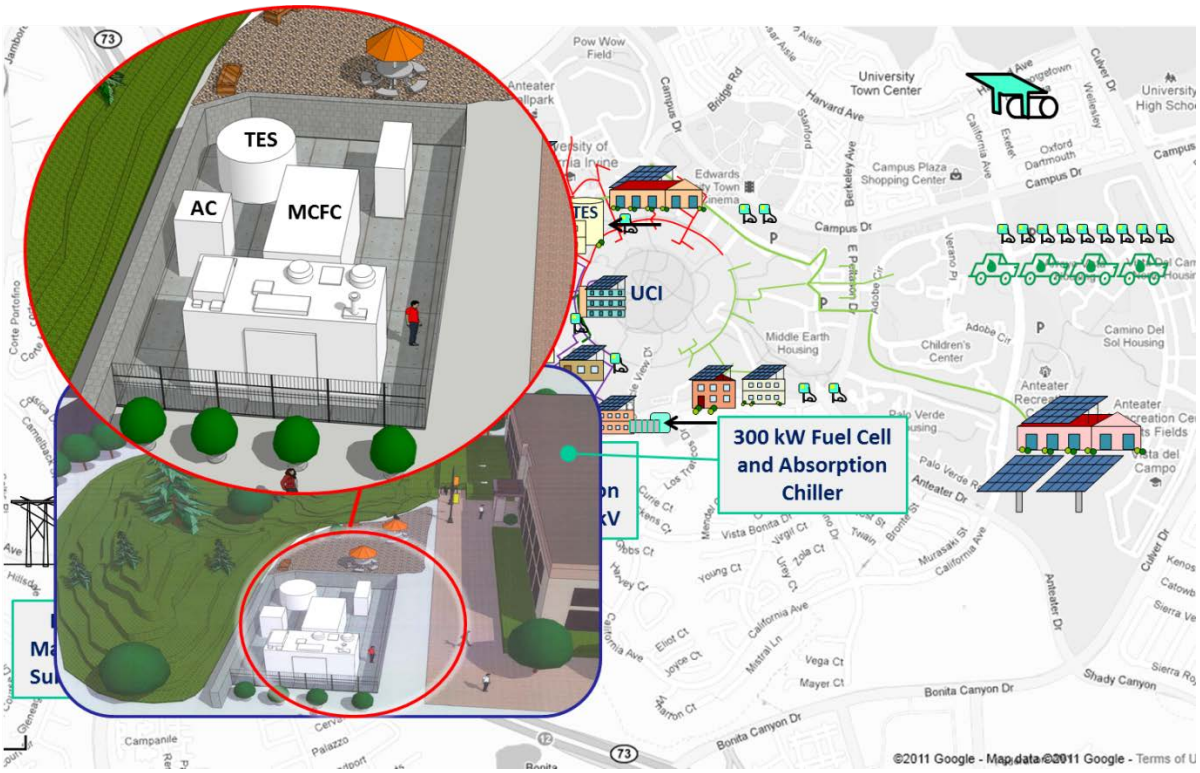

Energy Efficiency and Demand Response

UCI Campus Pilot Project Summary

The UCI Community represents a special opportunity for testing how communities operate internally to become RESCOs as well as how they interface with the rest of the future smart grid to enhance renewable deployment. The relationship between APEP and UCI FM has enabled the UCI community to become a test bed for different technologies through the development of the UCI Community model, deployment of advanced metering, and various pilot projects. In addition, the same substation that serves the UCI Community also serves the Irvine Smart Grid Demonstration project allowing the UCI Community to be tested in the context of smart grid features. The history of the UCI community is also fundamental to its capability as a test bed. The historical design of the campus circuits has left a reasonable amount of flexibility to accommodate various technologies and circuit configurations. Table 2 lists the major attributes of the UCI Community.

Table 2: UCI Community Attributes

Attributes	Description
Substation	69kV to 12kV using two 15 MVA transformers.
Cogeneration Plant	13.5 MW natural gas fired gas turbine. Heat Recovery Steam Generator with Duct Burner. 5.5 MW steam turbine.
Enterprise Energy Management System	MelRok, LLC EnergiStream system. Capable of sub-metering building loads
Central District Heating/Cooling	Maintains 5 million square feet of conditioned space as well as high temperature water to make steam for laboratory use, domestic hot water, and industrial hot water
Thermal Energy Storage	4.5 MM gallons. 65% load shifting on average. 60,000 ton-hours of chilling storage when fully charged.
Electric Vehicle Charging	5 smart chargers on campus. 15 BEVs deployed. 10 PHEVs deployed.
Renewable Power	Fixed PV on 11 campus rooftops for 895kW total. 113 kW dual axis tracking concentrated PV. 3MW additional fixed PV planned for 2014.
Energy Efficiency	Building Retrofits. 10% load reduction despite adding one million square feet. UCI has received national recognition for its energy efficiency work on laboratories.
Hydrogen Fueling Station	Capable of delivering 180 kg-H_2/day. Can fill at 350 bar and 700 bar.
Advanced Building Level Combined Cooling Heating and Power	300 kW Molten Carbonate Fuel Cell (FuelCell Energy) integrated with 40 ton absorption chiller (Yazaki) and thermal energy storage tank to serve needs of Multi-Purpose Science and Technology Building
Demand Response	Nomination of 700 kW through EnerNOC. Multiple strategies using the TES tank, chillers, HRSG and steam turbine.

This chapter provided a brief overview of the project, its goals, and the approach that was taken to fulfill the requirements of this project. To fully understand the details of this project, the UCI electric grid and its resources were briefly introduced. The interactions between various tasks and pilot projects were also introduced. More details are provided in the Appendices.

CHAPTER 3:
University of California, Irvine Roadmap

In this chapter, the UCI roadmap for achieving high renewable penetration and eventually becoming a RESCO is introduced. The challenges that arise with increasing renewable resources are identified, and the complementary technologies that can offset the impacts of increasing renewable penetration and/or allow for greater uptake of renewable generation are introduced. The potential of each technology on the UCI campus is discussed.

The central theme of the roadmap is that high renewable penetrations can be achieved at UCI. Penetrations well beyond the 33% goal set forth by the state of California are attainable; however, to achieve these levels of renewable penetration while maintaining system reliability at the minimum LCOE, the UCI campus must adapt the dispatch of its central plant and heighten its already proactive role in reducing demand and integrating advanced technologies.

Major advances in the deployment of renewable generation correspond to reductions in fossil fuel generation and GHG emissions. Pursuing the deployment of large-scale regional renewable resources, energy efficiency and other demand-side management tools, along with transportation electrification and both thermal and electrical energy storage devices, present opportunities to increase the achievable renewable penetration level.

Results show that, while each technology mentioned above can support the integration of renewables, each must be installed at the appropriate time and place and must be coordinated with other UCI campus resources to reduce dependence on fossil fuels at the minimum LCOE while ensuring electric reliability. As mentioned previously, cooperation and coordination between community and grid-wide energy resources is critical to enabling each system to attain high renewable penetration levels. These concepts are illustrated in Figure 10 which shows the different levels of interaction required for a RESCO. These include the RESCO level interaction managing the resources and the loads in the RESCO, and the RESCO interaction with the grid to access the grid's resources (e.g., large regional renewables, peakers, load followers). This figure emphasizes the importance of the interaction between the community and the grid, which will assure the reliability of the electric system.

Figure 10: Integration of community distributed energy resources with regional renewable resources

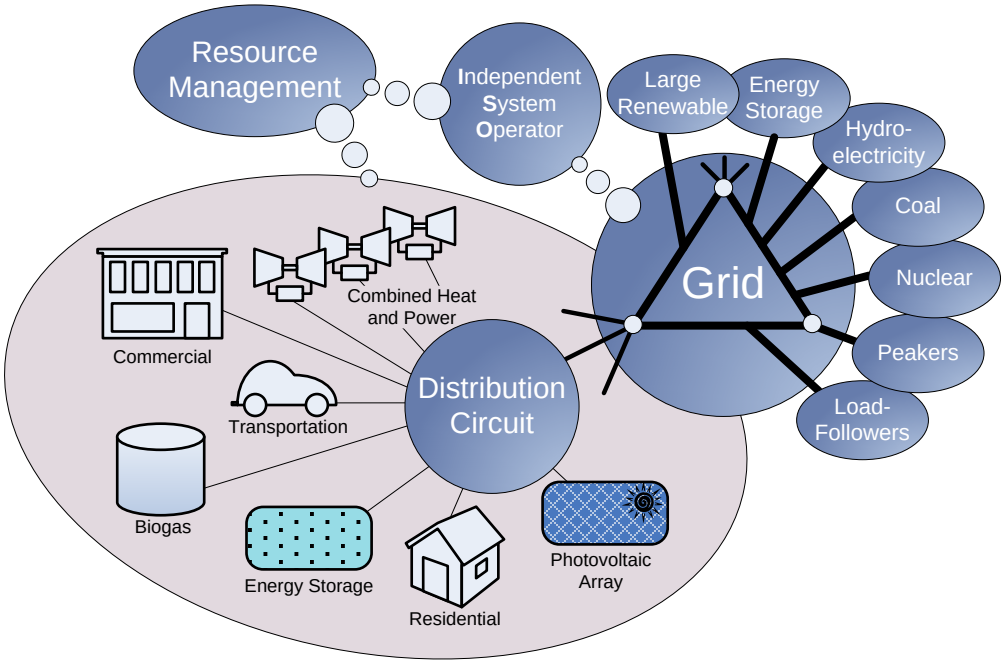

UCI is very aggressive and innovative in energy design. Large investment in the state-of-the-art energy technologies and infrastructure has been made and the UCI campus has 13 LEED certified buildings two of which were added in 2012 with LEED-Platinum certification. Conversion of UCI into a RESCO cannot be done overnight. The transition to secure energy supplies using renewables occurs over time; various policy initiatives and incentives will be required to move communities such as UCI in the direction of reduced dependence on fossil fuel resources. Securing energy supplies with renewables cost effectively is challenging because fossil fuel solutions in many cases will continue to be the simpler and lower cost solutions. The success of communities to reduce GHG emissions and decrease dependency on fossil fuels, cost-effectively, will require state and regional innovation in addition to advancement within the community. Cost effective opportunities within a community are limited and MUST BE COMPLEMENTED with regional and state renewable generation, dispatchable generation, and electric transmission advancements. Nonetheless, advancements in building efficiency and operating flexibility, electric distribution, urban layout, public transportation at the community are essential building blocks to enable cost-effective regional and state renewable deployment on the path to developing RESCOs.

The purpose of the UCI roadmap is to provide the first building block in identifying a path that would allow any community to become a RESCO. Thus, the primary substance of these research program findings have been expressed as just such a 'roadmap' for the deployment of renewable and complementary technologies on the UCI campus, as a function of increasing renewable penetration level (Figure 11).

Figure 11: UCI Roadmap for Achieving High Renewable Penetration

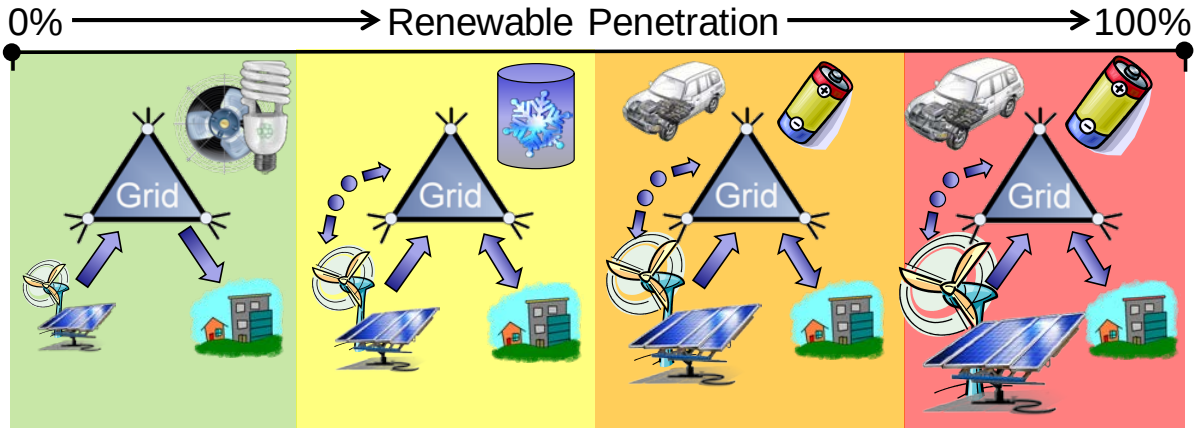

Techs	Energy Efficiency Local Renewables	Demand Response Dynamic Chiller Dispatch Regional Renewables	Energy Storage Generator Flexibility Alternative Transportation	All Complementary Techs., Renewable Dispatchability
Paradigm	Minimal Effects, System operation is ***nearly transparent***	Coordination **required** between community energy resources	Coordination required between community resources and grid, Dispatchable generation **critical** to avoid excess generation	Full dispatchability of energy supply and demand, scientific advances

Before discussing the composition of this roadmap, it is important to understand that the different stages displayed in Figure 11 are not to scale across the renewable penetration level range. For example, the green stage does not necessarily end at 25%, and the yellow stage does not necessarily refer to actions that need to be taken between 25% and 50%, and so on. The different sections represent a continuum of changes in the paradigm of the design of the UCI campus energy system that will become necessary as the renewable penetration level is increased. The exact boundaries of these stages will depend on the renewable and complementary technology mix, as well as on interaction agreements with the grid. Additionally, the technologies listed to achieve the evolving paradigms are cumulative from one stage to the next. For example, reaching the orange stage requires all of the technologies listed in that stage in addition to all of those technologies listed in earlier stages.

At low renewable penetration levels (green stage), renewable capacity levels are low enough such that renewable generation is essentially noise in the system. Renewable generation has minimal effects on the system in this stage. To aid the accommodation of renewable generation in this stage, energy efficiency is beneficial, relatively easy to implement, and many types are cost competitive. Reliance on local renewables is beneficial in this near-term stage to defer required investment in the construction of transmission lines.

At moderate renewable penetration levels (yellow stage), renewable generation becomes large enough to affect the operation of the system. On-campus generation may be required to turn

down to part-load or minimum operating points and slight curtailment of renewables may occur. To mitigate these issues and keep the system stable, the UCI campus will have to enable dynamic dispatch of the system load. The chiller/TES system may be required to dispatch the cooling load in response to renewable generation and the operation of other complementary technologies instead of simply in response to the fixed time-of-use rate structure schedule. Demand response is beneficial from both technical and cost standpoints if coordinated with renewable generation and the operation of other on-campus resources. Additionally, to increase the renewable penetration level, reliance will need to shift from local towards regional renewable resources. Regional renewable resources are less peak-dominated and are of higher quality than local resources, and provide more benefit to the UCI campus even with transmission losses. The use of non-variable renewable power will begin to reach its limit.

At high renewable penetration levels (orange stage), renewable generation severely impacts the operation of the system. The capacity of renewables is high enough such that large amounts of curtailment may occur if actions are not taken, and variable renewables make up the vast majority of the renewable mix. The on-campus gas turbine operates essentially at its minimum level for the entire time if it is not allowed to shut off. To mitigate these issues, more complementary technologies begin to make more economic sense and need to be brought in to manage the system. These technologies include energy storage and smart electric transportation. All of these complementary technologies must be coordinated with each other to ensure the most appropriate response to an event. To advance the renewable penetration in this stage, non-renewable base-load generation must be removed or replaced with flexible generation. For the UCI campus, this entails installing on-campus generation with lower minimum power levels and better ramping capabilities and acceptance of lower capacity factors. If this is not accomplished, the renewable penetration level will be extremely difficult to increase. At this point, the UCI community is becoming essentially an integrated element of the larger grid and must coordinate the operation of its resources heavily with that of the larger grid.

At very high renewable penetration levels (red stage), renewable generation makes up the large majority of the energy supply used to serve the load. To reach and advance the renewable penetration level at this point, the scale of the installed complementary technologies will need to be increased significantly to effectively render the supply and demand profiles as completely dispatchable. Achieving this requires scientific advances in generating and complementary technologies to increase technical capabilities while keeping cost to a minimum.

3.1. Renewable Penetration Potential

The UCI community has a variety of available alternatives to provide utility (i.e., electricity, heating and cooling) requirements to the campus. Local solar photovoltaics or wind are options for power generation, while solar thermal could provide heating for the campus.

Installation of any equipment, including renewables, must comply with voltage guidelines and standards. Results show that significant installation of distributed generation on campus does not infringe on voltage limitations (Task 2.3). Additionally, the UCI campus is well positioned

to create loop circuits to improve system reliability; however, implementing such an architecture is not considered critical to the development of UCI as a RESCO.

Campus buildings, parking structures, parking lots and additional open space represent opportunities to install rooftop solar photovoltaic (PV) or solar thermal heaters. Buildings, parking lots and parking structures at UCI have roughly 65 acres of space available for either solar PV or solar water heaters. Using this space, solar PV could provide 21.7% of the yearly electrical demand of the UCI campus, assuming that all of the solar PV energy could be used. Solar water heaters using that same space could provide 77.1% of the yearly campus heating load, assuming that all solar energy could be used, which would require a very large hot water storage tank, capable of providing seasonal shifting. The installation of solar PV and solar water heaters compete for the same space. In addition to space on buildings, UCI has roughly 110 acres of open land available for installation of concentrated PV; 19.7 acres are on-campus and 90.5 acres are off-campus. This land could generate 33.37% of the yearly electricity demand for the UCI campus if all of the generation could be used. Because of the generation profile of solar power, utilizing all of the generation on campus is challenging, as is shown in Task 7.2.1. As a result, on- and near-campus resources alone are insufficient to provide high renewable penetrations for the UCI campus.

This research finds that regional resources provide a significant advantage over local resources, both technically and economically (Task 7.2.1). The challenge with regional resources is the time required for permitting and installation of new transmission lines, if required. As such, regional resources should be pursued as quickly as possible. Local resources, though not as competitive as regional resources, are valuable to accelerate renewable rollout in the near-term because of the more localized permitting requirements and no need for transmission.

Without storage, renewable generation from these intermittent sources must occur at the time of demand but some renewables can provide some dispatchability. Biofuels, such as those from the OCSD tri-generation facility, represents an opportunity to increase renewables provided to the UCI campus but provided in a dispatchable manner. They can be provided as a fuel for use in a combustion generator, as a fuel to be electrochemically reacted in a fuel cell, or for transportation as a synthesis gas or hydrogen (Task 4.3).

3.2. Integration with UCI Central Plant

The UCI campus has a central co-generation plant that operates on natural gas to supply campus electricity (supplementing imports from SCE) as well as the heating and cooling needs. Electric chillers are operated to provide the chilled water needs for the campus and work in tandem with a large TES tank. The TES tank is capable of providing the entire cooling load for most days if charged fully at night. The TES tank is a proven cost competitive technology that dispatches the campus cooling load demand to reduce SCE demand charges and shifts cooling load from on-peak to off-peak. With proper coordination, the TES tank can increase the achievable renewable penetration on the UCI campus (Task 3.4).

While the TES tank is a valuable, proven resource for UCI, the competitiveness of this technology in other communities would be specific to community cooling needs. The TES tank

is particularly competitive at UCI because the centralized cooling loop allows the aggregation of multiple loads; however, the development of small TES systems continues and can prove beneficial for communities with different sized loads.

The co-generation plant at UCI cannot reduce its electricity generation below 8 MW, without completely shutting off. Added starts reduce the life of the equipment and, to minimize air quality impacts; there are restrictions on the number of times that this plant can be started per year. Because of this limitation, any renewable generation that would cause the co-generation plant to have to operate below 8 MW will likely be curtailed. To ensure the least cost operation with renewables, care must be taken to ensure that the installed renewable generation capacity does not cause the co-generation plant to drop below 8 MW as shown in Task 7.2.1.3. This can be done several ways including by tailoring the mixture of renewables to suit the UCI demand, by dispatching the available resources on campus, or by integrating other technologies that can provide flexibility.

As a result, with sufficiently high renewable penetration, the inclusion of inflexible or marginally flexible generation (i.e., that have startup limitations or must operate at a minimum operating point) on the UCI campus negatively affects the achievable level of renewable penetration. This is because, lacking the ability to export electricity or being penalized for exporting electricity, inflexibilities in the on-site co-generation plant at UCI can result in curtailment of renewable generation. This research finds that if additional non-renewable generation is to be installed on campus, it should be as flexible as possible to maximize the achievable renewable penetration.

3.3. Role of Complementary Technologies

Complementary technologies are those that do not provide renewable electricity but allow for greater uptake of renewable generation by using a variety of techniques. This research explores the impacts of energy efficiency, demand response, energy storage, and electric transportation on the operation and cost of the grid across a wide range of renewable penetrations.

Some complementary technologies provide technical and economic benefit over a wide range of renewable penetrations while others do not provide benefit until high renewable penetrations.

3.3.1. Energy Efficiency

Energy efficiency (EE) measures are those that permanently improve the efficiency of equipment on the UCI campus and thereby reduce both electricity demand and consumption. Retrofit of the campus with extensive EE measures, as presented in Task 6.3, has the capability to reduce the electricity demand by an average of nearly 2.5 MW. All EE measures reduce the electricity demand but the economic competitiveness of any specific EE measure depends on the cost to install and operate the equipment and how the shape of the demand reduction profile coincides with the demand profile itself. Heating, ventilation and air conditioning (HVAC) measures are competitive at a wide range of renewable penetrations, but interior lighting and exterior lighting retrofits are not cost competitive (Task 7.3.2.)

3.3.2. Demand Response

Demand response (DR) is when a customer reduces the consumption of electricity for an end-use device temporarily in response to a market signal or at critical times. Reduced electricity consumption can come from any number of pieces of equipment including building fans, pumps, lights, etc. Several DR techniques are explored to reduce campus electricity demand including: lighting reduction, ventilation fan turndown, pre-cooling, night purge, night cool, morning cool and day cool (Task 6.4). Of these techniques the most promising are lighting reduction and ventilation fan turndown. Both of these techniques result in a nearly instantaneous response with little impact to the building occupants and a significant resulting reduction. Nearly one-third of UCI's total modeled electricity consumption is considered controllable and can be dispatched using DR.

Utilizing the capacity available for DR can reduce the electricity imported by the campus and the resulting demand charge from SCE. For the maximum energy and cost savings, the DR must be coordinated with other campus resources, particularly with the operation of the chillers and TES tank.

Pursuing both EE and DR results in an interesting trade-off. The capacity that is made unnecessary by EE measures is unavailable to use for DR and therefore EE in effect reduces the ability of DR to shift or shed load. In addition to reducing the available capacity of DR, EE lighting retrofits can lower the installed cost for DR lighting retrofits due to the use of similar technologies in both applications, so if EE lighting retrofits are being pursued then care should be taken to enable the use of DR. However, HVAC control measures do not greatly impact the cost of pursuing DR.

3.3.3. Energy Storage

The effects of installing vanadium redox flow battery (VFB) systems of different energy and power capacities on the UCI campus are modeled in Task 3.2.8. Use of any energy storage system results in an associated energy penalty for charging and discharging the system. The benefit provided by shifting the energy must outweigh the energy penalty for the energy storage system to be beneficial. Inclusion of energy storage on the UCI campus improves the campus operation and enables greater uptake of renewable generation over a wide range of renewable penetrations. To retain these benefits, systems need to be appropriately sized in terms of their power capacity and duration. Also, to ensure the most effective use of the energy storage system it must be coordinated with the other dispatchable resources on campus, namely the chillers and TES tank, as well as the natural gas turbine (Task 7.3.1.3).

Despite the technical benefits of installing a VFB, the system is not cost competitive at UCI. Though energy storage on campus is not cost competitive at current energy storage costs (Figure 385) and under the current SCE rate structure, as the renewable penetration increases and the on-campus generation profile is increasingly influenced by renewables, the value of dispatchable and flexible resources will climb. This effect will be seen at both the UCI level and the grid level, again emphasizing the need for cooperation and coordination between community and grid-wide energy resources.

3.3.4. Electric Transportation

Electric transportation presents a unique opportunity to shape the UCI campus electricity demand profile. The behavior of electric transportation differs from the other complementary technologies such as VFB and other energy storage technologies. Energy efficiency and DR reduce electricity demand, and energy storage shifts electricity demand, but electric transportation actually adds electricity demand to the system.

Based on the National Household Traffic Survey (NHTS 2009), it was determined that more than 80% of the dwelling time of vehicles occurs at detached homes. This implies that recharging vehicles in a garage is the most likely option for drivers and the most favorable option will be home chargers (Task 3.3.2).

The model used to implement electric transportation at UCI and some of the model's results are shown in Task 3.3. The implementation of electric vehicles improves operation and the uptake of renewable generation, and the charging strategy of the vehicles can provide either more or less benefit. "Smart" charging provides the best performance of the three charging strategies investigated, with the "Immediate" and "Delayed" charging exhibiting similar results. When calculating the LCOE of the system, it was assumed that the costs of the electric infrastructure, the vehicle and communication equipment are completely shouldered by the consumer and as a result have no impact on the campus LCOE. The cost impact of electric transportation on the campus LCOE is solely due to the impact that each charging strategy has on the cost of meeting the new electricity demand profile. Under this assumption, the campus LCOE is reduced the most for "Smart" charging and less so but nearly the same for both "Immediate" and "Delayed" charging (Task 7.3.4.3).

In order to achieve the prescribed benefit, the electric transportation system must be coordinated with other available generating and complementary resources. Immediate charging does not require any information beyond the charging start and stop time and since it represents the most convenient charging strategy for users it need not be incentivized. Delayed charging requires information about the next planned trip of the vehicle owner and since it is less convenient for the user it likely will need to be incentivized. Lastly, Smart charging requires not only information about the next planned trip but also a signal from the UCI campus about the best time to charge. A real-time price signal can be used in conjunction with the user's trip information to incentivize smart charging as discussed in Task 3.1.

3.4. Public Transportation and Land-Use design

A survey of students, faculty and staff was taken that captured the behavior of individuals who utilized different types of transportation alternatives. For transit to campus, public transportation and biking have the lowest energy per person-mile and carbon dioxide (CO_2) emissions per person-mile of any of the alternatives. Walking and carpooling have the second lowest energy and CO_2 per person-mile, and single occupant conventional vehicles have the highest energy and CO_2 emissions per person-mile (Task 5.1).

The best way to reduce transportation emissions is to live close to the workplace. Reducing vehicle size and increasing vehicle efficiency can reduce energy intensity and cut CO_2 emissions

as much 50%. Riding a bike or walking to campus can reduce CO_2 emissions although required travel time renders human-powered alternatives unable to replace all forms of transportation (Task 5.2).

3.5. Community Role in Supporting the Grid

For a single community trying to become a RESCO, any unwanted electrical fluctuations introduced by intermittent renewables can likely be absorbed by the grid; however, if every community wishes to become a RESCO, it may not be possible for the grid to support all of the fluctuations associated with high renewable penetrations without significant investment in flexible generating and complementary technologies. Additionally, as more utility customers begin to provide self-generation from intermittent renewables, the utilities will be asked to provide less energy and to accommodate larger system dynamics. Thus communities must be prepared to either pay more in utility rates to be provided the necessary flexible generation or do their part in reducing those fluctuations.

The UCI community currently has a significant collection of resources that can provide buffering for intermittent renewable fluctuations including the co-generation plant, the TES tank, DR and a limited but growing electrified vehicle population. It has been shown that DR, energy storage and electric transportation can provide some dispatchability to support renewables.

In summary, to achieve high renewable penetrations characteristic of a RESCO at UCI, the first building block is identification of optimal technology deployment scenarios by evaluating many of them. This enables roadmap development that identifies necessary actions that need to be taken at each stage of increasing renewable penetration. At UCI, the interactions between the renewable resources and the central plant were noted, and it was concluded that in order to avoid renewable curtailment, additional non-renewable generation must be installed and should be as flexible as possible. Energy efficiency, demand response, energy storage, and electric transportation were identified as viable complementary technologies that allow increased uptake of renewables and help achieve a RESCO.

CHAPTER 4:
Roadmap for Aspiring Communities

Communities aspiring to be RESCOs have a wide variety of differing characteristics, including available resources, meteorological conditions, installed equipment and electric demand. Additionally, communities can vary in size from the size of a neighborhood with a few dozen homes, to the size of a college campus like UCI, to an electric utility such as Los Angeles Department of Water and Power or Southern California Edison, or even the entire state of California. This means that the ideal roadmap for aspiring communities is heavily dependent on their specific location and characteristics. As a result this research program explores what measures "generic" communities in California should pursue to reduce their fossil fuel consumption, and to increase their renewable generation penetration to provide reliable operation at the lowest LCOE.

California has significant renewable generation potential representing nearly 250 times the current renewable and non-renewable generation capacity of the state (CEC-150-2011-002). The potential capacity is primarily solar photovoltaic, concentrated solar power, and biomass; small hydroelectric and geothermal capacity is nearly halfway to the maximum potential capacity already. As a result, solar and wind power are selected as the renewable technologies to be installed to meet California's 33% renewables mandate.

If many communities in California wish to become RESCOs and install large amounts of intermittent renewables including wind and solar, the results of this research show that the resulting generation fluctuations will be challenging for the grid to support, particularly at high renewable penetrations (Task 7.2.2).

The approach to examine generic communities is to use the HiGRID model and apply it to the state of California. HiGRID separates the major generation technology types by duty cycle including intermittent (e.g., wind, solar), baseload (e.g., coal, nuclear, geothermal), hydroelectric, load-following (e.g., combined cycles, combustion turbines) and peaking (e.g., combustion turbines). The state's hourly electricity load is met by each generation type as that generation type's operating parameters will allow as shown in Task 7.1. In this way, the impacts of installing renewable generation on the grid can be explored, and recommendations can be made for a "generic" community within California.

The resulting recommendations for achieving high renewable penetrations for generic communities are presented in Figure 12. Recommendations are based on enabling greater renewable penetration while also respecting grid reliability requirements and state renewable penetration goals with the least cost alternatives.

Figure 12: Roadmap for Achieving High Renewable Penetration

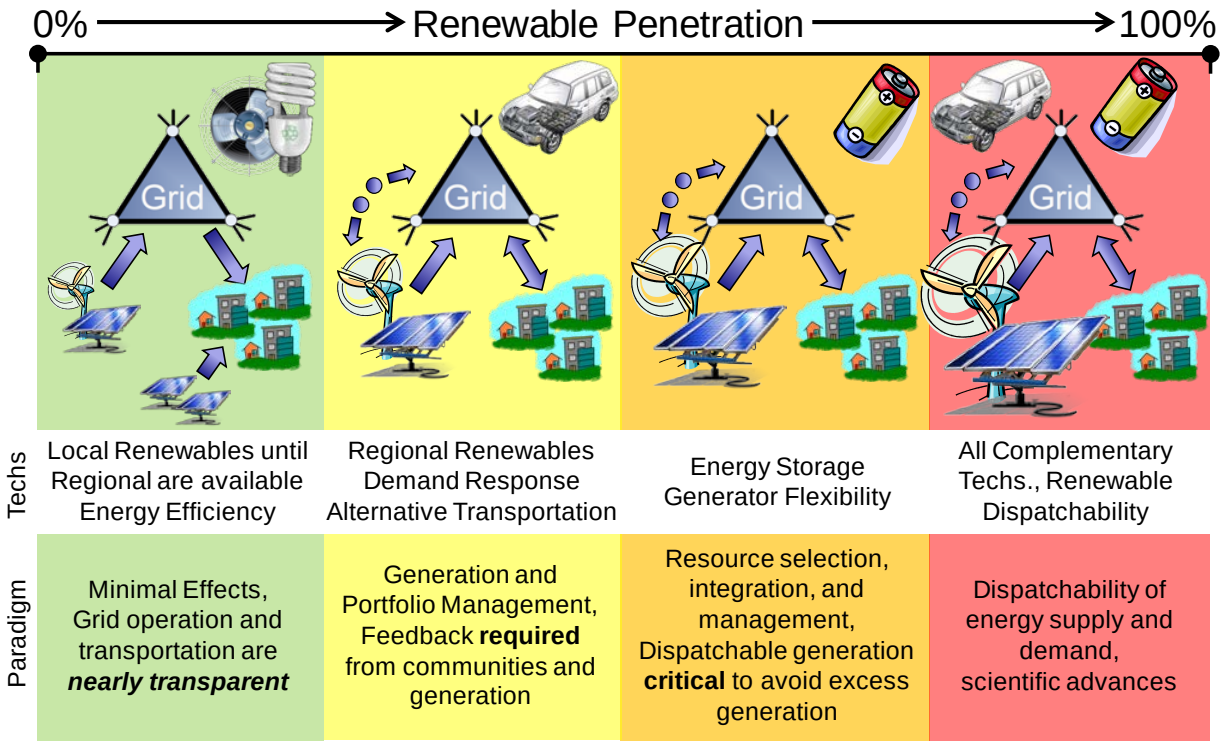

Similar to the UCI roadmap, the different stages displayed in the community roadmap are not to scale across the renewable penetration level range. For example, the green stage does not necessarily end at 25%, and the yellow stage does not necessarily refer to actions that need to be taken between 25% and 50%, and so on. The different sections represent changes in the paradigm of the design grid energy system components that will become necessary as the renewable penetration level is increased. The exact boundaries of these stages will depend on the renewable and complementary technology mix as well as on interconnection agreements with the grid. Additionally, the technologies listed to achieve the evolving paradigms are cumulative from one stage to the next. For example, reaching the orange stage requires all of the technologies listed in that stage as well as all of those technologies listed in earlier stages.

At low renewable penetration levels (green stage), renewable capacity levels are low, and renewable generation is noise in the system. The operation of both the electric grid and the transportation sector is essentially transparent to the end user. The focus should be on enabling regional renewables and in particular wind generation. While the necessary permitting is completed and transmission lines come online, local solar can be pursued. Utilizing EE measures is beneficial for accommodating renewables in this stage by reducing electricity demand and allowing the small amount of energy obtained from these renewables to serve a larger fraction of the (remaining) load. Energy efficiency measures are also relatively easy to install and many types are cost competitive.

At moderate renewable penetration levels (yellow stage), renewable capacities are large enough to affect the operation of other resources on the grid. The results of the research show that the renewable portfolio should focus on installation of regional wind power with at least twice as much installed wind power capacity as solar power. The balance generation fleet required to keep the grid in balance will be tasked with operating more dynamically in the face of power dynamics from intermittent renewables and will also likely exhibit decreased capacity factors. Utilization of peaking generation may increase to handle short-term renewable generation decreases during periods of high load. To help alleviate this behavior, DR and alternative transportation measures can be deployed. Demand response measures can be cost effective on the grid-wide scale and require minimal equipment upgrades but provide additional dispatchability. Similarly, alternative transportation (e.g., PEVs and FCVs) can help introduce more dispatchability into the electricity demand that the balancing generators must meet. For these benefits to be garnered, however, feedback from the communities where these measures are installed must be provided to grid operators such that generation can be intelligently dispatched to minimize the LCOE of the grid portfolio. This feedback can include scheduling the operation of these measures as well, based on forecast electricity demand.

At high renewable penetration levels (orange stage), renewable capacity levels are high, and the intermittency of the corresponding generation severely impacts the operation of the system. The capacity of renewables is high enough such that large amounts of renewable curtailment may occur in the absence of adequate management capability. The load following power plant fleet consists of generation capacity that is mostly in place to meet reliability and reserve margin requirements on the grid and that can consequently have very low capacity factors. Selection of the renewable portfolio mix has a strong impact on how the system will have to respond at this stage. To mitigate these issues and advance the renewable penetration level in this stage, implementing measures such as energy storage and flexible generation is required. The presence of high base load levels presents the primary limiting factor to increasing the renewable penetration level, causing renewable curtailment to increase exponentially. Therefore, the replacement of this generation capacity with flexible generation capacity is required. The benefits of using energy storage are more valuable at this stage, start to make economic sense, and can provide substantial benefits for managing the system.

At very high renewable penetration levels (red stage), renewable generation makes up the large majority of the electricity supply used to serve the load. Similar to the UCI roadmap, reaching and advancing the renewable penetration level at this point requires that the scale of the installed complementary technologies be increased significantly to effectively render both the supply and demand profiles as completely dispatchable. Achieving this requires scientific advances in both generating and complementary technologies to increase the grid's technical capabilities while keeping costs to a minimum.

4.1. Renewable Penetration Potential

Several types of renewable generating technologies are examined for the state, including local and regional solar photovoltaics as well as local and regional wind (Task 7.1). Regional

resources are located in areas of high resource potential, and local resources are located close to population centers based on the best local resource potential.

Renewables affect the resulting electrical load signal in unique ways. Wind generation, on average, is slightly focused in the nighttime hours of winter and spring while solar generation is focused in the afternoon of the summer and fall and does not provide any generation during the evening and early morning. Because of the variability in the generation signal even with large and well-dispersed renewable sites there can be rapid increases or decreases in generation and on the worst day even no generation. As a result, installing intermittent renewables capacity does not guarantee that other generation capacity can be removed, as shown in Task 7.2.2.3. 1 MW intermittent renewables $\neq$ 1 MW of load-following or 1 MW of peaking or 1 MW of baseload.

Increasing the size of a renewable site is shown to reduce the magnitude of the power fluctuations, and dispersing renewable sites through a geographic region decreases the relative magnitude of power fluctuations, as shown in Task 7.1.3.

With the current renewable "must-take" strategy in place in California, electric generation fluctuations from intermittent renewable generation must be absorbed by the grid. However, if the grid is to continue providing the required balancing generation to meet the load and the ancillary services to maintain reliability even with high renewable penetrations, this strategy must be re-evaluated.

Changes in the load shape and how renewables are handled in the market must be considered when developing time-of-use or real-time rate structures. Appropriate design of these rate structures can help support grid operation and incentivize greater uptake of renewables. Similarly, greater differentiation between the prices offered to flexible versus non-flexible generation can help incentivize an increase in the amount of flexible generation capacity installed, as required to balance increasing levels of intermittent renewables.

In all cases explored, without incentives renewable generation increased the portfolio LCOE of the grid-wide system and the increase varied with the resource type and the selection of complementary technologies. This is because of the still relatively high capital costs of the renewable technologies and because of how their intermittency affects how the other generation on the grid must operate (Task 7.2).

Among the renewable resource types analyzed, this research finds that regional resources provide more energy at a lower LCOE than do locally cited resources. Despite the efficiency penalty for transmission and the cost associated with adding transmission lines, higher capacity factors and less intermittency contribute to higher achievable renewable penetrations and a lower portfolio LCOE, as shown in Task 7.2.

While regional wind on its own provides the best performance and lowest LCOE of any single renewable resource, it is recognized that combining different types of renewable resources can further improve the performance and lower the LCOE in comparison to a single resource. Four separate optimizations were performed to determine the renewable resource mixture resulting

in the minimum LCOE, maximum capacity factor, minimum CO_2 emissions and maximum grid efficiency (Task 7.2.3). The optimal wind to solar power mixture varies based on the cost function; however, in all cases more wind should be installed than solar power by at least 2.5 times.

4.2. Design Decisions

Historically, dispatchable generation (e.g., load-following, peaking and hydroelectric) provides the majority of ancillary services (AS) to the grid because of its ability to operate below rated capacity and reserve the remaining capacity for AS (Task 7.1.4). As the renewable penetration increases, dispatchable generation must still provide AS while also balancing renewable intermittencies. This is compounded by the fact that increases in renewable generation will necessarily reduce the amount of generation provided by dispatchable plants, since baseload generation cannot change operation much. The result is that the dispatchable generation fleet operates less often (i.e., at a lower load factor) and more dynamically, as shown in Task 7.2.2. Gas turbines and combined cycle plants are designed to operate at full load, so operating these plants at part load reduces the plant efficiency (Task 7.1.6.2) such that the more dynamically these plants are operated the lower their efficiency.

Three techniques are explored in this research to combat the reduction in efficiency and capacity factor for the load-following fleet that is associated with installing increased amounts of renewable generation (Task 7.2.2.4).

Find other ways to provide AS

Ancillary services previously provided by load-following generation could be provided by other sources including DR and energy storage. This would increase the amount of load-following (i.e., flexible) generation available to balance renewable fluctuations and thereby increase the achievable renewable penetration, all while lowering the system-wide LCOE.

Increase the operating flexibility of dispatchable generation

If the turndown capability of dispatchable generation was increased and the part-load efficiency was improved, the result would be an enhanced ability of dispatchable generation both to compensate for generation fluctuations and to provide AS, increasing the achievable renewable penetration and lowering the system-wide LCOE in the process.

Remove baseload generation

By removing baseload generation, additional dispatchable generation can be installed, which will increase the available flexible generation for addressing intermittent renewables and meeting AS requirements. Because the capital for legacy (i.e., pre-existing) baseload plants is assumed to have been fully depreciated, leaving only fuel and the operations and maintenance portion of costs, the system-wide LCOE will increase for low renewable penetrations but for high renewable penetrations, the added system flexibility overcomes the additional capital investment required, resulting in a lower system-wide LCOE.

4.3. Role of Complementary Technologies

Complementary technologies include EE, DR, energy storage and electric transportation, all of which shift, shape or shed load and do not behave as a typical generator (Task 7.3).

Technologies operating to support a single community's on-site renewables can reduce the impact of renewable fluctuations; however, each community mitigating its own renewable fluctuations does not capitalize either on the benefits of large, dispersed renewables and or on the benefits of aggregation. Thus for the greatest overall benefit, complementary technologies should be located and dispatched to support the entire grid instead of based on each community's individual needs. This is not common practice today but to make installed renewables as effective as possible this change in strategy should be pursued.

4.3.1. Energy Efficiency

Energy efficiency (EE) measures are those that permanently improve the efficiency of equipment in the community and thereby reduce both electricity demand and consumption. All EE measures reduce the electricity demand but the economic competitiveness of any specific EE measure depends on the cost to install and operate the equipment and how the shape of the demand reduction profile coincides with the demand profile itself.

4.3.2. Demand Response

From the UCI results it was shown that the cost competitiveness of DR is dependent on the resources selected and the number of events for which the DR resources are dispatched. In addition to supporting fluctuations on the community level, DR can also support operation of the grid. DR can be used to reduce the energy demand for a period of time or to provide AS. This research finds that at low renewable penetrations DR should focus on reducing the energy demand with less focus on providing AS, as shown in Task 7.3.3. Both strategies will reduce the system-wide LCOE. However, as the renewable penetration increases, it becomes more valuable for DR to provide AS exclusively.

The ability to provide DR depends heavily on the types of loads in each community. As renewable penetrations increase and the value of flexible resources rise, communities should explore the ability to use DR to improve their system's performance, as shown in the UCI community section, as well as for supporting the grid.

From the government and regulatory point of view, current DR programs should be expanded to include the provision of AS, and DR program participation should be encouraged. DR can offer a cost-effective alternative to dispatchable generation for supporting the implementation of intermittent renewables.

Current DR programs administered by SCE are dispatched an average of 71 times per year. This dispatch is to support the grid during times of high load on the system, which predominantly occur during the summer months (Task 7.3.3.3).

As the renewable penetration increases, both the time-of-day and the season that DR events are called will change. Results suggest that maximum DR reductions will shift from late afternoon

to late morning as well as occurring from summer to fall. These anticipated changes should be considered when utilities and regulatory organizations are developing DR programs.

4.3.3. Energy Storage

Electrical energy storage is explored in this report (Task 7.3.1). Storage devices use the technical and economic arbitrage potential of energy produced during different time periods to realize a benefit. Because the round-trip technical efficiency of storing energy and later releasing it is always less than 100%, the economic benefit of storage devices must outweigh the technical charge/discharge penalty.

Appropriate sizing is critical to the effectiveness of energy storage. The two most important features to balance are the power capacity (i.e., installed capacity) and the energy capacity (i.e., duration). Increasing the power capacity eventually results in diminishing performance increases for capacity factor, efficiency, ramp rates, and starts without an increase in energy capacity. Similarly, if the power capacity is too low then the energy capacity will never be fully utilized.

In addition to increasing the achievable renewable penetration, appropriately sized energy storage has the ability to provide an additional reduction in CO_2 emissions, improve system capacity factor and grid efficiency, despite the efficiency penalty, as well as reduce balance fleet ramping and starts.

The value of energy storage is a balance between reduction in generator dynamics and the energy penalty for storing energy. Storage acts to reduce generator dynamics, which becomes more important with increasing renewable penetrations. As a result, the value of energy storage rises with increasing intermittent renewable penetration.

Capital cost and O&M costs vary for each type of energy storage. This research finds that energy storage technologies are not generally cost competitive at low renewable penetrations, but as the renewable penetration is increased energy storage technologies become increasingly competitive.

4.3.4. Electric Transportation

Electrifying vehicles increases the demand for electricity on the grid and reduces the demand for petroleum. The additional electricity demand must be met with additional generation. A model is developed using the National Household Traffic Survey (NHTS 2009) that determines the resulting increase in the electrical load profile for transitioning a user-defined portion of the vehicles to electric, as described more fully in Task 3.3.2.2. To achieve some dispatchability with the electric vehicles, the charging strategy is adjusted from an immediate strategy, where the vehicle charges as soon as it is connected, to either a delayed strategy (where the vehicle waits to charge until the latest possible) or a smart strategy (where the charging is based on an external cost function, e.g., real-time grid electric demand or time-of-use rate structure).

Benefits from integration with electric transportation, just like the other complementary technologies, are maximized by shaping the grid profile, as opposed to shaping a community's load profile. With the advent of "smart" meters that are capable of measuring real-time load

consumption and of advanced communication systems, the foundation is in place to incentivize charging of electric transportation at specific times through real-time price signals.

Optimal charger location selection is dependent on aligning vehicle owner needs with the needs of the grid. For the optimal results, chargers should be installed at a vehicle owner's home or workplace. Installing chargers at home well aligns with the time-of-day that drivers are home and the duration required to both charge the vehicle and support the grid, particularly for high wind and low solar capacity renewable portfolios. Installing chargers at work well aligns with the time-of-day drivers are at work and, to a lesser extent, the duration required to both charge the vehicle and support the grid, particularly for high solar and low wind capacity renewable portfolios (Task 7.3.4).

Without consideration of the charger location, the ideal electric vehicle charging profile smoothes the demand at low renewable penetrations and transitions to smoothing the renewable generation profile as the renewable penetration increases. The three most likely charging strategies are 1) immediate, where the vehicle charges as soon as it is connected, 2) delayed, where the vehicle waits to charge until the latest possible and 3) smart, where the charging is based on an external cost function (e.g., real-time grid electric demand or time-of-use rate structure). No information is required for the immediate charging strategy, while information about the next trip is required for the delayed strategy, and both next trip information and some cost function are required for the smart strategy.

This research found that smart charging most closely represents the ideal profile while considering each vehicle's location and charging needs throughout the day. Delayed charging is the second best, followed by immediate charging. Depending on the selected strategy, electric transportation can either improve grid operations or aggravate current balancing challenges and future challenges from intermittent generation.

Smart charging improves grid performance and can reduce the system-wide LCOE for all renewable penetrations. Delayed charging results in a slight and sometimes negligible improvement in performance and is generally not cost competitive until high renewable penetrations are achieved. Immediate charging either reduces or has a negligible effect on performance characteristics and increases the system-wide LCOE. It should be noted that the cost of the vehicle, charging equipment and any electrical infrastructure needs are not included in this analysis and all such costs are assumed to be shouldered by the vehicle owner. An improvement in performance and reduction in system-wide LCOE means that electric vehicles, if charged appropriately, provide value to the grid and are valuable enough to the utility that it could shoulder some of the customer-incureed costs.

Additionally, increasing the number of electric vehicles with smart charging will lower CO_2 emissions; however, the value of electric transportation for grid operations diminishes as the numbers of vehicles increase.

In this chapter, the UCI RESCO roadmap was expanded to those generic communities in California that aspire to become RESCOs. Although, wind power provides the best performance with the lowest LCOE, results show that a mix of solar and wind renewable resources improve

overall renewable portfolio performance and decrease costs. Therefore, solar and wind resources should be the primary candidate renewable technologies for installation and an appropriate ratio of installed wind capacity to installed solar capacity is at least 2.5. The intermittency of the solar and wind resources pose challenges for the generic RESCOs as well as the grid. The intermittencies introduce more dynamic operation of dispatchable generation causing reduced efficiency. Complementary technologies used to mitigate these impacts were discussed. The analyses performed indicate that complementary technologies shared between various communities can result in the greatest benefit for the entire grid.

CHAPTER 5:
Issues for Policy Makers and Industry Leaders

One of the three research program goals was to identify issues for policy makers and industry leaders that must be addressed to facilitate the implementation of renewable-based energy secure communities throughout the state. The nine major project findings listed in the Executive Summary are presented here. For each finding, related policy issues are discussed, and policy recommendations are proposed.

4. Communities must contribute to, communicate and coordinate with other utilities and the system operator or other communities to achieve a high-penetration of renewables.

Communities working alone to achieve renewable energy goals may produce negative, unintended consequences such as accentuating challenges in system-wide energy balancing or negatively impacting system-wide reliability. Furthermore, incorporation of energy resources located outside of the community into a comprehensive energy strategy will tend to result in a more efficient solution by allowing for technology diversity and optimally located renewable power generators, which can increase capacity factors and improve performance.

To properly utilize community energy resources when appropriate, but also incorporate energy resources located outside communities when appropriate, the state should provide guidance to communities with respect to when it may be appropriate to tap into resources that lie beyond the local region. To accomplish this, the state may consider providing utilities access to local resources at the community scale and facilitating resource utilization discussion between utilities and communities within their territory. The state may also consider placing minimum performance requirements on distributed generation and also on local grid performance at the community scale.

A smart-grid system will be necessary to access the information required to make decisions on whether community-scale renewable generation will tend to have overall positive or negative impacts on the electrical system. The state should incentivize the deployment of smart-grid technologies, and also assure that information obtained by those technologies is reaching the appropriate stakeholders in management of the state and regional electrical system.

Policy recommendations summarized:

Provide guidance to communities with respect to when it may be advantageous for the electrical system to be served by renewable power generation at the regional scale versus at the local, community scale;

Facilitate utility involvement in the decision-making process for deploying community-scale generation versus utility-scale generation. Giving utilities access to renewable generation resources at the community scale may lead them to be engaged more objectively on the decision making for community-scale versus utility-scale generation; and

Incentivize deployment of smart-grid technologies and assure, through appropriate policies, that information obtained by smart-grid technologies is reaching the appropriate stakeholders that are involved in managing the electric power system.

5. New economic mechanisms such as dynamic rate structures must be developed to incentivize dispatch of community resources in response to the behavior of the larger electric grid.

Renewable penetration on a large scale, in regions that lie outside of communities, is limited by land availability, transmission constraints, balance generator flexibility, and cost. Therefore, communities will play an essential role in meeting California's state and regional goals for emissions, environmental impact, and renewable penetration. The state should consider if and how guidance or incentives can be provided to communities so that those communities contribute constructively to these goals.

Strategies that can help communities contribute to California's energy and environment goals include three principal facets: (1) design and planning of communities, (2) distributed generation and other community-scale energy strategies, and (3) advanced information and controls for buildings. Existing programs in California help encourage community contributions in this area:

SB 375 requires community-scale integration of planning processes for transportation, land-use, and housing leading to more efficient communities that provide residents with alternatives to using single occupant vehicles. The goal is to reduce GHG emissions from automobiles and light duty trucks.

Feed-in Tariffs, incentives for distributed generation such as the Self-Generation Incentive Program, and the Renewable Portfolio Standard encourage communities to adopt low carbon, and renewable distributed generation strategies, including solar and fuel cells operating on biogas.

Title 24 for Zero Net Energy buildings and homes encourages communities to implement smart information systems and controls for buildings and homes.

However, while these policies begin to address the three facets, a more comprehensive policy approach should be implemented to incentivize community contribution – one that effectively incorporates the existing policies and programs listed above. Finally, accountability needs to be factored into a comprehensive strategy. In other words, the state should consider a policy that systematically tracks whether a community's contribution is continuous and whether it is producing the desired outcomes with respect to state and regional goals for emissions, environmental impact, and renewable penetration.

Policy recommendations summarized:

Determine how to guide or incentivize communities to contribute to state and regional goals for emissions, environmental impact, and renewable penetration;

Implement a comprehensive policy approach, which incorporates existing policies and programs, to address three principal facets of community strategies that can help contribute to energy and environment goals: (1) design and planning of communities, (2) distributed generation and other community-scale energy strategies, and (3) advanced information and controls for buildings; and

Maintain accountability by systematically tracking whether strategies that communities have implemented are producing the desired outcome.

6. Integration of electricity generation and transportation load provides synergistic benefits at both the community and regional level through:
    - Plug-in Electric Vehicle (PEV) charging
    - H_2 production for Hydrogen Fuel Cell Electric Vehicles (FCEVs).

Transportation is expected to shift away from petroleum-based fuels in the future towards more use of electricity and hydrogen (in addition to other forms of energy) to meet our transportation energy demands. If appropriately designed, shifting transportation energy towards more plug-in or hydrogen fuel cell powered vehicles can have two potential advantages:

It can improve a community's energy performance with respect to efficiency, GHG emissions, and criteria pollutant emissions; and

It can offer a new resource that can support grid stability and reliability by managing loads via either strategic charging of plug-in vehicles, or use of excess renewable electricity for hydrogen production for fuel cell electric vehicles (FCEVs).

However, these advantages are only made possible when appropriate controls and information technology are implemented to assure optimized charging and/or hydrogen production. For example, uncontrolled electric vehicle charging can strain the grid, or increase GHG emissions if vehicles are charging at peak times of the day.

It is therefore important that the state incentivize and regulate the adoption of electrified transportation and hydrogen infrastructure such that charging of electric vehicles is integrated into the grid intelligently. For plug-in vehicles, smart-grid technologies will help "corral" vehicle charging to those times of the day when it is helpful to the grid rather than challenging, or help plan for electrified rail. Existing policies that call for advanced planning of transportation solutions for communities (such as those related to SB 375) should always be cognizant of the need for electrified transportation to be "smart." Public education regarding the importance of smart charging should play an important role in building driver acceptance of charging strategies other than the most convenient strategy of immediate charging. Energy storage can help ensure grid reliability and stability as the capacity of intermittent renewables on the grid increases, as well as allow higher renewable penetration levels to be reached. The application and dispatch of energy storage, however, will need to be evaluated for optimal value at each renewable penetration level. To help mitigate the effects of intermittent renewables, diversifying the portfolio of energy storage options is especially important given

that intermittency can occur seasonally, diurnally, and instantaneously; different amounts of storage will be needed as well as different dispatchability characteristics. A portfolio of energy storage types including but not limited to: pumped hydropower, batteries, flywheels, and hydrogen storage should be considered, since each different type has unique characteristics which allow each to be better suited to fulfill certain roles in grid management compared to others. It is therefore important that energy storage policies created by the state be comprehensive with respect to the wide array of intermittency needs and be adoptive of a diverse array of storage technologies accordingly.

Policy recommendations summarized:

Continue to embrace increased electrification of transportation, either through plug-in vehicles, or hydrogen powered FCEVs, because with appropriate planning it can be an asset with respect to environmental impact and grid stability.

State incentives and regulations that affect the electrification of transportation should, without exception, require that plug-in electrified transportation be integrated with the grid intelligently and should include associated public education programs to build support for strategic charging strategies.

The state should explore policies that encourage the storage of energy from otherwise curtailed solar/wind electricity, and the production of electric power from this stored energy when solar/wind electricity is most valuable.

7. Reducing the capacity of carbon-fueled inflexible (base load) generation must be prioritized for meeting renewable utilization goals.

Among all of the strategies considered in this study for increasing the achievable utilization of renewable resources on the electric grid, the most effective single measure was the reduction of inflexible generation capacity in the system. The load must be balanced by generation at every hour. When renewable resources are producing a large amount of power, inflexible generation sourced from coal or nuclear power plants are not capable of physically of responding to renewable dynamics (i.e. turning down) to allow renewable generation to serve the load demand. To prevent overgeneration and keep the load demand balanced, this forces the curtailment of renewable generation.

For a given capacity of inflexible generation on the grid, a hard limit is imposed regarding the maximum achievable renewable penetration. Since inflexible generators cannot respond to renewable variability and decrease their power output, their contribution towards serving the load demand is fixed. This reduces the available electric load that can be satisfied by renewable generation, setting an upper limit on the achievable renewable penetration. Complementary technologies such as energy storage allow increases in renewable penetration compared to a renewable-only case up to this limit, but these technologies do not remove it.

It is therefore important that the non-renewable resources which support the electric grid evolve to increase their ability to respond to renewable dynamics and allow renewable generation to serve larger fractions of the load demand. Utilities will need to begin procuring

electricity from resources which exhibit this ability. Additionally, it is important that the provision of flexibility by supporting generators be incentivized and valued to offset decreased revenue from a decreased energy contribution.

Policy recommendations summarized:

Incentivize the reduction in energy procurement from power plants with limited dynamic capabilities (i.e. coal-fired steam turbines) as more renewable capacity is installed.

Alter the valuation of products in the CAISO electricity market to place increased value on flexibility services relative to bulk energy provision from non-renewable power plants as more renewable capacity is installed.

Incentivize the turnover of the conventional power plant fleet to increasingly adopt technologies with increased dynamic capabilities (ramping, start up, part-load operation).

8. Avoiding curtailment of renewable generation is critical for reaching renewable utilization goals in a cost-effective manner.

Curtailment of renewable generation occurs at times when the total electricity generation exceeds the available electric load demand, typically occurring after flexible generators have reduced their power output to the extent possible. Due to the characteristics of intermittent renewables, large capacities of wind and solar are required to provide a significant energy contribution to the load demand. This causes curtailment to occur during periods of peak renewable generation.

The costs associated with renewable generation are dominated by capital costs which scale with installed capacity. Revenue for the owners of these systems scales with energy sold. Once curtailment begins to occur, the increase in renewable penetration per unit of increased renewable capacity diminishes. Curtailed renewable generation is not bought since it does not serve the load demand. This means that increasingly large renewable capacities will become required to increase renewable penetration by a given amount. The overall effect is for costs to increase at an exponentially faster rate compared to revenue, causing the cost of electricity from renewable resources to increase in tandem.

To reach renewable utilization goals in a cost-effective manner, steps should be taken to prevent the cost of electricity from renewable resources from increasing in this manner. By avoiding curtailment through the use of complementary technologies or increased power plant fleet flexibility, the cost of electricity from renewable resources can be maintained at reasonable levels.

Policy recommendations summarized:

Incentivize the increased flexibility of the non-renewable power plant fleet (see Finding #5) to allow higher renewable capacities to be installed before curtailment occurs.

Adopt policies that encourage the installation of load shifting technologies to reduce or prevent curtailment through strategic investments.

Adopt appropriate policy targets for the installed capacity of load shifting technologies as a function of installed renewable capacity.

5. Complementary technologies such as energy storage and demand response are required to meet renewable utilization goals, but their preferred operation will change with renewable penetration.

Energy storage can help ensure grid reliability and stability as the capacity of intermittent renewables on the grid increases, as well as allow higher renewable penetration levels to be reached. The application and dispatch of energy storage, however, will need to be evaluated for optimal value at each renewable penetration level. To help mitigate the effects of intermittent renewables, diversifying the portfolio of energy storage options is especially important given that intermittency can occur seasonally, diurnally, and instantaneously; different amounts of storage will be needed as well as different dispatchability characteristics. It is therefore important that energy storage policies created by the state be comprehensive with respect to the wide array of intermittency needs and be adoptive of a diverse array of storage technologies accordingly.

As part of a comprehensive policy on energy storage, the state should also consider restructuring past incentives on energy storage as well as how incentives are administered. For example, CAISO may be best suited to determine how, when, and where energy storage is needed, and how it is dispatched; however, it has limited control of resources such as energy storage today.

Demand response (DR) is shown to provide a valuable reduction in load with little or no impact on facility occupants and can be a useful tool in stabilizing the grid and enable higher achievable renewable penetrations. Due to solar and wind intermittencies, the ability for demand response to stabilize the grid will likely increase. However, coordination of DR on a statewide, systematic basis has not been done before. The state should consider how demand response could best be coordinated throughout the state using the stakeholders and tools that are available. The nature of DR suggests that CAISO could be most effective in harnessing DR for load control. The state should explore ways in which CAISO could use the market structure to implement DR.

The most beneficial application of DR will also change as more renewable capacity is installed on the grid. DR operation strategies which provide the best cost and emissions benefits with low renewable capacity levels will not be the optimal option with high renewable capacity levels. The state should consider policies for incentivizing the evolution of DR operation strategies to best suit the changing needs of the system as higher renewable penetration levels are reached.

The Federal Energy Regulatory Commission (FERC) is also developing guidelines on pricing for DR technologies. The state should develop its demand response policies in coordination with the guidelines developed by FERC, and even provide input and guidance to FERC based on California's lessons learned.

Finally, energy storage and demand response both have unique advantages and disadvantages with regard to supporting the integration of renewable resources in terms of technical capabilities, capacity potential, and cost impacts. The state should adopt policies that integrate the deployment and utilization of both energy storage, demand response, and other complementary technologies (i.e. electric vehicle smart charging) to be more effective at mitigating the challenges associated with reaching higher renewable penetration levels.

Policy recommendations summarized:

Assure that policy created for energy storage is comprehensive with respect to the wide array of intermittency challenges (e.g., seasonal, diurnal, instantaneous), and is adoptive of the diverse array of available energy storage technologies accordingly;

Consider restructuring past incentives on energy storage as well as how those incentives are administered to meet today's goals and needs.

a. Explore how demand response could best be coordinated throughout the state. In particular, explore how CAISO could use the market structure to implement demand response

b. Consider how the optimal application of DR changes with increasing renewable penetration and incentivize the shift in DR operation accordingly.

c. Coordinate with FERC regarding guidelines on DR.

Adopt policies that integrate the deployment and use of energy storage, demand response, other methods that help mitigate the challenges associated with a higher penetration of intermittent renewable energy.

6. Significant cost, energy, and greenhouse gas savings are available through the widespread implementation of energy efficiency measures, but their impact on demand response potential must be considered.

Energy efficiency can today provide significant cost savings to communities, and reduce GHG emissions overall. The state should continue to require and/or incentivize community adoption of EE measures, and provide guidance for how best to implement EE measures by capturing and showcasing lessons learned or case studies for how EE has been implemented successfully. This includes equipment efficiency, resource management, novel building and grid controls, and integrated management of dispatchable resources such as energy storage and distributed generation.

However, EE must also be considered within the context of the overall electrical grid and energy system. For example, implementing EE strategies reduces the degree to which DR can be controlled, thereby reducing the potential contribution of the demand side in balancing the grid. Less control of DR will limit the degree to which intermittent renewables (wind and solar) can be absorbed by the grid and place more pressure on the supply side in balancing the grid. This may produce cases in which EE in the community should be sacrificed to support the reliability of the grid. The state should consider policies that incentivize *grid support* as part of

EE considerations along with the cost savings and carbon emissions reductions incentives that already accompany EE today.

Policy recommendations summarized:

Continue to require and/or incentivize community adoption of EE measures.

Provide guidance for how best to implement EE measures by capturing and showcasing lessons learned or case studies.

Incentivize *grid support* as an additional consideration of EE in addition to the cost savings and reduced carbon emissions incentives that already accompany EE today.

7. To support and complement a planning roadmap, a pragmatic planning and design tool is required for community planners and policy makers.

Deployment of energy infrastructure requires significant capital investment and once in place, the infrastructure is expected to operate for a lifetime of 15 to 30 years (or sometimes longer). Before making investments in the next generation of energy infrastructure, it is important to establish a clear analytical understanding of how a community's electrical system will be affected, both positively and negatively, depending on the types of technologies that are deployed and how and when they are utilized.

A planning tool, if properly developed and utilized, can help target investments more effectively towards achieving the desired outcome by allowing for an *a priori* evaluation of how the system will be affected by a variety of technologies prior to actually investing in and installing them. With advanced planning and understanding of how technologies affect the performance of and operate within the overall system, desired outcomes (e.g., reduced GHG emissions, improved air quality, increased penetration of renewables) can be maximized and required investment minimized.

The information produced through the use of an advanced planning and design tool is essential to creating a planning roadmap for transforming communities into RESCOs at minimized cost.

Policy recommendations summarized:

Work with researchers, engineers, and planners to develop and then parametrically apply a pragmatic planning and design tool to:

Understand from an analytical perspective the strategies and technologies that will maximize desired outcomes (e.g., reduced GHG emissions, improved air quality, increased penetration of renewables) and minimize required investment prior to deploying the next generation of energy infrastructure.

Support and complement a planning roadmap for transforming communities into RESCOs.

8. A planning roadmap is desirable for community planners to determine the options for their specific community to qualify as a RESCO.

For a community to understand the local resources available for renewable power generation is straightforward. However, for a community to understand how and when it is best to use those resources in the context of the entire California electrical grid, how smart grid technologies work to interact with distributed, renewable resources, and when it may be more advantageous to tap into community-scale renewable power versus rely on utility-scale renewable power resources can be daunting. To help a community qualify as a RESCO, including the need for the community to provide a benefit to the collective California electrical grid and the state's renewable and GHG goals, it will be important for the state to develop a planning roadmap that provides guidance for a community to qualify. Given the complexity of developing this roadmap, a pragmatic planning and design tool will be needed.

Policy recommendations summarized:

a. The state should consider creating a planning roadmap to assist community planners in determining options for their specific community to qualify as a RESCO.

b. A pragmatic planning and design tool should complement this planning roadmap.

CHAPTER 6:
Conclusions and Recommendations

6.1. Conclusions

The UCI community has established itself as a RESCO through its leadership in installing a wide variety of advanced technologies to provide electricity, heating, cooling and transportation fuels and services for the UCI campus. Technologies include: nearly 900kW of rooftop solar PV, 113 kW of Amonix high concentration PV panels, a central co-generation plant (13.5 MW gas turbine, 5.5 MW steam turbine, and Heat Recovery Steam Generator), a TES tank (4.5 million gallons), a hydrogen station (25 kg/day), FCVs, PEVs, a bio-diesel bus fleet, ZEV•NET, other shared-use vehicle programs, EE, and DR (700kW nomination) measures. These technologies are all integrated on UCI's micro-grid to explore the potential to provide reliable, secure and environmentally friendly energy sustainably and at the lowest cost. These deployments also enabled the development of a holistic energy integration and management methodology for RESCOs designated as the Holistic Grid Resource Integration and Deployment tool. All these activities achieved the quantitative goals of the project: (1) develop holistic Energy Integration and Management methodology and (2) demonstrate the deployment and integration of: 1 MW of PV, 24/7 production of renewable hydrogen and 300kW of electricity using a high temperature fuel cell for sustainable transportation, electric vehicles (plug-in electric and all electric), battery electric vehicle charging that utilizes dynamic price signals to incentivize the charging of EVs to help manage the energy balance, and the energy storage that will be required to achieve a RESCO.

Based on the operation of pilot projects and other resources at UCI, many alternatives have been explored for communities desiring to become RESCOs. Analyses were performed with the understanding that securing renewable generation while also considering the effect on system reliability and LCOE is essential to distinguishing the true value to a community. Additionally, consideration of the impacts on the grid from community operation and renewable generation is essential to understanding how RESCO concepts can be duplicated across the state and the world.

This research resulted in nine major findings that should be considered for any community interested in becoming a RESCO:

1. Communities must contribute to, communicate and coordinate with other utilities and the system operator or other communities to achieve a high-penetration of renewables.

Solely prioritizing community needs over that of the larger grid can inhibit progress towards reaching renewable utilization goals on the larger statewide scale. Willingness and ability to dispatch community resources to respond to the larger grid should be a requirement to obtain a RESCO designation.

2. New economic mechanisms such as dynamic rate structures must be developed to incentivize dispatch of community resources in response to the behavior of the larger electric grid.

Communities have the ability to help achieve the energy goals of the state. Energy goals can be supported through the integration of renewables and EE measures. This research shows that the regional grid can absorb fluctuations from some intermittent renewables; however, this becomes more and more challenging as the amount of installed renewables increases, which comes with greater community adoption of renewables. As a result, communities can help the grid achieve greater renewable penetration if community resources are used to support the grid (e.g., flexible generation, DR, energy storage, electrification of transportation). Community goals and grid goals are not always aligned; however, there are ways for the community to be incentivized to support the grid. Installation of smart electric meters provides one method for incentivizing grid support through strategic structuring of utility rate schedules.

Emissions goals can be supported through the use of more public transportation, carpooling, human powered transportation and transition to alternative fueled vehicles. All of these steps are shown to reduce emissions at UCI.

3. Integration of electricity generation and transportation load provides synergistic benefits at both the community and regional level through:
    - Plug-in Electric Vehicle (PEV) charging
    - H_2 production for Hydrogen Fuel Cell Electric Vehicles (FCEVs).

Electrifying transportation within the community is shown to provide a benefit with community performance and offers a resource to support the grid. The best results occur when chargers are placed at vehicle owner's homes and a "smart" charging strategy is employed instead of immediate or delayed charging.

4. Reducing the capacity of carbon-fueled inflexible (base load) generation must be prioritized for meeting renewable utilization goals.

The capacity of inflexible generation in operation sets a hard limit on the maximum achievable renewable penetration both within a community and on the statewide scale. Complementary technologies such as energy storage, demand response, and electric vehicles aid the system in increasing renewable utilization up to this limit, but they do not remove it. For California, the maximum achievable renewable penetration increased by about 1.6% per GW of inflexible capacity removed for a diverse renewable mix.

5. Avoiding curtailment of renewable generation is critical for reaching renewable utilization goals in a cost-effective manner.

Before curtailment occurs, the rate at which the levelized cost of electricity increases with renewable penetration increases linearly – in the range of an 0.7% to 6.5% increase in cost per percent increase in renewable penetration. Once curtailment starts to occur, this rate increases exponentially, reaching as high as a 350% increase in cost per percent increase in renewable

penetration. The benefit of avoiding this behavior must be considered when determining the cost-effectiveness of complementary technologies aimed at reducing curtailment.

6. Complementary technologies such as energy storage and demand response are required to meet renewable utilization goals, but their preferred operation will change with renewable penetration.

Energy storage, demand response, and electric vehicles each have unique constraints and characteristics which determine how well each can respond to different types of grid behavior. For example, the most beneficial operation of demand response at low renewable penetrations was to provide energy savings, but at high renewable penetrations using this service to provide spinning reserve became the most beneficial.

7. Significant cost, energy, and greenhouse gas savings are available through the widespread implementation of energy efficiency measures, but their impact on demand response potential must be considered.

Installing energy efficiency measures provides significant benefits regarding greenhouse gas emissions, renewable utilization, and electricity cost. Since these measures reduce the size of loads types available for demand response such as lighting and HVAC, however, they also reduce the extent to which demand response strategies can respond to grid events.

8. To support and complement the planning roadmap, a pragmatic planning tool and design tool is required for community planners and policy makers.

The variation in community characteristics (i.e., layout, available space, climate, current and planned renewable portfolio/penetration, complementary technologies, utility generation mix, etc.) requires a planning tool to develop community specific roadmaps that can evolve as the community evolves.

9. A planning roadmap is desirable for community planners to determine the options for their specific community to qualify as a RESCO.

The development of this roadmap initially requires support from a practical planning tool to ensure all options and variables are evaluated in a holistic way. Additionally, continuing support from the planning tool is required to re-evaluate and alter, if necessary, the roadmap as the community evolves toward a RESCO. Community planners need effective planning roadmaps, and a planning tool secures the roadmap effectiveness.

6.2. Recommendations

Through the pilot project demonstrations, development of the HiGRID modeling tool, and the development of roadmaps for the UCI community as well as generic communities, nine major findings were revealed. It is recommended that these findings be used to inform California policy decisions associated with renewables and RESCOs. In particular, it is recommended that the HiGRID modeling tool be considered for more widespread use by policy makers and communities. A graphical user interface has been developed to improve the ease of use. This type of use is currently being demonstrated. Finally, the roadmaps developed in this project

should be used by communities and policy makers when making decisions related to renewable energy. In addition, policy makers should be familiar with the issues outlined in Chapter 5.

6.3. Benefits to California

The benefits to California are realized in three ways: 1) pilot project demonstrations at the UCI campus have initiated the path toward zero carbon for this particular UC campus, 2) development of the HiGRID modeling tool portends immense value in its effective examination of resource impacts whether those resources are renewables or another technology such as energy storage (in fact, this tool has already been applied to several other issues facing California, e.g., pollutant emissions, San Onofre Nuclear Generating Station retirement, etc.), and 3) the generic roadmap provides communities in California with a pathway to achieving high renewable penetration and thereby reducing carbon emissions.

GLOSSARY

Term	Definition
APEP	Advanced Power and Energy Program
BEV	Battery Electric Vehicle
CEC	California Energy Commission
CHP	Combined Heat and Power
CPV	Concentrated Photovoltaic
Delayed Charging	The Plug-in Electric Vehicle waits to charge until the latest possible
DER	Distributed Energy Resource
DR	Demand Response
EE	Energy Efficiency
EV	Electric Vehicle
FM	Facilities Management
GHG	Greenhouse Gas
HiGRID	Holistic Grid Resource Integration and Deployment
HRSG	Heat Recovery Steam Generator
HVAC	Heating, Ventilation, and Air Conditioning
Immediate Charging	The Plug-in Electric Vehicle charges as soon as it is connected
LCOE	Levelized Cost of Electricity
NHTS	National Household Travel Survey
NREL	National Renewable Energy Laboratory
PHEV	Plug-In Hybrid Electric Vehicle
PV	Photovoltaic
RESCO	Renewable-Based Energy Secure Community
SCE	Southern California Edison. An investor-owned utility serving southern California

Smart Charging Strategy	The charging of the vehicle is based on an external cost function, e.g., real-time grid electric demand or time-of-use rate structure
TES	Thermal Energy Storage
UCI	University of California Irvine
USGS	United States Geological Survey
VFB	Vanadium redox Flow Battery
ZEV-NET	Zero Emission Vehicle – Network Enabled Transportation

REFERENCES

Publications Emanating from the RESCO Project

Eichman, J.D., Mueller, F., Tarroja, B., Schell, L.S., Samuelsen, S., "Exploration of the integration of renewable resources into California's electric system using the Holistic Grid Resource Integration and Deployment (HiGRID) tool", Energy, 2013. 50(1): p. 353-363

Chang, M.K., Eichman, J.D., Mueller, F., Samuelsen, S., Buffering intermittent renewable power with hydroelectric generation: A case study in California. Applied Energy, 2013. 112: p. 1-11.

Publications Emanating from the use of HiGRID in Support of other Projects

Tarroja, B., Eichman, J.D., Zhang, L., Brown, T., Samuelsen, S., "The Effectiveness of Plug-in Hybrid Electric Vehicles and Renewable Power in Support of Holistic Environmental Goals: Part 1 - Evaluation of Aggregate Energy and Greenhouse Gas Performance", Journal of Power Sources, 2014. 257(1): p.461-470

Tarroja, B., Eichman, J.D., Zhang, L., Brown, T., Samuelsen, S., "The Effectiveness of Plug-in Hybrid Electric Vehicles and Renewable Power in Support of Holistic Environmental Goals: Part 2 – Design and Operation Implications for Load-Balancing Resources on the Electric Grid", Journal of Power Sources, 2014. 278: p.782-793

Tarroja, B., AghaKouchak, A., Samuelsen, S., Sobhani, R., Feldman, D., Jiang, C.S., "Evaluating Options for Balancing the Water-Electricity Nexus in California: Part 1 – Securing Water Availability", Science of the Total Environment, 2014. 497-498: p.697-710

Tarroja, B., AghaKouchak, A., Samuelsen, S., Sobhani, R., Feldman, D., Jiang, C.S., "Evaluating Options for Balancing the Water-Electricity Nexus in California: Part 2 – Greenhouse Gas and Renewable Energy Utilization Impacts", Science of the Total Environment, 2014. 497-498: p.711-724

Shaffer, B., Tarroja, B., Samuelsen, S., "Dispatch of Fuel Cells as Transmission Integrated Grid Energy Resources", Applied Energy, 2015. 148: p.178-186

Tarroja, B., Shaffer, B., Samuelsen, S., "The Importance of Grid Integration for Achievable Greenhouse Gas Emissions Reductions from Alternative Vehicle Technologies", Energy, 2015. 87: 504-519

References Accessed in Support of the RESCO Project

3TIER, Development of Regional Wind Resource and Wind Plant Output Datasets. 2007-2008, U.S. Department of Energy.

Aalborg University. "EnergyPLAN: advanced energy system analysis computer model." Retrieved 04/20/2012, <http://energy.plan.aau.dk/>.

Akashi, Y., Neches, J., Detectability and Acceptability of Illuminance Reduction for Load Shedding. Journal of the Illuminating Engineering Society. 2004.

Amos, W.A., Costs of Storing and Transporting Hydrogen. NREL/TP-570-25106. NREL: 1998

ANSI/ASHRAE Standard 55 – 2010. Table 5.2.5.2. Page 14.

Ardehali, M., Smith, T., Evaluation of HVAC System Operational Strategies for Commercial Buildings. Energy Conservation and Management. Vol 38, No 3. 1997.

Argonne National Laboratory. "Energy and Power Evaluation Program (ENPEP-BALANCE)." CEEESA, ADICA Consulting, LLC, the U.S. D.o.E, The World Bank, and the International Atomic Energy Agency. Retrieved 7/23/2012, <http://www.dis.anl.gov/projects/Enpepwin.html>.

Asea Brown Boveri. "VENTYX: Market Analytics - Zonal Analysis." Retrieved 5/14/2012, <http://www.ventyx.com/en/enterprise/business-operations/business-products/market-analytics-zonal>.

Auld, A. E., J. Brouwer, et al. (2009). Effect of Distributed Generation on Voltage Levels in a Radial Distribution Network Without Communication. ASME Fuel Cell 2009, Newport Beach, CA USA.

Bauer, D., R. Marx, et al. (2010). "German central solar heating plants with seasonal heat storage." Solar Energy 84(4): 612-623.

Beckman, W. (1993). Detailed Simulation Methods and Validation. Active Solar Systems. G. Lof. Cambridge, MIT Press.

Bialobrzeski, R. (2007). Optimization of SEGS Solar Field for Cost Effective Power Output. Mechanical Engineering, Georgia Institute of Technology. Master of Science.

Black & Veatch Corporation. (2010). Renewable Energy Transmission Initiative (RETI) Phase 2B: FINAL REPORT. University of California, Office of the President, and California Institute for Energy and the Environment. RETI-1000-2010-002-F. <http://www.energy.ca.gov/reti/>.

Black & Veatch. (2008). Renewable Energy Transmission Initiative, Phase 1A Final Report. RETI-1000-2008-002-F.

Britton, E., "Carsharing? A roadmap and compass for this long trip," World Transport Policy and Practice, 1999, 5(3): 1-8

California Energy Commission. 2010. Database of California Power Plants. Last available update: September 2009. http://energyalmanac.ca.gov/powerplants/index.html

California Energy Commission. 2011. Staff Draft Report on Renewable Power in California: Status and Issues. August 2011. Publication No. CEC-150-2011-02.

California Independent System Operator. "Open Access Same-time Information System." Retrieved 04/20/2012, <http://oasis.caiso.com/mrtu-oasis>.

California Independent System Operator. (2003). 2003 Summer Assessment Report. April 11, 2003.

California Public Utilities Commission. (2011). Renewables Portfolio Standard Quarter Report. 3rd Quarter 2011.

California Senate Bill 107, Public Interest Energy Research, Demonstration, and Development Program, (2005-2006 Reg. Sess.)

California Senate Bill 1078, California Renewables Portfolio Standard Program, (2001-2002 Reg. Sess.), Public Utilities Code Section 399.11-399.20

California Senate Bill 2, California Renewable Energy Resources Act, (2011-2012 1st Ex. Sess.)

California State Assembly Bill 32, California Global Warming Solutions Act of 2006, (2005-2006 Reg. Sess.), Health and Safety Code Section 38500-38599

Chase, D.L. 2001. Combined-Cycle Development Evolution and Future. Schenectady, NY. General Electric Power Systems. GER-4206.

Connolly, D., H. Lund, B. V. Mathiesen and M. Leahy (2010). "A review of computer tools for analysing the integration of renewable energy into various energy systems." Applied Energy 87 (4): 1059-1082.

Contadini, J. F., Diniz, C. V., Sperling, D., Moore, R. M., Hydrogen production plants: emissions and thermal efficiency analysis. Presented at the Second International Symposium on Technological and Environmental Topics in Transports; October 2000 – Milan, Italy.

Duffie, J.A., Beckman, W.A., Solar Engineering of Thermal Processes. 1991: John Wiley & Sons.

Electricity Energy Storage Technology Options: A White Paper Primer on Applications, Costs, and Benefits. EPRI. Palo Alto, CA. 2010. 1020676.

EMFAC2007 release. California Air Resources Board. (September 2008, http://www.arb.ca.gov/msei/onroad/latest_version.htm)

Emissions inventory data. California Environmental Protection Agency, Air Resources Board. (January, 2009; http://www.arb.ca.gov/ei/emissiondata.htm)

Energy Exemplar Pty. Ltd. "PLEXOS: Power Market Simulation Software." (Software), Retrieved 04/26/2012, <http://www.energyexemplar.com/>.

Energy Information Administration (2012). Annual Energy Review 2011.

Energy Information Administration. (2003). "The national energy modeling system: an overview." Retrieved 7/23/2012, <http://www.eia.doe.gov/oiaf/aeo/overview/index.html>.

Eshel, Gidon, and Pamela A. Martin. "Diet, Energy, and Global Warming." Earth Interactions 10 (2006): 1-17. <http://pge.uchicago.edu/workshop/documents/martin1.pdf>.

Fallah, H.M., Integrated Energy Conversion Systems: A Mathematical Model of Extraction Steam Turbine, Energy Conversion 1978, Volume 18, pp. 11-15,

Federal Energy Regulatory Commission (2002). 2000-2001 Western Energy Crisis Database. October 18, 2011. <http://www.ferc.gov/industries/electric/indus-act/wec/enron/info-release.asp#directories>

Fuller, R. a. A., Lu (2007). Seasonal storage for solar thermal systems in Australia? . Australian and New Zealand Solar Energy Society 45th Annual Conference, Alice Springs, Australia.

GE Energy Consulting. "Concorda Software Suite - PSLF, MAPS and MARS." Retrieved 5/14/2011, <http://www.ge-energy.com/products_and_services/products/energy_consulting_software/concorda_software_suite.jsp>.

GE Energy Consulting. (2010). Integration of Renewable Resources: Operational Requirements and Generation Fleet Capability at 20% RPS. California Independent System Operator, Pacific Northwest National Laboratory, PLEXOS, Nextant.

GE Energy Consulting. (2010). Western Wind and Solar Integration Study. U.S.D.o.E. and National Renewable Energy Laboratory. NREL/SR-550-47434.

Gillette, A., Marks, J., Stoltzfus, E., Douglas, P., 33% Renewables Portfolio Standard Implementation Analysis Preliminary Results. 2009, California Public Utilities Commission.

Gordon, J.L., "Hydraulic turbine efficiency," Canadian Journal of Civil Engineering, 28(2):238-253, 2001.

Gou, X., W. Sun, et al. (2010). "A dynamic multi-timescale method for combustion modeling with detailed and reduced chemical kinetic mechanisms." Combustion and Flame 157(6): 1111-1121.

Hawkins, D., CAISO Overview and Role of Integrating Renewable Resources. 2007.

Heling, M.G., ASSESSMENT OF THE ZERO-EMISSION VEHICLE, SHARED-USE STATION CAR (ZEV-SUSC) MOBILITY CONCEPT WITH A FOCUS ON ENERGY AND ENVIRONMENTAL SUSTAINABILITY in Mechanical and Aerospace Engineering. 2008, University of California, Irvine: Irvine.

Heller, et al. Multifamily Billing Analysis: New Mid-Rise Buildings in Seattle. Ecotope Consulting Research and Design. December 2009.

Hendron, et al. Building America Performance Analysis Procedures. Revision 1. Building America. U.S. Department of Energy. National Renewable Energy Laboratory. June 2004.

HOMER Energy LLC. "Hybrid Optimization Model for Electric Renewables." Retrieved 04/20/2012, <http://www.homerenergy.com/>.

Huang, Y.J., et al., 481 Prototypical Commercial Buildings for 20 Urban Market Areas. Lawrence Berkeley National Laboratory. 1991.

Ibrahim H, Ilinca A, Perron J. Energy storage systems – Characteristics and comparisons. Renewable and Sustainable Energy Reviews. 2008;12(5):1221-50.

Instituto Superior Técnico; University of Zagreb. "H2RES: Energy Planning of Islands and Isolated Regions." Retrieved 04/20/2012, <http://powerlab.fsb.hr/h2res/index.html>.

Jansen, K.H., Brown T.M. and Samuelsen G.S. , "Emissions impacts of plug-in hybrid electric vehicle deployment on the U.S. western grid." Journal of Power Sources 195 (16): 5409-5416. 2010.

Kalogirou, S.A. (2003). "The potential of solar industrial process heat applications." Applied Energy 76(4): 337-361.

Kalogirou, S.A. (2004). "Solar thermal collectors and applications." Progress in Energy and Combustion Science 30(3): 231-295.

Kalogirou, S.A. (2009). Solar Energy Engineering: Processes and Systems. London, Elsevier.

KEMA Inc. (2010). Research Evaluation of Wind and Solar Generation, Storage Impact, and Demand Response on the California Grid. Prepared for the California Energy Commission. CEC-500-2010-010.

Kim, B. Neff, R. Measurement and communication of greenhouse gas emissions from U.S. food consumption via carbon calculators, Ecological Economics (2009), doi:10.1016/j.ecolecon.2009.08.017

Klein, J. 2010. Cost of Generation Model User's Guide Version 2. California Energy Commission. CEC-200-2010-002.

Klein, Joel. (2010). Cost of Generation Model User's Guide Version 2. California Energy Commission. CEC-200-2010-002.

Leal, E.M., and Brouwer, J., "A Thermodynamic Analysis of Electricity and Hydrogen Co-Production using a Solid Oxide Fuel Cell", ASME Journal of Fuel Cell Science and Technology, 3(2):137-143, 2006

Liu, H.H. "Analysis and Performance Optimization of Commercial Chiller/Cooling Tower Systems." Masters Thesis, Georgia Institute of Technology, June 1997.

Loutan, C. and D. Hawkins. (2007). Integration of Renewable Resources: Transmission and operating issues and recommendations for integrating renewable resources on the California ISO-controlled Grid. November 2007. California Independent System Operator.

Lowe, H.J. and D.G. Christie. "Heat Transfer and Pressure Drop Data on Cooling Tower Packings, and Mode Studies of the Resistance of Natural Draft Towers to Airflow." ASME Heat Transfer Proceedings, Paper 113, 1961.

Lozano, M., A. Anastasia, et al. (2010). Thermoeconomic Cost Analysis of Central Solar Heating Plants Combined with Seasonal Storage. ASME International Mechanical Engineering Congress & Exposition Vancouver, Canada ASME.

Lund, P. D. (1989). "A general design methodology for seasonal storage solar systems." Solar Energy 42(3): 235-251.

Meier, et al. Low-Power Mode Energy Consumption in California Homes. Lawrence Berkeley National Laboratory. Prepared for the CEC: PIER. 2008.

Morehouse, J. (1993). Optimum Design Techniques. Active Solar Systems. G. Lof. Cambridge, MIT Press.

Motegi, et al. Introduction to Commercial Building Control Strategies and Techniques for Demand Response. DRRC, LBNL. 2007.

Newsham, G.R., Brit, B., Demand-Responsive Lighting – A Field Study. NRCC-53233. 2010

NREL, National Solar Radiation Database. 1991-2005, U.S. Department of Energy.

NREL, Western Wind and Solar Integration Project. 2008, U.S. Department of Energy.

NREL, Wind Energy Resource Atlas of the United States. 1986, U.S. DOE.

NREL/GE (2003). DG Power Quality, Protection and Reliability Case Studies Report, submitted to NREL by GE CRD, Contract No NAD-1-30605-01, Program: Reliable, Low Cost Distributed Generator/Utility System Interconnect, August 2003

NSRDB (2005). National Solar Radiation Database 2005, National Renewable Energy Laboratory.

Nyberg, Michael. (2009). 2008 Net System Power Report. Staff Report. California Energy Commission. CEC-200-2009-010. <http://energyalmanac.ca.gov/electricity/total_system_power.html>.

Office of Integrated Analysis and Forecasting. (2008). Annual Energy Outlook. Washington, DC. Office of Integrated Analysis and Forecasting. DOE/EIA-0383.

Perez, R., Ineichen, P., Modeling daylilght availability and irradiance components from direct and global irradiance. Solar Energy, 1990. 44(5): p. 271-289.

Piette, M.A., Development and Evaluation of Fully Automated Demand Response in Large Commercial Facilities. Lawrence Berkeley National Laboratory. CEC PIER program. 2005.

Porter, K. and Intermittency Analysis Project Team. (2007). Intermittency Analysis Project: Summary of Final Results. California Energy Commission; PIER Research Development & Demonstration Program. CEC-500-2007-081.

Ralph S, Mercado P, Krewitt W, Bhuyan G, Flynn D, Holttinen H, et al. Integration of Renewable Energy into Present and Future Energy Systems. In IPCC Special Report on Renewable Energy Sources and Climate Change Mitigation [O. Edenhofer, R. Pichs-Madruga, Y. Sokona, K. Seyboth, P. Matschoss, S. Kadner, T. Zwickel, P. Eickemeier, G. Hansen, S. Schlömer, C. von Stechow (eds)], Cambridge University Press, Cambridge, United Kingdom and New York, NY, USA. 2011.

Razeghi, G., T. Brown, G.S. Samuelsen. The impact of plug-in vehicles on greenhouse gas and criteria pollutant emissions in an urban air shed using a spatially and temporally resolved dispatch model. J.Power Sources 2011, 196(23), 10387-10394

Razeghi G, L. Zhang, T. Brown, G.S. Samuelsen. Impacts of plug-in hybrid electric vehicles on a residential transformer using stochastic and empirical analysis. J.Power Sources 2014, 252, 277-285

Rudston, J. (2011). Techno-Economic Analysis of Sustainable Energy Systems for Meeting the Energy Demand of a Greenhouse in South Australia. School of Energy Resources, Australia, University College London. MSc.

Smith, C. (1993). System Performance. Active Solar Systems. G. Lof. Cambridge, MIT Press.

Snook, J., Papamichael, K., Koyle, B., Pierce, M., Lighting California's Future: Cost-Effective Demand Response. Public Interest Energy Research Program. California Energy Commission. March 2011.

Spath, P. L., Mann, M. K., Life cycle assessment of hydrogen production via natural gas steam reforming. NREL/TP 570-27637. NREL; February 2001

Tarroja, B., Characterization and Evaluation of Utility-Scale Intermittent Renewable Generation Variations and Implications for Electric Grid Load Balancing, in Mechanical and Aerospace Engineering. Masters Thesis, University of California, Irvine: Irvine, 2011

Tarroja, B., F. Mueller, J. D. Eichman and S. Samuelsen (2011). "Metrics for evaluating the impacts of intermittent renewable generation on utility load-balancing." Energy 42 (1): 546-562.

Tarroja, B., F. Mueller, J. D. Eichman, J. Brouwer and S. Samuelsen (2011). "Spatial and temporal analysis of electric wind generation intermittency and dynamics." Renewable Energy 36 (12): 3424-3432.

U.S. Energy Information Administration (2011). Net Generation by Energy Source: Total (All Sectors). EIA-906, EIA-920, EIA-923. August 19, 2012.

University of Wisconsin-Madison. "A TRaNsient SYtems Simulation program." Retrieved 04/20/2012, <http://sel.me.wisc.edu/trnsys/>.

Walker, G., EVALUATING MPPT CONVERTER TOPOLOGIES USING A MATLAB PV MODEL. Journal of Electrical & Electronics Engineering, 2001.

Weiss, W., Mauthner, F. (2012). Solar Heat Worldwide: Markets and Contribution to the Energy Supply 2010, International Energy Agency.

Wilcox, S. (2007). National Solar Radiation Database 1991-2005 Update. National Renewable Energy Laboratory. U.S.D.o.E., Office of Energy Efficiency and Renewable Energy. NREL/TP-581-41364.

Yin, et al. Study on Auto-DR and Pre-cooling of Commercial Buildings with Thermal Mass in California. LBNL. 2010.

Zhang L, Brown T, Samuelsen GS. Fuel reduction and electricity consumption impact of different charging scenarios for plug-in hybrid electric vehicles. Journal of Power Sources. 2011;196(15):6559-66.

APPENDIX A: Task 2:
Substation and distribution circuit infrastructure

TABLE OF CONTENTS

Task 2.1. Preferred RESCO Substation and Distribution Circuit Configurations A-3

Task 2.1.1. RESCO substation and distribution operating requirements A-3

Task 2.1.2. Common substation and distribution circuit components A-4

Task 2.1.3. RESCO substation and distribution circuit alternatives A-6

2.1.3.1. Fault current limiters A-6

2.1.3.2. Reactive power management A-8

2.1.3.3. Loop circuits A-9

Task 2.1.4. Preferred RESCO substation and distribution circuit configurations A-10

Task 2.1.5. Conclusions A-10

Task 2.1.6. References A-11

Task 2.2. UCI Substation and Distribution Circuit Infrastructure A-12

Task 2.2.1. UCI Electric System A-12

2.2.1.1. Electric Service History A-12

2.2.1.2. Monitoring Capabilities and Sample Data A-14

2.2.1.3. Installed Distributed Generation A-18

2.2.1.4. Campus Circuit Model Development A-18

Task 2.2.2. Development of UCI Campus Model Methodology A-21

2.2.2.1. Model Overview A-21

2.2.2.2. Model Methodology Description A-22

2.2.2.3. Verification of Modeling Approach A-23

2.2.2.4. Analysis Parameters A-24

2.2.2.5. Model Evaluation A-24

Task 2.2.3. Capacity of the Existing UCI Infrastructure A-28

2.2.3.1. Substation A-29

2.2.3.2. Distribution feeder circuits A-29

2.2.3.3. Building secondary distribution transformers A-30

2.2.3.4. Campus growth and flexibility A-31

Task 2.2.4. Cost and Performance of Infrastructure Improvements A-31

2.2.4.1. Campus Metering A-31

2.2.4.2. Electricity Export Allowance A-38

2.2.4.3. Campus Islanding A-38

Task 2.2.5. Conclusions A-39

Task 2.2.6. References A-39

Task 2.3. Interconnection of DER on UCI Distribution Circuit A-39

Task 2.3.1. Impact of Increased Distributed Generation on Circuit Operating Characteristics A-40

Task 2.3.2. Potential UCI Infrastructure Challenges A-50

Task 2.3.3. Conclusions A-51

Task 2.3.4. References A-51

UCI is a micro-grid with a collection of generation resources and diverse loads. In order to determine how renewables can be implemented at UCI an understanding of the electrical infrastructure currently in place and any adjustments that need to be made to provide electricity in a safe, reliable and cost competitive manner must be acquired. This section explores the current electrical infrastructure at UCI, the impacts of installing distributed energy resources (DER) on the UCI grid and technologies that can help support increases in DER.

Task 2.1. Preferred RESCO Substation and Distribution Circuit Configurations

Task 2.1.1. RESCO substation and distribution operating requirements

The electric distribution system is designed with the goal of providing end-users with electricity at end-user service entrance that is of a specific quality in a manner which is cost-effective, reliable, and safe. Some of the guidelines and standards defined for the quality of power at the electric service entrance are:

- Voltage within an allowable range of +5% of nominal (ANSI C84.1-2006)
- Frequency of 60 + 0.05 Hz during normal operation
- Voltage harmonic distortion within <5% THD (IEEE Std 519-1992)

For a grid-connected distribution system, the frequency is determined by load-generation balancing on the bulk transmission system and thus roughly independent of the local substation and distribution system. Poor distribution planning can, however, result in unacceptable customer voltage magnitude and harmonic levels. A RESCO should be capable of continuing to meet the voltage guidelines and standards.

The reliability of the electric power system is defined as having sufficient power available for the customer usage as well as minimizing the frequency of customer outages and the duration of customer outages when they occur. Common indices to quantify electric power system reliability are system average interruption frequency index (SAIFI), system average interruption duration index (SAIDI), and customer average interruption duration index (CAIDI). Many utilities report short-term power outages below a given threshold (e.g. less than five minutes) as a power quality problem and not a reliability one. The momentary average interruption frequency index (MAIFI) is used to count these separate interruptions. These indices will vary by utility, location, population density, and customer type (Willis 2004). A reasonable objective for a RESCO would be at least as reliable as the existing system, or a comparable community for the case of new construction.

The distribution system must also be safe, which means that faults should be avoided where possible, but when they inevitably occur, the fault is quickly detected and the affected line section de-energized and isolated. Standard fuses and reclosers have minimum pickup ratings below which they will not detect a fault, and maximum current ratings beyond which they will not be able to open the circuit and de-energize the fault. Thus the circuit must be designed to have no possible fault condition that exceeds the protection ratings. A RESCO must have

similar requirements for protection coordination that will allow the system to pickup faults that occur and clear them within a reasonable time.

Historically, these operating requirements have been achieved using robust components that have limited communication and control. The current distribution system is still effective, and the product results from tradeoffs between cost and reliability while maintaining safety. These features cannot be overlooked when considering advances to the distribution system to enable a renewable based energy secure community.

Task 2.1.2. Common substation and distribution circuit components

A typical distribution substation with associated circuit feeders is illustrated in Figure 13. The basic components and operation of a distribution system is rather simple:

- Substation Transformers: Transformer banks at the substation reduce the voltage from transmission and sub-transmission levels to distribution circuit feeder voltages (commonly 4 to 33 kV). Some transformers have a fixed turns-ratio, where the distribution secondary voltage is determined proportionally to the high-voltage and the transformer impedance losses. However, other transformers have load tap changing capability and thus the flexibility to change the outlet voltage independent of the transmission voltage. This helps decouple the distribution circuit voltage levels from transmission voltage variations. Each transformer bank typically feeds multiple distribution feeder circuits (e.g. 4 or 5) that are connected to the low-voltage side of the transformer through circuit breakers (Pansini 1992).

- Switchgear: Switches are installed at the substation and along the circuit to disconnect portions of the distribution circuit feeder and allow circuit reconfiguration to accommodate future load growth. Many substations can be fed from multiple sources so that if the main sub-transmission line is removed from service, a normally open switch to another sub-transmission line could be closed and service resumed. Switches must be designed to accommodate for arc flash conditions.

- Protective devices: Protective devices, such as circuit breakers, fuses, and reclosers, are installed at the substation and along the distribution circuit to protect equipment and customers against potential contingencies such as line-line and line-ground fault conditions. Protective devices throughout the distribution circuit must be coordinated to isolate and de-energize system faults with minimal impact on the rest of the system.

- Substation capacitors: Capacitors may be placed at the substation to control the amount of reactive power drawn from the sub-transmission system. Reactive power can cause large voltage sags in the transmission system. Hence, reactive power flow onto the transmission system must be controlled.

- Circuit feeder capacitors: Additional capacitors can be placed along the distribution circuit to provide reactive power locally and thus improve regulation of the distribution circuit voltage profile. Both substation and circuit feeder capacitors may be fixed or

switched. Approximately 60% of utility-installed capacitors are on the circuit, 30% at the substation, and 10% in sub-transmission/transmission banks (Rustebakke 1983).

- Distribution transformer: Distribution transformers reduce the distribution circuit voltage to the customer service entrance voltage, such as 120V single-phase or 480V three-phase. This is the final stage of voltage change before the customer service entrance. Distribution transformers are typically not capable of changing taps while energized, but often have five different low voltage taps that can be manually adjusted when not in service. Distribution transformers have losses of around 1 to 2%, which means they account for approximately 27% of all transmission and distribution losses (Barnes, Van Dyke et al. 1995).

Figure 13: Conceptual schematic of a standard distribution system

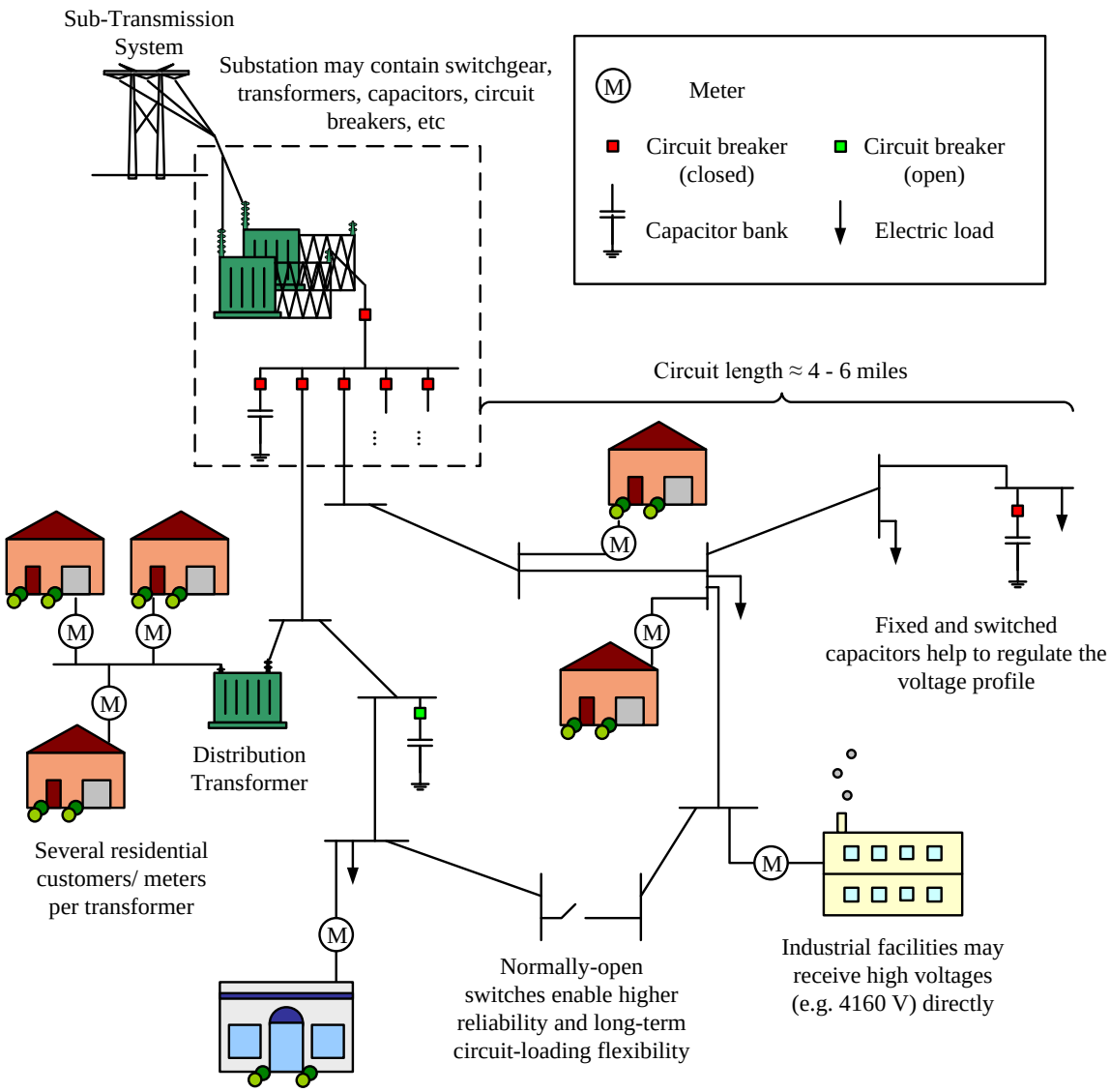

Task 2.1.3. RESCO substation and distribution circuit alternatives

Any substation and/or distribution circuit alternative technologies should be considered for one or more of the following reasons:

- Improve electric reliability indices
- Decrease operating and maintenance costs
- Enable increase in DER
- Increase efficiency and line capacity

However, trade-offs will always exist between the reliability indices, complexity, cost, and efficiency. For example, installing more fuses and reclosers on the distribution circuit will reduce the number of customers affected by a single fault, but increase the infrastructure and maintenance cost. Some advanced circuit configurations are designed to improve distribution system reliability, but if poorly implemented could actually decrease the reliability. As a result, early field tests typically install a new technology in parallel with the traditional such that the new device can be disconnected and still maintain standard operation. This redundancy will certainly increase the cost of these first prototype circuits, but allow the electric utility to field test distribution circuit technology to ensure that they behave as anticipated.

The current philosophy is that substations and distribution feeders represent a major infrastructure investment and will not be completely overhauled. However, when components fail or reach the end of their useful lifetime, there is an opportunity to provide system upgrades and install more effective equipment. Similarly, as new circuits are built they can utilize more advanced technology and incorporate flexibility for future expansions, but must remain compatible with the existing system. On the other hand, new requirements on the existing electric system, such as distributed generator installation or increased electric vehicle load, could possibly require circuit reorganization or new equipment. It is desired to minimize this invasiveness into the distribution system infrastructure, but minimize the impact where it is unavoidable. Three innovative distribution circuit alternatives are emerging as summarized below.

2.1.3.1. Fault current limiters

Transformers represent a significant infrastructure cost and efficiency penalty—substation transformers typically account for ½ to ⅔ of the total substation cost (Willis 2004) and distribution transformers alone account for 27% of all transmission and distribution losses (Barnes, Van Dyke et al. 1995). While technology advances have steadily improved the efficiency of small distribution transformers from 98% to upwards of 99% (Barnes, Van Dyke et al. 1995), large transformers ranging in size from 500 kVA to 5 MVA have impedance requirements that are determined by short circuit concerns. Depending on the voltage levels, the required impedance varies from 5.75% to 7.0% (IEEE Std C57.12.51-2008). Substation transformers have impedance that is typically around 8.0%, but can be specified higher to reduce the fault current limit (Short 2003).

Limiting the system fault current is important because a circuit with zero impedance would be extremely efficient during standard operating conditions, but would cause infinite short circuit current in the case of a line-to-ground fault. Circuit breakers have maximum current ratings past which the switch will be incapable of opening (the highest limited rating is around 100,000 A (Leung 2000)), and consequently, minimum system impedances. As circuit breakers take a few cycles to open, limiting the short circuit current will also reduce the total energy released into the fault, which is another valuable safety consideration (Short 2003). The use of high impedance transformers is one of the main ways that electric utilities reduce fault current, though this method causes inefficiency and loss of voltage stiffness, which can result in voltage sags (Leung 2000).

Concerns over the solution to mitigating fault current have led to interest in fault current limiters (FCL) using superconducting materials. Such an FCL would have nonlinear impedance characteristics to show virtually zero impedance during normal operation, but would move out of the superconducting region during an overcurrent and create a higher impedance (Leung 2000). There are a variety of strategies to implement such functions, including uses of both the mature low temperature semiconductor (LTS) and the newer high temperature semiconductor (HTS), though the HTS is gaining favor due to difficulties in thermal management during fault recovery for LTS materials (Leung 2000). An extremely simple and fail-safe FCL is to place an HTS element in series with the regular line. During a fault, the increased current heats the material up from superconducting to non-superconducting region (also referred to as the quench) to limit the fault current (Noe and Steurer 2007). A disadvantage of the series resistance method is a slow recovery time. Another HTS-type FCL is a shielded core, which is constructed like a transformer with the primary winding in series with the main circuit and the second winding shorted. A superconducting cylinder in between shields the primary from the secondary during normal operation, but during excessive currents will allow the flux to penetrate and thus create an additional inductance on the primary. A disadvantage of the shielded core FCL is large size—typically on the order of size and weight of a comparable transformer (Noe and Steurer 2007). There are many other types of FCL in development, and while early tests have been promising, they are not yet considered a commercial technology (Noe and Steurer 2007).

In addition to enabling the use of lower impedance power systems infrastructure (Noe and Steurer 2007), fault current limiting technology could be incorporated directly into a system transformer (Hayakawa, Kagawa et al. 2001). Such a superconducting fault current limiting transformer (SFCLT) would have near zero impedance during normal operation, but increase to a high impedance during fault overcurrent (Hayakawa, Kagawa et al. 2001). A SFCLT would improve efficiency, improve system stability, and lower fault current during a contingency. The technology is tested at a laboratory scale in (Kurupakorn, Hayakawa et al. 2004).

Dedicated fault current limiters and fault current limiting transformers are promising technologies for a future efficient and robust power system, though further field demonstrations and commercialization will be required before their widespread use.

2.1.3.2. Reactive power management

While consumer loads may have either a leading or lagging power factor, in general aggregated loads tend to be lagging and thus consume reactive power. The transmission of reactive power along power lines causes voltage drops, efficiency loss, and decreases the capacity of the line available for real power transmission. Thus reducing the flow of reactive power will provide a number of benefits for the system. Reactive power generation is traditionally accomplished through the installation of AC capacitors, which may either be located on a radial feeder/branch circuit or at the substation. The capacitor is most effective at improving efficiency and providing voltage support when located close to the source of the reactive power load. However as the utility already owns the substation property, it is easier to locate equipment there, particularly for underground distribution systems where pole-mount overhead capacitor banks are not feasible. These concerns have led to installation of roughly 60% of utility capacitors in the field, 30% at substations, and 10% on the transmission system (Rustebakke 1983).

At present, shunt capacitors are either connected directly (fixed) or through a mechanical breaker switch (switched). The capacitors are usually installed in sets of three single-phase banks and common ratings for each phase are 50, 100, 150, 200, and subsequent 100 kVAR increments (Short 2003). The difficulty with this method of supplying reactive power is that it is very coarse. The capacitor banks are large and switched as an entire unit. Once the capacitor bank is sized and installed, the rating is set and cannot be changed in future. As it is reactive power balancing that is important—not just the production of reactive power—better control of reactive power generation could improve the efficiency, capacity, and voltage of the system. Three candidate technologies that may be able to improve the management of reactive power on the feeder and at the substation are (1) thyristor-switched capacitor bank, (2) STATCOM, and (3) local power factor correction.

An alternative technology to traditionally switched capacitors is a thyristor-switched capacitor (TSC) bank. Such a bank includes several smaller capacitor banks that are each connected through a bi-directional thyristor switch with an inrush current limiting inductor. As thyristors are solid-state devices, each bank can be switched a nearly unlimited number of times in comparison to standard breakers (Torseng 1981), which are subject to mechanical wear and tear. Thus intelligent control of a TSC provides much finer control of the reactive power produced on a system by turning the banks on and off to provide variable levels of reactive power. In addition, the lower inrush is expected to increase the lifetime of the capacitors themselves, and the TSC could also be used for load balancing (Torseng 1981).

Another technology for reactive power management on the distribution system is the static synchronous compensator (STATCOM). While traditional utility capacitors are directly-connected AC capacitors, a STATCOM utilizes a DC capacitor connected through an AC/DC converter to provide the same capability within a smaller footprint. Also, the active control associated with the AC/DC converter allows the STATCOM to provide a continuum of reactive power outputs, both generation and consumption (Rao, Crow et al. 2000). Another benefit for STATCOM technology is that reactive power output can be controlled independent of the local voltage. Shunt-connected AC capacitors produce reactive power as a function of the local

voltage squared, yet they are used to level the voltage. For voltage leveling, more power should be produced at low voltages and less at higher, though in practice the inverse of this occurs in a passive capacitor system. Active control of a STATCOM could decouple voltage from reactive power output, which would increase the stability of the technology.

The main disadvantage of a thyristor-switched capacitor bank and STATCOM is the increased cost. Also, traditional semiconductor technologies used for a STATCOM cannot connect directly to the high voltage distribution line and will require a step-up transformer. New materials, such as silicon carbide (SiC), may enable solid state switches that can reliably be used at higher voltages (10 kV to 25 KV) and high frequency (20 kHz). The commercialization of power converters utilizing SiC materials would dramatically increase the applications for power electronics in the electric power utility, though this technology is still under development (Hefner, Sei-Hyung et al. 2006).

Other solutions may involve a combination of all these reactive power management strategies. The Tennessee Valley Authority successfully used an 8 MVA STATCOM paired with an 8 MVAR capacitor bank to prevent voltage sags and defer construction of an upgraded line in the Leake substation (Grant 2004). The combination responded to over 500 voltage events in its first 19 months of operation and exhibited an availability of 99.66% (Grant 2004). Also, the best location to compensate for reactive power is at the load itself. New Energy Star specifications would require solid-state lighting and AC/DC power supplies to meet power factor requirements as high as 0.95 at full load (Conner 2010). Thus in future, encouraging use of Energy Star appliances and lighting will also aid the problem of reactive power management in addition to end-use efficiency.

2.1.3.3. Loop circuits

Present day distribution circuits branch out from the substation radially. In practice, each distribution feeder circuit is connected to at least one other feeder circuit through one or more open switches. This connection makes it possible to (1) manually close the switch and back feed a portion of the distribution circuit in the case of a long term failure (Pansini 1992) and (2) allow portions of an existing circuit to be transferred to a new one for future load growth (Rustebakke 1983).

The flexibility provided by the inter-feeder switches is desirable for the establishment of long-term infrastructure and to increase reliability of the system, but the circuits are never simultaneously connected at both the substation and in the field. Such a configuration creates a closed-loop, which has the benefit of increasing distribution efficiency and increasing line capacity. These attributes occur because the neutral voltage point of the loop will float at its optimum point, which is dictated by the spatial loading of the loop. However, in the case of a fault, the entire loop will be de-energized and thus all customers would be affected compared to only the customers on the faulted feeder circuit. Thus circuits are not normally connected in a closed-loop configuration.

Advanced circuit protection technology could enable the benefits of an open-loop circuit for efficiency and line capacity, while also increasing the reliability of the circuit instead of

diminishing it. In this strategy, several circuit interrupters would each sense the direction and magnitude of current at their location and communicate to the other interrupters. During a fault, the interrupters would detect the faulted line section and open on either side to isolate and de-energize it. Reliability is increased by reducing the number of customers affected by a single fault, as now only the portion of a circuit closest to the fault will lose electric service. Circuits with this type of automatic reconfiguration ability are sometimes referred to as self-healing.

Loop circuits can result in improved efficiency. However, more complex circuit protection strategies must be implemented to maintain the same electric reliability. There is trade-off in efficiency and reliability versus operation complexity.

Task 2.1.4. Preferred RESCO substation and distribution circuit configurations

The main objective of the project is to securely enable increased penetration of renewable energy for community integration. There are advancements at the distribution substation and feeder circuit level that can improve distribution efficiency, reliability, and enable streamlining of distributed generation installation. However, as many of these technologies are still early in their development and field testing, the trade-offs between efficiency, complexity, reliability, and cost of a mature system are not yet fully understood. A key take-away is that the current infrastructure is elegant in simplicity, and while not optimal for efficiency and reliability, can support a renewable-based energy secure community.

Task 2.1.5. Conclusions

- Installation of renewables must comply with voltage guidelines and standards
    - Voltage within an allowable range of +5% of nominal (ANSI C84.1-2006)
    - Frequency of 60 + 0.05 Hz during normal operation
    - Voltage harmonic distortion within <5% THD (IEEE Std 519-1992)
- Fault avoidance, detection and isolation can increase the reliability of a system and becomes more important with the installation of renewables at UCI
- Circuits connected with switches is a solution to enable:
    - Back feed circuit in the event of long term failure
    - Transfer of load to accommodate future load growth
- Loop circuits can result in improved efficiency but require more complex circuit protection strategies to maintain the same electric reliability

Task 2.1.6. References

ANSI C84.1-2006 American National Standard for Electric Power Systems and Equipment--Voltage Ratings (60 Hertz).

Barnes, P. R., J. W. Van Dyke, et al. (1995). The Feasibility of Replacing or Upgrading Utility Distribution Transformers During Routine Maintenance. Oak Ridge, TN, Oak Ridge National Laboratory. Report No. ORNL-6804/R1. <http://www.ornl.gov/~webworks/cpr/v823/rpt/78562.pdf>.

Conner, M. (2010). New power regulations bring power-factor correction to lower-power supplies. EDN, August 26, 2010

Grant, I. (2004). STATCOM Postpones the Need for 161-kV Line. Transmission and Distribution World.

Hayakawa, N., H. Kagawa, et al. (2001). "A system study on superconducting fault current limiting transformer (SFCLT) with the functions of fault current suppression and system stability improvement." Applied Superconductivity, IEEE Transactions on 11(1): 1936-1939.

Hefner, A., R. Sei-Hyung, et al. (2006). Recent Advances in High-Voltage, High-Frequency Silicon-Carbide Power Devices. Industry Applications Conference, 2006. 41st IAS Annual Meeting. Conference Record of the 2006 IEEE.

IEEE Std 519-1992 "IEEE Recommended Practices and Requirements for Harmonic Control in Electric Power Systems."

IEEE Std C57.12.51-2008 "IEEE Standard for Ventilated Dry-Type Power Transformers, 501 kVA and Larger, Three-phase, with High-Voltage 601 V to 34 500 V; Low-Voltage 208Y/120V to 4160 V--General Requirements."

Kurupakorn, C., N. Hayakawa, et al. (2004). "Development of high temperature superconducting fault current limiting transformer (HTc-SFCLT) with Bi2212 bulk coil." Applied Superconductivity, IEEE Transactions on 14(2): 900-903.

Leung, E. M. (2000). "Superconducting Fault Current Limiters." IEEE Power Engineering Review(August).

Noe, M. and M. Steurer (2007). "High-temperature superconductor fault current limiters: concepts, applications, and development status." Superconductor Science and Technology 20: R15-R29.

Pansini, A. J. (1992). Guide to Electrical Power Distribution Systems. Englewood Cliffs, New Jersey, Prentice Hall.

Rao, P., M. L. Crow, et al. (2000). "STATCOM control for power system voltage control applications." Power Delivery, IEEE Transactions on 15(4): 1311-1317.

Rustebakke, H. M. (1983). Electric Utility Systems and Practices, John Wiley & Sons, Inc.

Short, T. A. (2003). Electric Power Distribution Handbook, CRC Press.

Torseng, S. (1981). "Shunt-connected reactors and capacitors controlled by thyristors." Generation, Transmission and Distribution, IEE Proceedings C 128(6): 366-373.

Willis, H. L. (2004). Power distribution planning reference book. New York, NY, Marcel Dekker, Inc.

Task 2.2. UCI Substation and Distribution Circuit Infrastructure

UCI's campus contains many buildings and a wide array of loads. some of which are not monitored. This task describes the electrical makeup of the campus along with information about key loads and distributed generation on campus. Additionally, available metered data is collected and analyzed in preparation of the UCI circuit model developed in the following tasks.

Task 2.2.1. UCI Electric System

2.2.1.1. Electric Service History

The electric service for the UCI campus has already experienced a history of change and steady growth that defines its present characteristics. The early campus was historically served directly from two SCE 12 kV circuits that entered the UCI central plant. Each of these two circuits separated into sub-circuits that fed the portion of campus around the central plant. A third SCE 12 kV circuit fed the East Substation, which was located on the opposite side of campus. This third line also connected to a bus bar that energized more sub-circuits to serve the east side of campus.

Around 1990, the UC Substation was built to accept a SCE 66 kV service directly and step the voltage down to 12 kV locally. The three old SCE lines were replaced with three circuits from the new UC Substation. Because these circuits were installed to replace an electric source in a different location, they run directly and unloaded from the UC Substation to the central plant or East Substation. To avoid voltage drop concerns, these circuits were installed with two conductors per phase to reduce the impedance. Most buildings in the main UCI campus are still served by infrastructure derivative of these three main circuits.

A conceptual schematic of the UCI electric service is presented in Figure 14. The primary feed for the UC Substation is an SCE 66 kV line with a single billing meter. The UC Substation has two 15 MVA transformers, which cannot be paralleled, that each serve 5 circuits and a capacitor bank. The 12 kV sides of the two substation transformers are connected with a tie-line switch. Originally, the tie-line was open and the two transformers were operated independently with their respective loads. However, as the on-campus combustion turbine produces more real power than the load served by either transformer, connecting it with this configuration would cause real power to be exported to SCE through one transformer. Thus when the turbine is producing power, the second transformer is disconnected and tie-line connected so that the first transformer serves the entire campus load. When the turbine goes offline, the tie-line is automatically opened and the second transformer reconnected. This occurs because a single 15

MVA transformer is insufficient to support the entire campus load without the local generation. At present, the two capacitor banks at the UC Substation are disconnected, presumably due to a resonance issue that occurred when the turbine generators were installed. The turbines do generate reactive power to augment this need.

There are another two circuits from the UC Substation that serve only the central plant loads. These loads are associated with normal plant operation, chillers and thermal energy storage, and the gas turbine generator. The circuit that connects to the gas turbine and steam turbine (UC-4) exports power back to the UC substation during normal operation. A third circuit is planned to connect the substation to the central plant for another generator in future.

In addition to the three main campus circuits, two central plant circuits plus future circuit, there are another four circuits—UC-2 and UC-5 connect to the health sciences buildings, UC-8 connects to a few large facilities in biological and physical sciences, and UC-10 feeds the Environmental Health and Safety building by the UC Substation. As additional circuits are built and loads shifted to new feeders, the previous cables are disconnected through switches but left otherwise intact. This legacy infrastructure allows for flexibility to easily move loads around and enable further capacity expansion. In addition, the circuits tend to radiate in interleaved pairs where each transformer can be easily switched from one feeder circuit to another.

Figure 14: Conceptual schematic of UCI electric service

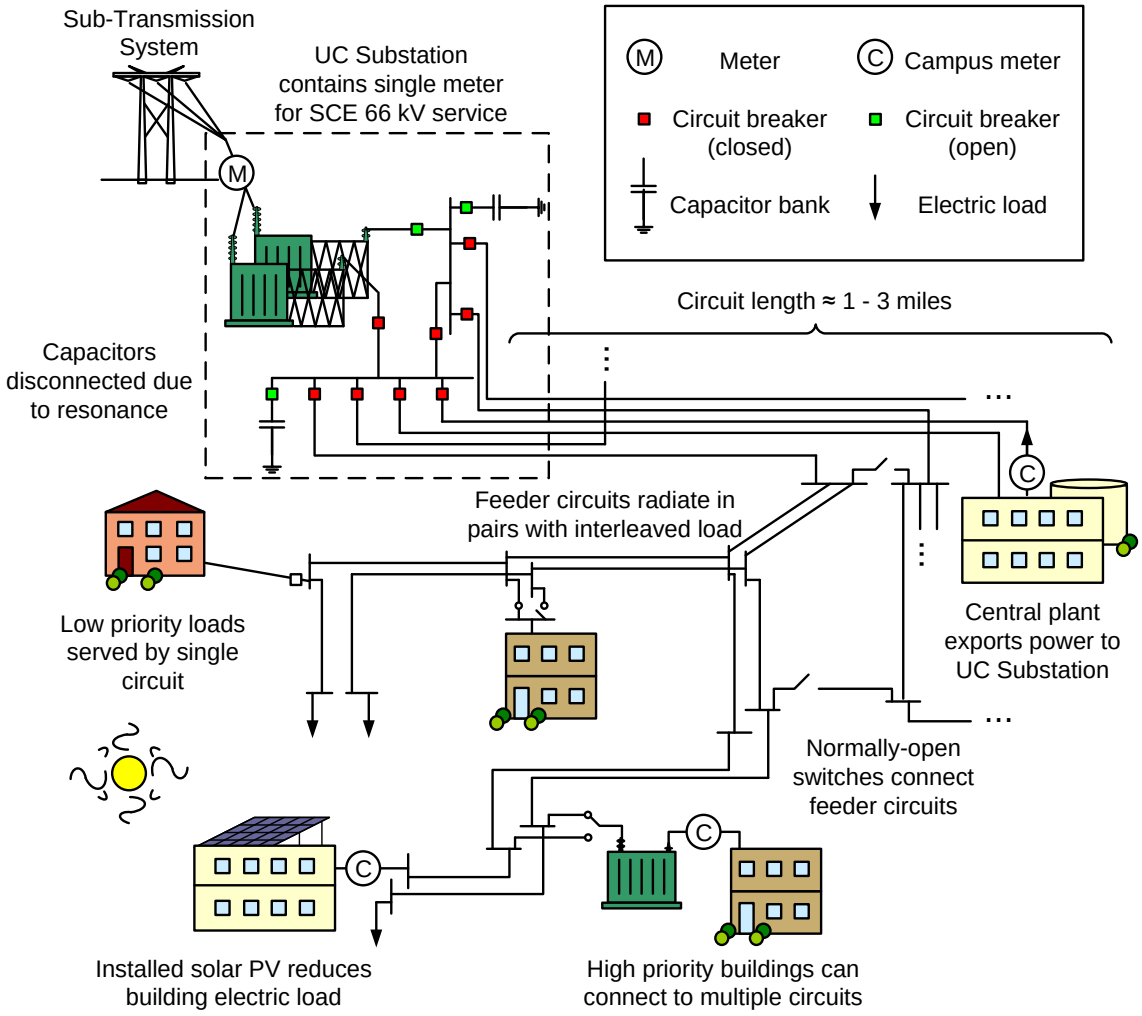

2.2.1.2. Monitoring Capabilities and Sample Data

The only SCE billing meter is installed on the 66 kV side of the 66/12 kV transformer, thus all loads downstream of this location are monitored for internal campus use only. Thus the campus meter network is extensive but not complete. As the meters are generally installed along with the construction of each building, a variety of meter types are located around the campus with older buildings tending to have older meter technology. As of November 2008, there were 83 facilities with KYZ pulse output meters that can transmit real power usage at 15 minute intervals with no further capabilities, and 31 facilities with either Schneider Electric ION 7330, 7650, or Siemens 9330 Power Quality Meters. Approximately 24 facilities have their own stand-alone sub-meter and 58 small facilities (i.e. trailers, interim buildings, and sheds) have no recorded metering. Both the 7330/9330 updated meters and historical KYZ meters communicate with an ITRON EEM system that allows access to the historical kWh data by meter.

In parallel with the ITRON EEM system, there is interest to take advantage of the increased capabilities of the 7330/9330 meters to also communicate reactive power, voltage, and transient

power quality events. An additional Schneider Electric PowerLogic™ ION Enterprise™ network has been established that to-date has thirteen active nodes at the locations and associated transformers given in Table 3.

Table 3: Location and associated transformer of ION Enterprise™ nodes

Location	Transformer
UC-3 HV Breaker	-
UC-9 HV Breaker	-
Engineering Gateway 480V	T055
Engineering Gateway 120V	T057
Chiller 1	T114
Chiller 5A	T114
Chiller 5B	T114
Chiller 6A	T114
Chiller 6B	T114
MSTB and Trailers	T117
MSTB Only	T117
Natural Sciences 1	T126
Natural Sciences 2	T127

Detailed voltage and real and reactive power flow are available for these UCI campus locations. Chiller 1, Chiller 5A/5B, and Chiller 6A/6B are all connected to a 4160V feed off of transformer T114 at the central plant. UC-3 primarily serves the central plant chiller loads and UC-9 serves the East Substation, which subsequently supplies power to most of the west side of campus including social sciences, engineering, and Verano Place housing. As the UC Substation mains are close together, the voltage is the same for both UC-3 and UC-9 feeders, though it will vary at the other three remote locations. Additionally, the UC-3 and UC-9 measurements are directly from the primary 12 kV system, the chillers are at 4160V, and the building measurements are on the distribution secondary 120V or 480V system.

Some of the voltages are normalized to a per-unit basis to enable direct comparison over a period of a week and the resulting voltages are presented for the initial 4 nodes in Figure 15. The UC main voltage is measured on the 12 kV side of the substation transformer and would be affected by the power flow through the transformer, but if this power flow is not manipulated the substation voltage can be taken as the input voltage to the system. As anticipated, the voltage at T127 (Natural Sciences 2) is a bit lower than the substation voltage due to line and transformer drop. The voltages at T117 and T126 are, however, much higher than the input voltage. This indicates that these transformers are set to a turns-ratio that puts them in a boosting mode. In general, distribution transformers have five taps on the low-voltage secondary to allow changes in the distribution voltage. Common tap settings might be +/- 2.5% and +/- 5% for voltage.

The voltages for the two transformers that serve the Engineering Gateway research, office, and instructional building are also normalized and presented in Figure 16. For this case, the UC Main voltage is below both transformers and both transformers are probably connected in a boosting configuration. As T055 and T057 are both much further from the UC Substation than the other transformers, the voltage drop is probably similarly larger than in the other cases.

Figure 15: Normalized voltage at four circuit locations over a week period

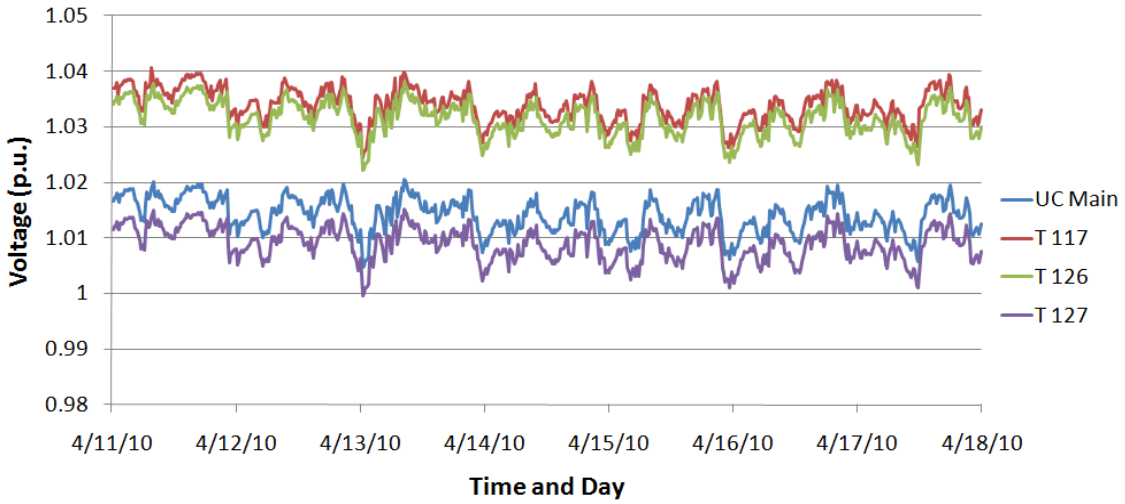

Figure 16: Normalized voltage at Engineering Gateway transformers T055 and T057

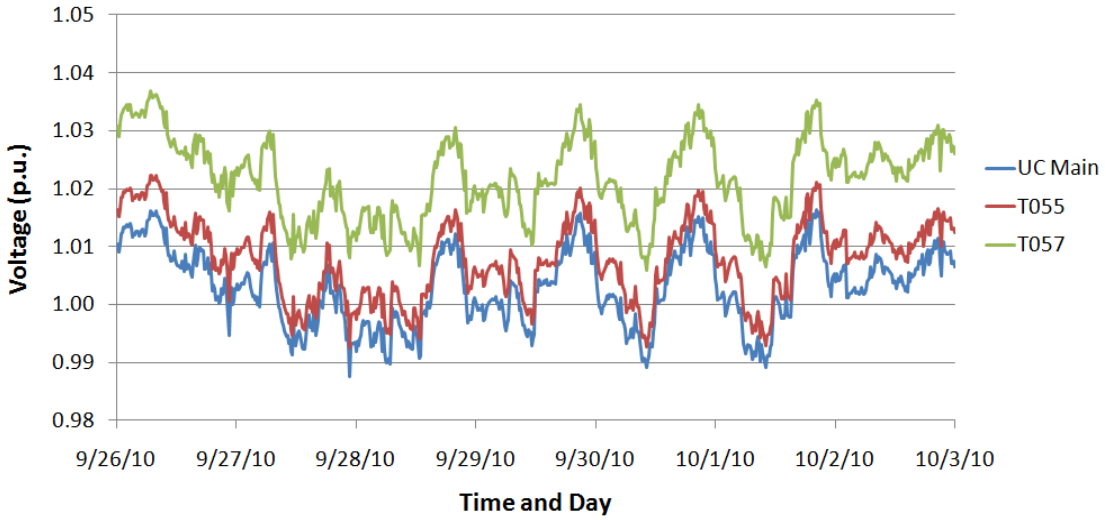

In addition to voltage, the ION Enterprise™ system also records real and reactive power for the connected nodes. The real power for the three monitored chillers is presented for a week period in Figure 17 and the associated reactive power is similarly presented in Figure 18. As the chillers

are large, individual loads their on/off cycle causes major step changes in the power usage for the UCI campus. The figure indicates a chiller power factor of about 0.9.

Figure 17: Real power monitoring for selected central plant chillers

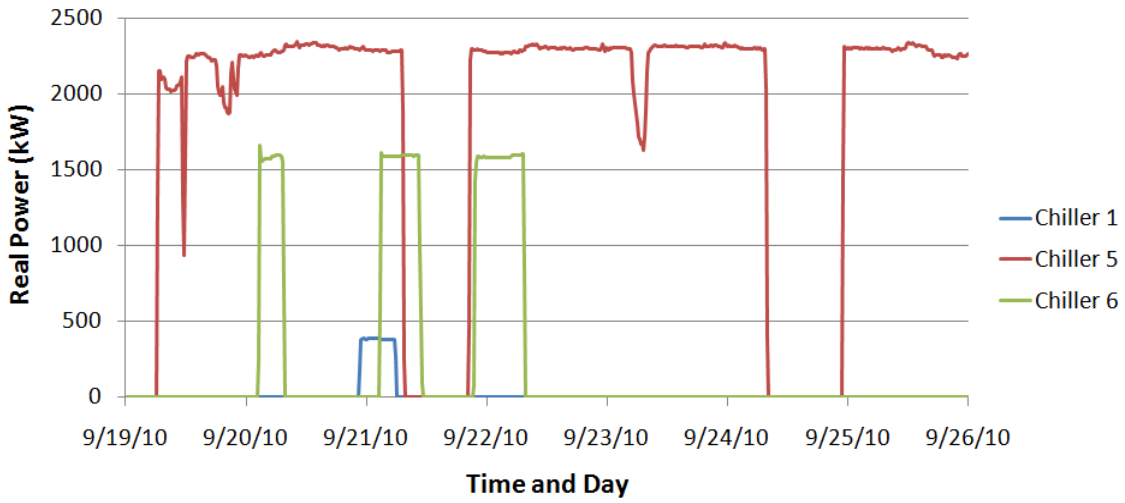

Figure 18: Reactive power monitoring for selected central plant chillers

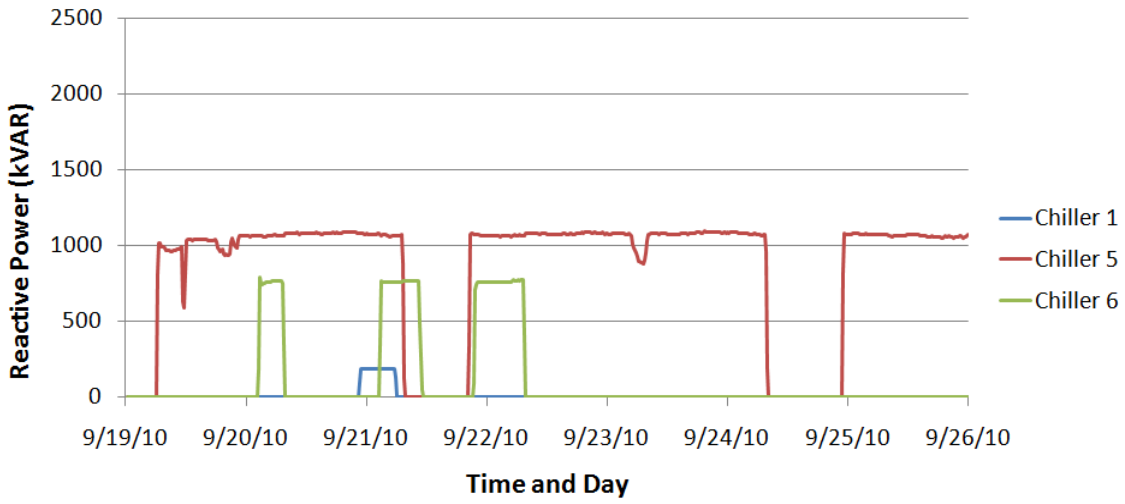

Building real power information at 15-minute intervals can help to determine the spatial and temporal distribution of load on the UCI campus, but reactive power information is needed to completely characterize the load flow and the local voltage required to begin to validate the campus model. Thus the data collected by the ION Enterprise™ system are focused on and used where possible. Additional plans for the metering of the UCI campus includes connecting additional 7330/9330 meters and upgrading the KYZ meters to include advanced capabilities.

2.2.1.3. Installed Distributed Generation

The UCI campus already meets the majority of its load through on-campus generation sources that include combustion and solar PV. The bulk of the power is provided by a synchronous combustion turbine generator rated at 13.5 MW and a co-generation steam turbine rated with a maximum capacity of 5.5 MW. Both turbines are located at the central plant and connect directly to the substation through circuit UC-4.

Recent interest in increasing on-campus generation of renewable electricity caused UCI to sign a power purchase agreement with SunEdison for several solar PV installations totaling 887 kW of electricity. The physical campus locations, installed capacity, and electric circuit location for each array is presented in Table 4.

Table 4: Location and rated capacity of UCI solar PV installations

Location	Capacity (kW DC)	Circuit
Anteater Recreation Center	150	ES-7
Biological Sciences 3	63	UC-8
Bren Events Center	118	UC-3
Engineering Gateway	48	ES-5
Environmental Health and Safety	118	UC-10
Multipurpose Science and Technology Building	92	CP2-3
McGaugh Hall	65	CP1-4
Natural Sciences 1	37	UC-8
Natural Sciences 2	56	UC-8
Sprague Hall	55	UC-2
Student Center 1	29	CP1-4
Student Center 2	56	CP1-4

The campus plans to expand its energy generation portfolio to include a 300 kW molten carbonate fuel cell, which would be located at the Multipurpose Science and Technology Building on CP2-3. Other future plans include an additional generator at the central plant (connected using the future UC-7 circuit) and a large solar concentrating PV system located near the Bren Events Center that would likely connect to the electric service on UC-3.

2.2.1.4. Campus Circuit Model Development

To develop the model each individual circuit is identified in the entire system map along with transformer loads and information on the landmarks (e.g., switchgear identification numbers, vault locations). Reserve circuits and branches of active circuits that are not loaded are ignored for simplicity. The critical bus locations on each circuit are identified and assigned to a number. A bus is defined when (1) a circuit branch occurs or (2) where a transformer load is located. If multiple load transformers are located very close to each other, these are all assumed to be at

the same voltage and the intermediary impedance between them is neglected. As each of the sub-circuits (e.g. CP1-3, CP1-4, and CP1-5) extending from the central plant or the East Substation can each serve dozens of transformers, they are each considered a separate "circuit" for identification and circuit representation. The difference between these sub-circuits and a normal circuit is the aggregate power flow of all the sub-circuits feed into the main circuit to determine the initial starting voltage.

Analysis of the one-line diagram yielded a total of fourteen circuits, 168 buses, and 136 transformers. The geographical location of each circuit can be roughly illustrated in Figure 19 where each color represents a distinct circuit. The multiple colors clustered next to a single main circuit name in the legend identify those as the associated sub-circuits. The bus locations and connections are used to build a model for first each individual circuit, then the aggregate for the entire campus. Because all loads connect back to one main transformer, the behavior of any part of the system will affect the entire system.

Figure 19: Geographic mapping of UCI electric service to campus locations

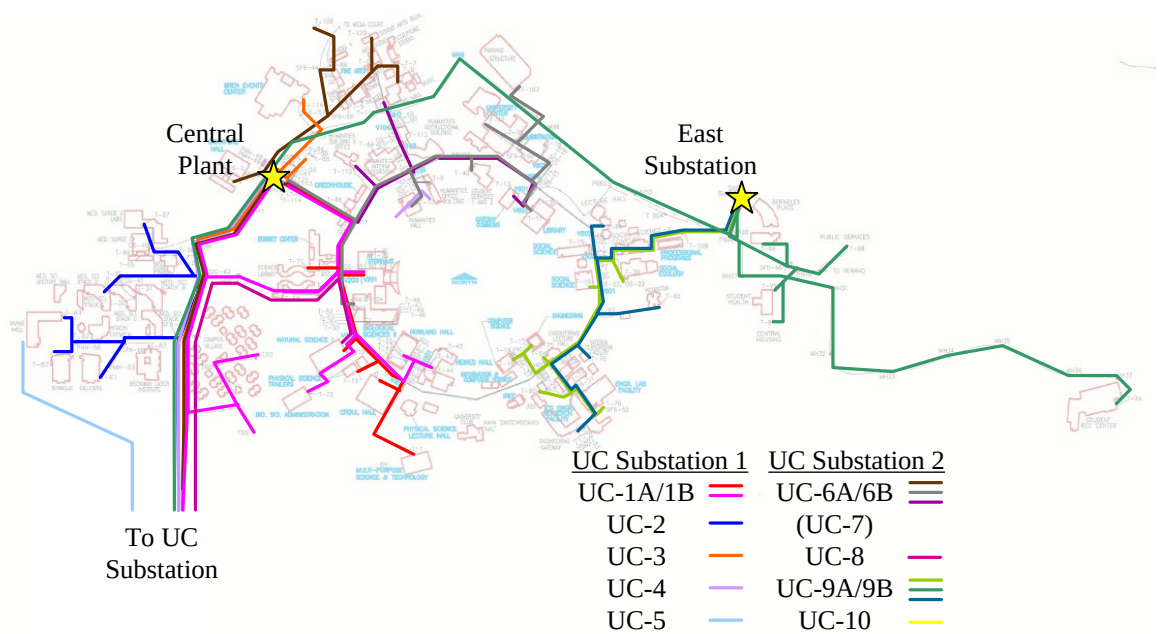

An SKM Arc Flash study conducted by Power Engineering Services Incorporated utilizes data on the conductor types and impedances along with transformer data (Power Engineering Services Incorporated 2009). The conductor information is used to approximate the impedance of each branch and this information is added to the previous model.

To both pare down the requirements of modifying parameters throughout the campus and optimize use of a small initial budget for meter infrastructure upgrades, initially two circuits are chosen for in-depth analysis. All of the main circuits are examined for a variety of parameters that include (1) a variety of load types (e.g. classroom, research, residential), (2) extensive existing metering infrastructure, and (3) high penetration of renewable energy. Due to the existence of a PV installation and future plans for a 300 kW molten carbonate fuel cell, the CP2-3

circuit was the prime candidate for early work. This circuit also serves a variety of loads that include research and classroom and all buildings have existing ITRON EEM-connected meters for power metering. Circuit CP2-3 historically also served three other buildings: Natural Science 1, Natural Science 2, and Biological Science 3. These loads have more recently been shifted over to the new UC-8 circuit, but the switch and associated cable that connected these loads to CP2-3 still remain. In addition, all of those three buildings also have solar PV. For these reasons, both CP2-3 and UC-8 are studied (1) in detail separately and (2) combined into a normally-closed loop. The circuit schematic for the actively loaded portions of CP2-3 and UC-8 is presented in Figure 20. The red color for CP2-3 and the magenta color for circuit UC-8 are both consistent with the campus-wide electric map from Figure 19.

Figure 20: One-line diagram for UCI circuit CP2-3 and UC-8

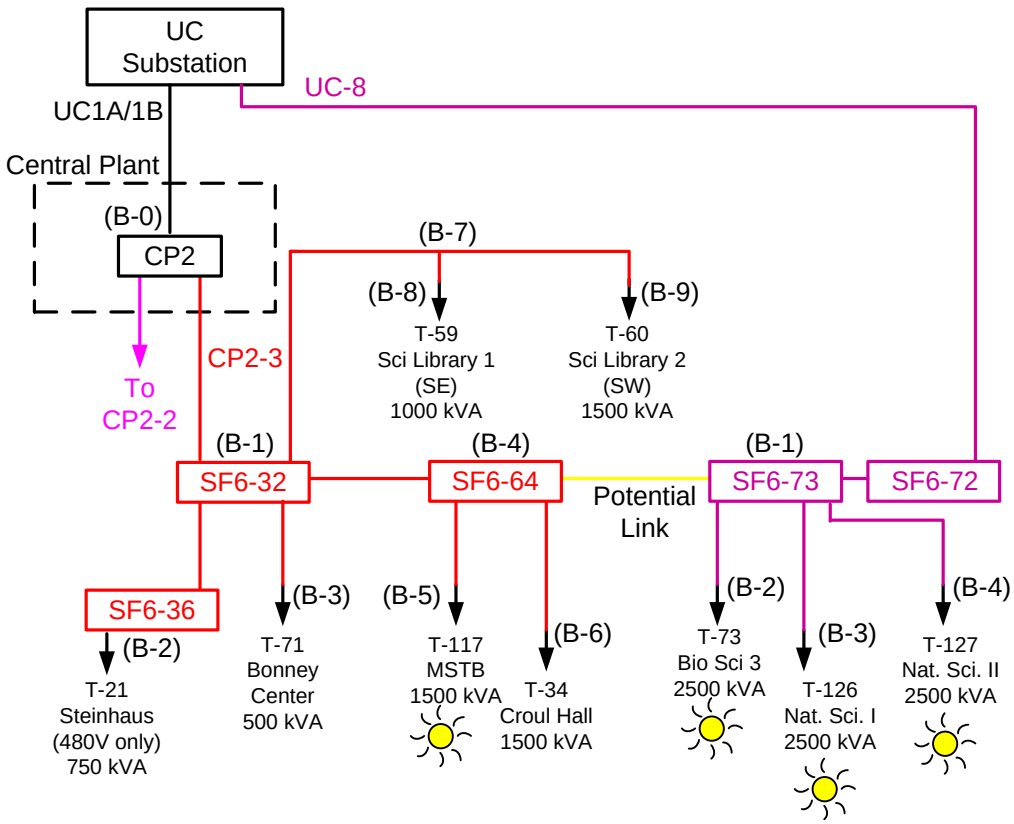

CP2-3 is primarily composed of three branches: the Steinhaus branch, the science building branch, and the Science Library branch. UC-8 has only one load nexus that is connected directly to the UC Substation, while CP2-3 is connected via the central plant.

Due to the limited early detailed metering information, CP2-3 and UC-8 are the focus of early work on model evaluation and analysis of alternative circuit scenarios. They were, however, selected early in the project due to their lucrative characteristics in capturing a high penetration of renewables and variety of campus load types. Thus CP2-3 and UC-8 are concentrated on at this stage in the project. A Matlab/Simulink™ model for the rest of the sub-circuits and UCI

campus has been built and populated with available load information, but the model description focuses on the two circuit with sufficient data for verification.

Task 2.2.2. Development of UCI Campus Model Methodology

2.2.2.1. Model Overview

The model used to explore the UCI campus electric circuits is developed in Matlab/Simulink™ according to a modified version of the ladder iterative technique (Grigsby 2007). Inputs for the model are the 66 kV incoming voltage and time-based real and reactive power information for the campus buildings. Where reactive power information is not available, it is approximated from the known real power and an assumed power factor, which is 0.9 for most buildings. Outputs are the voltage at each bus and the current at each generator, load, bus, and line segment. The model is built and solved entirely in the time domain and provides voltage and current waveforms as outputs. The time-based data are run through a post-processing Matlab code to produce voltage magnitudes, angles, and real and reactive power flow. This method lacks the optimization of more commonly used load flow analysis software, but it has a major advantage in providing flexibility for design of an interface between DG and the grid, as well as control and communication throughout the feeder. A circuit schematic of the simulated radial distribution model that shows two sample buses is presented in Figure 21.

Figure 21: Circuit schematic of distribution model

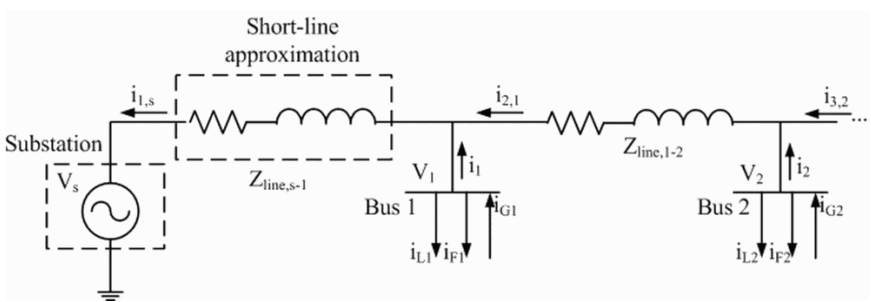

Several ideal assumptions are used for the campus model in order to be consistent with the limited information on non-ideal behavior that is available. These ideal assumptions are:

- Balanced loads and generation
- Symmetrical components
- Linear loads and transformers

Electric power is typically transmitted and distributed in three phases. Ideally, the load on each phase is balanced, but most real systems are unbalanced. Detailed data on the individual phases of the campus load and symmetry of the distribution system infrastructure is not available, so they are assumed to be balanced and symmetrical. This assumption allows the campus to be simulated with one active phase that is extended to the other two phases. This significantly reduces the simulation time and does not reduce accuracy given the limited information on the individual phases of the campus electricity demand.

Another set of ideal assumptions is that the loads and transformers only exhibit linear behavior. Many electronic loads are non-linear because they utilize diode rectifiers or other power electronics-based converters that generate harmonics at frequencies in addition to the line frequency. The iron core in transformers will exhibit a hysteretic non-linear relationship between applied voltage and resultant magnetic flux. The campus meters do not measure line harmonics, and a non-linear model of a transformer is highly dependent of geometry and thus manufacturer specific. Due to the lack of information on harmonics in the UCI campus system, the loads and transformers are assumed to be purely linear.

2.2.2.2. Model Methodology Description

As seen in Figure 21, the campus system model consists of three types of components: substation source, distribution line segment, and bus location. The model for each of these components is described in the following sections.

2.2.2.2.1. Substation source

The substation source is also the swing bus for the system—it is defined as having a voltage angle of 0° and provides the balance of real and reactive power on the system. The 66 kV side of the transformer is assumed to have a fixed, uncontrolled voltage that is externally defined by the rest of the electric power system. The 66/12 kV transformer that feeds the UCI campus has a fixed turns ratio, so the low-side voltage will be a function of the transformer impedance, high-side voltage, and loading of the transformer. The transformer core magnetizing reactance is neglected, which allows the impedance model to be the resistive loss in series with the leakage reactance. This simplification is commonly used in power systems analyses except where a detailed analysis of the transformer is required (Fitzgerald, Kingsley et al. 2003). The differential equation for the transformer model is presented below, where v_{drop} is the per-unit voltage drop for the transformer, "i" is the current, and f is the line frequency in Hz.

$$v_{drop} = iR + \frac{X}{2\pi f}\frac{di}{dt} \qquad (1)$$

Each of the UCI Substation transformers have a 15 MVA rating. One has an impedance of 6.75% with an X/R ratio of 19.7 and the other has an impedance of 6.90% with an X/R ratio of 19.7.

2.2.2.2.2. Line

The primary distribution lines can be either overhead or underground and either in the wye-configuration or delta. The simplest model of a distribution line is a reactance (X) and resistance (R) in series, and typical values for the X/R impedance ratio are around 0.5 to 2. In general, the X/R ratio is higher for overhead lines and large underground lines, and lower for small underground lines as resistance becomes more significant. A more complex model adds a capacitance term between the line and ground, but in general this capacitance can be neglected for short lines of less than 80 km (Glover 2002). The short line approximation, which neglects the capacitance, is used for the distribution system model herein. The line model has the same differential equation as the transformer except that the X/R ratio is much closer to 1 and the impedance values will vary with the cable type.

2.2.2.2.3. Bus location

Each bus location may have up to three types of connections: load demand, power generation, and filter element. A load consumes real power and a generation source produces it. A filter element does not consume or generate real power on average. Two examples of a filter element could be an AC capacitor or a storage battery. There are no filter elements installed in the UCI campus and this connection is therefore not used. A bus location may also define a branch in the system and have no local connection. However, a physical structure that has no local building connection and no loaded branches is consolidated into a series element in the model and not identified as a bus location.

Even for a linear and balanced load, another characteristic is how the load reacts to deviations in frequency and voltage. As frequency deviation is not explored or varied, this aspect is not considered. However, new generation will modify load voltages, which will affect the loads. Most loads can be considered a combination of constant impedance and constant power loads (Willis 2004). For simplicity, all loads are considered to be constant power in this model and will draw the same power regardless of voltage at the input. This assumption is conservative from the perspective of checking for overvoltages—increasing the voltage for a constant power load will decrease the drawn current, which would exacerbate the voltage rise. Generation is also considered to be constant power, but this well represents the physical characteristics of power generation and grid-connected inverters.

2.2.2.3. Verification of Modeling Approach

For verification of the modeling approach, a sample 4-bus system is created with a base power of 10 MVA and a base voltage of 12 kV. Values for the line and load impedance are chosen to be arbitrary, but realistic. For simplicity of hand calculation, the loads are all assumed to be constant impedance with overhead distribution lines, which means capacitance can be neglected. The Matlab/Simulink™ model is then compared to the same 4-bus system in both PowerWorld, which is a conventional load-flow simulation program, and to hand calculations for the same bus. The comparison of bus voltages and angles are shown below in Table 5 and Table 6, and the close agreement between results of all three methods indicates that the Matlab/Simulink™ method is a valid way to simulate load flow in a three-phase power system. A comparison of line power flow shows similar agreement, and an additional comparison between Matlab/Simulink™ and PowerWorld for constant power loads is consistent, indicating that both constant power and impedance loads are represented realistically by the Matlab/Simulink™ model.

Table 5: Bus voltage comparisons in p.u.

	Theoretical	PowerWorld	Simulink
Bus 1	0.969	0.97	0.969
Bus 2	0.953	0.95	0.953
Bus 3	0.946	0.95	0.946

Table 6: Bus angle comparison

	Theoretical	PowerWorld	Simulink
Bus 1	-2.85°	-2.85°	-2.85°
Bus 2	-4.55°	-4.56°	-4.55°
Bus 3	-5.50°	-5.51°	-5.50°

2.2.2.4. Analysis Parameters

The output parameters of interest across the various studies include maximum/ minimum voltage and substation real/ reactive power input. The voltage extremes must be between the 0.98 to 1.05 p.u. boundaries set on the power system. Ideally, the voltages will be within a narrow band at the lower end of the acceptable range. This is because lower voltage will reduce the power requirement for constant current and constant impedance loads and indirectly provide an efficiency benefit. The real and reactive power should have an export/ import pattern that is more desirable than without DG. For real power, this is assumed to be within the confines of load-leveling: power import at heavy load is less than or equal to that without DG, and power import at light loads is greater than or equal to the nominal power on the circuit. Similar conditions are also applied to reactive power consumption, as it is assumed that this resource is added with switched capacitor banks. At present, one third of utility capacitor banks are fixed and the other two-thirds switched to meet changing load requirements. A reduced swing in the reactive power usage would reduce the number of switches and extend component lifetime. The reactive power usage should not extend outside of the range, as adding reactive power need would directly equate to an increase in infrastructure investment, and a reduced reactive power load might recede below the permanent demand met by the base 1/3 of non-switched capacitors. The basic comparison metrics are summarized in Table 7.

Table 7: Analysis metrics for comparing control strategies

	Model Citizen	Good Citizen	Poor Citizen
Voltage Max	Vmax < 1.05	Vmax ≤1.05	V > 1.05
Voltage Min	Vmin = 0.98	Vmin ≥ 0.98	V < 0.98
Real Power	Load leveling	Pdem ≤ Pdem, max	Pdem > Pdem, max
Reactive Power	Load leveling	Qdem ≤ Qdem, max	Qdem > Qdem, max

2.2.2.5. Model Evaluation

The model is evaluated by using the known loads and UC Main voltage as inputs to the simulation, then calculating the predicted transformer voltages and comparing these data to the measured voltage where available.

Due to the ION metering system, the real power, reactive power, and voltage for Natural Sciences 1 and 2 are known. These data are presented for a 24-hour interval in Figure 22. These parameters are not known for the third building on UC-8, Biological Sciences 3, but the load is

estimated to be 850 kW with a power factor of 0.85. This estimation is used because it is consistent with the size and function of the building, and allows excellent agreement between the model results and observed voltages. This comparison is presented in Figure 23, where the y-axis is the difference in voltage between the UC main and the distribution secondary. This metric is used because the input voltage to the system changes substantially throughout the interval. For both T126 and T127, the voltage difference is accurately predicted with the model, though the lack of measured information at Biological Sciences 3 precludes this from being a true model validation.

Figure 22: Data from UC-8 for real power (a), reactive power (b), and voltage (c)

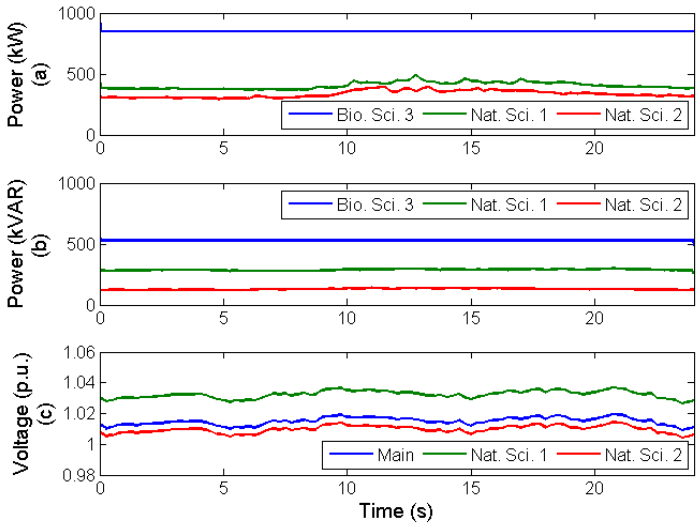

Figure 23: Comparison of model and measured voltage change between main substation and T126 and T127 for UC8 circuit

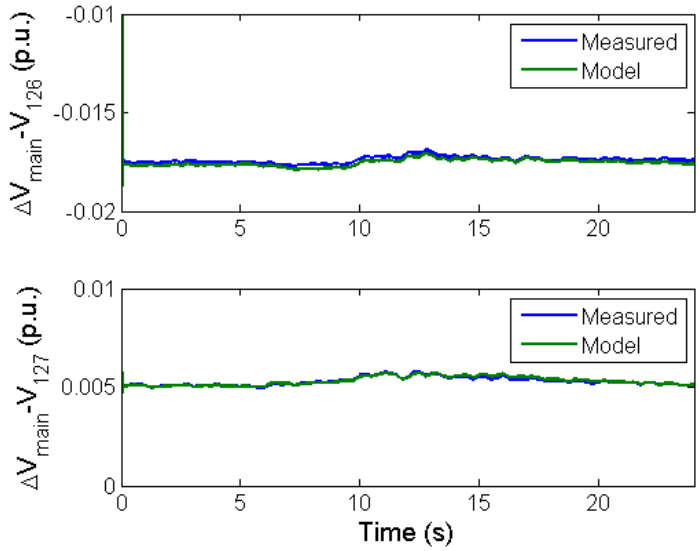

Circuit CP2-3 is more difficult to characterize than UC-8 because it has more loads, less ION monitoring, and a connection to CP2-2. All the loads on CP2-3 are connected to the ITRON system, but this only provides 1-hour interval data and no reactive power information. Also, the loads on CP2-2 will determine the voltage drop between the UC substation and the central plant, and these loads are not all included in the ITRON system. The best available real power information for the CP2-3 circuit is used along with an assumption of a 0.9 power factor. The net demand of all CP2-2 loads is estimated and included at the appropriate interconnection. Detailed information is available for MSTB, and the real and reactive power is presented in Figure 24 along with the measured main and local voltage.

Figure 24: Data for MSTB for load power (a) and voltage (b)

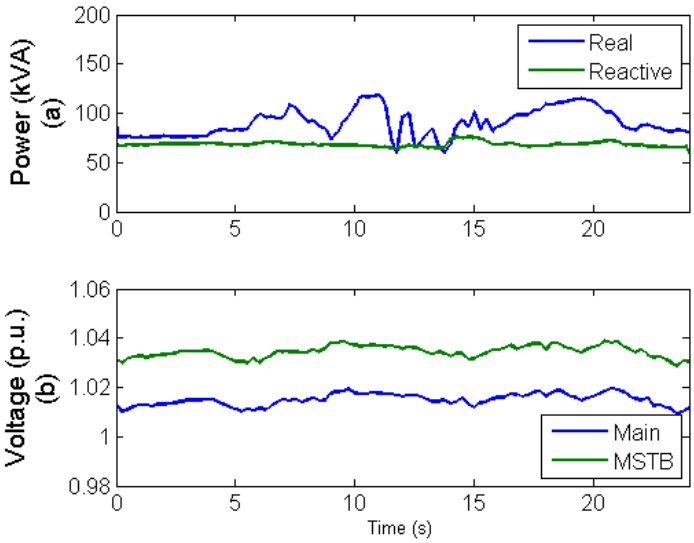

The comparison of model and measured voltage is presented in Figure 25 and does not exhibit the close agreement as for the UC-8 loads. This is likely to the high level of uncertainty of the CP2-3 and CP2-2 reactive power load data and lower data resolution for these loads. The input real power data from the other loads on the CP2-3 circuit are presented in Figure 26 along with the 15-minute interval real power data from MSTB located at T117. The sharp discontinuities in the MSTB data indicate the hour-interval power monitoring is an insufficient representation of the load dynamics and would cause the smoothing of the voltage profile for the model result versus the measured one that was noted in Figure 25. This result indicates that at a minimum, 15-minute ITRON data should be used in future.

Figure 25: Comparison of model and measured voltage change between main substation and T117 for CP2-3 circuit

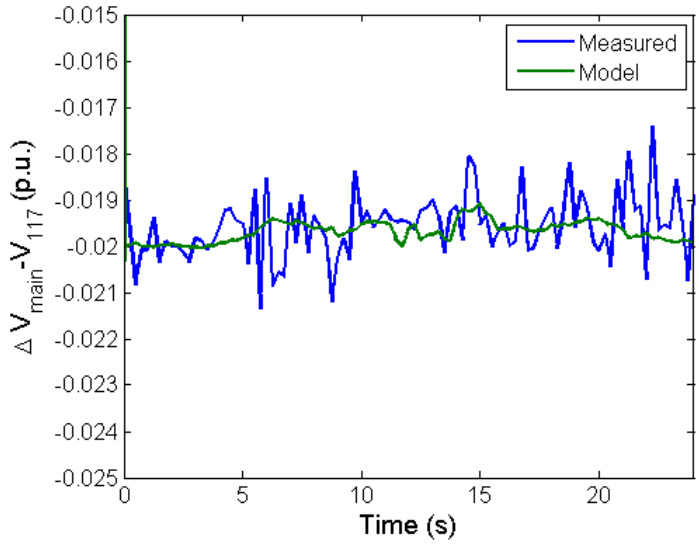

Figure 26: Model input power demand for the six transformers on circuit CP2-3

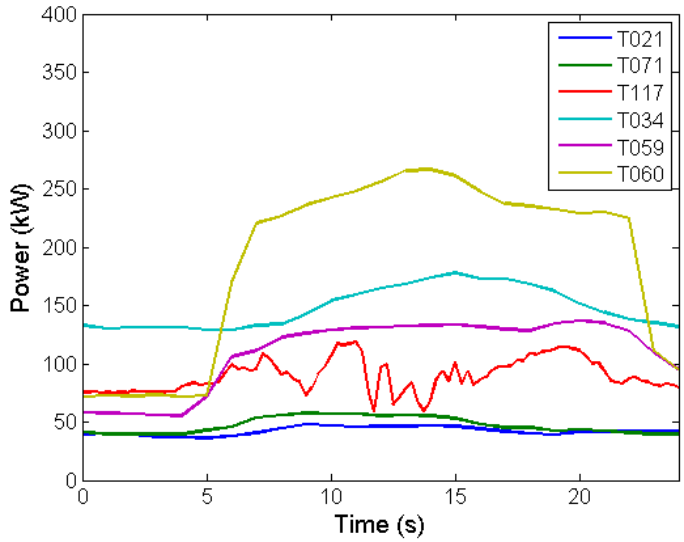

While the existing monitoring is insufficient to fully validate and populate the UCI circuit model, the available results are sufficiently promising to allow an exploration of alternate scenarios with different generation installations, and alternative circuit layouts.

Task 2.2.3. Capacity of the Existing UCI Infrastructure

The electric capacity of a distribution circuit must be assessed in several locations. The UC Substation is fed from a single SCE source through two 15 MVA transformers. Thus the first capacity concern is that the balance of electricity at the UCI transformers is within the allowable thermal limits. Next, the ten 12-kV circuits radiating from the substation each have a 720 A breaker and limitation on their maximum loading. Then finally, the individual transformer at

the load location must be capable of importing/exporting power between the primary distribution circuits and the building level.

This section is mainly focused on the thermal capacity of the components, which is the maximum power/current they can transfer without overheating. Concerns on limitations of voltage rise and voltage drop are addressed separately.

2.2.3.1. Substation

The UC Substation is the only connection between the UCI campus electric infrastructure and the rest of the electric power system. Thus the two 66/12 kV transformers located at the substation transfer the balance of power generation and loads/losses to the campus from SCE. This capacity analysis must take into account that the two transformers cannot be connected in parallel. Thus when assessing the campus while both transformers are loaded, each transformer must be analyzed separately. Transformer 1 feeds Capacitor Bank 1 and circuits UC-1 to UC-5; Transformer 2 feeds Capacitor Bank 2 and circuits UC-6 to UC-10.

When the gas turbine is in service and producing power, the gas turbine significantly reduces the amount of power through the substation. However, for reliability, the campus must be able to meet the whole campus load in case the turbine trips off-line. When the gas turbine is not producing power, both transformers are required to support the electric needs of the campus. When both transformers are connected, the entire UCI electric system is split into two based on the source transformer. Thus the sum of load on circuits UC-1 to UC-5 must be less than 15 MVA and the sum of load on circuits UC-6 to UC-10 must be less than 15 MVA. Ideally, these circuit pairs should be balanced to maximize the overall capacity of the campus. If a substantial unbalance is observed, portions of the distribution feeders should be transferred to balance the loading on each transformer. Load balancing would also decrease the load-losses of the two substation transformers.

Having significant generation capacity, the campus generation capacity is limited by the SCE requirement that the campus import 1 MW of electricity at all times from the substation. Due to the thermal energy storage tank, offsetting daytime chiller loads, the campus could actually export power during peak power periods. Additionally, the campus could potentially install additional equipment to further support utility grid operation. Such concepts are the subject of work in distributed energy resource analysis in other tasks.

2.2.3.2. Distribution feeder circuits

The capacity of the distribution feeder circuits will vary based on the type and size of conductor used in each section of the campus. The most common conductor used for the main UCI campus feeder circuits is 500 kcmil copper conductor triplexed in an underground non-metallic duct. The exact ampacity (current carrying capacity) will vary due to the local thermal resistivity and load factor, but is approximately 300-400 amperes per phase (IEEE Std. 835-1994). Some feeders are composed of two sets of conductors, such as the span between the UC Substation and the central plant for UC-1 and UC-6, and the UC Substation and East Substation for UC-9. This would increase the overall ampacity to 500-600 amperes per phase. While the existing load of all the feeders is unknown without further monitoring, the current in UC-9

generally ranges from 175 to 300 amperes per phase, which is significantly below the 500-600 ampere capacity for this feeder. After the East Substation, UC-9 separates into 2 major and three minor sub-circuits. A snapshot of this division is 85 A, 95 A, and 40/15/15 A for an input of 250 A. Thus the UC-9 feeder has plenty of spare capacity for additional loading in general and it is expected that the other major feeder circuits would have similar available capacity. In addition, two new circuits were recently brought into service to accommodate additional load growth in two areas of the campus: health sciences and biological/physical sciences.

The electric capacity of the UCI infrastructure will be affected differently by the addition of generation versus increased loading, yet the flexibility inherent in the design of the existing system can facilitate both types of expansion. Smaller DG installations, such as rooftop solar PV, will primarily offset local electric usage and increase the available thermal capacity of the infrastructure by reducing power flow. However, because it is not guaranteed that the DG is operating, the generation capacity typically does not offset the design capacity required from the distribution circuit. For example, solar is primarily coincident with load. However, large evening loads can be observed when the distributed solar generation is low. Hence, the capacity of the distribution circuit must be maintained, despite installation of the solar generation.

Increased electricity demand will reduce the available thermal capacity by increasing power flow. Yet the ability of most transformers to connect to two feeder circuits and the use of switches connecting the feeder circuits could allow a vast number of circuit reconfigurations. The flexibility in the circuit layout can help to avoid localized constrained sections of the feeder by moving transformers from heavily loaded portions to less heavily loaded ones in the case of excess load; and moving transformers onto lightly loaded circuit sections for the case of excess generation. Larger DG, such as the central plant generator, will cause a reversal of power flow and as a result the circuit feeder must be sized to accommodate this additional capacity.

2.2.3.3. Building secondary distribution transformers

Just as the substation transformers are a choke point between UCI campus and the regional electric power system, each secondary transformer is a limitation between the low voltage building load distribution system and the 12 kV UCI power system. Some buildings are served by multiple transformers—where low voltage loads could be shifted from one transformer to another—but the majority of buildings do not have such flexibility. However, one advantage of the secondary transformers over the UC Substation is that there are no explicit import/export requirements. Thus the allowable loading on any individual transformer could vary from rated load consumption to rated load generation. In aggregate, the campus must still meet the importation agreement, but having the distribution system behind a single utility meter allows flexibility in separating load consumption and generation.

As with the 12 kV distribution circuits, small amounts of generation will offset load locally and tend to increase the available capacity of a transformer. Large amounts of DG could exceed the local load demand and export real power, which is still constrained by the maximum transformer rating. Additional load would be subject to constraints on the transformer size and existing load, as it will tend to increase the transformer current.

The distribution transformers do not have the same flexibility as the 12 kV circuits for reconfiguration, but there are some mitigating measures available to improve capacity constraints. One is to implement power factor correction and/or harmonics compensation, which could maximize the real power capacity of the transformer by supplying the reactive power locally and/or reducing harmonics-based de-rating of the transformer. In addition, while moving a distribution transformer is a complicated undertaking, in theory a heavily loaded low capacity transformer could be swapped with a lightly loaded high capacity transformer. However, at some point an additional transformer or a transformer upgrade may be unavoidable for meeting campus electric scenario goals.

2.2.3.4. Campus growth and flexibility

The history and vision of the UCI electric service have already led to a power system that is as flexible for modifications as could be reasonably expected. The emphasis on reliability for campus buildings has led most transformers to have two circuit sources that can easily shift load. The circuits themselves are reconfigurable through existing switches that were installed to meet various stages of the campus growth. In addition, the utility tunnel provides convenient access to re-conductor critical circuits for increased capacity or to use high speed hard-wired fiber optic communications strategies in future. At present, most 12 kV circuit feeders appear to have considerable available capacity as well. There are also no exportation limitations for distribution transformers, which would significantly increase the local capacity constraints on DG. The flexibility elsewhere in the system may improve capacity challenges on the distribution and substation transformers, but these locations are not inherently suited to direct modification.

Task 2.2.4. Cost and Performance of Infrastructure Improvements

An integral part of enabling renewables and lowering cost is increasing the flexibility of current equipment, as has been discussed herein and will be further discussed in many of the sections. This section explores the cost and potential performance improvements for three main infrastructure improvement options: campus metering, electricity export allowance and islanding.

2.2.4.1. Campus Metering

Installing power metering equipment at key locations on campus, beyond the current infrastructure, has many benefits the students, faculty and staff using campus services as well as for campus operations. Sufficient metering on campus would allow facilities management to know how power is flowing across campus at all times. This can result in overall system improvements for how the loads are distributed between circuits as well as for improving fault detection and correction efficiency. This would also provide the ability for facilities management to more completely engage in intra-campus electrical billing, in which each group is billed for the electricity they consume. This would allow the campus to operate more sustainably as each group is appropriately charged based on their use and would motivate energy consciousness within each group.

To support this goal the university has submitted a request for quotation to supply 100 meters with revenue grade abilities or better to the campus. Additionally, the data should be stored

and the payment scheme will reflect a monthly fee for the period of five years with the capability to continue a service contract if desired.

The infrastructure of UC Irvine's Main Campus already provides vital support for research, administration, education, services, housing, entertainment, and recreation. With well over a hundred buildings and a student body of over 27,000 providing utilities of electricity, hot and cold water for this campus is quite challenging. The campus has at its disposal a multi-megawatt gas turbine and steam turbine central plant that also provides the hot and cold water for the campus, a large chilled water storage tank, nearly 900 kW of installed photovoltaic panels, and planned capacity for concentrated solar photovoltaic panels, and a FuelCell Energy 300kW fuel cell with an absorption chiller. These resources establish UC Irvine as a 'field laboratory' and test bed for research, alternative distributed energy technologies, and electricity generation and conservation. The UC Irvine campus is developing initiatives to both reduce operating costs and their carbon footprint. Meeting the goals associated with these initiatives is a challenge, but an essential first step is enabling a reliable system for determining how energy is used so that savings can be identified and progress tracked. In addition, this information can empower faculty, students and staff to understand their energy usage patterns.

At present, the UC Irvine Main Campus metering infrastructure is a collection of equipment and communications that was purchased as each building was completed and commissioned. Some of this equipment is working while others are not communicating with the campus' energy management software. There is no automatic notification for when or why an older meter loses communication. As a result, only approximately 28 of the 103 electrical meters and even fewer hot and cold water meters on campus are actively communicating data. Of the non-communicative meters, much of the legacy installation settings have been lost and reconnection is not simple.

The goal is to create a robust network of meters and communication that will (1) meet the needs of UCI Facilities in tracking energy and peak power usage, (2) allow for routine analyses of high voltage infrastructure effectiveness, (3) inform active campus research in smart grid technologies and energy integration, and (4) educate the campus community in both how their university is managing electric and thermal demands and how they can help. The data acquisition system functions automatically and also provides alerts when intervention is required to reconnect a non-communicative meter, replace a battery, or reset a system data server. The data collection software is flexible enough to connect a wide variety of meters—including future meter upgrades, existing up-to-date meters, and legacy meters until they are upgraded.

Requirements on the monitoring of this infrastructure include:

1. Ability for sub-metering and billing of individual campus facilities
2. Ability for tracking energy usage and quantifying conservation measures
3. Monitoring power flow on primary and understanding desired circuit re-configurations

4. Monitoring to increase campus electric reliability by detecting capacity overloads, overvoltages, power quality problems, and other infrastructure challenges

At present, the campus electric infrastructure is a combination of upgraded and legacy meters that communicate with two different pieces of energy monitoring software (i.e., ITRON EEM and ION). The legacy meters do not measure reactive power, or power factor; thus require upgrades. Additionally, many of the meters independent of their capability are not communicating with energy monitoring software. All meters, either not communicating or communicating to the ITRON EEM software must be transitioned to the ION EEM software, which was selected by the campus as the preferred solution. There are currently 137 transformers on campus and 103 meters installed of which around 30 are updated meters and the remainders are legacy. Table 8 summarizes the current status of UCIFL meters.

Table 8: Current Status of Campus Metering

Electric Meter Status	Updated type	Legacy type	Unknown	Total
Communicating	13 (ITRON) 8 (ION)	7 (ITRON)	-	28
Not communicating	9	58	8	75
Total	30 meters	65 meters	8 meters	103 meters

To adequately instrument the campus 118 meters will be needed. That includes 30 updated meters, 21 of which are communicating properly. The remaining 88 meters include substation meters, single building transformer meters and aggregated housing community meters. The figure below summarizes these numbers.

The provision of cold and hot water for buildings is the primary concern for the campus' central plant since the difference in electricity can be imported from the local electricity provider, Southern California Edison. Additionally, providing cold and hot water represents one of the major loads for each building. Though, there are relatively few installations of cold and hot water metering, many of which need to be calibrated now, the campus is investing in new meters. Table 9 summarizes the UCIFL water meter status:

Table 9: Water Meter Status

Water Meter Status	Cold water type	Hot water type	Total Meters
Total	29 meters	28 meters	57 meters

2.2.4.1.1. Category Approach

An ideal monitoring solution is a complete suite of meters and data that are easily accessible to inform and educate on the electric power usage on campus in both assessing the low voltage

power usage internal to individual buildings and the underground high voltage electric infrastructure.

The pursuit of this goal is divided into three categories. Each category is designed to build upon and learn from the previous category, in addition to expanding the capability and providing incremental benefits to the campus. Through the course of this project all three categories will be addressed. Category 1 is designed to provide information on the biggest and highest priority campus electrical loads along with facilities already sub-metered for the sake of billing. If a meter with any chance of campus electricity sub-billing is upgraded, it should be of revenue-grade accuracy at a minimum. It is expected that this additional capability will add little to no cost to the meter, but will increase the future flexibility of the infrastructure.

Category 2 involves installing upgraded meters on most of the transformers on campus and meters to aggregate the campus housing communities. The second category of the advanced monitoring infrastructure is to proceed with upgrading meters at buildings throughout the campus. This will include a meter at many transformers as well as one for feeder circuits leaving the central plant and the east substation. In addition to enabling a more thorough understanding of the demand usage of buildings on the campus, this level of monitoring will complement Category 1 equipment and enable real-time visualization of the power flows on the high voltage (12 kV) electric infrastructure. Such visualization will help to understand the relative line loading, detect high loss circuits, and further support the initiatives for the proposed work.

Category 3 develops portable monitoring capabilities for building load sub-metering, to break out the constituent loads, and high resolution electrical data for measurement of waveforms and capture of signal harmonics. The third category provides insight by sub-metering individual buildings off of a transformer, or even individual loads as desired, such as individual chillers or building equipment. The third category also includes a power quality test bed to both detect events, such as sags and swells, and provide power quality information to the field laboratory to analyze potential issues that may arise on fast timescales and available mitigation strategies.

The approach for all three categories is presented in Figure 27.

Figure 27: Comparison of model and measured voltage change between main substation and T117 for CP2-3 circuit

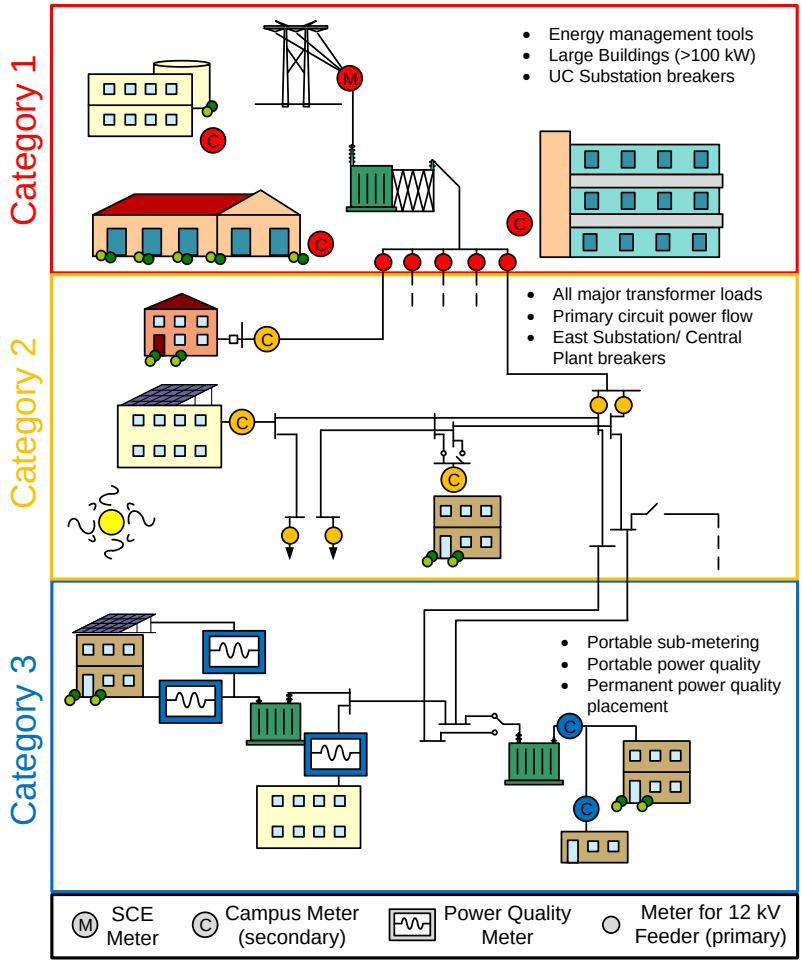

Category 1

1.1: Upgrading and connecting meters on high load (100 kW+) and high priority buildings

1.2: Commissioning and connecting of existing upgraded meters

1.3: Upgrade meters on UC Substation breakers

1.4: Determining optimal data collection suite for real-time data

Addressing the Category 1 activities will result in an 8.49MW increase in monitored power; including monitoring of the substation circuit breakers, which are critical for understanding power flow on campus. A portion of the load is already communicating to the campus energy management software. There is another portion that has upgraded electric meters but is not connected to the software. By establishing communications between those meters and the energy management software, 1.87MW can be monitored at a much lower cost than purchasing new meters and installing them. The campus has installed 28 updated meters and is currently

installing 10 more as well as 5 hot and 5 cold water meters on campus to contribute to the existing water metering infrastructure. Upgrading meters in buildings with loads greater than 100kW represents the remainder of demand captured in Category 1. Table 10 summarizes the findings for Category 1.

Table 10: Category 1 Summary

Category 1	Accounted power (MW)	Meter upgrades	ION Connections	CT/PT Installation
Updated and communicating	3.23	0	25	0
Upgrade to IONe Connection	1.87	0	13	0
100 kW+ building meter upgrade	3.39	18	18	5
UC Breakers	All	7	7	7
Total	8.49	30	68	12

Installing Category 1 metering infrastructure will account for 57% of the total power requirement for UC Irvine, of which 34% comes from connecting the currently installed updated meters to the new energy management suite. The remaining 23% will come from installing updated meters at buildings with over 100kW of load as shown in the figure below.

Figure 28: Category 1 Power Metering

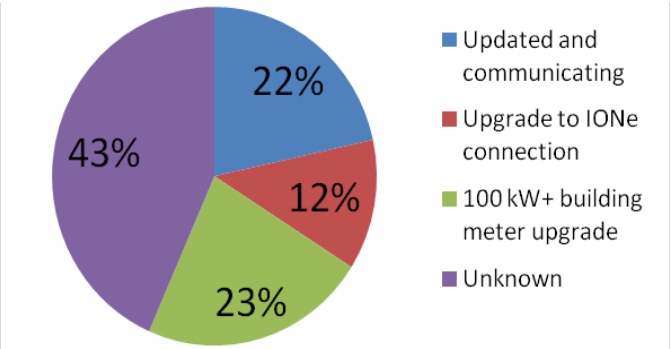

Category 2

2.1: Complete metering of nearly all transformers on campus

2.2: Install meters on central plant and east substation breakers

2.3: Meter aggregate on-campus housing loads

Addressing the Category 2 activities will result in a 5.41MW increase in monitored power. Nearly equal contributions to the accounted electrical power are provided from upgrading existing meters while using the same CT/PTs and aggregating the load from housing community transformers thereby reducing the number of meter installations required from 26 to 59. Table 11 summarizes the findings for Category 2.

Table 11: Category 2 Summary

Category 2	Accounted power (MW)	Meter upgrades	ION Connections	CT/PT Installation
Upgrade meters with CTs/PTs	2.75	38	38	0
Aggregate housing	2.66	5	5	5
CP/ES Breakers	UC-1, 6 & 9	12	12	12
Total	5.41	55	55	17

Similar to Category 1, installing meters for Category 2 further reduces the unknown load on campus from 43% following Category 1 to 7%. Eighteen percent comes from installing updated meters where there are already CTs/PTs installed with legacy meters. This reduces the cost of the installation and targets important buildings where meters were already installed. The final 18% comes from aggregating the housing community loads and installing one meter per community. Twenty-six meters would be required to instrument each transformer of the housing communities but by monitoring the main power line supplying the community the same amount of electricity can be monitored with only five meters. The breakdown is depicted in the figure below.

Figure 29: Category 2 Power Metering

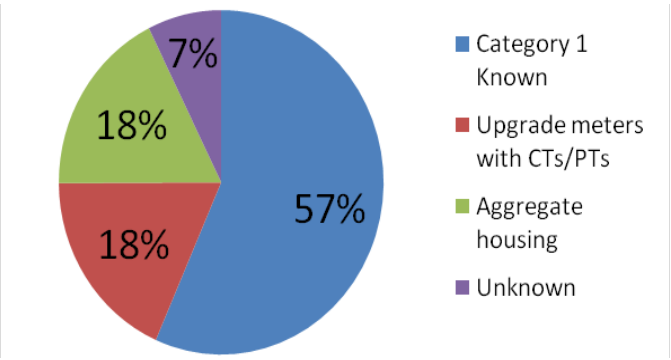

Category 3

3.1: Implement use of portable sub-metering equipment for relevant building loads

3.2: Implement use of portable power quality meters as necessary for other loads.

3.3: Install permanent power quality test bed at select locations such as substations, data servers, and UCI central plant.

Completing Category 3 activities will provide valuable information about the power quality and reliability of the system. Information provided form pursuing Category 3 cannot be derived from the typical building meters in Categories 1 and 2 and represents the other half of the picture of the effect from installing renewables onto a micro-grid such as UC Irvine. The

campus currently owns two sub-metering systems that are currently being used to compare the operation of two buildings. Providing another one of these systems for use on this project represents a key capability that can be used for dissecting the constituent components of a load signal, helping to target potential issues. The second element of Category 3 involves understanding the power quality of circuits on campus. With four portable power quality meters, the campus will have the ability to simultaneously monitor multiple locations to assess the health of the circuit. Additionally, with portable meters we will have the flexibility to move these meters to different locations, thereby maximizing the efficacy of the investment.

Once fulfilled the request for quotation for metering infrastructure at UC Irvine will be able to meet Category 1 and Category 2 requirements and provide real-time visualization of greater than 90% of campus loads. Addressing all three categories adds to the campus resource by providing additional capability to further support a micro-grid and to enable a more complete understanding of the effects of high penetrations of renewables on the system.

2.2.4.2. Electricity Export Allowance

While the campus infrastructure is reasonably flexible, allowing for shifting of load between building transformers and from circuit to circuit on campus using existing switches, the interconnection with the utility does not allow exportation. Moving to an interconnection agreement that allows for accidental export would increase the flexibility of the campus, by removing one of the constraints on the campus' central plant operators.

In an effort to enable electricity export from the campus, the university is planning to replace the switching equipment at the substation. $250,000 has already been paid to Southern California Edison and there are plans to spend an additional $300,000 for the required switching equipment and rental of generators to support the campus while the transition occurs. The backup generation is required to provide electricity to the critical loads on campus (e.g., research samples requiring specific environmental control).

2.2.4.3. Campus Islanding

Another technique to increase the campus' flexibility is to provide islanding capability. If the grid goes offline but the campus generator is operating it would be possible to maintain operation; however, if the grid goes offline and the campus generator is also shutdown, to restart that generator would take an additional generator capable of shouldering the load required to start the campus generator and support bringing the campus circuit's back online. This generator and the accompanying equipment to allow the campus grid to safely operate in island mode would cost significantly more than the substation retrofit required to allow export. Though a cost analysis of converting the campus to a standalone grid was not performed the tradeoff is between the additional requirement for equipment and the cost to operate and maintain the current backup diesel generators, which are located throughout the campus in key locations that serve critical loads.

Task 2.2.5. Conclusions

- Assessed the infrastructure supporting the electric system at UCI and collected data from available monitoring equipment
- Model was developed and verified for UCI distribution system

Task 2.2.6. References

Fitzgerald, A. E., J. Charles Kingsley, et al. (2003). Electric Machinery. New York, NY, McGraw Hill.

Glover, J. D. and M. S. Sarma (2002). Power System Analysis and Design. Pacific Grove, CA, Brooks/Cole.

Grigsby, L. L. (2007). Electric Power Generation, Transmission, and Distribution. New York, NY, CRC Press.

IEEE Std 835-1994 (1994). IEEE Standard Power Cable Ampacity Tables. IEEE Power Engineering Society, Insulated Conductors Committee. New York, NY, Institute of Electrical and Electronics Engineers.

Power Engineering Services Incorporated (2009). Arc Flash Hazard Study Report, for University of California, Irvine, PES Reference #: 4141-1.

Willis, H. L. (2004). Power distribution planning reference book. New York, NY, Marcel Dekker, Inc.

Task 2.3. Interconnection of DER on UCI Distribution Circuit

In the RESCO vision three key changes will impact the electrical power distribution system:

- Addition of distributed generation
- Electrification of the transportation sector
- Electrification of building heating and cooling

Each of these modifications may affect the distribution circuit infrastructure in different ways. Adding distributed generation will create electricity sources in the field and invalidate the previous assumption of uni-directional power flow from substation to customer. This is particularly true for cases where reversed power flow may cause overvoltages, or where disproportional amounts of real and reactive power could overload lines and reduce efficiency. Such problems have been extensively documented in the general case in (Auld, 2009; NREL/GE 2003). Increasing the electrification of transportation and heating/cooling sectors will add to the load on the system and could require capacity upgrades or load shifting between circuits. In

some cases, the distribution system may have to be retrofitted to accommodate the evolution to a renewable-based energy secure community.

Depending on site-specific installation, both operational changes and capacity upgrades could be required to support these advancements in renewable power generation and increased electrification while maintaining the goal of a safe, reliable, and high quality electric power service. These concerns are addressed on the UCI electric circuit infrastructure by first garnering an understanding of the campus electric service and then developing and evaluating a dynamic model that captures the key characteristics. A variety of RESCO scenarios can then be applied to the model and the appropriateness of the existing infrastructure and proposed modifications are then quantified and compared.

The recent history of the UCI campus electric system and current development of the campus electric model are described along with the model verification to-date. In addition, cases regarding the sensitivity of the UCI electric service to increased penetration of on-site solar PV, fuel cell, and turbine generator have been conducted and are described in detail herein.

Task 2.3.1. Impact of Increased Distributed Generation on Circuit Operating Characteristics

The following DG cases are explored: no PV, 300 kW MCFC, high renewable, and an additional combustion generator. In addition, all cases are analyzed with the same DER behavior and the formation of UC-8 and CP2-3 into a loop. The no PV case simulates the circuit behavior without the four existing PV arrays. The PV output is added to the measured load to give the actual electric power demand for the corresponding transformers. The 300 kW MCFC case simulates the installation of a fuel cell at the MSTB transformer as is planned for the near future. The high renewable case simulates all existing PV arrays increased to 5x capacity and the 300 kW MCFC installation. The generation at each bus for the high renewable scenario is presented in Figure 30. The additional combustion generator scenario adds a 10 MW power generation at the 12 kV side of the UC substation. This expansion is planned to be connected through the future UC-7 circuit, which would connect directly to the UC substation, and therefore has the equivalent effect on UC-8 and CP2-3 as injecting this real power directly at the substation bus as is modeled. The loop circuit scenarios examine all of these DER situations with the old connection between CP2-3 and UC-8 closed to form a loop. The impedance of this loop link branch is the same as the old cable connecting the two buses. All other DG scenarios are explored in the loop circuit configuration and compared to the standard radial configuration.

Figure 30: DG power at each bus for the high renewable UCI circuit scenario

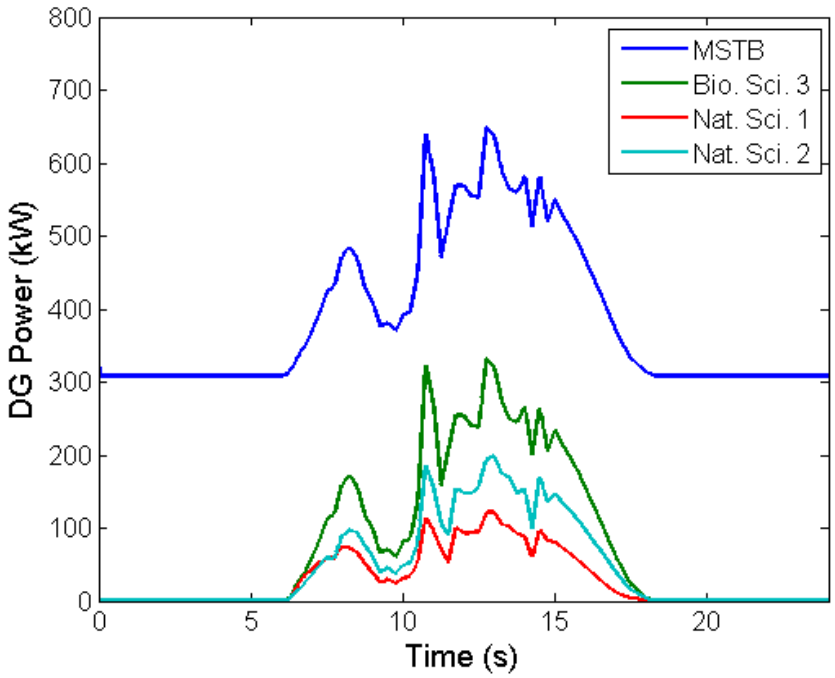

The voltage at each of the three transformers on the ION network is modeled for each electric scenario and presented in Figure 31, Figure 32, and Figure 33 for T117, T126, and T127 respectively. Similar voltage profiles can be obtained for the other system buses, but the turns-ratio of the distribution transformer—and hence actual secondary voltage—is only known for these three locations. These three transformers also represent three of the four DG sites on the focus circuits (excluding the central plant generator case). Overall, the various DG and electric service scenarios do not dramatically affect the voltage at each transformer. In all cases the new voltages are still well within the allowable limits of 0.98 to 1.05 p.u. For all locations, the no DG case decreases the voltage slightly during the midday time when PV produces electricity. Adding a 300 kW MCFC to the MSTB location on CP2-3 consistently raises the voltage of this bus, but does not noticeably affect the voltage at the other transformers over on UC-8. The high renewable case raises the voltage slightly over the 300 kW MCFC case at midday when the PV generation would be increased. When an additional generator is added at central plant, the voltage throughout the system is uniformly increased because this bulk power transfer across the substation 66/12 kV transformers will raise the input voltage at the UC Substation. It is assumed that the two generator scenario would still utilize a single substation transformer, even though the existing connections are set up solely to prevent export. Of course adding another generator would cause power exportation to the rest of the electric power system and may cause this decision to be reconsidered.

Figure 31: Voltage at T117 (MSTB) for alternate electric service scenarios

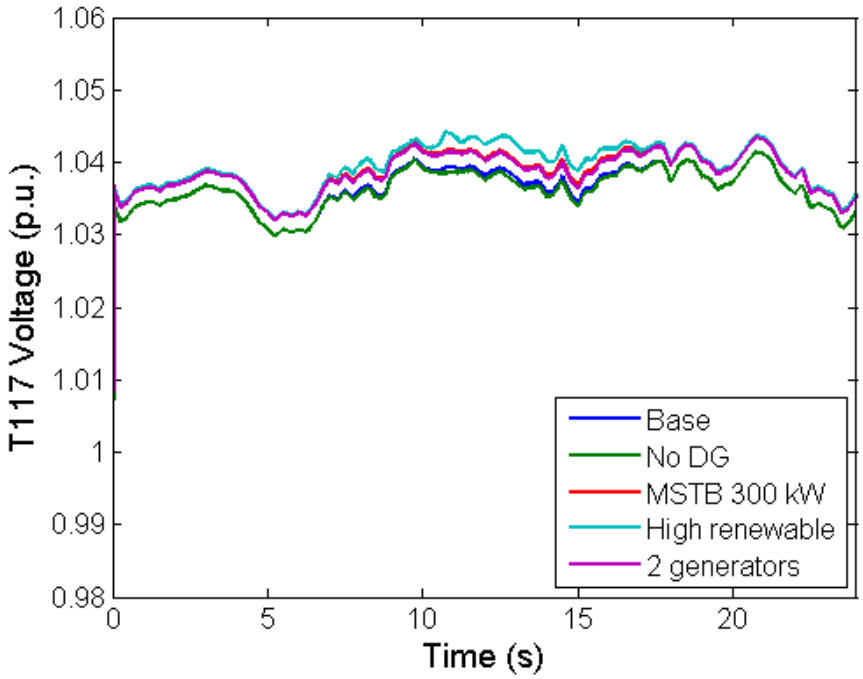

Figure 32: Voltage at T126 (Natural Sciences 1) for alternate electric service scenarios

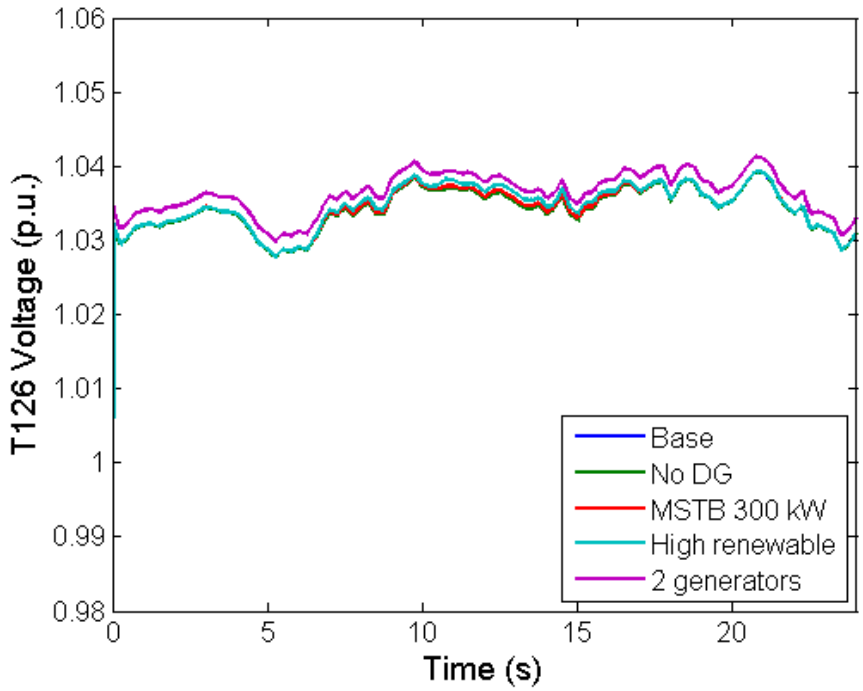

Figure 33: Voltage at T127 (Natural Sciences 2) for alternate electric service scenarios

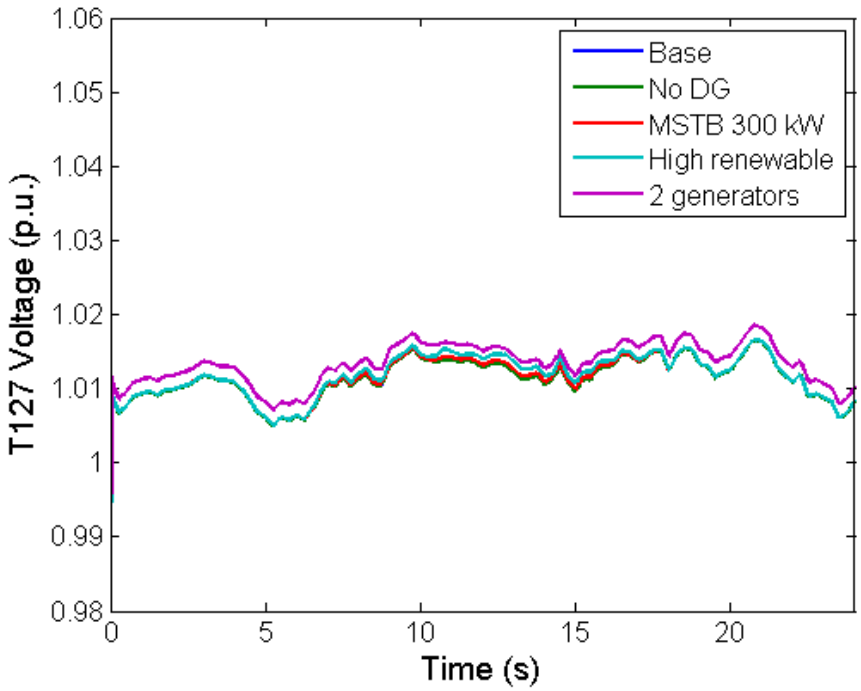

The real and reactive power flows from the substation are presented in Figure 34 and Figure 35. As expected, the addition of a constant generator as either fuel cell or combustion turbine uniformly decreases the real power importation, while increasing the PV generation only reduces the import at midday. It is assumed that all of these generation technologies operate at a power factor of one, so the only noticeable change in the reactive power is for the two combustion turbine scenario—for this case, the increased real power export through the transformer results in a higher overall reactive power demand.

Figure 34: Real power import for alternate electric service scenarios

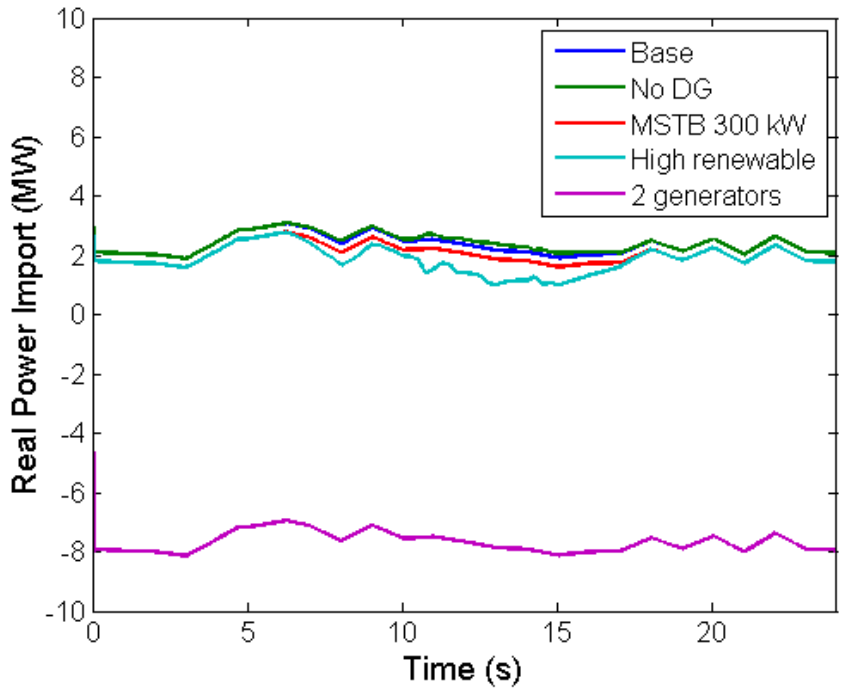

Figure 35: Reactive power import for alternate electric service scenarios

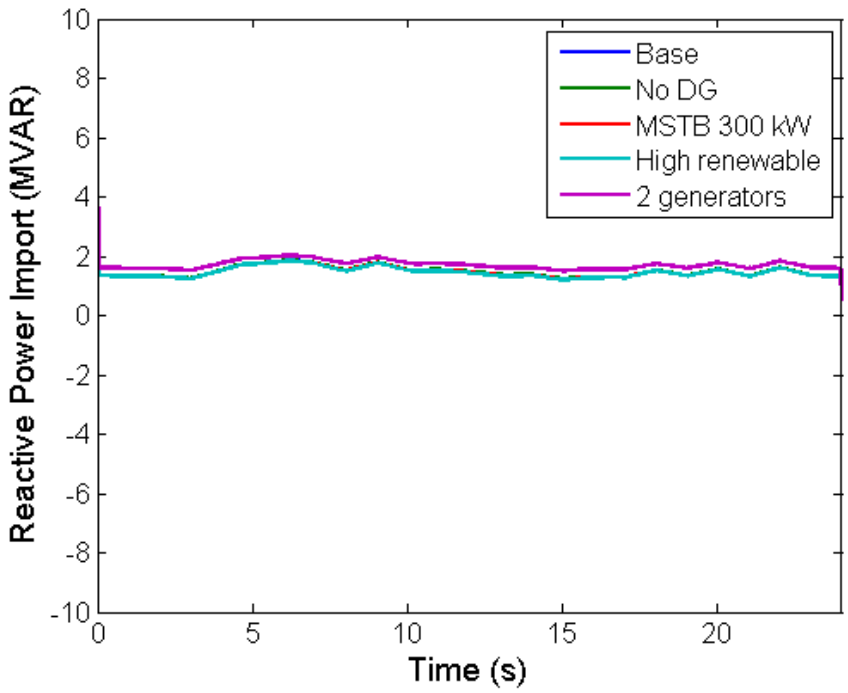

The addition of a 300 kW MCFC at the MSTB location causes a power reversal in the primary circuit connecting bus 1 to bus 4 on circuit CP2-3. This effect is presented in Figure 36, where the

base case is identical to that with 2 generators as the additional substation power flow does not affect the power flow on CP2-3. As expected, the subtraction of the existing generation increases the power flow to MSTB and Croul Hall, while the addition of generation reverses the power flow and causes it to be negative—meaning power flows from MSTB and Croul Hall to the rest of CP2-3. This effect is especially pronounced when the fuel cell is joined by more extensive solar PV. Still, as was previously observed, none of these cases cause undesirable voltage profiles, and the absolute power flow magnitude is reduced, which could lead to an efficiency benefit.

Figure 36: Power flow from bus 1 to 4 on CP2-3

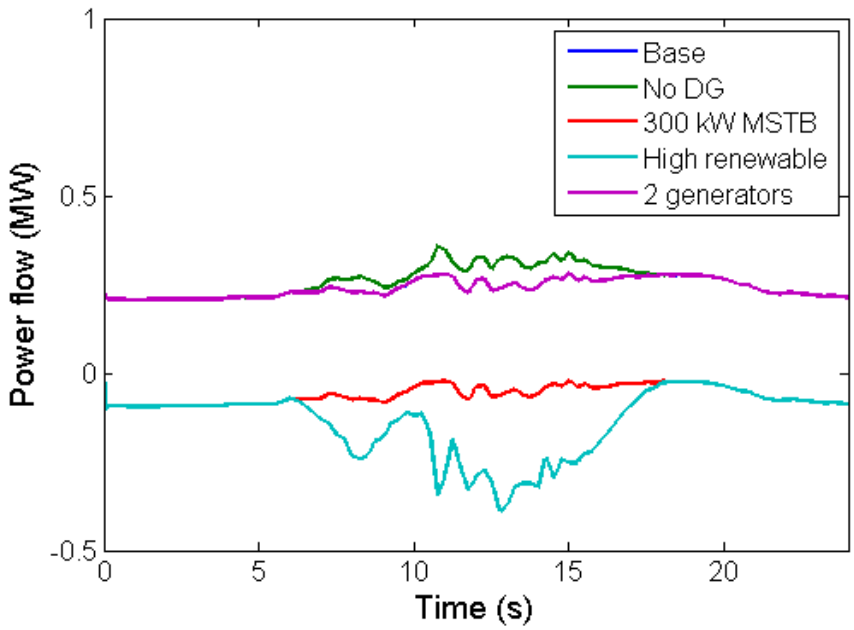

The efficiency of these circuits is presented in Figure 37. As before, the efficiency parameter is only concerned with the efficient local utilization of power and does not consider losses before the substation or beyond the building secondary transformer. The addition of DG as either fuel cell or solar PV tends to increase the efficiency due to the dispersed generation sources. The high renewable case has the most dramatic efficiency improvement, while the addition of a 300 kW MCFC is only marginal. This is likely because the solar PV power at the UC-8 loads is all consumed on the transformer secondary, while the excess from the 300 kW fuel cell has an efficiency penalty associated with travelling through the transformer, onto the primary, and then back to a neighboring secondary load. The worst efficiency is observed for the case with an additional 10 MW generator. As seen in the substation power flow from Figure 36, this case exhibits a high magnitude, reversed real power flow. This efficiency drop could probably be improved by adding an overall power factor correction function to the new generator so that the power leaves the campus at a power factor of 1. The simulation assumes that the new generator operates at a local power factor of 1 and neither produces nor consumes reactive power.

Figure 37: Efficiency for alternate electric service scenarios

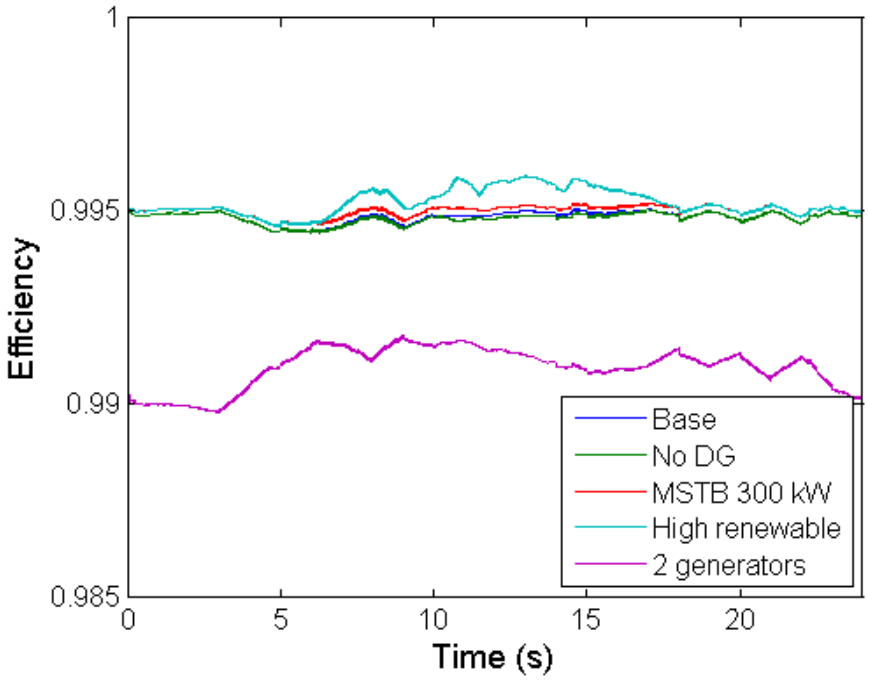

When UC-8 and CP2-3 are connected into a loop, the voltage effect varies based on the original feeder circuit. Because this link causes additional power to flow on UC-8 and back feed parts of CP2-3, the voltage is raised at T117 on CP2-3 and lowered on T126 and T127, which were previously on UC-8.

Figure 38: Voltage at T117 (MSTB) for alternate electric service scenarios (loop)

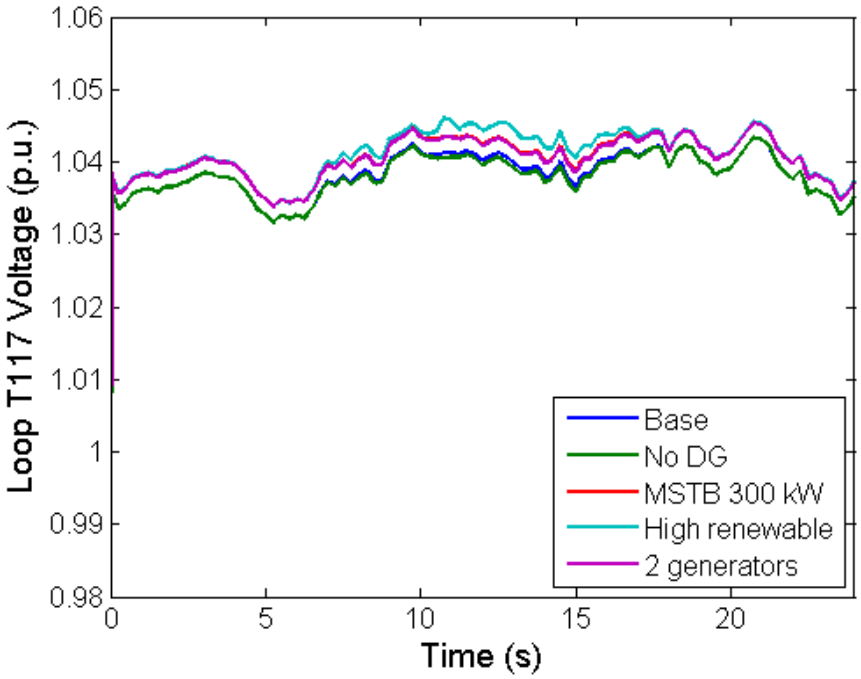

Figure 39: Voltage at T126 (Natural Sciences 1) for alternate electric service scenarios (loop)

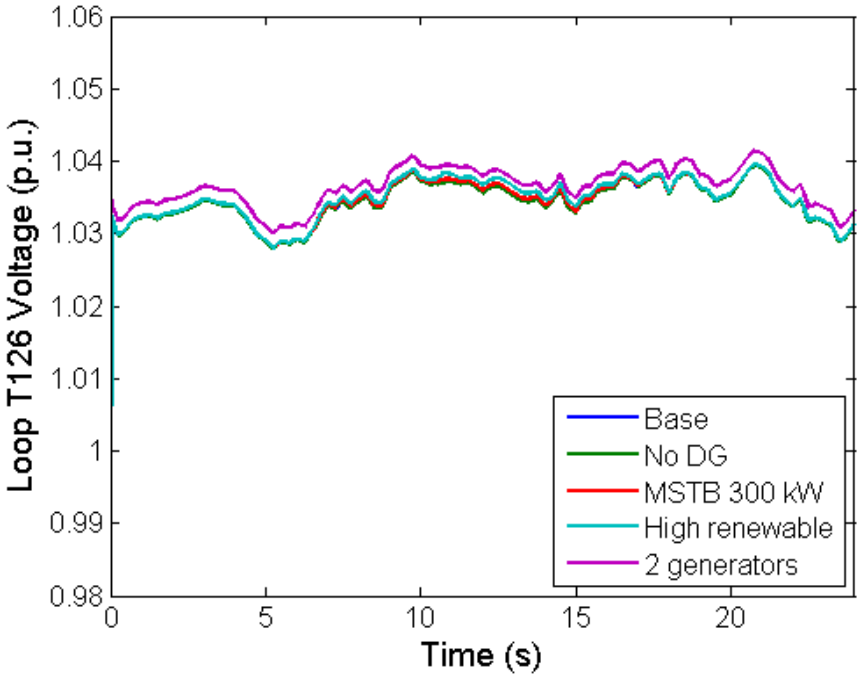

Figure 40: Voltage at T127 (Natural Sciences 2) for alternate electric service scenarios (loop)

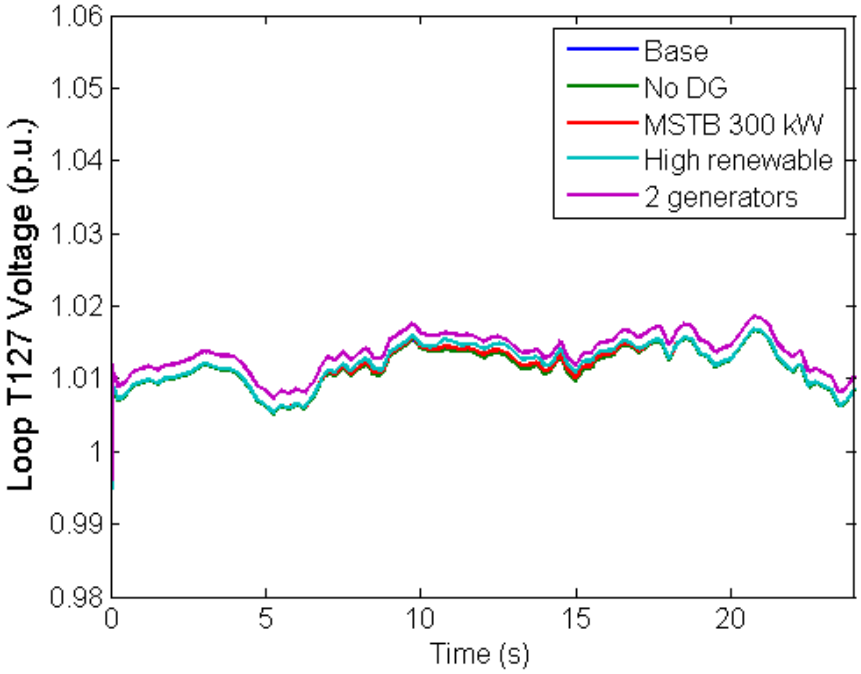

The average power flow through the loop link segment is quite low, generally less than 200 kW for the baseline case, as presented for all cases in Figure 41. As for the regular case, the second generator has no effect on the power flow and matches the baseline case identically. The addition of the fuel cell increases the link power flow by about 150 kW. That there is very low power flow through the link in the base case, this location likely represents the voltage minimum in the circuit and the excess generation from the 300 kW MCFC is roughly split between directions on the loop. The high renewable case reduces the link power flow slightly, but does not have a major effect on the power flow at the link.

The associated voltage on the primary is presented as a function of the distance along the loop that is traced from the main voltage to CP2, V1 and V4 on CP2-3, then V1 on UC-8 and back to the main voltage. The entire loop is 1.8 miles in length due to the short line lengths throughout the campus and the snapshot is taken at 12 s to include the effect of the PV generation. This loop voltage is presented in Figure 42 for all alternative loop scenarios and shows the overall voltage drop on the primary to be very minimal. The loop link occurs between bus 4 on CP2-3 at 1.094 miles and bus 1 on UC-8 at 1.187 miles along the loop. As predicted, this location is the voltage minimum, which explains the low power flow. The voltage drop is steeper on the UC-8 side of the loop because this circuit has only a single cable per phase, while the circuit connecting CP-2 to the main substation has two cables per phase and thus the impedance is halved. The main difference between the cases is in the voltage offset due to the transformer voltage drop. The power flow reversal for the 2 generator case raises the voltage throughout the loops, which is also observed in the individual load voltages of each transformer. The cases with 300 kW MCFC and additional PV both have a slight increase in voltage, but this is mostly uniform and due to the transformer drop, and not a result of the change in line power flow. Again, this is likely due to the low line impedance and minimal voltage drops anywhere in the UCI circuit lines.

Figure 41: Power flow from CP2-3 to UC8 through loop link

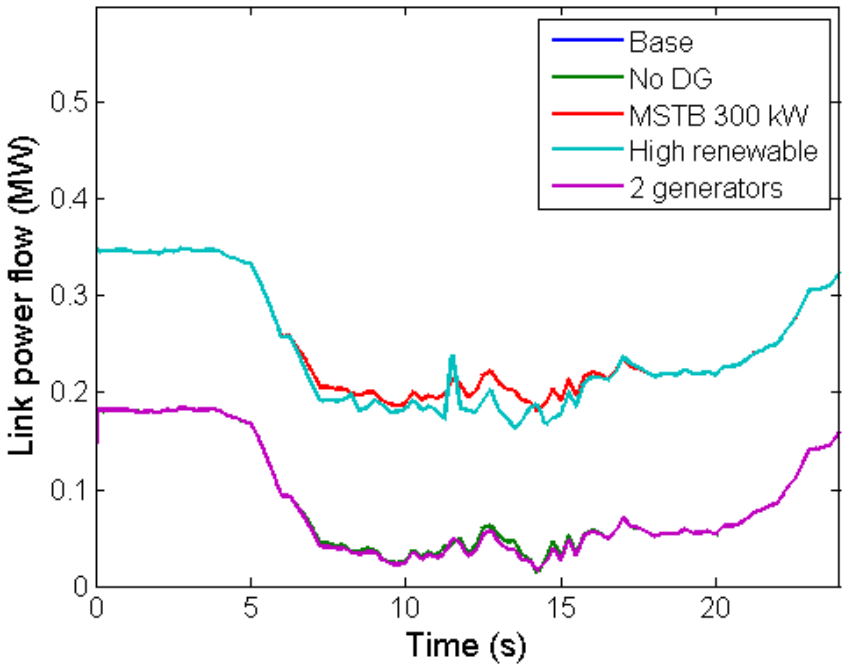

Figure 42: Primary loop voltage for alternative electric service scenarios

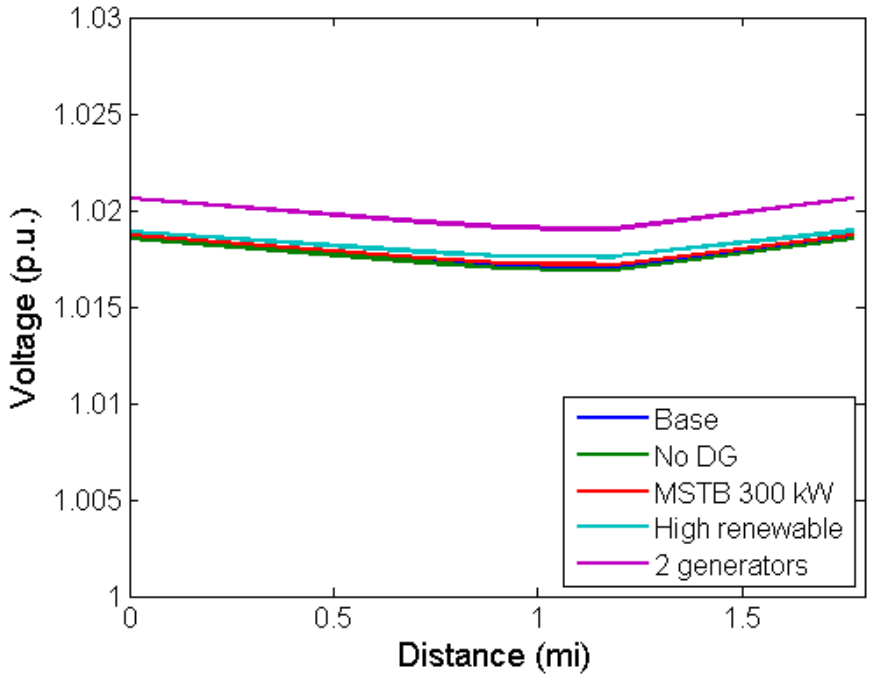

The efficiency for the loop cases is presented in Figure 43 and is nearly identical to that of the radial cases in Figure 37. Because the loop link power flow is quite low, the loop system acts very much as a radial system under normal operation. Thus the power flows, and hence

efficiencies, do not change noticeably. However, a properly implemented loop circuit would still have the added benefit of increased reliability.

Figure 43: Efficiency for alternate electric service scenarios (loop)

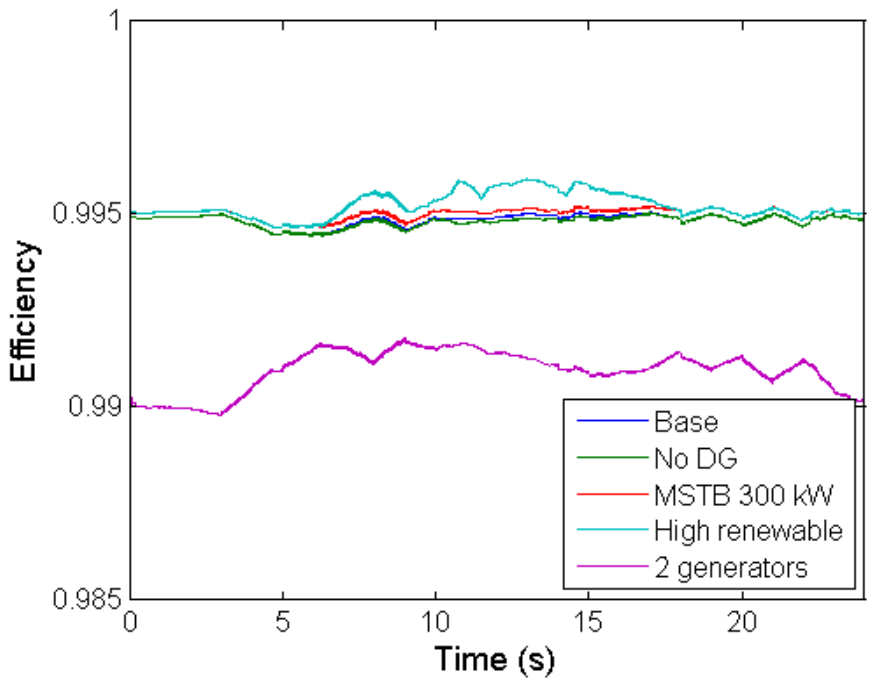

Task 2.3.2. Potential UCI Infrastructure Challenges

The UCI micro-grid electric infrastructure may have to support three energy advances in the future:

1. Increased distributed photovoltaic generation
2. Electric vehicle charging
3. Electric heat pump heating

Electric vehicle charging and electric heat pump heating are in essence conventional loads. In this respect both represent traditional loads, with the exception that they could potentially be dispatched, to improve the utilization of the electric infrastructure. None-the-less capacity could be added to support these loads.

The most interesting is an increase in distributed photovoltaic generation. The technology potentially represents a paradigm change in the design assumption that electricity is flowing from the substation to the end-user. Hence, the model of two UCI distribution circuits has been used to evaluate potential capacity and voltage limitations on the addition of DG.

No infrastructure barriers to the deployment of distributed generation have yet been identified for the UCI campus. As modeling and simulation scenarios proceed in this area, challenges may be identified and will be addressed as appropriate.

Simulation results of two UCI distribution circuits indicate that voltage limits should not be infringed with significant installation of distributed generation. When these two circuits were connected into a loop, the circuit neutral point remained near the location of physical interruption. Thus there is no explicit efficiency benefit to a loop configuration. Such a configuration may be capable of increasing reliability, but is not considered critical to the development of UCI campus into a RESCO.

Task 2.3.3. Conclusions

- UCI model for two distribution circuits has been used to evaluate potential capacity and voltage limitations on the addition of DG.
    - Voltage limits should not be infringed with significant installation of distributed generation
    - No explicit efficiency benefit to a loop configuration whose neutral point is near the location of physical interruption.
    - Loop connection may be capable of increasing reliability but is not considered critical to the development of the UCI campus into a RESCO.

Task 2.3.4. References

Auld, A. E., J. Brouwer, et al. (2009). Effect of Distributed Generation on Voltage Levels in a Radial Distribution Network Without Communication. ASME Fuel Cell 2009, Newport Beach, CA USA.

NREL/GE (2003). DG Power Quality, Protection and Reliability Case Studies Report, submitted to NREL by GE CRD, Contract No NAD-1-30605-01, Program: Reliable, Low Cost Distributed Generator/Utility System Interconnect, August 2003.

Appendix B:Task 3:
Distributed Energy Resource Management

TABLE OF CONTENTS

Task 3.1. Methods to use dynamic price signals to tailor electric loads B-4

Task 3.1.1. Dynamic Price Signaling B-5

Task 3.1.2. Smart Charging B-6

Task 3.1.3. Lessons learned on the benefits and challenges of utilizing dynamic price signals B-8

Task 3.1.4. Conclusions B-9

Task 3.2. Opportunities to Dispatch Heating and Cooling in Monitored Institution and Commercial Applications B-9

Task 3.2.1. Potentially dispatchable loads B-10

3.2.1.1. Electric chilling loads B-10

Task 3.2.2. Energy capacity of dispatchable loads B-10

Task 3.2.3. Available Data Types B-11

3.2.3.1. Hospital Complex Type B-11

3.2.3.2. Large Office Building Type B-11

Task 3.2.4. Statistical Analysis of Load Types B-12

3.2.4.1. Hospital Complex Type B-12

3.2.4.2. Load Distribution Analysis B-16

3.2.4.3. Sample Day Analysis B-19

Task 3.2.5. Office Building Type B-21

3.2.5.1. Monthly and Weekly Load Statistics B-21

3.2.5.2. Histogram Analysis B-25

3.2.5.3. Sample Day Analysis B-26

Task 3.2.6. Summary of Dispatchable Load Types B-28

3.2.6.1. Hospital Complex Type B-28

3.2.6.2. Large Office Building Type B-29
Task 3.2.7. Examples of Distributed Energy Management Opportunities B-30
3.2.7.1. Chiller Dispatch with Thermal Energy Storage B-30
Task 3.2.8. Electrical Energy Storage Model B-32
Task 3.2.9. Conclusions B-36
Task 3.3. Use of BEV Charging to Manage Intermittent Renewables B-37
Task 3.3.1. Feasibility of PEVs B-37
Task 3.3.2. PEV Charging Analysis B-39
3.3.2.1. Methodology B-40
3.3.2.2. Model B-40
3.3.2.3. Results B-42
Task 3.3.3. PHEV infrastructure requirement B-48
3.3.3.1. Immediate charging B-50
3.3.3.2. Delayed charging B-50
3.3.3.3. Average charging B-51
3.3.3.4. Smart charging B-51
3.3.3.5. Smart charging with the fuel price B-51
Task 3.3.4. Interaction between vehicles and the grid B-51
Task 3.3.5. New management strategies required to manage intermittent renewable power B-52
Task 3.3.6. PEVs impact on intermittencies B-56
Task 3.3.7. Conclusions B-57
Task 3.4. Dispatch of Cooling Loads to Manage Increased Renewables at UCI B-57
Task 3.4.1. Acquiring temporal resolution of the campus cooling load B-58
3.4.1.1. Chiller Model Description B-61
3.4.1.2. Electrical Centrifugal Chillers B-61
3.4.1.3. Cooling Tower B-63
3.4.1.4. Water pump B-63
3.4.1.5. Thermal Energy Storage Tank B-64

3.4.1.6. Integration of Chiller Plant B-64
Task 3.4.2. Cost Signal Types and Cost Function Optimization B-64
3.4.2.1. Cost Function Components B-65
3.4.2.2. Chiller Optimization Code B-66
Task 3.4.3. Results and Analysis B-75
3.4.3.1. Changes in Campus Load Characteristics B-75
3.4.3.2. TES Management of Increased Renewable Penetration Levels B-88
Task 3.4.4. Summary and Discussion B-98
Task 3.4.5. Conclusions B-99
Task 3.4.6. References B-100

The demand for electricity changes throughout each day and typically follows a diurnal cycle as shown in Figure 44. There is lower electrical load during the night and higher during the day. Also, the peak load occurs during the summer and the minimum during fall or winter. In California this is predominantly due to air conditioning load and other end uses loads that are focused during the daytime. As will be shown in more detail in Task 7, this diurnal nature requires that dispatchable generation be deployed to meet the changes.

Figure 44: Diurnal Electrical Load Pattern for UCI during each Season of 2005

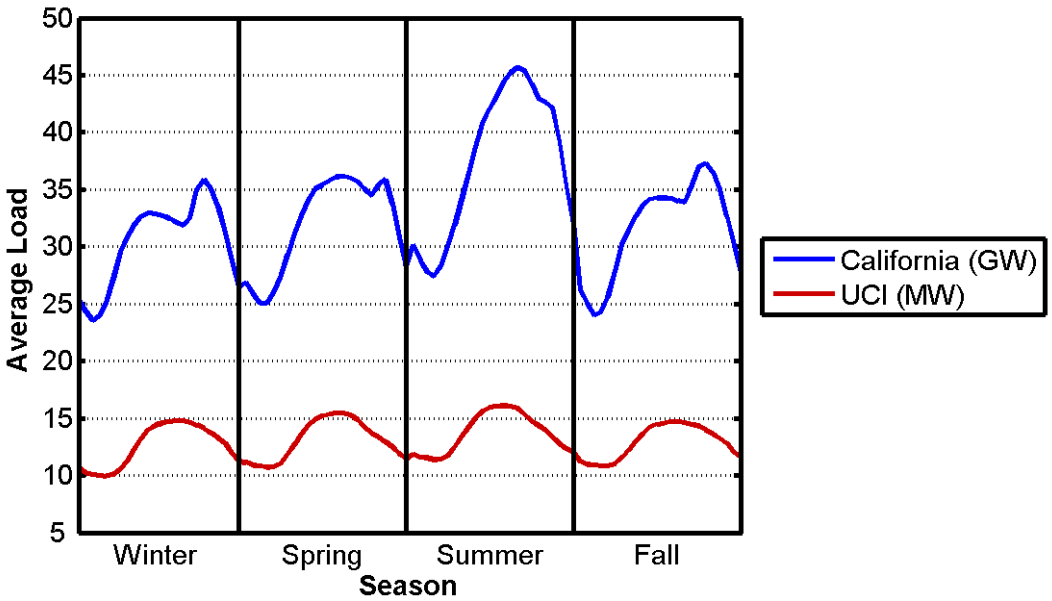

This task explores the value and challenges associated with both measuring and controlling loads. Some of the loads explored are plug load devices (e.g., laptops, cell phones), the campus electric, heating and cooling demand and electric vehicles. Understanding the dispatchability of these loads is paramount to determining energy management opportunities which will both ease management of the current grid and allow for greater integration of renewables.

Task 3.1. Methods to use dynamic price signals to tailor electric loads

Currently in California there are "time of use" (TOU) price signals which change the rate charged to customers based on the time of day (e.g., off-peak, mid-peak, on-peak). The next step after TOU pricing is moving to an even more dynamic signal, which is called real-time pricing. For real-time pricing there is a base rate and then a variable rate that is based on other factors like load on the grid and weather conditions. Use of real-time pricing allows customers to make a decision on how valuable the use of electricity is for them and to adjust their use accordingly based on a dynamic price signal. This section explores the several examples of using dynamic price signals to support real-time pricing related to plug-load devices like laptops and electric vehicles.

Task 3.1.1. Dynamic Price Signaling

The generated price of electricity changes according to meteorological conditions. The dynamic costs should be reflected onto the end-user's cost of electricity in order to reduce the overall electrical energy cost. To complete this task, an evaluation of dynamic price signaling should take place to enable effective dispatch of distributed energy resources to support the grid. The end-user shall be able to decrease his energy cost by using electricity that is not stored. With smart charging, electricity storage, such as batteries, and thermal energy storage (TES) would not be as necessary for the campus or utilities by producing and transmitting cheap energy directly to the end-user, transferring the savings from avoiding the use of storage to the consumer. To demonstrate the possibility and practicality of this task, the utilization of a relay controller and extension cord is necessary.

The 2-Channel 20 Amp SPDT USB Relay Controller used for this task is a switch that commands the activation of devices that require an outlet such as chargers, tools, or appliances which are connected to the controller. The relays are the communication components between the computer and the specified devices needed to be activated. After creating an incision into an extension cord, which is connected to both the outlet and the specified device, the wire underneath the insulation is spliced onto the relay to allow the computer the ability to control the flow of electricity to the device. The controller has LED status lights that indicate the activity of its relays, one of which remains illuminated while the controller is joined to an outlet, and another flashing light to indicate the transmission of data from the computer. The remaining status lights correlate with the relays, lighting up when the computer speaks to the controller to activate a specific relay. When the computer speaks to the controller to activate its relay, the controller permits the flow of electricity through that relay to initiate a command on the specified device. The computer requires a model known as "smart charging demo" to communicate to the controller; this will autonomously request when to activate each relay which corresponds to each action of the device (i.e. Relay 1 is to turn on; Relay 2 is to turn off).

The "smart charging demo" is a MATLAB model that may initiate the activation of a variety of charging devices; specifically, the model pertains to charging plug-in hybrid electric vehicles (PHEVs) at low electricity costs while the vehicle is not in use (dwelling). The model calculates the best time to begin charging based on predictions of weather and loading conditions within a 48-hour period.

The model first loads the various prices of electricity, which depend on three items: the utility companies (Southern California Edison (SCE) or Pacific Gas and Electric (PG&E)), the hours of the day, and the day of the week. Variables must then be inputted as energy usage differs among vehicles. Variables include oil price, utility rates (from either PG&E or SCE), vehicle information (i.e. approximate AC at full charge [kWh], electric vehicle (EV) range [miles], EV range remaining [miles], and average miles per gallon), trip information (i.e. start time, end time, dwelling time), current season of the year, day of the week, charging efficiency, and charging method (i.e. immediately, delayed, smart charging). After finding the remaining range in the battery and converting AC charge to DC in the battery of the vehicle, the code enters an

"if" statement to find the season and day to determine the cost of electricity. The calculations commence with location (home, work, school, or anywhere) and the trip information (trip number or last trip). Then it compares the price of oil per mile to the price of electricity per mile to find when the electricity rate is less than the oil rate.

The code enters another file called the "charging" function, which considers the trip destination, starting location, dwelling time, trip number, and state of charge using "switch" and "if" statements to account for different scenarios. In order to confirm the scenario, the model uses numbers to state its decision, employing 1 to translate as "yes" and 0 to translate as "no". If all conditions are satisfied, charging may take place at the desired time, and calculations are performed to find the amount of time needed to complete full charge. By comparing the amount of dwelling time to the time needed for full charge, the model produces charging options for the end-user: delay, immediate or smart charging. "Delay" postpones charging to the end of the dwelling time, and "immediate" begins the charging instantly. The "smart charging" option compares the oil price to the electricity price at the given time; when the price of electricity is less than the price of gasoline, and also if the time needed for full charge lies within the dwelling time, the code may utilize this option and begin charging the battery of the vehicle.

After the "charging" function is complete, power time and consumption computation completes in the "smart charging" program. If all requirements for "smart charging" have been satisfied, a serial port is opened and configurations to the port are adjusted for the computer to speak to the relay controller. A 48-hour period is needed for the end-user to be able to charge in the morning prior to beginning the work day (given the day is a weekday) and also overnight, which overlaps between the first day and the second day. Consistency within the time sequence is maintained by converting the 60-minute interval hours to 100-point interval hours; 100 points on the time scale is equivalent to one hour. Using this time format allows MATLAB to associate the output to the utility rate. The time point scale may reach up to 4800 points to represent 2 days. Real time is taken using the "clock" function to retrieve the current run-time that will correlate with the desired time to charge. An "if" statement compares the current time to the end of the dwelling time; If the statement is satisfied, another "if" statement is used to check if that time correlates with the output which would allow for charging. Fulfilling the statement will permit the computer to speak through the serial port to the controller and turn the relay on. If the statement is not satisfied, the model will continue running to verify when the controller will activate. The relay components remains off when the time sequence has surpassed the 48-hour period or the current time is not within the dwelling time. The serial port then closes communications with the controller after charging is complete.

Task 3.1.2. Smart Charging

As the PHEV is dwelling and depleted of energy, the charger is plugged into the vehicle but waits on standby while the charging device is inactive. A computer at the station contains the "smart charging demo" program along with the necessary utility data and vehicle information. The computer is connected to the relay controller, which is wired to the extension cord that is connected to the charging device. Both the extension cord and controller are powered by an

outlet. The end-user enters the required entries (explained on page 5) into the graphical-user-interface that will interact with the model. After the designated inputs, the code begins and runs the information and calculations while the conditions for charging are satisfied, finding the lowest cost of electricity within the vehicle's dwelling time. While the current time is not at the lowest cost of electricity at the desired time (within the dwelling time), the PHEV remains un-charged. As the current time coincides with the desired time, the computer will communicate to the relay controller to turn on a specified relay, activating the charger and charging the PHEV for an appropriate quantity of time as determined by the model. The model stops running and charging discontinues upon completion of determined time.

The completion of this task has produced a model that is capable of automatically activating a specified device that may result in saving both energy and money, and incentivize end-users to alter their power-usage behavior. When applied to a plug-in electric vehicle, the model programs the charging device to activate only at the moment the current time reaches the lowest cost of electricity within the vehicle's dwelling time. The model determines the optimum moment to charge by predicting price signals for the next 48 hours based on weather and load conditions; this will allow for control of distributed energy resources as they relate to price signals, providing cheaper resources and giving the end-user the ability to decide how to utilize their utilities. Figure 45 displays the correlation between the best time to begin charging (output) with the utility rates in dynamic price signaling for a Plug-In Hybrid Toyota Prius, given that the vehicle requires charging, the "smart charging" option is chosen, and dwelling time begins at 5pm and continues overnight for 12 hours.

Figure 45: Time of Charging

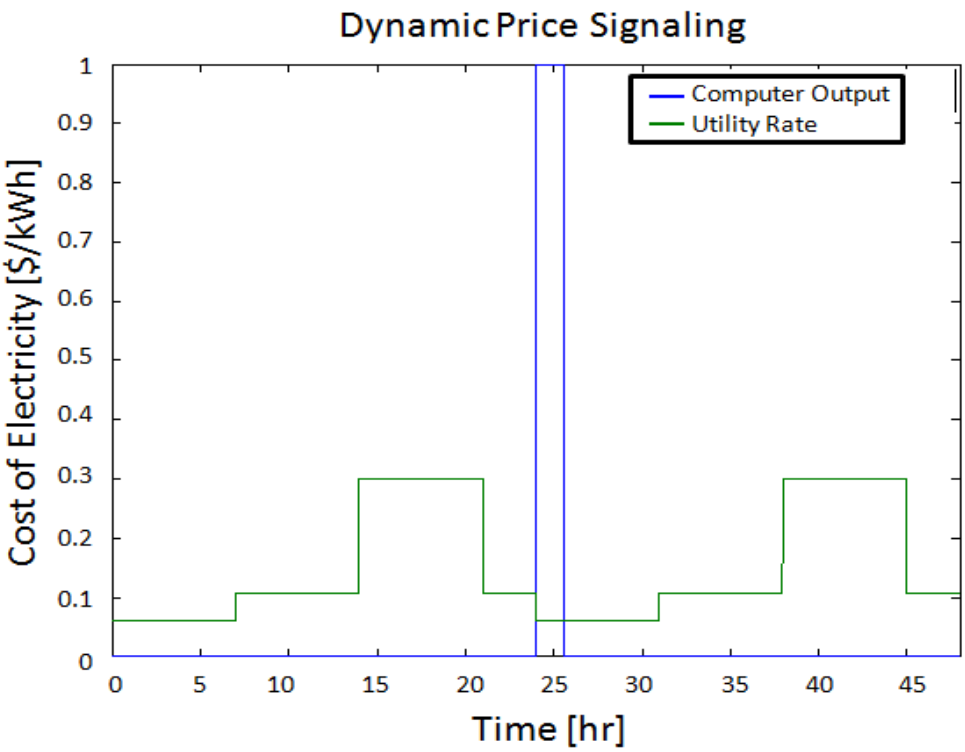

The figure demonstrates that the model finds the lowest time for cost of electricity over the 12-hour dwelling period after 5pm occurs at midnight. The utility rates illustrate a decrease in cost from 11 cents to 6 cents for electric energy, so the output, which reaches the value 1 at this time, explains that the most favorable moment to charge begins at 24 hours and ends at 26 hours. At 24 hours the computer will address the controller to activate its relay and charge automatically until the output drops to the value 0 at 26 hours. This will end the charging period for the current dwelling time.

The concept of automatic charging at the lowest energy cost also applies to laptop computers, phones, tablets, or other devices that require charging. The cumulative energy expense of modern technology can be greatly reduced if end-users were capable of controlling the costs of charging their devices with the relay controller. The application can expand to a larger scale such as facilities and infrastructures such as the University of California-Irvine campus, allowing the university to automatically manage its dispatchable loads with price signals.

Task 3.1.3. Lessons learned on the benefits and challenges of utilizing dynamic price signals

It is very important that the customers be made aware of their options and that the options are not overly complicated. For this idea to be feasible the complexities of turning equipment off, or delaying its use will need to be simple, intuitive and safe. To fully enable real-time pricing there must be communication between the utility and the customer. The deployment of smart

meters represents the best opportunity for the utility to communicate price signal information with their customers.

Just as the California Public Utilities Commission (CPUC) regulates the electricity rates, the CPUC will also have to regulate the implementation and use of real-time rates to ensure that the programs are not exploited. For example, proper measures need to be taken to account for on-site generation, demand side management (i.e., demand response), and energy storage devices (e.g., batteries, electric vehicles), which can adjust a customer's electric demand. If done properly dynamic price signals represent a valuable opportunity to shape the load, which will support grid operation and the integration of renewables as well as enhance the value proposition of advanced technologies like energy storage, electric vehicles and demand response.

Task 3.1.4. Conclusions

- Enabling real-time pricing requires communication between the utility and the customer
- Smart meters represent an opportunity for RESCOs to receive price signal information from the utility or ISO
- Real-time pricing will need the appropriate regulatory framework to be successful

Task 3.2. Opportunities to Dispatch Heating and Cooling in Monitored Institution and Commercial Applications

Different opportunities to dispatch building heating and cooling electric loads exist. If electricity is used to heat or cool a building it can be dispatched. However, depending on the equipment installed, and the duration and extent of the electric dispatch different occupancy impacts will be observed. Different occupancy impacts may be acceptable depending on the cost proposition of the electric dispatch and resulting consequence (e.g., grid failure) of not dispatching the loads. To evaluate opportunities of dispatch it is important to understand different applications and types of electric dispatch. A summary of electric dispatch is provided below:

Peak load reduction: Heating and cooling loads can be dispatched to reduce grid peak loads. This can help reduce distribution, transmission, and generator peak capacity.

Daily grid load variations: Heating and cooling loads can be dispatched to reduce daily load variations. This can enable supporting generators to operate less dynamically, improving thermodynamic efficiencies and amount of stress cycling on the generators.

Contingency conditions: Heating and cooling loads can be dispatched in cases of emergency. For example if a major transmission line fails, heating and cooling loads can be reduced to reduce strains on the system while new generation is brought online to reduce grid loss risks.

Load regulation: Heating and cooling loads can be dispatched to provide load balancing regulation. In this application heating and cooling loads can be varied in real time by the load balancing authority to balance grid loads.

Task 3.2.1. Potentially dispatchable loads

3.2.1.1. Electric chilling loads

By adding a thermal energy storage tank to an electric chilling system, it is possible to run the chiller with some independence of the cooling requirement. Figure 46, illustrates the system hardware upgrades that were needed to dispatch air conditioning chiller loads at UCI.

Figure 46: System hardware upgrade needed to dispatch air conditioning chiller loads

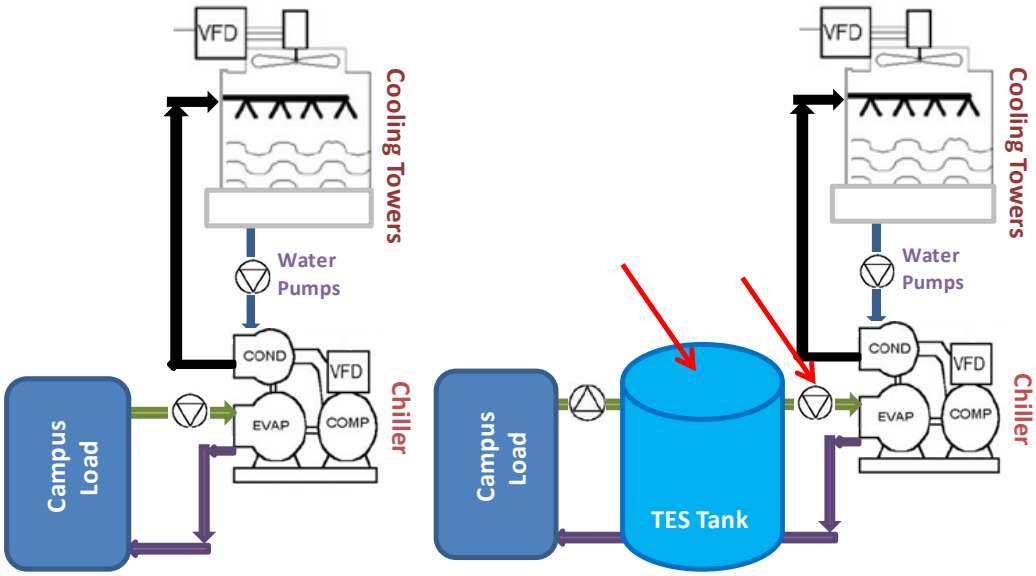

In total, only a cold water storage tank and a supplementary pump was required to dispatch the electric load. The total amount of supplementary pumping is minimal. In addition, since the tank is relatively large, limited heat losses are accrued from the tank. Without the cold water tank, the chillers will operate primarily during the day, during peak temperatures. However, with the tank, the chiller can operate at night with colder ambient temperatures. This will directly result in increased chiller operating performance - saving energy. The efficiency of the system is dependent on operating characteristic and ambient temperature conditions.

Task 3.2.2. Energy capacity of dispatchable loads

The UCI chilling plant total chilling power capacity can reach up to 6 MW, a substantial portion of the total campus load. The UCI TES tank holds 4.5 million gallons and can store 60,000 ton-hours of cooling and considering a chiller COP of 5 that is 0.7 kW per ton or 42 MWh of storage capacity. Running at full capacity, the tank can store 7 hours of chiller operation, or essentially one day worth of campus cooling.

Task 3.2.3. Available Data Types

In order to identify example energy management possibilities, load datasets of different natures were obtained for two different sites, such that an understanding of electric, cooling, and heating load behavior for different building and community types could be analyzed and understood. An outline of the data types used in this analysis is as follows:

3.2.3.1. Hospital Complex Type

The first site selected for this analysis is the Metropolitan Mental Hospital, a state prison for mental patients located in Norwalk, CA. This facility comprises a number of buildings which are collectively metered as an aggregate, with a total facility square footage of 1,215,750 and a typical average occupation of 600 people. Cooling and heating loads for this facility are met by an on-site cogeneration facility that provides steam and chilled water, however this facility is metered separately from the hospital complex itself. Therefore, the cooling load of this facility is not embedded within the electric load data. For this particular site, the following data was obtained:

Table 12: Availability Ranges for Electric, Heating and Cooling Data From a Hospital Complex

Data type	Resolution	Start Period	End Period	Units
Electric	15 minute	May 1, 2008 – 12:00 am	April 30, 2009 – 11:59 pm	kWh
Cooling	15 minute	May 1, 2008 – 12:00 am	April 30, 2009 – 11:59 pm	MMBTU/hr
Heating	15 minute	May 1, 2008 – 12:00 am	April 30, 2009 – 11:59 pm	MMBTU/hr

3.2.3.2. Large Office Building Type

The second site selected for this analysis is a 19-floor office tower occupied by The Irvine Company, with a total square footage of 400,000. This building encompasses typical electric loads, and also contains a separate but on-site central plant which provides cold water to meet cooling loads. The heating load of the building, however, is met by electric resistance heaters and is included with the electric load of the building. Therefore, for this building type it was not possible to separate the heating load explicitly. Load data for this site was presented in the form of three electric load data sets:

Table 13: Availability Ranges for Electric, Heating and Cooling Data From a Large Office Building

Data type	Resolution	Start Period	End Period	Units
Electric (E1)	15 minute	January 1, 2008 – 12:00 am	December 31, 2008 – 11:59 pm	kW
Electric(E2)	15 minute	January 1, 2008 – 12:00 am	December 31, 2008 – 11:59 pm	kW
Electric (Central Plant)	15 minute	January 1, 2008 – 12:00 am	December 31, 2008 – 11:59 pm	kW

The electric load of the central plant is used as the cooling load, since providing chilled water is the primary function of the central plant. The building electric load is split between two meters

– designated 'E1' and 'E2'. Both E1 and E2 meters monitor an aggregate load that contains a portfolio of typical office load types, however the breakdown of each respective portfolio was not available.

Task 3.2.4. Statistical Analysis of Load Types

3.2.4.1. Hospital Complex Type

The monthly and weekly minimum, maximum, and average demand values for each load type (chilling, heating, and electricity) for the hospital complex are displayed in Figure 47 and Figure 48, respectively. Note that the month index begins at 5, corresponding to the data set beginning during the month of May in 2008.

Figure 47: Monthly Cooling, Heating, and Electricity Trends: Hospital Complex Type

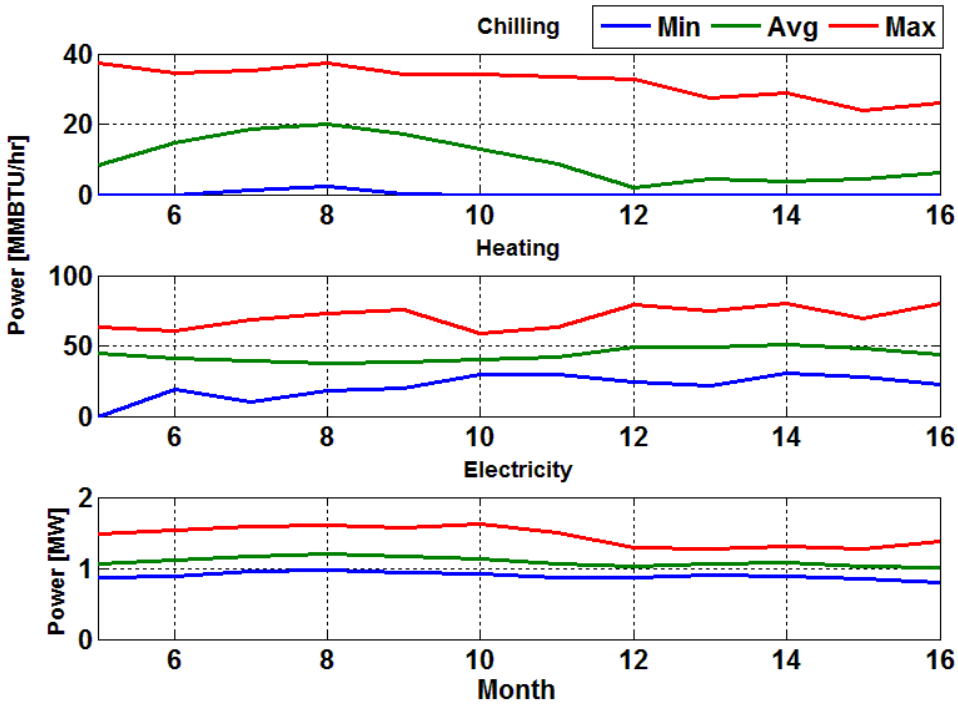

Figure 48: Weekly Cooling, Heating, and Electricity Trends: Hospital Complex Type

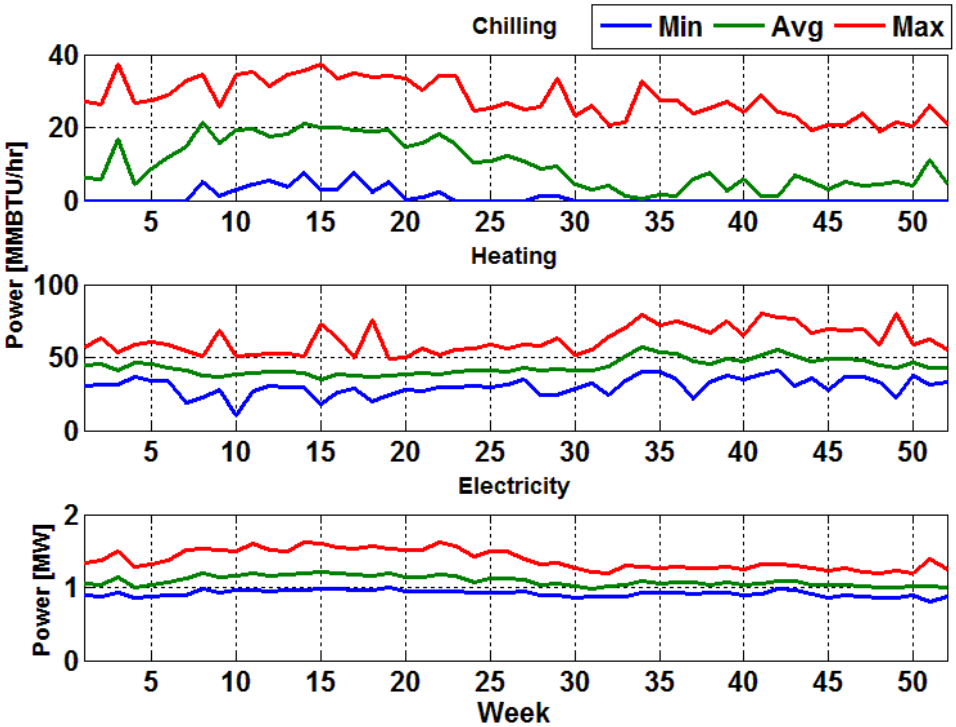

As expected, the average cooling demand distinctly rises during the summer months, with some months where the chiller plant is not allowed to turn off even during the nighttime hours, and the peak average cooling demand of 4.97 MMBTU/hr occurs during the month of August. As summer transitions into fall, the cooling load steadily decreases as average ambient temperatures at the facility decrease significantly, reducing the need for building cooling. Entering the winter months, the average monthly cooling load decreases to near-zero values with a minimum in December. As winter transitions into spring, the average cooling load rises with increasing ambient temperatures.

The minimum monthly cooling demand is nominally zero during all months except June through September. In normal operation, buildings within the complex determine set points for room temperature. The chiller plant is dispatched to provide cold water such that all of those set points are maintained. If the ambient temperature is such that the temperature set points for all buildings within the complex are already met, it is not necessary to activate the chiller plant. This effect typically occurs during the night time hours, where ambient temperatures tend to be low. The only period when the minimum monthly cooling demand is nonzero is during the summer months, where ambient temperatures during the night time hours are sufficiently high such that chilling must still be provided. In Norwalk, CA, for this time period, the ambient temperatures often do not drop below 80 degrees Fahrenheit even during the night time hours, which is still warm for most patients in the hospital. It is important to note that since this is a hospital complex, requirements for occupant comfort are generally more stringent than typical.

The maximum monthly cooling demand is not subject to the same magnitude of seasonal variability as the average monthly cooling demand. While the average monthly cooling demand exhibits a fairly large seasonal variability, the maximum monthly cooling demand remains relatively constant. Higher values are exhibited during the spring and summer months, after which the values decrease steadily for subsequent months and dodo not rise until the return of the spring months in April. The maximum monthly cooling load is mainly dependent on the operation paradigm of the chiller plant. Since this facility does not currently have any thermal energy storage capability installed, chiller plant operation must be directly matched to cooling load demand within a reasonable response time. In the non-summer months, the chiller plant is allowed to shut down during the cool night time hours and restart during the next day when temperatures rise above desired set points. During this restart, however, the chilling plant tends to operate initially at high capacity, in an attempt to restore temperature set points as quickly as possible. Additionally, if the ambient temperature increases very rapidly during the daytime, quick increases in chiller power usage occur. These types of events give rise to large maximum monthly cooling demands, even though on average the cooling demand is reduced during the non-summer hours.

The weekly chilling trends follow the same general trend as that of the monthly cooling demands as expected. Due to the finer resolution, however, the data displays more fluctuations compared to the monthly trends. The maximum weekly chiller demand exhibits the most fluctuations, primarily due to the tendency of the chiller plant to operate at high capacity when restarting or ramping up in response to violation of a temperature set point within the complex. On the weekly scale, however, the magnitude of this peak-biased operation is not the same from week to week, and therefore the maximum chiller power displays a slightly larger range of fluctuation.

The weekly average cooling demand trends also follow the trends exhibited by the monthly average cooling demand, with the exception of a few fluctuations. The spring months in this region are dominated by relatively warm days with intermittent rainstorms spread throughout the season. These weather patterns cause the ambient temperature to fluctuate from relatively high values during clear days to relatively low values during the onset of storm systems, and consequently the magnitude of the cooling demand will respond to this trend by increasing or decreasing cooling demand. In the summer months, the cooling demand is generally high due to the high ambient temperatures, however this region is also subject to periods of slightly higher temperatures due to intermittent heat waves that caused the small fluctuations during the summer months. During the winter and fall where the ambient temperature fluctuation appears to be more stable in the region, the fluctuations in the average cooling demand are not as pronounced.

The weekly minimum cooling demand trends also follow that of the monthly minimum cooling demand trends very closely and are due to the same drivers as extracted from examining the monthly minimum cooling demand trends.

The average monthly heating demand displays a trend that is opposite of that of the average monthly cooling demand as expected. The average heating demand tends to be lowest during

the summer months and highest during the winter months due to the respective changes in ambient temperature. The range of fluctuation of the average monthly heating demand is similar in scale to that of the average monthly cooling demand in absolute terms, however is much smaller as a percentage of the maximum demand. Chiller use and cooling demand in this type of complex is primarily used to meet occupant comfort needs for space cooling, and the fluctuations in the monthly average cooling demand reflect this use. The heating demand in this type of complex, however, encompasses much more than space heating and occupant comfort requirements. A hospital complex uses hot water to carry out a variety of process loads such as laundry, sterilization, and other processes relevant to medical facilities in addition to space heating demands. These process heating loads are relatively constant over the year from a monthly perspective, and therefore do not contribute to heating demand fluctuation on the monthly timescale. The fluctuations in the average monthly heating demand are therefore primarily due to occupant comfort and space heating requirements, which are a smaller fraction of the total heating load.

The maximum and minimum monthly heating demands show no apparent correlation with season on the monthly timescale. Since process loads are included in the heating demand and the breakdown of such loads is not specified in our data, the behavior of the monthly maximum and minimum heating demands are difficult to determine.

Compared to the scale of the heating demand, the fluctuations in the weekly heating demand trends are fairly small compared to that of the cooling demand. The maximum weekly heating demand is fairly stable with the exception of a few fluctuations during the summer and spring months which were driven primarily by increases in process loads as described from examination of the monthly trends. Contrary to the monthly heating demand trends, the weekly maximum heating demand does show a clear correlation with the season of the year, with slightly lower magnitudes during the summer months and slightly higher magnitudes during the winter months. This behavior is not significantly pronounced, however, due to the fact that space heating is only a small fraction of the total heating load in this complex. The average weekly heating demand is very stable and mirrors exactly the trend displayed by examination of the monthly heating demand trends.

The minimum weekly heating demand is also fairly constant due to the year-round occurrence of certain process loads, with the exception of a few fluctuations which tend to decrease the minimum weekly heating demand. These decreases coincide with instantaneous decreases in process load heating requirements that tend to occur at irregular intervals and are dependent on patient occupancy, treatment cycles and other factors which do not necessarily correspond with the season of the year.

The average monthly electricity use remains relatively constant over the course of 12 months and has a smaller relative range of fluctuation compared to the cooling and heating demands. This is expected since the electricity used for cooling is monitored separately from the aggregate of the other electric loads. Heating in this case is provided by natural gas as opposed to heat pumps or resistance heating. Cooling and heating loads are the major components of a given electric load that can have distinct seasonal variation, however both are monitored separately.

The electricity use in this case is therefore the aggregate of lighting and plug loads within the complex. The majority of the plug loads consisting of computers and medical equipment are often active for the entire year, and lighting loads may have a slight variation with season due to variations in daylight hours, however this complex may not necessarily have controls to take this into account. Additionally, contrary to a place like a school campus, the occupation of the complex does not vary with season: there are staff and patients occupying the complex in relatively constant numbers all year round.

The maximum and minimum monthly electricity use trends reflect the same relatively constant usage behavior as the average. A characteristic of note is that the average monthly electricity use is generally closer to the minimum values than the maximum values. The minimum load values occur during the night time hours when a minimum of staff is on site and medical equipment operation is at a minimum. The maximum load values occur during the daytime when the opposite is true, however this only occurs during a shortened time window of the day. The maximum values tend to be slightly higher in the summer and spring months compared to the winter and fall months. This behavior is primarily linked with the additional building equipment required to supplement the increased cooling demand. While the energy used to provide the chilled water is separate from the electric use of the buildings, each building must operate air handling units, pumps, and possibly reheat mechanisms in some cases to distribute the chilling throughout the building space. Operation of this auxiliary equipment to accommodate higher flow rates and increased chilling requires electricity, and therefore the electricity use is slightly higher during the summer months.

Paralleling the examination of the monthly electricity use trends, the weekly electricity use trends exhibit a very stable behavior throughout the course of the year. The average and minimum weekly electricity demand is essentially constant throughout the year, due to dominance by plug loads and other equipment which tends to operate year round. The maximum weekly electricity demand displays a slightly higher magnitude in the spring and summer months, reflecting the trend displayed by the monthly electricity usage data. The finer resolution in this case did not reveal any additional information about electricity use in the building, since the timescale of electricity use fluctuations tends to occur on the diurnal basis which will not be captured by a weekly examination.

3.2.4.2. Load Distribution Analysis

To obtain a sense of the distribution of the cooling, heating, and electric demand of the complex, the data for each load type was analyzed in terms of a histogram as follows. The histograms were created using the raw data for each load type with a 15-minute resolution. This will give a sense of the range of fluctuation and behavior of each load type. The distribution of the cooling load demand for the hospital type complex is presented in Figure 49:

Figure 49: Cooling Demand Distribution: Hospital Complex Type

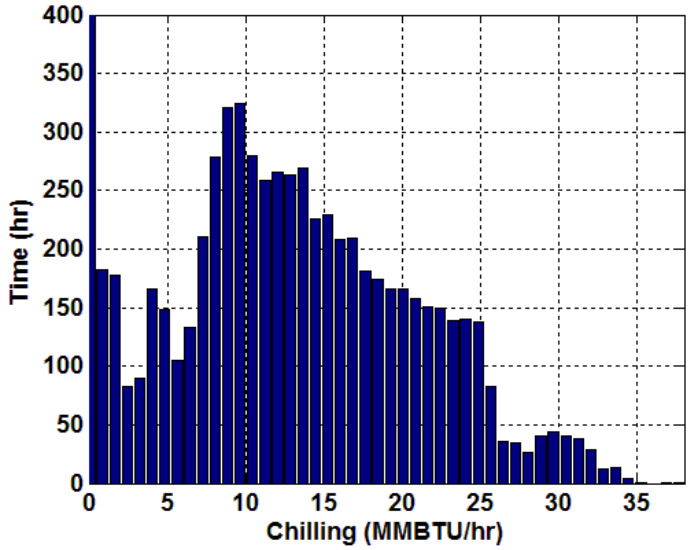

The histogram presented here displays an inset of the total histogram for this data. Since the chiller plant is offline for a large part of the year during the night time hours of each day and for the majority of the winter season, the amount of time that the cooling demand is equal to zero is very large compared to the amount of time that the chillers are actually operating. Therefore, this histogram displays the distribution of the cooling demand when it is nonzero.

The cooling demand tends to have a very continuous distribution. For this complex, the cooling demand tends to regularly vary over a wide range of values, characteristic of the cooling demand varying in real time and tending to occupy different typical magnitudes dependent on season and time of day. In general, there are distinct drop-off points, primarily below 6 MMBTU/hr and above 26 MMBTU/hr where the frequency that the chiller plant operating in those regions is relatively low. This complements the principle that cooling demand trends are due to distinct but regularly occurring events. The cooling demand is mainly governed by space cooling requirements and occupant comfort as described previously, and due to rotations of personnel throughout the day, the cooling demand will tend to increase from near-zero to a finite value on a daily basis and vice-versa without frequently operating at capacities in between such values. Additionally, the very large chilling values are either due to chiller response to violation of a temperature set point as described prior, or characteristically hot periods throughout the day that occur in the summer but last for only short periods of time. Therefore, the cooling demand is primarily contained within a given range of magnitudes, variance within which is dependent on diurnal weather patterns.

The distribution of the heating load demand for the hospital type complex is presented in Figure 50:

Figure 50: Heating Demand Distribution: Hospital Complex Type

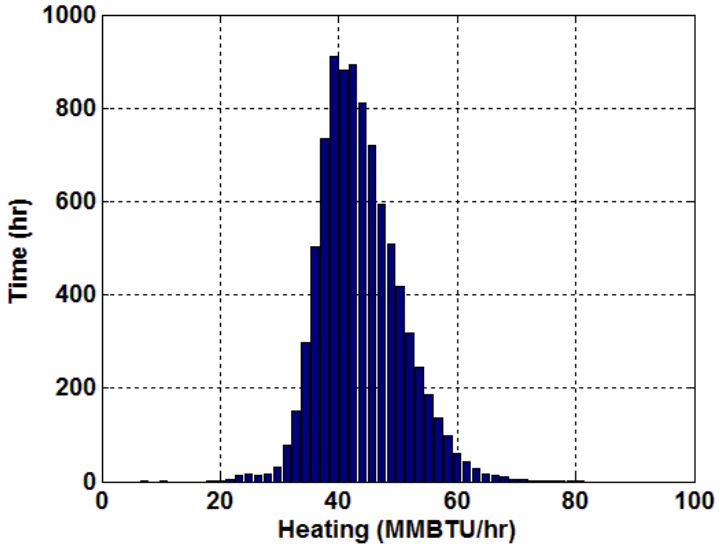

The heating demand displays a much more focused distribution compared to that of the cooling demand, closely matching a Gaussian distribution. The heating demand is primarily base-loaded and is strictly confined to a particular range of values between 30 MMBTU/hr and 60 MMBTU/hr. The variance within this range is due in small part to space heating requirements but is largely dominated by variations in process load behavior. Some of these process loads tend to operate year round such as hot water demand, which does not allow the heating demand to regularly fall below 30 MMBTU/hr, while other process loads such as laundry and sterilization are periodic and add to the heating demand but do not have a continuous duration. As implied by the weekly and monthly heating demand plots, the heating demand is very predictable and stable.

The distribution of the electric load demand for the hospital type complex is presented in Figure 51:

Figure 51: Electricity Demand Distribution: Hospital Complex Type

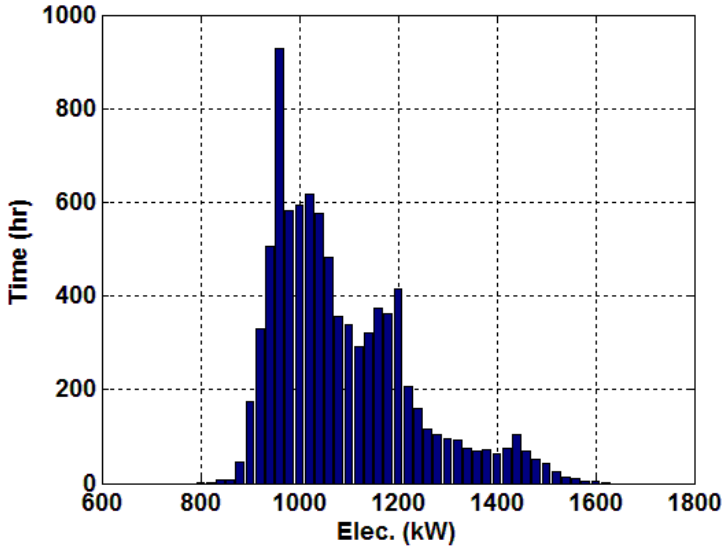

The electricity demand magnitude tends to fall within two magnitude ranges: between 900 kW and 1050 kW, and between 1100 kW and 1200 kW, with the higher electricity demand ranges showing steadily decreasing occurrences. The bimodal distribution of the electricity demand can be explained in terms of complex occupancy and staff rotations. First, the electricity demand is never zero or near zero, since systems within the complex which tend to patients, allows the night staff to operate, and provide lighting for the complex are active at night. Therefore, the electric demand has a large base load component, and additionally, it was shown previously that the electricity demand does not tend to vary with season. The first range of high occurrences is present due to these off-peak operating periods. The second range of high occurrences roughly reflects the slight increase in electricity usage due to staff rotations and occupancy of the building during working hours. Since the duration of the off-peak period is typically longer than the on-peak period of working hours (the majority of the staff has an 8-hour shift), the majority of electric demand occurrences fall within the first range.

Above both of the distribution foci is a small but regular amount of occurrences of electric demand that is greater than 1200 kW. These electric demand occurrences are typically due to the operation of air handling equipment for ventilation and to allow sufficient air and water flow to allow satisfaction of increased cooling demands. These periods happen regularly in the fall and summer months.

3.2.4.3. Sample Day Analysis

The behavior of the cooling, heating, and electric demand for a sample day within each season is presented in Figure 52:

Figure 52: Sample Daily Demand Profiles by Season: Hospital Complex Type

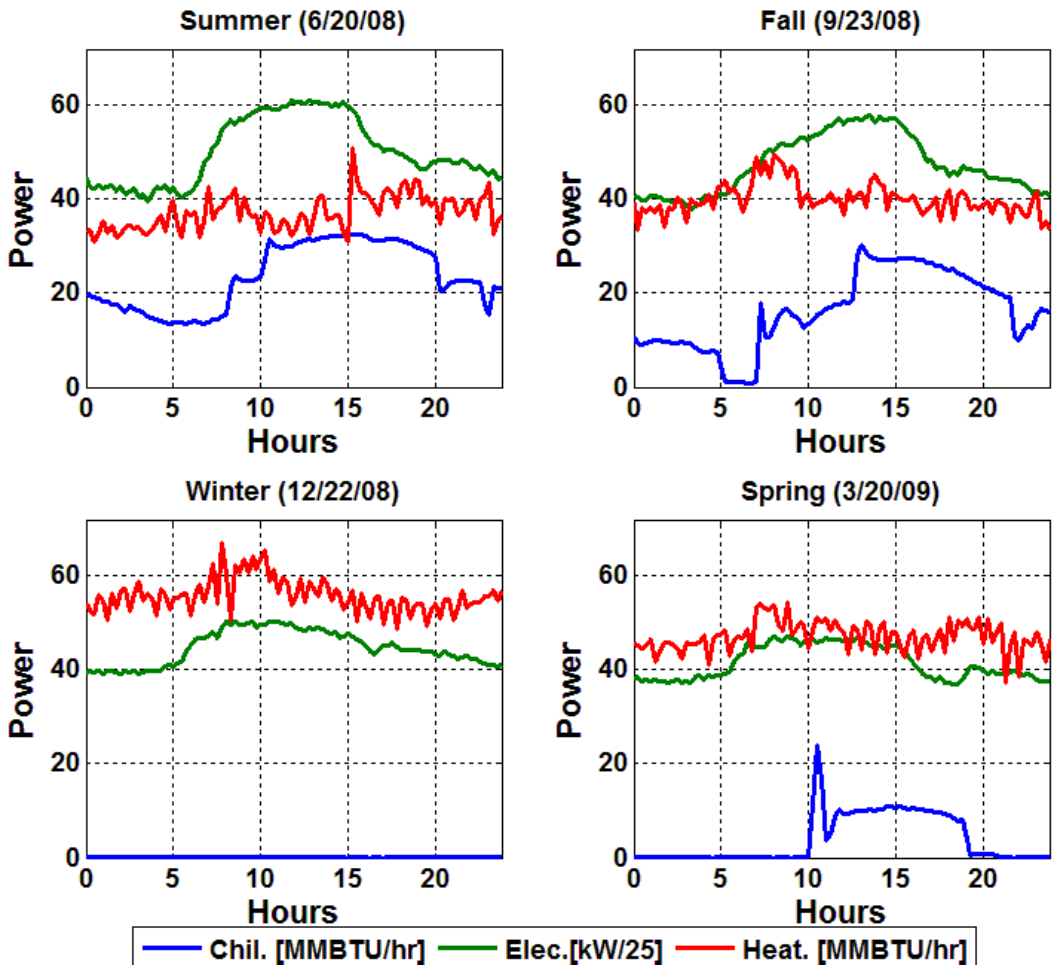

The electricity demand behaves predictably, with low magnitudes during the night time and early morning hours when occupation of the complex is at a minimum, indicating minimal usage of plug load equipment and requirements for ventilation and the operation of air handling equipment. The electric load magnitudes tend to be higher during the summer months due to air handling requirements to accommodate increased cooling, and are consequently lower during the winter and spring months. Small increases in demand during the onset of the night time hours occur due to lighting loads.

The heating demand behaves fairly predictably on average, although it exhibits a number of small magnitude fluctuations throughout the course of the day. These fluctuations represent the activation and deactivation of short term process loads which occur at semi-regular intervals throughout the day. The heating demand does not display any key differences in the diurnal profile between seasons with the exception that the average heating demand tends to be slightly higher during the winter months due to increased requirements for space heating and occupant comfort accommodations.

Of the three load types, the cooling demand appears to exhibit the most erratic behavior. Since the operation of the chiller plant in this complex is primarily in response to meeting temperature set points in the buildings for space cooling requirements, the chiller plant tends to operate with sharp increases or decreases, and also appears to lag by approximately 2 hours behind the occupancy trend of the complex as exhibited by the electric load demand. The latter effect is most likely due to the thermal mass of the buildings. In the morning hours, a finite amount of time is required for the effects of occupancy such as body heat and steadily increasing ambient temperatures to warm the buildings to the point where temperature set points are violated. This tends to occur across the entire complex simultaneously at the beginning of a day. Once this occurs, the chiller plant is activated or increased sharply in an attempt to restore the temperatures to desired set points as soon as possible. As activity in the buildings begins to vary throughout the day, violation of temperature set points across the complex begin to occur at different times in different buildings, with some exceptions, and the chiller plant behaves in a semi-continuous fashion. Additionally, at the end of the day, a finite time is required for the effects of lower occupation and lower ambient temperatures to cause the building to be cooled to the desired temperature set points, and therefore the chiller plant operates for about 2 hours beyond the drop in electric demand. Due to the control scheme of the chiller plant in this complex, the profile of the cooling demand is highly variable since it is governed by the number of violated temperature set points across the complex and ramping is determined by how many of these events occur simultaneously.

During the summer months, due to high ambient temperatures, the cooling demand is on average much higher than in any of the other seasons, and behaves more regularly with defined peaks and valleys since temperature fluctuations across the complex are not as prevalent. During the spring and fall months, the cooling demand can behave somewhat erratically, although features of higher daytime magnitudes and lower nighttime magnitudes are still present albeit superimposed with erratic behavior. During the winter months, the chiller plant does not tend to be needed due to the onset of low ambient temperatures.

Task 3.2.5. Office Building Type

3.2.5.1. Monthly and Weekly Load Statistics

The monthly and weekly minimum, maximum, and average demand values for each load type (chilling and electricity) for the office building type are displayed in Figure 53and Figure 54, respectively.

Figure 53: Monthly Cooling, Heating, and Electricity Trends: Office Building Type

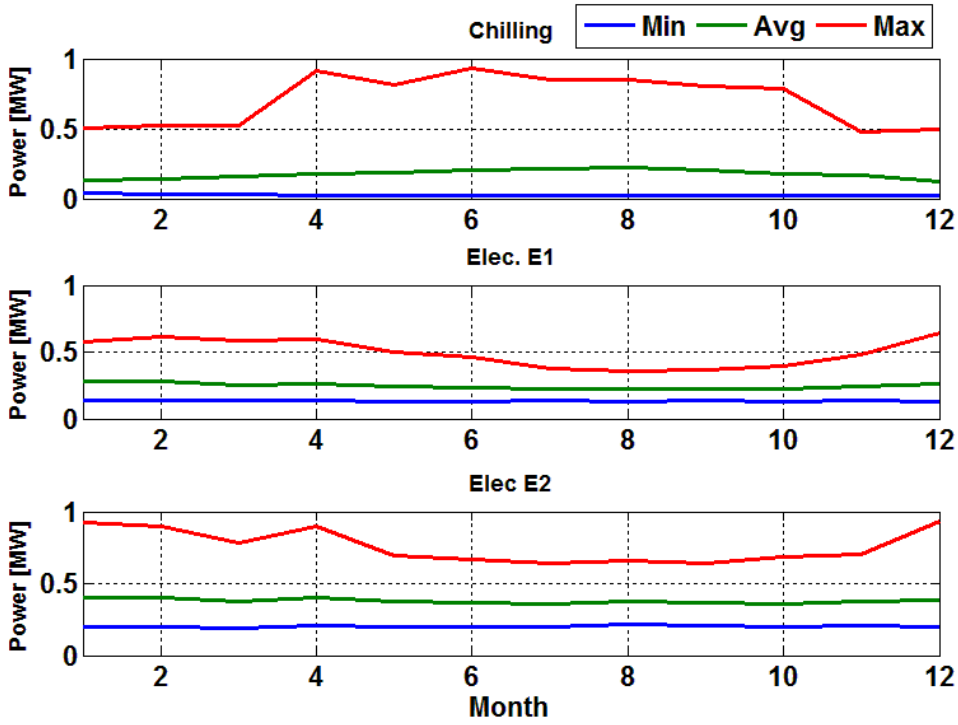

Figure 54: Weekly Cooling, Heating, and Electricity Trends: Office Building Type

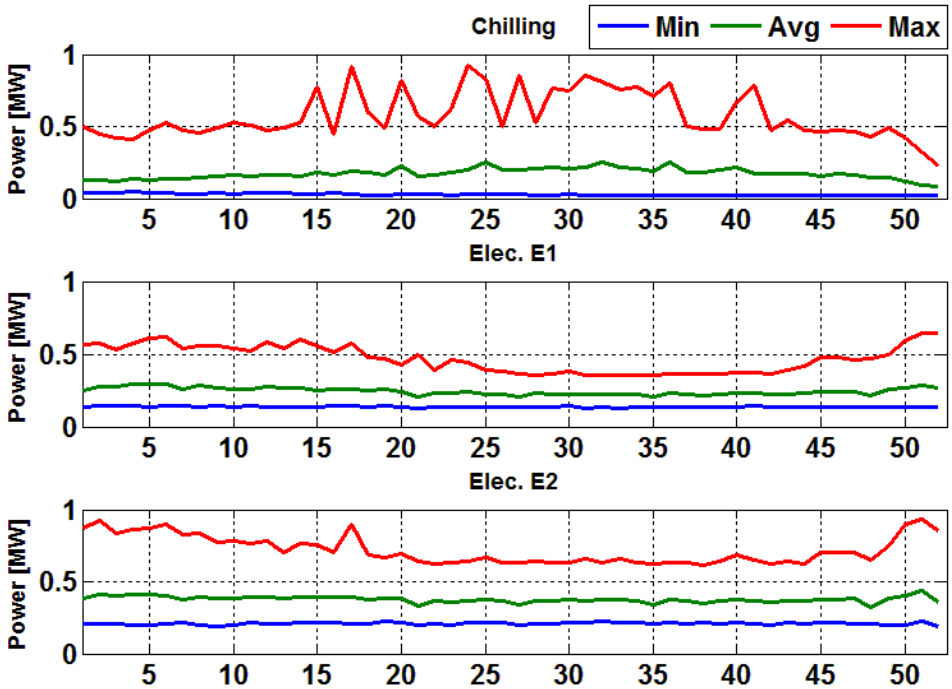

The average monthly cooling demand exhibits a distinct seasonal trend, with higher cooling demands present during the warmer months of the year and a peak value occurring during the month of August. Summer displays the highest cooling demands, spring and fall display slightly lower demands, and the winter months display the lowest cooling demands as expected, driven by occupant comfort requirements and seasonal fluctuations in the average ambient temperature.

The maximum monthly cooling demand appears to occupy two value ranges, one range for the winter months and another range for the remainder of the year. Similar to the hospital complex, the chiller plant at this building responds to violations of temperature set points and attempts to restore the temperature to the set point value as quickly as possible. This causes the chiller plant to operate at high values when it is activated or ramping up during a warm day for a short period, before ramping down as the temperature is restored. This behavior also causes the average monthly cooling demand to be more closely matched in magnitude to the minimum monthly cooling demand. The maximum monthly cooling demand has a similar value for the spring, summer, and fall months, since these values occur on days when the ambient temperature is high, the building is fully occupied, and a large amount of solar irradiance is present on the building, contributing to multiple heat sources for the building space. Days that exhibit these properties in the area of the building occur at least once during the summer, spring, and fall seasons due to events such as heat waves, contributing to nearly similar cooling demand levels on such days.

The minimum monthly cooling demand is essentially constant at a low magnitude throughout the entire year. During the night time hours when the building is not occupied and a minimum of heat-generating equipment is operational, meeting of the temperature set points for the building does not require the chiller plant to operate at a high power, and time periods with these properties occur regularly in all seasons over the course of any given month. Over the course of the year, however, the minimum monthly cooling demand is nonzero since a small amount of cooling must be maintained to meet the temperature set points in areas of the building with heat generating equipment that operate continuously, mainly data centers and servers in this particular case.

These trends are also reflected in the weekly cooling demand trends. The average weekly cooling demand tends to increase slightly during the summer months, with some perturbations along the year most likely corresponding to heat wave events. The minimum weekly cooling demand reveals no new information.

The maximum weekly cooling demand displays strong variability during the warm months of the year, with the maximum value fluctuating from week to week in the spring, summer, and fall months. These events occur due to the control scheme of the chiller attempting to restore temperature set points as quickly as possible, resulting in high power responses upon activation or ramping up. These events tend to occur more frequently during the summer months, but do not necessarily occur during every week and are dependent on the specific weather patterns of individual days.

Similar to the hospital complex, the average and minimum monthly electricity use of the building is fairly constant over the course of the year, since variations in the electric use occur over a diurnal timescale that is repeated within the course of any given month. The minimum monthly electricity use is nonzero due to the year round operation of data centers and servers, combined with night time lighting loads during minimum load points. This trend was exhibited by electric loads measured by both meters, E1 and E2, which meter separate loads within the building.

The maximum monthly electricity use does vary with season, however. In this case, maximum monthly electricity loads appear to be higher in the winter months, and somewhat higher in the spring months compared to the fall and summer months. This behavior is mainly due to the use of resistance heating for providing the heating needs of the building. In this office building, operation of plug loads is dependent on occupation which follows a diurnal timescale and would therefore appear constant from a monthly or weekly perspective. In addition, other plug loads such as data centers operate over the entire course of the year with relatively constant power usage. Heating loads, however, are seasonally dependent due to ambient temperature and irradiation fluctuations over the course of the year. The winter months exhibit the highest heating demands, translating in this case to higher electricity usage since heating loads are met by resistance heating.

These trends are also reflected in the weekly electricity use trends, which display a profile that very closely follows the monthly trend and reveals no new information.

3.2.5.2. Histogram Analysis

The distribution of the cooling load demand for the office building type is presented in Figure 55:

Figure 55: Cooling Demand Distribution: Office Building Type

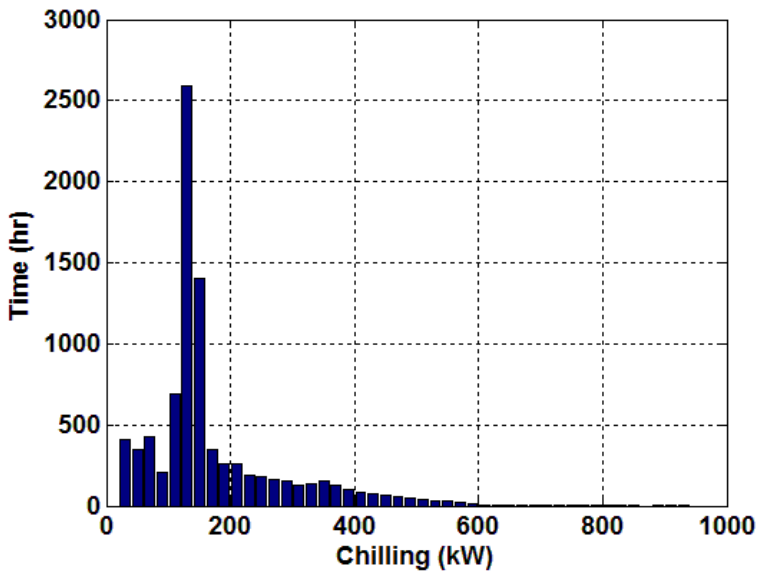

The distribution of the cooling demand over the year exhibits frequent occurrences of cooling demand magnitudes between 100 and 200 kW, with other occurrences being spread amongst a large range of values. Specifically, 130 kW is the most common value. The concentration of occurrences in the 100 kW to 200 kW range is most likely due to the fact that this happens to be the value of chilling power that is required to maintain temperature set points in the building in areas such as data centers and servers which operate continuously. Therefore, these values occur during essentially all of the non-work day hours, composing 15 hours of the day. Additionally, during days when the ambient temperature is low due to local weather patterns, this range of values occur since no additional cooling is required from the chiller plant. In the latter cases, the natural cooling of the building due to ventilation is enough to negate the heat sinks within building. This adds to the amount of time that the cooling demand values fall within the 100 kW to 200 kW range. Also, in contrast to the hospital complex which is represented by a series of buildings, this office building is a single establishment with a significantly lower thermal mass, indicating that the chiller plant does not have to operate for long periods of time at high values to meet temperature set points. This is exhibited by the low amount of occurrences at higher cooling demand values.

The distribution of the electric load demand for the office building type is presented in Figure 56:

Figure 56: Electricity Demand Distribution: Office Building Type

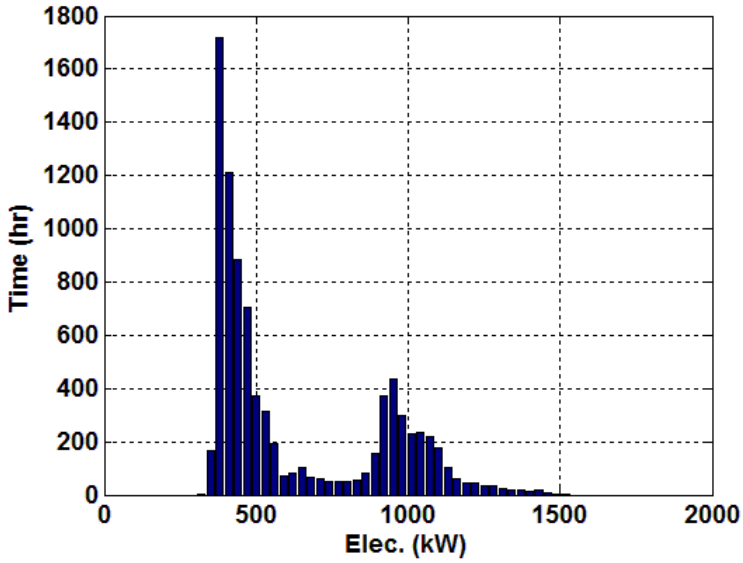

The electric usage distribution for this building displays a well-defined bimodal pattern, similar to that of the hospital complex but more pronounced. Note that the electric usage demand in this case displays the combined values of the E1 and E2 electricity meters. Electricity usage tends to fall within the ranges of 410 kW to 530 kW and 900 kW to 1150 kW. These values correspond to the periods of occupation and non-occupation of the building respectively. Many of the plug loads such as computers, lighting, and other office equipment are in operation during the typical work day schedule. Ventilation equipment also operates at higher load points during building occupancy. Heating loads also follow occupancy trends, and are also responsible for the higher electricity use values. Therefore, the 900 kW to 1150 kW range most likely represents periods of typical building occupancy. Variation in this range is dependent on occupant behavior. The range of values between 410 kW and 530 kW represents the typical periods of non-occupancy, when only data centers, night time lighting and a minimum of ventilation equipment is in operation. Small variance within this range depends on the variation in the operation of these components.

3.2.5.3. Sample Day Analysis

Sample representative daily profiles of the electric and cooling demand for the different seasons are displayed in Figure 57:

Figure 57: Sample Daily Demand Profiles by Season: Office Building Type

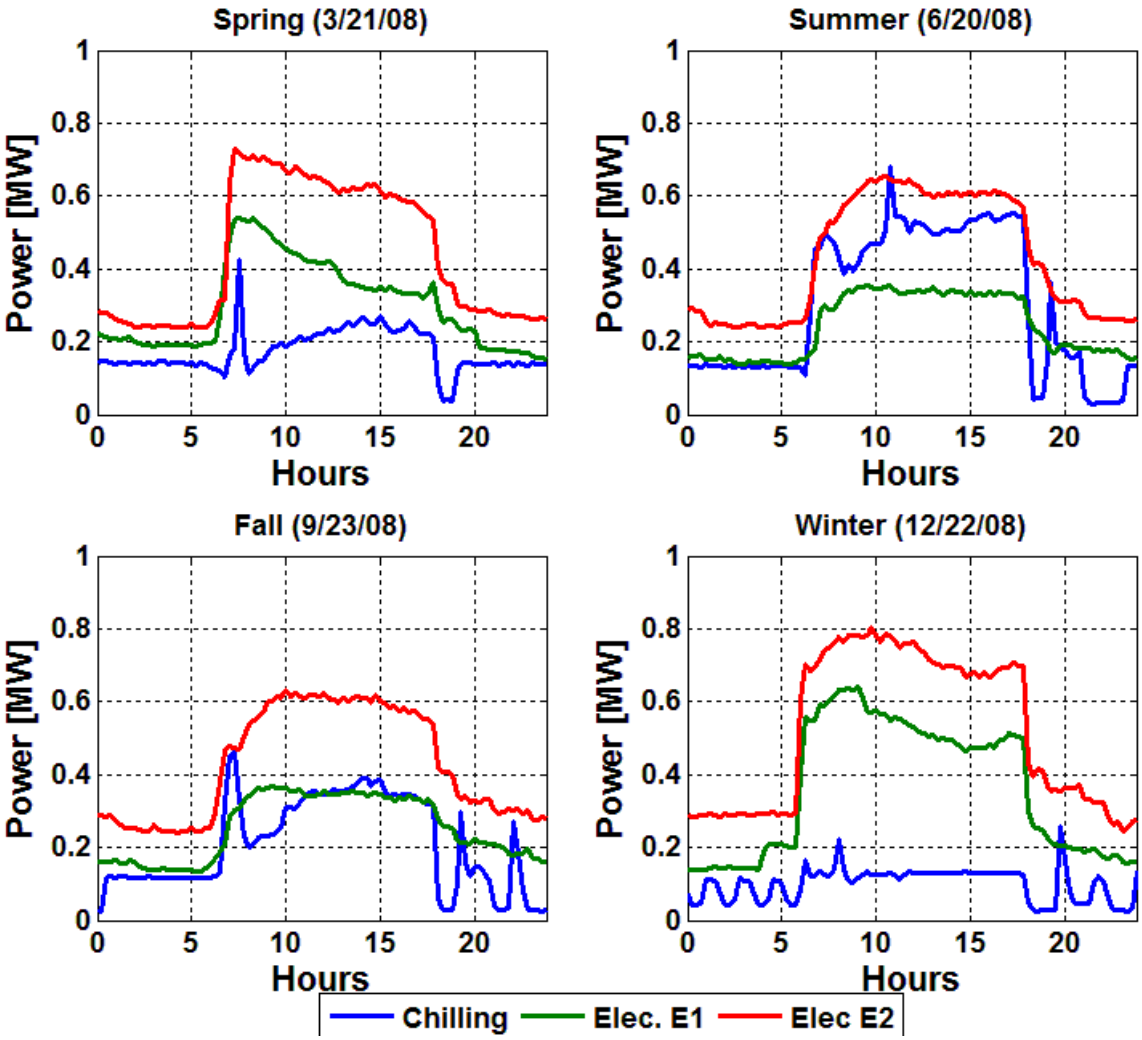

The cooling demand follows the building occupancy trend, with higher cooling demand values present during these hours in all seasons except the winter, when the cooling demand value settles around the minimum value required to cool the continuously operating data center and server equipment. The chilling profiles in the spring, summer and fall months display the characteristic high power, short duration response of the chiller plant during violations of temperature set points. This pattern is exhibited at the beginning of the day for all three of these seasons, due to building occupancy and operation of office equipment emerging as heat sources. After the initial increase in cooling demand in response to the onset of building occupancy, the chiller plant adjusts depending on ambient conditions. In the summer months, the high chiller power level must be maintained since ambient temperatures and solar irradiance values are high, whereas during the spring the chillers are allowed to ramp down. Depending on the weather pattern on a particular day, the chiller plant must either respond rapidly to more perturbations or settle on an acceptable value.

In contrast to the hospital complex, the cooling demand profile in this case is aligned with the occupancy profile in time. This is due to the fact that since this single building has a much lower thermal mass than the hospital complex, it does not require a long period of time for the building to restore temperature set points due to perturbations such as the beginning of the work day and end of the work day. The lower thermal mass allows the chiller plant to respond quickly to temperature perturbations within the building. Additionally, since this is a single, 19-floor building and the usage of the building space is similar on all floors, the violation of temperature set points within the building tend to occur simultaneously. Therefore, the cooling demand profile is less erratic than that of the hospital complex.

The daily electricity use trends represent building occupancy trends, increasing sharply at the beginning of the work day and decreasing sharply at the end of the work day during all seasons. The E2 electric meter appears to measure the larger fraction of the building electric loads. The magnitude of the electric use values are distinctly higher in the winter months and somewhat in the spring months during the periods of building occupancy due to the heavy use of resistance heating for occupant comfort during periods of low ambient temperatures and low solar irradiation values. The summer months exhibit the lowest electricity usage values due to the lack of heating needs. All seasons display nonzero electricity use during non-occupancy periods due to continuously operating equipment.

Task 3.2.6. Summary of Dispatchable Load Types

In this analysis, the three primary load types that have been examined are chilling, heating, and bulk electricity loads. The dispatchability of each load type in each building type will be discussed briefly herein.

3.2.6.1. Hospital Complex Type

For this complex type, examination of the chilling, heating, and bulk electricity loads was conducted separately. The cooling loads followed a distinct seasonal pattern, with higher values during the summer months compared to the remainder of the year. Dispatching cooling loads on these timescales – monthly and weekly – is very difficult in practice. The two main methods of dispatching cooling loads are via demand response or cold thermal energy storage. In the case of demand response, this would require allowing the temperature to float for certain periods to limit the maximum chiller power. This cannot be done on a seasonal or weekly timescale since the thermal mass of the building is not sufficient to maintain acceptable temperatures over such long periods of time. In the case of energy storage, weekly or seasonal thermal energy storage would require a very large scale system which would be impractical and difficult to operate.

It is more feasible to apply these methods to shape the diurnal profile to accommodate increased renewable penetration on the electric grid or within a given community, and attempt to minimize the total amount of energy required to meet the cooling demand. With thermal energy storage, the power usage of the chiller plant can be decoupled from the dynamics of the

cooling load demand within the complex, and can be shaped to accommodate an increased amount of renewable resources due to increased flexibility.

The heating loads are relatively constant on average across the day and the entire year. Periodic fluctuations in load, typically confined to a certain range, occur due to the activation and de-activation of process loads which occur on fairly short timescales. Due to the strong dependence of the heating load on process loads and the presence of a fairly constant profile on average, the heating load in this type of complex is difficult to dispatch. Techniques such as solar heating can be used to reduce the amount of fuel required by the natural-gas boiler that provides the heating energy, and hot water thermal energy storage can be used in combination to maintain the relatively smooth average profile of this load type. In this case, however, altering the heating load profile to reduce variability is not a likely option since the variability is already fairly low.

The bulk electricity loads are relatively constant over the course of the year, however this load type is characterized by a well-defined diurnal profile which represents the daily occupancy trend of the complex. This load type can be dispatched on the diurnal timescale by the use of electric energy storage, which can charge during periods of low load and discharge during periods of high load. This will create a smooth and predictable electric load profile and reduce peak demand charges, at the expense of requiring an increased amount of overall energy to meet the load. Additionally, the energy storage system can be dispatched to respond to variations in intermittent renewable resources, charging and discharging when necessary to create a smooth, more predictable effective load profile.

Therefore, for the hospital complex type, a list of the dispatchable loads and corresponding energy capacities are as follows:

Table 14: Dispatchable Loads: Hospital Complex Type

Load Type	Dispatchable	Energy Capacity	Units
Chilling	Yes	87,581*	MMBTU
Heating	No	382,595	MMBTU
Electricity	Yes	9.533	GW-hr

*Note that the Energy Capacity is displayed in terms of MMBTU, which is the cooling demand of the complex. The chiller power used to meet this demand is obtained by dividing this number by the coefficient of performance, indicated to have an average of 4 for this particular chiller plant.

3.2.6.2. Large Office Building Type

For this complex type, due to the use of resistance heating, the heating demand was grouped in with the electric demand. Therefore, it is only the chilling and electric demand that is examined separately.

The cooling demand in this building type is much more predictable due to the lower thermal mass and uniform behavior of temperature changes throughout different areas of the building. Following a strict diurnal profile that follows building occupancy trends, distinct periods of high and low demand ranges exist. Demand response measures can be used to shape the cooling load profile to accommodate the high power, short duration nature of many intermittent renewable resources on the electric grid or community. Cold thermal energy storage can be used to decouple the chiller power use from the cooling demand, and grant a degree of flexibility that allows the chiller power use to be shaped to accommodate intermittent renewable resources while still meeting the cooling demand.

The electricity demand can also be dispatched in the same manner as that of the hospital complex type, using electric energy storage. In this particular case, this also allows the heating demand to become somewhat dispatchable since it is tied to the electricity demand. This storage system can be dispatched to charge during periods of high renewable power generation and discharge during periods of low renewable power generation, contributing to a smooth and more predictable effective load profile.

For the large office building type, a list of dispatchable loads and corresponding energy capacities are as follows:

Table 15: Dispatchable Loads: Large Office Building Type

Load Type	Dispatchable	Energy Capacity	Units
Chilling	Yes	1.515	GW-hr
Electricity + Heating	Yes	5.486	GW-hr

Task 3.2.7. Examples of Distributed Energy Management Opportunities

Examples of the capabilities of utilizing certain distributed energy management strategies such as chiller plant dispatch and energy storage to respond to load signals which contain the behavior of intermittent renewable power fluctuations within the signal characteristics.

3.2.7.1. Chiller Dispatch with Thermal Energy Storage

The input load signal is the effective load demand that must be met by dispatchable generators on the electric grid, after the effects of intermittent renewable generation have been included. In this particular analysis, the load signal corresponds to a renewable penetration level of 33% on the electric grid of the state of California, and the effect of dispatching the chiller plant to respond to the behavior of such a load signal modeled using a dispatch optimization code which determines chiller operation periods based on a cost function. The specific details of the renewable power portfolio used in the load signal, details of the statewide load signal and the algorithm and description of the chiller optimization code are presented in detail in the report for Task 3.4, presented in another section of this deliverable report.

For the chiller dispatch example, the hospital complex type is used. The cooling demand is converted to the electric demand equivalent using a coefficient of performance of 3.5, as provided in the available data. The equivalent of implementing chiller dispatch at 2000 complexes of this type across the state of California is used to examine the effect of chiller dispatch on supporting increased renewable penetration levels on the statewide electric grid. A sample time series demonstrating the effect of utilizing chiller dispatch to respond to load signal fluctuations in an attempt to support renewable power generation is presented in Figure 58:

Figure 58: Sample Time Series of Chiller Dispatch Effects on Utility Grid at 33% Renewable Penetration Level

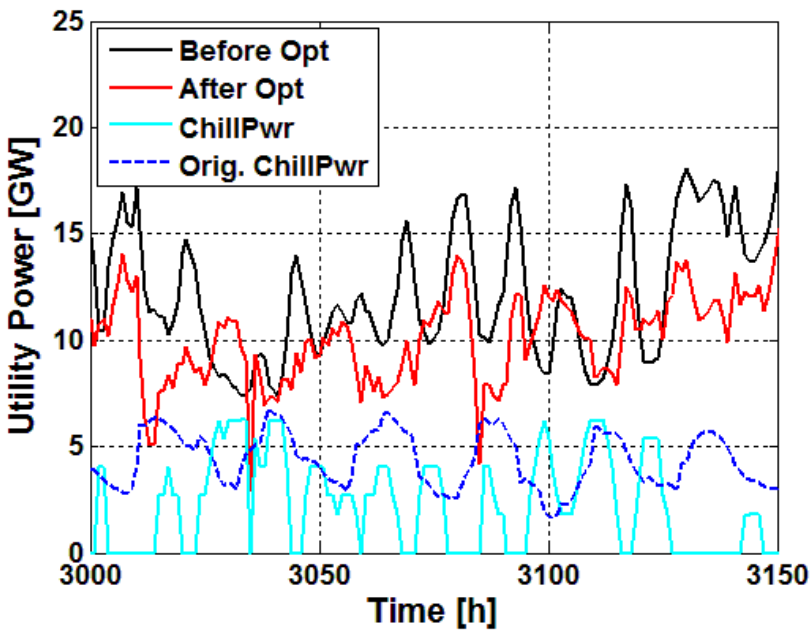

Displayed are the load profiles on the utility grid before and after the use of chiller dispatch at 2000 hospital complexes at a 33% statewide renewable penetration level, the original aggregated chiller power usage (which matches the cooling demand exactly) and the chiller power usage after dispatch. Both cases satisfy the cooling demand of the hospital complexes. The effective load profile on the electric grid before the use of chiller dispatch is fairly erratic due to a high penetration of intermittent renewable power resources which exhibit intermittent high power, short duration generating characteristics. This causes the effective load profile to contain many large fluctuations. After the use of chiller dispatch, however, the effective load profile on the electric grid still displays fluctuations but to a reduced extent compared to the case before chiller dispatch utilization. The dispatch of the chillers in this case is able to remove cooling load from periods of high electric grid loads and re-introduce such loads during periods of low electric grid loads, effectively responding to the combined variability of intermittent renewable resources and the raw load demand. On average, the grid load profile after chiller dispatch displays regular power fluctuations confined to a smaller range of values compared to the non-dispatch case.

Task 3.2.8. Electrical Energy Storage Model

This section investigates the use of electricital energy storage at a building. The electrical energy storage model is a physically-driven, rule-based model. It uses the system's physical behavior and operation to advise the rule-based constraints imposed (following the logic in Figure 59). It can be applied to several electrical energy stoage systems by simply changing some of the model parameters as shown in Table 16.

For this electric energy storage example, the large office building type is used since all of the load types for this building are given in terms of electricity usage. In this example, the chilling, heating, and plug and light loads are combined into a single electricity demand profile for the entire building. The building is then subject to 800 kW of installed solar power generation, representing an approximately 16% solar penetration level by energy. Assuming that no solar power is curtailed, an effective load demand profile is created, taking into account the combined variability of solar power and load demand, defined as the load demand at each point in time minus the instantaneous solar power generation at the corresponding time. This effective demand profile is subject to an energy storage module described as follows:

The energy storage model is a physically-driven, rule-based model. It uses the system's physical behavior and operation to advise the rule-based constraints imposed. Following the logic in Figure 59, any signal can be inputted into the model including demand, renewable signal, etc. Next, the maximum load value in the demand signal is reduced by a small increment while the nearest earlier minimum is increased and assessed an energy penalty due to inefficiencies of charging the system. The ramp rate, power capacity, energy capacity and other operational constraints are checked to ensure they are not violated for the resulting signal. If these conditions are violated then the current iteration resets to the initial values and reruns. This process continues until the available power and energy capacity for every available time step is exhausted.

Figure 59: Flowchart of Energy Storage Model

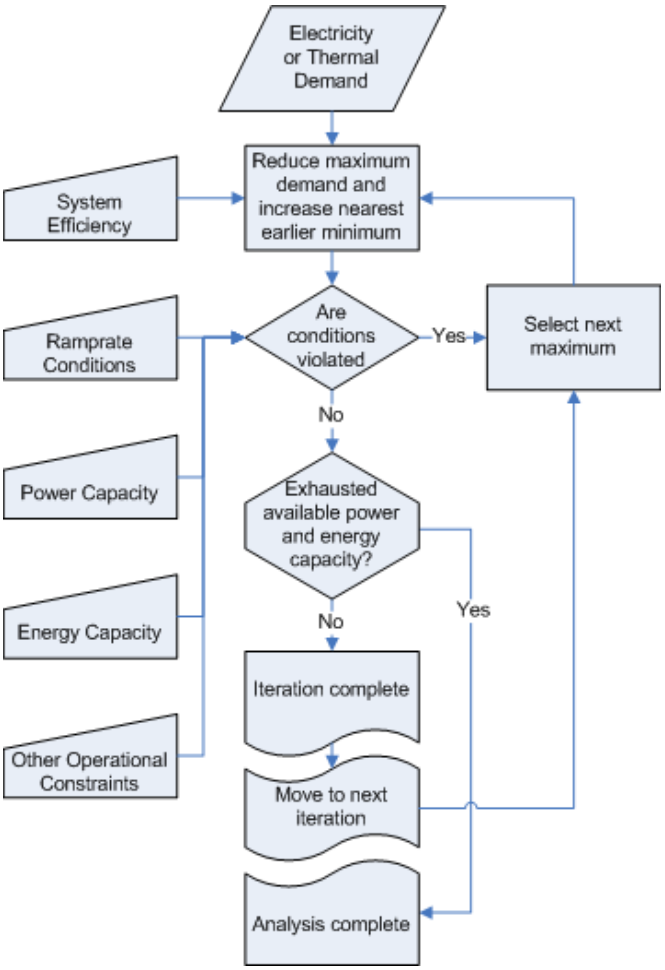

This control strategy shifts the maximum amount of load without violating any of the system constraints. The figures below show one example of the energy storage process that is modeled. Figure 60 depicts the peak to trough shifting described. Figure 61 and Figure 62 show the cumulative energy capacity and power demand, respectively. Notice the associated energy penalty for charging the system. This penalty is the energy that is lost in conversion or storage and does not contribute to the amount of generation.

Figure 60: Energy Storage Model Effect on Demand Signal

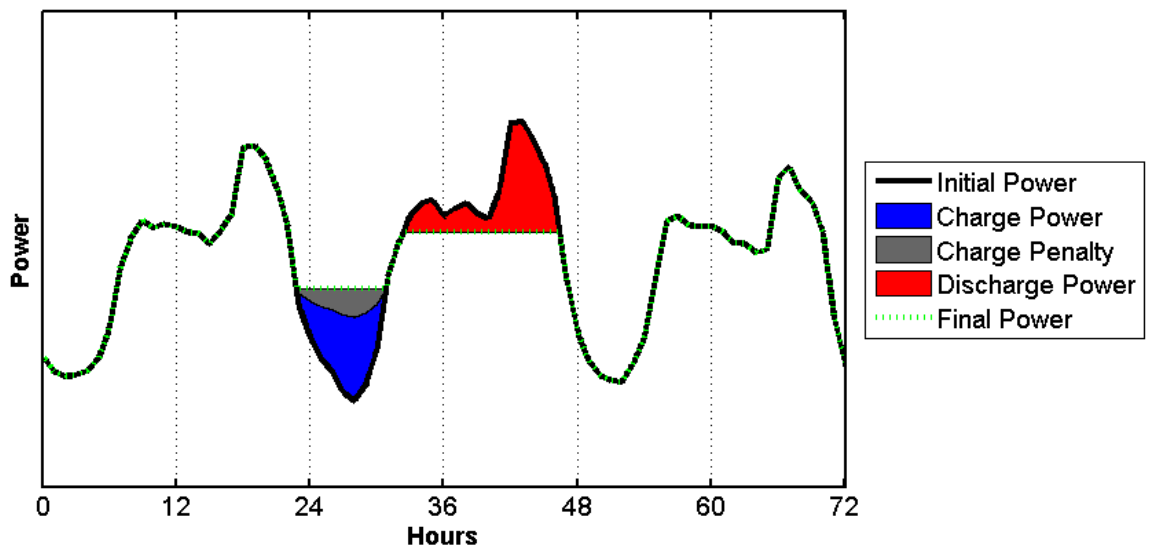

Figure 61: Cumulative Energy Capacity of Energy Storage System

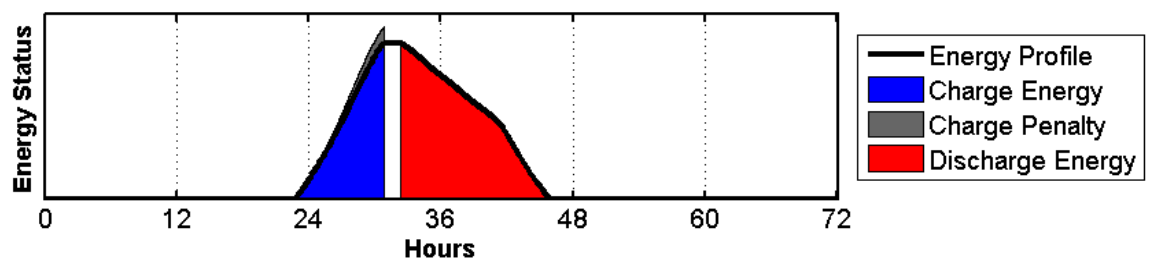

Figure 62: Power Demand of Energy Storage System

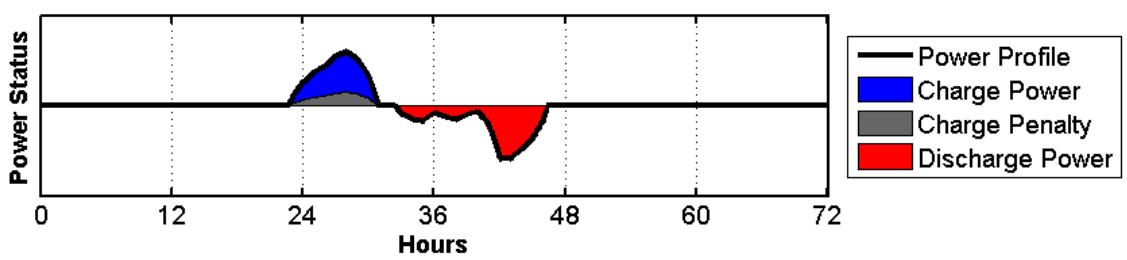

Information from the three figures above provides a complete picture of the operation of the model. While Figure 60 shows the resulting effect on the initial demand signal, Figure 61 provides information about the current and total energy capacity of the device. Lastly, the information used to generate Figure 62 constrains the charging and discharging power capacity

as well as the ramp rate of the system, since the derivative of the power status signal is the ramp rate.

In addition to the efficiency, power capacity, energy capacity and ramp rate of the system, the model considers variable charging and discharging power and has the ability to include additional operation characteristics dependent on the technology type. While the methodology is similar for all technologies, differing values for each parameter and the inclusion of additional operating characteristics are used to distinguish between technologies. Three examples of additional operating characteristics considered for pumped hydroelectric storage are 1) a constant "charging" of the system caused by the input of water from streams and runoff, 2) reservoir capacity and 3) flood and other safety constraints. Modeling energy storage in this way ensures that the storage system is operated to the greatest extent of its operating range while accounting for the critical operation characteristics of the system.

In this particular example, the energy storage system is assumed to be a Vanadium Flow Battery with the following parameters:

Table 16: System and Case Parameters

Parameter	Value
Storage System Efficiency	85%
Charge : Discharge Ratio	0.8
Power Capacity	50% of Max. Load
Duration Capacity at Rated Power	2 hours

A sample time series displaying the effect of applying electrical energy storage to manage intermittent renewable variability at a large office building is presented in Figure 63:

Figure 63: Sample Time Series of the Effects of Energy Storage in Managing Solar Variations

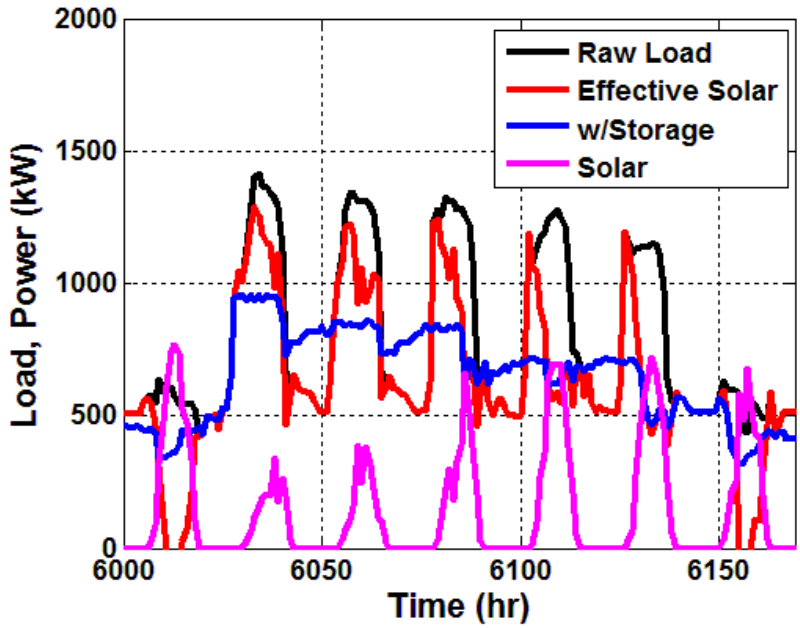

During this sample week, the presence of solar power introduces increased variability in the effective load demand profile. The presence of a high amount of installed solar power capacity introduces small fluctuations into the effective load demand. Additionally, the quick ramping characteristics of solar power subjects the effective load demand, which must be met by electric grid imports, to very quick changes in load point. During the weekends, the electric load in the building is very low, and the presence of solar power causes the effective load demand to drop to zero, necessitating the curtailment or export of excess solar power. Overall, the presence of solar power increases the range of variability of the effective load demand and can pose issues for generators that must meet this load.

The presence of energy storage allows smoothing of the electric load profile during periods when the building is subject to quick fluctuations in raw load demand (chilling, heating, plug) or quick variations in solar power. During periods of high effective load demand, the energy storage system is able to discharge to level such load peaks and prevent the peak grid import power from reaching large values. During periods of low effective load demand, the energy storage system is able to charge and impose a load on the system, preventing the electric load demand from decreasing to very low values, especially on the weekend days where it is able to prevent the onset of excess solar power generation. The implementation of energy storage system essentially allows the effective load demand characteristics to resist perturbations due to increased renewable power penetration.

Task 3.2.9. Conclusions

- Collected and analyzed monitored data from several institutions
- Using advanced chiller dispatch reduces the fluctuations in the load profile compared to the case before chiller dispatch utilization

- Cold thermal energy storage offers the ability to smooth the electric load profile when a building is subject to quick fluctuations in load demand
- Cold thermal energy storage systems are able to level load peaks and prevent the peak import power from reaching large values during periods of high load demand
- Thermal energy storage systems are able prevent the electric load demand from decreasing to very low values during periods of low load demand

Task 3.3. Use of BEV Charging to Manage Intermittent Renewables

Task 3.3.1. Feasibility of PEVs

Vehicle electrification has been proposed to address the issues of oil independence, air quality improvement, and GHG emission reductions. Automobile manufacturers have been working on different electrified vehicles, such as plug-in hybrid electric vehicles (PHEVs), battery electric vehicles (BEVs), and fuel cell electric vehicles (FCEVs).

Fuel cell vehicles consume only pure hydrogen and do not have any limitation of function compared to conventional internal combustion engine vehicles. However, the cost of the vehicle and fuel, and the installation of the hydrogen refueling stations and the hydrogen supply are still potential barriers for the deployment of FCEVs.

PHEVs, from the perspective of energy consumption, may rely on gasoline or grid electricity, depending on the driving and charging behavior. Due to the dual powertrains, there is no limitation of function when compared to conventional ICE vehicles. Because there are two complete powertrains, vehicle capital cost can be very high compared to conventional vehicles. For example, the Chevrolet Volt costs $40,000 compared to a comparable Chevrolet Cruze at roughly $20,000. The dilemma for PHEVs is that designing vehicles with a large battery would increase the cost and underutilize the mechanical propulsion system, while using a small battery would not distinguish their performance significantly from HEVs.

BEVs, with the highest tank-to-wheel efficiency of any light duty vehicle technology, provide another option. Unfortunately, the limitation of range and the availability of the charging infrastructure have always been considered to be a barrier to the mass deployment of BEVs to the consumer market. However, as shown in Figure 64, statistical data shows that BEVs are feasible for a significant portion of the drivers in California.

Figure 64: Average daily VMT for different types of vehicles for weekday driving.

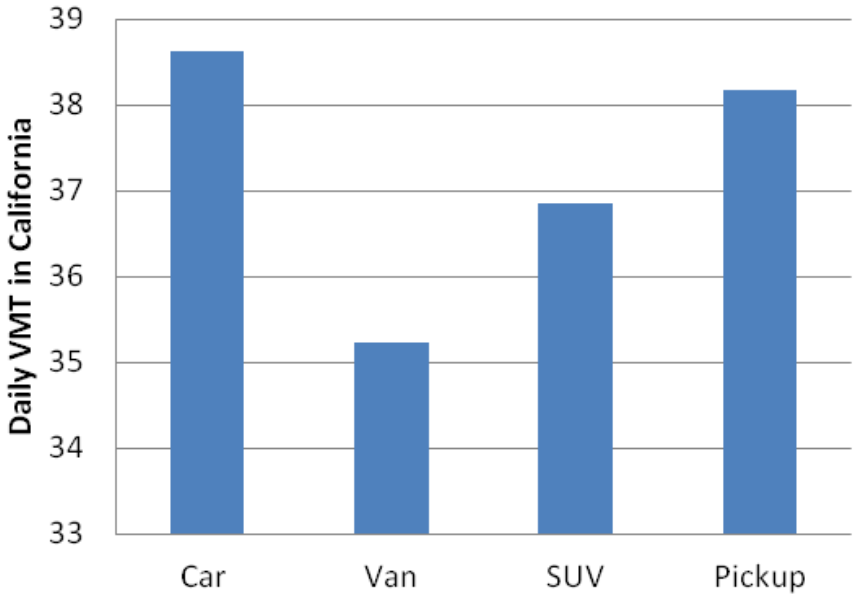

Figure 64 shows the average VMT from different types of vehicles when considering work trips during weekdays. The average daily VMT is lower than 40 miles for all four types of light duty vehicles, and current BEVs generally have ranges of 70 to 80 miles (e.g., Nissan Leaf). So, the limitation of range may be faced by few of the drivers for work trips.

Figure 65 shows the distribution of different types of vehicles. The cars (all sizes) contribute around 60% of the amount. Cars are clearly the most likely to be replaced by BEVs due to the size constraints of battery vehicles and the current manufacturer offerings. Consequently, it is likely that nearly 60% of petroleum powered light duty vehicles could be replaced by BEVs based on a simple vehicle size constraint. As shown in Figure 66, vehicles residing primarily at detached homes account for more than 80% of the dwelling time, implying that home recharging in a garage is likely for most drivers.

Figure 65: Distribution of light duty vehicle types in the California market.

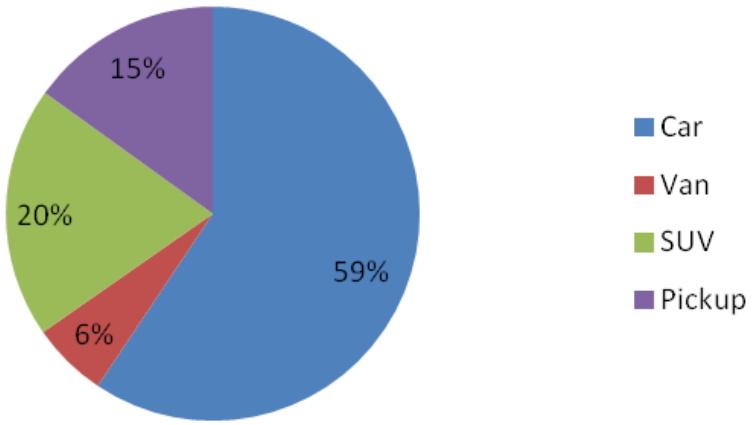

Figure 66: Distribution of California driver dwelling types.

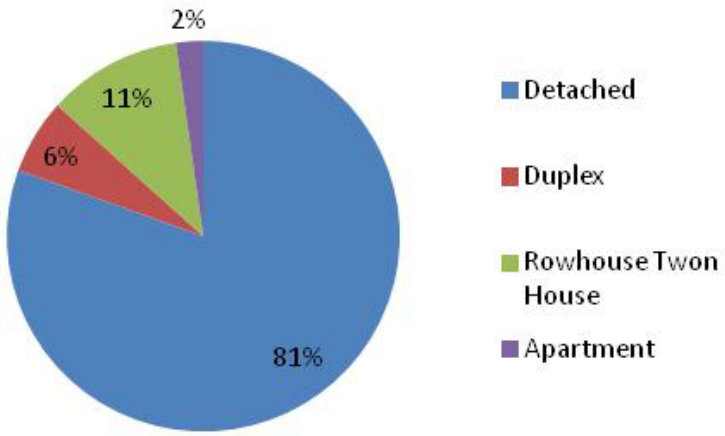

From the statistical data shown above, a rough judgment may be that BEVs can be used for the majority of work trips and that most drivers have the accessibility to recharge a BEV at home. As a result, these vehicles must be seriously considered in future energy plans.

Task 3.3.2. PEV Charging Analysis

In general, the analysis of charging infrastructure is complicated because: 1) recharging vehicle batteries takes a relatively long time, which usually is some amount of hours compared to a few minutes for gasoline refueling, and 2) due to the difficulty and expense in storing electricity, the generation and consumption of the electricity is simultaneous, which poses temporal challenges.

Charging infrastructure can support both PHEVs and BEVs. But, for BEVs, the only off-board energy source is from charging infrastructure while PHEVs may not have such a critical need

for charging because of the ability to use gasoline. In both cases, the proper infrastructure has to exist to support the utilization of PEVs without compromising mobility.

The goal of this work is to evaluate the energy and economic impacts of different charging profiles governed by time-of-use utility rates, and find the optimal scenario.

3.3.2.1. Methodology

1. Observe current vehicle operation
10. Assume people will not change the driving behavior when driving BEV
11. Assume there is charging infrastructure at specific locations depending on the scenario (home, work, other)
12. Quantify the cost of installation of the infrastructure (level 1, level 2, level 3)
13. Quantify the cost of 24-hour electricity; this process can be related to other properties of the electricity, such as GHG or pollutant emission
14. Minimize the operation costs and greenhouse emissions;
15. Sum up to a statistical result for a vehicle fleet.

3.3.2.2. Model

Figure 67 shows a schematic diagram of the Matlab model flow chart depicting inputs of infrastructure parameters, and output of total system cost.

Figure 67: Matlab PEV model flow chart

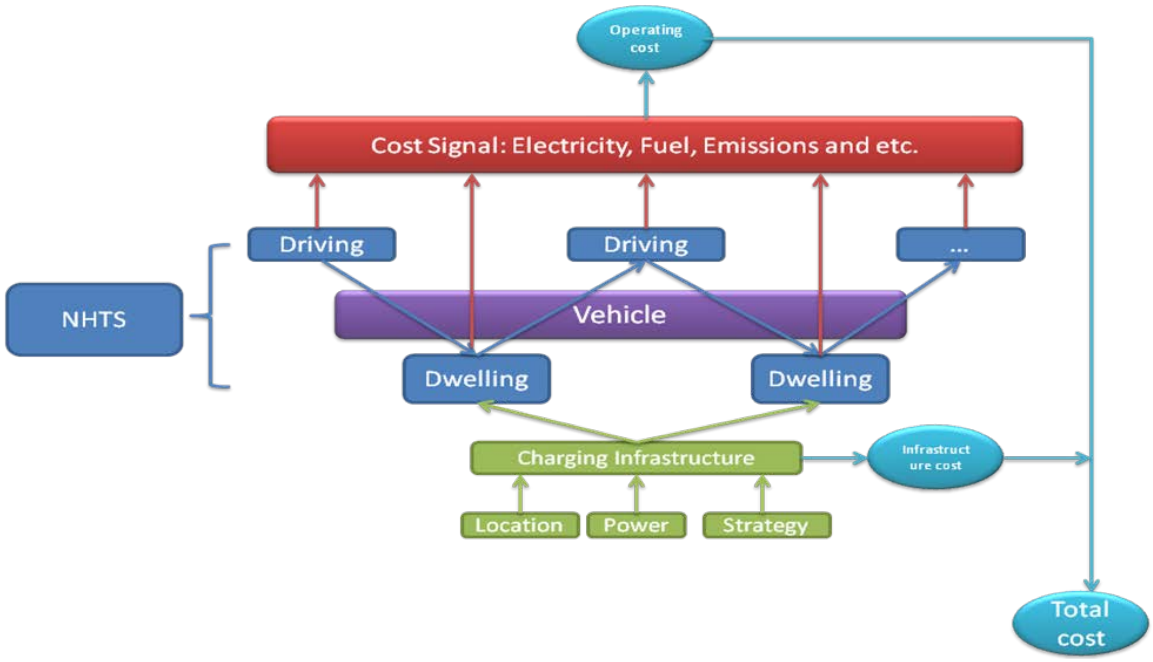

The model is based on the 2009 National Highway Travel Survey (NHTS2009), which provides a large amount of vehicle operation samples nationwide. All of the charging scenarios

combining different locations (home, work, other), different powers (1.44 kW Level 1, 2.88-7.2 kW Level 2) and different charging strategies (smart, immediate, delayed, and average) are evaluated based on different cost signal inputs.

Three cost signals are used in the model based on the SCE proposed EV charging rate and the generated charging rate from CAISO weekday load profiles. The SCE rate separates peak and off-peak rates, which are 10 cents/kWh from 9 p.m. to 12 p.m. and 20 cents/kWh from 12 p.m. to 9 p.m. The CAISO generated charging rate is proportionally scaled by the load profile in the range of 10 cents/kWh to 20 cents/kWh, as shown in Figure 68.

Figure 68: Real-time electric vehicle price signal generated by scaling CAISO load data between $0.10 and $0.20 per kWh.

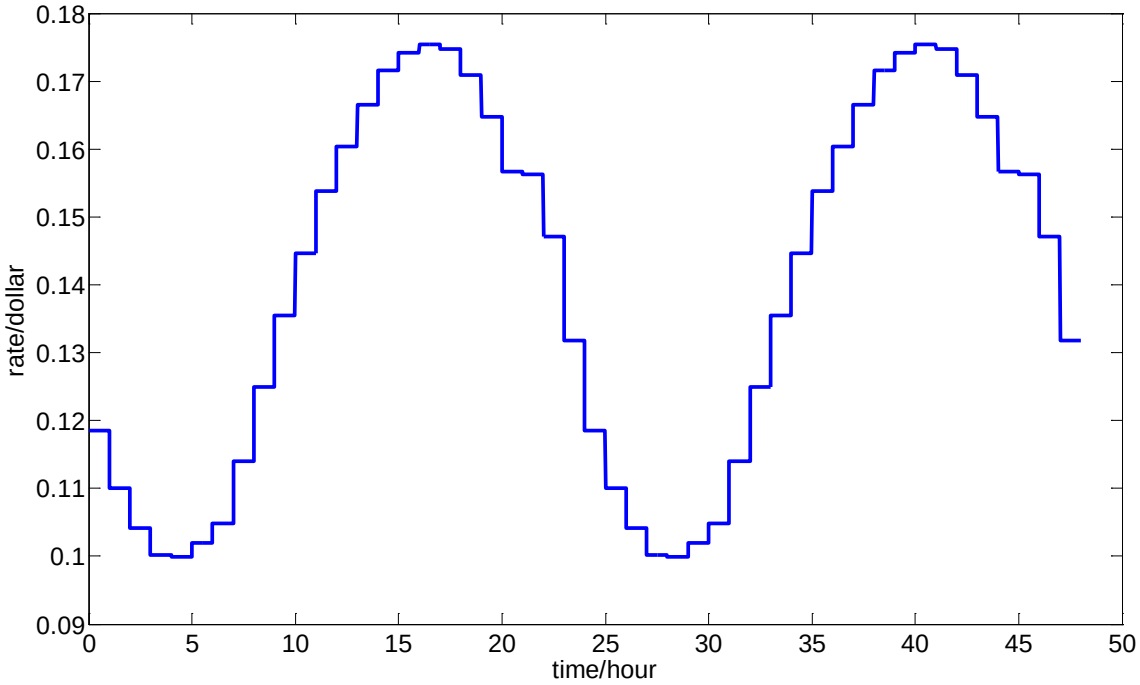

Some early information from utilities suggests that the variation of the electricity rate can be wider than that described in the previous section, so a third cost signal was developed to broaden the span. As shown in Figure 69, the new signal ranges from roughly 10 cents/kWh to 55 cents/kWh.

Figure 69: Real-time electric vehicle price signal generated by scaling CAISO load data between $0.10 and $0.55 per kWh.

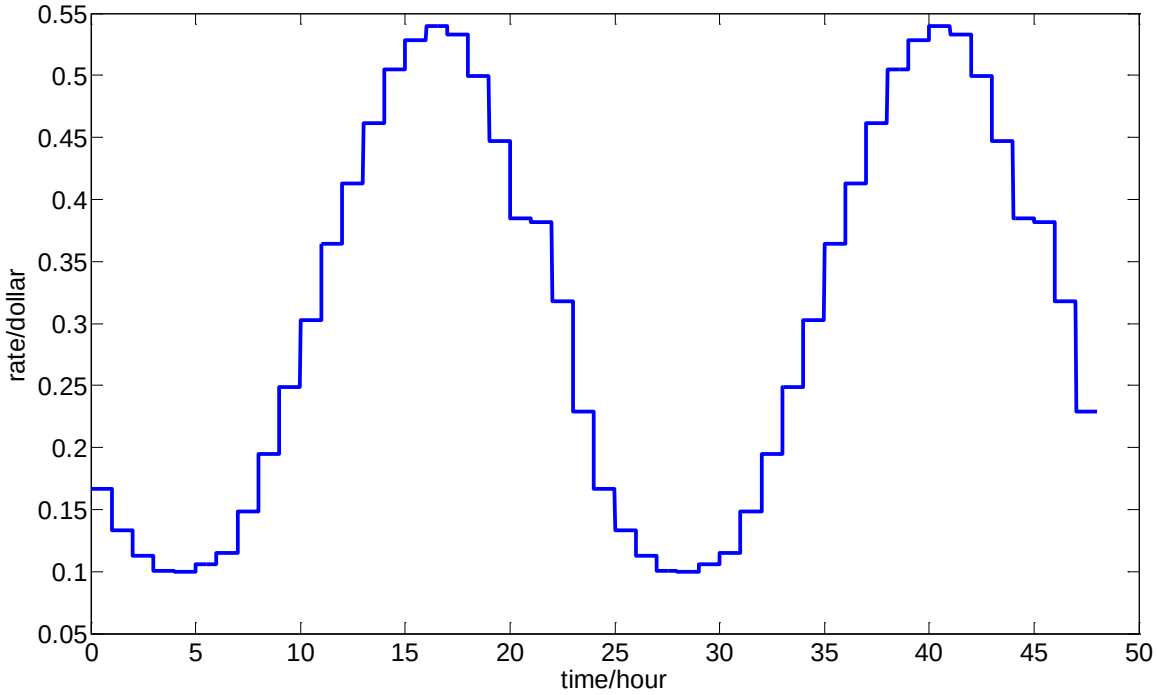

The cost of charging infrastructure must also be taken into account. An assumption is made that Level 1 charging, NEMA-15 based 1.44 kW, does not require additional infrastructure capital due to the ubiquitous nature of standard power outlets. This is likely true for home based charging, but likely a conservative estimate for workplace charging. Level 2 charging, based on SAE J1772, does require additional capital at all locations for the electric vehicle supply equipment (EVSE). This extra cost is assumed to be 10 cents/day for each vehicle based on the $3,000-$5,000 investment, with a 10 to 20 year lifetime.

3.3.2.3. Results

Work trips account for the largest portion of personal vehicle usage in the U.S. as indicated by the National Household Travel Survey. Additionally, the nature of work trips implies that this driving pattern is temporally repeated each weekday.

As described in the methodology section, all the charging scenarios are evaluated in the model; only a small portion of the most interesting results are shown herein.

3.3.2.3.1. Battery size

The first result shows the battery size requirement in order for BEVs to adequately satisfy consumer's normal driving behavior. The three lines in Figure 70 provide three different

scenarios. The black line shows the accumulated distribution of the battery size needed based on smart charging, in which the charging cost is minimum compared to all the other charging scenarios. The green line shows the scenario in which the minimum battery size can be achieved no matter what charging infrastructure will be needed. The red line is an intermediate scenario which describes the minimum battery size based on a smart charging strategy having realistic charging infrastructure scenarios.

Figure 70: Percentage of work trips achievable with minimum battery size or minimum charging cost.

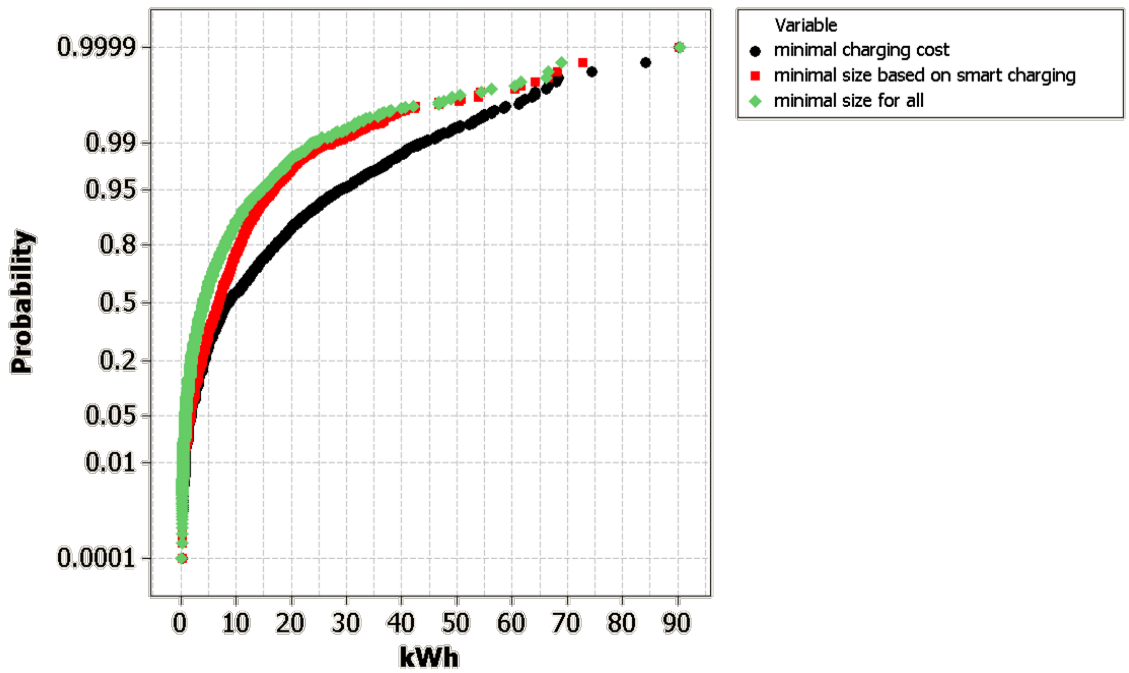

In general, the minimum battery size scenarios are very similar and distinct from the minimum cost scenario. The battery size for the early production EVs is around 25 to 30 kWh, corresponding to 80 to 100 miles electric range. Based on 80% battery usable capacity at the end of the vehicle life, the final capacity will range from 20 to 24 kWh, corresponding 65 to 75 miles all electric range.

With these numbers, it can be shown that more than 80% of vehicle trips can be performed by electric vehicles while minimizing the charging cost at the same time (black line in Figure 70). In the minimal battery size case, the percentage can reach up to 95% of trips.

3.3.2.3.2. Charging infrastructure requirement

The charging infrastructure needed to fulfill the scenarios shown in Figure 70 varies based on charging locations and charging power. Figure 71 shows the charging infrastructure distribution for the scenario of minimal charging cost. For the 7,028 home-based weekday work trips, all have home and work dwelling activities, and more than 60% have dwelling activities at some other locations. It is clear that home charging is needed for almost all the vehicles, with 55% requiring only 1.44 kW Level 1 charging, while the others rely on 7.2 kW Level 2 charging.

As for work locations, roughly 20% of the vehicles can achieve cost benefits from workplace recharging. Surprisingly, most workplace charging requires only Level 1 charging. For the locations other than home and work, less than 5% charging requirement can be observed where all of them are 1.44 kW Level 1 charging.

Figure 71: Charging infrastructure locations and power capacities required for minimum charging cost scenario for work trips.

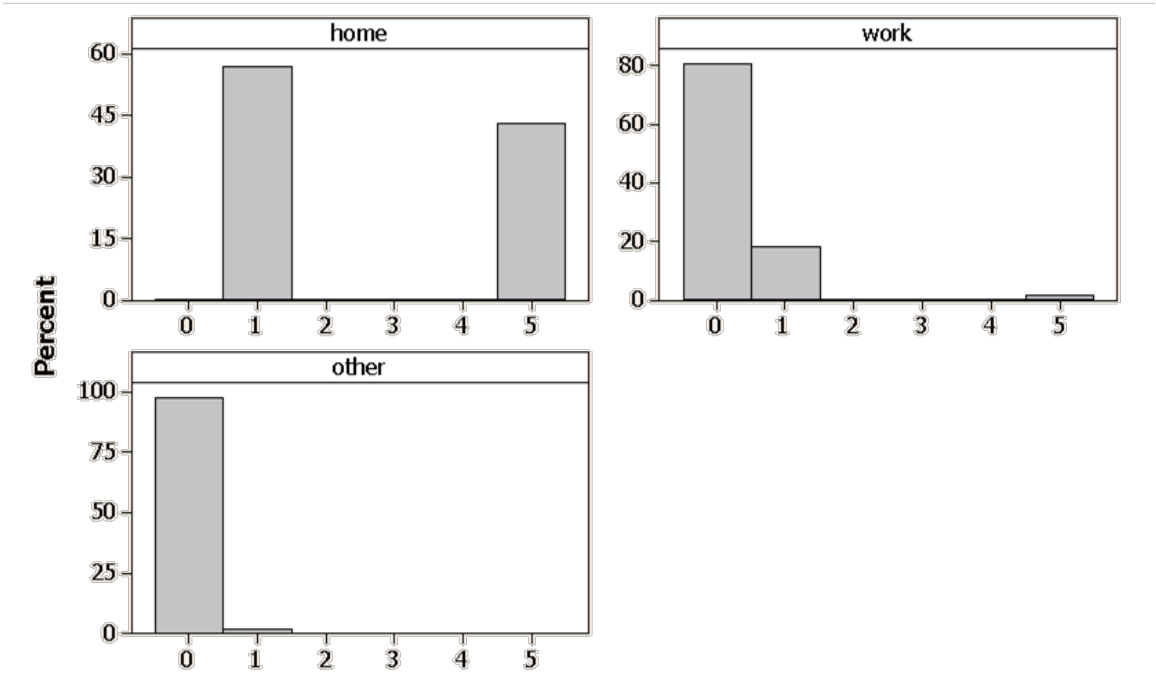

Figure 71 is somewhat misleading with respect to the charging requirements for "other" locations since some of the vehicles may not dwell at these locations. Thus, Figure 72 shows results for only vehicles which dwell at these locations and therefore provides a more explicit view of the requirement of charging infrastructure. Among the over 4,000 survey vehicles that stopped at other locations, less than 200 need 1.44 kW charging, and less than 5 require 7.2 kW charging.

Figure 72: Charging infrastructure required at non-home and non-work locations for minimum charging cost scenario.

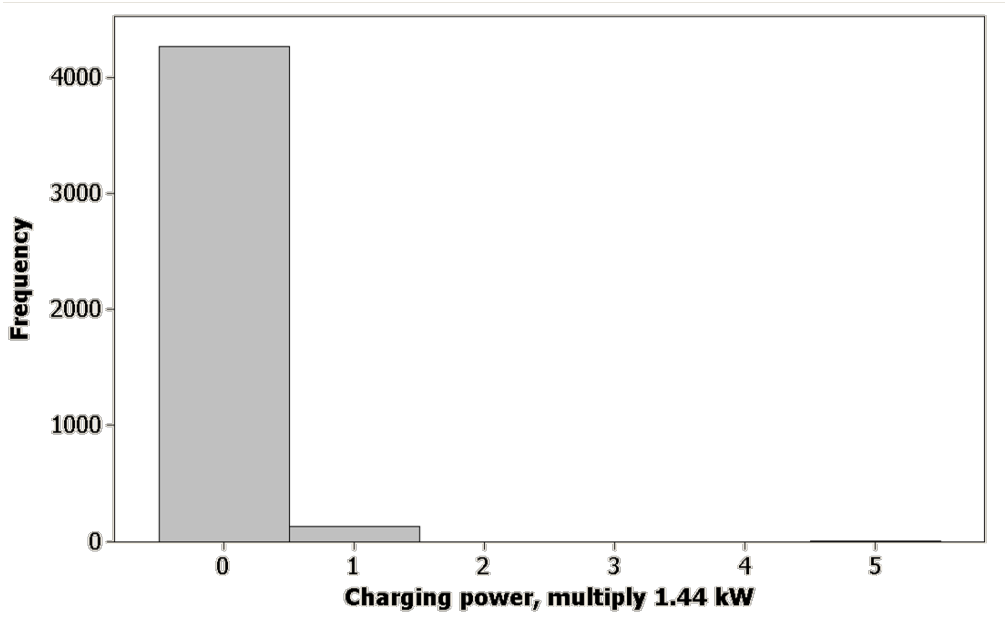

To summarize the requirement of charging infrastructure for weekday work trips, more than 80% of vehicles may be replaced by battery electric vehicles with battery sizes smaller than those announced by major auto manufacturers, while still able to minimize the charging cost from both electricity consumption and charging infrastructure installation. The corresponding requirement of charging infrastructure shows a clear trend that home charging is the most heavily utilized and work place charging is secondary. Charging at the other locations is minimal.

3.3.2.3.3. Infrastructure requirement for non-work trips on weekdays and weekends.

In general, the two results from weekday and weekend are very similar. Even compared to weekday work trips, these results do not show a substantial difference. Only a slight variation of battery size exists for the minimal charging cost scenario, as shown in Figure 73. For non-work trips, more vehicles can be replaced by electric vehicles with the same battery size compared to work trips because non-work trips have a shorter daily range than work trips, on average.

Figure 73: Percentage of non-work weekday trips achievable with minimum battery size or minimum charging cost.

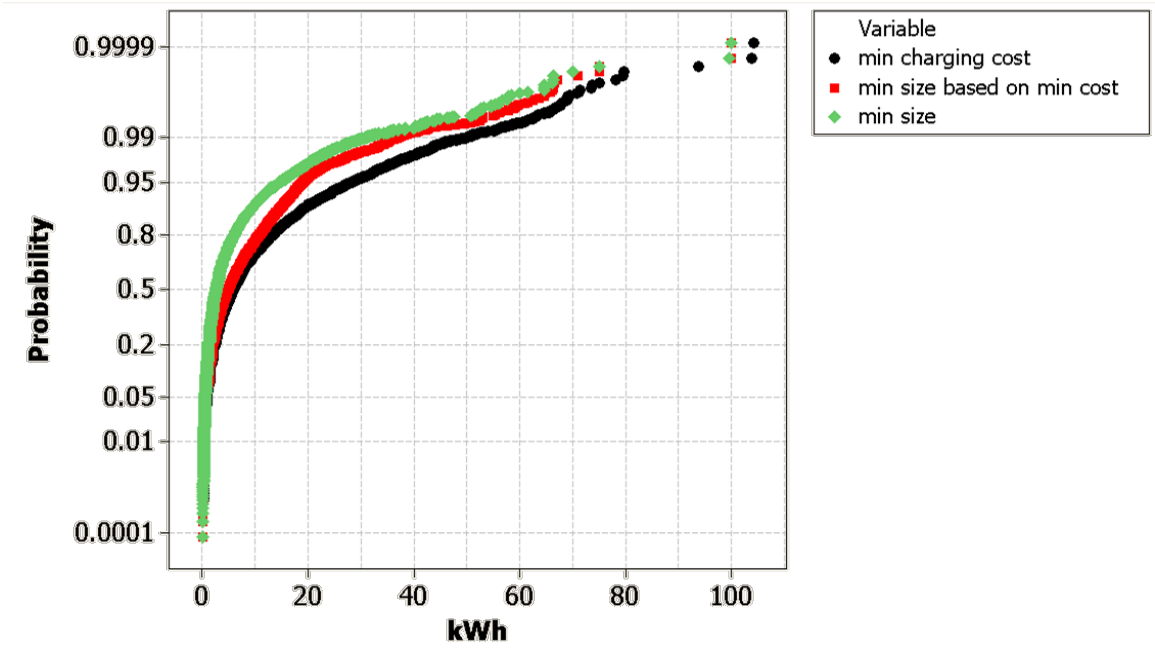

Another slight variation in terms of charging infrastructure is for home charging. The requirement for Level 1 and 7.2 kW Level 2 charging is 30% and 70%, respectively as shown in Figure 74. As a result, the non-work trips require fewer 7.2 kW, Level 2 chargers compared to work trips.

As for the charging infrastructure at other locations, non-work trips also shows the same trend as the work trips, which indicates that less than 5% of vehicles require charging at these locations. Figure 75 and Figure 76 show similar results for non-work weekend trips.

Figure 74: Charging infrastructure locations and power capacities required for minimum charging cost scenario for weekday non-work trips.

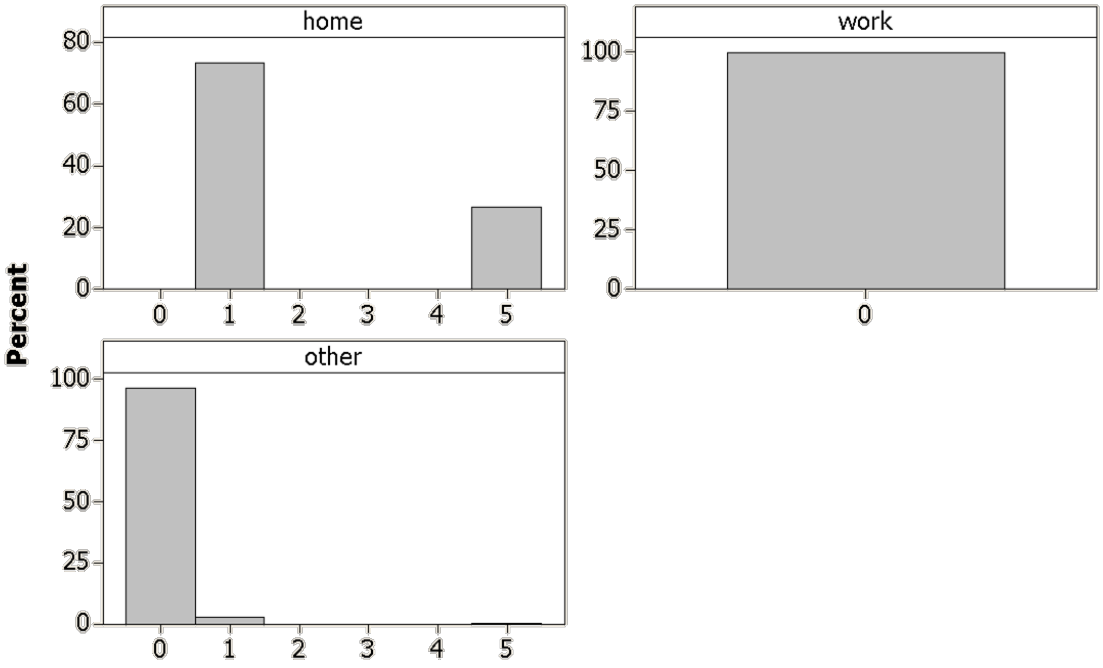

Figure 75: Percentage of non-work weekend trips achievable with minimum battery size or minimum charging cost.

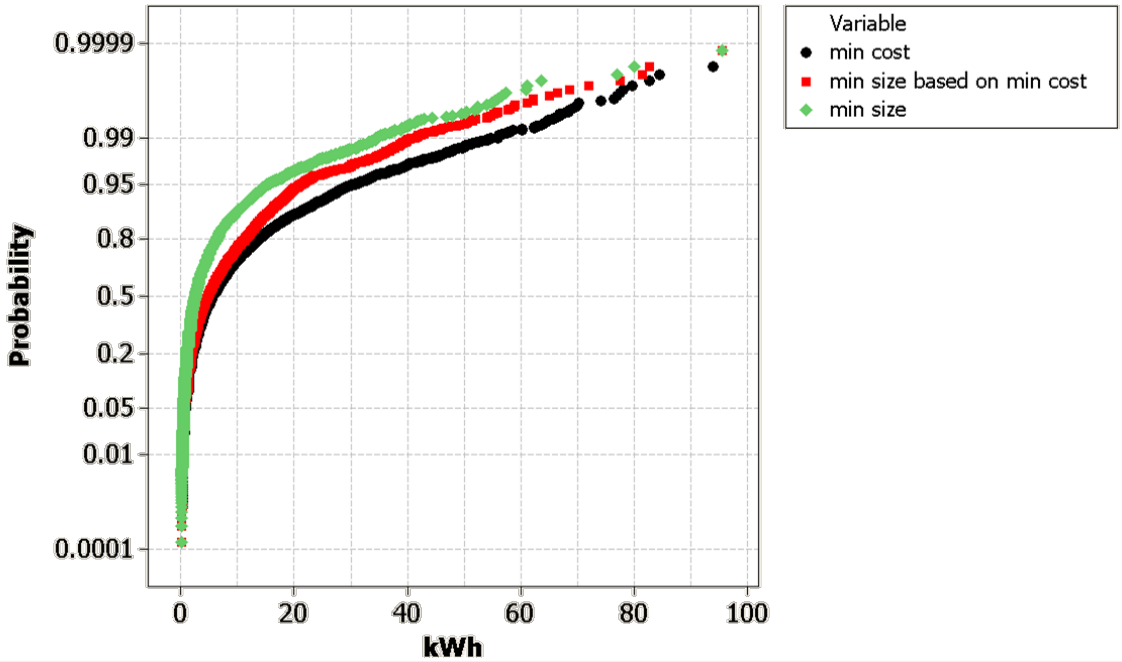

Figure 76: Charging infrastructure locations and power capacities required for minimum charging cost scenario for weekend non-work trips.

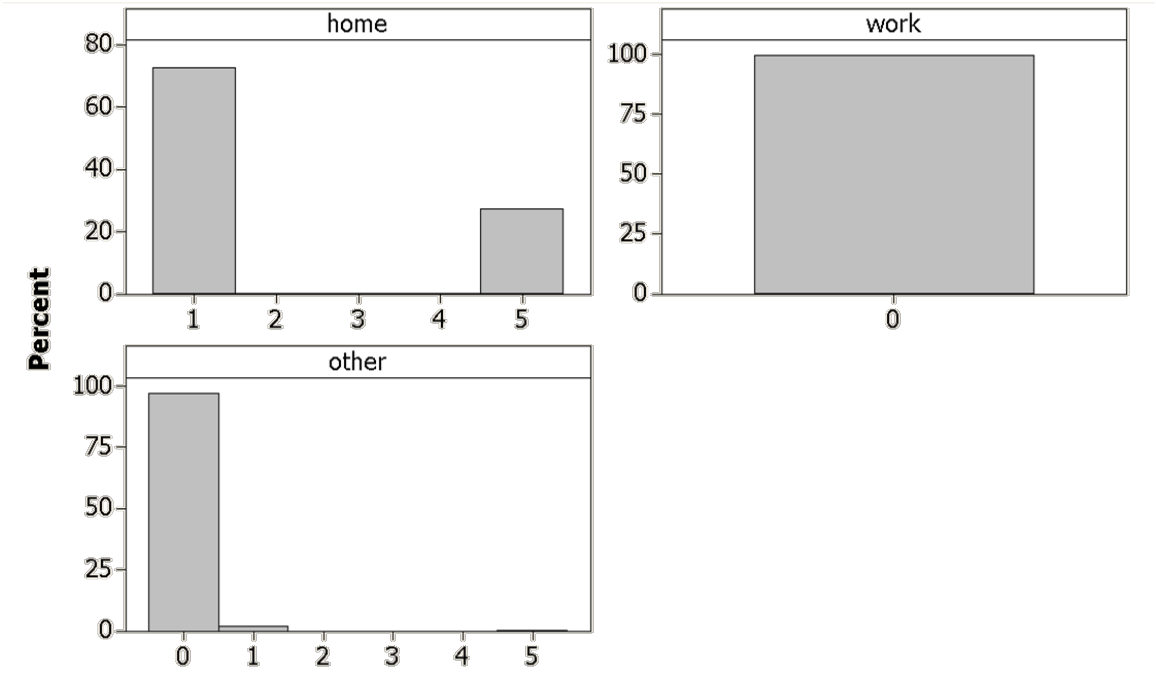

In summary, the infrastructure needed for non-work trips does not differ from that needed for work trips.

Task 3.3.3. PHEV infrastructure requirement

As stated previously, PHEVs do not solely rely on charging infrastructure to operate, and are able to satisfy travel demands due to the dual propulsion systems.

There exists an intuitive sense that PHEVs should be recharged as much as possible because more changing means more electric drive, higher efficiency, lower emissions, and lower cost. This statement is generally correct if the average characteristic parameters are used to calculate the emissions and operating cost. However, the generation and the consumption of the electricity are simultaneous, and the emission factor and the cost factor vary from time to time. The transmission and distribution cost changes from location to location as well. Take the electricity rates for example; the peak rate is at times more than the off-peak rate on a typical summer day. The residential EV charging rate from PG&E (Figure 77) gives a more specific example, which is 30 cents/kWh during the peak hour in summer. In this case, driving on electricity is more expensive than driving on gasoline, with current gasoline prices. The results similarly vary for the other products of the transportation system, such as GHG and pollutant emission.

Figure 77: Summer weekday electricity rates for PG&E.

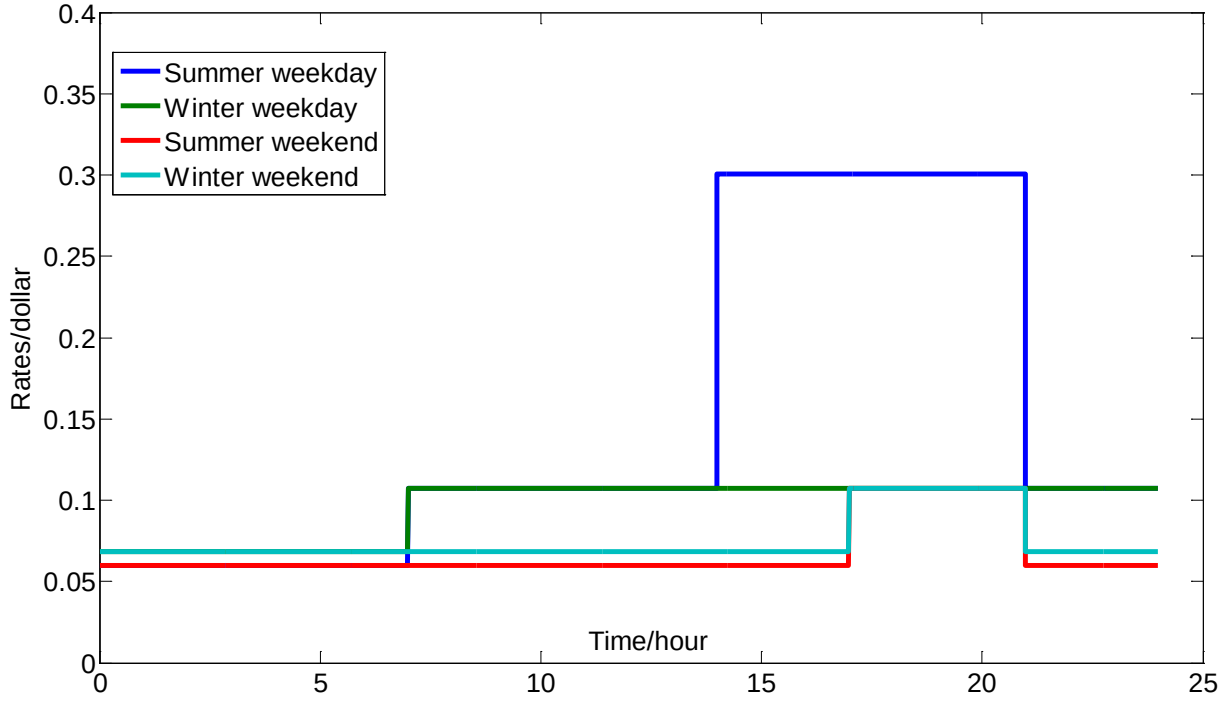

Figure 78: Summer Weekday Cost for Different PHEV Charging Scenarios

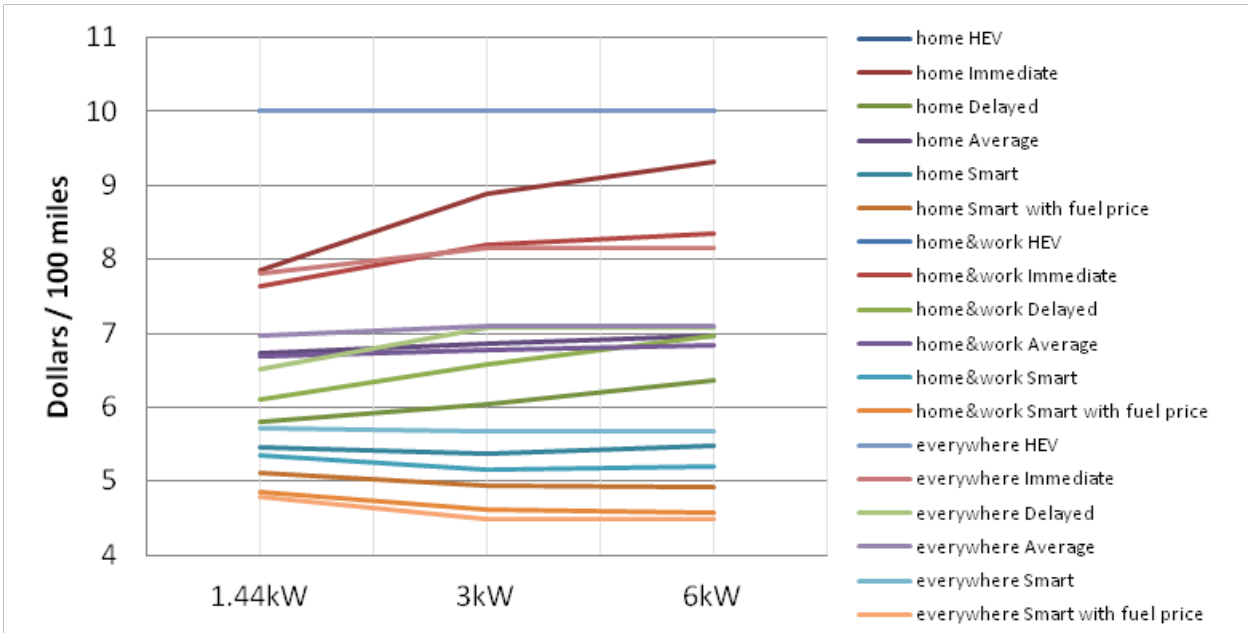

When PHEVs operate as simple HEVs, the cost is only dependent on gasoline expense and it is determined by the fuel efficiency and the fuel price. In Figure 78, a 40 MPG HEV requires a constant 10 dollars per 100 miles driven based on a fuel price of 4 dollars per gallon.

In this figure, all the other charging strategies for PHEV35 show a result of lower cost compared to the HEV case, which is considered to be one of the attractions for the potential PHEV consumers. However, the cost reduction varies widely. In general, the cost decreases from immediate charging, to average charging, to smart charging, and finally to smart charging with fuel price consideration.

3.3.3.1. Immediate charging

As shown in the set of red lines, one obvious trend is while increasing the charging power, the cost increases as well for all the locations, which means upgrading the charging infrastructure with higher power capability would increase the net charging cost. When the infrastructure cost is taken into account, high power charging is more expensive than 1.44kW Level 1 charging.

For the 1.44 kW case, charging strategies for all three locations show a very close cost result with a difference of less than 5% compared to the HEV cost. While for 3 kW and 6 kW cases, the costs of home & workplace and everywhere charging are close to each other; around 10% lower than home charging only. The reason is that high power immediate charging at home will increase the cost because most home immediate charging time would occur in the peak hour (before 9 p.m.) of the electricity rates. Contrarily, workplace charging can utilize the low rates in the morning and shift some of the charging load away from the home.

3.3.3.2. Delayed charging

As shown in the set of green lines, delayed charging assumes the driver knows the start time of the next trip so that the charging load can be delayed as much as possible. In general, in the

comparison with the immediate charging strategy, the delayed one shows 20% more reduction. However, like immediate charging, increased charging power consistently increases the cost for all the charging locations. The increase is from 5% to 10% while the power is from 1.44 kW to 6 kW.

3.3.3.3. Average charging

As shown in the set of purple lines, average charging cost displays low sensitivity to charging power, but the cost does climb as the charging power increases. Less than 5% difference can be observed, and adding more charging locations, especially those other than home and work, slightly raises the cost. In general, the average charging at different powers and locations shows a cost result with relatively small variation.

3.3.3.4. Smart charging

As shown in the set of light blue lines, the cost of smart charging is not sensitive to the charging power while the locations make a larger difference. The home & work place charging and the everywhere charging have the minimum and maximum cost respectively while the cost of the home charging lies in between. Compared to the other non-smart charging strategies, the smart charging shows a cost reduction of more than 40% compared to an HEV.

3.3.3.5. Smart charging with the fuel price

As shown in the set of orange lines, the cost reduction of smart charging with fuel price can be up to 50%. It is the only charging strategy that consistently has more cost benefit when increasing the charging locations, while from home & work place to everywhere charging the extra cost reduction can be ignored. When it comes to the charging power, higher power does not show a significant benefit compared to 1.44 kW Level 1 charging.

In summary, it is obvious that smart charging benefits cost reduction significantly more than non-smart charging strategies. The greatest difference can be as much as 30% and 40% when the charging powers are 1.44 kW and 6 kW respectively. Higher charging power could increase the cost for non-smart charging strategies and benefit only slightly the smart charging strategies. Adding workplace charging would only be beneficial for the smart charging, and more locations would either increase cost or provide only a small benefit.

Task 3.3.4. Interaction between vehicles and the grid

The integration of electric drive into passenger vehicles has been increasing dramatically. From standard hybrid vehicles having relatively small battery packs and motors that can mitigate the efficiency impacts of vehicle dynamics on combustion engines, to plug-in hybrid vehicles (PHEVs) enabling some portion of vehicle energy to be derived from the electric grid, to pure battery electric vehicles (BEVs) that rely entirely on grid electricity, and ultimately to fuel cell electric vehicles (FCEVs) capable of generating electricity cleanly onboard via a fuel cell, the advantageous transition to full electric drive appears inevitable. Electric drive offers substantial vehicle performance benefits including increased efficiency, improved torque and power characteristics, improved power density leading to advances in vehicle architecture for safety and comfort, reduced noise, and few moving parts for greater reliability.

As vehicles rely more heavily on electric drive, traditional electric generation energy sources and transportation energy sources will become much more intertwined. PHEVs and BEVs, collectively known as plug-in electric vehicles (PEVs), directly require grid electricity at increasing levels proportional to the number of electric miles travelled. Historically, coal, natural gas, nuclear, hydroelectric, and more recently, renewable wind and solar energy have been dedicated to the domain of electricity generation while petroleum has been predominately utilized for transportation. The advent of PEVs opens the door to allow transportation to utilize the wide array of energy sources previously available only to stationary power devices. Similarly, hydrogen powered FCEVs will require the same energy sources as electric generation. For example, hydrogen can be generated from reformation of natural gas, gasification of coal, or electrolysis of water using any electricity source. Resultantly, regardless of the eventual market proportioning of PEVs and FCEVs, transportation and stationary power will ultimately rely on the same sources of energy. AAs society aims to reduce GHG emissions, improve urban air quality, and provide secure energy resources, it is imperative that future vehicle and electricity generation technologies be assessed as a parallel, integrated system.

Task 3.3.5. New management strategies required to manage intermittent renewable power

The average electric generation mix in the United States currently consists of 68% combustion of coal and natural gas. Renewable wind, solar, biogas, and geothermal sources account for just 4.5%. Greenhouse gas reduction goals such as California's AB32, Renewable Portfolio Standards (RPS) mandated in 29 states to increase renewable energy sources, and increased siting, permitting, and operating costs for combustion technologies are driving a shift to greater portions of renewable power. Though environmentally preferable to traditional sources, wind and solar electricity sources are intermittent. The inability to accurately predict or control this power production will become increasingly troublesome as the portion of renewable power grows.

New energy management strategies are necessary to best utilize intermittent power which can lead to supply disruptions on a number of timescales.

Yearly: Peak loads are challenging for the utility to meet (Figure 79)

Seasonally: Significant seasonal variation exists in wind and solar availability

Daily: Diurnal load variation requires most generation facilities to considerably turn down at night; this ability and operating profile increases costs, emissions, and fuel consumption (Figure 80)

Minutes: Intermittency of solar and wind resources will become an additional significant challenge as Renewable Portfolio Standards (RPS) push renewable penetrations to 20% or higher (Figure 80)

<Seconds: Power quality

Three solutions exist that can address the short term intermittency problems: (1) load shedding, (2) energy storage, or (3) dispatchable power generation. Careful integration of transportation

and the grid can allow vehicles to serve as any, or all, of these 3 intermittency solutions. A vehicle charged by the grid represents a potential load that can be removed (1, load shedding), reducing the peak grid power demand and relieving the stress caused by temporary low renewable output. Additionally, the battery packs onboard vehicles can serve as energy storage (2, energy storage) if drivers can be coordinated to charge at times when excess renewable electricity is generated. Charging during times of excess will in turn reduce the need to charge during peak times. Future technology enabling vehicle energy to supply the electric grid, often referred to as vehicle-to-grid, or V2G, may enable vehicles to serve as dispatchable electricity sources (3, dispatchable power generation) that could be called upon as needed in times of low renewable output. However, the technology, economics, and overall attractiveness of V2G is still uncertain and likely decades from implementation, even in a best case scenario given the coordination necessary between consumers, automakers, and utilities.

PEVs can be used as load shedding devices based on existing mechanisms between utilities and customers. During peak load demand times (e.g. hot summer day with high air conditioner use), or during periods of low renewable power generation (e.g. when the wind is not blowing) the utility can either reduce the load, or supply more power. Current methods for reducing load include contractual agreements whereby consumers agree, for example, to turn off air conditioning or stop industrial operations when directed by the utility. In exchange, the customers receive monetary incentives. Homes and businesses are currently being retrofitted with "Smart Meters" in many markets throughout the U.S. which can access real-time rate information provided by the utility and communicate with appliances. Consumers will then have the opportunity to pre-program these appliances to run only when it is economical. By controlling rates, the utility ultimately controls load. A PEV could interface with the utility in the same way, allowing the utility to provide some control over when the vehicle is charged.

PEVs could be used as dispatchable power plants. The current method of supplying additional dynamic power is to call on peaker plants which can provide more power on short notice. Currently, natural gas fired turbines supply the bulk of peak power with a portion coming from hydro-electric facilities. In the future, V2G strategies may enable stored energy onboard vehicles to supply power to the grid if the vehicle is plugged-in, if the proper smart metering is established, and if the utility and EV owner agree on timing and pricing. The need to use PEVs to meet peak loads would be rare, likely on the order of only a few hours of each year, as shown in Figure 79.

Figure 79: Hourly California system load ordered from highest to lowest.

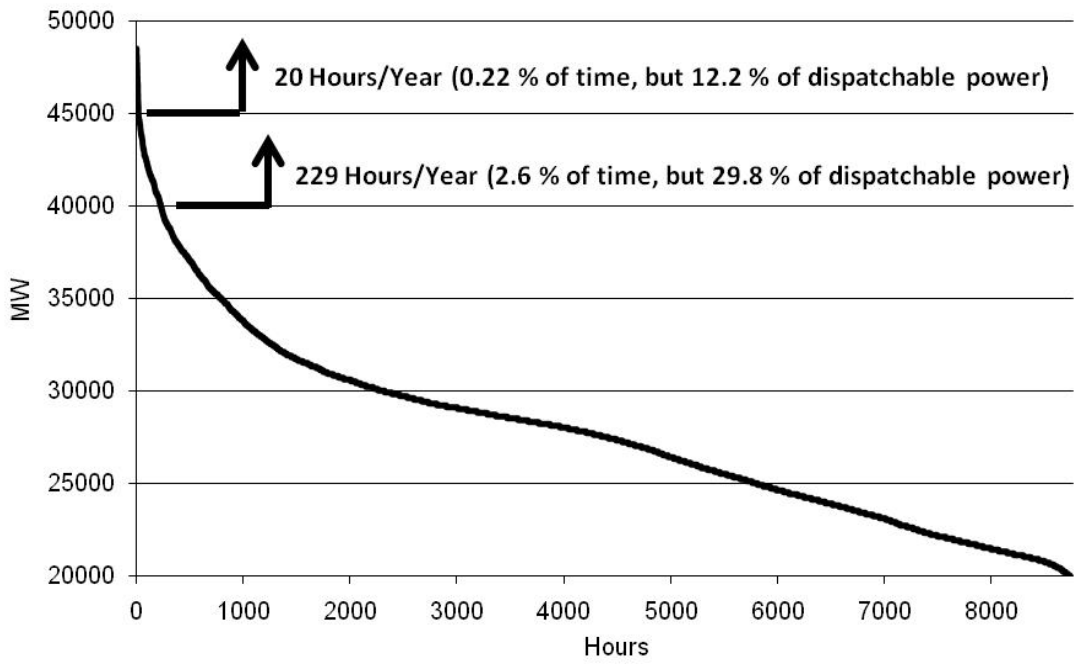

Figure 79 shows California electric load in MW versus each hour of the year (8,760 hours). The hours are arranged in order of highest to lowest load. This clearly shows that the high peak power requirements only occur for a few hours each year. Nearly 1/3 of dispatchable generation capacity is required to meet the load demand for just 229 hours each year. 12% of the dispatchable generation is only used for 20 hours each year.

Figure 80: California system load for one week showing diurnal variation and impact of 33% wind power on other generation types.

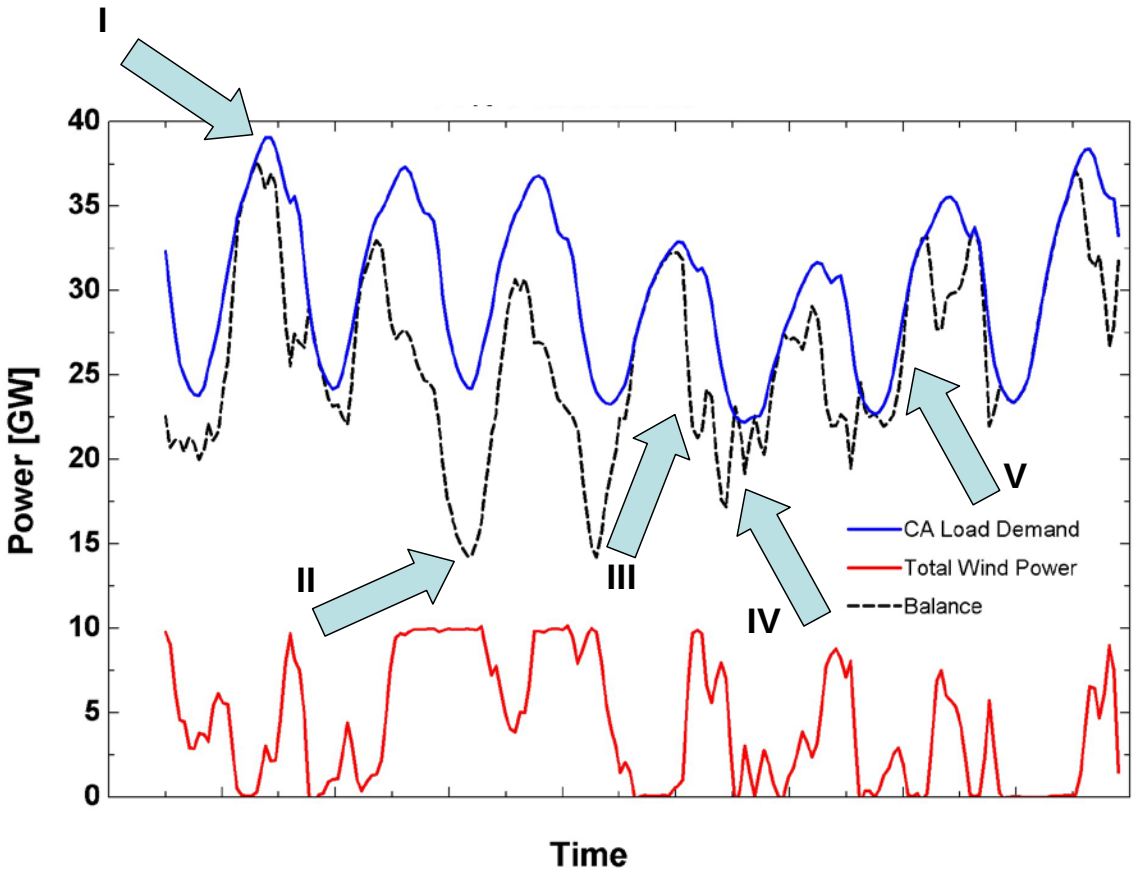

Figure 80 shows California load dynamics over a 7 day period assuming a 33% penetration of wind power (33% renewable is mandated in California for the year 2020).

- Arrow I shows a situation where wind power is low and load is high; other generation is forced to meet the load requirements.
- Arrow II shows a situation with high wind power and low statewide load. The power output required by other generators at this point is less than half of what is required at Arrow I.
- Arrow III shows wind power output increasing very rapidly. In order to utilize this wind resource, the power output of other generators must drop very rapidly.
- Arrow IV shows a series of significant power level changes required in a short time period.
- Arrow V shows the steep power increase required of other generators when wind power is very low.

As utilities strive to meet RPS goals with non-dispatchable solar and wind resources, dispatchable power sources and controllable loads will become even more valuable.

Task 3.3.6. PEVs impact on intermittencies

PEVs have the opportunity to play a major role in the integration of renewable power sources into the existing grid mix. Figure 81 shows the Southern California Air Basin electrical load profile for a peak summer day having a characteristic dip in the early morning hours corresponding to low activity and lower temperatures, and an early afternoon peak corresponding to high activity and air conditioner power consumption.

Figure 81: Temporal electricity power demand for extreme summer day in southern California.

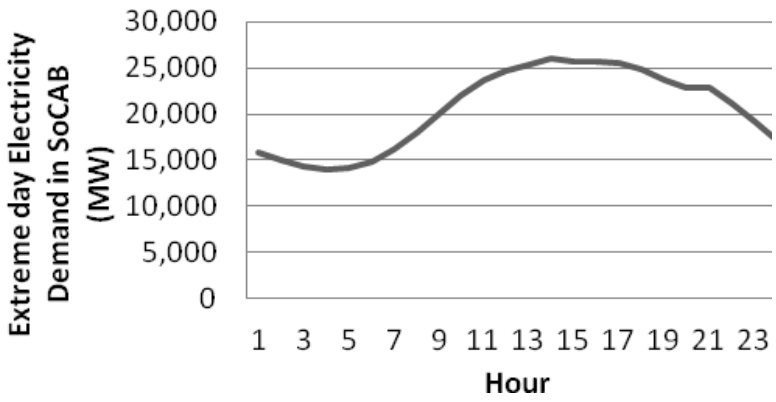

In a longer term outlook, the intermittent peak-and-valley nature of wind and solar power will tend to shift the daily occurrence of the minimum and maximum effective load demand to unconventional times, affecting the compatibility of the electric grid system with technologies that have time-constrained dispatchable loads. As a result, the grid-preferred optimum charging times may change from what they are today, and may even change from one day to the next based on wind and solar irradiation occurrences.

At present, the maximum load demand occurs typically during the daytime hours when commercial and industrial sectors become active, or during the early evening hours when residential loads peak as a result of people returning home from work and utilizing their in-home appliances. Rate structures for the price of electricity, forecasting of load demand, and the scheduling dispatch of electric generators are highly dependent on knowledge of this pattern. As intermittent renewables are added in large amounts to the system, however, this pattern changes and at certain renewable penetration levels, the occurrence of the maximum load demand becomes unpredictable. Solar power will act to reduce the daytime peak, shifting the maximum to evening or morning hours. Wind power may, or may not, occur during the time of the new peak depending on region and strength of intermittency, and therefore the peak of the effective load demand that must be managed becomes difficult to predict.

This has implications for technologies which rely on being able to provide benefit by acting during certain time periods. For example, one assumption is that PEVs should charge during the nighttime hours when the effective load demand is at a minimum. With increased intermittent renewable penetration levels, however, the nighttime hours designated for charging may or may not necessarily be a time of minimum load, especially when other time-constrained dispatchable loads are considered.

Therefore, in order to address these challenges, the load-balancing infrastructure must be refined such that the utilization of installed generator resources remains high while maintaining system robustness, reliability, and higher renewable penetrations. Energy management strategies such as the implementation of energy storage at different scales, and implementing and increasing the flexibility of dispatchable loads such as PEV charging present a multi-faceted set of options for helping to mitigate these challenges when implemented synergistically.

Task 3.3.7. Conclusions

- Vehicles residing primarily at detached homes account for more than 80% of the dwelling time, implying that home recharging in a garage is likely for most drivers
- For weekday work trips, more than 80% of vehicles may be replaced by battery electric vehicles with battery sizes smaller than those announced by major auto manufacturers, while still able to minimize the charging cost from both electricity consumption and charging infrastructure installation
- The infrastructure needed for non-work trips does not differ from that needed for work trips

Task 3.4. Dispatch of Cooling Loads to Manage Increased Renewables at UCI

The Goal of this task is to evaluate how dispatchable air conditioning system can help manage intermittent renewable generation.

The University of California, Irvine is currently equipped with a 4.5 million gallon, 60,000 ton-hour, thermal energy storage system working in parallel with a centralized chilling system. The system is dispatched to minimize the campus chilling cost under the current electrical energy rate structure which is not an optimal strategy for managing high penetration of renewables. Just like battery electric vehicles, air conditioners can be dispatched to support the grid. Models of the University of California, Irvine cooling loads, air conditioning units, and thermal energy storage are to be developed. The model will provide a platform to evaluate the extent to which the system can be operated to support the grid with high renewable penetration.

Management of building loads is a critical enabling element needed to facilitate the deployment of cost effective RESCOs. Much of the intermittency associated with renewable resources can be

cost effectively handled with building and ultimately community load management with the appropriate controls and communications between utilities, buildings, and DER.

This report addresses the following tasks:

1. Acquire temporal UCI campus cooling load.

16. Model UCI cooling system including the thermal-energy-storage system.

17. Evaluate the extent to which loads can be tailored by dispatching air conditioning loads.

18. Quantify cold water thermal energy storage advantages in managing increased renewable penetration.

Task 3.4.1. Acquiring temporal resolution of the campus cooling load

Two sets of data have been obtained for the UCI campus cooling load. The first data set is the most complete and has better resolution; however, it is outdated in that it is from the year 2000. Since then the campus has experienced significant growth making this data set less desirable. Therefore, more current data from the year 2010 were to be acquired, but there were challenges associated with achieving 15-minute resolution for these cooling load data. The cooling load data are currently recorded every two hours by plant operators, which meant that these data would need to be extracted manually from the plant operator logbook. Therefore, the cooling load from two representative summer and winter months in 2010 were recorded from the plant operator logbooks (See Figure 82, Figure 83, and Figure 84). In both data sets, the cooling demand was calculated based on the recorded cold water return and supply temperatures from which the return and supply enthalpies could be determined and the difference between these enthalpies provided the cooling load:

$$P_{cool} = \frac{\dot{m}\left(h_{ret} - h_{sup}\right)}{COP} = \frac{\dot{m}C_p(T_{ret} - T_{sup})}{COP} \tag{2}$$

Therefore, the temporal profile of this data set represents the raw cooling demand of the UCI campus without the effect of the thermal energy storage system installed at the UCI central plant. In the absence of the TES system, chillers would have to operate in real time to meet this cooling demand. Obtaining the raw cooling load profile allows the analysis to compare the differences between the behavior of the aggregate load demand with and without thermal energy storage.

The year 2000 data set has been used in most of the following analyses because of its high resolution, but some insights can be made from examining the 2010 (two-hour resolution) data. As expected, the heating load is higher in the winter than in the summer where the reverse is true for the cooling load. The electric load profile is similar for the summer and winter months. This may seem unexpected at first, but it is important to remember that in these data the cooling load has been separated from the electric load. The relationship between the ambient temperature and the cooling load appears to be predictable to an extent (See Figure 84), which

may be useful in developing control strategies as well as strategies to mitigate the adverse effects from high renewable penetration.

Figure 82: University of California, Irvine campus electric, heating, and cooling load profiles for January 2010

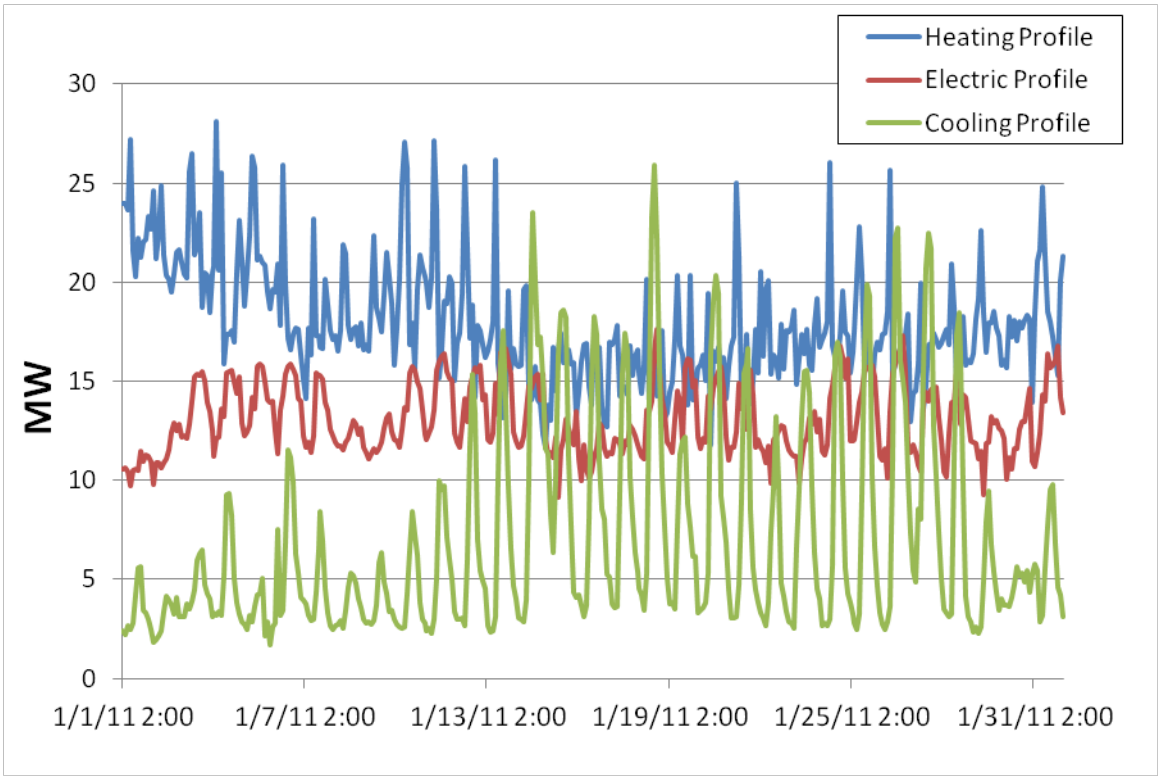

Figure 83: University of California, Irvine campus electric, heating, and cooling load profiles for July 2010

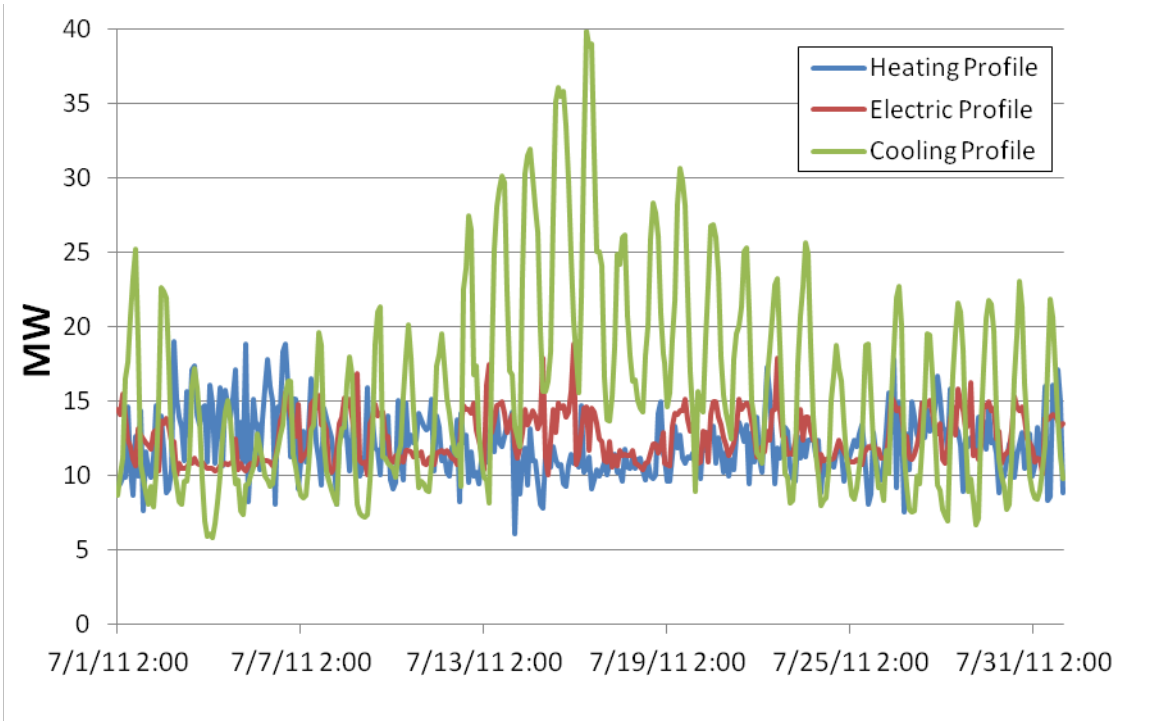

Figure 84: Relationship of the University of California, Irvine campus cooling load to the ambient temperature for the months of January and July of 2010

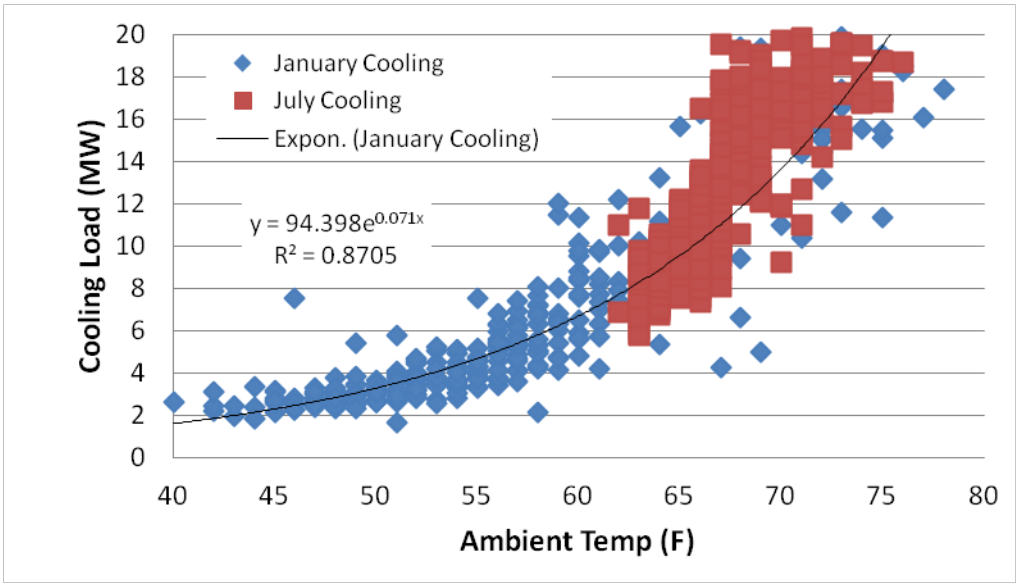

3.4.1.1. Chiller Model Description

The campus cooling system consists of eight centrifugal chillers in parallel, a multiple-cell cooling tower with a common sump, and a stratified water thermal energy storage (TES) tank (4.5 million gallon; 60,000 ton-hour). Figure 85 shows the cooling system's primary-secondary loop schematic.

Figure 85: University of California at Irvine's central plant primary-secondary loop schematic

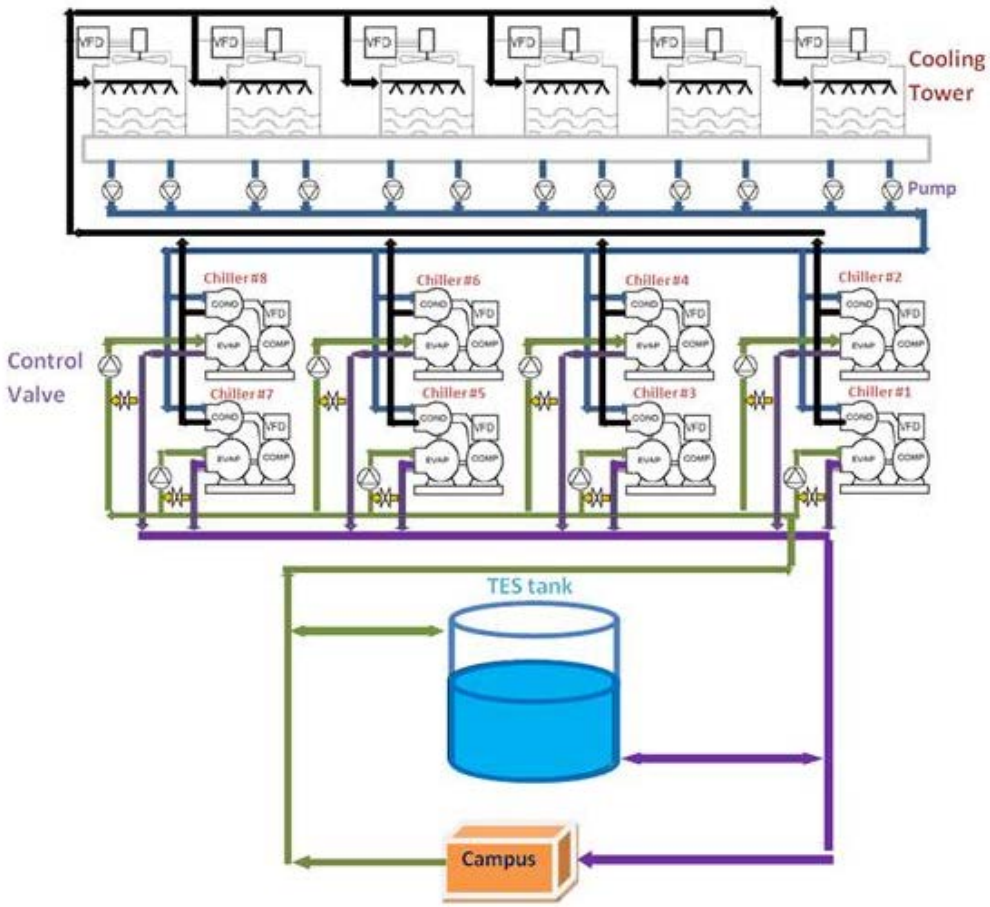

A quasi-steady thermodynamic model of the campus cooling system has been developed by modeling each of the plant components based on models in the literature. Each of the component models are developed based on conservation of mass, momentum and energy and resolving the key transport phenomena (e.g., heat transfer). Details of each of the component models are shown below:

3.4.1.2. Electrical Centrifugal Chillers

Each centrifugal chiller consists of compressor, condenser, evaporator and expansion valve.

3.4.1.2.1. Modeling of Compressor

Figure 86 gives the vapor compression cycle of the centrifugal chillers studied.

Figure 86: Vapor compression cycle pressure-enthalpy diagram

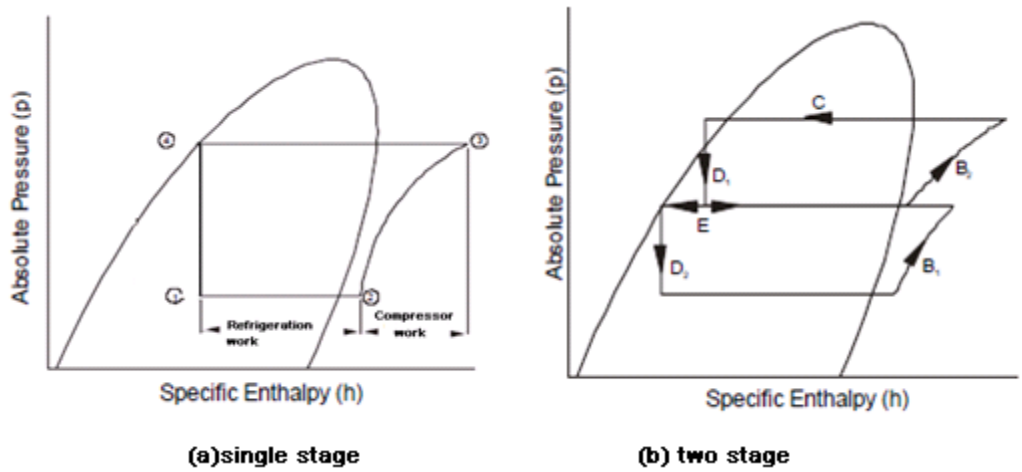

The isentropic approach is used for compressor analysis. The isentropic work for the single stage compressor is given as:

$$\boldsymbol{w = c_1 m_r (h_3 - h_2) + c_2} \quad \textbf{(3)}$$

The two-stage compressor uses an economizer which flashes a portion of the refrigerant. It is assumed that the inter-stage saturated temperature in the economizer T_{int} is:

$$T_{\text{int}} = \frac{T_{ev} + T_{cd}}{2} \quad \textbf{(4)}$$

And the isentropic work is given by:

$$W = c_1 m_r [(1-x)\Delta h_{B1} + \Delta h_{B2}] + c_2 \quad \textbf{(5)}$$

3.4.1.2.2. Modeling of Evaporator and Condenser

The chilled water flows through the evaporator and condenser of the chiller. The evaporator is a heat exchanger where the chilled water gives up its sensible heat (the water temperature drops) and transfers the heat to the refrigerant as latent energy (the refrigerant evaporates or boils). The condenser is also a heat exchanger, where the heat leaves the refrigerant (condensing the refrigerant) and enters the condenser water (raising its temperature).

As in the previous study (Liu, 1997), the method of log mean temperature difference (LMTD) is adopted to model the heat transfer performance of the shell-and-tube flooded type evaporator and condenser. The mathematical expressions to determine the cooling load, heat exchanger conductance (AU), and LMTD are summarized in following equations:

$$\dot{Q}_{evap} = \dot{m}_{chw} C_w (T_{chwr} - T_{chws}) \quad \textbf{(6)}$$

$$\dot{Q}_{evap} = UA_{evap} LMTD_{evap} \quad \textbf{(7)}$$

$$LMTD_{evap} = \frac{T_{chwr} - T_{chws}}{\ln(\frac{T_{chwr} - T_{evap}}{T_{chws} - T_{evap}})} \quad \textbf{(8)}$$

It is assumed that the overall UA is a function of chilled water flow rate and cooling load. And the following equation is used to determine the overall AU.

$$AU_{evap} = \frac{1}{c_1 m_w^{-0.8} + c_2 Q_{cl}^{-0.745} + c_3} \quad \textbf{(9)}$$

3.4.1.3. Cooling Tower

The NTU-effectiveness analysis is engaged to model the cooling tower. The number of transfer units (NTU) can reflect the cooling tower performance, which is given by the equation developed by Lowe and Christie (1961):

$$Ntu = c(\frac{m_{cdw}}{m_a})^{1+n} \quad \textbf{(10)}$$

The fictitious specific heat C_{paf} is defined as the enthalpy difference over the temperature difference of the leaving and entering condition of the saturation air as:

$$C_{paf} = \frac{h_{awbe} - h_{awbl}}{T_{awbe} - T_{awbl}} \quad \textbf{(11)}$$

The LMTD method is adopted to describe the effective heat transfer coefficient (AU_{ct}) of the cooling tower:

$$AU_{ct} = \frac{Q_{cd} C_{pa}}{C_{paf} LMTD_{ct}} \quad \textbf{(12)}$$

$$LMTD_{ct} = \frac{(T_{ctwe} - T_{ctwl}) - Approach}{\ln((T_{ctwe} - T_{ctwl}) / Approach)} \quad \textbf{(13)}$$

The mass flow rare air m_a is computed by the given relationship between Ntu and AU_{ct}:

$$Ntu = \frac{AU_{ct}}{m_a C_{pa}} \quad \textbf{(14)}$$

The cooling fan power is determined by mass flow rate of air:

$$w_{fan} = \exp(A + B \cdot \ln(m_{air})) \quad \textbf{(15)}$$

3.4.1.4. Water pump

The following equations are used to model constant speed pumps. The efficiency and shaft power are a function of flow rate.

$$W_{shaft} = A_1 + B_1 \cdot GPM \quad \textbf{(16)}$$

$$\eta_{pump} = A_2 + B_2 \cdot GPM + C_2 \cdot GPM^2 \quad \textbf{(17)}$$

$$W_{pump} = \frac{W_{shaft}}{\eta_{pump}} \quad \textbf{(18)}$$

When variable speed pumps are used, the pump power is computed by use of the 'affinity laws'.

3.4.1.5. Thermal Energy Storage Tank

It is assumed that the mass flow rate entering the tank is equal to the mass flow rate exiting the tank. The tank can operate in two modes: charging and discharging. If the flow rate of chilled water produced by chillers is greater than campus flow rate, the difference will be charged into TES tank.

A dynamic modeling of the physical TES tank has been developed. The model simulates the TES tank with 50 control volume nodes – discretized in the longitudinal direction–of the same dimension. Each node simulated a well-mixed tank volume at constant temperature. Energy balance and mass balance are considered within each node. Mass balance expression is of a continuity nature of the flows into and out of a node. The energy balance is governed by the rate of change of stored energy in each node caused by the difference in the thermal energy flow (in and out of the node), and the difference in the thermal conductive heat transfer between the nodes. Energy contribution from liquid mixing is assumed to be negligible.

3.4.1.6. Integration of Chiller Plant

The overall chiller plant model is developed by integration of each component's model as the arrangement of the cooling system's primary-secondary loop (Shown in Fig.1).

A single chilled water pump is dedicated to each chiller. An automatic modulating bypass control valve is installed at each chiller to accommodate variation in chilled water return temperature and maintain the minimum allowable leaving chilled water temperature by returning part of the chiller outlet to the chiller inlet.

Task 3.4.2. Cost Signal Types and Cost Function Optimization

To examine the effects of dispatching cooling loads at the community scale on influencing the properties of the bulk grid load, cost functions were developed to simulate different dispatch behaviors. The different dispatch behaviors are then simulated via the use of an optimization code which provides an augmented chiller load profile based on an attempt to minimize the value of these cost functions.

3.4.2.1. Cost Function Components

The dispatch behavior of the central plant chillers with TES capability was simulated by allowing the system to respond to different cost functions, which weighted certain metrics that pertain to the utility-grid behavior or campus demand behavior with more or less priority.

The cost function used in this analysis has two components.

1. A **utility component** which represents a real-time electricity rate that is designed to promote chiller dispatch to benefit the transmission grid by penalizing peak campus power use and increasing power demand during periods of high electric load on the bulk transmission grid. More specifically:

$$\boldsymbol{Cost_u = k_u\left(\frac{P_{grid}}{P_{grid,max}} + max\left(\frac{P_{chil}}{P_{chil,max}}\right)\right)} \quad \textbf{(19)}$$

Where P_{grid} is the load demand on the bulk transmission grid, P_{chil} is the power demand of the aggregated chiller plant, and k_u is a constant which weights the priority of this behavior and can translate this component into a dollar per kilowatt hour amount. The first fraction represents the normalized load demand on the bulk transmission grid. Therefore, during periods of high grid load, the associated cost penalty is higher. The second fraction represents the normalized power demand of the aggregated chiller plant on the UCI campus and penalizes excessively high power use. Setting this component to a high priority (high k_u value) will promote the dispatch of the chiller plant to operate during periods of low grid load and minimize absolute power demand requirements.

19. An **energy component** which evaluates the energy required to provide the cooling necessary to prevent the TES tank from becoming empty:

$$\boldsymbol{Cost_e = k_e(P_{chil})} \quad \textbf{(20)}$$

Where k_e is a constant which weights the priority of this behavior and can translate this component into a dollar per kilowatt hour amount. While the amount of cooling required is set by the cooling load, the magnitude of the actual power used to provide that cooling is dependent on the coefficient of performance (COP) of the chillers in the chiller plant. The COP is unit specific and generally depends on the mass flow rate of water and the wet-bulb or ambient temperatures. When this component is given a high priority (high k_e), the chiller plant will be dispatched to minimize the total amount of energy consumed to provide the required cooling demand, operating in the most efficient manner possible.

The cost function is a combination of these two components:

$$\boldsymbol{Cost = k_u\left(\frac{P_{grid}}{P_{grid,max}} + max\left(\frac{P_{chil}}{P_{chil,max}}\right)\right) + k_e(P_{chil})} \quad \textbf{(21)}$$

Using this cost function, isolated and combined dispatch behaviors can be simulated. Setting either of the k constants to zero eliminates the corresponding component from influencing the cost, therefore the chiller plant will not respond to the behavior prioritized by that component. In this analysis, three cases are examined in particular.

1. **Utility-Biased:** In this case, the priority of the chiller dispatch is to benefit the electric grid, and cooling loads at the community level are dispatched in response to transmission grid load characteristics. The local considerations of chiller efficiency are not addressed, and the primary controlling entity is the electric utility. This case represents a limiting scenario where community cooling loads can be used as distributed, dispatchable energy resources by the utility or balancing authority to mitigate issues on the bulk transmission grid.

20. **Chiller-Biased**: In this case, the priority of the chiller dispatch is to minimize the energy used to provide the necessary cooling. The behavior of the bulk transmission grid is not considered, and the campus operates independently of the properties of the electric grid load. To achieve this, the chiller plant will operate in the most efficient manner possible, regardless of the effect that it has on influencing the characteristics of the electric grid load. This represents a limiting scenario where community resources are not controlled by any extent by the electric utility or balancing authority, and communities act independently of each other.

21. **Combined Case**: In this case, the chiller dispatch responds to electric grid load characteristics and energy use considerations with equal priority. This is a compromise between the chiller-biased and utility-biased cases where both considerations are addressed.

A summary of the three cases as implemented in the optimization code is presented in Table 17:

Table 17: Chiller Dispatch Behavior Parameters

Case	k_u	k_e
Utility-Biased	1	0
Chiller-Biased	0	1
Combined	1	1

3.4.2.2. Chiller Optimization Code

The cost functions and associated dispatch behaviors described previously are simulated by the use of a chiller dispatch optimization code which determines the temporal operation of the aggregated chiller plant such that the case-specific cost function is minimized.

3.4.2.2.1. Dataset Inputs and Code Outputs

3.4.2.2.1.1. Inputs

To utilize the following chiller optimization code, a number of data sets and model tables are required as inputs:

1. Temporally resolved cooling demand for the UCI campus for an entire year (Tons).

22. Temporally resolved building electric loads for the UCI campus for an entire year (MW).

23. Temporally resolved wet-bulb temperature at the UCI campus for an entire year (F/C).
24. Model table that determines the combined coefficient of performance of the aggregated chiller plant as a function of wet-bulb temperature and water flow rate (Unit-less).
25. Model table that determines the aggregated chiller plant power as a function of COP and water flow rate (MW).

The temporally resolved data sets were obtained from UCI campus facilities and associated measurements. The model tables were obtained from results produced by the UCI campus cooling system model described previously.

3.4.2.2.1.2. Outputs

Once the code is executed, it will provide the following outputs:

1. Temporally resolved chiller plant power for the entire year (MW).
26. Temporally resolved total campus load demand for the entire year (MW).
27. Temporally resolved TES level profile for the entire year (%).
28. Total chilling energy consumption for the entire year (MWh).

3.4.2.2.2. Optimization Strategy

The basic operation of the code that determines the chiller power profile associated with different dispatch behaviors is described herein.

1. At the first time-step in the beginning of the year, the TES tank is assumed to be full. As time moves forward, the corresponding raw cooling demand at each time-step is subtracted from the TES capacity until a point is reached where the TES tank becomes empty. The chiller power profile is initialized as being zero at all times.
29. The time step before the TES tank is expected to be empty and the last time step when the TES level was full is recorded. Between these two points in time, the chiller plant must be activated to prevent the TES tank from becoming empty and unable to meet the cooling demand. Therefore, this creates a window where the cost of providing a certain increment of chilling can be evaluated.
30. In this window, the cost (according to the specified cost function) of using the chiller plant to provide a fixed increment of cooling is evaluated at each time step. The increment of cooling is specified by the user as a fraction of the cooling capacity of the chiller plant. The time step at which the increment of cooling can be provided at lowest cost is selected, and the chiller power is increased at that particular time step. The TES level is constrained such that the capacity of the TES tank cannot be exceeded, that is, time steps where adding one increment of cooling would cause an overflow of the TES tank are automatically assigned an extremely high cost function value and are therefore disregarded.

31. The chiller power profile is updated, and the process described in steps 1-3 are repeated, with the new initial time step starting immediately after the last time step when the TES tank was full as evaluated in the previous process iteration.

32. Steps 1-4 are repeated until the end of the year is reached, producing an updated chiller power profile for the entire year. The updated chiller power profile for the campus is added to the decoupled electric load for the campus to produce a new campus load profile.

3.4.2.2.3. Electric Grid Effects Model

Once the updated campus load profile is obtained, the effect of large scale chiller dispatch is examined by displacing the original chiller power profile with the updated chiller power profile in the bulk electric grid load that dispatchable generators must meet in time.

Balance Signal:

The bulk electric grid load that dispatchable generators must meet in time is referred to as the 'balance' signal, and is defined as:

$$\boldsymbol{P_{Bal} = P_{Load} - P_{Ren}} \quad \textbf{(22)}$$

Where P_{Load} is the total electrical load demand at a single instant and P_{Ren} is the corresponding total renewable power generation that is actually delivered to meet the load at that time, after the effects of power curtailment and losses, if applicable, have been accounted for. The balance signal is the load demand profile that is fed to the community chiller plants in the cases where the bulk grid load profile is a consideration in the cost functions ($k_u \neq 0$).

On the utility grid, the balance signal represents the power profile that generators in the electric system in combination with any auxiliary technologies must be able to meet at all times and follow dynamically in order to ensure that the total power generation is always matched to the load demand. The properties of this signal have direct implications for the required temporal behavior of electric generators in a system such as the utility grid. The generators which are tasked with meeting the balance power are called "balance generators". Since this particular study does not incorporate any auxiliary technologies such as energy storage, the balance generators are the primary load-balancing element that must meet the effective load demand in this case. Therefore, all of the metrics presented as follows are properties of the balance signal that pertain to a different aspect of balance generator fleet behavior or design. This signal has the same significance for any scale of internally balanced systems, where the load demand of the system is met mostly by energy resources internal to the system.

In this analysis, the following properties of the balance signal are used to characterize the effect of large scale community cooling load dispatch on supporting the bulk electric grid in supporting increased renewable penetrations:

Maximum Balance:

This is the maximum value of the balance signal over the time period considered.

The maximum balance value indicates the minimum balance generator fleet rated power capacity that is required to meet the load demand of the system.

For a balanced system, the balance generator fleet must be sized to provide at least this amount of power to prevent blackouts even if only for one time instant throughout the time period considered. This generator fleet size does not take into account the additional margins for safety and reliability. However, the inclusion of these margins serves only to increase the required generator fleet size, and therefore the metric indicates a minimum required generator fleet capacity.

Balance Capacity Factor:

The balance capacity factor is defined as the ratio of the average balance power to the maximum balance power. The balance capacity factor measures the utilization of the installed balance generator fleet assets.

For a self-balancing system, this quantity gives an indication of how much of the total installed capacity of the balance generators is typically used over a given time period. Generator cost is directly related to this metric, since capital investment must eventually be recovered by revenue garnered by producing and delivering power. A large maximum balance indicates a large installed capacity and therefore a large capital investment, while the average balance is indicative of the typical power delivered and is therefore tied to the financial return on the investment. High capacity factor values are preferable, since this indicates that the installed assets are being fully or mostly utilized for the intended purpose.

Surplus Renewable Generation (%): This is the fraction of the available renewable energy that cannot be used to immediately serve the load of the system in question.

The surplus renewable generation measures the extent of utilization of the installed renewable energy resources.

The obtained renewable energy that cannot be used to serve the load of the system in question due to the presence of excess power in the absence of sufficient demand must be transmitted to another balancing area, stored, or curtailed. In the case of curtailment, a high surplus renewable fraction indicates wasting of the potential to generate renewable power. The significance of this metric is the same for all scales of load balancing systems. Low values are preferable, as that indicates that the installed renewable resources are utilized to the highest extent possible within the system that such resources were installed to serve.

3.4.2.2.3.1. Wind Power, Solar Power and Bulk Grid Load Demand Datasets

The balance signal is determined for each statewide renewable penetration level. The renewable power profiles for each penetration level are determined from NREL databases. A spatially and temporally resolved wind speed and power dataset was developed by the NREL Western Wind and Solar Integration Project (GE Energy Consulting, 2010 (WWSIS)). The dataset provides wind speed and potential power output at a 10-minute resolution for potential wind sites across the United States for the years of 2004 through 2006 with a spatial resolution of 2 km by 2km areas. Each square kilometer area of the study is assumed to contain ten 3-MW wind turbines.

Details of the dataset compilation are presented in the report presented by the 3TIER Corporation (3Tier, 2008). The electrical power output and effective wind speed from each of these areas were determined using a mesoscale model developed by 3TIER Corporation. The performance curve for the Vestas V90 3.0 MW turbine was used to determine the wind power output potential of each block.

The interface to the NREL database is presented in Figure 87 for the Tehachapi Region in Southern California. Each wind turbine icon or colored dot on the map is representative of one 2 km by 2 km block. The icon colors represent the effective capacity factor of each block at a height of 100 meters as shown in Table 18.

Table 18: Legend for NREL Wind Potential Map Capacity Factors

Icon Color	Wind Potential Capacity Factor
Blue	< 25%
Green	25 – 30%
Yellow	30 – 35%
Orange	35 – 40%
Red	> 40%

Figure 87: NREL Wind Farm Potential Map in the Tehachapi region of Southern California

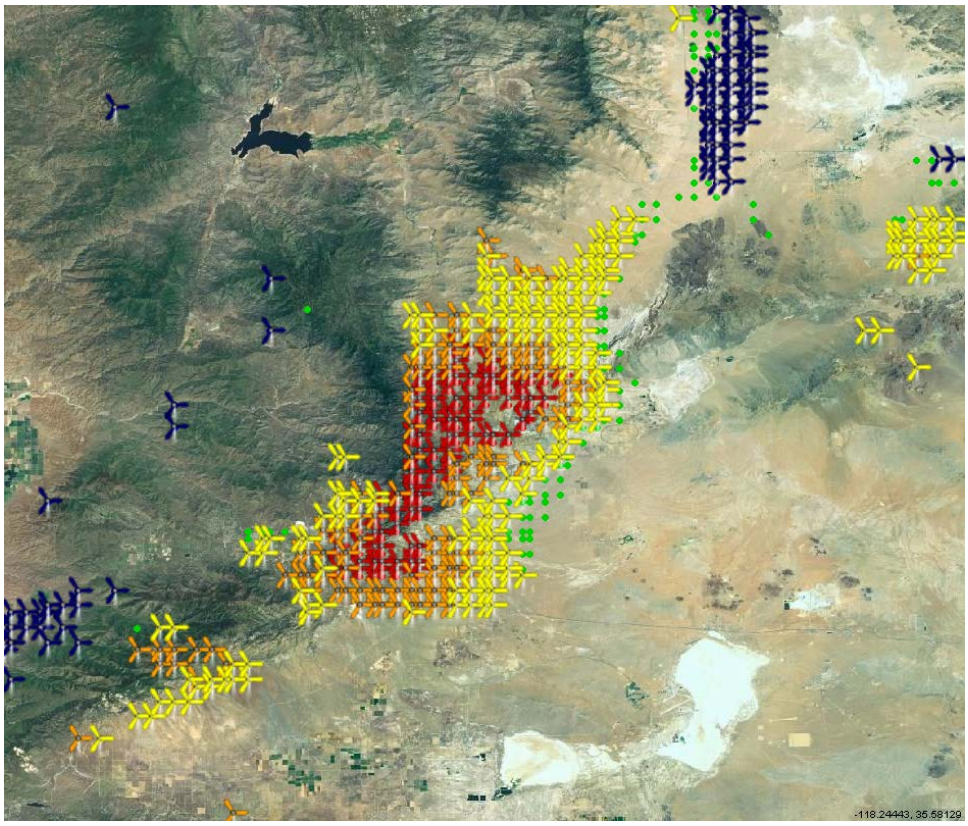

For the current study, the wind potential region in the Tehachapi region in California is examined due to its high wind potential (NREL-Wind, 1986), regional proximity to major population centers in the Southern California region, as well as its potential to support a large capacity of wind power generation. Data from the NREL model was obtained and uploaded into a SQL data server, where it was extracted by applying SQL database queries. One example of such a query was used to effectively calculate the sum of the power output from every turbine block confined to a user-specified set of spatial coordinates (latitude and longitude). This approach allows the user to obtain wind power data for different sizes of wind farms within the potential map or for the entire potential map itself. Wind power data was also obtained for different geographical regions, allowing the evaluation of wind power characteristics as a function of regional dispersion. Note that due to the nature of the source data, the effect of wind turbine shadowing is not captured.

For solar power profiles, a solar irradiation dataset is used such that it is measured from a region consistent with that of the load data and wind power data for the Southern California region. Solar power production is modeled by utilizing irradiation data obtained from the National Solar Radiation Database (NSRDB), (NREL-NSRDB, 2005) developed by NREL as inputs to first-principles-based models of solar photovoltaic panels. The dataset includes the different components of irradiation (direct, diffuse) and is converted into an effective total (in-plane) irradiation, after which it is fed to a first-principles solar photovoltaic model (Tarroja, 2011). Data from the NSRDB is available for most sites from 1991 through 2005. The database

contains hourly-resolved irradiation measurements from a variety of sites spread throughout the U.S, as shown in Figure 88:

Figure 88: Location of NSRDB Solar Irradiation Measurements (Yellow)

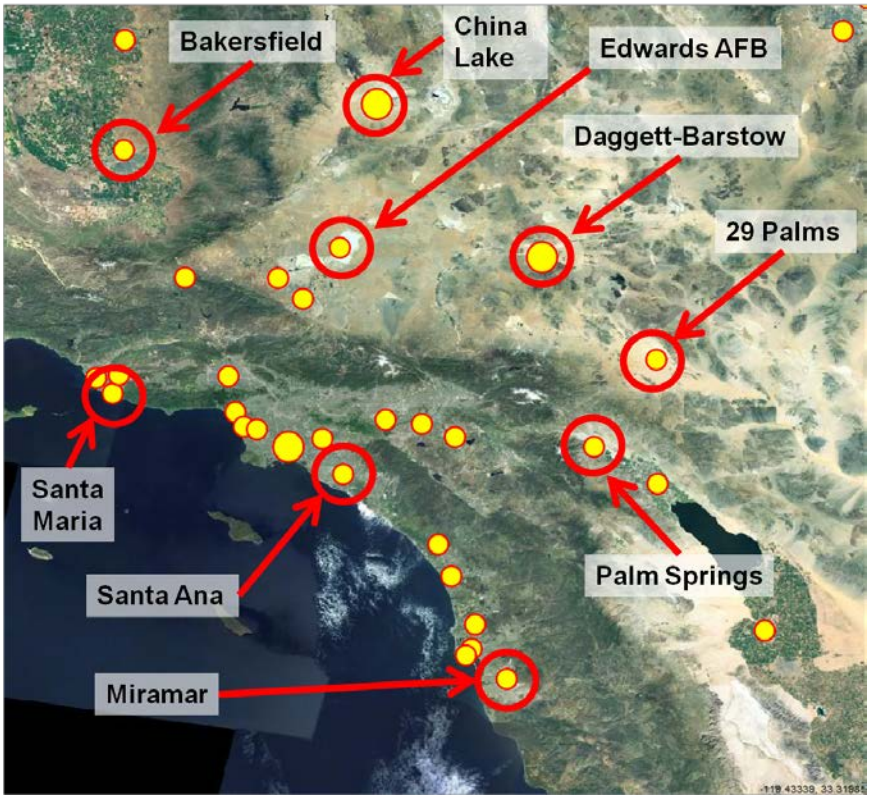

This particular study uses solar irradiation data from a spatially diverse array of sites, as located across Southern California as shown.

For raw electric grid load data, this particular analysis uses the load demand of the entire state of California as the load profile to be served. A dataset for the aggregated load demand as reported by the three major investor-owned utilities (Southern California Edison, Pacific Gas & Electric, and San Diego Gas & Electric) to the California Independent System Operator (CAISO) was obtained for the year 2005. While a multitude of smaller utility entities exist within California, these three major utilities account for the vast majority of the electrical demand within the state. This dataset has a 1-hour resolution and spans the entire year. Wind and solar data was obtained for the same time period, and the wind data was converted to a 1-hour resolution to match the data. This was found to be reasonable given that the scale of the spatial diversity of the wind resources and the scale of the system are sufficiently large such that very fast timescale fluctuations in wind power are very small compared to the longer timescale fluctuations. For this particular analysis, it is assumed that there exists no base load, that is, the balance generator fleet is assumed to be completely flexible and no non-zero power level is required to be maintained at all times.

3.4.2.2.3.2. Renewable Deployment Curve

The properties of the renewable power generation profile and therefore the effective load demand profile will depend on the mix of renewable resources used to serve the load demand at any given renewable penetration level. As a state, California has set a renewable portfolio standard goal for reaching a 33% renewable penetration level on the statewide system by the year 2020. As a result, a number of studies have been carried out to determine the feasible deployment of different renewable resources between the current time and the target year, taking into account planning, policy, permitting, and transmission construction issues. To develop the first part of the deployment curve used in this analysis, renewable resource capacities and capacity factors specified by the reference case roadmap in the 33% RPS Implementation Preliminary Report (Gillette, 2009) are used as inputs to the renewable power generation module to define renewable penetration levels up to 33% in this study. Above the 33% renewable penetration level, the deployment of renewable resources was projected based on capacity limitations presented by the NREL WWSI (GE Energy Consulting, 2010 (WWSIS)) and the following assumptions:

1. Wind power is sourced primarily from the Southern California Region. This is based on data displayed in the WWSIS which seems to indicate that the majority of the state's wind power potential is based in this region.

33. Wind power is assumed to be cheaper than solar power in the near term, until most high wind areas have been utilized. Therefore, wind power will be used to increase the renewable penetration level until it nears its capacity limit, after which solar power will become the primary means of increasing the penetration level.

34. Small Hydro, Biomass, Biogas, and Geothermal are not assumed to increase in capacity beyond their amounts at the 33% renewable penetration level. This assumption is based on capacity limitations for each of these individual resources.

35. Solar power becomes cost competitive by the time relatively high renewable penetration levels are reached (50% +), and the solar portfolio is assumed to be comprised of 70% desert azimuth tracking PV systems and 30% coastal fixed PV systems.

Combining all of these factors produces the deployment curve presented in Figure 89, and this curve is used as the basis for this analysis.

Figure 89: Renewable Deployment Projection based on assumptions.

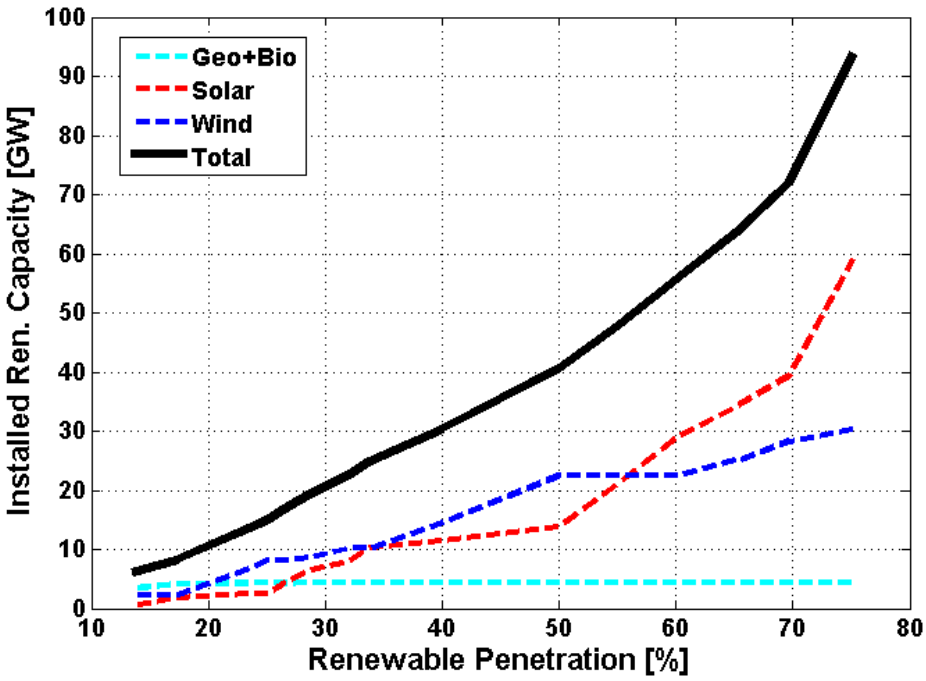

After the 33% penetration level, cases are evaluated at the 40%, 45%, 50%, 55%, 60%, 65%, 70% and 75% penetration levels.

3.4.2.2.3.3. Interface with Campus Chiller Dispatch

Once the updated campus load profile and pre-chiller effect balance signal has been determined, the effect of large scale cooling load dispatch on the characteristics of the balance signal at different renewable penetration levels can be examined. Therefore, the potential for community cooling load dispatch to complement and accommodate increased renewable penetration levels can be examined.

The effect of the new cooling load dispatch is captured by augmenting the original balance signal and creating a new balance signal, defined as the following:

$$\boldsymbol{P_{Bal} = P_{Load} - P_{Ren} - (N_{comm} * P_{chil-orig}) + (N_{comm} * P_{chil-new})} \quad \textbf{(23)}$$

Where the parameters are as follows:

- N_{comm} is the number of communities exhibiting cooling load dispatch across the entire state. UCI is used as the model community, and the peak cooling demand capacity of the campus is approximately 8.34 MW. Therefore, a N_{comm} value of 1 corresponds to an 8.34 MW cooling demand capacity displacement.
- $P_{chil-orig}$ refers to the original cooling load. Since the updated chiller load profile replaces this load, this component is subtracted from the balance signal.

- $P_{chil\text{-}new}$ refers to the updated cooling load. This replaces the original cooling load profile and is added to the balance signal.

Inherent in this approach is the assumption that all communities with cooling load dispatch capability across the state have the same pre-TES and post-TES cooling load profiles. In practice, this is not necessarily true due to the difference in temperature profiles and cooling needs between locations. However, this approach still provides a good estimate of the potential for cooling load dispatch to support the electric grid with increased renewables.

In this particular study, an N_{comm} value of 2000 is used, indicating that the equivalent cooling load of 2000 UCI-sized communities can be dispatched (about 16.6 GW of peak cooling load capacity). This figure is very aggressive, however it was picked such that the full potential of cooling load dispatch on aiding the electric grid with increased renewable penetration levels can be examined, even if such potential may not be completely realized.

Task 3.4.3. Results and Analysis

3.4.3.1. Changes in Campus Load Characteristics

The implementation of cooling load dispatch at a community will alter the characteristics of the local community load demand, which may or may not be beneficial depending on the dispatch strategy. These changes are examined herein.

A yearly snapshot of the cooling electric load and total campus load demand before and after optimization of chiller operation for the utility-biased case with a 13% baseline renewable penetration level on the grid is presented in Figure 90 with a 1-week inset in Figure 91:

Figure 90: Campus and Cooling Loads Before and After Dispatch - Utility Biased Case at 13% Grid RE

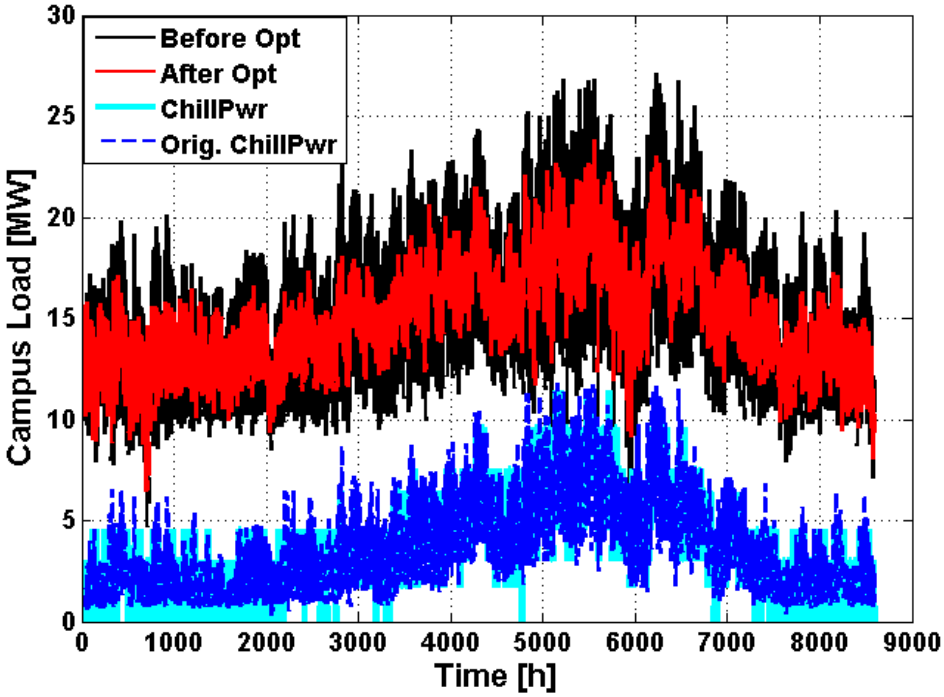

Figure 91: Campus and Cooling Loads Before and After Dispatch Inset - Utility Biased Case at 13% Grid RE

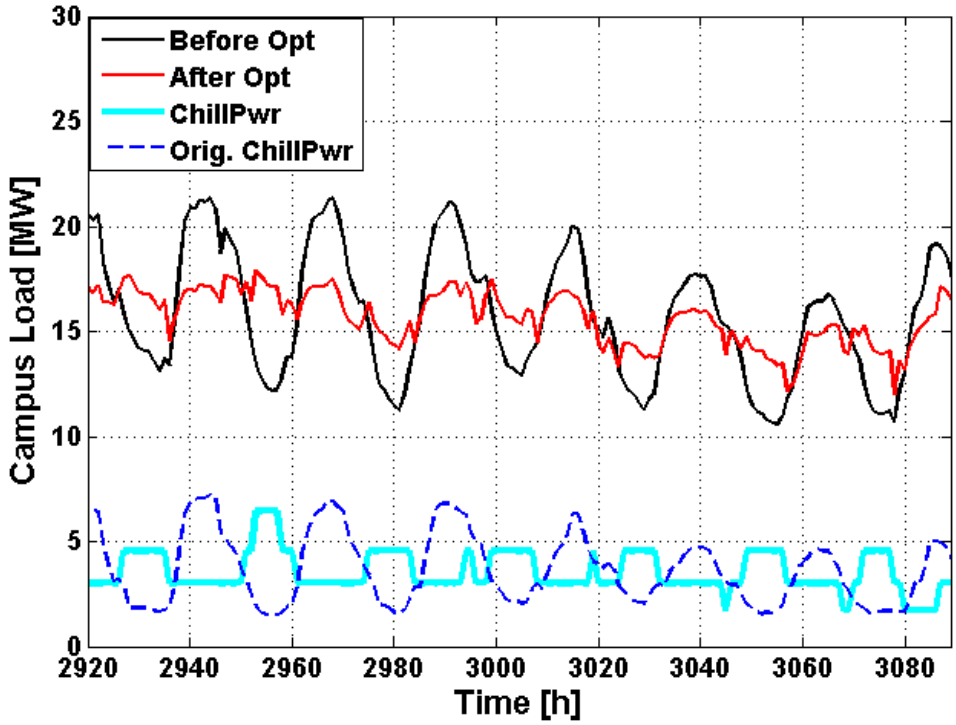

In this case, the use of chiller dispatch typically works to smooth out the campus load demand compared to the case without chiller dispatch. Note that this trend only occurs since the campus load demand profile is similar to the balance power profile at this renewable penetration level. The typical daily peaks of the campus load, especially during the summer months, are significantly decreased while load valleys during the winter and spring tend to be increased somewhat. The component of the utility-biased cost function component which penalizes not only power use during high grid load periods but also the peak power demand within an evaluation window prevents the chiller plant from operating at full capacity as much as possible while still meeting the cooling demand.

The general trend of chiller plant operation in the utility biased case is to shift the majority of the peak cooling load to the night-time hours, when the electric load of the bulk grid tends to be low. This also coincides with the time periods when the campus electric load tends to be low, therefore the total campus load peaks are also decreased significantly. Consequently, the time periods of previously low load demand exhibit increased electric loads after the chiller dispatch. Combined, both of these trends act to create a relatively smoother load profile for the campus which varies within a smaller range of power, given that the campus load profile is similar in character to that of the bulk-grid load demand.

Since peak power use is penalized in the cost function, the chiller plant tends to operate at part load capacity for longer periods of time rather than near full capacity for short periods of time to keep the TES tank filled and cooling demand satisfied. The result is a more predictable and

less dynamic chiller plant operation, although this may decrease the efficiency of the chiller plant and require a more-than-optimal amount of energy to meet the cooling demand.

As the renewable penetration level increases, however, the characteristics of the campus load demand and the balance profile on the electric grid begin to deviate from each other due to the effect of bulk renewable generation on the balance profile. Since the chiller dispatch in this case responds to the characteristics of the balance profile (effective utility load), this behavior may increase the variability of the campus load at higher renewable penetrations. A yearly snapshot of the cooling electric load and total campus load demand before and after optimization of chiller operation for the utility-biased case at the 55% renewable penetration level is presented in Figure 92 with an inset in Figure 93:

Figure 92: Campus and Cooling Loads Before and After Dispatch - Utility Biased Case at 55% Grid RE

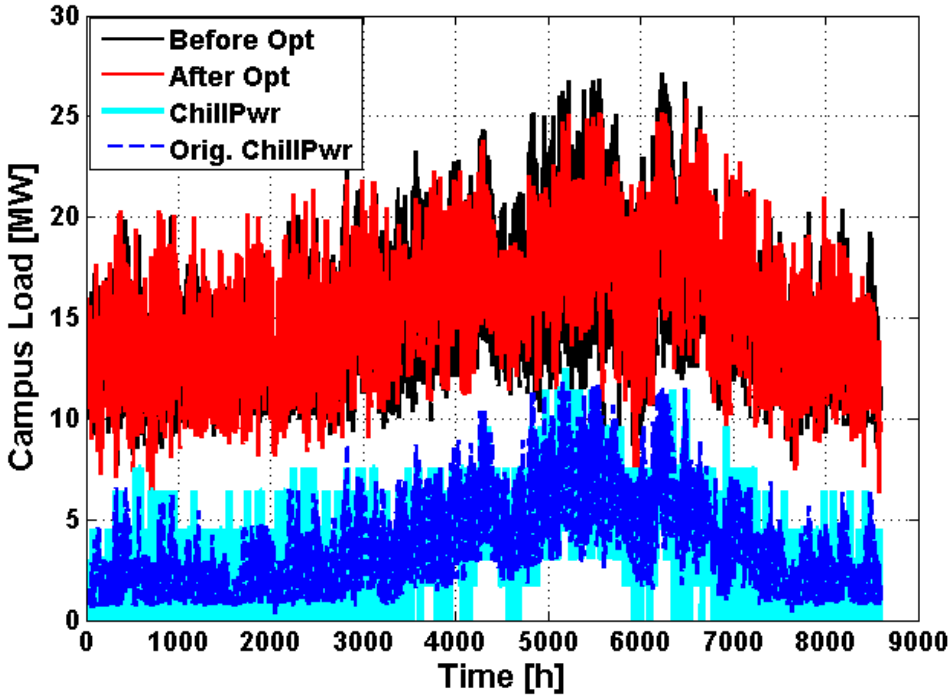

Figure 93: Campus and Cooling Loads Before and After Dispatch Inset - Utility Biased Case at 55% Grid RE

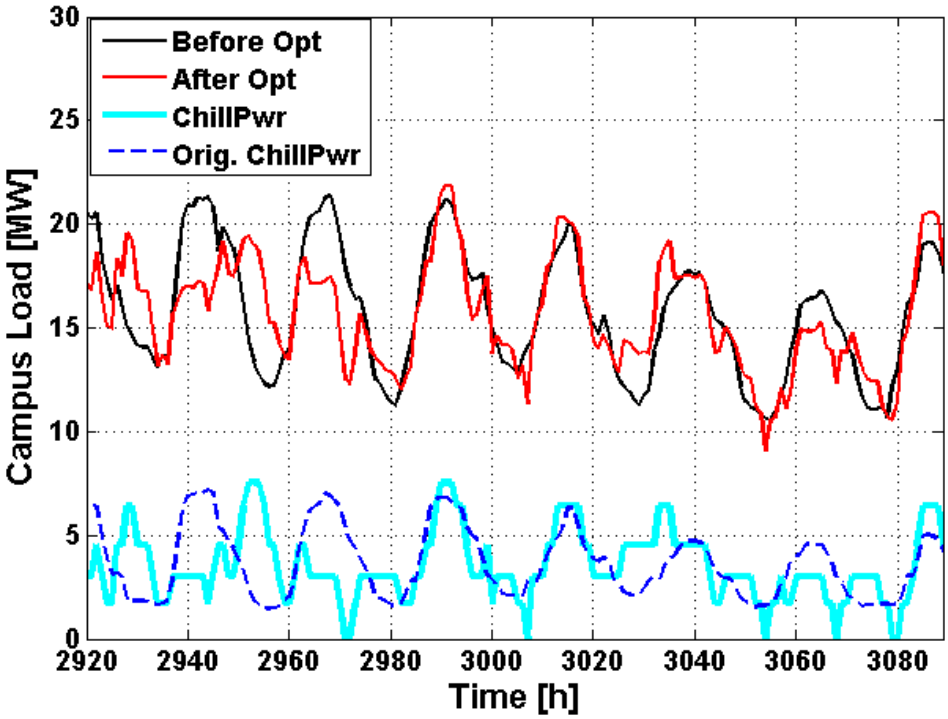

In this case, the chiller plant behaves in a manner that does not necessarily reduce the variability and range of fluctuation of the campus load. At high renewable penetration levels with large installed intermittent renewable capacities, the balance profile on the electric grid begins to exhibit large power fluctuations which occur at irregular intervals for varying periods of duration due to the behavior of the intermittent renewables. In order to attempt to level such variations, the chiller plant at the community level will be required to respond with a similar level of dynamics in order to counter such variability and level the balance power profile. Since the character of the balance profile in terms of typical maximums, minimums and duration periods between extremes no longer coincides with that of the campus load, the extent to which utility-biased chiller dispatch reduces campus load variability is decreased and eventually mitigated at high renewable penetration levels.

A yearly snapshot of the cooling electric load and total campus load demand before and after optimization of chiller operation for the chiller-biased case is presented in Figure 94 with a 1-week inset in Figure 95:

Figure 94: Campus and Cooling Loads Before and After Dispatch - Chiller Biased Case

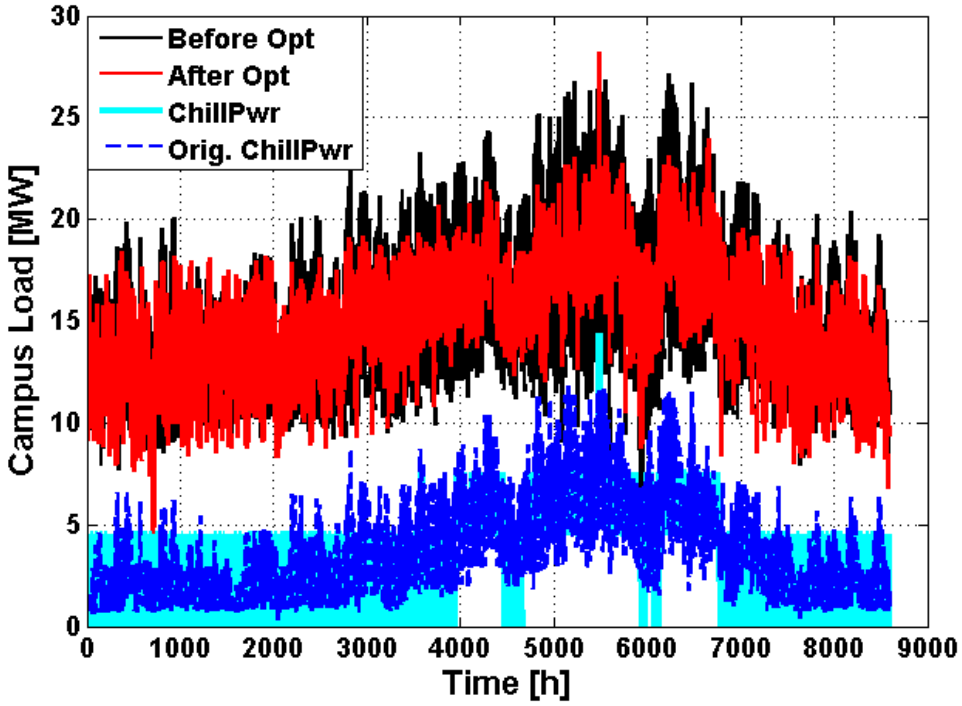

Figure 95: Campus and Cooling Loads Before and After Dispatch Inset - Chiller Biased Case

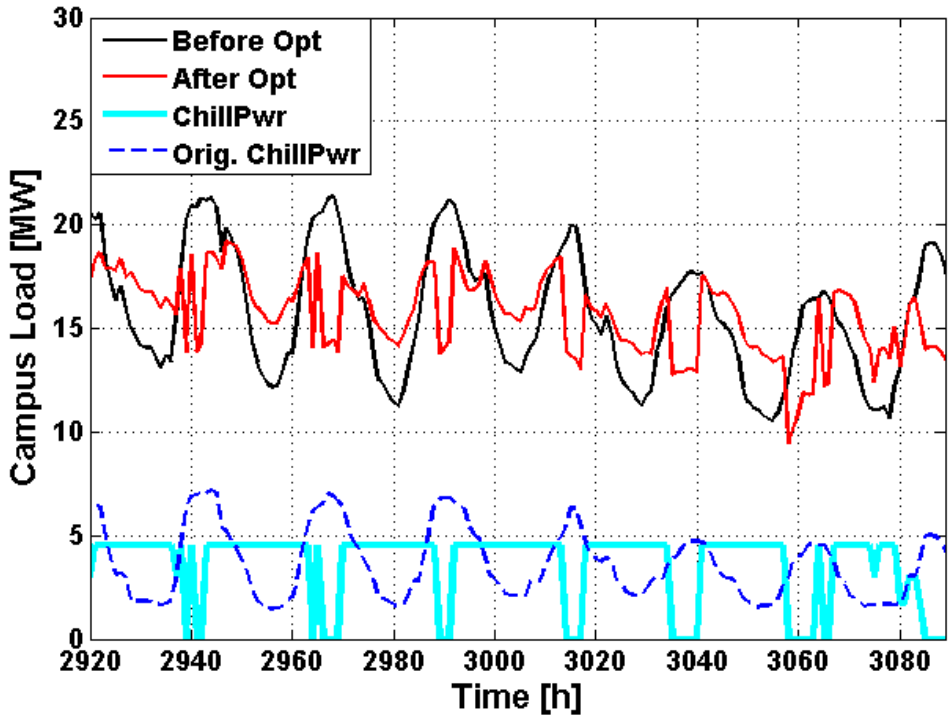

In this case, the chiller dispatch works to maximize the efficiency of the chiller plant without regard for the conditions of the load on the electric grid, therefore the effect on the campus load does not change with renewable penetration. Therefore, the chillers will turn on when the conditions for such units minimize the power required to provide an increment of cooling. These particular units tend to operate at highest efficiency when the wet-bulb temperature is low (increased cooling tower effectiveness) and when the required flow rate for a given chiller is high. Note that the chiller units tend to operate efficiently when the required flow rate of each individual chiller is high, and that this does not necessarily correspond to points when the required flow rate of the aggregated chiller plant is high. An extra chiller activating at low part load decreases the efficiency of the entire plant.

Operating in this manner, the cooling load tends to be shifted off of typical peak hours, but is not necessarily shifted towards low-load hours. The occurrence of chiller activation during the night time hours is simply due to the fact that the wet-bulb temperature tends to be very low during such hours; however the wet bulb temperature is not necessarily correlated to the load demand. As shown in Figure 95, the chillers do often activate during periods of high (although not necessarily peak) campus electric load, which loosely corresponds to high electric grid load. The activation of chillers during high load but off-peak hours can decrease the peak load compared to the non-dispatch case, however this effect is not completely systematic and during some days, the peak load is increased.

Since low efficiency is penalized when utilizing this dispatch behavior, the chiller plant attempts to avoid operation of any of its chiller units at part load capacity. As a chiller plant and

at a given wet bulb temperature, the highest total efficiency occurs when the total mass flow rate required of the aggregated plant matches that of a certain integer number of chiller units operating at full capacity. Therefore to maximize efficiency, the chiller plant will choose to operate at certain, specific flow rate levels. For the window displayed in Figure 95, the chiller plant operates at a power level around 4.9 MW, which corresponds to four of the UCI chiller units being active and near full capacity. Since the individual chiller units in the UCI central plant are somewhat different in their performance characteristics, the 4.9 MW level appears to be the overall point of highest efficiency for the entire plant. Activation of another chiller unit would cause the overall plant efficiency to decrease, and bringing the corresponding chiller unit to full capacity would cause the TES tank to overflow in these cases. When the chilling demand is large, however, the 4.9 MW level is not sufficient to meet the demand and a different set point is used that still corresponds to individual chillers operating at full capacity. Overall, the chiller plant will not only attempt to operate during periods of low wet-bulb temperatures, but it will also attempt to settle on set points that correspond to individual chillers being at or near full capacity. Therefore, the chiller plant tends to operate at a certain set points for the power level for a given period of time when required, and shuts off completely otherwise. The result is the shape of the chiller power profile in Figure 95, where discrete windows of chiller operation are present and are of different duration periods.

Overall, the 'on-off' behavior of the chiller plant tends to render the temporal profile more variable than that in the utility-biased dispatch case on a day to day basis. However, the tendency of efficient periods of operation to often occur during low campus load periods allows chiller-biased dispatch to garner some reduction of typical fluctuation range compared to the case without chiller dispatch. On the seasonal timescale, the use of efficiency-based chiller dispatch does display the benefit of decreasing peak campus loads somewhat during the summer months. This effect is primarily due to the fact that high wet-bulb temperatures during this season tend to occur during the daytime when cooling loads are the highest, therefore chiller operation is shifted toward off-peak hours. Additionally, maximizing efficiency decreases the total amount of energy used to provide the high cooling loads during this period, indirectly decreasing chiller power peaks.

In addition, contrary to the utility-biased case, the effect that the chiller-biased case has on the variability of the campus load does not change with renewable penetration level, since the temporal behavior of the chiller plant is not influenced by bulk renewables. Therefore, the effect of the chiller-biased dispatch on the campus load demand is constant with renewable penetration level, and always serves to increase the variability of the campus load demand profile.

A compromise between the two limiting cases presented previously is to consider both chiller efficiency and bulk grid load characteristics in the chiller dispatch behavior simultaneously. The yearly snapshot of the cooling electric load and total campus load demand before and after optimization of chiller operation for the combined case is presented in Figure 96 with a 1-week inset in Figure 97 for the 13% baseline renewable penetration level:

Figure 96: Campus and Cooling Loads Before and After Dispatch – Combined Case at 13% RE

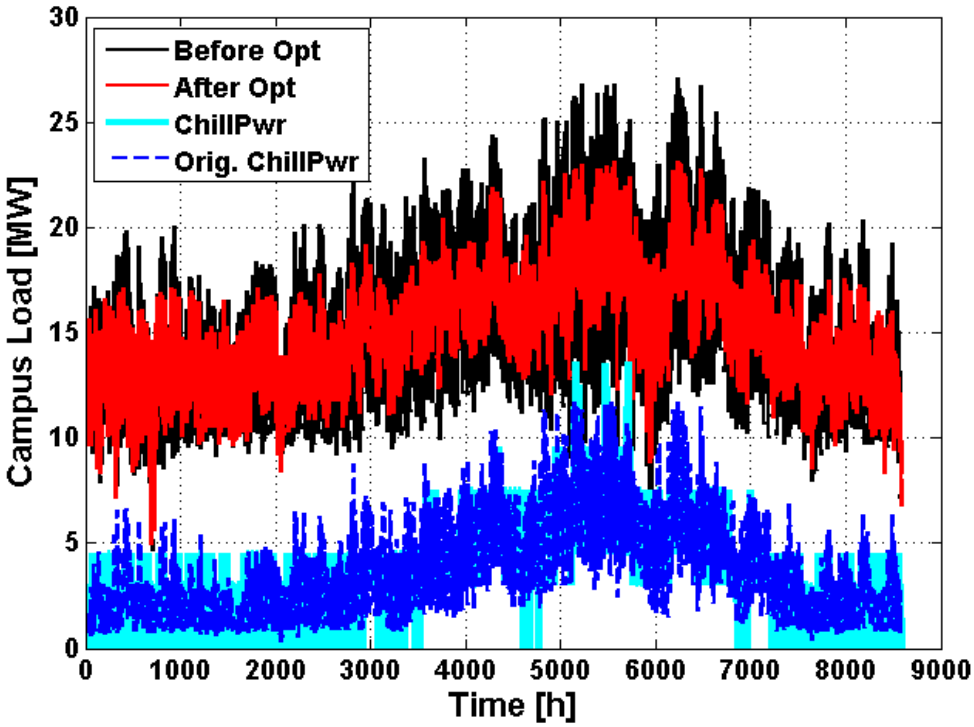

Figure 97: Campus and Cooling Loads Before and After Dispatch Inset - Combined Case at 13% RE

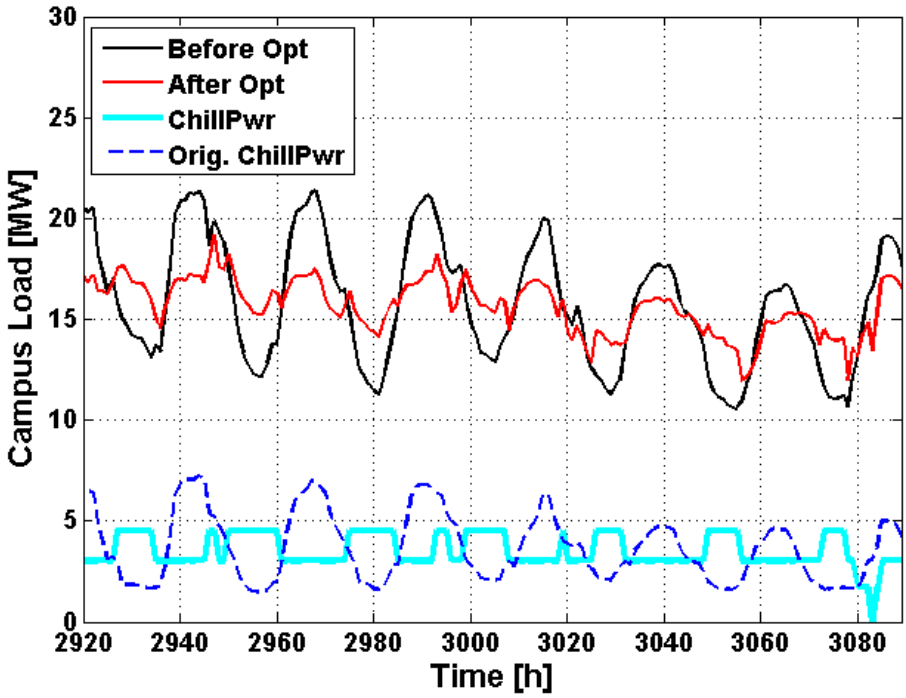

The combined case considers the effect of bulk grid load characteristics and chiller efficiency with equal priority, and therefore exhibits a compromise between the advantages and disadvantages of each. The temporal chiller power profile exhibits combined characteristics. The influence of considering chiller efficiency causes the chiller plant to operate at discrete power outputs and tending to settle on certain set points due to efficiency considerations, often preventing high power levels due to efficiency decreases. The influence of considering the utility grid load profile causes increases in chiller power to nominally coincide with load valleys. In addition, the shape of the chiller power profile does not exhibit the 'on-off' characteristic of the chiller-biased case as strongly: the effect of considering grid conditions causes the chiller plant to operate at part load during periods of high bulk grid load demand.

This operating schema tends to allow the chiller plant to partially maximize efficiency while being able to provide some benefit to the electric grid. The effect of considering both utility and local needs simultaneously also drives the majority of the chiller power demand to take place during the night hours, since wet bulb temperatures and bulk grid load magnitudes are low during these times. With both criteria considered, the chiller power profile saves a small bit of energy while limiting the quick dynamics of the chiller plant. Overall, this serves to save energy in meeting the same chilling demand while also reducing the typical fluctuation range of the total campus electric load from the case without chiller dispatch.

A comparison of the three different chiller dispatch behaviors in terms of their effect on the average daily campus load fluctuation range is presented in Figure 98:

Figure 98: Average Campus Daily Load Range vs. Renewable Penetration Level

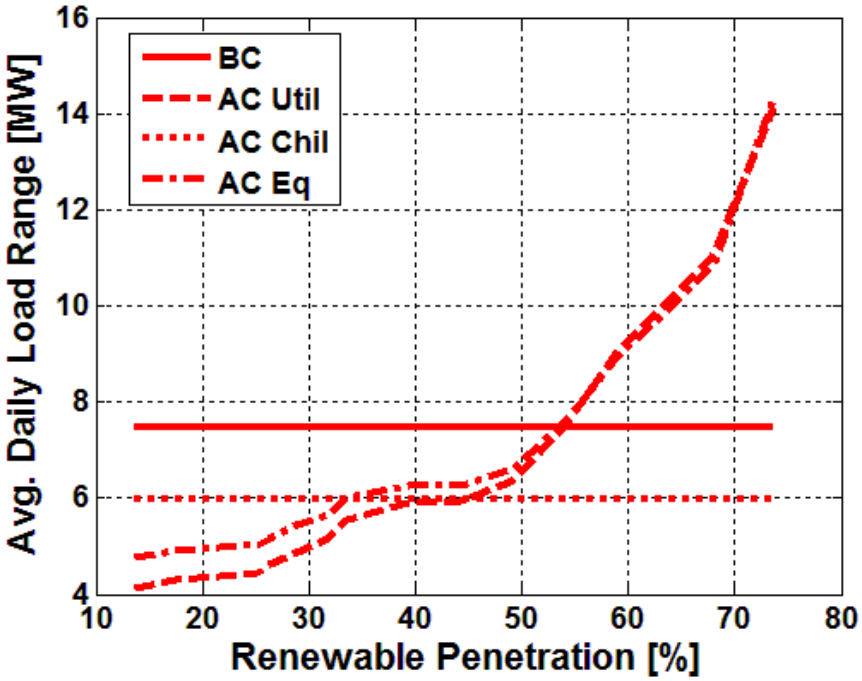

By this measure of variability, the chiller-biased case shows a constant but small reduction in the typical load fluctuation of the campus. The utility-biased case shows a significant reduction in typical campus load fluctuation; however this reduction diminishes with increasing renewable penetration level and is completely mitigated by the 53% renewable penetration level, after which it displays an increase in typical load fluctuation. This occurs due to the need for the campus chillers to operate at very high power outputs in order to respond adequately to the strong fluctuations of intermittent renewable resources on the electric grid. The combined case represents a compromise between the extreme cases, where the reduction in typical load fluctuation range at low renewable penetration levels is not as significant and the benefit is mitigated at a lower renewable penetration level.

Notable trends are also displayed when examining the total amount of electric energy that has been used by the chillers to meet the cooling demand per campus for the entire year with different chiller dispatch priorities at different transmission-grid renewable penetration levels, as displayed in Figure 99:

Figure 99: Chiller Energy Use for Different Dispatch Priorities vs. Renewable Penetration Level

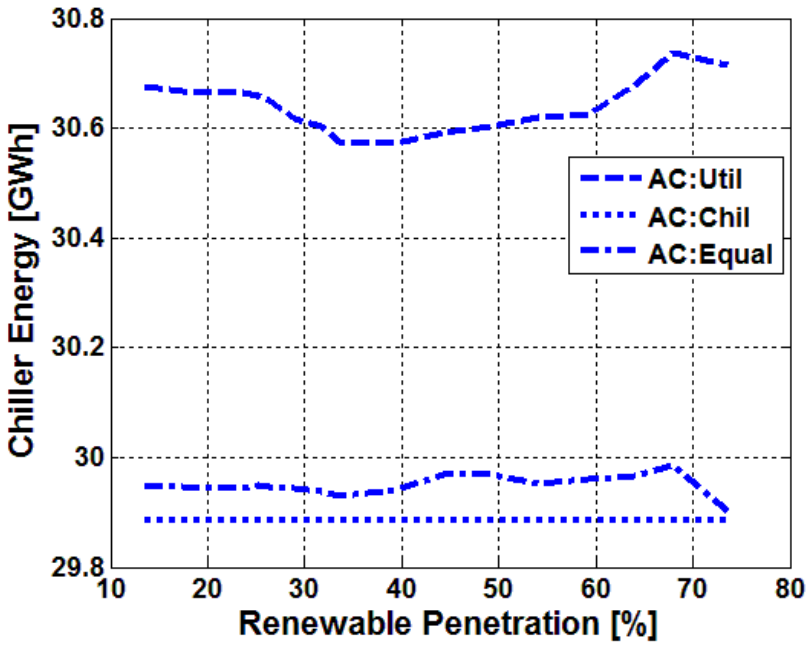

The chiller-biased case requires the lowest total energy use to meet the same cooling demand. This is expected since with the chiller-biased dispatch priority, the chiller plant operates strictly to maximize efficiency and utilize the minimum energy necessary to meet the cooling demand for all time. The chiller energy use in this case is also constant with renewable penetration level, since the chiller behavior is not influenced by the characteristics of the balance load profile that is heavily affected by increases in intermittent renewable capacity and changes in the renewable power portfolio on the grid. This energy use value of 29.89 GWh is the minimum amount of energy that can be used to meet the campus cooling demand with the given temperature profile of the UCI location.

By contrast, the utility-biased case requires the highest total energy use to meet the same cooling demand. With this dispatch behavior, the chiller plant will operate to decrease the variability of the balance load and therefore may not necessarily be allowed to operate during periods of low wet-bulb temperatures or with the individual chiller units at close to their individual maximum flow rate. Periods of low wet-bulb temperature do not systematically occur during periods of low balance magnitudes, and depending on the magnitude of the required increase or decrease in the balance power due to a renewable or load fluctuation, the corresponding response of the chiller plant may require one of its units to operate at part load, which significantly decreases the total plant efficiency. For example, at a single point in time, the balance power may fluctuate such that a large balance power decrease occurs. To level this fluctuation, the chiller plant must increase its power usage by an amount proportional to the difference between the running average balance power and the extremum of the fluctuation, which may not necessarily correspond to chiller units within the plant operating near full capacity. This decreases total plant efficiency significantly, especially at low overall power levels.

The required chiller energy use for the utility-biased case is also relatively constant, with some slight fluctuations. These occur due to changes in the renewable power portfolio at each penetration level moving the periods of operation of the chiller plant to points which may correspond to different wet bulb temperatures and different part-load conditions. The chiller energy use decreases slightly until about the 40% renewable penetration level, after which the chiller energy use steadily increases. The increase in renewable penetration level at this point is first dominated by wind power growth until 50%, after which solar power becomes the primary driving force. Solar power and wind power in this region tend to exhibit power output profiles with intermittent periods of high power and short duration. Therefore, as the capacities of these resources are increased in the renewable power portfolio, the associated variability is translated to the balance power profile of the transmission grid as relatively short periods of very low or zero balance power. When responding to the balance profile, the chiller plant will operate with high power output during these periods in an attempt to level the balance profile. The operation of the chiller plant complements this characteristic well, since the chiller plant is more resistant to the efficiency decrease due to part load operation of a unit when the aggregate plant is operating at high power. The efficiency decrease in allowing one chiller to operate at part load has a reduced impact on plant efficiency when more chiller units are already operating at full capacity. In addition, periods of low wet-bulb temperature are constrained to limited time windows.

The combined case exhibits some characteristics of both the chiller-biased case and the utility-biased case. In this case, the chiller energy use remains relatively constant, with small increases or decreases depending on which priority tended to be more dominant for a given renewable penetration level. One interesting characteristic to note is that the chiller energy use of the combined case is very close to the minimum required as shown by the chiller biased case. In the chiller biased case, in addition to the behavior of the cooling demand, the power set point of the plant is determined such that part load operation of individual units are minimized and the time of operation is influenced by the wet bulb temperature. In the combined case, however, the efficiency consideration due to part load operation still influences the chiller power set point, but the times of operation are influenced by the utility grid balance. The main element that changes between the two cases is the time of operation and not so much the power set point. For this particular system, the chiller plant efficiency is generally more sensitive to the part-load operating condition as opposed to the wet bulb temperature. Therefore, the combined case is able to retain the majority of the efficiency benefit due to minimization of individual unit part load operation, but is able to place the times of operation at periods that can benefit the utility grid.

It is important to note, however, that all three of these cases exhibit reduced chiller energy consumption compared to the case without thermal energy storage, where the cooling demand must be met in real time with no flexibility for dispatch control. The chiller energy use of the previous three cases with respect to the case without thermal energy storage is presented in Figure 99:

Figure 100: Chiller energy use compared to case w/o TES. BC: Before Chiller Dispatch.

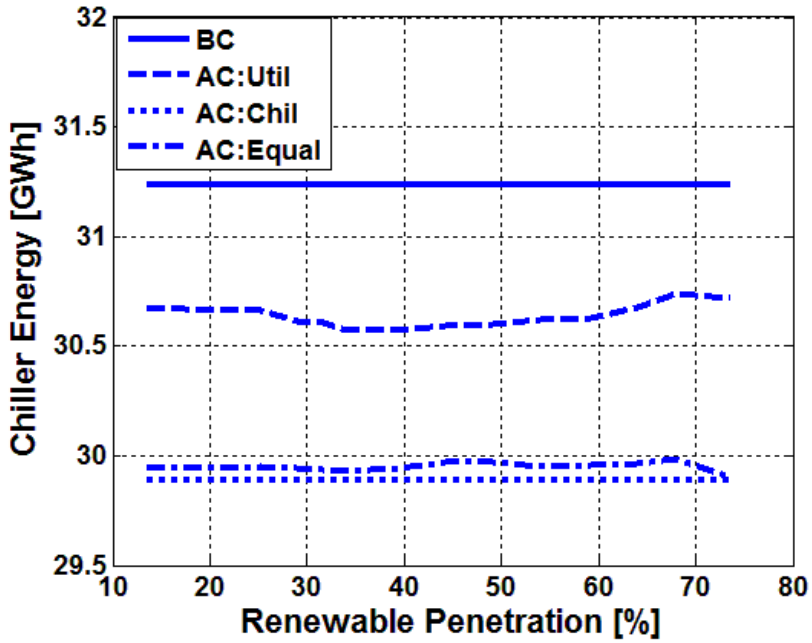

Without thermal energy storage and the ability to dispatch cooling loads, the total chiller energy consumption for the year is approximately 31.25 GWh, and is constant with renewable penetration level since the cooling demand is not a function of the balance power profile. All three of the TES dispatch cases explored in this analysis present slight energy savings compared to the no-TES case, regardless of dispatch behavior priority. The disparity in energy consumption is due to the fact that the periods of peak cooling demand tend to correspond with periods of high ambient temperature and therefore high wet-bulb temperatures, reducing chiller plant efficiency. Additionally, the continuous nature of the cooling demand causes the chiller plant to operate with chiller units at part load if no dispatch strategy is used, reducing chiller plant efficiency further.

3.4.3.2. TES Management of Increased Renewable Penetration Levels

When integrated into a sufficient amount of communities or in large enough capacities, the use of thermal energy storage has the ability to affect the management load balancing resources on the transmission grid. Combined with the increased penetration of renewable energy resources, the use of TES can be a key complementary technology for assisting the electric grid in accommodating the characteristics of intermittent renewable resources. The effect of large-scale TES implementation is examined herein.

The effect of TES implementation on the maximum, minimum, and capacity factor of the balance power profile as a function of renewable penetration level is presented in Figure 101:

Figure 101: Balance Parameters vs. Renewable Penetration Level for Different Chiller Dispatch Cases

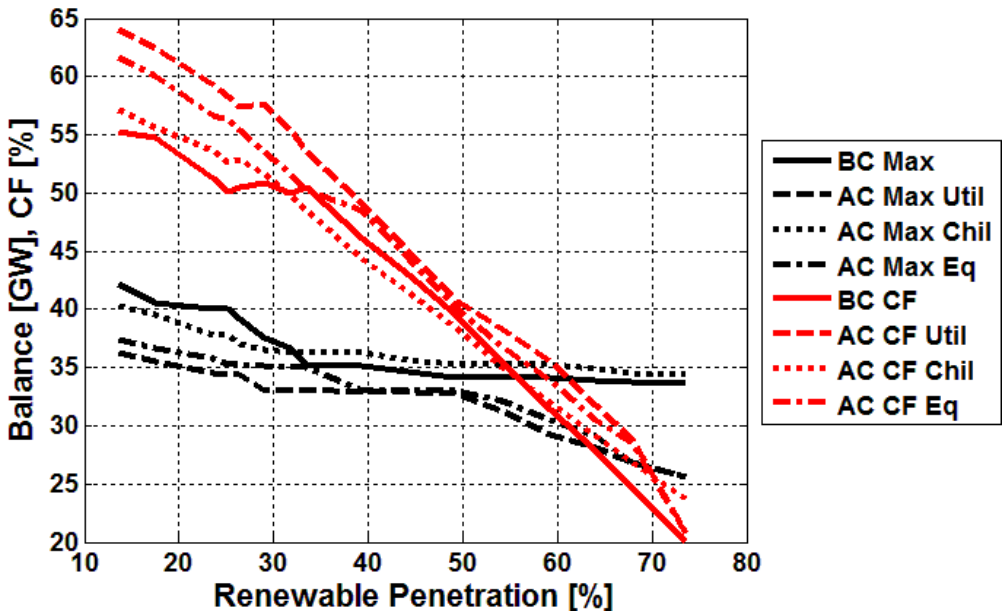

The black lines correspond to the maximum balance value and the red lines correspond to the capacity factor of the balance generator fleet. BC corresponds to the value of such parameters before the implementation of large scale chiller dispatch (no TES), while AC corresponds to the respective chiller dispatch cases as described prior. The behavior of the parameters before the implementation of TES is described in Tarroja (2011) and will not be described in detail herein.

3.4.3.2.1. Effect on Balance Capacity Factor

Depending on the chiller dispatch priority, the implementation of thermal energy storage can either increase or decrease the capacity factor of the balance generator fleet.

The utility-biased case tends to increase the balance capacity factor. In this case, the chiller plant is given information about when the pre-TES balance power is high or low and is therefore well equipped to level variability in the balance load profile. By using the thermal energy storage system to shift cooling loads from originally high balance periods to low balance periods, the chiller dispatch contributes to creating a more smooth balance profile where the maximum deviation from the average balance value is reduced within a given chiller operation window, increasing the utilization of the balance generator fleet. With this dispatch behavior, the current balance capacity factor value (56% at 13% RE penetration) can be maintained until about the 33% renewable penetration level.

There are limits on the ability of thermal energy storage dispatch to shift loads, however, and such is the reason that while utility-biased TES dispatch is able to shift cooling loads, the capacity factor of the balance generator fleet still decreases monotonically with increasing renewable penetration level. This limitation is a function of a number of factors. First, the TES tank can only influence a specific type of load – the cooling load, and therefore cannot affect the

portions of the balance profile that correspond to other electric loads. Second, the primary priority of the chiller plant and TES tank is to meet the campus cooling demand. The chiller plant and TES tank cannot be operated in a manner that does not allow the campus cooling demand to be met at any point in time, even if such an operation method would allow the system to benefit the electric grid to the maximum extent. Therefore, the chiller plant and TES tank is constrained in its ability to level balance signal fluctuations even if it is dispatched to do so.

The benefit garnered by using utility-biased chiller dispatch changes magnitude with renewable penetration level. This behavior is a function of the characteristics of the renewable mix and the effect on the predictability of the balance profile.

The largest increase in capacity factor compared to the base case is present at renewable penetration levels below 33%. In this range, the capacity of the renewable resources is still low enough such that the temporal pattern of the balance signal is still predictable in terms of the occurrence of its peaks and valleys. Since solar power tends to peak in the daytime and wind power in this region tends to peak approximately 12 hours beforehand in the middle of the night, balance peaks and valleys start to form 12 hours apart as opposed to the typical 24 hour increment present in the raw load demand. This pattern, while having a different timescale than the raw load demand, reliably occurs every day since renewable capacities are also low and the fluctuations in the variable renewables do not distort it. Therefore, the chiller plant simply shifts from charging and discharging on a 24 hour timescale to a 12 hour timescale on a regular basis, and is still capable of leveling balance peaks and valleys to limit the variability of the balance signal and retain a high balance capacity factor.

Above 33%, the benefit steadily decreases until the 50% penetration level. This occurs due to the dominance of wind power in the renewable mix in these ranges and the fact that the renewable capacities start to become large enough such that fluctuations in power output severely affect the balance profile. Wind power is used as the main resource to increase the renewable penetration level in this range, which reduces the balance power to very low levels during the nighttime and also brings about the onset of over-generation during these periods. Comparatively, the solar power capacity is only increased slightly. The decrease in balance power during periods of peak wind power becomes much higher than that during periods of peak solar power. This causes the chiller plant to become limited in its ability to increase the balance power magnitude during periods of peak wind power, since it may be capable of completely leveling balance valleys during peak solar power periods but not as much during peak wind power periods because the magnitude is too high. This relative difference between these magnitudes combined with the limited size of the TES tank reduces the effectiveness of the chiller-TES system, since being able to level one type of balance valley (solar induced) but not the other (wind induced) does not restore the capacity factor as strongly as if both were affected by the full capacity of the chiller plant. Therefore, the balance capacity factor does not see as much of a benefit. In addition, the wind power profile tends to exhibit more small fluctuations compared to solar power on a typical basis, and the large capacity of wind power in these cases allows these fluctuations to severely distort the balance power profile. This causes the balance power profile to become somewhat unpredictable in terms of daily trends, and

while the chiller plant is allowed to operate dynamically in this study, the TES tank reaches its limits more often due to the irregularity of the chiller dispatch and the difference in the relative magnitudes of wind-induced balance valleys and solar-induced balance valleys. Combined, these factors reduce the effectiveness of chiller dispatch in reducing variability for increasing the balance capacity factor.

Above 50%, the benefit increases until a sharp decrease negates the benefit at the 75% penetration level. This behavior occurs because of the sharp increase in solar power in this penetration range and the onset of massive amounts of over-generation due to both wind and solar power. Since in this range, peak solar power periods are also causing over-generation in addition to the wind power periods, the respective decrease in the balance power profile for each type of event becomes more similar to each other, and equal to each other at the higher end of the range since the balance power cannot be decreased below zero. This restores some level of daily regularity to the balance profile which the chiller plant take advantage of: a restoration of the 12-hour variability experienced at the lower renewable penetration levels. In this case, the chiller plant is not capable of completely leveling the balance valleys caused by wind or solar power. Since the respective decreases are near equal, however, it is able to provide a near-equal contribution towards leveling both types of events to the extent possible and is able to reduce balance variability similar to the trend displayed below the 33% penetration level, albeit to a smaller extent during periods when the over-generation power is not too large. At the upper end of the penetration range, however, the over-generation is so large that the chiller plant operating at maximum capacity cannot prevent the balance power from dropping to zero during even off-peak wind and solar power periods, and the benefit is negated by the 75% level.

The chiller-biased case tends to decrease the capacity factor of the balance generator fleet compared to the case without thermal energy storage, except at renewable penetration levels below 30%, where the capacity factor is increased due to energy savings. The decrease is linear with renewable penetration. Since the dispatch of the chiller plant is not influenced by balance profile characteristics, the chillers will tend to operate at certain, specific power levels during periods of low wet-bulb temperatures as discussed previously. This manner of operation adds load to the grid with no consideration for on-peak or off-peak balance periods. Since this load profile is not complementary to the intermittency of wind and solar power, the chiller dispatch often introduces additional variability into the balance profile, increasing the typical range of balance power variability and causing the typical deviation from the average balance value to increase within that window. The result is a decreased utilization of the balance generator fleet at all renewable penetration levels compared to the case without thermal energy storage until the 75% renewable penetration level, where the benefit is garnered by energy savings alone, however this effect is limited.

The combined case necessarily constitutes a compromise between the effects of the utility-biased and chiller-biased cases. During the time periods where minimizing energy use is a higher priority due to the fact that chilling must be deployed at those times to fill the TES tank and the conditions at that time render the chiller units to be less efficient, the effect of the chiller dispatch likely contributes to a decrease in the balance capacity factor. Other time periods where dispatch to level fluctuations in the balance power profile takes precedence contributes

to an increase in the balance capacity factor. The net result is that a small benefit compared to the case without thermal energy storage until the 50% penetration level, where due to the strong variability and over-generation, the utility-biased factor takes precedence.

Overall, the large scale implementation of thermal energy storage and chiller dispatch capability to enable cooling loads to be a dispatchable resource has the potential to aid the balance generator fleet on the electric grid in terms of counteracting the decreased utilization of such resources. This benefit can be realized only if communication between communities and the electric grid is installed, and if dispatch behavior to respond to fluctuations in the balance profile is given at least equal priority to other dispatch behavior. The extent of the benefit depends on the weighting of the grid-response priority compared to other constraints.

3.4.3.2.2. Effect on the Maximum Balance Value

Depending on the chiller dispatch priority, the implementation of thermal energy storage has a tendency to decrease the maximum balance value, however in certain cases it can also cause it to increase.

The utility-biased case decreases the maximum balance value at all renewable penetration levels. This effect is expected, since the cost function governing this dispatch priority penalizes operation of the chillers during periods of high balance power, and additionally penalizes excessive chiller power demand. Therefore, the chiller plant will be dispatched to operate during periods of low balance and will attempt to minimize the maximum chiller power demand for each respective operating window. This has the effect of removing load demand during periods of originally high balance values, reducing the maximum balance values. Since the displaced load is then added during periods of originally low balance values, the balance value at such times is generally not increased above that of the daily peak values and therefore does not contribute to increasing the maximum balance value. This case is shown to be capable of decreasing the maximum balance value by between 5.9 GW (13.9%) at the 13% renewable penetration level, 8.05 GW (23.9%) at the 75% renewable penetration level and any range in between depending on penetration level. The benefit is increased at higher renewable penetration levels since the onset of over-generation weights the priority to respond to the load higher than the penalty for high chiller power use, and therefore the chiller plant is used to full capacity.

The chiller-biased case tends to decrease the maximum balance value at lower renewable penetration levels and slightly increases the maximum balance value at higher renewable penetration levels. The initial decrease occurs since the periods of low wet-bulb temperatures tend to occur during the nighttime hours, when the balance values tend to be lowest (for renewable penetration levels below 33%). Therefore, even though the chillers are not communicating with the electric grid directly, the effect is similar to the utility-biased case since the cooling demand is displaced from typically high balance value periods, albeit to a smaller extent. As the renewable penetration level increases and the balance profile becomes more and more unpredictable, the chiller-biased case is unable to adjust to the change in the occurrence of high and low balance power periods. In addition, the chiller plant in this case tends to operate

at certain power set points to maximize efficiency and take advantage of the times of lowest wet-bulb temperatures. This behavior has the effect of removing cooling loads from a given time period of variable length and introducing the same energy content of the removed load at another time period. If the chiller plant operates at a period of originally high balance values, it will significantly increase the balance value during that time and changes in the renewable penetration level will not alleviate such an effect since the balance profile does not influence the chiller plant. Therefore, only minimal decreases in the maximum balance value is garnered by utilizing chiller-biased dispatch, after which the value will remain constant and eventually end up higher than that in the case without thermal energy storage implementation. The effects range from a 1.87 GW (4.4%) decrease at the 13% renewable penetration level to a 0.67 GW (1.98%) increase at the 75% renewable penetration level.

The combined case naturally represents a compromise between the chiller-biased and utility-biased cases in terms of effectiveness. This dispatch behavior tends to decrease the maximum balance value for all renewable penetration levels, albeit to a lesser extent than that of the utility-biased case. The decrease in the maximum balance value is closer to that of the utility-biased case compared to the chiller-biased case, since the utility component penalizes the peak power use during chiller operation windows directly in addition to penalizing the general use of power during high balance power periods. Therefore, in terms of addressing the maximum balance, the combined case will be slightly more likely to follow the utility-biased case rather than the chiller-biased case. At very high renewable penetration levels, the effect of the combined case converges on that of the utility-biased case. This occurs since the period at which the maximum balance values occur at these penetration levels tended to coincide with periods when the chiller plant must operate at high power capacities due to the high capacity of intermittent renewable resource penetration, rendering the efficiency criteria essentially met. Therefore, the combined case will be heavily biased toward the utility-biased case.

3.4.3.2.3. Effect on Surplus Renewable Generation Value

The effect of implementing thermal energy storage with chiller dispatch on a large scale on the amount of surplus renewable generation for the three different dispatch behaviors is presented in Figure 102:

Figure 102: Surplus Renewable Generation vs. Renewable Penetration Level for Different Chiller Dispatch Cases

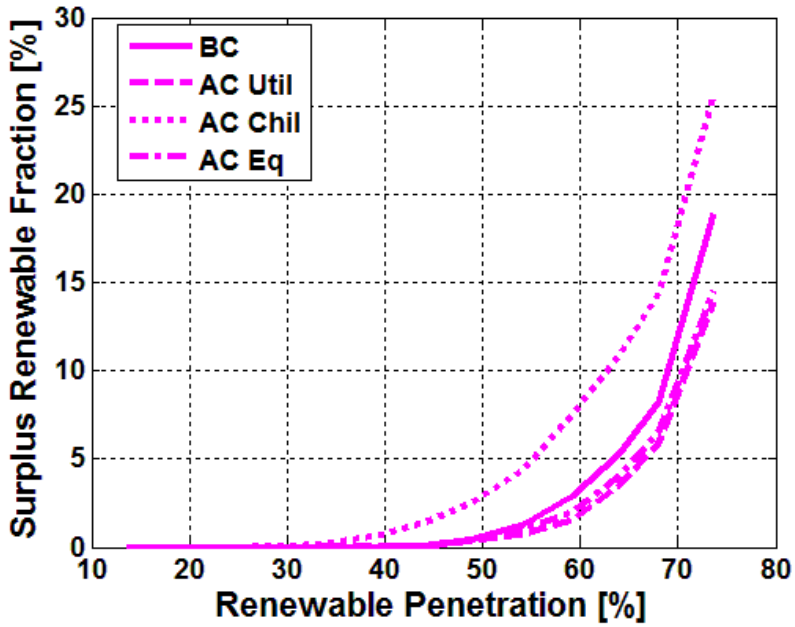

In general, the use of large scale chiller dispatch does not reduce the amount of surplus renewable generation compared to the case without thermal energy storage and in certain cases can actually increase it.

The utility-biased and combined cases show only a small effect on altering the amount of surplus renewable energy obtained compared to the case without thermal energy storage for all renewable penetration levels. This behavior is unexpected, given that the chiller plant will attempt to operate when the magnitude of the balance signal is relatively low in an attempt to level the load profile. In this case, however, the limitations on the TES tank in terms of capacity, the need to meet the local cooling load as a first priority, and the large power requirements to level the effect of the high power, short duration nature of intermittent renewables prevents utility-biased chiller dispatch from decreasing the amount of surplus renewable energy. Time series plots for the TES charge level, surplus power generation, and balance profiles with chiller power and renewable generation for a representative 300 hour period at the 55% renewable penetration level is presented in Figure 103:

Figure 103: Representative TES Charge, Surplus Power Generation, Balance and Renewable Power Profiles at the 55% Renewable Penetration level for the Utility-Biased case.

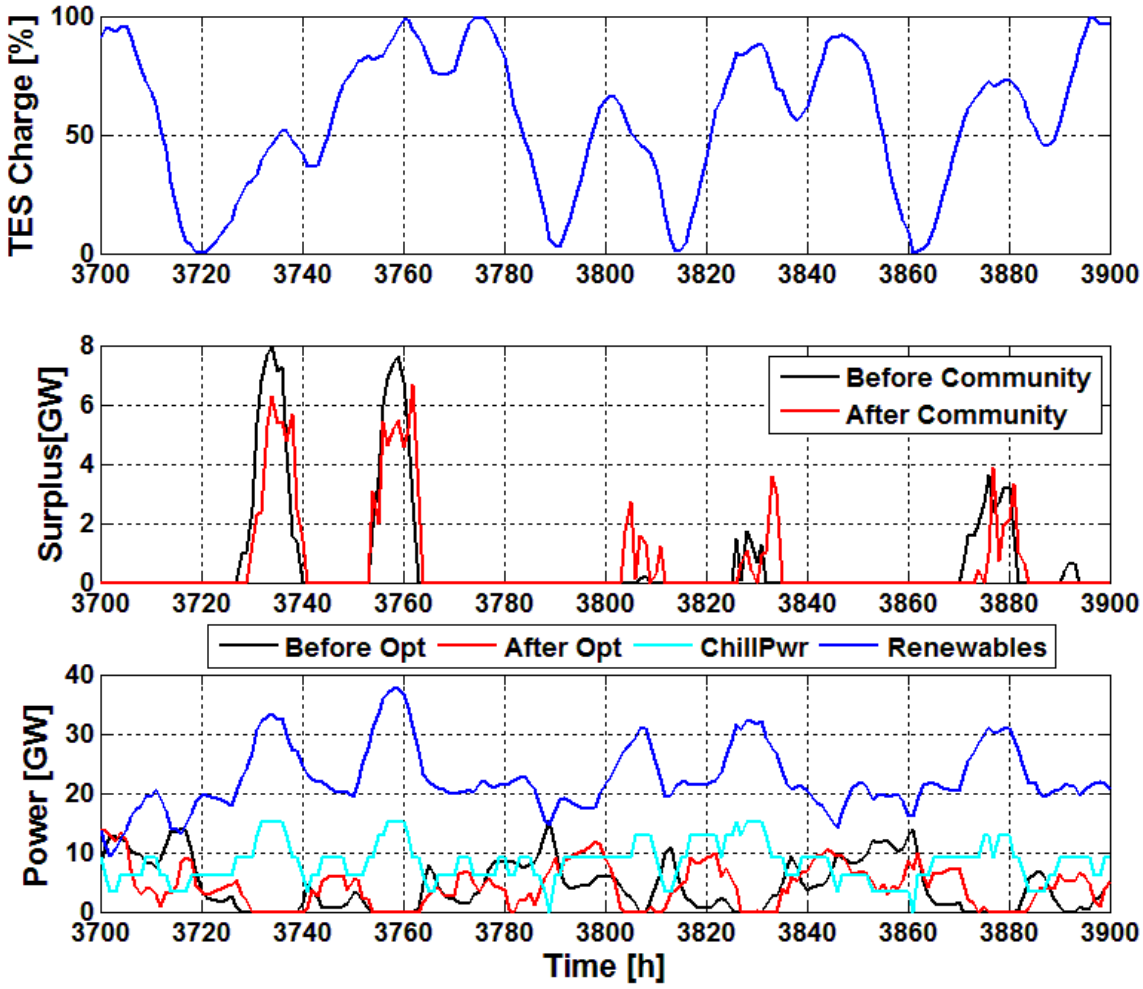

The cooling system must meet the local cooling demand as a priority and additionally, the cooling load is only a fraction of the electric load. This implies that the TES tank will be sized to meet the cooling demand of the campus. It would not make sense to oversize the TES tank in order to supposedly help the grid as would be the case with an electrical energy storage system. Doing so implies that an excess amount of cold water would be produced that would not be used to meet the local cooling load, indicating unnecessary energy usage. The preferred sizing of the TES tank limits the magnitude of the load that the chiller plant introduces during any given time period, since it is sized based on an energy consideration primarily, with the power consideration of the chiller plant as a secondary criterion.

An example of such a limit is displayed between hours 3750 and 3765. During this period, the renewable power generation peaks, and chillers are dispatched to introduce load and mitigate the drop in the balance power magnitudes during this period. Since the TES tank reaches near full charge before the point when renewable generation drops off, however, the chiller plant is prevented from reaching its full capacity and is forced to turn off early, leaving a period of high

renewable generation and low balance power which cannot be leveled. During these periods, a significant amount of surplus energy is still present. These periods happen regularly throughout the year, especially since renewable power production tends to increase quickly without expectation to very high magnitudes. While chiller dispatch is able to reduce the amount of surplus energy present compared to the case without thermal energy storage, the extent to which it does so is limited.

In addition to this effect, the chiller plant is penalized for excessive power use during any given chiller operation window, and will be more reluctant to utilize its full capacity unless explicitly necessary. The effect of spreading what was originally a high magnitude, short duration cooling load over a long duration period with smaller magnitudes effectively reduces the cooling load at a time when renewable power generation may be high. This causes the amount of surplus power produced after applying renewable generation to be increased over that in the case without thermal energy storage for such periods.

Overall, the net effect is only a small decrease in the amount of surplus renewable energy obtained for a given renewable penetration level compared to the case without thermal energy storage. The reductions in surplus energy obtained by operating chillers during low balance periods is countered by increases in surplus energy obtained by spreading cooling load over longer periods of time. In this particular case, the two components of the utility cost function – the load sensitive component and the peak power penalty – act to counter each other and no net benefit or disadvantage is garnered.

The chiller-biased case displays a marked increase in the amount of surplus renewable energy obtained compared to the case without thermal energy storage. Surplus energy starts to become present by as low as the 29% renewable penetration level, and by the 75% renewable penetration level, the surplus renewable fraction is approximately 26% compared to 19% without thermal energy storage. This once again is an artifact of the lack of influence that the behavior of the balance power signal on the electric grid has on the chiller dispatch and operation. Time series plots for the TES charge level, surplus power generation, and balance profiles with chiller power and renewable generation for a representative 300 hour period at the 55% renewable penetration level for the chiller-biased case is presented in Figure 104:

Figure 104: Representative TES Charge, Surplus Power Generation, Balance and Renewable Power Profiles at the 55% Renewable Penetration level for the Chiller-Biased case.

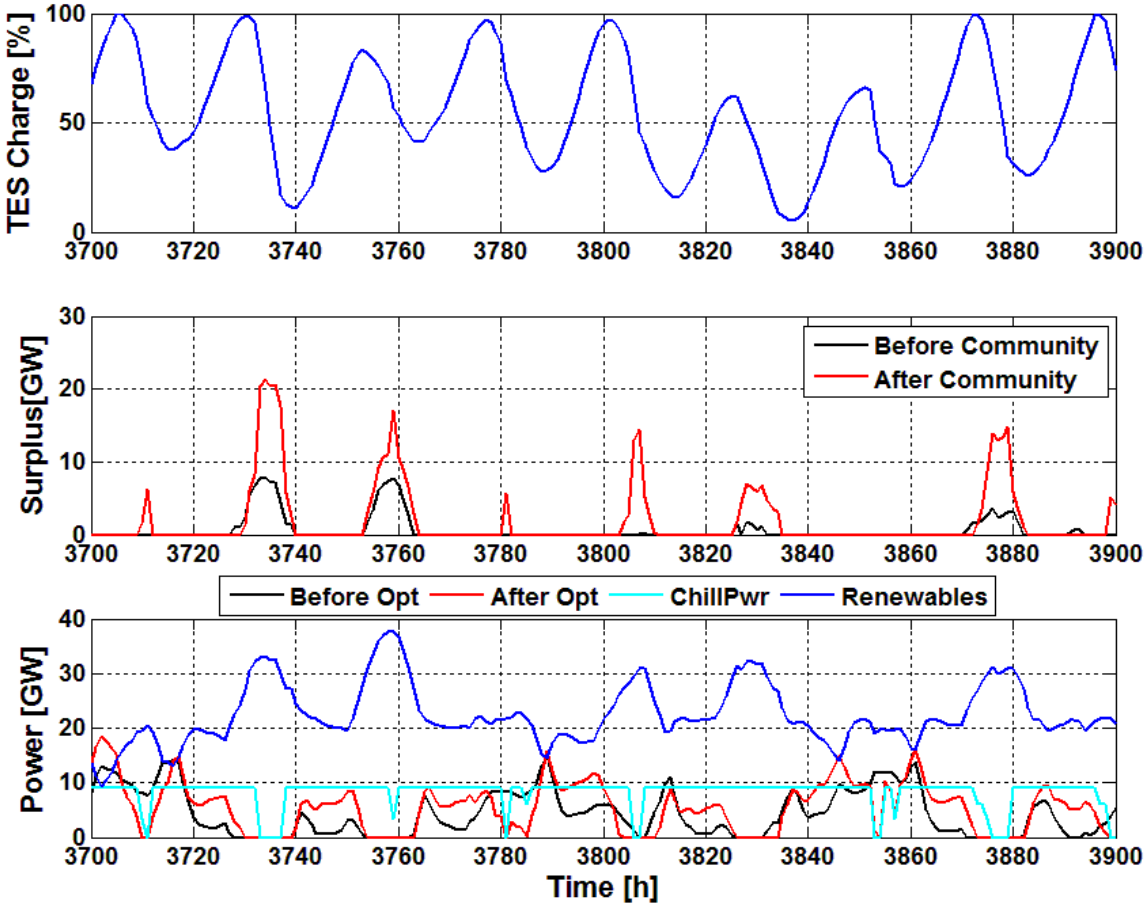

As discussed previously, to maximize efficiency, the chiller plant will tend to operate at certain set points corresponding to any active units being at full capacity without any consideration of the behavior of the balance profile. Therefore, the chiller power demand will introduce additional load during periods of peak and near-peak balance power, and activation will occur with no solid correlation to the effective load demand (balance). This introduces an extra degree of variability into the balance signal, and as shown in Figure 104, the chiller power demand may remove cooling load from periods of high renewable power generation if it is not efficient to operate the plant at that time and move load to a later time period. This effect can essentially remove the entirety of the cooling demand during such periods. This causes the amount of surplus renewable generation obtained during this period to be greatly increased, however contrary to the utility-biased case, this effect is not countered explicitly since the time period when the cooling load is re-introduced may not necessarily correspond to a time period when it is beneficial.

Overall, the lack of information or influence from balance profile characteristics renders this dispatch behavior ill equipped to manage high renewable power penetration levels from the standpoint of reducing the amount of over-generated renewable energy.

Task 3.4.4. Summary and Discussion

Overall, converting cooling loads from a static load to a dispatchable load by means of implementing thermal energy storage at the community level has the potential to aid in the management of the electric grid at increased renewable penetration levels to a significant but limited extent. The extent to which this ability can be garnered is dependent on the manner by which the chillers at each community are dispatched. Depending on the chiller dispatch behavior, the implementation of cooling load dispatch via thermal energy storage can either provide a significant benefit or end up worsening the issues already associated with managing high renewable penetration levels, or any effect in between.

Cooling load dispatch in the utility-biased case reduced campus load variability, and this condition applies as long as the campus load shares similar characteristics to that of the bulk-grid balance profile. As the campus load and grid balance profiles start to deviate from each other due to the effect of centralized renewables, the variability may not necessarily be reduced. This deviation tends to occur at higher renewable penetration levels when intermittent renewable behavior renders the signal to which the chillers respond to as somewhat unpredictable. While this may reduce the combined dynamics of the bulk electric grid, it can either maintain the current level of campus load variability or increase such variability at higher renewable penetration levels. Therefore, in the utility-biased case there is also a tradeoff between the bulk electric grid and the community in terms of load fluctuation range. At very high renewable penetration levels, the typical fluctuation range of the campus load can well exceed original levels and that of the chiller-biased case. It is important to note, however, that all three chiller dispatch behaviors display a reduction in campus load variability for a large but limited renewable penetration level range.

In terms of energy use, cooling load dispatch shows reductions compared to the case without thermal energy storage in all three cases examined herein. In the case of chiller-biased operation, the reduction is systematic since the chiller plant actively searches for the most efficient time periods to operate. In the case of utility-biased operation, the reduction occurs since the erratic nature of the balance signal causes the chillers to operate during time periods of slightly lower wet-bulb temperatures compared to the case without chiller dispatch, when most of the cooling load was supplied during the hot daytime hours. The combined case is once again a compromise between these cases.

At the campus level, there exist tradeoffs between the three different cases, and the preferred chiller dispatch strategy will depend on the priorities of the community.

From the utility-grid perspective, however, the difference in effectiveness between the three cases is clear. The utility-biased case is capable of providing significant benefit to the ability of the electric grid to manage increased renewable penetration levels, especially at the low levels. The increase in capacity factor and reduction in the required balance generator fleet capacity allows current levels of balance generator fleet utilization to be maintained, aiding to keep the overall levelized cost of electricity within acceptable ranges and reduces the need for near-term changes in grid operations. These two factors are current major obstacles to the accommodation of increased renewables on the electric grid. The reduction in the minimum required balance

generator fleet capacity can potentially reduce the capital investment into the system on the generator side, although this cost will have to be weighed against the cost of implementing chiller dispatch. Additionally, while utility-biased chiller dispatch only slightly reduced the amount of surplus renewable energy obtained, it did not exacerbate the issue.

By contrast, the chiller-biased dispatch case exacerbated many of the issues associated with accommodating high renewable penetration levels on the electric grid. Since this type of operation is not directly sensitive to balance profile characteristics, it is incapable of adapting to the changes in the balance profile brought about by increases in intermittent renewable capacity that act to decrease balance generator fleet utilization and increase the minimum required balance generator fleet capacity. Additionally, the inability of chiller-biased dispatch to adapt to changes in balance profile characteristics causes a larger amount of renewable energy obtained to be wasted and requires an increased amount of renewable capacity to meet a given renewable penetration level.

Task 3.4.5. Conclusions

A study which examined the potential for the conversion of cooling loads from a static load to a dispatchable load at the community level to aid the electric grid in managing increased renewable penetration levels has been examined. Effects on community load characteristics as well as bulk grid load characteristics were highlighted for three different dispatch behaviors, each with corresponding priorities, advantages, and disadvantages. The conclusions of this study are as follows:

- **The implementation of thermal energy storage to enable cooling load dispatch provides a reduction in local chiller energy use almost regardless of chiller dispatch behavior.** The extent of reduction, however, depends on chiller dispatch behavior.
- **The effect of cooling load dispatch on campus load variability depends on dispatch behavior:** If the chillers respond to utility-load characteristics, large reductions in typical load fluctuation range occur when the character of the campus load matches that of the balance profile on the utility grid. As these two load profiles deviate in character, the reduction in campus load fluctuation is diminished or eliminated. If the chillers do not respond to utility-load characteristics, a small but constant reduction in campus load fluctuation is garnered.
- **Cooling load dispatch can aid in the management of increased renewable penetration levels on the electric grid only if community chillers communicate with and respond to utility-load characteristics.** If the operation of community chillers is influenced by the character of the utility-grid load demand (post-renewables), it is capable of adapting to the increased dynamics brought about by increased renewable penetration levels. If the operation of community chillers is not influenced by the character of the utility-grid load demand (post-renewables), it is ill-suited to complement high installed intermittent renewable capacities.
- **The benefit of utility-responsive chiller dispatch is diminished at higher renewable penetration levels. Therefore at very high renewable penetration levels, other energy**

management strategies must be implemented along with cooling load dispatch to accommodate such penetration levels. Inherent limitations of cooling load dispatch on helping the electric grid include the fact that meeting the local cooling load is the first priority, and the fact that the cooling load is only a fraction of the total electric load. Therefore, cooling load dispatch is unable to significantly influence the balance profile beyond a given extent.

Overall, cooling load dispatch can be considered as an important part of the energy management strategy portfolio that will be required to allow the electric grid to accommodate increased renewable penetration levels. The benefit of such a strategy, however, is highly dependent on the manner in which it is implemented. Consideration of the control strategy for operation, and tradeoffs between effects on the community load vs. the utility-load must be taken into account.

Task 3.4.6. References

3TIER, Development of Regional Wind Resource and Wind Plant Output Datasets. 2007-2008, U.S. Department of Energy.

Gillette, A., Marks, J., Stoltzfus, E., Douglas, P., 33% Renewables Portfolio Standard Implementation Analysis Preliminary Results. 2009, California Public Utilities Commission.

Liu, H.H. "Analysis and Performance Optimization of Commercial Chiller/Cooling Tower Systems." Masters Thesis, Georgia Institute of Technology, June 1997.

Lowe, H.J. and D.G. Christie. "Heat Transfer and Pressure Drop Data on Cooling Tower Packings, and Mode Studies of the Resistance of Natural Draft Towers to Airflow." ASME Heat Transfer Proceedings, Paper 113, 1961.

NREL, Western Wind and Solar Integration Project. 2008, U.S. Department of Energy.

NREL, Wind Energy Resource Atlas of the United States. 1986, U.S. DOE.

NREL, National Solar Radiation Database. 1991-2005, U.S. Department of Energy.

Tarroja, B., Characterization and Evaluation of Utility-Scale Intermittent Renewable Generation Variations and Implications for Electric Grid Load Balancing, in Mechanical and Aerospace Engineering. Masters Thesis, University of California, Irvine: Irvine, 2011.

Appendix C:Task 4:
Renewable Generation Deployment

TABLE OF CONTENTS

Task 4.1. UCI MW Solar PV System and Capacity C-2

Task 4.1.1. The campus photovoltaic installation and monitoring equipment C-2

Task 4.1.2. Monitored effects of a megawatt PV installation on UCI micro-grid C-3

4.1.2.1. Diurnal Variation C-4

4.1.2.2. Morning Cloud Cover Effects C-4

4.1.2.3. Intermittent Cloud Passes / Cloud Passes at Peak C-6

4.1.2.4. Storm Events C-8

Task 4.1.3. Simulated interactions between the campus PV installation and Solar turbine C-11

Task 4.1.4. Analysis results of campus solar photovoltaic capacity C-14

4.1.4.1. Available Area for Installation C-14

4.1.4.2. Local versus Regional Renewable Generation C-18

Task 4.1.5. Conclusions C-19

Task 4.2. Installation of Concentrated PV on Campus C-20

Task 4.2.1. Conclusions C-30

Task 4.3. Biogas Poly-generation Renewable Energy Station C-30

Task 4.3.1. The Orange County Sanitation District biogas tri-generation energy station C-32

Task 4.3.2. Guidelines for other tri-generation biogas energy station C-35

Task 4.3.3. The analysis results of campus biogas generation capacity C-36

Task 4.3.4. Modeling of biogas poly-generation system C-37

Task 4.3.5. Conclusions C-43

Task 4.3.6. References C-44

The University of California Irvine and the Advanced Power and Energy Program, are very progressive in implementing advanced and environmentally friendly technologies on campus. In addition to UCI supporting the construction of Leadership in Energy and Environmental design (LEED) certified buildings, and a multi-megawatt central generation plant with thermal energy storage tank for providing electricity, heat and cooling to meet campus demand, there is a growing amount of renewable generation on campus. There are currently large rooftop solar photovoltaic (PV) arrays on buildings throughout the campus, two advanced high concentration photovoltaic (HCPV) panels at the recreational facility and a tri-generation station operating on anaerobic digestion gas at the Orange County Sanitation District (OCSD) facility. Table 1 lists each pilot project and whether it was implemented under this RESCO project. The several pilot projects investigated in this section are listed in Table 19 below. This section provides information and analysis about the renewables as well as explores the challenges that UCI faced with land use, availability, aesthetics, interconnection and operation.

Table 19: Task 4 Renewable Pilot Projects

System	Capacity
UCI Fixed Plate PV	893 kW
UCI Concentrated PV	113 kW
OCSD Tri-Gen Fuel Cell	300 kW

Task 4.1. UCI MW Solar PV System and Capacity

Task 4.1.1. The campus photovoltaic installation and monitoring equipment

The University of California at Irvine has installed 893 kW of solar PV capacity across the breadth of its campus area. This consists of multiple arrays of varying sizes, each having been installed on the rooftops of different buildings within the campus vicinity. These arrays are connected to the appropriate distribution circuit on which their host building resides.

Power data for each of the installed arrays are made available by the Client Connect interface provided by Sun Edison. A running total of solar energy production, as well as electrical power production at a temporal resolution of up to 15 minutes are provided. Data can be extracted for individual building arrays or for the aggregate of all of the arrays representing the entire campus.

Currently, the UCI campus has PV panels installed on 11 buildings as part of the campus-wide array. The location of each of these arrays on the campus grounds is displayed in Figure 105, with the corresponding nameplate capacity of each array listed in Table 20:

Table 20:

Figure 105: Location of UCI Campus Solar PV Resources

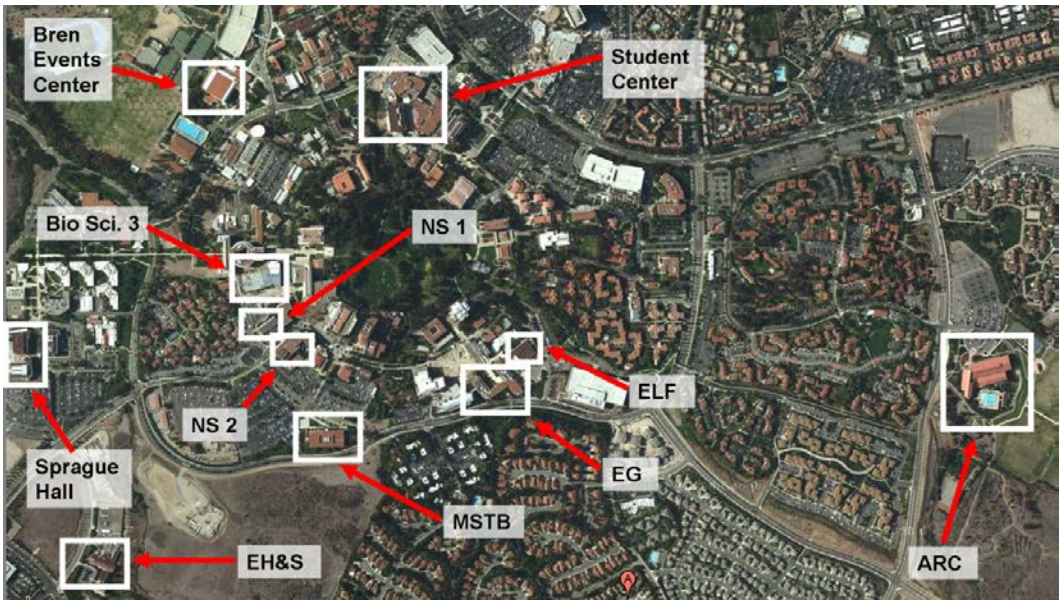

Table 20: Nameplate Capacity of Individual PV Arrays

Campus Building	PV Array Nameplate Capacity (kW DC)
Anteater Recreation Center (ARC)	150
Biological Sciences 3	63
Bren Events Center	118
Engineering Gateway (EG)	48
Environmental Health and Safety (EH&S)	118
Multipurpose Science and Technology Building (MSTB)	92
McGough Hall	65
Natural Sciences 1 (NS 1)	37
Natural Sciences 2 (NS 2)	56
Sprague Hall	55
Student Center (SC)	84
Engineering Laboratory Facility	5
Total UCI Campus	893

Task 4.1.2. Monitored effects of a megawatt PV installation on UCI micro-grid

The campus has not yet captured any monitored effects on the voltage or power quality on the UCI micro-grid circuit. This is due to two primary factors:

Peak day time loads are at the same time as peak building loads. The solar installation ~1 MW is a small fraction of the 15 MW campus load (<8%). At these penetration levels the impact of PV on distribution circuits is similar to efficiency measures to decrease peak loads.

As discovered from analysis in Task 2, the UCI circuits are short. Consequently the campus could handle a significant amount of solar penetration without impact to the circuit voltage profile.

However, with increased solar penetration, solar can have an impact on the operation of the electric distribution circuits. This is especially true on longer circuits operating closer to capacity operating limits. For example the power can flow backward on the circuit. Such impacts are evaluated in more detail in Task 2.

Field data from the UCI rooftop PV installation was used to evaluate and characterize solar intermittencies. Solar irradiation in the southern California region exhibits four key types of intermittencies that are relevant to the operation of the supplementary electrical infrastructure and balancing of demand. These types are listed as follows:

4.1.2.1. Diurnal Variation

Solar irradiation varies according to the cycle of the earth's rotational period, and is only present in any measureable magnitude during the daytime hours. The time period of the daytime hours where significant solar irradiation is present on a given area of land varies with its location, season and local characteristic weather phenomena. This type of intermittency is generally well understood: there is no solar power during the night hours, and therefore an example of this intermittency is not displayed herein.

4.1.2.2. Morning Cloud Cover Effects

In the Southern California region as well as other coastal areas, a common weather occurrence is the formation of a marine layer due to the cooling effect of the ocean surface on the relatively warm air mixture. This cloud blanket moves inland due to a pressure gradient caused by the heating of inland air, often forming fog. The marine layer tends to form in the late night or early morning hours, when the ocean surface is the coldest, after which it moves inland during the morning hours, where it resides until there is sufficient radiant input from the sun to burn off the layer.

This effect has strong implications for the utilization of solar power, especially on coastal buildings which are attempting to make use of solar power as part of their distributed generation portfolio. Since this effect occurs in the morning hours and can last up to slightly past noon, when the solar irradiation is the highest, this type of intermittency has the potential to induce very large ramp rates in solar power which the supplementary system must compensate for. The power output from a given PV array may increase from very low power to near maximum power in the timescale required for the final section of the marine layer to burn off. An example of this effect on the UCI campus PV array is shown in Figure 106.

Figure 106: Marine Layer Effect on UCI PV Arrays: 8/19/09

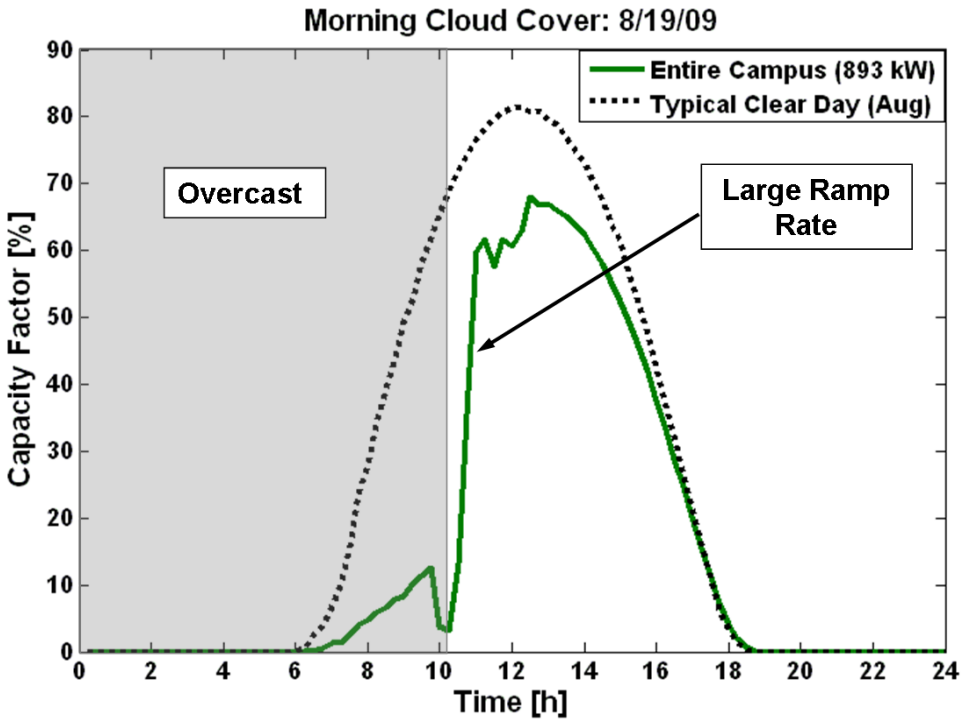

The overlay of the overcast period was obtained by extracting cloud cover data from the NOAA weather database for weather stations in the vicinity of the UCI campus. The power data exhibits a large ramp rate of solar power production from about 3% of nameplate capacity to about 60% in approximately 30 minutes. The increase from about 11% to 60%, which constitutes the final section of the large ramp, occurred in one 15 minute interval. It must also be noted that due to the temporal resolution of the data, it is possible that the power fluctuations which occur on the sub-15 minute timescale may be more erratic than displayed in Figure 106.

At the current time, the total nameplate capacity of the UCI PV array is about 6% of the average electrical load of the campus, therefore this effect is not disruptive to the operation of the current campus energy management strategy. However, if the level of solar PV penetration was significantly higher, which may be required as part of the plan to secure the UCI campus with renewable energy, this effect may result in voltage instability in the distribution circuits and a temporary inability to balance the campus load demand if strategies are not in place to accommodate for it. This is analogous to the electrical grid of the southern California region if it utilizes a high penetration of stand-alone solar power.

The marine layer effect is also one which simultaneously covers a large land area, and therefore cannot be avoided to any significant extent by using local regional dispersion of PV resources. In the August 19 event, all of the individual PV arrays on campus exhibited a profile which matched that of the aggregate, indicating that this effect was simultaneous. This is expected due to the nature of the weather phenomena.

4.1.2.3. Intermittent Cloud Passes / Cloud Passes at Peak

This type of intermittency refers to that caused by a cloud pattern that consists of numerous but relatively small clouds which pass over a given area. The cloud pattern is not as coherent as it would be during a storm or an overcast day, rather, it displays spots of clear sky amongst spots of covered sky or vice versa. It is possible for this type of intermittency to occur during the hours of peak solar irradiation, in which case it would introduce unfavorable dynamics in the power output of a PV array, namely, it will cause the power output to exhibit large negative and positive ramp rates which the supplementary energy management components will have to compensate for. The strategies for mitigating the effects of a large positive power ramp rate and a large negative power ramp rate may differ, however both may need to be in place to buffer this type of intermittency.

It is important to note that it is difficult to quantify exactly how strong of an effect that an intermittent cloud pattern will have on the output of a solar PV array. Depending on the fraction of the hemisphere of sky surrounding the array that is covered by clouds, the size of the array, and the distribution of the clouds, different cases are possible. It is possible that an intermittent cloud pattern may not affect the power profile of the PV array to any significant degree. This case refers to the presence of a large, widely dispersed solar array and a relatively low hemispherical cloud coverage fraction. On the other hand, it is also possible for an intermittent cloud pattern to cause large distortions in the power profile of a PV array, usually in the case of high hemispherical cloud coverage and/or small array sizes. Developing a correlation between the hemispherical cloud coverage fraction as provided in the NOAA (National Oceanic and Atmospheric Administration) weather databases and the magnitude of the unfavorable dynamics introduced into a power profile for different array sizes and dispersions may be possible.

An example of the latter case, relatively high hemispherical cloud coverage fraction (5/8ths to 7/8ths) for the UCI campus array and two individual buildings, is displayed in Figure 107:

Figure 107: Intermittent Cloud Pass: High Hemispherical Sky Coverage + Cloud Pass at Peak – 11/21/09

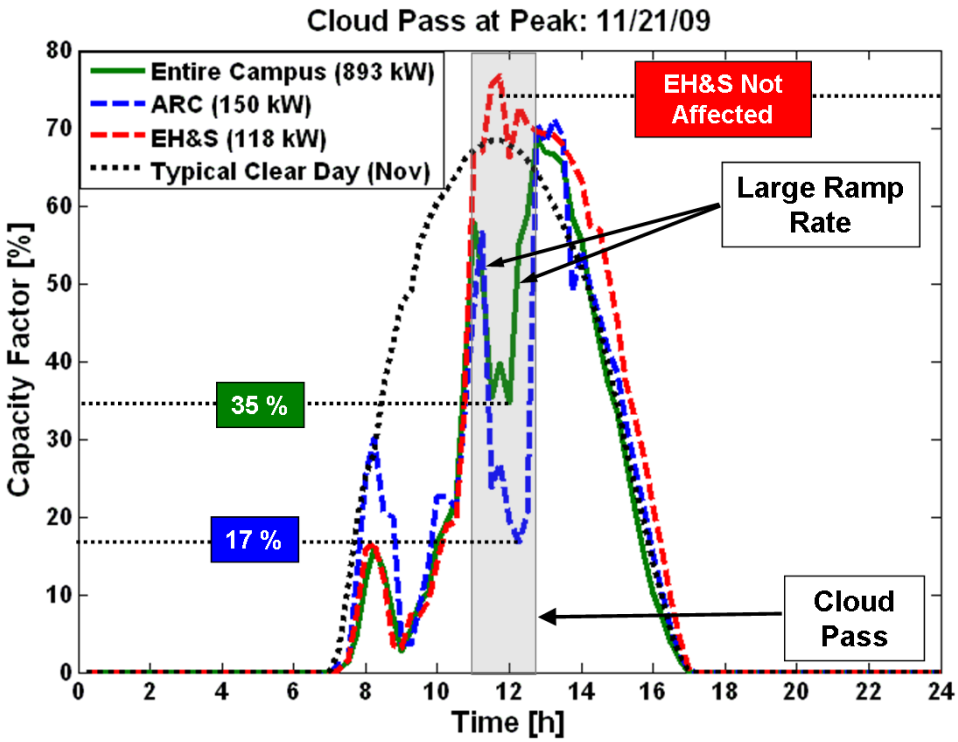

Figure 107 displays a number of notable characteristics about the power output profile of a PV array that is subjected to an intermittent cloud pass, and a cloud pass at peak. This particular day shows two distinct cloud passes, one which occurs at approximately 8:30 am and one at 11:00 am.

The first cloud pass lasts for about 1.5 hours, and simultaneously covers all of the arrays on campus, as they exhibit similar decreases in the magnitude of their power output for the duration of the pass.

The second cloud pass which occurs during the hours of peak solar irradiation, lasts for approximately the same duration, but did not affect all of the arrays on campus. The array on the rooftop of the Anteater Recreation Center (ARC) displays the expected profile of a PV array being subject to a cloud pass at peak: a distinct, quick drop in power output at the onset of the cloud cover, small power oscillations during the cloud pass due to the patched nature of a scattered cloud pattern, and a quick increase to near maximum power levels as soon as the cloud passes. However, the Environmental Health and Safety building, which is located on the other side of the campus grounds, was not affected by the second cloud pass. This array, as well as some of the others, maintained peak power output throughout the duration of the pass as indicated by the fact that the drop in total campus power output was not as large as some of the individual buildings such as the array at the ARC.

This result indicates that there is a benefit to the dispersion of PV resources across a large land area, since when intermittencies of this type occur, a smaller fraction of the entire capacity of the

solar PV system needs to be backed up by auxiliary strategies such as energy storage or ramping of supplementary generators. The power output of the aggregated arrays still maintained a reasonable value during the second cloud pass of 35% of nameplate capacity due to utilization of land area dispersion. This benefit occurs because such dispersion decouples the power output from one section of the array from another, therefore decreasing the degree to which the onset of some intermittency types affect the total power output.

Figure 107 also displays an additional trait of the behavior of solar irradiance. In the time period after the second cloud pass (and during for the EH&S array), the power output of each of the individual arrays as well as that of the entire campus exceeded the expected power output from a typical clear day. This is due to the silver lining effect, when light is diffracted by the vapor droplets along the outer edge of the cloud, creating a very slight concentrating effect which struck some of the campus PV arrays.

It is also important to note that the degree of power oscillations displayed in Figure 107 is slightly smoothed out due to the 15-minute resolution of the data. The data measured from any individual array at smaller time intervals may display a higher degree of power oscillations.

4.1.2.4. Storm Events

The final type of intermittency that is relevant to the operation of the supplementary electrical infrastructure and balancing of demand is the types of intermittencies that occur during storm events. The morning cloud cover effect discussed the power profile of a solar PV array exposed to a coherent fog in the morning hours, while the intermittent cloud pass type discussed the power profile during the onset of a broken cloud pattern. The discussion of the current type of intermittency will involve the power profile of a PV array during a completely overcast sky with precipitation.

On the UCI campus, a strong storm event was present over the campus land area on three days during December 2009. December 7th consisted of a completely overcast day with heavy rainfall, December 11th consisted of alternating cloud cover between heavily broken and complete overcast with no rainfall, while December 12th consisted of a similar alternating cloud cover pattern, but with light rainfall. The power profiles of the aggregated PV arrays during these three days are presented in Figure 108:

Figure 108: UCI PV Power Profiles During Storm Events: a) Overall, b) Inset

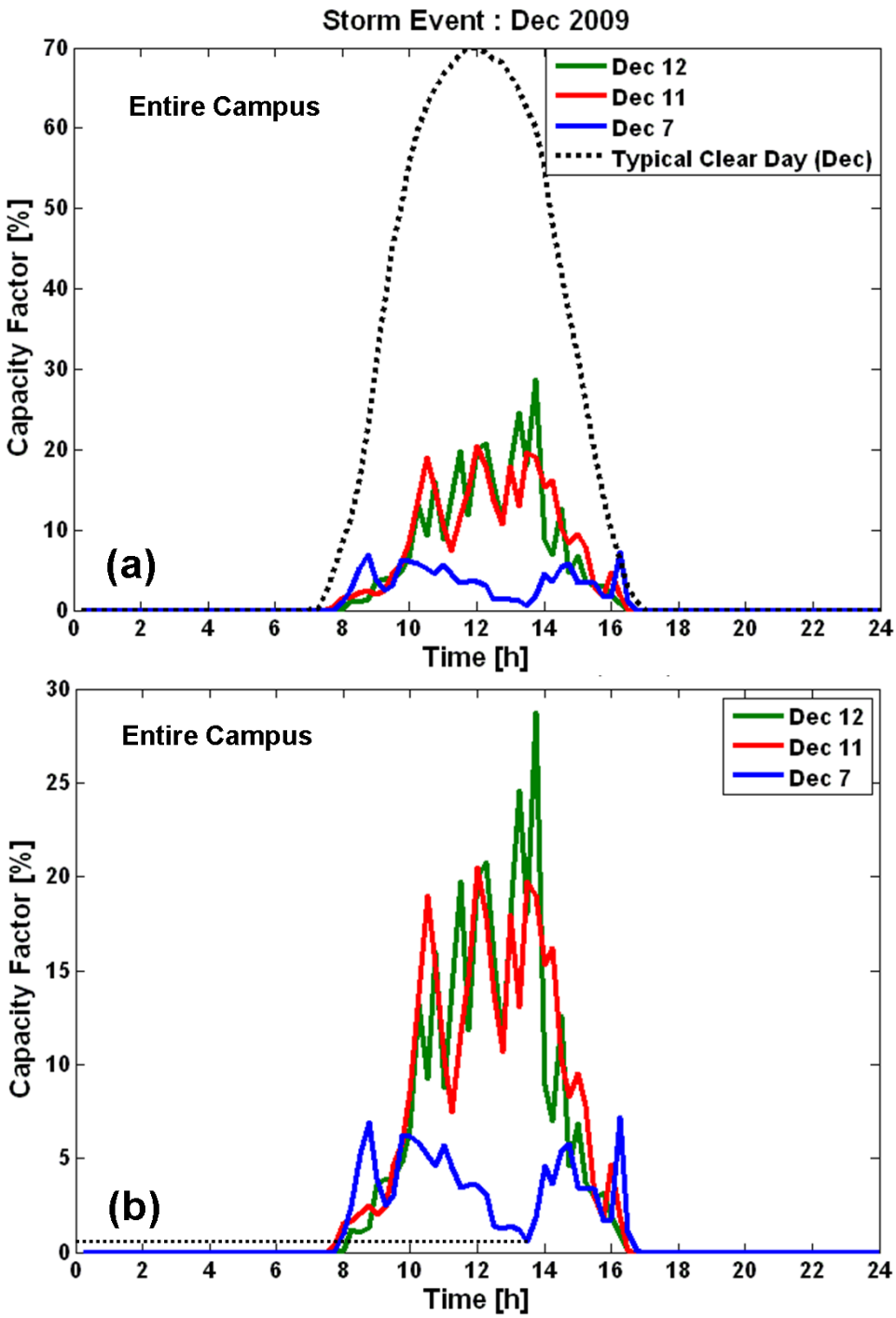

From Figure 108, it is apparent and expected that the power output of the PV array during the storm events is significantly reduced when compared to that of a typical clear day. However, it is important to note that while it is reduced by a very significant extent, the power output of the array never reaches zero, even during the heavy storm that occurred on December 7. During a completely overcast day, the solar arrays are still capable of generating a small amount of

power due to the absorption of diffuse irradiation. The effective amount of irradiation that strikes a given PV array is composed of two components:

1. Direct "beam" irradiation: the component of the sun's radiation which arrives on a horizontal surface at ground level without interruption, in a straight line from the sun.

36. Indirect "diffuse" irradiation: the component of the sun's radiation which arrives at a horizontal surface at ground level after being reflected from atmospheric objects such as clouds and airborne particles.

The onset of clouds essentially eliminates the direct component, however, the indirect component is still present with a magnitude that is dependent on the thickness of the cloud layer. During a heavy storm event when the cloud layers are the thickest and the diffuse irradiation is further reduced by absorption and re-radiation by the water droplets, the power output is reduced to less than 5%, reaching as low as 1% which is practically zero from a power generation standpoint. Due to the small range of maximum and minimum power output levels during a heavy storm event, the dynamics are present but of a small magnitude overall, rendering its output more or less steady.

From a dynamic standpoint, a more severe case arises during storm events where the cloud cover alternates between a heavily broken state (7/8ths hemispherical sky coverage) and a completely overcast state (8/8ths hemispherical sky coverage). The profiles for these types of events are displayed in Figure 108 for December 11 and 12. Overall, the power output from the panel is essentially chaotic, showing relatively large oscillations in power as the cloud cover state and thickness of the cloud layers alternate. It is important to note that if the data was of a finer temporal resolution, the magnitude and frequency of the power oscillations may indeed be larger than that displayed herein. During light storm events, the power output appears to oscillate regularly between 10% and 20% of nameplate capacity power in a fashion that is difficult to predict.

However, while these profiles may seem disturbing by their shape, it is important to note that these fluctuations are much smaller in magnitude than those exhibited by the campus PV system during times of intermittent, broken cloud patterns (5/8ths to 7/8ths). During a storm event, the upper limit of the power profile is decreased significantly, and even though the power will oscillate widely in the remaining power range, the overall ramp rates are relatively small in comparison. During the presence of broken cloud patterns, the power range within which the output from a PV system can oscillate is very large, since the upper limit is even slightly higher than the peak clear day power, while the lower limit can be close to zero. Due to the nature of an intermittent cloud pattern, the frequency of power fluctuation is expected to be higher during intermittent cloud patterns than during storm events.

In addition, it should be noted that all of the storm events which impacted the UCI campus during the current lifetime of the PV installation affected the entire campus simultaneously. This is expected since storms are regional events: storm events typically affect an entire region (such as the entire South Coast Air Basin), and therefore a very large degree of dispersion of

solar PV resources would be required to reduce the effect of this type of intermittency to even a small, measurable degree.

Task 4.1.3. Simulated interactions between the campus PV installation and Solar turbine

To minimize operation costs, the campus operates a 13.5 MW Solar gas turbine (GT) distributed generator, with heat recovery to provide campus heat, cooling or supplementary electricity (as shown in Figure 109). Even though the campus could export power to the grid, the electric utility currently requires that the campus never export power unless new substation equipment is installed. Due to this limitation, solar PV generation dynamics may have to be compensated for by the turbine to ensure no power from the campus is exported onto the grid.

Figure 109: Campus central plant, and solar installation

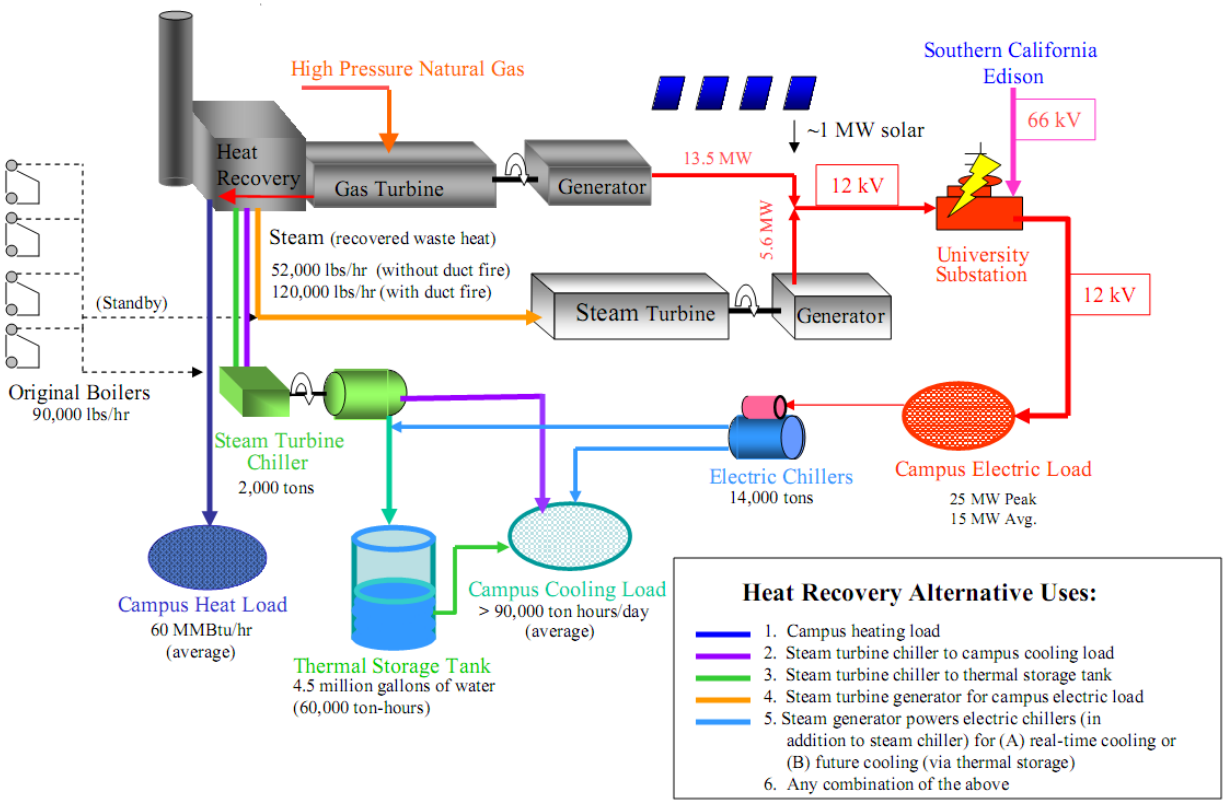

To evaluate interactions between the campus PV and the Solar gas turbine, the campus energy balance was simulated using hourly measured campus load for a whole year. The PV output was simulated using a PV model verified to field data. This allows for a sensitivity analysis based on the amount of solar installed. An example spanning case is shown in Figure 110.

Figure 110: Campus energy balance simulation. Spanning case- peak summer day with 10 MW of installed PV capacity.

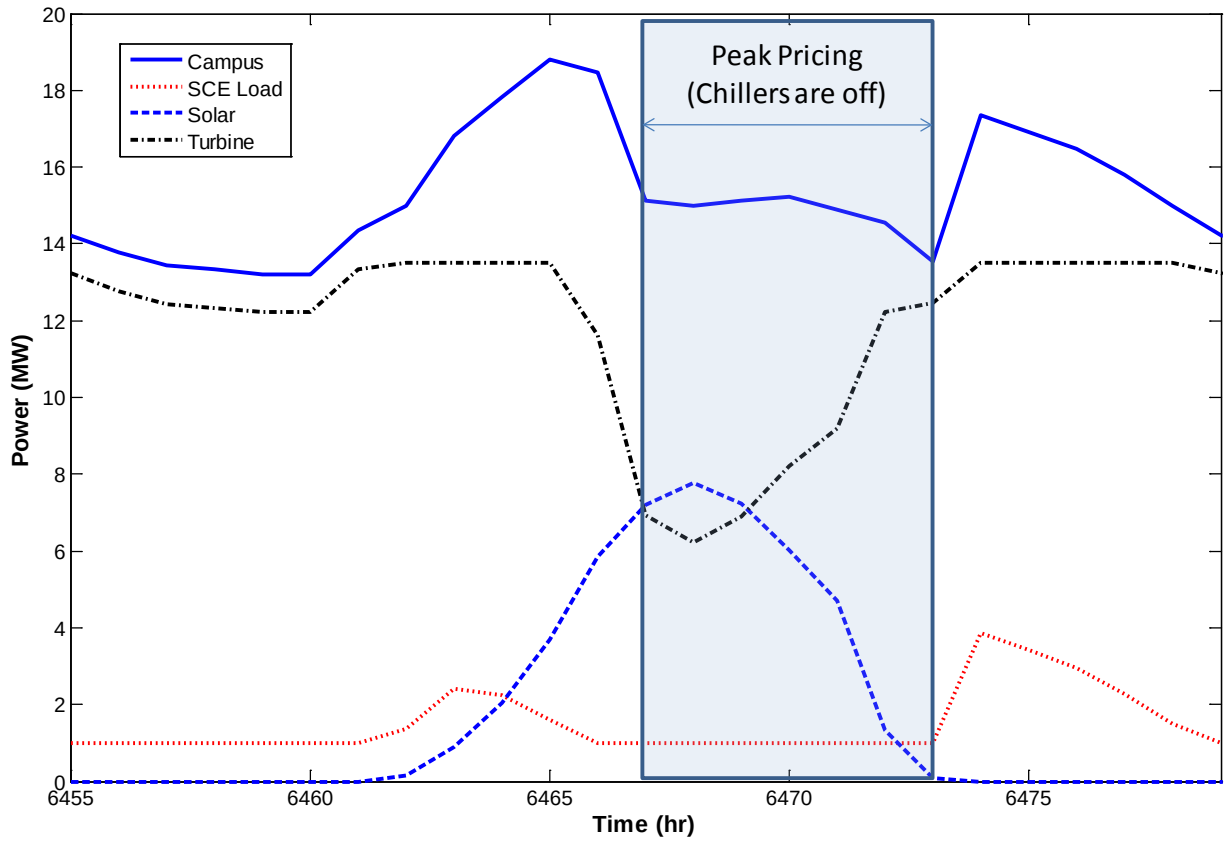

The campus load is different than one may expect. With the cold water thermal energy storage tank, the campus is able to turn off chillers during peak electric pricing by generating and storing cooling water at off peak electric prices. From the simple simulation, many important points can be made about the impact on future grids and communities with increased renewables.

- Price of electricity dictates how the central plant operates the system to minimize the cost of electricity. Using the price-of-electricity, it is possible for the utility to impact end-uses of electricity.
- With a significant amount of solar, gas turbines balancing loads will have to turn down during the day. If the campus installed new equipment, then the campus could actually export electricity in the future spanning scenario
- Electric demands may still be high at dusk when solar irradiance is gone.

This last point is further illustrated in Figure 111, showing that utility load demands are still high at dusk when people are still using electricity, with the lights on because the sun is down.

Figure 111: Comparison of daily power produced between a 2-axis tracking 24 kWac Amonix panel and a typical flat-plate panel (normalized)

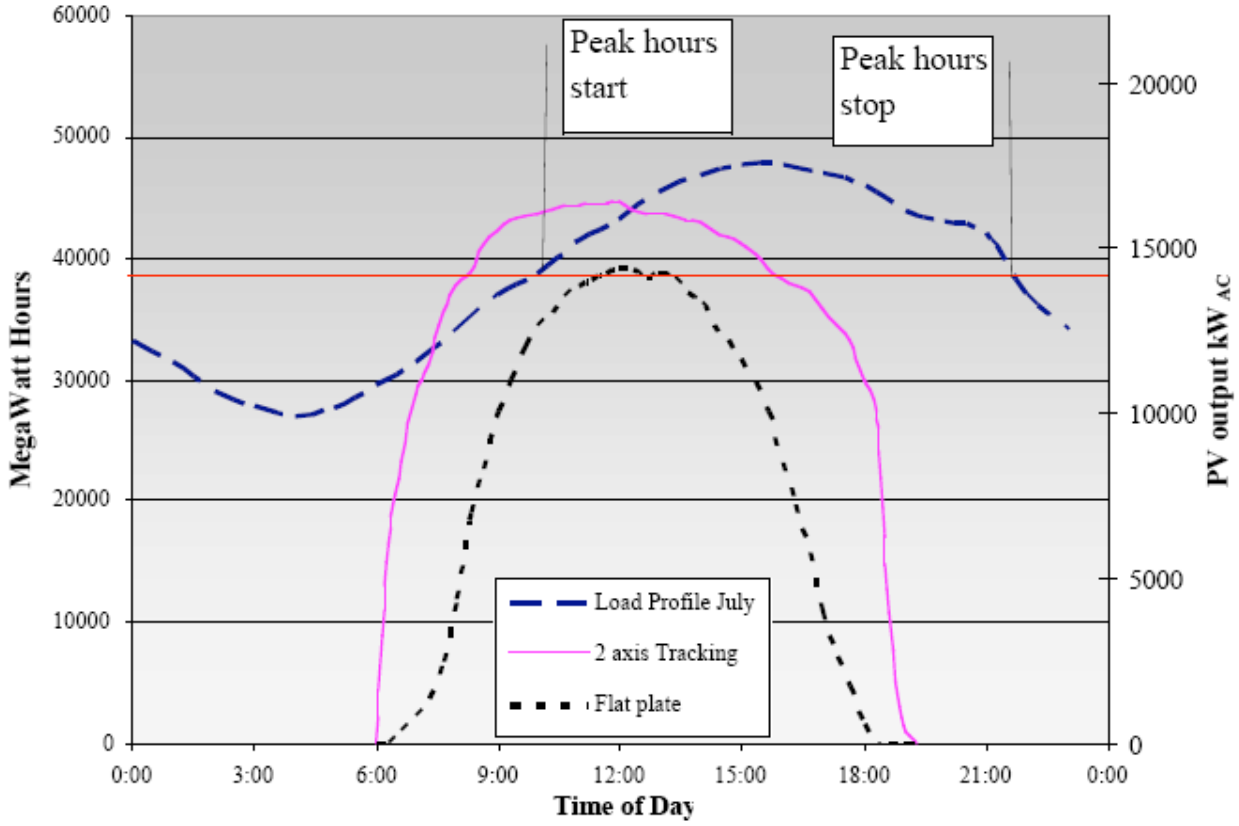

This is particularly important for the grid. Even though solar is correlated with load, energy will have to be dispatched in the morning and evening. This could result in two daily max peaks for dispatchable generation rather than one without solar as was captured in Figure 110. The developed model was used to evaluate the sensitivity to this. Specifically, the GT capacity factor, SCE peak import, and GT time at full power was evaluated for increased solar peak capacity in quarter megawatt increments. The results shown in Figure 112 indicate that as more solar is installed the GT capacity factor decreases. Peak imports from the utility decreased with more solar, but with diminishing returns. Peak utility loads shifted to dusk, when loads are still high but the sun is down. This indicates that even though solar can be installed on distribution circuits, dispatchable generation, transmission, substation and distribution circuit capacity must be maintained to serve high dusk loads and loads during cloudy days.

It is clear that load balancing will become increasingly difficult with increased intermittent renewables,. Finding the most economical means to balance load is an important secondary cost to renewable generation, which can significantly impact the cost-of-electricity. Assumptions regarding the renewable cost of electricity must carefully evaluate what complementary capacity must be maintained to balance grid loads.

Figure 112: Solar impact of Gas Turbine operation.

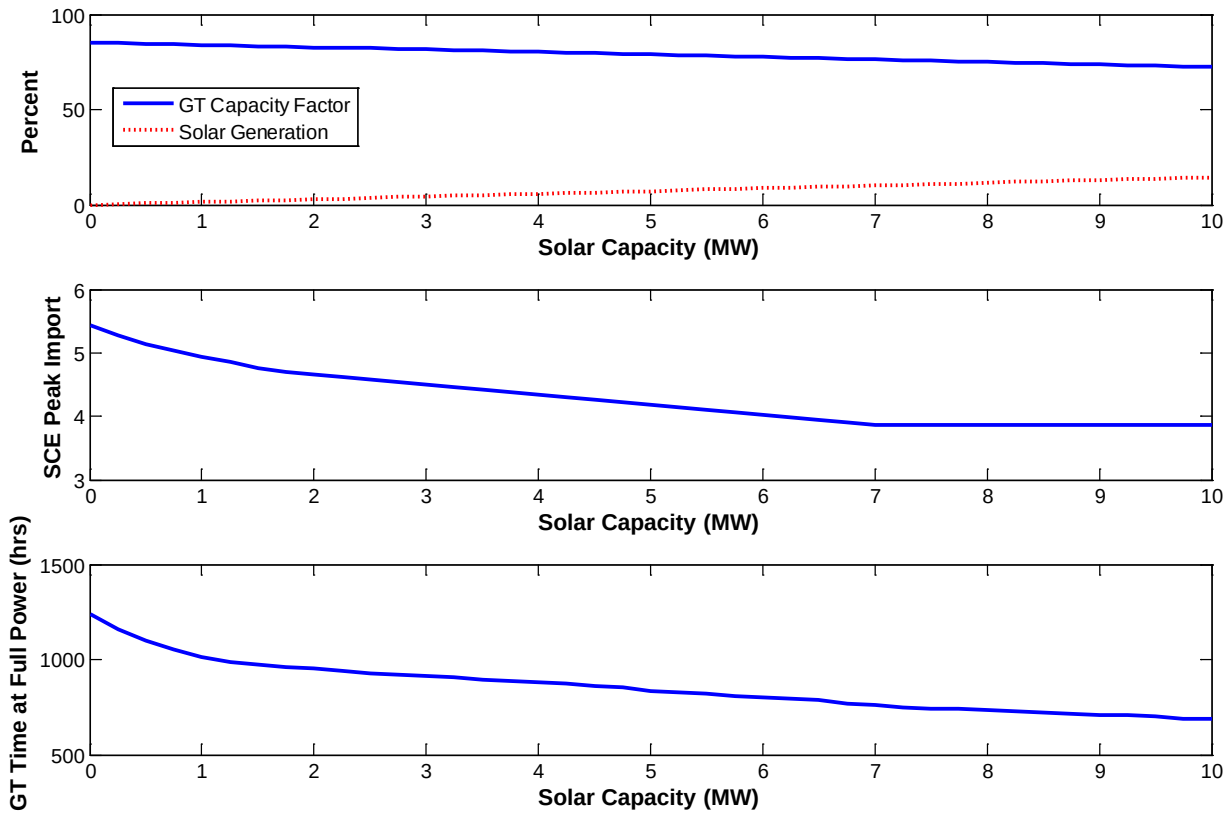

Generator capacity factors will be shown to further dictate what generation technology is most economical. This can have implications on the overall gas turbine fleet efficiency, since more efficient generators tend to be more expensive but with decreased fuel costs. However, with lower capacity factor, the gas turbine installation cost becomes more dominant over fuel costs in the overall generator cost-of-electricity. Further, less efficient generators may burn more fuel and thereby emit more GHG emissions as well as pollutant emissions. Hence, the generator capacity factor and load balancing can have broad implications and trade-offs (See Task 7 for more discussion).

Task 4.1.4. Analysis results of campus solar photovoltaic capacity

Technically, the main factor limiting the campus photovoltaic capacity is the available area to install the solar PV panels. Economically, installed PV is not cost effective for the campus without incentives.

4.1.4.1. Available Area for Installation

Solar photovoltaics can be installed within the campus either on the rooftops of buildings or on open land. Both rooftops and open land have pros and cons. The primary benefits and drawbacks of rooftop and open land installations are summarized below:

Rooftop Benefits:

- Once building HVAC equipment is installed, rooftop space is generally available.
- Generally building rooftops are "shadow-free."
- Rooftop PV is "Out of sight, out of mind." Limited to no visual aesthetic concerns.

Rooftop Drawbacks:

- Each rooftop can hold only a small amount of cells.
- Installation on a rooftop is much harder than installation on open land (e.g., a crane is needed to raise the equipment to the roof).
- Typically only fixed PV can be installed (with decreased power density).
- Supporting structure must be integrated with building.

Open land Benefits:

- Larger centralized location, allows for economies-of-scale.
- Can utilize both fixed and tracking PV. Tracking PV systems have improved power densities.
- Can be installed into the ground. No need for "fancy" supporting structures.

Open land Drawbacks:

- Community land is valuable. Utilized land cannot be used for "other" purposes.
- Ground level installations tend to have more visual aesthetic issues.

A study to examine the available land area for solar photovoltaic deployment was carried out to determine the maximum capacity available for this size of community. Using GIS with land and building data for the UCI campus, the land area available for photovoltaic deployment was determined. The following assumptions were used:

- Fixed PV is deployed on building rooftops, ground level parking lots (in the form of a car shade), and parking structure terraces.
- Fixed PV power density is 15 Watts/m^2
- Fixed PV tilt angle is 33.64^o and azimuth is 0°
- 20% of the building rooftop area is available for solar installations

- 15% of the ground level parking lot area is available for solar installations at
- 70% of the parking structure terrace area is available for solar installations
- Concentrated PV is deployed on exposed ground within the campus domain.
- Concentrated PV power density is 40 Watts/m^2 (4-6 acres per MW)

Note that the power density of concentrated PV is substantially higher than fixed PV because concentrated PV has a higher efficiency and hence more effectively utilizes land.

Figure 113: Rooftop PV assumed dimensions (from Natural Sciences II building PV Installation)

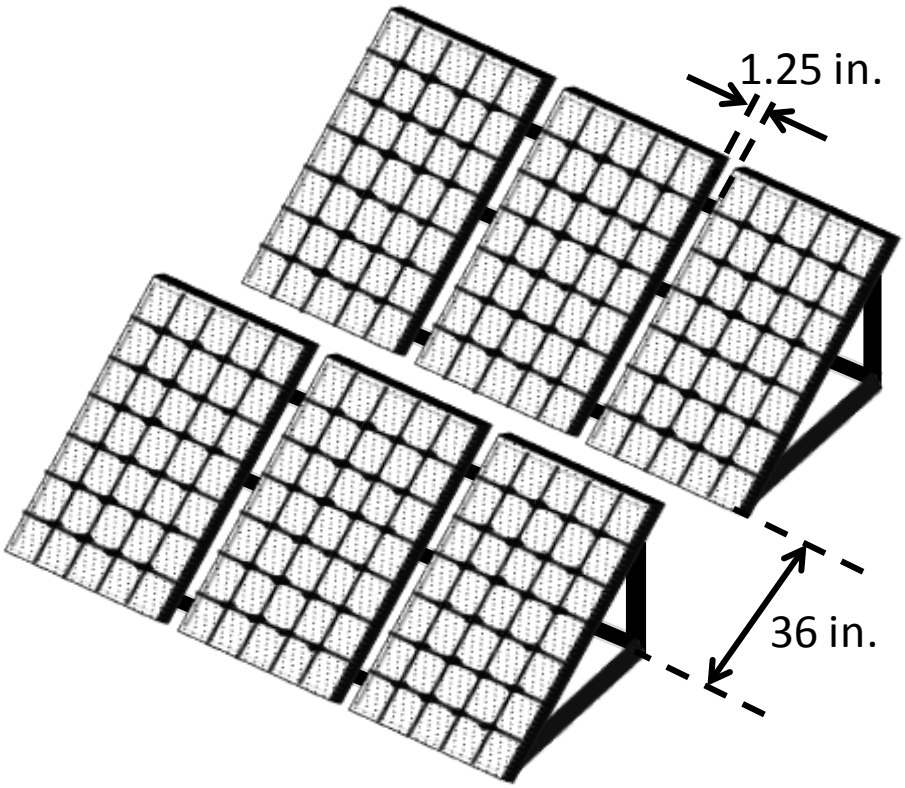

The results of the land use study and parameters for the fixed PV are drawn from Table 21 and Figure 114.

Table 21: Fixed PV Land Use Study Results

Fixed PV						
Sr. No.	Site Type	Area (acre)	Fixed (MW)	Fixed (GW.hr/year)	% of UCI peak load	% of UCI energy
1	Building rooftops	37.0	8.3	13.7	43.9	12.35
2	Parking lots	21.3	4.8	7.9	25.2	7.10
3	Parking structures	6.6	1.5	2.4	7.8	2.21
	Subtotal	64.9	14.6	24.0	76.9	21.66

Figure 114: Geographic Location of On-site Fixed PV Potential

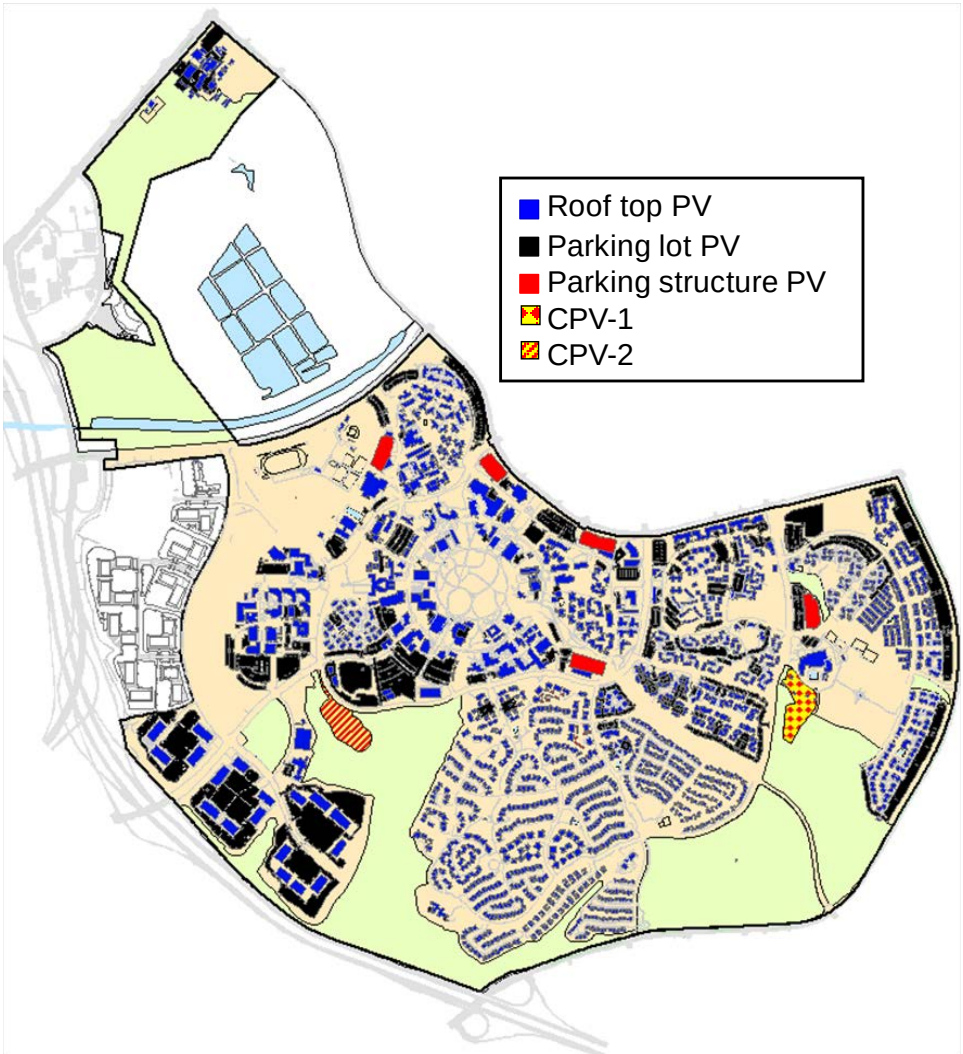

Overall, it was determined that a maximum of 14.6 MW of fixed solar photovoltaic panels can be deployed on the UCI campus; however, the utilization of this amount of renewables is the topic of following sections.

4.1.4.2. Local versus Regional Renewable Generation

The difficulty in siting PV in limited areas within the community raises the question why not install solar in local 'desert' environments? Sensitivity analysis was conducted comparing the delivered electricity capacity factor of the same panel installed at UCI or Barstow-Daggett assuming a range of transmission losses.

Results indicate a that the capacity factor could be increased 20% to more than 25% for installing the same panel in the desert versus the coast. Considering a worst case scenario of 12% Transmission losses the delivery of PV electricity from the desert to the coast results in a 19% increase in delivered capacity factor (see Figure 115).

Figure 115: Local versus regional renewable generation: Comparing PV delivered capacity factor

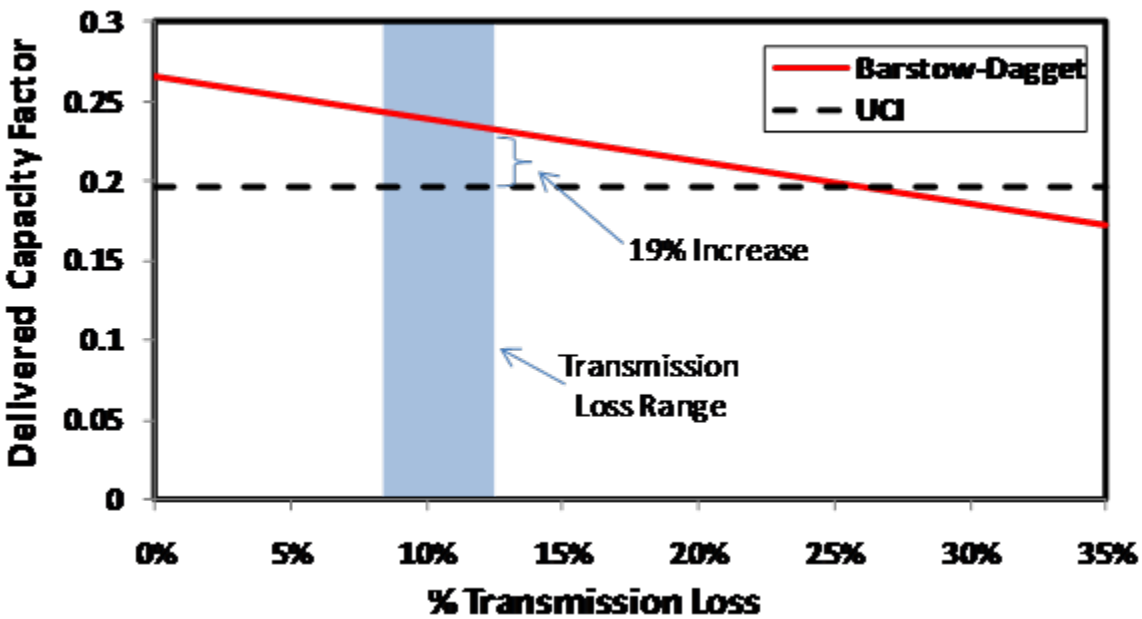

Significantly more electricity can be generated from the panel in the desert compared to the coast. This result is attributed to higher "clear-day" irradiation as well as less cloud cover in the desert. For example the desert is not subject to a coastal marine layer.

Such a result motivates regional renewable generation at the highest quality resource locations with transmission to loads. A similar analysis was conducted comparing the delivered capacity of local wind generation versus generation of wind at a high wind resource site. A comparison with Tehachapi is shown in Figure 116. The benefit to install wind at a regional high renewable

resource site is even greater than solar. A 335% increase in delivered capacity factor is expected for regional versus local wind installation even with 12% transmission loss.

Figure 116: Local versus regional renewable generation: Comparing wind generation delivered capacity factor

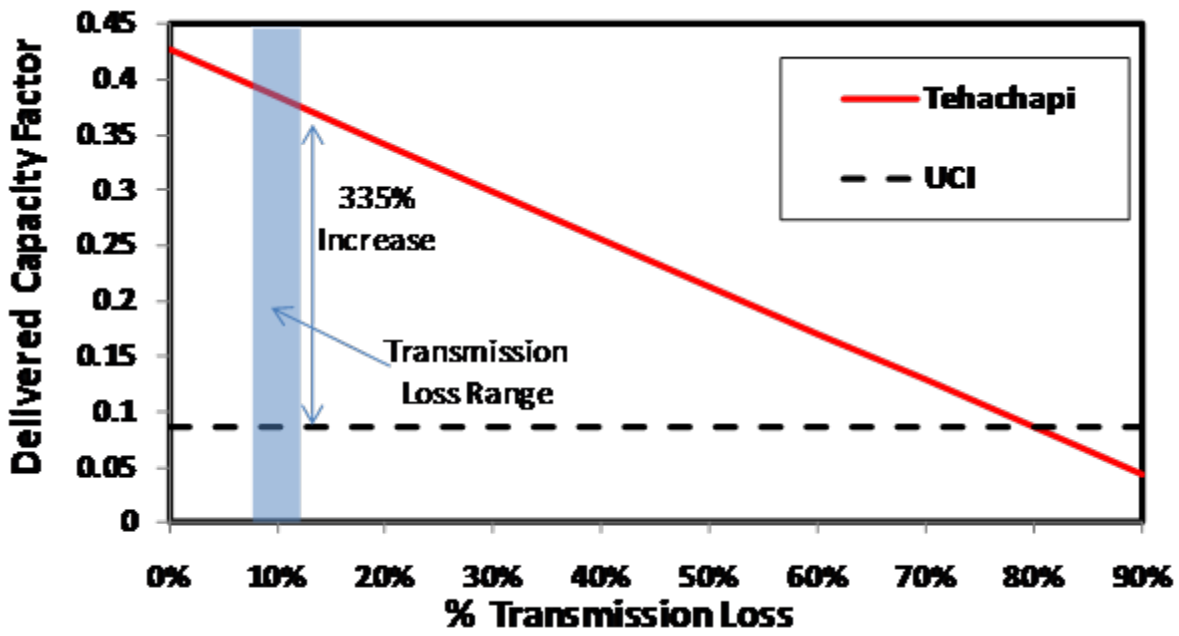

In addition to increased power output per equipment installed, it is projected regional lands will be more open with less economic value. Further, larger plants serving many customers can be developed taking advantage of economies-of-scale. As will be shown in Appendix F:Task 7:, decreased generation costs of regional renewable generation will outweigh increased transmission costs. Further, spatial diversification of renewable sites serving load points will make balancing loads more manageable, particularly when considering community distributed energy resource management.

One economic advantage of local generation is that local sites can finance or invest in local electric generation. Available capital can be used to offset future electric cost by installing local generation. Electricity consumers represent a significant installation opportunity for renewables via local generation. Today, limited programs or policy exist to provide individual electricity consumers the opportunity to purchase regional renewable installations or invest in them in return for reduced electric rates or electricity credits. Such programs or policy could provide necessary revenue for capital intensive renewable installations.

Task 4.1.5. Conclusions

- UCI has 893 MW of rooftop solar PV installed on campus. These sites were monitored to explore their behavior.
- UCI has space on campus to install additional PV generation.

- Building rooftops: 8.3 MW of PV
- Parking structures: 1.5 MW of PV
- Open parking lots: 4.8 MW of PV

- Solar panel operation at UCI is impacted by diurnal variation, marine layer effects, cloud passes, and storm events.

Task 4.2. Installation of Concentrated PV on Campus

High Concentration Photovoltaic (HCPV) is a very promising technology as it achieves industry leading system efficiencies with less silicon (see Figure 117 for field efficiency measurements). The technology can potentially be installed (a) centrally, e.g., MW scale desert installations, or (b) distributed within the community in smaller 100 kW installations.

Figure 117: Amonix performance to field conditions.

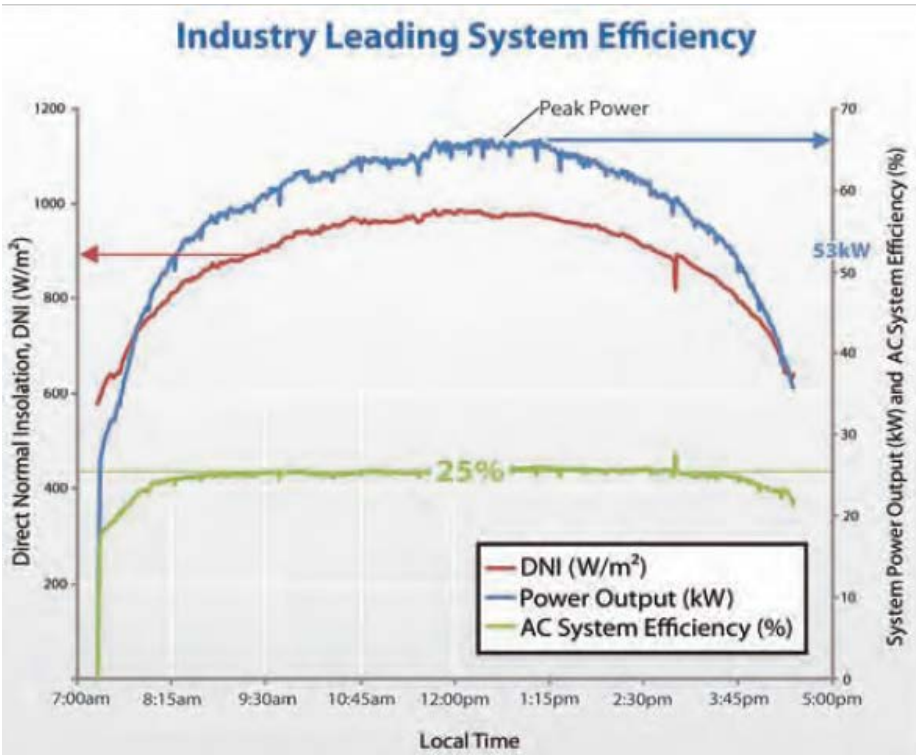

Source: Amonix 7700 datasheet

As part of the project, UCI has been working to install up to seven Amonix 7700 solar power generators on campus. The installation would result in 371371 kW net AC. While the campus has been very aggressively pursuing the installation of the seven panels, locating seven panels

on campus is an arduous process. While very efficient, power densities the panels are also very high. For cost reduction purposes, the panels are made large as shown in Figure 118. The rated power of the pictured panel is 53 kW AC PTC (PVUSA test conditions: 850 W/m2 DNI, 20 degrees Celsius ambient, 1 m/s wind speed) and uses 7,560 high efficiency (almost 40%) multi-junction solar cells. Approximately 3 acres are needed to site the seven panels. Several sites have been evaluated in detail. An example site evaluation is presented in Figure 119.

Figure 118: Amonix 7700 array installed at the University of Nevada, Las Vegas.

Figure 119: Schematic of proposed 7 HCPV panel installation at UC Irvine

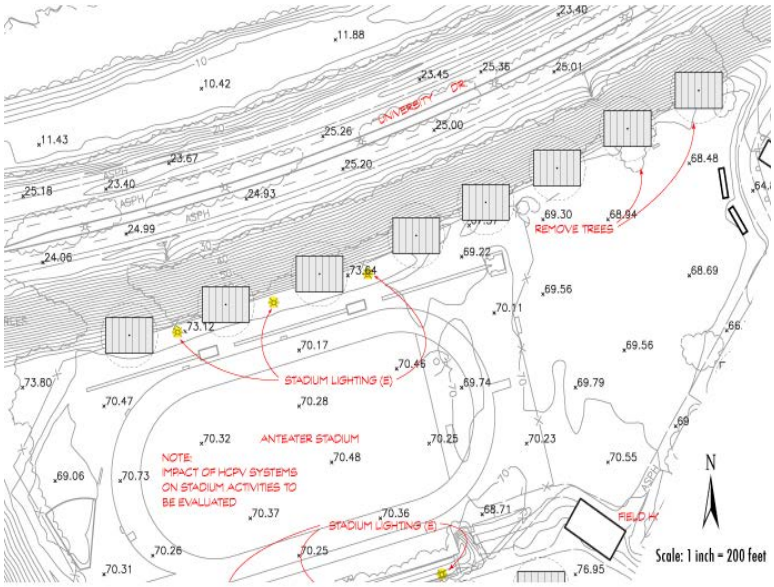

Locating renewable generation within the community is difficult. Particularly, each site within the community may have various challenges including:

- 10 year plus land availability
    - Max 3% slope
    - Minimum to no shading of the panels
    - Safe from vandalism

    - Must be on the ground (i.e., not suitable for rooftop installations)
- Electric connectivity to 480 V transformer (i.e., to building or distribution circuit directly)
- Public approval (e.g., Aesthetic and safety)

Each site will have to be evaluated and reviewed individually. Of course the most promising site will be selected;; but the installation can be difficult, and the process can be expensive. It is necessary to "stream-line" the installation approval process to minimize installation cost. Technology advances can aid in the approval process. For example, depending on the length of the "pole" the panels must be "fenced-off". However, Amonix is evaluating longer poles to enable access to the ground below the panels. One interesting trade-off is the panel size. Larger panels make use of economies-of-scale, but affect aesthetic concerns as a result. Efforts to deploy concentrated PV around the campus have shown this point to be very difficult. Extensive effort was made to understand visual impacts of the panels as part of the installation review process. For example, the visual impacts of the most promising demonstration project site were evaluated from different viewing areas. The project site and viewing areas are illustrated in Figure 120..Example site views can be found in Figure 121, Figure 122, Figure 123, Figure 124, Figure 125 and Figure 126.

Figure 120: HCPV demonstration Project site and viewing areas.

Figure 121: Potential HCPV Site 1

Figure 122: Potential HCPV Site 2 (With no panel glare)

Figure 123: Potential HCPV Site 2 (With panel glare)

Figure 124: Potential HCPV Site 3 (With no panel glare)

Figure 125: Potential HCPV Site 3 (With panel glare)

Figure 126: Potential HCPV Site 4 (with no panel glare)

The panels are large, and can change the aesthetics of a community. Smaller panels could have less of an aesthetic impact, but could result in higher equipment costs. This negative experience of the installation review process also favors installation of renewables at central regional locations with transmission of electricity to the community.

The potential capacity for HCPV panel installation on the UCI campus is presented in Figure 127.

Table 22: Concentrated PV Land Use Study Results

Concentrated PV							
Sr. No.		Site Location	Area (acre)	Conc (MW)	Conc. (GW.hr/year)	% of UCI peak load	% of UCI energy
1		California Ave and ARC service Rd	5.4	1.1	1.8	5.7	1.63
2		Bison and E Peltason Dr	5.8	1.2	2.0	6.1	1.77
3		University Dr and MacArthur Blvd	8.5	1.7	2.9	9.0	2.59
4		Jamboree/Fairchild and Campus Dr	90.5	18.1	30.4	95.2	27.38
		Subtotal	110.2	22.0	37.0	116.0	33.37

Figure 127: Geographic Location of On-site Concentrated PV Potential

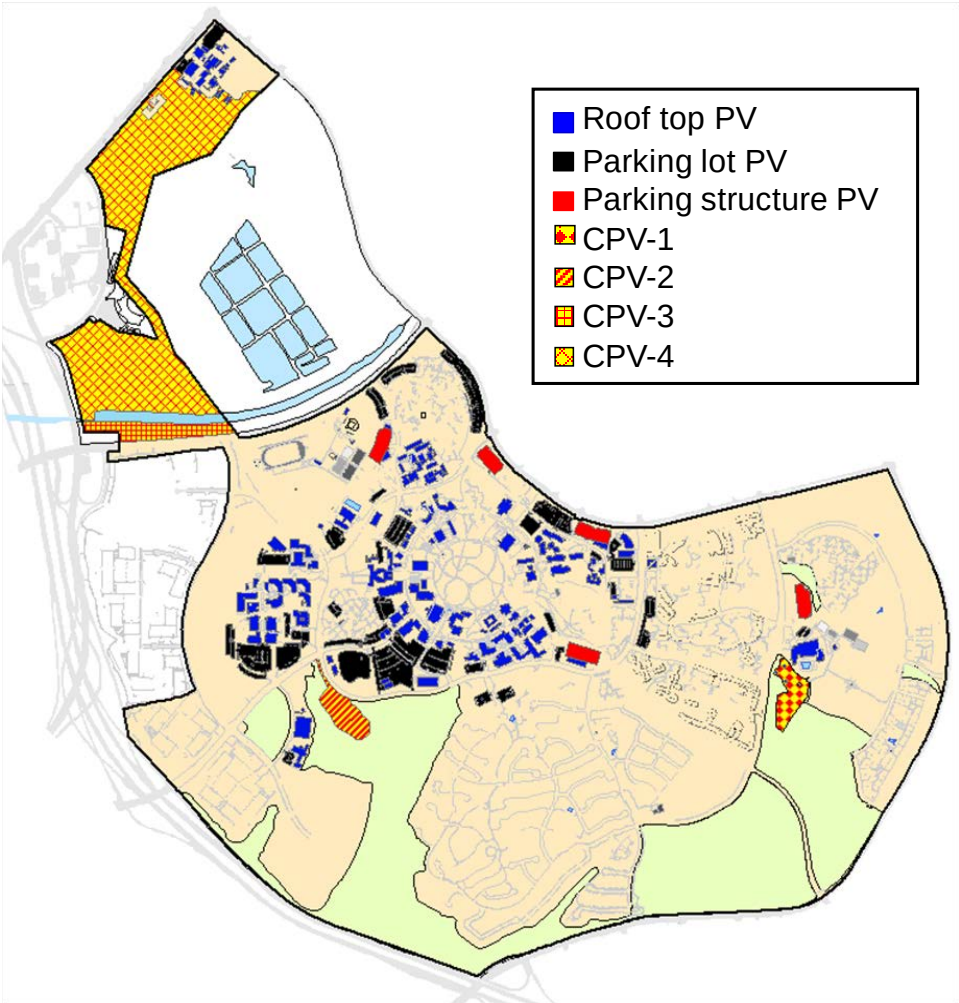

It was determined that a maximum of 22.0 MW of concentrated solar photovoltaic capacity can be deployed on the UCI campus and surrounding area.

After exploring several site alternatives, two Amonix HCPV panels were installed near the Anteater Recreational Center (ARC). One of the panels is Amonix's older model and has 53kW of peak power, while the other panel is one of Amonix's new products with a peak power of 60kW for the exact same footprint.

Several pictures are presented below. Figure 128 illustrates the tower during construction. Figure 129 and Figure 130 show the panels after being installed during their commissioning phase. Lastly, Figure 131 shows both panels generating electricity during an August evening.

Figure 128: Amonix HCPV Panel During Construction

Figure 129: Amonix HCPV Panel During Commissioning (back view)

Figure 130: Amonix HCPV Panel During Commissioning (front view)

Figure 131: Amonix HCPV Panels During Operation

Task 4.2.1. Conclusions

- HCPV achieves industry leading system efficiencies with less silicon than many other types of PV panels.
- The technology can potentially be installed both centrally (e.g., large scale desert site), or distributed (i.e., within a community).
- Available area, aesthetics, and panel requirements must be considered when installing HCPV systems.
- UCI has space on and near campus to install additional HCPV generation.
    - On campus: 4 MW of HCPV over 3 different sites
    - Near campus: 18.1 MW of HCPV
- Two Amonix HCPV panels, totaling over 110MW of capacitywere installed on the UCI campus near the Anteater Recreational Facility.

Task 4.3. Biogas Poly-generation Renewable Energy Station

In collaboration with FuelCell Energy (FCE) and Air Products and Chemicals, Inc. (APCI), the Advanced Power and energy Program (APEP) is leading the installation of a biogas poly-generation renewable energy station at the Orange County Sanitation District. The installation is being sponsored by the California Air Resource Board, Air Quality Management District, the Orange County Sanitation District and the U.S. Department of Energy. The technology is very attractive from an air quality and thermodynamic efficiency perspective. By electrochemically reacting the fuel rather than combusting it, the system avoids high temperatures and thereby

pollutant emissions. Further, by producing both hydrogen and electricity, the energy station can be made more thermodynamically efficient.

Figure 132: Concept, sponsor and participants of the OCSD poly-generation energy station

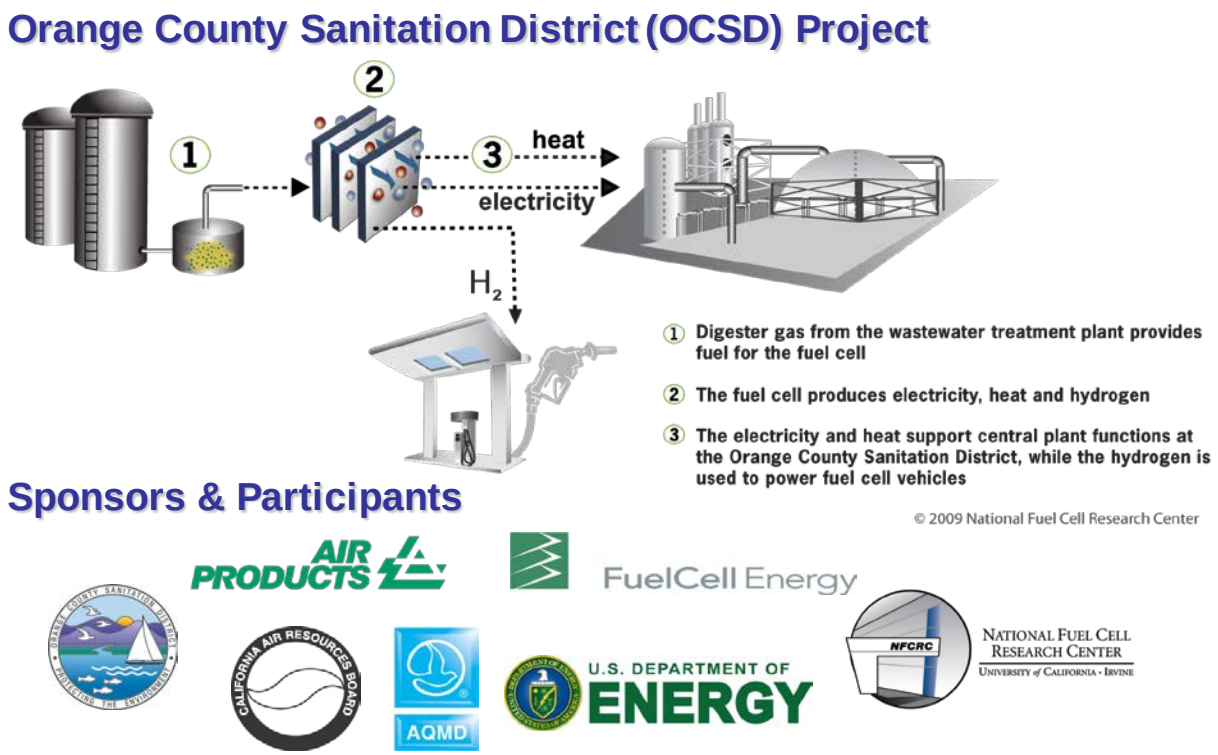

Solid oxide fuel cells (SOFC) and molten carbonate fuel cells (MCFC) operate at high enough temperature and produce enough heat from electrochemical reactions to provide heat to internal endothermic reformation processes to produce H_2 (i.e., internal reformation). Usually, H_2 is produced in quantities sufficient only for electrochemical reactions that produce electricity but these systems can be re-designed to make excess hydrogen as a co-product. Such systems (H_2-FCS) can provide H_2 with lower marginal costs, fuel use, and emissions than conventional H_2 production methods (Leal, 2006). Remarkably, since hydrogen is produced in a distributed generation fashion there is no energy penalty associated with the transport and delivery of the hydrogen to its point of use. Recent studies performed at the APEP demonstrate that less energy is needed to transport and deliver hydrogen to vehicles compared with distributed and centralized steam methane reforming (SMR), and distributed and centralized electrolysis (see Figure 133).

Figure 133: Energy requirements to produce and deliver hydrogen with different technologies

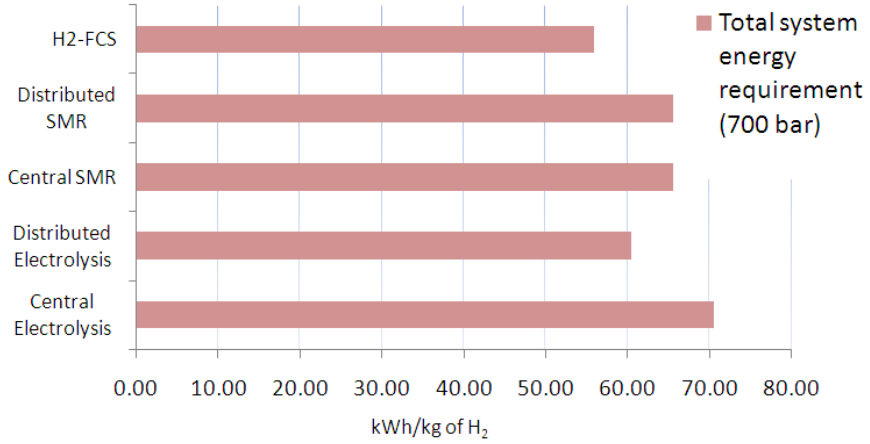

Task 4.3.1. The Orange County Sanitation District biogas tri-generation energy station

A first-of-a-kind tri-generation energy station has been developed and installed by the team comprised of UCI APEP, FuelCell Energy, and Air Products and Chemicals, Inc. The system is currently undergoing demonstration testing and evaluation for the generation of electricity and hydrogen from anaerobic digester gas at the Orange County Sanitation District. The team believes that this tri-generation technology may become very important for commercial deployment of local hydrogen production around the world. The initial testing phase of the current effort was accomplished by operation on natural gas and simulated digester gas at the FuelCell Energy headquarters. Pictures of the tri-generation system as it was tested at FuelCell Energy are presented in Figure 134 and Figure 135.

Figure 134: Fuel cell subsystem of hydrogen poly-generation unit

Figure 135: Hydrogen separation and processing subsystem of hydrogen poly-generation unit

Following successful initial testing at FCE, the tri-generation system was disassembled and prepared for shipment and subsequent deployment at the Orange County Sanitation District. At OCSD the system has been installed so that it can provide hydrogen for hydrogen fuel cell

vehicles. The site of the tri-generation system (Direct FuelCell ® hydrogen production unit) and the hydrogen refueling station is illustrated in Figure 136.

Figure 136: Installation overview for the poly-generation unit at the Orange County Sanitation District

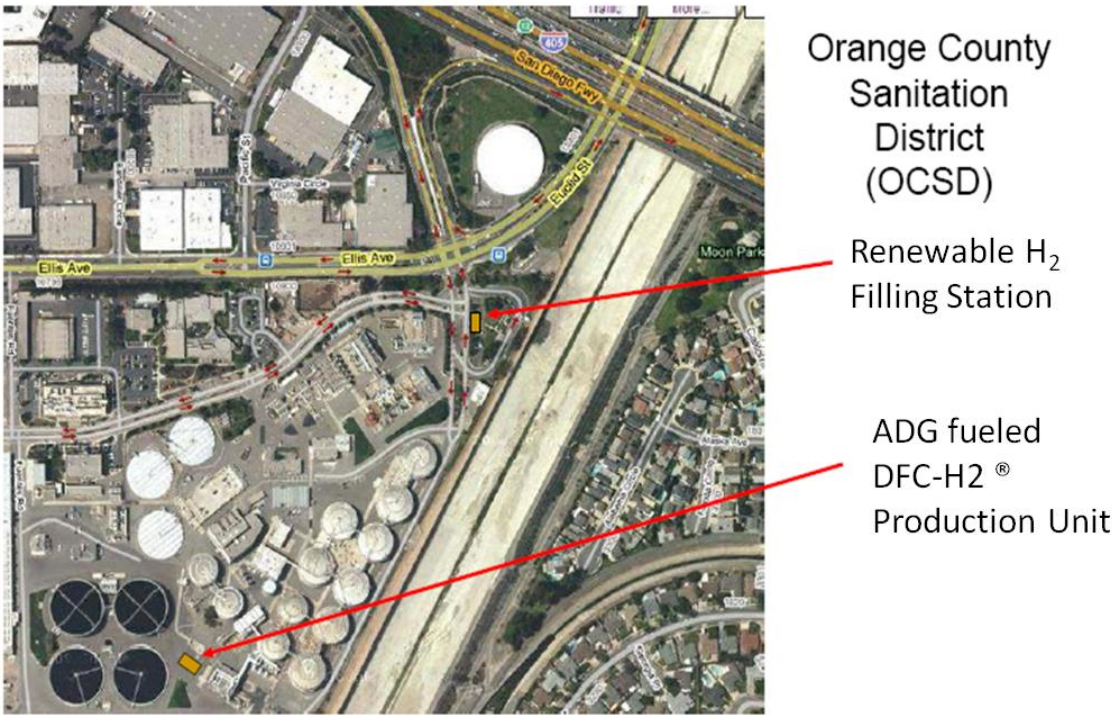

The system that is installed at OCSD is the world's first hydrogen co-production system installed at a customer site. In addition, this installation comprises the first time ever that an electricity, heat, and hydrogen poly-generation system has been operated on a renewable digester gas fuel. The installation was completed (except for the digester gas clean-up skid) in January of 2011. The anaerobic digester gas clean-up skid was delivered and installed in June of 2011, allowing operation on digester gas to occur at that time. The prime contractor in the effort is Air Products and Chemicals, Inc., who is working with FuelCell Energy, APEP, and OCSD on the project. The main funding agencies are the U.S. Department of Energy, California Air Resources Board, and the South Coast Air Quality Management District.

An overview photograph and description of the installation is presented in Figure 137. The novel tri-generation system is comprised of nine major system components: (1) anaerobic digester gas clean-up skid, (2) fuel cell mechanical balance of plant, (3) Direct FuelCell ®, (4) electrical balance of plant, (5) anode exhaust skid, (6) syngas compressor, (7) pressure swing adsorption hydrogen purification, (8) high pressure compressor, and (9) hydrogen storage tubes.

The equipment shown in Figure 137 is all that is required for the tri-generation of power, heat and hydrogen..The system is connected via a stainless steel pipeline to the hydrogen fueling

station that is installed outside of the OCSD fence-line near an off-ramp of the I-405 freeway. The hydrogen storage tanks and hydrogen pipeline store and deliver hydrogen to the fueling station at a pressure of about 6,500 psig (45 MPa).

Figure 137: Overview photograph and description of the OCSD Tri-Generation installation

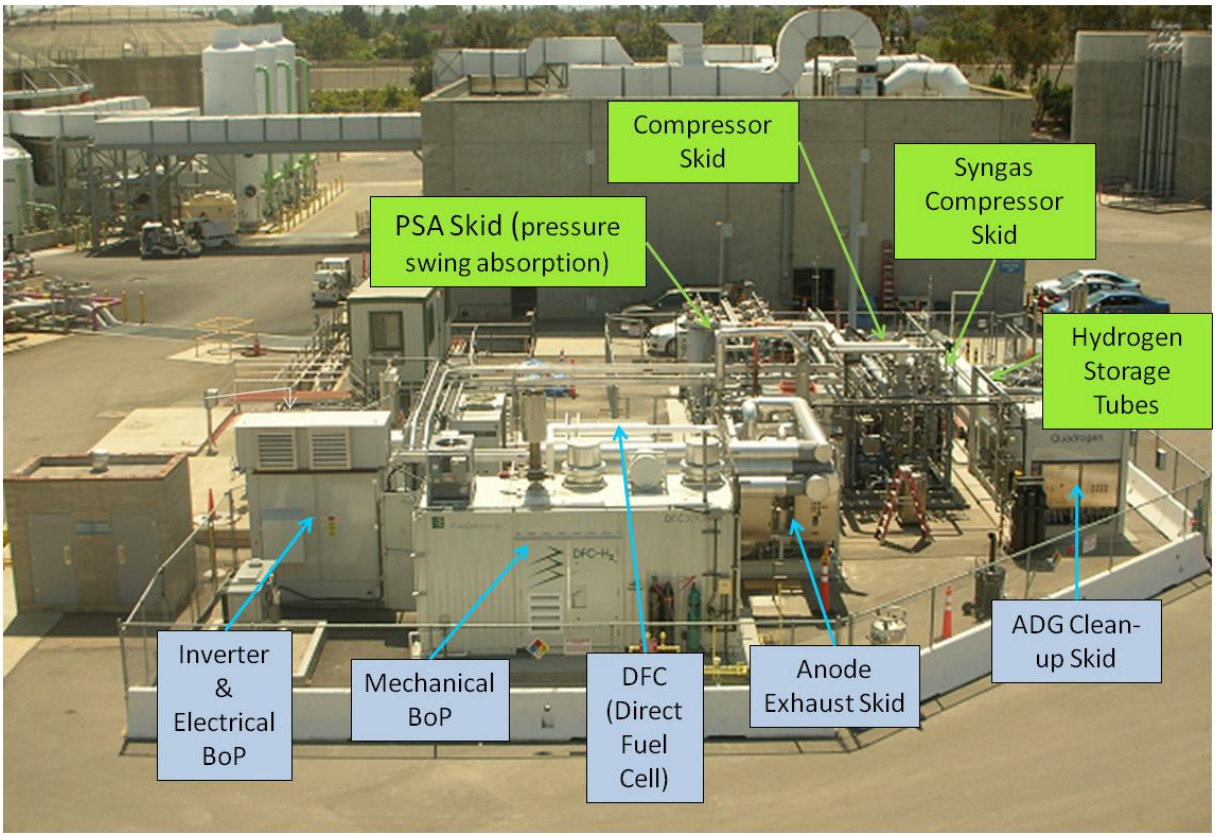

Task 4.3.2. Guidelines for other tri-generation biogas energy station

The preliminary guidelines and recommendations that have been determined from the first full year of operation of the tri-generation biogas energy station are as follows:

1. <u>Electrical Interconnection:</u> Interconnection challenges should be expected when fuel cell installations are interconnected via inverters with complex facilities with many motors and other non-linear loads (such as those present at a waste-water treatment plant). One should make sure that proper equipment is installed including: electric isolation transformers, robust inverter systems and inverter controls with good "ride-through" capabilities, and possibly even load banks and energy storage that is capable of managing and operating the fuel cell system as interconnected with a facility with power quality issues.

37. <u>Anaerobic Digester Gas Clean-Up</u>: Fuel cells can be contaminated by and are very sensitive to sulfur compounds, higher hydrocarbons, and siloxanes. One of the most challenging components and functions of the current project is that of the ADG clean-up

system, which must continuously remove all of these potential contaminants to very low levels (less than 10 ppb). The current system contains some novel clean-up strategies and multiple systems for the removal of each contaminant which are recommended for any subsequent implementation of an ADG-fueled poly-generation system.

38. Intermittency of Fueling Events: The fact that fueling is intermittent and not consistently placing a demand for hydrogen upon the poly-generation system requires controls for dynamic dispatch of the co-products (power, heat and hydrogen). Such controls and dynamic operating principles remain a subject of active research that is recommended for future poly-generation systems development and implementation.

39. Variability of Flow and Composition of ADG: Since digester gas is produced in a manner that leads to variations in pressure and flow rate as well as composition, all future systems should be designed for dynamic operation on pure ADG, pure natural gas, and various combinations of ADG and natural gas.

Task 4.3.3. The analysis results of campus biogas generation capacity

Table 23 contains the calculated efficiency for the coproduction of hydrogen and electricity from natural gas using a DFC®300 molten carbonate fuel cell. Significant improvement in PSA performance was achieved as a result of the engineering development work. Preliminary estimates from Phase 1 indicated the hydrogen recovery from the PSA would be 75% with a 300 psig inlet pressure. Through innovative cycle design work and the selection of optimal adsorbents, PSA recovery was improved in Phase 3 to over 85% with a 150 psig inlet pressure. Achieving a higher recovery with less compression power significantly improves the economics of the co-production system. The improved PSA performance was verified with pilot plant runs at Air Products' Adsorption Technology Center.

Table 23: Projected Performance of Hydrogen Energy Station by Phase of U.S. DOE Program – Natural Gas Feed

	Units	Phase 1	Phase 2	Phase 3
Overall Efficiency (Net Power + H_2 Product) / (Fuel)	LHV	60%	63%	**66%**
Power Efficiency Net Power / (Total Fuel – H_2 Product)	LHV	49%	49%	**50%**
Hydrogen Efficiency (H_2 Product – Purification Power) / H_2 Product	LHV	68%	71%	**77%**
Hydrogen Product	Kg/day	~ 88	~ 125	**~ 175**
Net Power w/o & w/ Hydrogen	kW	~ 247 / 207	~ 300 / 250	**~ 300 / 250**
Natural Gas Flow	Nm^3/hr	~ 55	~ 66	**~ 74**

From the previous results, it can be stated that co-production of hydrogen and electricity improves the operating economics as well as the asset utilization compared to conventional technologies for power and hydrogen generation. It holds promise to facilitate hydrogen

infrastructure for a range of applications. It stands to benefit the stationary, transportation, material handling, and portable power sectors through increased fuel efficiency, ultra-low emissions and fuel flexibility. DFC® power plants are operating on digester gas at over a dozen sites, providing a source of low-cost renewable hydrogen.

Process simulations have predicted that, for every 100,000 people, approximately 1 MW of electricity plus 500 kilograms per day of hydrogen can be produced at wastewater treatment plants. However, it is important to note that most recent research performed by APEP scientists demonstrates that the hydrogen production potential is higher than previously estimated. Therefore, although successful demonstration of the Hydrogen Energy Station at OCSD will allow for the rollout of a means to produce renewable hydrogen and electricity at high efficiency and at virtually zero emission of criteria pollutants, there is a vital need to continue improving the system design based on learning derived from research and demonstration efforts.

Task 4.3.4. Modeling of biogas poly-generation system

Optimal cycle design configurations for making excess hydrogen have been investigated and modeled with ASPENPlus®. These designs thermally integrate both MCFCs and SOFCs with hydrogen separation units (HSU). Hydrogen from the anode-off gas has to be separated and purified before the fuel cell after-burner. The purification technology selected for these analyses is Pressure Swing Absorption (PSA) which requires the anode-off gas to be pressurized and cooled down. Importantly, hydrogen concentration has to be increased by shifting CO and steam to H_2 and CO_2 and/or by condensing steam in the anode-off gas before the PSA unit. For this reason, our models include a water-gas shift reactor (WGSR). Figure 138 shows the schematics of one of the designed HSUs.

Figure 138: Hydrogen Separation Unit AspenPlus® schematics

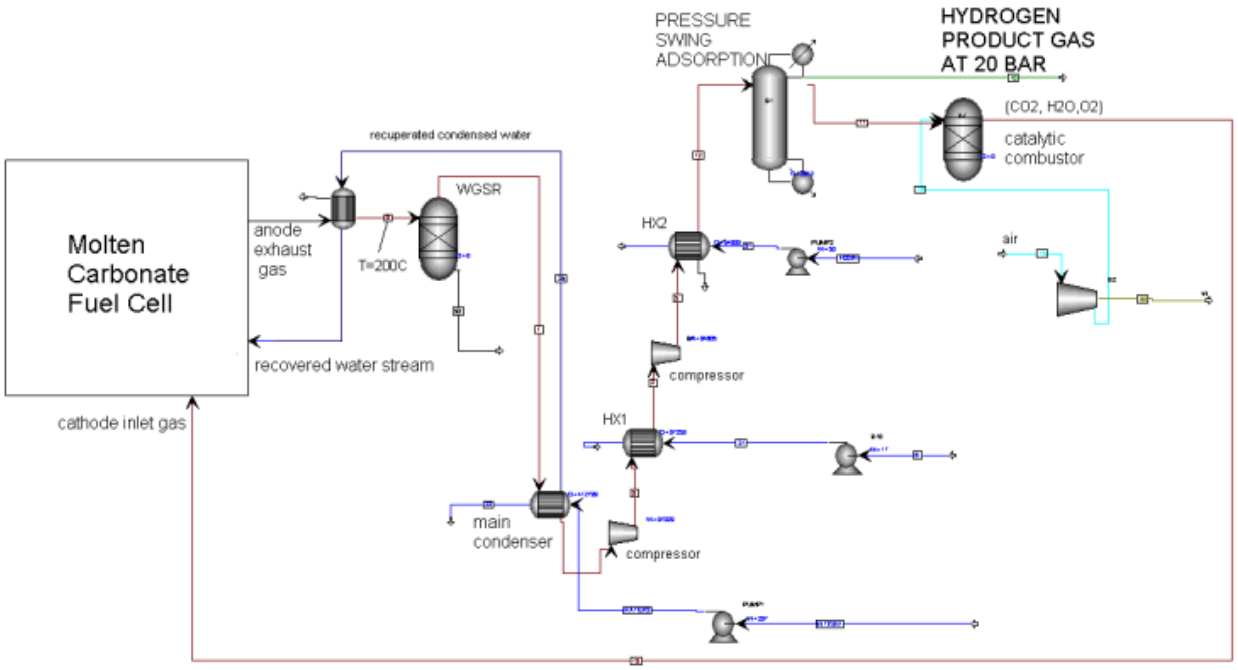

As shown in Figure 138, the anode-off gas is cooled down through heat exchangers to the optimal temperature for the gas shift reaction. Studies at the APEP demonstrate that the H_2 concentration peaks at T=200200 C. After the WGSR, the gas is cooled to lower temperatures before the compression stage in order to compress it more efficiently. After compression, the gas is cooled down again due to the temperature rise during the compression stage. Once the gas is at the right temperature (T=50 C), pressure (P=20 bar) and H_2 molar concentration ([H_2] = 30%) it passes through the PSA unit where hydrogen is extracted from the stream for its dispensing to vehicles. Once the hydrogen has been separated, the remaining anode-off gas, a mixture of CO, CO_2, H_2O, and some traces of CH_4 and H_2, is oxidized in the catalytic combustor. The exhaust gas, a mixture of CO_2, H_2O and O_2, is then inserted to the cathode compartment to complete the fuel cell electrochemical reactions.

Recent studies performed at the APEP demonstrate that hydrogen yield and overall system efficiency can be optimized by operating the fuel cell at lower utilization factors. Several synergies were previously anticipated and associated with lower fuel utilization factors. Among these synergies, lower polarization losses and lower parasitic loads associated with lower cooling air demand are expected. When working at lower utilization factors, higher cell voltages are observed because higher concentrations at the anode outlet increase the Nernst voltage and decrease the anode activation losses. Consequently, since the cell operates at higher cell efficiencies, less electrochemical heat is generated which reduces the cooling air requirements. In addition, when operating at lower utilization factors, the endothermicity associated with the internal reformation reactions absorbs most of the heat generated during the exothermic fuel cell reactions, lowering the air cooling requirements even more. By reducing the cooling air requirements, significant energy savings associated with the air compressors are observed and

increase the overall system efficiency. Significant modeling efforts have been conducted in order to incorporate these synergies into the SOFC model developed with ASPENPlus®. Importantly, with the developed SOFC model, it is possible to obtain VI curves at different utilization factors, as best seen in Figure 139. The main goal of this modeling effort is to capture the synergies previously cited.

Figure 139: SOFC VI and power densities curves at different utilization factors

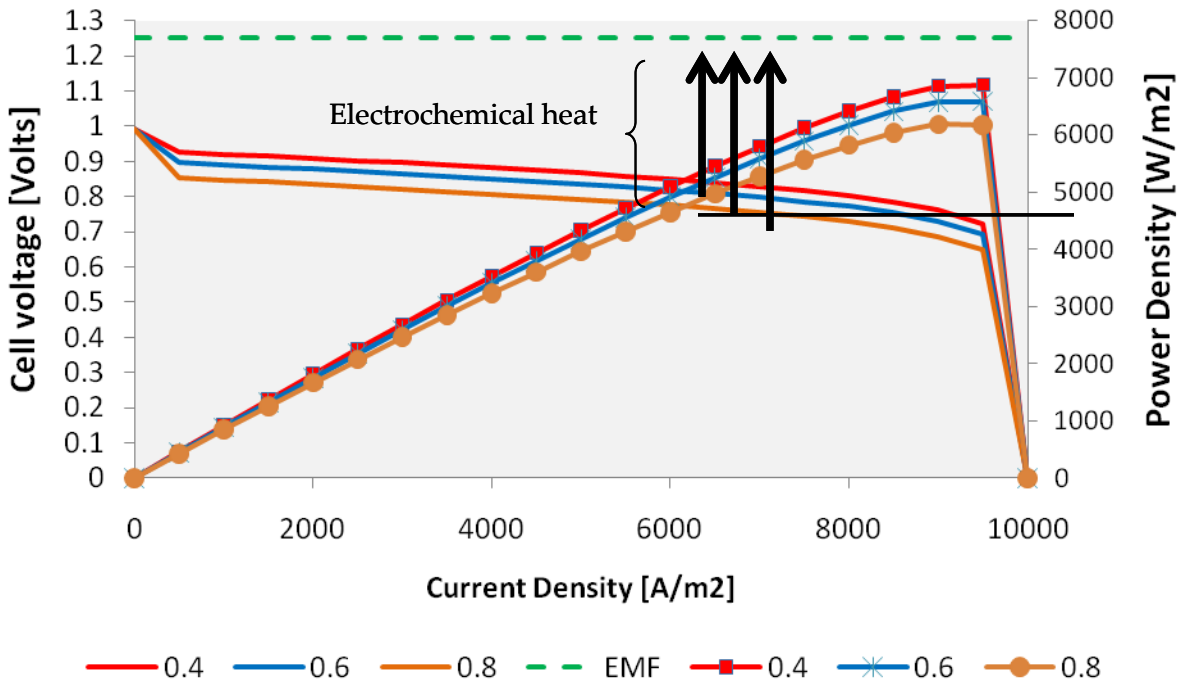

Figure 139 shows the VI curves and power densities of the SOFC at different utilization factors. In this figure, the first synergistic effect can be appreciated (less electrochemical heat generated). As seen, at the same power density (e.g. 5000 A/m^2), the operating voltage is higher at lower utilization factors demonstrating that the fuel cell produces electricity more efficiently when it operates at lower utilization factors. It is also important to realize that the electrochemical heat generated is proportional to the distance between the maximum electromotive (EMF) force and the operating voltage. Therefore, as observed in Figure 139, less heat is generated at lower utilization factors. Consequently, less cooling air will be required.

To capture the first synergistic factor, the electrochemical heat is calculated as a function of the operating voltage. The electrical efficiency is defined as the ratio between the operational voltage (V_{op}) and the theoretical voltage

$$\eta_{FC,elec} = \frac{V_{op}}{V_{th}} \tag{24}$$

where the operation voltage (V_{op}) is obtained from the SOFC model and the theoretical voltage (V_{th}) is

$$\boldsymbol{V_{th}} = \frac{-\Delta\bar{h}_f}{\boldsymbol{2F}} \tag{25}$$

Since $\Delta G = \Delta H - T\Delta S$, the theoretical voltage is calculated with the change in enthalpy of formation instead of the Gibbs energy in order to account for all the chemical energy of the fuel which includes entropy generation.

All the chemical energy of the fuel is transformed either into electricity or heat. Therefore, the thermal efficiency of the fuel cell can be defined as

$$\boldsymbol{\eta_{FC,thermal} = 1 - \eta_{FC,elec}} \tag{26}$$

At the same time, the thermal efficiency of the fuel cell can be determined by the following expression

$$\boldsymbol{\eta_{FC,thermal} = \frac{q}{\Delta\bar{h}_{R,comb}}} \tag{27}$$

Where q is the electrochemical heat generated and $\Delta\bar{h}_{R,comb}$ is the enthalpy of combustion which corresponds to the maximum amount of thermal energy that can be extracted from the fuel. If the previous equations are combined, an expression to determine the electrochemical heat as a function of the operating voltage is obtained

$$\boldsymbol{q = \left(\frac{V_{th} - V_{op}}{V_{th}}\right)\Delta\bar{h}_{R,comb}} \tag{28}$$

As seen in Figure 139, the operation voltage is higher at lower utilization factors. Therefore, at lower utilization factors less electrochemical heat is generated. As a result, less cooling air is required to cool down the fuel cell stack. To calculate the amount of air required to dissipate the electrochemical heat $\dot{n}_{air}$, the following expression has been derived:

$$\boldsymbol{\dot{n}_{air}\bar{c}_p\Delta T_{stack} = \dot{n}_{fuel}q} \tag{29}$$

Where ΔT_{stack} has been fixed at 200 C and $\dot{n}_{fuel} = f(u_f)$ corresponds to the necessary amount of fuel to produce 1MW of electric power at different utilization factors. Table 24 shows the results of the described analysis at a current density equal to 5000A/m^2.

Table 24: Synergistic effect related with less electrochemical heat generated at lower utilization factors (j=5000A/m2)

Utilization Factor	0.4	0.6	0.8
Operation Voltage (V from Figure 133)	0.85	0.81	0.76
Theoretical voltage V_{th} (V)	1.25	1.25	1.25
Fuel input (kmol CH_4/hr)	14.43	10	7.9
Enthalpy of Combustion $\Delta\bar{h}_{R,comb}$ (LHV) (kJ/mol)	-241.8	-241.8	-241.8
Electrochemical Heat (q) (kJ/mol)	-77.81	-85.52	-95.17
Cooling air required $\dot{n}_{air}$ (kmol/hr)	70.17	80.18	93.98

As seen in Table 24, the necessary amount of air $\dot{n}_{air}$ to dissipate the electrochemical heat decreases at lower utilization factors. Therefore, parasitic loads associated with the air compression are lower at lower utilization factors.

The second synergistic effect relates to the fact that at lower utilization factors there is a higher proportion of endothermic reactions (i.e. steam reformation) that may absorb more heat released during the exothermic fuel cell reactions. To capture the effects of this synergy the following expression has been derived

$$\Delta\dot{\boldsymbol{n}}_{\boldsymbol{air}}\bar{\boldsymbol{c}}_{\boldsymbol{p,air}}\boldsymbol{T}_{\boldsymbol{FC}} = (\dot{\boldsymbol{n}}_{\boldsymbol{fuel,u_f}} - \dot{\boldsymbol{n}}_{\boldsymbol{fuel,0.8}})\Delta\bar{\boldsymbol{h}}_{\boldsymbol{R,ref}} \quad \textbf{(30)}$$

where $\Delta\dot{n}_{air}$ represents the air decrement due to the additional endothermic reforming reactions of the extra amount of fuel that has to be used to produce the same amount of power at lower utilization factors ($\dot{n}_{fuel,u_f} - \dot{n}_{fuel,0.8}$) when compared with the baseline case (uf = 0.8). Fuel cell temperature (TFC) is assumed to be 1173K. Results associated with this synergistic factor are shown in Table 25.

Table 25: Synergistic effect related with additional endothermicity at lower utilization factors at (j=5000A/m2)

Utilization Factor	0.4	0.6	0.8
Additional fuel in (with respect u_f = 0.8) (mol CH_4/s)	1.813889	0.583333	0
Enthalpy of reformation $\Delta\bar{h}_{R,ref}$ (kJ/mol)	-206.1	-206.1	-206.1
Cooling air decrement (kmol/hr)	-35.8545	-11.5305	0

As seen in Table 25, there is a significant air decrement when the fuel cell operates at a fuel utilization factor equal to 0.4. Both synergistic factors are independent to each other and may be added up. Figure 140 shows the air flow versus the fuel utilization factor. As seen, the total amount of air is reduced as the utilization factor decreases.

Figure 140: Air flow versus fuel utilization – Synergistic effects

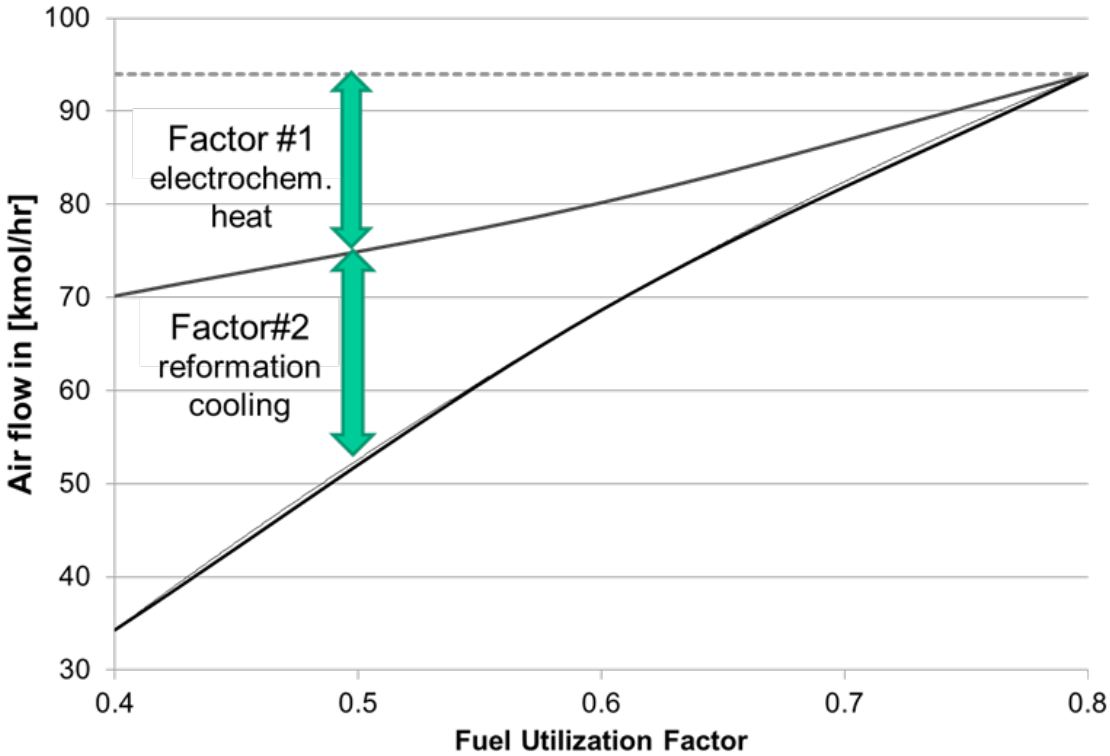

Table 26 presents the main results of a 1MW SOFC operating at 5000 A/m² at different fuel utilization factors. A control strategy has been incorporated to the SOFC AspenPlus® model in order to optimize the amount of air as a function of the utilization factor. This control strategy captures both synergistic factors: (1) less electrochemical heat generated; (2) more endothermic reactions to absorb the fuel cell reactions' exothermic heat.

The effect of the described synergy can be appreciated in the Net Electric Power (before PSA) column. As seen, at lower utilization factors, the net electricity is higher than at high utilization factors due to the lower parasitic loads associated with the air compression.

Table 26: Summary results for hydrogen production and separation using a high temperature fuel cell

Fuel Utilization Factor	Energy Input (LHV) (KW)	Gross Electric Power (KW)	Net Electric Power (before PSA) (KW)	Hydrogen output (kg H_2/hr)	Net electric power (after PSA) (KW)	Overall efficiency (after PSA)
0.4	3206.7	1038.4	979.0	48.7	635.7	0.70
0.5	2649.7	1053.0	982.3	33.0	700.8	0.68
0.6	2222.2	1038.5	957.8	21.8	723.6	0.65

0.7	1924.2	1023.8	934.6	13.9	733.3	0.62
0.8	1755.5	1033.2	936.8	8.3	754.6	0.59
0.9	1716.4	1036.4	934.2	3.9	757.5	0.51

Interestingly, the energy input value is higher at lower utilizations in order to maintain the power output. Therefore, if only electricity is produced, the system efficiency drops considerably since more fuel is necessary to produce the same power output. However, if hydrogen is separated from the anode off gas, the total energy output including electric power and hydrogen power (LHV) is higher at lower utilization factors. As observed, the overall efficiency when hydrogen is separated including the energy penalties associated with the Pressure Swing Adsorption reaches 70% in the case of operating at 40% utilization factor. It is important to note that the potential use for residual heat is not taken into account in this calculation. If so, the efficiency would be even higher. Also, it is important to note that although the air flow is decreased as the system works at lower utilization factors the oxygen stoichiometry is always maintained at permissible levels.

Task 4.3.5. Conclusions

- A biogas poly-generation renewable energy station is installed and operating at the Orange County Sanitation District.
- This technology is very attractive from air quality and thermodynamic efficiency perspectives.
- Guidelines for other tri-generation biogas energy stations are developed
    - Interconnection challenges were overcome with the installation of the proper equipment including electric isolation transformers, robust inverter systems and inverter controls
    - Properly functioning ADG clean-up system is essential to operation with a fuel cell, which continuously reduces all potential contaminants to very low levels
    - Poly-generation systems require controls for dynamic dispatch of the co-products (power, heat and hydrogen) if there is not consistently a demand for hydrogen.
    - Systems should be designed for dynamic operation on pure ADG, pure natural gas, and various combinations of ADG and natural gas.

Task 4.3.6. References

Leal, E.M., and Brouwer, J., "A Thermodynamic Analysis of Electricity and Hydrogen Co-Production using a Solid Oxide Fuel Cell", ASME Journal of Fuel Cell Science and Technology, 3(2):137-143, 2006.

Appendix D:Task 5:
Land-Use Design and Mobility

TABLE OF CONTENTS

Task 5.1. UCI Public Transportation Energy Intensity and Climate Footprint Benefits D-2

Task 5.1.1. UCI and APEP Transportation and Urban Layout Research Resources.....D-3

Task 5.1.2. ZEV-NET, Zip-Car and Battery Electric Vehicles.....D-3

Task 5.1.3. Hydrogen Fuel Cell Vehicles and Hydrogen Refueling.....D-6

5.1.3.1. Biodiesel Shuttle (B20).....D-10

5.1.3.2. On-Campus Housing.....D-11

Task 5.1.4. Transportation Alternatives Survey D-12

Task 5.1.5. Survey participants D-15

Task 5.1.6. Analysis Approach.....D-15

5.1.6.1. Analysis Summary D-16

5.1.6.2. Survey and Analysis Results D-19

Task 5.1.7. Public Transportation Benefits D-20

Task 5.1.8. Conclusions.....D-22

Task 5.1.9. References.....D-23

Task 5.2. Land-Use Design Effect on Transportation Intensity D-23

Task 5.2.1. Distance vs. Time Comparison.....D-23

Task 5.2.2. The analysis results of energy and carbon footprint of on campus residence D-24

Task 5.2.3. Personal Transportation.....D-26

Task 5.2.4. Comparison of FCVs and Hydrogen Technologies D-29

Task 5.2.5. BEVs and Grid Electricity D-29

Task 5.2.6. Conclusions.....D-29

Task 5.2.7. References.....D-30

UCI has nearly 30,000 students, faculty and staff, which regularly commute to work. Many factors influence the choices that people make when deciding the transportation method that suits them; however, there are some methods that are less energy intensive and/or polluting than others.

This task explores the energy intensity and climate footprint for transportation alternatives of the students, faculty and staff at UCI. A survey is administered to gather data about the different transportation methods for both on- and off-campus residents, and the results are analyzed to determine the most beneficial methods for transportation at UCI.

Task 5.1. UCI Public Transportation Energy Intensity and Climate Footprint Benefits

To quantify the benefit of community planning and to compare various transportation alternatives, a well-to-wheel analysis was conducted. UCI, as well as APEP, has been demonstrating emerging transportation alternatives including hydrogen fuel cell vehicles, battery electric vehicles, and biodiesel shuttles. To provide as realistic data as possible, various APEP staff and students utilizing various available transportation alternatives were surveyed. The data gathered from the survey was then taken and used to conduct a well-to-wheel analysis. Results from the survey and analysis are used to aid in the development of a roadmap for transportation and community planning. The overall research approach is illustrated in Figure 141.

Figure 141: Flowchart of the methodology for using UC Irvine as a living laboratory in conjunction with previous research to collect data on energy use and greenhouse gas emissions for various modes of transportation

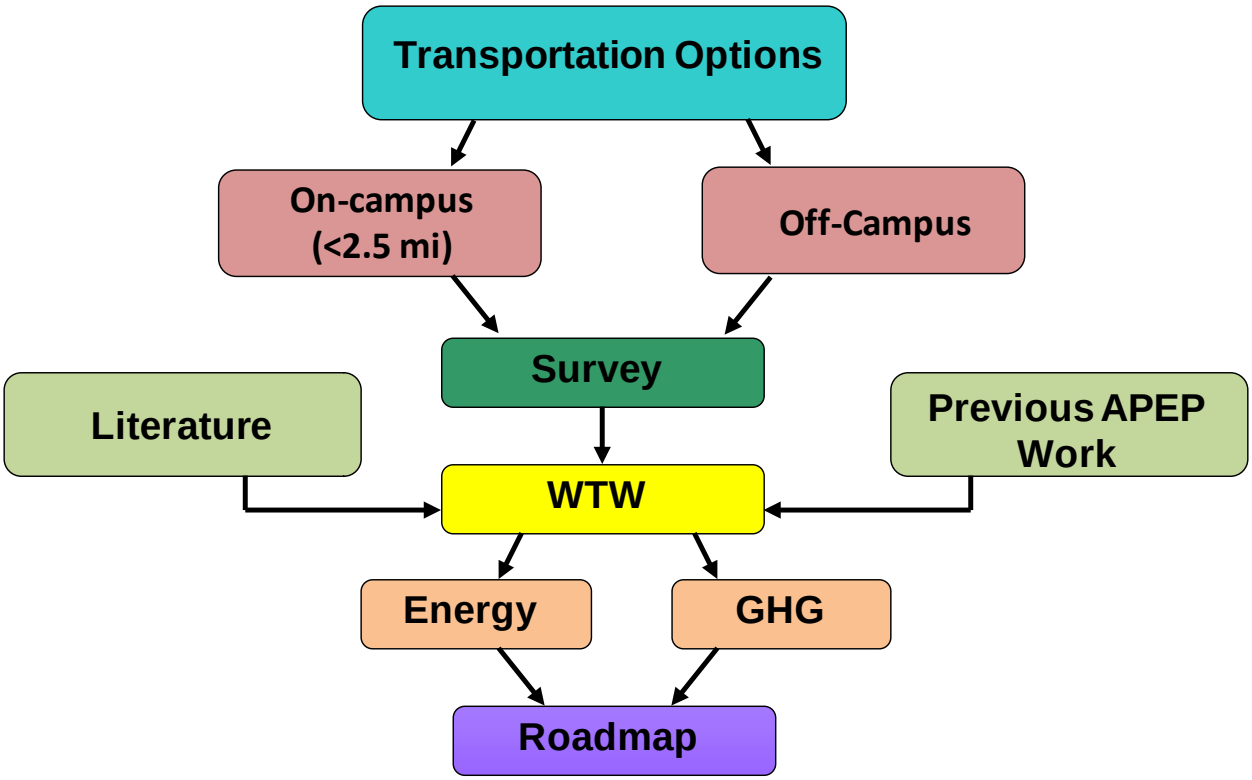

Task 5.1.1. UCI and APEP Transportation and Urban Layout Research Resources

The UCI campus and the Advanced Power and Energy Program have a unique set of research resources and campus infrastructure. This section of the report summarizes the key resources used in the survey.

Task 5.1.2. ZEV-NET, Zip-Car and Battery Electric Vehicles

As part of APEP's Zero Emission Vehicle Network Enabled Transportation (ZEVNET) program, APEP is evaluating the opportunity of network based zero emission vehicle sharing as well as the performance of emerging zero emission vehicles themselves. However, the ZEV NET primary fleet has been Toyota RAV 4 battery electric vehicles.

A key objective of the ZEVNET program is to promote increased public transportation, by providing electric vehicles for the last leg of a commute. The concept is illustrated in Figure 142 with a picture of the ZEVNET station at the Irvine transportation center presented in Figure 143.

Figure 142: The ZEV•NET Shared Use Station Car concept

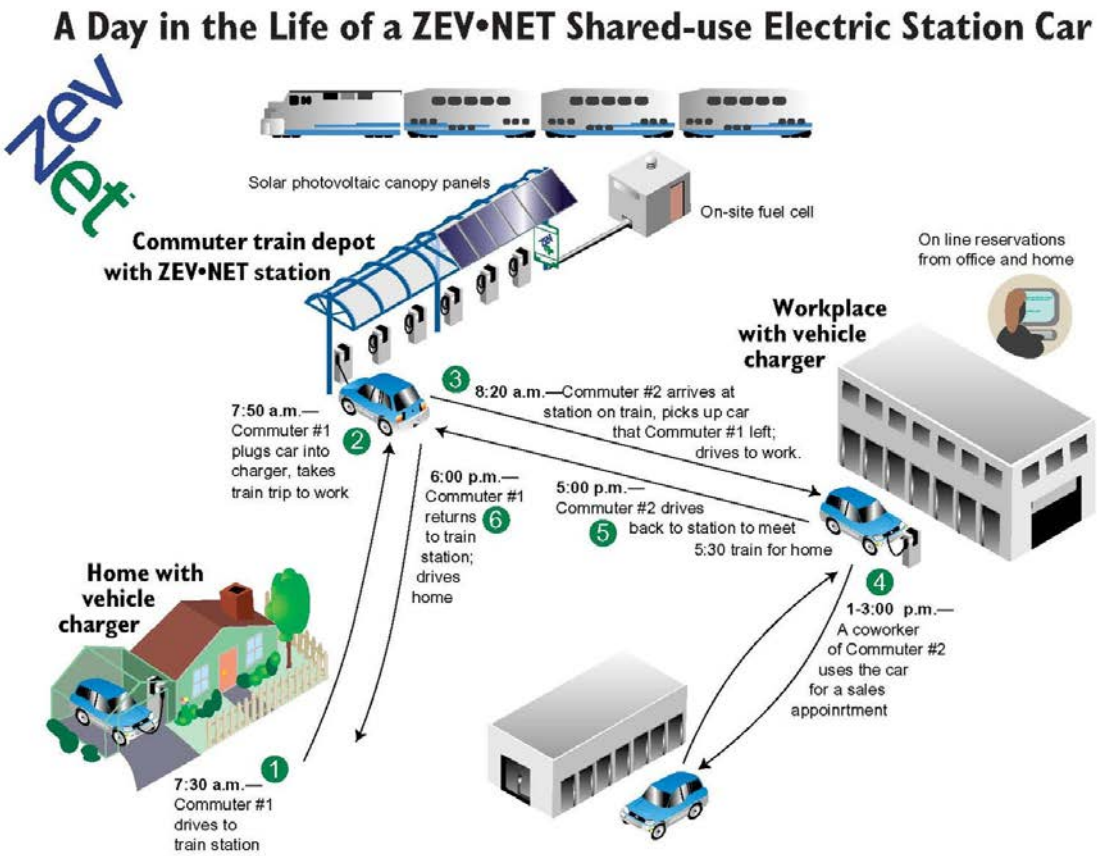

Figure 143: Portion of Electric Vehicles operated as part of the ZEV•NET program

Recently, the ZipCar program has become available at UC Irvine as a commercial car sharing program. Continued interactions between ZEVNET and ZipCar have taken place since the introduction of ZipCar to UCI. There are 8 stations located throughout the campus. There is no membership fee for faculty and staff. However, there is a $35 membership fee for students which goes toward a $35 driving credit. The cost to use the ZipCar is $8/hour or $66/day and includes the cost of renting the car, gas, mileage (up to 180 miles/day), plus the cost of insurance. As a commercial industry, ZIPCAR currently supports a fleet of small sedans.

Though the price may appear steep to students, ZipCar remains a viable alternative for those who may not own a car on campus, but may need an automobile on an occasional basis. At its core, the ZipCar program is a form of car sharing in which a small number of vehicles meet the transportation needs of many individuals (Heling, 2008). As depicted in Figure 144, several alternative transportation modes cannot match the mobility enabled by a personal automobile (Heling, 2008). However, car sharing programs provide an efficient means to fill this gap.

Figure 144: Illustration of Car-sharing's role among transportation alternatives

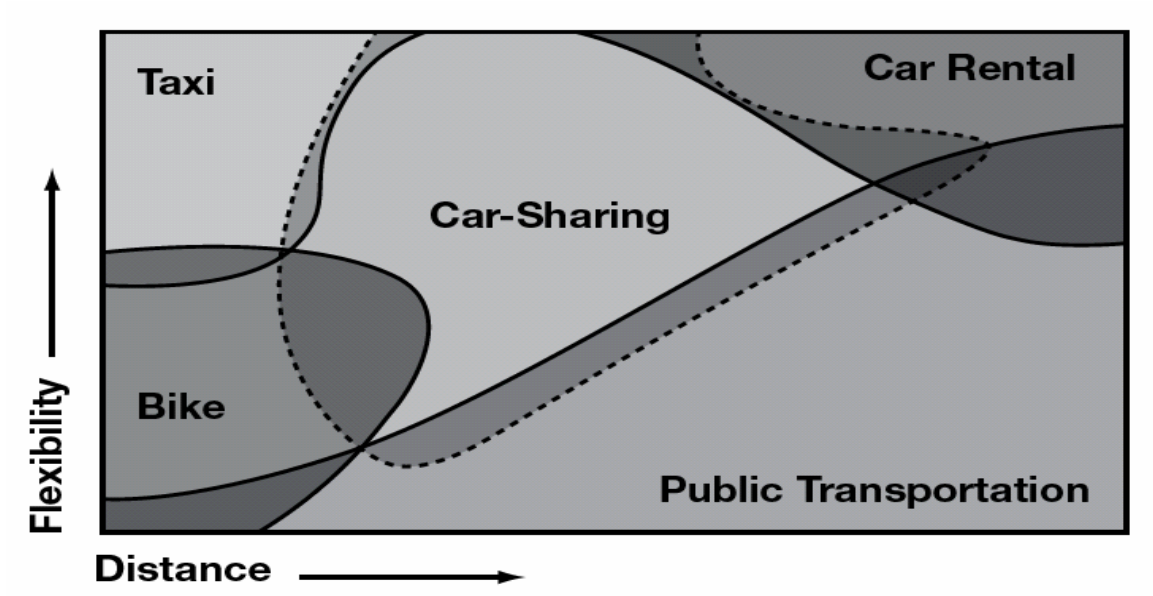

Source: Britton, 1999

Task 5.1.3. Hydrogen Fuel Cell Vehicles and Hydrogen Refueling

In addition to the ZEVNET program, part of APEP's collaboration with Toyota involves the management of a fleet of 2008 to 2010 Highlander fuel cell hybrid vehicles (FCHV). These vehicles are intended to be leased out to qualified drivers within the campus and the surrounding community.

Along similar pursuits, General Motors with the California Air Resources Board teamed up the National Fuel Research Center to begin deploying Chevy Fuel Cell Equinox vehicles to the general public.

In order to deploy fuel cell automobiles to the public, APEP has had to proactively pursue and lead the deployment of hydrogen refueling for California. Working with Air Products, APEP installed a cutting-edge hydrogen fueling station on the UC Irvine campus. The station was constructed as part of the DOE Hydrogen Infrastructure Project and the Hydrogen Highway Initiative and its three year evolution is pictured below.

Figure 145: Hydrogen Storage and Dispensing System (taken January 2003)

Figure 146: Hydrogen Electrolyzer System (taken March 2004)

Figure 147: Hydrogen Fueling Station at the Intersection of Campus and Jamboree (taken September 2006)

Hydrogen is delivered to the UCI station as a liquid and is stored onsite as a liquid in a 1500 gallon insulated vessel, as depicted in Figure 148. As needed, the liquid is vaporized and compressed by the main compressor to 54 MPa and stored in three equally sized storage tubes capable of holding 52 kg of 54 MPa hydrogen. Contemporary hydrogen vehicles are either equipped with onboard storage tanks pressurized to 35 MPa or 70 MPa, depending on the vintage and the manufacturer. When a 35 MPa vehicle refuels, hydrogen is cascaded directly from the 54 MPa storage tubes to the vehicle's tank. Hydrogen is drawn from the lowest pressure storage tube first. As the vehicle tank pressure nears parity with the first station tube, the second storage tube is called upon. If this pressure is insufficient to completely fill the vehicle, the third tank is used. Two additional steps are required to fill a 70 MPa vehicle. The stored 54 MPa hydrogen is further compressed with a RIX reciprocating piston compressor up to a final pressure of nearly 80 MPa. However, the extra compression and high pressure require that the fuel be cooled substantially in order to accomplish quick vehicle refueling safely. The high pressure hydrogen therefore passes through a heat exchanger (cooling block) which cools the gas just before it enters the vehicle. The cooling block is cooled by an onsite refrigeration unit. The cooling block and refrigeration are each sized to work in tandem.

Figure 148: Schematic of UC Irvine hydrogen station showing liquid and gaseous hydrogen storage, 35 and 70 MPa compression and dispensing, and 70 MPa pre-cooling.

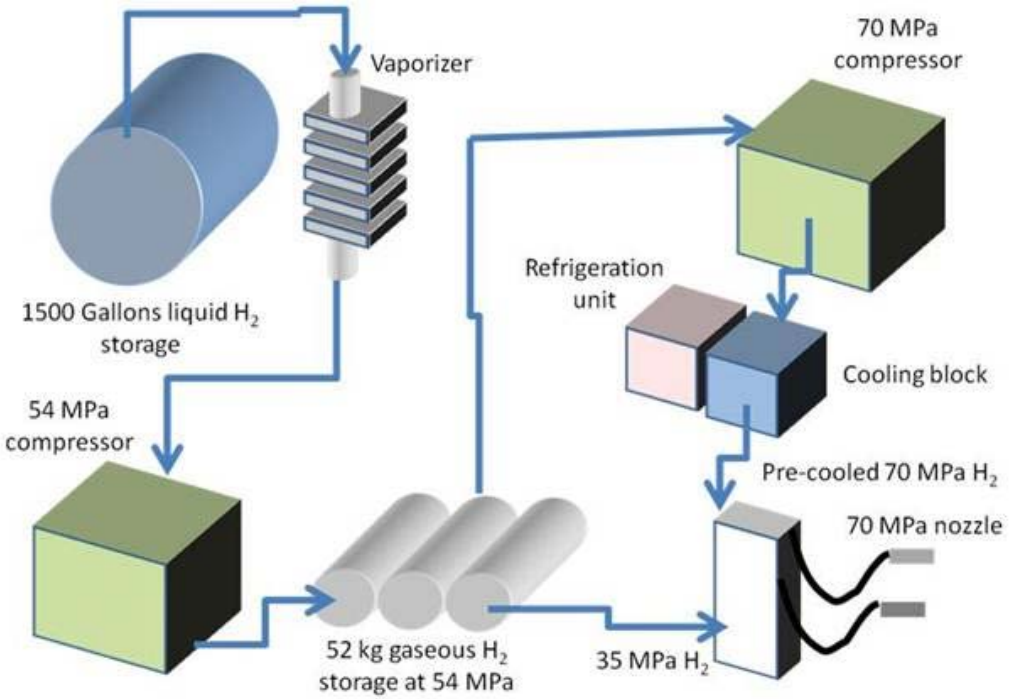

The station has a nominal daily maximum capacity of 25 kg which is limited by the 54 MPa compressor (capable of compressing roughly 1 kg per hour). However, as shown by actual usage data, vehicle fueling does not take place consistently throughout a 24 hour period. As a result, even though the station only dispenses an average of 16.5 kg per day, the 52 kg of onsite 54 MPa storage is often depleted at a rate greater than 1 kg/hour during common refueling times, resulting in a shortage of hydrogen. Additionally, as more vehicle manufacturers have adopted 70 MPa technology over the past two years, the distribution of 35 MPa and 70 MPa refueling has changed as shown in Figure 149. The higher proportion of 70 MPa filling results in a greater dependence on the refrigeration and cooling system.

Figure 149: Plot showing increase in proportion of 70 MPa filling compared to 35 MPa.

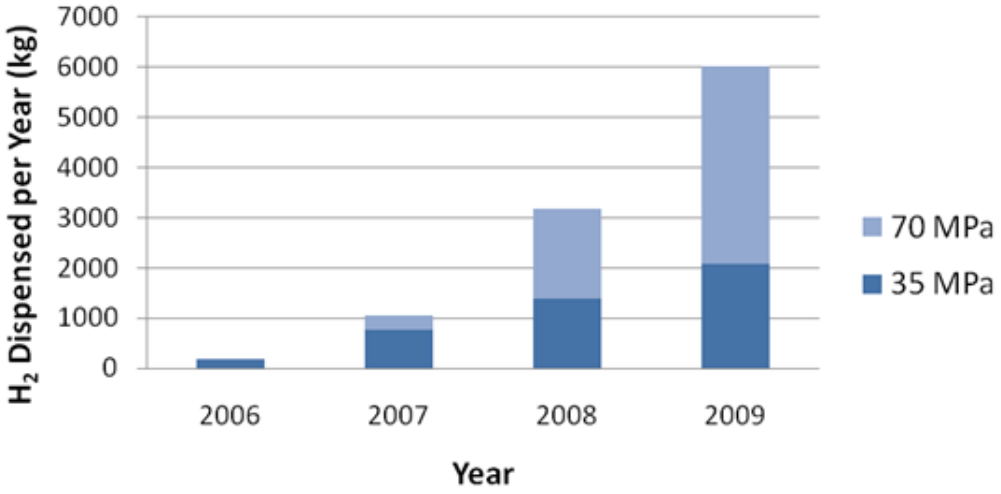

5.1.3.1. Biodiesel Shuttle (B20)

In 2006, the Associated Students of UC Irvine (ASUCI) began a campaign to retrofit its fleet of shuttle buses servicing on campus housing communities to run on 100% biodiesel (B100). See Figure 150 for a picture of the passenger bus operated. Unfortunately, due to high maintenance costs the retrofitted fleet was evaluated to only be suitable for use with 20% biodiesel (B20). Nevertheless, the B20 buses were operated for four years and demonstrated a commitment by the campus towards sustainable initiatives. The shuttles had a large ridership impact with approximately 12 shuttles operating each hour resulting in approximately 1,000,000 passengers per year (UC Irvine Transportation, UC Irvine Business and Administration Services).

Figure 150: Biodiesel powered passenger bus operated at UCI

5.1.3.2. On-Campus Housing

In an effort to recruit and provide convenience for students and faculty, the University of California, Irvine subsidizes on campus housing. A Google aerial map of the campus is shown in Figure 151 highlighting undergraduate, graduate, faculty and staff housing. The on campus housing allows students and faculty to live close to the university to decrease car trips and commuting time. Housing near the work/school place will be shown to be very effective at decreasing GHG emissions and energy consumption for transportation. However, much of Southern California is not planned to minimize car trips.

Figure 151: On-campus housing for Faculty, Staff and Students at UCI

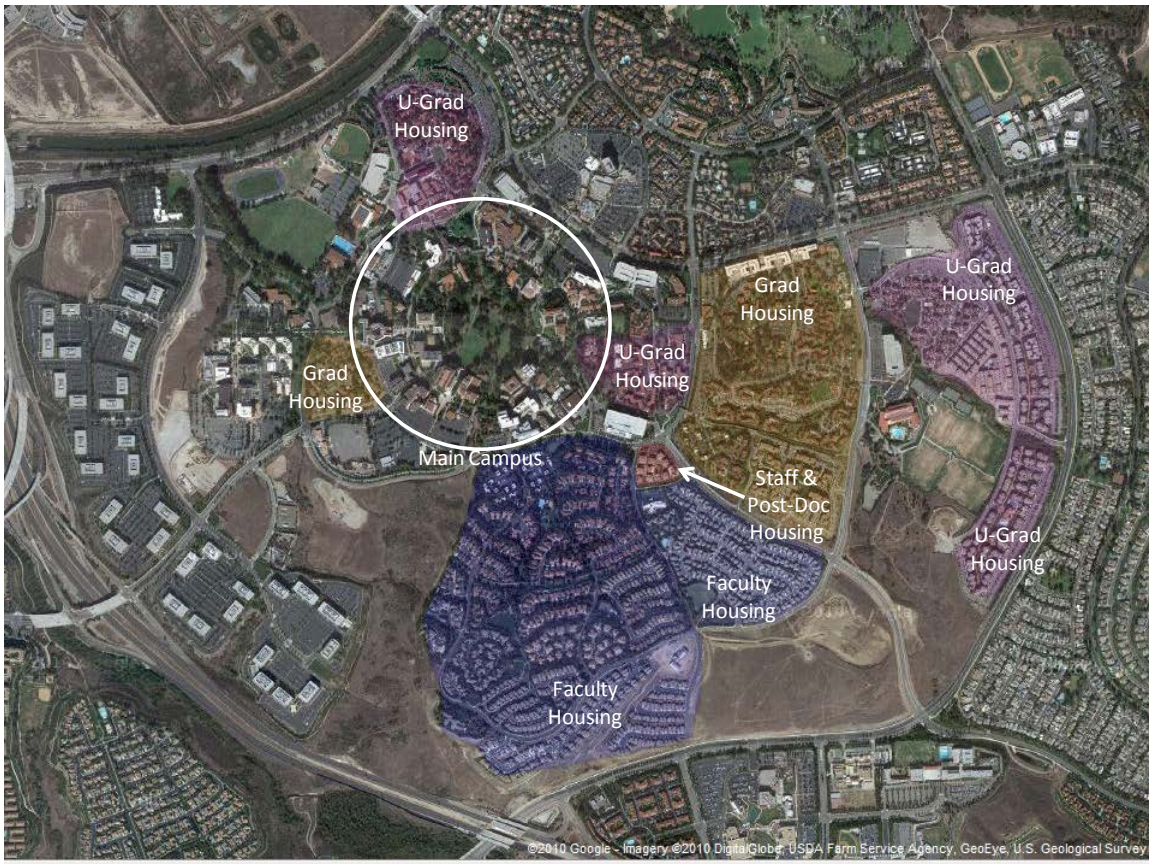

Task 5.1.4. Transportation Alternatives Survey

To obtain vehicle performance and use data, students and faculty who commuted from home to campus utilizing various transportation modes available through the Advanced Power and Energy Program and the University of California, Irvine were comprehensively surveyed for a period of two weeks. The survey pool included:

- Three drivers of conventional internal combustion vehicles,
- one driver of a hybrid electric vehicle,
- two drivers of fuel cell vehicles,
- four people who biked to campus,
- one person who alternated between the on-campus biofuel powered shuttles and biking,
- two people who walked,
- one ZEVNET commuter who utilized electric vehicles and the Orange County Metrolink rail system

A nice balance was maintained amongst the poll takers as approximately 50% resided on campus while the other 50% resided off campus.

Due to unique differences between transportation alternatives, three different surveys were required to obtain necessary information: motor vehicle, mass transit, and human powered transportation. Survey participants were given one of three questionnaires specially designed for their transportation methods (i.e. motor vehicle, mass transit, or human powered). In some cases, survey participants were given two survey types (for example: mass transit and human powered) if they utilized more than one option during the two week survey period.

The surveys consisted of two parts: 1) a front-end requesting basic and specific vehicle information (see Figure 152) and 2) tables to log individual trip information (see Figure 153). The front-end was developed to obtain basic information including name, contact information, and residential address (relevant for commute distance). Vital information specific to a particular mode of transportation was also requested. For instance, the motor vehicle front-end asked participants to record vehicle information (make, model, year, initial odometer reading), vehicle type (fuel-cell, hybrid, internal combustion engine), percentage of driving distribution (street or highway), and refueling (date, odometer reading, gallons filled, octane #, cost, calculated MPG). The mass transit front-end requested the type of mass transit (bus or train), the company that provided the transit (ASUCI, Metrolink, etc.), the route #, and the intersections/stops used. Lastly, the front-end for the human powered transportation asked users to select whether they walked or biked and to include body mass index data (weight, height) which were to be used for calculations of caloric consumption.

The tables for logging individual trips were all similar in that they all asked the survey taker to note the date, the start and stop time of their commute, and the number of passengers. For each trip, the user placed a mark noting whether they had started and/or ended a trip from home (H), other (O), or work (W). This method made it possible to track and separate trip chaining – stops made en route from home-to-work and vice versa. Also, all three survey versions left room for the participant to mention any anomalies in their typical commute (i.e. traffic, an accident, a flat tire, weather, or some atypical driving behavior).

With respect to the table for the motor vehicle survey, the participants had to additionally record the change in their odometer after each trip and provide a rough illustration of their fuel gauge and/or battery storage (HEV and BEV) at the start. The mass transit log did not require this additional information requested on the motor vehicle survey. It only asked the rider to confirm what type of vehicle and fuel the transit system was using for that particular commute (i.e. petroleum-P, natural gas-NG, biofuel-BF, hydrogen-H, electricity-E, or diesel-D). Lastly, as can be presumed, the human powered travel log needed no additional information on fuel or mileage. However, we did ask for the survey takers to subjectively note whether they had felt that their travel pace had been light-L, brisk-B, or intense-I during a particular commute trip.

Figure 152: Front-end of the three survey versions.

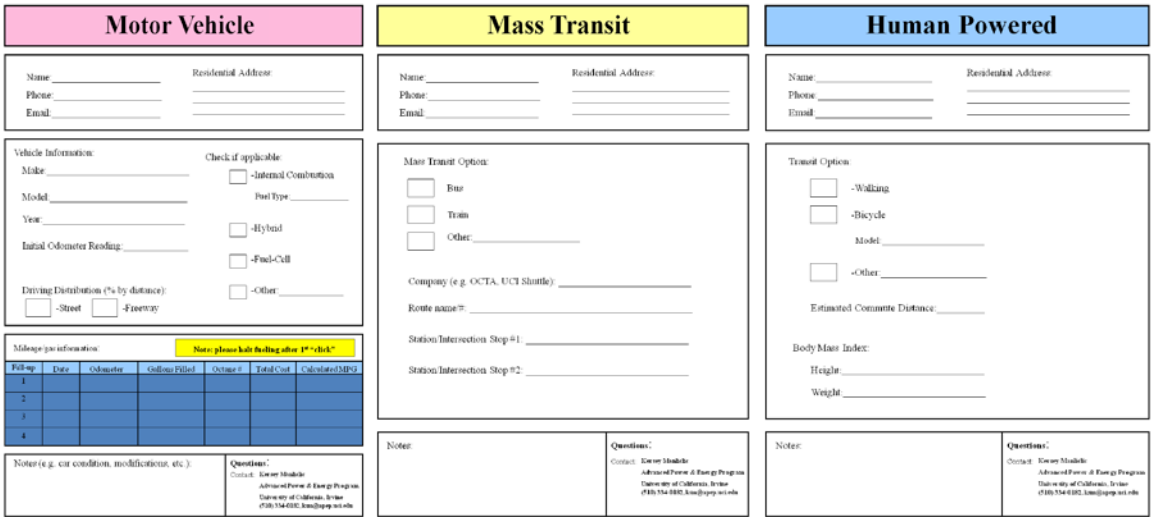

Figure 153: Tables of the three survey versions

Task 5.1.5. Survey participants

Each of the survey participants' transportation characteristics is summarized below.

Three internal combustion engine vehicles were surveyed for the study. These included a 2005 Honda Civic coupe traveling approximately 2 miles with a calculated MPG of 26, a 1998 Lexus ES 300 commuting about 12 miles with a calculated MPG of 24, and a 2006 Toyota Corolla that commuted roughly 8 miles, had a calculated MPG of 31, and partially carpooled during the 2 week period. The survey also included a 2007 Toyota Prius hybrid that commuted about 21 miles with an approximate MPG of 47.

For the human powered transportation, our study had 5 people that rode their bikes. 4-out-of-the-5 had commutes to campus less than 2 miles in distance. The remaining person traveled roughly 7.5 miles. 2 people walked to campus. The first person was nearby having to walk only 0.25 miles. Conversely, the second person was much further living 2 miles away.

For the fuel cell study, two drivers of the 2008 Toyota FCHV Highlanders were surveyed. One driver commuted about 38.25 miles, partially carpooled during the 2 weeks period, and refueled with liquid H_2 at 70 MPA. The second driver also used the same vehicle. However, that person was closer to campus having to commute only 1 mile, did no carpooling, and refueled at only 35 MPA (refueling at 70 MPA required extra training). They obtained roughly 46 MPGGE and 44 MPGGE, respectively.

For the biofuel study, our survey taker was one of our four local bike riders. During the two weeks, the participant commuted roughly 37% of the time (10 trips) via bike and the remainder of the time (17 trips) via the campus shuttle. The shuttle service at UC Irvine operates on 20% biodiesel (B20) and services all of the campus-run housing communities. According to data provided by UC Irvine Transportation Services, the shuttles had a budgeted MPG of 4.75 and an approximate ridership of 25 passengers. This number was on par with the average counted by our survey taker.

Lastly, we had one survey taker whose commute consisted of using two 1998 Rav4 EV's and the Southern California Metrolink rail system which operates on diesel fuel. The participant would drive one of the Rav4's approximately 3.5 miles from home to the train station in West Corona, CA. He would then proceed to take the 803 train in the mornings (804 on the return trip) to the station in Irvine, CA. The distance between stations was approximated to be 34 miles using Mapquest.com. Lastly, our survey taker used the second Rav4 to make the 9.55 mile trip from the Irvine station to the UCI campus.

Task 5.1.6. Analysis Approach

Survey data was used to quantify (a) Energy [MJ/mile] and (b) GHG emissions [kgCO2equivalent/mile] for various transportation options. In conducting the analysis of various transportation modes, both well-to-tank (WTT) and tank-to-wheel (TTW) was resolved. Well-to-tank encompasses all processes required to deliver a given amount of fuel from the source to the vehicle. For example, a gasoline pathway follows oil extraction, refinement, and

the transportation associated with finally delivering a gallon of gasoline to a gas station. In order to compare all pathways on a similar basis, energy use and emissions of the WTT portion were measured on a per gasoline gallon equivalent (GGE) basis, the equivalent energy of a gasoline gallon. The tank-to-wheel (TTW) portion captured energy use and GHG emissions as a result of operating the vehicle. TTW measurements account for the efficiency of a vehicle, typically measured by a vehicle's mileage per GGE. As such, the well-to-wheel (WTW) analysis combines the WTT and TTW portions of a pathway into a complete study of a fuel supply chain and consumption.

5.1.6.1. Analysis Summary

To obtain WTT data, various available life cycle analyses (LCA) conducted on the fuels studied in the RESCO project were referenced. These LCAs, conducted by research laboratories such as the Argonne National Laboratory (ANL) and the National Renewable Energy Laboratory (NREL) provided the comprehensive data of energy use and emissions for various fuels that occur between energy feedstock recovery (well) and delivery to the general public (tank). It should be noted that a WTW analysis does not encompass a fuel's entire lifecycle (such as construction or disposal factors).

5.1.6.1.1. ICEs, HEVs, and Gasoline

For the analysis, three internal combustion engine (ICE) vehicles were included: a 2006 Toyota Corolla, a 2005 Honda Civic, and a 1998 Lexus ES 300. Additionally, one hybrid electric vehicle (HEV), a 2007 Toyota Prius, was also studied. For conventional gasoline, the June 2001 study conducted by Argonne National Laboratory – with the participation of BP, ExxonMobil, and Shell - under the commission of General Motors reported a WTT energy use of 230,000 BTU/mmBTU of fuel delivered. In conjunction with that value was the 21,125 gCO2e (grams of CO_2 equivalent) emitted per mmBTU of fuel delivered. For diesel, the WTT energy use and GHG emissions were 175,000 BTU and 16,500 gCO2e, respectively, per mmBTU of fuel delivered.

The figure below shows the calculation logic for WTT energy use and emissions. At a given stage, energy use by fuel type is estimated by using energy efficiency and fuel type shares. Following that, emissions are calculated by using energy use by fuel type, emission factors by fuel type, and combustion technology shares (GM-ANL, 2001).

Figure 154: Calculation Logic for Well-to-Tank Energy Use and Emissions of Transportation

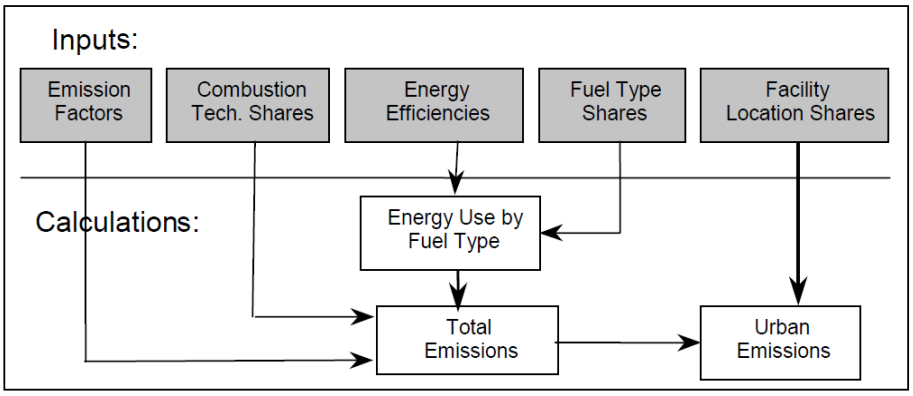

Source: GM-ANL, 2001

5.1.6.1.2. Train and Diesel

One survey taker rode a Southern California Metrolink train with an approximate mpg of 0.3 and an average ridership of 600. This mpg was verified indirectly by utilizing information on the diesel gas tax from the Southern California Rail Authority and the American Petroleum Institute. From 2009-2010, the diesel motor fuel tax was approximately $0.615. During 2009, Metrolink spent roughly $7,832,000 for fuel taxes. Thus, with the assumption that all of the trains in the Metrolink fleet are the same, around 12,734,959.35 gallons of diesel fuel were used to travel nearly 25,488,786 miles (25,488,786 miles/12,734,959.35 gallons ≈ 0.2 mpg).

5.1.6.1.3. Human Powered

Well to tank energy and GHG emissions of walkers and bikers was evaluated by approximating the calories exploited making the trip and further calculating the corresponding energy use and emissions associated with agricultural food production and transport. In other words, assuming that calories burned during the commute meant that the survey taker had to have a higher caloric intake in their diet equivalent to the calories burned for the commute, the amount of food a person needed to consume could be estimated. That amount then corresponded to energy use and emissions associated with agricultural food production.

Using body mass data coupled with travel speed and distance, the calories burned by our survey takers were referenced from available calculators – average value from WEBMD and Healthstatus.com. From those values, the calories burned while under resting heart rate were subtracted. This would make the energy use and emissions comparable to the other modes of transportation. Using research conducted by Eshel and Martin on energy use and emissions from agricultural food production, the efficiency of food production and consumption could be calculated to be around 7.6% (Eshel, 2006). Kim and Neff reported on emissions data for the agricultural industry gathered from the EPA and from previous work done by Weber and Matthews (Ecological Economics, 2009). A range for the annual per-capita GHG emissions was presented and spanned from 1.56 metric tons of CO2e to 3.1 metric tons of CO2e. This range

was then converted to approximately 1.99 to 3.95 gCO2e per kcal of food consumed and the average, 2.97, was used for our calculations.

5.1.6.1.4. Shuttle and Biodiesel

The WTT energy used for the UC Irvine campus shuttles was drawn from a study conducted by NREL - An Overview of Biodiesel and Petroleum Diesel Life Cycles – and was approximately 1.2414 MJ per MJ of fuel (Spath, 2001). The WTT emissions were derived from a consultation – Assessment of Biodiesel and Ethanol Diesel Blends, Greenhouse Gas Emissions, Exhaust Emissions, and Policy Issues - prepared by Levelton Engineering for Natural Resources Canada in 2002 (Levelton, 2002). Since the shuttles utilize B20 (20% biodiesel, 80% conventional diesel), the WTT emissions are derived by multiplying the biodiesel WTT value by 0.2 and diesel WTT value by 0.8. Our TTW study of the shuttles was verified and supplemented with actual ridership data supplied by UC Irvine Transportation Services. UC Irvine Transportation Services also provided the mpg for their shuttle fleet to be roughly 4.75 mpg. Lastly, the TTW emissions were assumed to be 80% of the emissions that come from diesel fuel (8.0672 kg CO2/gallon) with the reasoning that carbon from the 20% biofuel is carbon neutral.

5.1.6.1.5. FCEVs and Hydrogen

Eight pathways were investigated for H_2 production. This consisted of four base supply chains for two fuel cell electric vehicles (FCEVs) using H_2 compressed to 70 MPa and 35 MPa. The FCVs used were Toyota Highlander FCHVs, or fuel cell hybrid vehicle, the Toyota naming variant for their FCVs. Of the four base chains, two produced H_2 by natural gas in a central SMR plant and transported by truck to a H_2 fueling station, with one of the plants liquefying the H_2 prior to transportation. A third chain used natural gas in an onsite HTFC at the H_2 fueling station. The fourth supply chain used digester gas in an onsite HTFC. All pathways used grid electricity to compress the H_2. Additionally, liquefaction used grid electricity. The grid was assumed to be the CA grid mix used (see next paragraph). All trucks were assumed to use diesel.

5.1.6.1.6. BEVs and Grid Electricity

Three different pathways were investigated for grid mix combinations. The first was based on the assumption that the additional charging load of a battery electric vehicle (BEV) is insignificant enough on the grid as a whole that only marginal power plants supply the electricity, thus the grid mix consists entirely of natural gas steam turbines and peaker plants, called the CA marginal mix. This would entail charging that occurs at peak hours of the day. The second pathway is based on the 2007 CA grid mix as given by the CEC (Jensen, 2009). The third was based on the 2007 US grid mix, also from the CEC. All three pathways were taken on yearly averages, and were not time dependent. CA and US grid mix numbers were validated in comparison to EPA eGRID data for 2005, and the CA marginal mix was validated in comparison to CEC data from 2005 (Heling, 2008). Two BEVs were used with the three pathways for a total of six cases. The BEVs were identical in all respects, including driver, the only difference was the distance traveled and use of carpooling. Both BEVs were Toyota RAV4 EVs. Since the RAV4 EVs were approximately 12 years old, in order to gauge advances in BEV

technology, the storage capabilities and energy efficiency of a Nissan LEAF BEV were modeled under the same operational conditions as the RAV4 EV using available information from Nissan.

5.1.6.2. Survey and Analysis Results

Each vehicle technology type surveyed is compared based on recorded survey data. Figure 155 and Figure 156 do not take into account passenger occupancy in order to focus on the technologies themselves rather than driver choices. Public transportation options yielded extremely high energy consumption values in comparison to the other alternatives, and are limited in the figures. Instead, the maximum for each is numerically represented at the top of both figures. The TTW portion in these pathways are missing as they would be off the graph, not be confused with not having any TTW energy use. Both FCVs show higher energy use than the Corolla and the Prius, suggesting long distance liquid hydrogen delivery is inefficient. In later sections, hydrogen production alternatives will be explored in order to see if advancements can yield better results in comparison to current ICE technology.

Figure 155: Comparison of energy consumption as Surveyed on a Per Mile Basis

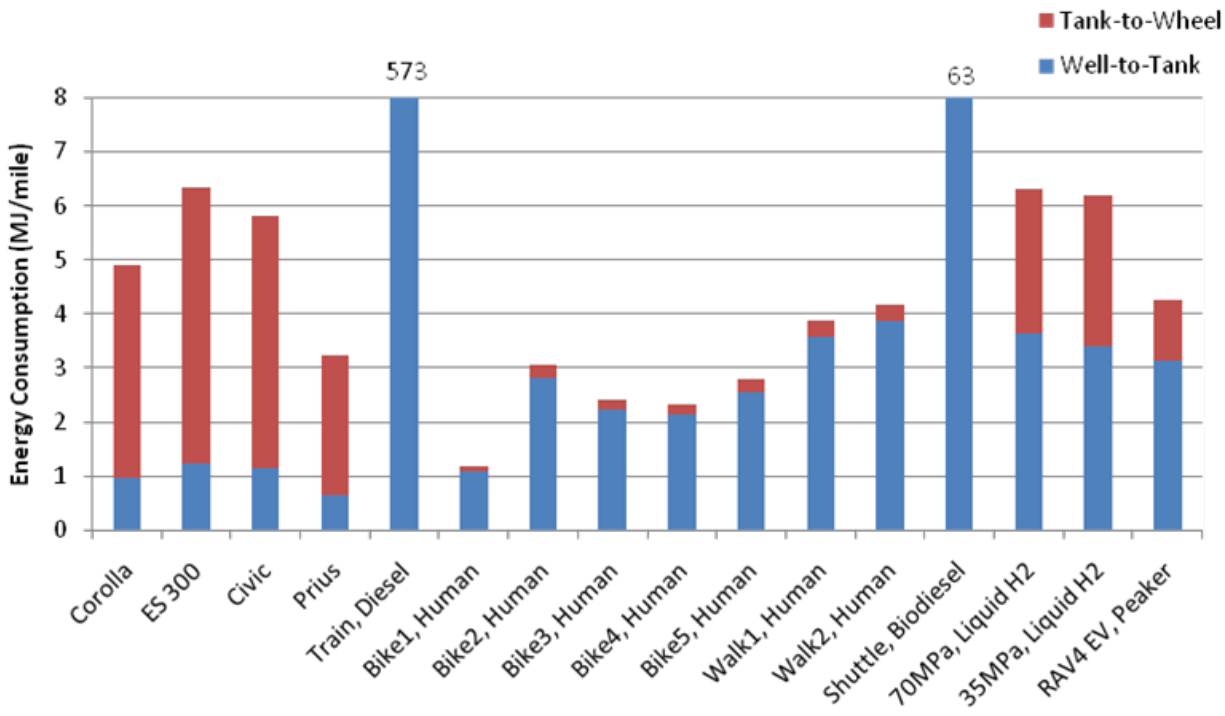

Figure 156: Comparison of GHG Emissions as Surveyed on a Per Mile Basis

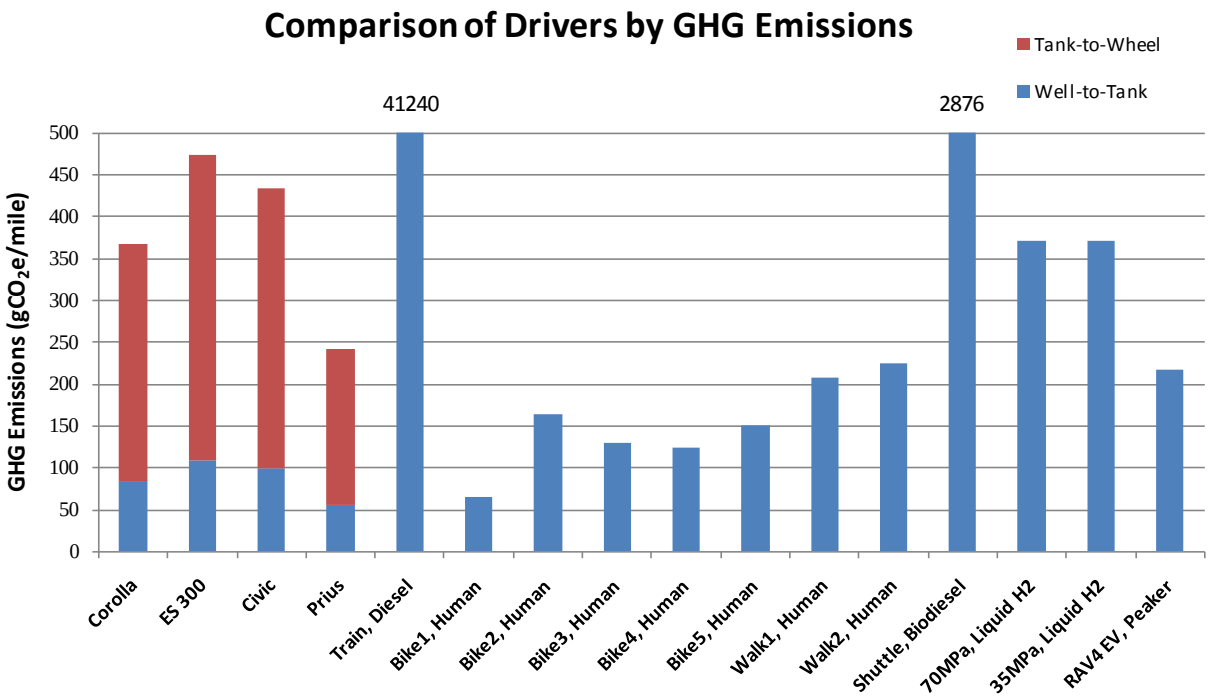

Proportionally, the GHG emissions presented in Figure 156 are similar to energy differences in Figure 154. Again, the HEV performed better than the FCVs, however vehicle size plays an important role due to the aerodynamics and weight. The Toyota FCHV Highlanders are medium sized sport utility vehicles, while the Toyota Prius used is a smaller sedan. Additionally, all ICEs surveyed were sedan type cars. Greater fuel economy could be expected from the FCVs had they been with smaller vehicles.

Task 5.1.7. Public Transportation Benefits

Figure 157 and Figure 158 present the same data as in Figure 155 and Figure 156 but on a per person mile basis accounting for vehicle occupancy. Considering trip sharing and vehicle occupancy, the benefits of carpooling and public transportation are clear. A single train consumes high amounts of energy and has high emission rates. However, each train trip carries 100's of passengers making trains one of the most attractive options for long distance transportation. The Corolla performed better than certain 35 MPa FCV pathways as the former did more carpooling. Efforts to promote carpooling and public transportation can be very beneficial. It is also worth investigating the use of alternative energy in public transportation, such as electricity from the grid or fuel cells in the use of public buses or trains, as the high passenger capacity would likely yield a very low energy use and CO_2e emission on a per person-mile basis.

Figure 157: Comparison of Trip energy use per mile

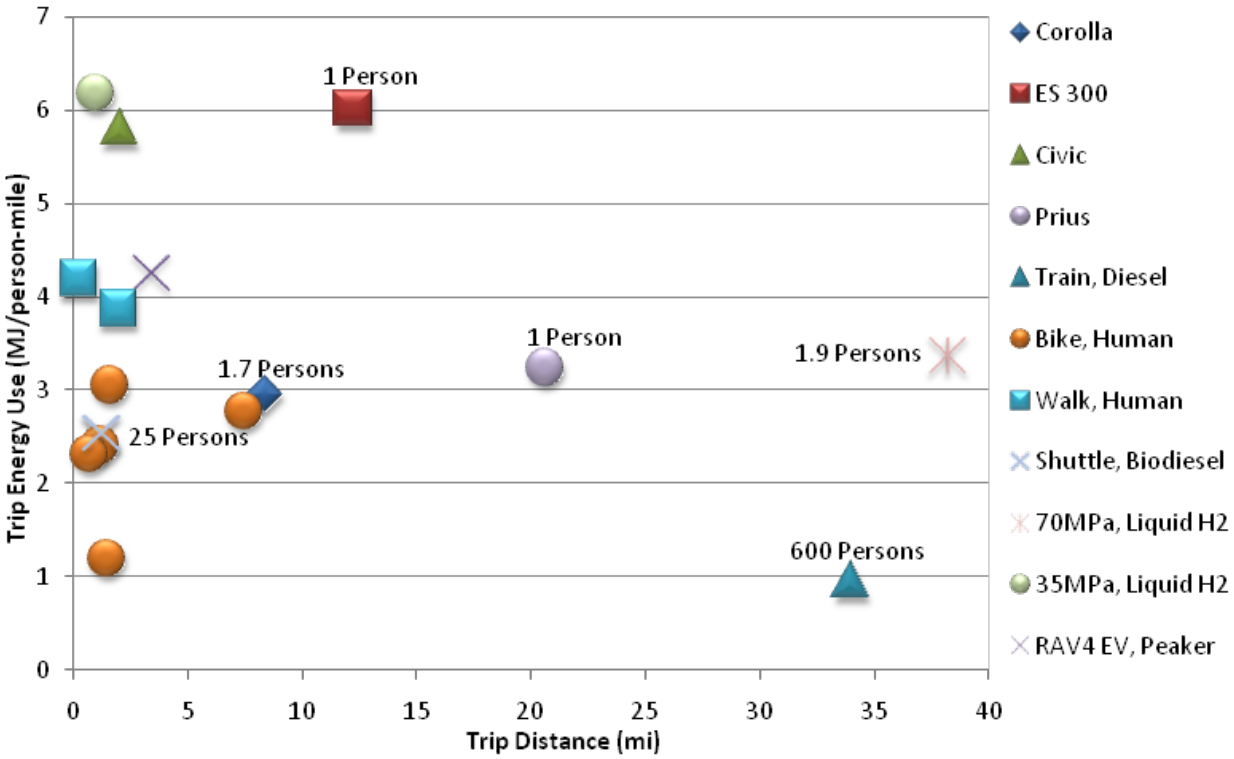

Figure 158: Comparison of Trip greenhouse gas emissions per mile

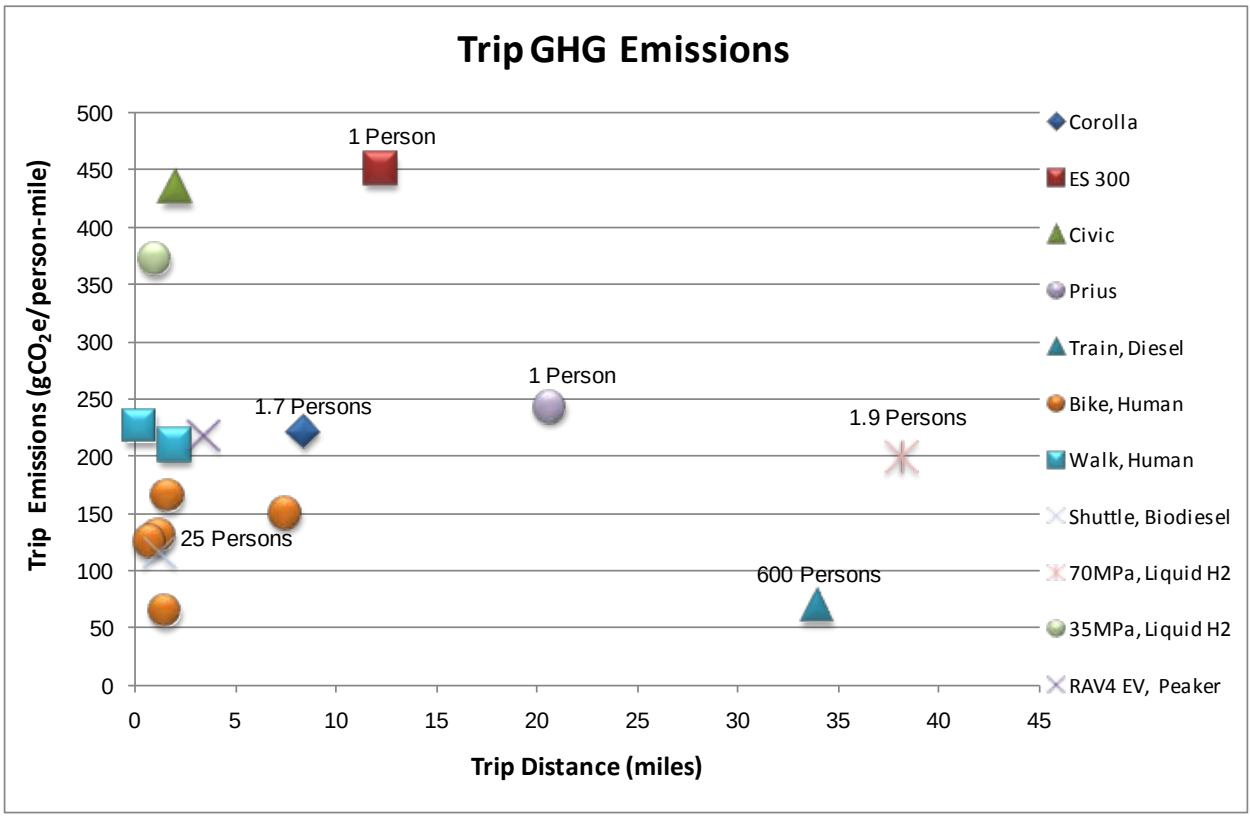

Task 5.1.8. Conclusions

- Different transportation alternatives are explored including: electric vehicles, hydrogen fueled vehicles, hybrid (gas-electric) vehicles, biodiesel shuttle, train, biking and walking.
- Students, faculty and staff were surveyed on their transportation options and these options were compared.
    - Public transportation (train and shuttle) and biking have the lowest energy and CO_2 emissions per person-mile.
    - Walking and carpooling (conventional and fuel cell vehicles) result in the second lowest energy and CO_2 emissions per person-mile.
    - Conventional vehicles (single occupant) have the highest energy and CO_2 emissions per person-mile.

Task 5.1.9. References

Britton, E., "Carsharing? A roadmap and compass for this long trip," World Transport Policy and Practice, 1999, 5(3): 1-8.

EMFAC2007 release. California Air Resources Board. (September 2008, http://www.arb.ca.gov/msei/onroad/latest_version.htm) Emissions inventory data. California Environmental Protection Agency, Air Resources Board. (January, 2009; http://www.arb.ca.gov/ei/emissiondata.htm)

Eshel, Gidon, and Pamela A. Martin. "Diet, Energy, and Global Warming." Earth Interactions 10 (2006): 1-17. <http://pge.uchicago.edu/workshop/documents/martin1.pdf>.

General Motors Corporation, Argonne National Laboratory, BP, ExxonMobil, and Shell. Well-to-Tank Energy Use and Greenhouse Gas Emissions of Transportation Fuels - North American Analysis - . Vol. 3. June 2001.

Heling, Matthew G. Assessment of the Zero-Emission Vehicle, Shared-Use Station Car (ZEV-SUSC) Mobility Concept with a Focus on Energy and Environmental Sustainability. UCI, 2008.

Jansen, Karel H. The Impact of Plug-In Hybrid Electric Vehicles on the Western Grid of the United States . UCI, 2009.

Kim, B. Neff, R. Measurement and communication of greenhouse gas emissions from U.S. food consumption via carbon calculators, Ecological Economics (2009), doi:10.1016/j.ecolecon.2009.08.017

Levelton Engineering Ltd. and (S&T)2 Consultants Inc.. Assessment of Biodiesel and Ethanol Diesel Blends, Greenhouse Gas Emissions, Exhaust Emissions, and Policy Issues: Prepared for Natural Resources Canada. September 30, 2002.

National Renewable Energy Laboratory (NREL). An Overview of Biodiesel and Petroleum Diesel Life Cycles. May 1998.

Spath, P. L., Mann, M. K., Life cycle assessment of hydrogen production via natural gas steam reforming. NREL/TP 570-27637. NREL; February 2001.

Task 5.2. Land-Use Design Effect on Transportation Intensity

Task 5.2.1. Distance vs. Time Comparison

The trip distances and times were compared between all survey participants in Figure 159. Of interest are the marginal increases in trip time in order to travel similar distances between transportation alternatives. For example, the Corolla travels marginally further than the furthest bike, and only 10 minutes faster. As mentioned earlier too, the Civic, which traveled a similar distance to some human powered options will also take a similar amount of time, due to the increased stopping frequency and the lack of a freeway at short distances.

Figure 159: Trip Distance and Time Comparison

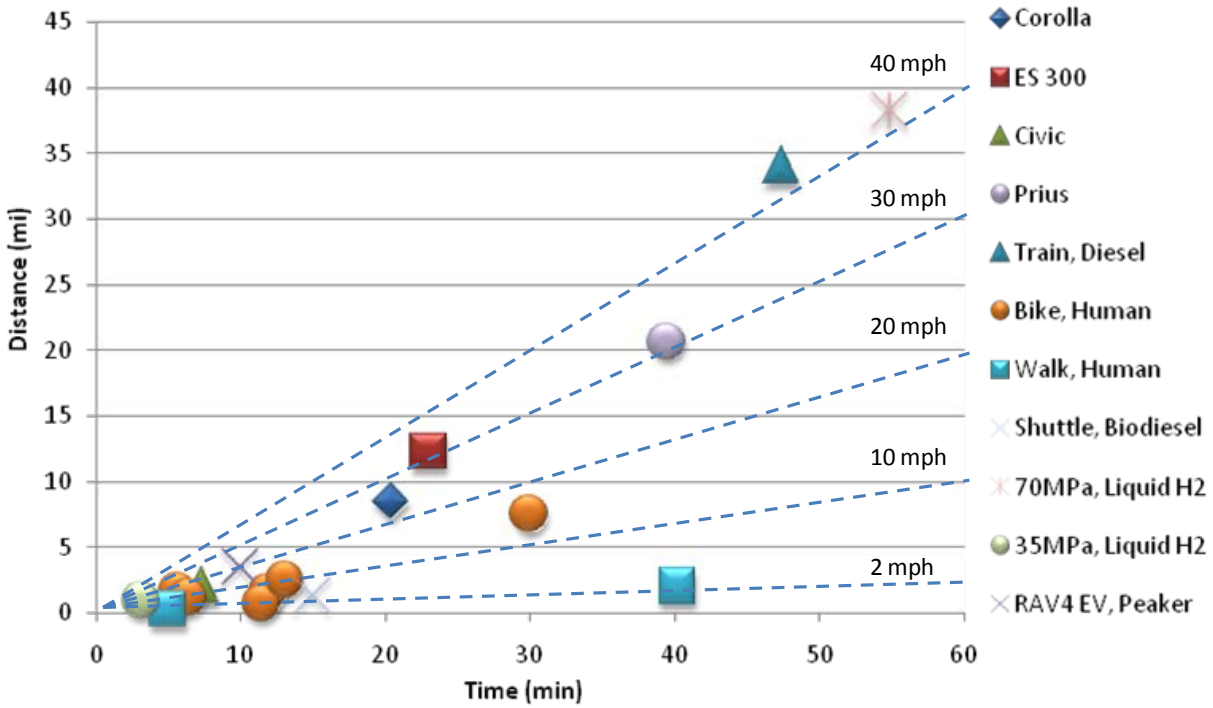

A general trend of increasing time associated with increasing trip distance can be seen in this plot. Human powered transportation follows this trend albeit with a slope that renders this form of transportation unfeasible due to the long travel times. Given that this form of transportation has the smallest environmental impact, this highlights the need for community planning to enable personal transportation.

Task 5.2.2. The analysis results of energy and carbon footprint of on campus residence

Results compared on a per person basis indicate the lowest energy and GHG emissions can be achieved by living close to where you live and work. Public transportation has a great benefit for longer trips, but living close to work leads to the lowest GHG emissions even for individuals driving a short distance. Biking or carpooling longer distances is better than not doing so, but the best alternative is to live close to where one works.

Figure 160: Survey Results for Energy Use versus Distance Travelled

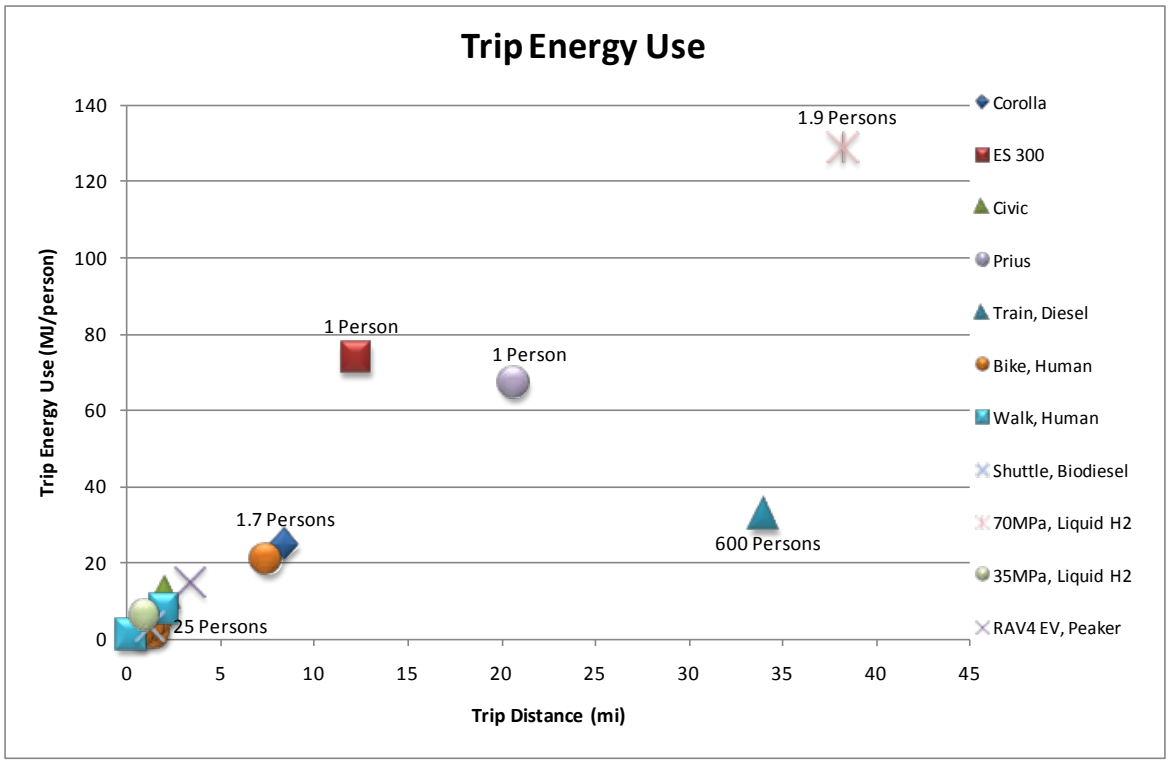

Figure 161: Survey Results for Emissions versus Distance Travelled

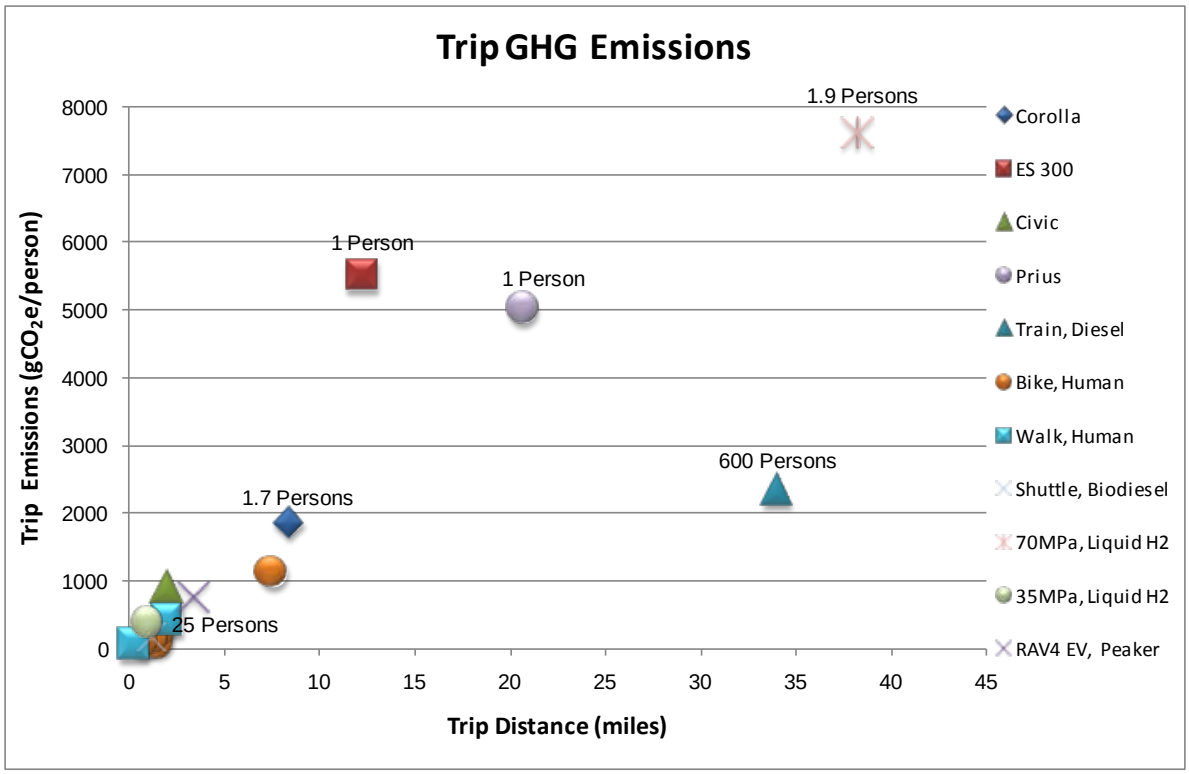

Task 5.2.3. Personal Transportation

Despite the clear benefits of living near work, carpooling, and public transportation, southern California commuting is primarily based on personal transportation. While personal transportation is not the preferred mobility solution, advances in personal transportation alternatives can reduce GHG emissions and improve security by reducing reliance on imported petroleum.

To better compare the personal vehicle pathways, vehicles were not only compared on a basis of energy use, but also by vehicle weight since greater weight is typically related to larger size and interior space. Technology alternatives were explored for H_2 production and grid electricity generation in order to see how future advancements and infrastructure changes compare to existing ICE technology. Public transportation and human powered transportation are not shown in Figure 162 and Figure 163.T The fuel economy of both FCVs were averaged for this analysis. Additionally, the current 2010 Toyota vehicle lineup was added in order to give a better sense of surveyed data in comparison to EPA data.

Figure 162: Comparison of Vehicle and Fuel Type by Energy Use and Vehicle Weight

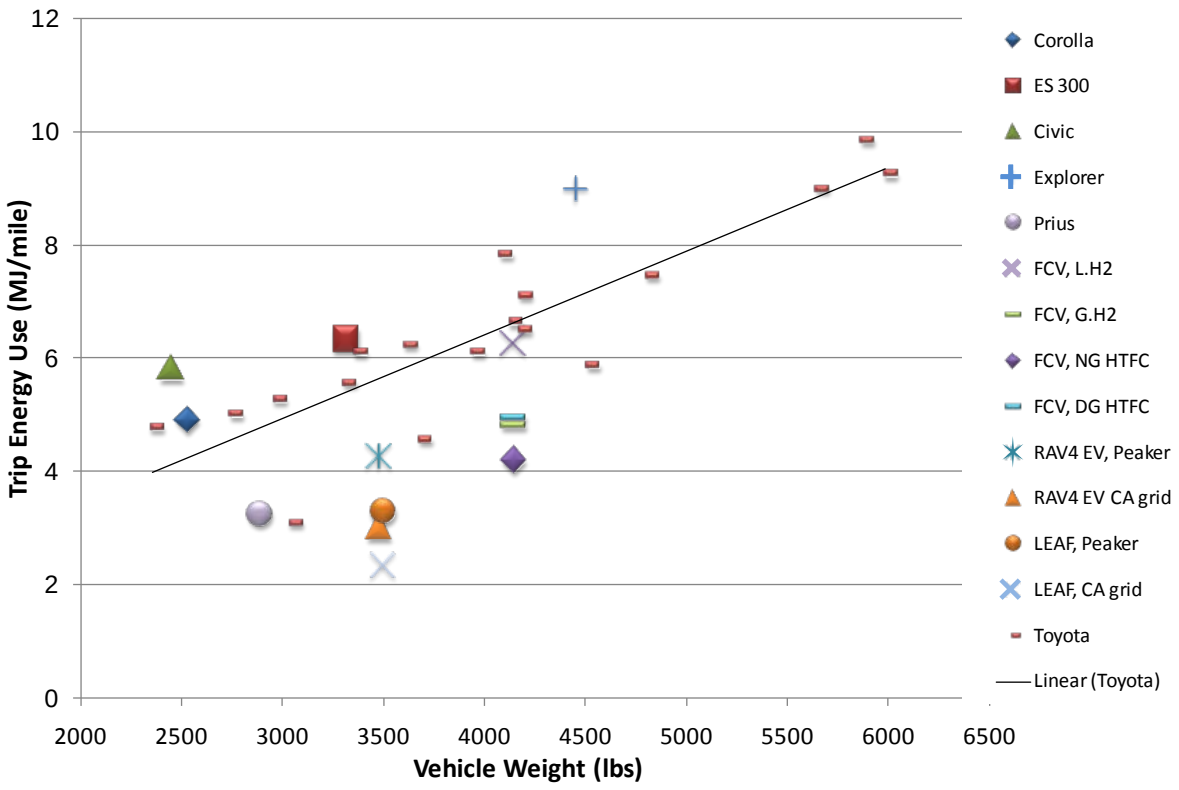

Figure 163: Comparison of Vehicle and Fuel Type by GHG Emissions and Vehicle Weight

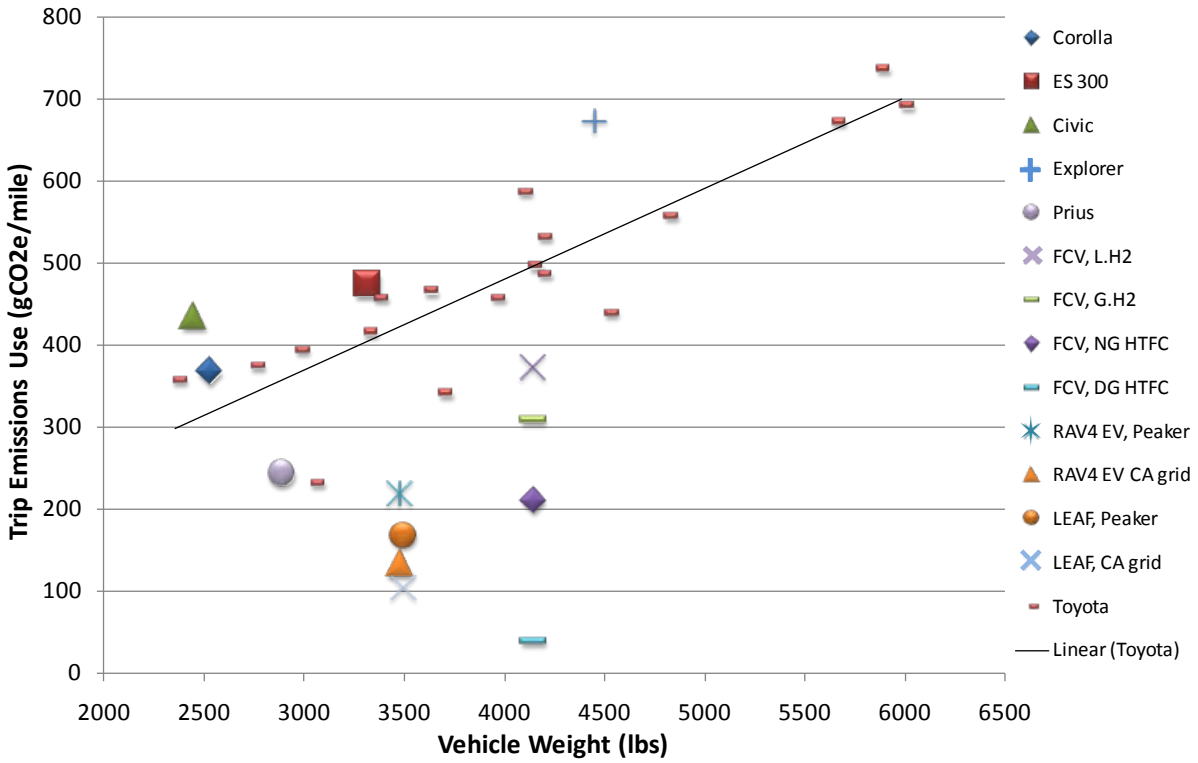

Here, the vehicle size differences can be seen as a major influence on fuel economy. In the prior analyses, the FCVs were not appealing alternatives to the three ICEs surveyed whereas in this comparison they are competitive in their respective weight class. The evolution of H_2 production methods for the FCVs should be noted given the associated decreasing emissions and energy use with improved, newer technologies with the exception of energy use by digester gas HTFCs. The higher energy use by digester gas HTFCs is necessary to purify the more contaminated digester gas into methane suitable to be processed in the HTFC. This increase in energy use by DG HTFC is marginal however when compared to the associated decrease in GHG emissions.

Here, the LEAF was added in order to get a better idea of current emerging BEV models in comparison to the older RAV4 EV. For the BEV grid mixes, the US grid mix was excluded since it is very similar to the marginal mix. Working off the CA marginal mix (or US grid mix), RAV4 EV emissions per mile were only slightly higher than FCVs using NG HTFC H_2. The CA average grid scenario compared well against other technologies being surpassed only by digester gas HTFCs, which rely on the limited number of locations for deployment, whereas grid electricity infrastructure is already established and can be expanded to accommodate increased BEV usage.

While both the BEVs and FCVs present attractive alternatives, it should not be overlooked that simply switching to smaller cars is an immediate solution to reducing energy use and emissions. One could nearly halve emissions by driving a smaller car when suitable as

compared to a heavy truck. Similarly, the use of smaller vehicles with fuel cell or battery technology holds potential for even more efficient vehicles.

Task 5.2.4. Comparison of FCVs and Hydrogen Technologies

In comparing the different H_2 pathways, the 35 MPa data showed less energy consumed and lower emissions on a per GGE basis. However, the 3535 MPa tank has a smaller H_2 capacity and therefore decreased range compared to the 70 MPa tank. When the four base pathways are compared against their respective energy use, SMR with liquefaction of H_2 performed the worst, followed by digester gas HTFC, then SMR for gas H_2, and finally natural gas HTFC. With regards to GHG emissions, the order was the same with the exception that digester gas performed the best. The liquefaction process consumes nearly 30% of the total energy use in the first pathway, which negates the benefit of being able to transport more H_2 in liquid form per truck than in gas form. Both onsite HTFC pathways save the energy and emissions resulting from transportation. W. While this may help decrease transport truck traffic , data show that the contribution transport has to the WTT energy use and emissions is insignificant, less than 1%.T The transportation of liquid hydrogen on an average trip of 50 miles requires only 0.092 kWh of energy per kg of H_2 delivered. However, the energy used by SMR, liquefaction, and pumping at 70 MPa have much higher energy use magnitudes at 48.11, 22.91, and 8.33 kWh/kgH_2, respectively (Amos, 1998; EMFAC, 2007; Contadini, 2000; Spath, 2001; EPA, 2009). The digester gas HTFC requires more energy to produce each kg of H_2, but does not have the emissions of natural gas extraction, hence the H_2 production via this pathway has a much lower emission rate compared to the other 3 base pathways. While liquid H_2 was the earliest pathway implemented, current advancements show a favorable progression to gaseous H_2, as well as the transition to onsite HTFC stations instead of central SMR plants.

Task 5.2.5. BEVs and Grid Electricity

Of the three electricity pathways, the CA grid mix performed the best in both energy use and emissions, followed by the US grid mix, and last the CA marginal mix. The CA grid mix performs the best due to the largest percentage of renewable energy generation. In this study, hydroelectric energy was combined with renewable on the basis that they have zero or negligible operating emissions and were taken to have 100% efficiency in terms of energy use rates. The CA marginal mix performed the worst as it used a combination of the least efficient generation technologies. However, the only reason a BEV would be powered by the CA marginal mix is when charging occurs during the peak electric demand hours of the day, requiring the use of marginal power plants. This warrants a look at the influence of charging time on energy and emissions footprints, which is not discussed in this study but subject to future work.

Task 5.2.6. Conclusions

- Living close to the workplace is the best way to reduce transportation emissions.
- Reducing vehicle size from a large to a small vehicle can halve energy intensity and CO_2 emissions.

- Use of alternative fueled vehicles (BEC, FCV, hybrid) can significantly reduce CO_2 emissions.
- Although the environmental impact of human powered transportation is low, the time for travel is not feasible to replace all forms of transportation.

Task 5.2.7. References

Amos, W.A., Costs of Storing and Transporting Hydrogen. NREL/TP-570-25106. NREL: 1998

Contadini, J. F., Diniz, C. V., Sperling, D., Moore, R. M., Hydrogen production plants: emissions and thermal efficiency analysis. Presented at the Second International Symposium on Technological and Environmental Topics in Transports; October 2000 – Milan, Italy.

EMFAC2007 release. California Air Resources Board. (September 2008, http://www.arb.ca.gov/msei/onroad/latest_version.htm)

Emissions inventory data. California Environmental Protection Agency, Air Resources Board. (January, 2009; http://www.arb.ca.gov/ei/emissiondata.htm)

Eshel, Gidon, and Pamela A. Martin. "Diet, Energy, and Global Warming." Earth Interactions 10 (2006): 1-17. <http://pge.uchicago.edu/workshop/documents/martin1.pdf>.

Kim, B. Neff, R. Measurement and communication of greenhouse gas emissions from U.S. food consumption via carbon calculators, Ecological Economics (2009), doi:10.1016/j.ecolecon.2009.08.017

Spath, P. L., Mann, M. K., Life cycle assessment of hydrogen production via natural gas steam reforming. NREL/TP 570-27637. NREL; February 2001.

Appendix E:Task 6:
Building Design and Operation

TABLE OF CONTENTS

Task 6.1. RESCO Tailored Building Design and Operations Criteria E-4

Task 6.1.1. Background E-4

Task 6.1.2. Approach E-4

Task 6.1.3. Project Deliverables E-5

Task 6.1.4. Project Overview E-5

Task 6.1.5. Conclusions E-7

Task 6.2. Temporal Models for Building Load Demand E-7

Task 6.2.1. The Quick Energy Simulation Tool (eQUEST) E-7

6.2.1.1. eQUEST Model Inputs E-8

6.2.1.2. eQUEST Model End-Use Outputs E-9

Task 6.2.2. Model Calibration E-9

6.2.2.1. Multipurpose Science and Technology Building E-10

6.2.2.2. Natural Sciences II E-11

6.2.2.3. High Rise Engineering Tower E-12

6.2.2.4. Humanities Instructional Building E-14

6.2.2.5. Middle Earth Dormitories – Valimar E-15

6.2.2.6. Apartment Building – Verano 2100 ..... E-16

Task 6.2.3. CEUS and DEER Standard Building Models E-17

6.2.3.1. California Commercial End-Use Survey E-17

6.2.3.2. Database for Energy Efficient Resources E-18

Task 6.2.4. Extrapolating a Campus-Wide Load Profile by End-Use E-18

Task 6.2.5. Integrating Model with HiGRID Code E-25

Task 6.2.6. Conclusions E-25

Task 6.2.7. References E-25

Task 6.3. Tailoring Building Load Profile through Passive Building Energy Efficiency Measures E-25

Task 6.3.1. Interior Lighting E-26

Task 6.3.2. Exterior Lighting E-27

Task 6.3.3. HVAC Systems E-28

Task 6.3.4. Energy Efficiency – Total Effect E-30

Task 6.3.5. Energy Efficiency – Cost Analysis E-31

Task 6.3.6. Other Opportunities for Energy Efficiency E-32

Task 6.3.7. Energy Efficiency vs. Demand Response E-32

Task 6.3.8. Conclusions E-32

Task 6.3.9. References E-33

Task 6.4. Demand Response and Load Management E-33

Task 6.4.1. Existing Demand Response Programs and Compensation E-33

Task 6.4.2. Technical Literature Review E-35

6.4.2.1. Lighting Reduction E-36

6.4.2.2. Ventilation Fan Turn-Down E-36

6.4.2.3. Pre-Cooling E-38

6.4.2.4. Night Purge E-39

6.4.2.5. Plug Load Control E-40

6.4.2.6. Automated Demand Response E-40

Task 6.4.3. Building Model Analysis and Results: MSTB E-40

6.4.3.1. Night Purge E-41

6.4.3.2. Pre-Cooling E-41

6.4.3.3. Fan Turn-Down E-42

Task 6.4.4. Building Model Analysis and Results: Natural Sciences II E-43

6.4.4.1. Pre-Cooling and Night Purge E-43

6.4.4.2. Lighting Reduction E-49

6.4.4.3. Fan Turn-Down E-51

6.4.4.4. Comparison of Demand Response Measures: Natural Sciences II E-53
Task 6.4.5. Experimental Demand Response Testing E-54
6.4.5.1. Test 1: 15% Fan Turn-Down E-55
6.4.5.2. Test 2: Pre-Cool to 70°F E-61
6.4.5.3. Test 3: 30% Fan Turn-Down E-67
6.4.5.4. Full Building Response to Demand Response Tests E-74
6.4.5.5. Conclusions from Demand Response Experiments E-75
Task 6.4.6. Demand Response Model Characterization E-77
6.4.6.1. Lighting Reduction E-77
6.4.6.2. Pre-Cool E-77
6.4.6.3. Fan Turn-Down E-79
6.4.6.4. Demand Response Cost Analysis E-79
6.4.6.5. Conclusions E-80
Task 6.4.7. Further Research beyond RESCO E-80
Task 6.4.8. References E-81

Understanding how buildings can support renewables is as important as understanding the operation of renewables. This section explores current demands for electricity from building loads by developing models for UCI campus buildings and modeling end-use profiles for the entire campus. Then these results are used to determine how building design and operation can support the implementation of renewables.

Task 6.1. RESCO Tailored Building Design and Operations Criteria

Task 6.1.1. Background

Building electricity and fossil fuel use account for 2,400 million metric tons (a total of 40%) of U.S. carbon dioxide emissions. In order to establish a renewable-based energy secure community, it is essential to minimize building energy use and the environmental impact associated with building energy use. Simple and cost-effective efficiency measures can substantially decrease energy needs. Aspects of building design and operations that control energy usage include:

- Lighting fixtures and controls
- Heating, ventilation, and air conditioning (HVAC) systems and controls
- Building envelope (insulation materials, windows)
- Appliance (plug) loads

The integration of renewable generation into the building infrastructure can, if carefully accommodated, dramatically increase the effectiveness of renewable resources. This research focuses on how building controls, feedback, and system integration can play a role in enabling higher penetrations of cost-effective renewable power onto the electric grid.

Task 6.1.2. Approach

The approach of this research effort is to utilize dynamic models of building demand to evaluate building designs that can tailor building loads to be responsive to intermittent power generation. Steady-state and temporal models of building energy use will be developed and applied to research (1) the amount and type of renewables that can be integrated into common building designs, (2) the building designs that optimize the penetration of renewable resources, (3) the impact of direct and indirect demand response mechanisms on load curves and renewable intermittency, and (4) the integration of continuous power storage and generation that is required to assure that the intermittency associated with large fractions of renewables is buffered to reach the high goals of reliability, availability, maintainability, and low COE demanded by the energy future.

Lessons learned from various renewable deployment and sustainability studies and the practical operating experience in the deployment of distributed renewable and continuous power generation resources at UC Irvine are reviewed, evaluated, documented, and utilized to inform forward trending dynamic analyses. The impacts of various demand response

mechanisms such as price signals, automatic setback thermostats, and communication with advanced metering infrastructure are also explored and modeled.

The primary analysis platform for modeling the supply of renewable energy and building demand is the Holistic Grid Resource Integration and Deployment tool or HiGRID. The code is written in Matlab. The goal of the HiGRID tool is to assess the challenges associated with integrating renewable resources into communities of different scales – campuses, cities, and states. On an hourly timescale, the renewable energy generation model includes geothermal, large wind farms, rooftop PV, 1 and 2 axis tracking PV, concentrating solar thermal power, and small-hydro. The HiGRID tool utilizes hourly end-use load profiles derived from detailed temporal building energy models and has the ability to manipulate the profiles to model the aggregated, large-scale implementation of demand response and energy storage technologies in order to alter or shift the load shape to accommodate intermittencies in renewable energy generation. The platform thus provides an interface to explore the technical and economic limitations for demand response, energy storage, and integration of renewable resources.

Task 6.1.3. Project Deliverables

CTG Energetics (now The Cadmus Group) led the Building Design and Operation component of the RESCO research project. The final deliverables included in the RESCO tailored building design and operations criteria report include:

- Model: Temporal model of building load demand
- Model Test Plan: Building efficiency and passive building load tailoring
- Model Test Plan: Demand response and load management scenarios
- Analysis Result: Beneficial building design and operating criteria.

Task 6.1.4. Project Overview

The Cadmus Group calibrated and aggregated modeled building load profiles and has made significant progress in evaluating demand response strategies applicable to the UCI campus buildings. Six representative UCI campus buildings were modeled, four of which were calibrated to historical metered data. These building end-use load profiles have been normalized with respect to building area and combined with data gathered by the California Commercial End-Use Survey (CEUS) and the Database for Energy Efficient Resources (DEER) to build a campus-wide load profile by end use. The following buildings have been modeled:

Table 27: Modeled buildings used to develop UCI's campus-wide load profile.

Building	Building Class (Allocated)	Data Source
Natural Sciences II	Lab, Office, Study	ION, Itron
Multipurpose Science and	Classroom, Lab,	MelRok, ION,

Building	Building Class (Allocated)	Data Source
Technology Building	Office, Study	Itron
High Rise Engineering Tower	Classroom, Lab, Office, Study	ION
Humanities Instructional Building	Classroom, Office, Study	ION
Verano Apartments	Residential	No metered data available
Middle Earth (Valimar)	Residential	No metered data available
Restaurant	General Use	CEUS
Health	Healthcare	CEUS
Unrefrigerated Warehouse	Support	CEUS
College	General Use, Special Use, Support	CEUS
Assembly	General Use, Special Use	DEER
Conditioned Storage	Support	DEER
Primary Education	General Use	DEER

The end-use profiles generated from the models specified above were allocated by square footage to the major building types documented for the UCI campus in order to establish a campus-wide load profile for use in the analysis of building operation response to intermittent energy generation by renewable resources.

Throughout the research, peak energy reduction strategies were identified as either static energy efficiency measures or dynamic demand response strategies. Depending on the results derived from integrating these load profiles with the HiGRID tool, it could be necessary to re-define the particulars of energy efficiency and demand response measures within the context of volatile grid energy supply with high renewable penetration.

Energy efficiency measures were integrated into the HiGRID model by utilizing the industry experience of The Cadmus Group from recent energy efficiency projects to project theoretical future scenarios in which energy efficiency is optimized amongst interior lighting, exterior lighting, and HVAC systems. The respective reduction in the overall load profile was characterized qualitatively before integration into the HiGRID model. Cost analysis for these energy efficiency measures was also incorporated to assist in determining optimal energy solutions for integrating high penetrations of renewable energy resources.

Demand response techniques have been studied and documented in a large body of literature. Based upon published and modeled results, the viability of five different strategies has been initially assessed. The eQUEST modeling engine provided good strong results for lighting reductions, but is limited in its capability for modeling HVAC demand response strategies including pre-cooling, night purge, and fan turn-down. Based upon night purge power consumption results obtained through available literature and building model responses, the night purge demand response strategy has been dismissed. Empirical fan turn-down and pre-cooling tests have been conducted at the MSTB and NatSciII buildings at UCI in order to experimentally characterize the effectiveness of each measure.

Task 6.1.5. Conclusions

- UCI and generic community data was collected to develop end-use profiles from a variety of sources including:
    - ION: building data
    - ITRON: building data
    - MelRok: sub-metered building data for MSTB
    - DEER: Database of energy efficient technologies and measures containing performance, costs, and lifetime estimates
    - CEUS: Commercial end-use profiles for the state of California

Task 6.2. Temporal Models for Building Load Demand

Building models have been developed for six buildings on the UCI campus in order to simulate their end-use load profiles and allocate these results to relevant building areas in extrapolating a campus-wide load profile. The Quick Energy Simulation Tool (eQUEST), based on the DOE-2.2 simulation engine, has been chosen to create these models for its ease of calibration and relevant end-use outputs. Commercial building end-use load profiles were generated from data collected by the California Commercial End-Use Survey (CEUS) and the CEC Database for Energy Efficient Resources (DEER) to represent the building types that have not been modeled in eQUEST. Following their completion, the building models will be run with a customized 2005 weather file from the Santa Ana (John Wayne) Airport weather station.

Task 6.2.1. The Quick Energy Simulation Tool (eQUEST)

The Quick Energy Simulation Tool "eQUEST" v3.64 was released in August, 2010 with enhancements to the program and the DOE-2.2 simulation engine. It is designed to provide a simple comprehensive energy simulation tool capable both of smart defaults and detailed

modifications, including hourly schedules for lighting, heating, cooling, ventilation and load control. Its inputs allow the model to be accurately calibrated to metered data and its outputs include the end-use profiles relevant to the HiGRID code manipulation.

6.2.1.1. eQUEST Model Inputs

eQUEST allows the user to match almost every single modeled building characteristic to the actual building. Because the on-campus buildings are all connected to a central plant for chilled water, the loop is monitored for heat energy transferred at each building site. All usage schedules can be adjusted on an annual, weekly, or hourly basis. The relevant input categories are summarized below:

- Building Shell and Internal Loads
    - Geometry
    - Occupancy
    - Lighting
    - Daylighting
    - Equipment
    - Internal Energy Sources
    - Infiltration
    - Thermal Mass
- Water-side HVAC
    - Chilled Water Loop / Meter
    - Hot Water Loop / Meter
    - Domestic Hot Water Loop / Meter
- Air-side HVAC
    - Thermostat Control
    - Air Flow
    - Outside Air and Exhaust
    - Heating and Cooling Systems and Specifications
    - Layout of Air Handling Units

6.2.1.2. eQUEST Model End-Use Outputs

Within eQUEST, the user chooses specifically which end-use loads to output and extracts those outputs to an excel file. These files are accumulated, processed and incorporated into the HiGRID tool. Below are the outputs chosen to be included in the HiGRID code analysis:

- Lighting end-use energy
- Task lighting end-use energy
- Miscellaneous end-use energy (plug loads, equipment, etc.)
- Heat rejection end-use energy
- Auxiliary end-use energy
- Vent fan end-use energy
- Exterior total end-use energy (exterior lighting, elevators, etc.)
- Total end-use energy
- Heating end-use energy (Btu)
- Cooling end-use energy (Btu)
- Domestic hot water end-use energy (Btu)

Task 6.2.2. Model Calibration

The NatSciII, MSTB, High Rise ET, and HIB buildings were metered using digital electric meters and recorded the total building power consumption at 15 minute intervals. MSTB was submetered and its data collected via a MelRok Energy Management System, providing end-use power consumption data for all major air handlers and auxiliary pumps as well as portions of lighting and plug loads. These data were averaged on hourly intervals and compared side-by-side to the total end-use energy calculated in eQUEST (the auxiliary and heat rejection end-use energies were removed from the modeled energy usage because these end-uses are found at the buildings since the campus uses a centralized district energy system). The eQUEST model was built to reflect all of the known building envelope and HVAC system specifications. The output data was then compared with the metered data at various intervals of time (days, weeks, months) to ensure that it achieved a high degree of accuracy during all periods of the year and particularly that it maintained a similar shape to the metered load.

The daily calibrations compared the difference between total modeled and metered energy usage to the lighting, miscellaneous, and vent fan power consumption on an hourly basis. The miscellaneous and lighting power schedules were changed directly when they appeared to significantly contribute to the disparity, while the vent fan control set points were modified to limit the minimum and maximum fan power consumption when it contributed to a disparity with observed operation. This process was repeated iteratively, and in the absence of detailed

end use metered data, was adjusted using a combination of known operational parameters, observed conditions, and intuitive assessment based on experience. Days during the summer that best represented the average power consumption and load shape were chosen for calibration.

The building load profiles were flatter than expected in many cases, indicating high baseline miscellaneous and lighting power consumption compared to eQUEST defaults. Given their use as science/engineering labs, the 24/7 operation schedule makes some sense considering possible student work schedules, but leaves some room for improving HVAC efficiency. The level of exterior lighting was approximated by visual observations of the fixtures at 7-10 kW for each building, further contributing to the nighttime power consumption.

6.2.2.1. Multipurpose Science and Technology Building

The following figures display the final results for the Multipurpose Science and Technology Building eQUEST model calibration using the metered data archived from the building's MelRok Energy Management System. In determining the individual end-use calibrations, the lighting and supply fan power meters were disaggregated based on individual submeter locations, and the remaining unaccounted load was distributed accordingly to approximate and account for all non-metered loads.

Figure 164: Total metered and modeled data calibration for MSTB during July, 2011

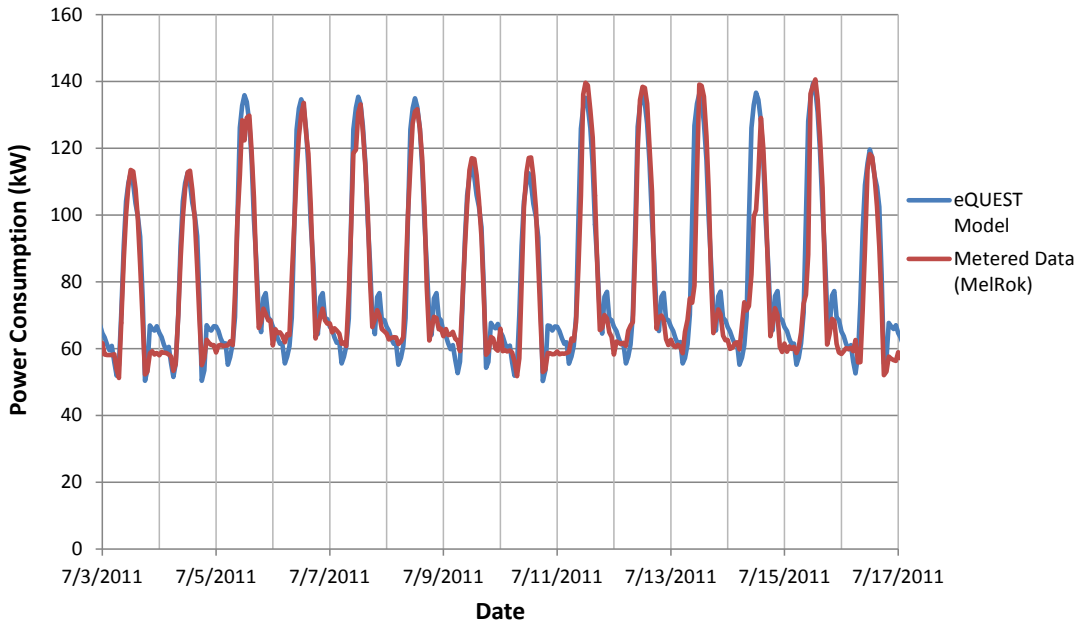

Figure 165: Metered and modeled end-use power for MSTB on May 2nd, 2011 – a weekday

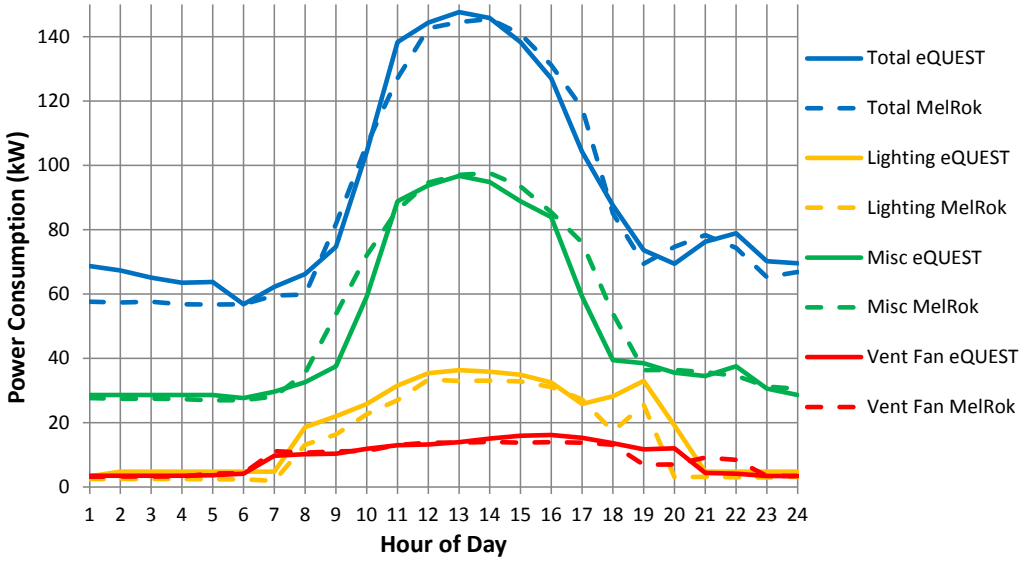

6.2.2.2. Natural Sciences II

The following figures display the final results for the Natural Sciences II eQUEST model calibration using the metered data archived from the building's ION Energy Management System. In determining the individual end-use calibrations, the fan power was calculated based on the known operational equipment and schedule, while the lighting and miscellaneous power consumptions were directly modified to reflect the metered data.

Figure 166: Total metered and modeled data calibration for the Natural Sciences II building during July, 2009

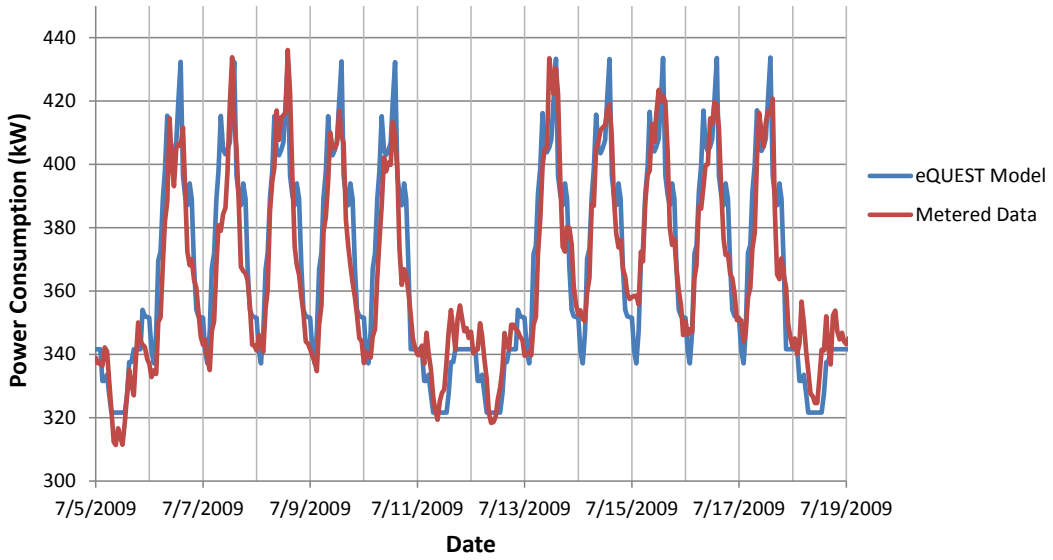

Figure 167: Metered and modeled end-use power for the Natural Sciences II building on August 10th, 2009 – a weekday

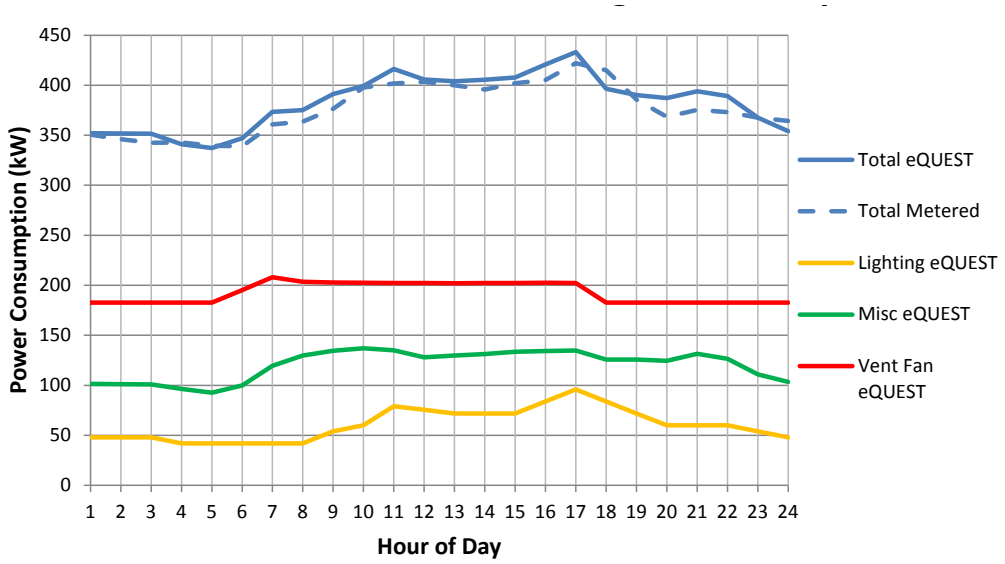

6.2.2.3. High Rise Engineering Tower

The following figures display the final results for the High Rise Engineering Tower eQUEST model calibration using the metered data archived from the building's ION Energy Management System. In determining the individual end-use calibrations, the fan power was

calculated based on the known operational schedule, while the lighting and miscellaneous power consumptions were directly modified to reflect the metered data.

Figure 168: Total metered and modeled data calibration for the High Rise Engineering Tower during June, 2009

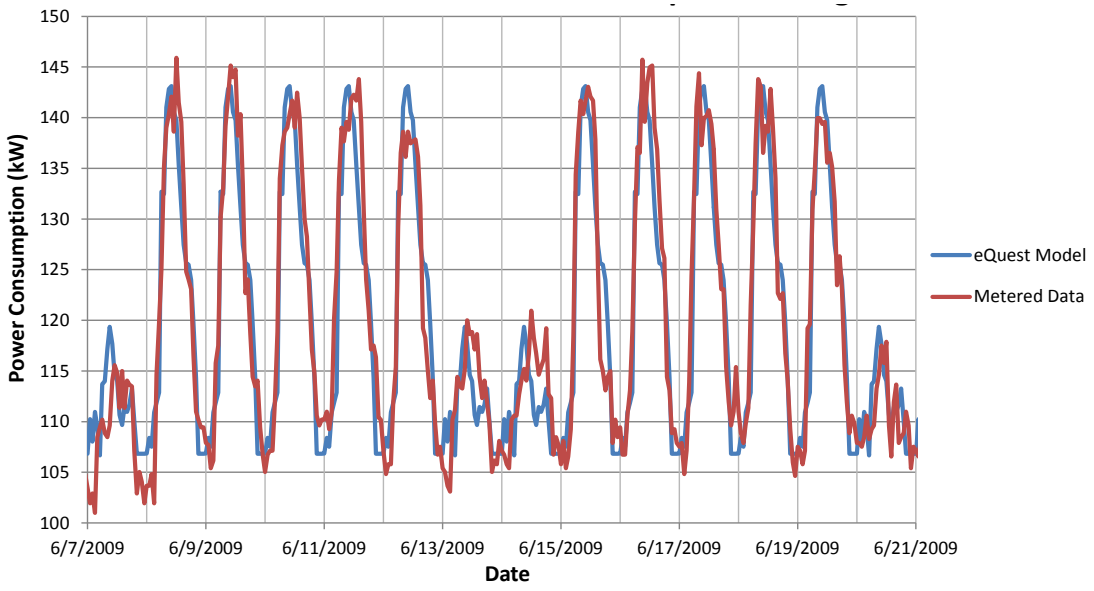

Figure 169: Metered and modeled end-use power for the High Rise Engineering Tower on August 10th, 2009– a weekday

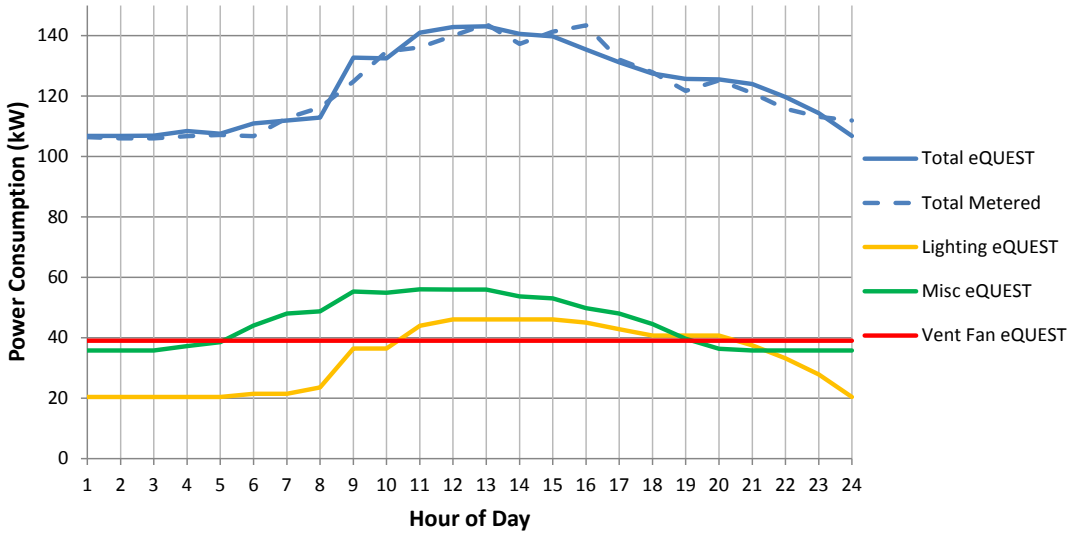

6.2.2.4. Humanities Instructional Building

The following figures display the final results for the Humanities Instructional Building (HIB) eQUEST model calibration using the metered data archived from the building's ION Energy Management System. In determining the individual end-use calibrations, the fan power was calculated based on the known operational schedule, while the lighting and miscellaneous power consumptions were directly modified to reflect the metered data.

Figure 170: Total metered and modeled data calibration for HIB during January, 2009

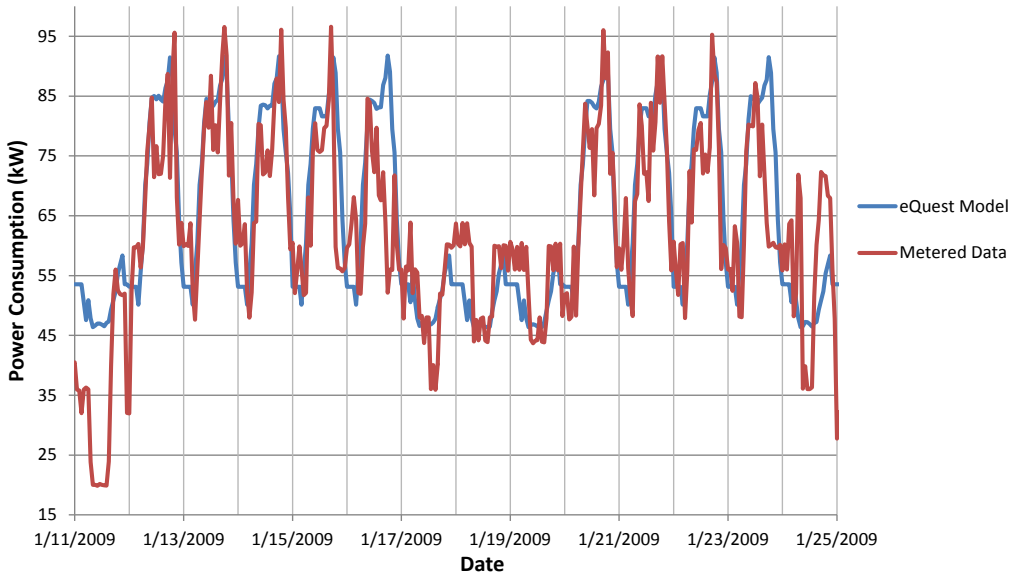

Figure 171: Metered and modeled end-use power for HIB on January 13th, 2009– a weekday

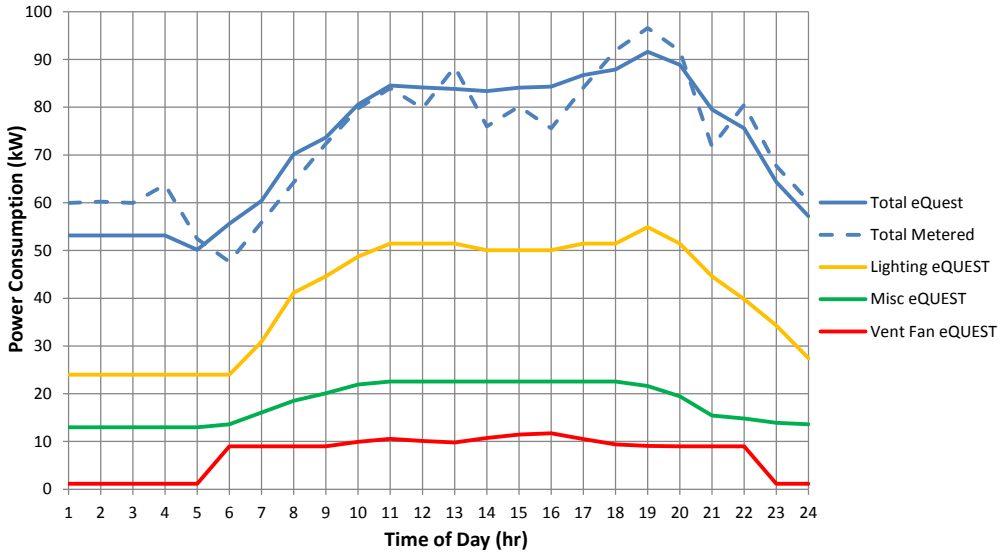

6.2.2.5. Middle Earth Dormitories – Valimar

The following figures display the final modeled eQUEST results for the Valimar dormitories. The eQUEST model was built to reflect all of the known building envelope and HVAC system specifications. The fan power was estimated based on a 24/7 operational schedule, while standard occupancy, lighting, and plug load schedules were derived from multi-family residential research by DOE's Building America (Hendron, 2004), along with reasonable assumptions regarding dorm life.

Figure 172: Total modeled power for Valimar dormitory in Middle Earth in September, 2005, using the final weather file

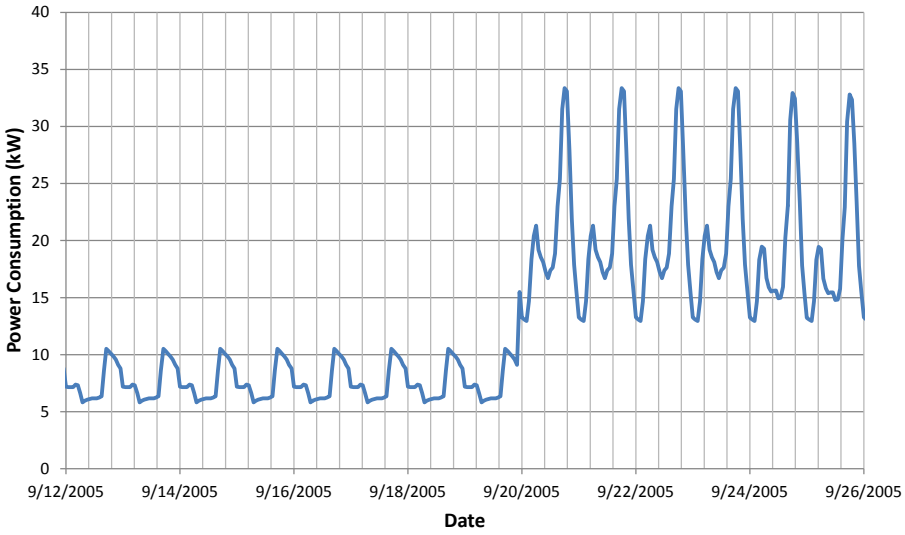

Figure 173: Modeled end-use power for Middle Earth Valimar on June 12th, 2009– a weekday.

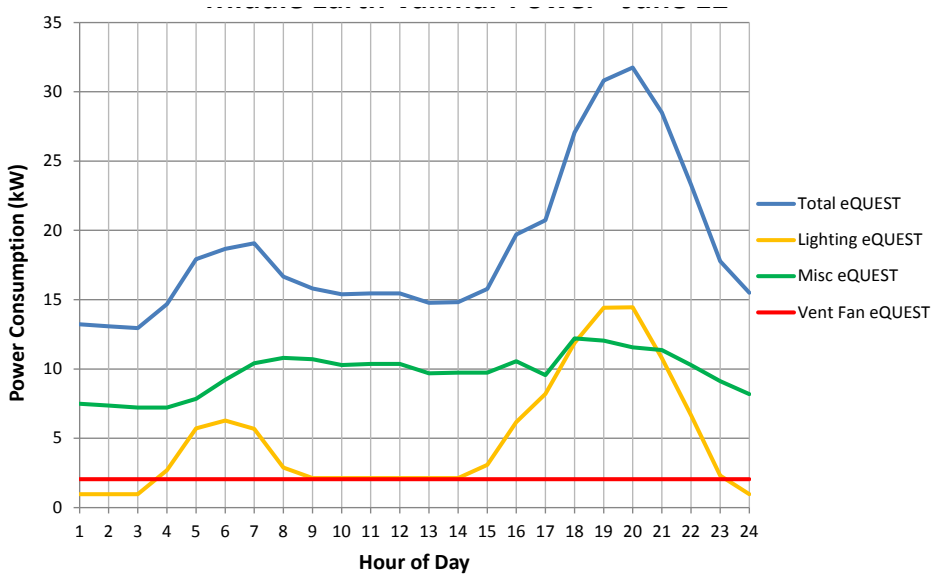

6.2.2.6. Apartment Building – Verano 2100

The following figures display the final modeled eQUEST results for the Verano apartments. The eQUEST model was built to reflect all of the known building envelope and HVAC system specifications. The fans were modeled to run for heating-only, while standard occupancy, lighting, plug load, and domestic hot water schedules were derived from multi-family residential research by DOE's Building America (Hendron, 2004) and Ecotope (Heller, 2009).

Figure 174: Total modeled power for the Verano 2100 apartment building in September, 2005, using the final weather file.

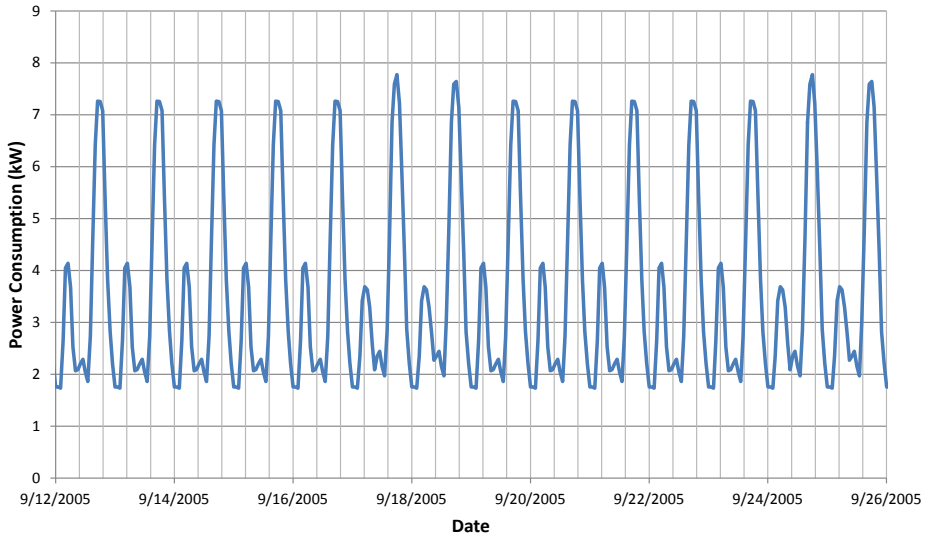

Figure 175: Modeled end-use power for Verano 2100 on March 3rd, 2005– a weekday with heating.

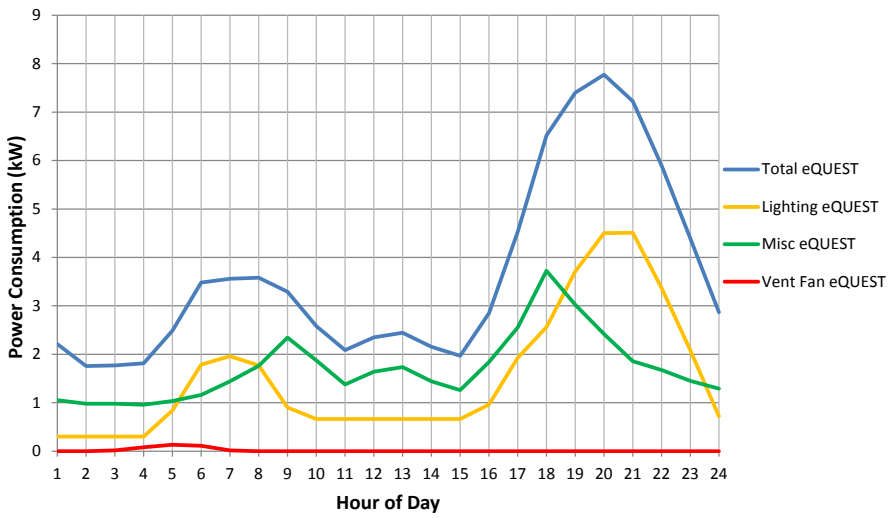

Task 6.2.3. CEUS and DEER Standard Building Models

The California Commercial End-Use Survey and the Database for Energy Efficient Resources were used as data sources for the generic end-use profiles that could not easily be approximated using the detailed and calibrated eQUEST models described above. The results of these analyses were allocated to building space as noted in Table 27 to construct the overall campus energy end use profile.

6.2.3.1. California Commercial End-Use Survey

The California Commercial End-Use Survey is a comprehensive study of commercial sector energy use, primarily designed to support the state's energy demand forecasting activities. Data were gathered from a random sample of 2,790 commercial facilities and were stratified by utility service area, climate region, building type, and energy consumption level. One of many useful outcomes from this survey was the characterization of end-use load profiles for a variety of commercial buildings in each climate zone, including those used to help construct the UCI baseline:

- Restaurant
- Unrefrigerated Warehouse
- College
- Health

The end-use profiles for the buildings above were mapped to the General Use, Special Use, Support, and Healthcare building classes used in the campus-wide building characterization.

6.2.3.2. Database for Energy Efficient Resources

The Database for Energy Efficient Resources was built to accumulate information on selected energy-efficient technologies and measures. In order to provide estimates of the energy-savings potential for these technologies in numerous applications, DEER applies these measures to a set of 23 commercial prototype building models. In order to fill in the end-use profiles for these particular building types, the following prototype models were used:

- Primary Education
- Assembly
- Unconditioned Storage

The end-use profiles generated from these models were mapped to the General Use, Special Use, and Support building classes specified in the campus-wide building characterization.

Task 6.2.4. Extrapolating a Campus-Wide Load Profile by End-Use

The UCI campus was entirely characterized by allocating all of the building square footage on campus to one of ten distinct building classes. The square footage in each of the six modeled buildings was also allocated to a building class. The percentage of normalized end-use building data allocated to each class was determined proportionally to the allocated area in each building divided by the total modeled, allocated area for each class. The residential allocations were determined by the known proportion of residential square footage that was dormitories and apartments for Valimar and Verano respectively, taking into account that some residences are not accounted for on the main campus meter. The mapping chart below illustrates the allocation of normalized end-use data to each building class.

Figure 176: Mapping chart illustrating the allocation of the modeled normalized end-use profiles to each building class

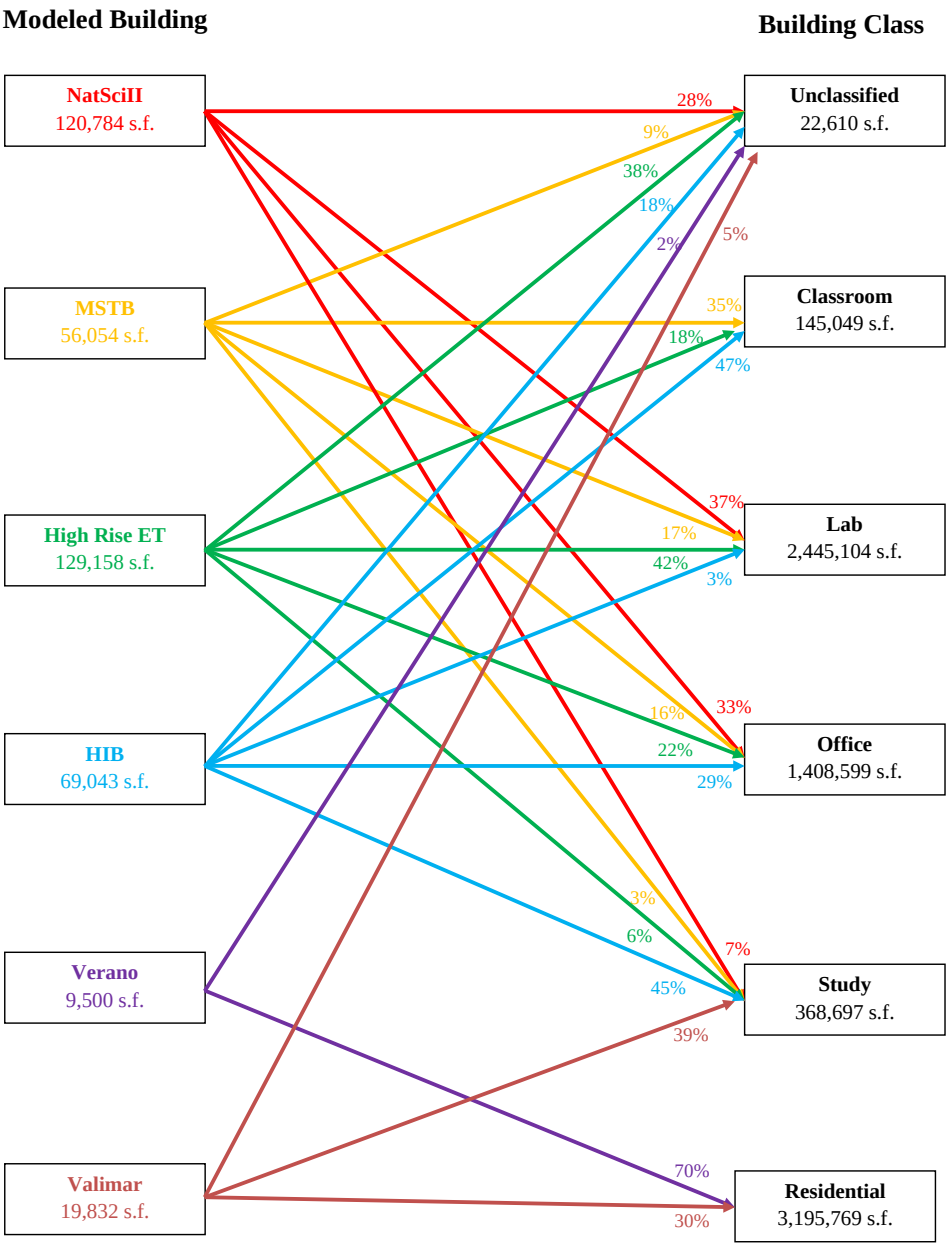

The Special Use, General Use, Support, and Healthcare categories did not match any modeled space, so the CEUS and DEER prototype models representing a known percentage of each class were allocated proportionally to these classes. The following mapping illustrates the allocation of normalized end-use data to each building class.

Figure 177: Mapping chart illustrating the allocation of the prototype normalized end-use profiles to each building class

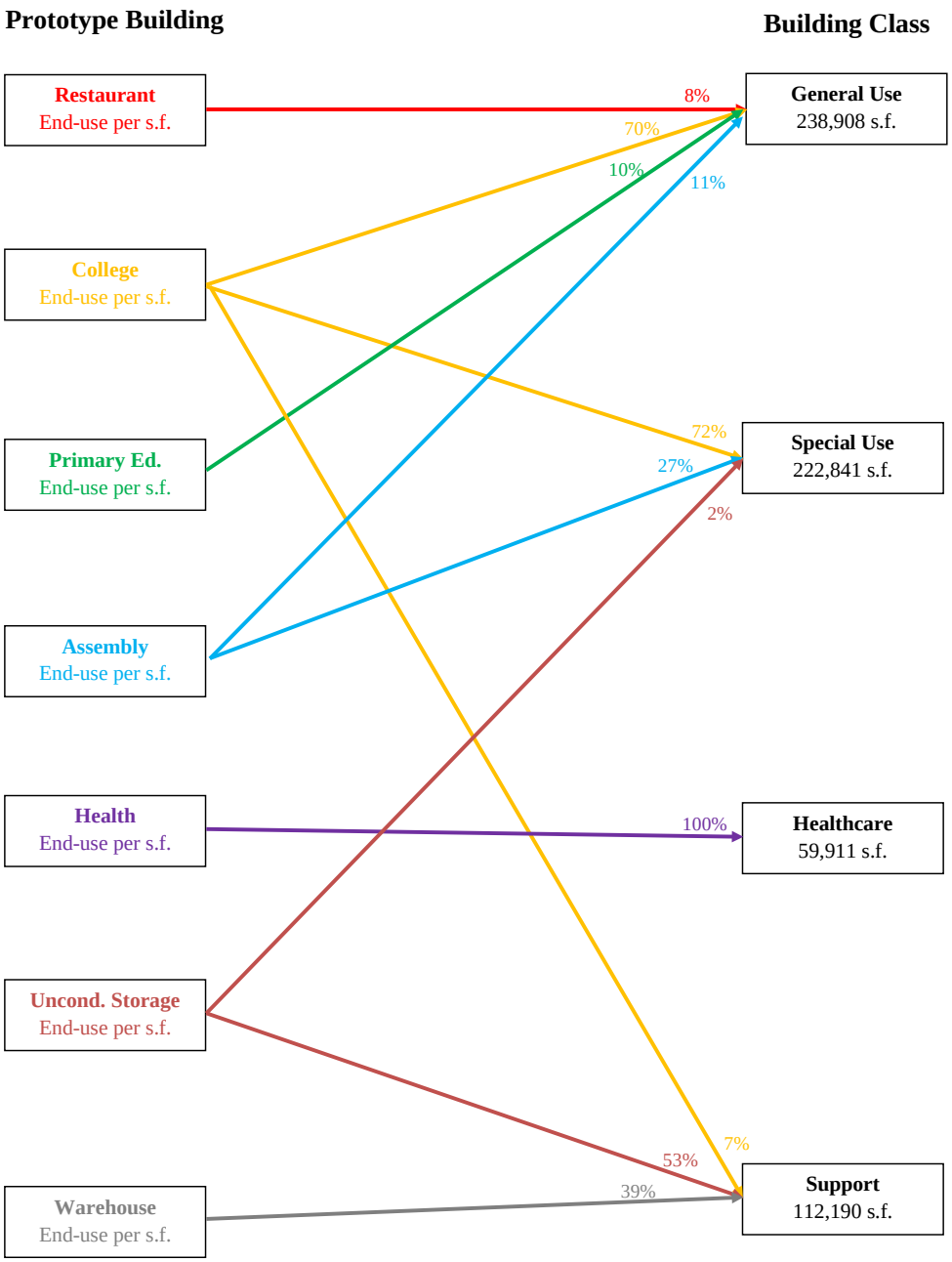

Each of the modeled building end-use profiles have been normalized by square footage. Based upon the building allocations specified above, the normalized end-use loads have been multiplied by their allocated fraction and summed to complete the load profile for each of the

ten specified building classes. The normalized building class load profile was then multiplied by its total square footage to provide the total campus-wide load profile for each building class.

The figure below shows the extrapolated campus power consumption results including lighting, miscellaneous, and vent fan end-uses. These results are an aggregation of each of the ten building class load profiles, allocated to modeled buildings proportional to used space.

Figure 178: One week of modeled, extrapolated hourly energy consumption for UCI campus in May

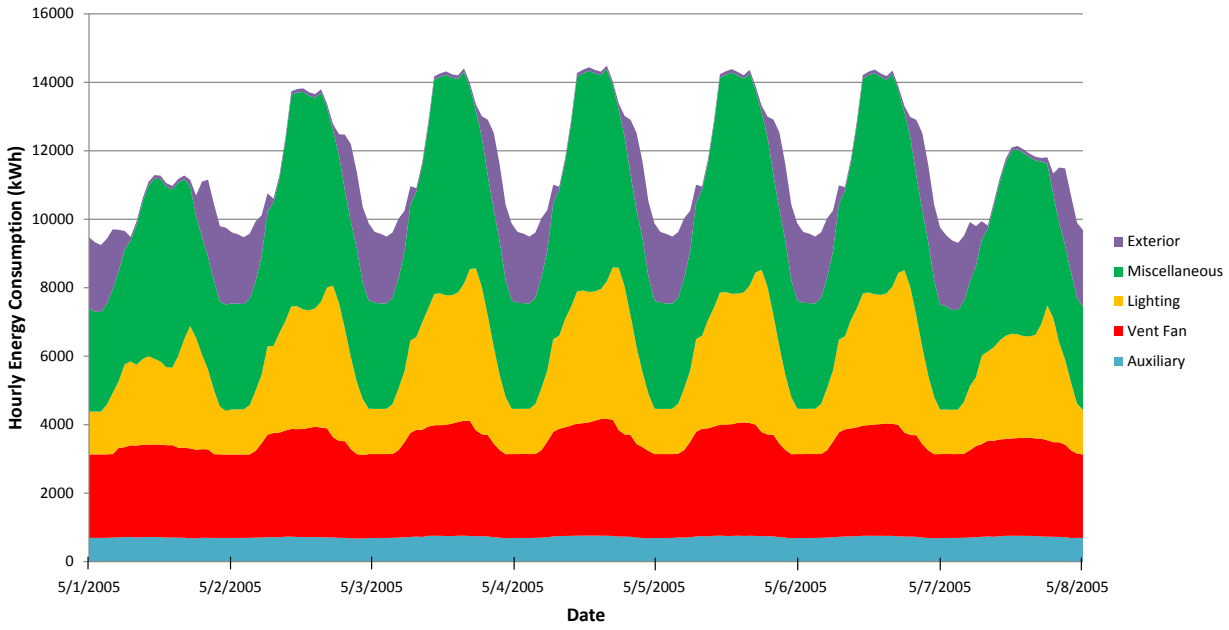

The load shape results from a combination of educational, residential, and commercial usage schedules. The peak power consumption of the extrapolated data is slightly lower than the expected 15-25 MW peak demand for the UCI campus. However, the lighting and vent fan power consumption shown above is a conservative estimate for the amount of controllable loads on campus and should suffice for the quantification of dispatchable loads.

Figure 179: The hourly energy consumption and chilled water load for the UCI campus during 2005's peak temperature day of September 29th

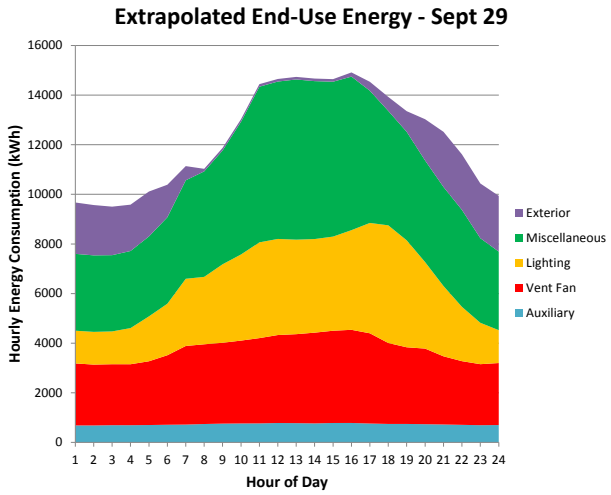

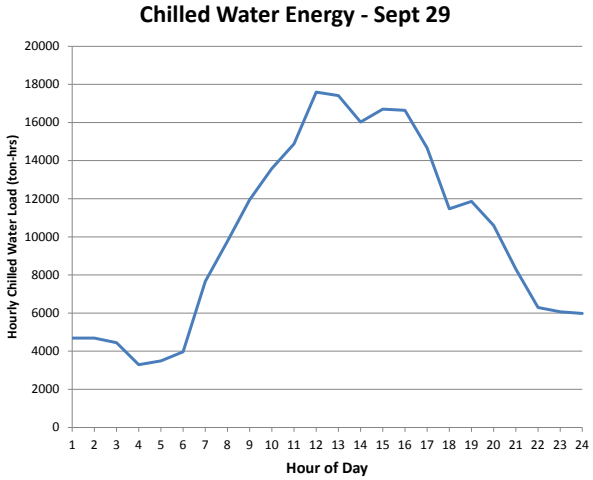

Above, the hourly end-use profile and chilled water energy consumption is shown for the hottest day in 2005, to demonstrate the load incurred on the campus and central plant during peak load conditions. The data for chilled water use helps quantify the magnitude of thermal loads, but does not accurately reflect the time during which the load is incurred, because the campus thermal energy system will not respond within the same timeframe as the modeled individual water chillers. Below, the total chilled water usage is shown by month.

Figure 180: The modeled, extrapolated total chilled water usage of the UCI campus in 2009

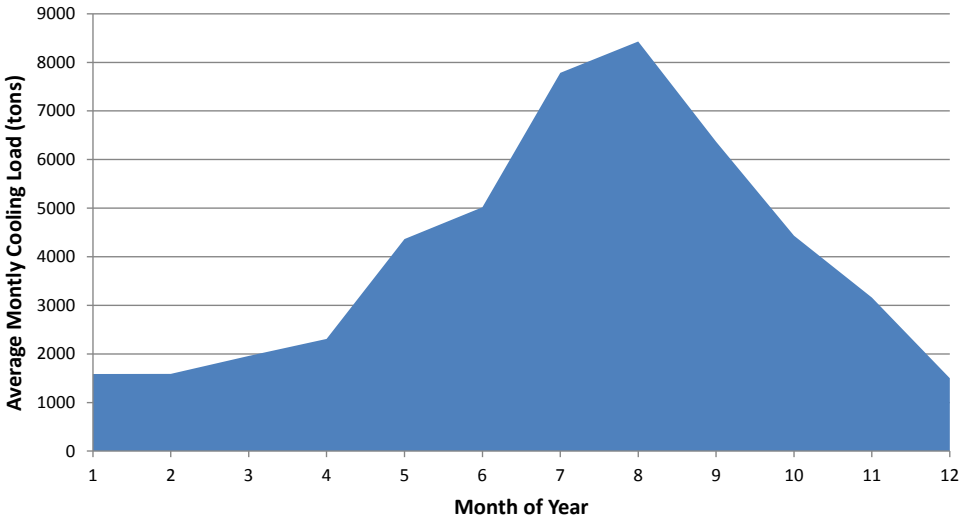

The distributions of annual energy consumption by end-use and building class are shown in the figure below. The end-use distributions of the extrapolated data are reasonable given typical building energy performance in southern California and the detailed metered outputs of MSTB.

Figure 181: Distribution of total end-use energy consumption at UCI using the extrapolated building model results

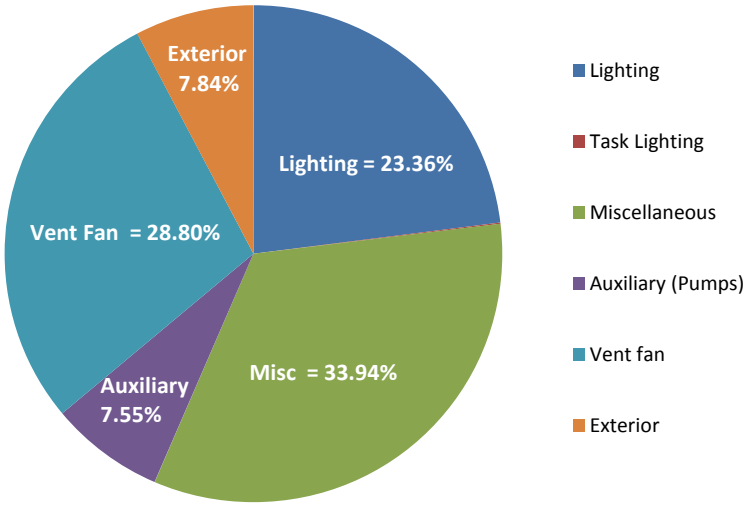

The magnitude of controllable building loads, however, does not include the entirety of the modeled vent fan and lighting power consumption. HVAC demand response measures are not applicable in laboratories and hospitals due to stringent ventilation requirements and are not easily executable with residential air handling units. Lighting demand response may be applicable to all buildings, but this strategy requires centralized lighting control which, realistically, will not be achievable for 100% of on-campus buildings.

Figure 182: Distribution of total annual energy consumption at UCI by building class. Laboratory use composes the greatest energy consumption component

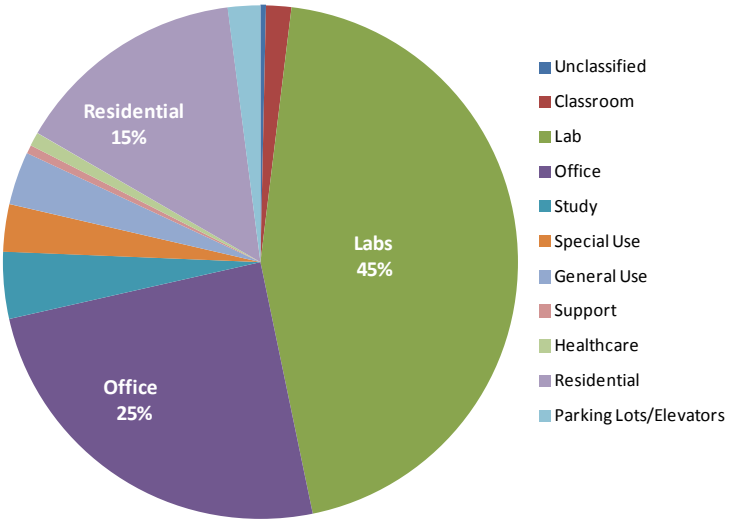

Therefore, assuming 100% penetration of the DR measures throughout the campus, the maximum dispatchable load is composed of all lighting end-use power and the vent fan end-use power excluding the laboratory, residential, and healthcare building classes. This dispatchable load is compared to the total modeled power consumption in the figure below.

Figure 183: Total controllable loads which may be dispatched for demand response, composing approximately 1/3 of UCI's total modeled power consumption

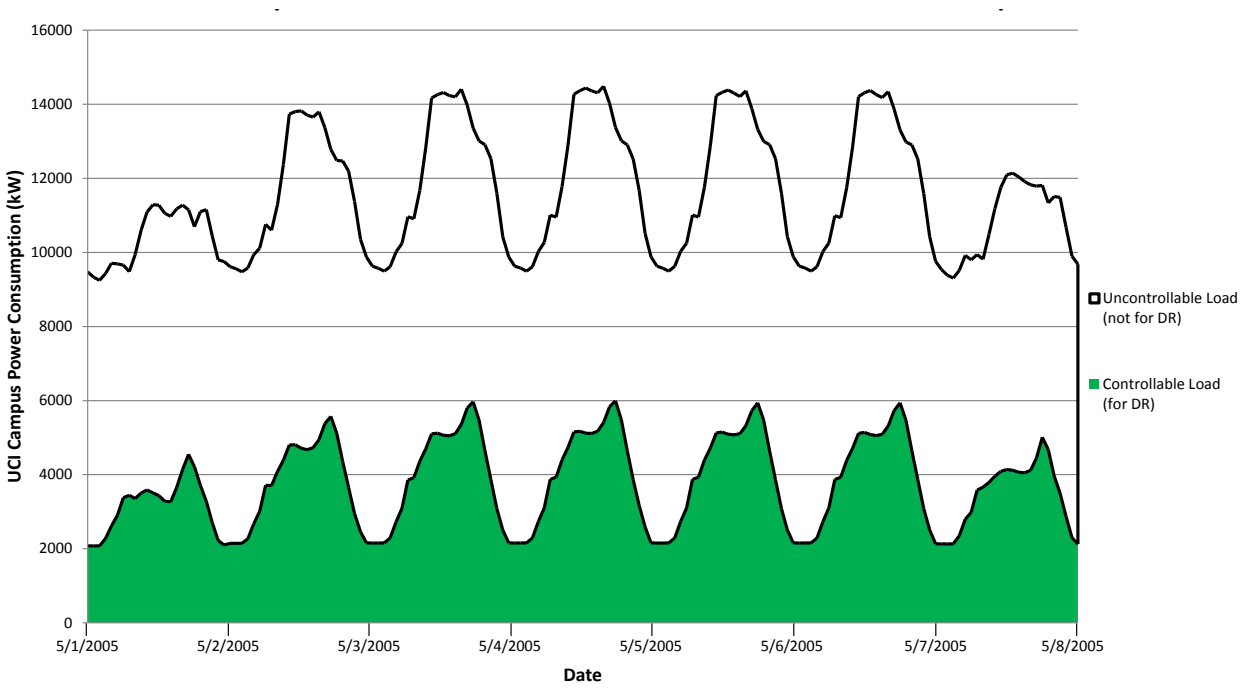

Task 6.2.5. Integrating Model with HiGRID Code

The total end-use load profiles for each building class were put in database matrices for manipulation within the HiGRID code. Fundamental alterations may be made to the building load profile through energy efficiency measures which will apply to the lighting and vent fan end-uses for certain building classes on a daily basis. Strategic changes to the daily load profile may be developed to accommodate high levels of renewable penetration.

When the HiGRID code detects the need for a demand response event, temporary energy reduction measures will modify lighting and vent fan end-uses for particular levels of penetration into each building class. The load reductions will be characterized for each strategy at multiple levels of required load shedding and may include combinations of multiple demand response measures.

The fiscal value of this demand response power reduction gained by the energy provider may be quantified by the average cost of providing this additional power to meet the baseline building demand through renewable resources. This value can provide an upper bound for the amount of money that participants in the demand response program might be compensated. By demonstrating the value of large-scale implementation of automated demand response, a major goal of the research is to motivate building operators and utilities alike to progress toward smarter power utilization strategies.

Task 6.2.6. Conclusions

- Building data was input into eQUEST to develop end-use profiles.
- Nearly one third of UCI's total modeled power consumption is considered controllable and can be dispatched using demand response.

Task 6.2.7. References

Heller, et al. Multifamily Billing Analysis: New Mid-Rise Buildings in Seattle. Ecotope Consulting Research and Design. December 2009.

Hendron, et al. Building America Performance Analysis Procedures. Revision 1. Building America. U.S. Department of Energy. National Renewable Energy Laboratory. June 2004.

Task 6.3. Tailoring Building Load Profile through Passive Building Energy Efficiency Measures

As renewable power generation becomes more prevalent and exerts greater influence over the profile of the total grid power supply, building demand profiles may also change significantly due to the application of energy efficiency measures. As an industry, energy efficiency in buildings is progressing at a rapid rate due to improvements in low-wattage lighting technology and controls, advanced HVAC system controls, and many other efficient technologies resulting from better understanding of energy end-uses and application of

advanced digital controls. Therefore, in consideration of future energy supply/demand scenarios within the HiGRID model, the building load profiles must also be evaluated assuming some optimization of the previously modeled end-uses through energy efficiency measures.

A number of energy efficiency measures have been evaluated by modifying the eQUEST building models used to characterize the end-use profiles for the actual buildings on the UCI campus (MSTB, NatSciII, HIB, High Rise ET, Valimar, Verano):

1. Replace installed interior lighting systems with technologies capable of 0.50 W/s.f.
40. Integrate photocell controls to all perimeter zones capable of reducing lighting output in response to daylight.
41. Replace installed exterior lighting systems with technologies capable of providing equal lighting output at 50% power consumption.
42. Perform air balance and optimize supply and return fan duct static pressure set points.
43. Implement a discharge air temperature reset strategy between 55 °F and 65 °F based on building load, utilizing airside economization.

The standard CEUS and DEER building models were not modified as part of the energy efficiency analysis. Due to the lack of knowledge and lack of controllability associated with the *General Use, Special Use, Healthcare,* and *Support* building classes, the application of energy efficiency measures was assumed to be infeasible. For the *Classroom, Lab, Office, Study,* and *Residential* building classes, however, energy efficiency cases were analyzed assuming the application of the aforementioned measures to all of the associated on-campus square footage.

Because the application of different energy efficiency measures will affect the building demand profile in different ways, changes to interior lighting, exterior lighting, and HVAC energy end-uses have been evaluated separately – to characterize the value of these strategies, independently and together – to generically characterize the value of energy efficiency under theoretical future scenarios. The following subsections describe these measures in detail and illustrate their associated reductions in demand.

Task 6.3.1. Interior Lighting

Significant opportunities for energy efficiency in interior lighting systems are currently on the market and are becoming more cost effective over time due to optimization of manufacturing for light-emitting diode (LED) technologies and advanced digital lighting controls. Many high performance buildings are capable of achieving lighting power densities below 0.5 W/s.f. with these technologies, which is considered to be on the leading edge of energy efficiency. Therefore, this benchmark value was chosen to be the basis for the adjustment to total lighting power. The ratio of the energy-efficient LPD (0.5 W/s.f.) to the initially modeled LPD was used as a scaling factor applied to the lighting system wattage modeled by eQUEST in the energy efficiency (EE) case.

Occupancy controls are becoming widely prevalent, yet the analysis of the energy efficiency case for interior lighting systems assumes that occupancy controls were already integrated throughout these buildings to drive the standard lighting end-use profiles. Photocell-based daylight controls which are capable of continuous dimming or light switching are also becoming prevalent, and have not been integrated in most of UCI's buildings. Therefore, automatic photocell controls were implemented to all perimeter zones in the UCI eQUEST models to quantify additional energy savings achievable through the application of energy efficiency measures.

Figure 184: Average daily power consumption – baseline and with interior lighting efficiency measures.

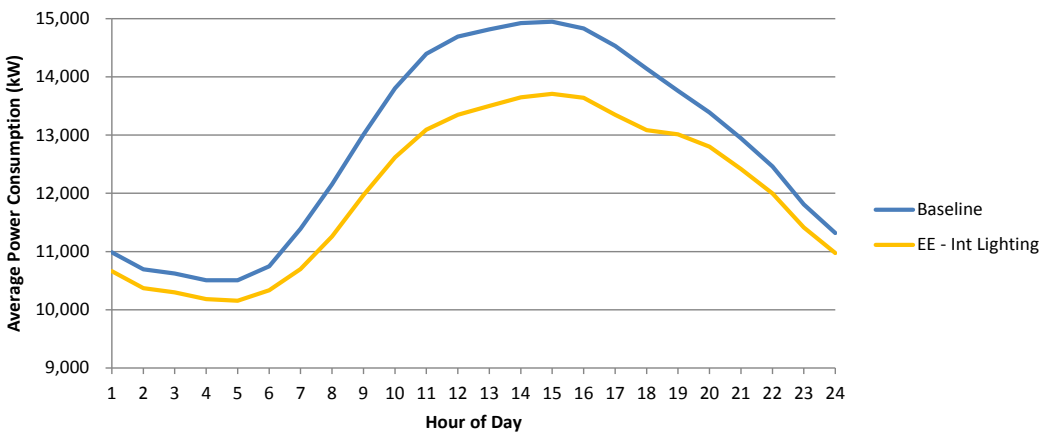

The figure above demonstrates the reduction in lighting power on average due to energy efficiency measures for interior lighting systems. Specifically, this figure reflects data extrapolated from the revised eQUEST models with absolute lighting power densities of 0.5 W/s.f. and daylight controls in all perimeter zones. As can clearly be inferred from this figure, internal lighting energy efficiency measures reduce significantly more power during the normal operating day between 8:00 a.m. and 8:00 p.m. The overall effect of internal lighting efficiency measures is therefore to *flatten* the average daily demand profile. Peak demands are significantly lower, but the base load is only marginally reduced through interior lighting efficiency measures.

Task 6.3.2. Exterior Lighting

Opportunities for energy efficiency in exterior lighting systems are also progressing rapidly, with low-wattage metal halide technologies being integrated to existing fixtures and LED options becoming more and more cost effective as the technology develops within the marketplace. Depending on the power requirements of existing systems, it is estimated that approximately 50% of exterior lighting power can be reduced by installing LED technologies capable of producing equivalent lighting outputs. Therefore, the net installed exterior lighting capacity (kW) was reduced by 50% for each UCI eQUEST building model. Parking lot light and

street light power models were also reduced by 50%, assuming that the LED replacements are implemented throughout the entire campus. The only exterior lights assumed to run during the day are the parking lot lights.

Figure 185: Average daily power consumption – baseline and with exterior lighting efficiency measures.

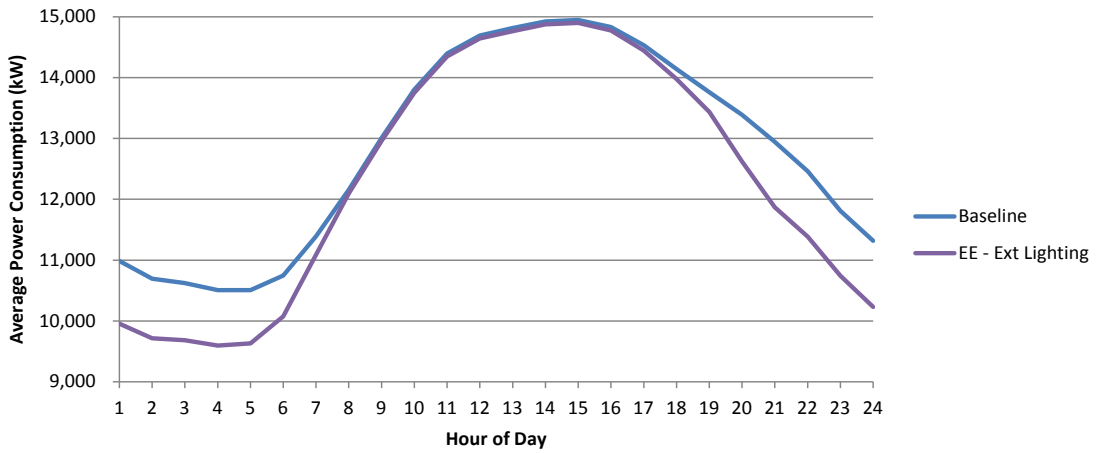

Exterior lighting functions primarily at night for campus visibility and security. Therefore, energy efficiency in exterior lighting systems applies almost entirely to the base load, whereas the peak demand remains relatively unaffected.

Task 6.3.3. HVAC Systems

The operational logic for heating, ventilation, and air conditioning systems can be optimized to reduce net power consumption. Many optimized control strategies for HVAC systems are being implemented across the high performance buildings industry as building automation system controls become more sophisticated.

At the simplest level, operating schedules can be tailored to building usage such that the HVAC system operation is aligned with building occupancy. Currently, an effort is underway to align HVAC equipment schedules to actual occupancies at UCI; this effort is expected to reduce annual energy use on campus by nearly 12 million kWh. The energy efficiency analysis model assumes that all such changes have been applied.

Duct static pressure set point controls determine operating fan speeds producing a significant impact on fan power consumption. Supply fan duct static pressure set points can be optimized with respect to building air balance and ventilation requirements to minimize this fan power. The duct static pressure set points for the air handling systems in all UCI eQUEST building models are based on reasonable assumptions for airflow reductions in each building. The modeled duct static pressure set points were determined based on typical baseline industry controls with respect to typical optimized (high performance) industry control set points.

- All buildings with lab space were modeled with duct static pressure set points of 2.5″ w.c. rather than 3.5″ of w.c.
- The Multipurpose Science & Technology Building was modeled with a duct static pressure set point of 0.5″ w.c. based on actual building demand response tests and airflow requirements.
- All other office/residential models implemented a duct static pressure set point of 1.5″ w.c.

Especially in the comfortable climate of Irvine, CA, supply (discharge) air temperature controls can be optimized to save significant power and energy. HVAC controls allow the supply air temperature set points to modulate in response to building load. By doing so, design air temperatures can be supplied at peak loads while higher temperatures can be supplied at partial loads to meet the space thermal requirements. Implementing a discharge air temperature reset will also significantly reduce zone reheat power consumption and enable greater utilization of airside economizer operation. Airside economizer controls can be applied to systematically reduce HVAC energy usage by optimizing outdoor air intake in response to the outside and return air temperature measurements. Discharge air temperature resets of 55 °F to 65 °F were implemented in each of the UCI eQUEST building models.

Figure 186: Average daily power consumption – baseline and with HVAC system efficiency measures

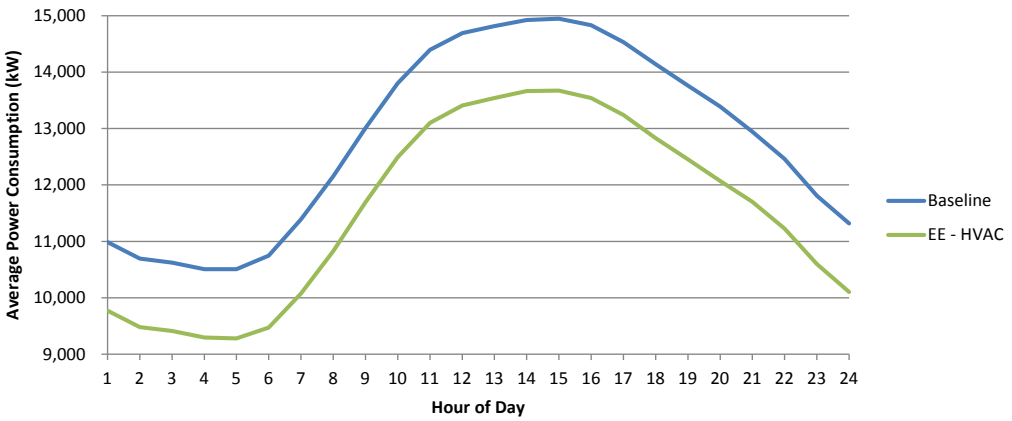

Throughout the UCI campus, HVAC power consumption and the associated auxiliary power is relatively flat. Therefore, energy efficiency in on-campus HVAC systems reduces the total load profile by an approximately constant amount, only slightly (~100 kW) greater in the daytime. The peak demand and the total base load are reduced through energy efficiency in HVAC systems.

Task 6.3.4. Energy Efficiency – Total Effect

With the implementation of all of the above-mentioned energy efficiency measures to full capacity, the effect on the total load profile on net is an approximately flat reduction in total building demand. However, the demand reduction profiles for the energy efficiency measures vary significantly by energy end-use. Energy efficiency in HVAC system controls enables a relatively flat reduction in demand, suitable for integration with almost any energy generation or storage system. Energy efficiency in exterior lighting systems will focus the demand reductions to nighttime (base load) power consumption, while energy efficiency in interior lighting systems will focus demand reductions to daytime (peak) power consumption. Therefore, energy efficiency policy focus towards internal versus external lighting may drive power reductions focused toward peak demand reductions or base load demand reductions respectively. Depending on the integration of renewable power systems and trends in research, technology, and market forces, one may be significantly better suited as a policy outcome.

Figure 187: Average daily power reductions due to interior lighting, exterior lighting, and HVAC energy efficiency measures

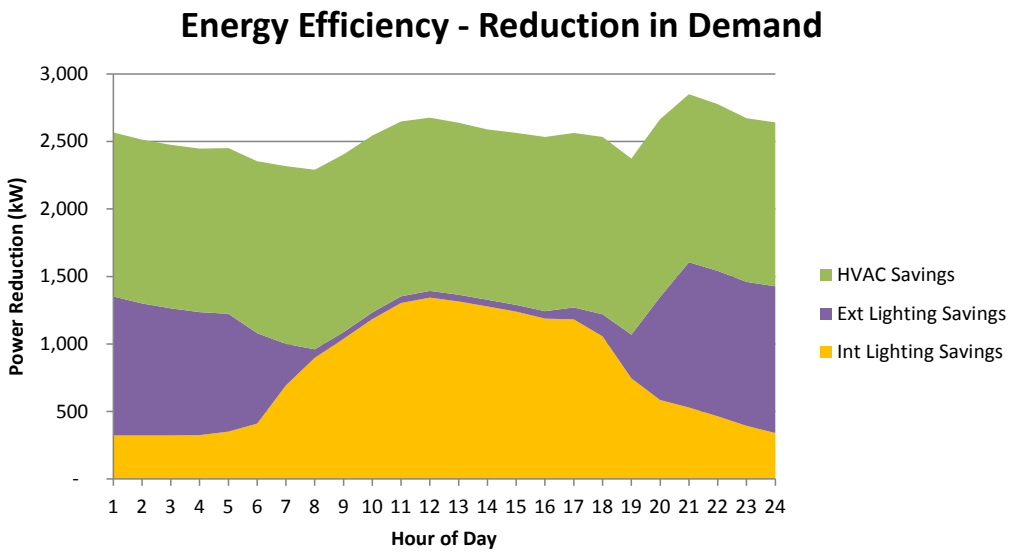

Figure 188: Average daily power consumption – all energy efficiency measures

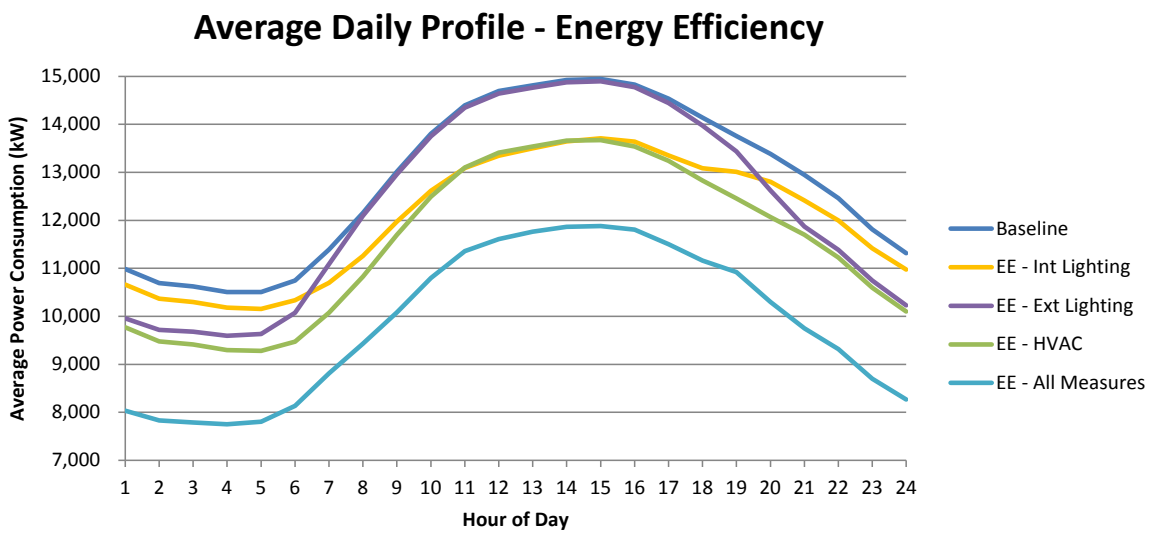

Task 6.3.5. Energy Efficiency – Cost Analysis

The following cost table describes the inputs and assumptions used to determine the cost of implementing each category of energy efficiency measures, broken out by cost component (Table 28). These inputs were normalized by the total demand reduction and used in the HiGRID model to determine the cost-effectiveness of the various solutions for integrating a higher penetration of renewable energy sources. Negative cost values represent savings due to reduction in the cost of maintenance.

Table 28: Energy Efficiency Cost Breakdown for each Technology

EE Measure	Cost Component	Cost	Justification
Interior Lighting	Installed Cost	$4.00/s.f.	Current LED costs (recent projects) & trajectory
	Fixed O&M Cost	-$50/fixture/yr	Savings due to fluorescent ballast/lamp maintenance
Exterior Lighting	Installed Cost	$1,000/fixture	Current LED costs; assumed avg. 200W/lamp baseline
	Fixed O&M Cost	-$43/fixture/yr	Savings due to incandescent ballast/lamp maintenance
HVAC	Programming Cost	$48,000 total	8 weeks of programming time at $120/hour
	Controls Eqt. Cost	$15,000 total	Fixed expenses for additional controls hardware
	Air Balance Cost	$0.40/s.f.	Current air balancing costs (recent projects)
	Fixed O&M Cost	$6,000/yr	One week of controls maintenance at $120/hour

Task 6.3.6. Other Opportunities for Energy Efficiency

In addition to lighting and HVAC energy efficiency measures, there are also some growing opportunities to reduce miscellaneous loads. For instance, a very large amount of power is consumed unnecessarily by plug standby loads. Based on state research, 13% of total residential electric demand is attributed to equipment standby load (Meier, 2008). Some plug loads are uncontrollable, such as computers, Ethernet hubs, phones, refrigerators, clocks, and battery chargers; they must remain on continuously in almost all cases. Many others can be controlled with occupancy sensors, such as task lighting, monitors, audio/video appliances, and portable fans/heaters. Some plug load control systems exist to turn off power to certain appliances when they are not needed; these systems are nascent in the market and still relatively expensive. Plug load controls should be evaluated in future research efforts as a mechanism for reducing the total base load.

Task 6.3.7. Energy Efficiency vs. Demand Response

Reductions in power consumption may be classified either as energy efficiency or demand response, both of which are addressed in this report and incorporated in the HiGRID model analysis. Energy efficiency refers to static, systematic control of building loads to reduce net building energy usage/costs, while demand response refers to dynamic load adjustments/alterations as a function of grid energy supply or pricing. When a power reduction measure can continuously minimize the building energy load without noticeably affecting the building operation and occupant comfort, there is no reason for which the measure should not be employed full time – which distinguishes it as an energy efficiency measure. When a power reduction measure eventually does affect the building operation and occupant comfort, it is distinguished as a measure of demand response and should therefore only be employed over shorter (1-5 hour) time periods to minimize or negate negative effects on occupant comfort.

There are inevitable trade-offs between load reduction efforts in energy efficiency and demand response. As systems are optimized to systematically consume less energy through energy efficiency measures, the capacity for those systems to make further reductions through efforts in demand response is significantly decreased. On a temporary basis, demand response measures may still be applied to optimized, energy-efficient systems, yet the depth to which their power can be reduced from the energy-efficient baseline is less than the depth of reducible power from the baseline of current operations. Therefore, the associated effect of optimizing energy efficiency is to decrease the net grid supply requirements yet also to decrease the controllability of these optimized systems through measures of demand response, accommodating lower fluctuations in the available grid supply.

Task 6.3.8. Conclusions

- Energy efficiency measures including interior lighting, exterior lighting and HVAC system balancing and optimization are explored for use on UCI's campus

- Average power reductions total around 2,500 kW.
    - HVAC savings are nearly a baseload reduction.
    - Exterior lighting savings are focused in the evenings.
    - Interior lighting savings are focused in the afternoons.
- There are trade-offs between EE and DR. As systems incorporate energy efficiency measures, the capacity for those systems to make further reductions through demand response are decreased.

Task 6.3.9. References

Meier, et al. Low-Power Mode Energy Consumption in California Homes. Lawrence Berkeley National Laboratory. Prepared for the CEC: PIER. 2008.

Task 6.4. Demand Response and Load Management

Due to the volatile nature of renewable power supply, dynamic response to high-demand events must be employed at the building level to most effectively utilize the available power. Under the scenario of automated demand response, it is critical to temporarily shed building load during high-demand events and to utilize excess energy generation during high-supply events to negate the effects on personal comfort due to the response. Many studies have been conducted to determine the validity of various demand response strategies, and many programs currently exist through public utilities to implement these strategies and compensate the participants.

Task 6.4.1. Existing Demand Response Programs and Compensation

Current demand response programs exist at various levels of demand reduction and consumer commitment in order to cost-effectively flatten the load imposed on the utility. Each program requires participants to use particular meters installed by the utility and, in most programs, manually adjust system controls to meet their pledged demand reduction. Compensation rates increase with the certainty by which demand will be shed, the amount of power shed during the event, and the quickness of response. The advantage to automated demand response is that buildings can instantaneously respond to events as they occur, and thereby provides additional value to customers and utilities. However, the only compensation currently offered for automated demand response is a technology incentive for the installation of automated demand response systems.

Table 29: Demand Response programs and compensation levels by utility

Program(s)	Monthly Compensation	Event Compensation	Technology Incentive

Program(s)	Monthly Compensation		Event Compensation	Technology Incentive
SCE Demand Response Programs				
Critical Peak Pricing CPP	N/A – Pay CPP electricity rates		Higher rates during CPP events	N/A
Base Interruptible Program BIP (below 2kV)	15 min, On-peak		$21.11/kW	$125/kW up to 50%
	15 min, Mid-peak		$6.45/kW	$125/kW up to 50%
	15 min, Winter Mid-peak		$1.32/kW	$125/kW up to 50%
	30 min, On-peak		$19.74/kW	$125/kW up to 50%
	30 min, Mid-peak		$6.02/kW	$125/kW up to 50%
	30 min, Winter Mid-peak		$1.22/KW	$125/kW up to 50%
Demand Bidding DBP	N/A – Voluntary		$0.50/kWh	N/A
Capacity Bidding Program CBP (day-of, 1-4pm)	May	$4.66/kW	Market energy price	$125/kW up to 50%
	June	$7.25/kW	Market energy price	$125/kW up to 50%
	July	$17.08/kW	Market energy price	$125/kW up to 50%
	August	$19.67/kW	Market energy price	$125/kW up to 50%
	September	$10.87/kW	Market energy price	$125/kW up to 50%
	October	$2.56/kW	Market energy price	$125/kW up to 50%
Real Time Pricing RTP	N/A – Pay RTP electricity rates		Higher rates during hi-temp RTP events	N/A
Auto-DR	Reduction in electric bills		$0	$300/kW up to 100%
Optional Binding Mandatory Curtailment	Customers exempt from rotating outages		15% of load available for reduction during every rotating outage	N/A
PG&E Demand Response Programs				
Peak Day Pricing PDP	N/A – Pay PDP electricity rates		Addtl. charges during peak hrs	N/A
Base Interruptible Program BIP	< 500 kW red.	$8.00/kW	$0	$125/kW up to 50%
	500-1000 kW red.	$8.50/kW	$0	$125/kW up to 50%
	> 1000 kW red.	$9.00/kW	$0	$125/kW up to 50%
Under Frequency Relay UFR	$0.67/kW total on-peak demand		Subject at all times to automatic service interruptions	N/A
PeakChoice (committed)	2-day notice	$4.00/kW	$0.15/kWh	$125/kW up to 50%
	1-day notice	$5.00/kW	$0.15/kWh	$125/kW up to 50%
	4.5 hr notice	$7.00/kW	$0.15/kWh	$125/kW up to 50%

Program(s)	Monthly Compensation		Event Compensation	Technology Incentive
	30 min notice	$10.00/kW	$0.15/kWh	$125/kW up to 50%
Capacity Bidding Program CBP (day-of, 1-4pm)	May	$2.85/kW	Market energy price	$125/kW up to 50%
	June	$6.47/kW	Market energy price	$125/kW up to 50%
	July	$19.41/kW	Market energy price	$125/kW up to 50%
	August	$24.43/kW	Market energy price	$125/kW up to 50%
	September	$14.30/kW	Market energy price	$125/kW up to 50%
	October	$6.33/kW	Market energy price	$125/kW up to 50%
Auto-DR	Reduction in electric bills		$0	$250/kW up to 100%
Optional Binding Mandatory Curtailment	Customers exempt from rotating outages		5-15% of load available for reduction during every rotating outage	N/A
Scheduled Load Reduction Program	$0.10/kWh per month of actual energy reductions during SLRP days		$0	N/A
Demand Bidding DBP	Voluntary	Day-ahead	$0.50/kW per hr	N/A
	Voluntary	Day-of	$0.60/kW per hr	N/A

Typical existing demand response programs compensate participants via some combination of monthly rates, event rates, and technology incentives. They primarily require participants to shed more than 30-100 kW during demand response events and, depending on the level of commitment, may penalize participants who fail to meet their pledged peak demand event power usage, or Firm Service Level (FSL). Some programs are entirely voluntary, some are bid upon within 24 hours of an event, and some require an FSL to be met during any event with limited to no notice. While automated demand response programs and their associated software do exist, they have not yet sufficiently penetrated the market to effectively streamline the process of large-scale demand response. In theory, when these systems are deployed on a large scale, utilities could effectively eliminate the need for more convolved, less efficient DR programs.

Task 6.4.2. Technical Literature Review

Various techniques for implementing demand response at the building level have been investigated in scientific journal articles. These methodologies include lighting reduction, fan turn-down, pre-cooling, night purging, thermal storage, and plug load control.

6.4.2.1. *Lighting Reduction*

Many commercial facilities are illuminated at levels significantly higher than necessary for required tasks. Studies have shown that workers in office environments are generally satisfied with lower levels of ambient lighting. The factors influencing the acceptability of light dimming are:

- The amount of daylight incident on workspace
- The speed of the dimming process
- The level of lighting reduction

Empirical studies agree that dimming the lights at a slow rate (about 1% per minute) is best to avoid the detection of illuminance reduction (Newsham, 2010). The level of illuminance reduction has also been studied in various papers within the context of occupant response and energy reduction. The table below proposes illuminance reduction levels under different conditions of (grid demand) urgency and daylighting. Estimated energy reduction percentages have been calculated through the calibrated NatSciII eQUEST building model.

Table 30: Proposed levels of illuminance reduction for daylit and non-daylit office spaces and their associated occupant acceptability as well as NatSciII's total energy reduction.

Urgency	Daylighting	Illuminance Reduction	Acceptability (Akashi, 2004)	Total Energy Reduction (NatSciII)
Level 1	None	20%	80%	5%
	Low	40%	80%	9%
	High	60%	80%	14%
Level 2	None	35%	70%	7%
	Low	50%	70%	12%
	High	70%	75%	16%
Level 3	None	50%	50%	12%
	Low	60%	60%	14%
	High	80%	70%	19%

Lighting reduction can reduce a building's total energy demand by 5-20% with minimal effects on occupant comfort. Where dimming is applicable, lighting control will be integrated into the software. The dimming rate may depend on the amount of notice and magnitude of the DR event.

6.4.2.2. *Ventilation Fan Turn-Down*

It has been shown in numerous studies that decreasing the duct static pressure (DSP) and limiting the ventilation fan variable frequency drive (VFD) speed can lead to significant reductions in fan power usage. A case study performed by the Demand Response Research

Center (LBNL) on the UC Santa Barbara Library showed a 17% total fan power reduction when the supply fan VFD was limited to 70%, and a 35% total fan power reduction when the supply fan VFD was limited to 60% and the DSP reset to 0.4 IWC (Motegi, 2007). The supply fan power during the case study is shown below, with the moderate price (70% limited) period between 1:15-2:15pm and 3:15-4:15pm and the high price (60% limited) between 2:15-3:15pm.

Figure 189: Power consumption of the supply fan given two different levels of demand response between 1:15-4:15pm

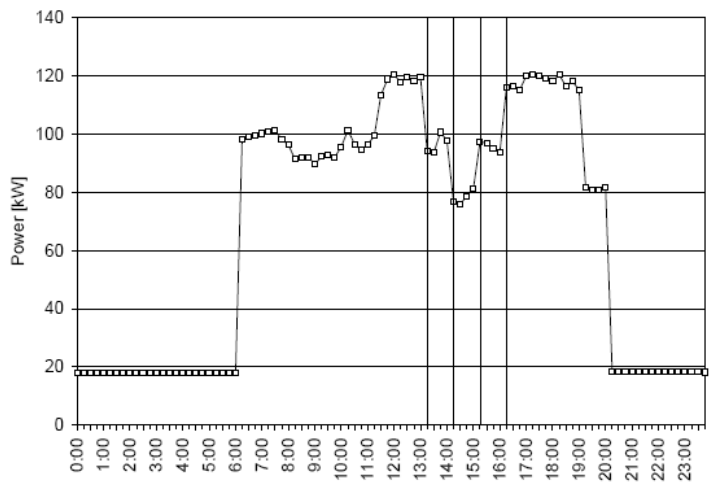

Source: Motegi, 2007

While reductions in peak power consumption due to fan turn-down can be simply modeled in the HiGRID code, the temperature response of the building space and the effect on occupant thermal comfort is nonlinear in nature and difficult to estimate. Not enough research has been published to attempt to characterize the temperature response for non-specific building types. In order to thoroughly characterize the demand response measure, limits must be set for the degree to which the variable frequency drive and duct static pressure are lowered. Different levels of fan limitation with corresponding effects on thermal comfort will be specified based upon the urgency of the demand response event and the occupant acceptability. ASHRAE Standard 55 (ANSI, 2010) recommends that the maximum change in operative temperature allowed during a period of time is the most restrictive of the values in Table 31:

Table 31: Maximum change in operative temperature per ASHRAE Standard-55 requirements

Change in Temperature	
Degrees F	**Time Period**
± 2.0	15 min
± 3.0	30 min
± 4.0	1 hour
± 5.0	2 hours

± 6.0	4 hours

Reducing fan power consumption during demand response events is the researched strategy with the largest potential to reduce peak power usage. The ASHRAE standards provide reasonable criteria for determining the limit to which fan power is curtailed during urgent demand response events. Taking these limiting factors into account, variable speed fan control is a key component for effectively applying demand response through the building automation system.

6.4.2.3. Pre-Cooling

Research into the pre-cooling of large commercial buildings indicates that significant chiller savings can be achieved during peak demand hours. This strategy forces the building to cool to lower temperatures prior to an event and allows temperatures to rise during the event to reduce the HVAC load. It is most effective on buildings with high thermal mass, which helps delay increases in temperature. Amongst pre-cooling strategies, the most energy efficient method of saving energy during a DR event is to implement an exponential step temperature reset. In 2010, LBNL modeled four different temperature reset methods using the Demand Response Quick Assessment Tool (DRQAT) and then tested the exponential step temperature reset method on an office building (Yin, 2010). The reset schedules and results are shown in the figures below.

Figure 190: Temperature reset points and simulated results for four different temperature reset strategies utilizing pre-cooling to reduce the thermal impact of temperature reset schedules. The exponential step temperature reset is named "step temp reset" for this study.

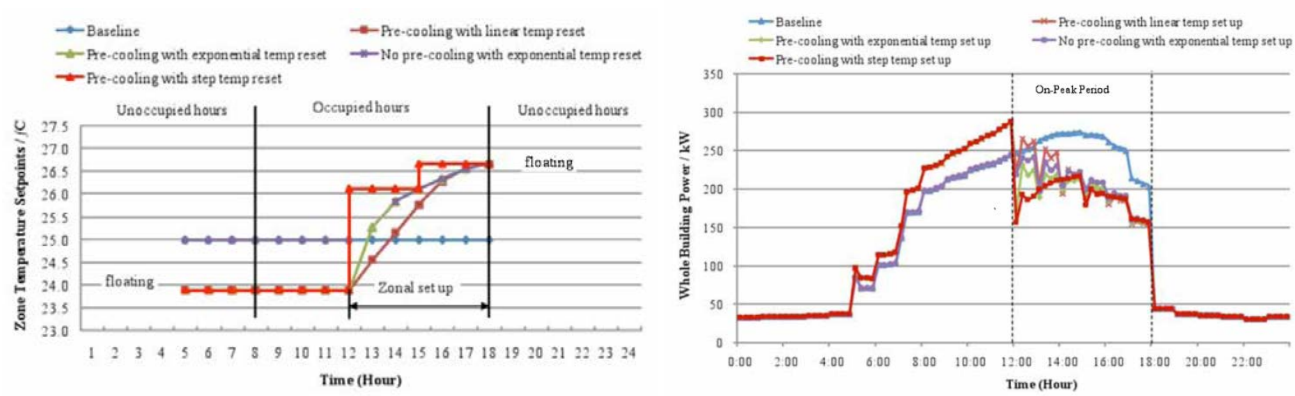

Source: Yin, 2010

Figure 191: Automatic pre-cooling demand response on an office building compared to two baseline models for the building.

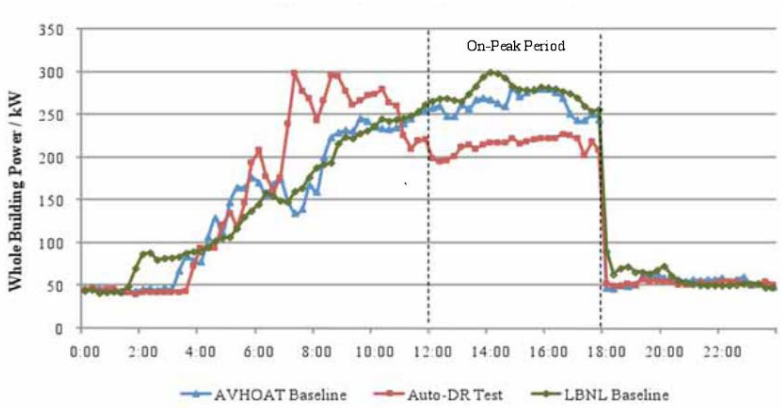

Source: Yin, 2010

The results indicate that whole building power reductions can be made on the order of 20-25% by utilizing pre-cooling and exponential step temperature reset demand response strategies. The net energy usage is approximately equal to the baseline taking into account the pre-cooling period. It must also be considered that in this study, the temperature was allowed to drift up to 80°F, which is well outside of the comfort range targeted in this research. Maintaining temperatures under 77°F, it is expected that RESCO's modeled pre-cooling load reductions will be lower than LBNL's results.

Pre-cooling demand response techniques to date have only been applied to on-peak periods during the early afternoon. Pre-cooling is primarily useful as a strategy for maintaining comfort and shifting loads, and the HiGRID code may indicate that different utilization techniques be employed under high renewable generation scenarios.

6.4.2.4. Night Purge

The night purging demand response strategy is very similar to that of pre-cooling, and in fact many studies use these terms interchangeably to describe methods of reducing peak cooling loads. However, for the purposes of this research night purging will be considered a strategy which does not involve air conditioning but instead uses only mechanical ventilation to drive the building's temperature down during the night and reduce morning-afternoon HVAC load. When the outdoor air reaches a pre-defined temperature, the controller activates the main supply fan in order to introduce outdoor air into the building.

One of few studies to empirically quantify the potential for cooling energy reduction by night purge determined that the strategy was altogether ineffective in reducing energy usage, and actually increased annual energy consumption by 0.2% (Ardehali, 1997) due to the increase in supply fan load during the night. While the net energy use is not as important as the shift in load, preliminary simulations have shown that the demand savings are actually quite

insignificant. The night purging demand response strategy will not be applied in the RESCO pilot study.

6.4.2.5. Plug Load Control

Plug load control was originally researched as a potential demand response strategy, yet the research has indicated that sufficiently economical candidates still do not exist. Most plug loads are too small or too vital to turn off in demand response events (Snook, 2011). Despite this fact, plug load control should be considered a measure of energy efficiency because when devices are not being used they should ideally not consume energy.

While this option is to be deferred to the future research, large single-device loads such as large water pumps are an option that could be economically shed during a demand response event with dedicated receivers that actuate existing device shut-down controls. It is less a part of building operation in essence but should be considered as a viable option future demand response research projects.

6.4.2.6. Automated Demand Response

Automated demand response techniques show potential for advanced controls to reduce the implementation cost of demand response, aid in informed decision making, and with higher levels of customer participation could revolutionize the market for demand response to provide additional value to both consumers and power generators.

A field study conducted by LBNL on five disparate commercial building sites utilized an automated demand response system to generate an XML price signal from a single internet source. The buildings monitored the common price signal and automatically shed site-specific electric loads when the price increased beyond pre-determined thresholds. The program was successful as a whole with aggregated peak power reductions averaging around 350 kW between 1:15pm and 4:15pm. Key technical challenges in the implementation of the field study – including software compatibility, time zones (price servers), IT failures, energy management control system (EMCS) failures, and hardware issues – were identified and the resolutions summarized (Piette, 2005). This study will be an important reference for the development of automated demand response control logic in RESCO.

Task 6.4.3. Building Model Analysis and Results: MSTB

In March of 2011, preliminary demand response strategies were applied to a standard uncalibrated eQUEST model for the Multipurpose Science and Technology Building. This initial analysis was useful in interpreting the achievable peak demand reductions of particular strategies as well as off-demand power consumption and effects on thermal comfort. August 20th was modeled in each scenario.

6.4.3.1. *Night Purge*

The night purge strategy was evaluated using the MSTB model under the schedule of 24/7 fan operation in order to drive down nighttime temperatures and reduce chiller and fan power load during the day when demand response events would be likely to occur. The advantage of the night purge strategy is that fan and chiller power does decrease during the day, but a very large amount of energy is consumed during the night in fan power. Overall, the strategy round trip efficiency was evaluated to be 43%.

Figure 192: Evaluation of the night purge strategy for electricity and chilled water consumption

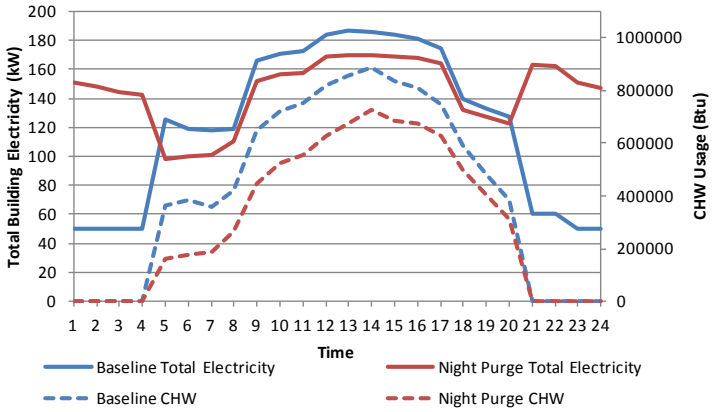

6.4.3.2. *Pre-Cooling*

The pre-cooling strategy was also applied to the MSTB model using eQUEST, assuming that the temperature set point was decreased from 73°F to 70°F for one hour mid-day in order to reduce the chiller load during the afternoon. The total energy savings using this strategy were quite small, yet its overall efficiency was 64%, better than that of the night cool strategy.

Figure 193: Evaluation of a 1-hour pre-cooling strategy for electricity and chilled water consumption

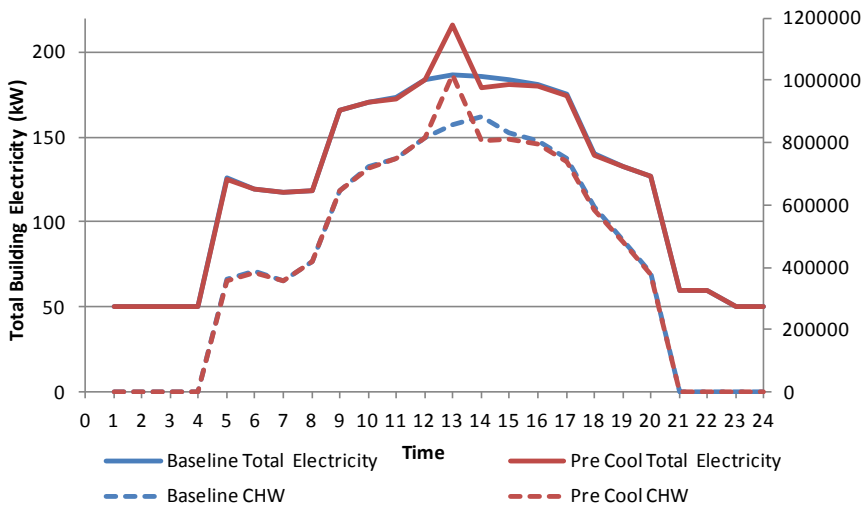

6.4.3.3. Fan Turn-Down

The fan turn-down strategy is an effective and currently utilized method for demand response, yet it cannot be modeled within eQUEST. However, the maximum savings gained and change in temperature can be modeled in eQUEST to estimate the best-case power reduction and worst case temperature response in a fan turn-down scenario as shown in the figure below.

Figure 194: Evaluation of 2-hour fan OFF reduction measure for electricity and chilled water consumption and temperature response

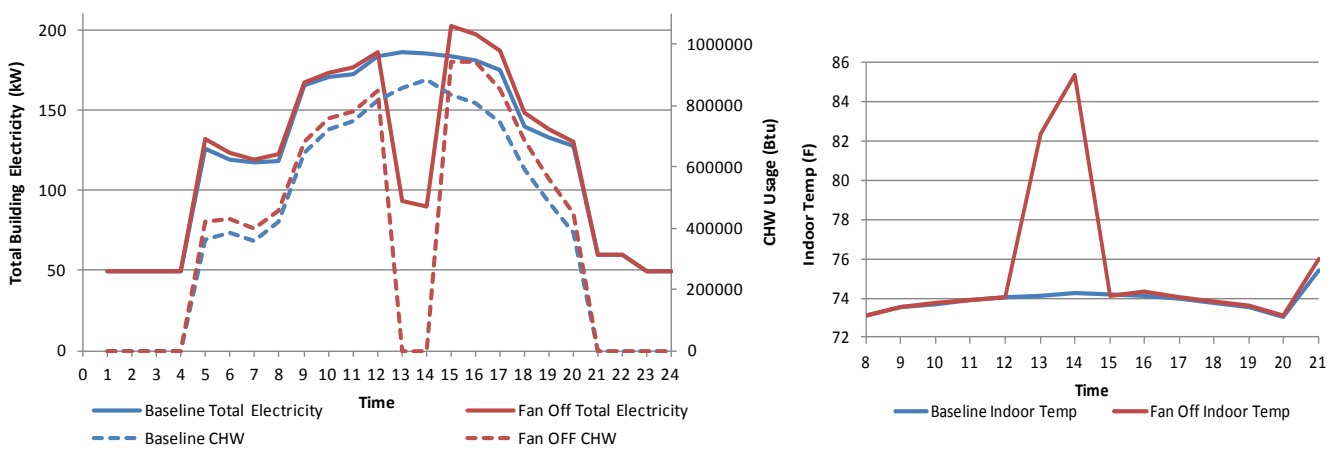

The initial modeled results showed that only small savings could be achieved using the night purge and pre-cooling strategies, and that these strategies would require large additional amounts of energy prior to the demand response event. While fan turn-down could not be

modeled precisely, it was shown to reduce peak demand significantly and instantaneously. Along with the application of pre-cooling and/or night purge, this strategy would be particularly effective for an automated demand response program.

Task 6.4.4. Building Model Analysis and Results: Natural Sciences II

While tailored demand response techniques have not yet been applied to all calibrated building models, an informed analysis has been made for some promising demand response strategies and their relative magnitudes of demand reduction have been compared. Analysis was made for six different demand response strategies using the mostly calibrated Natural Sciences II building model.

6.4.4.1. Pre-Cooling and Night Purge

There were a variety of options for operational strategies to pre-cool building space the night before, the morning of, and the day of a demand response event. The goal of the preliminary model analysis was to determine which strategies were appropriate for events with and without limited lengths of notice prior to the event. Trade-offs included the additional energy expenditure prior to the event, the magnitude of peak load reduction, and the temperature response of the building space. The strategies were defined as night cool, morning cool, and day cool, as shown in Figure 195.

Figure 195: Hourly temperature set point schedules for baseline operation, night purge, and three pre-cooling strategies

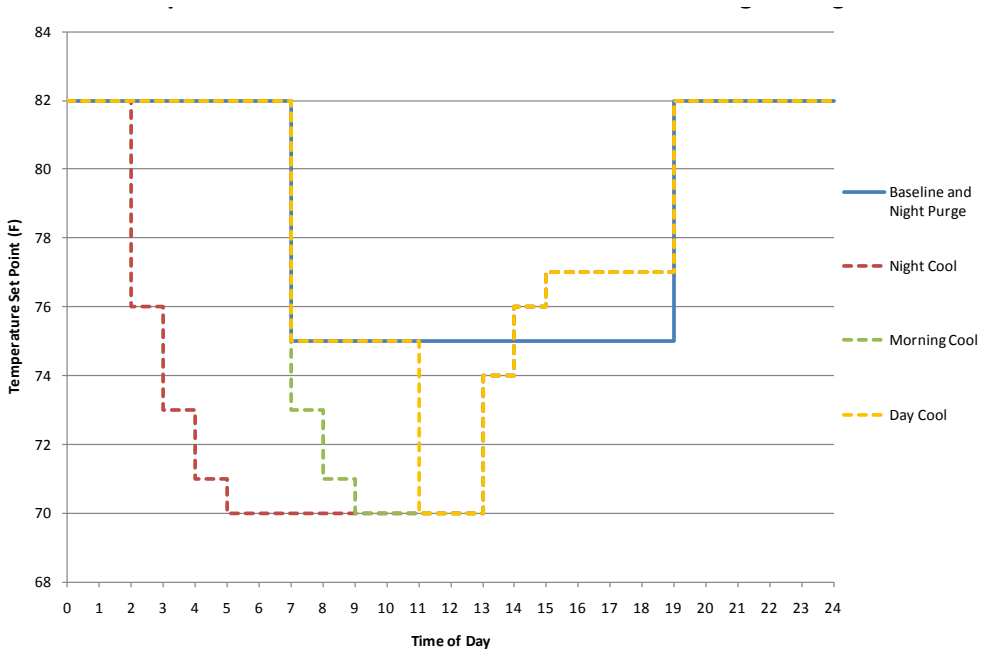

The change in temperature set points during the temperature step-up period all followed an exponential trend over the 6-hour DR event consistent with LBNL's field test. The temperature turn-down prior to the event was also implemented in a step-by-step method in order to reduce the initial energy expenditure for the cooling periods for which greater cooling time was allotted.

The results – modeled for August 18, 2009 – indicated a relatively small quantity of load reduction during the demand response event and initial energy expenditures exceeding the actual energy reductions for a net increase in building load. The night purge strategy did not noticeably decrease energy usage during the event, and longer cooling periods did not appear to significantly reduce afternoon load. The electrical power consumption did not drop more than 2% during the floating period.

Figure 196: Hourly power consumption with four different HVAC control demand response measures

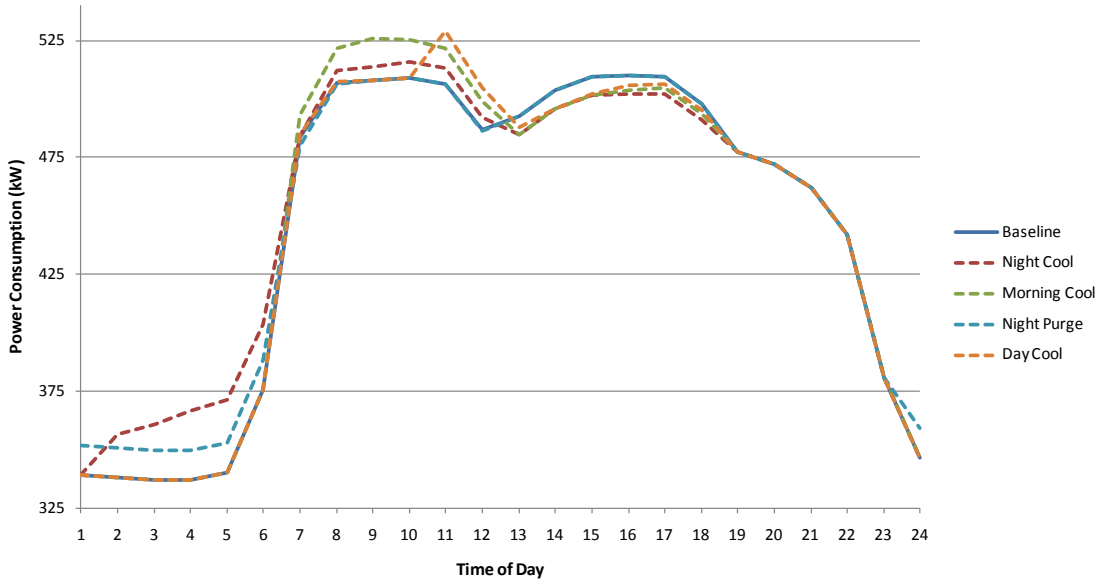

Reductions in chiller power were also observed and were much more efficient on average – with net chiller energy reductions for the night purge, day cool, and morning cool strategies. The total chiller energy reduction during the event averaged from about 7-10% for the morning cool and day cool strategies and 1-2% for the night cool strategy. The chiller energy usage is summarized for each strategy below.

Figure 197: Energy usage incurred on building's chilled water plant under four HVAC demand response measures

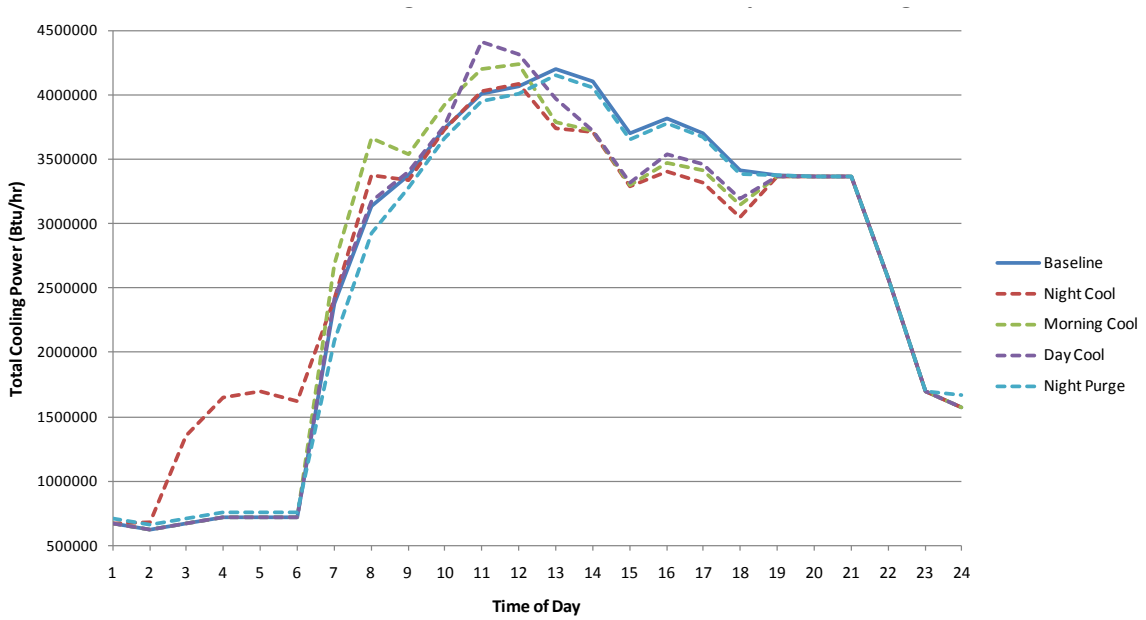

Figure 198: Zone temperature response to the four HVAC pre-cooling strategies. During August, the night cool strategy fails to lower the zone temperature to below the occupied set point

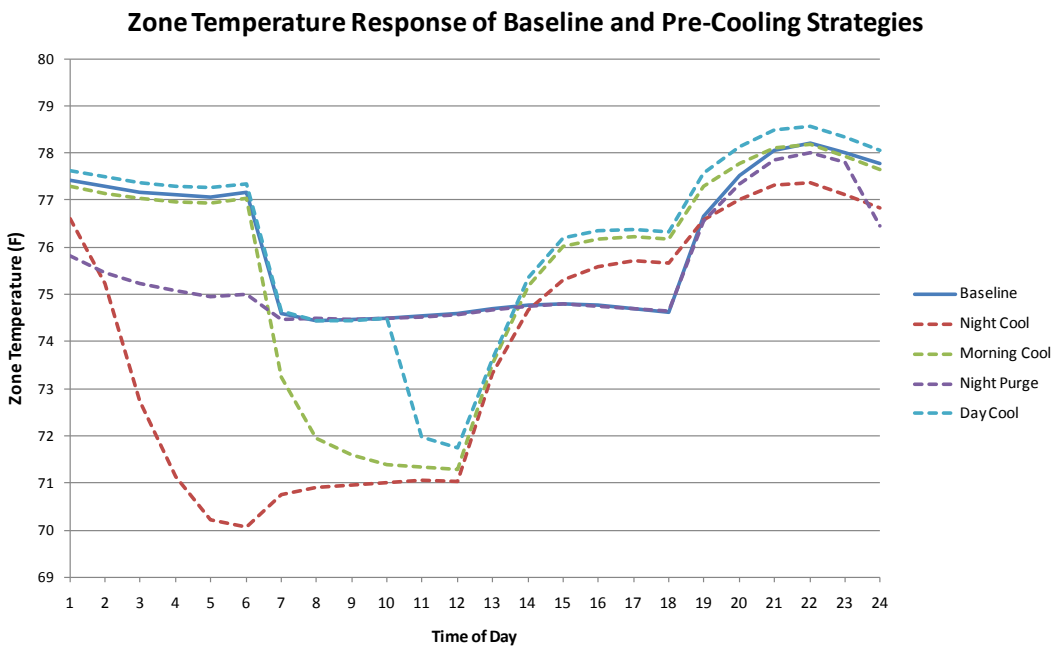

Reductions in HVAC power consumption during the demand response period were relatively small, yet the preliminary analysis revealed some important strategic design aspects. First,

without changing the temperature set point, only trivial peak power reductions are achievable using the night purge demand response strategy. The night purge strategy only has the potential to work when the outdoor temperatures are cool enough to drive the building temperature to below the cooling set point. The results indicate that Irvine's diurnal swings are insufficient for this strategy to effectively reduce afternoon demand. The night cool and morning cool strategies do not have a significant effect on peak power reductions, and depending on the notice/urgency for a demand response event, may not be feasible for automatic implementation. The day cool strategy may be effective, in combination with other demand response measures, in utilizing peaks in solar generation to reduce cooling demand during the later afternoon when future demand response events might be more likely to occur.

The energy savings calculated by eQUEST tend to be underestimated for pre-cooling strategies because the DOE-2.2 calculation engine has flaws in dealing with building thermal mass. In order to accurately estimate power reductions for the HiGRID code, eQUEST results will be compared with results from LBNL's Demand Response Quick Assessment Tool (DRQAT) – which is programmed to better estimate thermal mass effects and results from empirical testing on the UCI buildings.

6.4.4.1.1. Pre-Cooling Analysis Using the Demand Response Quick Assessment Tool

DRQAT is a modeling program tailored for the assessment of demand response strategies applied to building models with limited specified detail. It is based on EnergyPlus simulations of prototypical buildings developed by J. Huang et al. (Huang, 1991) and HVAC equipment. It incorporates prototypical buildings and equipment and allows the user to specify a relatively small number of parameters in order to make a quick assessment of demand response strategies (Yin, 2010). Using DRQAT, initial demand response strategy assessments were re-evaluated based upon the morning cool and day cool procedures. Below, Figure 199 and Figure 200 show the power consumption and average zone temperatures for each strategy. The average peak demand reduction for both figures was approximately 15 kW.

Figure 199: Power consumption and temperature response for a morning cool demand response strategy modeled in DRQAT during an event on August 5, 2009.

Figure 200: Power consumption and temperature response for a day cool demand response strategy modeled in DRQAT during an event on August 5, 2009

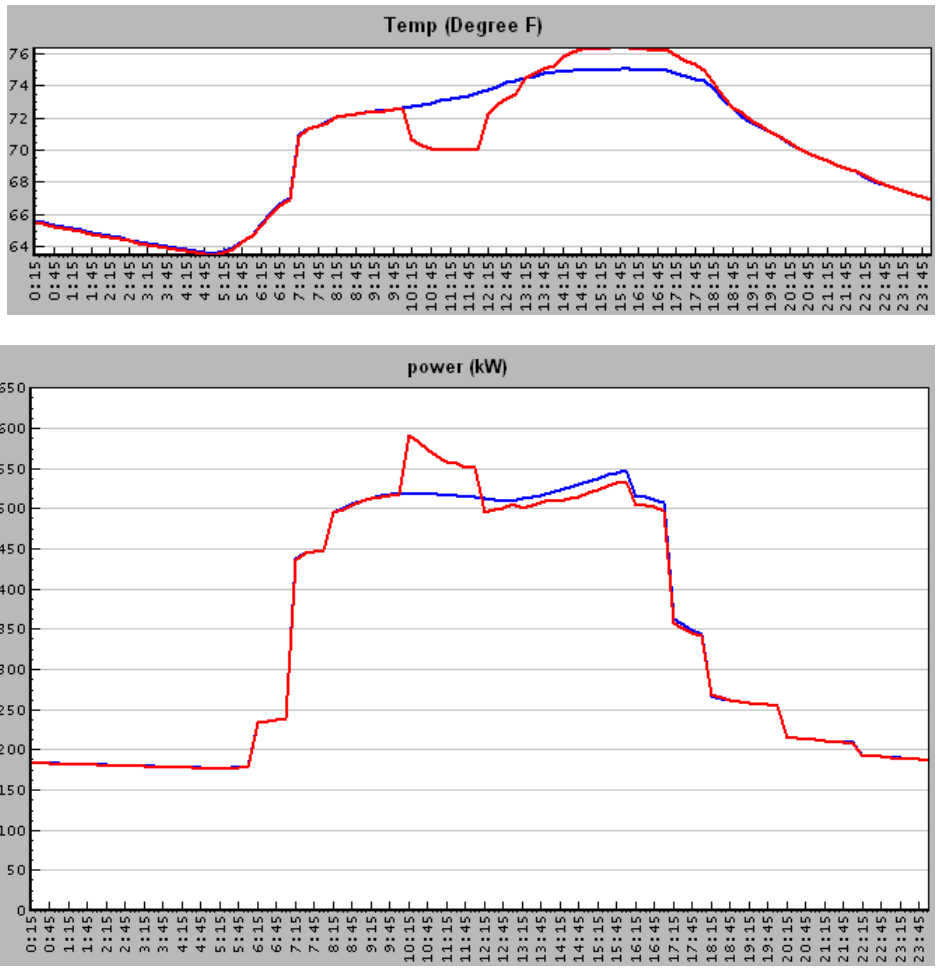

The simulation results presented above implement the same HVAC schedules and set points modeled in eQUEST. The results from the DRQAT confirm that there is no real advantage to implementing longer pre-cooling periods, and indicate savings approximately twice that of those estimated by eQUEST, ranging from 3-4% of total power consumption. The temperature response remains within a reasonable range of comfort in both analyses. However, Cadmus implemented the day-cool procedure on a UCI building to confirm the potential for demand reduction and temperature response in a real building and to verify the eQUEST and DRQAT model results.

6.4.4.2. Lighting Reduction

Lighting reduction in buildings is significantly easier to model than pre-cooling strategies and yields better results for reducing total building peak power consumption. For the purposes of preliminary analysis, a mid-level lighting reduction was applied to the Natural Sciences II building model, limiting lighting illuminance to 60% of its maximum power consumption. The

hourly lighting schedule for the baseline and demand response events are shown below in Figure 201.

Figure 201: Lighting schedules for the baseline Natural Sciences II building and with applied lighting reduction

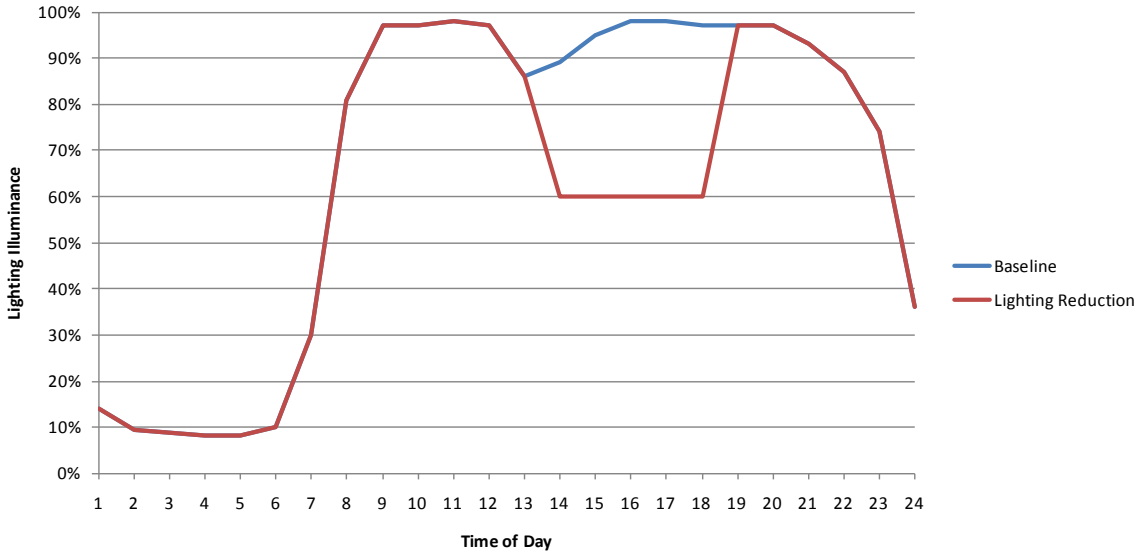

The reduction in power consumption utilizing the lighting reduction demand response strategy is much more significant than reductions estimated for the pre-cooling HVAC demand response strategies. A 35-40% reduction in lighting corresponds to a 7-9% reduction in total building demand, or 35-45 kW. This accounts for a significant portion of achievable peak demand reduction, and while levels of reduction will be tailored to acceptable specifications and changed over longer periods of time, lighting reduction will certainly be incorporated as a primary measure to reduce peak demand in the HiGRID code.

Figure 202: Demand reduction of lighting strategy compared to reductions achievable using HVAC pre-cooling strategies

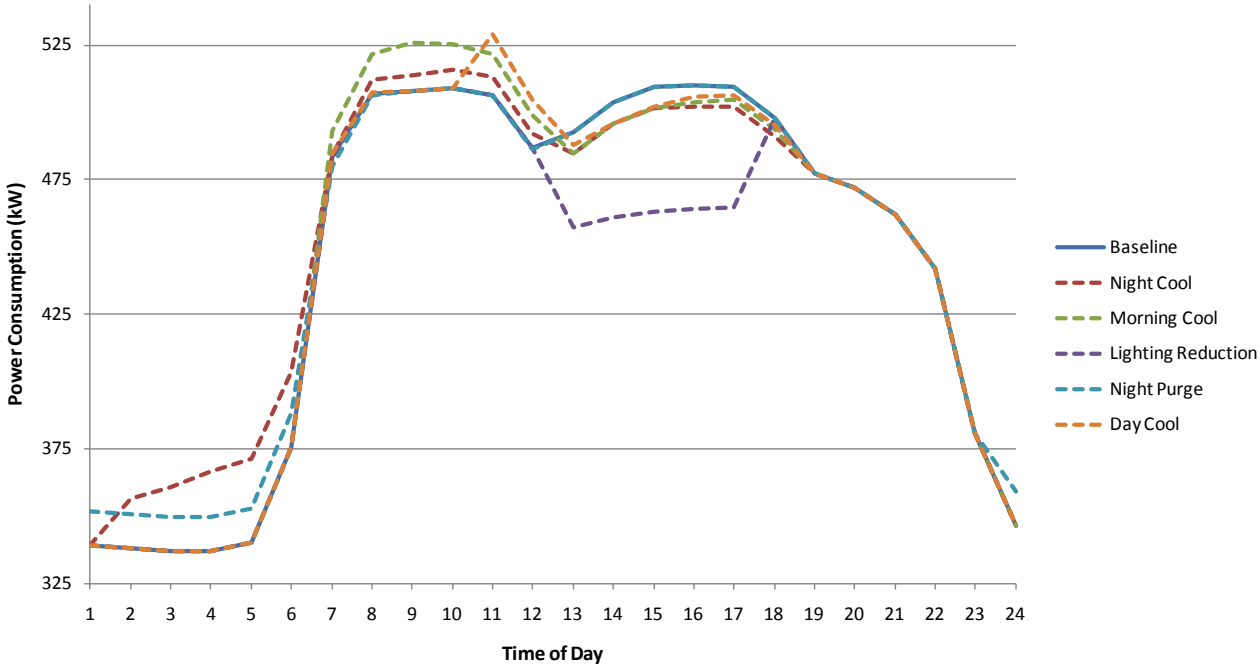

6.4.4.3. Fan Turn-Down

The eQUEST modeling software is not compatible with fan turn-down methodologies because it allows the user only to specify Fan ON/OFF on an hourly basis rather than as a percentage of maximum flow. However, given known fan power consumption, the reduction in power associated with a percentage turn-down can be calculated given the approximate relationship

$$\frac{P_2}{P_1} = \left(\frac{n_2}{n_1}\right)^a \qquad (1)$$

where a is a constant around 2.5, given the non-ideal characteristics of normal air, to calculate the power during a demand response event, P_2, given the change in fan speed, n_2/n_1. The power reduction achieved using fan turn-down, compared to lighting reduction and day-cooling, is shown in Figure 203. Due to the non-linear relationship between power consumption and fan speed, a 15% reduction in the VFD corresponds to a 33% reduction in fan power. With the Natural Sciences II building model, this strategy can potentially reduce total peak demand by over 10%. Fan speed reduction is a potent measure for demand response and a reliable strategy for significantly reducing total power on a temporary basis.

Figure 203: Total building power consumption under multiple (simultaneous) demand response strategies. Over 20% of the total peak demand can be reduced with the combination of fan turn-down and lighting reduction

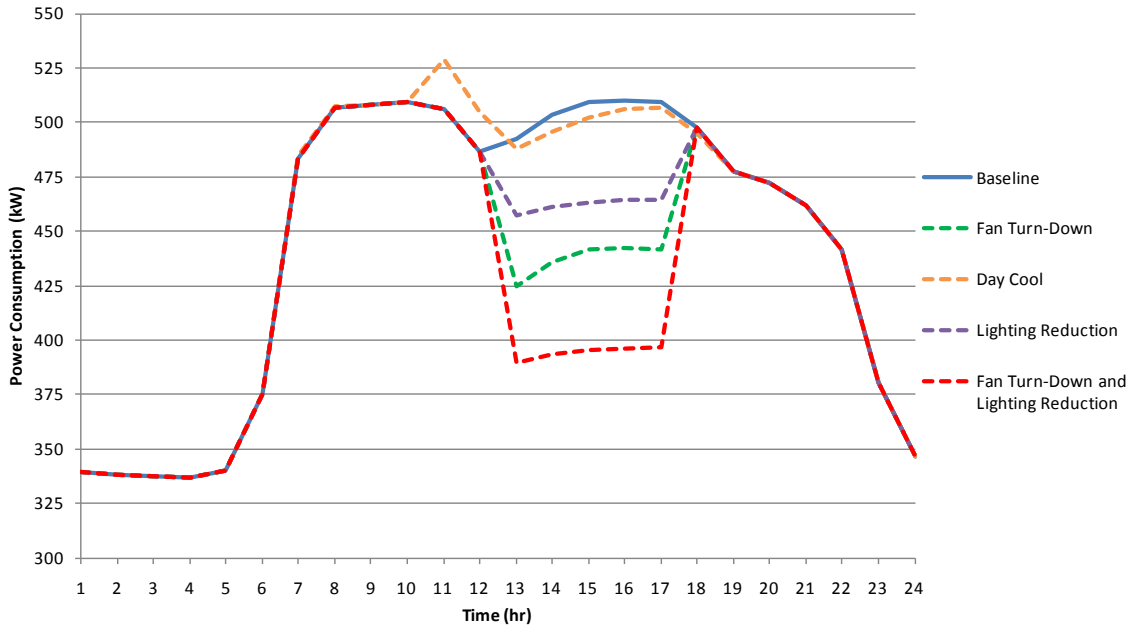

If, however, the building is to maintain its default temperature set points during the implementation of a fan turn-down, a greater load will be incurred on the chilled water plant serving the building. If a temperature set point change is made, then the temperature response of the building space must be monitored to ensure that it remains within acceptable values. Evaluating the trade-offs of such issues cannot precisely be done in eQUEST, but the worst-case temperature response is shown in Figure 204.

Figure 204: Floating zone temperature response for when fans are turned OFF at noon, representing the worst-case thermal effects for a fan turn-down procedure

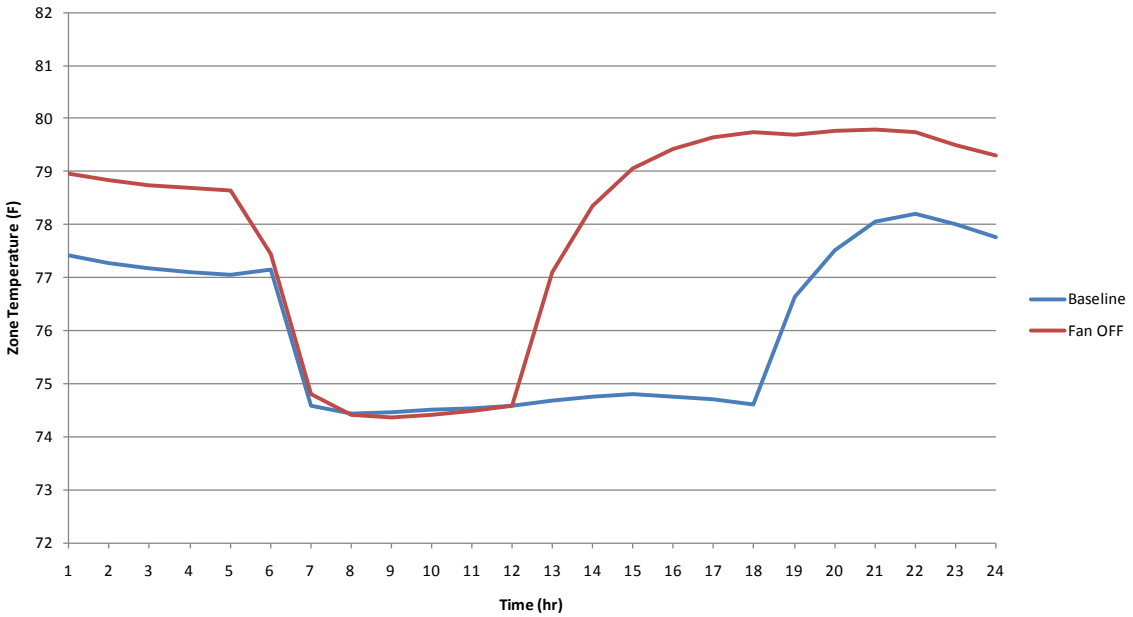

In order to appropriately define levels of fan turn-down while maintaining zone temperatures within acceptable levels, the thermal response of the building zones must be understood. Alternatively, temperature set points could be maintained by increasing the thermal load on the central chiller plant, in which case the thermal energy usage must be understood. For UCI, this latter technique presents a unique opportunity to shift the chiller power consumption hours after the demand response event due to the central plant's large thermal reservoir. Because these thermal responses cannot be modeled within eQUEST, these strategies are to be tested on either the Natural Sciences II building or the Multipurpose Science and Technology Building. It is important that the fans maintain minimum outside air and thermal comfort requirements as specified by the ASHRAE standards. Working within these limitations, however, the fan turn-down demand response strategy holds significant potential to meet the requirements of renewable-based energy supply and demand.

6.4.4.4. Comparison of Demand Response Measures: Natural Sciences II

In comparing the relative magnitudes of demand reduction by each of the proposed strategies and the levels of comfort that they can maintain, priorities can be made regarding the specific numerical levels of each type of reduction and the integration of multiple demand response measures. From the preliminary analysis, it is clear that pre-cooling does not lead to significant energy savings alone, but qualitatively it stands to reason that integrating pre-cooling with fan turn-down could help to make significant demand reductions while maintaining a more acceptable environment for thermal comfort. Lighting is a clear and easy demand reduction measure for buildings that have some type of control integrated into their automation systems

(on/off or dimming), but would require a greater cost for buildings without the required control infrastructure. Below, Figure 205 summarizes the demand reductions observed with each modeled strategy.

Figure 205: Average demand reduction for each demand response strategy for each quarter of the day, assuming the peak reduction occurs between 1pm and 5pm

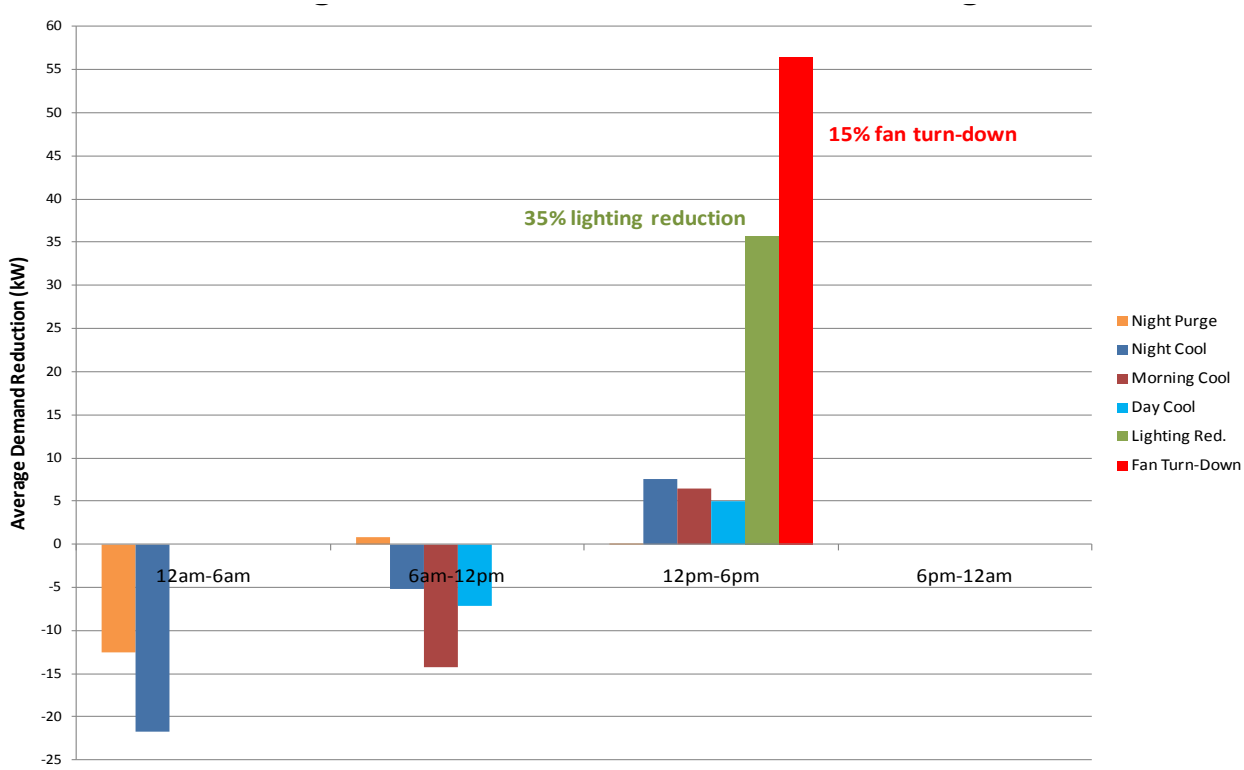

Task 6.4.5. Experimental Demand Response Testing

Before the demand response strategies detailed above can be integrated into the HiGRID code and applied to the modeled end-use load profiles, the thermal effects observed and energy reductions achieved with the fan turn-down and pre-cooling strategies needed to be verified with real UCI building load reductions. Cadmus worked with UCI Facilities personnel to run three demand response tests on MSTB and the office portion of NatSciII. The goals of these tests were to track fan power consumption, chilled water load, and zone temperatures during the demand response event and to compare the building response with historical baseline data to quantify feasible levels of fan turn-down and pre-cooling demand reduction while maintaining reasonable levels of occupant comfort. The testing followed the schedule:

Table 32: Demand Response Testing Schedule

Test	Date	Test Procedure	Day Temp	Night Temp
1	10/10/2011	15% Fan Turn-Down	74°F	57°F
2	10/12/2011	70°F to 77°F Pre-Cool	98°F	68°F

3	10/14/2011	30% Fan Turn-Down	81°F	62°F

The following points were trended for each of MSTB's two air handling units between 9/19/2011 and 10/15/2011 and for one of NatSciII's three air handling units between 10/3/2011 and 10/15/2011:

- Supply Fan Power Consumption (kW)
- Exhaust Fan Power Consumption (kW)
- Supply Fan Speed (%)
- Chilled Water Valve Position (%)
- Supply Fan Static Pressure Drop (IWC)
- Supply Air Temperature (°F)

The baseline comparison data were determined by averaging trend data from multiple days with similar temperatures and scaling the averaged trend data to meet the pre-test and post-test data on the day of the demand response test. Applied levels of fan reduction were pre-determined by a different set of baseline data, so the actual fan speed limitations are not exactly 15% and 30% reductions for Test 1 and Test 3. All test parameters were controlled automatically through the Building Automation Systems except the NatSciII supply fan speed, which was controlled manually at the air handler due to the system's limitations for automated control.

Prior to testing the fan turn-down strategy, UCI Facilities warned researchers that the supply fans serving MSTB and NatSciII ran with static pressure reset control designed to optimize the demand controlled ventilation (DCV) to the building spaces. Because these fans were already running efficiently, the amount of feasible load reductions would be lower than was originally expected. However, while static pressure control strategies are implemented for some buildings on campus, many run with constant static pressure set points of 1.5-2.5 IWC and therefore campus-wide models will need to account for buildings both with and without static pressure resets. For the purpose of experimental research, however, testing the fan turn-down strategy on supply fans with DCV would validate the strategy's applicability to every available air handling system on campus.

6.4.5.1. Test 1: 15% Fan Turn-Down

The first test was designed to implement a 15% fan turn down for AHU-1 and AHU-2 at MSTB and AHU-3 at NatSciII between 1:00 pm and 5:00 pm. Based on data gathered between 9/19/2011 and 10/8/2011, fan speeds were limited to 53% for AHU-1, 65% for AHU-2, and 58% for AHU-3. The figures below demonstrate the fan speed limitation compared to a baseline average composed of the following days:

Table 33: Days used in baseline average compared with the testing day, shown on the right

Day	Mon	Wed	Fri	Mon	Thur	Mon	Fri	Sat	Mon
Date	9/19	9/21	9/23	9/26	9/29	10/3	10/7	10/8	10/10
High	76°F	74°F	76°F	76°F	77°F	76°F	71°F	76°F	74°F
Low	62°F	62°F	61°F	64°F	61°F	63°F	55°F	52°F	57°F

Figure 206: Supply fan turn-down compared to historical baseline

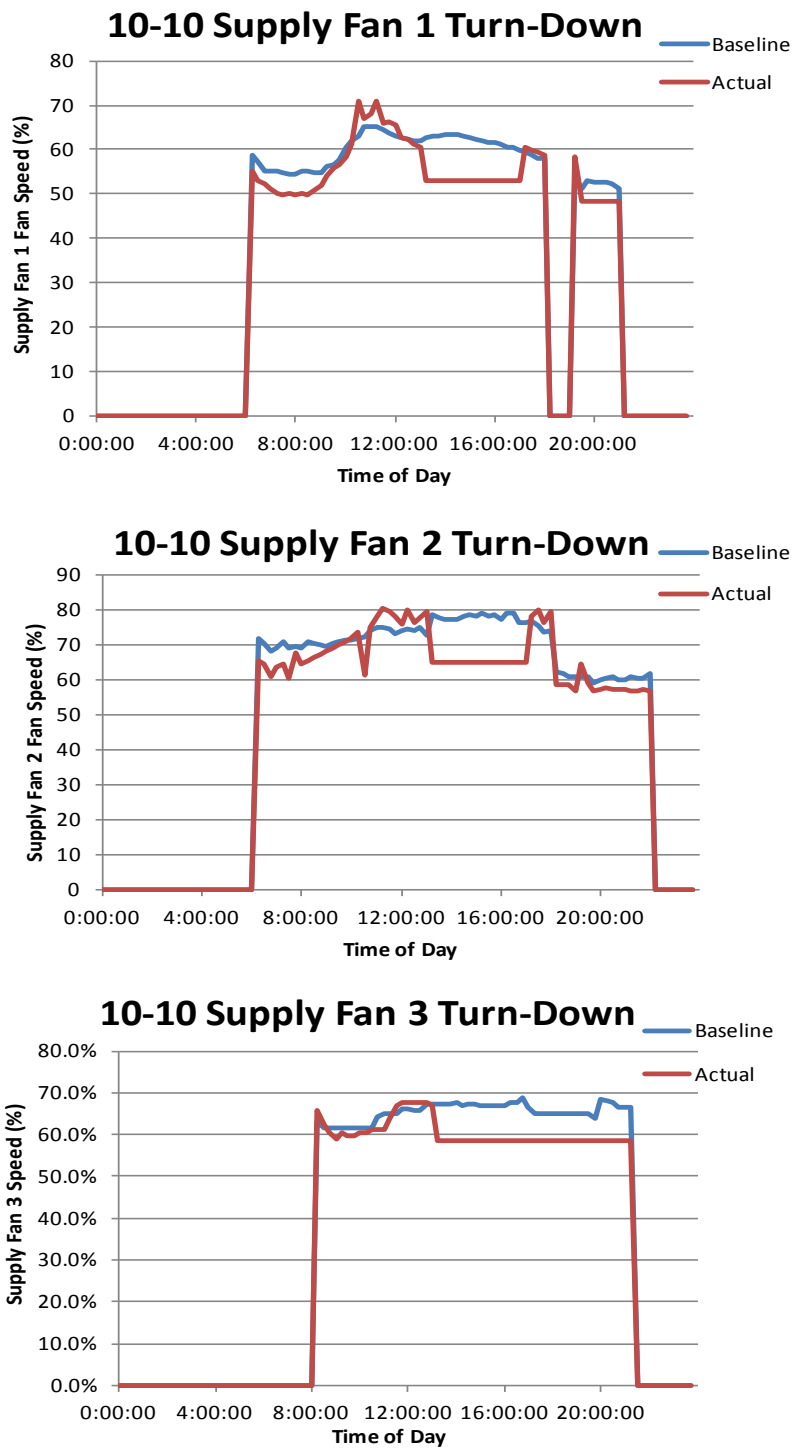

Following the test, the detailed baseline comparison indicated that Supply Fans 1 and 2 at MSTB achieved 14.7% and 16.5% reductions respectively and Supply Fan 3 at NatSciII achieved a

13.3% reduction. These fan speed limitations resulted in power savings of 1.4 kW, 2.5 kW, and 5.7 kW at Supply Fans 1, 2, and 3 respectively, as shown in the following figures:

Figure 207: Supply fan power compared to historical data for 10-10 fan turn-down

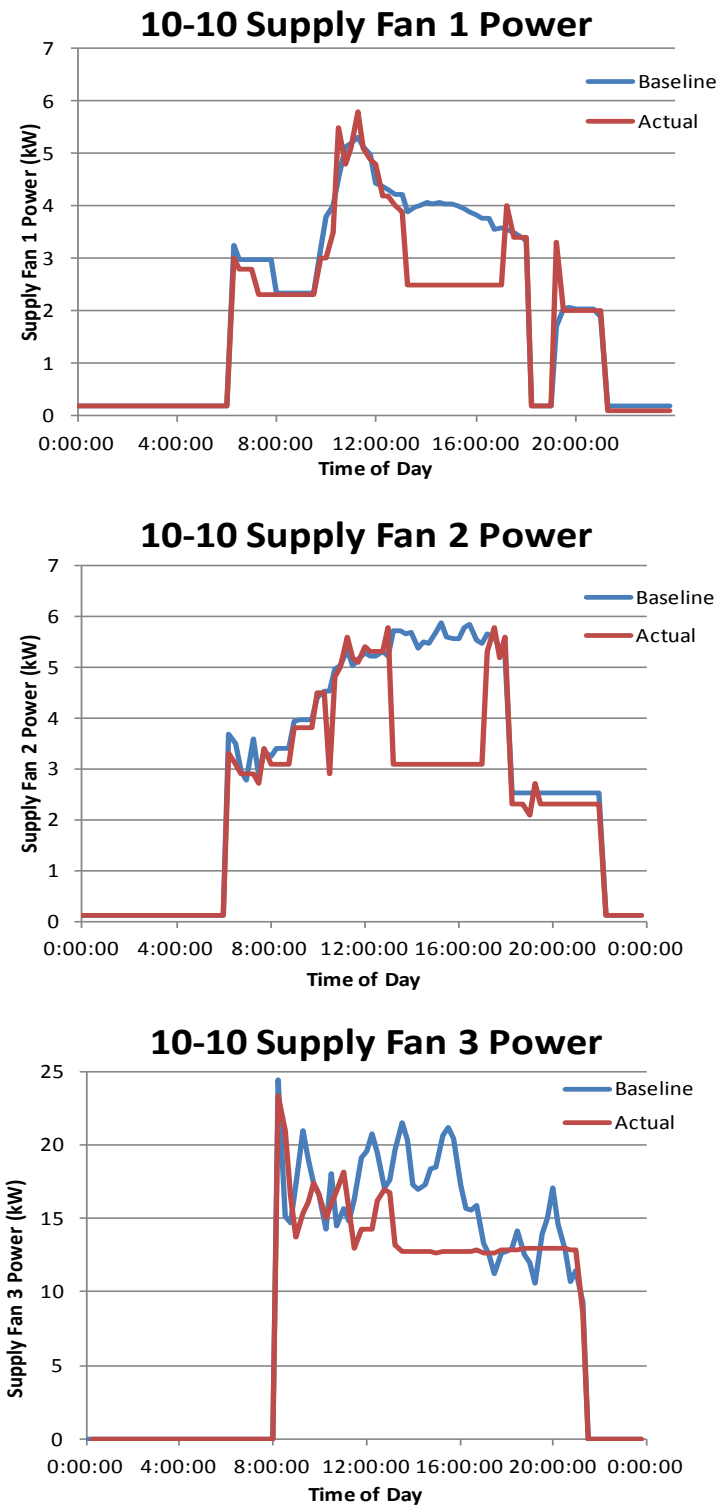

During the 1:00 pm to 5:00 pm testing period, the fan static pressure was set back to 0.2-0.24 inches of water column in the MSTB air handlers and 1.1-1.2 inches of water column in the NatSciII air handler. In normal operation, the MSTB air handlers average 0.5-0.6 IWC and the NatSciII air handler averages 1.9-2.0 IWC, indicating approximately 50% reduction in static pressure. No noticeable changes were seen in chilled water consumption or in supply air temperatures, indicating that no significant additional thermal loads were incurred during the test. The space temperature reports showed no considerable change over the period of the turn-down, as shown in the figures below.

Figure 208: Temperature change of all zones in MSTB and office portion of NatSciII. Shown are the minimum, mean, maximum, first quartile, and third quartile of the data

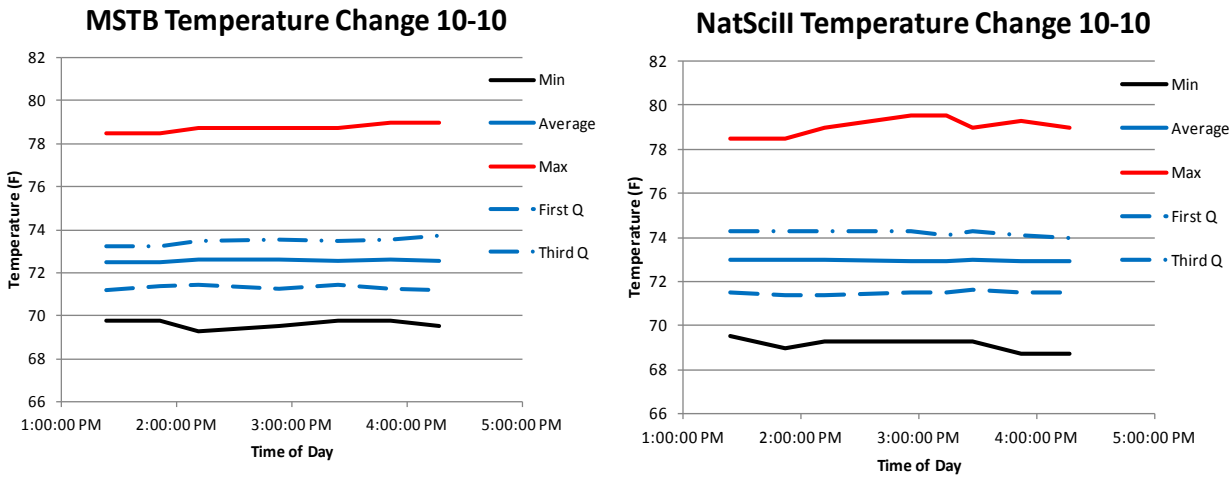

Because the buildings were running with static pressure reset control prior to the fan limitation, one primary concern regarding the indoor air quality of the building space was whether the spaces were able to meet minimum ventilation requirements. During the test, the amount of air supplied to a sample of spaces was verified at the Building Automation System and, in some spaces, at the exit of the duct. The following tables summarize the actual and minimum levels of flow to these spaces.

Figure 209: Actual flow rates and minimum rates of flow for a sample of spaces in MSTB.

MSTB 10-14 VAV Flow Rates				
Time	**Room**	**Flow (CFM)**	**Min Flow (CFM)**	**Room Type**
13:57	100	148	152	Lobby
13:58	104	828	849	Phys Lab
13:59	103M	152	152	Meeting Room
13:59	112	504	44	Mac Lab
14:00	114	688	200	Classroom
14:01	139	860	860	Phys Eq

14:02	210	1424	420	Classroom
14:03	205	132	128	Reception
14:04	217	580	152	Office
14:05	256	116	116	Meeting Room
14:05	242	104	112	Computer Class
14:09	246	1320	800	TA Suite

Figure 210: Actual flow rates and minimum rates of flow for a sample of spaces in NatSci II

Flow Rates in NatSci II				
Time	**Room**	**Flow (CFM)**	**Min Flow (CFM)**	**Room Type**
14:34	4109	232	240	Office
14:35	4121	0	100	Conference
14:36	4125	80	80	Reception
14:37	5103	240	220	Accounting Office
14:45	3141	0	240	Work Room
14:47	3113	448	172	Office
14:49	3260	536	240	Open Office
14:50	3120	error	error	Reception
14:57	1107	248	240	Office
14:58	1115	324	212	Office
14:59	1120	112	132	Reception
15:00	5000	240	244	Lobby
15:00	5137	312	320	Work Room
15:56	5120	144	200	Reception

Figure 211: Cell shading key for flow rate tables.

Minimal ventilation
Over-ventilated
Slightly under-ventilated
Under-ventilated
Not ventilated (acc. to BAS)

The apparent lack of flow in two of the sampled spaces in NatSciII caused some initial worries, but after coordination was made with the Facilities managers, it was discovered that the many

of the damper motor actuators in NatSciII were severely out of calibration and that they were in the process of being replaced. These spaces were identified to Facilities to ensure that they were on the list to be tested and/or replaced. The ventilation performance of the first turn-down test was determined to be satisfactory and deeper fan limitations feasible.

6.4.5.2. Test 2: Pre-Cool to 70°F

The second test involved pre-cooling each of the building spaces to 70°F and then gradually resetting the temperature set points to 77°F until 5:00 pm. The temperature reset schedule is shown below:

Figure 212: Temperature reset schedule for the 10-12 pre-cooling test

Time	Testing Procedure
11:00 am	Reset all (applicable) zone temperatures to 70°F.
1:00 pm	Reset all (applicable) zone temperatures to 74°F.
2:00 pm	Reset all (applicable) zone temperatures to 76°F.
3:00 pm	Reset all (applicable) zone temperatures to 77°F.
5:00 pm	Restore temperature set points to default schedules.

The figures below demonstrate the fan speed limitation compared to a baseline average composed of the following days:

Figure 213: Days used in baseline average compared with the testing day, shown on the right

Day	Thur	Tue	Fri	Mon	Tue	Thur	Wed
Date	9/22	9/27	9/30	10/3	10/11	10/13	10/12
High	81°F	81°F	81°F	76°F	78°F	85°F	98°F
Low	62°F	61°F	64°F	63°F	58°F	62°F	62°F

During the demand response period, an average of 2.1 kW of peak demand was shed on MSTB's AHU-1, and averages of 3.0 kW of peak demand were shed for MSTB's AHU-2 and NatSciII's AHU-3. During the pre-cooling period, averages of 1.2 kW, 7.2 kW, and 34.8 kW of demand were added for supply fans 1-3, respectively. The overall efficiencies of the pre-cooling strategy is defined as

$$\boldsymbol{Efficiency} = \frac{\boldsymbol{Energy\ Shed\ During\ Demand\ Response\ Event}}{\boldsymbol{Energy\ Consumed\ During\ Pre-Cooling\ Period}} \quad \textbf{(2)}$$

were 337%, 171%, and 35% for supply fans 1-3, respectively. The power consumption of the supply fans is shown in the figure below:

Figure 214: Supply fan power compared to historical data for 10-12 pre-cool

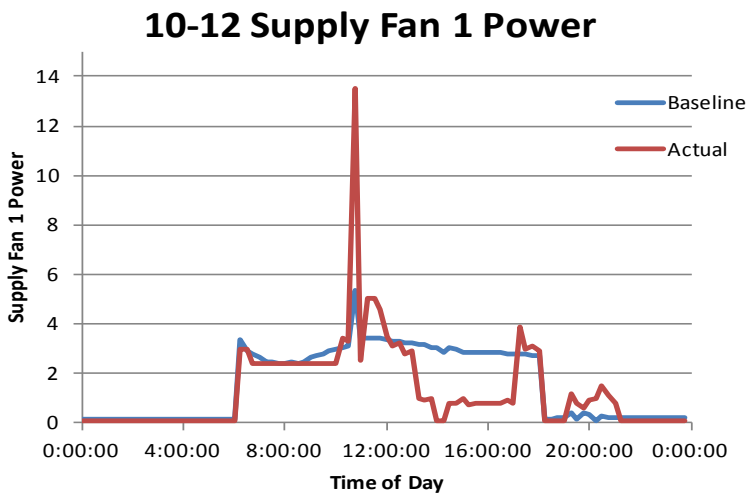

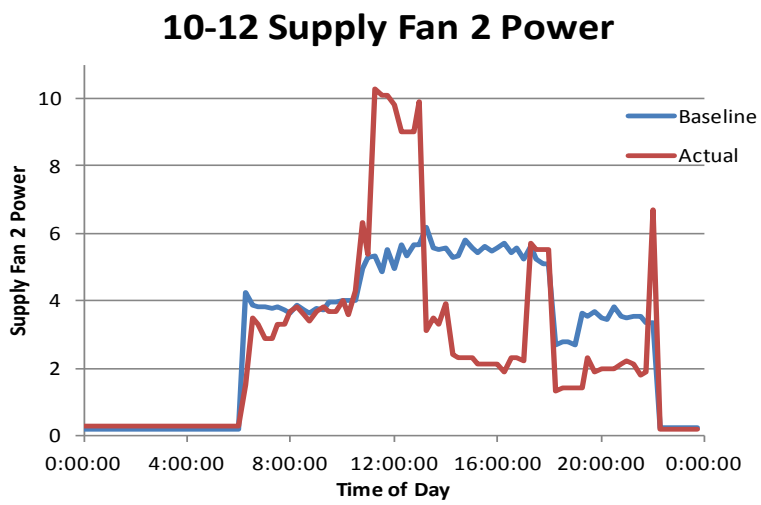

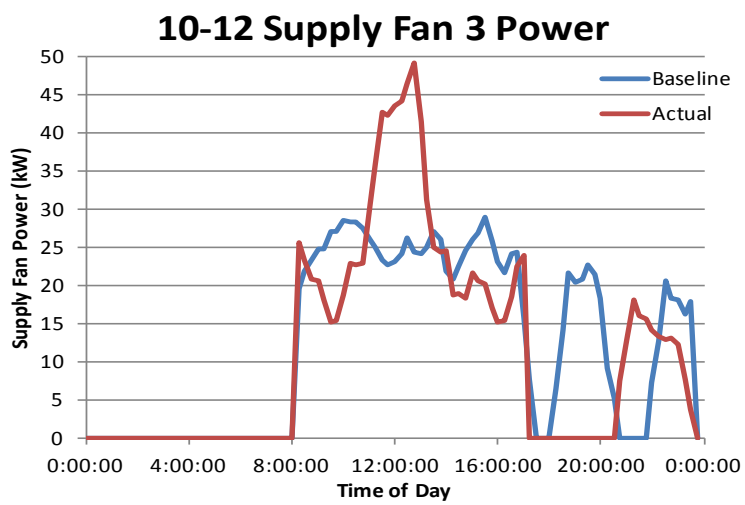

The chilled water consumption followed a similar trend, with efficiencies of 124%, 112%, and 556% for air handlers 1-3 respectively. For MSTB's air handlers, the trade-off between supply fan power and chilled water energy is relatively equitable, while at NatSciII, the fan power takes the bulk of the load during the pre-cooling period and the chiller recovers most of the load during the temperature reset.

Figure 215: Chilled water valve position – indicating thermal load – compared to historical data for 10-12 pre-cool

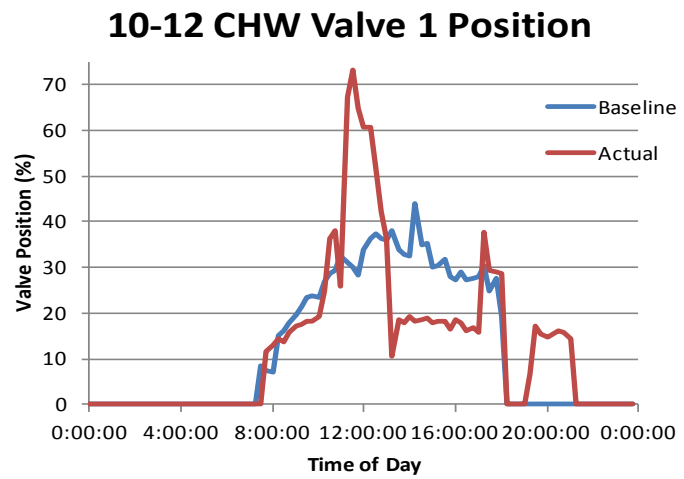

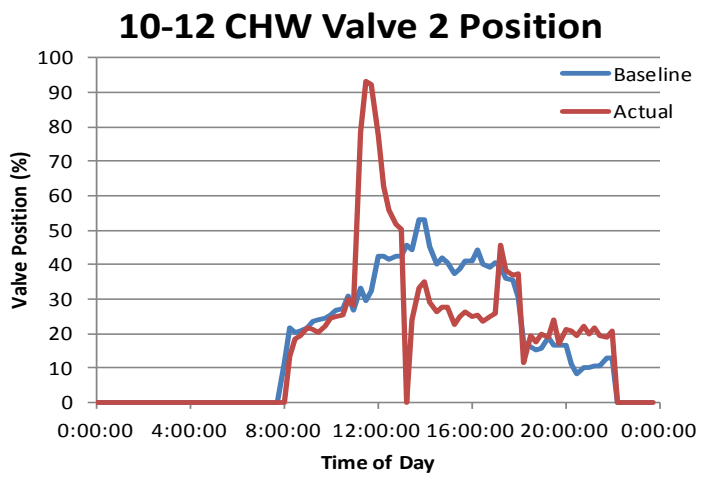

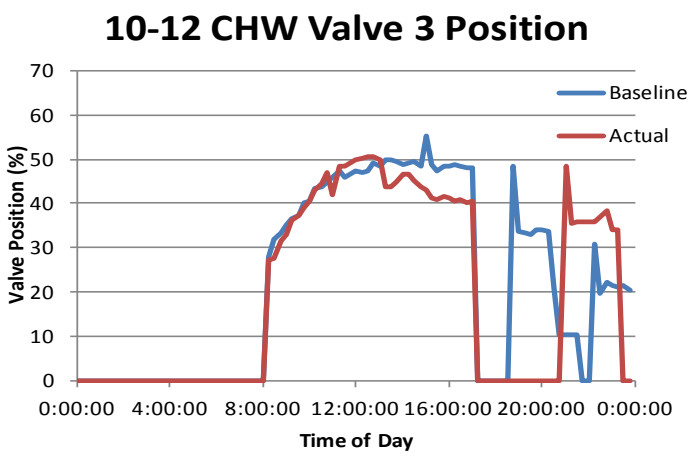

Overall, each of the air handlers reduced chilled water usage. While the consumption of chilled water during the pre-cool event will be a primary demand response concern for buildings with individual water chillers, thermal loads incurred at UCI will affect electric consumption at the central plant only during the night due to its thermal capacity and operational schedule. The supply air temperature (SAT) from the MSTB air handlers was reset during both the pre-cooling period and the temperature step-up period, while the SAT from the NatSciII air handler remained constant at 58°F for the duration of the test. As the night-time operation commenced, however, the chilled water valve at NatSciII closed and the SAT rose for four hours until its temperature set backs were exceeded. The control sequence allowing for the reset of SAT at MSTB is the mechanism by which the loads were shared between the chilled water and fan power.

Figure 216: Supply air temperature compared to historical baseline data for 10-12 pre-cool

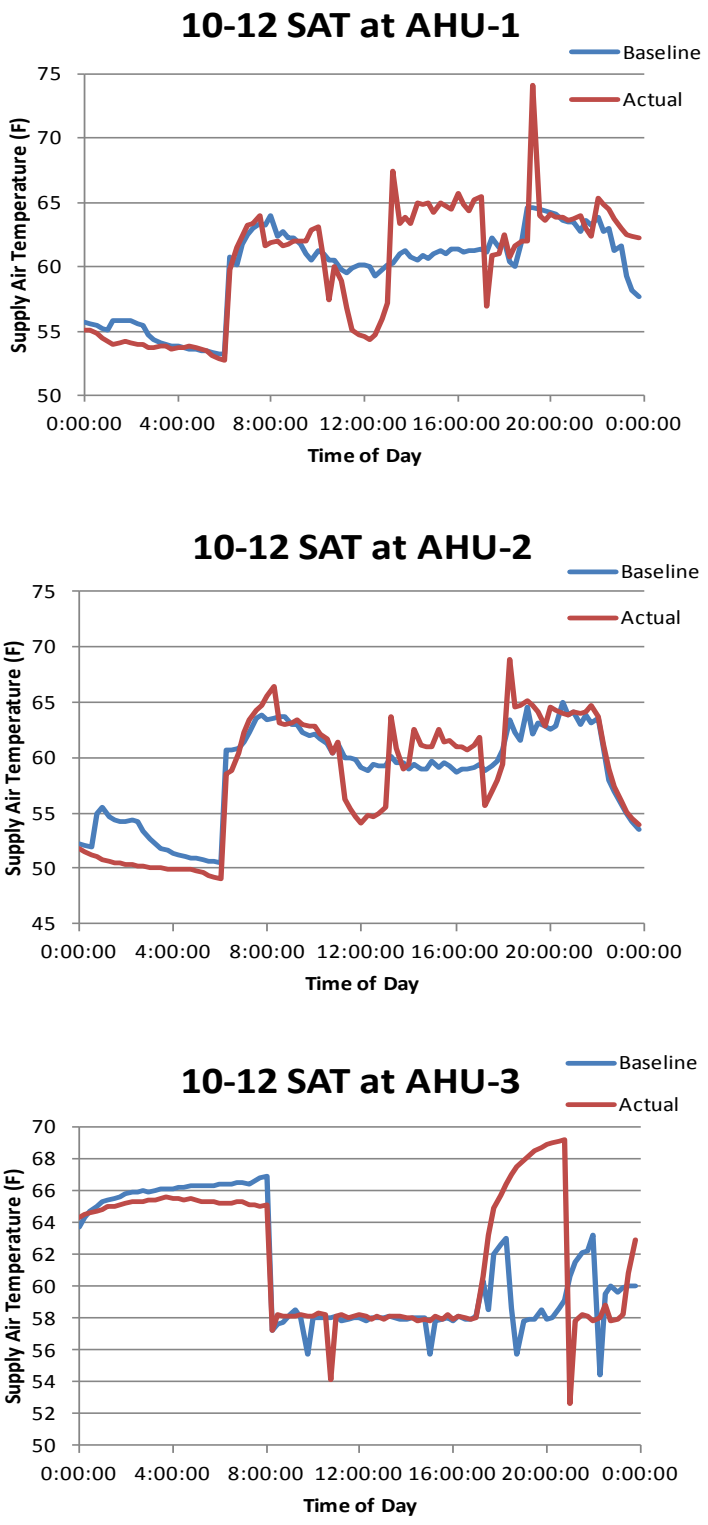

Compared to the fan turn-down tests, the zone temperatures tracked during the pre-cooling test underwent significant changes due to the reset of the zone temperature set points. However, despite outdoor temperatures peaking around 100°F on the testing day, the indoor temperatures remained within reasonable boundaries considering the buildings' pre-existing air balancing issues.

Figure 217: Temperature change of all zones in MSTB and office portion of NatSci II. Shown are the minimum, mean, maximum, first quartile, and third quartile of the data

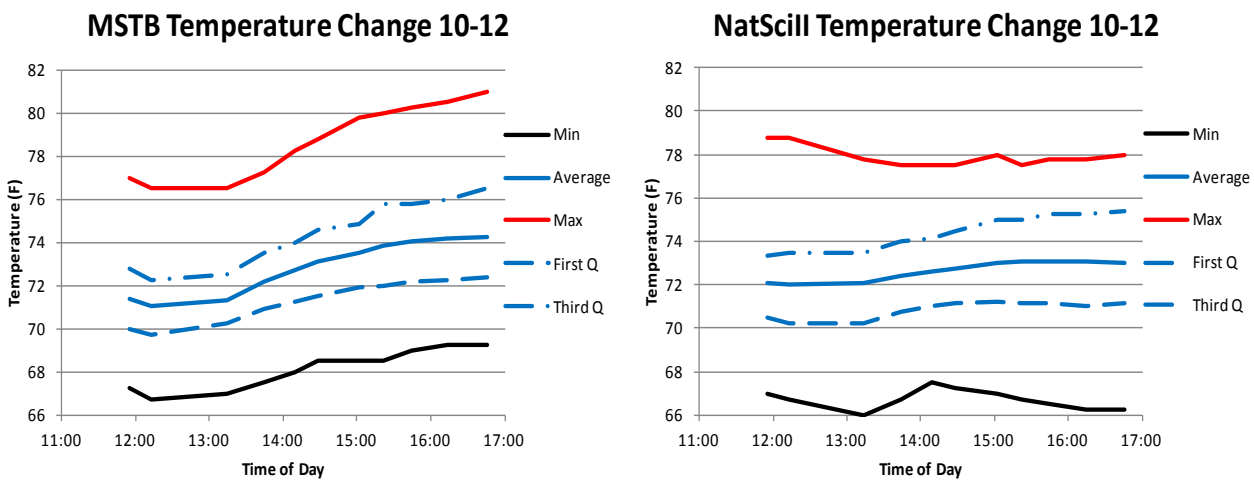

During the step-up period, temperatures raised by an average of 3°F in MSTB yet only by 1°F at NatSciII. According to ASHRAE 55 Thermal Comfort standards, temperature changes of less than 6°F over a four-hour period are acceptable, indicating that the temperature responses observed at each building were satisfactory. It is expected that NatSciII would retain lower temperatures longer than MSTB because it has higher thermal mass, yet the lack of temperature response coupled with NatSciII's fan power trend indicate that the test was unsuccessful at NatSciII. The fan and temperature control mechanisms at NatSciII did not allow for sufficient temperature drift during the period of 1:00-5:00pm. This is due to the fact that NatSciII doesn't allow for SAT resets and that its VAV boxes are poorly calibrated, so certain zones never reach their minimum air requirements. Despite the fact that most zones remained far under the temperature set points, airflow cannot decrease sufficiently during the step-up period because some zones remain below minimum airflow requirements, thereby increasing the supply fan power consumption. If a fan speed limitation or SAT reset was applied to NatSciII during the DR event, then significant savings would be realized and the thermal response would be more akin to that of MSTB.

6.4.5.3. Test 3: 30% Fan Turn-Down

The third test was designed to implement a 30% fan turn down for AHU-1 and AHU-2 at MSTB and AHU-3 at NatSciII between 1:00 pm and 5:00 pm. Based on data gathered between 9/19/2011 and 10/13/2011, fan speeds were limited to 44% for AHU-1, 53% for AHU-2, and 48%

for AHU-3. The figures below demonstrate the fan speed limitation compared to a baseline average composed of the following days:

Table 34: Days used in baseline average compared with the testing day, shown on the right

Day	Thur	Tue	Fri	Tue	Fri
Date	9/22	9/27	9/30	10/11	10/14
High	81°F	81°F	81°F	78°F	81°F
Low	62°F	61°F	64°F	58°F	62°F

Figure 218: 10-14 Supply fan turn-down compared to historical baseline

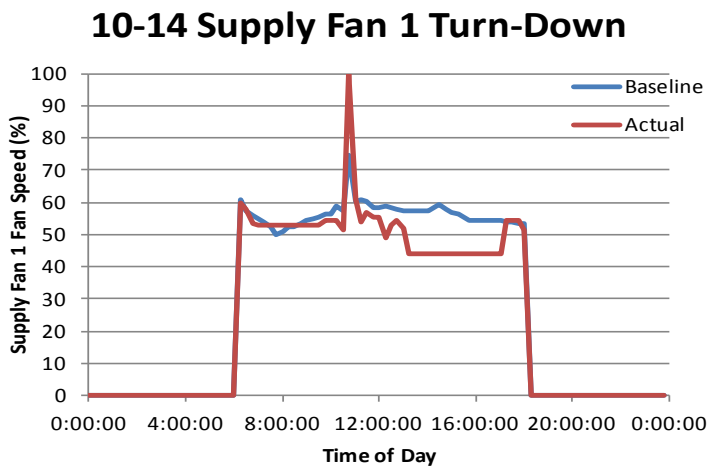

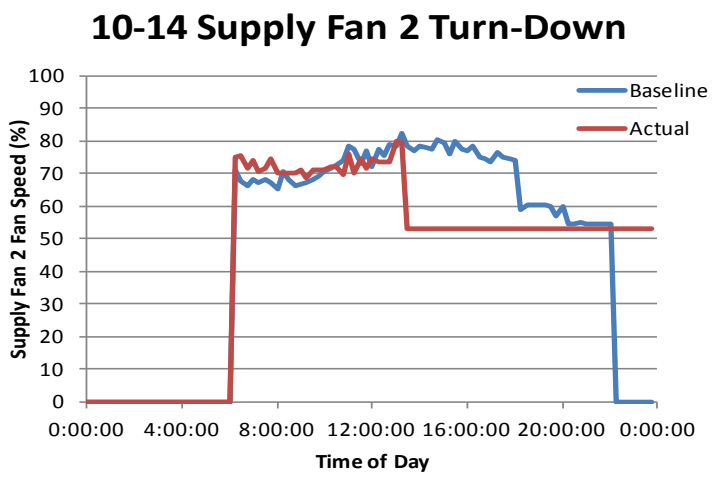

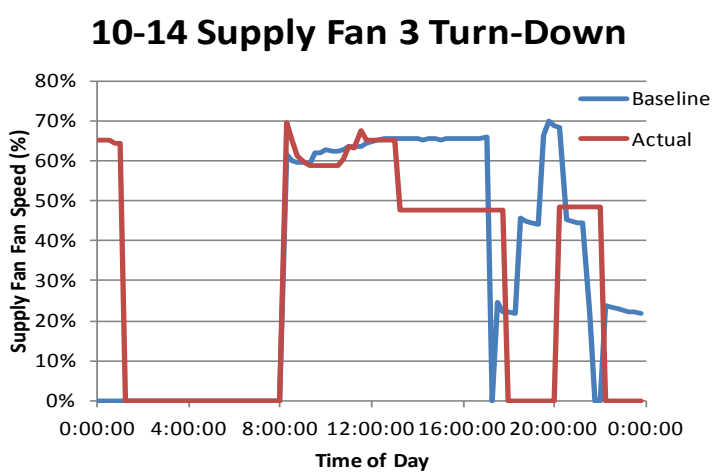

Following the test, the detailed baseline comparison indicated that Supply Fans 1 and 2 at MSTB achieved 21.8% and 31.4% reductions respectively and Supply Fan 3 at NatSciII achieved a 27.0% reduction. These fan speed limitations resulted in power savings of 1.7 kW, 3.3 kW, and 11.6 kW at Supply Fans 1, 2, and 3 respectively, as shown in the following figures:

Figure 219: 10-14 Supply fan power compared to historical baseline

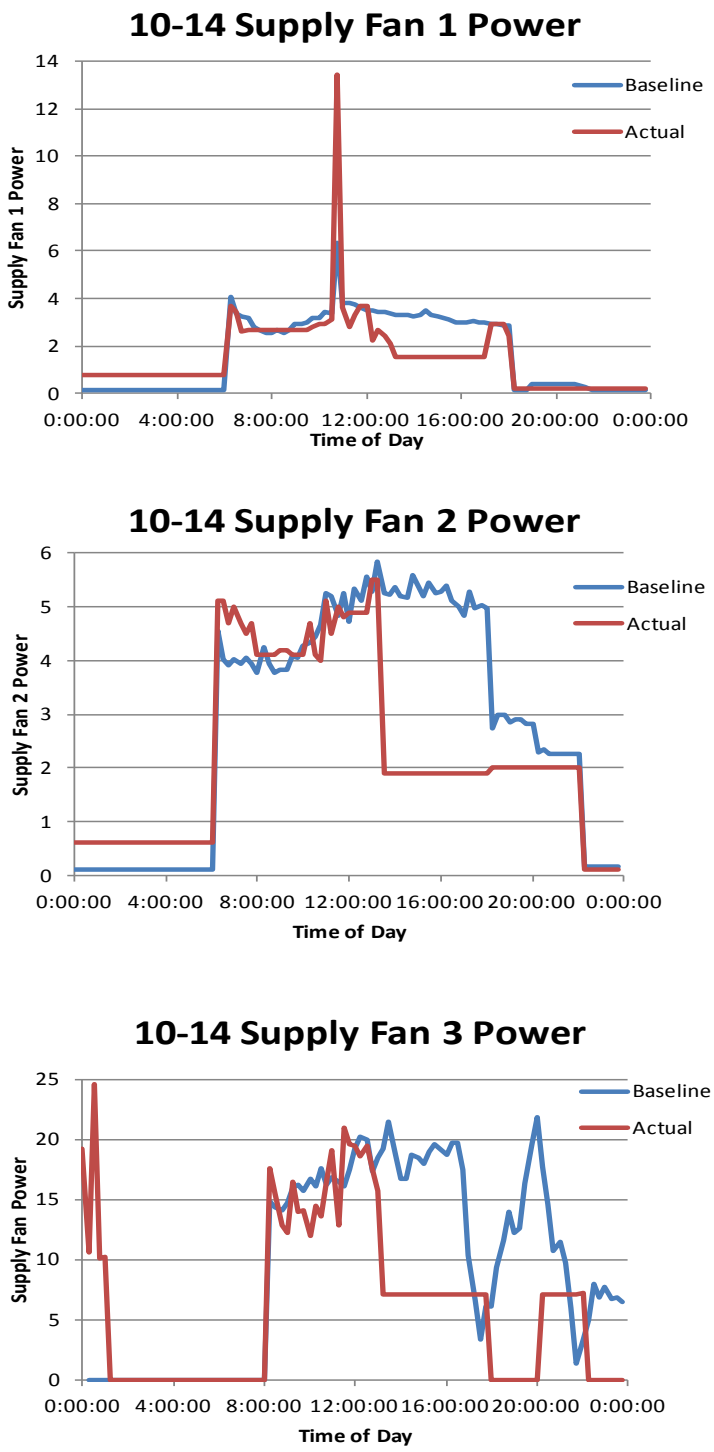

During the 1:00 pm to 5:00 pm testing period, the fan static pressure was 0.08-0.10 inches of water column in the MSTB air handlers and 0.27-0.32 inches of water column in the NatSciII air handler. In normal operation, the MSTB air handlers average 0.5-0.6 inches of water column and the NatSciII air handler averages 1.7-1.8 inches of water column. No significant changes were seen in chilled water consumption or in supply air temperatures, indicating that no significant additional thermal loads were incurred during the test. The space temperature reports showed no considerable change in average zone temperature but the zones that had the highest temperatures became warmer.

Figure 220: Temperature change of all zones in MSTB and office portion of NatSci II. Shown are the minimum, mean, maximum, first quartile, and third quartile of the data

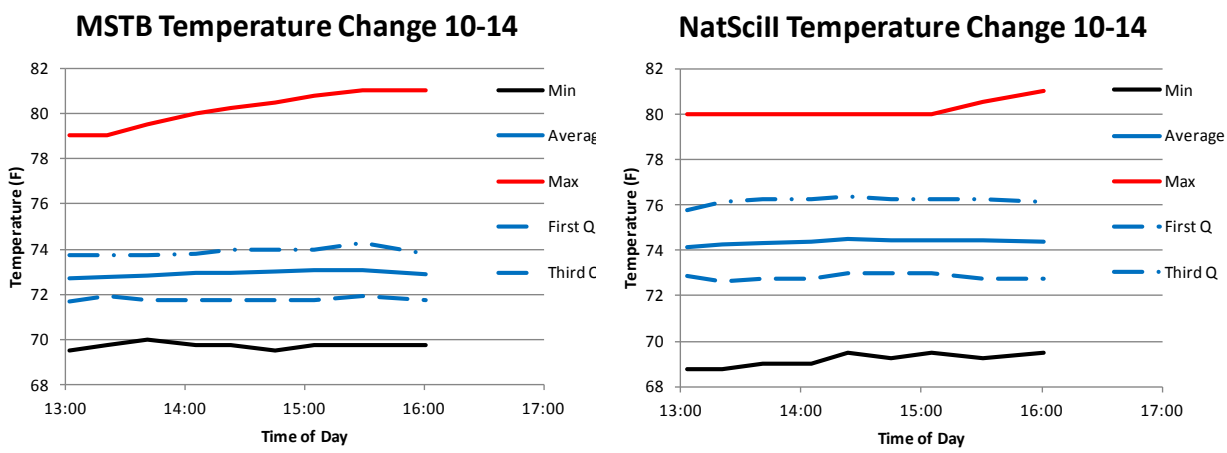

The changes in temperature were acceptable but they indicate that the zones with the highest temperatures were unable to maintain their temperature due to a lack of airflow. Because the buildings were running with static pressure reset control prior to the fan limitation, one primary concern regarding the indoor air quality of the building space was whether the spaces were able to meet minimum ventilation requirements. During the test, the amount of air supplied to a sample of spaces was verified at the Building Automation System and, in some spaces, at the exit of the duct. The following tables summarize the actual and minimum levels of flow to these spaces.

Table 35: Actual flow rates and minimum rates of flow for a sample of spaces in MSTB

MSTB 10-14 VAV Flow Rates				
Time	**Room**	**Flow (CFM)**	**Min Flow (CFM)**	**Room Type**
13:57	139	724	720	Office
13:58	141	304	300	Phys Lecture
13:58	124	1024	300	Classroom
13:59	114	704	200	Classroom
13:59	136	238	232	Phys Prep

14:00	143	432	700	Phys Fab
14:00	100	680	900	Lobby
14:01	101	400	400	Phys Electronic
14:01	103	232	232	Math Lobby
14:02	103H	136	140	Office
14:02	105	1076	1440	Phys Lab
14:03	103M	148	152	Meeting Room
14:03	111	184	180	Phys PC Lab
14:04	112	636	44	Mac Class
14:04	283	456	440	Office
14:04	269	380	160	Office
14:07	265	500	500	Office
14:08	253	484	160	Office
14:08	241	812	380	Office
14:09	256	116	116	Meeting Room
14:09	254	196	200	Reading Room
14:10	242	0	112	Research Computer Class
14:10	246G	476	252	Office
14:11	246	912	800	TA Suite
14:11	201	456	500	Bio Med Class
14:12	210	1024	420	OAC Class
14:12	205	376	128	Reception
14:13	205E	276	152	Office
14:13	217	412	152	Office
14:13	220	256	260	EE Class
14:14	224	500	260	EE Class
14:14	229	764	700	Office
14:15	224A	132	128	Office

Table 36: Actual flow rates and minimum rates of flow for a sample of spaces NatSci II

NatSciII 10-14 VAV Flow Rates				
Time	**Room**	**Flow (CFM)**	**Min Flow (CFM)**	**Room Type**
13:26	1202	124	112	Office
13:26	1000	0	900	Lobby
13:27	1201	1392	700	Conference
13:28	1102	180	180	Main

13:28	1120	132	132	Reception
13:29	1139	172	172	Assistant's Office
13:30	2000	976	320	Lobby
13:30	2202	108	112	Kitchen
13:31	2210	228	160	Work Room
13:32	2201	352	592	Conference
13:32	2121	196	112	Mail
13:33	2139	0	200	Office
13:34	2145	0	200	Office
13:35	3000	320	324	Lobby
13:35	3120	76	200	Reception
13:36	3202	112	112	Kitchen
13:36	3212	200	200	Lab Tech
13:37	3201	592	592	Conference
13:38	3101	400	552	Office
13:39	3145	296	172	Office
13:39	3141	0	240	Work Room
13:40	3260	164	164	Open Office
13:43	4000	0	324	Lobby
13:44	4202	148	112	Kitchen
13:44	4210	0	80	Work Room
13:44	4201	604	592	Conference
13:45	4101	404	420	Office
13:45	4141	0	224	Work Room
13:45	4131	60	100	Office
13:46	5000	400	244	Lobby
13:46	5120	68	72	Reception
13:47	5133	204	200	Office
13:47	5211	272	220	Office
13:48	5212	204	200	Work Room

Table 37: cell shading key

Minimal ventilation
Over-ventilated
Slightly under-ventilated
Under-ventilated

Not ventilated (acc. to BAS)

The lack of flow observed in about 20% of the sampled spaces in NatSciII caused some worries, and casted doubt that the damper motor actuators were actually damaged. These spaces were identified to Facilities to ensure that they were on the list to be tested and/or replaced. However, during normal operation 19 of the total 91 boxes are either 100% open or closed, indicating that up to 21% of NatSciII's VAV motor actuators could be in need of replacement. The ventilation performance of the third turn-down test needs to be verified by the VAV-space correlation but initial observations indicate that the 30% turn-down is feasible in MSTB, but perhaps not in NatSciII. Furthermore, it demonstrates that MSTB can operate at static pressures as low as 0.1 inches of water column and maintain temperatures and flows at reasonable levels. Therefore, Cadmus has recommended to Facilities that they modify the static pressure control set point from 0.5 to 0.1 or 0.2 inches of water column at MSTB during setback hours (6:00pm – 6:00am) as a measure of energy efficiency.

6.4.5.4. Full Building Response to Demand Response Tests

Given the levels of pre-existing fan power for the air handling units in MSTB and the office portion of NatSciII, the full building power trends show small relative energy savings during the event. When applied to buildings whose air handlers compose a more significant portion of total building energy use, the tested DR strategies will show much greater overall savings. Below, the total building power trends are shown for MSTB and NatSciII for each of the testing days.

Figure 221: Total building power compared to baseline consumption for each of the three DR testing days

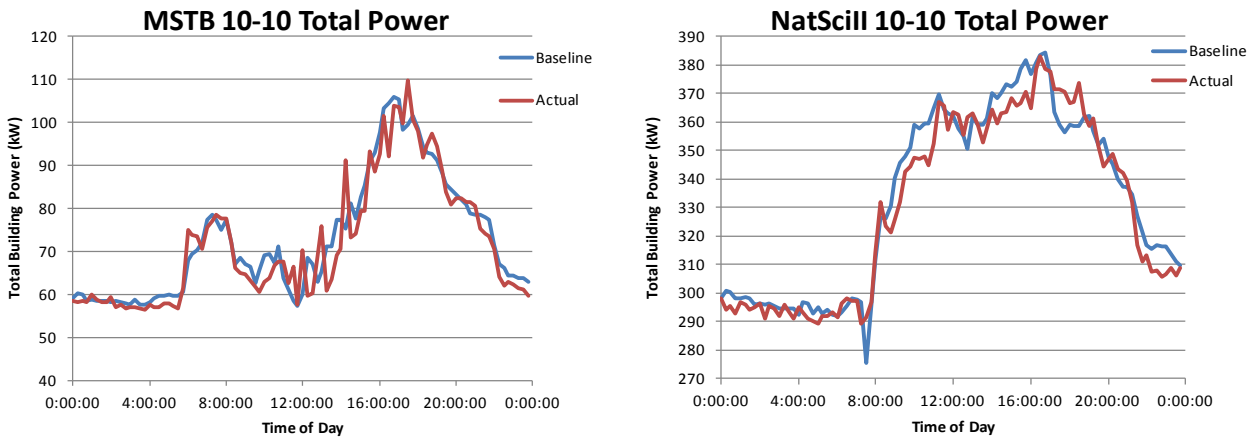

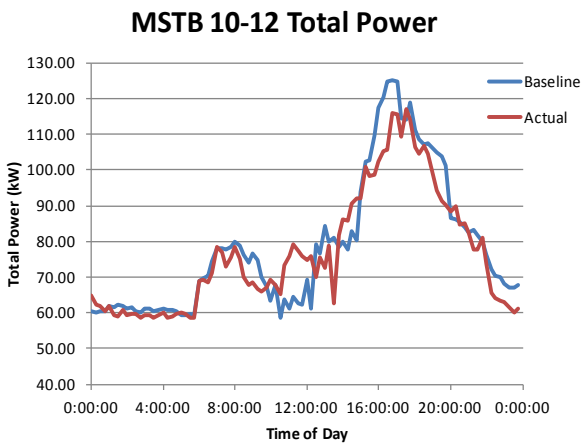

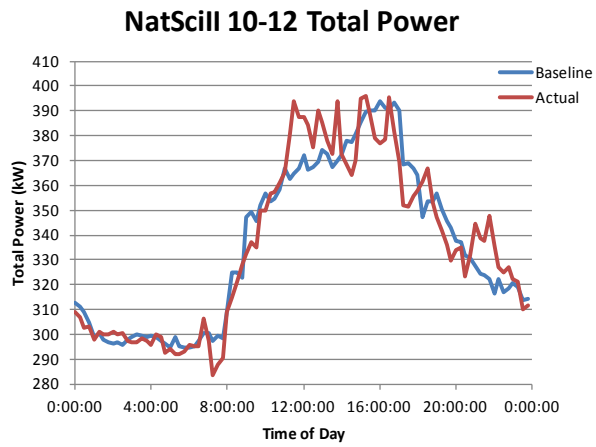

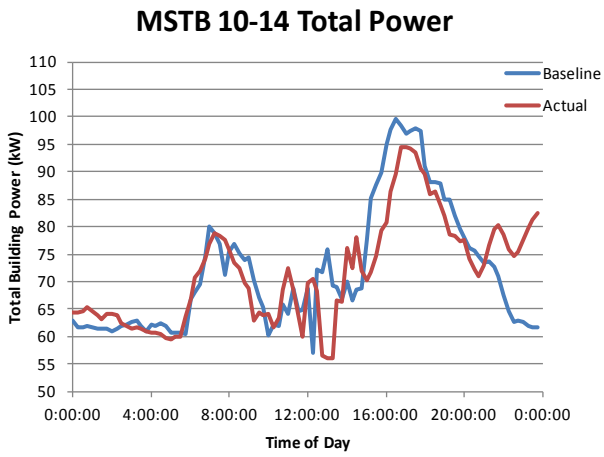

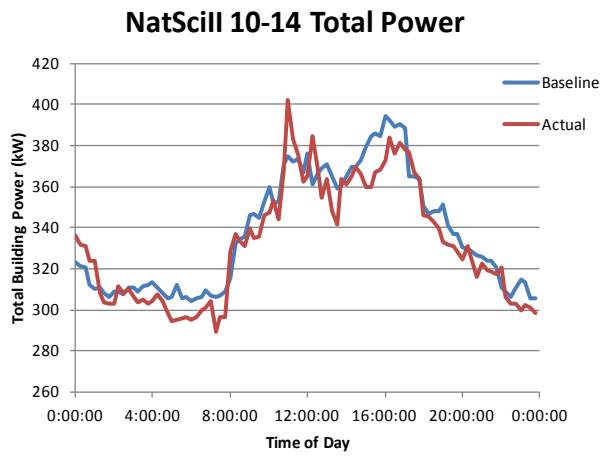

6.4.5.5. Conclusions from Demand Response Experiments

The demand response tests demonstrated that significant savings could be achieved with pre-cooling to 70°F as well as 15% and 30% fan turn-downs. The pre-cooling experiment showed that MSTB's supply fan power could be reduced by as much as 60% during the demand response period with a 53% increase in fan power during the pre-cooling period and a 3°F rise in average temperature. For NatSciII, however, the supply fan power could only be reduced by 13% and was increased by 71% during the pre-cooling period. Average temperatures were only raised by 1°F, so a supply air temperature reset or fan speed limitation could be applied at NatSciII in conjunction with the pre-cooling to further limit peak demand.

The fan turn-downs achieved similar percentage savings to the pre-cooling experiment with little to no adverse effects on zone temperatures and ventilation. The average fan speed reductions are shown below with their corresponding power reductions:

Table 38: Average fan power reductions observed for each fan speed reduction applied

Fan Speed Red. (%)	Fan Power Red. (%)

13.3%	30.7%
14.7%	35.9%
16.5%	44.9%
21.8%	52.7%
27%	62%
31.4%	63.8%

Figure 222: Fan turn-down speed fraction plotted against power fraction with power fit applied

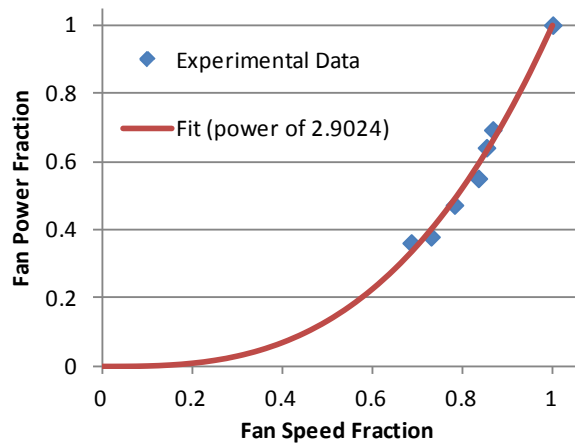

Fitting to the empirical results, the non-ideal power relationship between fan speed and power consumption is determined to be

$$\frac{P_2}{P_1} = \left(\frac{n_2}{n_1}\right)^{2.9024} \tag{3}$$

where P_2/P_1 is the fan power fraction of normal operation and n_2/n_1 is the fan speed fraction of normal operation. These results verify the theoretical power relationship between fan speed and fan power, and provide an empirical basis for evaluating fan power reduction to any modeled fan turn-down.

The application of the demand response tests at MSTB and NatSciII also resulted in the identification of an appropriate energy efficiency measure at MSTB – namely that significantly lower static pressure reset control set points could be applied at MSTB on a regular basis. This discovery highlights the nature of the relationship between demand response and energy efficiency measures. Certain strategies might be applicable to some buildings as DR measures and others as EE measures depending on the specific building design's ability to carry out the strategy on a regular, non-temporary basis. Therefore, in evaluating DR measures, appropriate EE measures may be identified for the specific building and vice versa.

Most importantly, however, the demand response tests demonstrated that different levels of pre-cooling and fan turn-down are appropriate for different buildings. When a DR event occurs,

buildings will need to have pre-designed HVAC response strategies specific to their building design and system capabilities. Depending on the building design, certain strategies may be significantly more potent demand shedders than others. While specified community-wide DR strategies would achieve reductions in peak demand, they can only be designed to the level of the worst-performing HVAC system. In order to optimize the total potential for community-scale implementation of HVAC demand response, it would be necessary to apply a set of DR testing procedures to each applicable building.

Task 6.4.6. Demand Response Model Characterization

Based on the technical literature review, the modeled demand response results and the empirical demand response experiments, the following demand response characterizations were integrated into the HiGRID model. The total capacity of each demand response strategy was determined under current operations and under the modified energy-efficient baseline. Supply fan reductions of 30% and lighting reductions of 45% were not enabled under the energy-efficient condition due to the fact that they did not satisfy the ventilation and comfort requirements of these measures.

Demand Response Strategy	Reduction	Gross Capacity	Gross Capacity: *Energy Efficiency*
Lighting Reduction	15%	711 kW	560 kW
	30%	1,423 kW	1,120 kW
	45%	2,134 kW	
Pre-Cool	NA	834 kW	652 kW
Fan Turn-Down	10%	414 kW	324 kW
	20%	750 kW	587 kW
	30%	1,015 kW	

6.4.6.1. Lighting Reduction

To characterize the lighting demand response potentials for lighting reductions, flat scaling factors were applied to the campus lighting end-use profile based upon the required demand response reduction. Depending on the required lighting reduction, the % reduction by dimming (achievable with reasonable levels of occupant satisfaction) and the % penetration into the total building stock will be defined. The lighting power during a demand response event is defined as:

$$P_{DR} = P_{baseline} * [1 - (\%Penetration) * (\%Reduction)] \quad (4)$$

6.4.6.2. Pre-Cool

Three different data sources were consulted to characterize the power reduction for pre-cooling demand response. The primary calibration points for the fan power characterization were

drawn from the empirical tests conducted on October 12th, 2011. The trends recorded for the NatSciII building indicated that zones in a number of places were unable to meet ventilation or temperature set points, running out of control and invalidating the test results for a functional characterization. Therefore, the average 52% increase in fan power during the pre-cooling period and the average 53% fan power reduction during the temperature reset period for MSTB's two air handlers were used as reference points for the scaling factors applied to baseline fan power consumption.

The Demand Response Quick Assessment Tool (DRQAT) was tested for pre-cooling using prototypical defaults for a medium-mass office building in a suburban area in Irvine. Results for days of various temperature were compared to baseline performance and the exponential temperature dependence of the % increase and % reduction were determined. The temperature differentials were analyzed in reference to the space temperature set points during the pre-cooling and temperature reset periods respectively. Thus, the temperature dependence of the pre-cooling performance was modeled:

$$P_{pre-cool} = P_{baseline} * \left(1 + 0.52\left(\frac{T_{out} - 70°\text{F}}{28°\text{F}}\right)^{0.489}\right) \quad (5)$$

$$P_{temp\ reset} = P_{baseline} * \left(1 - 0.53\left(\frac{T_{out} - 77°\text{F}}{21°\text{F}}\right)^{0.563}\right) \quad (6)$$

The NatSciII and MSTB buildings were modeled and calibrated in eQUEST, and pre-cooling schedules were applied to the buildings parametrically and the results compared to the baseline fan power. The eQUEST results were used to characterize the time-dependence of fan power with respect to the durations of the pre-cooling and temperature reset periods.

As expected, the average increase in fan power during the pre-cooling period was lower for tests with longer durations (more shock to the fan power is absorbed in the first hour or two and later in the day) for the NatSciII model. However, due to the nature of the finely calibrated air handler model, MSTB's increase in fan power did not follow the same trend and was omitted from the calibration of the time-dependence of pre-cooling.

The average reduction in fan power during the temperature reset period was also lower for runs with longer reset durations due to the engagement of temperature control systems over time. The exponential fit was estimated based on the affected model results and applied to the empirically-determined scaling factor. The final relationships are:

$$P_{pre-cool} = P_{baseline} * \left(1 + 0.52\left(\frac{T_{out} - 70°\text{F}}{28°\text{F}}\right)^{0.489}\left(\frac{2hr}{Duration}\right)^{0.168}\right) \quad (7)$$

$$P_{temp\ reset} = P_{baseline} * \left(1 - 0.53\left(\frac{T_{out} - 77°\text{F}}{21°\text{F}}\right)^{0.563}\left(\frac{4hr}{Duration}\right)^{0.383}\right) \quad (8)$$

6.4.6.3. Fan Turn-Down

To characterize the potential for reduction in fan power by fan speed limitation, flat scaling factors were applied to the campus controllable fan energy end-use profile based upon the required demand response reduction. Depending on the required HVAC reduction, the % fan speed reduction (up to 30% achievable to remain above minimum ventilation levels) and the % penetration into the total building stock was defined.

As determined with respect to empirical fan turn-down tests, the experimental fan power relationship applicable to buildings at UCI is given by:

$$Fan\ Power_2 = Fan\ Power_1 \left(\frac{Fan\ Speed_2}{Fan\ Speed_1}\right)^{2.9} \tag{9}$$

Therefore, the fan turn-down power during a demand response event is defined as:

$$P_{DR} = P_{baseline} * [1 - (\%Penetration) * (1 - (1 - \%Reduction)^{2.9})] \tag{10}$$

6.4.6.4. Demand Response Cost Analysis

The following cost table describes the inputs and assumptions used to determine the cost of implementing each demand response strategy, broken out by cost component. These inputs were normalized by the total demand reduction and used in the HiGRID model to determine the cost-effectiveness of the various solutions for integrating a higher penetration of renewable energy sources.

Table 39: Demand Response Cost Breakdown for each Technology

DR Measure	Cost Component	Cost	Justification
Lighting Reduction	Installed Cost	$50/ballast	Current ballast costs (recent projects). 10 ballasts/kW
	Fixed O&M Cost	$30/ballast/yr	Current ballast costs & lifespans. 10 ballasts/kW
	Variable O&M Cost	$0.50/kWh	Demand response compensation (DBP)
Pre-Cool	Programming Cost	$48,000 total	8 weeks of programming time at $120/hour
	Equipment Cost	$15,000 total	Fixed expenses for additional controls hardware
	Fixed O&M Cost	$12,000/yr	Two weeks of controls maintenance at $120/hour
	Variable O&M Cost	$0.40/s.f.	Current air balancing costs (recent projects)
Fan Turn-Down	Programming Cost	$48,000 total	8 weeks of programming time at $120/hour
	Equipment Cost	$15,000 total	Fixed expenses for additional controls hardware
	Fixed O&M Cost	$6,000/yr	One week of controls maintenance at $120/hour

	Variable O&M Cost	$0.50/kWh	Demand response compensation (DBP)

6.4.6.5. Conclusions

Significant research has been accomplished in modeling, calibrating, and extrapolating building load end-uses across the UCI campus as well as defining and characterizing demand response strategies and energy efficiency measures. The total extrapolated power consumption has been calibrated to real UCI data and the energy efficiency and demand response measures characterizations have been finalized, so the HiGRID code can be engaged to parametrically test specific load reduction strategies for buildings to effectively respond to variations in high-penetration renewable supply and demand.

- Experiments are performed to examine pre-cooling and fan turndown strategies at MSTB and Nat Sci II buildings.
    - Different levels of pre-cooling and fan turn-down are appropriate for different buildings.
    - Energy shifting and savings can be achieved with pre-cooling with only a minimal rise in temperature.
    - Significant savings can be achieved with 15% and 30% fan turndown with little to no adverse effects on zone temperature.
- Several DR strategies are explored including lighting reduction, ventilation fan turndown, pre-cooling, and night purge.
    - Night Purge: Fan and chiller power decrease during the day but a large amount of energy is required to power the fan during the night and longer cooling periods did not appear to significantly reduce afternoon load.
    - Pre-cool: Total energy savings were small, yet it allowed for shaping of the load.
    - Fan Turndown: Reduces demand significantly and instantaneously.
    - Lighting Reduction: Reduces demand significantly and instantaneously.
- Fan turndown and lighting reduction are the most beneficial of the techniques explored.
- Based on the experiments performed expressions are developed to calculate the controllable portion of lighting and ventilation fan based on desired DR penetration and reduction.

Task 6.4.7. Further Research beyond RESCO

Given limitations in the scope of RESCO's Building Design and Operation research and technologies that currently are economically feasible, this research leaves some interesting and

promising power utilization strategies untouched. The strategies that have been discussed to improve energy efficiency and demand response are to be applied solely to commercial buildings in this study, primarily because it is commercial buildings for which it will be financially viable in coming years. Some large industrial loads and time-flexible process loads can be practically implemented in demand response, and future studies should focus more deeply on these possibilities. In residential applications, plug load control has the potential to reduce up to 13% of total residential electric demand by just eliminating unused standby loads. Finally, because the study is primarily focused on the moderate climate of Irvine, CA, demand response and energy efficiency strategies such as night purging and thermal energy storage are relatively insignificant, whereas in climates with large diurnal swings and extreme weather, they could be used as potent demand reducing measures.

Task 6.4.8. References

Akashi, Y., Neches, J., Detectability and Acceptability of Illuminance Reduction for Load Shedding. Journal of the Illuminating Engineering Society. 2004.

ANSI/ASHRAE Standard 55 – 2010. Table 5.2.5.2. Page 14.

Ardehali, M., Smith, T., Evaluation of HVAC System Operational Strategies for Commercial Buildings. Energy Conservation and Management. Vol 38, No 3. 1997.

Huang, Y.J., et al., 481 Prototypical Commercial Buildings for 20 Urban Market Areas. Lawrence Berkeley National Laboratory. 1991.

Motegi, et al. Introduction to Commercial Building Control Strategies and Techniques for Demand Response. DRRC, LBNL. 2007.

Newsham, G.R., Brit, B., Demand-Responsive Lighting – A Field Study. NRCC-53233. 2010

Piette, M.A., Development and Evaluation of Fully Automated Demand Response in Large Commercial Facilities. Lawrence Berkeley National Laboratory. CEC PIER program. 2005.

Snook, J., Papamichael, K., Koyle, B., Pierce, M., Lighting California's Future: Cost-Effective Demand Response. Public Interest Energy Research Program. California Energy Commission. March 2011.

Yin, et al. Study on Auto-DR and Pre-cooling of Commercial Buildings with Thermal Mass in California. LBNL. 2010.

Appendix F:Task 7:
Holistic Energy Integration and Management

TABLE OF CONTENTS

Task 7.1. Intermittent Renewable Integration and Management Modeling F-5

Task 7.1.1. Background F-5

7.1.1.1. Conventional Generation F-6

7.1.1.2. Renewable Generation F-7

7.1.1.3. System Resource Mixtures F-8

7.1.1.4. Grid Modeling Techniques F-11

7.1.1.5. Historical Operation F-15

Task 7.1.2. Holistic Grid Resource Integration and Deployment (HiGRID) tool F-17

7.1.2.1. Approach F-19

Task 7.1.3. Renewable Module F-21

7.1.3.1. Wind Modeling F-21

7.1.3.2. Solar Power Modeling F-27

7.1.3.3. Calculation of in-plane beam irradiation and in-plane reflected irradiation F-30

7.1.3.4. Fixed-Plate Solar Photovoltaic Module F-31

7.1.3.5. Solar Thermal Power Modeling F-37

7.1.3.6. Other Renewables F-46

Task 7.1.4. Dispatchable Load Module F-47

7.1.4.1. Common Models F-47

7.1.4.2. UCI Specific Models F-47

7.1.4.3. California Specific Models F-47

7.1.4.4. Hydroelectric Generation Module F-48

7.1.4.5. Hydroelectric Verification F-52

Task 7.1.5. Baseload Generation Module F-55

7.1.5.1. Baseload Verification F-57

Task 7.1.6. Balance Generation Module F-58

7.1.6.1. UCI Community Model F-58

7.1.6.2. California Model F-68

7.1.6.3. Balance Generation Verification F-81

Task 7.1.7. Emissions F-82

Task 7.1.8. Curtailment F-83

Task 7.1.9. Cost-of-Generation Module F-84

Task 7.1.10. California Model Verification Summary F-93

Task 7.1.11. Conclusions F-95

Task 7.1.12. References F-96

Task 7.2. Renewable Integration Results F-99

Task 7.2.1. UCI Community Results F-100

7.2.1.1. Description of Cases F-100

7.2.1.2. Technical Analysis – GT Trips Allowed F-104

7.2.1.3. Technical Analysis – GT Trips Not Allowed F-128

Task 7.2.2. California Results F-141

7.2.2.1. Spanning Results F-141

7.2.2.2. Solar Thermal Trough Power Plant Results F-158

7.2.2.3. Balance Fleet Installed Capacity Results F-165

7.2.2.4. Generator Flexibility Results F-167

Task 7.2.3. California Optimization Results F-180

7.2.3.1. Optimization Technique F-180

7.2.3.2. Increment Study F-181

7.2.3.3. Optimization Results F-184

7.2.3.4. Conclusions F-192

Task 7.3. Complementary Technology Integration and Management F-192

Task 7.3.1. Energy Storage F-193

7.3.1.1. Introduction F-193

7.3.1.2. Approach F-195

7.3.1.3. UCI Campus Results F-195

7.3.1.4. California Results F-212

Task 7.3.2. Energy Efficiency F-249

7.3.2.1. Approach F-249

7.3.2.2. ResultsF-250

7.3.2.3. Energy Efficiency Cases – Lighting and HVAC F-252

7.3.2.4. Energy Efficiency Cases – HVAC Only F-260

7.3.2.5. Energy Efficiency Cases – Different Renewable Rollout Strategies F-262

Task 7.3.3. Demand Response F-265

7.3.3.1. Approach F-265

7.3.3.2. UCI Campus Results F-268

7.3.3.3. California Results F-284

Task 7.3.4. Electric transportation F-297

7.3.4.2. Approach F-299

7.3.4.3. UCI Campus Results F-300

7.3.4.4. California Results F-315

Task 7.3.5. References F-337

Task 7.4. Solar Heating in RESCO F-337

Task 7.4.1. Model of Residential Water Solar Heater F-341

Task 7.4.2. Model Central Solar Heating System F-341

Task 7.4.3. Evaluate Hot Water Storage F-344

Task 7.4.4. Comparison of combined heat and power and centralized solar heating F-348

Task 7.4.5. Conclusions F-349

Task 7.4.6. References F-350

Task 7.5. UCI Campus Roadmap Toward RESCO Vision F-351

Task 7.6. Generic Community Roadmap Toward RESCO Vision F-351

The authors consider task 7 as the heart of the RESCO program. All of the models and results developed in the other tasks support the goal of this task, which is to determine the most effective and cost-competitive techniques for the UCI campus and generic communities to achieve high penetrations of renewables. It is important that not only can UCI achieve high renewable penetrations but that neighboring communities can do the same. As such, the impacts of renewable generation on the operation of grid resources serving UCI and generic communities are considered during this analysis, which provides valuable insight into what communities can do to support the state of California reaching its renewable goals.

This section presents an integrated model for both UCI and generic communities. Subsequent results are shown for a variety of scenarios including spanning results, which explore the implications for different types of renewable resources, and complementary technology results which explore the impacts of energy efficiency, demand response, energy storage and electric vehicles on the system.

Task 7.1. Intermittent Renewable Integration and Management Modeling

In recent years, California legislation has passed legislation that will require changes to the electric power system. Assembly Bill 32 (AB32), voted into law in 2006, requires that the state of California reduce GHG emissions to 1990 levels by 2020 (AB32, 2005-06). Additionally, Senate Bill 1078 was passed thereby establishing California's Renewable Portfolio Standard (RPS). The RPS establishes renewable penetration goals for the state. Senate Bill 107 in 2006 and Senate Bill 2 in 2011 both accelerate the RPS timetable and require that retail sales of renewable electricity constitute 20% of all electricity sales within California by 2013, 25% by 2016 and 33% by 2020 (SB107, 2005-06; SB1078, 2001-02; SB2, 2011-12). The current renewable percentage of electric sales for the major investor-owned utilities in California is 17% (CPUC, 2011). While some of the renewable resources, such as geothermal and biomass, have predictable or even dispatchable behavior, other renewable resources, including wind and solar, are less predictable and present unique integration challenges but are crucial to meeting the RPS goals (CEC-150-2011-02, 2001). Additionally, renewable resources vary with respect to cost competitiveness as compared to traditional generators (AEO, 2008). Understanding the optimal technical and economic deployment strategies is essential to ensuring reliable, low-cost provision of electricity while meeting AB32 and California's RPS goals. This section presents a model to explore the technical and economic constraints of integrating renewable resources into both the UCI micro-grid and generic communities in California while considering the impacts on the larger system-wide grid.

Task 7.1.1. Background

To correctly assess the implications of renewable resources for communities and the larger grid alike, it is important to understand how the grid dispatches resources to provide electricity for communities to import while maintaining system reliability.

The predominant resources used to generate electricity include natural gas, nuclear, coal, conventional hydroelectric, hydroelectric pumped-storage, petroleum liquids, petroleum coke,

other gasses, biomass, geothermal, solar, wind, tidal and wave. Each of these resources can be used in a different subset of generation equipment. A breakdown of the major resource mix serving California for 2005 is depicted in Figure 223.

Figure 223: Breakdown of Net Generation Meeting California's Electricity Demand for 2005

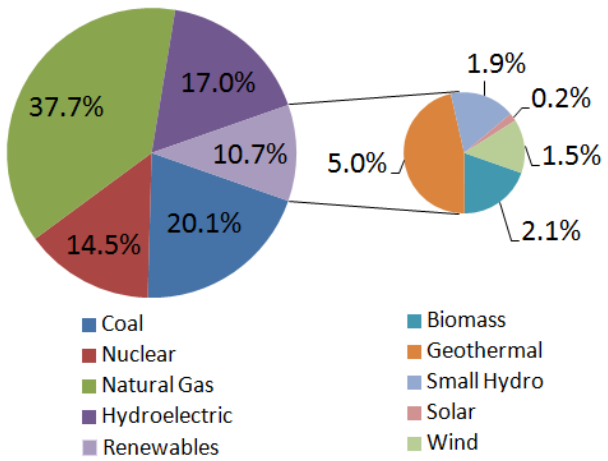

Source: CEC-200-2009-010

Net generation consists of in-state generation, plus imports, less exports. The largest contributor to the generation mixture in California is natural gas at 37.7% of which 88.4% is generated in-state. Coal is the second largest contributor, of which 48.6% was from in-state generation. Additionally, imports are separated by the region they come from (i.e., Northwest and Southwest). Over 42% of the total coal imports come from the Southwest. Hydroelectric is the next largest contributor at 18.9%. Conventional hydroelectric provided 17.0% and small hydro provided 1.9% of the net generation to California. Pumped-storage hydro is the last type of hydro and due to the efficiency penalty with pumping up water and then generating with it later, the resulting generation appears negative since it takes more electricity to pump the water into an upper reservoir than can be extracted from it for generation. The fourth largest contributor to California generation is from Nuclear. There are two operating nuclear power stations in California, San Onofre and Diablo Canyon, which provide 86.7% of the nuclear generation. Most of the remaining generation comes from the Southwest (i.e., 11.7% of total nuclear generation). The last category is renewables, which consist of biomass (both wood derived and other), geothermal, small hydro, solar and wind. In 2005 renewable generation accounted for 10.7% of net generation.

7.1.1.1. Conventional Generation

The major types of equipment for conventional resources include combustion turbines, steam turbines, and water turbines. Natural gas or any other gas can be used as the feedstock for combustion turbines, steam turbines, or a hybrid system, i.e., combined-cycle, that integrates both combustion and steam turbines to increase efficiency. Coal, nuclear and geothermal resources typically use steam turbines to convert the heat from either combustion or nuclear reactions to electricity. Hydroelectricity is separated into three categories, conventional hydro,

small hydro and hydro pumped-storage. The distinction between conventional hydro and small hydro is defined in Senate Bill 1078 as generation facilities that do not require a "… new or increased appropriation or diversion of water…" (SB1078, 2001-02). Pumped-storage provides generation just as does conventional hydro; however, it has the capability to bring the water from a lower reservoir to an upper reservoir for storage until it will be used. This is particularly useful for shifting electric demand to a more desirable time, as will be shown herein.

Each technology is operated differently based on its technical ability and the preferred economic behavior. Figure 224 presents the major generation technologies from the Western Energy Crisis data set released by the Federal Energy Regulatory Commission (FERC). This data set contains the hourly resolved generation profile of every in-state generator for the years of 2000 and 2001. All generators of each type are collected and their total generation is shown in Figure 224.

Figure 224: Resource Use Breakdown for Four Consecutive Days of California In-State Generation

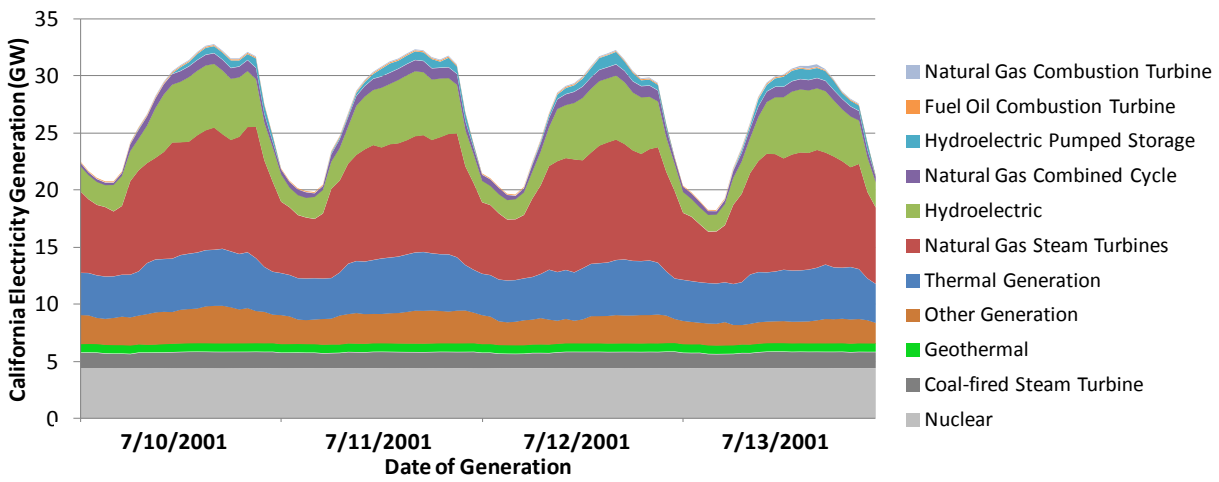

Source: FERC Western Energy Crisis Database, 2002

7.1.1.2. Renewable Generation

According to the California Energy Commission (CEC) in its CEC-150-2011-002 report released in 2011, there is a significant technical potential for renewable generation in California. In the report, calculations of the technical or theoretical potential of renewable generating capacity consider geographical restrictions, both natural and climatic parameters, and technical limitations (i.e., energy conversion efficiencies). Currently installed solar, wind, wave and tidal power represent a very small fraction of the technical potential at 0.0075%, 2.6%, 0.0% and 0.0%, respectively. Meanwhile, small hydro, geothermal and biomass are relatively close to their theoretical potential with 28.2%, 64.0%, and 53.9%, respectively, of the capacity already installed (CEC-150-2011-02, 2011).

Table 40: Technical Renewable Capacity Potential Predictions

Renewable Generation Technologies	Installed Capacity (MW, 2010)	Potential Capacity (MW)
Concentrating Solar Power	1,356	1,061,362
Photovoltaic		17,000,000
On-shore Wind	2,819	34,000
Off-shore Wind		75,400
Wave and Tidal	demonstrations	32,763
Biomass	1,077	3,820
Small Hydro	1,380	2,158
Geothermal	2,600	4,825
Total	9,232	18,214,328

Source: CEC-150-2011-02

The values presented in the report are power capacity so the ability for these resources to provide electrical energy will depend on their capacity factor. The CEC report does not discriminate the efficacy with which the installed capacity can provide electrical energy to the grid. The capacity factors for renewables are very site dependent for example the solar radiation in a region with many overcast days will be less than a similar region with less overcast days. The present research will provide the link between power capacity and resulting energy capacity. Changes in the capacity factor with increasing installed power capacity are important to consider as the sites with highest capacity factor will be taken first leaving sites that will provide progressively less and less energy for the same installed capacity.

7.1.1.3. System Resource Mixtures

The generation mixture and total generation requirement changes with each year. Figure 225 shows California's generation from 2002 to 2010. Notice that the generation does not significantly increase over this 8 year period with the largest increase of 2.39% from 2006 to 2007.

Figure 225: Breakdown of Total California Generation for 2002 to 2010

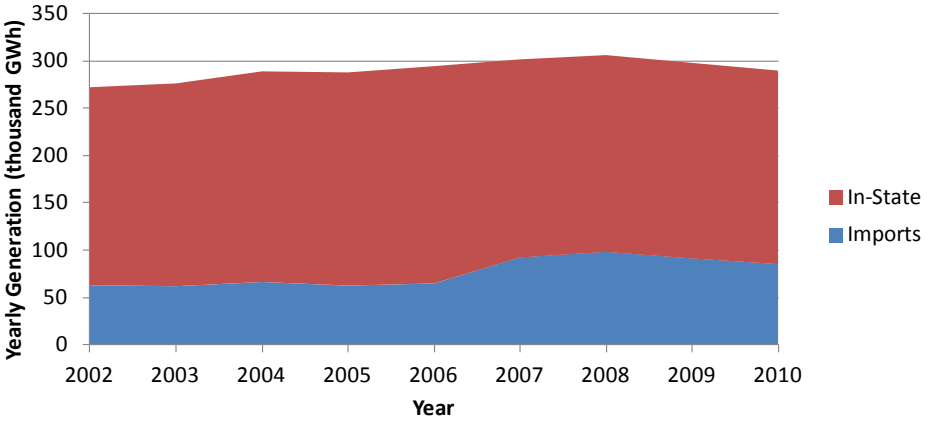

Source: CEC-200-2009-010

The generation mixture for California from 2002 to 2010 is presented in Figure 226. All the categories are similar except for the "Unspecified" group, which was started in 2009 and contains import generation from unknown generation sources. The apparent decline in coal generation between 2008 and 2009 appears to be largely the result of the 2009 changes in how imported generation is categorized. California has issued a moratorium on all new nuclear production facilities so the relative contribution stays the same as no new plants are installed. The state also does not allow new coal plants and has been slowly reducing the coal generation in-state.

Figure 226: Breakdown of Generation Meeting California's Electricity Demand for 2002 to 2010

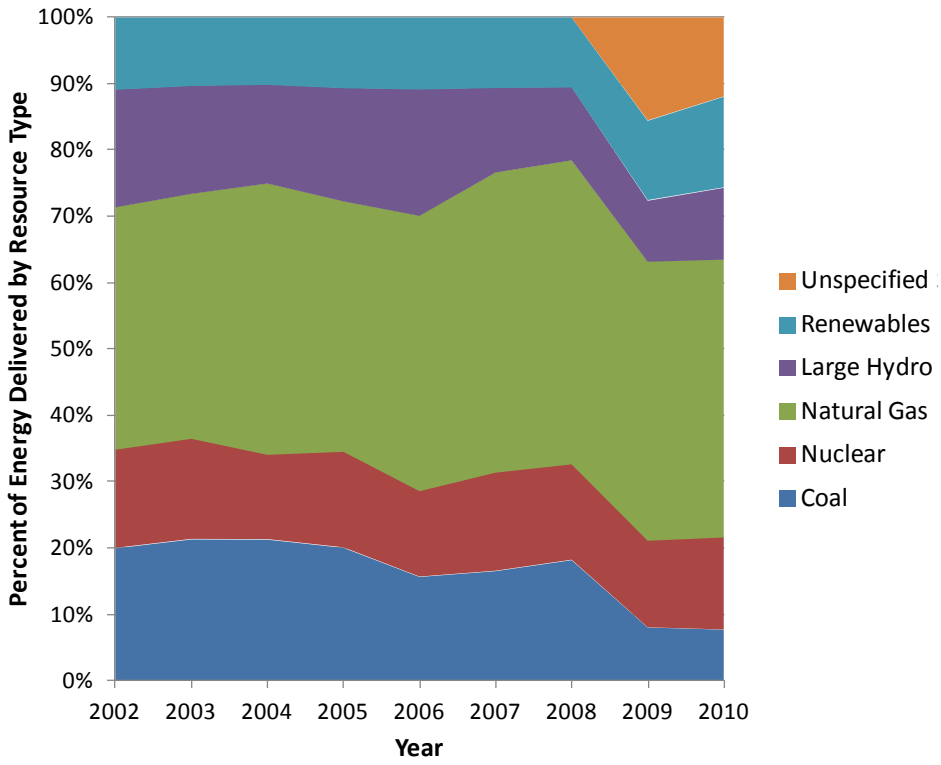

Source: CEC-200-2009-010

When compared to the entire United States, California has much less coal generation and much more natural gas and renewable generation than the national average. Another interesting difference is the contribution to generation from biomass as the leading renewable generation technology.

Figure 227: Breakdown of Generation Meeting the United States' Electricity Demand for 2008

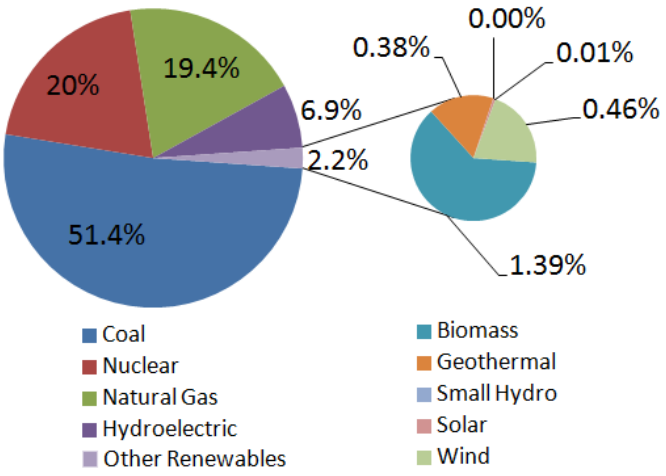

Source: EIA-906, EIA-920, EIA-923

With the leadership of AB32 and the RPS, California is making significant strides toward meeting their renewable goals. The purpose of this work is to explore the implications as the renewable penetration continues to increase and to identify technologies, operating strategies, etc. that can complement renewable generation and mitigate any challenges that arise.

7.1.1.4. Grid Modeling Techniques

The term "Grid Modeling" can represent a variety of topics. Grid models can include applications ranging from resource planning and projection to seasonal resource adequacy to operation and reliability; each with their own specialties and associated benefits and shortcomings. Additionally, understanding the scope and time resolution requirements is very important when selecting a methodology to pursue.

7.1.1.4.1. Applications

There are many models available to explore the effects of changes in an energy system. Changes can include types of equipment (i.e., renewables, energy storage, electric transportation) or the operation strategy for current or retrofitted equipment (i.e., once-through cooling, optimized economic dispatch). The types of applications can be generally separated into the following three categories. Oftentimes a single model can address multiple applications.

- Long-term Projection
- Dispatch
    - Market-based
    - Statistical

- Network / Load flow

Long-term projection models, are oftentimes used to model load-growth and the resources that will meet the additional load, policy or regulation implications or other long-term phenomenon that affect energy systems. These models typically span multiple years or even decades. These analyses can additionally be used to determine resource adequacy for a grid system, which is done quarterly in California, to ensure that enough there is enough generating capacity to provide electricity to customers on the highest consumption day of the year.

Dispatch models predict the behavior of generation or demand signals. These signals can include a wide array of sources and are developed using a number of different techniques. The most common techniques for determining dispatch of generation signals are Market-based or statistical methods. While both techniques require historical data for tuning and verification of the models, the amount of data required is dependent on the technique selected.

Statistical methods rely on the statistical patterns of a reference signal to predict the behavior of that signal for different criteria. One example developed by Jansen et.al. uses an hourly average for every day of a given month to determine an approximate hourly generation profile for that month (Jansen, 2010), then, scales the generation for that month to the typical monthly capacity factor (i.e., average power generated divided by the potential maximum power generation). This process is repeated for every month of the year to develop a model that exhibits daily load changes and seasonal generation patterns. Another technique is to develop a set of load-duration curves that can be used to predict the load shape for a given period. The EMPS, MARKAL/TIMES, STREAM and WASP models are examples of tools that use such an approach. Connolly's 2009 paper entitled "A review of computer tools for analyzing the integration of renewable energy into various energy systems" provides a good review of different computer models for exploring each of these applications (Connolly, 2010).

Market-based grid dispatch models reconstruct the market using information about market components (e.g., day ahead, hour ahead, real-time, ancillary service), market participants and constraints of participants (e.g., maximum and minimum operating power, ramp rate, minimum operating time) . In the United States, Independent System Operators (ISOs) modify and manage the market according to regulation established by the FERC. To perform a market-based analysis, information must be gathered from both ISOs and FERC; however, depending on the desired granularity of the analysis the amount of data required can be very different. Some tools like ENPEP-BALANCE and NEMS have a time resolution of one year. Thus, they cannot capture the dynamics that occur on the hourly or sub-hourly timescale and as such will not generally require market data at that resolution (ANL, 2012; EIA, 2003). PLEXOS, Ventyx Market Analytics and Concorda MAPS model market dynamics on the hourly and sub-hourly timescale and can calculate locational marginal prices and a wealth of additional information for each market modeled (e.g., day ahead, real-time) (PLEXOS, 2012; GE MAPS, 2011; VENTYX, 2012). The price of electricity, generator dispatch and reserve requirements to maintain grid reliability is accomplished with a combination of unit commitment and economic dispatch analyses, where unit commitment determines which generation units should turn on or off and

when they should do so and economic dispatch ensures that the most cost effective solution is reached by determining the power set point for each generator at every time point.

Network/Load flow models simulate the transmission and distribution characteristics of a grid system. They can be highly detailed to include substations and transmission line characteristics or less detailed to look at the bulk electricity flow for import and export. There is a particular need for this type of modeling with the increase in renewable electricity generation and advanced technologies including electric vehicles and energy storage that can change the conditions that transformers operate. Several studies have been performed within California including one specifically looking at transmission requirements from the Renewable Energy Transmission Initiative (RETI) (RETI-1000-2010-002-F, 2010), two renewable integration reports from the California Independent System Operator (CAISO) and GE Energy Consulting (GE Energy Consulting, 2010 (CAISO 20%); Loutan, 2007) and a few other integration studies from the CEC, KEMA and the National Renewable Energy Laboratory (CEC-500-2010-010, 2010; CEC-500-2007-081, 2007; GE Energy Consulting, 2010 (WWSIS)).

7.1.1.4.2. Scope

Models can be generally classified as either large-scale or small-scale. Large-scale grid models can encompass regional, state, provincial, national or global perspectives. Coincident with geographic scope, consideration must be included for the quantity and type of equipment included. This can include hundreds or thousands of generators, miles of transmission lines, electrical infrastructure equipment, load and generation aggregators, energy efficiency measures and demand requirements as well as reserves to maintain reliability. Small-scale analyses predominantly focus on communities, islands or single-sites. In terms of equipment small-scale can include large equipment and all the elements of large-scale analyses but are typically less in number (e.g., from thousands of generators to dozens). Additionally, small-scale can include distributed generation that may not be considered in large-scale analyses since generation less than one megawatt is not included in CEC energy almanac capacity calculations and is small enough that it can be absorbed into a community's demand (CEC-200-2009-010, 2009).

It is recognized that both types of analyses provide valuable information and with California's push to increase renewables it is imperative that work be continued in both groups; however, particularly for the small-scale analyses, it is important that implications on the larger grid be considered. It is not sufficient to say that the balance between generation and demand can be absorbed by the grid, especially under high renewable scenarios where increased intermittency will propagate to the interconnection between the customer and the utility.

7.1.1.4.3. Time Resolution

Grid models heavily rely on collected data for verification and selection of time resolution is very important for grid-scale modeling. The time resolution greatly affects the time and resources required to both develop a model, as well as run the model. Most applications of grid modeling have a typical time resolution used when modeling. Long-term projection analyses typically use months as the highest resolution and years or multiple years for the lowest.

Dispatch strategies can use as low as daily or even monthly resolution (e.g., hydro modeling) and extend to as high as sub-minute. There is a significant amount of hourly data available so many dispatch models use hourly values; however, to accurately model ramping characteristics of generators and regulation, resolution should be *at least* at 5 minutes to mirror the 5-minute market parameters used by ISOs like in California (CAISO, 2012 (OASIS)). Network/Load flow analyses time resolutions are similar to dispatch and are often used with dispatch models to assess the minimal cost generating solution that does not violate transmission congestion constraints. The lowest resolution for Network/Load flow analyses can be on the order of days for state wide import/export information or to the sub-second level for looking at frequency regulation on the grid. As collected data becomes more resolved there is an ever increasing challenge with storing, manipulating and distributing that data. These topics should be considered when assessing the appropriate time resolution for each modeling application.

Figure 228: Considerations at Different Time Resolutions

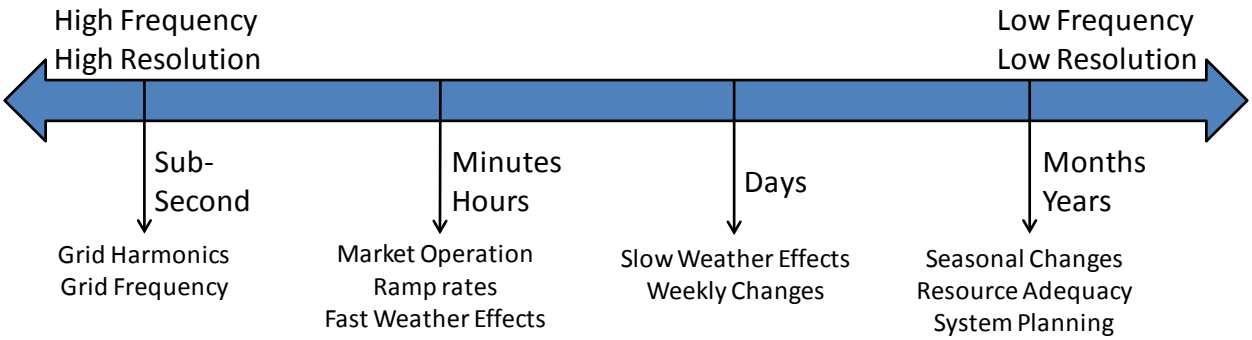

Grid modeling applications require different types and amounts of data. For instance long-term projection analyses require relatively coarse data on the yearly operation totals, which is often available in the United States from the Energy Information Administration (EIA), or other agency, including state entities (e.g., Air Resources Board, CEC). However, dispatch and network/load flow analyses can require a much more substantial set of data depending on the scale of the analyses. For instance, a single or islanded community may include less than ten generators and not include any import or export from outside sources while to model the state of California would require hundreds of generators, and dozens of transmissions lines that allow for import and export with outside sources. The accuracy of grid models can be highly dependent on the source and quantity of data acquired. Primary proprietors of these data are Independent Service Operators (ISOs), electricity and gas utilities and government agencies. While these groups currently provide access to some of the data, continued and increasing support from these agencies is an important part of stimulating additional research and innovation for grid modeling.

Historically, 15 minute time resolution has been used when collecting data for utility billing but as more renewables are installed on the grid and the value of flexible generation increases higher resolution data could provide significant benefit to customers, market participants, and research institutions alike. Higher resolution data can enable additional markets and rate structures that can provide incentives for communities to reduce, shift or shape their electrical

consumption to more appropriately reflect the needs of the grid with the goal of reducing the cost of generating electricity. With higher resolution data, institutions conducting research on grid operations, just as with billing, can explore advanced markets and operating strategies for equipment.

7.1.1.5. Historical Operation

The electricity generation and distribution system must continually generate electricity to balance the electricity demand on the grid. In addition there must be additional generation capable of turning on quickly or changing its load point to ensure that grid stability is maintained. To do this those who own generation, own and operate transmission lines and serve customers work together with balancing authorities to ensure sufficient generation capacity is acquired to meet the peak daily generation as well as the oscillations in demand. These balancing authorities are under the jurisdiction of the FERC and the North American Electric Reliability Corporation (NERC). Additionally, in California, the California Public Utilities Commission (CPUC) works with investor owned utilities to establish the rates charged to the customers. With the cooperation of FERC, NERC, CPUC and CAISO, electricity can be provided reliably at a low cost to the ratepayer.

An electricity market is in place in California to balance generation and consumption of electricity along with additional services to ensure reliability (i.e., ancillary services). This market was partially deregulated in 1996 and was further deregulated in 2009 with the "Market Redesign and Technology Upgrade" (MRTU) program in an effort to lower cost of electricity to the ratepayers.

7.1.1.5.1. Market Structure

It is recognized from many sources in the literature that increase in renewables will cause changes in the need for specific types of market resources (GE Energy Consulting, 2010 (CAISO 20%); Loutan, 2007; CEC-500-2010-010, 2010; CEC-500-2007-081, 2007; GE Energy Consulting, 2010 (WWSIS)) so an understanding of the market is essential when modeling either the technical or economic impacts of renewables. This section provides a description of the California energy markets. Additional details can be gathered from the literature including the previously mentioned reports and a variety of additional material on CAISO's website (http://www.caiso.com/).

The energy market settles demand, import, export and generation of electricity on a variety of timescales including day ahead, hour ahead and real-time. The day-ahead is a prediction of the needed generation as calculated approximately 14 hours before the desired operating day. Similarly, the hour-ahead is a prediction around 75 minutes ahead of the beginning of the hour and the real-time economic dispatch program provides information every 5 minutes to support balancing of the generation and load. Figure 229 and Figure 230 present examples of the differences between each market. The differences between a day-ahead and hour-ahead prediction (i.e., hour-ahead adjustment) are depicted in Figure 229, while the differences between the hour-ahead and real-time markets (i.e., load-following) are illustrated in Figure 230. Notice that all market results can be larger or smaller than the other markets meaning that

there is a need to purchase capacity to increase or decrease the resulting signal. In the case of the real-time signal this is called load-following up and load-following down. Using just the day-ahead, hour-ahead and real-time markets the final load does not equal the actual load. This is accomplished with regulation.

Figure 229: Day-ahead to Hour-ahead Scheduling with Hour Adjustment Example

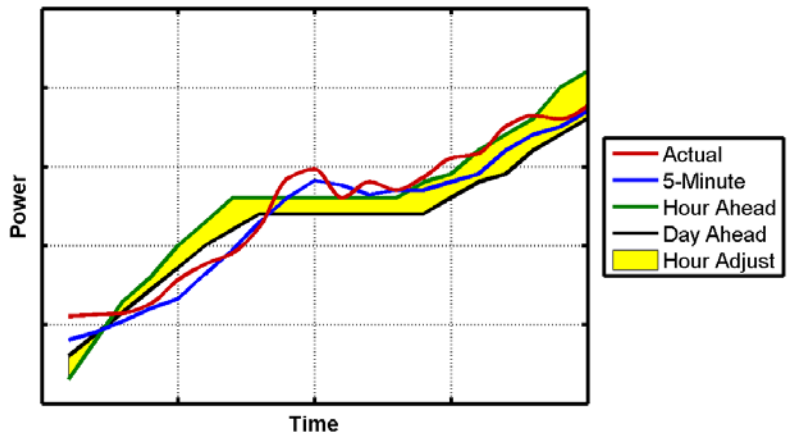

Figure 230: Hour-ahead to Real-time Scheduling with Load-following Adjustment Example

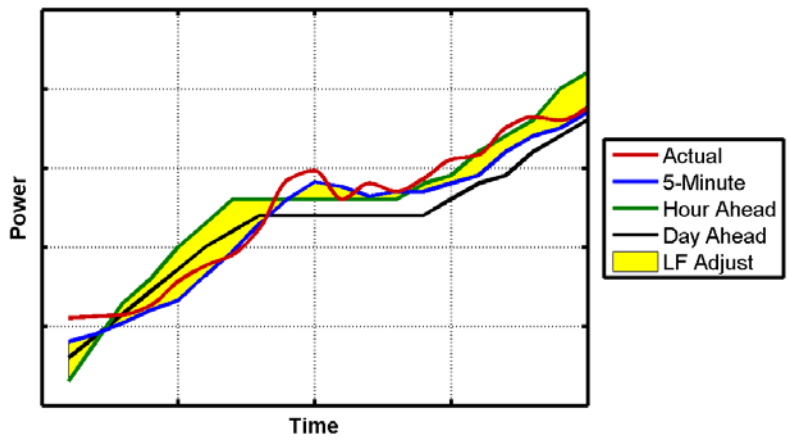

In addition to energy markets there are ancillary services markets, which include regulation up, regulation down, spinning reserve, and non-spinning reserve. These markets have a similar bidding time-scale as energy markets: two day-ahead, day-ahead and hour-ahead. By bidding into an hour-ahead market, for instance, a generator pledges that it can provide the given resource during that hour. Regulation normally provides the final, second-by-second balancing of the load to ensure that the generation matches the demand. This is accomplished with an automatic generation control (AGC) signal. Each generator can bid a portion of their generation into regulation up or down. Based on the AGC signal that each generator is sent, the generator

must turn up or down in response to the signal. This ensures that grid frequency is maintained while generation compensates for load demand. Figure 231 presents an example case where regulation up and down meets the remaining difference between the real-time market and the actual demand.

Figure 231: Example Regulation up and Down Acquisition

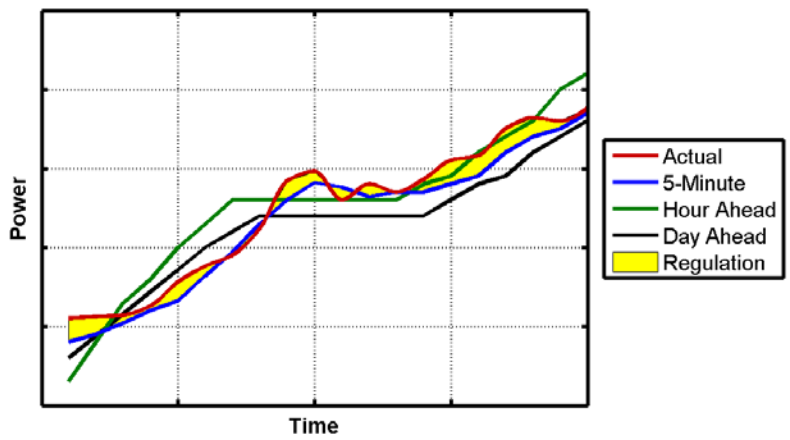

Spinning reserve, non-spinning reserve and any other reserves are called in the event that regulation does not have enough capacity to prevent demand/generation imbalance. This can occur for several reasons including load scheduling errors, supply scheduling errors and generator outages. Spinning reserves are resources that are online, synchronized to the grid and can meet electric demand in a short amount of time (i.e., 10 minutes for CAISO). Non-spinning reserves are resources that are off-line but can be turned on, synchronized and ramping to meet load within 10 minutes. Additionally, non-spinning reserve must be able to provide electricity for two hours. Selection of reserve needs is based on the system-wide operating reserves and must be settled for each node of the system.

The energy and ancillary service markets are the current mechanism for the balancing authority to meet system loads on a second-by-second basis while providing reliability in the event of scheduling imbalances or generator failures. Intermittent generation can change the requirements of the grid to maintain reliability. In the CAISO 20% renewable penetration study, CAISO explores additional adjustments to the real-time and regulation markets that are likely to result from higher renewable penetrations (GE Energy Consulting, 2010 (CAISO 20%)).

Task 7.1.2. Holistic Grid Resource Integration and Deployment (HiGRID) tool

The unpredictable behavior of intermittent renewables like solar and wind power makes their integration into the grid challenging, because energy and reliability requirements must be simultaneously satisfied. A significant amount of effort has been focused on exploring this topic as is evidenced by work commissioned by the CAISO (including two Integration of Renewable Resources reports (Loutan, 2007; GE Energy Consulting, 2010 (CAISO 20%)), and the

CEC (including a report from KEMA (CEC-500-2010-010, 2010), and the Intermittency Analysis Project (CEC-500-2007-081, 2007) as well as for the entire United States (GE Energy Consulting, 2010 (WWSIS)) and groups like the International Panel on Climate Change (IPCC) that have prepared a review of renewable technologies and the implications for their integration into grid systems (Ralph, 2011).

The research presented herein leverages lessons learned from the previous studies to capture the behavior of renewable resources and implications for integration into larger grid systems, while providing reliable and secure power. Past studies are used to advise this work on the appropriate strategy to incorporate operational changes from renewables relating to spinning and non-spinning reserve margin and regulation, for example. In this way, highly detailed grid modeling information can be incorporated while additional and more diverse analyses can be performed.

Various tools have been developed to analyze energy systems and grid load balancing. Connolly et al. compiled a list of the most prominent energy analysis tools available (Connolly, 2010). The available tools and their features were cross-referenced against the requirements for this work to establish a list of appropriate tools. Of the 37 tools explored by Connolly, only four tools include modeling of conventional generation and renewable energy and the ability to explore energy storage and demand response at a sufficiently high resolution (1 hour or less) to capture the interactions between each resource. The four tools are HOMER, H_2RES, TRNSYS and EnergyPLAN. The first three of those tools are best suited for small, remote or islanded systems (Instituto Superior Técnico, 2012; HOMER, 2012; University of Wisconsin-Madison, 2012) and while they can be stretched to analyze larger systems, they do not have the functionality required to incorporate many generators and many resource types adequately. EnergyPLAN has many of the desired features including hydroelectric modeling and the ability to look at transportation constraints and CO_2 emissions for large systems; however, one of the main goals of this work is to explore the implications that installing renewables have on the other generators including baseload, peakers and load-followers. While EnergyPLAN separates the geothermal and nuclear from other generation, it lumps the remaining generation (predominantly coal and natural gas) into a single category (Aalborg University, 2012). A key finding from this work is understanding how intermittent renewables impact small communities like UCI but also understand implications for larger communities. Thus, none of the reviewed tools could adequately provide this functionality.

There are a number of tools that have the potential to model the breakdown between every type of generation both renewable and non-renewable and the externalities associated with increasing renewable penetrations, including PLEXOS, VENTYX and GE MAPS (Energy Exemplar, 2012; Asea Brown Boveri, 2012; GE Energy Consulting, 2011 (GE MAPS)). These tools use a combination of unit commitment and economic dispatch to calculate the price of electricity and generator dispatch for a large grid system. PLEXOS and VENTYX include both types of constraints, while GE MAPS considers mainly generator operating constraints and transmission constraints to a lesser degree. All three of the above-mentioned tools rely on data from the utilities and grid system operators and operate on hourly or sub-hourly timescales and are able to represent a diverse range of renewable generation coupled with conventional

generation, while simultaneously satisfying reliability requirements. However, they are not very amenable to implementation of complementary technologies (e.g., energy storage, demand response, electric transportation), except when the response of complementary technologies directly aligns with market bidding strategies. In an effort to maintain the required functionality and have greater control over the implementation of complementary technologies, an energy modeling tool was developed that allows for analyses of large (i.e., statewide, regional) and small (i.e., city or community) systems on an hourly timescale.

7.1.2.1. Approach

The HiGRID model was developed to resolve interaction between different types of generation (e.g., gas turbines, combined cycle plants, renewable generators) and supporting equipment (e.g., electric energy storage, thermal energy storage, chillers) in an effort to evaluate the cost and benefit of installing renewable generation capacity. The time resolution is hourly and the analysis area can range in size from a college campus like UCI, to a city, to the entire state of California depending on the input data.

If applied to UCI this modeling tool has the ability to integrate local and regional renewable resources, the UCI cogeneration plant (i.e., combined cycle), chillers, boilers, thermal energy storage and other complementary technologies. Similarly, if this tool is applied to the state of California, it has the capability to integrate conventional generators including coal, nuclear, natural gas and hydroelectric with an array of both local and regional renewable generation.

Each resource data signal is temporally coincident, because many of the phenomenon that contribute to intermittencies of renewable generation like wind speed, temperature, cloud cover, and humidity also affect the operation of other generators as well. For example, on a cloudy day, while the solar power generated will be lower than on a clear day, the ambient temperature will be lower as well and can result in lower cooling needs. Figure 232 presents the flow diagram for the HiGRID model. The systems modeled in HiGRID are composed of generation resources, both renewable and conventional, and additional complementary resources such as energy storage and demand side-management strategies that all act to balance the system by not only providing sufficient energy to meet the demand, but in the case of the model for California, also must provide sufficient generation reserves to maintain reliability.

Figure 232: HiGRID Model Flowchart

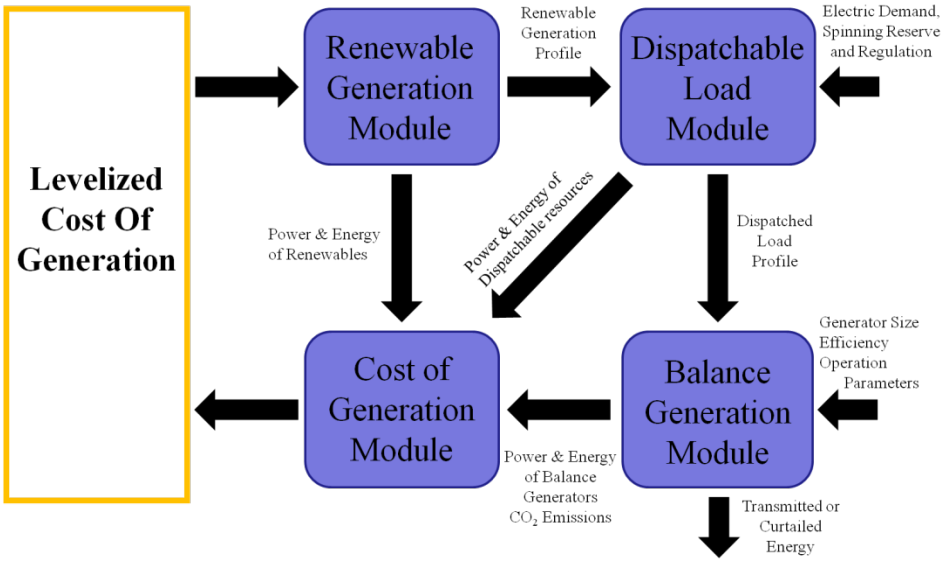

The first module described is the "Renewable Generation Module," which includes all renewable generation except for geothermal, small-hydro and biomass/biogas. Next, the "Dispatchable Load Module" will be described, which includes complementary technologies and hydroelectric for use with the California model. Then, the "Balance Generation Module," which is required to meet the remaining energy that cannot be met by the previous generation and includes a combined cycle plant, in the case of the UCI model and many gas turbine, steam turbine and combined cycle plants for the California model. Lastly, the "Cost of Generation Module" takes inputs from all other modules and calculates the portfolio levelized cost of electricity (LCOE) that is used to compare different technology mixtures and different renewable penetrations in the HiGRID tool.

A summary of the technologies used in the HiGRID model are presented in Table 41. The HiGRID tool can operate for UCI and for the entire state of California and has separate technologies available for each adaptation. Notice that for UCI, resources are included that are both local to the campus as well as regionally generated and transmitted. Similarly, the California model includes regional resources as well as distributed wind and solar generation plants (i.e., local to the point of use). UCI resolves the heating and cooling demand using the thermal energy storage tank, chillers, boilers and the combined cycle generator, while the California model does not include the heating and cooling demand. Additionally, UCI must import some electricity, while the California model includes all generation, in-state or out-of-state, that is required to meet the electric demand.

Table 41: Technologies Included in HiGRID Tool

HiGRID Technologies		
	UCI Model	**California Model**
Renewable Generation	Local and regional wind Local fixed axis PV	Local and regional wind Local fixed axis PV

	Regional 1-axis tracking PV	Regional 1-axis tracking PV Regional 2-axis tracking PV Solar Thermal Trough Plant Small-hydro Geothermal Biomass/Biogas
Dispatchable Generation	Energy Efficiency Demand Response Electric Transportation Electrical Energy Storage Thermal Energy Storage Chillers Boilers	Demand Response Electric Transportation Electrical Energy Storage
Baseload Generation		Nuclear Coal Geothermal
Balance Generation	Imports from Grid Combined Cycle Plant	Gas Turbines Combined Cycles

Task 7.1.3. Renewable Module

7.1.3.1. Wind Modeling

Wind generation is modeled following the process described in Tarroja (2011), with data drawn from the Wind Integration Dataset developed by 3TIER in collaboration with the National Renewable Energy Laboratory (NREL) (Wilcox, 2007). The area selected to support this work includes predominantly California with resources in Tehachapi, Beaumont, Palmdale and Granite Mountain as well as wind resources in Colorado and New Mexico. Resource limitations are calculated from the WWSIS study and from the Renewable Energy Transmission Initiative report released in May 2010 that describes the current status and future possibilities for siting renewables and transmitting their power (GE Energy Consulting, 2010 (WWSIS); Black and Veatch, 2010).

7.1.3.1.1. Wind Data Acquisition and Characteristics

The specific wind power dataset implemented for use in the HiGRID code has been obtained from the NREL Western Wind and Solar Integration Study (GE Energy Consulting, 2010 (WWSIS)). Specifically, the data provides 10-minute temporal wind speed and potential power for 2 km by 2 km potential wind sites across the United States for the years of 2004 through 2006. Each 4 kilometer square area of the study is assumed to contain ten 3-MW wind turbines. Details of the dataset compilation are presented in the report presented by the 3TIER Corporation (3TIER, 2007). The electrical power output and effective wind speed from each of these areas were determined using a mesoscale model developed by 3TIER Corporation. The

performance curve for the Vestas V90 3.0 MW turbine was used to determine the wind power output potential of each block.

The WWSI interface is presented in Figure 233. Each wind turbine icon or colored dot on the map is representative of one 2 km by 2 km block. The icon colors represent the effective capacity factor of each block at a height of 100 meters as shown in Table 42.

Table 42: Legend for NREL Wind Potential Map Capacity Factors

Icon Color	Wind Potential Capacity Factor
Blue	< 25%
Green	25 – 30%
Yellow	30 – 35%
Orange	35 – 40%
Red	> 40%

Figure 233: NREL Wind Farm Potential Map in the Tehachapi region of Southern California

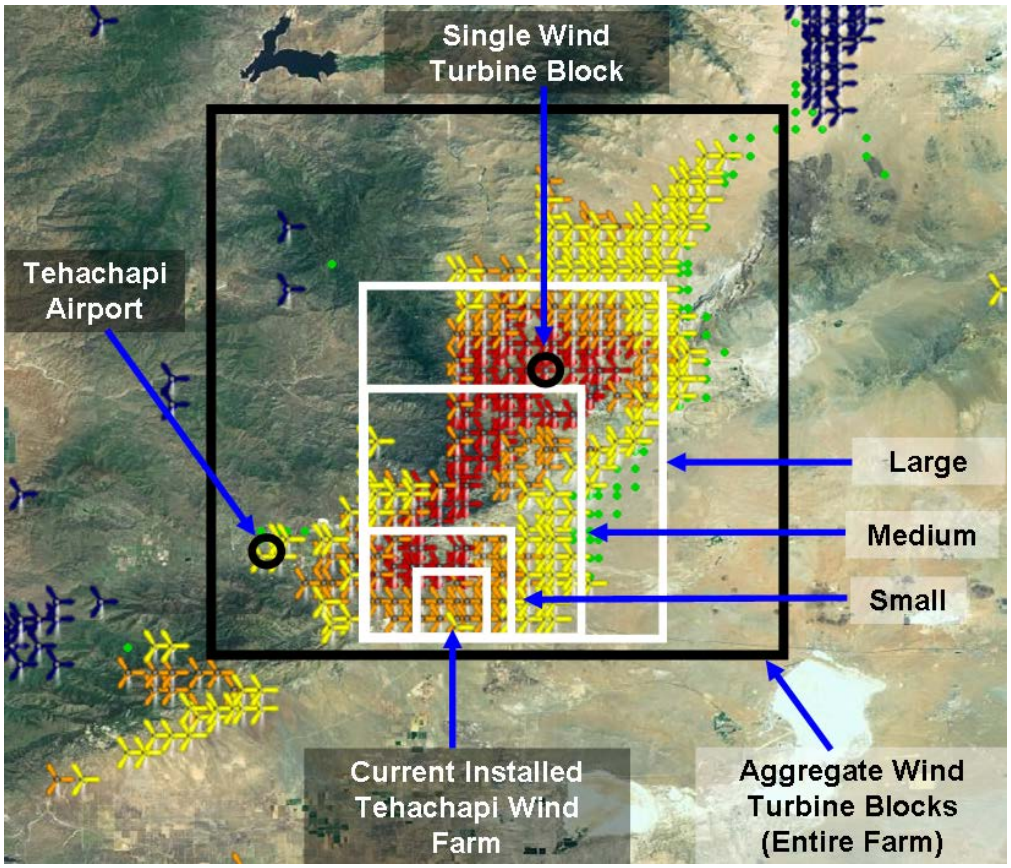

Source: NREL Western Wind Dataset (3TIER, 2007)

Data from the NREL model was obtained and uploaded into a SQL data server, where it was extracted by applying SQL database queries. One example of such a query was used to effectively calculate the sum of the power output from every turbine block confined to a user-specified set of spatial coordinates (latitude and longitude). This approach allows the user to obtain wind power data for different sizes of wind farms within the potential map or for the entire potential map itself, allowing the evaluation of wind power characteristics as a function farm size. In addition, simple mathematical operations such as calculating the mean and standard deviation of each wind turbine block were also implemented using an SQL query. Note that due to the nature of the source data, the effect of wind turbine shadowing is not captured.

The use of this dataset allowed the synthesis of wind power profiles of different spatial scales, capturing an important aspect of modeling wind power on the transmission grid from a dynamic energy balancing perspective. The wind power output and severity of power fluctuations exhibited by a single wind turbine or small group of tightly clustered wind turbines is significantly higher than that exhibited by a large, spatially diverse group of turbines. An example of wind power profiles composed from data representing different scale measurements is presented in Figure 234 and Figure 235:

Figure 234: Power profiles of different wind farm representation: 4th week of July 2005

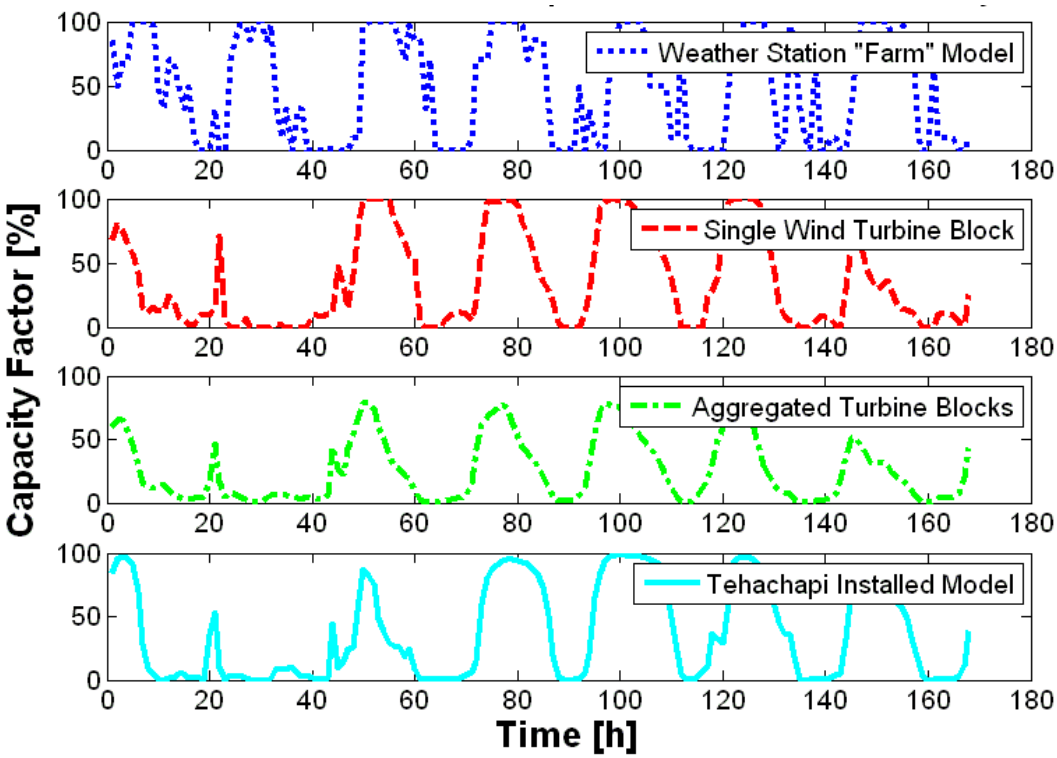

Figure 235: Corresponding Power Spectral Density Relative to Aggregated Turbine Block Model

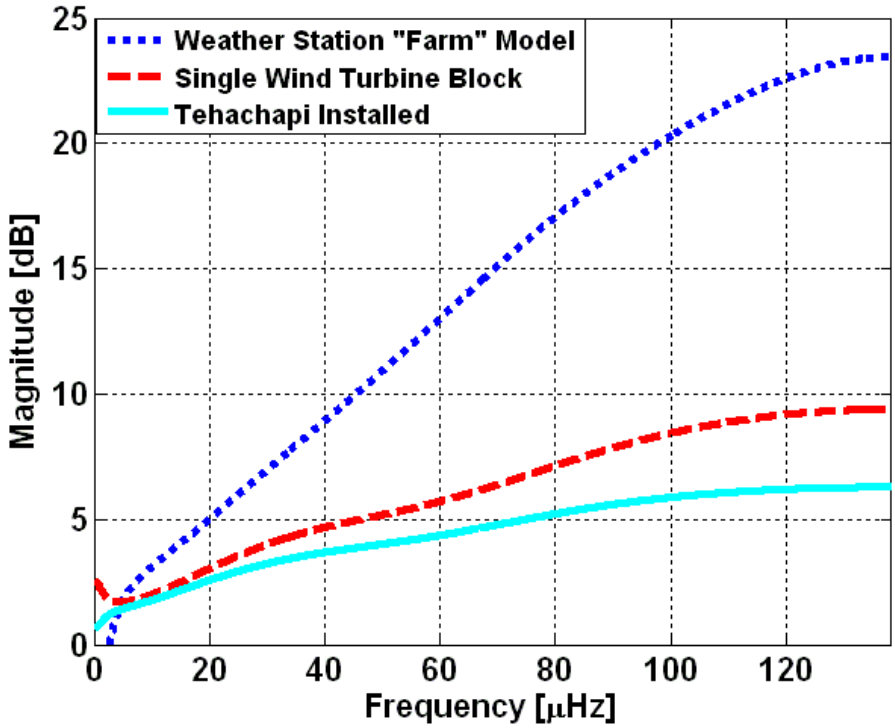

Four different scales of wind power measurements were compared:

1. A wind farm subject to measured wind speeds from Tehachapi airport weather data (single point) using the Vestas V90 Power curve
2. A single wind turbine block (10 simulated turbines)
3. The currently installed Tehachapi wind farm (small simulated wind farm)
4. Aggregated wind turbine blocks (large simulated wind farm), as shown in Figure 233.

From Figure 235, it is apparent that wind power output determined from data measured at smaller scales yield more severe power dynamics than that determined from large-scale data. This is due to the buffering effects of the rotational inertia of the turbine and the finite time required for a prevailing wind disturbance to propagate or affect the total output of a wind farm covering a large land area. A separate, power spectral density-based analysis examined and confirmed the presence of these effects, and the use of this particular dataset allows these characteristics to be taken into account when creating wind power profiles for the HiGRID model.

Wind power data was also obtained for different geographical regions, allowing the evaluation of wind power characteristics as a function of regional dispersion, allowing the use of decoupled wind power profiles to create aggregate wind power profiles in addition to simple scaling of power output. Total wind power profiles created in this manner is believed to be

more representative of the actual wind power profile that will be imposed onto the transmission grid since wind power potential from different regions is likely to be utilized.

In the HiGRID tool, the total nameplate capacity of wind farms installed in different regions is specified as an input, and the resulting time-resolved power profile (MW vs. time) is calculated and produced from computation of the wind data.

7.1.3.1.2. Wind Data Verification

Wind power results from this model were verified against wind power production data from the currently installed Tehachapi wind farm as shown in Figure 236 and Figure 237. Data was provided by Southern California Edison (Hawkins, 2007) for the month of April 2005 as presented by the solid lines. The modeled wind profile which encompasses the currently installed wind farm is dubbed the "Tehachapi installed model", and is based upon the known areas of wind turbine installations and estimates of wind turbine sizes and dispersion in this region as coupled to the NREL 2 km X 2 km wind data (3TIER, 2007). Model results are presented as dashed lines for the representative days (Figure 236) and average diurnal profiles (Figure 237). The Tehachapi installed model well represents the daily production from April, 2005 and the average diurnal profile (Vick, 2008) for the month of July 2005. In addition, the current analyses considered the entire Tehachapi area wind resource as represented by the "Tehachapi Farm Model" curve, and shown for comparison in Figure 237.

Figure 236: Current Wind Power Model Verification with Tehachapi Wind Farm Power Data for April 2005

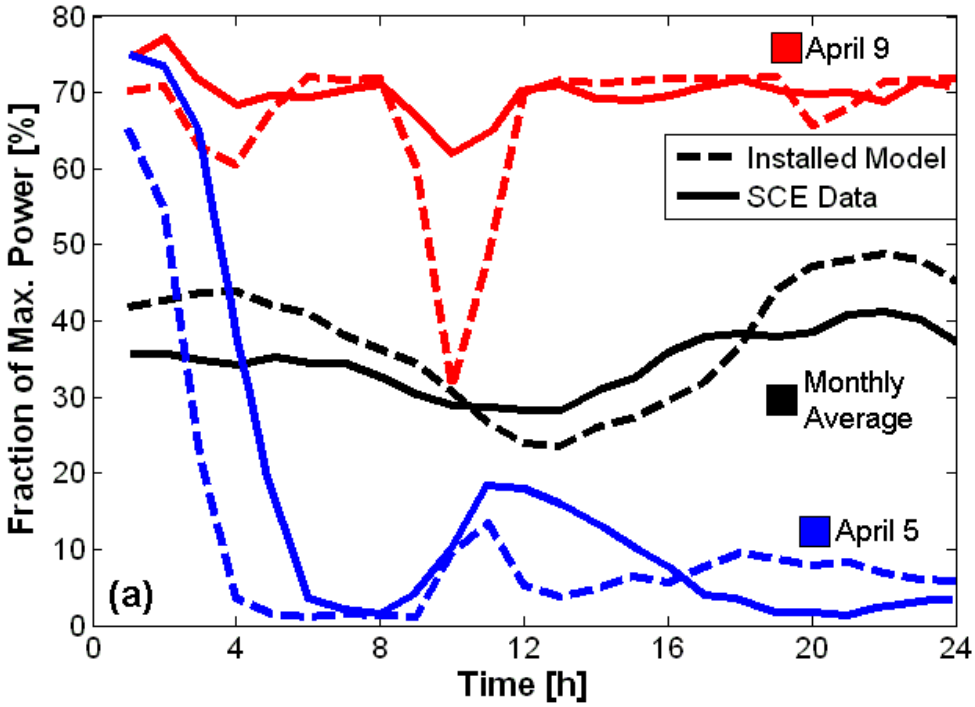

Figure 237: Current Wind Power Model Verification with Tehachapi Wind Farm Power Data for July 2005

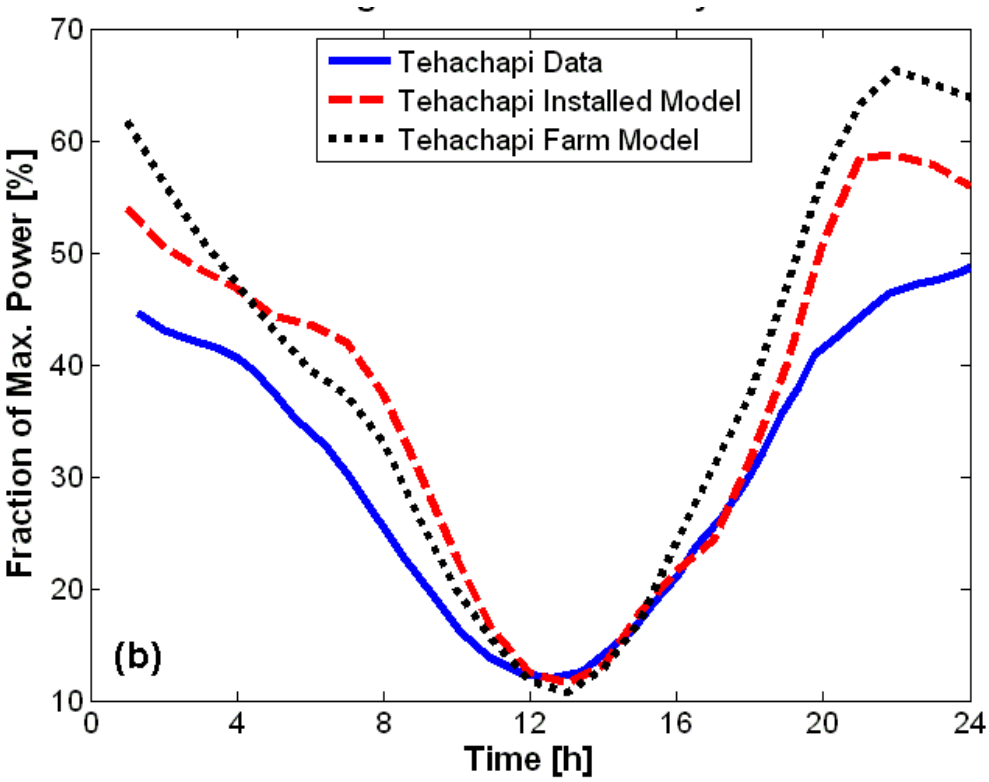

The Tehachapi installed model well simulates the average measured power production profiles, sharing the same qualitative characteristics and shape. Wind power is lowest during the day and peaks during the early morning and late night hours. However, the predicted average diurnal profile has higher capacity factors during the peak hours and lower capacity factors during the daytime hours than the SCE data. This trend is displayed to a reduced extent for the July 2005 results of Figure 237. This discrepancy is most likely due to differences between the wind turbine units assumed in the model and the actual wind turbine units currently used in the Tehachapi Wind Potential region. The model determines power output using the power curve of the Vestas V90 3.0 MW turbine, which is larger than most of the installed units. The currently installed units exhibit significant variation due to the diversity of wind turbine units from various manufacturers. The various cut-in speeds of the installed turbines compared to the single higher cut-in speed of the Vestas turbine lead to the more dynamic model responses to wind speed (especially for low wind velocity) compared to the data. The rated speed of the Vestas turbine is about 15 m/s, which is generally higher than that of the installed turbines allowing modeled power to take advantage of the higher wind speeds at night, explaining the higher nighttime capacity factor of the model.

The model is also not expected to exactly predict the data due to other factors not considered in the model such as the diversity in the technology level of the currently installed wind turbines and wider variations in hub height (100 m in the model versus 60-100m in the data). Nonetheless, Figure 237 the figures present comparisons of wind power measured and

predicted for two days in the year 2005, April 5 and April 9 that adequately verify essential intermittencies, day-to-day variability, dynamics and ramp-rate features of wind power in this region are captured.

7.1.3.2. Solar Power Modeling

Solar power includes both photovoltaic and solar thermal technologies. For solar photovoltaic technologies radiation data from the NSRDB were selected for different sites in California including: 1) coastal sites like Santa Ana, Santa Maria and Miramar, 2) desert sites like Daggett-Barstow, Palm Springs, Twenty-nine Palms and Edwards Air Force Base, and 3) inland sites like Bakersfield Meadows and China Lake. Transmission and resource restrictions are considered in a similar manner as that for wind generation. Technologies include fixed plate, 1-axis tracking and two-axis tracking photovoltaic panels.

Additionally, a single-axis tracking solar thermal power plant is modeled. The system is modeled after the Solar Energy Generation Systems (SEGS) VIII plant in Harper Lake, California. The solar thermal power plant model was developed in the Matlab/Simulink environment and uses a different tracking model than the solar photovoltaic plants for determining the incident radiation. A model was developed to calculate the power generation of a solar thermal system. The selected plant architecture is based on the SEGS VIII solar thermal power plant, which uses a trough to concentrate the sun's energy onto a tube that delivers the heated working fluid to a heat exchanger. Heat is then drawn from the heat exchanger to power a steam turbine, which can also use natural gas to raise steam for the turbine. This model is based on the thesis of Robert Bialobrzeski (Bialobrzeski , 2007).

7.1.3.2.1. Solar Data Acquisition

For the purposes of the HiGRID code, solar power production is modeled by utilizing irradiation data obtained from the National Solar Radiation Database (NSRDB) developed by NREL as inputs to first-principles-based models of solar photovoltaic panels and solar thermal power cycles. The dataset includes the different components of irradiation (direct, diffuse) and is converted into an effective total (in-plane) irradiation via a model constructed in house. Data from the NSRDB is available for most sites from 1991 through 2005. The database contains hourly-resolved irradiation measurements from a variety of sites spread throughout the U.S, as shown in Figure 238:

Figure 238: Location of NSRDB Solar Irradiation Measurements (Yellow)

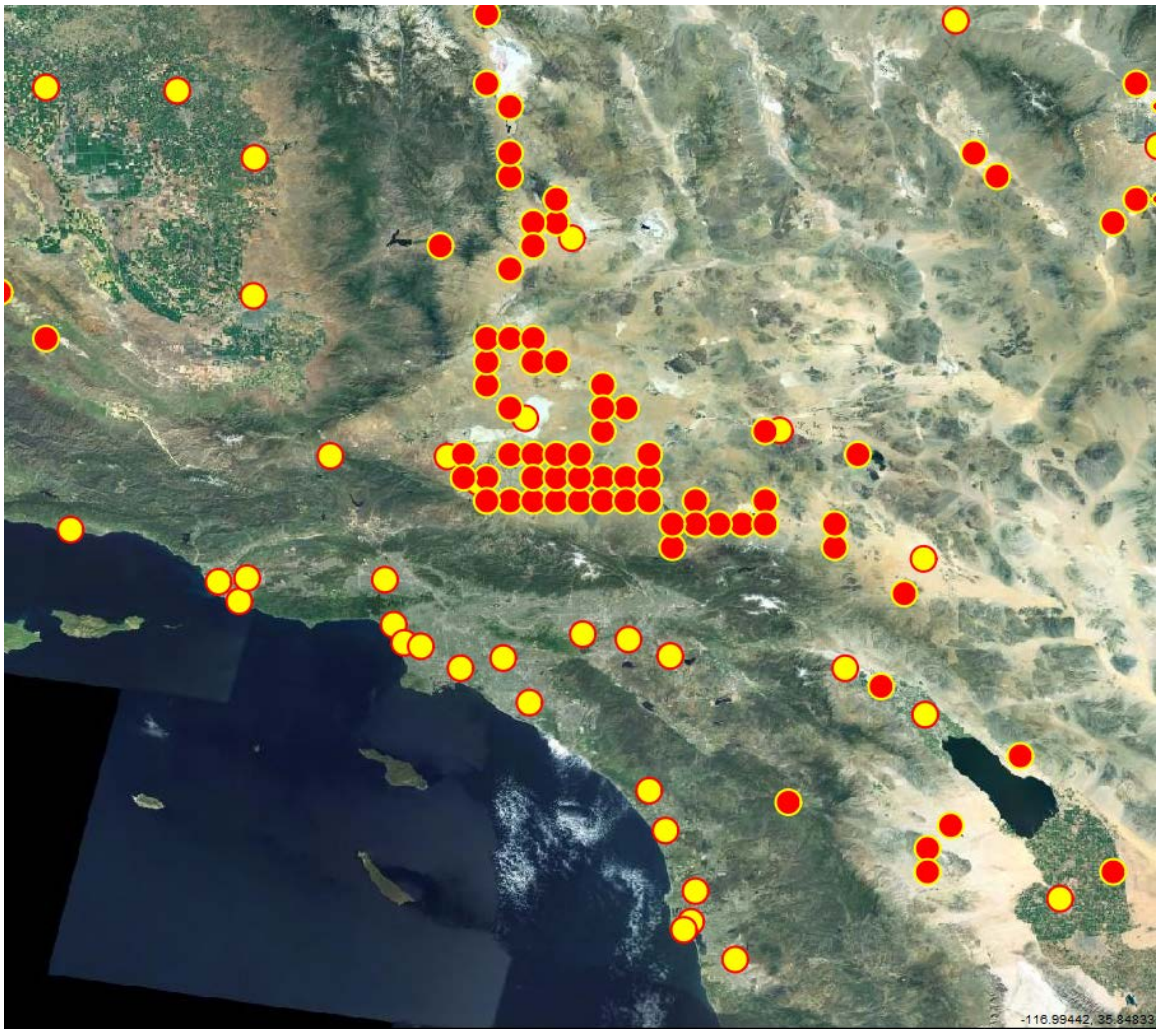

A separate, in-house analysis showed that for solar power profiles composed of a large amount of solar farms that are spaced apart by a sufficient amount such that their cloud-pass sequences are decoupled, the fast-timescale fluctuations in irradiation become a smaller and smaller fraction of the total solar power output and the total profile converges towards its longer-timescale average. This effect is presented in Figure 239 utilizing irradiation data with a 5-minute resolution for the case of a) 1 site, b) 3 sites, c) 5 sites, and d) 8 sites spread across the state of Oregon, respectively.

Figure 239: Decrease in Magnitude of Fast-Timescale Fluctuations in Irradiation Profiles based on a) 1 site, b) 3 sites, c) 5 sites, d) 8 sites

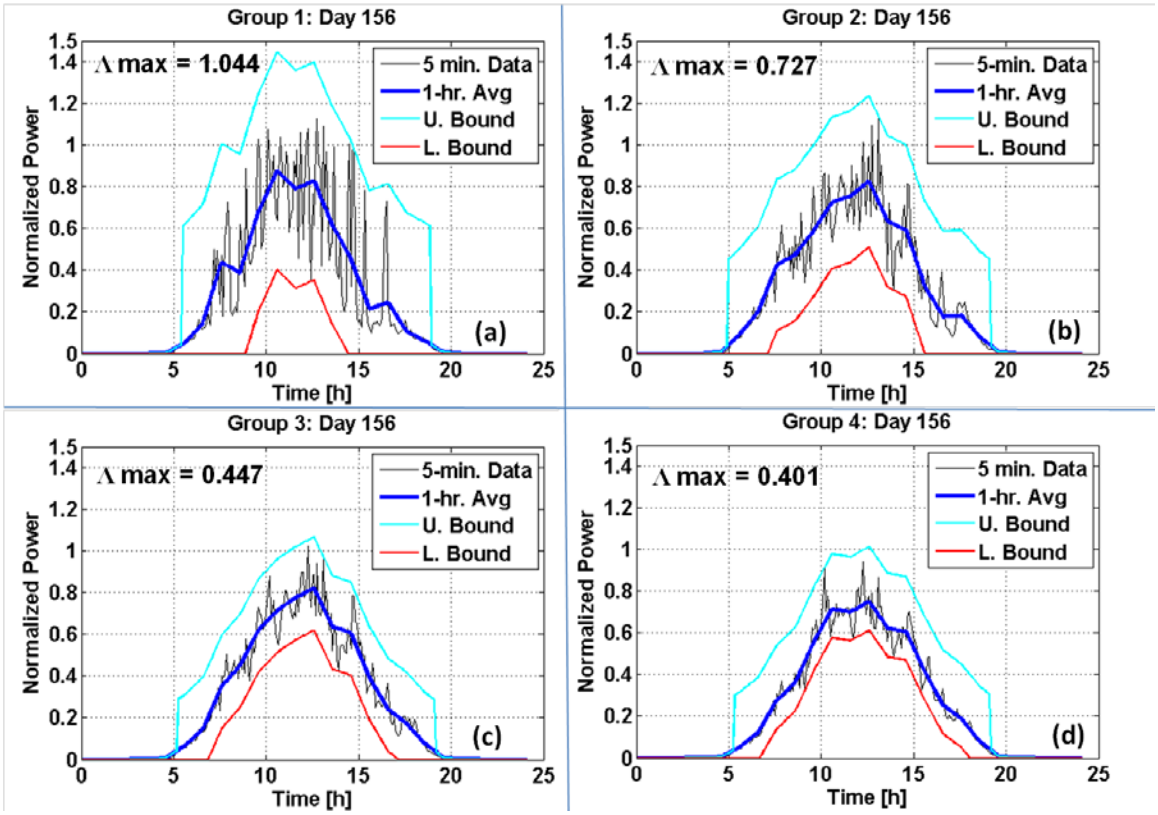

Therefore, for a large-scale system such as the transmission grid that utilizes multiple solar farms that are spread across large distances, it is reasonable to utilize hourly resolved irradiation data as the input to model solar power production.

The use of this dataset allows for the construction of total solar power profiles from solar farm installations that may be present at a variety of sites ranging from large desert installations to distributed coastal installations such as the rooftops of buildings. In the HiGRID code, the nameplate capacity of solar farms at different sites is specified as an input, and appropriately scaled profiles from the different regions are combined to create the aggregate solar power profile. Different technologies such as fixed-plate, 1-axis tracking, and 2-axis tracking can be specified for each individual solar farm, and the different technologies utilize slightly different power profiles produced by in-house models.

7.1.3.2.2. Solar Irradiation Module

Solar power-producing devices such as photovoltaics are capable of producing electrical power from both direct and indirect light inputs. Therefore, the total irradiation that is incident on the photovoltaic cell must be calculated from the different irradiation components.

Calculation of the in-plane irradiation on the solar array is done using the exact model constructed in Heling (Heling, 2008). The model reads files containing hourly data for different types of solar insolation for a given location:

Direct "beam" insolation (B) is the component of the sun's radiation which arrives on a horizontal surface at ground level without interruption, in a straight line from the sun.

Indirect "diffuse" insolation (D) is the component of the sun's radiation which arrives at a horizontal surface at ground level after being reflected from atmospheric objects such as clouds and airborne particles.

An additional given parameter is the global horizontal irradiation (H), which is the amount of total (beam and diffuse) irradiation striking a horizontal surface at ground elevation.

The model uses the different types of insolation to calculate in-plane beam irradiation (I_b), the in-plane diffuse irradiation (I_d), and the in-plane irradiation that is reflected from the ground. (I_r). The total in-plane irradiation on the solar panel is then:

$$I = I_b + I_d + I_r \tag{11}$$

7.1.3.3. Calculation of in-plane beam irradiation and in-plane reflected irradiation

The in-plane beam irradiation is calculated according to the following method using the solar declination and the true solar time:

The solar declination, which is the angle between the earth's equatorial plane and a straight line drawn between the center of the earth and the center of the sun, is calculated for locations north of the equator as:

$$\delta = 23.45^\circ \sin\left[\frac{360(d_n + 284)}{365}\right] \tag{12}$$

where d_n is the serial number of the day of the year.

The true solar time, which is the difference between noon and the considered hour of the day in terms of a complete revolution of the earth, is calculated as:

$$\omega = 15 \times (TO - AO - 12) - (LL - LH) \tag{13}$$

where TO is the local time, AO is the time by which the clocks are advanced ahead of local time zones, LL is the longitude of the site in consideration, and LH is the reference longitude of the local time zone encompassing the site in consideration. Note that TO and AO are in hours, and LL, LH are in degrees.

The solar declination and true solar time are used to calculate the angle of solar incidence θ_s, which is the angle between the sun and the line that perpendicular to the face of the photovoltaic array:

$$\cos\theta_s = \sin\delta\sin\phi\cos\beta - \sin\delta\cos\phi\sin\beta\cos\alpha + \cos\delta\cos\phi\cos\beta\cos\omega + \ldots$$
$$\cos\delta\sin\varphi\sin\beta\cos\alpha\cos\omega + \cos\delta\sin\alpha\sin\omega\sin\beta. \quad \textbf{(14)}$$

where Φ corresponds to the latitude of the site under consideration,

The total in-plane beam irradiation is then calculated by:

$$I_b = B\max(0, \cos\phi_s) \quad \textbf{(15)}$$

The total in-plane reflected irradiation can also be calculated by:

$$I_r = \rho_g H \frac{1-\cos\beta}{2} \quad \textbf{(16)}$$

where ρ_g is the reflectivity of the ground.

7.1.3.3.1. Calculation of the in-plane diffuse irradiation

The in-plane diffuse irradiation is calculated according to the model presented by Perez (Perez, 1990), represented by:

$$\theta_Z = \cos\phi\cos\delta\cos\omega + \sin\phi\sin\delta \quad \textbf{(17)}$$

$$I_d = D\left[\frac{(1-F_1)(1+\cos\beta)}{2} + F_1\frac{a}{b} + F_2\sin\beta\right] \quad \textbf{(18)}$$

Where F1 and F2 are functions of the sky condition, found from tables presented in Perez, 1990, and θ_z is the solar zenith angle as calculated by Duffie, 1991. The values for a and b are calculated according to:

$$a = \max(0, \cos\theta_s) \quad \textbf{(19)}$$

$$b = \max(0.087, \cos\theta_Z) \quad \textbf{(20)}$$

7.1.3.4. Fixed-Plate Solar Photovoltaic Module

The PV model captures the effect of solar irradiance, cloud cover, and ambient temperature on the array outlet power, dynamically capturing the intermittent nature of solar PV power. The model integrates (1) a power equivalent circuit model and (2) an energy balance based PV cell temperature model. The developed model is tuned to represent experimentally measured data of a Solarex MSX-60 panel installed on top of the Engineering Laboratory Facility at the University of California, Irvine. The developed module model output is scaled to simulate any sized solar installation parametrically.

7.1.3.4.1. Power module

The model was developed based on an equivalent circuit representation of a solar cell as presented in Walker, 2001, with temperature dependence of the diode saturation current (I_o) and photo-current (I_L), and the inclusion of a series resistor. The circuit diagram is presented in Figure 240.

Figure 240: Equivalent Circuit Representation of a Solar Cell

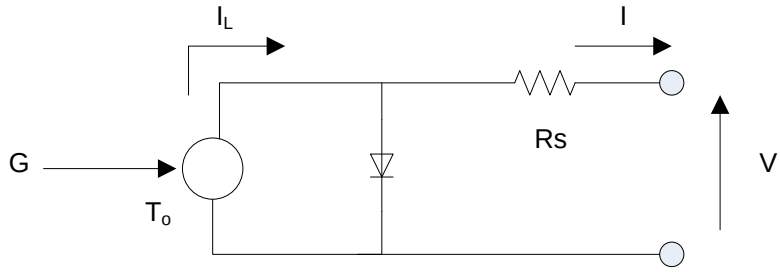

The operating current throughout the panel circuit is determined from the Shockley diode Equation and Kirchoff's current Law:

$$I = I_L - I_o(e^{q(V+IR_S)/nkT} - 1) \quad \textbf{(21)}$$

The limiting current of the panel is assumed to have a linear temperature dependence, where the slope is determined from the short circuit current at different temperatures:

$$I_L = I_{L(T1)}(1 + K_o(T - T_1)) \quad \textbf{(22)}$$

$$K_o = (I_{SC(T_2)} - I_{SC(T_1)})/(T_2 - T_1) \quad \textbf{(23)}$$

The reference limiting current is assumed to have a linear dependence on the magnitude of the incident solar irradiation:

$$I_{L(T1)} = G \cdot I_{SC(T_1,nom)} / G_{(nom)} \quad \textbf{(24)}$$

The diode saturation current is dependent on temperature and is given by:

$$I_o = I_{o(T_1)} \cdot (T/T_1)^{3/n} \cdot e^{-qVg/nk\cdot(1/T - 1/T_1)} \quad \textbf{(25)}$$

$$I_{o(T_1)} = I_{SC(T_1)} / (e^{qV_{OC}(T_1)/nkT_1} - 1) \quad \textbf{(26)}$$

Where the variables are as follows:

Table 43: Power Module Variables

Variable	Quantity	Value	Units
I	Operating Current	--	A
I_o	Diode Saturation Current	--	A
I_L	Photo-current	--	A
T	Temperature	--	K
T_1	Reference Temperature	298	K
G	Irradiation	--	W m^{-2}
R_s	Series Resistor	0.003	Ohm
I_{SC}	Short Circuit Current	3.8	A
K_o	Slope of Current vs.	--	A/K

	Temperature curve		
V_{OC}	Open Circuit Voltage	0.585	V
q	Charge	--	C
n	Diode Quality Factor (1 < n < 2)	1.2	--
V_g	Band Gap Voltage	1.12	V
k	Boltzmann's Constant	1.38×10^{-23}	$J\ K^{-1}$
V	Operating Voltage	--	V

7.1.3.4.2. Cell Temperature Module

The temperature of the solar cell was determined by applying conservation of energy to a control volume encompassing the entire 5 kW solar array. Heat transfer due to convection and radiation was resolved, however conduction was assumed to be negligible since the contact area of the panel interconnects with the roof is very small.

$$\rho \forall C_v \frac{dT_s}{dt} = Q_{rad} - Q_{conv} - Q_{rad,loss} - W \quad \textbf{(27)}$$

Convective heat transfer was determined using a turbulent-flow Nusselt number approach for a flat plate:

$$\overline{Nu} = \frac{\overline{h}L}{k_f} = 0.664\, Re_L^{0.5}\, Pr^{0.33} \quad \textbf{(28)}$$

Where Re_L is the Reynolds number of the ambient flow, Pr is the Prandtl number, k_f is the thermal conductivity of the ambient air, L is the length of the plate, and A_s is the surface area of the array.

The density, dynamic viscosity, thermal conductivity and Prandtl number are all temperature dependent. The velocity of the ambient air is taken from measured wind speed data in the Santa Ana region for the appropriate time period.

Radiative heat transfer was modeled using the grey body assumption, where the temperature of the grey surface is set to the ambient temperature:

$$Q_{rad} = \left(G_{measured} - \varepsilon\sigma\left(T_s^4 - T_\infty^4\right)\right)A_s \quad \textbf{(29)}$$

where $G_{measured}$ is the in-plane solar irradiation on the panel, calculated from the irradiation module. In addition, a radiative heat loss was included to account for the absorptivity of the ambient atmosphere and any cloud cover that might be present. This loss is also modeled with a grey body, where the temperature of the grey body is set to the ambient temperature minus 2 degrees Kelvin, and the emissivity of the grey body is dependent on the ambient relative humidity and cloud condition:

$$Q_{rad,loss} = \varepsilon(\%RH, \text{Cloud})\sigma A_s\left(T_s^4 - (T_\infty - 2)^4\right) \quad \textbf{(30)}$$

Where:

$$\varepsilon(\%RH, \text{Cloud}) = 1 - \left(\frac{\varepsilon_{\text{RH}} + \varepsilon_{Cloud}}{2} \right) \quad \textbf{(31)}$$

Where ε_{RH} and ε_{Cloud} are the emissivity indices of the grey surface due to relative humidity and cloud cover, respectively:

Table 44: Relative Humidity Emissivity Indices

Relative Humidity (%)	Relative Humidity Index
RH < 65%	0
65%< RH < 70%	0.1
70% < RH < 75%	0.25
75% < RH < 80%	0.4
80% < RH < 85%	0.5
85% < RH	0.8

Table 45: Cloud Condition Emissivity Indices

Cloud Condition	Cloud Condition Index
Clear	0
Few	0
Scattered	0.05
Broken	0.25
Overcast	0.65
Haze	0.8

This approach greatly simplifies the calculations needed to determine the temperature of the solar cell. Notice that as the cloud cover or relative humidity increases, the radiation loss decreases, representing the effects of atmospheric radiation absorption and re-radiation. This assumption was made since it was deemed unnecessary to develop a physics of weather simulation for the purpose of determining the temperature of the solar cell, since the variation in the performance of the cell over the temperature range considered is relatively small, however it is significant enough to be included.

7.1.3.4.3. Fixed Plate Photovoltaic Model Verification

The model was constructed to simulate the performance of a Solarex MSX60 60W solar panel array. Model validation of the power module was carried out by comparing simulation results to power data obtained from a 3.85 kW solar array on the rooftop of the Engineering Laboratory Facility at the University of California, Irvine. The simulated irradiation and cell temperature were used as inputs to the power module, and the results were compared to the measured power data. The individual 60W panel was scaled up to 3.85 kW for comparison.

The combined model was validated against measured power, cell temperature, and irradiation data from a 3.85 kW solar panel array on the roof of the Engineering Laboratory Facility at the University of California, Irvine.

Figure 241: Solar Model Validation: Power Module

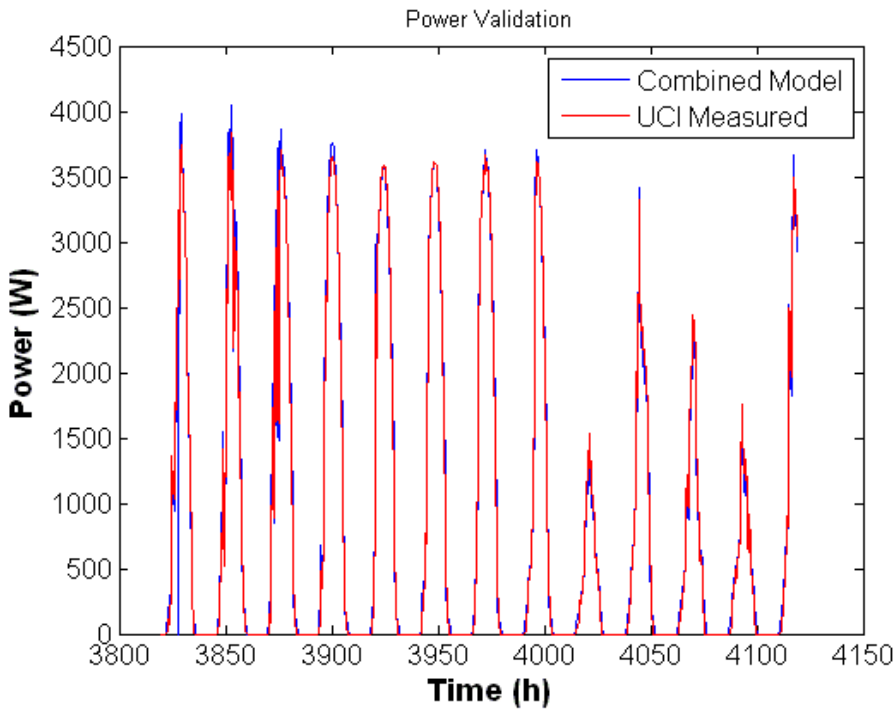

Figure 242: Solar Model Validation: Temperature Module

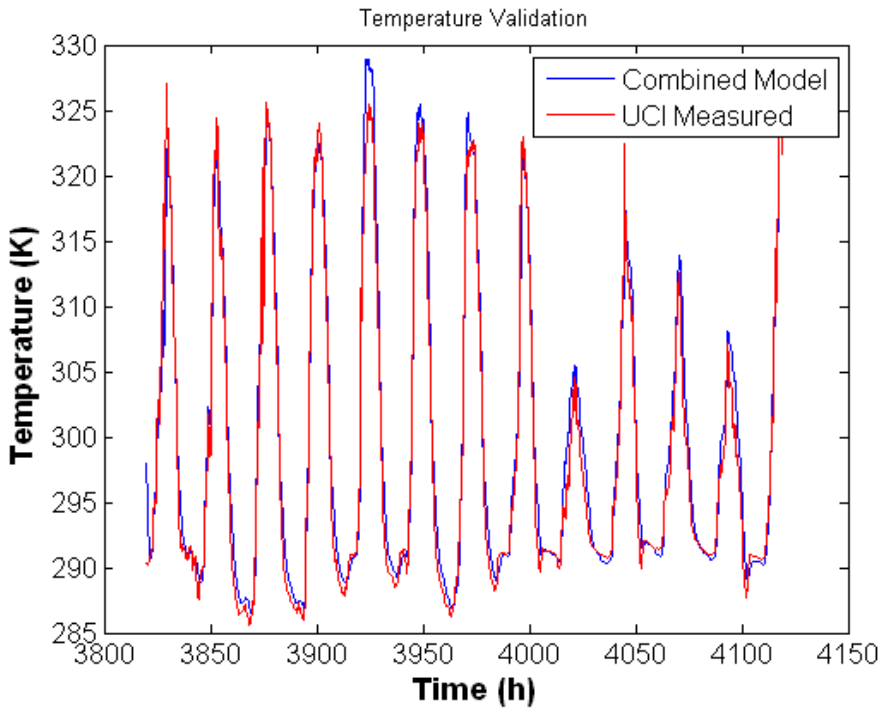

Figure 243: Solar Model Validation: Irradiation Model

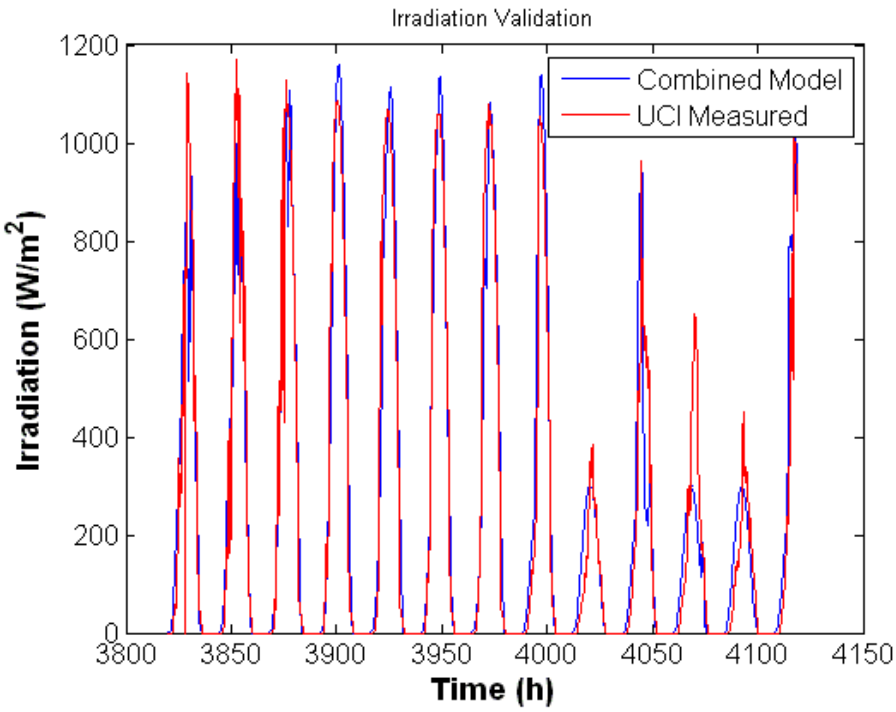

From Figure 241, Figure 242 and Figure 243, the combined model results match with the measured data with an average error of 1.36%. Therefore, it is safe to assume that a more detailed model for determining the effective irradiation, power output, or cell temperature is not necessary for this level of analysis.

7.1.3.5. Solar Thermal Power Modeling

Solar thermal power generation relies on the concentration of solar radiation to heat a fluid that is used by a heat engine to generate electricity. The concentration of sunlight is required to reach temperatures sufficient for use in a heat engine. Three mirror configurations for the concentration of sunlight are commonly considered: parabolic trough, parabolic dish and heliostat with central receiver.

Table 46: Comparison of the different concentrating solar thermal power technologies

Concentrating Solar Thermal Technology	Tracking	Concentration ratio	Operating temperature (C)
Linear Fresnel reflector	Single-axis tracking	10 - 40	60 - 250
Parabolic trough collector	Single-axis tracking	10 - 85	60 - 400

Parabolic dish reflector	Two-axis tracking	600 - 2000	100 - 1500
Heliostat field collector	Two-axis tracking	300 - 1500	150 - 2000

Each configuration is typically designed for integration with a particular thermodynamic cycle. Parabolic trough and heliostat technologies typically use steam cycles, although some heliostat technologies may be configured as Brayton cycles. Parabolic dish systems utilize the Stirling cycle. The most efficient of these configurations is the parabolic dish/Stirling system with average solar to electric efficiencies over 20%. Although these systems are the most efficient, they are not as well proven and do not currently exist in large installations . The parabolic trough and heliostat systems have been demonstrated at large scales in California and Nevada. The parabolic trough system accounts for the largest solar installation in the world: the Solar Energy Generating System (SEGS). This installation consists of nine separate arrays installed in California totaling 354 MW of capacity. However, an installation currently under construction in Ivanpah Dry Lake, CA using the heliostat technology will surpass the SEGS with a 370 MW installed capacity. Despite that the efficiency of a parabolic trough system is the lowest of the three concentration technologies, it is the specific technology modeled for the assessment of solar thermal power in HiGRID given that most concentrating solar thermal power is currently generated in California using the parabolic trough technology.

Table 47: Summary of the SEGS installations

Unit	I	II	III	IV	V	VI	VII	VIII	IX
Solar Field Aperture Area (hectares)	8.3	19	23	23	25.1	18.8	19.4	46.4	48.4
Rated Capacity, MWe	13.8	30	30	30	30	30	30	80	80
Annual Net Electricity Production (GW-hr)	30.1	80.5	91.3	91.3	99.2	90.9	92.6	252.8	256.1

Source: Bialobrzeski 2007

The parabolic trough model focuses on one of the larger SEGS installations, SEGS VIII. SEGS VIII has a peak capacity of 80 MW (89 MW when supplemented with natural gas) and began operation in 1989. The solar field consists of many loops of several solar collector assemblies (SCAs) connected in series (See Figure 244). Each of these loops are connected in parallel, and the heat transfer fluid (HTF) in the supply/return headers to each loop is maintained at a nominal temperature such that the temperature difference across each loop is the same. When the HTF returns from the field it enters several heat exchangers, which produce steam for the steam turbine. After steam production, the HTF then returns to the field. The HTF is Therminol-VP1. The heat exchanger configuration in SEGS VIII consists of a pre-heater, a steam generator, and a super-heater. The steam produced in these heat exchangers expands through a steam

turbine. When steam exits the turbine, it is condensed and sent back through the heat exchangers. The heat exchangers, steam turbine, and condenser are referred to as the power block of the system.

In HiGRID, the solar thermal power model was developed based on modeling work done by Bialobrzeski (2007). Bialobrzeski developed this model to investigate the cost effectiveness of SCA replacement throughout the solar field given that expensive, high efficiency SCAs may not be cost effective in the lower temperature regions of the SCA loops. With this motivation in mind, simple, empirical models were developed for computationally efficient simulation of the entire solar field and the power block. A model such as this will work well for use in HiGRID given its computational efficiency.

Figure 244: Schematic of the SCA loop within the solar field

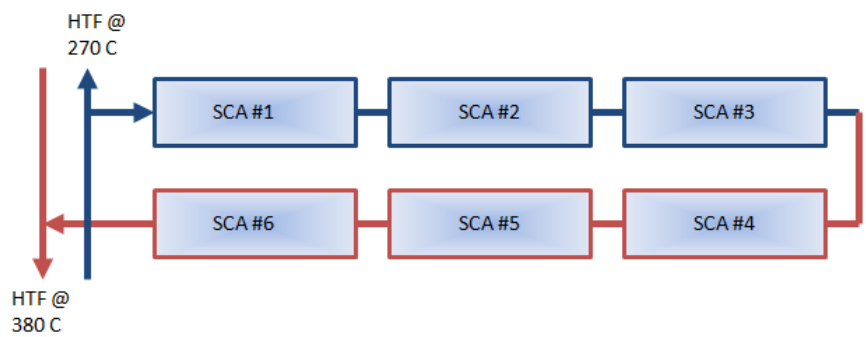

7.1.3.5.1. Angle of Incidence

The incident solar irradiation will result only from direct beam irradiation because of the high concentration ratio in parabolic troughs. It can be determined from the angle of incidence for a north-south axis orientation with single axis east-west tracking. The angle of incidence was determined using the following equations:

$$\boldsymbol{\omega = 15\,(solar\ time - 12)} \tag{32}$$

$$\boldsymbol{\delta = 23.45\ \sin\left(360\ \frac{284 + day}{365}\right)} \tag{33}$$

$$\boldsymbol{solar\ time = time + 4\,(\psi_{ST} - \psi) + EOT} \tag{34}$$

$$\begin{aligned}\boldsymbol{EOT} \\ \boldsymbol{= 229.2\,(0.000075 + 0.001868\cos B - 0.032077\sin B} \\ \boldsymbol{- 0.014615\cos(2B - 0.04089\sin 2B)\,)}\end{aligned} \tag{35}$$

$$\boldsymbol{B = (day - 1)\frac{360}{365}} \tag{36}$$

$$\boldsymbol{\theta = \cos^{-1}\left(\sqrt{1 - (\cos\alpha - \cos\alpha(1 - \cos\gamma))^2}\right)} \tag{37}$$

where $\alpha = 90 - \theta_z$ and $\theta_z = \cos^{-1}(\cos\delta\cos\omega\cos\psi + \sin\delta\sin\psi)$

If $\sin\omega > 0$ then

$$\boldsymbol{\gamma = 2\pi - \cos^{-1}\left(\frac{\cos\psi \sin\delta - \cos\delta \cos\omega \sin\psi}{\cos\alpha}\right)} \quad \textbf{(38)}$$

otherwise

$$\boldsymbol{\gamma = \cos^{-1}\left(\frac{\cos\psi \sin\delta - \cos\delta \cos\omega \sin\psi}{\cos\alpha}\right)} \quad \textbf{(39)}$$

Table 48 lists the symbols used in the equations above along with their corresponding meanings.

Table 48: Angle of incidence equation parameters

α	Solar Altitude
φ	Latitude
ψ	Longitude
γ	Solar Azimuth
ψ_{PST}	Time Zone Reference Longitude

The incident irradiation can then be determined using the angle of incidence using the following equation:

$$\boldsymbol{\dot{G}_{inc,rad}[W/m^2] = I_b \cos\theta} \quad \textbf{(40)}$$

7.1.3.5.2. Solar Field Model

The solar field model considers a single loop within the field to be representative of the rest. It also assumes the temperature distribution in the loop is linear such that an equivalent temperature rise occurs in each SCA. The thermal energy collected per unit aperture area is calculated using the following equation:

$$\dot{G}_{coll}\,[W/m^2] = X_{end}\,\eta_{opt}\,\dot{G}_{inc,rad} - f_{HL}(C_1\Delta T + C_2\Delta T^2) \quad \textbf{(41)}$$

where

$$\eta_{opt} = f_{opt}\,C_{off-axis}\,\eta_{opt,nom} - f_\theta\,\theta\left(\frac{1}{\cos\theta} - 1\right) \quad \textbf{(42)}$$

$$X_{end} = 1 - \frac{f}{L_{SCAstring}}\tan\theta \quad \textbf{(43)}$$

$$\Delta T = T_{HTF} - T_{ambient} \quad \textbf{(44)}$$

T_{HTF} is the average of the inlet and outlet temperatures of each SCA in the loop, determined by assuming a linear temperature distribution across the loop. Given that there are 6 SCAs in each loop, there will be a temperature rise of 18.5 C across each SCA in the loop when the header temperatures are 271 and 382 ºC. Table 49 defines the variables used within the equations for determining the thermal energy collected by the solar field.

Table 49: Definition of variables for solar thermal power model

$L_{SCAstring}$	Length of Loop	571.2	m
f	Focal Length	1.71	m
$\eta_{opt,nom}$	Nominal optical efficiency	0.733	-
C_1	Sandia Linear Heat Loss Coefficient	0.05145	W/m^2-K
C_2	Sandia Quadratic Heat Loss Coefficient	0.00069	W/m^2-K
$C_{off-axis}$	Off-axis Correction Coefficient	1	-
f_θ	Incidence Angle Modifier	0.004	-
B_{const}	Gross Power Constant	-13.1995	MW
C_{coeff}	Gross Power Coefficient	0.381957	-
D_{const}	Net Power Constant	0.119574	MW
F_{coeff}	Net Power Coefficient	0.917813	-
Loops	Number of Loops	142	-
A_{SCA}	SCA aperture area	548.4	m^2
f_{opt}	Optical Efficiency Modifier		-
f_{HL}	Heat Loss Modifier		-
θ	Incidence Angle		-
X_{end}	End Effect Coefficient		-

The optical and heat loss modifiers are determined using a vector that defines the value for each heat collection element (HCE) type and a matrix that defines the percentage of a specific HCE type (e.g., broken, cloudy, washed, etc.) at each of the six SCA locations within the loop. The transpose of the column vector in Table 50 can be multiplied by the matrix in Table 51 to determine the appropriate optical and heat loss modifiers at each SCA in the representative loop. The matrix used for model verification against experimental data is displayed below in Table 51. Bialobrzeski (2007) does not explicitly state what percentages he assumed, therefore, the values used within this report could be different. The values in Table 51 were chosen such that there is agreement between experimental data (Bialobrzeski 2007) and the model predictions. It is important to note that for the HiGRID simulations the matrix in Table 51 was altered to resemble a completely new plant, i.e., values of 1 were placed in the last row of Table 51.

Once the thermal energy collected by a single loop is calculated, it can then be multiplied by the total number of loops (142) to determine the total thermal energy collected by the solar field.

Table 50: Optical and heat loss modifiers for the various heat collection element (HCE) types considered in Table 51

HCE type	f_{OPT}	f_{HL}
Broken	1	6
Cloudy	0.43	3
Washed	0.5	2.5
Lost Vacuum	0.98	2.1
Refurbished	0.91	2.3
Used Luz	0.98	1.9
New UVAC	1.03	1.5

Table 51: Fraction of each heat collection element (HCE) type in each location of the SCA loop

	SCA # in loop					
HCE type	1	2	3	4	5	6
Broken	0.1	0.1	0.1	0.1	0.1	0.1
Cloudy	0.05	0.05	0.05	0.05	0.05	0.05
Washed	0.05	0.05	0.05	0.05	0.05	0.05
Lost Vacuum	0.1	0.1	0.1	0.1	0.1	0.1
Refurbished	0.1	0.1	0.1	0.1	0.1	0.1
Used Luz	0.6	0.6	0.6	0.6	0.6	0.6
New UVAC	0	0	0	0	0	0

7.1.3.5.3. Power Block Model

The power block is modeled using curve fits to data collected from the SEGS VIII plant. It was found by (Bialobrzeski 2007) that the gross power output could be defined by the following equation:

$$\dot{E}_{gross} = B_{const} + C_{coeff}\dot{Q}_{total} \quad (45)$$

The net power output can then be calculated from the gross power output using this equation:

$$\dot{E}_{net} = D_{const} + F_{coeff}\dot{E}_{gross} \quad (46)$$

The coefficients in the above equations are defined in Table 49.

7.1.3.5.4. Natural Gas Use

Natural gas is used to supplement the heat collected by the solar field only during on-peak periods. The on-peak period is defined as 12pm to 6pm on weekdays from May 12 to September

28 (Bialobrzeski 2007). During these on-peak periods, natural gas will be used to attain the target on-peak gross power output of 97 MW with the constraint that the maximum thermal energy production of the natural gas heaters is 200 MW. The total target thermal energy production is determined using the following equation:

$$\dot{Q}_{tot,target} = \frac{\dot{E}_{gross,target} - B_{const}}{C_{coeff}} \tag{47}$$

Once the target thermal energy production is defined, the total thermal energy to be produced from the natural gas heaters can be defined:

$$\dot{Q}_{gas} = \dot{Q}_{tot,target} - \dot{Q}_{field} \tag{48}$$

The total thermal energy provided to the power block is then:

$$\dot{Q}_{total} = \dot{Q}_{gas} + \dot{Q}_{field} \tag{49}$$

The rate at which the natural gas heaters can change output is set to 35 MW (increase or decrease) per hour.

7.1.3.5.5. Model Verification

The model described in the previous sections was verified against SEGS VIII operational data presented in Bialobrzeski (2007). The data include annual net power generation, natural gas usage, and solar heat collected as well as diurnal variation for a full week in the summer from July 2, 2005 to July 9, 2005. The data are presented in Figure 245 along with model predictions. The model seems to agree reasonably well in spite of two major issues. The first is that in the model natural gas is used on day 185 when in the data natural gas usage is shown to be zero. This is a result of the model's inability to account for holidays, which will introduce some error into the annual results that should be negligible. The other major issue is that the model's natural gas use begins after the time that the data suggest it should, and in the evening the model's natural gas use continues after the data suggest it should have been shut down. After further examination, it can be proposed that although the on-peak period is from 12pm to 6pm, the operators may begin turning the gas heaters on an hour before the on-peak period started in order to allow them time to warm up before the on-peak period begin. Similarly for shutdown, the operators likely begin shutdown before the on-peak period ended to account for the max ramp rate of the gas heaters.

Figure 245: Comparison of model predicted performance to SEGS VIII measured data from Bialobrzeski (2007)

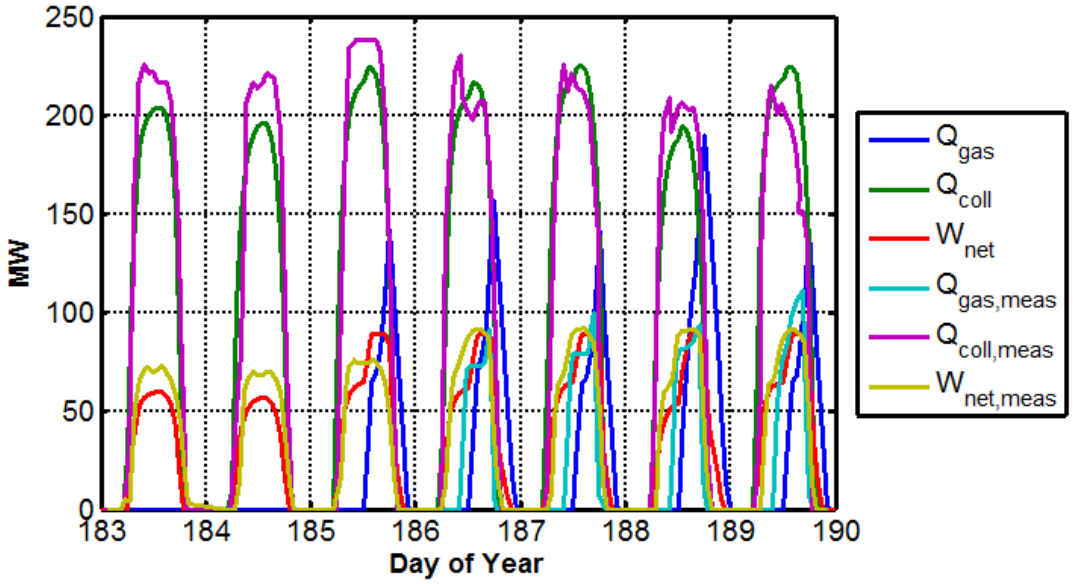

Based on data from Figure 245 regarding the gas heater operation schedule, the operation schedule in the model was modified such that the gas heaters would begin start-up and shutdown an hour prior to 12pm and 6pm, respectively. The model results and the corresponding SEGS VIII plant data are shown in Figure 246. After modifications to the gas heater schedule, the model's predictions of the actual plant performance improved. There are still issues with the gas heaters in the model increasing to much higher values than seen in the data. The gas heaters have a maximum heat supply rate of 200 MW, which has not been exceeded in these cases. It is possible that the operators were using different logic than implemented in the model. Recall that the model is designed to maximize electricity production without regard for issues such as increased degradation resulting from high ramp rates. Nonetheless, the model predicts the dynamics of a parabolic trough solar thermal power plant reasonably well and is sufficient for use in HiGRID.

Figure 246: Comparison of model predicted performance after modifications to the gas heater operation schedule to SEGS VIII measured data from Bialobrzeski (2007)

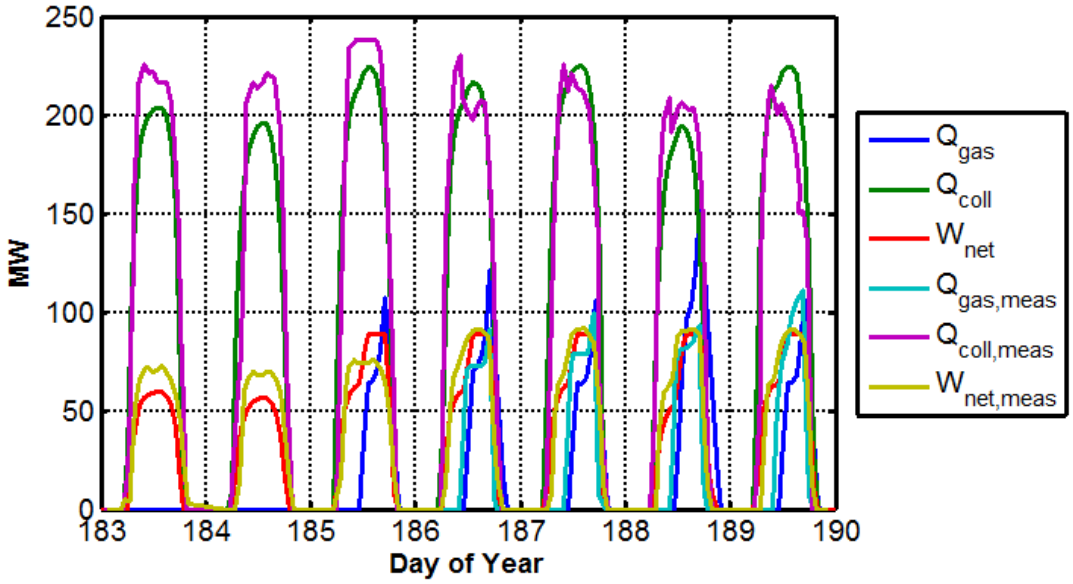

The model was also compared to the annual data available from the SEGS VIII plant. The weather and solar irradiation data used for input into the model were obtained from NREL's 2005 National Solar Radiation Database (Wilcox, 2007). The location used was Dagget-Barstow, which is about 25 miles from the SEGS VIII site in Harper Lake, CA. Table 52 shows the comparison between the model's prediction of annual plant performance with the annual data collected from the SEGS VIII plant. The natural gas usage is over-predicted by the model, which could be expected given the results from Figure 246. The discussion relating to Figure 246 stipulates possible reasons for this in the paragraph above. Although the gas heater use is not predicted well, the solar field heat collection is well predicted, which is expected because the matrix in Table 51 was tuned to achieve this result. Additionally, the net power output still well predicts the plant's power output for 2005 in spite of the error associated with the gas heaters.

Table 52: Comparison of model's predicted annual plant performance for 2005 with annual SEGS VIII plant data

	Model	Measured	% Error Model
Net Electric Power (MW-hr)	141,474	138,212	2.36%
Total Gas Heat (MW-hr)	73,492	61,250	19.99%
Total Field Heat Collection (MW-hr)	452,809	438,605	3.24%

7.1.3.5.6. Solar Thermal Power Plant Model

The model used for the simulations in HiGRID differs from the model used for verification in that the HiGRID simulations model approximates a new plant which uses new HCEs in all the SCAs (See Table 53). These new HCEs are universal vacuum collectors (UVAC) as identified in

Table 50. This new plant will be more suitable for use in the HiGRID simulations where the grid impacts of new renewable energy installations are considered.

Table 53: Fraction of each heat collection element (HCE) type in each location of the SCA loop for the solar thermal power plant for use in HiGRID

	SCA # in loop					
HCE type	1	2	3	4	5	6
Broken	0.1	0.1	0.1	0.1	0.1	0.1
Cloudy	0.05	0.05	0.05	0.05	0.05	0.05
Washed	0.05	0.05	0.05	0.05	0.05	0.05
Lost Vacuum	0.1	0.1	0.1	0.1	0.1	0.1
Refurbished	0.1	0.1	0.1	0.1	0.1	0.1
Used Luz	0.6	0.6	0.6	0.6	0.6	0.6
New UVAC	0	0	0	0	0	0

7.1.3.6. Other Renewables

Geothermal, biomass, biogas and small-hydro generation are also considered in HiGRID. These resources are not used for the UCI community model but when assessing impacts of renewables on larger communities and on the entire state it is important that these other renewables be considered.

7.1.3.6.1. Geothermal

Geothermal plants exhibit a relatively constant output as is evidenced from the data provided by FERC for 2000 and 2001 (FERC, 2002). Monthly capacity factor-based operation is used to incorporate planned outages. Dry steam, flash steam and binary cycle power plants are available technologies and can be selected for analysis with each plant type introducing unique operation and cost parameters.

7.1.3.6.2. Small-Hydro

In California, hydroelectric generation is only considered renewable if it is does not introduce diversion or require increased appropriation of water, as defined by Senate Bill 1078 (SB1078, 2001-02). This means that only a portion of the total hydroelectric generation is considered renewable. HiGRID determines this portion based on the historical state generation percentage of total hydroelectric. The details of hydroelectric generation will be discussed in the "Dispatchable Load Module" section.

7.1.3.6.3. Biomass and Biogas

Lastly, biomass and biogas are included as renewable resources. On the state-level there is very little in-state coal generation, therefore it is assumed that all of the biomass and biogas is used as fuel for advanced combined cycle power plants. HiGRID captures CO_2 impacts of using biomass and biogas. Combustion of biomass or biogas will reduce the CO_2 emissions in

comparison to burning natural gas since the combustion of those fuels has a low net CO_2 impact.

Task 7.1.4. Dispatchable Load Module

Dispatchable loads include boilers, chillers and thermal energy storage as well as electrical energy storage, demand response and electric transportation. Just like the renewable module, all of the models are shared between the UCI and California models except the chillers for UCI and hydroelectric generation for the California model.

7.1.4.1. Common Models

The common models between both the UCI and California models include energy storage, demand response and electric transportation. The energy storage model is presented in Task 3.2.8 and the results are presented in Task 7.3.4. Similarly, the demand response model approach has been presented in Task 6.4 and is presented along with the results in Task 7.3.3. Lastly, the electric transportation modeling approach was presented in detail in Task 3.3.2.2 and again briefly with the results in Task 7.3.4.

7.1.4.2. UCI Specific Models

The UCI specific models have been presented previously in this document in support of other tasks. The energy efficiency model was presented in detail in Task 6.3 and is presented along with the results in Task 7.3.2. Also, the operation of the chillers and TES tank was presented in Task 3.4.1.

7.1.4.3. California Specific Models

The dispatchable load module for the California model includes generation that supports system balancing and must be calculated before the balance generation. Dispatchable loads include hydroelectricity, energy storage, demand response and electric vehicle charging. Each of these technologies affects the generation or demand in a unique way.

The dispatchable load module compares the load demand with the available renewable generation and then dispatches to complement the renewable generation and improve general grid performance. Time-resolved load demand data are drawn from CAISO's OASIS site (CAISO, 2012 (OASIS)) and are scaled to reflect total California demand (CEC-200-2009-010, 2009). The HiGRID tool is meant to assess changes in operation and not as a planning tool, as such HiGRID operates for a single year so the load demand will not change. Managing ancillary services requires that sufficient capacity be available to meet the load and to adjust in the event of a generator failure or a sudden reduction in demand. This effectively creates a margin of operation for each power plant that is considered in this module. The time-resolved ancillary services (spinning reserve and regulation) values are drawn from OASIS and scaled just as the load vector was scaled to reflect statewide demand as opposed to in-state generation. While it is assumed that spinning reserve will remain constant over the course of a single year even with increasing renewables, regulation requirements will change with increasing renewable penetration. Using values from CAISO's Integration of Renewables report,

regulation is increased proportionally according to the profiles shown in Figure 247 with increasing renewable penetration (GE Energy Consulting, 2010 (CAISO 20%)).

Figure 247: Effect of Increasing Renewable Mixture on Regulation Up and Down

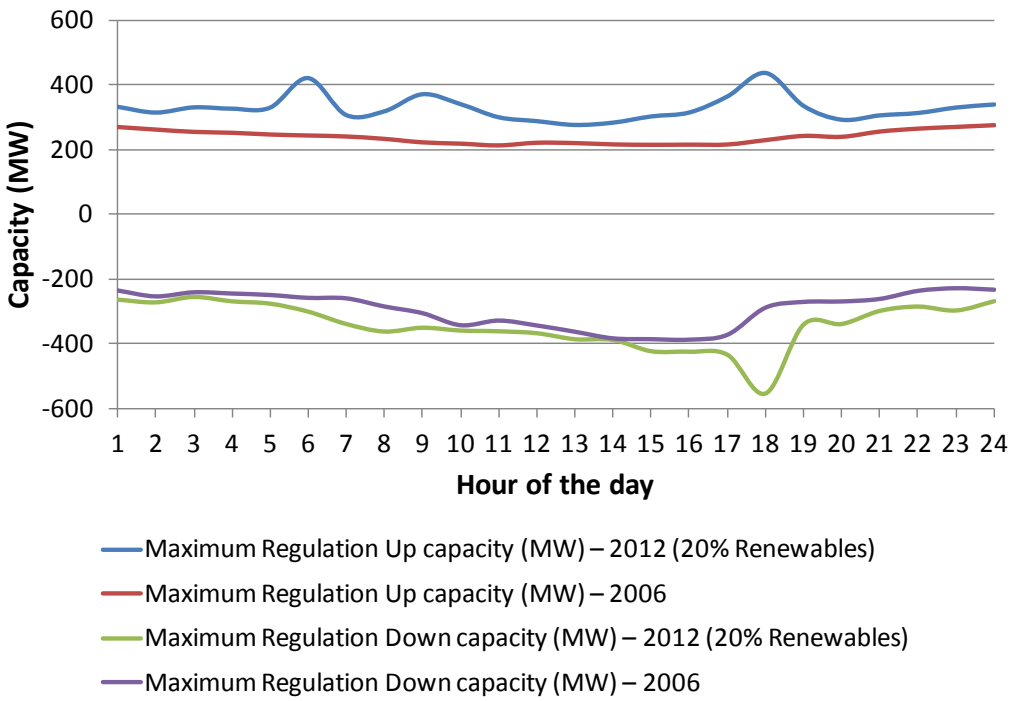

Source: GE Energy Consulting, 2010 (CAISO 20%)

The only dispatchable generation module that is specific to the California model is the hydroelectric generation module.

7.1.4.4. Hydroelectric Generation Module

In California, hydro generation provides a significant amount of dispatchability to the grid given its ability to quickly increase and decrease generation. From Table 59 and Table 60 it can be seen that conventional hydroelectric (HY) combined with Hydroelectric Pumped Storage (HYPS) contributes over 70% of the spinning reserve capacity, over 60% of the non-spinning reserve capacity and nearly 40% of the regulation reserve while only contributing 15.8% to the generation capacity for 2000 and 2001.

Hydroelectricity is modeled using several components including run-of-the-river, conventional hydro, daily hydro and pumped hydro and is scaled to the total hydro generation in California. Figure 248 depicts the methodology employed for the hydro model.

Conventional hydroelectric power (i.e., non-pumped hydro) is divided into seasonal hydro, daily hydro, and baseload hydro. The aggregate of these sub-models represents the total conventional hydro power. Seasonal hydro refers to power generated from water to prevent flooding as a result of seasonal rain patterns. Daily hydro is water that is required to pass

through on a daily basis to meet water supply needs, such as agriculture or human consumption. Base load hydro represents power generated from run-of-the-river hydro sites that generate electricity proportional to the flow of the river. Pumped storage resources are divided into the *seasonal* and *pumped* portions of pumped hydro. The seasonal portion of pumped hydro is the water that is dispatched through pumped storage turbines that accumulates from upstream flows and rain water for the same reason as conventional hydroelectric plants, such as water level regulation. The pumped portion hydro refers to the remaining capacity that can be pumped back up from the lower to the upper reservoir and be used to generate at a later time. All the categories for hydro modeling should not be considered as rigidly defined. For example, baseload hydro may sometimes contain water that would be more properly defined as daily hydro. Rather, these categories are implemented in the code to ensure that all the requirements are met by breaking the system down into smaller, more manageable components. The model was verified to hydro plant generation data released by the FERC during the Western Energy Crisis in 2000 and 2001. Hourly resolved data for every in-state hydro plant participating in the energy market was collected for this dataset. Based on the models created using 2000 and 2001 data the hydro operation in 2005 can be predicted, as will be shown.

Figure 248: Methodology for Hydroelectric Model

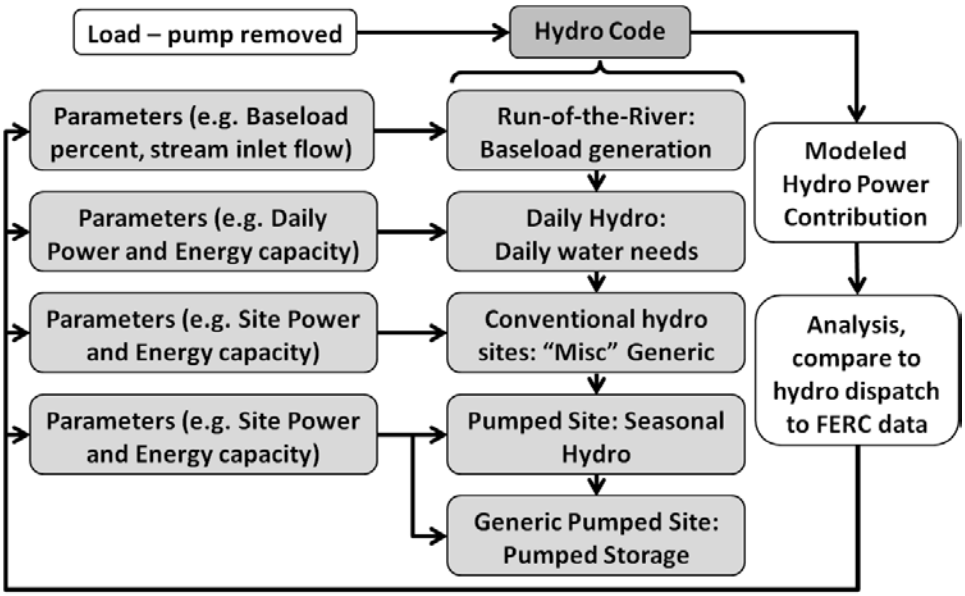

Two large power plants in California are selected to be explored in greater detail. Castaic Power Plant, located between Pyramid Lake Castaic Lake, and Helms Power Plant, located Northeast of Fresno. Stream flow data for both sites were obtained from the United States Geological Survey (USGS) Annual Water Data Reports. By using stream flow data, evaporation losses are included in the analysis.

To calculate the energy resulting from the stream flow, the pressure head, efficiency, stream flow and other operating conditions must be known. Every site is different and not all are

tracked by USGS sensors, which makes inclusion of this detail challenging when considering around 300 plants are in-state alone.

Since each site is supplied by a different inlet stream, each with unique time-resolved stream flow rates which are dependent on a number of meteorological factors, a representative inlet stream flow was used to represent the total flow from all rivers in California that lead to generation stations. This was achieved by using a combination of multiple stream flow data obtained from the USGS. Three different stream patterns were chosen to reflect the state-wide stream flow patterns. These rivers were chosen for their relatively large flow volumes and their potential contribution to the total generation within the state, as recorded in FERC's eLibrary. The selected locations are the Feather River, the American River, and the Yuba River. The patterns for the three rivers are different on a yearly basis, for example, peak flow may occur in winter, while another year it occurs in summer. This is caused by a variety of factors, such as human use and regulations, rainfall, snow melt, evaporation and other losses. It is assumed that a combination of the three rivers yields a seasonal pattern that approximates the water input into the hydro energy system. Only the pattern is of concern here, as the magnitude is proportional to the total energy generation from hydro in the state (i.e., 18.9% of the total for 2005), as shown in equation (80). Portioning of the combination was obtained through error minimization by comparing the modeled hydro dispatch with the actual generation data for the year 2001. The composition and the available maximum capacity for each stream were varied, and the lowest error result was used as a representative stream flow. Using this approach and aggregating the hydroelectric fleet alleviates the need to track each site's specific parameters such as pressure head, installed capacity, turbine efficiency, and reservoir size. As a result the pressure head is selected to ensure a representative energy stored per unit volume of water and all turbines were assumed to have identical efficiencies of 80% and the efficiency for pumped storage was set at 75% (Gordon, 2001).

Four separate models exist: run-of-the-river hydro, daily hydro, seasonal hydro, and pumped hydro. The first two types of hydro generation behave similar to baseload generation as there is little to no control over their operation. Run-of-the-river hydro generation is proportional to the stream flow vector. The daily hydro model ensures that there is a minimum of hydro generation each day. This value is selected based on the baseload hydro and historical operation of hydro power plants. When the generation occurred is a function of the load profile to be met subject to generation ramp rate and installed generating capacity constraints. The most substantial contribution to conventional hydro power generation comes from the seasonal hydro model. This category reflects large generating stations with reservoirs and how they must operate throughout the year. Consequently, this model must be run for an entire year to capture these properties. The model sequentially reduces the demand signal by bringing on additional hydro generation subject to system and generator constraints and starts with the output from the daily hydro and run-of-the-river models. In this way, baseload constraints are integrated into the conventional hydro model. Additional constraints include an aggregated reservoir level (initial fill, final fill, minimum fill and maximum fill), provision for spinning reserve, fleet ramp rate and installed generation capacity. All reservoirs are modeled as one large reservoir from which water can be drawn to generate electricity. To address level

constraints, the reservoir is converted from volume capacity to energy capacity using equation (80) where $\dot{\forall}(t)$ is the time-resolved stream flow rate and E_{Hy} is the total electrical generation from hydro for the concerned system (i.e., the state of California for this analysis). Then the level is constrained by first taking the vector of stream flows converted to energy and calculating the cumulative fill level, using equation (81), and second by applying equations (82) and (83) as constraints. For equation (82), $\forall_{cap}$ is a constant that represents the maximum system reservoir capacity. This term is calculated by comparing with several years of historical data to determine how it changes with changing values of E_{Hy}. Equation (83) is used to ensure that the level from one year to the next returns to its original level.

$$\frac{\dot{\forall}(\boldsymbol{t})}{\sum \dot{\forall}(\boldsymbol{t})} \cdot \boldsymbol{E_{Hy}} = \dot{\forall}_{\boldsymbol{energy}}(\boldsymbol{t}) \tag{50}$$

$$\forall_{\boldsymbol{fill}}(\boldsymbol{t}) = \sum_{\boldsymbol{1}}^{\boldsymbol{t}} \dot{\forall}_{\boldsymbol{energy}}(\boldsymbol{t}) \tag{51}$$

$$\boldsymbol{max}\left(\forall_{\boldsymbol{fill}}(\boldsymbol{t})\right) \leq \forall_{\boldsymbol{cap}} \tag{52}$$

$$\forall_{\boldsymbol{fill}}(\boldsymbol{t}_{\mathbf{initial}}) = \forall_{\boldsymbol{fill}}(\boldsymbol{t}_{\boldsymbol{final}}) \tag{53}$$

The hydro system is constrained to a maximum installed capacity value such that equation (84) is satisfied, where $P_{Hy}(t)$ is the time-resolved conventional hydro generation signal and $P_{Hy\ Max}$ is the maximum installed capacity. Spinning reserve capacity is subtracted from $P_{Hy}(t)$ thereby reducing the available capacity for dispatch. Additionally, the fleet ramp rate is applied during each incremental increase in generation as the model solves. The fleet ramp rate is a tuned parameter based on the hydro generation data from the 2000 and 2001 FERC data.

$$\boldsymbol{max}\left(\boldsymbol{P_{Hy}}(\boldsymbol{t})\right) \leq \boldsymbol{P_{Hy\ Max}} \tag{54}$$

$$-\boldsymbol{R_{down}} \leq \frac{\boldsymbol{d}}{\boldsymbol{dt}}\left(\boldsymbol{P_{Hy}}(\boldsymbol{t})\right) \leq \boldsymbol{R_{up}} \tag{55}$$

The last model is the pumped hydro model. This model reflects the behavior of pumped hydro generating stations and is comprised of two parts, the seasonal component and the pumping component. The seasonal model is the same as is used with conventional generation and allows for consideration of stream flows into the reservoir in addition to just pumping water from a lower reservoir. For the pumping model, generation is sequentially turned on and pumps required to offset the generation are turned on at a time before the generation is needed. Rather than depleting water from the reservoir, the model locates the nearest earlier local minimum value and raises the load at that time. By including the generation and pumping efficiencies (80% and 75%, respectively) the penalty associated with pumping the water to the upper reservoir and using it later is assessed. This process is repeated and subject to similar constraints as those used for the other models like reservoir level, fleet ramp rate and installed capacity of generators. Because there is an ability to pump, additional constraints on the pumps are included like fleet ramp rate and installed pumping capacity. The majority of the data is drawn from the USGS in the form of daily volumetric flow measurements, in addition to general reservoir characteristics, such as size and height. The daily measurements had to be extrapolated into hourly data by assuming an average hourly value for each hour. Since the hydro model looks at the cumulative flow rate, this process was determined to be acceptable as

will be shown from verification against both 2000 and 2001 FERC data. This data allowed for matching of both the general shape that hydro power should create as well as the total energy.

7.1.4.5. Hydroelectric Verification

Absolute percentage differences are calculated as a measure of the error using equation (86) below. Using the absolute value ensures that signals that are less than the historical data being compared to do not skew the results. All values for percentage differences are presented as a percentage of the historical FERC signal.

$$\text{Percent Difference} = \frac{\sum \left| Model_{Signal} - FERC_{Signal} \right|}{FERC_{Signal}} \cdot 100 \qquad \textbf{(56)}$$

Hydro generator data was aggregated for 2000 and 2001 from the FERC data and used to verify the model results. The same model was used to compare both years with only three values changed, which include: 1) hourly-resolved load demand, 2) total yearly energy from conventional hydro and pumped hydro, and 3) normalized stream flow vector. While the amount of energy generated from hydro is strongly dependent on the weather for that year, the installed capacity stays relatively constant. According to the CEC in its power plant database, the installed capacity of hydro plants in California has risen less than 100 megawatts between 1994 and 2009, which represents a capacity increase of 0.667%.

Any hydro model must accurately represent different behaviors including, diurnal, as well as seasonal. That is why multiple criteria were considered when assessing the accuracy of the model. The four most important components are the hourly timeseries, daily average and monthly average. Hourly timeseries represents the hourly dispatch of both conventional and pumped generation. Daily average represents the average of each hour of the day for the entire year and captures the diurnal behavior. Lastly, the monthly average is the average power generation for each month and captures the seasonal behavior. Following equation (86), the absolute, percentage difference is calculated with comparison to the FERC data, and the results for 2000 and 2001 are shown in Table 54. Figure 249, Figure 250 and Figure 251 show the comparison between FERC hydro data and model runs for 2001 on an hourly basis, a daily average basis, and a monthly basis, respectively.

Table 54: Percentage Differences Between FERC Data and Modeled Hydro for 2000 and 2001

	Hourly Timeseries	Daily Average	Monthly Average
FERC 2000	15.7%	11.5%	11.0%
FERC 2001	14.9%	6.2%	4.4%

Figure 249: Hourly Timeseries of Model and FERC Data in 2001

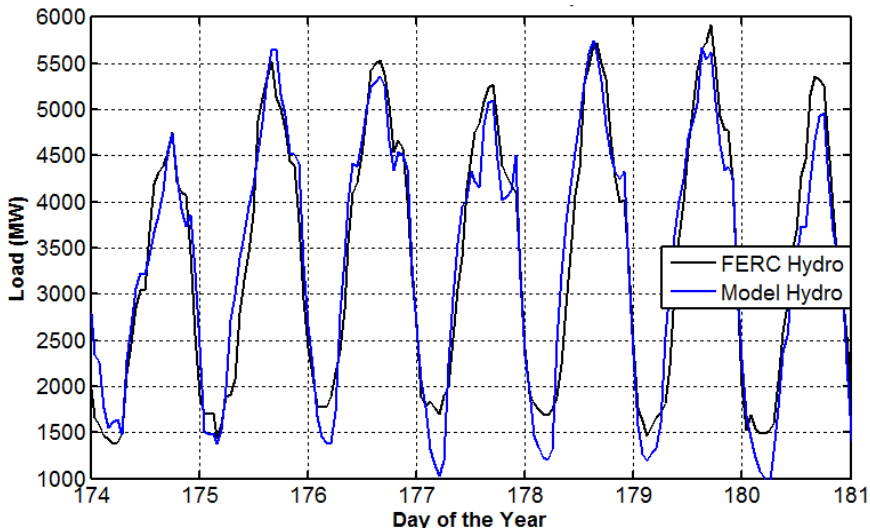

Figure 250: Daily Average of Model and FERC Data in 2001

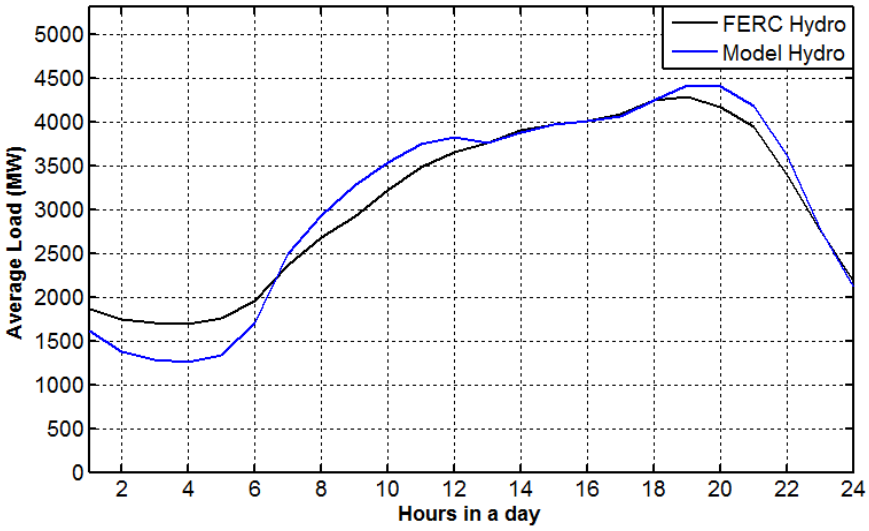

In comparison to FERC data, it can be seen the model tends to under-generate hydroelectricity during the night and early morning, predominantly between midnight and 7am. Additionally, past 7am there are higher than expected generation rates. Still, an error value below 15% on an hourly basis, paired with the decreased error when doing averaged comparisons, shows the model's potential to model other years.

Figure 251: Monthly Average of Model and FERC Data in 2001

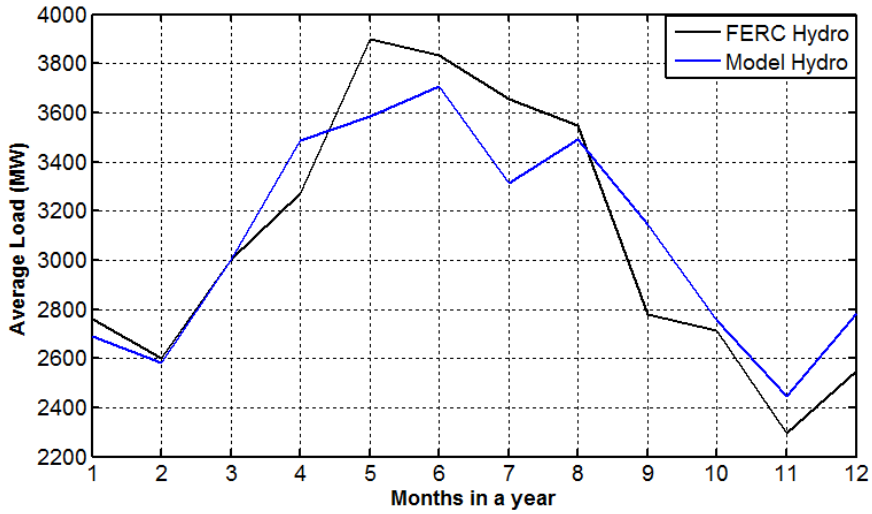

Once the model was verified for different years it was adjusted to reflect 2005 because the goal of this model is to represent how hydro generation can change with increasing renewables, and coincident renewable generation data for wind and solar is only available for 2005, thus the model must be able to function for any year. The larger model, HiGRID, is designed for 2005 based calculations of similar reasons, and as such, uses 2005 CAISO load and spinning reserve profiles. Unlike the FERC data, which looks at only generators, the CAISO data represents the electricity demand, which includes the increase in demand from pumping for pumped hydro sites. A separate methodology was designed to remove this consumption from the CAISO demand profile and prevent duplication of pumped storage electricity consumption. This method, termed pump removal, uses a feedback loop to arrive at the corrected load profile.

The feedback loop starts with the original load profile passing through the hydro code. The modified load profile was passed through the hydro code, and pumped storage energy consumption from the load balancing process could be outputted. Theoretically, adding this energy consumption back to the modified load should recreate the original load provided the consumption vector was accurate. A fraction of the error between the original load and this modeled utility load was then used in the next iteration, subtracted from the scaled CAISO data. However, later it was determined that regardless of gain, given enough iterations, the solution converges. The resulting modified CAISO load profile with pumped storage consumption removed could then be calculated for any year and used as an input into the HiGRID model. Thirty iterations of the pump removal code were run to demonstrate limit of lowest achievable error, shown in Figure 252. Notice that the load demand during the evening is lowered in accordance with the times that the pump generators are turned on (e.g., hours 25-30, 48-53, 72-78).

Figure 252: Resulting Total Generation Profiles for Pump Removal Code

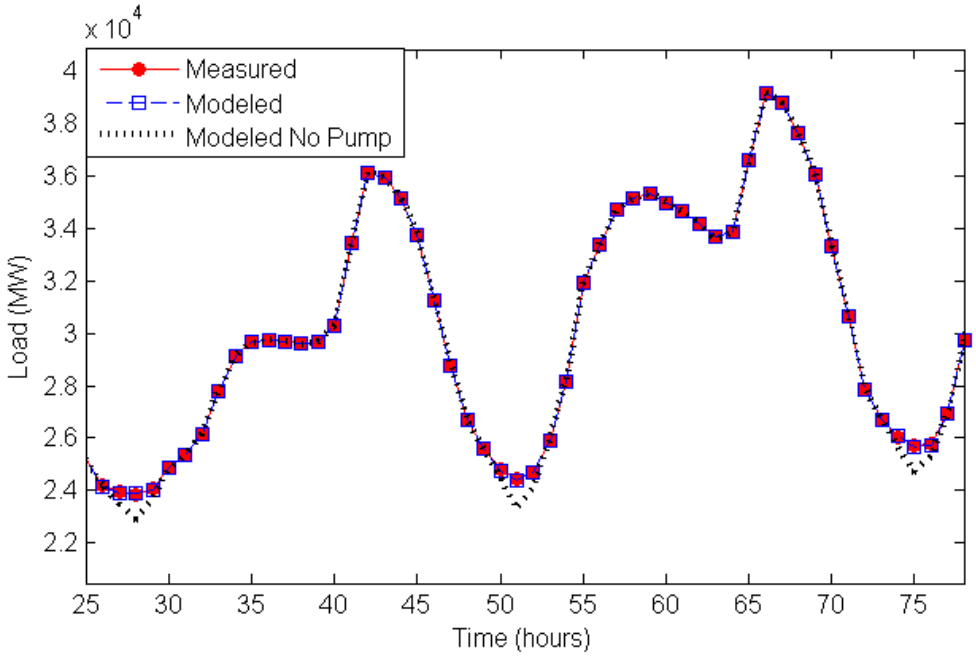

Task 7.1.5. Baseload Generation Module

Since the UCI community does not have any baseload generation this module is specifically for use with the California version of HiGRID.

After the dispatchable load has been exhausted, baseload generation is implemented. Baseload, predominantly consists of nuclear, coal, geothermal generation; however other fuels like natural gas can provide baseload power too. Plant operation is modeled as baseload generation based on an installed capacity and capacity factor. Baseload technologies have a high capacity factor, very few starts and a higher operating hour count for each year. Table 58 shows that baseload plants in 2001 had an average capacity factor of 71.6% with only 7 average starts per plant per year and an average number of operating hours of 8177. The daily average profile for baseload generation is nearly flat as shown in Figure 253.

Figure 253: Daily Average Baseload Generation for FERC 2001 Data

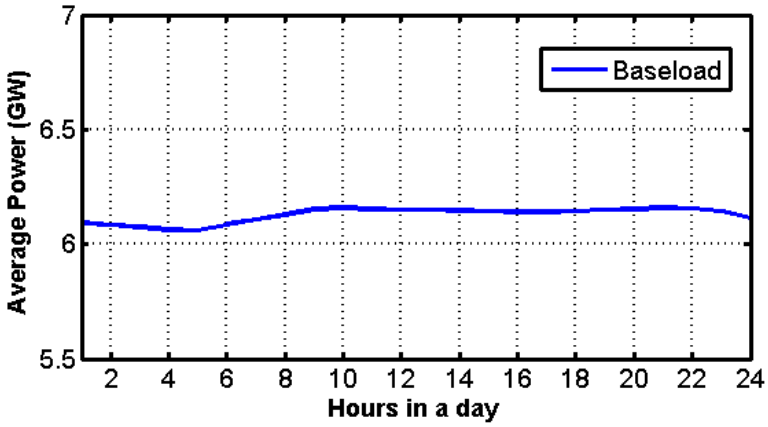

By examining the daily average profiles for each month in 2001 (Figure 254), it becomes clear that while there is little change each hour, the generation for a given month can drop substantially. Generation is lowest during April and May, which represents the lowest demand months of the year and allows planned outages for the baseload generation to ensure that they can provide the maximum power during the hotter months of June, July and August.

Figure 254: Daily Average Baseload Generation by Month for FERC 2001 Data

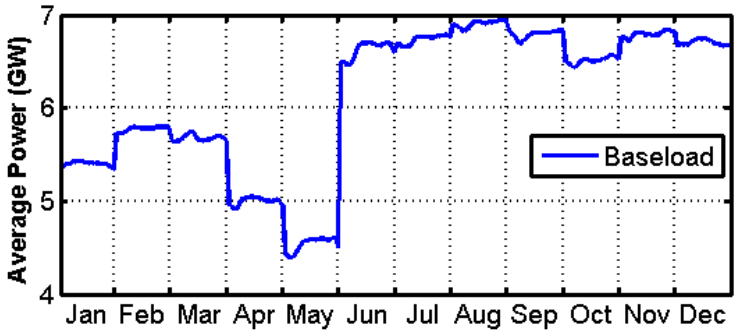

To capture this effect the baseload module uses a variable capacity factor to ensure that hours with low demand are preferentially selected for planned outages and that limited outages occur during hours with high demand. The variable step, "N", can conceptually be any value but was selected as monthly for this model; thus, N=12. The first step is to separate the system-wide load, vector M in length, into N consecutive groups and sum them creating a vector, N in length. This approach requires as inputs, the installed capacity of the baseload technology or technologies, baseload fleet capacity factor and the load data to be met, in part, by baseload generation. Additionally the variable step must be selected such that N is less than or equal to M.

$$E_{Load} = \sum_{i=1}^{N} \{Load(j) : j = M/N \cdot (i-1), ..., M \cdot i\} \quad \textbf{(57)}$$

The first step is to calculate the relative importance of each variable load step by taking a monthly average of the load signal as shown in equation (88), where E_{Load} is the load to be met by baseload generation.

$$B = \frac{(1 - E_{Load} / \max(E_{Load}))}{\sum_{i=1}^{N} (1 - E_{Load}(i) / \max(E_{Load}))} \quad \textbf{(58)}$$

The variable "B" represents the required monthly energy percentage reduction to achieve the ideal distribution of baseload generation for each month. The next step is to determine the available capacity for each month and is shown in equation (89) where Cap_{base} is the capacity available for each of the "X" number of baseload technologies.

$$C = E_{Load} / \max(E_{Load}) \cdot \sum_{i=1}^{X} Cap_{base}(i) \quad \textbf{(59)}$$

The next step is to calculate the capacity that should be reduced from variable "C" to achieve the desired capacity factor for the baseload generation. Variable "D" from equation (90) represents the total capacity across all 12 months that will be removed from "C".

$$D = \sum C - N \cdot \sum_{i=1}^{N} \left(Cap_{base}(i) \cdot CF_{base}(i) \right) \quad \textbf{(60)}$$

The final step is to remove a total of "D" capacity from "C" maximum capacity apportioned to provide the most generation during the months with the highest load demand ("B"). Equation (91) calculates the power at which the baseload fleet must operate for each of the twelve months to achieve the desired yearly capacity factor and while supporting the changing load on the grid and is denoted by the variable $Cap_{setpoint}$.

$$Cap_{\text{setpoint}} = C - B \cdot D \quad \textbf{(61)}$$

Using $Cap_{setpoint}$ This method could be refined to include historical data to approximate the daily average profile while also providing the planned outage characteristics; however, the actual operation with high renewable capacity will not be the same as historical operation. Thus based on the uncertainty with the ability of baseload generation to provide dispatchable power on an hourly basis, the method as described above is used and will be verified in the verification section below.

7.1.5.1. Baseload Verification

Using a monthly capacity factor driven model allows for variable generation that is not dependent on historical generation but rather considers the seasonal value of generating capacity and selection of planned outages to establish the hourly generation of baseload generation.

By comparing the hourly timeseries of the actual generation to the modeled generation for 2000 and 2001 the resulting error using equation (86) is 12% and 10.7%, respectively. Figure 255 and

Figure 256 show the daily average by month for the model compared to the FERC data. The model was developed to adjust generation to meet the inputted capacity factor while also providing more generation during months of high load.

Figure 255: Baseload Generation Comparison Using Daily Average by Month for HiGRID model versus 2000 FERC data

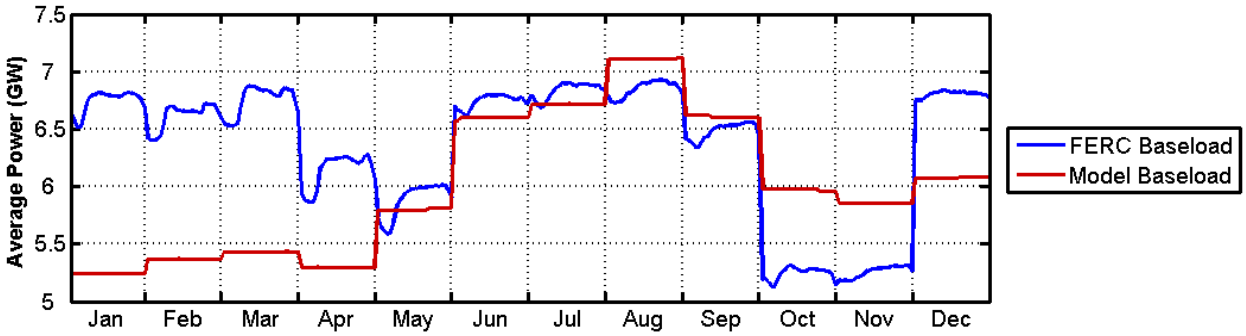

Figure 256: Baseload Generation Comparison Using Daily Average by Month for HiGRID model versus 2001 FERC data

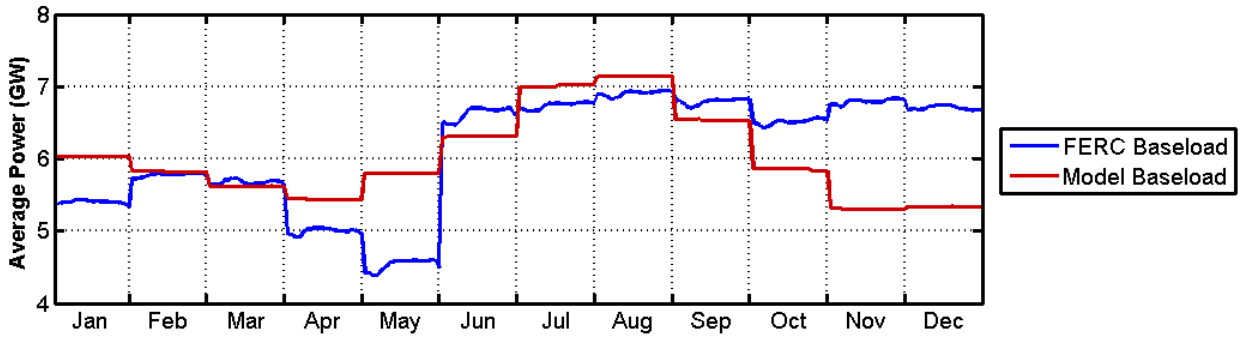

Differences from the FERC data are related to the use of contracts to purchase energy from baseload generation. These contracts must be fulfilled and their time horizons can vary based on the purchaser or the generator. Additionally, prediction of the load for the entire year is not possible thus the generation cannot determine the ideal time to turn on or off. This model reflects the ideal time for baseload generation to turn on such that it maximizes the flexibility of the balance generation fleet.

Task 7.1.6. Balance Generation Module

7.1.6.1. UCI Community Model

To accurately model the impact of increasing the renewable penetration level on the UCI campus and the effect of variable renewable power on the behavior of on-campus generation resources, a model of these on-campus resources was developed. A short description of the major generation resources is presented here.

7.1.6.1.1. Gas Turbine Model

The gas turbine is used to meet a portion of the electric demand of the campus, while providing exhaust heat to be used to meet the campus heating demand. The model is based on rigorous first principles quasi-steady state dynamics, contains thermodynamics equations that describe the simplified physics for each of the major components of the gas turbine. These component parts consist of a compressor, combustor chamber, turbine, power shaft, air handling system, and enclosure housing. A schematic of the single-shaft natural-gas fired gas turbine in component modules is shown in Figure 257. Synchronous operation is preferred for single-shaft configurations because the generator needs to reliably produce electricity at constant frequency (60 Hz). Under any operating condition other than start-up and shut-down, power produced by the turbine drives both compressor and the generator load.

Figure 257: Block diagram of gas turbine engine components

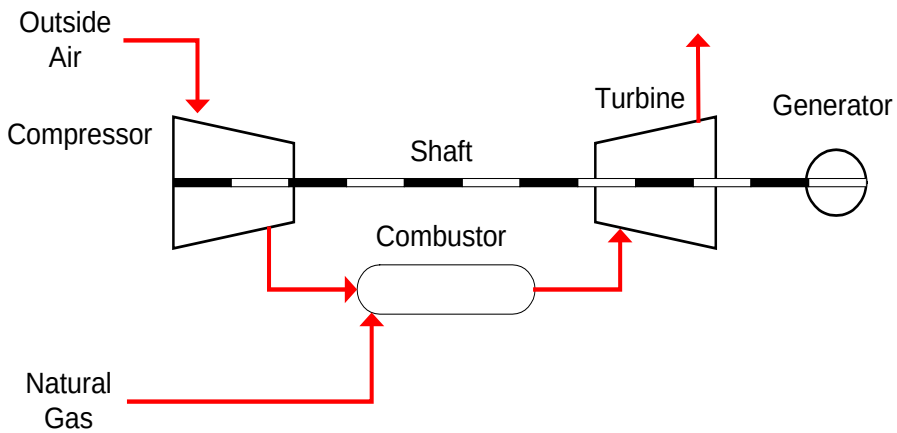

7.1.6.1.1.1. Assumptions

1. All gases are ideal gases
44. Heat transfer to the environment is assumed to occur primarily at the engine section
45. The generator is assumed to be well insulated.

7.1.6.1.1.2. Compressor and Turbine

The compressor and turbine work can be expressed as a function of their respective isentropic efficiency, rotor inlet temperature, compression ratio, and specific heat ratio, with the following expressions

$$\dot{W}_{\text{comp}} = \eta_{\text{comp}} \frac{kRT_{01}}{k-1}\left[\left(\frac{P_{02}}{P_{01}}\right)^{k-1/k} - 1\right] \tag{62}$$

$$\dot{W}_{\text{turb}} = \eta_{\text{turb}} \frac{kRT_{03}}{k-1}\left[\left(\frac{P_{04}}{P_{03}}\right)^{k-1/k} - 1\right] \tag{63}$$

where isentropic efficiency of the compressor and turbine can be determined, respectively, as

$$\eta_{\text{comp}} = \frac{T'_{02} - T_{01}}{T_{02} - T_{01}} \tag{64}$$

$$\eta_{\text{turb}} = \frac{T_{03} - T_{04}}{T_{03} - T'_{04}} \tag{65}$$

The energy balances for the compressor and turbine are given as,

$$\rho C_{mass} V_{cv} \frac{dT_{02}}{dt} = \dot{E}_{in} - \dot{E}_{out} + \dot{W}_{comp} \tag{66}$$

$$\rho C_{mass} V_{cv} \frac{dT_{04}}{dt} = \dot{E}_{in} - \dot{E}_{out} + \dot{W}_{turb} \tag{67}$$

where $\dot{E}_{in}$ and $\dot{E}_{out}$ are enthalpy terms representing the internal energy of flow at the inlet and outlet of the compressor and turbine. The flow enthalpy can be captured based on the sensible enthalpy of the fluid species and their respective heat of formation as follows:

$$\dot{E}_i = \sum^{i} m_i \left[\overline{h}^{o}_{f,i} + \left(\int_{T_{ref}}^{T} \overline{c}_p dT\right)\right] \tag{68}$$

7.1.6.1.1.2.1. Combustor

Most state-of-the-art combustors utilize dry lean-premixed combustion technology to achieve low levels of both nitrous oxides (NOx) and carbon monoxide (CO) emissions. The combustion chamber is characterized as a constant volume and perfectly mixed reactor where complete and instantaneous combustion reaction occurs. The key assumption here is chemical kinetic rates are 2 to 6 orders of magnitude greater than transport phenomena in a gas turbine engine (Gou, 2010). On the other hand, complete reaction is a reasonable assumption due to the inherent characteristics of dry lean-premixed technology to combust fuel with a large excess of air above the required stoichiometric level. In the model, the combustion is simulated as a complete combustion reaction of methane with the overall reaction,

$$CH_4 + 2O_2 \rightarrow CO_2 + 2H_2O \tag{69}$$

The conservation of mass in the combustion chamber is described by

$$\frac{dP}{dt} = \frac{RT}{V}\left(\dot{N}_{in} - \dot{N}_{out} + \sum R_i\right) \tag{70}$$

The energy conservation is

$$\rho C_p V_{cv} \frac{dT_3}{dt} = \dot{E}_2 - \dot{E}_3 - \dot{Q}_L \tag{71}$$

The pressure losses in the combustor is expressed as

$$P_2 = P_3\left(1 - \frac{\Delta p}{100}\right) \tag{72}$$

7.1.6.1.1.3. Power Shaft

The coupling of the shaft speed and torque of the compressor, turbine, and generator can be described by a torque balance performed on the rotating shaft. As shown in Figure 258, the torque produced by the turbine on the shaft is opposed by the torque of the compressor and the generator. The torque by the compressor and turbine, respectively τ_{comp} and τ_{turb}, are sometimes referred to as "developed torques." The opposing torque produced by the steady operation of the generator generally referred to as load torque, τ_{load}, is a resistive torque caused by the rotating motion of reduction-drive gearbox, generator shaft, and synchronous generator with permanent magnet exciter. The aggregated inefficiencies of these components inside the generator compartment amount to minimal efficiency loss.

Figure 258: Schematic of the torque diagram around the rotating shaft of single-spool

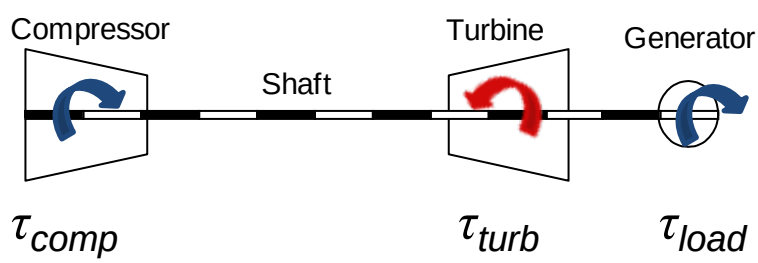

The torque analysis based on the rotating shaft relates the change in shaft speed, ω, and the rotating inertia to the torque balance

$$\tau_{turb} - \tau_{comp} - \tau_{load} = J\frac{d\omega}{dt} \tag{73}$$

Since the work being done, P, on a rotating body is a product of the exerting torque and the angular velocity,

$$P = \tau\omega \tag{74}$$

Power balance on the rotating shaft then becomes

$$P_{turb} - P_{comp} - P_{load} = J\omega\frac{d\omega}{dt} \quad (75)$$

where the power of the generator, P_{load}, is a controlled variable for the feedback control of the fuel inlet. The power of the compressor, P_{comp}, and turbine, P_{turb}, are output variables determined from thermodynamic relationships and part-load characteristic maps. Figure 259 shows the model representation of Equation (105) in Simulink.

Figure 259: Simulink representation of the shaft dynamics

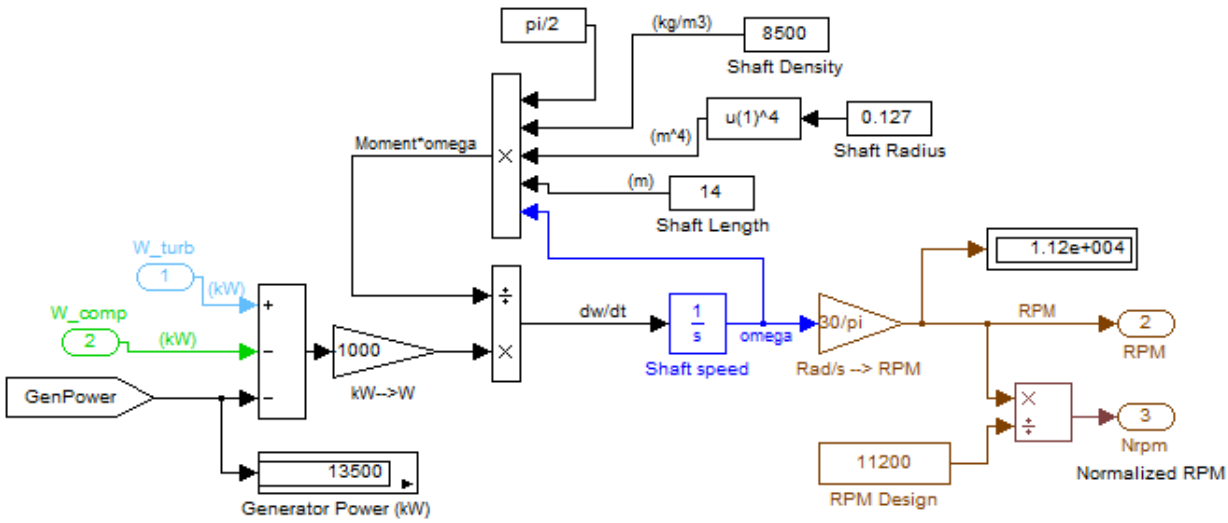

7.1.6.1.1.4. Air Handling Unit

As ambient temperatures rise, gas turbine efficiency and power output decrease due to a lower density of air. In conventional combined cycle plants, this effect is alleviated by installing air cooling systems to lower the compressor inlet temperature and effectively increase gas turbine performance. Standard air cooling systems can be quite complex but for simplicity, the model assumes a pressure loss across an air filter and cooling coil. The cooling coil module is simulated as a discretized counter-flow shell-and-tube configuration as shown schematically in Figure 262. Quasi-two-dimensional conductive and convective heat transfer using Fourier's law and Newton's law of cooling are considered and resolved at each node with control volumes for the shell side, tube side, and the heat exchanging wall.

Figure 260: Discretized counter-flow shell-and-tube cooling coil.

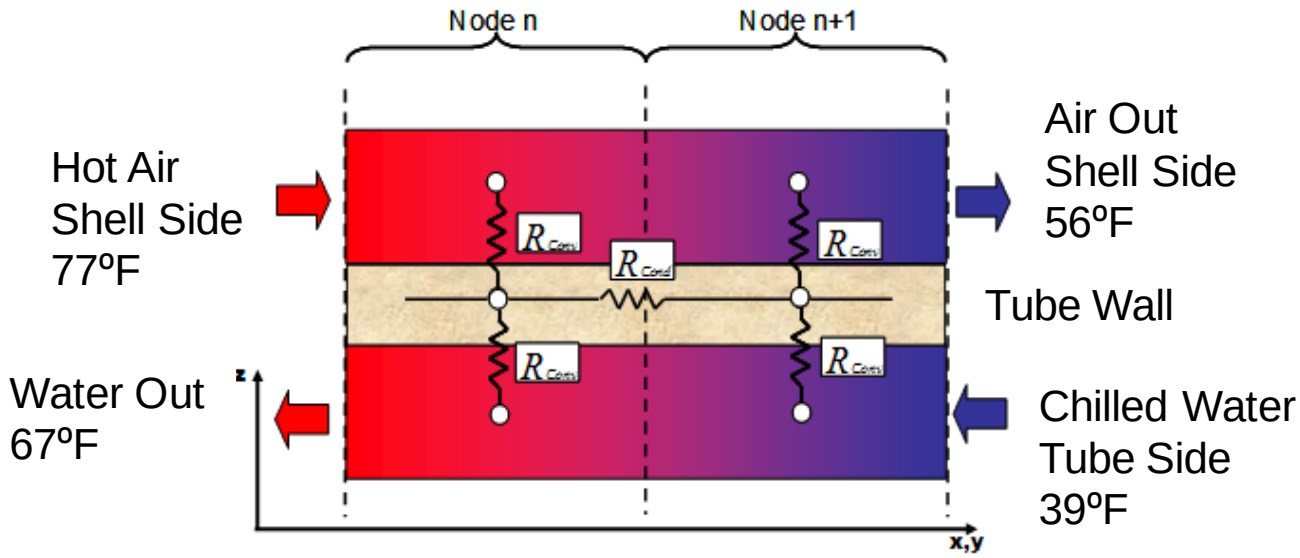

7.1.6.1.1.5. Control Logic

The control strategy of the gas turbine is modeled as having two active principal controllers: temperature control by variable inlet guide vane (VIGV) manipulation and power control by fuel flow manipulation. The temperature controller of gas turbine model has been tailored after recorded field data of a Solar Titan 130 at various part loads under steady state operation. As shown in Figure 261, the turbine exhaust temperature is controlled by manipulating the air flow rate with a proportional and integral action with a feed forward. The feed forward block contains recorded field data of the Titan 130 engine relating the turbine exhaust temperature to various part loads. In synchronous engines typically used in CCHP systems, the air flow rate is physically controlled by the closing action of the variable inlet guide vanes (VIGV). The VIGVs are connected together by a rod to an actuator. Thus, the closing action of the VIGVs can be simulated as a transfer function with a time delay constant. In the physical system, the closing of the VIGVs not only reduces the air flow but also changes the angle of incidence of the air flow into the compressor rotor blades. Since the compressor module contains a VIGV performance map, the deviation of the angle of incidence or VIGV angle (from off-design position) corresponds to a specific compressor air flow and pressure ratio.

Figure 261: Modeled Solar Titan 130 temperature controller.

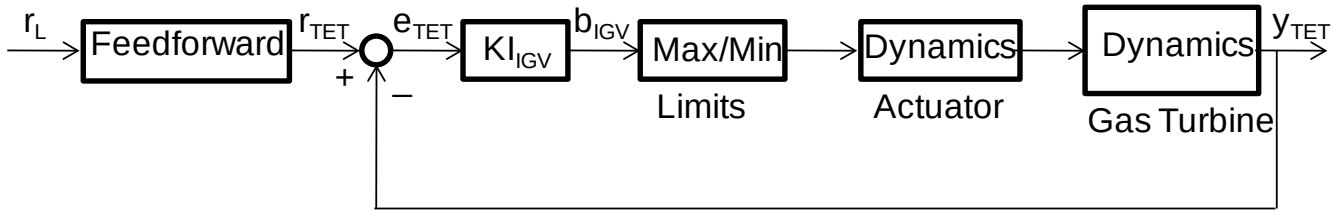

The gas turbine power is controlled by manipulating the fuel flow into the combustor with a proportional and integral action without a feed forward. This power controller is displayed in the block diagram in Figure 262. The dynamics of the fuel delivery system is represented by a first order transfer function with time delay constant. For synchronous gas turbines, while the load control is active during all operating conditions, speed control is only active during transient operation. The proportional and integral speed control loop serves as a curtailment or increase of fuel delivered to ensure constant shaft speed. This is especially important for the generator to maintain its frequency to that of the 60 Hz regulation. Also during transient operation, acceleration control by fuel manipulation becomes active when the acceleration of the generator exceeds the acceleration limit. This is an integral control feedback loop without feed forward. The output of the three control loops for the fuel delivery system are fed into a minimum value select gate where the loop with the lowest output will be the active controller of the fuel flow.

Figure 262: Modeled Solar Titan 130 power controller.

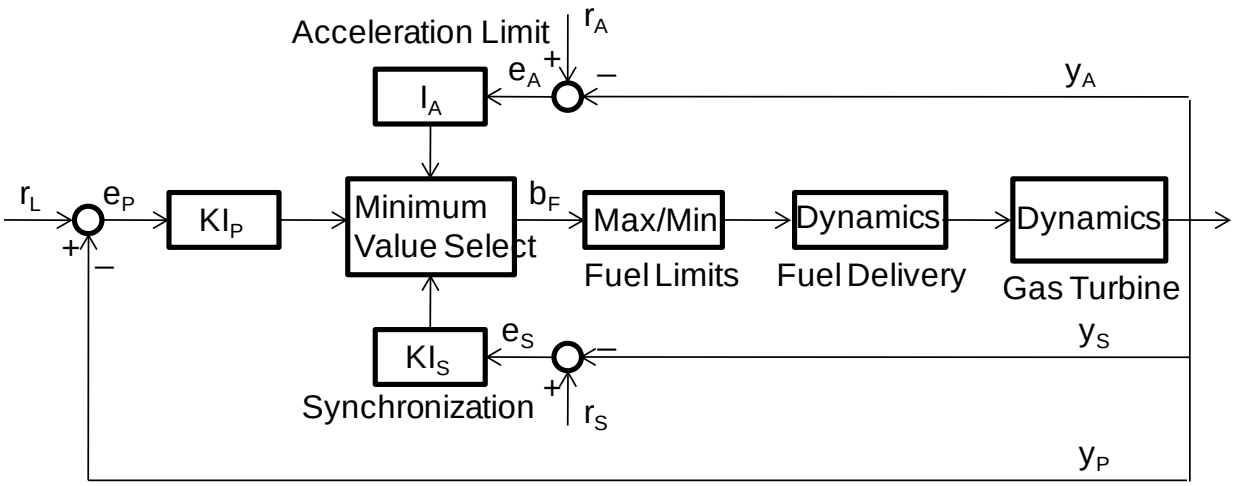

7.1.6.1.1.6. Design and Off-Design Characteristics

The off-design simulation of the engine performance requires the performance maps of the compressor and turbine for part-load characteristics. These performance maps of the compressor and turbine are generally not available for proprietary reasons. Performance maps of representative gas turbines are used in their places. The maps are then tailored to match the

design-point performance specifications (Table 1) of the Titan 130. Part-load performance is simulated by employing a controlling scheme to manipulate the fuel flow and the air flow according to observed field data and suggested turbine exit temperature (TET) control from the literature.

In part-load operation of the Titan 130, the inlet airflow is controlled by modulating the variable inlet guide vanes (VIGV). This is to ensure that the turbine exit temperature (TET) is at the highest level as possible. Maintaining the highest possible TET is critical for the efficiency of the heat recovery steam generation system in cogeneration plants. The first six compressor stages are equipped with VIGVs for the Titan 130. The setting angles of the variable vanes are actively controlled during part-load operation to change the airflow characteristics. Changing the angle of these vanes or VIGV modulation provides the closing effect on the air flow and changes the direction of the air flow being introduced into the rotor inlet. Both of these physical effects provide surge protection for the compressor by lowering pressure ratio and moving the operating point away from the surge line in part-load operation. In the model, the operating characteristics of the compressor are derived from empirical performance of a representative compressor at different IGV angles. The minimum operating power of the gas turbine is about 8 MW. If the gas turbine power is required to drop below 8 MW for any reason, the entire system must shut down or 'trip' offline.

Table 55: System parameters of Solar Titan 130 engine for design performance

Parameters	Design Specs	Field Data	Simulation
Electrical Power [MW]	13.5	13.5	13.5
Shaft speed [rpm]	11,200	--	11,200
Pressure Ratio	16	16	16
Fuel Flow (Natural Gas) [pph]	--	6600	6600
Air Flow Rate [pph]	396,390	--	418,260
Engine Efficiency [%]	33.3	32.6	32.6
Compressor Efficiency [%]	83	--	83
Turbine Efficiency [%]	--	--	85.6
Compressor Inlet Temperature [^{o}F]	59	55	55
Firing Temperature [^{o}F]	2050	--	1903.7
T5 Temperature [^{o}F]	--	1400	1400
Exhaust Temp [^{o}F]	913	926	926

7.1.6.1.2. Heat Recovery Steam Generator (HRSG) Model

The heat recovery steam generator (HRSG), which uses exhaust from the gas turbine to produce steam that is used to meet the heating demand of the campus and potentially produce additional electricity through the use of the steam turbine, is modeled using the Number of

Transfer Units (NTU) method. The expressions for the heat exchanger effectiveness are presented as follows:

$$\varepsilon = \frac{1}{C_r}\left[1-\exp\left\{-C_r\left[1-\exp(-NTU)\right]\right\}\right] \qquad C_{\min} \text{ unmixed } C_{\max} \text{ mixed} \tag{76}$$

$$\varepsilon = 1-\exp\left\{-\frac{1}{C_r}\left[1-\exp(-C_r\cdot NTU)\right]\right\} \qquad C_{\min} \text{ mixed } C_{\max} \text{ unmixed} \tag{77}$$

Where

$$NTU = \frac{UA}{C_{\min}} \tag{78}$$

C_r refers to the ratio of the heat capacity coefficients of the two fluids (C_{min}/C_{max}), U is the overall heat transfer coefficient, and A is the area of heat transfer.

The heat recovery steam generator (HRSG) model is an integrated dynamic model consisting of individual cross-flow dynamic models simulating the physical and transient performance of the major HRSG components. The simulated components are the economizer, two subsequent boilers, and the superheater. Under all operating cases, cross-flow configuration using the effectiveness-NTU method is modeled with the assumption that the air side is the mixed fluid and the water or steam side is the unmixed fluid. Thus, equations (106) and (107) are used to determine the effectiveness factor of each heat transfer component. Boiler #1 is simulated as a single-phase cross-flow heat exchanger with the key assumption that the colder fluid, in this case water, is heated up to the onset of evaporation. This is reasonable based on the observation that water still retains its liquid phase while moving through this section of the HRSG. Boiler #2 is simulated as a cross-flow heat exchanger with a phase change occurring on the colder and unmixed fluid side. Preliminary analysis indicated that the air side is generally the limiting factor in the heat transfer but the model has the intelligence to switch between equations (106) and (107).

7.1.6.1.3. Steam Turbine Model

If steam in excess of the amount required to meet the campus heating demand is present, this additional steam is routed through the steam turbine to produce additional electricity to meet the campus electric load. The on-campus steam turbine is a 5.5 MW unit that does not include any steam extraction, and is oversized for this application in anticipation of an expansion of the gas turbine capacity.

The steam turbine is modeled with a physical dynamic model of the steam turbine based on first-principle thermodynamics is developed and validated against in-field operation data. The mass balance for the steam turbine is given as,

$$V_{cv}\frac{d\rho}{dt} = \dot{m}_{in} - \dot{m}_{out} \quad \textbf{(79)}$$

The transient energy balance takes into account the enthalpy difference between the inlet and outlet steams, the work done on the turbine blades by the steam, and a constant heat loss to the surrounding. The governing equation for the energy balance is thus,

$$\rho C_p V_{cv}\frac{dT}{dt} = \dot{m}h\big|_{in} - \dot{m}h\big|_{out} - \dot{W}_{st} - \dot{Q}_L \quad \textbf{(80)}$$

where $\dot{W}_{st}$, the actual mechanic work, deviates from the ideal mechanic work according to its isentropic efficiency and is given by the expression,

$$\dot{W}_{st} = \eta_{isen}\left(\dot{m}h\big|_{in} - \dot{m}h\big|_{out}\right) \quad \textbf{(81)}$$

During the expansion stages, the steam loses some of its quality. The outlet enthalpy therefore is a function of quality and is expressed as

$$h_{out} = h_f + xh_{fg} \quad \textbf{(82)}$$

All thermodynamic properties for steam are obtained from steam tables derived from IAPWS IF-97. Peak isentropic efficiency of 0.9 was used for the model, representing the typical value for steam turbines. Important design characteristics for the central plant turbine are synchronous generator, inlet-pressure valve control, and operating pressure range of 230 psig inlet and 15 psig outlet.

The off-design performance of the steam turbine was simulated using a steam turbine performance curve derived from part-load study as reported by Fallah (1978). The resulting performance curve relates the isentropic efficiency to the steam flow.

7.1.6.1.4. Utility Interconnection Considerations

The UCI campus currently operates under an agreement with Southern California Edison (SCE) such that the campus is not allowed to export power, and must maintain a minimum import power level at all points throughout the year. Specifically, the UCI campus must import at least 1 MW of electricity at all times from SCE. This agreement is rooted in the notion that there is insufficient equipment to manage exported power or low imported power levels on the local distribution and sub-transmission systems. If the on-campus generation increases or the campus load demand decreases such that the imported power drops below this level, SCE will cause the on-campus gas turbine to trip offline and the entirety of the campus load demand at the time will be met by imported power.

To avoid this, the campus typically operates the gas turbine at a power level that is at least 2 MW below the load demand. If the load demand at a particular hour drops, the gas turbine will be turned down until it reaches its minimum power level. Additionally, the steam turbine will not produce any power if doing so would cause an import power violation.

7.1.6.2. California Model

Balance generation is broken into two groups based on the duty cycles as will be described in the following section. Load-following generation manages larger, diurnal electricity demand swings and provides a significant amount of ancillary services. Peakers provide energy for highly dynamic events including providing regulation and energy during the peak of the day when no other generator either can respond quickly enough or has the available capacity to meet the remaining load.

Understanding how the integration of renewables affects the other generation on the grid is vital to understanding the "true" cost and value of renewable generation. The balance generation model satisfies the remainder of the load not met by the renewables, baseload or other dispatchable generation.

7.1.6.2.1. Generator Duty Cycles

From the time-resolved FERC data (FERC, 2002) it is possible to calculate the general operating characteristics for each generation technology and fuel type combination, which is presented in Table 56. The average maximum and minimum plant size is shown along with plant capacity factor. Average unit count shows the average number of generators per plant as determined with the California System Operator's summer generation assessment, which contains information about which plants are an aggregation of multiple generators (CAISO, 2003 (summer assessment report)). Two values for the heat rate are provided both with units of (Btu/kWh). Rated heat rate is the heat rate at rated power, while the observed heat rate calculates the actual heat rate using the load point and a function that relates to the hourly load point to heat rate. When rated heat rate is different from the observed it is an indication that the generation type is operating away from the rated load point.

Table 56: California Fleet Generation Operating Parameters for 2001

Generator Type	Total Capacity (MW)	Avg Max Capacity (MW)	Avg Min Capacity (MW)	Avg. Capacity Factor	Energy (GWh)	Avg. Unit Count	Rated Heat Rate	Observed Heat Rate	Avg. Yearly Operating Hours	Avg. Starts
Hydroelectric	9557	49.0	0.0	34.0%	24261	1.7	-	-	5965	104
Hydro Pumped-storage	2538	193.3	0.0	20.6%	2618	5.6	-	-	3632	166
Nuclear Driven Steam Turbine	4414	1103	162.0	85.8%	33146	1.0	10479	10478	7591	5
Coal Fueled Steam Turbine	1520	760.0	176.9	76.6%	10199	1.0	10335	10361	7614	14
Geothermal Driven Steam Turbine	1767	53.5	2.7	69.1%	10173	1.3	17581	17633	8305	7

Natural Gas Combined Cycle	1257	62.2	28.8	32.3%	3551	2.4	10026	11568	3955	58
Fuel Oil Combustion Turbine	885	61.7	26.6	14.3%	1172	1.1	14704	14625	1832	108
Jet Fuel Combustion Turbine	15	15.0	13.0	2.3%	3	1.0	16003	16375	249	31
Natural Gas Combustion Turbine	692	33.8	17.7	10.6%	515	1.4	16894	17773	1212	138
Other Generation	9002	91.7	0.0	23.0%	16511	2.2	9330	10077	4274	125
Natural Gas Steam Turbine	15022	259	40.2	40.2%	63133	1.0	10348	11507	5526	17
Thermal Generation	6860	20.5	0.1	44.8%	30476	2.2	-	-	6348	70
Total	53529	74.2	1.8	38.2%	195756	1.9	12563	13735	5689	81

Using the information in Table 56 technologies that have similar operation (i.e., duty cycles) can be grouped together. Duty cycles are determined from the capacity factor, heat rates, operating hours and starts. The most generic duty cycles are baseload, dispatchable and intermittent. Baseload operation is characterized by very high yearly operating hours, few starts and high capacity factor. Nuclear, coal and geothermal all exhibit these characteristics. Intermittent generation is characterized by uncontrollable and less predictable generation that is dependent largely on geological conditions and includes wind, solar, wave, tidal and small-hydro. The remaining technologies are dispatchable; however, further classification of the dispatchable duty cycle results in three additional duty cycles: hydroelectric, load-following and peaking. Hydroelectric is comprised of both conventional hydroelectric and pumped-storage. Load-following and peaking categories are more difficult than the others to separate since their operations can often exhibit similar characteristics. Peakers can be characterized as generators that turn on during times of high load to meet the power demand, but also can provide regulation and some capacity to meet reserve margin. Load-followers can typically be characterized as generation that provides the bulk of the dispatchable power and changes power output throughout the day with a relatively small portion of the generation being turned off at night. Steam turbines take more time to turn on than combustion turbines and the nature of peakers is that they can quickly come online for a short amount of time so, combustion turbines are more likely to be peakers and systems with steam turbines are more likely load-following units, but this is not the case with all units and therefore must be analyzed on a plant-by-plant basis.

CAISO's summer assessment document classifies most the dispatchable generators as "peakers" or a combination of "cogeneration", "thermal" or "various," which are all considered as load-followers (CAISO, 2003). For those that are not defined from the summer assessment document their classification is established based on their capacity factor, yearly operating hours and starts in comparison to the plants that are defined. 46 out of 726 plants are not listed in the summer assessment document. The duty cycle for these plants is a peaker if two criteria are met 1), if the capacity factor for a plant is less than 12% or the operating hours are less than 40%

of the year and 2), if the average duration that the generation is operating (i.e., yearly operating hours / yearly starts) is greater than 55 hours per start; otherwise the plant is a load-following plant. Table 57 contains the resulting fleet operations separated by duty cycle and by generation type.

Table 57: California Fleet Operating Parameters for 2001 by Duty Cycle and Technology Type

Duty Cycle	TYPE	Energy (GWh)	Max Capacity (MW)	Avg Max Capacity (MW)	Avg Min Capacity (MW)	Avg Capacity Factor	Avg Heat Rate	Avg Operating Hours	Avg Plant Starts	Plant Count
BASE	GEO	10173	1767	53.5	2.73	69.1%	17633	8305	7	36
	NUKE	33146	4414	1103.4	162.00	85.8%	10478	7591	5	4
	STC	10199	1520	760.0	176.90	76.6%	10361	7614	14	2
BASE Total		53517	7701	223.6	32.59	71.6%	12824	8177	7	42
HY	HY	24261	9557	49.0	0.00	34.0%		5965	104	251
	HYPS	2618	2538	193.3	0.00	20.6%		3632	166	39
HY Total		26879	12096	55.4	0.00	33.4%		5861	107	290
LF	CCNG	3125	903	64.2	16.67	46.6%	10786	5927	30	13
	CTFO	756	216	108.0	18.00	53.0%	12510	7094	11	2
	CTNG	150	25	25.0	14.00	68.3%	16239	6846	74	1
	OTHER	14683	7200	154.7	0.00	31.7%	10449	5332	62	66
	STNG	62846	14548	279.8	43.08	44.1%	11766	6035	15	52
	TH	28733	6140	19.7	0.00	46.6%		6520	56	481
LF Total		110293	29032	78.8	4.75	44.5%	11735	6296	49	615
PK	CCNG	426	355	60.2	41.00	18.1%	13832	1983	86	6
	CTFO	415	669	54.0	28.08	7.9%	15993	955	124	13
	CTJF	3	15	15.0	13.00	2.3%	17558	249	31	1
	CTNG	365	667	34.3	17.94	7.0%	18003	860	142	23
	OTHER	811	1208	40.2	7.49	7.6%		1096	83	59
	STNG	287	474	79.0	15.25	5.6%	13290	1118	32	6
	TH	42	66	22.1	5.00	6.1%		1397	69	3
PK Total		2350	3454	45.0	16.90	7.8%	16286	1068	100	111
INT	OTHER	1017	594	15.1	0.00	22.1%		5691	312	45
	TH	1700	653	32.5	0.00	24.8%		4625	307	42
INT Total		2717	1247	22.8	0.00	23.3%		5224	310	87
Grand Total		195756	53529	74.2	1.78	38.2%	13735	5689	81	1145

Notice that the load-following duty cycle has a combination of every kind of plant but is more heavily focused on the steam turbine, thermal, other and combined cycle plants where as the peaker duty cycle is more focused on natural gas, jet fuel and fuel oil combustion turbines than the load-following breakdown. Table 58 compares only the total for each duty cycle.

Table 58: California Fleet Operating Parameters for 2001 by Duty Cycle

Duty Cycle	Energy (GWh)	Max Capacity (MW)	Avg Max Capacity (MW)	Avg Min Capacity (MW)	Avg Capacity Factor	Avg Heat Rate	Avg Operating Hours	Avg Plant Starts	Plant Count
BASE	53517	7701	223.6	32.59	71.6%	12824	8177	7	42
HY	26879	12096	55.4	0.00	33.4%		5861	107	290
LF	110293	29032	78.8	4.75	44.5%	11735	6296	49	615
PK	2350	3454	45.0	16.90	7.8%	16286	1068	100	111
INT	2717	1247	22.8	0.00	23.3%		5224	310	87
Total	195756	53529	74.2	1.78	38.2%	13735	5689	81	1145

Based on the duty cycles established above and with the FERC data the resulting generation and purchased bids can be collected. Table 59 shows the energy and ancillary service market results based on the market construction in 2001. Though the construction is different from the MRTU program there are still some strong similarities. This information was extensively used for the development and verification of the HiGRID model as will be described later. Reviewing this chart provides a wealth of information about the type of resources that bid into certain markets. For instance, HY provides the majority of spinning reserve and non-spinning reserve, while LF provides the majority of regulation, both down and up. For comparison, results from 2000 are included in Table 60. Creating Table 59 and Table 60 represents a significant time investment because to compile this data the information was first inserted into an SQL database, then generation were classified by their duty cycles and then finally could be queried to develop the two tables seen below.

Table 59: California Market Bidding Results for 2001 by Duty Cycle

Generation and Bid Quantities for 2001 (GW)	Duty Cycle						Grand Total
	PK	LF	HY	HYPS	BASE	INT	
Actual Generation	2,604	110,041	24,261	2,618	53,517	2,717	195,758
Hour-ahead Generation	1,783	109,193	24,553	2,043	52,841	2,682	193,096
Day-ahead Spinning Reserve	13	1,500	6,824	984	0.0020	-	9,321
Hour-ahead Spinning Reserve	20	1,967	6,949	1,003	0.0020	-	9,939

Day-ahead Non-Spinning Reserve	553	1,212	2,127	2,752	-	-	6,644
Hour-ahead Non-Spinning Reserve	733	1,521	2,192	2,882	-	-	7,327
Day-ahead Replacement Reserve	265	490	133	1,114	-	-	2,002
Hour-ahead Replacement Reserve	396	802	242	1,172	-	-	2,611
Hour-ahead Regulation Up	145	2,246	1,296	629	-	-	4,316
Hour-ahead Regulation Down	182	3,665	1,501	37	-	-	5,385
Supplemental Energy Incremental Bid	5,482	19,778	291	4,937	0.75	-	30,488
Supplemental Energy Decremental Bid	(26)	(17,009)	(5,786)	(1,082)	(2,732)	-	(26,634)

Table 60: California Market Bidding Results for 2000 by Duty Cycle

Generation and Bid Quantities for 2000 (GW)	Duty Cycle						Grand Total
	PK	LF	HY	HYPS	BASE	INT	
Actual Generation	3,543	102,167	32,863	2,676	55,944	2,701	199,894
Hour-ahead Generation	3,088	92,937	31,845	3,600	55,033	2,431	188,934
Day-ahead Spinning Reserve	41	1,437	2,171	389	156	-	4,193
Hour-ahead Spinning Reserve	44	1,957	2,465	475	156	-	5,098
Day-ahead Non-Spinning Reserve	1,013	624	287	1,810	-	-	3,734
Hour-ahead Non-Spinning Reserve	1,154	1,006	451	2,055	-	-	4,667
Day-ahead Replacement Reserve	299	971	251	465	1.3	-	1,986
Hour-ahead Replacement Reserve	477	1,789	405	570	1.3	-	3,243
Hour-ahead Regulation Up	235	2,601	1,953	778	-	-	5,567
Hour-ahead Regulation Down	176	2,454	2,477	92	20	-	5,219
Supplemental Energy Incremental Bid	3,336	17,091	3,875	2,833	750	-	27,884
Supplemental Energy Decremental Bid	(197)	(9,231)	(6,759)	(447)	(3,158)	-	(19,791)

7.1.6.2.2. Balance Generation Model

Load-followers provided over half of the generation, nearly half of the regulation and a large portion of spinning reserve over the years of 2000 and 2001 as was shown in Table 59 and Table 60. Peakers provide a small fraction of the energy at around 1.6% of the total generation while providing 0.4% of the spinning reserve and around 3.6% of the regulation.

Dispatch of balance generation will be affected as increases in renewables change the system requirements to maintain stable operation and reliability as is evidenced from the literature (GE Energy Consulting, 2010 (CAISO 20%); Porter, 2007; GE Energy Consulting, 2010 (WWSIS). Understanding the effects on these generators requires that their generation is not constrained to historical operating behavior but is allowed to change operation to the extent that its operating constraints allow.

Figure 263 depicts the process by which the HiGRID tool dispatches load-following and peaking generation. In this way, peaking and load-following generator characteristics and reserve constraints are considered. Once complete, the generator operation results in a balanced system that is able to provide the sufficient amount of power to meet the demand and reserve without violating operating constraints. The outputs from the module include time-resolved number of peaking and load-following generators and output power, as well as the heat rate, fuel use, and average startups for each type of generator.

Figure 263: Balance Generation Module Flowchart

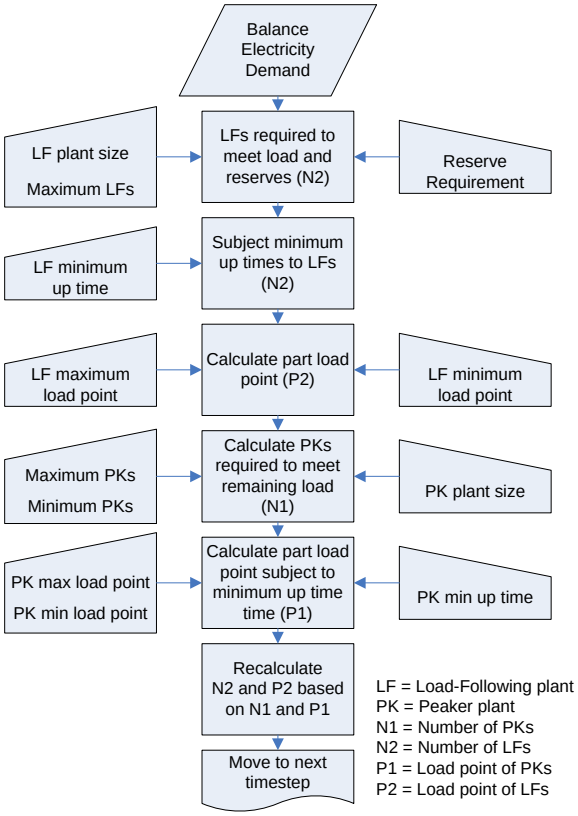

The model assumes that there are two classes of generation (i.e., load-following and peaking) and that all plants are comprised of identical generators with operation characteristics that represent the fleet average. Characteristics that are considered in the balance generation module are listed in Table 61. The minimum and maximum load points represent the maximum and minimum achievable generation for the generator. The minimum load point for load-follower has two values. 75% is the nominal minimum value but the load point can dip as low as 60% in extenuating circumstances and for very short times (i.e., related to the maximum ride through time). Minimum up time represents the fewest hours that a generator must be turned on to maintain economic competitiveness and limited impact on unit lifetime. These values are gathered from generator data collected by the WECC in the Transmission Expansion Planning Policy Committee document library. Maximum ride through is applied to load-followers only and is used to mitigate situations when a generator would turn off and then turn on the next few hours. The value represents the number of hours that the generator will "ride

through" an event that draws its load point below 75% so that it will not have to turn off and on the next hour. The maximum of these two characteristics determines the minimum load prediction required to operate this model. For instance, if the minimum up time of load-following generation is the highest of all generator times and it has a value of 5 hours then the load 5 hours in advance must be either known or predicted for the model to operate. This establishes a balance between degradation, efficiency loss and ability to meet emission limits. Rated power and rated efficiency are based on the fleet average drawn from FERC data. The minimum and maximum unit operating values established a range for the total number of units that can operate. Notice that the maximum is set to infinity but the capability is coded into the model to consider a limit to the number of generators. The minimum number of peakers is set to two to correspond with the FERC data, which had a few peakers on for very long periods of time. Lastly, the heat rate versus load-point curves allow for variable heat rate calculations. These curves along with the rated efficiency determine the plant efficiency at part load.

Table 61: Generator Operating Characteristics Considered for Balance Generation Module

Generator Operation Characteristics	Variable	Peaker	Load-Follower
Minimum Load Point	jL	70%	75% (60%)
Maximum Load Point	Jh	98%	98%
Minimum Up Time	UP_{min}	2 hours	8 hours
Maximum Ride Through (max down) Time	$Down_{max}$	0 hours	1 hour
Generator Rated Power	P	50 MW	70 MW
Generator Rated Heat Rate	η	17.1 MMBtu/MWh	11.4 MMBtu/MWh
Minimum Units Operating	U_{min}	2	0
Maximum Units Operating	U_{max}	∞	∞
Plant Losses	L_{plant}	3.4%	2.9%
Transmission Losses	L_{TX}	2.09%	2.09%
Transformer Losses	L_{XFMR}	0.5%	0.5%
Heat Rate vs. Load-Point Curve		Based on Solar Titan 130 Gas Turbine	Based on GE STAG 209E (Chase, 2001)

Three strategies can be employed for dispatching the generation based on the desired outcome: 1) maximum efficiency, 2) minimum efficiency, 3) minimum starts. The maximum efficiency strategy turns on the minimum number of generators to provide both the load and ancillary services while meeting all other generator parameters. The first step to calculating the number of generators and their load point is to calculate the minimum number of generators as shown in equation (113). Where the "Load" represents the remaining load, "SP" is the remaining

spinning reserve and "REG" is the remaining regulation to be met by the balance generation. The naming for N2 and P2 as well as N1 and P1 come from Figure 263.

$$N2_{\min}(t) = \left\lceil \frac{Load(t) + SP(t) + REG(t)}{jL_{LF} \cdot P_{LF}} \right\rceil \quad \textbf{(83)}$$

Equation (114) presents the maximum number of generators that is allowed such that the minimum up time is not violated ($N2_{\min up}$), where N is a vector the length of the load, SP and REG vectors.

$$N2_{\min up}(t) = \min\left(_{i=1}^{N}\{N2_{\min}(t) : t = i,\ldots,i + Up_{\min}\}\right) \quad \textbf{(84)}$$

The number of load-following generators required to operate the system without violating any constraints ($N2_{\max eff}$) can be developed by comparing $N2_{\min}$ and $N2_{\min up}$ as shown in Figure 264. The minimum up time and the maximum efficiency lines bound the resulting profile such that operation in that region meets as much load as possible and provides the necessary ancillary services.

Figure 264: Maximum Efficiency Example Calculation for Load-Followers

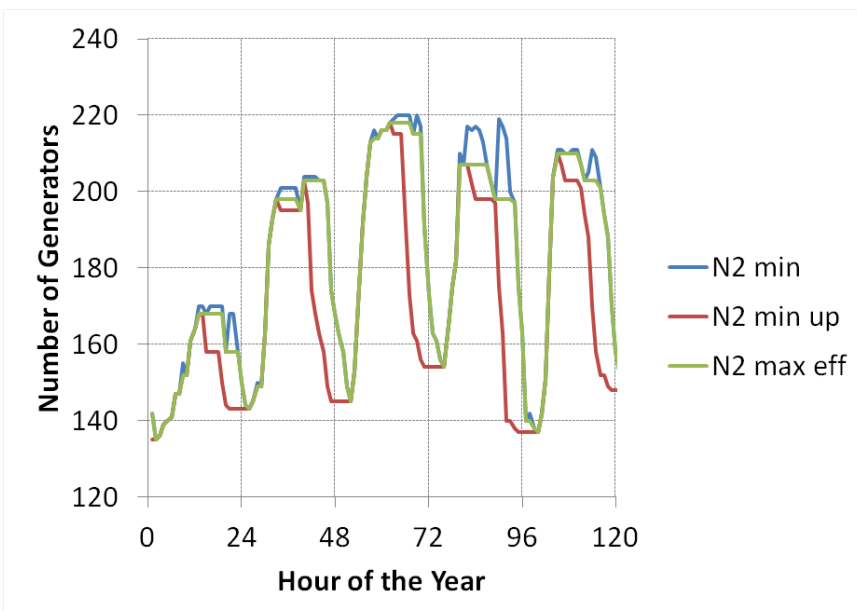

Calculating the resulting load point is a back calculation of equation (113) with replacing jL_{LF} for N2 as shown in equation (115).

$$P2(t) = \frac{Load(t) + SP(t) + REG(t)}{N2_{\max eff}(t) \cdot P_{LF}} \quad \textbf{(85)}$$

In the event that load-followers cannot meet all of the load peakers are called to generate. Peakers are subject to generator operating constraints, just as the load-followers, so a similar process is repeated for peakers. The number of operating peaker plants and their load point is

calculated using equations (116) and (117) similar to the load-followers; where the number of peakers is calculated as the highest efficiency operation using jh_{PK} in the denominator.

$$N1(\mathrm{t}) = \left\lceil \frac{Load(t)}{jh_{PK} \cdot P_{PK}} \right\rceil \tag{86}$$

$$P1(t) = \frac{Load(t)}{N1(t) \cdot P_{PK}} \tag{87}$$

If the peaker minimum-up time is set for the same increment as the resolution of the data (i.e., 1 hour in this case) then the model is complete as the peakers can meet all of the remaining load requirements. However, if the minimum-up time is more than this amount then there is a possibility that the peakers will over generate. To resolve this issue the model is iterated. The load-following generation is run again with the peaker generation removed, then the peakers are run again. This process can be repeated as many times as is necessary to settle on a result where all load is met with the minimal amount of peaking generation.

The second scenario is the minimum efficiency scenario. Maximum efficiency represents one extreme and minimum efficiency represents the other extreme in terms of operation envelope. While minimum efficiency is not a case that is of practical interest it represents the maximum number of generators that can support the load and ancillary services and in so doing bounds the solution set to achievable values. As it turns out the minimum efficiency calculation is essential to calculating the minimum starts scenario.

Minimum efficiency closely mirrors maximum efficiency except the jL is replaced with the jh and Up_{min} is replaced with $Down_{max}$. The resulting profiles for the number of generators are shown in Figure 265.

Figure 265: Minimum Efficiency Example Calculation for Load-Followers

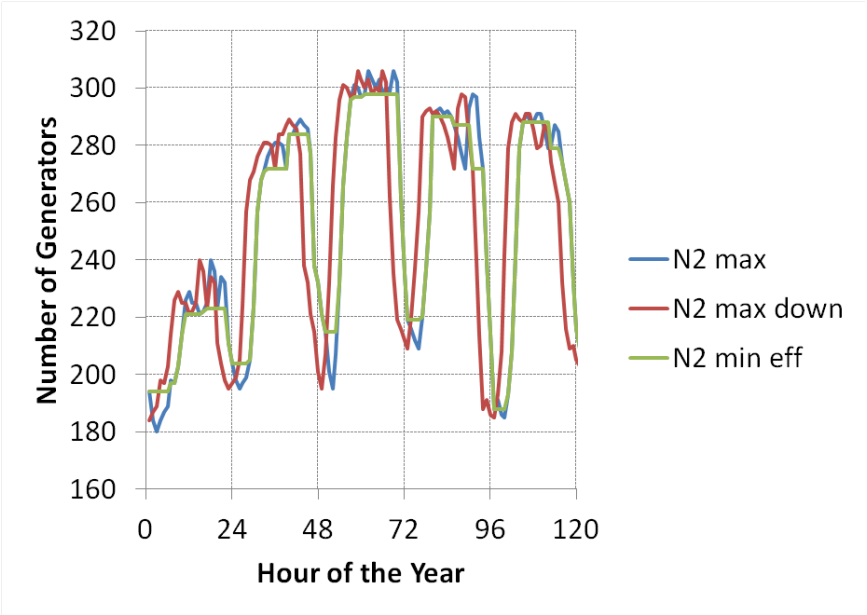

Maximum efficiency represents the least number of generators and minimum efficiency represents the most generators on at any given time. The minimum starts scenario represents a hybrid of both cases such that all generators stay on the longest time possible. Figure 266 shows the comparison of the minimum starts scenario in comparison to the maximum and minimum efficiency scenarios. Notice that to minimize the starts the number of generators oscillates between the minimum and maximum efficiency. As will be shown in the verification section, the minimum starts signal results in less error from the measured data.

Figure 266: Minimum Starts Example Calculation for Load-Followers

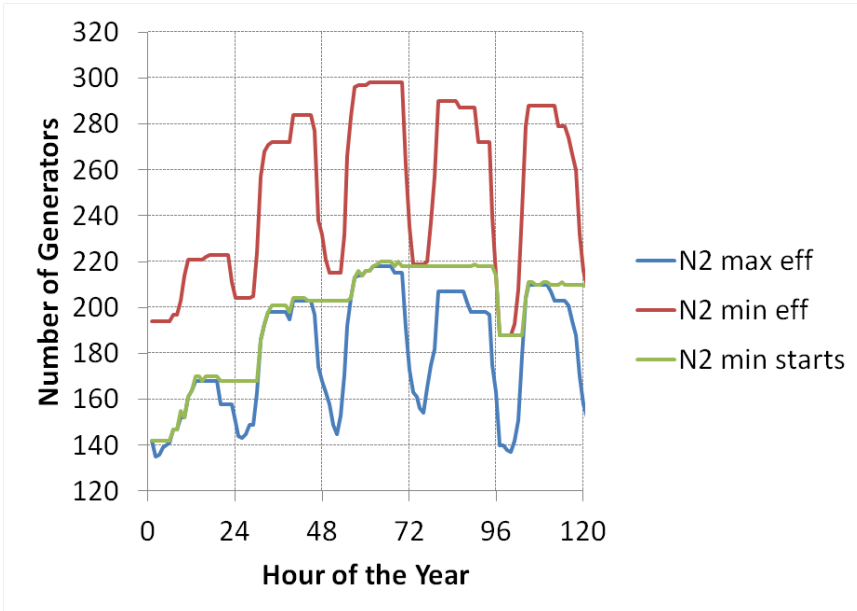

The final values for N1, P1, N2 and P2 represent the number of generators and load point required to meet the generation requirements on the system; however, to calculate the electricity delivered to load equations (118) and (119) are used for peakers and load-followers, respectively.

$$E1_{\text{Delivered to load}}(t) = N1(\text{t}) \cdot P1(t) \cdot P_{PK} \cdot (100 - L_{plant}) \cdot (100 - L_{TX}) \cdot (100 - L_{XFMR}) \quad \textbf{(88)}$$

$$E2_{\text{Delivered to load}}(t) = N2(\text{t}) \cdot P2(t) \cdot P_{LF} \cdot (100 - L_{plant}) \cdot (100 - L_{TX}) \cdot (100 - L_{XFMR}) \quad \textbf{(89)}$$

Now that the number of generators and the load point of each generator are calculated, the time-resolved heat rate can be calculated. Part load performance data for a GE STAG 209E combined cycle generator is used to model load-following heat rate as shown in Figure 267 (Chase, 2001). The curve exhibits two unique regions that define the operation of the plant. For high plant output (i.e., 100-80%) the heat rate increases slowly. Below 80% plant output the heat rate rises rapidly equivalent to rapid reduction in the efficiency.

Figure 267: Part-Load Performance of a GE STAG 209E Combined Cycle Generator (two turbines)

Source: GER-4206 (Chase, 2001)

A similar process is used for representing the heat rate of the peaking fleet. UC Irvine's 13.5 MW Solar Titan 130, gas turbine generator is normalized and then used to model the peaker operation as shown in Figure 268. There is a similar linear region from 100% to 90% part load then a rapid increase for 90 and below.

Figure 268: Part-Load Performance of a Titan 130 Simple Cycle Gas Turbine Generator

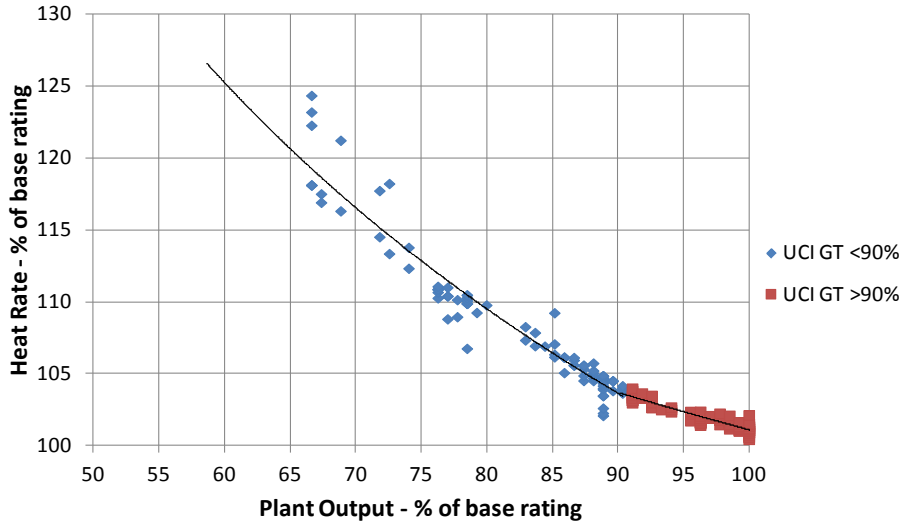

Figure 267 and Figure 268 represent the performance as a function of the base rating and the base power ratings used for this equipment is shown in Table 61. In particular, the nominal plant size for the entire fleet, based on FERC data, is 50MW for peakers and 70MW for load-followers with heat rates of 17.1 and 11.4 MMBtu/MWh, respectively. A piece-wise function was

used to model the heat rate relationship with load point. The high load point region uses a linear curve fit, while the low load point region uses an exponential curve fit.

To calculate the fuel consumed during each time step the expression in equation (120) is used, where HR_{LF} is the heat rate based on the load point, P2. A similar expression can be used to calculate the fuel use for peakers.

$$Fuel_{LF}(t) = N2(t) \cdot P2(t) \cdot P_{LF} \cdot HR_{LF}(t) \quad \textbf{(90)}$$

Converting a heat rate to fuel to electrical efficiency can be done using equation (121), where 3.413 is a constant conversion factor from MMBtu and MWh. A similar expression is used to calculate the fuel to electrical efficiency for peakers.

$$\eta_{LF}(t) = \frac{3.413}{HR_{LF}(t)} \quad \textbf{(91)}$$

The following assumptions were made in the development of the model.

1. Balance generation is represented by two types of generators (i.e., peakers and load-followers). These generators are representative of a fleet of generators operating with a similar duty cycle.

46. All peakers have the same operating parameters (i.e., peak power, heat rate) and all peakers operating during a given time step behave in the same manner (e.g., power output), based on the fleet average.

47. All load-followers have the same operating parameters and all load-followers operating during a given time step are dispatchable and behave in the same manner. This means that typical operational parameters for load-following and peaking generation are used to represent the entire fleet of each generating type, independent of the size of that fleet. This simplification from actual operations, where each plant's operation is unique, is based on the use of historical data to verify the general operating assumptions.

48. Transmission constraints are not modeled. For small-scale systems this assumption means that transmission/congestion issues do not cause a change in operation. That is to say, no transmission congestion occurs for small-scale systems and sufficient power can be provided to meet the demand. Large-scale systems are handled differently. The first three assumptions remove the need for considering spatial resolution and dispatch order for each specific generator but also remove the ability to directly calculate any congestion constraints. This is addressed by integrating results from previous studies and historical data and by including an additional inefficiency resulting from violations of transmission system constraints. Previous studies include WWSIS by NREL and a report by CAISO that details the effects of renewables at 20% renewable penetration within California (GE Energy Consulting, 2010 (CAISO 20%); GE Energy Consulting, 2010 (WWSIS)).

49. Historical load demand, reserve margin and regulation are known and maintained in the model. Baseload generation is independent of the need for load prediction,

hydroelectricity operates to meet seasonal constraints with daily dispatchability, and peaker and load-follower operations need an accurate prediction of the load to satisfy their respective operational constraints.

7.1.6.3. Balance Generation Verification

Comparing the three scenarios establishes which scenario should be used to minimize error and best reflect the behavior of load-following and peaking generation. The best match for both peakers and load-following generation is the minimum starts profile as shown in Figure 269 and Figure 270. It is especially clear with the peaker generation but also evident from the daily average profile.

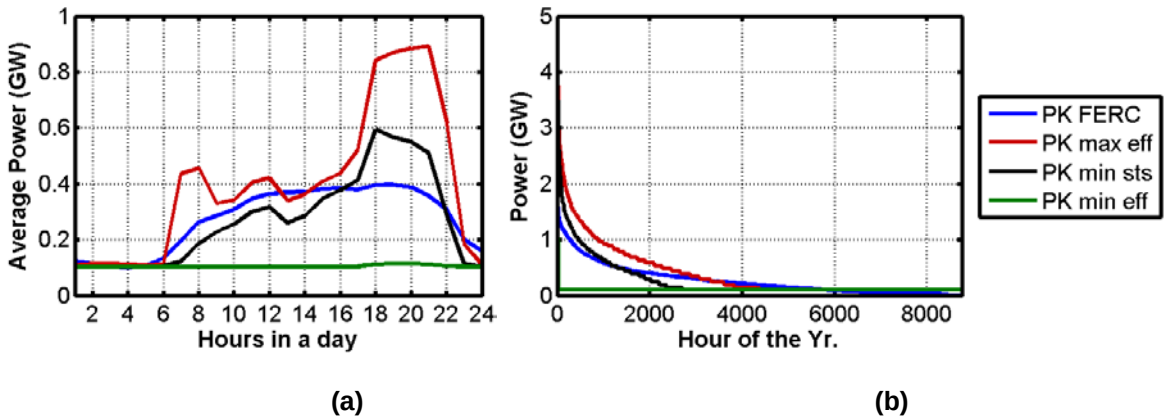

Figure 269: Comparison between model PK scenarios and 2001 FERC data (a) daily average, (b) load duration

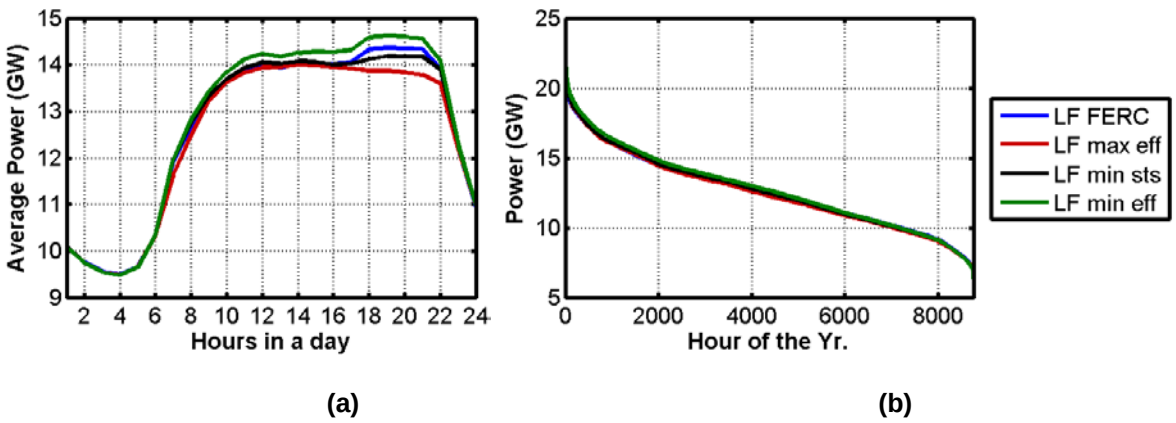

Figure 270: Comparison between model LF scenarios and 2001 FERC data (a) daily average, (b) load duration

Using equation (86) the percentage difference can be calculated for each of the time-resolved signals. Additionally, the error calculations are applied to the daily average and load duration signals for both the peakers and the load followers.

For the results in Table 62 the baseload and hydro generation signals were set equal to the FERC results, which isolate the remaining balance generation signals. In the following sections verification results from the combined model will be presented and discussed.

Table 62: Balance Generation Module Verification

Category Percentage Difference	2000	2001
Peaker Timeseries	86.5%	74.6%
Peaker Daily Average	34.2%	23.5%
Peaker Load Duration	37.5%	37.2%
Load-follower Timeseries	2.9%	1.6%
Load-follower Daily Average	1.1%	0.48%
Load-follower Load Duration	1.6%	0.56%

Additionally, the number of starts for the peakers are 140 and 122 from the model and 132 and 100 from FERC for 2000 and 2001, respectively. The starts for load-following are 29 and 26 compared to 45 and 49 for FERC 2000 and 2001 values.

Table 2 shows how well the peaker signal correlates to other generation signals for both the historical FERC data and the model data. Notice that the FERC peaker signal when compared with the FERC signals for hydro, baseload, load-following and total does not well correlate meaning that the other signals are not good predictors of the peaker behavior. Similarly, the HiGRID peaker signal does not well relate to any of the other generation signals, which explains, in part, the reason for the error in the modeled peaker signal.

Table 63: Peaker Signal Correlation with Other Generation Signals for FERC data and Modeled Results

Peaker Signal	Hydro	Baseload	Load-Follower	Total
FERC	0.469	-0.170	0.584	0.559
HiGRID	0.397	-0.033	0.278	0.363

The ability for peakers to rapidly turn on and respond to load changes and peakers non-correspondence with other generation signals are the three main reasons that determining when peakers turn on is challenging and the cause of the resulting error.

Task 7.1.7. Emissions

The balance generation module provides information about the number of generators operating their condition (i.e., hot (very recent start), warm (recent start), cold (not recent start)) part-load operation and fuel used emissions can be calculated. While the HiGRID model only calculates

CO_2 emissions, other GHG and criteria pollutants emissions can be calculated if the emission factors are known.

Carbon dioxide emissions are calculated in two parts. There are associated CO_2 emissions from the use of fuel for nominal operation and there are additional fuel consumption requirements for startup events. Emissions from nominal operation are calculated using fuel consumption and a CO_2 emissions factor shown in Table 64. Natural gas and coal are the sole contributors to CO_2, while nuclear, geothermal, hydroelectric, biomass, biogas and other renewables are not included.

Table 64: CO_2 Emission Factors for Different Fuel Types

Technology	CO_2 Emission factors (EF_{CO2})
Natural Gas	0.0585 (tons CO_2/MMBtu fuel)
Coal	0.1134 (tons CO_2/MMBtu fuel)

The startup fuel emissions are based on the number of starts a generator performs during a given time period, the installed capacity of that generator and a startup fuel factor. Based on the CEC Cost of Generation model inputs, a value of 2.8 MMBtu/MW/start is used to assess the fuel consumption due to start-ups (Klein, 2010).

Total CO_2 emissions are calculated using equation (122), where EF_{CO2} is the CO_2 emissions factor for a given fuel type, $Cap_{installed}$ is the installed capacity of a generator(s) and $Fuel_{startup}$ is the startup fuel use value.

$$Emissions_{CO_2} = \left(\sum_{t=1}^{N} Fuel(t) + Cap_{installed} \cdot Fuel_{startup} \cdot \sum_{t=1}^{N} Starts(t) \right) \cdot EF_{CO_2} \qquad \textbf{(92)}$$

Task 7.1.8. Curtailment

Generation that exceeds the demand on the grid must be transmitted to another entity that can use the electricity (i.e., exported), or curtailed assuming that it cannot be stored. In the early stages of renewable adoption export of unwanted system generation dynamics could be absorbed by the larger grid; however, as more and more communities begin to integrate renewables to meet state RPS requirements, it will no longer be possible to export those dynamic generation changes to the grid. Additionally, based on the current market structure in California, renewables are must-take (i.e., every MWh must be purchased, independent of the time of generation); however, as renewables increase, this research shows that there is a point at which the grid can no longer support a must-take approach. Thus the more renewable capacity that is integrated into the grid the greater the potential need for curtailment.

For each renewable mixture the other modules calculate the necessary curtailment, considering system reliability requirements. The challenge is to appropriately distribute that curtailment between the resources that generate them. This challenge is complicated by the fact that

different technologies are better able to curtail than others. For instance wind turbines must engage their brakes to stop the blades from spinning. Depending on the braking mechanism, additional use can degrade the equipment faster. Solar photovoltaic power will retain the voltage potential whether or not current is drawn so curtailment on solar photovoltaics is relatively easier. While solar photovoltaic technologies would have an easier time curtailing generation, it is not reasonable that the burden of curtailment based on wind turbine generation be placed on the PV plants. For this model it is assumed that each technology shoulders curtailment throughout the year based on the proportion of total renewable energy that it contributes. There are exceptions if a selected power line was overloaded and curtailment of a particular resource is essential from a grid stability point-of-view. Energy apportioned curtailment calculations must be calculated at the resolution of each time step and keeps track of the energy generated for the year. In this way the curtailment is fairly distributed between renewable resources.

Task 7.1.9. Cost-of-Generation Module

The purpose of the HiGRID Cost of Generation module is to calculate the levelized cost of electricity ("LCOE") for any given portfolio of generating capacity. The LCOE represents the discounted revenue per MWh that would be required to recover all of the costs incurred over the life of the generating technology to produce all of the MWh. In this regard, the term costs includes capital costs, operations and maintenance costs, fuel costs, financing costs, and all taxes. The levelized cost of electricity yields a single value for each generating technology that takes into account the costs, operating parameters, and economic life of that generating technology. The primary purpose of the levelized cost of electricity calculation is to allow a comparison of different generating technologies on a cost per MWh basis despite different costs, operating parameters, and economic lives.

The HiGRID Cost of Generation module calculates the portfolio LCOE for any given portfolio of generating technologies as the MWh-weighted average of the technology-specific LCOE for each generating technology in the portfolio. The portfolio of generating technologies is determined by the interaction of the Load Module with the Renewable Generation Module and Dispatchable Generation Module. Calculation of the portfolio LCOE enables a dynamic comparison of different generating portfolios that, in turn, allows for least cost portfolio optimization within specified technical and operating constraints.

The cost of generation module is, in part, based on the CEC's model for determining the LCOE of generation technologies (Klein, 2010). The cost of generation module draws on performance information for each technology including installed capacity, electricity generated, fuel consumed, starts and hours of operation to calculate the LCOE from each generator type and the portfolio as a whole. Some of the impacts of intermittent renewables are not evident from the direct cost of installing renewables, but rather, manifest themselves in an increased need for conventional generation capacity that causes a rise in the cost of those technologies needed to support the intermittency of the renewables. Figure 271 depicts the flow chart for the cost of generation model.

Figure 271: Cost of Generation Model Flowchart

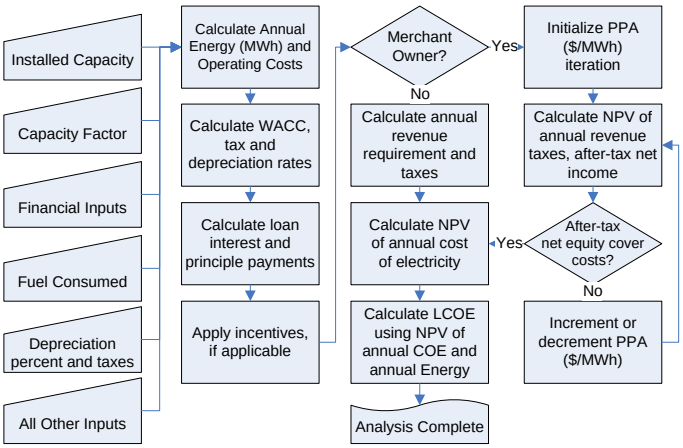

Model inputs are shown in the left of Figure 271 and include:

- Gross capacity
- Capacity factor
- Instant cost
- Fixed O&M cost
- Variable O&M cost
- Heat rate
- Heat rate degradation
- Capacity degradation
- Debt term
- Economic life
- Tax life
- Ad valorem tax rate
- Tax incentives
- Buy-downs
- Feed-in tariffs
- Annual starts
- Start-up fuel
- Plant losses

- Transmission losses
- Transformer losses
- Transmission cost
- CO_2 emission factors

The LCOE for private (merchant) ownership is calculated using an income cash flow methodology whereas the LCOE for investor- and publically-owned utilities is calculated using a revenue requirement methodology. The two methodologies differ in many respects, including in their treatment of taxes, depreciation, and required rates of return. Each generating technology may have only one type of owner per run in the current HiGRID Cost of Generation module, and all results to-date are based on merchant (private) ownership of generation, assuming 60% equity and 40% debt.

The HiGRID Cost of Generation module currently includes cost and initial operating parameters for over 40 different generating technologies, both fossil-fueled and renewable. Costs include, among others, capital costs, fixed and annual operations and maintenance ("O&M") costs, fuel costs, tax rates, and financing costs. Initial operating parameters for each generating technology include the nameplate capacity, annual load factor, initial heat rate, annual heat rate degradation, and annual capacity degradation. The annual number of starts and required start-up fuel are included, where applicable. Table 65 and Table 66 include the cost and initial operating parameters for the technologies included in the UCI community analysis. Table 67 and Table 68 include the parameters for the technologies that serve California load.

Table 65: Initial Costs and Operating Parameters for Technologies Serving UCI Load (1 of 2)

	Combustion Turbines	Rooftop PV	1-Axis Tracking PV	Regional Wind	Parabolic Trough	2-Axis Tracking PV	Flow Battery (Va Redox)	DR - Lighting Turndown	DR - Fan Turndown	DR - Building Precool	Electricity Imports
Gross Capacity	49.9	0.01	25	50	250	25	10	0	0	0	100
Annual Capacity Factor	0.05	0.2	0.27	0.37	0.27	0.32	0.1	0.333	0.167	0.167	0.65
Instant Cost ($/kW)	1292	6600	4500	1975	3687	4650	3100	0	0	0	0
FOM ($/kW-yr)	23.94	25	50	13.7	51	55	32	0	0	0	0
VOM ($/MWh)	4.17	0	0	5.5	2	0	0	0	0	0	0
HR (MMBtu/MWh)	9.266	0	0	0	9.266	0	0	0	0	0	0
HR Degradation	5e-4	0	0	0	5e-4	0	0	0	0	0	0
Capacity Degradation	5e-4	5e-3	5e-3	0.01	5e-3	0.005	0	0	0	0	0

Debt Term (Yrs)	12	20	15	20	15	15	5	0	0	0	0
Economic Life (Yrs)	20	25	20	30	20	20	10	20	40	40	20
Federal Tax Life (Yrs)	15	5	5	5	5	5	10	0	0	0	0
State Tax Life (Yrs)	15	20	20	30	20	20	10	0	0	0	0
Ad Valorem Tax Rate	0.011	0	0	0.011	0	0	0.011	0.011	0.011	0.011	0
Annual Starts	120	0	0	0	365	0	0	0	0	0	0
Start-Up Fuel (MMBtu/MW)	2.8	0	0	0	0	0	0	0	0	0	0
Plant Losses	0.034	0	0.064	0.01	0.224	0.09	0	0	0	0	0
TX Losses	0.021	0	0.05	0.05	0.05	0.05	0.05	0	0	0	0
Transformer Losses	5e-3	0	5e-3	5e-3	5e-3	5e-3	5e-3	0	0	0	5e-3

Table 66: Initial Costs and Operating Parameters for Technologies Serving UCI Load (2 of 2)

	Natural Gas Boiler	Small GT (13.5MW)	Small ST (6.0MW)	Electric Chiller	Steam Chiller	Thermal Energy Storage (TES)	Local Wind	Ext/Garage Lighting	Interior Lighting	HVAC Control, Opt, balancing
Gross Capacity	2.1	13.5	6	200	300	10	50	0	0	0
Annual Capacity Factor	0.5	0.8	0.45	0.25	0.25	0.75	0.37	0	0	0
Instant Cost ($/kW)	40	1200	1000	400	600	600	1975	0	0	0
FOM ($/kW-yr)	5	25	30	10	15	1.75	13.7	0	0	0
VOM ($/MWh)	1	5	7.5	48	92	1	5.5	0	0	0
HR (MMBtu/MWh)	3.412	12	0	0	0	0	0	0	0	0
HR Degradation	0.05	1e-3	1e-3	0	0	0	0	0	0	0
Capacity Degradation	0	1e-3	1e-3	5e-3	5e-3	5e-3	1e-2	0	0	0
Debt Term (Yrs)	10	12	12	20	20	20	20	0	0	0
Economic Life (Yrs)	20	20	20	20	20	30	30	40	40	40
Federal Tax Life (Yrs)	15	15	15	20	20	20	5	0	0	0
State Tax Life (Yrs)	15	15	15	20	20	30	30	0	0	0
Ad Valorem Tax Rate	0.011	0.011	0.011	0.011	0.011	0.011	0.011	0.011	0.011	0.011
Annual Starts	0	150	100	0	0	0	0	0	0	0
Start-Up Fuel (MMBtu/MW)	0	2.8	0	0	0	0	0	0	0	0
Plant Losses	0	0.034	0.034	0	0	0	0	0	0	0

TX Losses	0	0	0	0	0	0	0	0	0	0
Transformer Losses	0	0	0	0	0	0	0	0	0	0

Table 67: Initial Costs and Operating Parameters for Technologies Serving California Load (1 of 2)

	Adv. Combustion Turbines	Rooftop PV	1-Axis Tracking PV	Regional Wind	Nuclear	Adv. Combined Cycle	Parabolic Trough	2-Axis Tracking PV	Legacy Nuclear	Legacy Coal	Legacy Hydro
Gross Capacity	200	0.01	25	50	960	200	250	25	4456	5061	12392
Annual Capacity Factor	0.1	0.2	0.27	0.37	0.865	0.75	0.27	0.32	0.926	0.791	0.326
Instant Cost ($/kW)	827	6600	4500	1975	3950	989	3687	4650	0	0	0
FOM ($/kW-yr)	16.33	25	50	13.7	147.7	7.17	51	55	109.6	36.64	16.94
VOM ($/MWh)	3.67	0	0	5.5	5.27	2.69	2	0	2.5	5.25	3.02
HR (MMBtu/MWh)	8.55	0	0	0	10.4	6.47	9.266	0	10.48	10.36	0
HR Degradation	5e-4	0	0	0	2e-3	2.4e-3	5e-4	0	2e-3	2e-3	0
Capacity Degradation	5e-4	5e-3	5e-3	0.01	2e-3	2.4e-3	5e-3	5e-3	2e-3	1e-3	0.02
Debt Term (Yrs)	12	20	15	20	20	12	15	15	0	0	0
Economic Life (Yrs)	20	25	20	30	40	20	20	20	20	20	20
Federal Tax Life (Yrs)	15	5	5	5	20	20	5	5	0	0	0
State Tax Life (Yrs)	15	20	20	30	30	20	20	20	0	0	0
Ad Valorem Tax Rate	0.011	0	0	0.011	0.011	0.011	0	0	0	0	0
Annual Starts	120	0	0	0	0	25	365	0	2	30	0
Start-Up Fuel (MMBtu/MW)	2.8	0	0	0	0	2.8	0	0	2.8	2.8	0
Plant Losses	0.034	0	0.064	0.01	0.022	0.029	0.224	0.09	0.1	0.1	0.05
TX Losses	0.021	0	0.05	0.05	0.021	0.021	0.05	0.05	0.021	0.021	0.021
Transformer Losses	5e-3	0	5e-3	5e-3	5e-3	5e-3	5e-3	5e-3	5e-3	5e-3	5e-3

Table 68: Initial Costs and Operating Parameters for Technologies Serving California Load (2 of 2)

	Legacy Geothermal	Legacy Combined Cycles	Legacy Combustion Turbines	Pumped Hydro	Compressed Air Energy Storage	Flow Battery (Va Redox)	Flow Battery (ZnBr)	DR - Lighting Turndown	DR - Fan Turndown	DR - Building Precool	Local Wind
Gross Capacity	2545	21420	3750	5000	200	10	10	0	0	0	50
Annual Capacity Factor	0.645	0.511	0.086	0.285	0.3	0.1	0.1	0.333	0.167	0.167	0.37
Instant Cost ($/kW)	0	0	0	2500	1250	3100	2000	0	0	0	1975
FOM ($/kW-yr)	134.1	17.78	12.19	35	24.6	32	22	0	0	0	13.7
VOM ($/MWh)	11.9	4.21	10.19	7	65	0	0	0	0	0	5.5
HR (MMBtu/MWh)	0	12.72	19.44	0	4.163	0	0	0	0	0	0
HR Degradation	0	2.4e-3	5e-3	0	5e-4	0	0	0	0	0	0
Capacity Degradation	0.04	2.4e-3	5e-3	0	0	0	0	0	0	0	0.01
Debt Term (Yrs)	0	0	0	20	20	5	5	0	0	0	20
Economic Life (Yrs)	20	20	10	40	20	10	10	20	40	40	30
Federal Tax Life (Yrs)	0	0	0	20	20	10	10	0	0	0	5
State Tax Life (Yrs)	0	0	0	20	20	10	10	0	0	0	30
Ad Valorem Tax Rate	0	0	0	0.011	0.011	0.011	0.011	0.011	0.011	0.011	0.011
Annual Starts	15	30	120	0	250	0	0	0	0	0	0
Start-Up Fuel (MMBtu/MW)	0	2.8	2.8	0	2.8	0	0	0	0	0	0
Plant Losses	0.05	0.058	0.068	0	0	0	0	0	0	0	0
TX Losses	0.05	0.021	0.021	0.05	0.05	0.05	0.05	0	0	0	0
Transformer Losses	5e-3	5e-3	5e-3	5e-3	5e-3	5e-3	5e-3	0	0	0	0

Most of the costs for new capacity included in the HiGRID Cost of Generation module are derived from the generation plant costs developed in the CEC Cost of Generation model. In addition, the HiGRID Cost of Generation module includes so-called "legacy" generating technologies. Legacy generating technologies are included to reflect already existing electricity generating capacity that may be largely or fully depreciated. Such legacy generating technologies include all generating capacity serving California. The installed capacity for each legacy generating technology included in the integrated HiGRID model is based on the estimated capacity mix serving the electrical load for California in 2005, determined, in part, by a review of the CEC's Database of California Power Plants (CEC, 2010).

The initial legacy generating technologies included in the HiGRID Cost of Generation module are nuclear capacity, large hydro capacity, coal-fired capacity, natural gas-fired baseload capacity, natural gas-fired intermediate load capacity, and natural gas-fired peaking capacity. The parameters for each legacy generating technology are considered to be representative of the aggregate capacity included within that technology and are included to allow for a full representation of the generating capacity serving California. The purpose of including a full representation of all generating capacity is to allow for future analysis that might include dispatching off even legacy baseload generation as the level of renewables penetration increases to very high levels. Fuel price forecasts are based on mid-range values in the CEC Cost of Generation model and may readily be changed to reflect changing long-term market conditions.

Because of their assumed age, all capital costs associated with the legacy generating technologies are assumed to be fully depreciated, i.e., there are no capital costs included in the LCOE. The LCOE for each legacy generating technology is based solely on its fuel costs and on its specified fixed and variable O&M costs. Each legacy generating technology has a specified aggregate heat rate and capacity factor, as well as heat rate and capacity degradation factors representative of that technology.

System balancing will become increasingly difficult as the penetration level of intermittent renewable generating technologies increases. Changes in annual load factors of natural gas-fired generating technologies may change as a result of changes in, for instance, the renewable penetration level and the associated natural gas-fired generation required for system balancing. All of the initial operating parameters of the HiGRID Cost of Generation module are dynamic and subject to change based on the output from the Renewable Generation Module and Dispatchable Generation Module. This is an important feature that enables the integrated HiGRID model to find the most economical means of system balancing through the iterative calculation of the LCOE of different generating technology portfolios.

Annual capacity factors are an important factor in determining the LCOE for any given generating technology. The impact on the LCOE of changing the annual capacity is clearly illustrated in Figure 272, which shows the LCOE (excluding all incentives) over the full theoretical range of capacity factors for four of the generating technologies listed in Table 67 and Table 68. i.e., advanced natural gas combustion turbine ("Adv CT"), advanced natural gas combined cycle ("Adv NGCC"), onshore wind, and 1-axis tracking photovoltaics ("1-Axis PV"). As the annual capacity factor increases, more and more MWh are generated. Since everything else is held constant, increasing the capacity factor leads to a continually declining LCOE.

Figure 272: Impact of Annual Capacity Factor on LCOE (Excluding all Incentives)

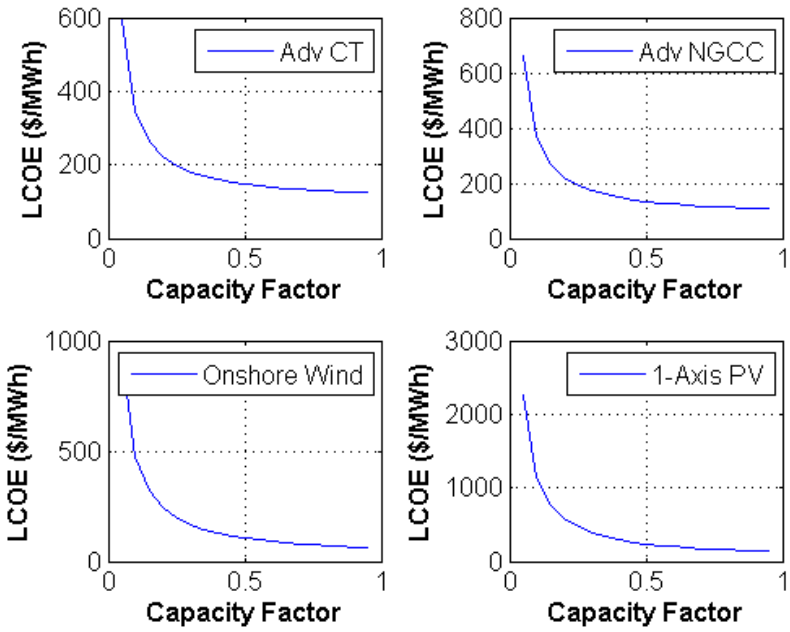

The importance of the LCOE for any given generating technology is that it, in turn, impacts the portfolio LCOE. The LCOE of different generating portfolios are compared and any changes in a portfolio's LCOE have important implications for determining the optimal portfolio to meet California's load. At a lower capacity factors, capital costs become more dominant relative to fuel costs. In addition, lower capacity factors generally result in higher heat rates and increased emissions of all types. These effects have important implications for the true costs of system balancing as renewable penetration levels increase.

The economic life of a generating technology also impacts its LCOE, as illustrated in Figure 273. Figure 273 illustrates the LCOE for the same four generating technologies as above, this time changing the theoretical economic life over a range of 5 to 40 years. As the economic life of a technology is extended, there comes a time where the (negative impact) reduction in MWh generated due to cumulative capacity and heat rate (where applicable) degradation factors outweighs the positive impact of the extended economic life. Said differently, fuel costs become more dominant relative to capital costs. This effect is particularly dramatic for the 800 MW advanced NGCC generating technology due to the combined effect of an ever-increasing heat rate in the face of rising natural gas prices. The two renewable generating technologies show very little increase in the LCOE as their MWh generated in the later years wane because these technologies are immune from the impact of fossil fuel prices. The interaction of financing costs, taxes, and depreciation also contribute to the shape of the curves in Figure 273. Thus, the end of the twelve-year financing term for the advanced NGCC generating technology contributes to the upward turn of the LCOE as that technology's economic life is extended.

Figure 273: Impact of Economic Life on LCOE (Excluding all Incentives)

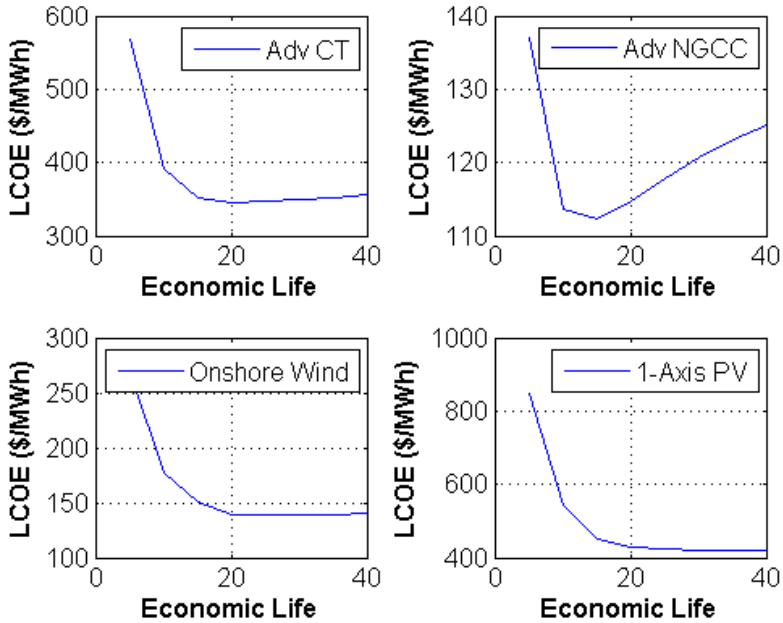

The issue of the appropriate level of transmission costs to allocate to new renewable generation is one that is widely debated in California and elsewhere. The integrated HiGRID model relies on the in-state per MWh transmission costs developed by the Renewable Energy Transmission Initiative for all renewable generating technologies (RETI-1000-2010-002-F, 2010). The capacity of each block of renewable generation installed by the HiGRID Renewable Generation Module is assigned to a California Renewable Energy Zone ("CREZ") based on the geographic location of the installed capacity. For each renewable generating technology included in the generating portfolio, a MWh-weighted average transmission cost is calculated, based on the location and generating profile of each block of installed capacity included in that generating technology category.

Transmission costs associated with fossil-fueled generation are based on CAISO wheeling charges and other transmission-related costs from the CEC Cost of Generation model. Rooftop solar photovoltaics (in 10 kW increments) have been included as a separate (distributed) generating technology with no transmission costs or associated losses.

Tax incentives and California Solar Initiative incentives may either be included in or excluded from the LCOE calculations in the HiGRID Cost of Generation module to allow for sensitivity analysis. Comparative results with and without such incentives will be provided at a later date.

The HiGRID Cost of Generation module is designed to allow all inputs to be changed as market conditions and other assumptions change. New generating technologies may be added to the model and the costs and initial operating parameters for generating technologies already included in the HiGRID Cost of Generation module may be changed with ease.

The HiGRID Cost of Generation module works in tandem with the other modules of the integrated HiGRID model, receiving revised portfolio definitions with associated capacities and operating parameters from both the Renewable Generation Module and the Dispatchable Generation and providing back to those modules a revised portfolio LCOE that measures the cost impact of changing the renewable energy capacity component of the generating mix serving California. The integrated nature of the HiGRID cost and generating modules and the relative ease with which the input parameters may be changed result in a powerful yet flexible analytical tool that will provide significant insights into the technical and cost impacts associated with the increased penetration of renewables.

Task 7.1.10. California Model Verification Summary

This work is not intended to advise utilities on the specific locations of power plants required in the future or on the capacity of transmission lines required to alleviate congestion constraints with additional renewables; rather, this study addresses the technical feasibility of installing renewables and indicates the resultant changes to costs and operation of the grid for any mixture of renewable technologies and the effect of including complementary technologies. The result of constructing the tool in the way described and subjecting it the aforementioned assumptions is a tool that can quickly span a variety of scenarios and can perform optimizations if desired to more accurately understand the cost and performance implications for installing renewable generation.

The California HiGRID model was verified using hourly resolved generation profiles for each generator within the state of California from the FERC data (FERC, 2002). Table 69 presents a comparison of the percentage differences between modeled values and historical FERC data for each specific resource type. Errors in baseload and hydro models, cascades to the load-following and peaking models because the total load demand and spinning reserve must be met regardless of any errors in previous models.

Table 69: Percentage Difference Between Modeled Generation and FERC Data

Model Year	Hydro	Baseload	Peaking	Load-Following	Total
2000	17.2%	12.0%	76.4%	7.5%	11.9%
2001	13.9%	10.7%	74.9%	5.6%	8.9%

While the percentage difference shows a measure of the total error it is also important to understand when the error occurs. Instantaneous generation profiles display when the error occurs, as shown in Figure 274.

Figure 274: Hourly In-State Generation Comparison to FERC Data for 2001

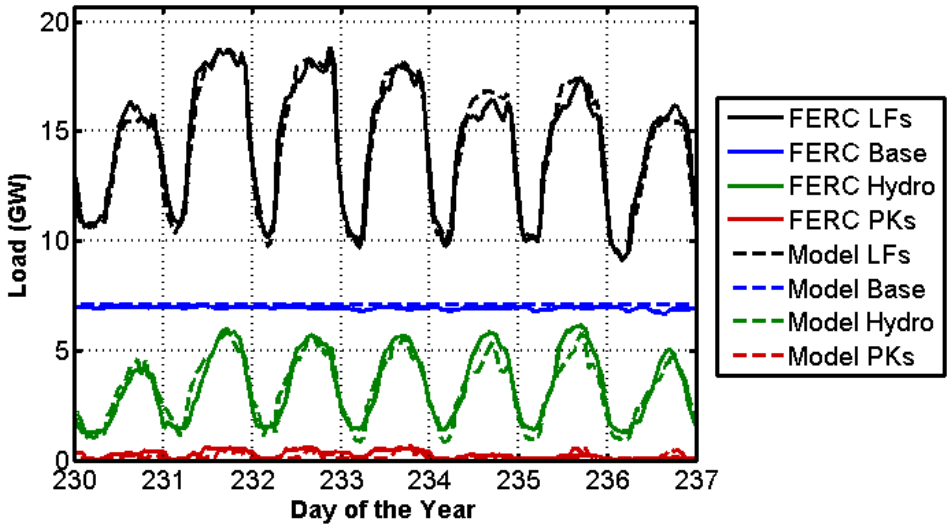

Additionally, daily average curves and load duration curves are included in Figure 275 and Figure 276, which present the distribution of generation throughout the year. The daily average represents the agreement to diurnal behavior by averaging each hour of every day together. The load duration curve is useful to ensure that the actual system and the modeled system have similar range and load distribution for the year.

Figure 275: Daily average Comparison to FERC Data for 2001

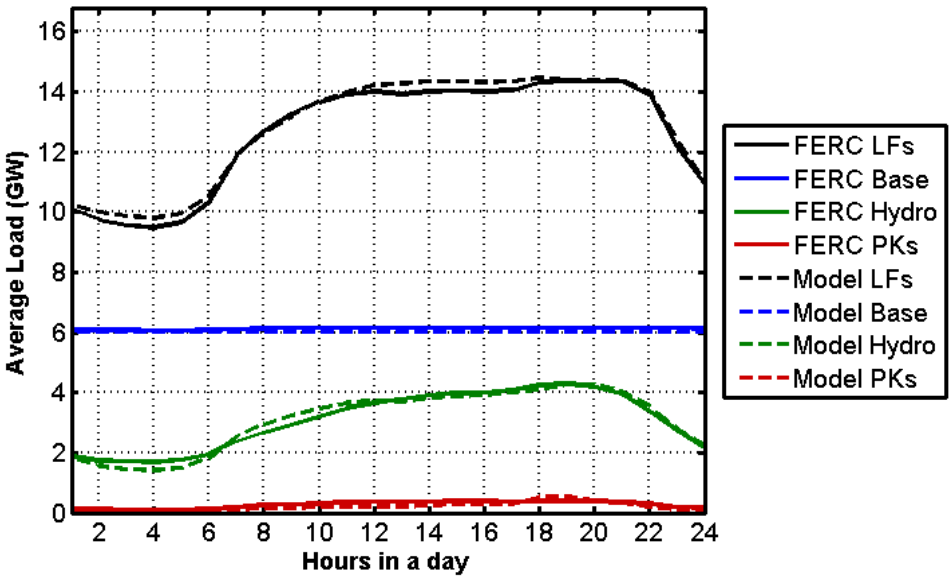

Figure 276: Load Duration Curve Comparison to FERC Data for 2001

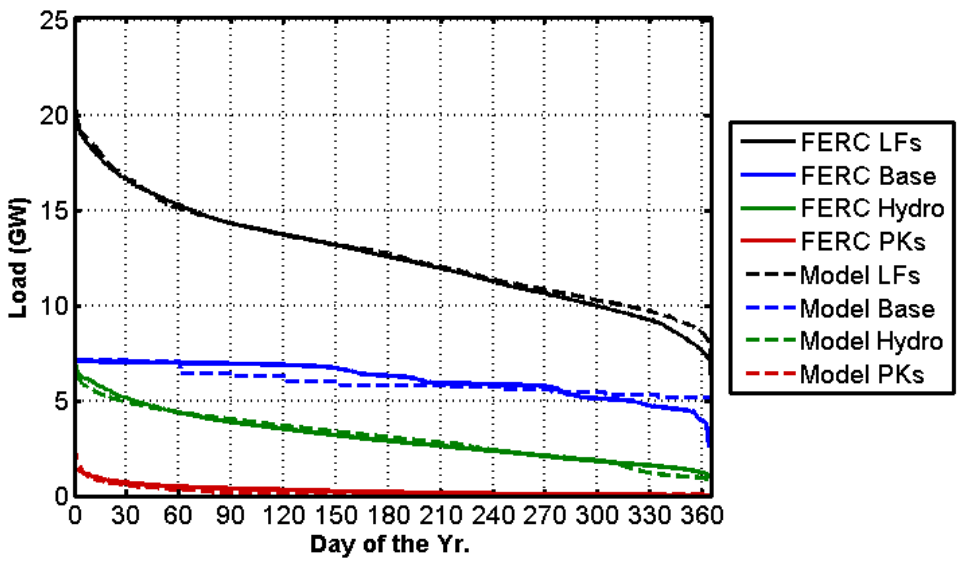

Agreement of the hydroelectric, baseload, and load-following modules with the FERC data is good; however, the error resulting from the peaker model appears high. Operation of peakers is necessary to assure grid stability during high load times and highly dynamic periods, but can be unpredictable. The amount of peaking is determined by the available capacity of the system and the operational characteristics of the generators. Peakers can turn on for a few hours each day, which is not feasible for large baseload or load-following plants that can take hours to start up. The utilization can change dramatically from one day to the next and they are often bid into the non-spinning reserve market because they have the capability to turn on very quickly. As the name suggests, non-spinning reserve is generation that is not currently on but can come on rapidly to meet demand. It is for these reasons that determining when peakers are turned on is challenging and the error for this module is high. While, the error for the peaker model is high, the contribution of peaking to the total energy is low at around 2% of all the supplied energy. Thus the three contributing factors to error of the peaker generation signal are 1) the dynamic requirements of peaker generation, 2) peaker's non-correspondence with the generation signals from other generation types and 3) compounding error for each successive resource model (i.e., hydro, baseload, load-follower and finally peaker).

Task 7.1.11. Conclusions

The development of the HiGRID model is essential to the progress of the RESCO project. This section describes the development and presents the verification for each section.

- Increasing the size of a renewable site can significantly reduce the magnitude of the power fluctuations
- Dispersing renewable sites through a geographic region decreases the relative magnitude of power fluctuations.

- Based on the reduction in the magnitude of fast-timescale fluctuations for multiple sites it is reasonable to use hourly resolved data as the input to model solar power production
- A solar PV model was developed which matched the historical data with an average error of 1.36%.
- Developed a solar thermal model using a similar approach outlined in Bialobrzeski (2007) with a resulting error of 2.36% compared to the net electrical generation.
- Baseload generation model inputs installed capacity and capacity factors for any mixture of baseload technologies to quickly calculate time-resolved dispatch
- Developed first principles model of UCI's gas turbine, steam turbine and heat recovery steam generator
- Developed physically-driven, rule-based generation model to balance the energy and reliability requirements of the grid using generator operating parameters as inputs
- Use of generator operating parameters for dispatch enables values to be adjusted to explore the effects of a more efficient fleet or a fleet with greater turndown
- Model developed to calculate CO_2 emissions for each fueled generator and includes emissions from both nominal operation and startup
- Cost of Generation Model is capable of calculating the portfolio LCOE for any mixture of renewable and conventional resources

Task 7.1.12. References

3TIER, Development of Regional Wind Resource and Wind Plant Output Datasets. 2007-2008, U.S. Department of Energy.

Aalborg University. "EnergyPLAN: advanced energy system analysis computer model." Retrieved 04/20/2012, <http://energy.plan.aau.dk/>.

Argonne National Laboratory. "Energy and Power Evaluation Program (ENPEP-BALANCE)." CEEESA, ADICA Consulting, LLC, the U.S. D.o.E, The World Bank, and the International Atomic Energy Agency. Retrieved 7/23/2012, <http://www.dis.anl.gov/projects/Enpepwin.html>.

Asea Brown Boveri. "VENTYX: Market Analytics - Zonal Analysis." Retrieved 5/14/2012, <http://www.ventyx.com/en/enterprise/business-operations/business-products/market-analytics-zonal>.

Bialobrzeski RW. OPTIMIZATION OF A SEGS SOLAR FIELD FOR COST EFFECTIVE POWER OUTPUT. Master of Science: Georgia Institute of Technology, 2007.

Black & Veatch. (2008). Renewable Energy Transmission Initiative, Phase 1A Final Report. RETI-1000-2008-002-F.

Black & Veatch Corporation. (2010). Renewable Energy Transmission Initiative (RETI) Phase 2B: FINAL REPORT. University of California, Office of the President, and California Institute for Energy and the Environment. RETI-1000-2010-002-F. <http://www.energy.ca.gov/reti/>.

California Energy Commission. 2010. Database of California Power Plants. Last available update: September 2009. http://energyalmanac.ca.gov/powerplants/index.html

California Energy Commission. 2011. Staff Draft Report on Renewable Power in California: Status and Issues. August 2011. Publication No. CEC-150-2011-02.

California Independent System Operator. "Open Access Same-time Information System." Retrieved 04/20/2012, <http://oasis.caiso.com/mrtu-oasis>.

California Independent System Operator. (2003). 2003 Summer Assessment Report. April 11, 2003.

California Public Utilities Commission. (2011). Renewables Portfolio Standard Quarter Report. 3rd Quarter 2011.

California Senate Bill 107, Public Interest Energy Research, Demonstration, and Development Program, (2005-2006 Reg. Sess.)

California Senate Bill 1078, California Renewables Portfolio Standard Program, (2001-2002 Reg. Sess.), Public Utilities Code Section 399.11-399.20

California Senate Bill 2, California Renewable Energy Resources Act, (2011-2012 1st Ex. Sess.)

California State Assembly Bill 32, California Global Warming Solutions Act of 2006, (2005-2006 Reg. Sess.), Health and Safety Code Section 38500-38599

Chase, D.L. 2001. Combined-Cycle Development Evolution and Future. Schenectady, NY. General Electric Power Systems. GER-4206.

Connolly, D., H. Lund, B. V. Mathiesen and M. Leahy (2010). "A review of computer tools for analysing the integration of renewable energy into various energy systems." Applied Energy 87 (4): 1059-1082.

Duffie, J.A., Beckman, W.A., Solar Engineering of Thermal Processes. 1991: John Wiley & Sons.

Energy Exemplar Pty. Ltd. "PLEXOS: Power Market Simulation Software." (Software), Retrieved 04/26/2012, <http://www.energyexemplar.com/>.

Energy Information Administration. (2003). "The national energy modeling system: an overview." Retrieved 7/23/2012, <http://www.eia.doe.gov/oiaf/aeo/overview/index.html>.

Fallah, H.M., Integrated Energy Conversion Systems: A Mathematical Model of Extraction Steam Turbine, Energy Conversion 1978, Volume 18, pp. 11-15,

Federal Energy Regulatory Commission (2002). 2000-2001 Western Energy Crisis Database. October 18, 2011. <http://www.ferc.gov/industries/electric/indus-act/wec/enron/info-release.asp#directories>

GE Energy Consulting. (2010). Western Wind and Solar Integration Study. U.S.D.o.E. and National Renewable Energy Laboratory. NREL/SR-550-47434.

GE Energy Consulting. "Concorda Software Suite - PSLF, MAPS and MARS." Retrieved 5/14/2011, <http://www.ge-energy.com/products_and_services/products/energy_consulting_software/concorda_software_suite.jsp>.

GE Energy Consulting. (2010). Integration of Renewable Resources: Operational Requirements and Generation Fleet Capability at 20% RPS. California Independent System Operator, Pacific Northwest National Laboratory, PLEXOS, Nextant.

Gordon, J.L., "Hydraulic turbine efficiency," Canadian Journal of Civil Engineering, 28(2):238-253, 2001.

Gou, X., W. Sun, et al. (2010). "A dynamic multi-timescale method for combustion modeling with detailed and reduced chemical kinetic mechanisms." Combustion and Flame 157(6): 1111-1121.

Hawkins, D., CAISO Overview and Role of Integrating Renewable Resources. 2007.

Heling, M.G., ASSESSMENT OF THE ZERO-EMISSION VEHICLE, SHARED-USE STATION CAR (ZEV-SUSC) MOBILITY CONCEPT WITH A FOCUS ON ENERGY AND ENVIRONMENTAL SUSTAINABILITY in Mechanical and Aerospace Engineering. 2008, University of California, Irvine: Irvine.

HOMER Energy LLC. "Hybrid Optimization Model for Electric Renewables." Retrieved 04/20/2012, <http://www.homerenergy.com/>.

Instituto Superior Técnico; University of Zagreb. "H2RES: Energy Planning of Islands and Isolated Regions." Retrieved 04/20/2012, <http://powerlab.fsb.hr/h2res/index.html>.

Jansen, K.H., Brown T.M. and Samuelsen G.S. , "Emissions impacts of plug-in hybrid electric vehicle deployment on the U.S. western grid." Journal of Power Sources 195 (16): 5409-5416. 2010.

KEMA Inc. (2010). Research Evaluation of Wind and Solar Generation, Storage Impact, and Demand Response on the California Grid. Prepared for the California Energy Commission. CEC-500-2010-010.

Klein, J. 2010. Cost of Generation Model User's Guide Version 2. California Energy Commission. CEC-200-2010-002.

Loutan, C. and D. Hawkins. (2007). Integration of Renewable Resources: Transmission and operating issues and recommendations for integrating renewable resources on the California ISO-controlled Grid. November 2007. California Independent System Operator.

Nyberg, Michael. (2009). 2008 Net System Power Report. Staff Report. California Energy Commission. CEC-200-2009-010. <http://energyalmanac.ca.gov/electricity/total_system_power.html>.

Office of Integrated Analysis and Forecasting. (2008). Annual Energy Outlook. Washington, DC. Office of Integrated Analysis and Forecasting. DOE/EIA-0383.

Perez, R., Ineichen, P., Modeling daylilght availability and irradiance components from direct and global irradiance. Solar Energy, 1990. 44(5): p. 271-289.

Porter, K. and Intermittency Analysis Project Team. (2007). Intermittency Analysis Project: Summary of Final Results. California Energy Commission; PIER Research Development & Demonstration Program. CEC-500-2007-081.

Ralph S, Mercado P, Krewitt W, Bhuyan G, Flynn D, Holttinen H, et al. Integration of Renewable Energy into Present and Future Energy Systems. In IPCC Special Report on Renewable Energy Sources and Climate Change Mitigation [O. Edenhofer, R. Pichs-Madruga, Y. Sokona, K. Seyboth, P. Matschoss, S. Kadner, T. Zwickel, P. Eickemeier, G. Hansen, S. Schlömer, C. von Stechow (eds)], Cambridge University Press, Cambridge, United Kingdom and New York, NY, USA. 2011.

Tarroja, B., F. Mueller, J. D. Eichman and S. Samuelsen (2011). "Metrics for evaluating the impacts of intermittent renewable generation on utility load-balancing." Energy 42 (1): 546-562.

Tarroja, B., F. Mueller, J. D. Eichman, J. Brouwer and S. Samuelsen (2011). "Spatial and temporal analysis of electric wind generation intermittency and dynamics." Renewable Energy 36 (12): 3424-3432.

U.S. Energy Information Administration (2011). Net Generation by Energy Source: Total (All Sectors). EIA-906, EIA-920, EIA-923. August 19, 2012.

University of Wisconsin-Madison. "A TRaNsient SYtems Simulation program." Retrieved 04/20/2012, <http://sel.me.wisc.edu/trnsys/>.

Walker, G., EVALUATING MPPT CONVERTER TOPOLOGIES USING A MATLAB PV MODEL. Journal of Electrical & Electronics Engineering, 2001.

Wilcox, S. (2007). National Solar Radiation Database 1991-2005 Update. National Renewable Energy Laboratory. U.S.D.o.E., Office of Energy Efficiency and Renewable Energy. NREL/TP-581-41364.

Task 7.2. Renewable Integration Results

With the models complete the first analysis is to explore the effects of renewables on the system for the UCI community and California. Spanning cases for each renewable technology are performed with the model such that impacts from each technology and the systems on which

they are installed can be isolated. While it is understood that installing a single technology is not technically practical and most likely not economically competitive, there is value to developing an understanding for the behavior of each resource and effectively showing that a single technology cannot adequately support high renewable penetrations.

Task 7.2.1. UCI Community Results

7.2.1.1. Description of Cases

The spanning cases for the UCI community include local and regional solar, local and regional wind and a case the combines local wind and local solar to make the maximum local resource case.

7.2.1.1.1. Local Solar Spanning Case

For the Local Solar spanning case, the proportion of fixed PV and concentrated PV is maintained and the total capacity is scaled up from zero to twice the maximum capacity. Twice the maximum capacity is used as the upper limit such that the analysis is not limited by the constraints of the UCI campus. Other communities may have more or less available land area for the deployment of solar photovoltaic systems, and may have a different peak load level and load profile. Therefore it was important to capture the possibility of utilizing a larger capacity of solar power such that the implications of the analysis can be applied to communities with more available land area than the UCI campus.

For this case, the radiation data input is sourced from the same data as that used in the larger-scale HiGRID model, with the exception that in order to represent solar resources installed on campus, only the radiation data for the Santa Ana location is used. Locations of the solar sites used in the HiGRID model are displayed in Figure 277:

Figure 277: Solar Irradiation Data Locations

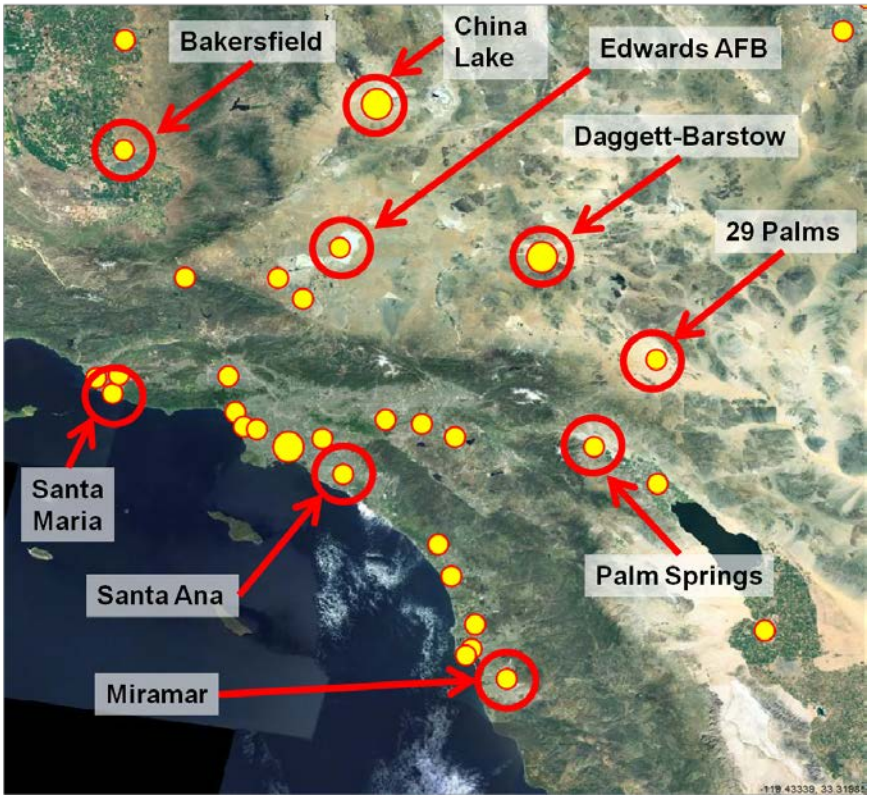

7.2.1.1.2. Regional Solar Spanning Case

As a comparison to the case that uses only local solar resources, a spanning case was used that utilizes off-campus solar resources only. Off-campus solar resources tend to have a higher capacity factor and allow the installation of large systems that take advantage of increased efficiencies, however, the produced power must pass through transmission lines to reach the UCI campus and incur a corresponding proportional loss. This case was used to determine the tradeoff between the benefits of increased capacity factors at more suitable sites and the losses due to transmission and distribution of the produced power.

For this case, the solar installation is assumed to be deployed in the Daggett-Barstow area in the desert region of Southern California, and radiation inputs to the relevant solar power models for this area were used. The technology used is assumed to be 1-axis (azimuth) tracking solar photovoltaic panels, installed as a part of a large installation in the region. The capacity of the system and increment of spanning is matched to that of the Local Solar spanning case for comparison. This assumes that a certain capacity proportion of a large solar power system installed in the region will be diverted towards the UCI campus, and the solar power potential of the region is very large. The capacity in this case refers to that proportion.

7.2.1.1.3. Local Wind Spanning Case

The Local Wind spanning case utilizes local wind power resources installed in relative proximity to the UCI campus. Since the wind potential in this region is quite low, data from the

NREL WWSIS study has revealed only one suitable site for wind turbine deployment in Newport Beach, approximately 5 miles from the UCI campus. Wind speed input from this site was acquired from the NREL WWSIS.

To more accurately represent the performance of wind turbines installed at a site with a lower wind speed, the performance curve of the Vestas V90 3.0MW turbine used to provide the wind power data in the NREL WWSIS database was modified to have a lower cut-in speed and lower overall capacity. Wind turbines are selected based on the suitability of their operating range to the wind speed distribution of the preferred area of deployment; therefore it would be misleading to utilize an oversized turbine for a low wind speed site such as Newport Beach. The performance curve of the original and modified turbines is presented in Figure 278:

Figure 278: Original and Modified Wind Turbine Power Curve for Low-Speed Area and Inset

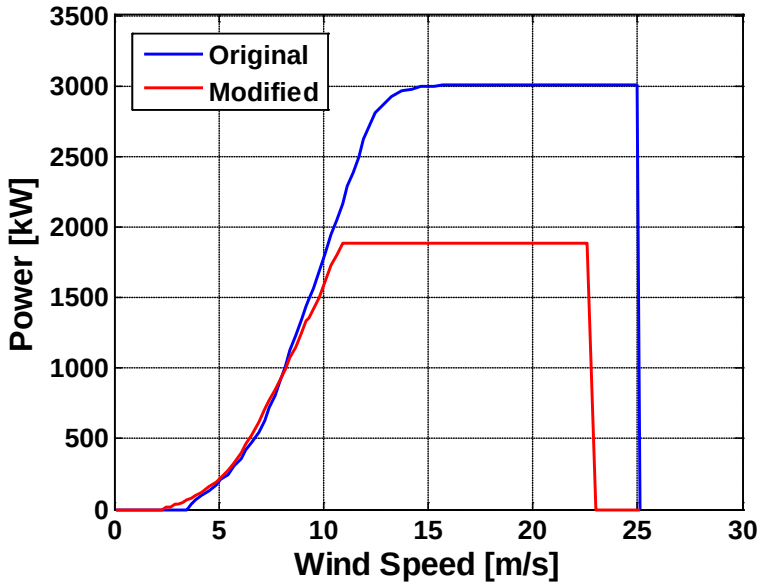

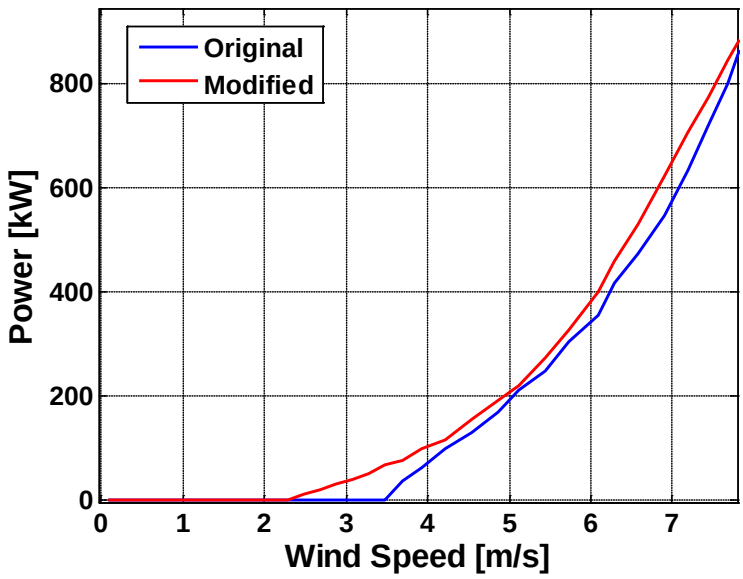

To produce the modified power curve, the efficiency (compared to the Betz power) at each point was maintained, but the cut-in speed was lowered to about 2.3 m/s (from 3.5 m/s originally), and the cut-out speed lowered from 25 m/s to about 23 m/s. This lowered the overall capacity from 3.0 MW to 1.8 MW per turbine.

For this case, the capacity increment and upper capacity limit are matched to those used in the Local Solar spanning case.

7.2.1.1.4. Regional Wind Spanning Case

To provide a comparison for the Local Wind spanning case, a case which exclusively utilizes off-campus wind power resources is examined for the same reasons that a regional solar spanning case was examined. In this case, wind power from the Tehachapi, Beaumont, Granite Mountain and Palmdale regions is produced and a certain proportion is delivered to the UCI campus. The delivered proportion is determined based on the ratio of the effective full-time population of the UCI campus to the population of the Southern California Air Basin, which the regional wind resources will primarily serve.

Unlike regional solar power resources, however, there exists a distinct limit on the wind power potential of regional wind resources, and the capacity of the regional wind resource cannot be scaled up in an arbitrary fashion. Utilizing the sites within the region that have a capacity factor of at least 30% in the NREL WWSIS data, the maximum wind power capacity is approximately 30,390 MW. Therefore, for this case the capacity of the regional resource is scaled up from zero to twice the available capacity, once again to represent cases for communities that are located near more substantial wind power resources. The effective wind power capacity as seen by the UCI campus is the regional resource power capacity multiplied by the population ratio.

The wind power data from the NREL WWSIS utilized in the larger-scale HiGRID model is used to provide the wind power output in this case.

7.2.1.1.5. Maximum Local Resource Spanning Case

As a final scenario for the set of baseline cases, a case which explores the maximum potential of utilizing exclusively local resources is explored. This case combines the Local Wind and Local Solar spanning scenarios to determine the extent to which using exclusively local renewable resources only can increase the renewable penetration range of the campus. To maintain the same resolution as that of the other cases, the increment of capacity for wind and solar power in this case is half of that used in the other cases.

7.2.1.1.6. Summary of Spanning Scenarios

A summary of the five cases described herein is displayed in Table 70. Note that the peak load of the UCI campus for the data used is 25 MW.

Table 70: Summary of Cases

Scenario	Local Wind Cap. [MW]	Regional Wind Cap. [MW]	Local Solar Cap. [MW]	Regional Solar Cap. [MW]
Local Solar	0	0	0 to 73.2	0
Local Wind	0 to 73.2	0	0	0
Regional Wind	0	0 to 60,780 (0 to 37.2 effective)	0	0
Regional Solar	0	0	0	0 to 73.2
Local Resource Maximization	0 to 73.2	0	0 to 73.2	0

This analysis will be presented in two scenarios. The first scenario allows the on-campus gas turbine to trip offline if the net load decreases to levels that cause it to operate below its minimum power level. This scenario implies that the capabilities of on-site generation have improved start up and shut down capabilities.

The second scenario will not allow the gas turbine to trip offline. In this case, the gas turbine will only decrease to its minimum power level and any generation above the load demand for that time will be curtailed. The strategies that attempt to mitigate potential gas turbine trips will still operate, however, since the curtailment of power is undesirable. Since power plants are limited in their ability to start up and shut down both physically and due to criteria pollutant emissions concerns, this scenario is more representative of an operating scheme that may be used under current standards.

7.2.1.2. Technical Analysis – GT Trips Allowed

7.2.1.2.1. Energy Analysis and Renewable Performance

7.2.1.2.1.1. Required Renewable Capacity vs. Renewable Penetration Level

The progression of renewable capacity with renewable penetration level is displayed in Figure 279:

Figure 279: Renewable Capacity vs. Renewable Penetration

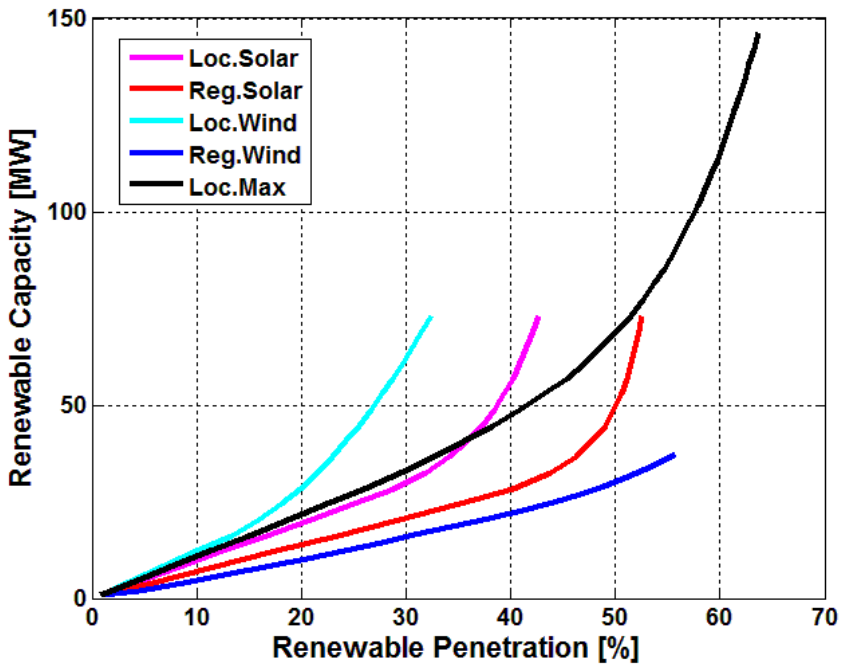

The progression of renewable capacity with renewable penetration level follows similar trends in all of the cases. Each case initially displays a linear relation between capacity and penetration level. After a certain point, however, the relation becomes exponential due to the effects of surplus renewable generation at higher renewable capacity levels, and increasingly larger increments of capacity increases become required to increase the penetration level. This change in relation is due to exponentially increasing curtailment, which is discussed in the next section.

Per unit of rated capacity, the use of regional wind power resources garners the largest increase in renewable penetration level. The use of regional wind power allows the UCI campus to reach a renewable penetration level of 55.73% with an effective capacity of 37.44 MW. Regional solar, local solar, and local wind are only able to reach penetration levels of 53.25%, 44.16%, and 32.42% respectively, and require more than twice the installed capacity to do so. The case that maximizes the use of local resources is able to reach higher penetration levels than the regional wind case, but requires significantly (more than 4 times) higher capacity to do so. This trend occurs due to the behavior of the power output of each renewable resource and location.

Of the four resources presented here, regional wind power tends to last at significant levels for longer periods of time in addition to having power peaks. By contrast, solar power resources are strictly high power and short duration, exhibiting high power output during the daytime with steep ramp up and ramp down rates and zero power during the night-time hours. Local wind resources in this case, tend to follow a somewhat similar trend: on-site wind power tends to peak considerably in short bursts with little to no power produced in between such times, even with the turbine being sized more appropriately for the region. For the particular local wind site used in this case, the power profile appears to exhibit this characteristic even more so than solar power, since the cycle of power peaking is not necessarily diurnal and can occur at

random. Therefore, when the nameplate capacity is increased past a certain point, the periods of peak generation will cause the onset of surplus renewable generation, whereas all other periods will not contribute significantly to serving the load demand unless the nameplate capacity is increased dramatically. This causes the required capacity to reach a given renewable penetration level to increase exponentially at this point. Therefore, resources with dominantly 'peaky' power profiles require large nameplate capacities to reach high renewable penetration levels.

Also, the use of regional resources tends to yield higher increases in renewable penetration level per unit nameplate capacity compared to the local resources. The onset of the exponential relation occurs at higher renewable penetration levels. This suggests that even with the 10% transmission loss assumed in this study, the increase in capacity factor garnered from siting renewable installations in high potential regions still yields more of a benefit. For the use of regional solar power specifically, the power output tends to have a longer diurnal power duration band compared to the regional resource, allowing power to be generated at off-peak hours whereas in the local case, there would be no power generated. This is due to the radiation profile at the regional location and also due to the azimuth tracking ability of the system. In addition, the solar radiation levels are simply higher, meaning that off-peak hours will generate more power than that of their local counterparts. From a practical standpoint, however, the siting of additional transmission capacity to accommodate using these regional resources can potentially be prohibitive.

7.2.1.2.1.2. Surplus Renewable Fraction

The surplus renewable fraction is the percentage of renewable energy obtained that is not used to serve the load demand of the system in question – the UCI campus in this case – since the renewable power generation exceeded the load demand at particular times throughout the year. The larger the fraction, the more energy is being exported if possible or curtailed otherwise. The progression of this metric with renewable penetration level is presented in Figure 280:

Figure 280: Surplus Renewable Fraction vs. Renewable Penetration Level

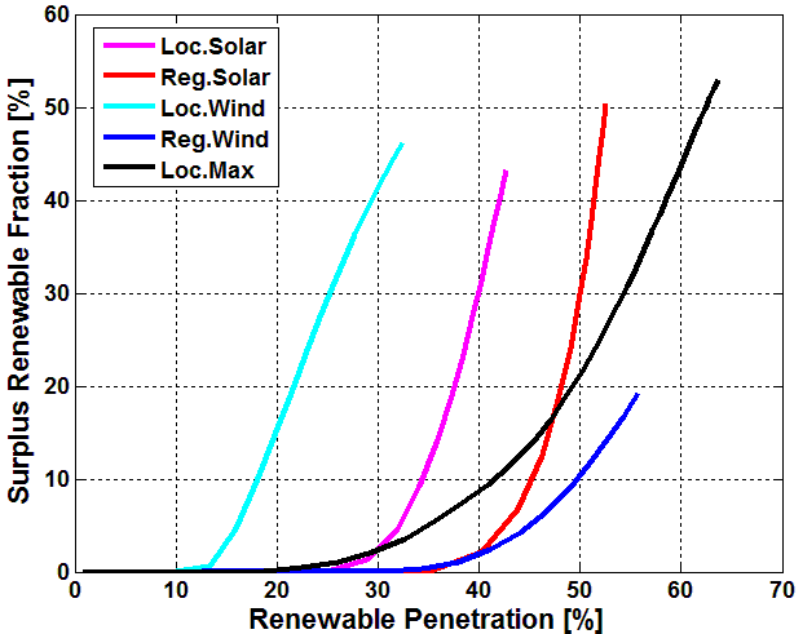

The behavior of the surplus renewable fraction for each resource tends to parallel that of the required renewable capacity. The use of regional wind resources yielded the lowest surplus renewable capacity per unit penetration level, since it is the least peak-dominated of the resources presented here. The use of regional solar tends to match regional wind up to about the 41% penetration level, after which the off-peak hours of regional solar power generation no longer tend to contribute significantly to serving the load demand. The local resources reach this point at lower renewable penetration levels, with the use of local wind reaching such a point at a 13.8% penetration level. The local resource maximization case has a more gradual increase in surplus renewable generation compared to the local wind and local solar. This is due to the fact that while the individual resources that compose this case are peak-dominated, they tend to peak during different times of the day. Therefore, a mix of wind and solar power allows the total renewable power generation profile to more effectively cover a larger portion of each day to some extent. After about the 50% penetration level, the regional solar case exhibits higher surplus renewable fractions than the local resource maximization case due to its reliance on a single (albeit higher quality) resource.

Overall, without the use of any energy management strategies such as exporting, energy storage, or demand response, increasing the renewable penetration level of a community will cause large portions of the obtained renewable energy to either be wasted or used elsewhere. The latter may occur if the community is allowed to export to the grid and act as a distributed renewable power plant, however, scheduling of power and interfacing with the transmission system operator can pose challenges.

7.2.1.2.2. Behavior of the On-Site Generation

The heating, cooling, and a large portion of the electric load demand on the UCI campus is served by the campus central plant. The introduction of large amounts of renewable power, however, will affect the manner in which the central plant operates and its ability to meet the respective campus loads, since the equipment of the plant can only operate within certain constraints as described in the model description. Therefore, in order to accommodate a large amount of renewable power in a community such as the UCI campus, the implications for the use of non-renewable on-site generation must be examined such that an understanding of how the characteristics and capability of on-site generation may need to be modified to accommodate renewable power.

7.2.1.2.2.1. Behavior of the Gas Turbine

Under the current operating scheme, it is preferred for the gas turbine to operate at full capacity for as much of the time as possible such that it will have sufficient exhaust output to meet the heating demand in addition to emissions and efficiency concerns. The SolarTitan 130 unit used in the central plant, however, cannot operate at a part load condition below 8 MW, and in addition, the campus is mandated to maintain a minimum import of at least 1 MW at all times from Southern California Edison. Therefore, the gas turbine must turn down in power if the load drops below a certain point in order to prevent violation of the minimum import condition, and it must turn off completely if it will be forced to operate below 8 MW. The introduction of large amounts of renewable power, however, can often decrease the balance – defined as the remaining load after utilization of renewable power - that the gas turbine must meet to levels below its minimum power, overall causing the gas turbine to operate for a lower amount of time throughout the year.

7.2.1.2.2.1.1. Gas Turbine Capacity Factor

The first measure of gas turbine operating duration is the capacity factor of the gas turbine which is a measure of equipment utilization, as displayed in Figure 281:

Figure 281: GT Capacity Factor vs. Renewable Penetration Level

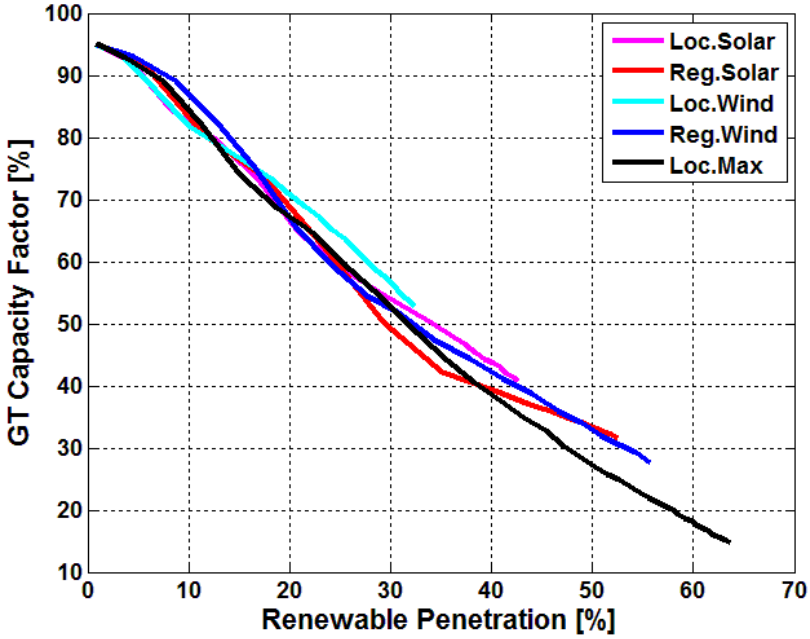

As the renewable penetration level increases, the gas turbine capacity factor decreases due to excessive shut-offs caused by very low effective load conditions. At current, the gas turbine operates with a capacity factor of about 95%. For renewable penetration levels below about 18%, the regional wind resource still allows the highest gas turbine capacity factor, since it is the least peak-dominated of the resources considered, and every renewable power peak is likely to be associated with a gas turbine shut-off. By contrast, the local wind case in this penetration level range exhibits the lowest gas turbine capacity factors. This occurs since the local wind case has the largest installed capacity of any of the individual resources for those given penetration levels and is also the most peak-dominated of the resources considered. The large capacity indicates that any power peak will cause a gas turbine shut down and therefore a decrease in capacity factor. The local resource maximization case has a similar total installed capacity in this penetration level range, but the combined renewable profile is not as peak-dominated. At the 18% renewable penetration level, the regional wind resource case starts to exhibit gas turbine capacity factors similar to the other cases, since the off-peak hours start to cause gas turbine shut offs. In this penetration range, the most peak-dominated resources cause the highest decreases in gas turbine capacity factor.

The local wind resource case then exhibits the highest gas turbine capacity factor from the penetration level range between 18% and 32%, after which its capacity maxes out. This is an inverted trend as compared to that displayed in the low renewable penetration range, and occurs since the local wind resource is the most peak-dominated resource. In this range, since the off-peak hours of local wind power generation tend to still exhibit very low power generation levels, those intermediate hours do not contribute to additional gas turbine trips. The intermediate hours of regional wind, by contrast, still exhibit relatively high power levels and causes additional gas turbine shut offs.

Above the 32% penetration level, the local solar case exhibits the highest gas turbine capacity factors. This is because it is nearing the point where it causes the highest amount of gas turbine shut offs that it can, since the peak and near-peak hours of solar power generation are already causing gas turbine trips, and the off-peak hours are generating essentially zero power and cannot contribute to additional gas turbine turndowns or trips. The regional solar case, due to its longer duration of power generation and higher power levels overall, starts to reach this point at a later renewable penetration level compared to its local counterpart. The regional wind case starts to follow a similar behavior, where the off-peak hours are already causing a gas turbine turndown or trip and the remaining hours are not likely to contribute to additional events due to extremely low power levels.

Overall, however, the decrease in the gas turbine capacity factor for all of the cases is relatively similar, and no one case shows a distinct advantage over another in contrast to the required capacity and surplus renewable fraction metrics displayed prior. The variable nature of wind and solar resources triggers many gas turbine trips and long periods of gas turbine turndown. While each resource may cause such events at different periods of the day, the net effect from this standpoint is the same.

By the 35% penetration level, the gas turbine capacity factor for all cases has essentially been reduced by half to between 43% and 48%, and by the 50% penetration level the capacity factor drops to near 30%. This indicates that large amounts of renewable power will severely decrease the utilization of on-site generation resources and may render electricity obtained from such resources as more expensive in order to pay off the capital cost of such equipment. This occurred, however, due to the constraints placed on the particular system of the UCI campus. The minimum import constraint forces the gas turbine to turndown or trip. If the campus were allowed to export power, the gas turbine might be able to remain running during periods of very high renewable power generation. Additionally, the particular unit used in the UCI central plant had a minimum operating power of 8 MW (from a maximum of 13.5 MW). If the campus utilized a unit or technology which was capable of ramping dynamically in response to renewables and operating at lower part load conditions, the capacity factor may not decrease as significantly with increased renewable penetration.

7.2.1.2.2.1.2. Gas Turbine Downtime

A more explicit examination of the gas turbine downtime is presented in Figure 282:

Figure 282: GT Downtime vs. Renewable Penetration Level

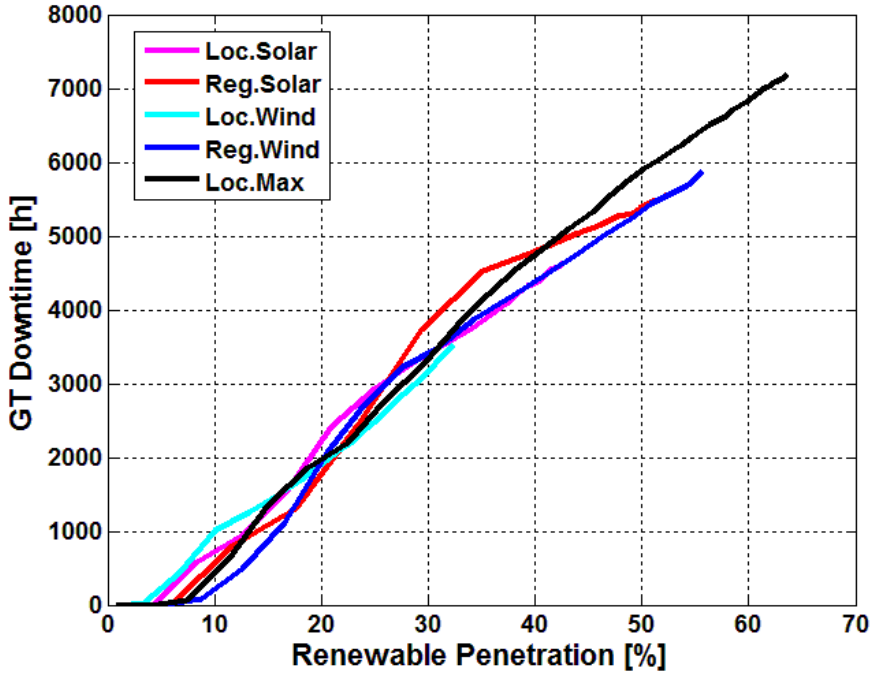

The gas turbine downtime increases with renewable penetration level, essentially mirroring the trend of the gas turbine capacity factor for the same reasons. By the 40% penetration level, all cases have a gas turbine downtime which exceeds 4300 hours out of the year, indicating at this point the gas turbine is essentially shut down for more than half of the yearly operating hours. By the 50% penetration level, the shutdown portion approaches two thirds of the year, rendering the gas turbine to be a mostly dormant piece of equipment.

7.2.1.2.2.1.3. Gas Turbine Start-Up Events

In addition to gas turbine capacity and downtime, another concern for the gas turbine power plant is the amount of times that it starts up per year. Since combustion engines exhibit very high criteria pollutant emissions during startup procedures – in excess of that emitted during typical yearly operation – the South Coast Air Quality Management District (SCAQMD) sets limitations on the amount of times that the gas turbine (or any power plant) can start up every year. In the case of the gas turbine at the UCI central plant, the unit is limited to 13 start events. The count of gas turbine start up events vs. renewable penetration level for each of the cases is presented in Figure 283:

Figure 283: GT starts vs. Renewable Penetration

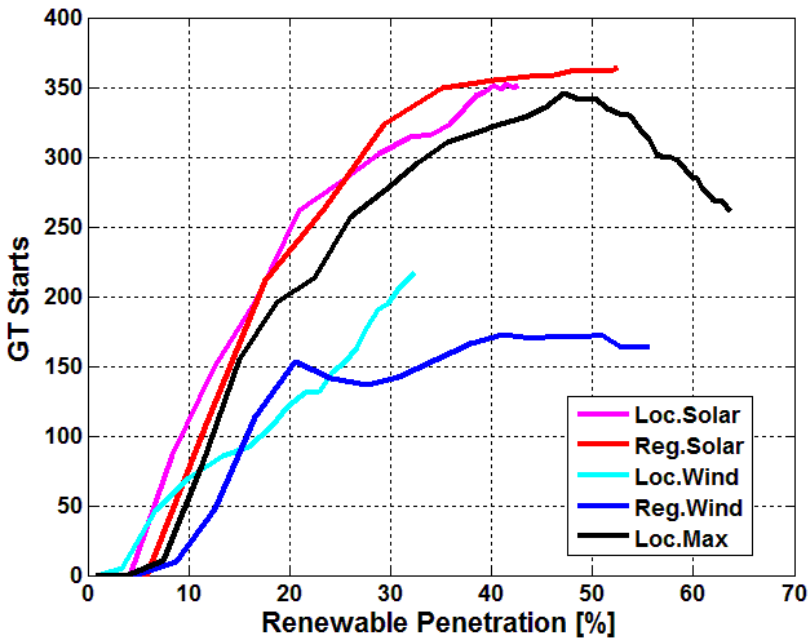

For all cases, the number of gas turbine start events increases steadily until a certain point where it starts to become somewhat constant. The regional wind spanning case displays the lowest amount of gas turbine starts due to the fact that it is the least peak-dominated of the resources considered. Due to the variability of wind power, many of the smaller peaks in the power generation profile occur in close temporal proximity to one another. The regional wind resource exhibits a large amount of smaller peaks and such events occur so close to one another such that the gas turbine is not allowed to re-start. In addition, the regional wind resource also exhibits long, continuous periods of part-load generation. When the gas turbine trips offline or shuts down, a certain time period is required for the plant to start back up. In this case, however, even if the gas turbine is ready to restart, small peaks or persisting part-capacity power production in regional wind power are high enough to cause the gas turbine to shut off as soon as it turned on, therefore the unit remains off.

For the local wind case, the number of gas turbine starts increases but not to the same extent as that of the solar cases. This is due to the fact that while the local wind resource is the most peak-dominated of the resources considered, the low capacity factor indicates that there are not many power peaks during the year to begin with. That is, while local wind power tends to be producing either near full power or near zero power at any given time, the majority of the time is near zero power. Solar power on the other hand, regularly peaks every day unless there is a storm event or other cloud pass that prevents solar power generation from reaching its capacity. Therefore, the number of peaks in solar power generation is very large, and since such peaks are spaced approximately 24 hours apart, they allow sufficient time in between for the gas turbine to become ready to restart.

The number of starts for all cases becomes level at a certain point. This occurs due to one of two reasons: 1) the renewable power resource may be exhibiting persistent power generation that does not allow the gas turbine to restart, or 2) the renewable resource cannot cause any more starts because it only affects a certain portion of the day.

Overall, however, it is shown that in all cases, the number of starts far exceeds the emissions-based limit of 13 starts. This violation occurs at a very low renewable penetration level: ranging from about 4.0% for the local wind case to about 8.7% for the regional wind case. This has strong implications for the criteria pollutant emissions associated with the increased penetration of renewable resources: since the variable nature of renewable resources may cause non-renewable generators to cycle or startup/shut down frequently, a large increase in criteria pollutant emissions may result. This issue can be solved at the community scale by allowing an export margin to allow the gas turbine to remain running, or by utilizing generator technology that does not have significant start up emissions.

7.2.1.2.2.2. Behavior of the Heat Recovery Steam Generator (HRSG), Fuel Use, and Steam Turbine

In the UCI central plant, the exhaust of the gas turbine is used to create steam in order to meet the heating demand of the campus. Steam in excess of the heat demand is used to run the steam turbine for additional electric power generation as long as doing so will not cause an import power violation. The introduction of renewable power, however, reduces the operating hours and average power level of the gas turbine as shown in the previous results, and therefore will reduce the ability of the system to meet the heating demand without the use of external boilers or a duct burner. The reduction in available steam also has implications for the operation of the steam turbine. This section examines the effect of implementing large amounts of renewable power on the HRSG and fuel use.

7.2.1.2.2.2.1. HRSG Contribution to the Heating Demand

At current, the exhaust stream from the gas turbine is used to provide essentially all of the energy required to meet the heating demand. As the gas turbine turns down or shuts off, however, the total available exhaust enthalpy will be decreased, and the contribution of the HRSG towards meeting the heating demand of the campus will be decreased. A plot of the HRSG contribution towards meeting the heating demand as a function of renewable penetration level for the different cases is presented in Figure 284:

Figure 284: HRSG Contribution to Heating Demand vs. Renewable Penetration

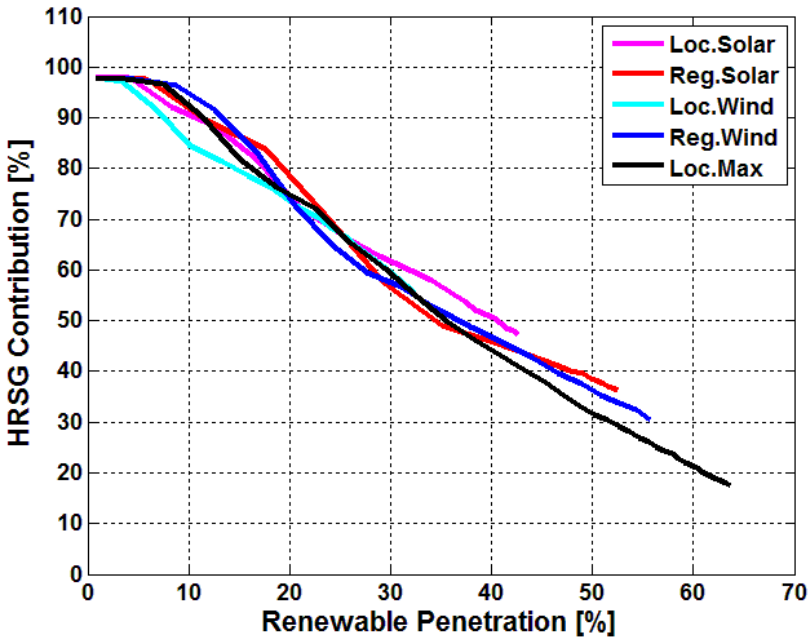

In the current system configuration, the HRSG is able to meet about 98% of the heating demand. As the renewable penetration level increases, the fraction of the heating demand that the HRSG can meet decreases with a trend that is essentially the inverse of that displayed by the GT downtime. This relation is expected, since any gas turbine turndown or downtime will prevent any contribution to the heating demand by the HRSG at that time, and therefore the behavior of the HRSG contribution for each case is motivated by the same driving factors as that of the GT capacity factor and GT downtime.

No case shows any significant advantages over any of the others after the 20% renewable penetration level. Below the 20% renewable penetration level, the local wind case shows the largest decrease in the HRSG contribution since it shows the largest decrease in gas turbine capacity factor. Above the 25% penetration level, local solar allows the highest HRSG contribution since it is reaching the point where it cannot cause many additional gas turbine shut offs.

Overall, the decreased ability of the HRSG to meet the heating demand indicates that additional fuel must be used through external boilers of increasing size to provide the steam necessary to meet the heating demand. This trend is displayed more explicitly in Figure 285, which displays the additional fuel use in the boilers needed to meet the heating demand.

Figure 285: Duct Burner / Boiler Fuel Requirement vs. Renewable Penetration

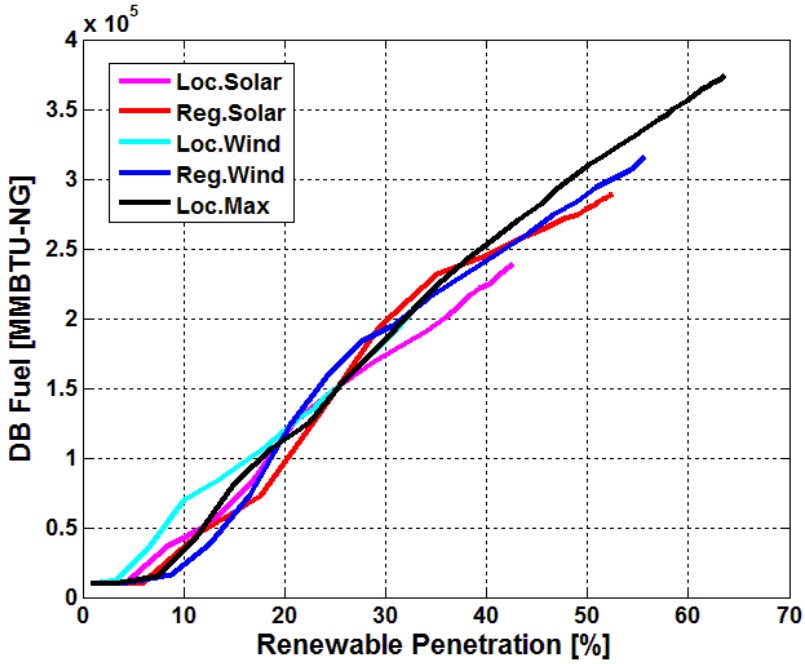

7.2.1.2.2.2.2. Campus Fuel Use

The behavior of the gas turbine fuel use and total fuel use with renewable penetration is presented in Figure 286 and Figure 287:

Figure 286: GT Fuel vs. Renewable Penetration

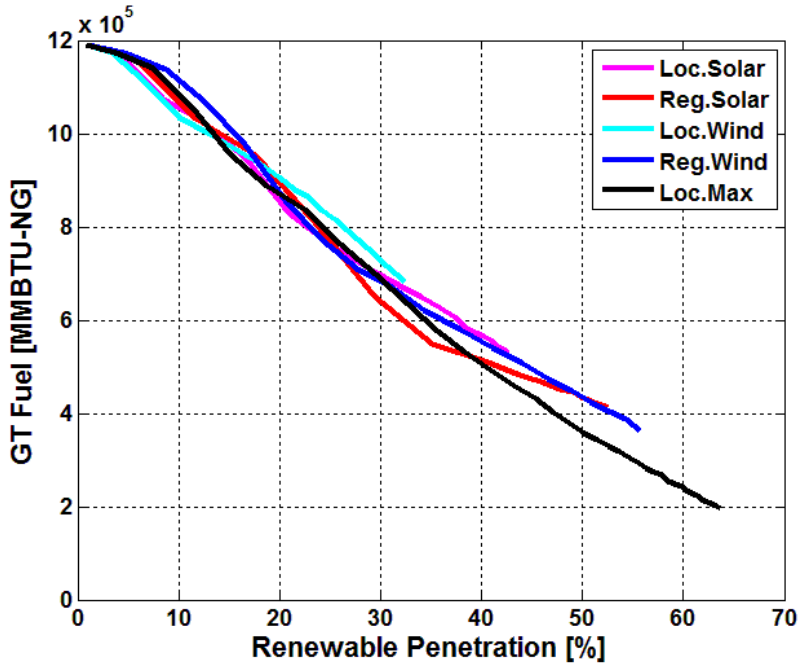

Figure 287: Total Fuel vs. Renewable Penetration

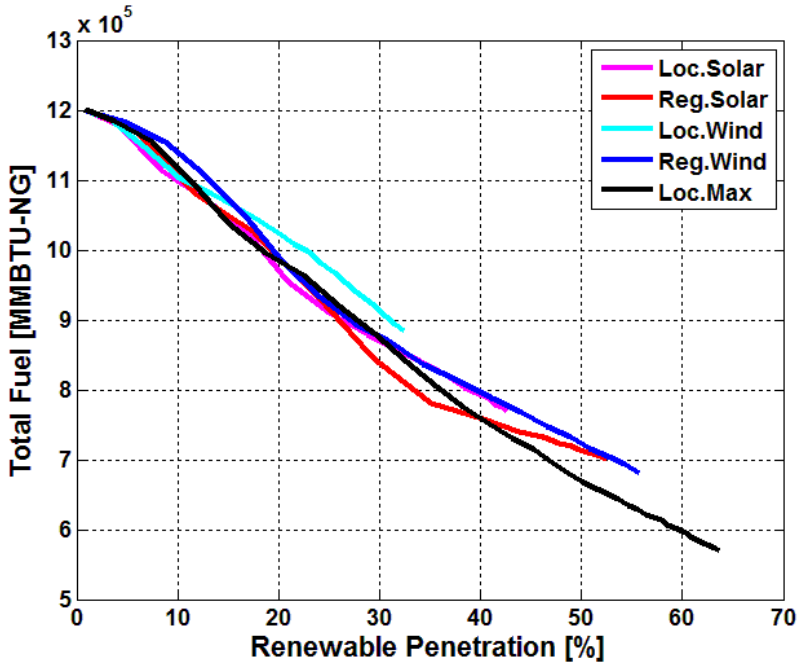

The required additional fuel use for the boilers as a function of renewable penetration level follows the trend displayed by the gas turbine downtime as a function of renewable penetration level, and is naturally an inverse of the HRSG contribution curve. By the 50% penetration level, almost 300,000 MMBTU of natural gas needs to be added to meet the heating demand of the campus. In this case, however, the total energy of the heating demand is smaller than the total energy input required to operate the gas turbine in the current operation scheme. Under current operating conditions, if the HRSG was not present, about 430,000 MMBTU of natural gas would be required to meet the heating demand, however, the gas turbine requires 1,190,000 MMBTU of natural gas to operate for 1 year, therefore the heating demand is only 1/3rd the energy content of the gas turbine fuel use. Due to this difference in scale, as the renewable penetration level increases, the total natural gas fuel use of the campus still decreases since the large periods of gas turbine downtime cause the gas turbine to require less fuel.

While the total annual energy in the gas turbine exhaust stream may be larger than the total annual energy required by the heating demand, however, temporally there still exist periods when insufficient steam is provided by the HRSG to meet the heating demand at that time. Excess steam produced at different times cannot be used to supplement deficits in steam at those given times.

7.2.1.2.2.2.3. Behavior of the Steam Turbine

As less steam becomes available to meet the heating demand, even less will be available to power the steam turbine after the fact, since meeting the heating demand takes priority over running the steam turbine. Therefore, the steam turbine capacity factor (utilization) will decrease as the renewable penetration level increases. This behavior is displayed in Figure 288:

Figure 288: ST Capacity Factor vs. Renewable Penetration

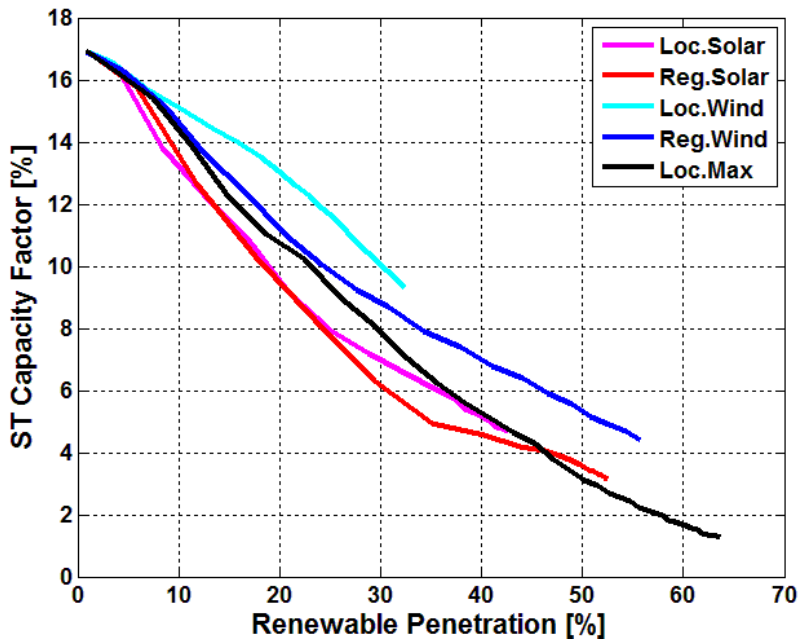

Compared to the gas turbine capacity factor, the steam turbine capacity factor is very low, about 16.9% under current operating conditions. This occurs due to two reasons: 1) the priority of the generated steam is to meet the heating demand, only steam in excess of the heating demand will be used to run the steam turbine and 2) the steam turbine is severely oversized for this application. The particular unit used in the UCI central plant is a 5.5 MW unit, which is designed to have steam input generated from a 30 MW gas turbine – roughly double the size of the gas turbine used in this application. Therefore, the capacity factor can be expected to be low overall.

As the renewable penetration level increases, the steam turbine capacity factor decreases to even lower levels. The shortage of steam is able to decrease the capacity factor to below 10% by the 30% renewable penetration level in all cases, and to as low as 3.5% by the 50% renewable penetration level. The local wind case allows the steam turbine to have the highest capacity factors since while it does tend to cause the most amount of gas turbine downtime at the lower penetration level ranges due to its peak-dominated behavior, the off peak periods essentially cause no turndown since local wind power generation during these periods are near zero. Therefore, when local wind power peaks, the steam generation is decreased to zero, decreasing the yearly HRSG contribution and shutting off the steam turbine, however during off peak hours, the gas turbine is allowed to operate at essentially full capacity and produce more than enough steam to meet the heating demand and run the steam turbine during those times.

The regional wind case shows the next highest steam turbine capacity factors. In the lower renewable penetration ranges, this generally occurs since regional wind power causes the lowest amount of gas turbine downtime. In addition, the regional wind resource peaks during the night time hours when the heating demand is the lowest, so the reduction in gas turbine power still allows sufficient steam to be produced to meet the heating demand and run the

steam turbine. This effect is limited by the fact that the electric load is also low at night, and the steam turbine cannot be activated if it will cause an import violation. The solar cases cause the lowest steam turbine capacity factors since solar power causes gas turbine shut downs during the early daytime, when the daily heating demand is the highest.

Overall, the decreases in steam turbine capacity to very low levels render it a much underutilized piece of equipment. At the higher renewable penetration levels where the capacity factor drops below 5%, for future communities it may not be worth justifying the cost associated with purchasing that size of equipment. This could be rectified by changing the operating scheme to prioritize electric power over the heating demand, which could only be done if the import margin on the UCI campus was lifted.

7.2.1.2.3. Behavior of the Import Power Signal

As very few communities are islanded and capable of meeting the entirety of their electric load demand using internal resources only, the UCI campus is similar to most communities in that it is at least partly dependent on the utility grid to meet some of its load. This interconnection to the utility grid is currently governed by certain rules and restrictions which are based in the utility's (Southern California Edison in this case) ability to manage its transmission and distribution system. The most prominent restriction on the interconnection of the UCI campus to the SCE utility grid is the minimum import restriction, which dictates that the UCI campus must import at least 1 MW of electric power at all times. Violation of such restriction gives the utility grid the right to disable (trip) the on-site generation (gas turbine) of the UCI campus. Such a scenario is undesirable for the UCI campus, as disabling of the gas turbine will cause all of the campus electric load demand to be met by imported power, incurring large demand charges and additionally higher energy use charges until the gas turbine is able to be restarted.

As communities such as the UCI campus seek to increase their respective renewable penetration levels the rules and restrictions of current interconnection paradigms may be a limiting factor in allowing communities to reach their sustainability goals. This is especially likely given the fact that prominent local renewable resources such as solar are very peak-dominated, and can only contribute significantly to increasing the renewable penetration level with high capacities. The behavior of the characteristics of the import signal for each of the spanning cases are examined in this section, such that some insight into changes in the interconnection rules that may be required may be garnered. The import signal is analyzed in a similar way to that of the chiller power signal, by way of a load duration curve, with the key difference being that the import power is allowed to become negative in the case that the campus will be required to either export or curtail power.

The import power distribution for the local solar and regional solar spanning cases is displayed in Figure 289 and Figure 290 respectively:

Figure 289: Import Power Distribution: Local Solar Case

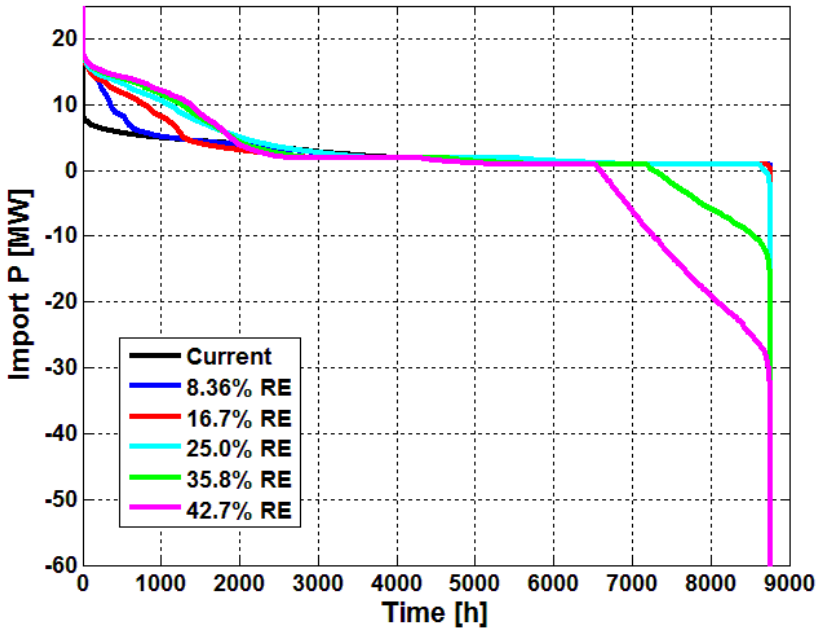

Figure 290: Import Power Distribution: Regional Solar Case

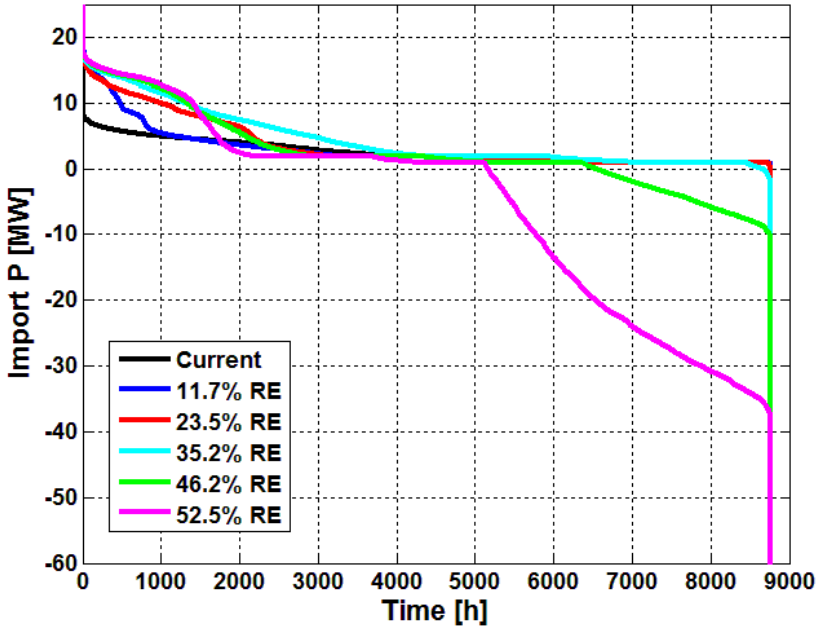

As the onset of increased solar power begins to cause more gas turbine trip events, the number of hours of high import power is increased, as are the number of export/curtailment hours and the magnitude of power export/curtailment. Negative import power values refer to power that is either curtailed or exported. The number of export hours can be determined by taking

distance on the time axis from the point where the load duration curve crosses the zero import power line to 8760, which is the number of hours in one year. For renewable penetration levels up to about 40%, the regional solar case exhibits a lower number of import hours compared to the local solar case. This occurs since the quality of the regional resource is higher in terms of magnitude and also in terms of time duration, and therefore does not need as much capacity to reach the same renewable penetration level compared to the local case. Therefore, the lower capacity indicates lower peak power levels, and subsequently a lower amount of export hours. At approximately the 35% renewable penetration level, the regional solar spanning case exhibits 87 export hours while the local solar case exhibits 1474 export hours. This advantage is mitigated at renewable penetration levels above 40%, since at this point the installed solar capacities are so high that the majority of off-peak hours start causing export events. This is expected from the exponential behavior region of renewable capacity curves presented prior. Above the 40% renewable penetration level, both solar cases exhibit essentially the same number of export hours.

For a given renewable penetration level, the regional solar case also exhibits a lower maximum export magnitude compared to the local case, mostly due in part to the lower installed capacity. The maximum export power for the regional case appears larger in the load duration curves, but this is due to the regional case being able to reach higher renewable penetration levels overall. At about the 35% penetration level, the regional solar case exhibits a maximum export of 2.3 MW, compared to 16.8 MW in the local solar case. This is also expected since the local solar case reaches the exponential capacity increase requirement at a lower renewable penetration level compared to the regional case.

The import power distribution for the local wind and regional wind spanning cases are displayed in Figure 291 and Figure 292 respectively:

Figure 291: Import Power Distribution: Local Wind Case

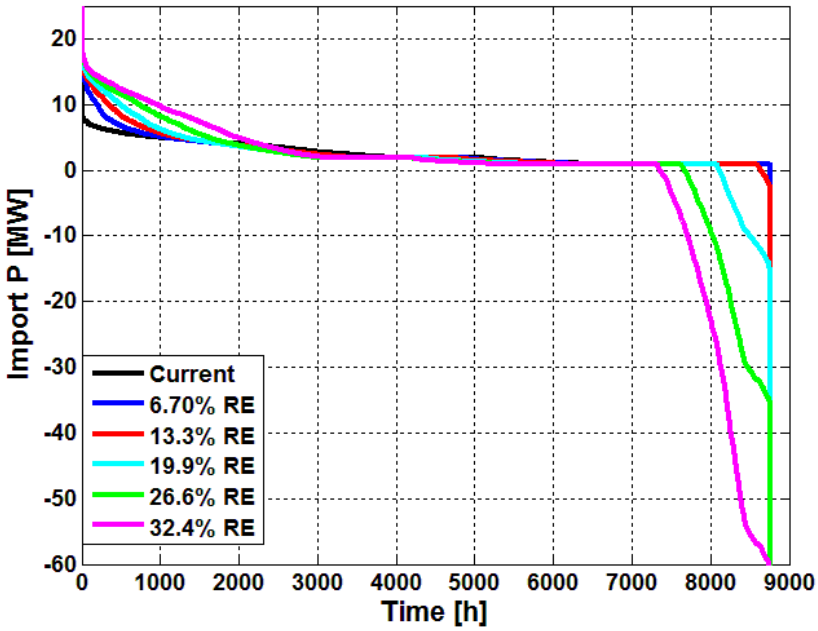

Figure 292: Import Power Distribution: Regional Wind Case

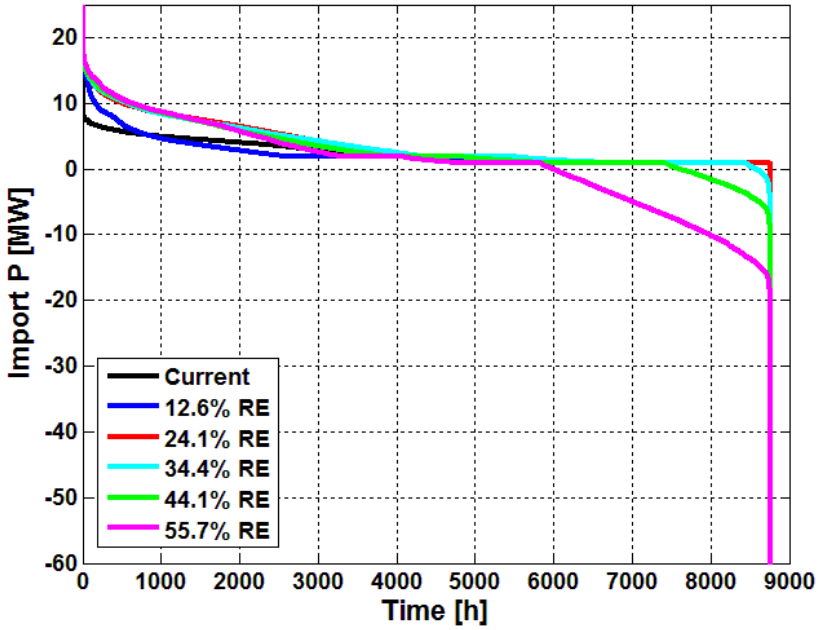

The local and regional wind spanning cases exhibit similar effects on the import power distribution as that shown by the solar cases, namely an increase in the maximum import power levels, maximum export power levels, and number of export hours, albeit to different extents. In general, for a given renewable penetration level, the regional wind case exhibits significantly lower export hours and maximum export magnitudes. This occurs primarily due to the strongly

peak-dominated nature of the local wind resources and the weakly peak dominated nature of the regional wind resource, which causes significant differences in the required capacity for each resource to reach a given renewable penetration level with the regional case requiring significantly less.

As an example, the local wind case exhibits a maximum export of 35.9 MW with 1083 export hours at the 26.6% penetration level. At a similar penetration level of 24.4%, the regional wind case exhibits a maximum export of only 5.7 MW with that event representing the only export hour.

The import power distribution for the local resource maximization case is displayed in Figure 293:

Figure 293: Import Power Distribution: Local Resource Maximization Case

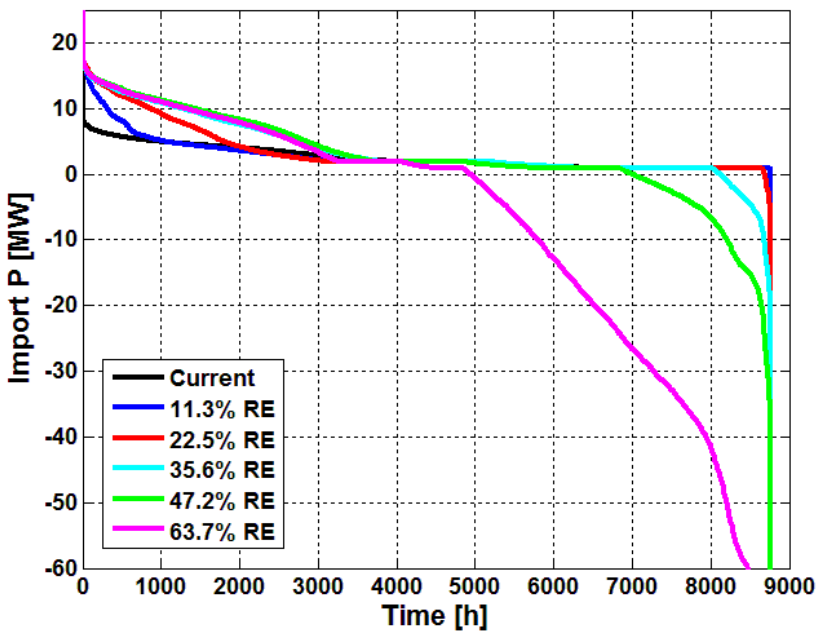

The local resource maximization case shows a combination of the local wind and local solar spanning case properties. In general for a given renewable penetration level, the local resource maximization case exhibits a lower maximum export power compared to the local wind spanning case, but a higher maximum export compared to the local solar spanning case. For example, at approximately a 35% penetration level, the maximum export power in this case is 19.8 MW, which is higher than that of the local solar case. The local wind case reaches higher maximum export power levels at lower penetration levels. These trends occur primarily due to the very high total installed capacity requirement at each renewable penetration level.

In the case of export hours, however, the combination of local wind and solar resources is slightly beneficial. At the 35% penetration level, the local resource maximization case exhibits 630 export hours, less than either local wind or local solar. This occurs primarily due to the fact that while both local wind and local solar resources are peak-dominated, the fact that each

resource tends to reach its peak during different periods of the day allow the capacity of each individual resource to not be as high to reach a given renewable penetration level. This has the effect of making the combination less peak dominated compared to the individual resources, and therefore yields less export hours.

A prominent characteristic is that for the UCI campus, the maximum import power is increased as the solar capacity is increased. This trend happens to be true for all of the spanning cases. A plot of the maximum import power as a function of renewable penetration level is displayed in Figure 294:

Figure 294: Maximum Import Power vs. Renewable Penetration

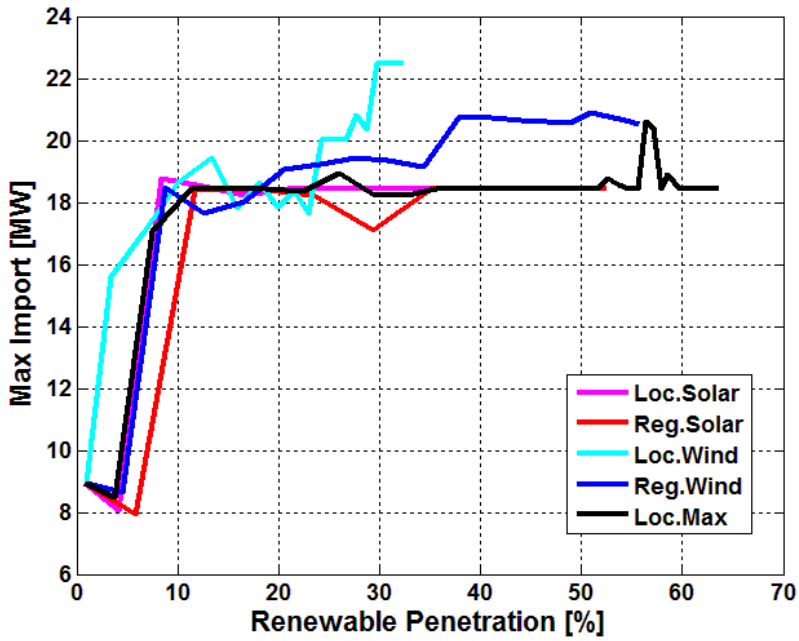

This is counter intuitive for solar power, since the peak load demand occurs during the daytime when solar power is at its highest. Due to interconnection arrangements, however, the increase in maximum import power occurs due to the gas turbine being shut down due to a violation of the minimum import arrangement due to the gas turbine not being able to operate below 8 MW. Therefore, during a trip event, at least an additional 8 MW of import power is instantly added. Additionally, the gas turbine does not follow the load demand exactly, since it attempts to leave a 1-2 MW margin in case of sudden load drops. Therefore, during a trip event under the current operating scheme, anywhere from 9 to 10 MW can be instantaneously added to the import power.

The maximum import power at the current renewable penetration level of 0.8% is about 8.95 MW. At renewable penetration levels between 3.7 and 8%, the maximum import power jumps to about 18.5 MW for essentially all of the cases. The local wind case shows an increase in maximum import power as soon as its capacity is increased. Additionally, the local and regional wind cases can cause the maximum import power to increase to even larger values in excess of 20 MW. This additional increase occurs due to the successive wind power peaks not allowing

the gas turbine to restart. For example, a wind power peak may cause the gas turbine to shut down. Subsequently after, the wind power may decrease quickly and the effective campus load demand therefore increases to high levels. If this occurs in close proximity to the trip event, the gas turbine may have not had enough time to restart, and therefore the increased load during the wind power drop is still completely met by imported power. Solar power does not have this problem since solar power peaks are temporally spaced far enough apart such that they always allow sufficient time for the gas turbine to restart.

Overall, this has significant implications for the evolution of utility interconnection rules with respect to the import margin. These results imply that the presence of a minimum import margin in the rules for community interconnection to the utility grid can severely limit the ability of a community to reach high renewable penetration levels with local generation. The large amount of export hours and large magnitude of export power may not be able to be accommodated for on the grid. Additionally, the increase in maximum import power for the UCI campus or similar communities will cause the campus to incur expensive demand charges. For the use of regional renewable resources, these concerns are not as strong since the renewable power flow is not originating on-site and possibly can be diverted to other loads or other communities if it would cause an issue when directed towards a target community. Additionally, the regional resources appear to exhibit the lowest amount of impact on the characteristics of the import signal compared to the local resource cases. In the case of regional resources, however, if all communities on the electric grid wished to reach the same renewable penetration level, in the event of an import/export issue there may not be another community or load to direct the excess renewable energy towards since all similar communities will have the same problem. A scheme must be implemented by grid operators to distribute regional renewable power generation amongst communities in a manner that allows each of them to reach their renewable penetration level goals but also leverages the larger grid and interconnection with other loads to prevent import/export issues from occurring at any one community.

7.2.1.2.4. Behavior of the Cost of Electricity

The behavior of the levelized cost of electricity for each of the renewable technologies is presented in Figure 295:

Figure 295: Change in Levelized Cost of Electricity vs. Renewable Penetration Level

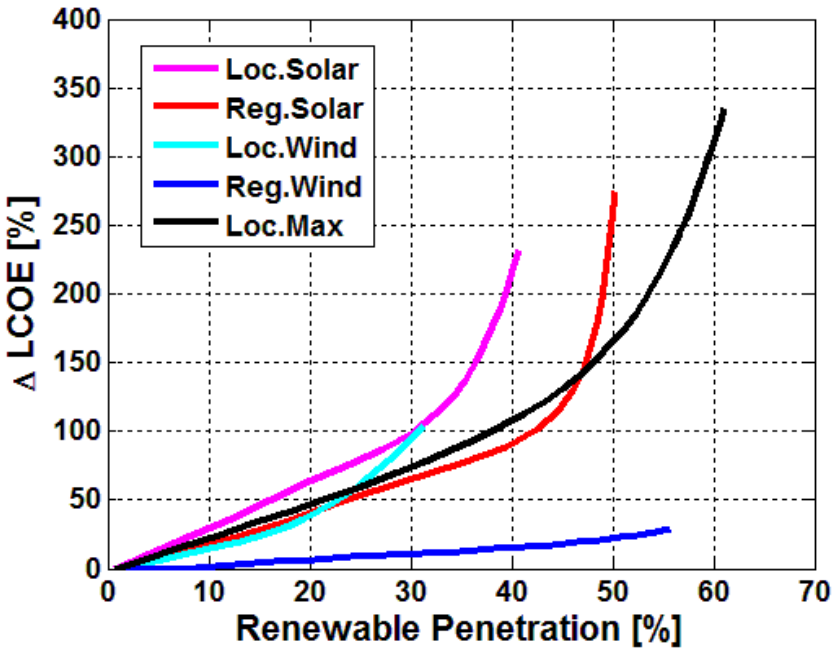

As the renewable penetration level increases, the levelized cost of electricity increases in a manner similar to the increase in renewable capacity. The behavior of the cost for each technology has a linear region and an exponential region, the latter of which reflects the effect of curtailed renewable power.

Of the technologies considered in this analysis, regional wind power displays significantly lower increases in cost compared to all of the other technologies. At the 53% penetration level for regional wind, the cost of electricity has only increased by approximately 35% compared to current levels. The local resource maximization case, which was the only other renewable mix which was able to reach the same renewable penetration level, shows an increase in electricity cost of 240% for the same renewable penetration level. The low cost of regional wind power in this case is due to three primary reasons.

First, regional wind power resources have much higher capacity factors compared to the other technologies. Solar power has a capacity factor between 18-25%, and local wind resources are of low quality with a capacity factor of about 13% with appropriately sized turbines. Regional wind power, on the other hand, has a capacity factor of about 38% on average.

Second, the profile of regional wind power in California's high quality resources renders it the least peak-dominated of the technologies considered. This delays the onset of excessive amounts of curtailment compared to the other technologies.

Third, wind power typically has low capital costs compared to the other technologies, since wind turbines require only conventional materials compared to solar power which requires exotic materials and manufacturing techniques. Modern wind turbines can extract a large

amount of energy per unit of land area and also take advantage of economies of scale. At current, regional wind power by itself has similar levelized costs levels to the on-campus gas turbine. Therefore, even when wind power starts to show a large amount of curtailed energy which causes the price to rise, compared to the other technologies, the increase is not as significant.

The most expensive technology for a given renewable penetration level is local solar. This occurs due to the relatively expensive capital costs of solar photovoltaic technology, low capacity factors and high required capacities due to curtailment. For a community, however, local solar photovoltaic is the most readily available technology due to its suitability for placement on existing rooftops.

The effect of capacity factor is present in the difference between local wind and regional wind. While both scenarios have fairly similar capital costs, the low capacity factor of local wind resources requires very large capacities to reach a given renewable penetration level. Additionally, the peak-dominated nature of local wind compounds on the issue. This is also displayed in the difference between local and regional resources in general. At the higher renewable penetration levels, regional resources show lower cost increases compared to the local resources.

7.2.1.2.5. Conclusions – GT Trips Allowed

In this analysis, five renewable resource spanning scenarios for the UCI campus were examined. The effects of increasing the community renewable penetration level while utilizing different resources of different quality, as well as a case which maximized the use of local resources. These effects were examined in terms of renewable performance, the effect of reaching different renewable penetration levels on the behavior of on-campus generation (gas turbine, HRSG, steam turbine), and the effects on the characteristics of the import power signal. The conclusions of this study are as follows:

- **The benefits of the high quality and profile characteristics of regional renewable resources outweigh the disadvantages of transmission losses from an energy standpoint.** The regional wind and solar resources outperformed their local counterparts in many of the metrics examined. These resources required much lower installed capacities to reach a given renewable penetration level and generate a lower amount of excess power, have similar or better impacts on the behavior of the on-campus generation resources, and allow for more flexibility for mitigating import/export interconnection issues. The use of local resources allow the attainment of similar renewable penetration levels, but require much higher capacities and have stronger impacts.
- **Regardless of resource type, the attainment of higher community renewable penetration levels has mostly similar effects on the behavior of on-campus generation resources.** All cases displayed a similar decrease in gas turbine capacity factor, HRSG heating demand contribution, steam turbine capacity factor, and fuel use as well as increases in gas turbine downtime. The exception to this is the fact that the wind

resources caused the lowest amount of gas turbine start up events due to their profile characteristics.

- **If supporting systems/technologies are not implemented in parallel, the capabilities of on-site electric generation resources must be increased to have the following characteristics:**
    - **Be capable of operating efficiently and cleanly at part load and have a large operating power band.** The introduction of high renewable power capacities will cause on-campus generation to often operate at various levels of turndown. Much of the gas-turbine downtime exhibited in these cases was due to the fact that the unit used on the UCI campus cannot operate below 8 MW. Since intermittent renewable resources tend to be peak dominated, with profiles exhibiting short duration, high power periods, attaining high renewable penetration levels will require high nameplate renewable capacities that will cause the balance to drop to very low (even zero or negative) levels. If an on-site generating technology was capable of operating at severe part load turndown, it would prevent excessive start and shut-down events.
    - **Be capable of load-following in a strongly dynamic manner.** The variable nature of intermittent renewable power will cause the balance to become very dynamic, and on-site generation must be able to keep up with such variation or be installed with additional systems that allow it to do so or decrease the dynamics of the balance.
    - **Be capable of starting up without excessive criteria pollutant emissions**. The high capacity of renewable resources at higher renewable penetration levels will often cause the balance to become zero or negative, in which case the on-site generation will be required to shut off unless an unlimited export margin was allowed. This can happen frequently during the course of a year, especially at high renewable penetration levels, and the number of start events can well exceed the 13-event limit placed on the campus gas turbine due to emissions constraints. Therefore, an on-site generator must become capable of starting up without emitting large amounts of criteria pollutants.
- **The presence of a minimum import requirement for interconnection to the utility grid is a severe limiting factor to the attainment of high renewable penetration levels in a community.** All resource types considered eventually caused a violation of the minimum import requirement at reasonably desirable renewable penetration levels. Additionally, the high power, short-duration nature of intermittent renewable resources indicates that in order to obtain a large amount of energy from such sources, the high peak generation must be accommodated. On the other hand, allowing full export of this power can cause issues for the transmission system operator. Methods for interfacing exported power with the transmission system operator need to be developed to minimize power curtailment.

- **It is difficult for a community to obtain high renewable penetration levels without strong interconnections with the utility grid/other communities and the presence of complementary technologies.** Overall, the small scale of a community renders it difficult for all of the energy management operations to be internal and adequate for accommodating large renewable power capacities. Exports and imports, as well as the use of regional resources allow communities to have an option for mitigating a problem that they may not be fully equipped to manage. The presence of complementary technologies such as energy storage is expected to aid in this manner, and the extent to which such technologies do so will be examined in a following analysis.

Overall, a number of challenges have been identified in the context of attempting to attain high renewable penetration levels at the community scale, and it is clear that additional steps need to be taken for a community to reach such renewable penetration levels. An analysis of some of the options available to a community for aiding in taking such steps need to be, and will be, examined in a following analysis.

7.2.1.3. Technical Analysis – GT Trips Not Allowed

7.2.1.3.1. Energy Analysis and Renewable Performance

7.2.1.3.1.1. Required Renewable Capacity vs. Renewable Penetration Level

The progression of renewable capacity with renewable penetration level is displayed in Figure 296:

Figure 296: Renewable Capacity vs. Renewable Penetration Level

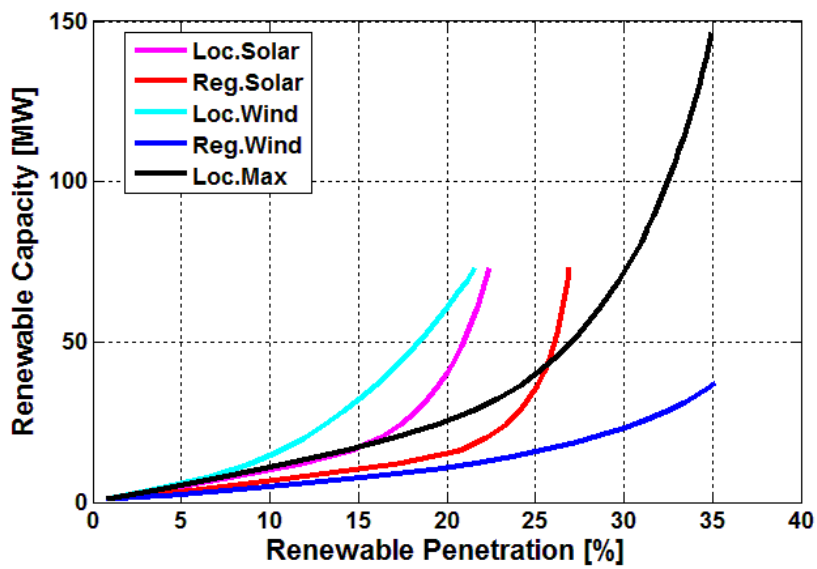

The required renewable capacity generally follows the same trends as that of the case with gas turbine trips allowed. A linear trend is displayed at low levels, transitioning to an exponential increase due to surplus renewable generation. Overall, however, the renewable penetration levels that are attained before the onset of exponential behavior are significantly lower. The gas

turbine remaining online introduces an uninterruptible base load that limits the ability of the system to utilize renewable power, since renewable power must be curtailed at a higher load level. Compared to the case with the gas turbine tripping offline, the achieved renewable penetration level is decreased by 10% and 20% for local and regional wind respectively, 19% and 23% for local and regional solar respectively, and 28% for the local resource maximum case.

Additionally, the relative renewable penetration levels achieved by each of the different technologies have changed. The use of regional wind power is able to achieve significantly higher renewable penetration levels relative to the other technologies compared to the case where gas turbine trips were allowed. The use of local wind, while not achieving higher penetration levels for a given capacity with the capacity levels used, appears to be on track to surpass local solar power. This occurs since wind power is able to contribute to serving the load outside of the daytime hours, a characteristic that is much more valuable with a high base load. Since regional wind power is the least peak-dominated, it is able to contribute much more to the load than any of the other technologies.

7.2.1.3.1.2. Surplus Renewable Fraction

The progression of the surplus renewable fraction with renewable penetration level is presented in Figure 297:

Figure 297: Curtailed Energy vs. Renewable Penetration Level

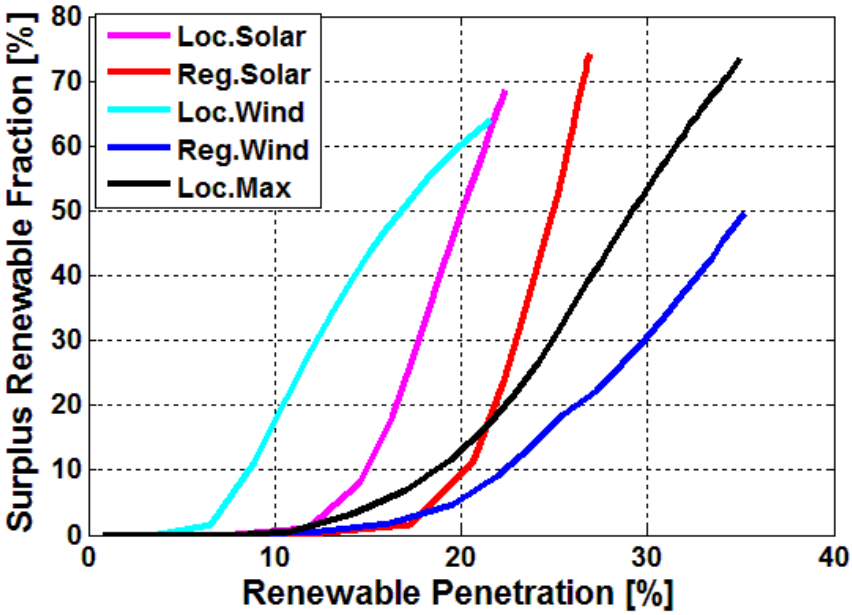

The behavior of the surplus renewable fraction for each resource tends to parallel that of the required renewable capacity, and with the exceptions noted in the previous discussion, generally follow similar trends to that of the case with gas turbine trips allowed. The onset of curtailment occurs at much lower renewable penetration levels, as low as 5% for local wind. The levels of curtailment are also significantly higher compared to the case where the gas turbine is allowed to trip offline. Whereas in the former case, the highest level of curtailment was about 53%, in this case the lowest level of curtailment exhibited by any of the resources is 50% for

regional wind. Solar power in particular reaches very high levels of curtailment since it is very peak-dominated and cannot serve the load outside of the daytime hours. For regional solar, approximately 74% of the energy produced is not used to serve the load. This trend is expected due to the presence of a higher uninterruptible base load level, and is the cause behind the lower renewable penetration levels achieved in this case.

7.2.1.3.2. Behavior of the On-Site Generation

As described previously, the introduction of renewable power can affect the behavior technologies in the central plant. With the gas turbine not allowed to trip off, however, the behavior of certain central plant technologies becomes more resilient to disruption by renewable power. The behavior of the on-site generation with the introduction of renewables is described here. It is important to note, however, that the behavior of the chillers does not change by allowing the gas turbine to stay online, since the chillers will still attempt to mitigate potential gas turbine trips to prevent the curtailment of gas turbine power. Additionally, gas turbine starts and downtime are no longer relevant metrics for this case.

7.2.1.3.2.1. Gas Turbine Capacity Factor

The progression of the gas turbine capacity factor with renewable penetration level is displayed in Figure 298:

Figure 298: GT Capacity Factor vs. Renewable Penetration Level

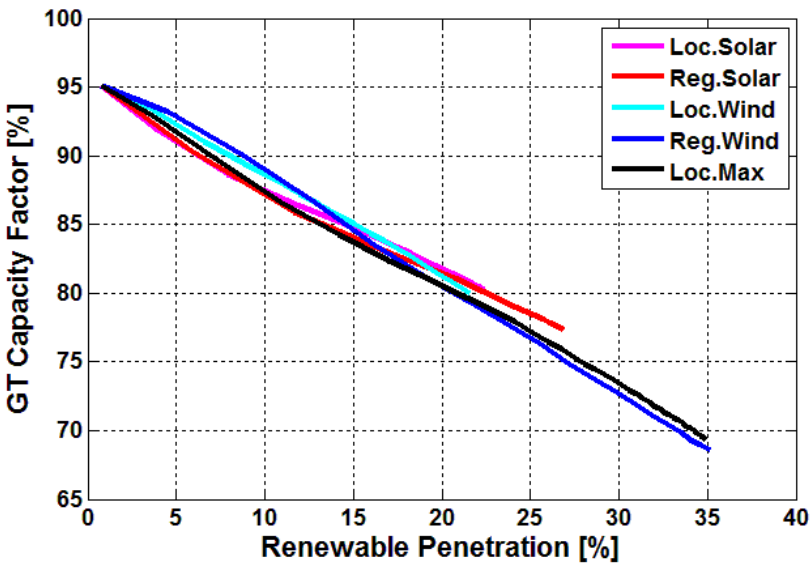

The decrease in gas turbine capacity factor is somewhat similar for all technologies considered and follows essentially a linear trend with renewable penetration level. This occurs since decreases in gas turbine capacity factor come from reduced power output only, and every turndown in gas turbine power corresponds to an equal increase in renewable power utilization. The main differences between technologies are due to the different times of the day that these technologies cause the gas turbine to turn down and the effect of the chillers. For example, solar power affects the load demand strictly during the daytime. The original load demand is typically at its highest during this time, however due to the effect of the chillers, the cooling load is moved to the nighttime hours, decreasing the daytime load. Therefore, at low penetration levels, solar can cause the balance during the daytime to become low enough to cause the gas turbine to turn down. Wind power on the other hand occurs primarily during the nighttime when the cooling load is placed, allowing the gas turbine power to remain relatively

high during the nighttime hours but not affecting it during the daytime. At penetration levels up to about 17%, this allows wind resources to maintain a higher gas turbine capacity factor.

Above 17% penetration, however, solar resources start to allow higher gas turbine capacity factors. This occurs because at this point, the renewable capacities are so large that any occurrence of renewable power drives the gas turbine towards its minimum power level. Since solar resources can only cause this to happen during the daytime hours, the gas turbine is still able to operate above minimum power during the nighttime hours and retain a higher capacity factor. Wind resources affect the load at all times during the day, especially regional wind, and cause the gas turbine to operate at minimum power more often than solar. The local resource maximum case, which can also affect the load at any point during the day, shows a similar trend.

Additionally, with the gas turbine forced to remain online, the gas turbine capacity factor levels remain at higher levels compared to the previous case even for similar renewable penetration levels. For example, at 30% penetration, the gas turbine capacity factor was between 50-56% in the previous case, compared to 72% in this case.

7.2.1.3.2.2. HRSG Contribution to the Heating Demand

As described prior, the exhaust stream from the gas turbine is used in an HRSG to provide almost all of the energy required to meet the heating demand. Turndown in the gas turbine may decrease the contribution of the HRSG towards providing energy to meet the heating demand. Since the gas turbine is not allowed to trip offline in this case, however, the ability of the HRSG to contribute to the heating demand is expected to be higher. The progression of the HRSG contribution to the heating demand with renewable penetration level is presented in Figure 299:

Figure 299: HRSG Contribution to Heating Demand vs. Renewable Penetration

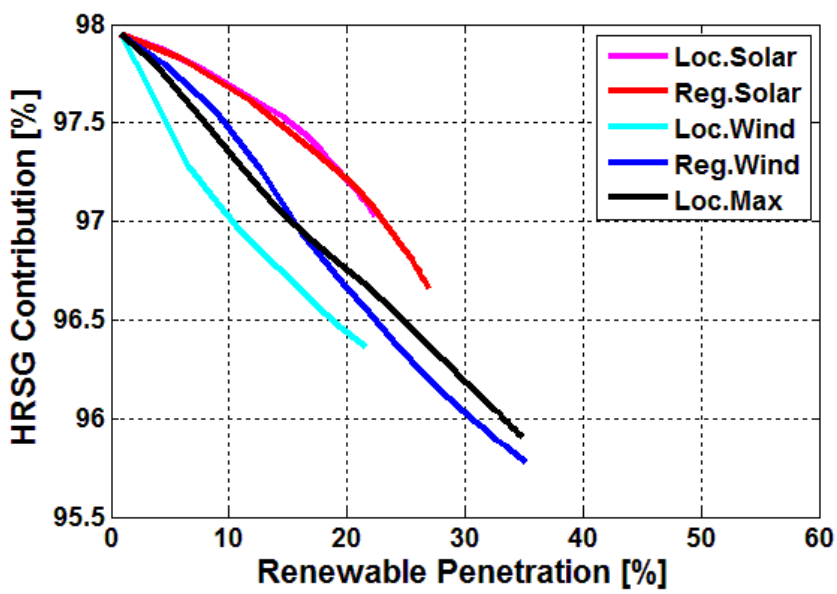

As the renewable penetration level increases, the contribution of the HRSG towards meeting the heating demand decreases only by a very small amount, from about 98% at current to 95.8% at

the 35% penetration level for regional wind and local resource maximization. This is in contrast to the case where the gas turbine is allowed to trip off, where the HRSG contribution decreased significantly. While there is less steam available in total, there is still enough to meet the heating demand. Additionally, at part load, the gas turbine exhibits decreased efficiency. While at part load the total input energy is decreased, this also indicates that more of the input energy is released as heat in the exhaust stream, slightly buffering the decrease in total available energy.

Comparing this result with the case where the gas turbine was allowed to trip offline, it is implied that disruptions to meeting the heating demand are primarily due to gas turbine shutdowns more so than gas turbine turndown.

7.2.1.3.2.3. Steam Turbine Capacity Factor

The previous result showed that with the gas turbine not allowed to trip offline, there was still sufficient steam left to meet the heating demand. Since the steam turbine only receives steam that is leftover after the heating demand is met, the gas turbine turndown may not leave enough steam to utilize the steam turbine. The progression of the steam turbine capacity factor with renewable penetration level is presented in Figure 300:

Figure 300: ST Capacity Factor vs. Renewable Penetration Level

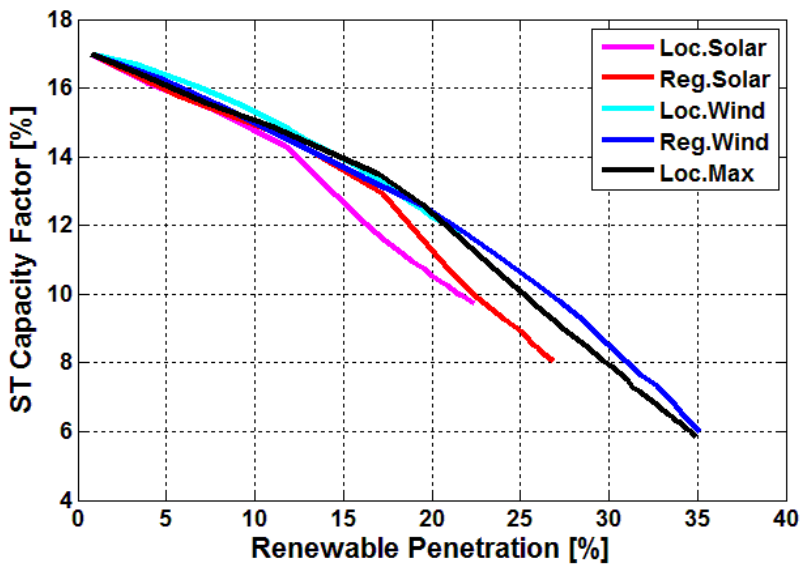

The steam turbine capacity factor decreases with renewable penetration level as less steam becomes available for use due to turndown of the gas turbine to accommodate renewables. All of the technologies show similar decrease up to the 12% level, where solar technologies show larger decreases in steam turbine capacity factor. This behavior overall mimics the trends displayed in the case where the gas turbine was allowed to trip offline.

Solar resources cause the gas turbine to turn down during the daytime when the campus heating demand is at its highest, therefore leaving even less steam available for the steam turbine. This decrease is not as significant at low solar capacities but becomes more significant at higher solar capacities. Although solar resources show higher gas turbine capacity factors at

high penetration levels, this doesn't necessarily reflect in higher steam turbine capacity factors. This trend occurs since the higher gas turbine capacity factors for solar power are due to allowing the gas turbine to operate above minimum power during the nighttime. While the heating demand is low during the nighttime hours, theoretically leaving more steam to be used in the steam turbine, the load is also low during these hours, and the steam turbine cannot be used if it will cause an import violation. This is especially true since at high solar penetration levels, the cooling demand is placed during the daytime to attempt to mitigate potential gas turbine trips. Therefore, the steam turbine is unable to use the extra steam leftover in the nighttime hours in the solar cases.

The steam turbine capacity factors in this scenario are of similar levels to the scenario where the gas turbine was allowed to trip offline for a given renewable penetration level. This may be unexpected, since with the gas turbine remaining online, more steam should be available to use even at high renewable penetrations. However, since the steam turbine cannot be activated if it will cause or worsen an import violation, the steam turbine is still limited to low capacity factors. Overall, the steam turbine remains an underutilized piece of equipment.

7.2.1.3.3. Behavior of the Import Power Signal

As described previously, the UCI campus is similar to most communities in that it is partly dependent on the utility grid to meet a part of its load. The previous scenario showed that with increased renewables, it may become difficult for a community to maintain a minimum import level at all times and that this requirement may be a limiting factor for the penetration of renewable power into a community such as UCI. With the presence of an uninterruptible base load as in this case, this issue is expected to be exacerbated. The behavior of the import signal for the different technologies is displayed here. A negative import value in this case refers to power being curtailed or exported if possible.

The import power distribution for the local solar and regional solar spanning cases is displayed in Figure 301 and Figure 302 respectively:

Figure 301: Import Power Distribution: Local Solar Case

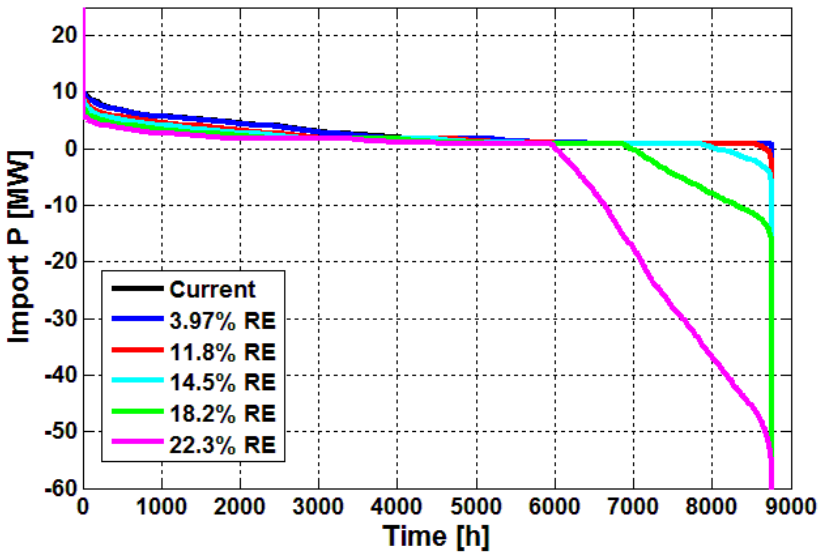

Figure 302: Import Power Distribution: Regional Solar Case

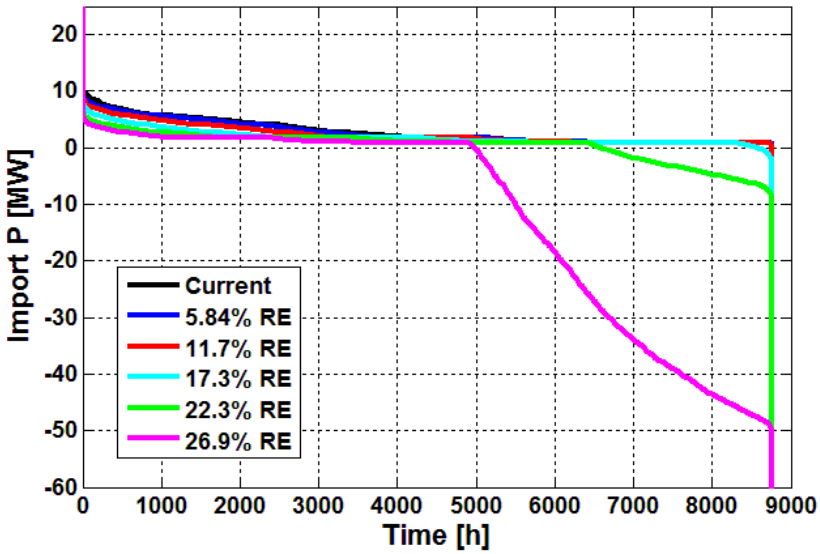

Qualitatively, the distribution of the import signal is similar to the trends displayed in the scenario where the gas turbine was allowed to trip offline. As the penetration level of solar power is increased, the import signal starts to become negative for more and more hours, signifying the need for export or curtailment. Local and regional solar cases show about 2800 and 2300 export hours respectively at the 22% penetration level, with a maximum export of 14 MW and 8 MW respectively. The regional solar case exhibits lower import hours and maximum

import levels compared to the local solar case, primarily due to the higher resource quality and broader time duration of power output compared to the local case.

There are a few differences compared to the scenario where the gas turbine was allowed to trip offline. First, the maximum import levels are not as high. Since the gas turbine is not allowed to trip offline, the import power never rises to encompass the entirety of the load demand at any time. While this prevents excessive demand charges for the campus, it comes at the cost of lower renewable penetration levels being achieved and high levels of curtailment. Second, the number of export hours and maximum export levels are higher than the previous scenario at significantly lower renewable penetration levels. With an uninterruptible base load, curtailment occurs at a higher load level and is exacerbated as shown through the other metrics. Notice for the regional solar case, to increase the renewable penetration level from 22.3% to 26.9%, the number of export hours increases to about 3800 from 2300 and the maximum export power increases to 49 MW from 8 MW, showcasing the diminishing returns with increased solar capacity.

The import power distribution for the local wind and regional wind spanning cases are displayed in Figure 303 and Figure 304 respectively:

Figure 303: Import Power Distribution: Local Wind Case

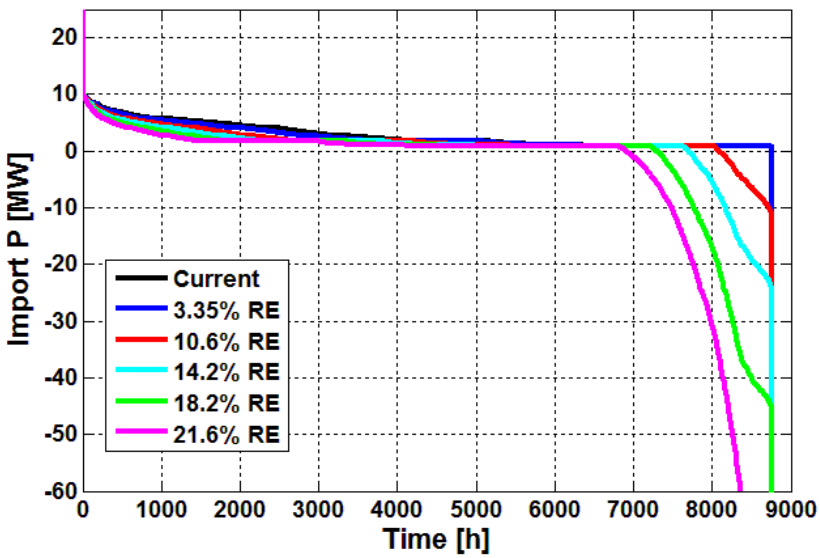

Figure 304: Import Power Distribution: Regional Wind Case

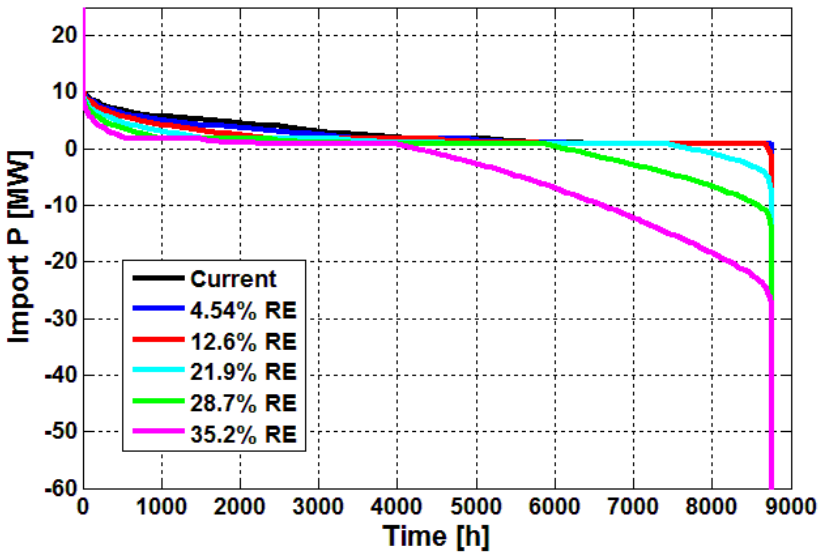

Qualitatively, the overall trends displayed by the wind cases are similar to that displayed in the scenario where the gas turbine was allowed to trip offline. The key differences between this scenario and the former are also similar to that displayed by the solar cases: increased export hours and maximum export power levels at lower renewable penetration levels. The regional wind case shows lower export hours and maximum export power levels than the local wind case for a given renewable penetration level. For example, at the 21% penetration level, the regional and local wind cases show 1200 and 1900 export hours respectively, and maximum export power levels of 26 MW and 70 MW respectively. By the 35.2% penetration level for regional wind, more than half of the hours of the year are export hours.

The import power distribution for the local resource maximization case is displayed in Figure 305:

Figure 305: Import Power Distribution: Local Resource Maximization Case

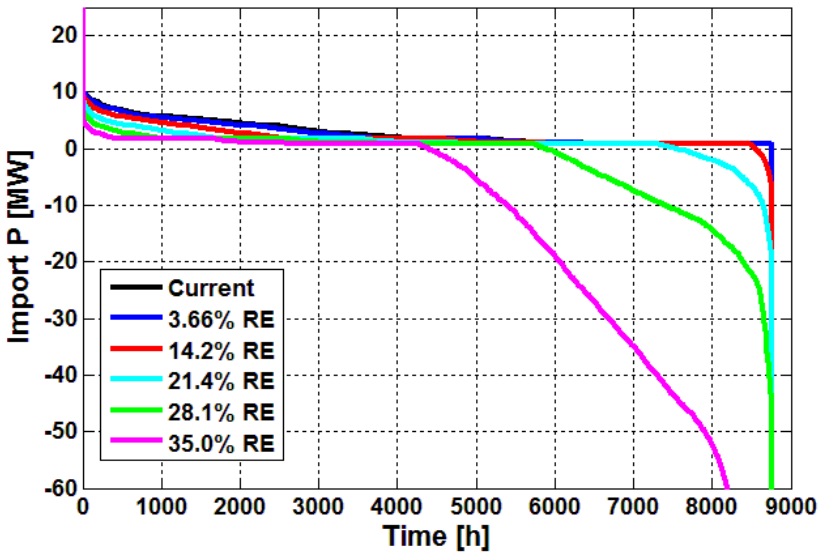

The local resource maximization case shows a combination of the local wind and local solar spanning case properties. The trends are similar to that displayed in the scenario where the gas turbine could trip offline. For a given renewable penetration level, the export hours tend to be higher than that of the local solar case but lower than that of the local wind case, and a lower maximum export power than both cases. For example, at about a 21% renewable penetration level, the local resource maximization case shows about 1400 export hours and a maximum export power of 19 MW. The lower maximum export power is due to the ability of the local resource maximization case to more evenly affect the load during both the daytime and nighttime hours. With utilization of local resources, however, the achievable renewable penetration level only just matched that of the regional wind case, albeit with significantly higher capacities and maximum export hours.

Another important characteristic of the UCI campus is the maximum import power, which sets the demand charge for the campus. A plot of the maximum import power as a function of renewable penetration level is displayed in Figure 306:

Figure 306: Maximum Import Power vs. Renewable Penetration

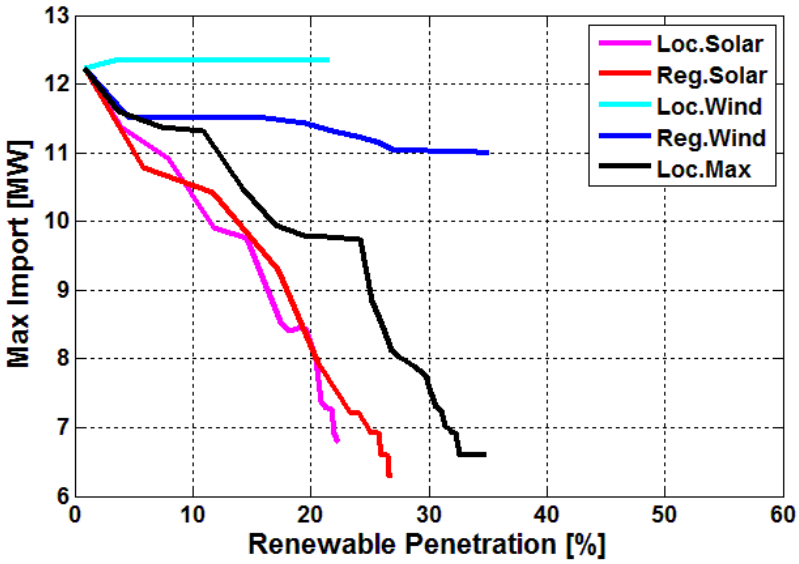

In contrast to the scenario where the gas turbine was allowed to trip offline, the maximum import power decreases with renewable penetration level for all cases with the exception of local wind. The maximum import power levels are also much lower than the former scenario as a direct cause of the gas turbine not being allowed to trip offline. In this case, the import power can never be increased to meet the entirety of the load due to the gas turbine remaining online.

The solar resources show the largest decreases in maximum import power. This is in contrast to results for the California model, which shows a limited extent to which solar power decreases the maximum import power. This difference is primarily due to the effect of the chiller and thermal energy storage system. The TES system prefers to place the cooling load during the nighttime hours unless potential gas turbine trips occur in the daytime. Additionally, when a potential gas turbine trip does occur, the chillers will only introduce enough cooling load at that point to mitigate the trip. At low renewable penetration levels, the capacity of solar power is not enough to cause a trip. Therefore, the balance is allowed to decrease during the daytime, reducing the maximum import since the chillers will place the cooling load entirely during the nighttime hours. At higher renewable penetration levels, the capacity of solar cause gas turbine trips during the daytime and the time of peak import to be shifted to the nighttime. The chillers then place the cooling load during the daytime to attempt to mitigate it, however, they are typically unsuccessful due to the high capacity of solar power. This has the effect of removing load during the nighttime hours to decrease the import power at that time but being unable to increase it during the daytime hours, continuing to decrease the maximum annual import power.

Wind resources on the other hand peak during the nighttime hours when the chillers prefer to operate. Additionally, the times when wind power will cause the gas turbine to trip will mostly be during the nighttime hours. Therefore, the cooling load is almost always placed during the

nighttime hours and the maximum import occurs during the daytime where it remains unaffected with increasing wind penetration.

7.2.1.3.4. Behavior of the Cost of Electricity

The behavior of the change in the levelized cost of electricity compared to current levels with renewable penetration level for the different renewable technologies is presented in Figure 307:

Figure 307: Change in Levelized Cost of Electricity vs. Renewable Penetration Level

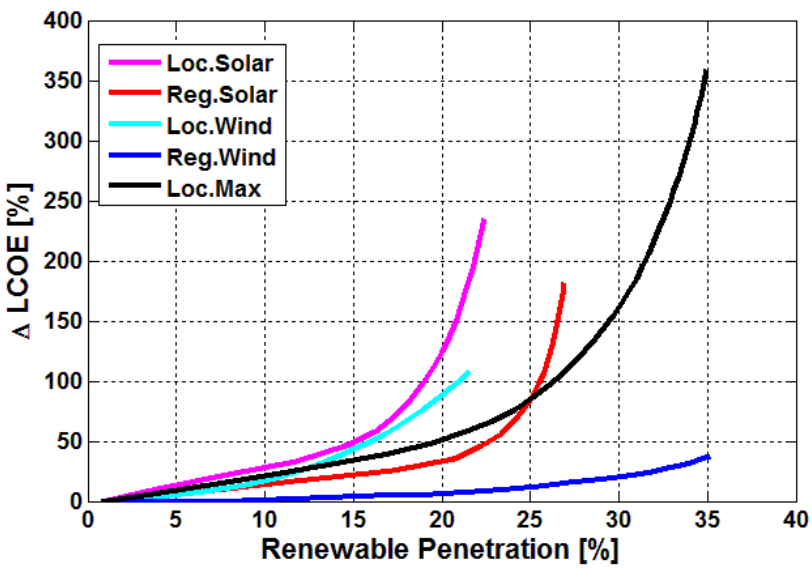

The trends exhibited by the levelized cost of electricity with renewable penetration level in the case without allowing gas turbine trips are essentially the same as that exhibited by the case with allowing gas turbine trips. This behavior occurs due to the same driving factors. The only primary difference between this case and the previous case is that the point at which exponential increases start to occur due to renewable curtailment is shifted towards much lower renewable penetration levels. This is consistent with the effects exhibited in the other metrics discussed for this case.

7.2.1.3.5. Conclusions – GT Trips Not Allowed

In this analysis, five renewable resource spanning scenarios for the UCI campus were re-examined with the condition that the gas turbine was not allowed to trip offline. In general, the qualitative effects of introducing renewables into the UCI campus were similar to the previous scenario where the gas turbine was allowed to trip offline. This case allowed some additional insight to be gained regarding the effect of installing high capacities of renewable power within a community such as the UCI campus. These insights are summarized here.

- **The presence of an uninterruptible base load severely limits the attainable renewable penetration level for a given installed renewable capacity.** Compared to the previous scenario, the attainable renewable penetration levels were decreased by an average of 20% for the same installed capacity. This emphasizes the need for generator flexibility in

terms of part load, cycling, and start-up performance to allow the attainment of high renewable penetration levels.

- **Maintaining the minimum operation of on-campus electric generation prevents disruption of combined heat and power resources at the cost of high levels of curtailment.** In the previous scenario, the erratic behavior of the gas turbine disrupted the ability of the HRSG to meet the heating demand, and boilers had to be increasingly relied upon. With the gas turbine allowed to stay online even at minimum power, the HRSG was able to meet the vast majority of the heating demand and high utilization of the CHP system remained. This utilization comes at the cost of curtailing large amounts of renewable power to reach the same penetration levels.
- **The presence of an uninterruptible base load significantly increases the cost of electricity at a given renewable penetration level.** In this case, the savings from allowing the gas turbine to remain online and inflexible do not outweigh the costs of curtailment when attaining high renewable penetration levels. This occurs because forcing the gas turbine to remain online renders it more difficult to reach a given renewable penetration level by requiring significantly increased renewable capacities to compensate for curtailment, increasing costs.

Overall, this scenario highlights the need for changes in balancing generator performance and operating scheme from current standards to accommodate renewable power. The extent to which improvements are necessary are a subject of future research and are also dependent on the technical and financial ability of complementary technologies to shape the load profile. The effectiveness of these options is discussed in later sections.

Task 7.2.2. California Results

Several different analyses are performed using the HiGRID model. 1) Similar to the analysis done for the UCI community model each renewable resource is spanned. 2) The solar thermal trough power plant model is run to explore the behavior of a solar thermal power plant on the grid. 3) Balance fleet installed capacity is compared for different scenarios to determine if renewables can replace balance fleet generation. Lastly, 4) effects of enhancing the flexibility of balance generation are explored.

7.2.2.1. Spanning Results

There is a significant technical potential of renewable capacity that could be installed in California. Based on a 2011 report released by the CEC there is over 18,000 GW of potential capacity in the state (CEC-150-2011-002, 2011). A breakdown of the capacity by resource type is presented in Table 71.

Table 71: Available Renewable Capacity in California

Renewable Resource	Installed Capacity (2010)	Potential (MW)

Concentrating Solar Power	1,356	1,061,362
Photovoltaic		17,000,000
On-shore Wind	2,819	34,000
Off-shore Wind	0	75,400
Wave and Tidal	demonstrations	32,763
Biomass	1,077	3,820
Small Hydro	1,380	2,158
Geothermal	2,600	4,825
Total	9,232	18,214,328

Source: CEC-150-2011-002

The single largest contributor is solar PV followed by concentrating solar power. All other resources have at least an order of magnitude less capacity available than solar. Also, biomass, small hydro and geothermal are nearing their capacity limits. It is for this reason that the following sections focus on the impacts of installing solar and wind technologies on California's grid.

7.2.2.1.1. Description of Cases

The California HiGRID model results include spanning for local and regional wind, local and regional solar (both 1- and 2-axis tracking), and a mixed case comprised of 50% installed capacity (i.e., MW) of regional wind and 50% of 1-axis tracking PV.

Each spanning scenario begins with no wind or solar generation. The hydro power profile is held constant based on the base case in 2005. The only renewables installed are the geothermal, small hydro and biomass supporting California's demand according to 2005 capacities. Initially each scenario has 8.95% renewable penetration and 0 MW of wind or solar and steadily increases to 300,000 MW.

Renewable generation profiles for each technology are shown below as a daily average throughout the year (Figure 308). Notice the diurnal cycle characterized by an afternoon peak of solar and the more flat profile from wind. Solar technologies with tracking are better able to make use of the incident radiation so their profiles begin before the fixed solar and typically extend to after the fixed solar. Local and regional wind profiles are more constant and typically have higher nighttime generation than daytime. The wind and solar mixture exhibits characteristics of both profiles as expected. While the daily average shows information about typical behavior the generation varies from hour to hour and season to season.

Figure 308: Daily Average Renewable Generation Profiles for 5GW of Installed Renewable Capacity

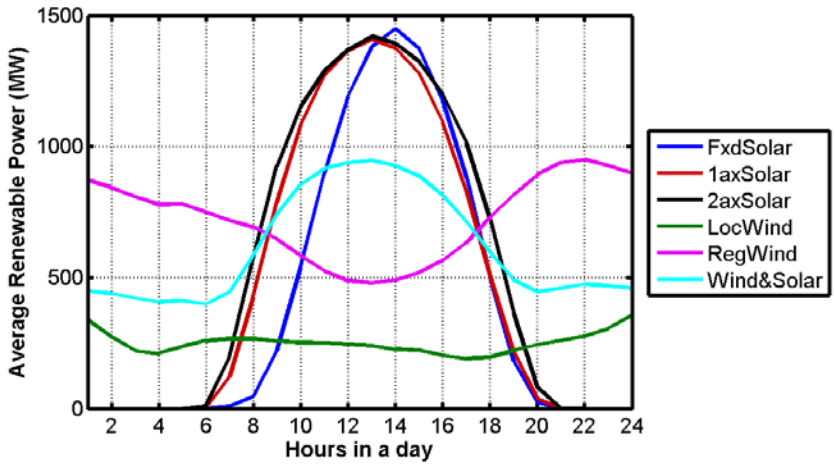

Figure 309 depicts the daily average for each season of the year. Solar profiles are greatest in the spring and summer, while wind profiles are greatest in the winter and spring.

Figure 309: Daily Average Renewable Generation Profiles by Season for 5GW of Installed Renewable Capacity

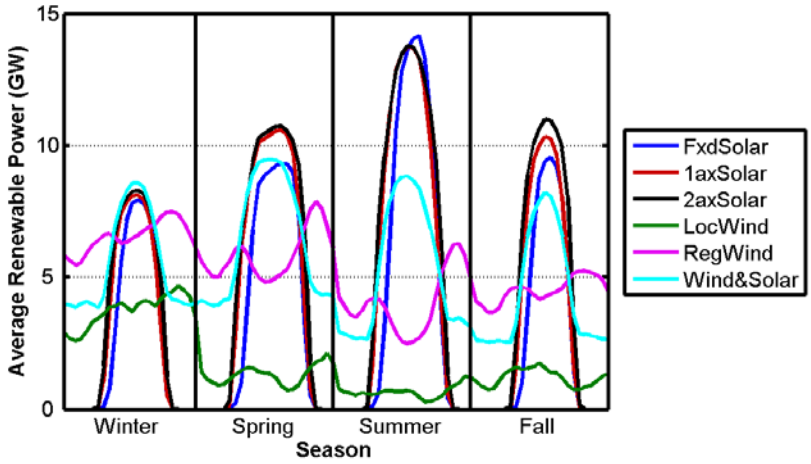

Load duration curves are presented in Figure 310 to show the distribution of generation points for each type of generation. Notice that wind generation is more distributed throughout the entire year, while solar generation only contributes around 4500 hours of generation due to the diurnal cycle.

Figure 310: Load Duration Curves for 5GW of Installed Renewable Capacity

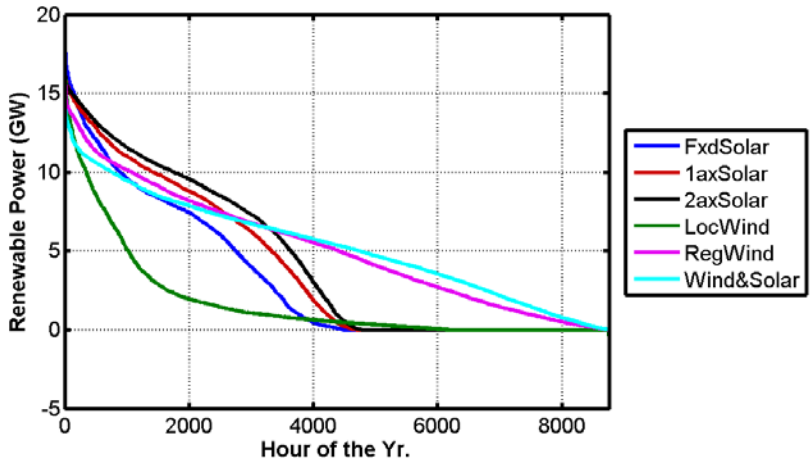

Each resource affects the load shape differently. Figure 311 shows the average load profile less the renewable portion. Notice that the shape for wind reduces nearly evenly across each hour. The solar generation, due to the concentration of generation during the afternoon hours a peak forms in the morning and in the late afternoon. The afternoon peak at 9PM does not receive any contribution from solar power. The formation of a "double peak" for solar presents interesting challenges, as will be discussed, and means that conventional thinking that the peak occurs in the afternoon and the minimum load point occurs in the night could be changed with enough solar power. Similarly, the time-of-use timeframes (e.g., on-peak, mid-peak, off-peak) would need to be adjusted to accommodate high renewable penetrations.

Figure 311: Load Less Renewable Generation for 22GW of Installed Renewable Capacity

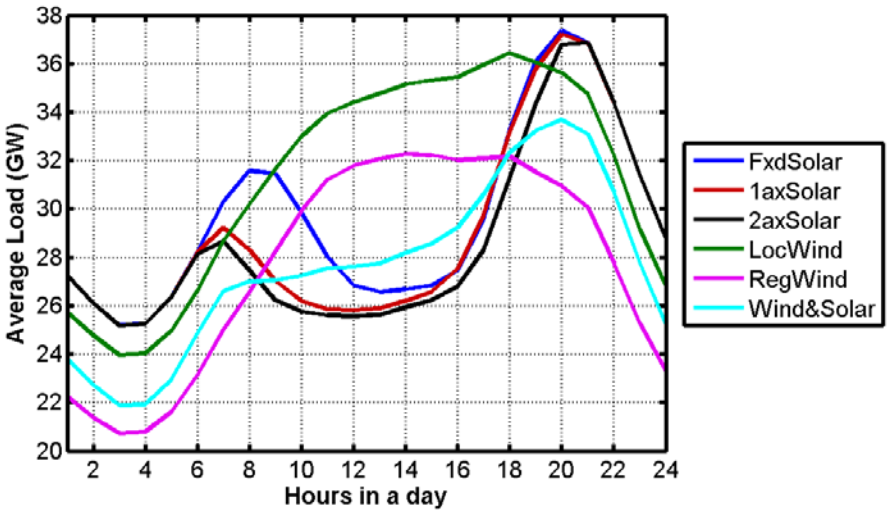

While the previous four figures present information on the renewable generation and load shape, the following section will show how the renewables interact with the grid.

Renewables affect the resulting load signal in unique ways. Solar power is concentrated in the afternoon of the summer and fall and does not provide any generation during the evening and early morning. Wind power is more even throughout the day with a slight focus in the nighttime hours of winter and spring.

- With sufficient solar power capacity the load shape can be shifted to form a "double peak," one in the morning and one in the early evening.
- Changes in the resulting load shape from renewables must be considered when developing time-of-use or real-time rate structures to support grid operation and incentivize greater uptake of renewables.

7.2.2.1.2. Operation Results

Figure 312 shows how the installed renewable capacity affects the renewable penetration for each technology and two different resource mixes since the resource mix has changed substantially since 2005. The major difference is that the 2005 resource mix includes a more substantial baseload component while the 2011 resource mix only has 2.2GW nuclear and 3.3 GW coal which is much lower than the 2005 case. This allows the reader to understand the the results in the context of changing resource mixes and inform their understanding for the rest of the figures in this report that consider the 2005 resource mix. Section 7.2.2.4 examines the effect of baseload resources in more detail.

Figure 312: Renewable Penetration versus Installed Capacity for Generation Technologies

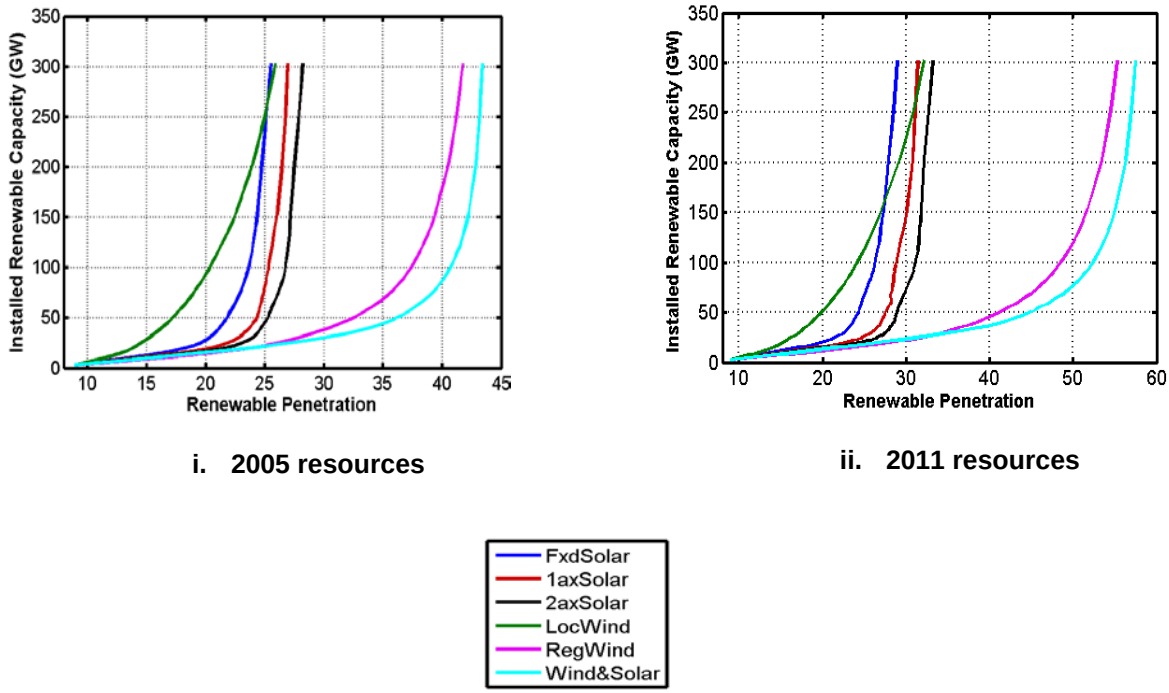

i. 2005 resources **ii. 2011 resources**

The curves are characterized by two regions. The first portion of each curve has a relatively low slope and represents a region of steadily increasing renewable penetration for installed renewable capacity. The second region exhibits a sharp increase in slope and represents a significant increase in capacity for a marginal gain in penetration. The location where the slope increases is based on when the available capacity of all other generation is reduced to the lowest possible value. No reduction is made to baseload generation, and complementary technologies (i.e., demand response, energy storage or electric transportation) are not included and hydroelectric, for this analysis, is non-dispatchable, which means that load-following, and peaking are the only remaining dispatchable resources. The 2011 resource mix shows a capability for higher renewable penetration for a given installed renewable capacity due to the removal of baseload resources (see Section 7.2.2.4 for more information on the effect of baseload).

As an example of how the load-following and peaking must change Figure 313 contains area charts for the generation buildup of renewable, peaker, load-following, hydro, geothermal and baseload generation. The black line represents the initial demand and the red section above the line represents generation that must be curtailed or transmitted to someone that can use it. Three renewable penetrations are presented including 8.9%, 20.4% and 26.9%. Notice that the baseload, geothermal and hydroelectric stay nearly the same for each run. The only differences result from the baseload model changing the monthly capacity factor as the load changes. Renewables replace load-following generation and occasionally cause an increase in the peaker generation requirement to meet ramping demands. Once for the 20.4% case and several times in the 26.9% case excess renewable generation is experienced. Load-following generation at

these times is the minimum amount that is possible while still providing enough capacity to meet spinning reserve and regulation requirements.

Figure 313: Generation Breakdown with All Regional Wind

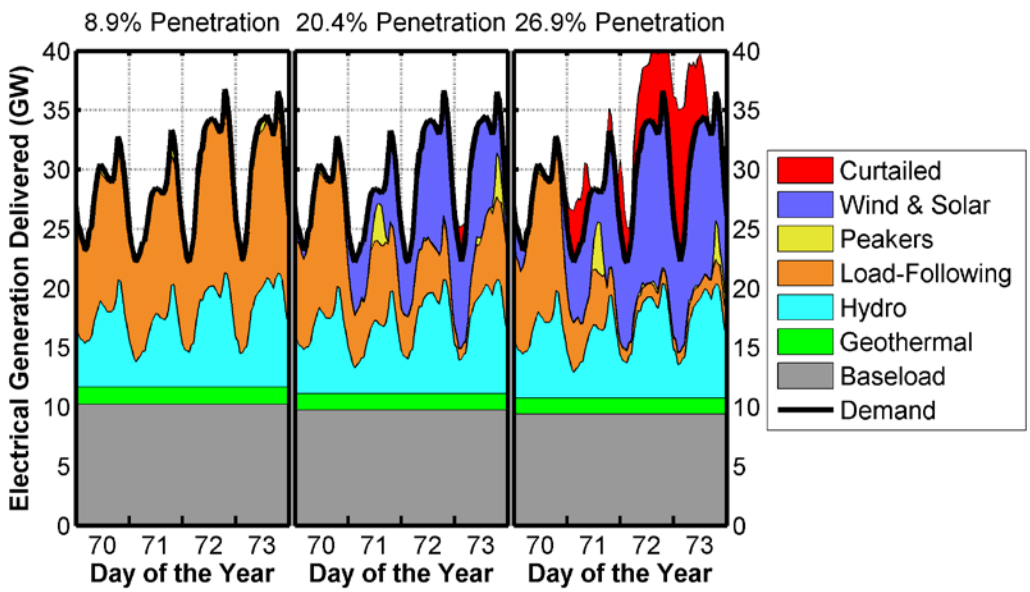

Similar to installed capacity, capacity factor provides an indication of how effectively the renewable resources are integrating into the system. Capacity factors are calculated using (123) where "t" is the timeframe of the analysis, in this case one year (i.e., 8760 hours).

$$\text{Capacity Factor} = \frac{\sum \text{Demand}(t)}{\text{Installed Capacity} \cdot \max(t)} \tag{93}$$

Wind has the highest system-wide capacity factor until around 22% where the 50/50 mixture of wind and solar becomes the highest capacity factor technology as shown in Figure 314. Combining the wind and solar allows for delayed onset of curtailment and almost always performs better than the best of either technology.

Figure 314: System-wide Capacity Factors for each Technology

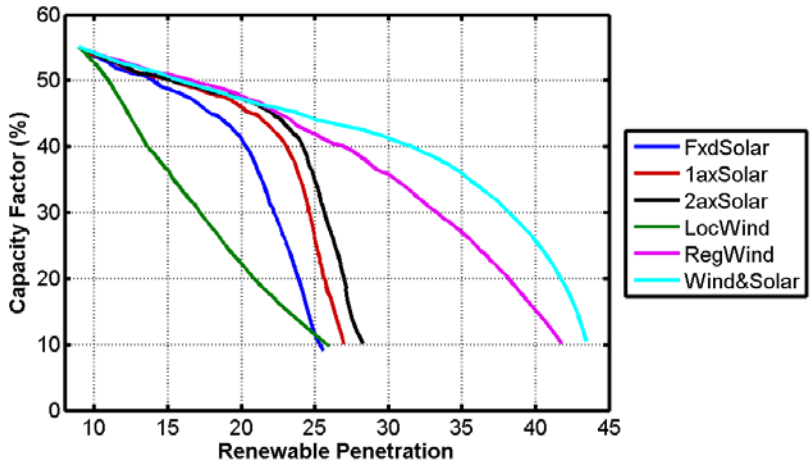

Installing renewables will reduce the fuel consumed to generate the electricity demand. The heat rate will fall because lower efficiency peakers and load-followers are removed with increasing renewable penetration leaving only renewables, which don't take any fuel and baseload technologies as evidenced by Figure 315.

Figure 315: System-wide Heat Rate for Generation Technologies

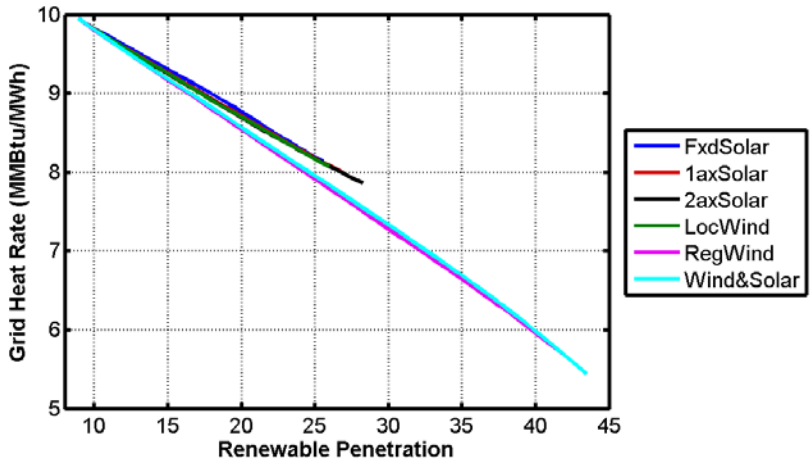

The maximum penetration is limited by the coincidence of each signal to the demand signal. Different generation technologies have different generation profiles as was demonstrated in Figure 309. Figure 316 shows the amount of curtailment resulting from each renewable technology rollout. As the renewable penetration increases for each technology the curtailment monotonically increases. The amount of curtailment and the penetration at which it reaches that point is a function of the coincidence of the demand signal to each renewable generation signal. Those that better coincide with the demand and are less likely to violate other system constraints have less curtailment at the same renewable penetration as other technologies.

Figure 316: Renewable Penetration versus Curtailment for each Technology

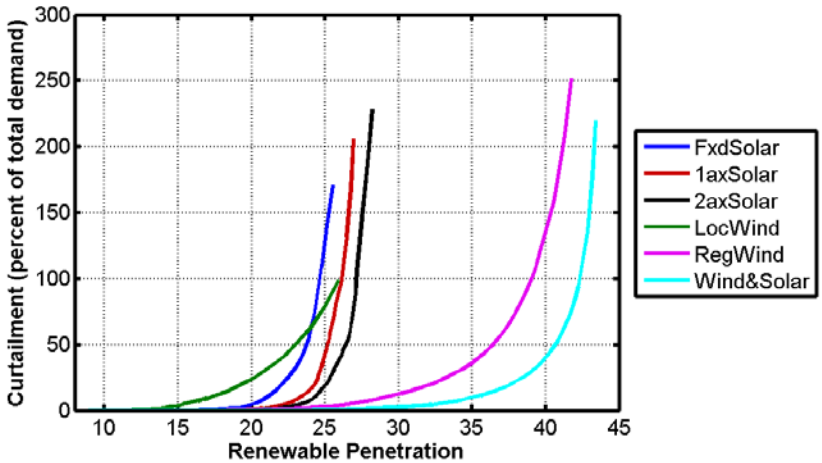

As renewables displace load-followers the efficiency of each generator falls because it must be operated at lower load points and more dynamically to accommodate the increased dynamics from additional intermittent renewables. Changes in load-following fleet efficiency are presented in Figure 317.

Figure 317: Load-Following Efficiency Comparison for Generation Technologies

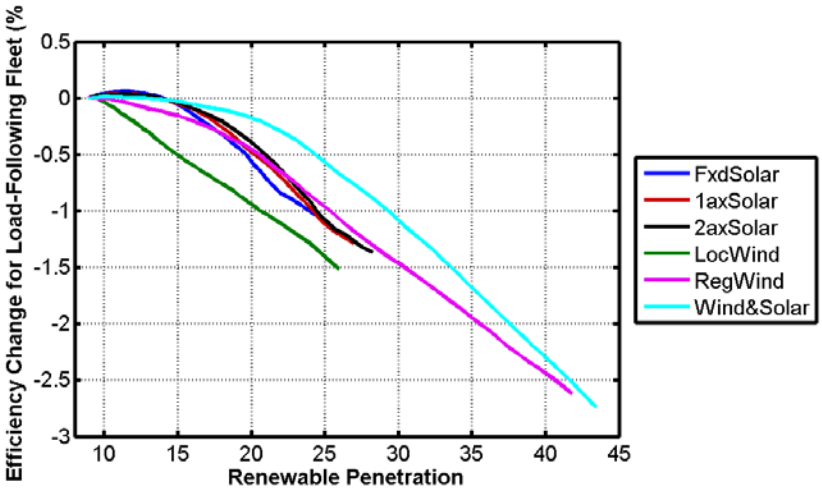

As renewables displace load-followers and change the operation of peakers, the number of starts generally increases for all technologies as shown in Figure 318. Wind technologies exhibit a smaller rise in starts than solar technologies and, again, the wind and solar mixture exhibits characteristics of both types. The turndown in starts for each technology is because once the grid is saturated with each resource, then sufficient curtailment exists to provide firming of that resource. Curtailment reduces the number of peakers and load-followers that must turn on or off to accommodate the changes in generation. In this way, curtailment actually firms the renewable signal and provides some dispatchability, at the expense of electricity that could be delivered to customers. While curtailing renewables will not increase the value proposition of

their installation, noting that some firming of the renewable signal is possible with curtailment is an interesting concept.

Figure 318: Comparison of Average Yearly Starts per Generator for Load-following and Peakers for each Technology

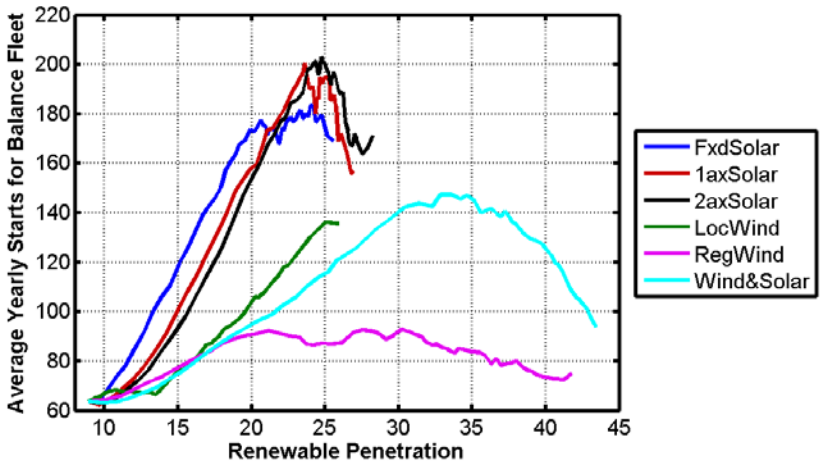

The average balance fleet ramp up and ramp down represents the average capacity that operating load-following and peaking plants must change their load point during the year. Notice that the solar technologies, cause a slight improvement initially (i.e., first 5%), since the solar signal well complements the demand signal. Following the initial region regional wind and the 50/50 mixture provide the smallest increase, while the other technologies cause a significant increase in the ramping (Figure 319 and Figure 320). The increase in ramping requirements for solar technologies is as a result of the concentration of the solar signal around the afternoon hours. For the first 5% it provides benefit by reducing the maximum; however, with greater solar capacity it results in a significant ramp down of the balance fleet each day as solar comes online and a significant ramp up as the solar goes offline in the late afternoon.

Figure 319: Fleet Ramp Up Comparison for Generation Technologies

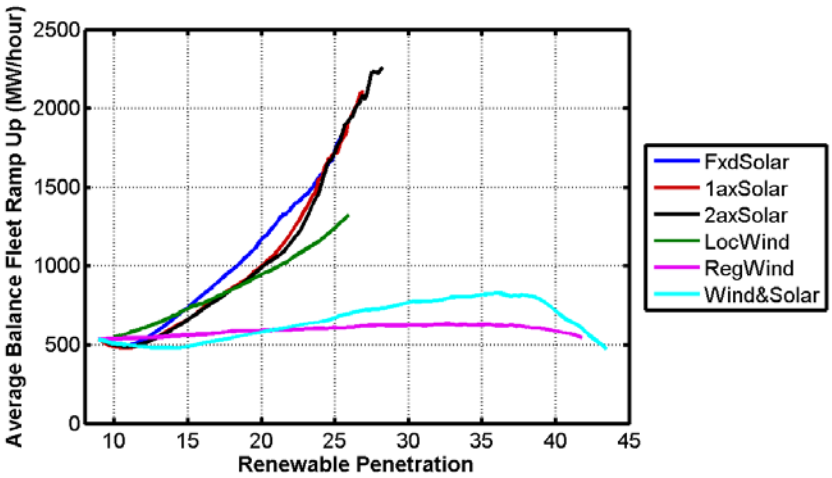

Figure 320: Fleet Ramp Down Comparison for Generation Technologies

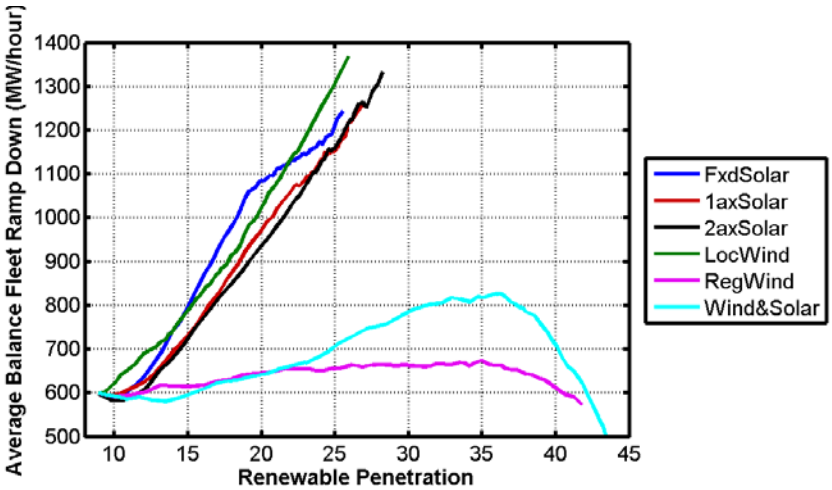

In addition to the operation measures, HiGRID uses the emissions module to calculate the carbon dioxide emissions related to the use of fuel and startup emissions for each technology. The CO2 reductions are presented as a percentage reduction from the initial case in 2005 and show the impact of increasing the renewable penetration without an increase in the load demand. Results, shown in Figure 321 and Figure 322, show that an increase in renewables will reduce the emissions of CO2. Figure 321 shows the effect compared to the renewable penetration (i.e., an energy measure) while Figure 322 shows the effect compared to the installed capacity (i.e., a measure of installed power). When compared to the renewable penetration the reduction in CO2 is nearly linear, while for installed power capacity, each marginal MW of capacity results in a diminishing reduction in CO2.

Figure 321: Carbon Dioxide Reduction Compared to Renewable Penetration for each Generation Technology

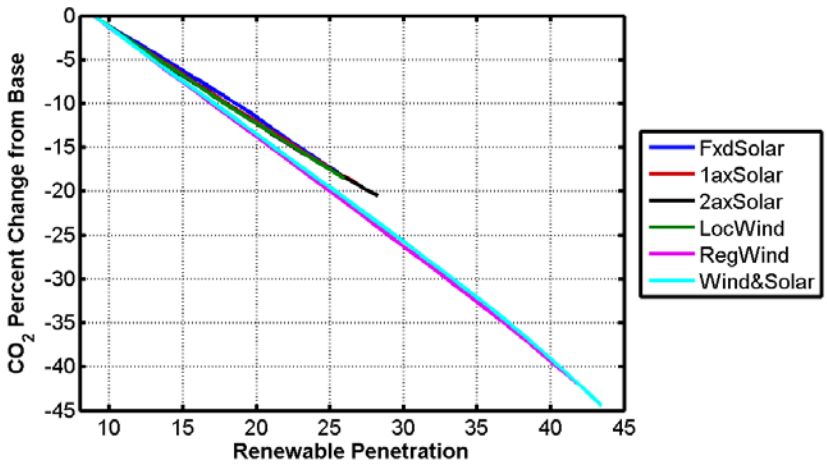

Solar technologies tend to more quickly approach their minimum value, while the wind and mixed scenarios more slowly approach their minimum value. Regional wind and the wind and solar combination allow for a much larger reduction than any other recognizing the value of wind with a higher capacity factor and the synergy of combining the resources.

Figure 322: Carbon Dioxide Reduction Compared to Installed Renewable Capacity for each Generation Technology

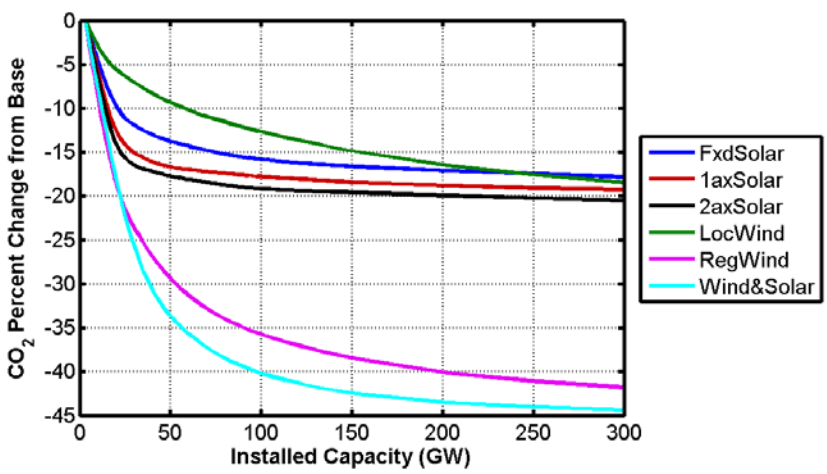

7.2.2.1.3. Cost Results

7.2.2.1.3.1. Technology Specific Cost Results

The last metric explored for the spanning cases is the levelized cost of electricity (LCOE). The cost of generation module provides both a technology-specific and a portfolio LCOE. As its name suggests, the technology-specific LCOE looks at the contribution of each resource to the

LCOE, while the portfolio LCOE is a calculation that weights the technology-specific LCOE values based on the lifetime energy provided.

To better explain the figures that will be shown later, two figures are presented that show how the technology-specific LCOE changes with renewable penetration for a mixture of 50/50 wind and solar. Figure 323 shows the LCOE breakdown at 8.9% renewable penetration, the lowest penetration only including geothermal, small-hydro and biomass/biogas. Notice that all the technologies are legacy and do not have a debt or equity portion since the plants are assumed to be fully depreciated. The LCOE values represent only the portion for generation and transmission but do not include distribution costs.

Figure 323: Technology-specific LCOE Breakdown at 8.9% Renewable Penetration for 50/50 Wind and Solar Mixture

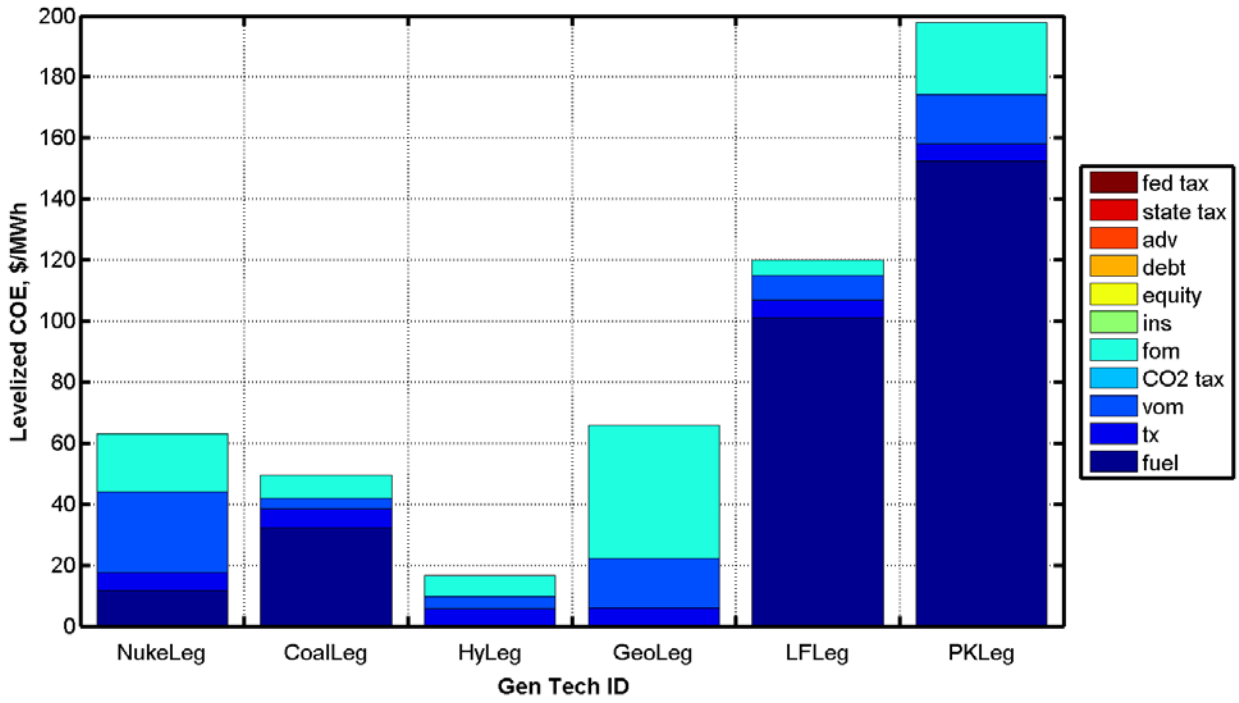

Once renewables are installed, the legacy technologies do not increase their LCOE; however, there is an additional need for peakers in the form of 200MW combustion turbines (i.e., CT200) as the renewable penetration increases to 20.4%. The peakers are required to support the added fluctuations from the installation of wind and solar. The need to install new peaking generation will increase the portfolio costs.

Figure 324: Technology-specific LCOE Breakdown at 20.4% Renewable Penetration for 50/50 Wind and Solar Mixture

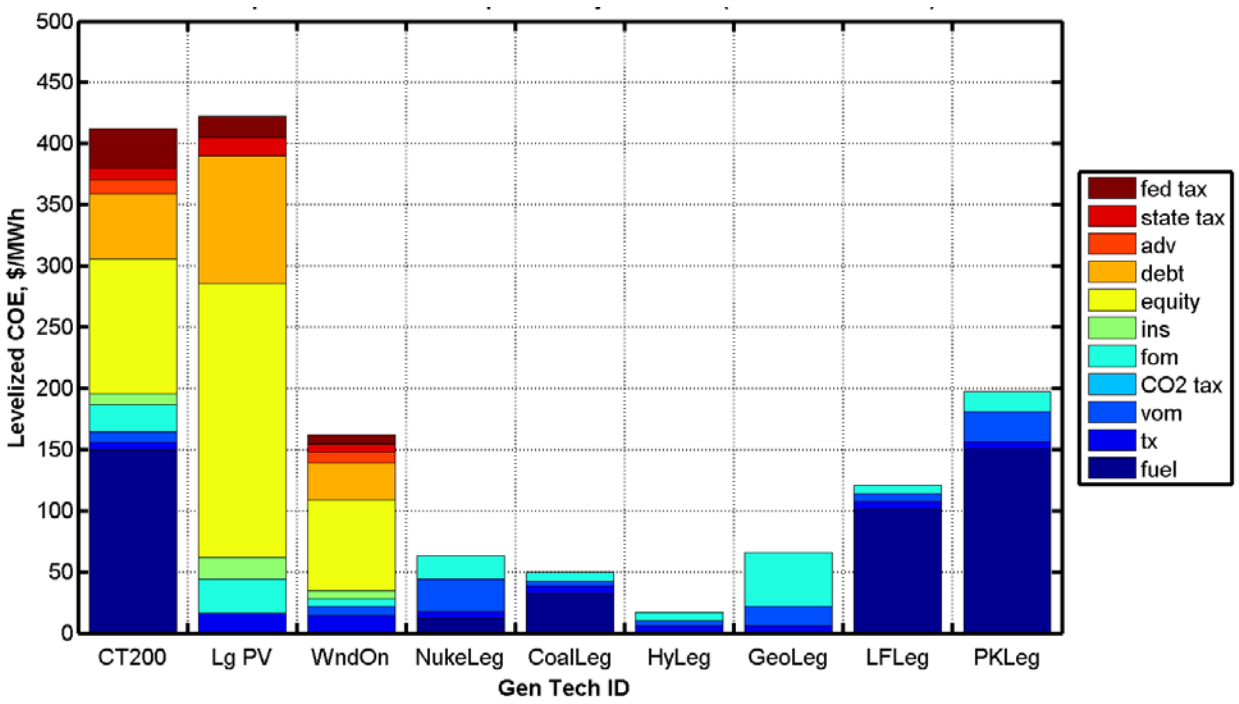

Now that the reader has been introduced to the concept of technology-specific LCOE values and seen the impacts with increasing the renewable penetration, three distinct cases will be presented to further show how the LCOE changes with penetration.

The progression of the technology-specific LCOE for three cases including 1-axis tracking PV, regional wind and 50/50 mixture of wind and solar is presented in Figure 325, Figure 326 and Figure 327, respectively. Notice that initially, the LCOE of for each technology in each of the three cases is the same but the LCOE for renewables changes dramatically, with increasing penetration. Initially, peakers, load-followers, hydro, nuclear, coal and geothermal are all legacy technologies, therefore they don't have the capital investment While the LCOE for baseload technologies and hydro is significantly less expensive than the renewables.

The load-following LCOE reduces for the first few penetrations of the 1-axis case because of the coincidence with the peak load and solar signal initially, however, as the renewable penetration increases the peaker and load-following LCOE values increase. Notice that the 1-axis PV only goes to 27% penetration, while the others increase to over 40%.

Figure 325: Technology-specific LCOE Progression for 1-axis Tracking PV

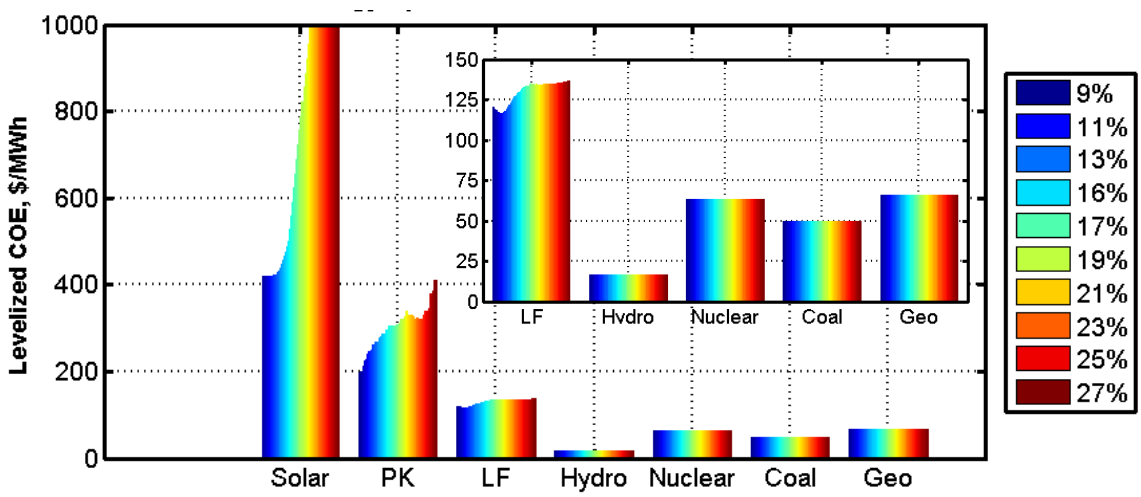

For 1-axis PV, the LCOE for solar power can climb to a very high value as excess generation forces curtailment, while the wind has a lower initial LCOE and a lower maximum LCOE.

Figure 326: Technology-specific LCOE Progression for Regional Wind

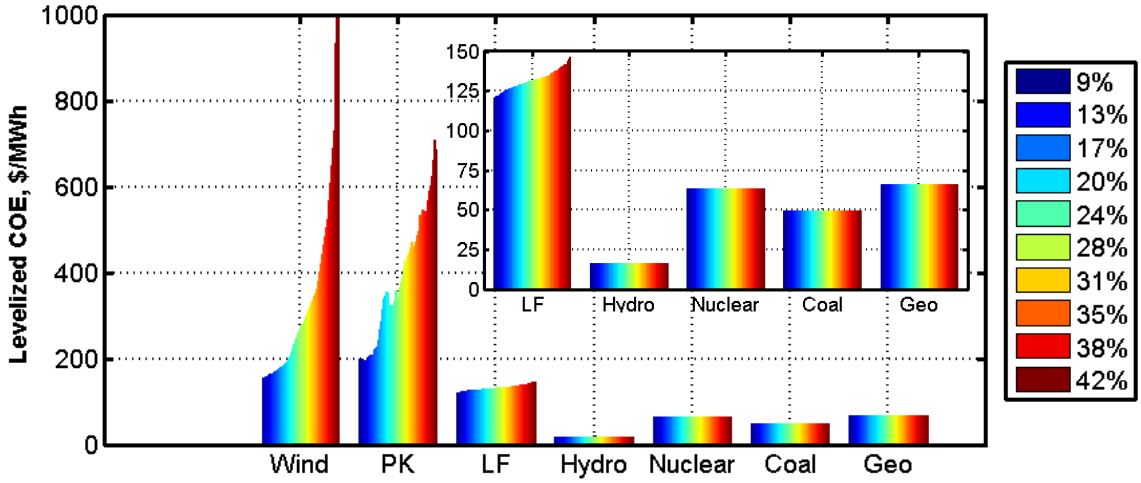

Combining both wind and solar results in lower LCOE values for both at high renewable penetrations and it also reduces the resulting peaker LCOE.

Figure 327: Technology-specific LCOE Progression for 50/50 Wind and Solar Mixture

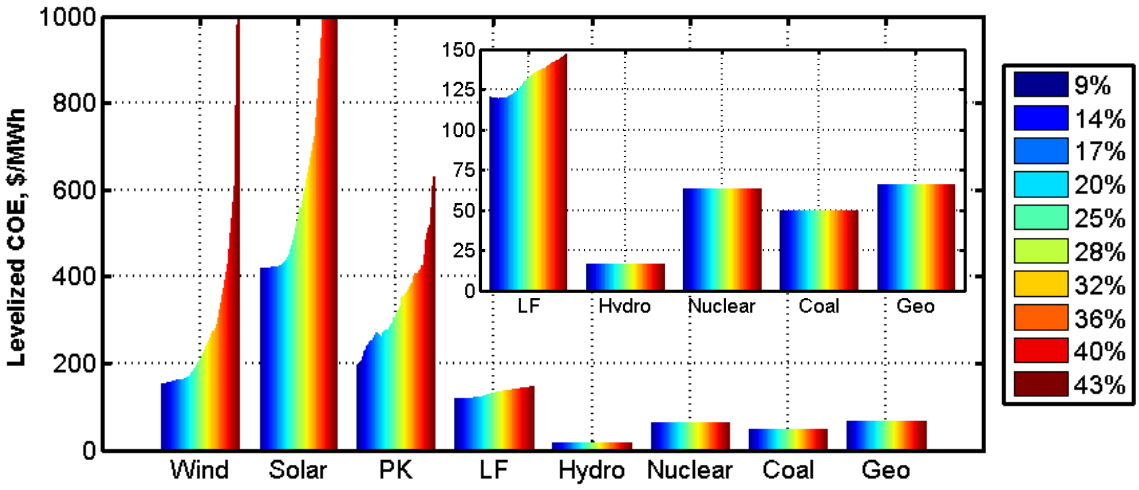

7.2.2.1.3.2. Portfolio Cost Results

The previous section provided a description for why the LCOE of each technology increases with increasing renewable penetrations. This section looks at the resulting portfolio LCOE values. Initially, the least competitive technology is the local wind. While the capital cost is low the capacity factor is also very low resulting in a high contribution to the LCOE. With higher renewable penetrations the local wind becomes more cost competitive than the fixed and 1-axis tracking solar because of the sharp curtailment with the solar technologies on account of their very focused generation pattern. Regional wind starts as the most economically competitive technology and is able to achieve significantly higher renewable penetrations with much less cost. Around 37% renewable penetration the 50/50 wind and solar has a lower LCOE than the regional wind rollout. As the wind penetration increases it experiences an increase in the LCOE due to curtailment; however, the 50/50 mixture rollout is able to improve system performance by relying on the benefits of both wind and solar profiles to meet the demand. Figure 328 presents the LCOE for each generation technology and Figure 329 presents the same information but only from 8 to 24% renewable penetration.

Figure 328: Levelized Cost of Electricity for Generation Technologies

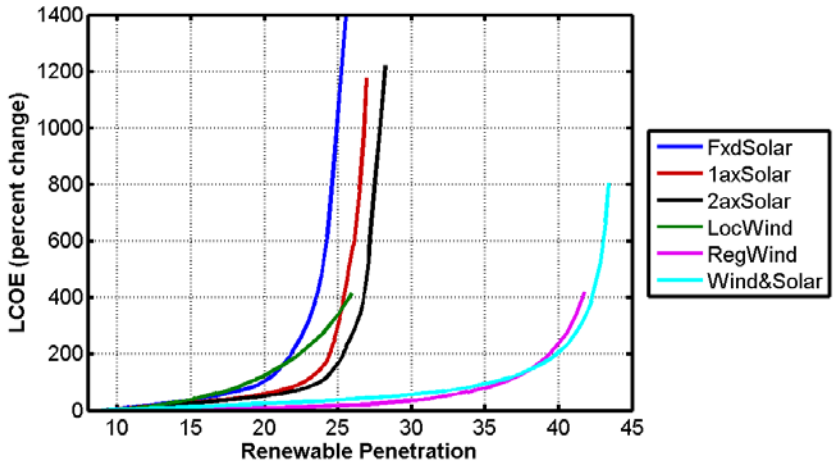

Figure 329: Levelized Cost of Electricity for Generation Technologies (RENPEN 8-24%)

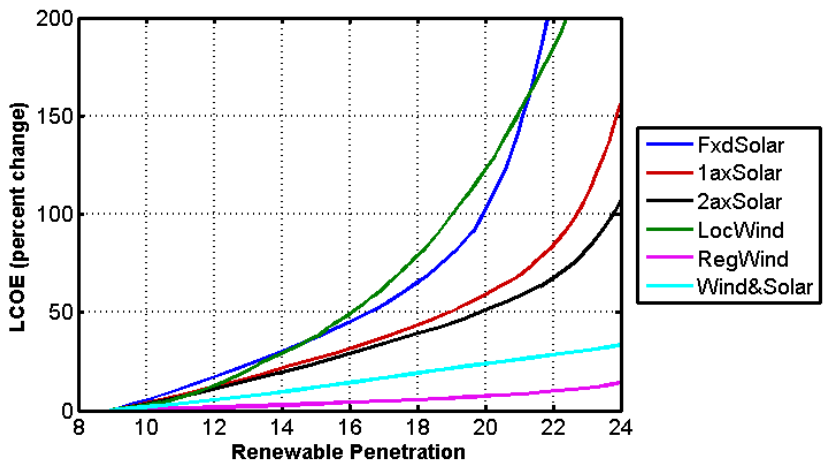

7.2.2.1.4. Conclusions

- **Regional resources provide more energy at a lower LCOE than locally cited resources.** Despite the efficiency penalty for transmission and the cost associated with adding transmission lines, higher capacity factor and less intermittence contribute to higher achievable renewable penetrations and lower portfolio LCOE.
- Export of unwanted renewable dynamics to the grid is allowed in California's market with the renewable "must-take" strategy; however as renewable installations increase eventually this strategy must be re-evaluated if grid stability is to be maintained.
- Curtailment can act to "firm" a renewable signal at the expense of increased LCOE.

- For the first 5% renewable penetration, the solar generation signal coincides well with the demand signal causing a reduction in balance fleet yearly starts, ramp up and ramp down as well as an increase load-follower fleet efficiency.
- **The technology-specific LCOE for renewables increases as the renewable penetration rises.** As the renewable penetration increases, the grid becomes saturated with renewable generation resulting in excess generation, which causes a rise in the LCOE.
- **The technology-specific LCOE for peakers and load-followers increases as the renewable penetration rises.** Peakers and load-followers must accommodate for the increased ramping requirements on the system, while still maintaining reliability in the face of rising regulation requirements. These increasingly stringent requirements cause a rise in the LCOE for peakers and load-followers.

7.2.2.2. Solar Thermal Trough Power Plant Results

This analysis explores the impacts of operating a solar thermal trough plant with and without an auxiliary burner.

First, the generation profile of the solar thermal power plant is explored. Then, the solar thermal model is run three times: 1) no additional fuel included, 2) natural gas can be used to fire an auxiliary burner to generate at full power during the summer and spring between 11AM and 5PM and 3) natural gas can be used to generate at full power during the summer and spring between 11AM and 8PM. These three cases are compared to one another to see how operating the plant differently affects the grid.

7.2.2.2.1. Solar Thermal plant operation without additional fuel

Without a thermal storage mechanism or the capability to supplement generation with a natural gas auxiliary burner, the solar thermal plant can only generate during the hours when the sun provides enough heat input to operate the steam turbine. As such, the average generation profile begins around 7AM and ends by8PM as shown in Figure 330 for four different renewable penetrations (on an energy basis). As the renewable penetration increases so does the generation profile; however, it does not increase uniformly, particularly at high renewable penetrations when there is the potential for excess generation.

Figure 330: Average Daily Generation Profiles for Solar Thermal Plant without Supplemental Burner

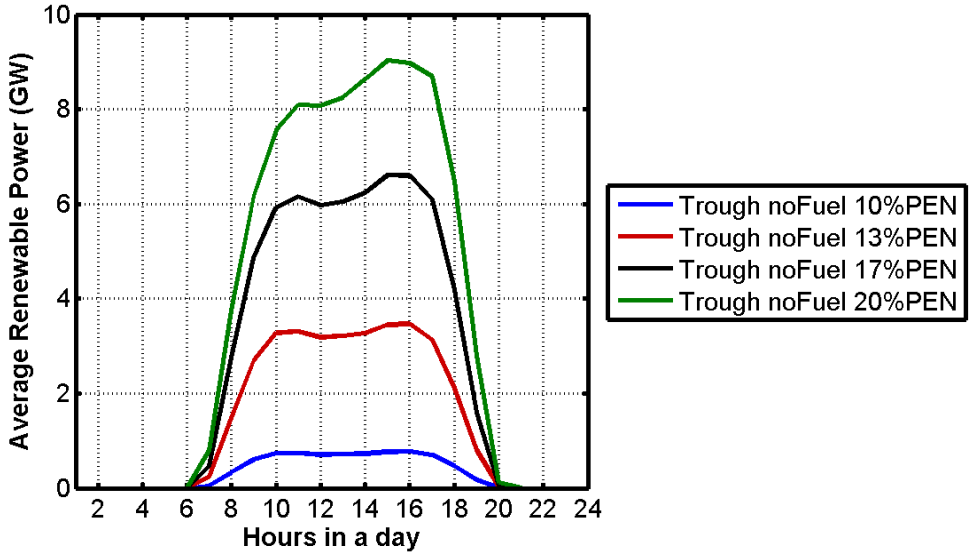

The intensity of the sun during the spring and summer allows for more generation during those two seasons than any other (Figure 331).

Figure 331: Average Daily Generation Profiles by Season for Solar Thermal Plant without Supplemental Burner

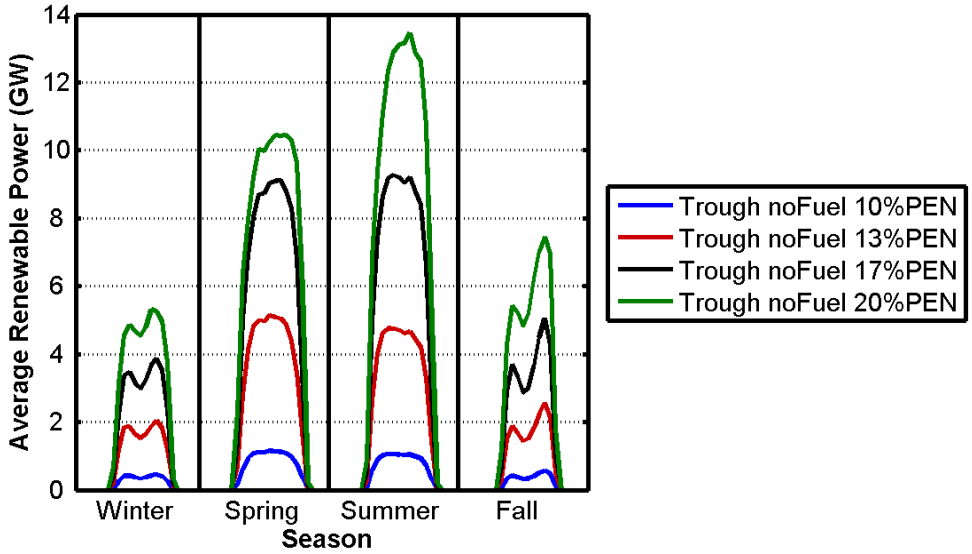

The solar thermal power plant is generating power for 45% of the hours in the year (Figure 332), but with the addition of thermal storage and supplemental burners this value can be increased. The next section explores the impacts including supplemental burners into the solar thermal power plant.

Figure 332: Load Duration Profiles for Solar Thermal Plant without Supplemental Burner

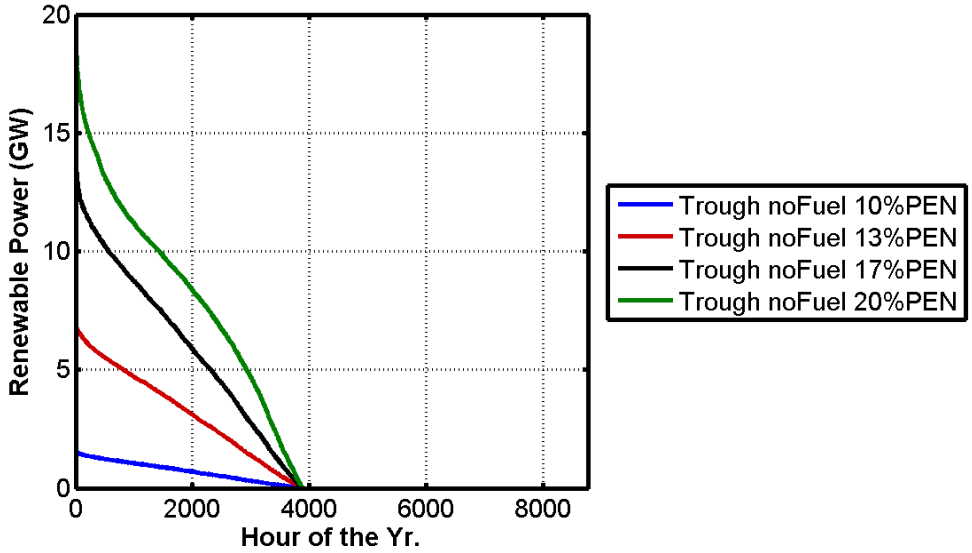

7.2.2.2.2. Solar Thermal plant operation with supplemental burner

Including supplemental burners allows the plant to smooth and extend its generation profile. Figure 333 shows the average generation profile for the modeled solar thermal plant with the ability to burn additional fuel to increase the heat sent to the steam turbine. The two cases that include supplemental burners can operate from 11AM to 5PM and 11AM to 8PM, respectively. The case allowing fuel from 11AM-5PM is used for smoothing and adds generation during peak load times. The case allowing fuel from 11AM-8PM provides smoothing, and adds generation during peak load times but also can increase the generation in the evening hours. Notice that using fuel allows the plant to be at a much higher average output power at 8PM and then the power gradually lowers over the following 4 hours.

Figure 333: Average Daily Generation Profiles for Solar Thermal Plant at 20% Renewable Penetration with Different Supplemental Burner Configurations

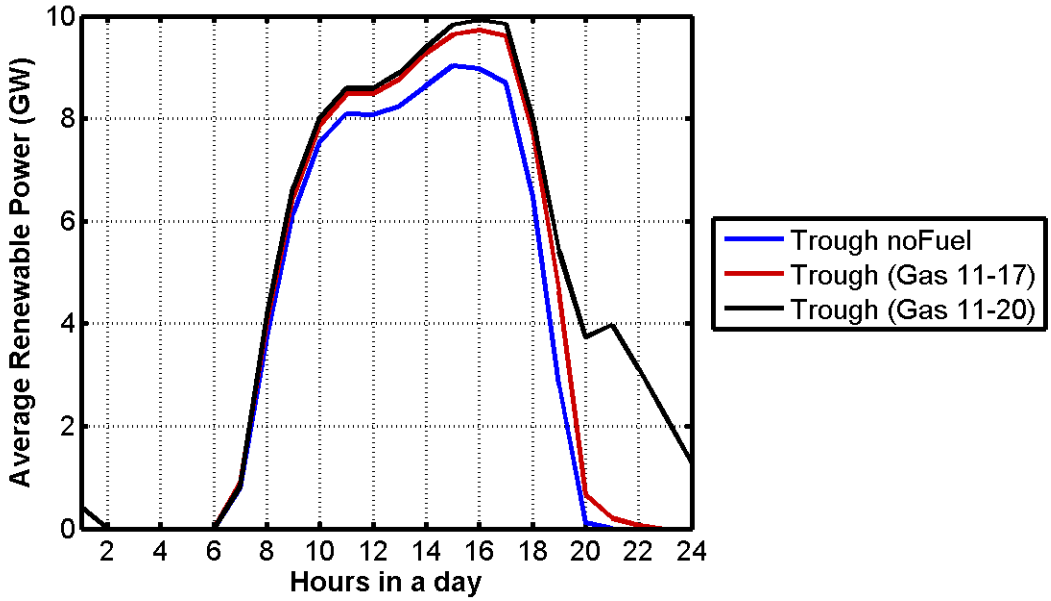

Inclusion of the burner, particularly the 11AM-8PM burner, increases the percentage of hours served by solar power from 45% to 51% by extending the hours of operation in the evening (Figure 334).

Figure 334: Load Duration Profiles for Solar Thermal Plant at 20% Renewable Penetration with Different Supplemental Burner Configurations

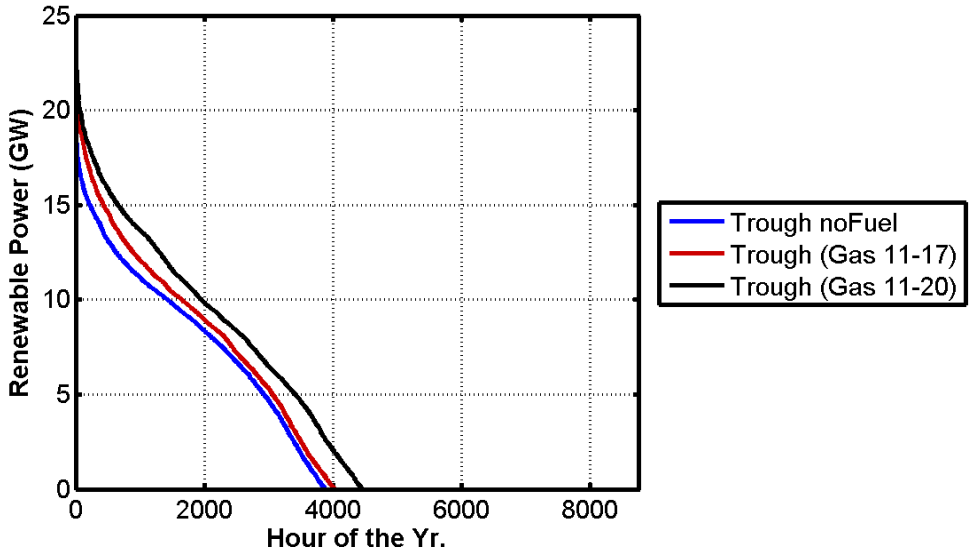

Comparing the three cases outlines a comparison of different generation properties, where each case contains the properties described below:

- No Fuel
    - Solar generation profile without modification
- Gas 11-17
    - Generation smoothing
    - Additional generation at peak load times
- Gas 11-20
    - Generation smoothing
    - Additional generation at peak load times
    - Extended evening generation

The most important property for increasing the renewable penetration is the ability to extend the hours of operation of a solar thermal power plant as shown in Figure 335. The Gas 11-17 case actually reduces its renewable penetration by increasing its generation during peak times. That is because providing fuel during peak hours does not enable additional renewables. Because there is baseload generation that will not turn off and there is a minimum load-following, peaker and hydroelectric capacity required to maintain reliability, providing only peak generation actually causes the solar thermal plant rollout to approach the point of excess generation more quickly than without. The Gas 11-20 case allows for additional uptake of renewable generation at the end of the day. This is because around 5PM, without a supplemental burner, the plant must turn off since it cannot generate enough heat to maintain operation of the steam turbine. However, if the plant is to supplement the heat from solar radiation with additional heat from a natural gas burner then it can increase the contribution from renewable generation by making use of the solar radiation that would otherwise be insufficient to operate the steam turbine. As a result the Gas 11-20 case enables higher renewable penetration.

Figure 335: Installed Renewable Capacity vs. Renewable Penetration with Different Supplemental Burner Configurations

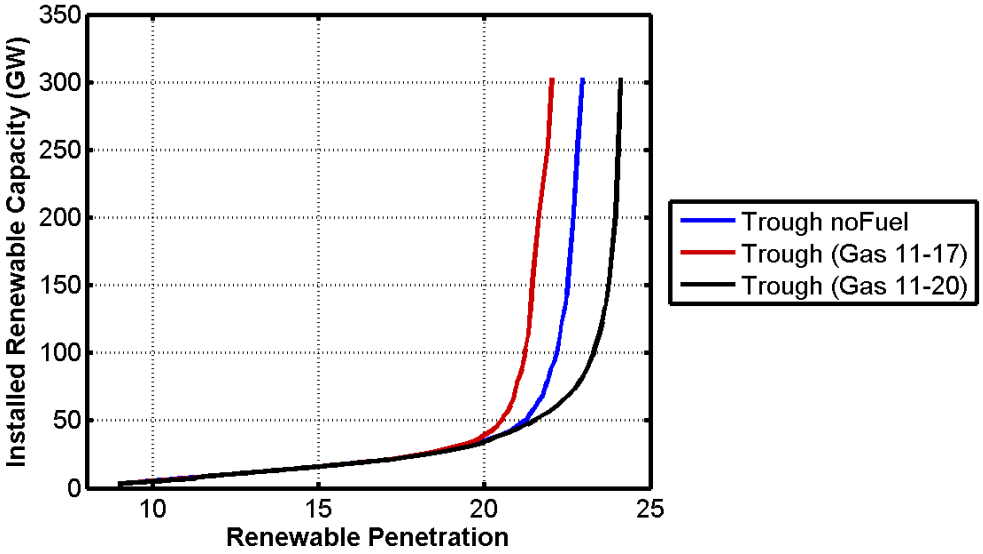

Carbon dioxide emissions are uniquely affected by the three different cases as well (Figure 336). While the other results are presented versus renewable penetration, the resulting reduction for CO_2 remains nearly linear for renewable penetration making the differences difficult to see so the results are presented on a per installed power capacity basis. All three cases reduce the emissions initially; however as the uptake of renewable generation on the grid becomes saturated (i.e., excess generation increases), the emissions reduction capability of each case diverges. The case with no auxiliary burner shows a reduction settling at between 12 and 15% CO_2 reduction from base. The Gas 11-17 case is interesting in that the more capacity of renewables installed the more the burner is used so the emissions will actually increase if the burner is not used appropriately. Lastly, the Gas 11-20 case shows a reduction greater than all other cases because of its ability to uptake additional renewable generation where the other plants would have to curtail their generation toward the evening hours because of the steam turbine limitations.

Figure 336: CO_2 Reduction from Initial Baseline vs. Installed Capacity (power basis) with Different Supplemental Burner Configurations

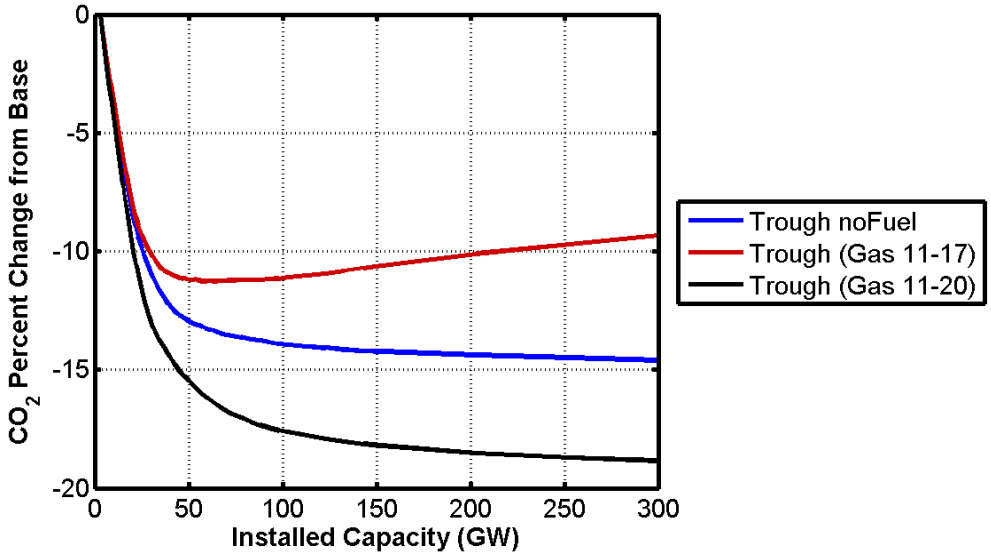

Based on the previous results it is not surprising that the Gas 11-20 provides the lowest LCOE of all three cases as shown in Figure 337. The Gas 11-17 case has a higher LCOE at each renewable penetration because use of the burner reduces the renewable penetration as shown in Figure 335.

Figure 337: LCOE Comparison with Different Supplemental Burner Configurations

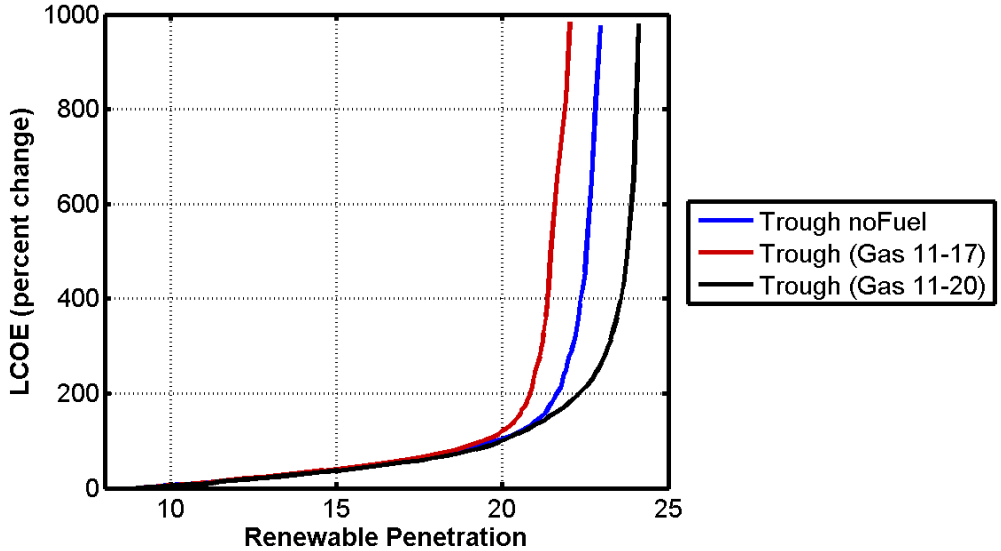

7.2.2.2.3. Conclusions

- Inclusion of a supplemental burner or thermal storage system can smooth the generation profile and extend the hours of operation
- Extending the hours of operation is the most important factor to increase the achievable renewable penetration

7.2.2.3. Balance Fleet Installed Capacity Results

Because of the intermittent nature of wind and solar, installing a megawatt of generation does not result in the removal of a megawatt of load-following generation. Even if it is only a few days a year, the sun will not be shining or the wind will not be blowing and the capacity of the renewable generator will need to be backed up by a dispatchable generator. To further explore this concept three scenarios were run using the HiGRID model for California using 1-axis tracking PV, regional wind and 50/50 wind and solar mixture (see Figure 314, Figure 315 and Figure 316, respectively). These three figures contain the maximum operating load-follower and peaker installed capacity values for the entire year as well as the average and minimum for each renewable penetration.

Two values for the maximum are included: the solid line is based on equation (123) and the dashed line is based on equation (126). The solid line represents the best case scenario (i.e., optimistic) where the traditional role of the peaker is replaced with advanced load-following generation with faster ramp rates, lower part load capability, and lower degradation from startups and part load operation. The maximum capacity will result from the single hour that the fleet generation is highest.

The dashed line represents the worst case scenario (i.e., pessimistic) where the peaker and load-following roles do not change and the highest capacity results from the hour of the year when peaker generation is highest and the hour of the year when load-following generation is the highest.

$$\boldsymbol{Max\ Capacity_{Solid} = max(N_{LF}(t) \cdot P_{LF} + N_{PK}(t) \cdot P_{PK})} \quad \textbf{(94)}$$

$$\boldsymbol{Max\ Capacity_{Dashed} = max(N_{LF}(t) \cdot P_{LF}) + max(N_{PK}(t) \cdot P_{PK})} \quad \textbf{(95)}$$

where, $N_{LF/PK}$ is the number of generators of that type operating as a function of time and $P_{LF/PK}$ is the rated generator power for each type of generation. The pessimistic capacity will always be less than or equal to the optimistic capacity.

The maximums for the solar case begin at 32.4 and 34.1 GW. The pessimistic case (i.e., dashed line) only reduces 3 GW over the entire renewable penetration and toward the highest renewable penetrations the capacity increases quickly. The rise in capacity is because the solar profile and the load profile are only partially coincident, which causes a morning peak and an evening peak that must be met by peakers. The optimistic case (i.e., solid line) follows a similar trend except for it quickly reaches the minimum point at 30.2 GW with only 3.9% contribution

from solar, because of the similarity of the diurnal load shape to the solar power profile. This reduction is only 2.2 GW and the capacity for the optimistic case rises at high renewable penetrations because of the partial coincidence of the signals.

Figure 338: Load-follower and Peaker Installed Capacity with 1-axis Tracking PV Rollout

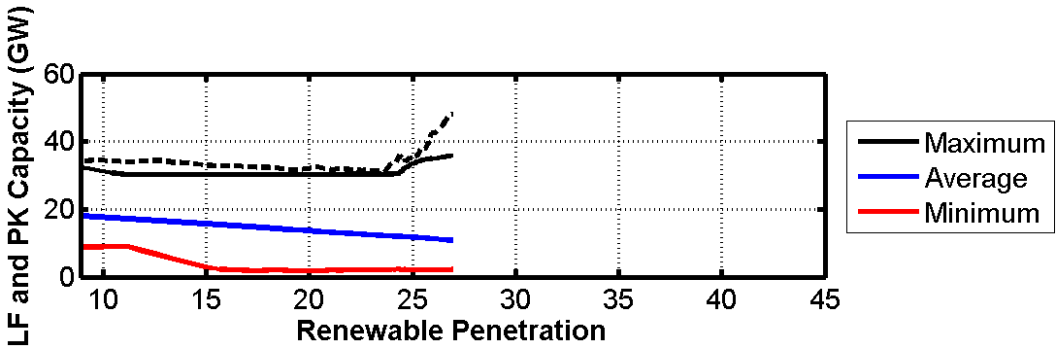

All three cases begin with the same capacity values of 32.4 GW for optimistic and 34.1 GW for pessimistic. The optimistic case reduces to 30.9 GW with 6.1% contribution from wind and then continues to decrease until 30.5 GW at 41.8% renewable penetration, a reduction of 1.9 GW.

Figure 339: Load-follower and Peaker Installed Capacity with Regional Wind Rollout

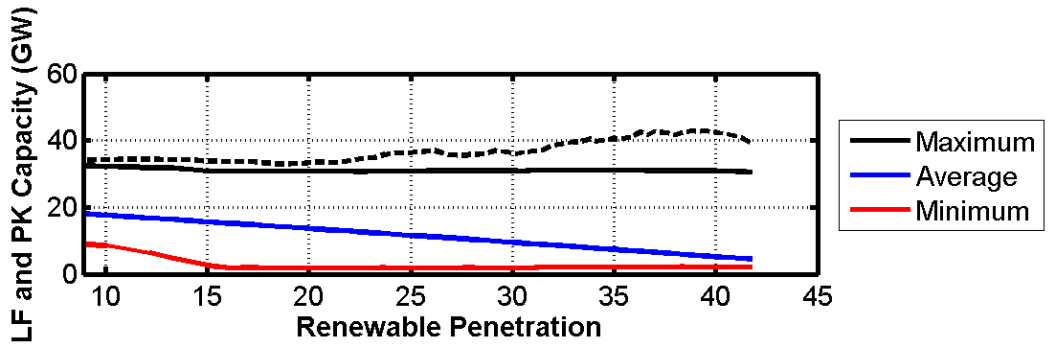

When wind and solar are combined, the resulting capacity reductions are the largest at 7.14 GW for the pessimistic and 10.0 GW for the optimistic case.

Figure 340: Load-follower and Peaker Installed Capacity with 50/50 Wind and Solar Mixture

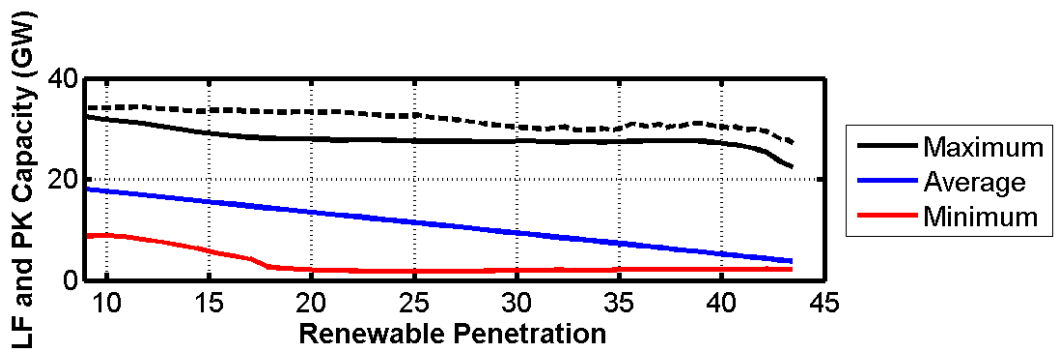

7.2.2.3.1. Conclusions

The behavior of each generator duty cycle is different and provide different value to the grid. As such 1 MW Intermittent Renewables ≠ 1 MW Load-follower ≠ 1 MW peaker ≠ 1 MW baseload.

- **Installing intermittent renewables does not significantly replace load-followers or peakers.** This is because of the few days a year when the renewable generator is not able to generate, another generator must take its place
    - **Improving balance fleet operating flexibility can improve the ability of renewables to displace capacity.** The balance fleet characteristics to improve include: ramp rates, part load capability and degradation from startups and part load operation.
    - Installing a mixture of wind and solar improves the ability to remove the balance generation capacity

7.2.2.4. Generator Flexibility Results

7.2.2.4.1. Description of Cases

Three analyses are performed. 1) Explore the implications for installing renewables if spinning reserve, regulation and other ancillary services were not required. While this is not a practical solution it provides valuable information on how renewables interface with the rest of the grid. 2) Explore providing advanced turndown for load-following and peaker generation. Increasing the turndown capability of balance generators will allow for higher efficiency operation at low load points and greater flexibility to balance the grid. Lastly, 3) Explore the effects on the grid if all baseload coal generation serving California is removed. Increasing renewables reduces the energy provided by load-following generation and is limited by the ability of load-followers to

provide system reliability while providing energy to balance the load. Removing baseload generation will alleviate some of the pressure on load-following as will be shown.

7.2.2.4.2. Approach

The HiGRID model ensures that sufficient regulation and spinning reserve capacity are maintained. As described in the balance generation module the method for acquiring this capacity is to reserve some of the capacity of load-following and hydro generation for provision of ancillary services (AS) and allowing the remainder to be used for providing energy to meet the grid electrical load. There are limitations to the amount that can be reserved for AS because capacity reserved cannot be used for anything else and the generator must be operating (excluding hydro power). As such, providing AS requires that the generator be able to lower its load point or turn down. Table 72 presents the operating parameters used by the HiGRID model to determine how the peakers and load-followers operate and the amount of AS that the balance generators can provide.

Table 72: Fleet Operating Characteristics for Conventional Peaker and Load-Follower used in HiGRID

Characteristics	Peaker	Load-Follower
Generating Power	50 MW	70 MW
Minimum Part Load	70%	60%
Maximum Part Load	98%	98%
Base Efficiency	20%	30%
Minimum Up Time	2 hrs	8 hrs

Maintaining reliability through the provision of AS has effects on the operation of the grid. While removing ancillary services is not an option if grid stability is to be maintained, the following analysis explores the effects that AS requirements have on the integration of renewables by removing the need for regulation and spinning reserve.

7.2.2.4.3. Results

7.2.2.4.3.1. Impact of Removing Ancillary Service Requirement

Two cases are run, one with AS requirements and one without. Both runs involve incrementally increasing the renewable capacity following a 50/50 mixture of regional wind and 1-axis solar PV from 0 to 300GW of total renewable capacity. The renewable penetration (energy basis) is tracked for both runs and the relationship between the installed capacity and the resulting renewable penetration is shown in Figure 341. Excess generation begins to increase around 35% renewable penetration and causes the exponential increase in installed capacity with a small contribution to increasing the renewable penetration. Removing the need for AS enables a higher renewable penetration because the dispatchability of balance generators must be split between providing AS and balancing renewable intermittencies. While this is not feasible if reliability is to be maintained, the concept that increasing or freeing up dispatchable

generation will allow for greater intermittent renewable management can be drawn from these results.

Figure 341: Installed Renewable Capacity Comparison with and without AS for 50/50 Wind and Solar Mixture

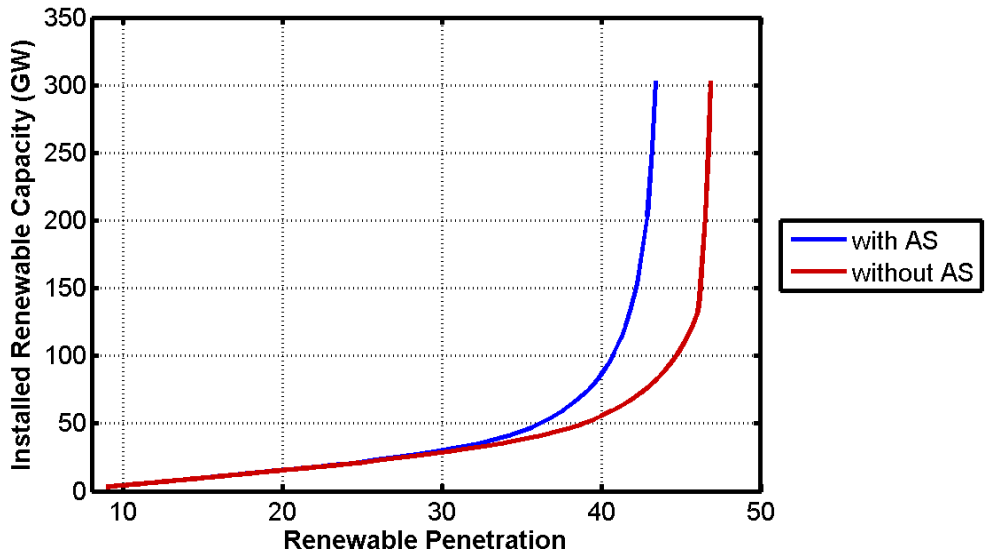

In addition to increasing the achievable renewable penetration the system-wide capacity factor would improve if dispatchable generation could be focused on increasing the renewable penetration. Notice that the capacity factor stays roughly the same until the curtailments starts because there is sufficient generation to provide both the energy required and the additional reserved capacity for AS; however, as the renewable penetration increases and displaces load-following generation and introduces more challenging system load changes, the two lines diverge and the difference between the two is as a result of the capacity that must be maintained to support system reliability while also providing dispatchable generation for meeting system load changes.

Figure 342: Capacity Factor Comparison with and without AS for 50/50 Wind and Solar Mixture

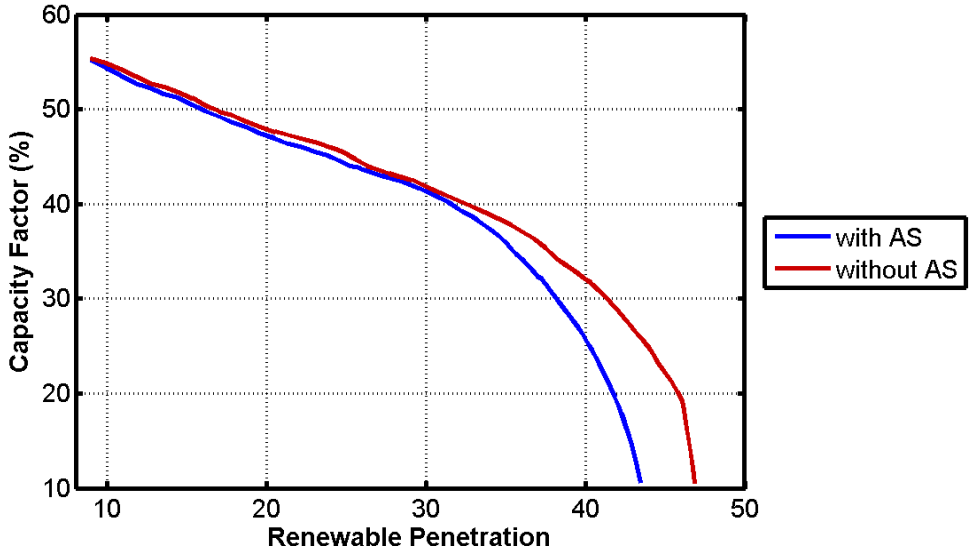

Following from the improvement in capacity factor and achievable renewable penetration the levelized cost of generation for the system will be lower for a system without AS versus a system with AS given the same installed renewable capacity as shown in Figure 343.

Figure 343: LCOE Comparison with and without AS for 50/50 Wind and Solar Mixture

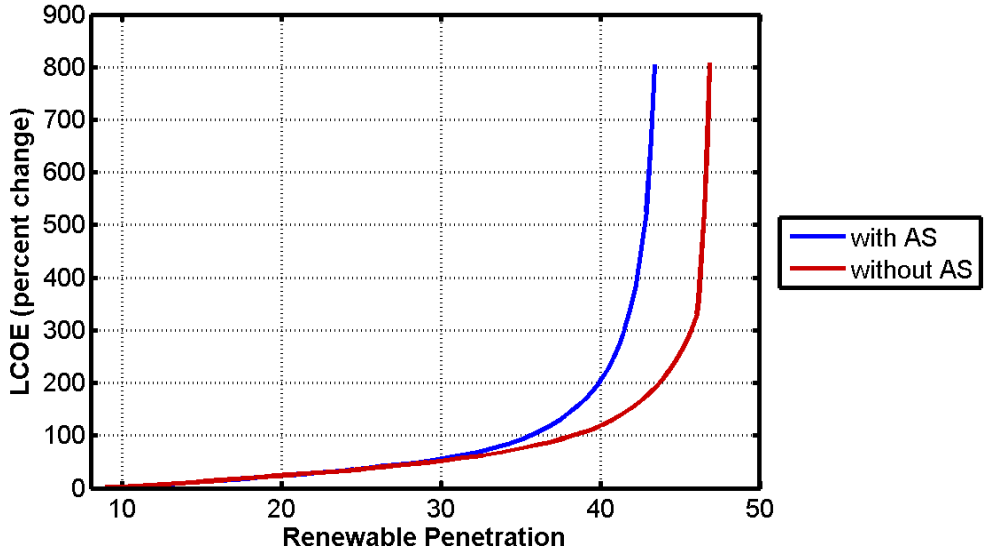

7.2.2.4.3.1.1. Conclusions

- Dispatchable generation must split their flexibility between providing AS and balancing intermittencies of renewable generation.

- Finding other ways to provide AS and freeing up dispatchable generation to balance renewables would allow for greater uptake of renewable generation

7.2.2.4.3.2. Impact of Advanced Generator Turndown on Renewable Implementation

While it is not possible to remove the need for ancillary service, there are opportunities to achieve some of the benefit while still providing ancillary services and maintaining system reliability. One technique to improve the performance of peakers and load-followers while simultaneously increasing the achievable renewable penetration is to improve the potential turndown of each generator.

Requiring flexible generation to operate below its rated power to provide ancillary service needs will reduce the generator's efficiency. However, if generators were better able to support this operation, there are opportunities to improve system efficiency for cases without renewables and allow for further integration of wind and solar for cases with renewables. Figure 344 shows the part load performance of a conventional GE STAG 209E combined cycle generator documented in 2001 (Chase, 2001) and a curve exhibiting advanced turndown.

Figure 344: Part Load Performance for a Conventional Combined Cycle and an Advanced Combined Cycle, both Operating with Two Gas Turbines

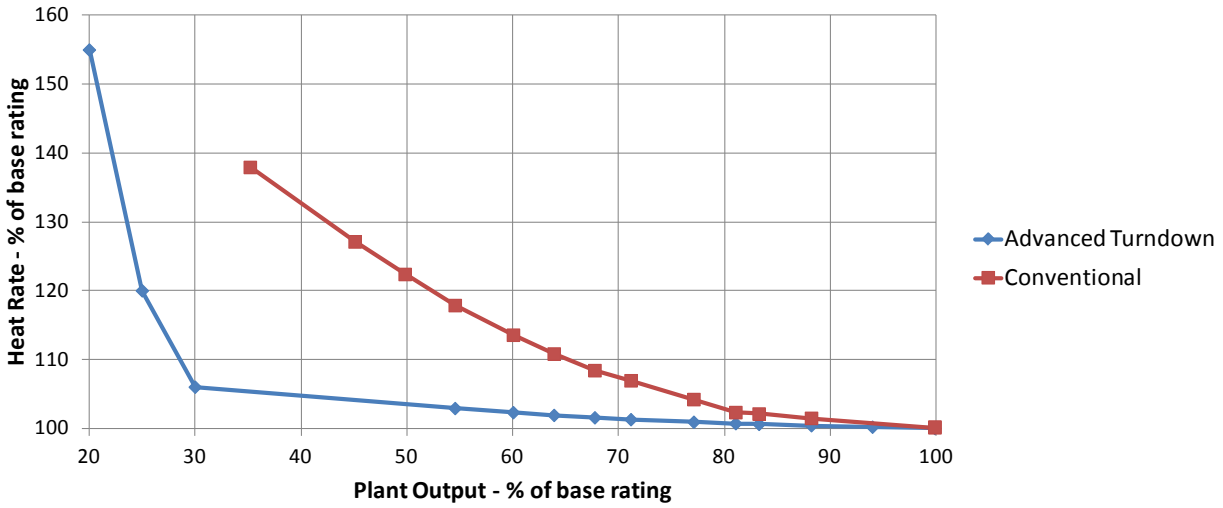

Similarly, University of California at Irvine has a 13.5MW gas turbine. Figure 345 shows a similar part load performance curve for operation of the installed gas turbine and a turbine with advanced turndown capabilities. Notice that the current generator has not historically operated at low part load conditions with the lowest point around 67% of full load capacity.

Figure 345: Part Load Performance Curves for UC Irvine's Solar Gas Turbine and a Turbine with Advanced Turndown Capabilities

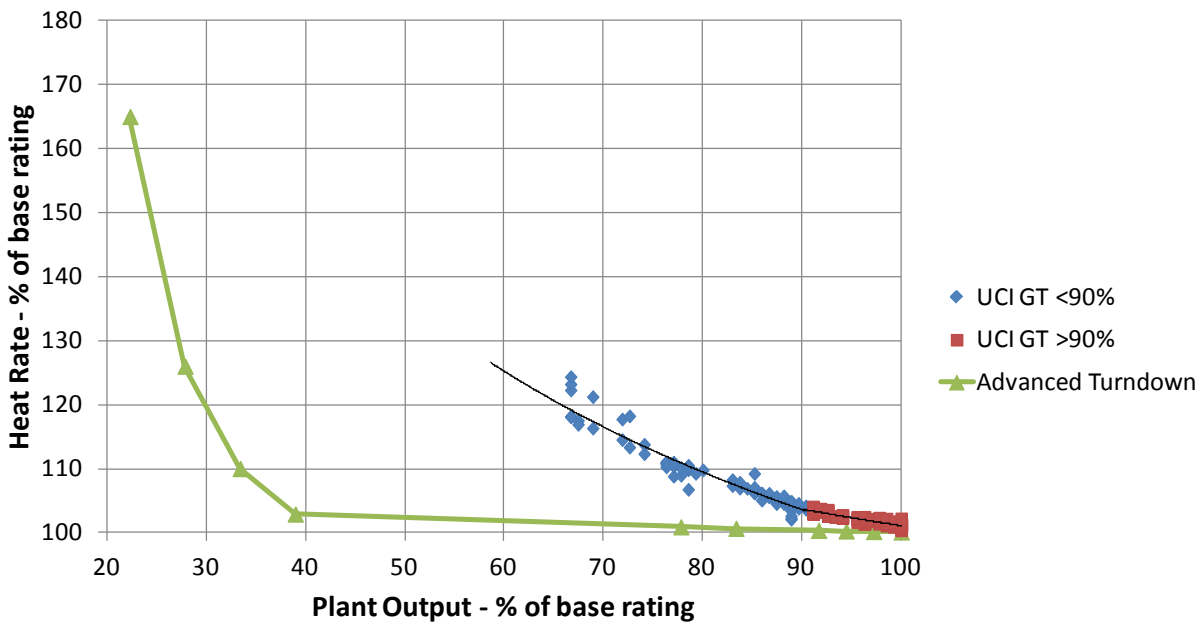

Both the GE STAG 209E and UCI's Solar Titan 130 exhibit a region where there is a relatively small reduction in heat rate ranging from 100% to 80% and 90%, respectively. Operating in this region provides the highest efficiency while still allowing for part load operation. In the context of ancillary services, a generator's ability to operate at part load can provide a value stream to the generator by selling additional capacity into the ancillary services market, which typically sells for a higher price than sale in the energy market.

The curves for both the combined cycle and the simple cycle turbines were developed by following an average of 15:1 reduction in percentage plant output power to an increase in percentage heat rate. This value represents over double that of the conventional technology (6:1), on account of expected advancement of the technology. This pattern occurs until 30% for combined cycle and 40% for simple cycle gas turbine at which point the effect on heat rate increases as a power series. The selected operating characteristics used are presented in Table 73.

Table 73: Fleet Operating Characteristics for Advanced Part Load Peaker and Load-Follower Modeling

Characteristics	Peaker	Load-Follower
Generating Power	50 MW	70 MW
Minimum Part Load	40%	30%
Maximum Part Load	98%	98%
Base Efficiency	20%	30%

Minimum Up Time	2 hrs	8 hrs

These values are used with the HiGRID code to represent the operation of the fleet of peaking and load-following generation that meets the state demand. Meeting ancillary service needs with high part load generators can be done more easily as evidenced by lower LCOE (Figure 346) and higher capacity factor (Figure 347).

Figure 346: Levelized Cost of Generation with Increasing Renewable Penetration for 50/50 Wind and Solar Mixture including Advanced Part Load Generation

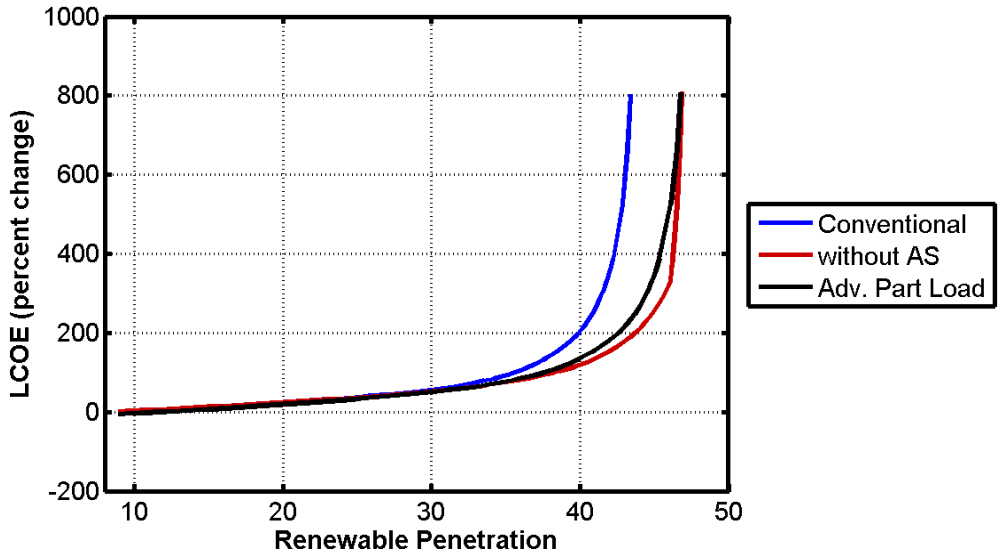

Notice that the implementation of advanced part load capable generation can provide a similar benefit as removing all AS, but unlike removing AS, high turndown generation is a practical solution and one that gas turbine and combined cycle plant manufacturers should pursue.

Figure 347: Capacity Factor with Increasing Renewable Penetration for 50/50 Wind and Solar Mixture Including Advanced Part Load Generation

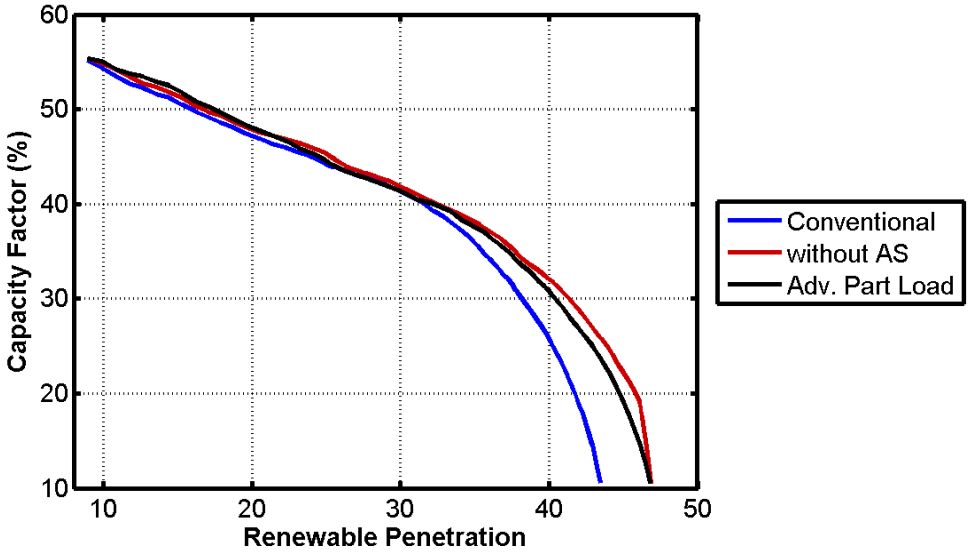

Additionally, without changing the peak efficiency of the generators, the average efficiency will improve as shown in Figure 348 and Figure 349 . This improvement occurs because generators necessarily have to operate below their rated power, even with the current amount of renewables, to maintain ancillary service capacity. Thus with better part load performance, efficiency will increase and will provide even more benefit as the renewable penetration increases.

Figure 348: Average Efficiency for Peakers with Increasing Renewable Penetration for 50/50 Wind and Solar Rollout Strategy

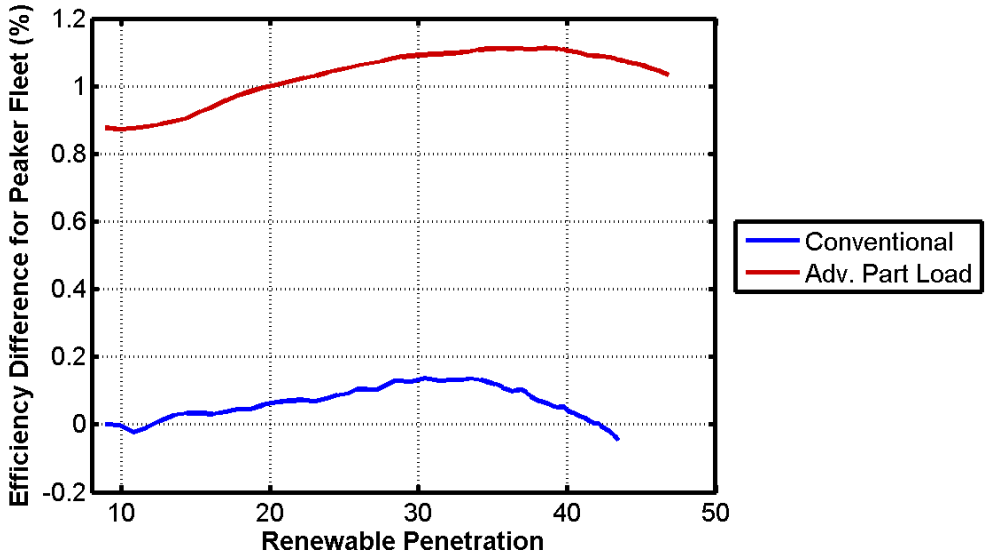

The efficiency of peakers increases around 1% and the efficiency of load-followers goes from an increase of 0.3% for low renewable penetrations to an increase of 2.5% compared to the use of conventional load-following generation at high penetrations. The increase in efficiency for the entire scenario is caused by lower efficiency loss at part load; however, the effects are more pronounced with higher penetrations as the dynamics caused by intermittent generation accentuate the importance of part load generation in this region.

Figure 349: Average Efficiency for Load-Followers with Increasing Renewable Penetration for 50/50 Wind and Solar Rollout Strategy

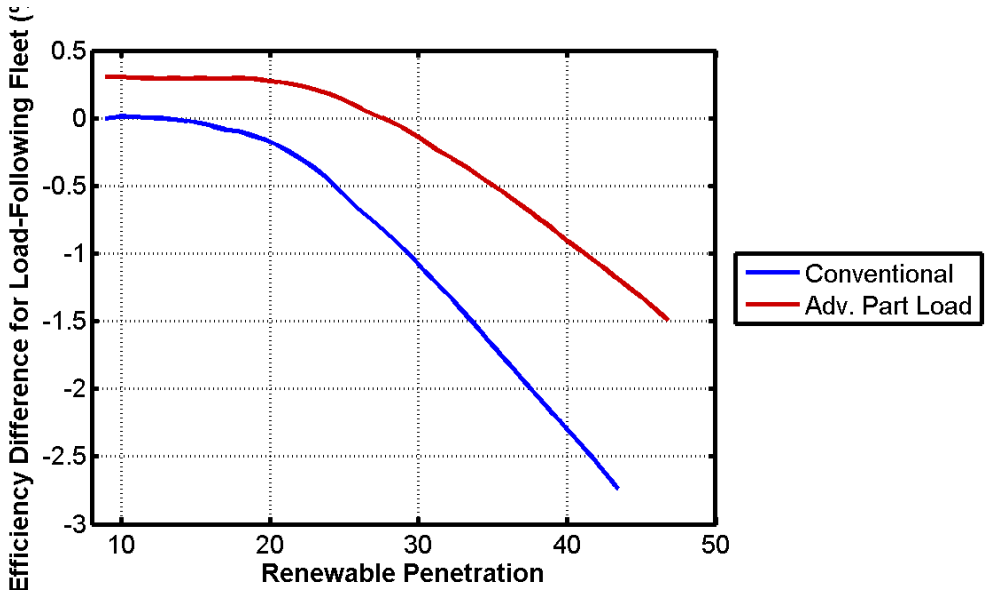

Another concern for flexible generation is the number of starts per year for each generator. Starts increase the wear on the equipment and cause a temporary increase in fuel use and criteria pollutant emissions. Improved part load performance has the potential to reduce the number of starts experienced for peakers and load-followers as shown in Figure 350. Greater part load allows generators to avoid turning off at times of low load only to turn on again during times of high load.

Figure 350: Average Starts for Peakers and Load-Followers with Increasing Renewable Penetration for 50/50 Wind and Solar Rollout Strategy

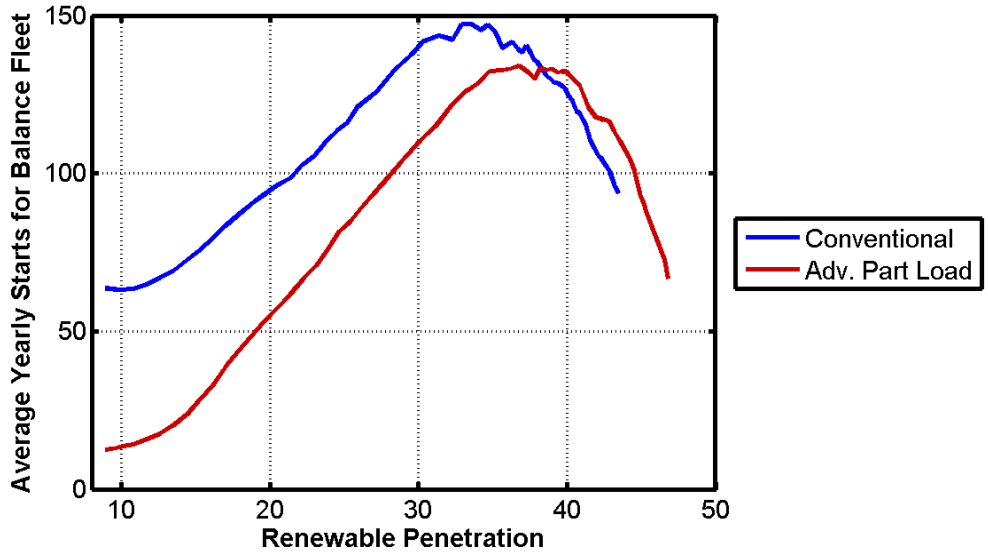

7.2.2.4.3.2.1. Conclusions

- Advanced part load generators have the ability to reduce the system-wide LCOE, and balance fleet starts, while increasing the balance fleet efficiency and capacity factor.

7.2.2.4.3.3. Effects of Baseload Generation on Renewable Implementation

A key contribution to the total energy consumed in California during 2005 comes from baseload generation with 20.1% coming from coal generation and 14.5% coming from Nuclear as shown in Figure 223. While the state has been reducing the purchase of coal generation and there is a moratorium on new nuclear plants, a significant portion of baseload still exists.

Baseload operation stays relatively constant with little dispatchability as shown in the baseload model description. An analysis to explore how removing coal baseload from the mixture affects the grid and renewable integration is performed. All of the existing coal generation for the analyzed year (i.e., 2005) is removed and replaced with the appropriate amount of load-followers to meet the load at all times. Replacing baseload with load-followers will add dispatchability that did not exist with the coal plants. The result is that without coal generation the achievable renewable penetration increase from 44% to over 60% (Figure 351). With the baseload, excess renewable generation must be curtailed; however, with the coal generation replaced with flexible load-following generators it is possible to turn down or turn off generators to compensate.

Figure 351: Installed Renewable Capacity Comparison with and without Coal Baseload for 50/50 Wind and Solar Mixture

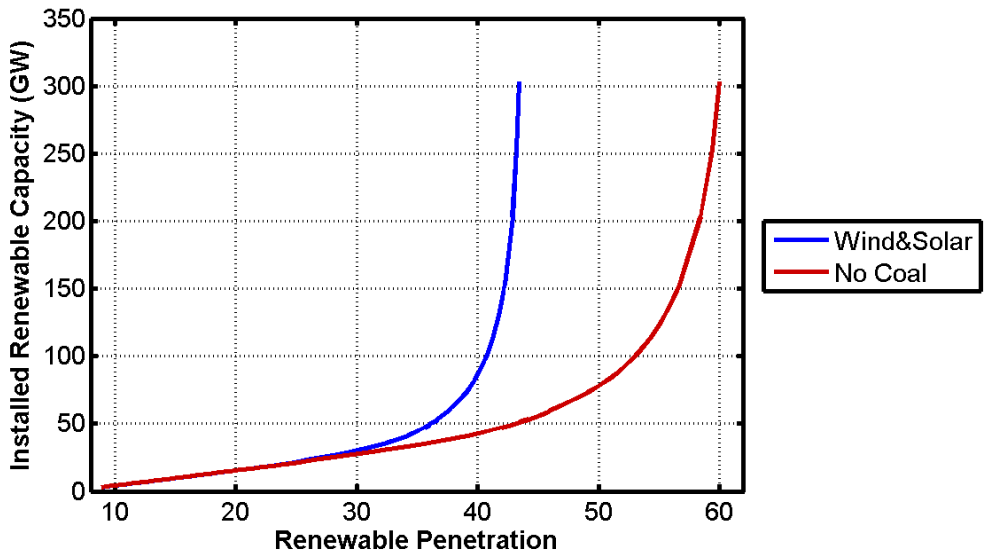

Wind and solar capacity excess generation causes a rapid decay in the capacity factor at around 30 to 40% renewable penetration. Removing the coal baseload provides greater access to flexible generation, which helps to buffer intermittencies caused by wind and solar generation.

As a result, the capacity factor with no coal baseload can remain higher for a longer time than the capacity factor for the case with coal baseload.

Figure 352: Capacity Factor Comparison with and without Coal Baseload for 50/50 Wind and Solar Mixture

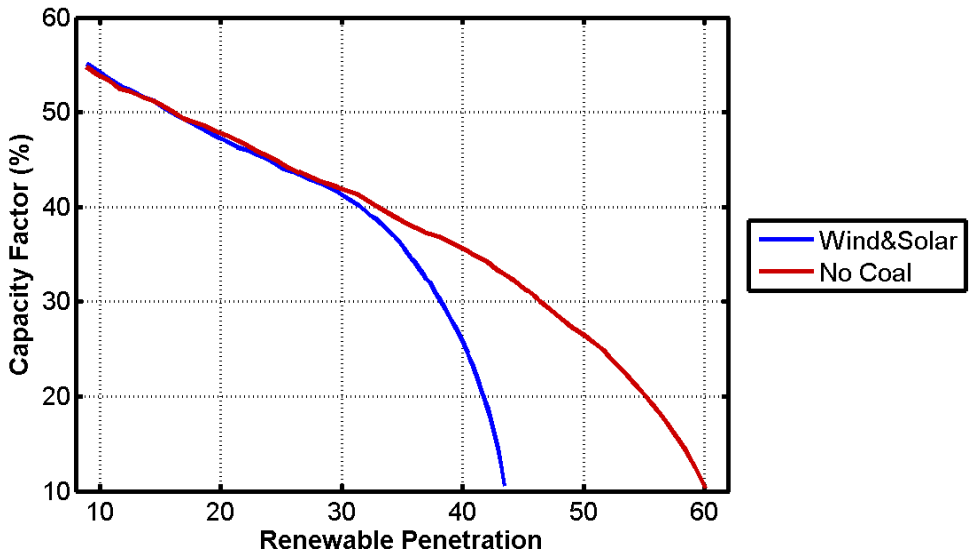

The current baseload generation in California has been installed for many years and is nearly or completely depreciated. As such, the costs to generate from these plants are related only to maintenance and fuel usage. The model assumes that for legacy technologies like nuclear and coal generation there is no capital cost (due to their age it has already been paid back). Thus, to be economically competitive with the current baseload technologies, a resource must be either very inexpensive or provide additional value to the grid (e.g., ancillary service). As a result, replacing coal baseload with load-following initially yields a 20% increase in the system-wide LCOE, compared to the base case with coal baseload (Figure 353). As the renewable penetration increases and the value of enhanced flexibility becomes more important, the LCOE without coal baseload drops below that of the with coal baseload case. The crossing point is at 33.4% renewable penetration.

Figure 353: LCOE Comparison with and without Coal Baseload for 50/50 Wind and Solar Mixture

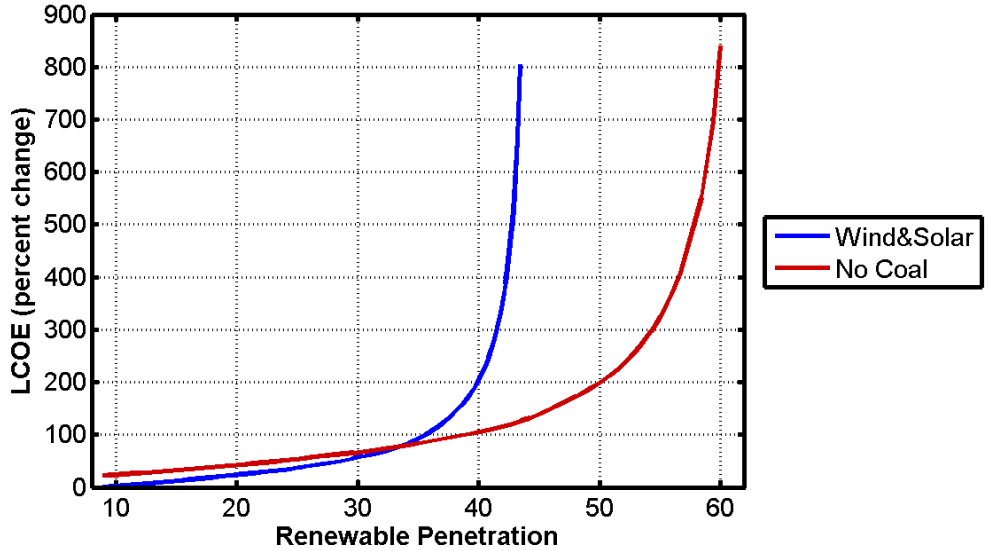

In addition to increasing the achievable renewable penetration and the capacity factor, removing coal baseload will reduce the CO_2 emissions. The analyzed 2005 case resulted in a 21.4% reduction as shown in Figure 354. Removing coal baseload can increase the achievable renewable penetration, and hence, the total CO_2 reduction increases from that of the case with coal baseload from 44.4% to 86.2%.

Figure 354: CO_2 Comparison with and without Coal Baseload for 50/50 Wind and Solar Mixture

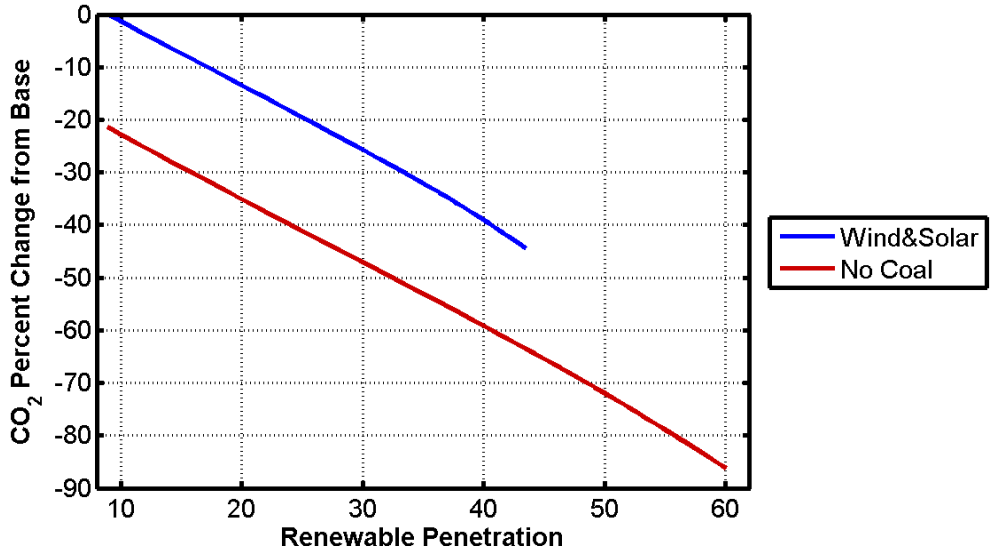

7.2.2.4.3.3.1. Conclusions

- **Removing baseload increases the achievable renewable penetration.** By increasing the percentage of dispatchable generation on the grid there is more system flexibility to accommodate the intermittent renewables signal.
- **Removing coal baseload and replacing it with natural gas plants will significantly lower CO_2 emissions.**
- Removing baseload will initially increase LCOE because of the cost to purchase new load-following generators; however, as the renewable penetration increases the value of added system flexibility will overtake the added equipment investment and can result in a significant LCOE reduction.

Task 7.2.3. California Optimization Results

An optimization of the ideal installation of renewable technologies given the system configuration and constraints is performed. The optimization incrementally increases the installed renewable capacity to satisfy one of four different cost functions. These cost functions include:

1. **Minimum Cost:** The technology that increases the portfolio LCOE the smallest amount is selected each iteration
2. **Maximum Capacity Factor:** The technology that reduces the system-wide capacity factor the least is selected each iteration
3. **Minimum Carbon Dioxide:** The technology that reduces the carbon dioxide emissions the most is selected each iteration. Emissions are strictly from the use of fuel and startup emissions.
4. **Maximum Grid Efficiency:** The technology that increases the system-wide grid efficiency the greatest amount is selected each iteration. The efficiency is based on the fuel to electrical conversion.

7.2.3.1. Optimization Technique

Performing the optimization involves incrementally increasing the capacity of each resource, selecting the optimal technology, and moving to the next increment. The optimal solution is determined by first running the model for all five technologies including rooftop PV, 1-axis PV, 2-axis PV, local wind and regional wind. Next, the results must be adjusted so that they are comparable because 1,000 MW of wind technology does not provide the same energy as 1,000 MW of solar power. As such, results are linearly scaled to the renewable penetration of the technology with the least renewable penetration. Figure 355 and Figure 356 present the technique graphically for the minimum cost and maximum capacity factor approaches, respectively. Notice that the second iteration has cyan lines representing the linear interpolation for that iteration. The circles are the result, given a 1,000 MW increase in capacity,

and the X's represent the interpolated values all aligned at the technology with the lowest penetration increase. For the second iteration of Figure 355 regional wind is the least cost alternative followed by local wind, then 2-axis, 1-axis and rooftop.

Figure 355: Minimum Cost Optimization Technique

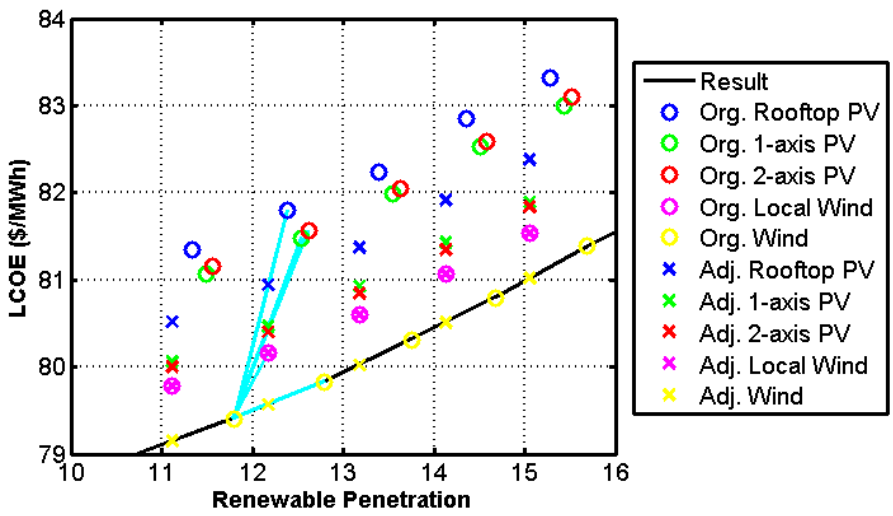

Figure 356: Minimum Cost Optimization Technique

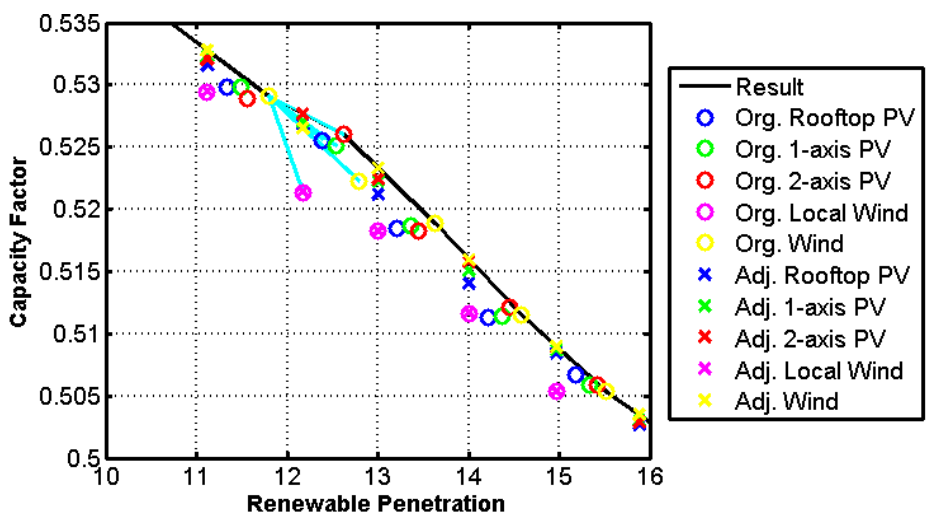

7.2.3.2. Increment Study

It is important to know the sensitivity of the results to the increment selected. Minimum cost optimization was explored for four different increment sizes for renewable capacity: 500, 1,000, 2,000, and 4,000 MW. Figure 357 and Figure 358 present the capacity rollout for wind and solar, respectively. Notice that all four increments result in the exact same results until around 22.5% renewable penetration when there are slight differences in capacity; however, these

discrepancies do not diverge, but rather, converge back on the same solution. There are points during the optimization where the cost, capacity factor, etc. causes a switch in the previously installed resource, while there is an exact location that this crossover will occur, occasionally the increment selection will not allow for the ideal location of the crossover to be selected. However, as the scenario develops it adjusts at other points and the solutions converge.

Figure 357: Installed Capacity of Wind Generation for Minimum Cost Optimization

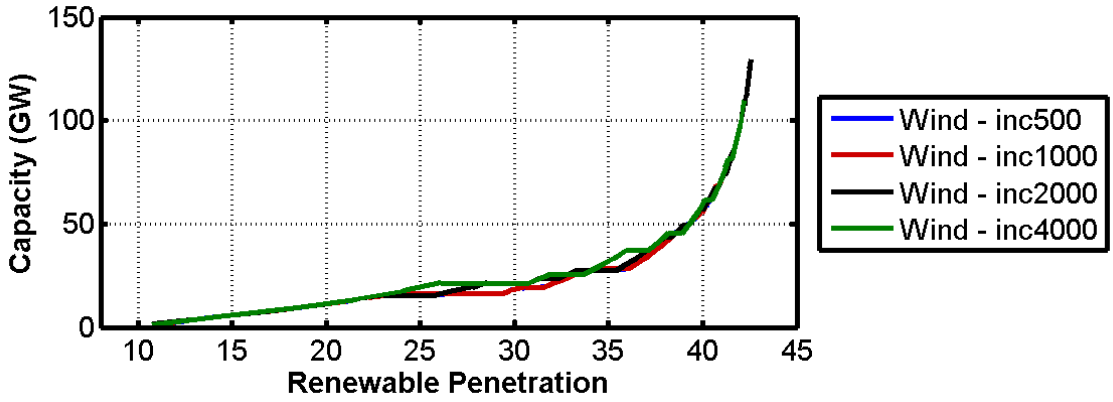

Figure 358: Installed Capacity of Solar Generation Type for Minimum Cost Optimization

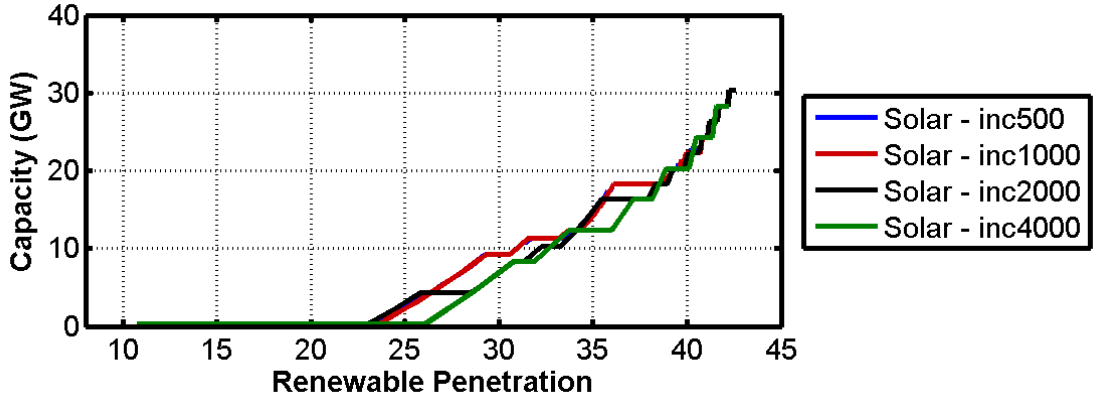

In addition to the capacity of each resource the increment also has a small impact on other aspects. The required installed capacity to achieve a given renewable penetration (Figure 359) has very little effect from the increment.

Figure 359: Installed Renewable Capacity Comparison for Minimum Cost Optimization

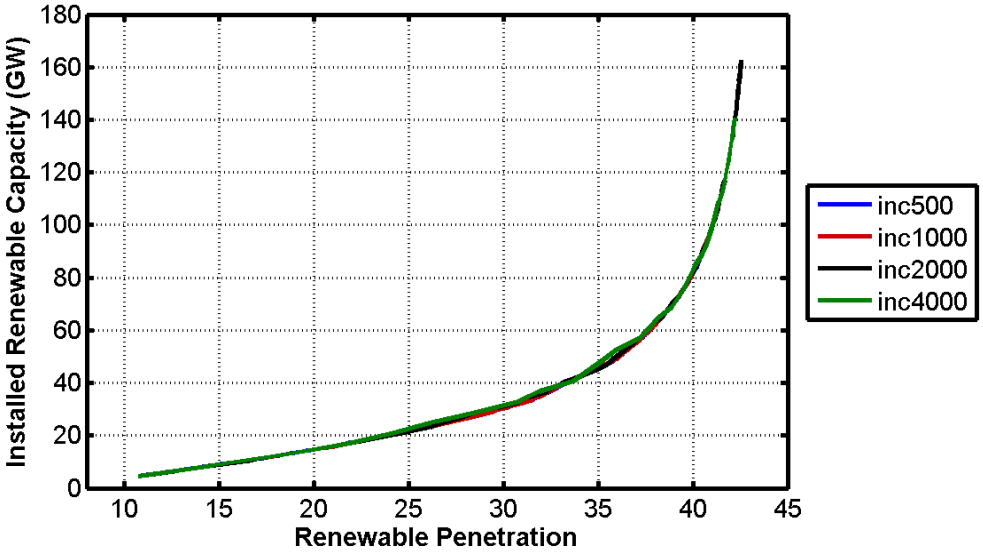

Similarly, different increments have little effect on the capacity factor and LCOE, particularly for 1,000 MW and below as shown in Figure 360 and Figure 361.

Figure 360: Capacity Factor Comparison for Minimum Cost Optimization

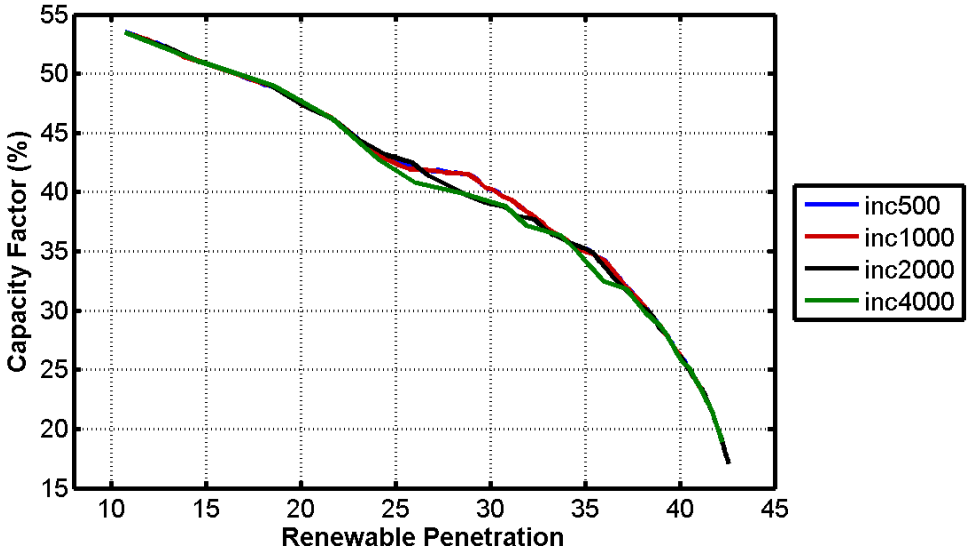

Figure 361: LCOE Comparison for Minimum Cost Optimization

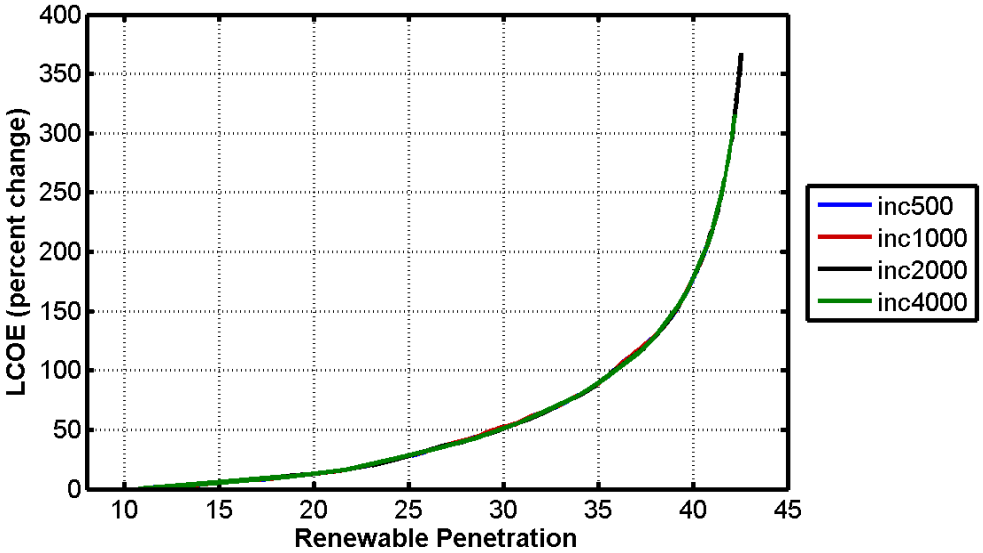

In an effort to minimize computation requirements and local error in the results, an increment of 1,000 MW is used for the optimization. That means that each step will involve installing 1,000 MW of each resource to determine which resource is the optimal and then proceeding to the next iteration.

7.2.3.3. Optimization Results

The regional HiGRID model was run four times one for each of the four different cost functions including minimum cost, maximum capacity factor, minimum carbon dioxide emissions and maximum efficiency. The solver selects from one of five renewable technologies for each iteration (i.e., rooftop PV, 1-axis PV, 2-axis PV, local wind and regional wind). Figure 362 presents the rollout for the minimum cost optimization strategy. Notice that the pattern is wind dominant with the next largest contribution coming from 2-axis PV. Figure 363, Figure 364 and Figure 365 present similar plots for maximum capacity factor, minimum CO_2 emissions and maximum grid efficiency cases.

Figure 362: Installed Capacity for Minimum Cost Optimization Strategy

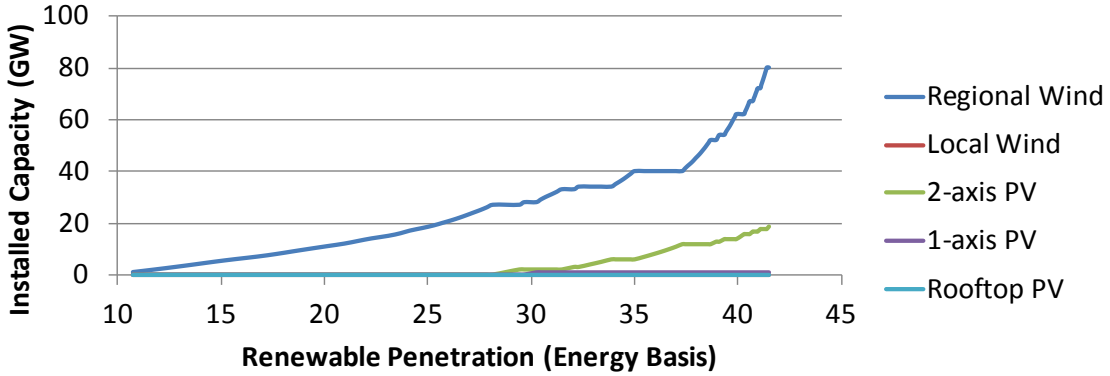

Figure 363: Installed Capacity for Maximum Capacity Factor Optimization Strategy

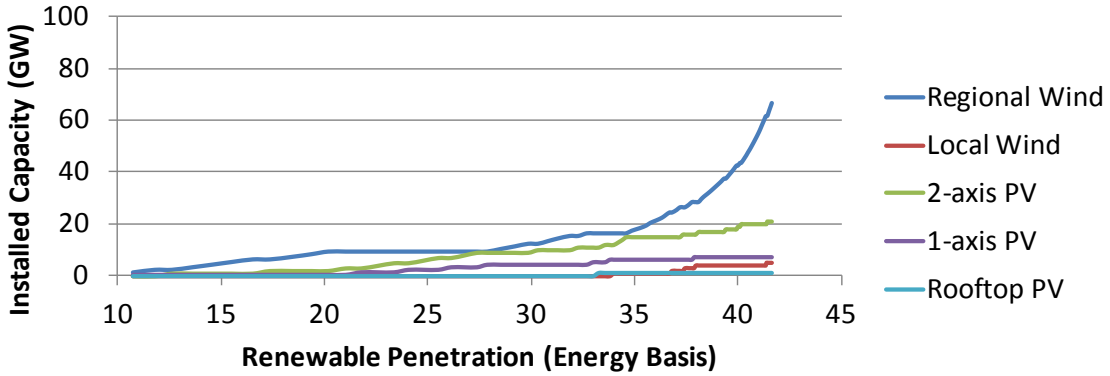

Figure 364: Installed Capacity for Minimum CO_2 Optimization Strategy

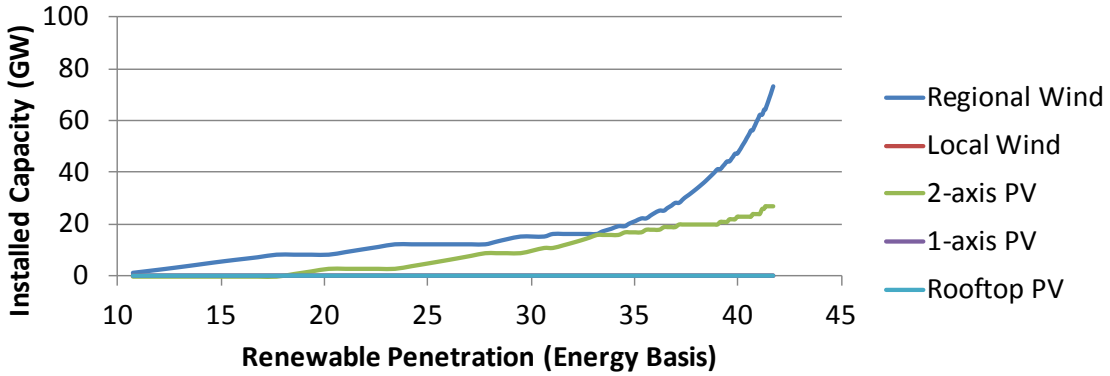

Figure 365: Installed Capacity for Maximum Efficiency Optimization Strategy

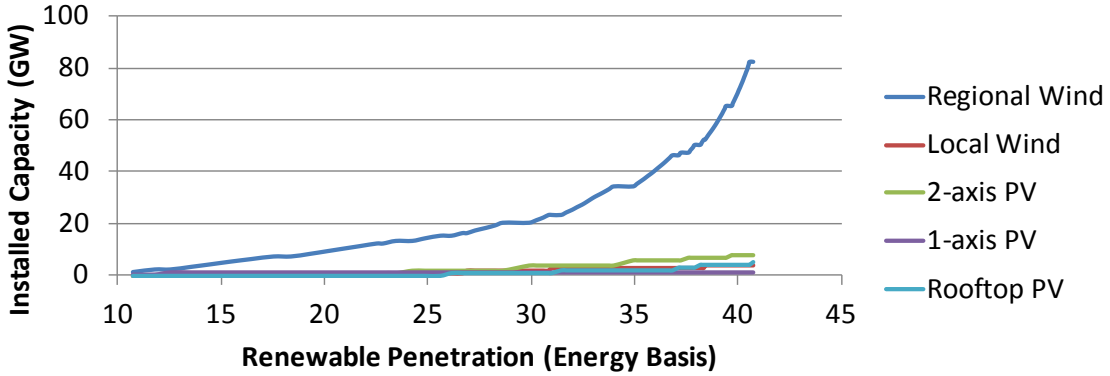

To simplify the previous figures and allow them to be compared, the material can be separated into two groups (i.e., wind and solar) instead of five technology groups. Figure 366 and Figure 367 present the rollout of wind and solar capacity installed for each cost function. Notice that all strategies have more wind than solar and that the cost function determines the optimal time and in what proportion the solar is installed. Notice that the maximum capacity factor and the minimum CO_2 strategies maintain the least amount of wind, in comparison to the maximum efficiency and the minimum cost approaches. The shape and pattern of this finding is repeated often in the results.

Figure 366: Installed Capacity of Wind Generation for Different Cost Functions

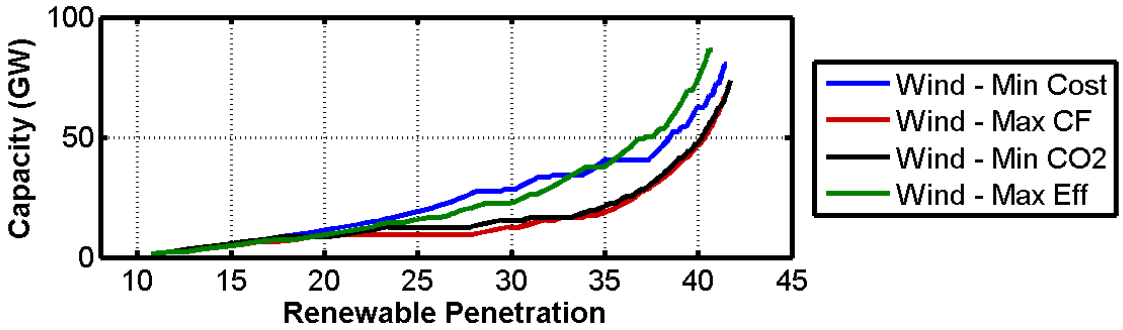

Figure 367: Installed Capacity of Wind Generation for Different Cost Functions

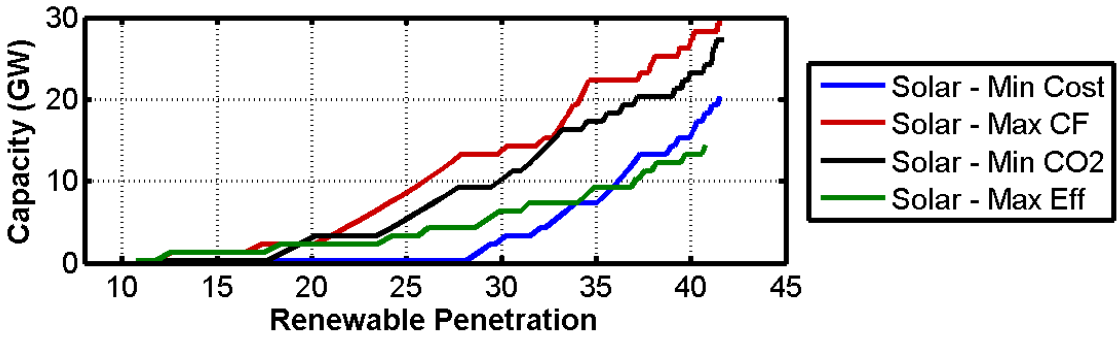

Looking at the installed wind and solar capacity as a ratio presents a unique perspective on the ideal rollout strategies for renewables. Figure 370 presents a ratio of installed capacity for wind and solar. The lines start at the point that additional capacity of solar is installed since all scenarios begin with installation of wind capacity. The minimum cost strategy relies on wind for longest of all strategies and then eventually builds up its solar portfolio. The maximum efficiency strategy nearly always maintains a 5:1 ratio of wind to solar capacity, while the maximum capacity factor and minimum carbon emissions begin around a 5:1 ratio but are most often a 2.5:1 ratio. It is apparent from the previous figures that for California a much larger portion of the installed renewable capacity should come from wind to maintain optimal power mixtures. This will be described in more detail in the following sections.

Figure 368: Optimized Wind to Solar Capacity Ratio for Different Cost Functions

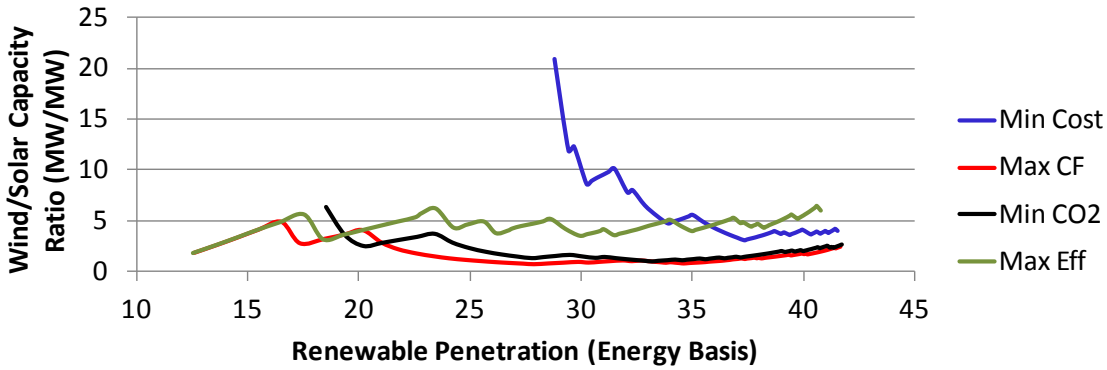

Since 100 iterations were run the total installed capacity of the renewables will be the initial installed capacity of small hydro, geothermal and biomass/biogas plus 100 GW of wind or solar capacity. Figure 369 contains a breakdown of the total installed renewable capacity for the four cost functions. The minimum cost approach and the maximum efficiency approach see an exponential increase in their capacity around 27% renewable penetration (energy basis). While the minimum cost approach converges with the max capacity factor and minimum CO_2, the maximum efficiency does not and results in a lower maximum achievable renewable penetration than the others.

Figure 369: Installed Renewable Capacity Comparison for Different Cost Functions

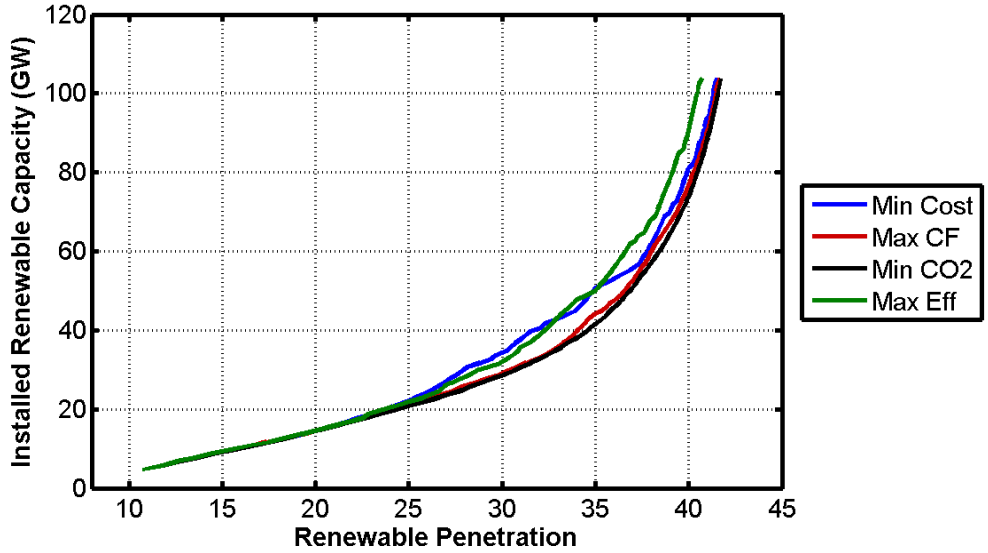

As expected the maximum capacity factor approach has the maximum capacity factor for each point of the analysis. The minimum CO_2 results in the next highest capacity factor..Although all optimization strategies begin the same, the minimum cost and maximum efficiency become nearly 5 points lower at higher renewable penetration.

Figure 370: Capacity Factor Comparison for Different Cost Functions

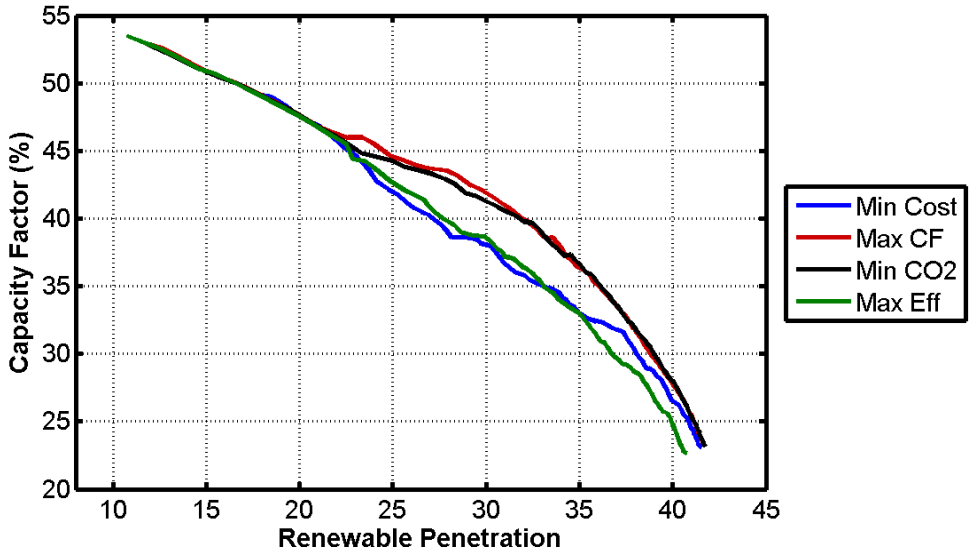

Figure 371 presents the resulting grid fuel to electrical efficiency for each scenario. The overall grid efficiency increases from 35% to nearly 60% as the fuel consumption is decreased by the use of renewable generation. As expected the highest efficiency is achieved by the maximum efficiency strategy. It is difficult to distinguish the overall pattern from Figure 371 so Figure 372

presents the same material that is in Figure 371 but is presented as a function of the percentage difference from the maximum efficiency case.

Figure 371: Grid Fuel to Electrical Efficiency Comparison for Different Cost Functions

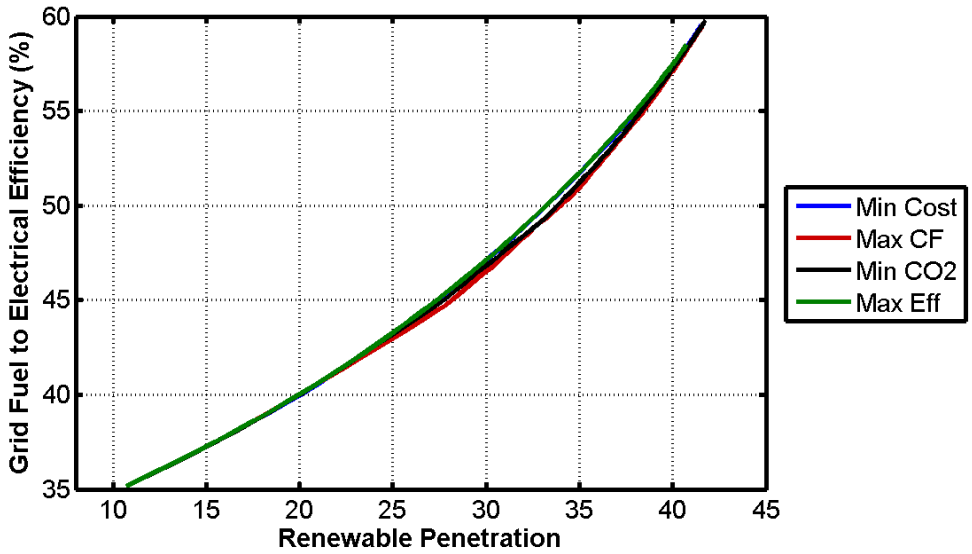

Figure 372: Grid Fuel to Electrical Efficiency Comparison for Different Cost Functions (max efficiency as the base case)

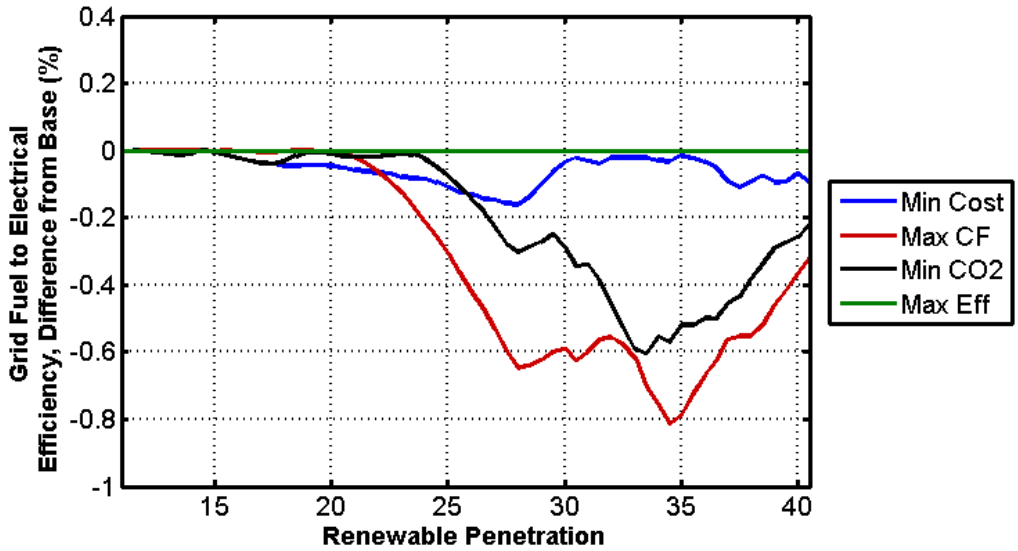

Exploring the resulting excess generation provides another perspective of the tradeoffs for pursuing different strategies as presented in Figure 373. Minimum cost starts with the greatest curtailment and then trades off with maximum efficiency, while the maximum capacity factor and minimum CO_2 have the lowest curtailment.

Figure 373: Curtailment Comparison for Different Cost Functions

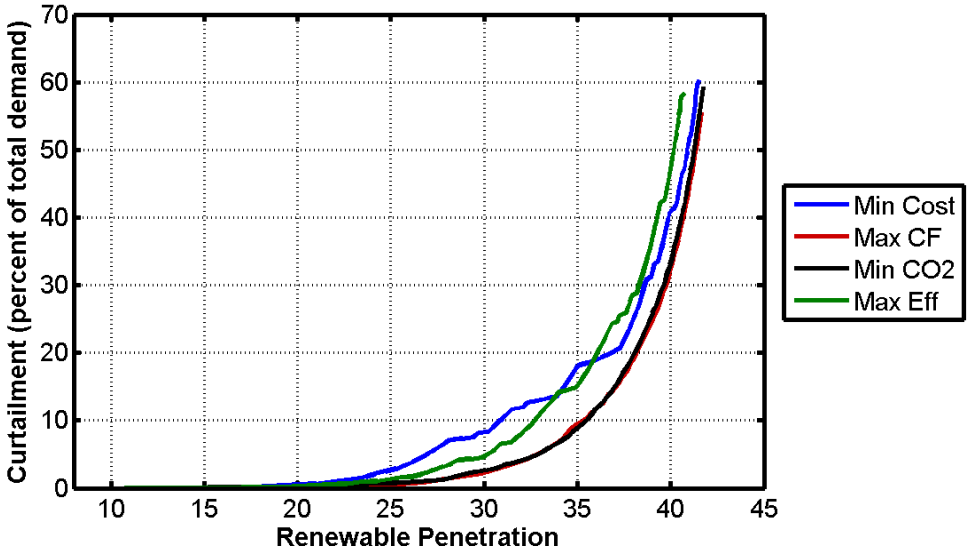

Comparing carbon dioxide emissions is particularly important in the context of California legislation. Figure 374 presents the resulting emissions reductions versus the installed renewable capacity. While most other figures compare the renewable penetration, the carbon emissions compare to the installed capacity, because an increase in renewable generation on an energy basis results in a nearly linear reduction in emissions. As such, carbon reduction optimization is performed on an installed capacity basis (i.e., power basis). The minimum CO_2 emissions strategy results in the lowest CO_2 emissions, as expected.

Figure 374: Carbon Dioxide Reduction versus Capacity (Power Basis) for Different Cost Functions

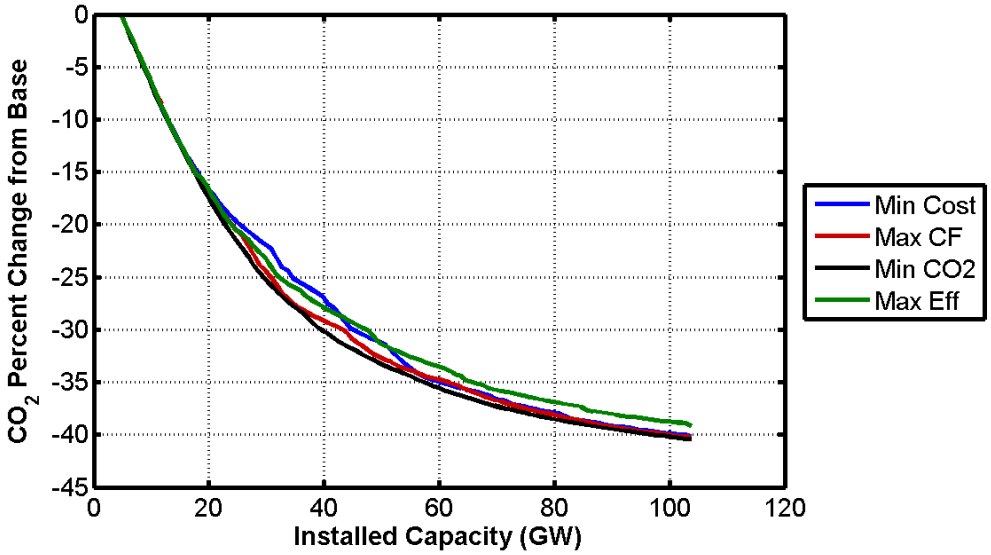

The final cost function is the portfolio LCOE. For each strategy the system-wide LCOE is calculated based on the installed equipment and its operation. The results are shown in Figure 375. Not surprisingly the minimum cost strategy results in the least cost approach followed by the maximum efficiency strategy, then the minimum CO_2 strategy and finally the maximum capacity factor strategy. The minimum cost maintains the most wind initially, which has a lower cost than its solar counterpart then the transition to solar occurs at the time that will minimize the increase to the LCOE.

Figure 375: Curtailment Comparison for Different Cost Functions

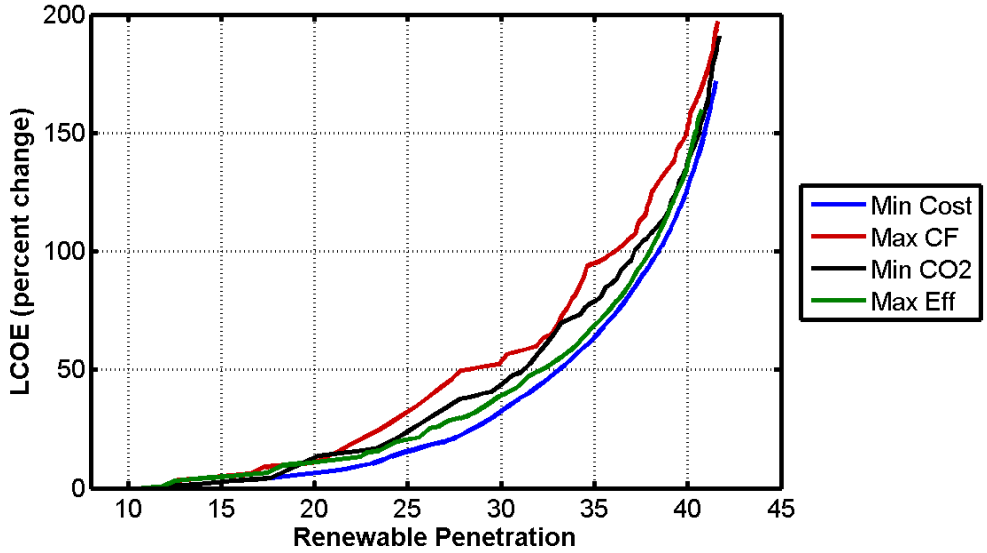

7.2.3.4. *Conclusions*

- Developed robust technique for optimizing renewable rollout strategies based on different cost functions.
- Analyzed the sensitivity to increment selection (i.e., 0.5, 1, 2 and 4 GW) for the optimization and found that the increment has little effect on the results and the results converge on the same values.
    - An increment of 1 GW is selected to minimize computational requirements and local error in the results.
- The optimal wind to solar power mixture varies based on the cost function; however, in all cases more wind should be installed than solar power by at least 2.5 times.
- Selection of a particular cost function has implications for the effects on the rest of the grid.

Table 74: Summary of Optimization Results

Optimization Strategy	Minimum Cost	Maximum Capacity Factor	Minimum CO_2	Maximum Efficiency
Achievable Renewable Penetration	Higher	Higher	Higher	Lower
System-wide Capacity Factor	Lower	Highest	Higher	Lower
Grid Efficiency	Higher	Lower	Lower	Highest
Excess Renewable Generation	Higher	Lower	Lower	Higher
CO_2 Emissions Reduction	Depends on renewable penetration region	Higher	Highest	Lower
Increase in LCOE	Lowest	Highest	2nd Highest	2nd Lowest

Task 7.3. Complementary Technology Integration and Management

As seen from Task 7.2 implementation of high penetrations of renewables becomes challenging from a cost and a performance point of view. Complementary technologies offer an opportunity to help support the integration of renewables and more generally, lower cost, and

increase reliable operation of the grid. The technologies considered in this section are electric energy storage, energy efficiency measures, demand response measures, and electric transportation. Each technology can support in different ways as will be discussed in the following sections.

Task 7.3.1. Energy Storage

With increasing levels of renewable energy, balancing the electrical energy demand becomes more challenging. Energy storage technologies represent one technique to mitigate increased intermittency of renewable generators. These technologies store energy for use at a later time. From a grid perspective, energy is typically stored during a time of low load and used during a time of high load at the expense of an energy penalty due to inefficiencies in charging and discharging an energy storage medium.

7.3.1.1. Introduction

Many storage technologies are available and can be separated into either potential or kinetic energy storage systems. Potential energy storage systems include pumped hydro, which uses the gravitational potential energy of water to store energy, and batteries, which use the chemical potential to store and later generate electricity. Even fuels like gasoline and natural gas are an energy storage medium since they can be stored and used whenever there is demand for their utility. Kinetic energy storage systems include thermal storage, where thermal energy is stored in a thermal mass and insulated from the environment then used later to either generate electricity or provide heating or cooling needs, and compressed air energy storage (CAES), where a fluid, typically air, is compressed and stored in a container (e.g., salt cavern) and then expanded through a turbine to generate electricity when it is needed. Understanding how a system behaves is dependent on its operating characteristics.

7.3.1.1.1. Energy Storage Characteristics

In many ways energy storage systems operate in a similar manner, shifting the load from one time to another. However, each technology has different operating parameters and timescales over which it operates. These parameters uniquely identify each technology type. Ibrahim et.al., developed a list of the most critical evaluation criteria for energy storage systems (Ibrahim, 2008).

- Storage capacity
- Available power
- Depth of discharge or power transmission rate
- Discharge time
- Efficiency
- Durability
- Autonomy
- Costs

- Feasibility and adaptation to the generating source
- Self-discharge
- Mass and volume densities of energy
- Monitoring and control equipment
- Operational constraints
- Reliability
- Environmental aspect
- Other characteristics

As an example of two of these characteristics the following figure shows how each of the technologies compares based on storage capacity (i.e., energy capacity) and available power (i.e., power capacity). Knowing the timescale over which each device operates is important for sizing and selecting the correct technology for your application. The devices in the lower left of Figure 376 have high power output compared to their energy stored so they are best suited to balance fast electricity demand changes, whereas the technologies in the upper right predominantly provide buffering on a longer timescale for large electrical systems. Thus matching the technology to the application is critically important and similarly, when modeling energy storage technologies, incorporating the essential evaluation criteria is pivotal to developing an accurate model.

Figure 376: Power Capacity versus Energy Capacity for Various Energy Storage Devices

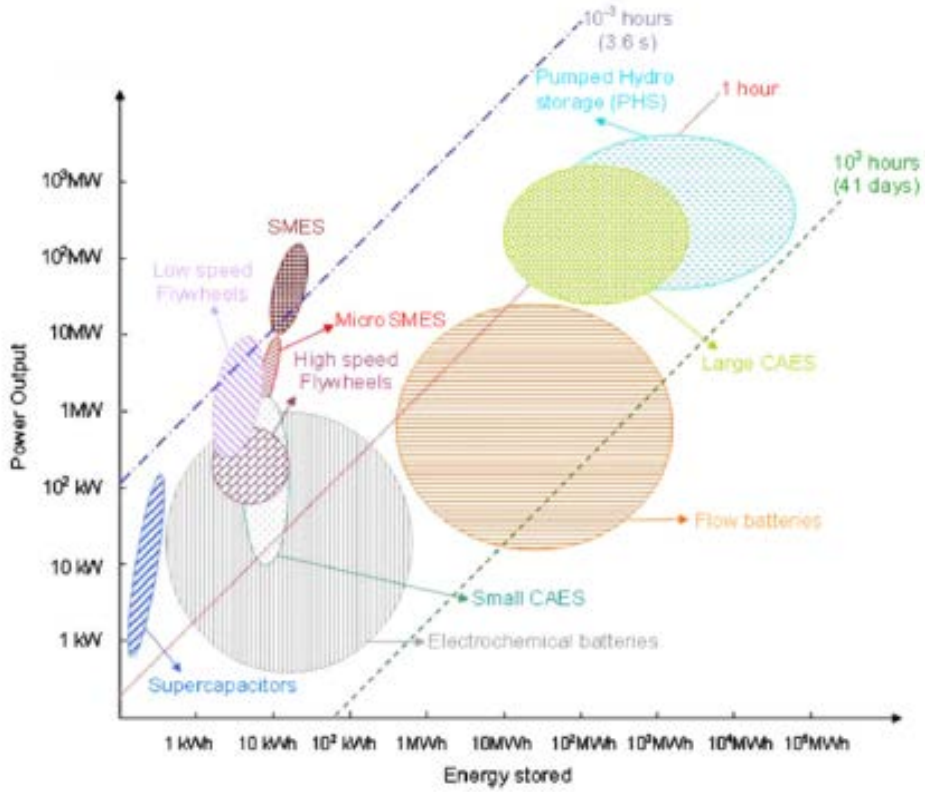

Source: Ibrahim, 2008

7.3.1.2. Approach

Hourly renewable and hourly load data are used to determine the electricity demand signal. The goal of this model is to explore the dispatch of energy storage systems and the resulting impacts on a grid system. Based on these model constraints, there is a subset of energy storage criteria that are important for the modeling of energy storage devices. The important characteristics to incorporate into an hourly timescale model include storage capacity, available power, discharge time, depth of discharge, efficiency, durability, and costs. An energy storage model was developed that integrates these characteristics and is presented in Task 3.2.8.

7.3.1.3. UCI Campus Results

7.3.1.3.1. Description of Cases

The energy storage model used to analyze the effects of implementing energy storage on the UCI campus is the same as that used to analyze grid-wide effects, but applied at the scale of the UCI campus. A description of this model is included in Task 3.2.8. The key difference between the application of the model at the grid-wide scale and the scale of the UCI campus are as follows:

1. The only energy storage technology considered for the UCI campus is the Vanadium-Redox flow battery (VFB). Pumped Hydroelectric Storage (PHS) and Compressed Air Energy Storage (CAES), which are the other two types included in the general energy storage model, are large scale, geographically constrained systems. Therefore, it would not make sense to apply these technologies exclusively for a smaller scale system such as the UCI campus.

50. The UCI campus analysis includes two operating strategies. The first is similar to that used in the grid-wide analysis, where the energy storage system acts to smooth the balance profile as much as possible, responding to the effects of renewable power generation. The second is similar to the first, but takes into consideration the priority of preventing the gas-turbine from tripping offline. The details of this application will be described along with the relevant cases in the following subsections.

This section will describe the cases examined to determine the effect of energy storage on the behavior of the UCI campus at increased renewable penetration levels.

7.3.1.3.1.1. Base Case without Energy Storage

To examine the effect of energy storage on the UCI campus, a base case is first established to determine the performance of campus resources without any energy storage measures present at a given renewable penetration level. The base case used in this analysis is the same as the 'Base Chiller Dispatch Case' described in the chiller dispatch sensitivity analysis (Task 3.4.3), since this case represents current operation of campus resources.

7.3.1.3.1.2. Demand Profile Smoothing (Standard) Energy Storage Cases

This analysis examines three standard energy storage cases that utilize different sizes of energy storage, applied solely to smooth the balance profile. In this application, the system will charge when the balance power is low (due to low load and/or high renewable generation) and discharge to level periods when the balance power is high. The size of the energy storage system in each case is defined by a power and energy capacity. The power capacity dictates the maximum charging and discharging power of the system, determining the extent to which the system can increase or decrease the balance at every hour. The energy capacity dictates how much energy the system can store.

This analysis varies the power capacity of the system and ties the energy capacity of the system to it by use of a rated discharge time. The rated discharge time is the amount of time that a fully charged system can discharge power at its discharge power capacity before it is emptied and is another method for expressing the energy capacity of the system. For example, an energy storage system with a discharge power capacity of 2 MW and a rated discharge time of 2 hours has an energy capacity of 4 MWh. Therefore, by varying the power capacity in these cases, the energy capacity of the system is also varied.

The power capacity is varied as a fraction of the peak raw campus load demand, which was 24.8 MW for the load data set used in this analysis. A summary of the system sizes for the three standard energy storage cases are as follows:

Table 75: Parameters for Standard Energy Storage Cases

Case	Power Capacity [MW]	Rated Discharge Time [h]	Energy Capacity [MWh]
20% of Peak Load	4.96	4	19.84
50% of Peak Load	12.40	4	49.60
100% of Peak Load	24.80	4	99.20

7.3.1.3.1.3. Demand Profile Smoothing w/GT Trip Avoidance (Modified) Energy Storage Case

This case applies energy storage on the UCI campus to smooth the balance profile, but with the added restriction of avoiding the tripping of the on-campus gas turbine. The on-campus gas turbine will trip when the balance is reduced below its minimum operating power plus the minimum import margin dictated by the utility. If renewable generation during a given hour will reduce the balance to levels that would cause the gas turbine to trip offline, the energy storage system focuses on charging in an attempt to charge and therefore increase the load to prevent the trip if possible. The occurrence of a potential gas turbine trip increases the priority to charge at that time compared to a simple drop in the balance profile. If the energy storage system is unable to prevent the trip, renewable generation will be curtailed to prevent the trip. Additionally, the energy storage system will not discharge energy to reduce the load to the extent that would create a trip event.

For this case, only the large energy storage size (100% of Peak Load) is used and contrasted with the standard 100% of Peak Load case.

7.3.1.3.1.4. Renewable Mix

The effect of complementary technologies such as chiller dispatch in this case will be carried out with the gas turbine not being allowed to trip offline. Since this scenario represents a more practical operating scheme under current standards, the ability of complementary technologies to mitigate potential issues can be more clearly examined.

Additionally, the renewable mix used for different renewable penetration levels parallels that used by the CPUC rollout strategy for attaining the 33% renewable penetration level, scaled down to the community level. The effective renewable capacities used are as follows:

Table 76: Renewable Mix used for Complementary Technologies

Targeted Renewable Penetration	Regional Wind Capacity [MW]	Local Fixed PV Capacity [MW]	Regional 1-Axis PV Capacity [MW]	Base Load Renewable Capacity [MW]	Local Wind Capacity [MW]
0	0	0	0	0	0
10.47 %	0.8655	0.0559	0.1134	1.6245	0
20.40 %	3.7644	0.3179	0.6455	2.2477	0
33.36 %	8.0111	1.3049	2.6493	2.4387	0

50.79 %	17.1297	2.2842	4.6376	2.4387	0

The base load renewables include geothermal, biomass and small hydroelectric. The 50.79% targeted penetration uses an extension of the 33% mix by energy. The targeted renewable penetration level represents the penetration level achieved with the corresponding capacity mix if all of the energy obtained from renewables is used to serve the load demand (i.e. no curtailment).

7.3.1.3.2. Analysis

7.3.1.3.2.1. Effect on Renewable Capacity Requirements

The progression of the required renewable capacity with renewable penetration level for the different demand response cases is displayed in Figure 377. The "100% P-T" case represents the 100% Peak Load case with avoidance of additional gas turbine trips.

Figure 377: Renewable Capacity vs. Renewable Penetration

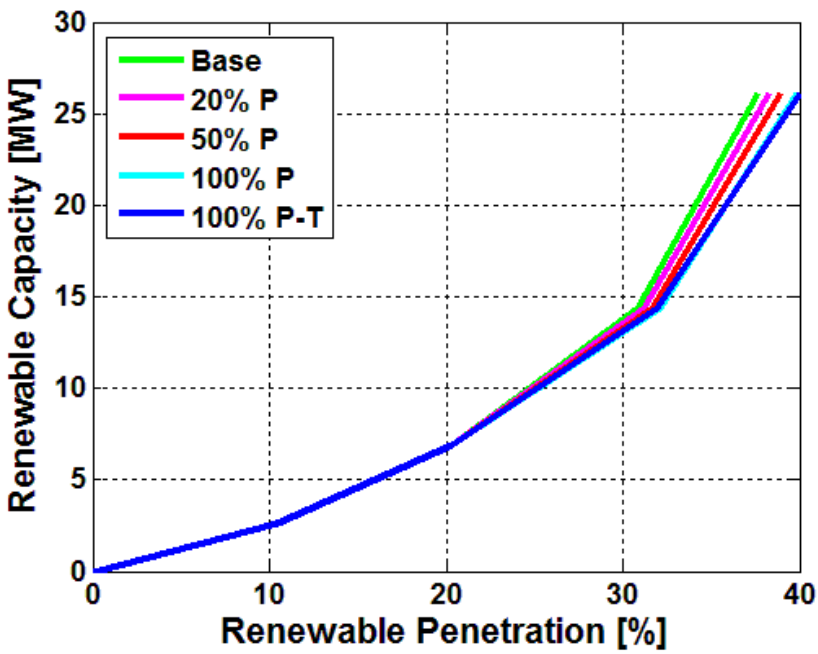

Similar to the trends displayed in the other complementary technology analyses, the total renewable capacity increases in an exponential manner with renewable penetration due to curtailment. None of the cases reach the targeted renewable penetration level dictated by the installed renewable capacity. This occurs for the same reasons as discussed in the other sensitivity analyses.

The effect of implementing energy storage on the UCI campus on the renewable capacity required to reach a given renewable penetration is dependent on the following factors:

1. **The efficiency penalty associated with using the energy storage system.** When a unit of energy is stored and discharged, a portion of it is lost to inefficiencies of the system.

Therefore, the amount available for discharge will be lower than the amount that was used to charge the system. To provide a given amount of energy towards serving the raw load demand, more generation is needed to overcome these inefficiencies. This essentially acts to increase the load demand by the amount consumed by these inefficiencies, and decreases the renewable penetration level for a given renewable energy contribution. It is important to note that only the fraction of energy that is shifted by the system actually passes through it and the efficiency penalty is only applied to this fraction and not the entire load demand.

51. **The smoothing of the balance profile allows renewable power that would otherwise be curtailed to contribute towards serving the load demand.** Energy storage can store excess renewable energy and discharge it during other periods, allowing this energy to contribute towards serving the load. This serves to increase the renewable penetration level for a given installed renewable capacity.

In this analysis, the energy storage system is used to smooth the balance profile, which is a more aggressive application of the system compared to using it for minimizing renewable curtailment only. This application indirectly accomplishes the latter, but will also use energy from non-renewable sources if needed.

At low renewable penetration levels when renewable curtailment is minimal or non-existent, the energy storage cases require more renewable capacity to reach a given renewable penetration level compared to the base case, but only by a very small amount. At these levels, the only factor present is the efficiency penalty. However, the increase in the load demand is very small compared to the energy of the load demand since only a small portion of the energy obtained is stored and discharged by the energy storage system. For the case with the largest energy storage size at the 10.47% targeted renewable penetration level, only 6.8% of the energy of the load passes through the storage system. Since the VFB system is assumed to have a round trip efficiency of 85%, the increase in the energy load demand for this case is only 1.03%. Therefore, the increase in required renewable capacity to reach a given renewable penetration level is very minimal.

At high renewable penetration levels when curtailment is significant, the energy storage cases require less renewable capacity to reach a given renewable penetration level compared to the base case. To the extent possible, the energy storage system charges during periods of low balance levels which tend to correspond to periods of high renewable power generation. This allows the campus to make use of otherwise curtailed energy. The system then discharges this energy during periods of high balance levels, which correspond to periods of low renewable power generation. The increase in the amount of renewable energy that is able to serve the load demand overpowers the increase in the load demand due to the efficiency penalty at high renewable penetration levels. Overall, the case with the largest energy storage size is able to increase the renewable penetration level by about 2.5% at the high end compared to the base case for the same installed renewable capacity.

7.3.1.3.2.2. Effect on Surplus Renewable Generation

The previous trends for the required renewable capacity are reflected in the progression of the surplus renewable fraction with renewable penetration level, presented for the different energy storage cases in Figure 378:

Figure 378: Surplus Renewable Fraction vs. Renewable Penetration Level

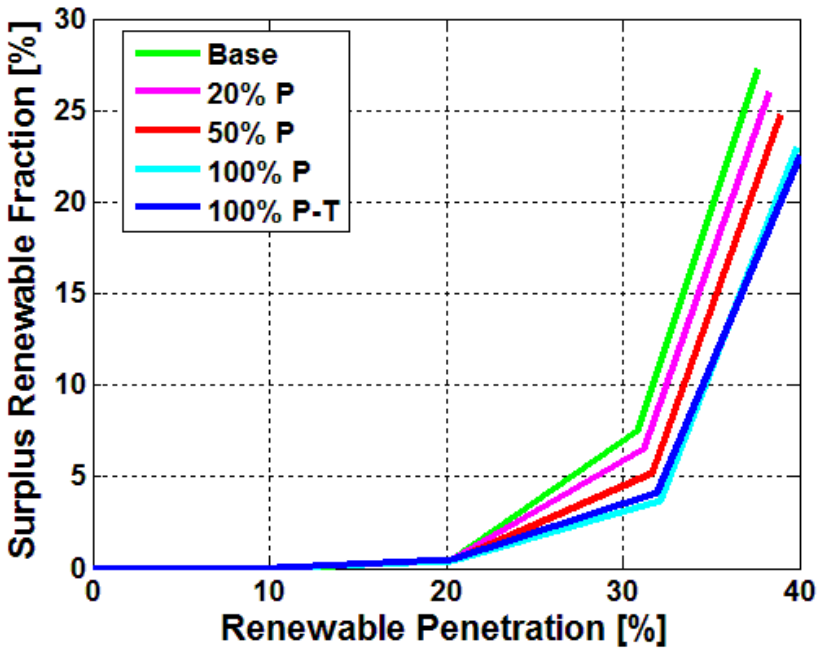

At low renewable penetration levels, curtailment is minimal or non-existent and energy storage reduces this amount where possible, but overall the differences between the cases are minimal. At high renewable penetration levels when curtailment in the base case is significant due to high variable renewable capacities, energy storage is able to reduce the surplus renewable fraction significantly. The cases with larger energy storage sizes are able to reduce curtailment by a larger extent, comparatively. At the 33.36% targeted renewable penetration, the base case curtails 7.5% of renewable generation and the actual renewable penetration level is only 30.85%. The 100% peak load energy storage case curtails only 3.7% of renewable generation and the actual renewable penetration level is only reduced to 32.12%. Smaller energy storage sizes garner smaller benefits.

The use of energy storage with the sizes considered in this analysis, however, is limited in their ability to mitigate renewable curtailment. At higher renewable penetration levels, the renewable capacity becomes very large. Therefore, during periods of peak renewable generation, the renewable power in excess of available load can exceed the power capacity of the energy storage system. This is especially applicable at the highest targeted renewable penetration level discussed in this analysis. Additionally, the energy storage systems are limited in the amount of energy that can be stored. Even if the excess renewable generation is within the power capacity of the system, it cannot be stored if the system is fully charged. Similarly, the energy storage system may not be able to reduce the balance over the full peak period since not enough energy

may be stored in the system to do so. The result is that with fixed energy storage sizes, curtailment still increases exponentially but the point at which this happens is delayed to a higher renewable penetration level. For energy storage to maintain renewable curtailment at or below fixed levels, the power and energy capacity of the system must be increased at higher renewable penetration levels.

At the high renewable penetration levels, there is also a very slight difference between the standard and modified 100% peak load energy storage cases. Initially, the standard case exhibits slightly lower curtailment levels than the modified case. This occurs since in the modified case, the energy storage system operates in a slightly different manner. Curtailment occurs when balance levels drop to levels that would cause the gas turbine to trip offline. The modified energy storage case highly prioritizes discharging at these times to prevent gas turbine trips, after which any remaining energy can be discharged to smooth the balance profile. In doing so, the energy storage system may exhaust itself by expending its stored energy to address more severe drops in the balance profile and be rendered ill equipped to address subsequent smaller events. The result is to allow smaller but more frequent drops in the balance profile that collectively causes more curtailment than the standard case which focuses on all balance profile drops proportional to severity.

As the renewable penetration level increases to very high levels, however, the trend is reversed slightly. For the 50.79% targeted renewable penetration level, the standard case exhibits slightly higher curtailment than the modified case. At this penetration level, the renewable capacity is so high that drops in the balance profile are much more severe. The energy storage systems in both cases are frequently exhausted, and focusing on mitigating more severe events is able to slightly reduce the curtailment levels.

Overall, however, the standard and modified cases only exhibit marginal differences in curtailment levels.

7.3.1.3.2.3. Effect on the Gas Turbine Capacity Factor

The progression of the gas turbine capacity factor with renewable penetration level for the different demand response cases is presented in Figure 379:

Figure 379: GT Capacity Factor vs. Renewable Penetration Level

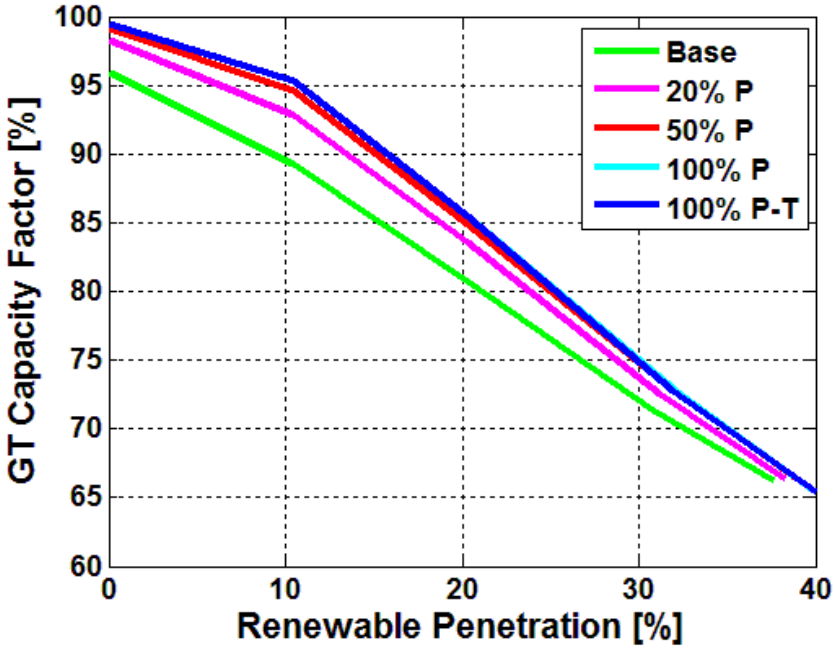

The implementation of energy storage of any of the sizes considered here is able to increase the capacity factor of the gas turbine compared to the base case. Cases that utilize larger energy storage sizes exhibit the largest benefit in terms of capacity factor. The increase in capacity factor compared to the base case is largest at lower renewable penetration levels, reaching as high as about 6% over the base case at the 10.47% targeted renewable penetration level and steadily decreasing to zero as the renewable penetration level increases.

The increase in gas turbine capacity factor is primarily due to the fact that when applied for balance profile smoothing, the energy storage system will attempt to charge during periods when the balance is low. On a day-to-day basis, this raises the minimum balance levels that the gas turbine and imports have to meet, allowing the gas turbine to operate above its minimum power levels. On the other hand, the energy storage system will discharge when the balance levels are high. However, the gas turbine has a maximum power level of 13.5 MW, the average load is typically higher than this amount for most of the year. Therefore any decrease in balance levels due to the discharging of the storage system that does not decrease the balance below 13.5 MW will not affect the gas turbine capacity factor. The net effect is to increase the daily minimum gas turbine power without extensively decreasing the daily maximum gas turbine power, increasing the gas turbine capacity factor. Naturally, energy storage systems with larger power and energy capacities are able to increase the daily minimum gas turbine power levels to larger extents and exhibit larger increases in the gas turbine capacity factor.

However, the capacity factor benefit of using energy storage in this manner diminishes as the renewable penetration level increases. By the 30% renewable penetration level, the increase in capacity factor drops to about 3% and continues to decrease as the renewable penetration level is increased. This occurs because as the renewable penetration level increases, large renewable

capacities cause large drops in balance levels. These drops are large enough to render the energy storage system unable to increase the balance levels above the minimum gas turbine power plus the import margin due to power capacity limitations or insufficient stored energy for many hours out of the year. Therefore, the gas turbine is restrained to operating at minimum power for most of the time. Additionally, in an attempt to smooth the balance profile, the energy storage system must discharge and decrease the balance levels where appropriate. Since balance levels are already significantly reduced due to high renewable capacities, these discharge periods do not allow the gas turbine to operate at full capacity as it did at low renewable penetration levels. While still able to garner increases in capacity factor compared to the base case, these factors contribute to decreasing the extent of this benefit at higher renewable penetration levels. Energy storage systems with larger power and energy capacities are required to maintain the benefit of using these systems in terms of increasing gas turbine capacity factor.

An interesting result is to note that the standard and modified cases show essentially no difference in terms of gas turbine capacity factor at any renewable penetration level. This is in spite of the fact that the modified case specifically focuses on preventing gas turbine trips. This result occurs because while the energy storage systems may operate slightly differently in these cases, the net effect on gas turbine capacity factor is the same. The modified case prevents severe drops in gas turbine power to the extent possible at any given hour but exhausts the system in doing so and allows more but smaller drops in the gas turbine power. The standard case does not prevent the severe drops as effectively, but therefore has enough energy stored to prevent turndown of the gas turbine due to less severe drops. The net effect in this case is similar.

These trends are also reflected in the behavior of the HRSG contribution towards serving the heating demand as presented for the different energy storage cases at different renewable penetration levels in Figure 380:

Figure 380: HRSG Contribution vs. Renewable Penetration Level

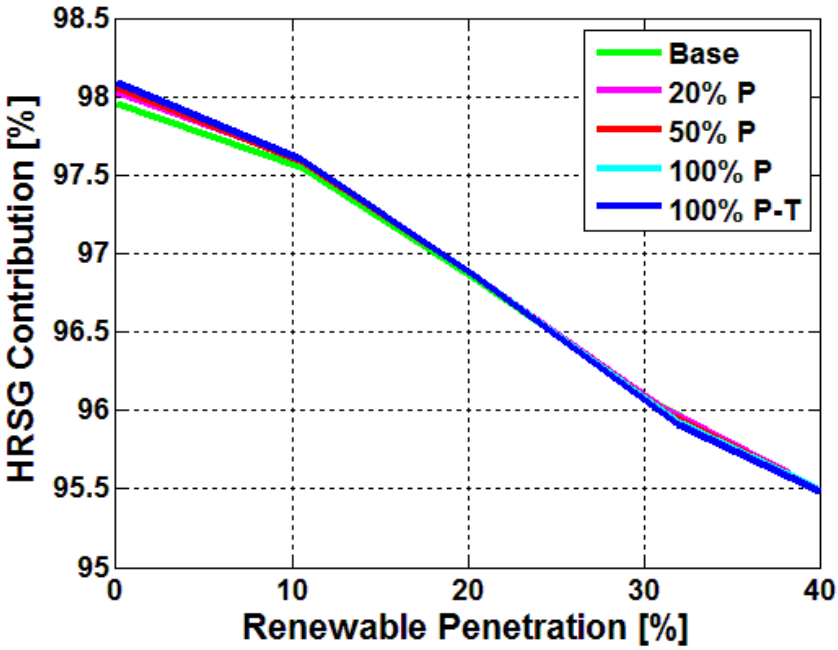

The contribution of the HRSG towards serving the heating demand of the UCI campus is not significantly altered with the implementation of electric energy storage of any size at essentially all of the renewable penetration levels compared to the base case. This occurs despite the fact that energy storage increases the capacity factor of the gas turbine, allowing more heat to be available for contributing towards serving the heating demand.

This trend occurs because in the base case, the contribution of the HRSG towards meeting the heating demand of the campus is not limited by the total availability of waste heat from the gas turbine throughout the year. Rather, it is limited by the fact that there is too much excess heat available during many hours of the year and there is no method for storing this heat for use at different times of the day when the available heat is insufficient to meet the demand. Energy storage increases the amount of heat available by increasing the gas turbine power, but this tends to happen during times when there is already excess waste heat available from the gas turbine. Therefore, the additional waste heat does not contribute to serving the heating demand.

Slight differences are present at different renewable penetration levels. At low renewable penetration levels, the HRSG contribution is higher for the energy storage cases. Larger energy storage sizes garner increased contributions from the HRSG towards serving the heating demand. This occurs because increases in gas turbine power more frequently occur when excess heat is not available. At high renewable penetration levels, this trend reverses as the increases in gas turbine power occur when excess heat is already available and decreases in gas turbine power during storage discharges reduce the amount of heat available during those hours.

Overall, however, the HRSG contribution towards serving the heating demand is not significantly affected by the use of electric energy storage.

7.3.1.3.2.4. Effect on the Import Power Signal

The use of energy storage also modifies the properties of the import power profile to the campus and therefore influences how the campus affects the utility grid when attaining higher renewable penetration levels. The distribution of the import power profile for the different demand response cases is displayed in Figure 381 for a low renewable penetration level (10.47% targeted penetration) and in Figure 382 for a high renewable penetration level (50.79% targeted penetration):

Figure 381: Import Power Distribution: 10.47% Target Penetration

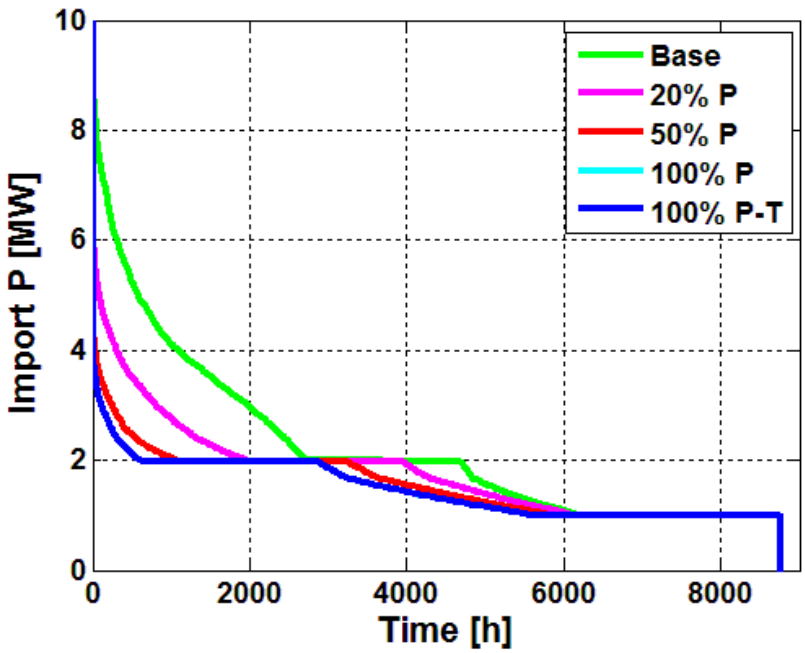

Figure 382: Import Power Distribution: 50.79% Target Penetration

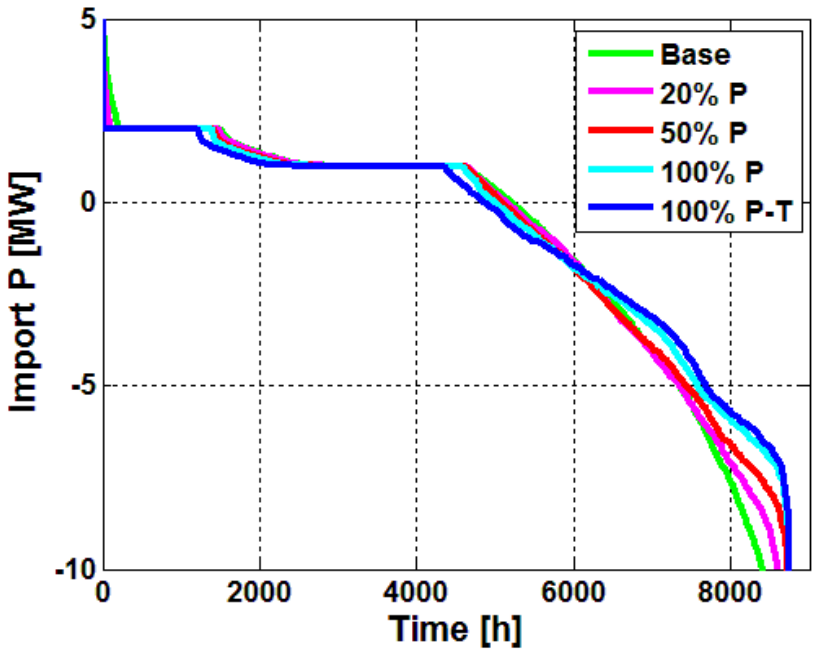

For a target renewable penetration level of 10.47%, the import power restriction for the campus is not violated for any of the cases. This is expected as the base case shows no violations and the implementation of energy storage acts to increase the daily minimum balance levels and consequently import power levels. The use of energy storage also decreases import power levels for many hours of the year, and overall decreases the total amount of imported energy to the campus. This occurs since energy storage is able to decrease peak balance levels and allow a larger fraction of the load during these times to be met by the on-campus gas turbine. Additionally, the minimum balance levels at this renewable penetration are not typically above the maximum power of the gas turbine, therefore increasing the minimum load level does not typically increase import power levels. This implies a decreased reliance on the electric utility for meeting the campus load demand.

At higher renewable penetration levels, the import power distribution changes significantly. For a target renewable penetration of 50.79%, all cases exhibit violations of the import power restriction for the campus for a significant number of hours out of the year. The cases that utilize energy storage with larger power capacities violate the import power restrictions for more hours compared to the lower sizes. The base, 20% of peak load, 50% of peak load, 100% of peak load standard and 100% of peak load modified cases violate the import power restriction for 4136, 4105, 4138, 4167, and 4402 hours respectively. In the standard cases, the energy storage system will respond by charging/discharging to valleys and peaks in the balance signal proportional to severity. Charging will be highest when balance levels are lowest and vice versa. At this renewable penetration level, however, the renewable capacity is so high that all of the drops in balance levels are severe. For the standard cases, the energy storage system will attempt to alleviate these drops by charging to larger extents but are often unable to do so to a large extent due to power or energy capacity limitations. The energy storage system is filled in

the process, rendering it unable to raise load levels in subsequent hours. With higher power capacities, however, the system will operate differently in that it will attempt to level larger drops in the balance profile since it has the capability to do so. This causes the system to exhaust itself more often without necessarily restoring import power levels to above the minimum restriction. When energy is expended in this manner, less energy is available for addressing hours when the import power could be restored to comply with the restriction. This is especially true for the modified case, which prioritizes more severe drops in the balance profile more so than the standard cases. The smaller energy storage cases focus on addressing smaller drops in the balance profile and are able to comply with the minimum import restriction for more hours out of the year.

This is also evidenced by the fact that the larger energy storage cases are able to reduce maximum export power levels and the number of hours of high export power compared to the cases with smaller energy storage sizes. This is expected from the trends displayed for the effect of energy storage on curtailment as described previously. Overall, energy storage sizes with larger power capacities reduce excess power levels but tend to increase the number of hours of excess power by a small amount.

The implementation of energy storage also has effects on the maximum import power, as displayed for the different cases with renewable penetration level in Figure 383:

Figure 383: Maximum Import Power vs. Renewable Penetration Level – Uncoordinated Dispatch

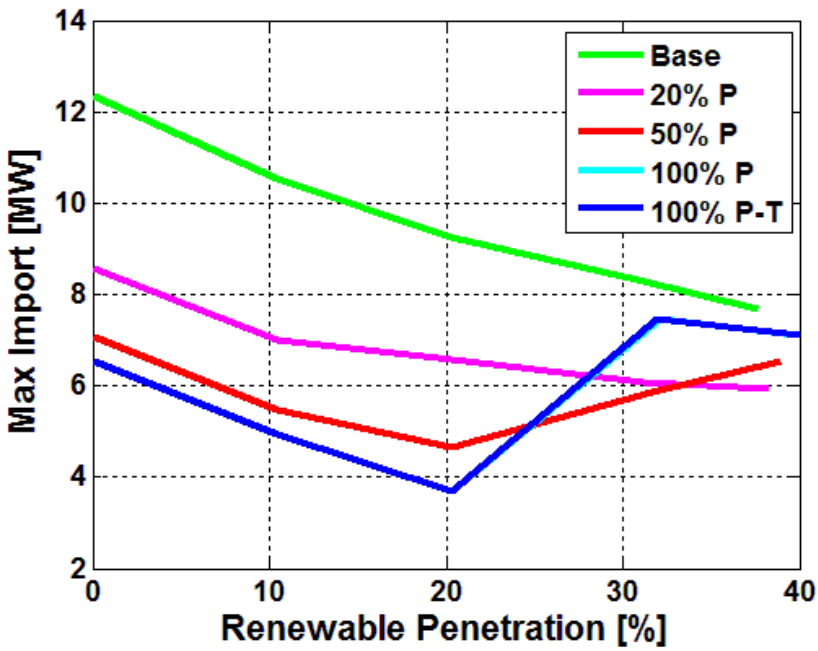

The first aspect to notice is that the maximum annual import level does not monotonically decrease with increasing the size of the energy storage system for all renewable penetration levels. At renewable penetration levels up to about 24%, larger energy storage systems reduce the maximum import power. By the 37% renewable penetration level, both the 50% and 100% of peak load cases exhibit higher annual import power levels than the 20% of peak load case. The

maximum import power level of the 100% of peak load case is almost as high as that of the base case.

This occurs exclusively due to the fact that with the base chiller dispatch case used in this analysis, the operations of the energy storage system and that of the chiller / TES system are not fully coordinated. With the base chiller dispatch strategy, the chillers are activated at 10 pm and shut down at 10 am with the only exception being the occurrence of a potential gas turbine trip, in which case the chillers will activate to prevent the trip. Otherwise, the chillers do not respond to the behavior of other complementary technologies.

Under this dispatch strategy, however, there exist a handful of hours out of the year where the operation of the energy storage system and chillers interfere with each other. The displayed trend occurs when the energy storage system charges during a particular hour to level a drop in the balance profile without knowledge that such an hour falls within the chiller activation window and the introduction of the cooling load would mitigate the drop in the balance profile anyway. Therefore, during that hour the load due to charging the energy storage system and the cooling load are accidentally stacked on top of each other, creating higher than necessary balance levels. Fortunately, this event only occurs for very few hours out of the year in this case and the chiller dispatch does not regularly interfere with the operation of the energy storage system, but only one occurrence is needed to raise the annual maximum import levels. However, only one hour of high import levels are required to incur a large demand charge, which is the case when the maximum import power level starts to increase after a certain renewable penetration level. This behavior occurs for all of the energy storage sizes for a small amount of hours out of the year, but is displayed with larger energy storage sizes since the power capacity of these systems, in addition to the chiller load, is able to significantly increase the load demand above levels experienced during the rest of the year.

For comparison, the progression of the maximum import power with renewable penetration level for the different energy storage cases using the free chiller dispatch strategy, which allows the operations of the chiller/TES and energy storage systems to be coordinated, is presented in Figure 384. These cases are compared to the free chiller dispatch case without energy storage to isolate the effect of energy storage alone. The free chiller dispatch case has lower maximum import levels than the base dispatch case as described in the chiller dispatch sensitivity analysis.

Figure 384: Maximum Import Power vs. Renewable Penetration Level – Coordinated Dispatch

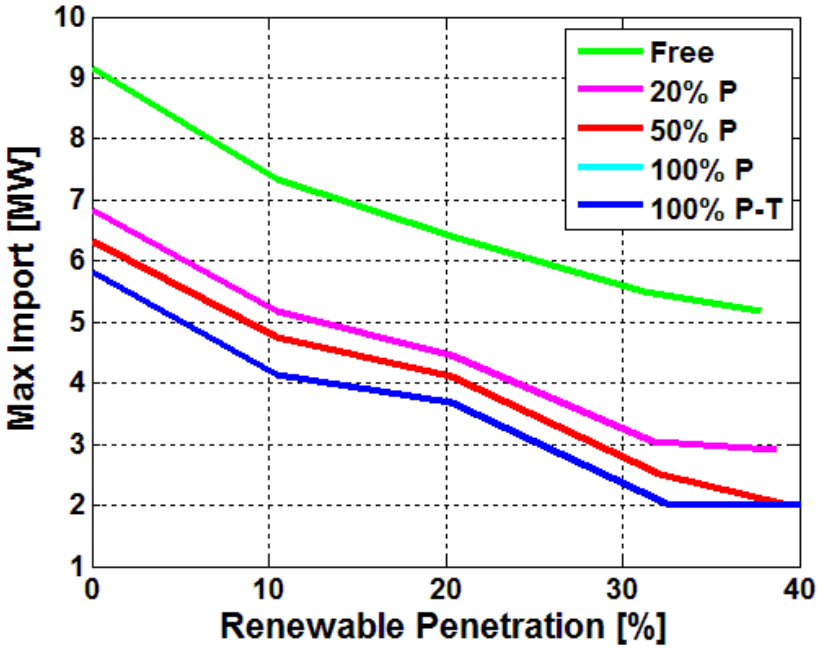

Without interference from the chillers due to smart dispatch of the system, energy storage is able to reduce the maximum annual import levels monotonically with renewable penetration level. The cases with larger energy storage sizes are able to reduce further the maximum annual import levels compared to the cases with the smaller energy storage sizes and the case without energy storage. This result highlights the importance of coordination between dispatchable loads and load-altering technologies. If the chillers were completely dispatchable and coordinated with the operation of the energy storage system, the maximum annual import power decreases monotonically with increasing renewable penetration level as expected. It is also important to note that the larger energy storage sizes show a decrease in the average import power as shown from the import power distributions previously, indicating that the average effect of energy storage implementation is still present and not mitigated by uncoordinated chiller/TES system usage.

Overall, this highlights the notion that in order to realize the benefits of implementing complementary technologies, the operation of these technologies need to be coordinated with each other. It can be insufficient for only one complementary technology to have a 'smart' dispatch.

7.3.1.3.2.5. Effect on the Cost of Electricity

The behavior of the levelized cost of electricity with renewable penetration level for the different energy storage cases compared to the base case is displayed in Figure 385. The base case is the same as that used in the chiller dispatch sensitivity analysis.

Figure 385: Change in LCOE of Different Energy Storage Cases Compared to Base Case

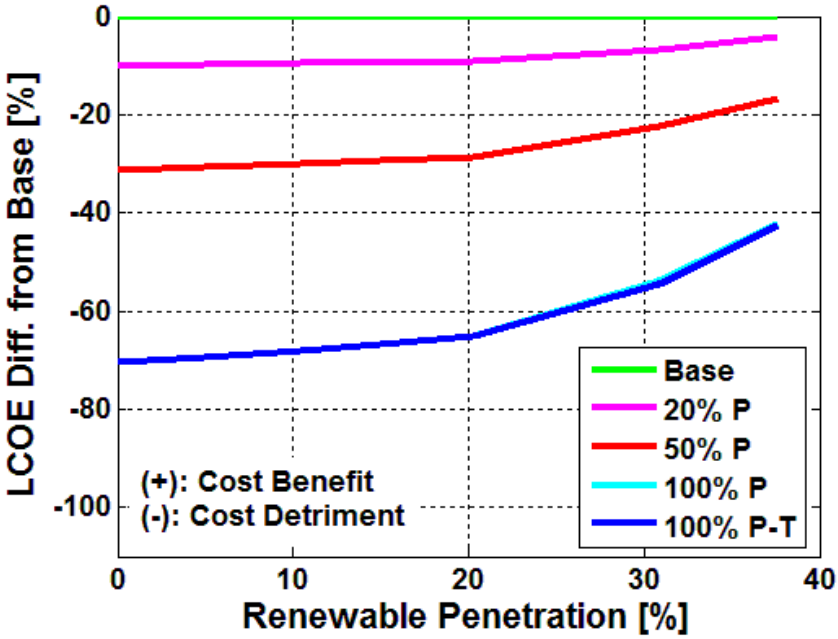

When interpreting the percentage difference from base, note that a positive difference indicates a cost benefit or decrease in the levelized cost of electricity compared to the base case and a negative value indicates a cost detriment or increase in the levelized cost of electricity.

Similar to the other complementary technology analyses, the cost model used in this analysis does not take into account the cost benefit of peak shaving. This was deemed appropriate when assuming connection to a utility grid with increased renewable penetration levels, since the times when the balance power on the utility grid as a whole is high will become unpredictable with increased renewable penetration levels.

For the UCI campus, all of the energy storage cases show increased costs of electricity compared to the base case, with the cases utilizing larger energy storage sizes exhibiting the highest increases in cost. As the renewable penetration level increases, however, the cost difference from the base case is diminished. While none of the cases are able to reach cost-competitiveness at any renewable penetration level, the cost difference from the base case is diminished by about 33% at the highest renewable penetration level. This decrease occurs due to the reduction in curtailment compared to the base case that occurs at the higher renewable penetration levels.

From the previous discussions, the use of energy storage provides many technical benefits for the UCI campus at high renewable penetration levels, all of which have cost benefits. These benefits include but are not limited to: increasing the capacity factor of the gas turbine, significantly minimizing renewable curtailment and requiring lower installed renewable capacities to reach a given renewable penetration level. All of these factors act to reduce the cost of electricity compared to the base case. However, these benefits must be weighed against the cost of installing and maintaining energy storage systems of the given power and energy capacities. The technology type considered for this analysis – the Vanadium Redox flow battery

– happens to require high capital costs due to the use of exotic substances and manufacturing techniques. Other factors also contribute to high costs such as short system lifetime, which requires more frequent replacement of the system and therefore more capital investment. Therefore, while the technical benefits of using these systems are significant, with current costs for VFB systems these benefits do not outweigh the capital and operating costs of the energy storage systems.

It is important to note, however, that this result would likely be changed if rate structures for imported electricity were in place that took into account factors such as peak shaving. Since energy storage is able to decrease peak balance levels on average, the cost benefit from a rate structure that took this into account could allow these systems to be more cost competitive at lower renewable penetration levels. Constructing a rate structure with these properties, however, can become increasingly difficult as higher renewable penetration levels are reached on the utility grid since peak balance periods may become difficult to predict.

7.3.1.3.2.6. Conclusions

This analysis examined the effect of implementing energy storage to smooth the balance profile on the ability of a community such as the UCI campus to accommodate increased renewable penetration levels. The key insights of this analysis are presented here.

- **The implementation of energy storage improves the operation of UCI campus energy resources and achieves increased renewable penetration levels.** The use of energy storage of any size was able to slightly mitigate many of the issues raised by the stand-alone integration of renewable resources. These benefits include: reduced required renewable capacities to reach given renewable penetration levels, decreased curtailment of renewable power, increased gas-turbine capacity factors and decreased reliance on the utility for meeting the load demand on an energy basis compared to the base case. These benefits were also present to some extent over a large range of renewable penetration levels. Depending on operating strategy, these systems may also reduce the maximum import power from the utility.
- **Energy storage systems need to be appropriately sized for a given renewable penetration level for the technical benefits to continue being significant.** At higher renewable penetration levels, renewable power generation often exceeded the power and energy capacity of the energy storage systems with the sizes considered here. This caused many of the benefits of using these systems to be diminished and eventually negated at higher renewable penetration levels. Systems with increased power and energy capacities are required to maintain the extent of these benefits at very high renewable penetration levels.
- **The operation of the chiller/TES system must be coordinated in real time with the operation of the energy storage system in order to make the most effective use of these technologies.** Since the base chiller dispatch strategy does not coordinate with the operation of the energy storage system, its operation interfered with that of the energy storage system for a few hours and increased the maximum annual import power in

some cases. This would cause a large but unnecessary demand charge on the campus, and highlights the importance of coordination between dispatchable technologies. With coordinated operations, the full benefit of implementing energy storage was realized.

- **The technical benefits of using a VFB energy storage system did not outweigh the high capital cost of this technology, but may do so if combined with an appropriate rate structure that takes the cost benefit of peak shaving into account.** Vanadium flow batteries are currently expensive due to multiple factors, contributing to high capital costs that nullify the cost benefits of the technical improvements that the system provided for the UCI campus. When combined with an appropriate rate structure that values services during load peaks more so than other hours, however, the use of a VFB system may become more cost competitive for a larger range of sizes and renewable penetration levels. Constructing this rate structure may be difficult, however.

Overall, the use of energy storage on the UCI campus provides many technical benefits for the operation of on-campus energy resources when achieving high renewable penetration levels. The realization of these benefits, however, requires overcoming practical and economic obstacles and appropriate sizing for different renewable penetration levels.

7.3.1.4. California Results

7.3.1.4.1. Description of Cases

Three types of energy storage will be analyzed including: pumped hydro (HYPS), compressed air energy storage (CAES), and Vanadium Redox flow battery (VFB). These types were selected because of their capability to provide utility-scale power and multiple hours of demand shifting. Several cases were explored for each technology as shown in Table 77. It is important to note that for this study the effect of energy storage will be explored for the renewable integration market only (i.e., how energy storage systems can increase the renewable penetration on the grid).

The installed power capacity represents the total capacity of all units, and values of energy capacity were selected to span the range of reasonable values for each technology. The efficiency reflects values found in the literature, particularly for the CAES, which uses similar values as to those found in the Ibrahim, et. al. paper entitled "Energy storage systems—Characteristics and comparisons" (Ibrahim, 2008). Lastly, the depth of discharge for each technology was selected at 80%, which represents the nominal amount of energy capacity that can be drawn from each technology.

Table 77: Selected Operating Parameters for Energy Storage Technologies

Technology	Total Rated Power Capacity (GW)	Energy Capacity (hours at rated capacity)	Efficiency
HYPS	0.5, 1, 2, 4, 8, 12, 16 and 20	2, 4, 8, 16, 24, 32 and 48	0.75

CAES	0.5, 1, 2, 4, 8, 12, 16 and 20	2, 4, 8, 16, 24, 32 and 48	0.51*
VFB	0.5, 1, 2, 4, 8, 12, 16 and 20	2, 4, 8, 16, 24, 32 and 48	0.75

* Combined efficiency: 1kWh electrical generation requires 0.75kWh of electricity for compression and 5,077 Btu of natural gas in a turbine with a heat rate of 4.16 Btu/kWh.

Selection of operation conditions, particularly energy capacity, was based on a paper released in December 2010 from the Electric Power Research Institute entitled "Electricity Energy Storage Technology Options: A White Paper Primer on Applications, Costs, and Benefits."

In addition to the operating parameters the following cost parameters were selected for this analysis (Table 78) (Klein, 2010; Electricity Energy Storage, 2010).

Table 78: Input Parameters for Energy Storage Technologies

	Pumped Hydro	CAES	Flow Battery (Va Redox)
Instant Cost ($/kW)	2500	1250	3100
Fixed O&M ($/kW-yr)	35	24.6	32
Variable O&M ($/MWh)	7	65	0
Heat Rate (MMBtu/MWh)	0	4.16	0
Heat Rate Degradation (%/year)	0%	0.05%	0%
Capacity Degradation (%/year)	0%	0%	0%
Debt Term (Yrs)	20	20	5
Economic Life (Yrs)	40	20	10
Federal Tax Life (Yrs)	20	20	10
State Tax Life (Yrs)	20	20	10
Ad Valorem Tax Rate	1.1%	1.1%	1.1%
Start-Up Fuel (MMBtu/MW)	0	2.8	0
Plant Losses	0%	0%	0%
TX Losses	5.0%	5.0%	5.0%
Transformer Losses	0.5%	0.5%	0.5%
TX Cost ($/MWh)	4.3	4.3	4.3

7.3.1.4.2. Operation Results

This discussion will first describe the effect of energy storage on the operation of the grid and integration of renewables then describe the effect on the levelized cost of electricity when integrating energy storage.

As stated previously, there are many characteristics that can change the effectiveness and life of energy storage technologies (e.g., Storage capacity, Available power, Depth of discharge, Discharge time, Efficiency, etc.). The following analysis shows the effects from different

combinations of storage capacities (i.e., energy capacity) and available power (i.e., power capacity). For this analysis, the energy storage is controlled such that it maximizes its use and maximizes the uptake of renewables on the grid. This can be seen in Figure 386 which describes the buildup of generating technologies for three different renewable penetrations with energy storage. While the algorithm stays the same (i.e., reduce maximum with nearest, earlier minimum) the role of energy storage changes. For 10.8% renewable penetration, energy storage can reduce a large portion of the on-peak energy while increasing the nighttime minimum; however, with increasing renewable penetration, energy storage focuses on the spikes that form from adding solar and wind profiles. For comparison, Figure 387 is presented, which is the same analysis only without any energy storage. Notice that for each day of the 32.9% case, the energy storage reduces the peaks, which are largely comprised of peaking units and is able to increase the demand at times when excess generation exists, thereby reducing curtailment.

Figure 386: Generation Buildup with 2GW of HYPS and 8h Energy Capacity for 10.8%, 20.4% and 32.9% Renewable Penetration Comprised of a 50/50 Mixture of Wind and Solar

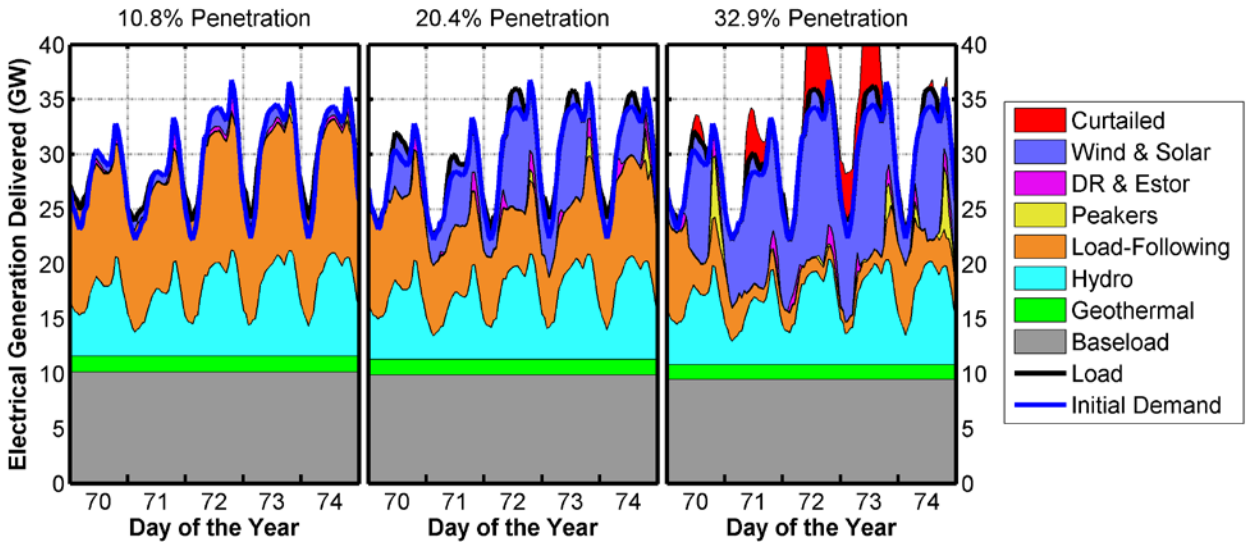

Figure 387: Generation Buildup without Energy Storage for 10.8%, 20.4% and 32.9% Renewable Penetration Comprised of a 50/50 Mixture of Wind and Solar

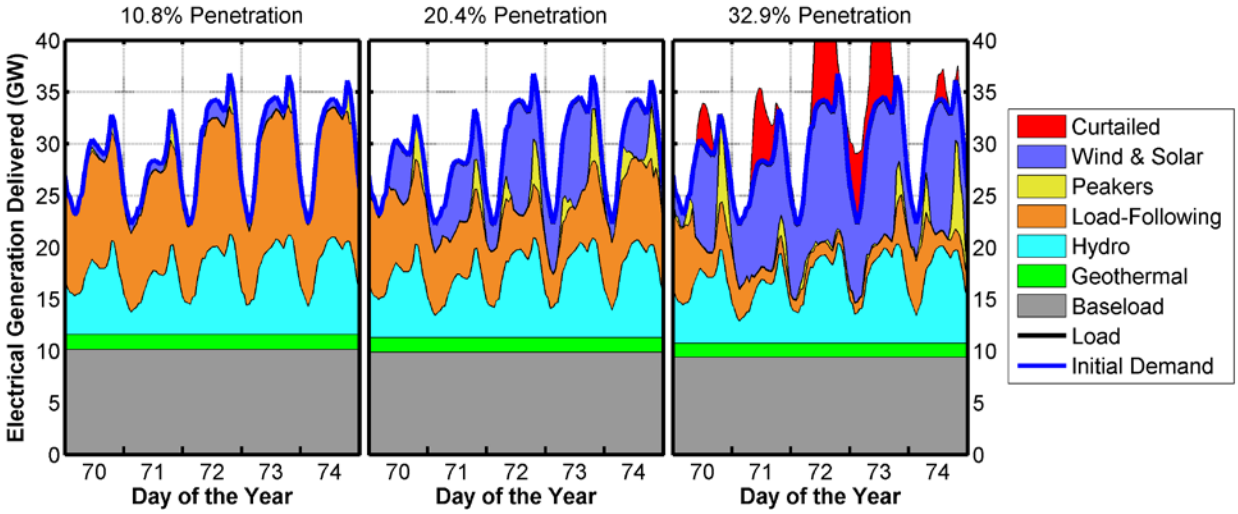

Increases in renewables will have effects on the hourly scale but typically have a similar effect from day to day as well. This can be explored by looking at the daily average renewable generation and storage profile for all days of the year, presented in Figure 388 and Figure 389.

Figure 388: Daily Average Renewable Generation of Every Day in the Year for a 50/50 Mixture of Wind and Solar

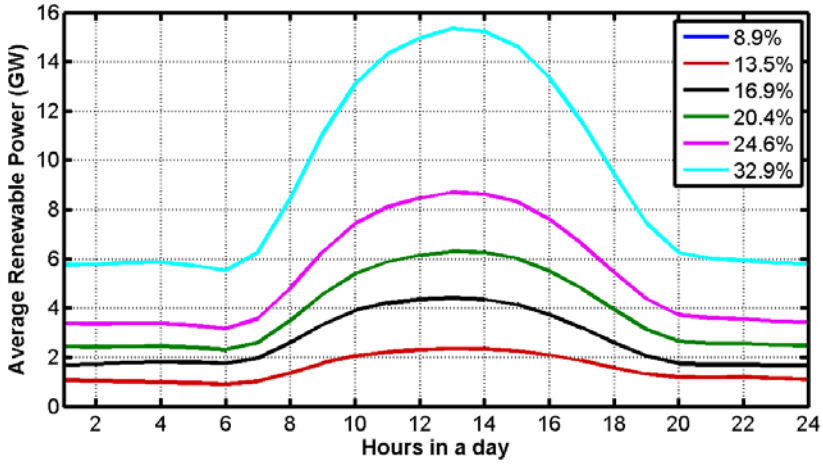

Figure 389: Daily Average Renewable Generation of Every Day of Each Season for a 50/50 Mixture of Wind and Solar

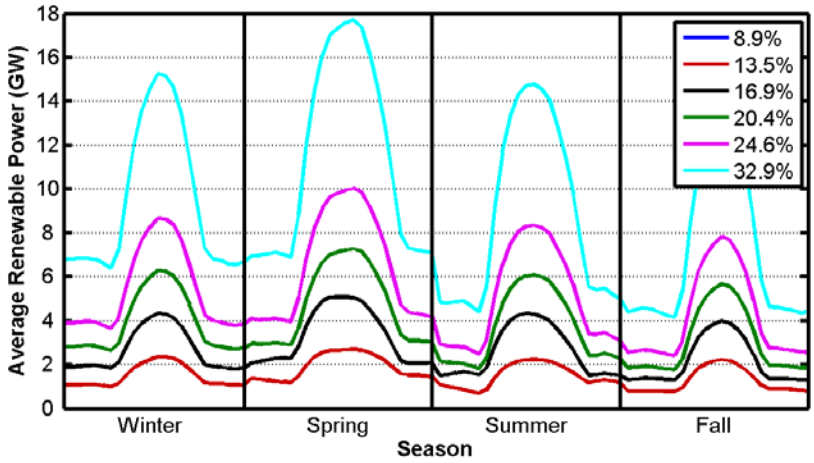

The wind portion contributes to the seemingly baseloaded value, while the solar contributes the peak each day. From a seasonal perspective, while solar generation is largest in the summer, wind generation is largest in the winter and spring so the overall profile shows a maximum in the winter and spring followed by the summer then the fall.

Understanding the power profile from wind and solar aids in understanding why the energy storage behaves as it does. In Figure 390 the daily average energy storage profile is shown. A negative value indicates charging and a positive power indicates discharging. Notice the shape of the curve changes very predictably about two inflection points around 9AM and 6PM from the 8.9% penetration case to the 32.9% case . These inflection points are caused by a combination of the hourly renewable profile and the initial shape of the demand curve.

Figure 390: Daily Average Storage Profile for Every Day of the Year with 2GW of HYPS with an 8 Hour Capacity for a 50/50 Mixture of Wind and Solar

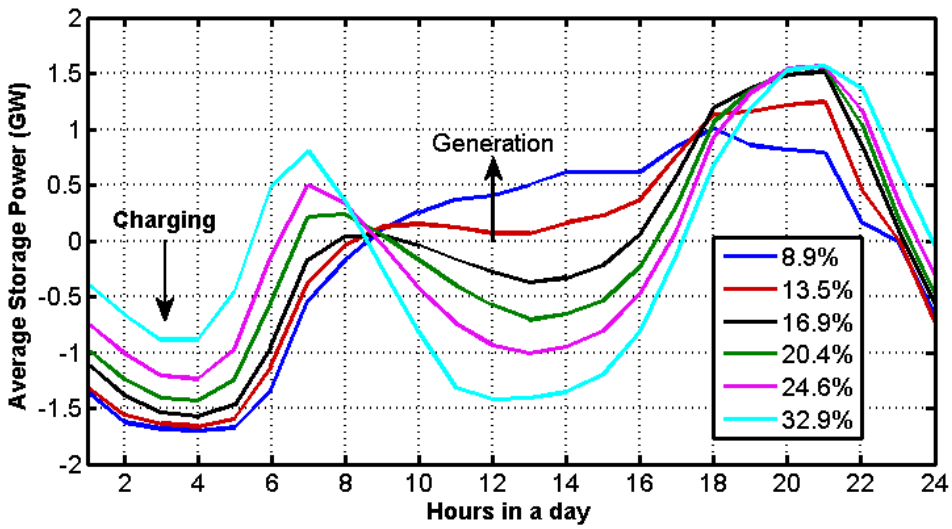

Now that the general profile for the energy storage has been established, sensitivities are performed on different metrics including power capacity, energy capacity, and cost. This enables a more complete perspective of how the operation of energy storage systems change to complement renewable generators and the benefits that it can bring.

7.3.1.4.2.1. Spanning Installed Power Capacity

The system-wide energy storage power capacity was varied from 0.5GW to 20GW while holding the energy capacity constant at 16GWh of storage in an effort to explore the importance of power capacity for the system. The runs for this sensitivity are summarized in Table 79.

Table 79: Power Capacity Sensitivity for Energy Storage

Total Rated Power Capacity (GW)	Energy Capacity (GWh)	Energy Capacity (hours at rated capacity)
0.5	16	32
1	16	16
2	16	8
4	16	4
8	16	2
12	16	1.333
16	16	1
20	16	0.8

Increasing the available power allows the system to more aggressively reduce peaks and enable curtailed energy to be used. Figure 391 depicts the storage profile for the average day for four different power capacities. Notice that between the hours of two and six, the system is nearly

operating at its maximum power point for 0.5, 1 and 2GW. At installed capacities above 2GW, the power never reaches its maximum value. This is an indication that the system is larger than can be used continuously. In the case of energy storage systems, it is acceptable that they do not operate at their maximum output power all the time, as that power may not always be required but can be very valuable for rapid dynamics if needed. Additionally, the profiles for systems with greater capacity than 4GW are nearly the same, indicating that adding an additional capacity does little to affect the shape. Figure 392 compares the same profiles for a higher renewable penetration, which experiences similar behavior, in terms of capacity limitations, as lower penetrations. Notice the change in shape to adjust for the increasing renewable generation, particularly, the charging peak moving from the night to the afternoon to complement solar power generation.

Figure 391: Daily Average Energy Profiles at 9% Renewable Penetration for different Installed Capacities of Pumped Hydro with 16GWh or storage for a 50/50 Mixture of Wind and Solar

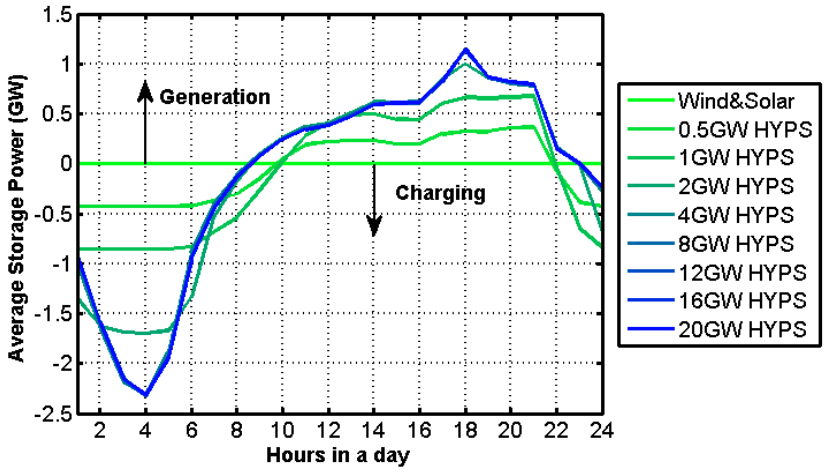

Figure 392: Daily Average Storage Profiles at 33% Renewable Penetration for different Installed Capacities of Pumped Hydro with 16GWh of storage for a 50/50 Mixture of Wind and Solar

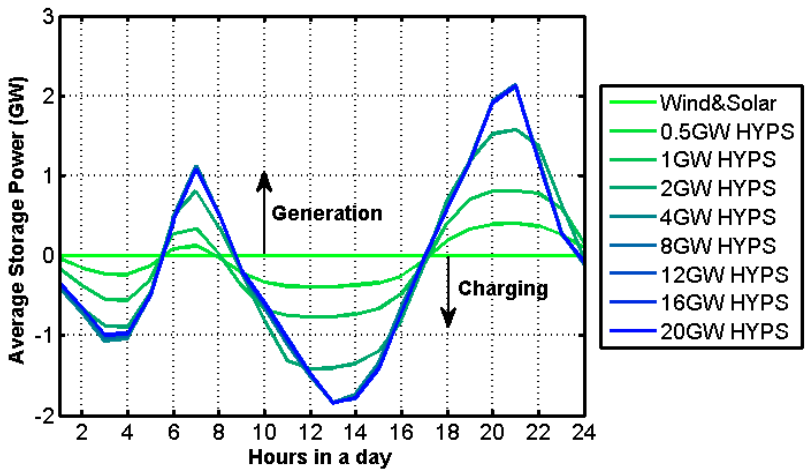

By examining the load duration curves for each power value in Figure 393, it is possible to see the profiles trending toward a maximum profile. The maximum profile signifies that the system is limited by the energy capacity because an increase in the power causes no change in the profile. Also for the 0.5GW and 1GW it is possible to see its line of maximum power. Each line actually is slightly below its maximum value because this figure shows the load duration profile, delivered to meet the demand, which includes the plant, transformer and transmission loss to move the power from the facility to a point of end use.

Figure 393: Load Duration Curve at 33% Renewable Penetration for different Installed Capacities of Pumped Hydro with 16GWh of storage for a 50/50 Mixture of Wind and Solar

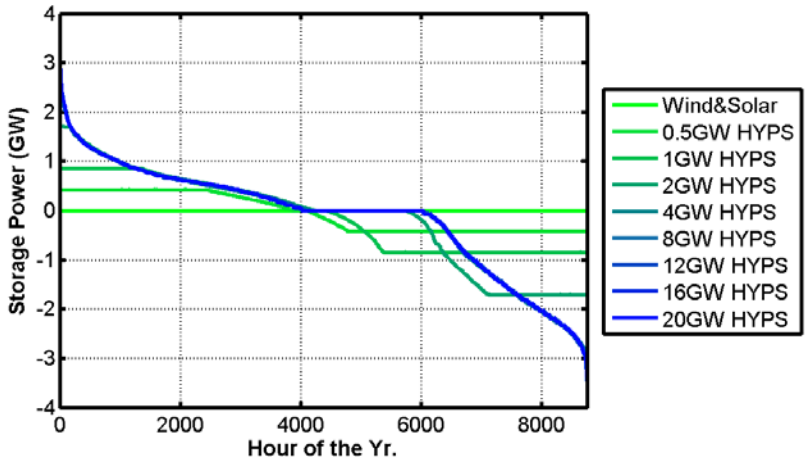

The limitations due to energy capacity can be shown in Figure 394 as well, which describes the additional amount of generation required to shift the load with energy storage (i.e., the energy penalty). Notice that as the power increases, the penalty increases; however at high powers, the energy shifted does not increase anymore and the energy penalty reaches a maximum value at roughly 4GW of installed capacity. Also, the energy penalty increases with greater renewable

penetration; however, because the operating strategy tries to reduce the highest peaks, whether they are renewable or not, the storage will be completely dispatched independent of the renewable penetration.

Figure 394: Energy Penalty for Different Installed Capacities of Pumped Hydro with a 50/50 Mixture of Wind and Solar

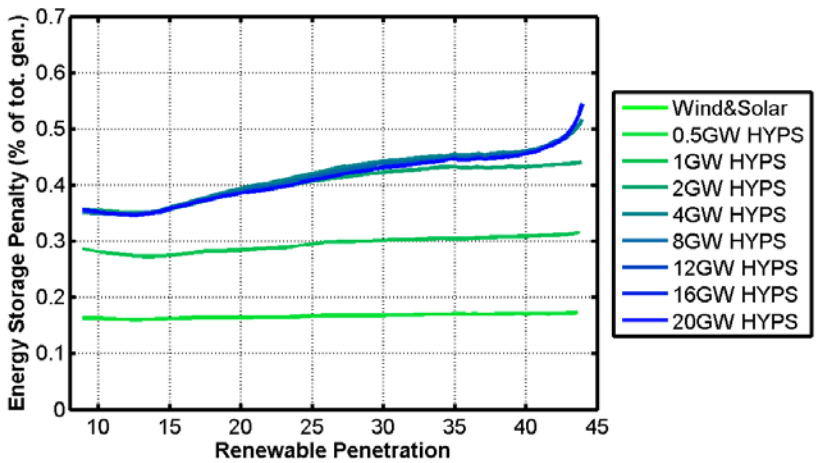

On account of the energy penalty, energy storage when operating in "renewable integration" mode will reduce the renewable penetration for the same installed capacity of renewables until enough renewables are installed such that the use of energy storage will be able to make use of excess renewable generation (i.e., energy penalty must be negated by the uptake of excess renewable generation). That is why the installed capacity in Figure 395 initially requires more renewable capacity to achieve the same renewable penetration but after the energy penalty has been balanced out (i.e., around 22%) energy storage helps increase the renewable penetration.

Figure 395: Installed Renewable Capacity for Different Power Capacities with 16GWh of Storage for a 50/50 Mixture of Wind and Solar

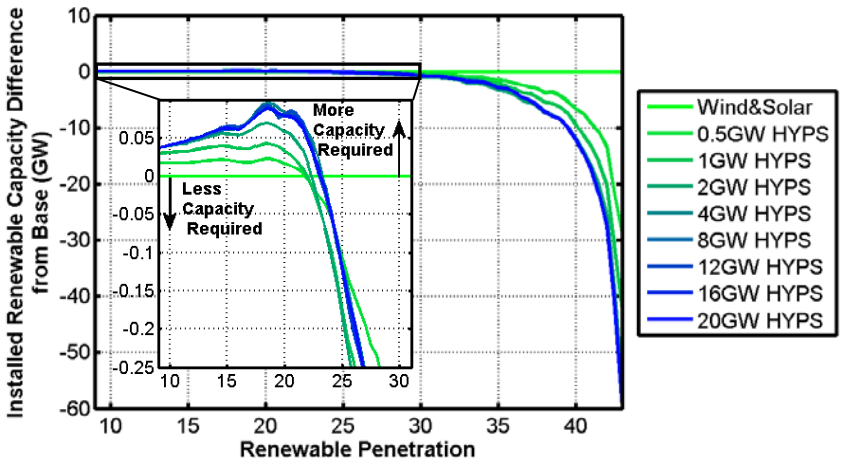

Despite incurring an energy penalty, increasing the power capacity improves the system performance for all renewable penetrations. This is expressed by Figure 396, which shows the system-wide capacity factor and how it increases with additional of energy storage. Installing 20GW of storage capacity would increase the system capacity factor by 3% at 9% renewable penetration.

Figure 396: Grid-wide Capacity Factor for Different Installed Capacities of Pumped Hydro with a 50/50 Mixture of Wind and Solar

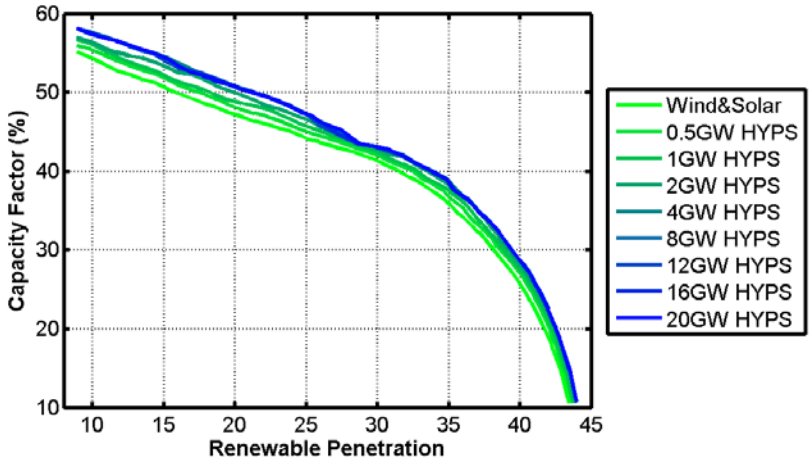

The fuel to electrical efficiency of the grid will increase with increasing renewables but it will not increase linearly. This non-linearity is due to several factors including:

1. Continued need for balance generation to complement the renewable generators when little wind or solar generation is available and there is high demand.

52. Changing mixture of resources with different heat rates changes the fuel consumption

53. Generators operating at a lower load-point result in less efficient operation

54. Increase in startups, caused by increased variability, result in greater startup fuel consumption

When energy storage is included in the grid mixture it further increases grid efficiency. Figure 397 shows the overall shape of the efficiency curve while Figure 398 shows the same information expressed as the difference from the "Wind&Solar" base signal, which is a 50/50 mixture of wind and solar. The up-turn in efficiency at high renewable penetrations occurs because significant increases in installed renewable capacity remove the need to operate balance generation by using curtailment to "firm" the renewables. Though this is technically possible, this behavior is not practical, particularly from a cost perspective. Figure 398 clearly shows that higher power capacities yield higher efficiency gains.

Figure 397: Grid-wide Fuel to Electrical Efficiency for Different Installed Capacities of Pumped Hydro with a 50/50 Mixture of Wind and Solar

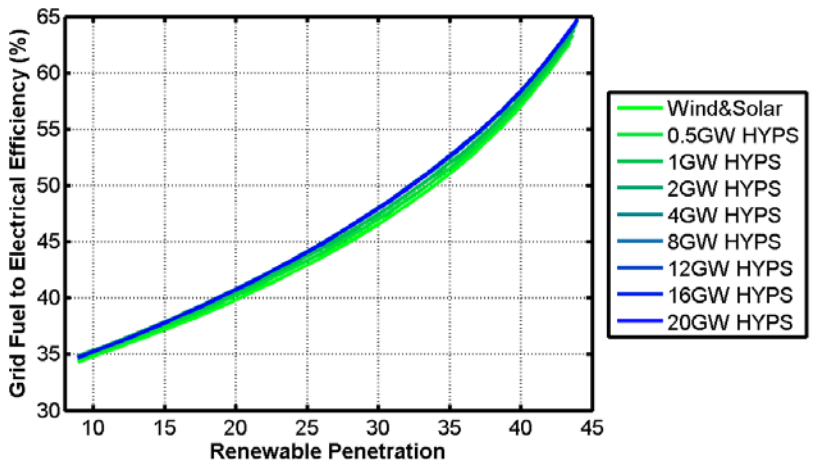

Figure 398: Grid-wide Efficiency as a Difference between Cases including Energy Storage and Those without Energy Storage for a 50/50 Mixture of Wind and Solar

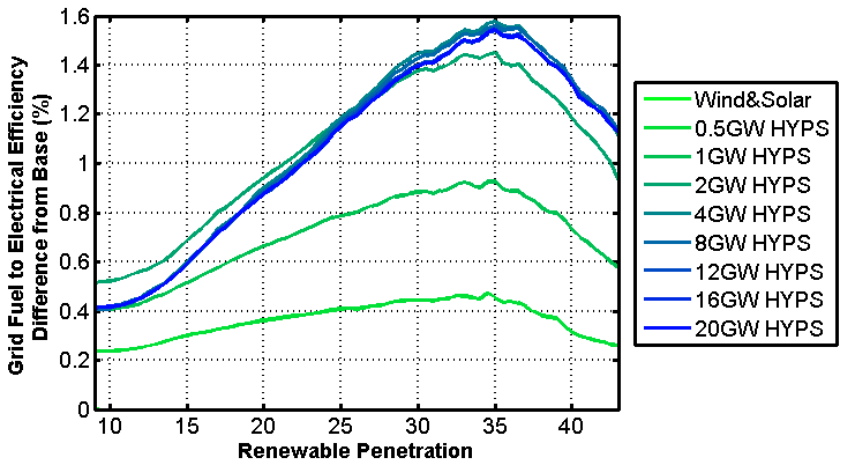

In addition to increasing the capacity factor and fuel to electrical efficiency of the grid, energy storage has the ability to reduce the required fleet ramp rate to integrate renewables. Balance generation includes peakers and load-followers and makes up the majority of generation that must ramp up or ramp down to accommodate both generation and demand changes on the grid. Figure 399 and Figure 400 show the ramp up and ramp down rates of the balance fleet for different installed capacities of energy storage. Ramp rates are similar in behavior and clearly show that with higher power capacity storage can reduce the ramping requirements of the fleet, when operating to maximize renewable generation uptake (i.e., renewable integration mode),.

Figure 399: Average Balance Fleet Generator Ramp Up for Different Installed Capacities with a 50/50 Mixture of Wind and Solar

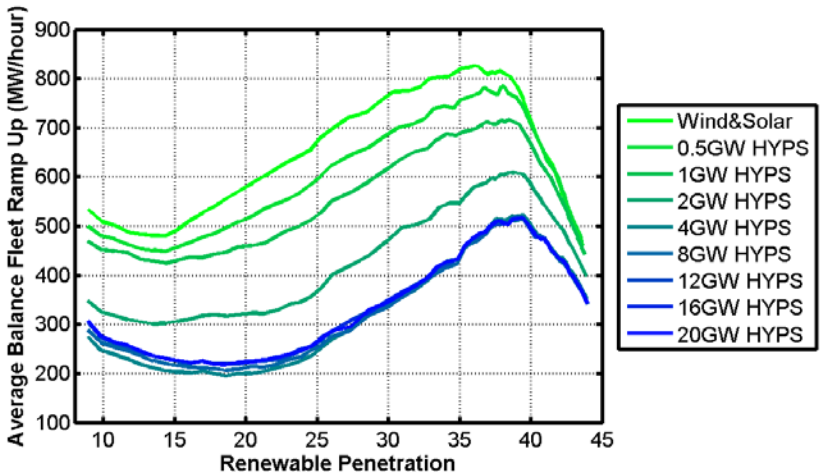

Figure 400: Average Balance Fleet Generator Ramp Down for Different Installed Capacities with a 50/50 Mixture of Wind and Solar

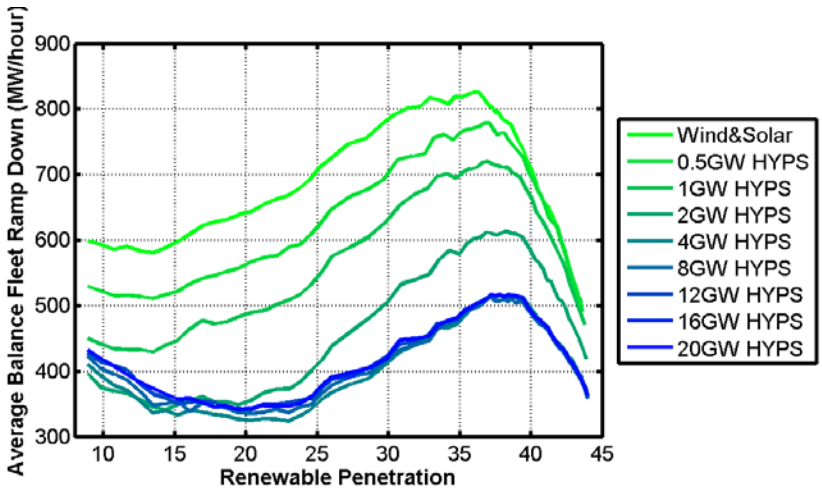

Average start count for the balance fleet could also be reduced on account of energy storage. Both peakers and load-followers experience a reduction in the average and total starts per year. The average starts are shown in Figure 401.

Figure 401: Average Balance Fleet Starts for Different Installed Capacities with a 50/50 Mixture of Wind and Solar

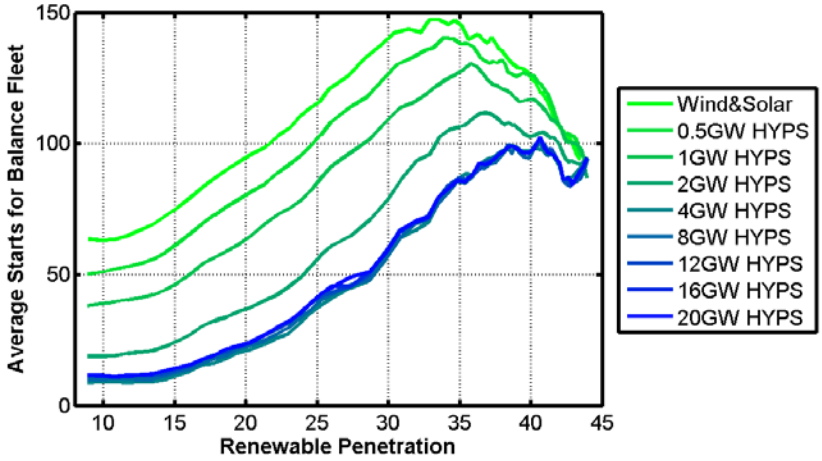

Another key consideration for the implementation of energy storage into the system is for carbon dioxide emissions. Energy storage generally reduces CO_2 emissions but there are occasions when implementing energy storage can increase the CO_2 emissions related to fuel consumption as shown in Figure 402. For high renewable penetrations there is such a large amount of excess generation that the energy storage ceases to be useful and if its operation is not managed appropriately (i.e., differently than for maximum renewable integration), it can cause an increase in the CO_2 emissions.

Figure 402: Carbon Dioxide Emissions for Different Installed Capacities with a 50/50 Mixture of Wind and Solar

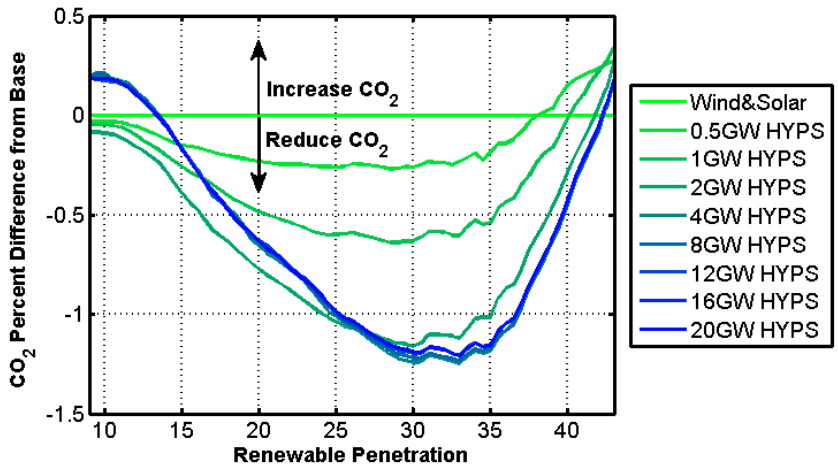

For low renewable penetrations, low capacities of energy storage reduce CO_2 emissions but beyond 2GW the initial emissions actually increase and are greater than that of lower power capacity systems until after 27% renewable penetration. This increase is related to the increase in emission from load-following units. Assuming that baseload devices experience little effect on their operation from increasing renewables, their emissions will remain unchanged; thus the two remaining CO_2 emitters are peakers and load-followers. Figure 403 shows the changing behavior of peakers due to energy storage. The CO_2 from peakers reduces because their power profile is reduced by the energy storage (Figure 404). Notice the profiles reduce dramatically with increased power capacity. This will reduce CO_2 emissions from peakers but is only half of the story.

Figure 403: Peaker Carbon Dioxide Emissions for Different Installed Capacities with a 50/50 Mixture of Wind and Solar

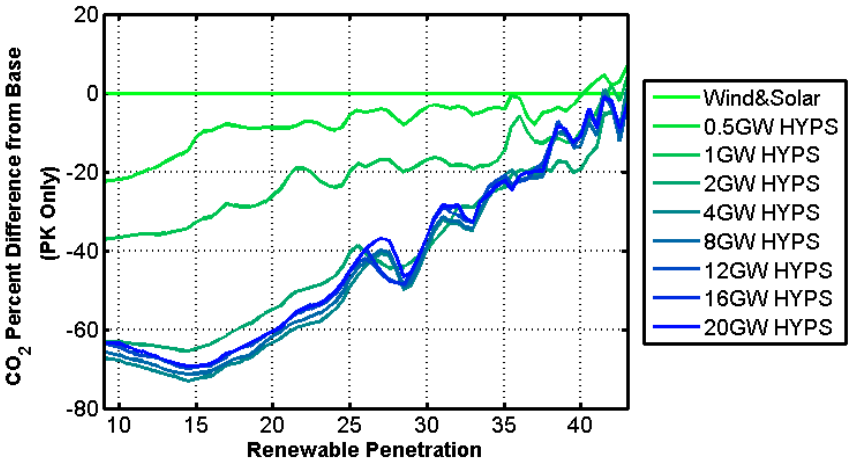

Figure 404: Daily Average Peaker Profiles at 9% Renewable Penetration for different Installed Capacities of Pumped Hydro with 16GWh of Storage for a 50/50 Mixture of Wind and Solar

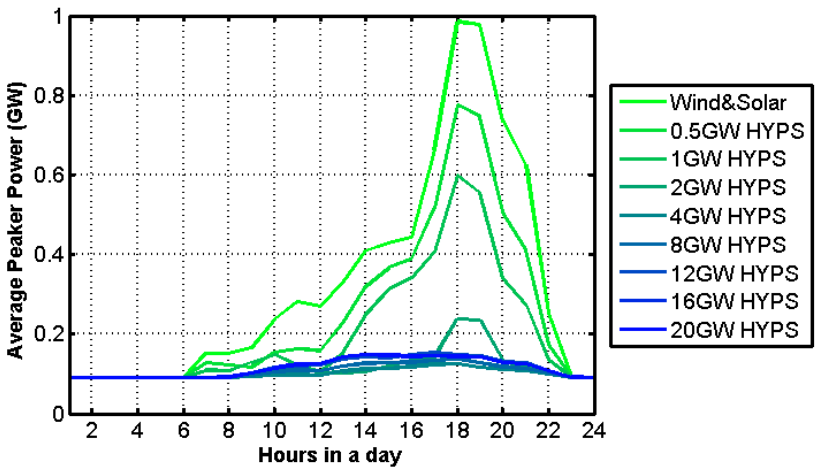

The other portion of emissions for low renewable penetration is from load-following plants. Load-following plants must generate additional power to accommodate the energy penalty associated with storage devices thus their CO_2 emissions will increase as shown in Figure 405. From Figure 406 it can be seen that the storage operates to smooth the load-follower operation and that as the power increases, the largest movement occurs in the nighttime hours due to charging.

Figure 405: Load-Follower Carbon Dioxide Emissions for Different Installed Capacities with a 50/50 Mixture of Wind and Solar

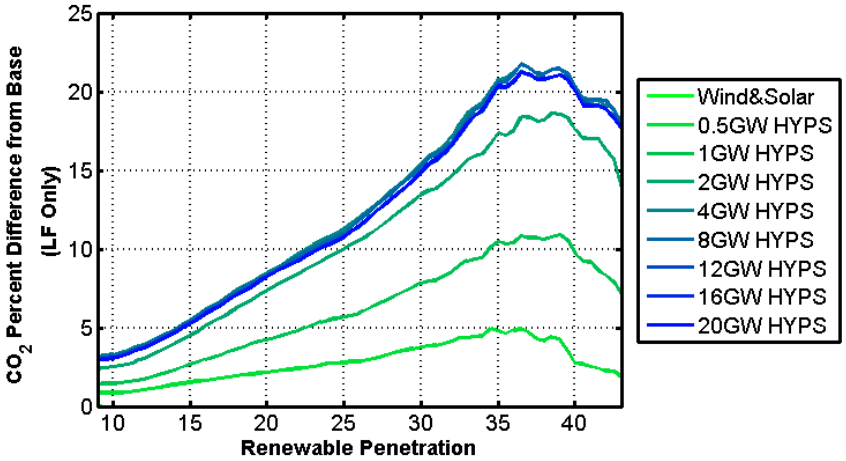

Figure 406: Daily Average Load-Following Profiles at 9% Renewable Penetration for different Installed Capacities of Pumped Hydro with 16GWh of Storage for a 50/50 Mixture of Wind and Solar

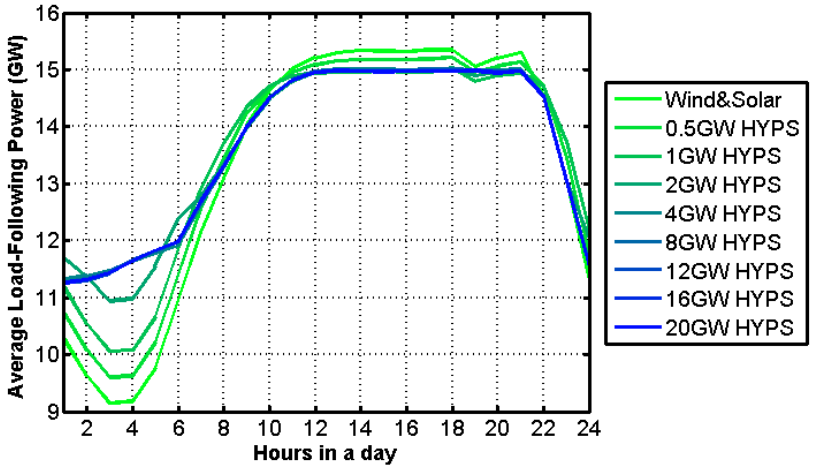

Energy storage has the potential to enhance the integration of renewables from the perspective of power capacity values, but it is important that its installation comes at a time and renewable penetration when it will improve system performance.

7.3.1.4.2.1.1. Conclusions

- Increasing power capacity increases the energy that can be shifted, until further utilization is limited by the energy capacity.
- Energy storage can increase the achievable renewable penetration but must first overcome the efficiency penalty for storing electricity.
- Energy storage can increase the system capacity factor and grid efficiency for all renewable penetrations
- Energy storage can reduce balance fleet ramping and reduce balance fleet starts for all renewable penetrations and particularly at low penetrations
- CO_2 emissions can be reduced from the use of energy storage but the power and energy capacity must be carefully selected to avoid a high energy penalty for using the storage.
- Value for energy storage is a balance between reduction in generator dynamics and the energy penalty for storing energy. Capacities below represent values after which the additional performance is greatly diminished or negligible:
    - 20 GW (maximum option) for maximizing the renewable penetration
    - 8 GW for maximizing capacity factor
    - 4 GW for maximizing grid efficiency, minimizing ramp rates and balance fleet starts

- 2 GW for minimizing CO_2 emissions

- For systems with the same energy capacity, increasing power capacity will eventually provide diminishing performance increases for capacity factor, efficiency, ramp rates and starts

7.3.1.4.2.2. Spanning Energy Capacity

Energy capacity for storage systems can extend over a wide range depending on the geographic shape and dimensions of the reservoirs, cavern or tank sizes. By spanning different energy capacities, sensitivities to energy capacity are explored. Table 80 presents the cases explored in this section.

Table 80: Energy Capacity Sensitivity for Energy Storage

Total Rated Power Capacity (GW)	Energy Capacity (GWh)	Energy Capacity (hours at rated capacity)
2	2	1
2	4	2
2	6	4
2	16	8
2	32	16
2	48	24
2	64	32
2	96	48

As shown in Figure 407 and Figure 408, greater energy capacity for the same power capacity allows the energy storage to shift more energy before it is depleted and must be recharged; however, the profiles approach a final shape as the energy capacity continues to increase. This signifies that the system is limited by the power capacity.

Figure 407: Daily Average Storage Profiles at 9% Penetration for different Energy Capacities of Pumped Hydro with 2GW Installed Capacity for a 50/50 Mixture of Wind and Solar

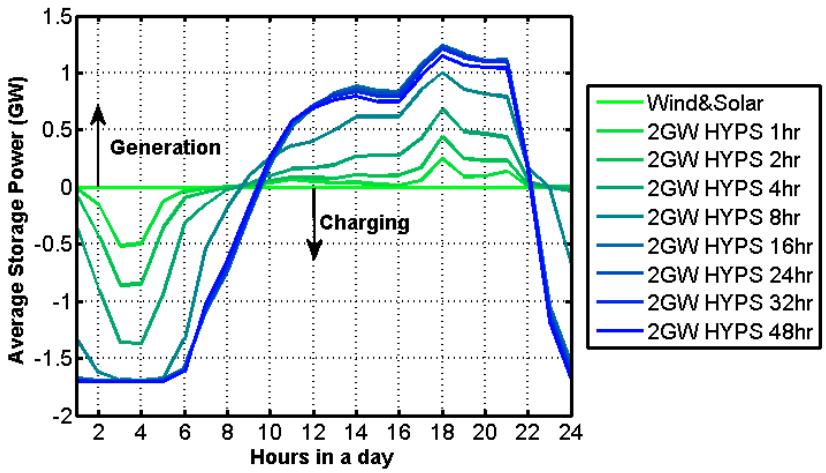

Figure 408: Daily Average Storage Profiles at 33% Penetration for different Energy Capacities of Pumped Hydro with 2GW Installed Capacity for a 50/50 Mixture of Wind and Solar

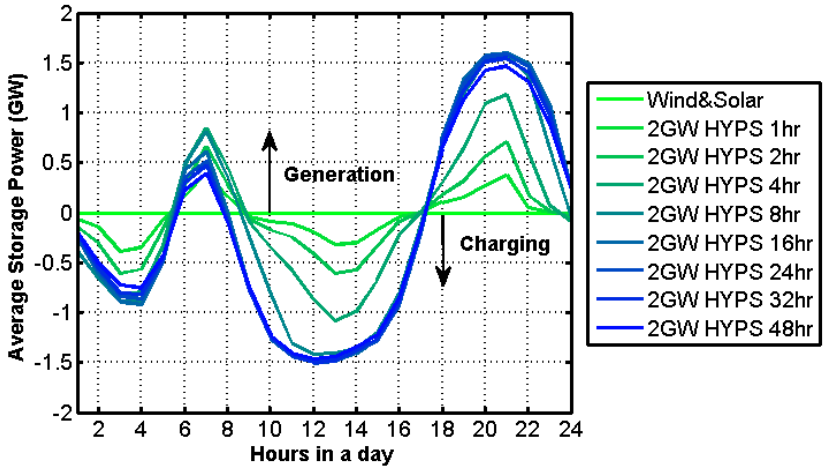

At 9% penetration the profile exhibits a similar shape to the demand, while at the 33% penetration value the profiles are shaped to complement the renewable generation and make use of as any excess generation that exists. As the energy capacity is increased the shape is less predictable than from an increase in the power capacity since the shifting can occur over progressively longer timeframes. However, just as with the power capacity cases, the energy capacity experiences an energy limitation at which point increasing the energy capacity will no longer greatly improve the ability of the system to uptake renewables. Figure 409 depicts this phenomenon with a load duration curve. The energy difference moving from one energy capacity to the next is progressively reduced, and the number of hours operating at maximum power increases because increasing the energy capacity allows for energy to be shifted over a

longer timeframe than a system with lower energy capacity. In addition, as the energy capacity is increased it experiences a higher energy penalty, as shown in Figure 410. The value of shifting load that another generator could have met (e.g., load-follower) must outweigh the associated energy penalty.

Figure 409: Load Duration Curve at 9% Penetration for Different Energy Capacities with a 50/50 Mixture of Wind and Solar

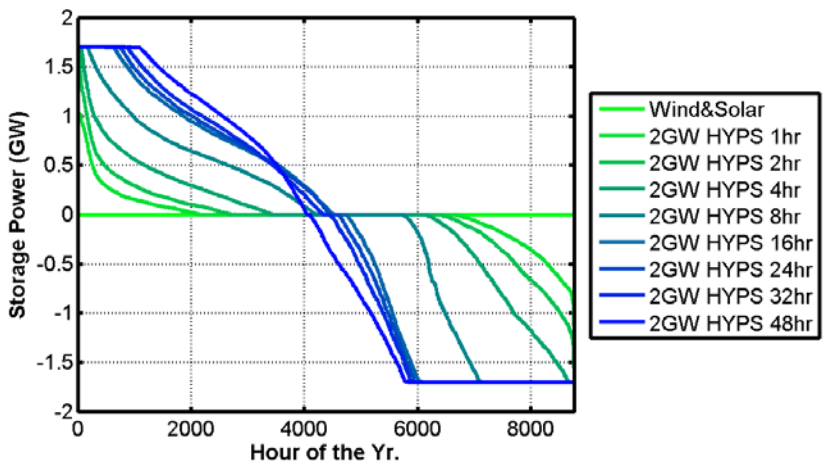

Figure 410: Energy Penalty for Different Energy Capacities of Pumped Hydro with a 50/50 Mixture of Wind and Solar

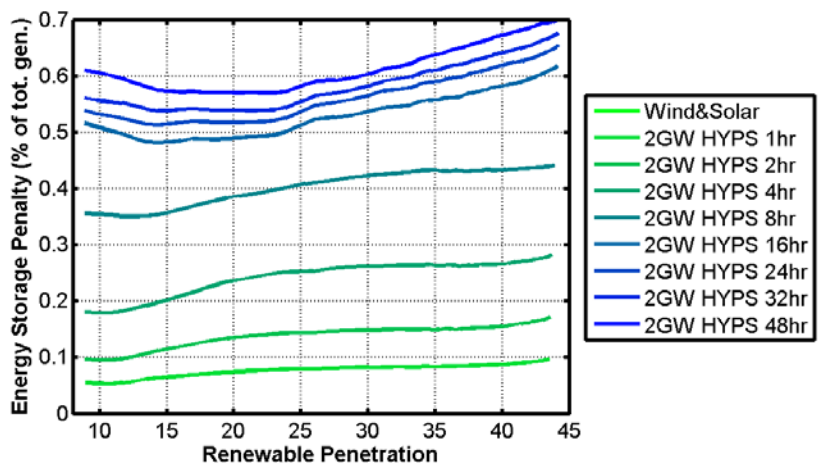

Similar to Figure 395, Figure 411 shows that due to the energy penalty, storage devices only increase the renewable penetration once excess renewable generation can be utilized. Larger energy capacities, increase the generation required to make up for the energy penalty so they also reduce the renewable penetration the most initially; however, as soon as sufficient excess generation is available (i.e., around 23%) high energy capacities quickly begin to reduce the required renewable capacity to achieve a given penetration.

Figure 411: Installed Renewable Capacity for Different Energy Capacities with 16GWh of Storage for a 50/50 Mixture of Wind and Solar

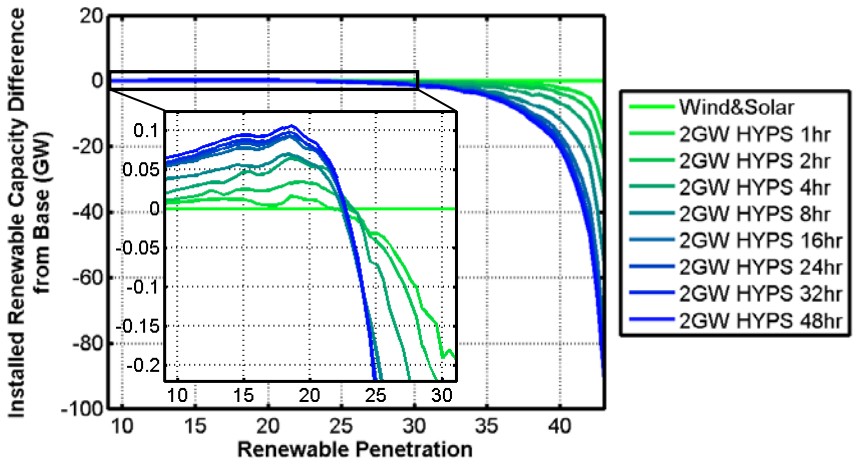

The capacity factor for cases with different energy capacities is similar to that of the power capacity cases. Figure 412 indicates that including energy storage will necessarily increase the system-wide, yearly capacity factor. Figure 413 presents the same information but as a difference from the base case with no energy storage, (i.e., "Wind&Solar").

Figure 412: Grid-wide Capacity Factor for Different Energy Capacities of Pumped Hydro with a 50/50 Mixture of Wind and Solar

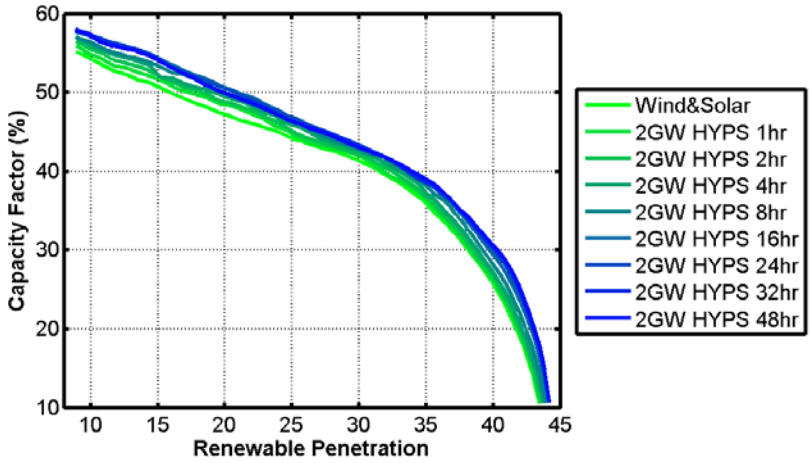

Figure 413: Grid-wide Capacity Factor as a Difference between Cases including Energy Storage and those without Energy Storage for a 50/50 Mixture of Wind and Solar

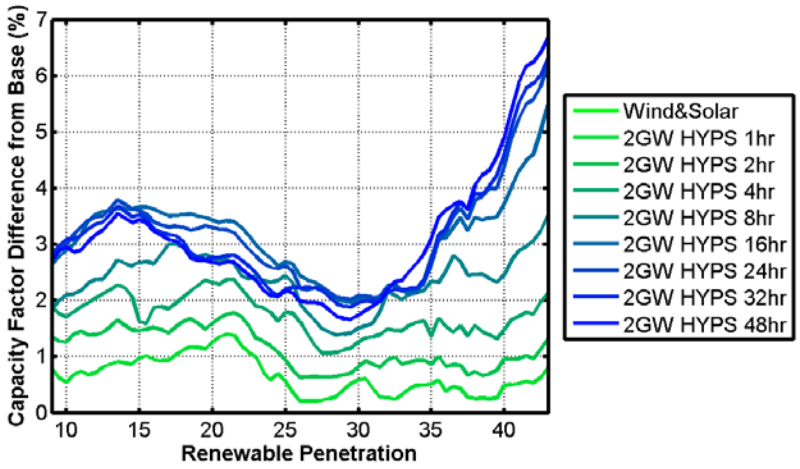

Comparing the grid efficiency energy capacity follows a similar trend as that of the power capacity sensitivity; however, just as with the capacity factor, the range over which the efficiency changes is limited as shown in Figure 414 and Figure 415. While, the high capacity values (16, 24, 32 and 48 hr) are tightly bunched, the greatest efficiency gain occurs with the 16 hour capacity case at 35% renewable penetration. This is because the 24, 32 and 48 hour cases increase the energy penalty without greatly improving the other generator's performance or enabling additional renewable generation. Thus, the highest energy capacity is oversized to provide the optimal support for integration of renewable generation in this system.

Figure 414: Grid-wide Fuel to Electrical Efficiency for Different Energy Capacities of Pumped Hydro with a 50/50 Mixture of Wind and Solar

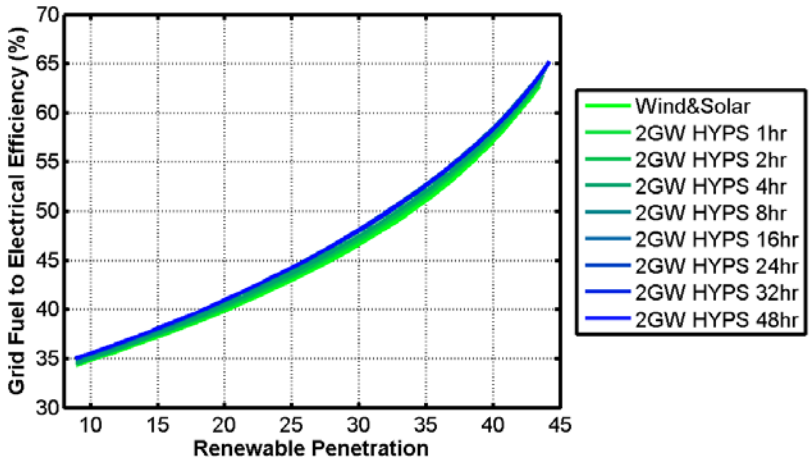

Figure 415: Grid-wide Efficiency as a Difference between Cases including Energy Storage and Those without Energy Storage for a 50/50 Mixture of Wind and Solar

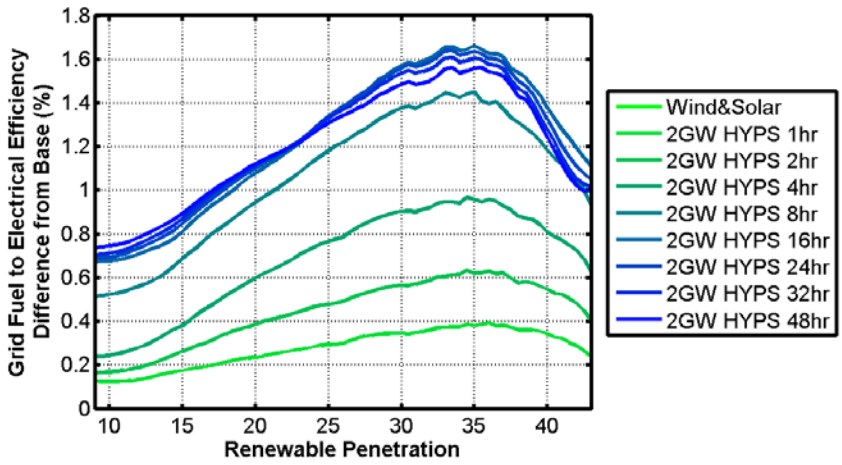

Varying the energy capacity results in a reduction of the average ramp rate up (Figure 416) and ramp rate down (Figure 417). Limiting the capacity to 2GW also limits the effectiveness of the ramp rate reduction. When compared with Figure 399 and Figure 400, it is apparent that power capacity is the most important factor to reduce the balance fleet ramp rate.

Figure 416: Average Balance Fleet Generator Ramp Up for Different Energy Capacities with a 50/50 Mixture of Wind and Solar

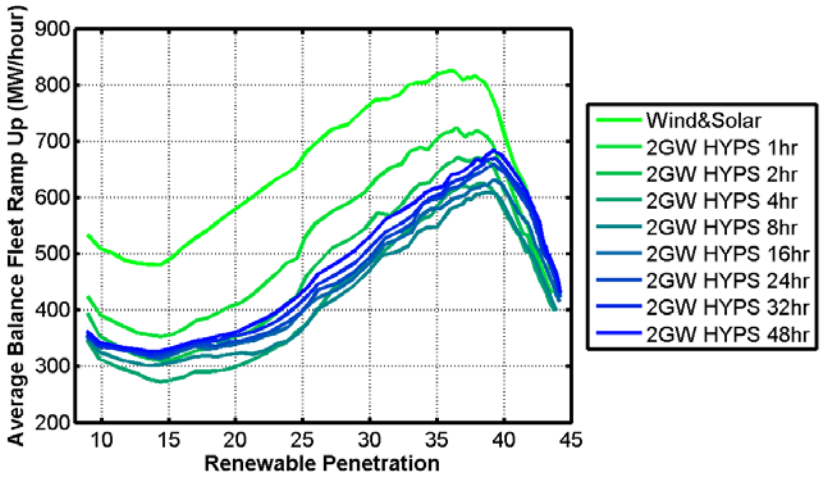

Figure 417: Average Balance Fleet Generator Ramp Down for Different Energy Capacities with a 50/50 Mixture of Wind and Solar

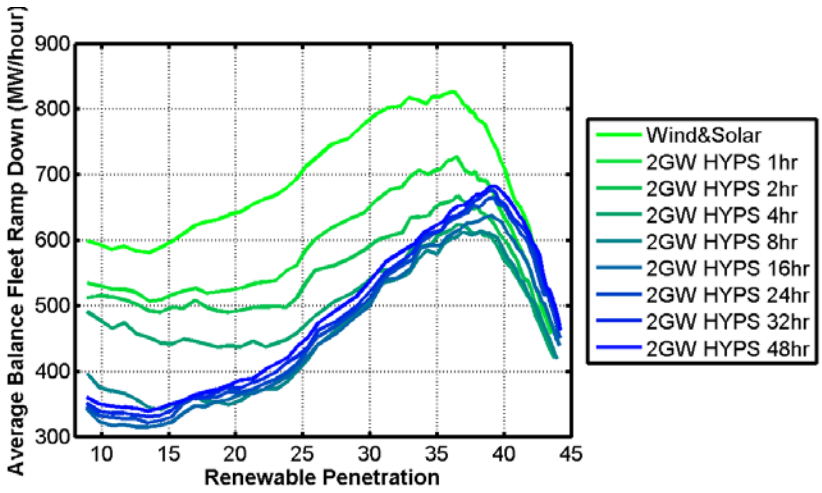

Reducing the average yearly starts for the balance fleet is achievable with all values of energy capacity; however, as the capacity is increased over 8 hours the starts do not reduce but rather stay around the same value. Thus selection of energy capacity is important when considering energy storage's effect on grid efficiency, capacity factor, fleet ramp rates and generator starts.

Figure 418: Average Balance Fleet Starts for Different Energy Capacities with a 50/50 Mixture of Wind and Solar

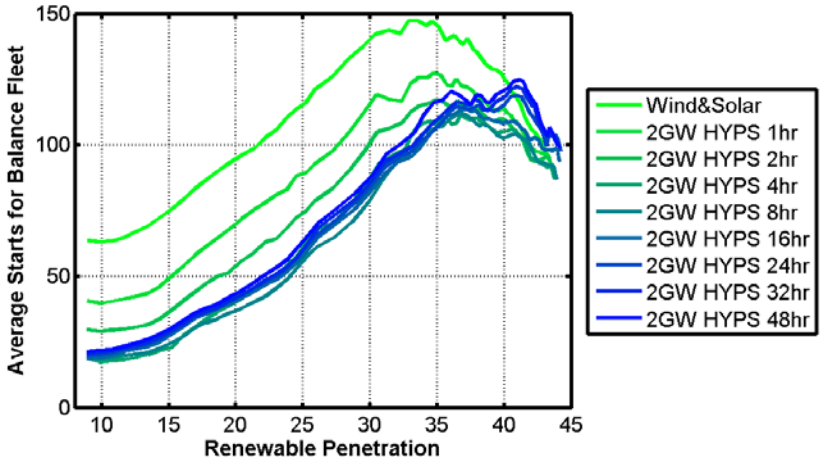

Figure 419 shows the effect of increasing energy capacity on CO_2 emissions. Similar to Figure 402, the selection of capacity can improve or deter CO_2 reductions. The maximum CO_2 reduction occurs for 8 hour capacity, while any larger capacity will cause the CO_2 emissions to increase initially and again at very high renewable penetrations. As described previously for the power capacity, this increase is as a result of the energy penalty that must be overcome initially and the large amount of excess generation at high penetrations.

Figure 419: Carbon Dioxide Emissions for Different Installed Capacities with a 50/50 Mixture of Wind and Solar

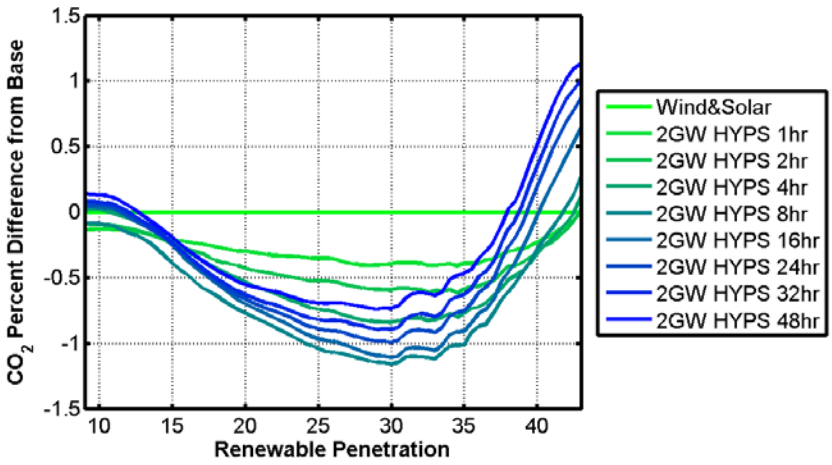

The next section will explore the cost implications for installing energy storage generation by again performing sensitivities on both the power capacity and the energy capacity.

7.3.1.4.2.2.1. Conclusions

- Increasing energy capacity increases the amount of energy that can be shifted by increasing the time window when energy is available to store.
- Larger energy capacities increases the additional generation required to store the energy (i.e., energy storage penalty)
- The benefits of increasing the energy capacity must outweigh the energy penalty for charging and discharging the storage system
- Larger energy capacities can increase the capacity factor and grid efficiency, reduce the ramp rates up and down, the average balance fleet starts and CO_2 emissions with respect to smaller capacities; however, there is a limit to the value of increasing the capacity. Capacities below represent values after which the additional performance is greatly diminished or negligible:
    - 48 hours at rated capacity (maximum option) for enhancing renewable penetration
    - 16 hours at rated capacity for increasing grid efficiency and capacity factor
    - 8 hours at rated capacity for minimizing CO_2 emissions
    - 4 hours at rated capacity for minimizing ramp rates and generator starts
- Energy Capacity is tightly tied with the power capacity

- Increasing the power capacity or energy capacity increases the use of an energy storage system and also increases the associated energy penalty with operating that system.
- Increasing power capacity increases the rate at which energy storage can shift energy but is limited by the energy capacity.
- Similarly, energy capacity affects the amount of energy that can be shifted and can be limited in its ability to shift if the power capacity is too low.

- Power capacity is the most important factor for reducing ramping requirements

7.3.1.4.3. Cost Results

Using the resulting power profiles along with the cost values, the effect on the levelized cost of electricity (LCOE) can be explored. Figure 420 shows the technology specific levelized costs for each generating technology that makes up the grid mixture with energy storage and Figure 421 represents the case without energy storage. "Complementary" represents a 4GW HYPS energy storage system. LCOE values for hydro, nuclear, coal, geo, and load-following generation represent fully depreciated assets (i.e., no capital investment is required only fuel and operation and maintenance (O&M) costs). Peakers initially, represent the all legacy generation but if additional plants must be installed to compensate for the changing demand shape, and then they are installed as new, non-depreciated plants and are assessed a capital cost.

Due to the operation strategy, the load-following LCOE is reduced for the energy storage case since greater energy from the renewables can be harnessed thereby reducing the number of required load-following plants and the load swings these generators must meet. The peaker LCOE is not always less for the energy storage case. This is due to several factors. First, energy storage acting to increase renewable penetration does not specifically focus on reducing peaker generation, though that is an important topic for future research and presents a valuable opportunity for energy storage devices.

As the penetration increases, the LCOE of energy storage reduces. This is on account of the ability to increase the amount of energy shifted as the penetration increases while maintaining the same capital cost and very similar O&M cost.

Figure 420: Technology Specific Levelized Cost of Electricity for each Generation Technology with 4GW of 8 Hour Pumped Hydro with a 50/50 Mixture of Wind and Solar

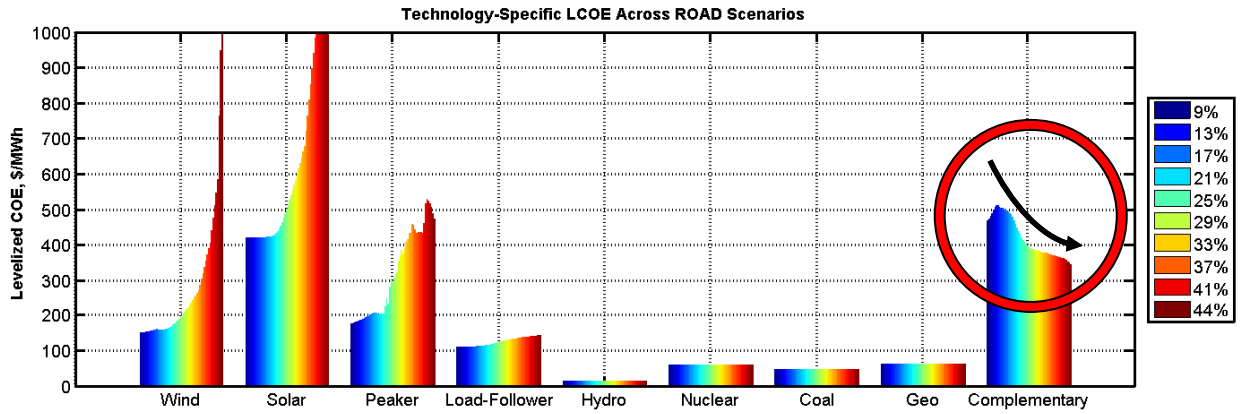

Figure 421: Technology Specific Levelized Cost of Electricity for each Generation Technology Excluding Energy Storage with a 50/50 Mixture of Wind and Solar

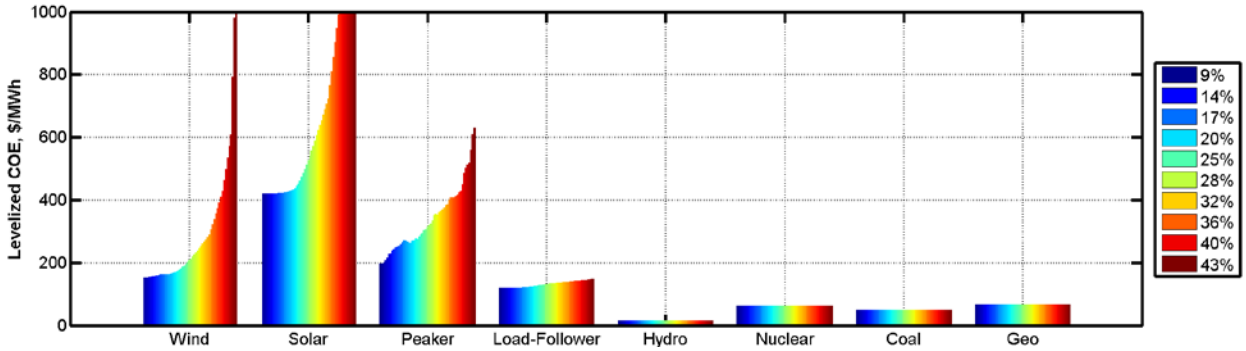

For energy storage systems to be cost competitive they must provide enough value to balance their capital and O&M costs including the energy penalty for storing energy. If the system-wide LCOE for the case with energy storage is less than that of the case without energy storage for a specific renewable penetration then energy storage is instantly valuable and should be installed. If the opposite is true then its value while operating in renewable integration mode does not warrant installation from a cost perspective. Fortunately for energy storage, as the renewable penetration increases the value of energy storage increases for a few reasons. First, energy storage LCOE generally reduces with increasing penetration due to an increase in the energy generated. Second, the cost of renewables increases non-linearly due to a number of reasons including 1) progressively lower capacity factor site availability with increasing installed capacity even when considering geographic diversification, 2) the need to maintain grid reliability by acquiring firm reserve capacity and additional regulation due to intermittent behavior, and lastly 3) high penetrations experience excess generation of renewables that, if not exported, can exponentially increase the LCOE.

The cost competitiveness for energy storage technology can be assessed by comparing the cost of the case without energy storage to the case with energy storage. For technologies that are not

cost competitive with the base case from the initial penetration, locating the crossover point (i.e., the renewable penetration after which the technology is competitive in the market) is critical to comparing different energy storage types and strategies from a cost perspective. Figure 422 presents the value of a 4GW, 8 hour capacity HYPS installation. Notice that initially, the value of the HYPS is negative, signifying that it is not cost competitive until the renewable penetration increases to 20.55% at which time the value of the HYPS with respect to the base case is zero. For greater penetrations the value of HYPS continues to grow, particularly as excess renewable generation becomes available for shifting.

Figure 422: Cost Competitiveness of Energy Storage with Increasing Renewables for 4GW HYPS and 8 Hour Capacity with a 50/50 Mixture of Wind and Solar

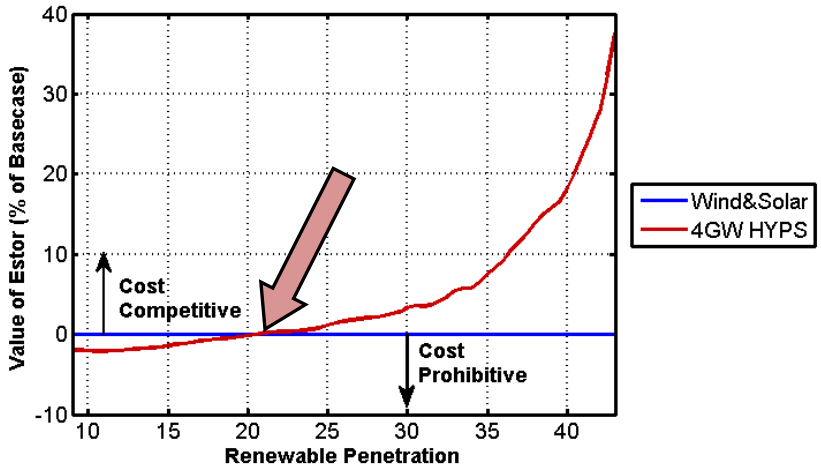

The cost competitiveness plot is derived by comparing the LCOE for two different cases. The LCOE values from which Figure 422 was developed are shown in Figure 423 as a percentage change from the initial, base case (Wind&Solar) LCOE value. This figure suggests that when the base case LCOE doubles (i.e., 100%), 1) including energy storage could reduce the LCOE by 16.5% and 2) including energy storage could increase the renewable penetration by 1.64% for the same LCOE as the base case.

Figure 423: Levelized Cost of Electricity Comparison between the base case and a 4GW, 8 Hour Capacity HYPS with a 50/50 Mixture of Wind and Solar

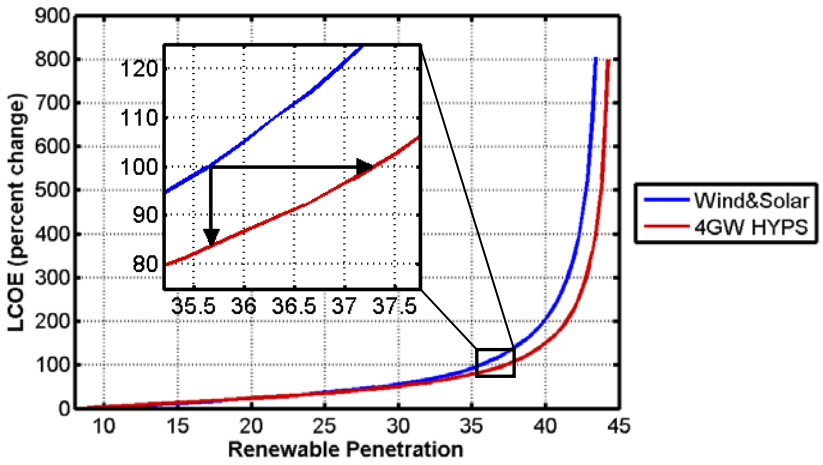

Using the same technique each power and energy capacity case can be explored to determine which cases are cost competitive. Figure 424 presents the value of energy storage compared to each power capacity value. Initially, larger power capacities are less competitive. 0.5 and 1 GW are always cost competitive and will lower the system LCOE in all cases. A 2GW installation starts cost competitive, dips slightly below the line around 11% and then increases in competitiveness beyond the 0.5GW for the remainder of the scenario. The other power capacities, though they provide superior performance advantages are not initially cost competitive. It is not until higher penetrations (24%, 35, etc.) that the storage becomes cost competitive with the current grid. As a reminder the competitiveness of each technology is based on operation to support renewable integration, not specifically for peaker support or ancillary service provision, though some of that behavior is experienced in the renewable integration strategy.

Figure 424: Levelized Cost of Electricity Comparison between All Power Capacity Cases for 16GWh Capacity with a 50/50 Mixture of Wind and Solar. Positive Values: Cost Benefit (cheaper), Negative Values: Cost Detriment (more expensive).

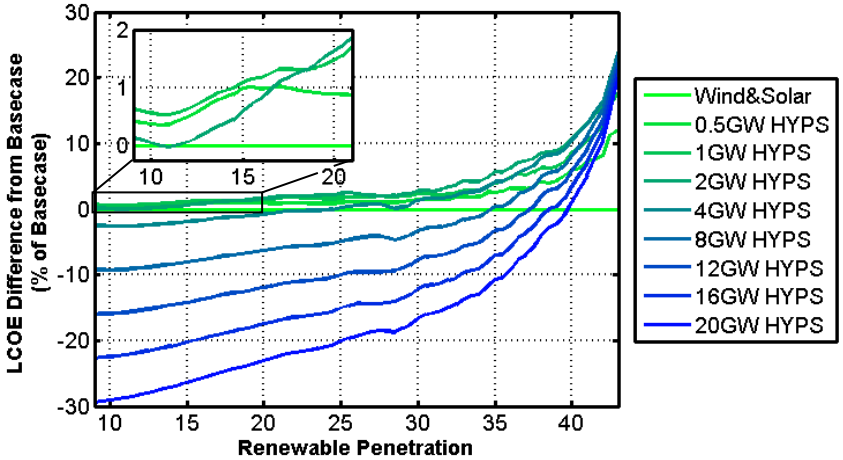

By averaging the LCOE difference value from Figure 424 for each renewable penetration, the average value for each scenario is calculated (Table 81). This shows that for different power capacities with 16GWh energy capacity, that 2GW is the preferred power capacity to achieve the maximum value over the lifetime of the system for all renewable penetrations. 16GWh would result in a system that has 8 hours of storage at rated power.

Table 81: Average Value for Various Power Capacities per Renewable Penetration

Total Rated Power Capacity (GW)	Energy Capacity (GWh)	Average LCOE difference from base case across all penetrations
0	0	0 (base case)
0.5	16	2.13
1	16	3.24
2	16	3.99
4	16	2.25
8	16	-2.43
12	16	-7.15
16	16	-11.82
20	16	-16.46

Smaller energy capacity systems are less cost competitive than larger capacity systems. The biggest reason for this is because the cost is assessed based on installed capacity (i.e., $/kW) and not on energy capacity. Variable operation and maintenance is charged on a per energy basis (i.e., $/kWh), and that is one reason that the larger capacities are very close and alternate for the most valuable in the 20%-35% penetration range. Increased generation from systems with larger energy capacity should reduce the LCOE for the system but from a combination of the

energy charge penalty and the variable O&M cost, the value of those systems can vary depending on the specific hourly operation of each system.

Figure 425: Levelized Cost of Electricity Comparison between All Energy Capacity Cases for HYPS with a 50/50 Mixture of Wind and Solar. Positive Values: Cost Benefit (cheaper), Negative Values: Cost Detriment (more expensive).

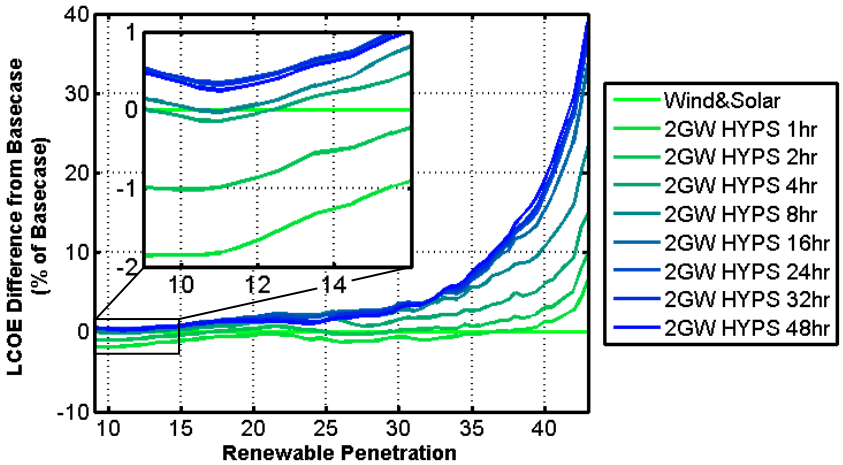

To find the most cost effective solution over the entire lifetime of the system, the average is taken for each energy capacity of the LCOE difference from the base case. The results are presented in Table 82. A system with 2GW has the greatest value at the highest energy capacity (i.e., 96GWh or 48 hours at rated capacity) for the reasons described in the previous paragraph.

Table 82: Average Value for Various Energy Capacities per Renewable Penetration

Total Rated Power Capacity (GW)	Energy Capacity (GWh)	Average LCOE difference from base case across all penetrations
0	0	0 (base case)
2	2	-0.41
2	4	0.71
2	6	2.26
2	16	3.99
2	32	5.32
2	48	5.68
2	64	5.74
2	96	5.88

7.3.1.4.3.1. Conclusions

- The technology-specific LCOE generally increases with increasing renewable penetration although the energy storage specific LCOE decreases with increasing renewable penetration

- Different operation strategies (e.g., renewable integration, ancillary service, peaker support) should be explored to compare the differences in value
- Energy capacity and power capacity should be sized appropriately to minimize cost, in addition to maximizing performance.
    - 2GW power capacity with 16GWh of storage is the most cost effective among the power capacity options
    - 48 hours at rated capacity (maximum option) is the most cost effective among the energy capacity options
- Energy storage must balance value to the grid with capital and O&M costs including the energy penalty for storing energy

Figure 426: Factors Affecting the Cost Competitiveness of Energy Storage

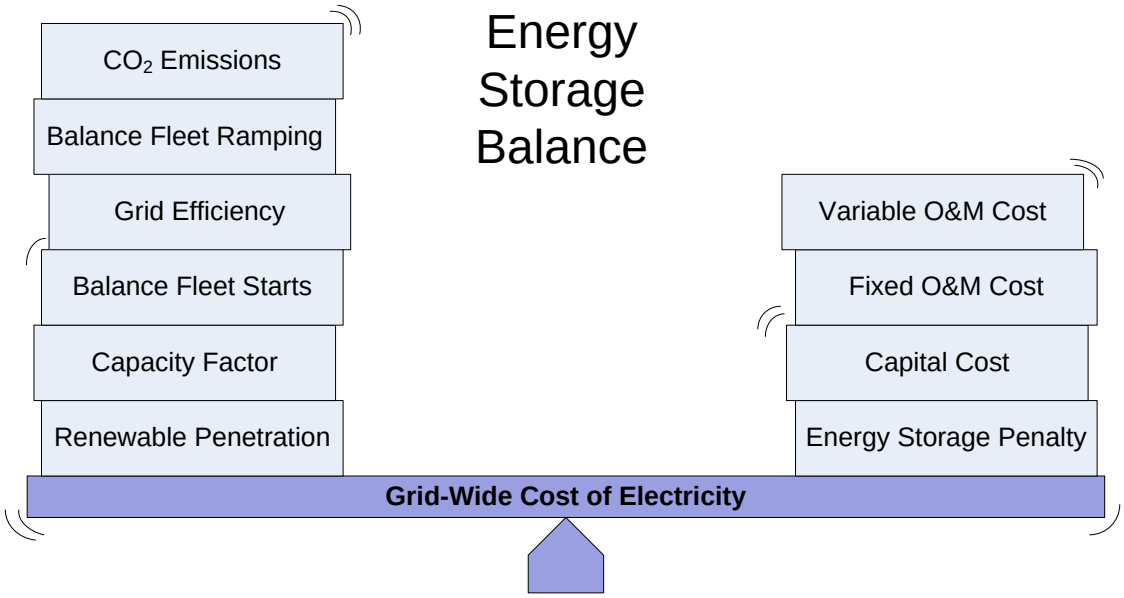

7.3.1.4.4. Technology Type Comparison Results

The previous sections have explored the implications of HYPS but this section will look at the two other technologies mentioned, compressed air energy storage (CAES) and vanadium redox flow batteries (VFB) along with HYPS.

While the operation is nearly the same there are a few slight differences. To compare the different storage types, first operating parameters must be selected. Based on the previous findings, 2GW with an energy capacity of 16GWh (8 hours) was selected. This represents a balance of low cost and performance improvements as well.

Figure 427 shows the daily average profile for a 2GW installation. The difference between HYPS and VFB is from a difference in the charge/discharge ratio that limits the charging rate of the VFB. CAES is larger because, though its overall efficiency is lower than the other types, it is able to generate electricity using a fueled generator so it has fewer restrictions on its ability to generate electricity. Similar behavior is exhibited for a renewable penetration of 33% except that the shape of the profile is adjusted to complement the renewable signal as shown in Figure 428.

Figure 428.

Figure 427: Daily Average Energy Profiles at 9% Renewable Penetration with 2GW of three different Storage Technologies for a 50/50 Mixture of Wind and Solar

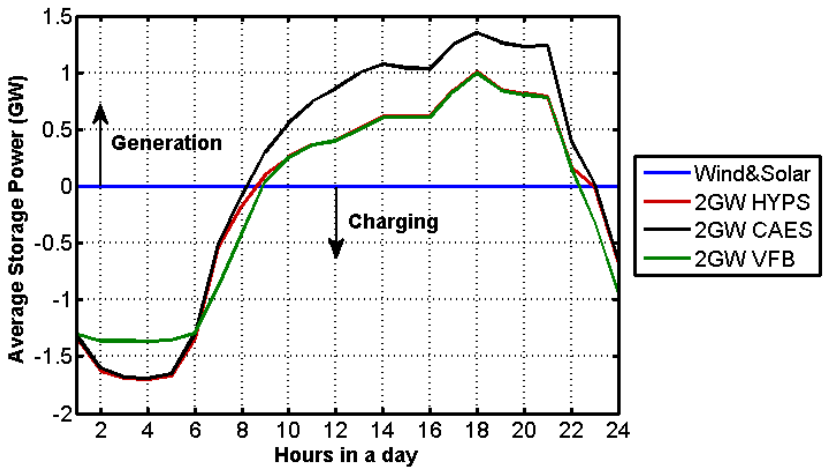

Figure 428: Daily Average Energy Profiles at 33% Renewable Penetration with 2GW of three different Storage Technologies for a 50/50 Mixture of Wind and Solar

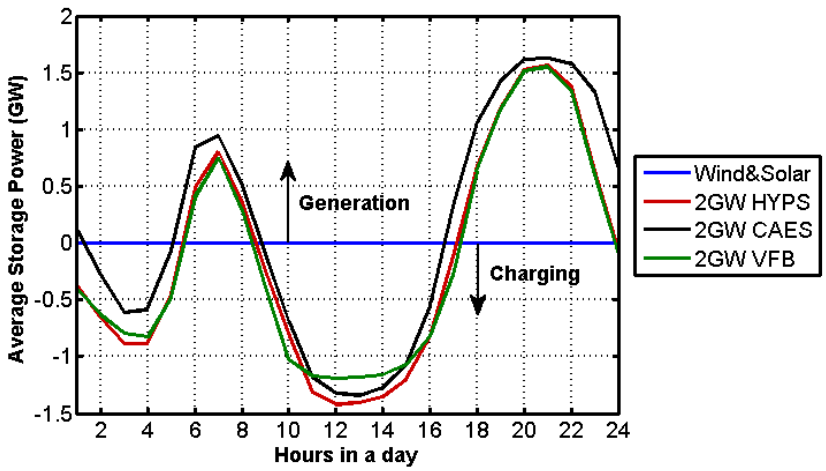

As a result of these differences in operation the CAES is able to generate more additional energy than the HYPS and VFB as shown in Figure 429.

Figure 429: Energy Generation with 2GW of three different Storage Technologies for a 50/50 Mixture of Wind and Solar

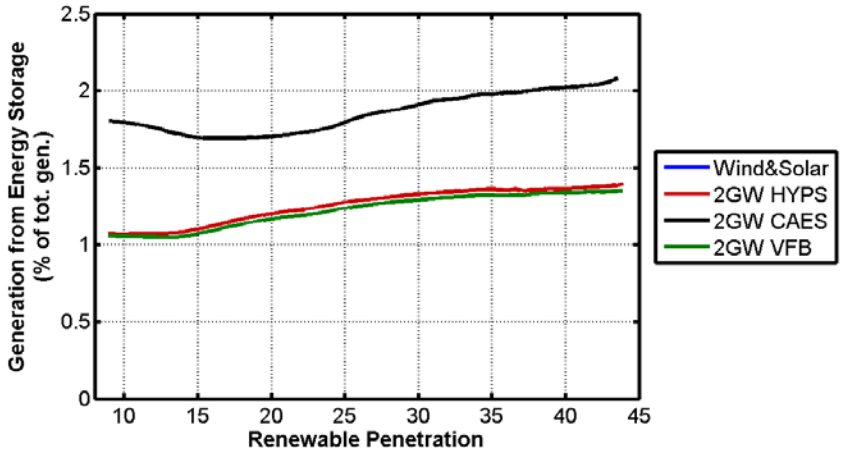

On account of greater total generation from CAES and lower overall efficiency, the energy penalty for CAES is larger than that of the HYPS and VFB as can be seen in Figure 430.

Figure 430: Energy Penalty with 2GW of three different Storage Technologies for a 50/50 Mixture of Wind and Solar

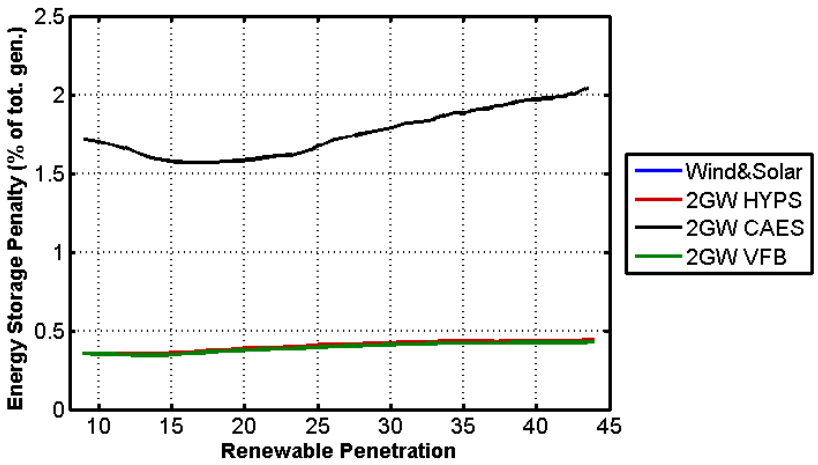

The system-wide efficiency is improved by all types of energy storage with 2GW of installed capacity; however, CAES experiences a slightly lower increase in the efficiency due to its lower overall efficiency. The total grid efficiency is shown in Figure 431 and again in Figure 432 as the difference from base case signal.

Figure 431: Grid-wide Fuel to Electrical Efficiency with 2GW of three different Storage Technologies for a 50/50 Mixture of Wind and Solar

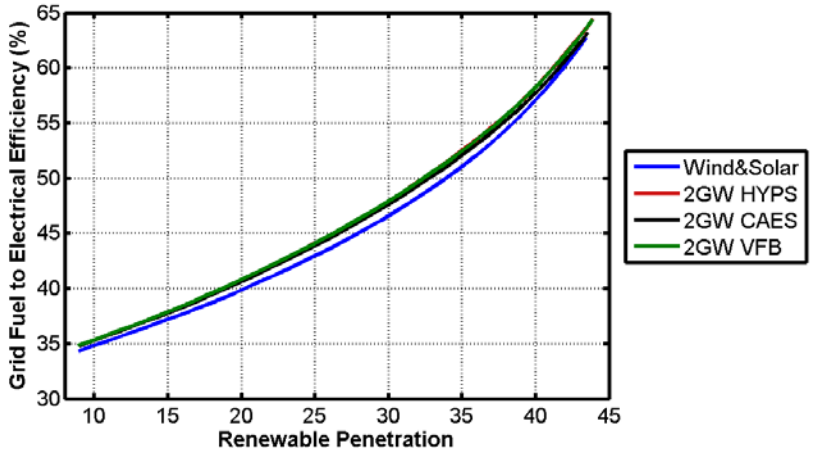

Figure 432: Grid-wide Efficiency with 2GW of three different Storage Technologies as a Difference from the case without Energy Storage for a 50/50 Mixture of Wind and Solar

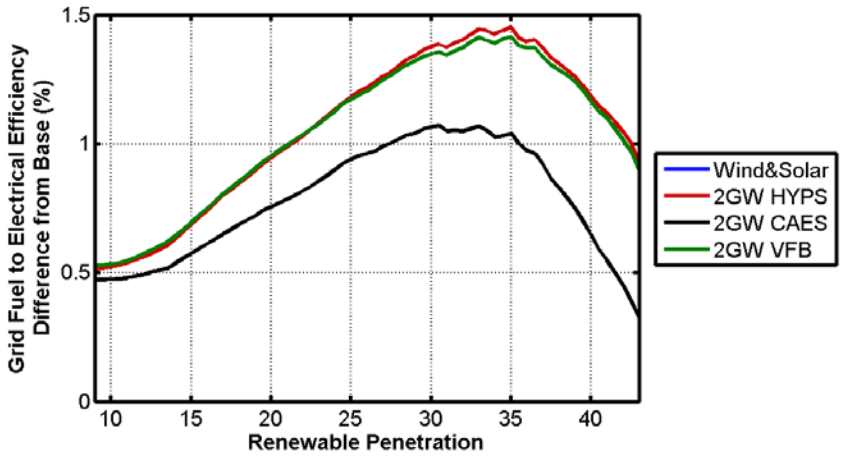

The balance fleet generator ramp rate up and down and yearly starts are very similar for all the three technologies as shown in Figure 433, Figure 434 and Figure 435.

Figure 433: Average Balance Fleet Generator Ramp Up with 2GW of three different Storage Technologies for a 50/50 Mixture of Wind and Solar

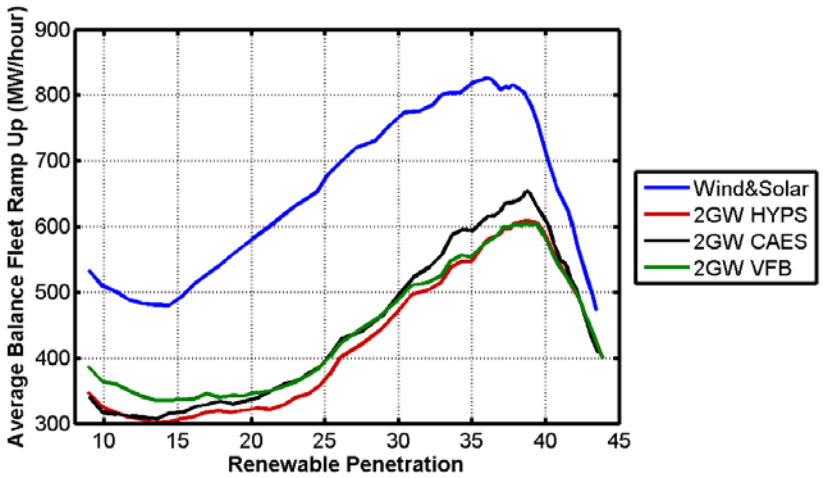

Figure 434: Average Balance Fleet Generator Ramp Down with 2GW of three different Storage Technologies for a 50/50 Mixture of Wind and Solar

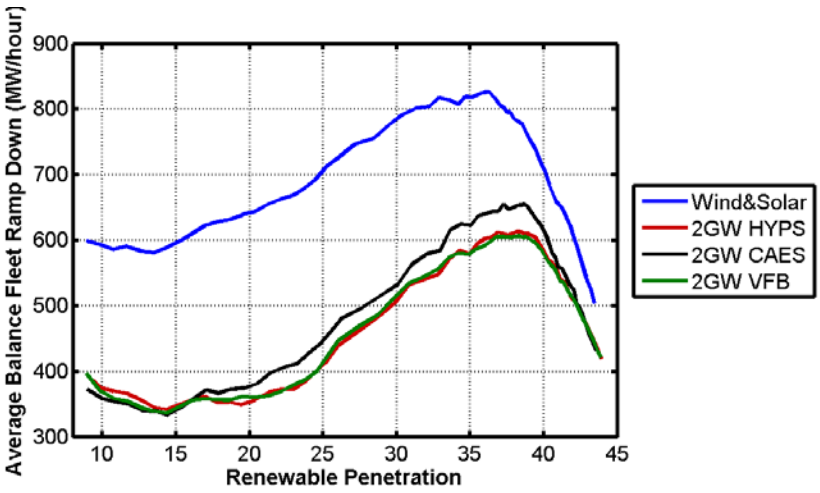

Figure 435: Average Balance Fleet Starts with 2GW of three different Storage Technologies for a 50/50 Mixture of Wind and Solar

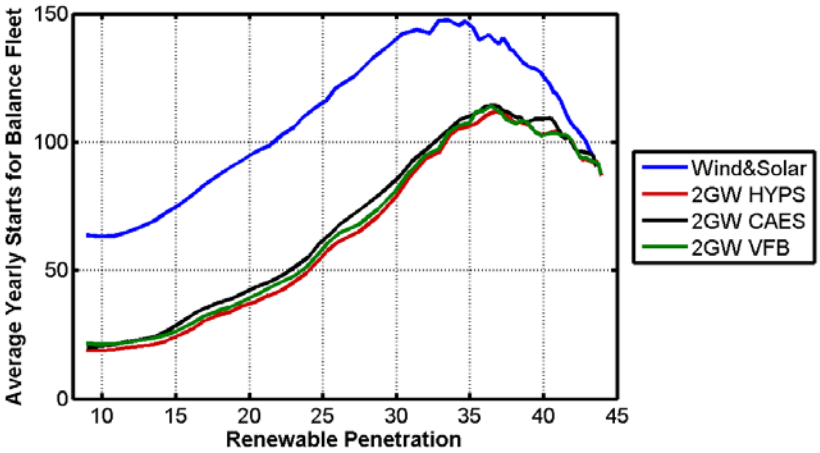

Carbon dioxide emissions for HYPS and VFB are very similar and the only really distinguishable difference comes from CAES. Unlike HYPS and VFB, CAES supplements its generation with a natural gas generator, which has CO_2 emissions. That is why the reduction for using CAES is the lowest.

Figure 436: Carbon Dioxide Emissions with 2GW of three different Storage Technologies for a 50/50 Mixture of Wind and Solar

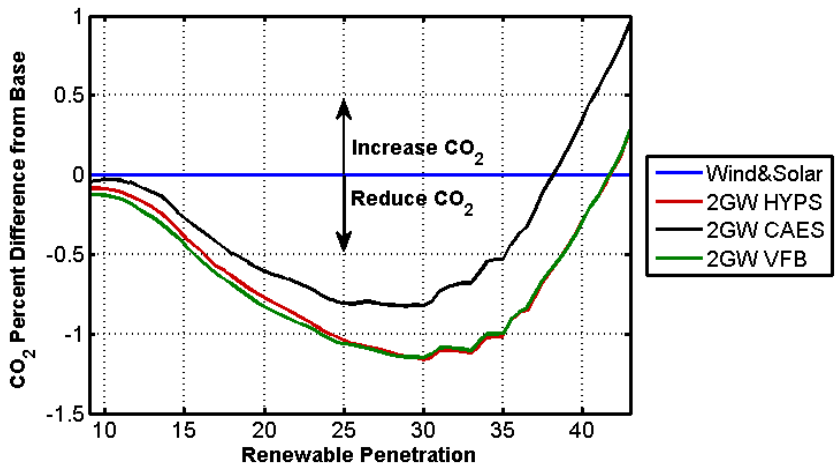

Lastly, the LCOE for each of the three technologies compared to the base case, "Wind&Solar" results in HYPS as the most cost competitive technology followed by CAES and then shortly after by VFB. The order is mainly a function of the capital and operation and maintenance costs and lifetime of the equipment. Equipment with a longer life is favored from a cost point of view. For capital and fixed O&M, CAES is the least expensive followed by HYPS and then VFB, and for variable O&M, CAES is much more expensive than the other two technologies. The balance of these factors results in LCOE values shown in Figure 437.

Figure 437: Levelized Cost of Electricity Comparison between 2GW of three different Storage Technologies for a 50/50 Mixture of Wind and Solar

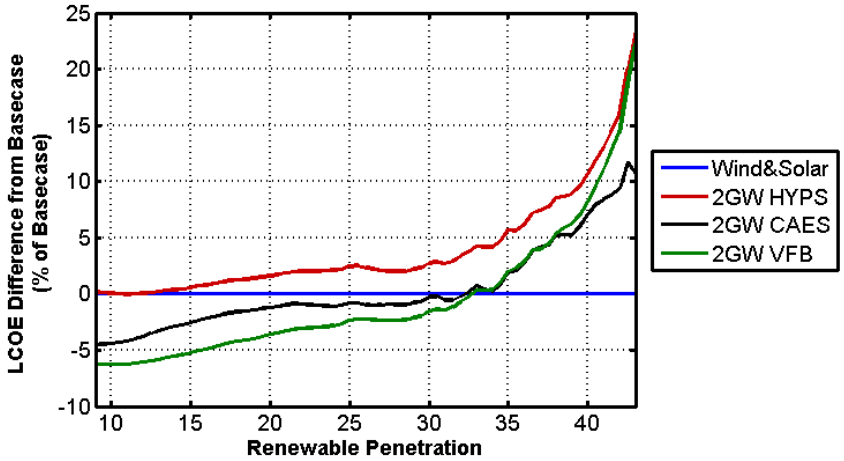

7.3.1.4.4.1. Conclusions

- Energy storage is a shifting technology and not a generating technology since the systems must first be charged.

- Shifting load results in a small increase in electricity demand because of the energy penalty associated with storing the energy (i.e., <100% efficiency). This will result in a small decrease in the renewable penetration by increasing the denominator while the numerator stays the same.
- Energy storage can change the operation of current generation and increases the uptake of renewables.
- Energy storage is likely not cost effective at low renewable penetrations but becomes more cost effective as the penetration is increased.
- Longer economic lifetimes contribute to why the HYPS technology is more attractive than the CAES and VFB.
- CAES has less restrictions on its generation because depending on the configuration CAES can have a fossil fueled generator to supply additional electricity
- CAES can provide more energy than the other types given the same energy capacity because it includes a fueled generator.
- CAES has a lower fuel to electrical efficiency, a higher energy penalty and higher CO_2 emissions because of the use a fueled generator while HYPS and VFB have similar behavior.

Task 7.3.2. Energy Efficiency

Energy efficiency (EE) represents an opportunity to reduce the electrical demand by installing higher efficiency or more flexible technologies than what was previously installed. A few examples include replacing lighting with low energy consumption bulbs, adding motion sensors to turn lights off in unoccupied areas, and balancing and optimizing Heating, Ventilating and Air Conditioning (HVAC) system.

There is an interesting interplay between the use of energy efficiency and demand response. An increase in EE reduces the electrical demand and will oftentimes reduce the available capacity of DR. Similarly, if capacity is reserved for DR then it will be inaccessible to perform EE measures. The interactions between DR and EE are explored for the simplified UCI community model.

7.3.2.1. Approach

The first step in developing a model of energy efficiency is to determine what the effect of installing selected technologies will have on the demand signal. UCI demand is separated by end-uses which are drawn from Task 6.3 and include:

- Lighting – All lighting fixtures within the building, including some task lighting (modeled together for UCI building models) and security/emergency lighting. Assume baseline lighting is incapable of automatic dimming.
- Task lighting – Task lighting energy modeled in CEUS and DEER building prototype models.
- Miscellaneous – Includes all plug loads from office equipment and other occupant-driven loads (i.e. everything that is unaccounted for in the other end-use categories).
- Auxiliary – Includes overhead process-based loads, which are primarily pump energies for the modeled buildings.
- Vent fan – All fan energy, primarily supply fan, but includes return and exhaust fan energy.
- Controllable vent fan – A subset of vent fan end-use energy which excludes all modeled ventilation for laboratory, healthcare, residential, or general (restaurants, schools, assemblies) because of constraints for ventilation requirements.
- Exterior total – Includes exterior lighting for buildings and parking lots, as well as elevator operation. Some load is attributed to exterior building lighting based on the model calibrations, while the rest has been estimated based on the observed quantity and operation of generic exterior lights and elevators throughout the campus.
- Total – The sum of all electric energy end-uses (excluding controllable vent fan energy, to avoid double-counting).
- Heating (Btu) – Modeled heating load served to the buildings by the central plant.
- Cooling (Btu) – Modeled cooling load served to the buildings by the central plant.
- Domestic hot water (Btu) – Modeled heating load for the domestic hot water systems serving each building.

The "lighting" category is used to consider the effects of interior lighting. The "Exterior lighting" category is used to assess the impacts of EE on exterior lighting. Finally, the "Vent Fan" category is used to determine the effects of EE on the HVAC system.

Reductions from energy efficiency are drawn from the results of Task 6.3 where each energy efficiency measure is analyzed for its capability.

7.3.2.2. Results

Three analyses are performed to explore the impacts of EE and combined EE/DR systems on the cost and performance of a grid system with increasing renewables. The first analysis involves looking at the impact of EE, EE with DR and DR alone for both lighting and HVAC. The second analysis is similar to the first but only includes HVAC technologies and focuses on the cost implications for performing HVAC only. The first two analyses are performed using a rollout

plan that incrementally installs a 50/50 mixture of wind and solar. The final analysis explores how different renewable mixtures influence the economic viability of installing EE technologies.

Cost values for EE technologies are determined (Table 83) based on the findings from Task 6.3. The gross capacity values are set by the analysis to determine the maximum amount of EE capacity that is available to the UCI campus. The instant cost for lighting is based on the purchase of a DALI interface, fixtures and controls. The instant cost for HVAC is based on 8 weeks of programming time, a fixed expense for controls and equipment, and a cost per gross square footage of the building. Notice that the fixed operation and maintenance (FOM) for lighting is negative meaning that installation of the new lighting will reduce the FOM, while the HVAC FOM value is positive representing an additional week of controls work each year.

Table 83: EE technology Costs

Capacity and Cost	Exterior/Garage Lighting Fixtures & Controls	Interior Lighting Fixtures & Controls	HVAC Controls Optimization & Balancing
Gross Capacity (kW)	1091.00	1648.00	1354.00
Instant Cost ($/kW)	$10,357.47	$11,990.29	$1,505.91
FOM ($/kW-yr)	-$453.66	-$50.00	4.43

Costs for DR technologies vary with the inclusion of EE. Table 84 shows the instant cost and FOM costs that are assessed to DR technologies without EE technologies included and Table 85 shows the cost of the same technologies with EE included. Notice the gross capacity falls, signifying a reduction in maximum available fan power and lighting power. The instant cost for the supply fan rose because the controls work for the fan will need to be done with or without EE and is a fixed cost so the same amount of controls spread over fewer kW of capacity causes an increase in the cost. Lighting saw a sharp reduction in the instant cost because the instant cost from EE directly contributes to lowering the DR lighting cost. The FOM cost increases for the supply fan and reduces for lighting for the same reasons that the instant cost is affected.

Table 84: DR Costs Without EE Technologies

Capacity and Cost	Supply Fan Limitation	Lighting Reduction
Gross Capacity (kW)	3758.00	4742.00
Instant Cost ($/kW)	16.76	500.00
FOM ($/kW-yr)	1.60	1.75

Table 85: DR Costs With EE Technologies

DR Costs with EE	Supply Fan Limitation	Lighting Reduction
Gross Capacity (kW)	2979.00	3730.00
Instant Cost ($/kW)	21.15	8.06
FOM ($/kW-yr)	2.01	0.00

7.3.2.3. Energy Efficiency Cases – Lighting and HVAC

7.3.2.3.1. Description of Cases

This analysis is performed on using the total electrical demand signal of UCI's campus (i.e., assuming that there is no on-site generation and all demand is met by import). All technologies are installed as a retrofit on existing buildings. Four signals are compared including:

1. 50/50 Wind and solar rollout without EE or DR
2. 50/50 Wind and solar rollout with EE and without DR
3. 50/50 Wind and solar rollout without EE and with DR
4. 50/50 Wind and solar rollout with EE and DR

The DR strategy for this analysis utilizes the DR model with the current Southern California Edison (SCE) DR program structure (see DR section for more details). Additionally, for DR, the occupant impact is set to two and the "grid smoothing" strategy is selected. To apply both EE and DR, first the EE is applied and, based on the remaining capacity, a new assessment of available DR capacity was developed.

7.3.2.3.2. Results

The way that each EE technology reduces the load is different. The daily average profile for each EE technology is presented in Figure 438. The interior lighting profile is able to reduce the demand the most during the day, when the most interior lights are on, and the exterior lighting profile is nearly the inverse of the interior profile. This is because most exterior lighting comes on during the night. Lastly, the HVAC profile is nearly linear except for a slight increase in the morning to accommodate cooling requirements in the morning.

Figure 438: Daily Average Profiles for Reduction using EE each Technology

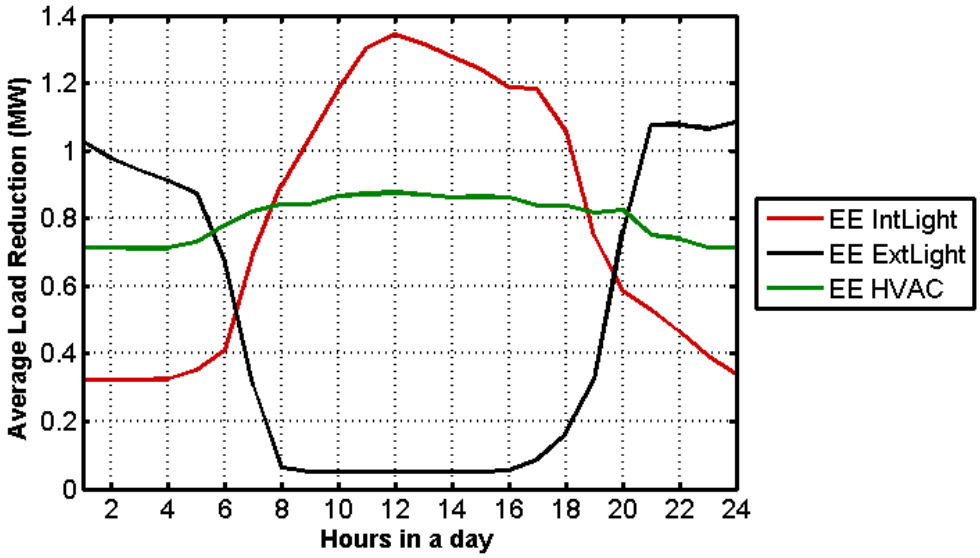

Figure 493 presents the daily average demand profile for each of the four signals compared. Notice the difference in the cases with EE and the cases without EE is large in comparison to the effect from DR and relatively constant throughout the day, and even though the individual components are different, the combination is nearly a baseload profile.

Figure 439: Daily Average Demand Profiles for UCI Campus at 9% Renewable Penetration for EE and DR Comparison with a 50/50 Mixture of Wind and Solar

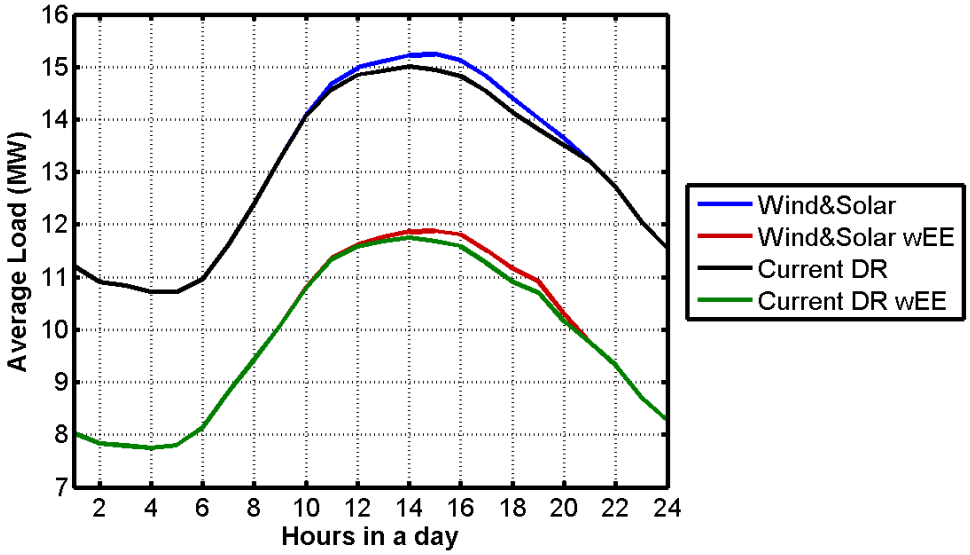

Separating the contribution to DR for the cases with EE and without EE shows that the dispatched DR reduces when EE is also implemented as shown in Figure 440. This is because the reduction in demand resulting from EE causes the hourly availability of DR to reduce in turn causing the average dispatched DR to reduce.

Figure 440: Daily Average Demand Response Profiles for UCI Campus at 9% Renewable Penetration for EE and DR Comparison with a 50/50 Mixture of Wind and Solar

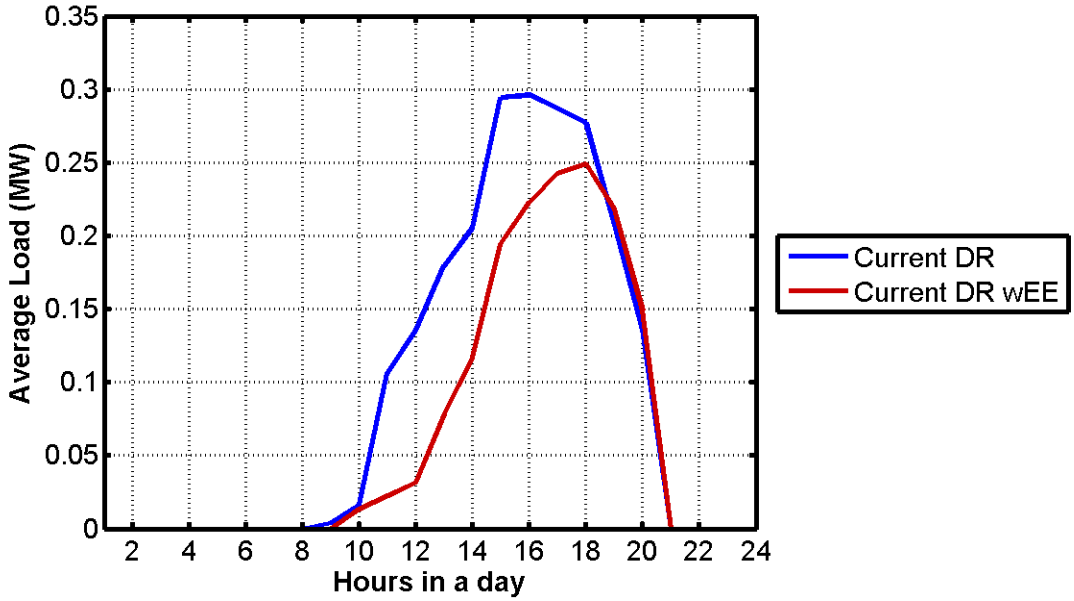

The achievable renewable penetration is 80% for the cases with EE and over 82% for the non-EE cases (Figure 502). Such a high achievable value is only because of the simplification of UCI's central plant for this analysis.

The EE cases begin with a lower installed renewable capacity than the non-EE cases for the same renewable penetration. After 73.6%, the relationship inverts and the non-EE case can provide lower installed capacity for the same renewable penetration. This is because of the energy efficiency reduction limiting the flexibility under high curtailment cases.

Figure 441: Renewable Penetration versus Installed Capacity for EE and DR Comparison with a 50/50 Mixture of Wind and Solar

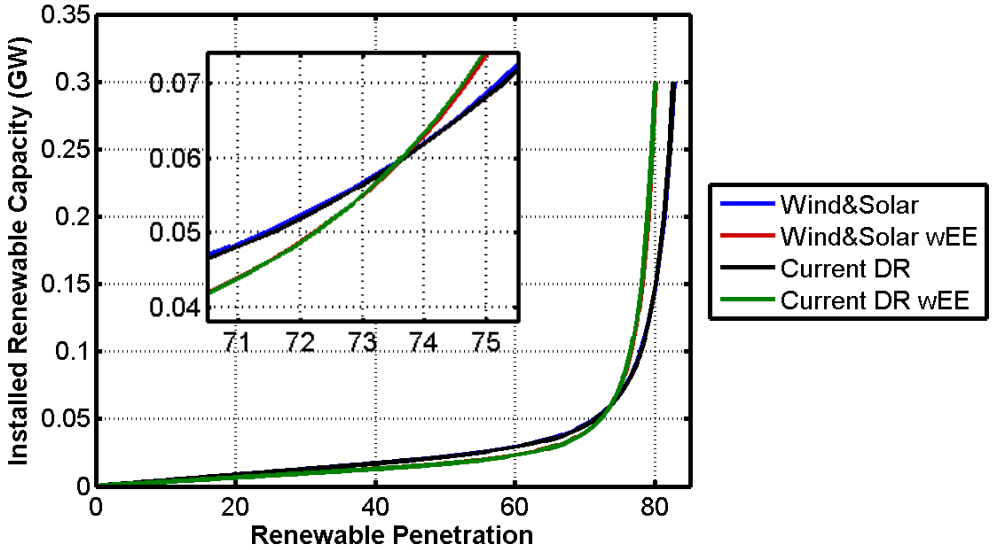

It is also interesting to look at the resulting effect on CO_2 emissions as shown in Figure 507. While the renewable capacity experiences an inversion of the EE and non-EE cases, carbon dioxide emissions for the EE cases are always lower than the non-EE cases, because of the reduced electricity demand requirements resulting from the EE measures; however the difference between the two reduces as the renewable penetration increases. Thus the value of EE for reducing CO_2 emissions reduces with increasing renewable penetration.

Figure 442: CO_2 Percentage Reduction from DR and EE cases for a 50/50 Mixture of Wind

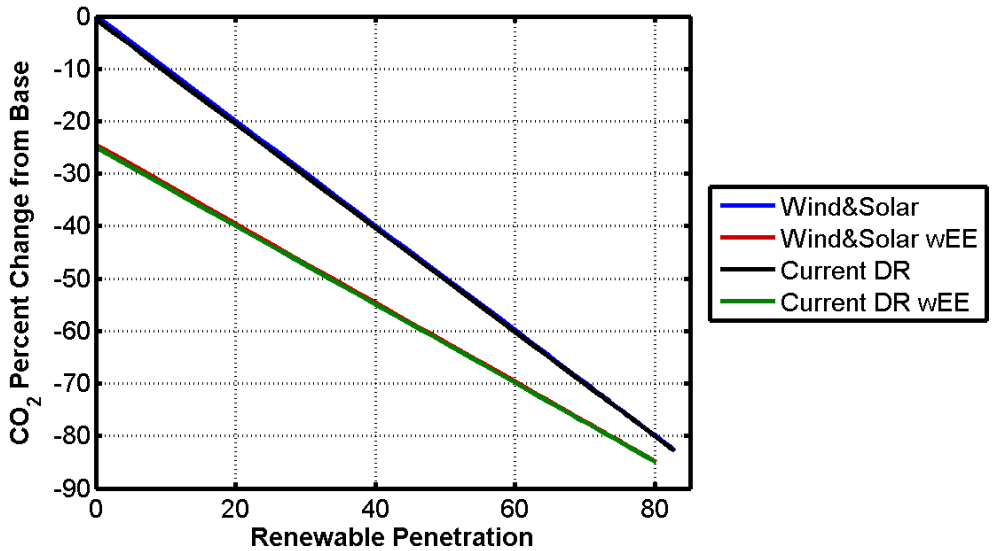

The impact on LCOE for different EE and DR cases is presented in Figure 509 as a percentage change from the zero point and as a percentage change from the base case (i.e., "Wind&Solar")

in Figure 444. Demand response operated with the current number of events begins slightly more expensive than the base case and steadily approaches the base case until it becomes more cost competitive than the base case at 76%. The energy efficiency cases require significant capital investment, particularly for the lighting technologies, as will be shown, and as result are not cost competitive.

Figure 443: LCOE Change for DR and EE cases with a 50/50 Mixture of Wind and Solar

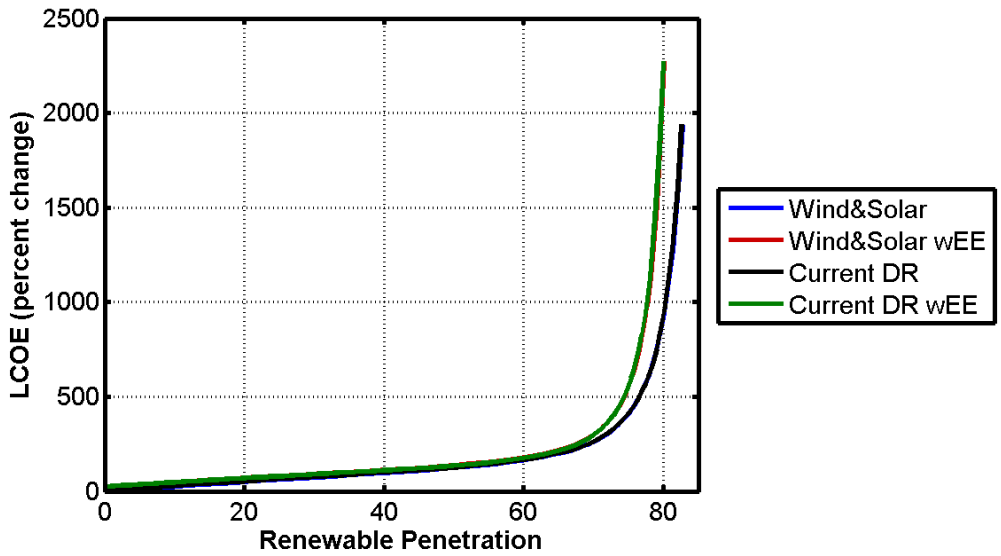

Figure 444: LCOE Percentage Change from the base case for DR and EE cases with a 50/50 Mixture of Wind and Solar

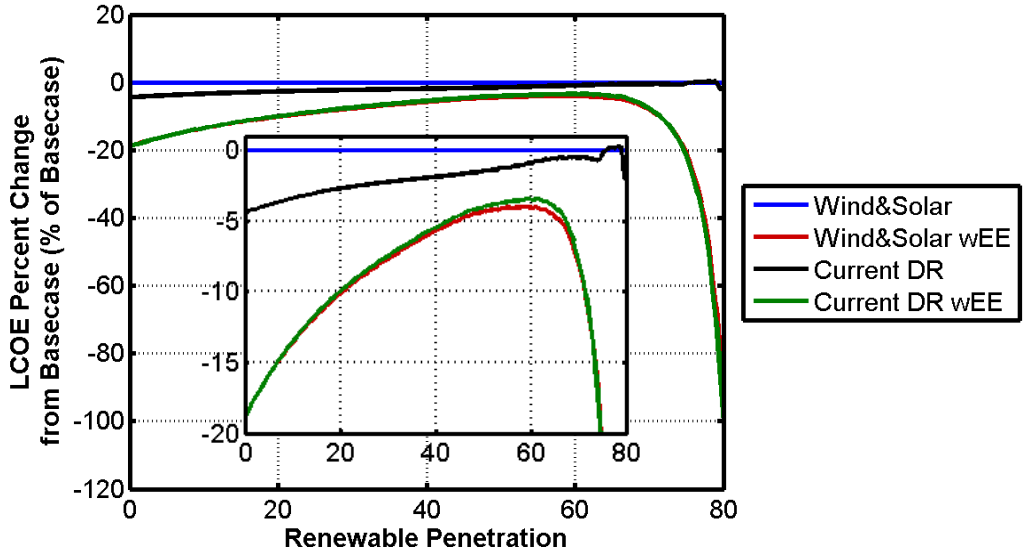

It has been shown that inclusion of EE affects the usage of DR and the performance the electric system with DR. EE also affects the relative value of DR. Figure 445, Figure 446, Figure 447 and Figure 448 show the levelized cost of electricity for each technology included in each of the four cases. The legend contains 11 items that breakdown the costs of each technology including: federal tax (fed tax), state tax, ad valorem tax (adv), debt and equity portion of investment, insurance (ins), fixed operation and maintenance (fom), CO_2 tax, variable operation and maintenance (vom), transmission (tx) and fuel. While the portfolio LCOE is developed by weighting each of these values with the energy contribution throughout each technology's lifetime the technology-specific LCOE is useful when comparing the effect of different technologies on the LCOE. Figure 445 represents the base case: 50/50 mixture of wind and solar at 38% renewable penetration. Notice that the import price is the lowest and both wind and solar are higher resulting in an increase in the portfolio price when more renewables are added.

Figure 445: Technology Specific LCOE at 38% Penetration from a 50/50 Mixture of Wind and Solar without DR or EE

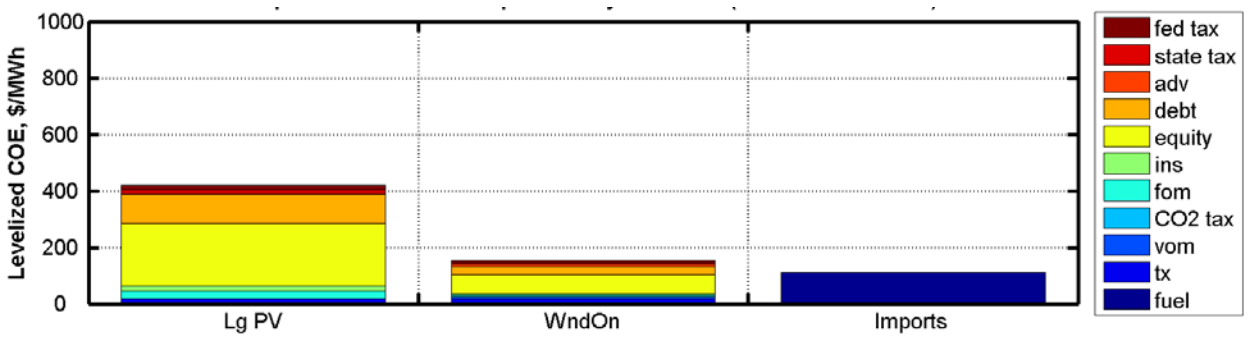

Once DR is added the technology-specific LCOE for each technology, excluding imports, will change slightly because of the change in the operation of each technology. From Figure 446 it is clear the lighting control is more costly than the other included technologies and that fan turndown is less expensive than the other technologies. This means that pursuing fan turndown alone will likely be cost effective, as will be explored in the next section.

Figure 446: Technology Specific LCOE at 38% Penetration from a 50/50 Mixture of Wind and Solar with DR and without EE

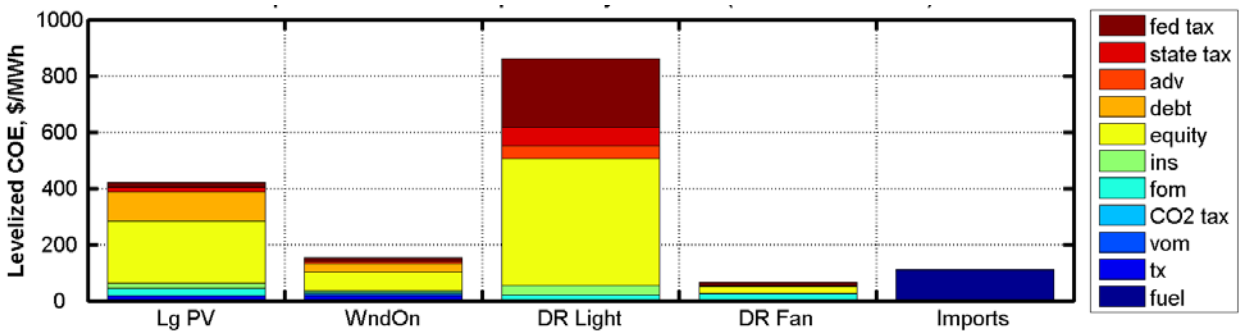

If the cost contribution for each of the EE technologies is separated, it is clear that the interior lighting is the most costly with respect to the resulting energy reduction that results. The second highest is exterior lighting and the HVAC is the least costly. Similar to the case with DR, the HVAC is lower than the price of all other technologies so it will likely lower the portfolio LCOE while the other technologies increase the LCOE.

Figure 447: Technology Specific LCOE at 38% Penetration from a 50/50 Mixture of Wind and Solar without DR and with EE

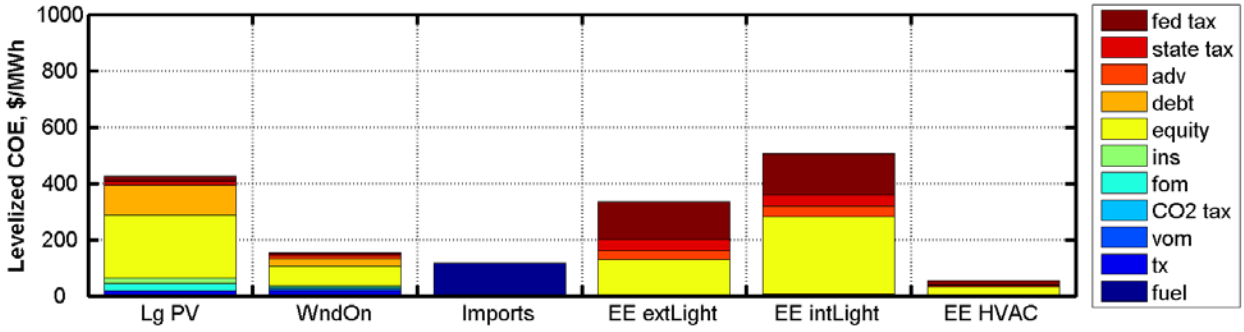

Several interesting things happen if we pursue EE and DR at the same time. The EE cost is the same for all cases; however, because advanced lighting is installed during the EE upgrades then the cost to perform lighting turndown is very marginal. Unlike lighting, the fan can be used less often but still costs a similar amount to instrument so its price per megawatt-hour of energy reduction actually increases.

Figure 448: Technology Specific LCOE at 38% Penetration from a 50/50 Mixture of Wind and Solar with DR and EE

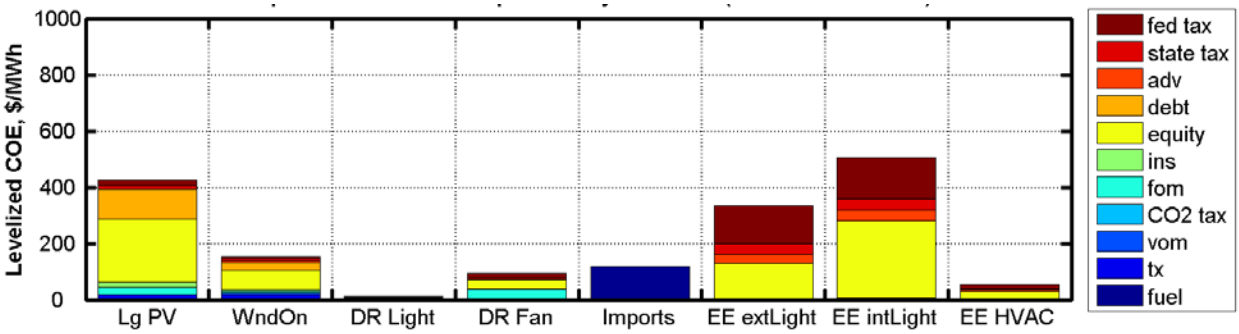

7.3.2.3.3. Conclusions

- The combination of interior and exterior lighting reductions and HVAC EE measures provides a reduction that is relatively flat and resembles baseload operation
- EE measures reduces the available capacity for DR.
- EE reduces the technology-specific LCOE to pursue DR for lighting turndown but increases DR for fan turndown's LCOE.
- Pursuing EE HVAC will cause little change to the DR HVAC costs while lighting EE will dramatically reduce the DR lighting costs.
- EE can provide a significant reduction to CO_2 emissions which is more pronounced at low renewable penetrations and less so at high penetrations.

7.3.2.4. Energy Efficiency Cases – HVAC Only

7.3.2.4.1. Description of Cases

The previous section recognized that the cost of each EE technology varies with renewable penetration and that the cost of high efficiency lighting is much more than that of the cost of HVAC. This section explores the value of pursuing only energy efficient HVAC and excluding the interior and exterior lighting reductions.

7.3.2.4.2. Results

The EE cases show lower cost than the base case as shown in Figure 449. While the additional impact of DR is small, the current DR case does become cost competitive at 19.6% renewable penetration.

Figure 449: LCOE Percentage Change from base for DR and EE cases using only HVAC with a 50/50 Mixture of Wind and Solar

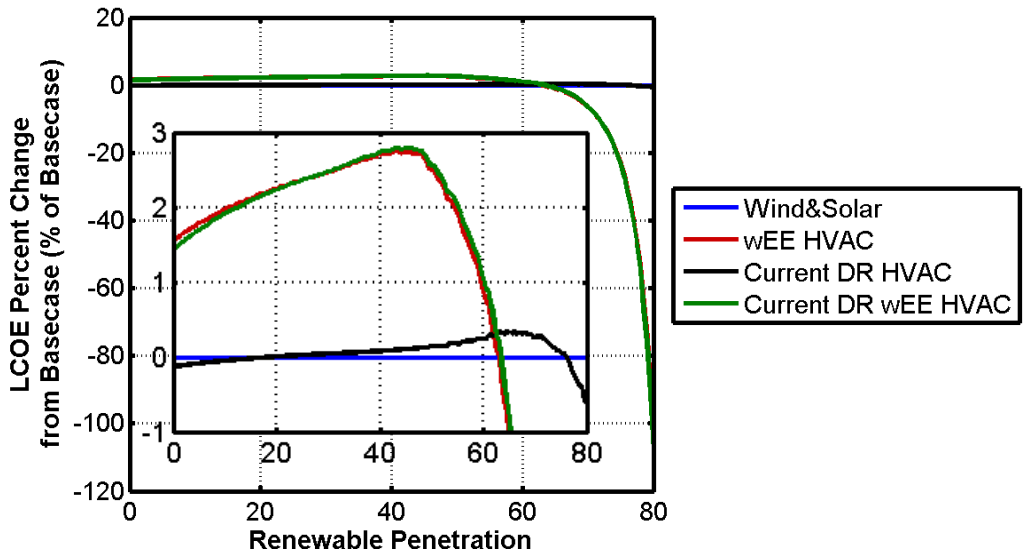

Looking at the technology-specific LCOE shows a similar story. The base case LCOE components are shown in Figure 450 where the legend contains 11 items including: federal tax (fed tax), state tax, ad valorem tax (adv), debt and equity portion of investment, insurance (ins), fixed operation and maintenance (fom), CO_2 tax, variable operation and maintenance (vom), transmission (tx) and fuel. Wind and solar are both more expensive than the imports and therefore cause an increase in the LCOE with increasing renewables.

Figure 450: Technology Specific LCOE at 38% Penetration from a 50/50 Mixture of Wind and Solar without DR or EE

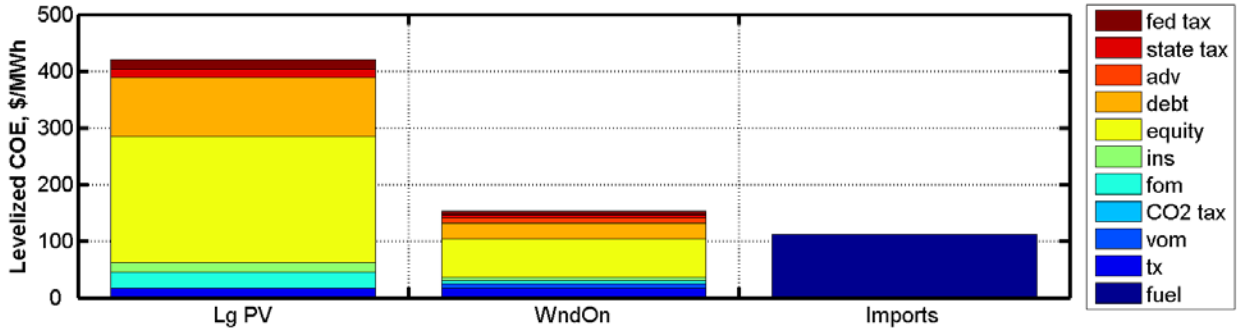

The technology specific cost of renewable technologies increases with increasing renewable penetration due predominantly to excess generation. In addition, dynamics on the grid can be reduced with the use of DR. As a result of increasing renewable LCOE and the increasing value of the reduction capability of DR, the value of fan reduction DR is initially not cost competitive but as the renewable penetration grows there is a crossover point, at which, the cost of fan turndown DR is cost competitive and reduces the system-wide LCOE. Figure 451 presents the technology-specific LCOE values at 38% renewable penetration.

Figure 451: Technology Specific LCOE at 38% Penetration from a 50/50 Mixture of Wind and Solar with DR (HVAC only) and without EE

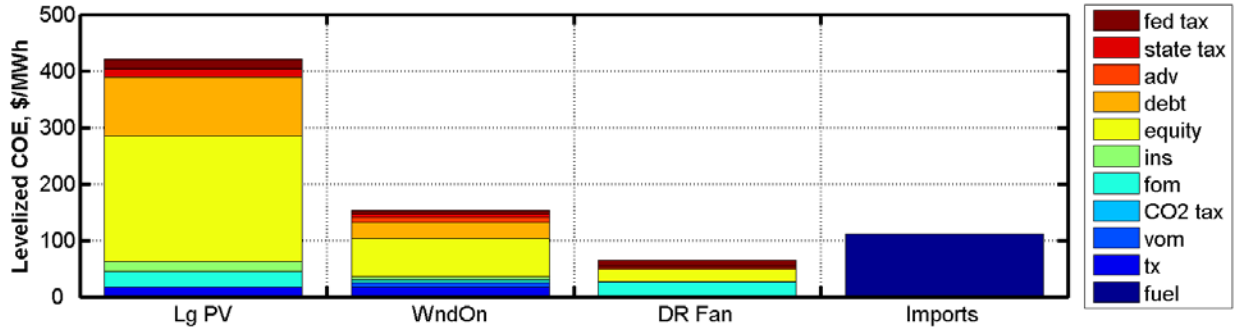

A similar phenomenon happens for HVAC energy efficiency; however EE provides value until a 73% renewable penetration and only at around 50% does the value begin to drop as shown in Figure 449. The drop occurs because of the baseload nature of the excess generation from renewables and the baseload shape of the EE signal. Figure 452 shows the technology specific breakdown for each resource at 38% renewable penetration.

Figure 452: Technology Specific LCOE at 38% Penetration from a 50/50 Mixture of Wind and Solar without DR and with EE (HVAC only)

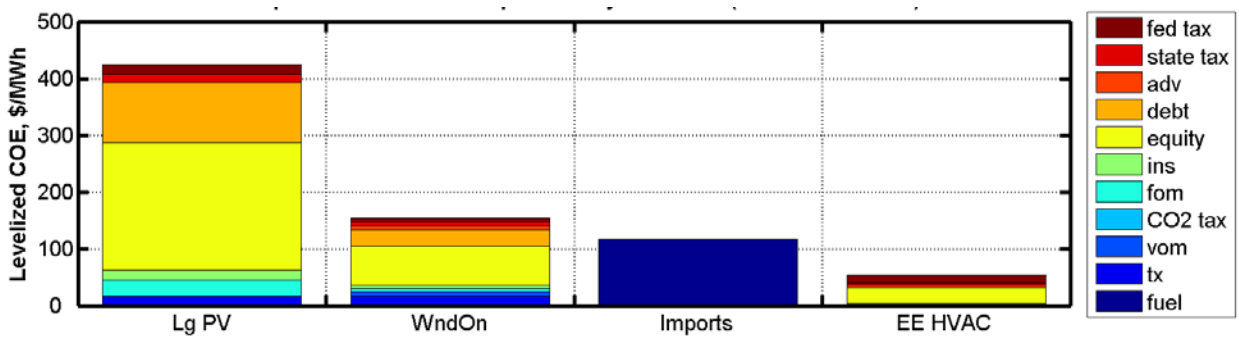

When both HVAC for EE and DR are applied (Figure 453) the LCOE of DR fan turndown increases from that of the DR only case. The LCOE of EE does not change but due to the reduction in capacity and energy provided by DR while the cost stays the same results in a more expensive technology specific cost for DR fan turndown. Just as with the DR only case the value of the EE with DR case becomes even more cost competitive than the EE only case around 25% renewable penetration.

Figure 453: Technology Specific LCOE at 38% Penetration from a 50/50 Mixture of Wind and Solar with DR and EE (HVAC only)

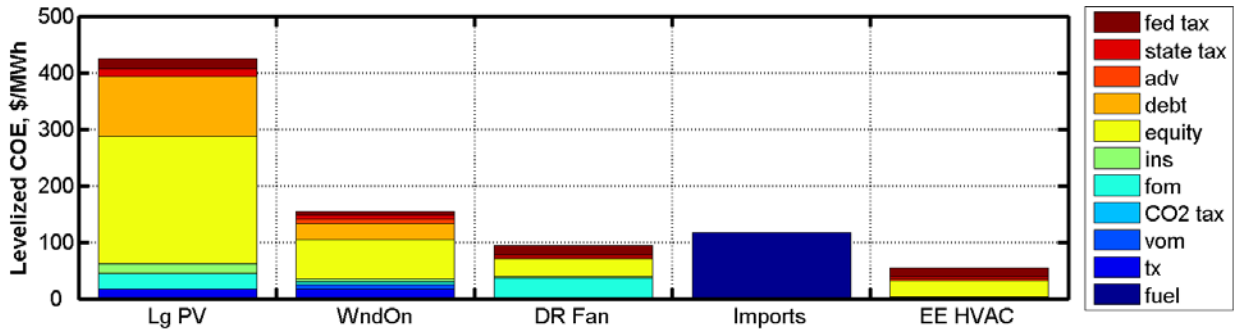

7.3.2.4.3. Conclusions

- Pursuing only HVAC for EE greatly improves the value proposition for EE, while pursuing both HVAC and lighting for EE does not prove cost competitive for any renewable penetration.
- Using only fan reduction for DR proves more cost competitive than pursuing both fan and lighting reduction.

7.3.2.5. Energy Efficiency Cases – Different Renewable Rollout Strategies

7.3.2.5.1. Description of Cases

The final section in the EE analysis explores the impact of EE technologies on different rollout strategies. The previous analyses only looked at a 50/50 mixture of wind and solar. This section explores the impacts of a 20/80 and an 80/20 mixture of installed wind and solar capacity.

7.3.2.5.2. Results

Figure 454 shows the behavior of the three EE technologies. The interior lighting and exterior lighting are in many ways opposite, i.e., the peak of one is the valley of the other, while the HVAC is relatively constant only increasing slightly in the morning hours to accommodate the HVAC demand.

Figure 454: Daily Average Profiles for Reduction using EE each Technology

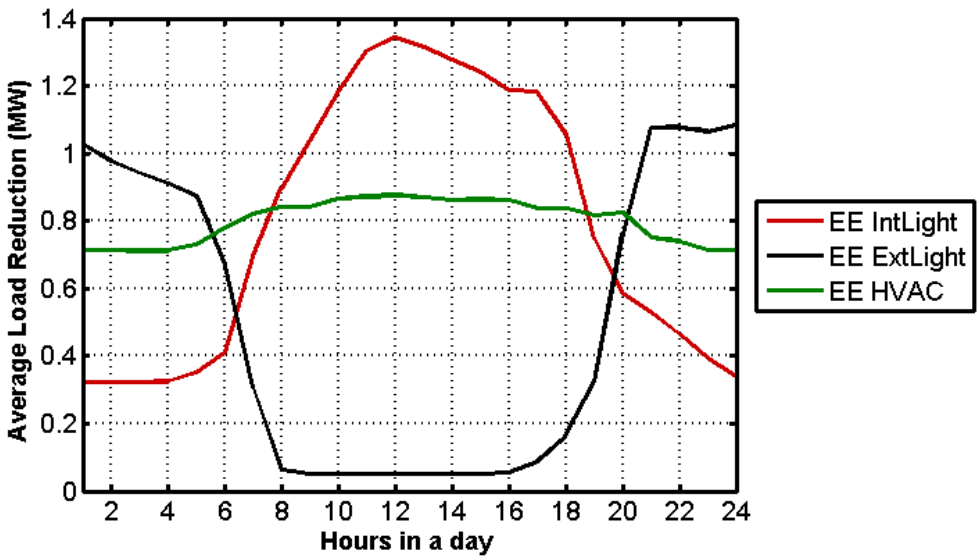

The previous sections have established that the EE HVAC provides the best economic advantage for a 50/50 mixture of wind and solar; however, there can be different impacts for different renewable penetrations. The two following figures (Figure 455 and Figure 456) present the system-wide LCOE percentage change from base case for a range of renewable penetrations based on a mixture of wind and solar in the proportions of 20/80 (on a power basis) for Figure 455 and 80/20 for Figure 456.

Figure 455: LCOE Percentage Change from base for EE Technologies with a 20/80 Mixture of Wind and Solar

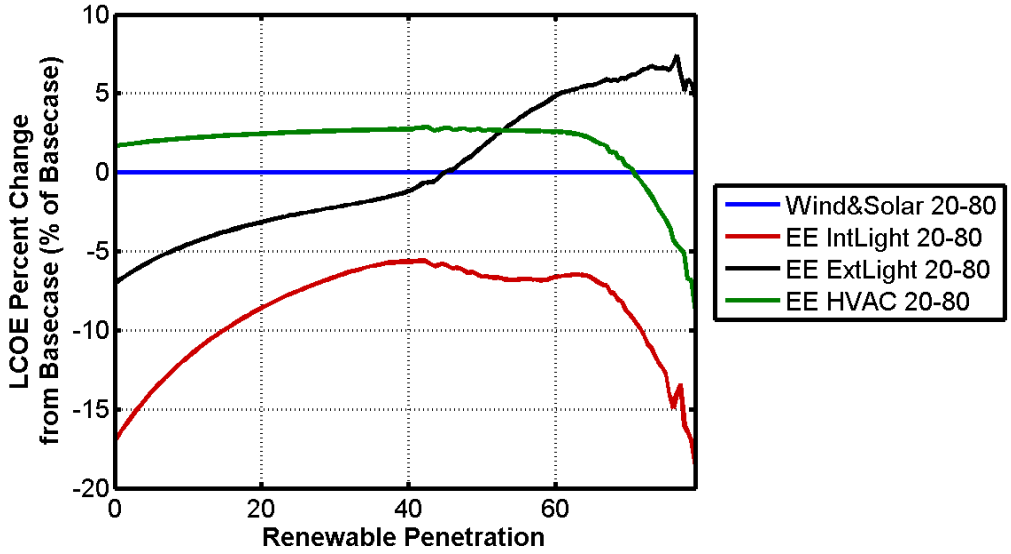

Figure 456: LCOE Percentage Change from base for EE Technologies with an 80/20 Mixture of Wind and Solar

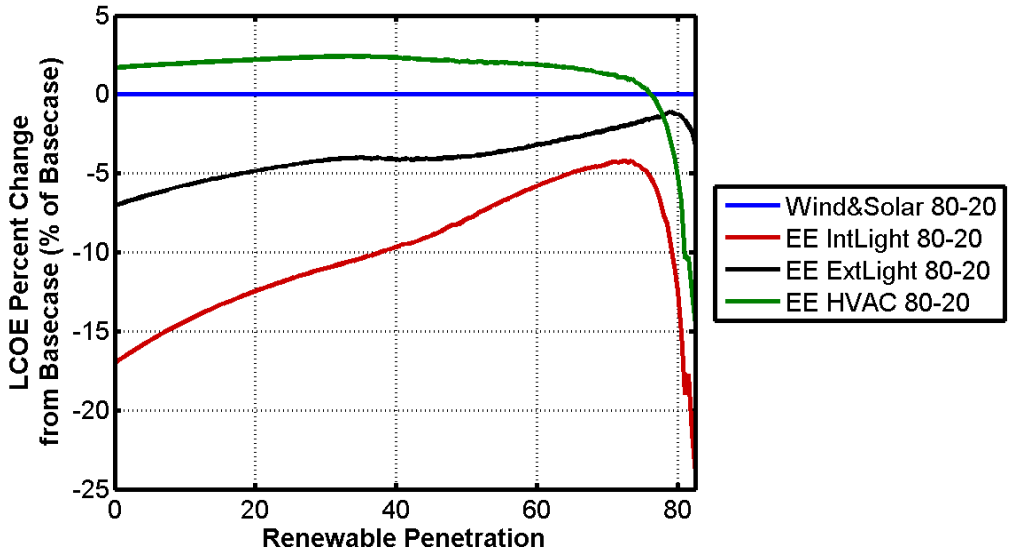

For both mixtures, EE HVAC is cost competitive until high renewable penetrations, at which point, the need for a baseload reduction such as EE HVAC is not incentivized. Notice that for the 20/80 mixture exterior lighting becomes cost competitive while for the 80/20 mixture it does not. This is because of the load reduction profile for exterior lighting presented in Figure 454. Solar generation is focused in the afternoon and early evening hours and does not generate at night, while the wind profile is more constant but slightly favors the evening and early morning

hours. As a result, a mixture of resources that favors solar can benefit more from a reduction in demand at a time when solar cannot provide generation (i.e., evening and early morning hours).

7.3.2.5.3. Conclusions

- **The mixture of renewable resources can affect the selection of EE technologies.**
    - Exterior lighting EE measures can be cost competitive for renewable scenarios that favor solar capacity.
    - HVAC EE measures are cost competitive for a wide range of renewable mixtures.

Task 7.3.3. Demand Response

Demand side management tools like demand response (DR) represent a method to reduce the demand for electricity at a specific time. Some DR will not impact its occupants (e.g., turning off the pumps for fountains), while others can affect the occupants (e.g., light dimming, cooling system turndown). The challenge is to assess the available capacity for DR, to implement DR changes that provide the most energy and minimal impact to customers, and to weight its value against other technologies and energy efficiency measures.

7.3.3.1. Approach

The first step to developing a DR model for the UCI community and the state of California was to determine the end use electricity profiles by type. This was performed for UCI campus by the Cadmus Group, Inc. and the data for the entire state was drawn from the Commercial End Use Survey (CEUS) database and is shown in Task 6.4.

The end use categories considered for this analysis are as follows:

- Lighting – All lighting fixtures within the building, including some task lighting (modeled together for UCI building models) and security/emergency lighting. Assume baseline lighting is incapable of automatic dimming.
- Task lighting – Task lighting energy modeled in CEUS and DEER building prototype models.
- Miscellaneous – Includes all plug loads from office equipment and other occupant-driven loads (i.e. everything that is unaccounted for in the other end-use categories).
- Auxiliary – Includes overhead process-based loads, which are primarily pump energies for the modeled buildings.
- Vent fan – All fan energy, primarily supply fan, but includes return and exhaust fan energy.

- Controllable vent fan – A subset of vent fan end-use energy which excludes all modeled ventilation for laboratory, healthcare, residential, or general (restaurants, schools, assemblies) because of constraints for ventilation requirements.
- Exterior total – Includes exterior lighting for buildings and parking lots, as well as elevator operation. Some load is attributed to exterior building lighting based on the model calibrations, while the rest has been estimated based on the observed quantity and operation of generic exterior lights and elevators throughout the campus.
- Total – The sum of all electric energy end-uses (excluding controllable vent fan energy, to avoid double-counting).
- Heating (Btu) – Modeled heating load served to the buildings by the central plant.
- Cooling (Btu) – Modeled cooling load served to the buildings by the central plant.
- Domestic hot water (Btu) – Modeled heating load for the domestic hot water systems serving each building.

The CEUS data does not come with exactly the same categories as the above items so it must be adapted to match the above list. Thirteen end-uses are used in the CEUS study including 3 HVAC end-uses and 10 non-HVAC end-uses. Seven of the end-uses are electric only and six can be both electric or natural gas. The categories available are as follows:

- HVAC End-uses
    - Space Heating – Electric and Gas
    - Space Cooling – Electric and Gas
    - Ventilation
- Non-HVAC End-uses
    - Water Heating – Electric and Gas
    - Cooking – Electric and Gas
    - Refrigeration
    - Inside Lighting
    - Office Equipment
    - Outdoor Lighting
    - Miscellaneous Equipment – Electric and Gas
    - Process – Electric and Gas
    - Motors
    - Air Compressors

7.3.3.1.1. Demand Response Measures

For the purpose of the present analysis, the ventilation end-use category draws from the "ventilation" category in the CEUS database. The lighting category draws from the "inside lighting" and "outdoor lighting" categories in the CEUS database.

The next step is to determine the capacity of generation that is able to be reduced and the associated occupant impact. This analysis was performed for the campus by the Cadmus Group, Inc., and the results were extended to California by using the load shedding capacity of the campus for each end use type and scaling up to state level using the CEUS data.

Fan turndown and lighting turndown were selected for further analysis. These categories draw from the vent fan, lighting and exterior lighting end-uses. The instant cost and fixed operation and maintenance (fom) costs are calculated for each technology as shown in Table 84. The gross capacity is derived from the DR availability signals. The instant cost for the supply fan is based on the time for programming and a fixed cost of $4/kW. The instant cost for lighting reduction is derived from a $50/ballast price with approximately 10 ballasts/kW. FOM costs for the supply fan represent the time for programming, support, testing and maintenance, while for lighting, FOM costs represent random replacement for failed bulbs over the course of 20 years.

Table 86: DR Costs Without EE Technologies

Capacity and Cost	Supply Fan Limitation	Lighting Reduction
Gross Capacity (kW)	3758.00	4742.00
Instant Cost ($/kW)	16.76	500.00
FOM ($/kW-yr)	1.60	1.75

7.3.3.1.1.1. Lighting Turndown

Lighting turndown involves installing lighting technologies with dimmable ballasts and the necessary control equipment to reduce the power consumption. For the model, the desired power reduction is selected based on the desired occupant impact of either 15, 30 or 45% (designated occupant impact levels 1, 2 and 3). These three values were selected to span the achievable dimming, while maintaining sufficient lighting in the area.

The lighting energy available for DR is a combination of the "lighting" and "exterior lighting" end-use values. The total available lighting energy must be scaled by the occupant impact ($DR_{occ\ impact}$) and the effective penetration ($DR_{penetration}$) of the DR technology into the market (e.g., 50% of light fixtures in a building). Lastly, all other constraints must be applied to the signal. Important constraints to consider are weekday/weekend usage, holiday usage and time-of-day. The DR lighting model allows for the exclusion of the weekend days (as many of the DR programs do not call events on weekends due to lower electricity demand). Also the model considers time-of-day exclusions. For instance, buildings on UCI's campus turn off in the

evening and back on in the morning. When the building lighting is turned off it is incapable of providing DR and some level of lighting is required at night. The following equation is used to calculate the DR available from lighting.

$$\boldsymbol{DR_{Lighting} = EndUse_{Lighting} \cdot DR_{occ\ impact} \cdot DR_{penetration} \cdot TimeOfDay_{constraint}} \quad \textbf{(96)}$$

The resulting vector represents the DR available from lighting for every hour of the year.

7.3.3.1.1.2. Fan Turndown

Fan turndown involves reducing the power consumption of the fans supporting HVAC in the building using control equipment. Some buildings are more amenable to turndown than others. For instance lab buildings on UCI's campus require more air changes per day than other types of buildings and as such the fan power cannot be lowered for these buildings. There are a significant number of building air conditioning systems on campus and throughout the rest of California that can operate with a reduction in fan power. For the fan turndown model the occupant impact level is selected from 1 to 3 representing turndown of the fan 10, 20 and 30% power. The reduction in fan power follows one of the affinity laws, which provides an approximation for the discharge characteristics of a fan at different fan speeds, as shown in the following equation.

$$\boldsymbol{Power_{Fan2} = Power_{Fan1}\left(\frac{Speed_{Fan2}}{Speed_{Fan1}}\right)^{2.9}} \quad \textbf{(97)}$$

Just as with the other DR events, important constraints to consider are weekday/weekend usage, holiday usage and time-of-day ($TimeOfDay_{constraint}$). In addition the penetration of the given technology is considered as well ($DR_{penetration}$). The final energy available to DR from fan turndown including all constraints is calculated using the equation below:

$$\boldsymbol{DR_{Fan} = EndUse_{Fan} \cdot DR_{penetration} \cdot \left(1 - \left(1 - DR_{occ\ impact}\right)^{2.9}\right) \cdot TimeOfDay_{constraint}} \quad \textbf{(98)}$$

The resulting vector represents the DR available from fan turndown for every hour of the year.

7.3.3.2. UCI Campus Results

7.3.3.2.1. Description of Cases

The demand response model used to analyze the effects of demand response on the UCI campus is the same as that used to analyze grid-wide effects but without the scaling up of the effects to encompass the entire state. A description of this model is included with that for the HiGRID model in another portion of Task 7. This section will describe the cases examined to determine the effect of demand response on the behavior of the UCI campus at increased renewable penetration levels.

7.3.3.2.1.1. Base Case without Demand Response

To examine the effect of demand response on the UCI campus, a base case is first established to determine the performance of campus resources without any demand response measures

present at a given renewable penetration level. The base case used in this analysis is the same as the 'Base Chiller Dispatch Case' described in the chiller dispatch sensitivity analysis (Task 3.4.3), since this case represents current operation of campus resources.

7.3.3.2.1.2. Standard Demand Response Cases

This analysis examines three standard demand response cases: Low Impact, Medium Impact, and High Impact. The standard cases use demand response measures to reduce the energy consumption of buildings on campus to a limited extent. While demand response can be used to perform other functions, the use of demand response to decrease energy consumption is representative of the primary application at current. Other applications may be more appropriate for aiding the campus in integrating renewable energy resources. The difference between this application and pure energy efficiency measures is that demand response measures cannot be utilized all of the time since doing so would violate occupant preferences. Therefore, this application applies the measures as much as possible, but not necessarily at every hour or to the same extent. These measures are assumed to be present on all relevant equipment on the UCI campus. Two primary demand response measures are utilized:

1. **Lighting reduction.** This involves the dimming of interior lighting in campus buildings to reduce electric energy consumption. Profiles for lighting loads have been obtained from building data on the UCI campus.

55. **Ventilation fan turndown.** This involves reducing the speed of ventilation fans and air handling equipment in campus buildings.

The use of demand response measures is limited by occupant preferences. Occupants in any given building may only be able to tolerate certain levels of reduced illumination or ventilation rates before it violates their preferred comfort levels or interferes with their ability to work.

The Low Impact case assumes that occupants are very sensitive to lighting and ventilation conditions and therefore demand response measures can only utilized to a modest extent. Specifically, lighting reduction was limited to power reductions of 15% and ventilation fan turndown was limited to a 10% power reduction. These figures correspond with maximum allowable levels for buildings with sensitive occupant tolerances from the literature.

The Medium Impact case assumes that building occupants are more tolerant of reduced illumination and ventilation rates, and therefore lighting reduction and ventilation fan turndown are used to increased extents. Lighting reduction is limited to power reductions of 30% and ventilation fan turndown is limited to power reductions of 20%. These figures correspond with allowable levels for buildings with average occupant impact tolerances from the literature.

The High Impact case assumes that building occupants are even more tolerant of reduced illumination and ventilation rates compared to the Medium Impact case. Lighting reduction is limited to power reductions of 45% and ventilation fan turndown is limited to power reductions of 30%. These figures correspond with allowable levels for buildings with high occupant impact tolerances from the literature.

7.3.3.2.1.3. High Impact Demand Response with no Additional GT trips (Modified).

The four cases described thus far apply demand response measures to reduce the energy consumption of buildings on campus as much as possible. The UCI campus, however, has on-site resources which have minimum operating levels such as the gas turbine. If demand response reduces the load demand at a particular hour that causes it to drop below the minimum power of the gas turbine, either the gas turbine will have to shut down or renewable power would need to be curtailed or wasted. Both of these options are highly undesirable for the campus due to technical and financial concerns.

This case takes those concerns into account and prevents the use of a demand response measure from decreasing the campus load demand below the minimum operating level of the gas turbine. The maximum reductions from the High Impact case are used as the limiting factor during hours when the minimum gas turbine power is not a potential issue.

7.3.3.2.1.4. Renewable Mix

The effect of complementary technologies such as chiller dispatch in this case will be carried out with the gas turbine not being allowed to trip offline. Since this scenario represents a more practical operating scheme under current standards, the ability of complementary technologies to mitigate potential issues can be more clearly examined.

Additionally, the renewable mix used for different renewable penetration levels parallels that used by the CPUC rollout strategy for attaining the 33% renewable penetration level, scaled down to the community level. The effective renewable capacities used are as follows:

Table 87: Renewable Mix used for Complementary Technologies

Targeted Renewable Penetration	Regional Wind Capacity [MW]	Local Fixed PV Capacity [MW]	Regional 1-Axis PV Capacity [MW]	Base Load Renewable Capacity [MW]	Local Wind Capacity [MW]
0	0	0	0	0	0
10.47 %	0.8655	0.0559	0.1134	1.6245	0
20.40 %	3.7644	0.3179	0.6455	2.2477	0
33.36 %	8.0111	1.3049	2.6493	2.4387	0
50.79 %	17.1297	2.2842	4.6376	2.4387	0

The base load renewables include geothermal, biomass and small hydroelectric. The 50.79% targeted penetration uses an extension of the 33% mix by energy. The targeted renewable penetration level represents the penetration level achieved with the corresponding capacity mix if all of the energy obtained from renewables is used to serve the load demand (i.e. no curtailment).

7.3.3.2.2. Analysis

7.3.3.2.2.1. Effect on Renewable Capacity Requirements

The progression of the required renewable capacity with renewable penetration level for the different demand response cases is displayed in Figure 457. The "High-T" case represents the high impact case without allowing additional gas turbine trips.

Figure 457: Renewable Capacity vs. Renewable Penetration

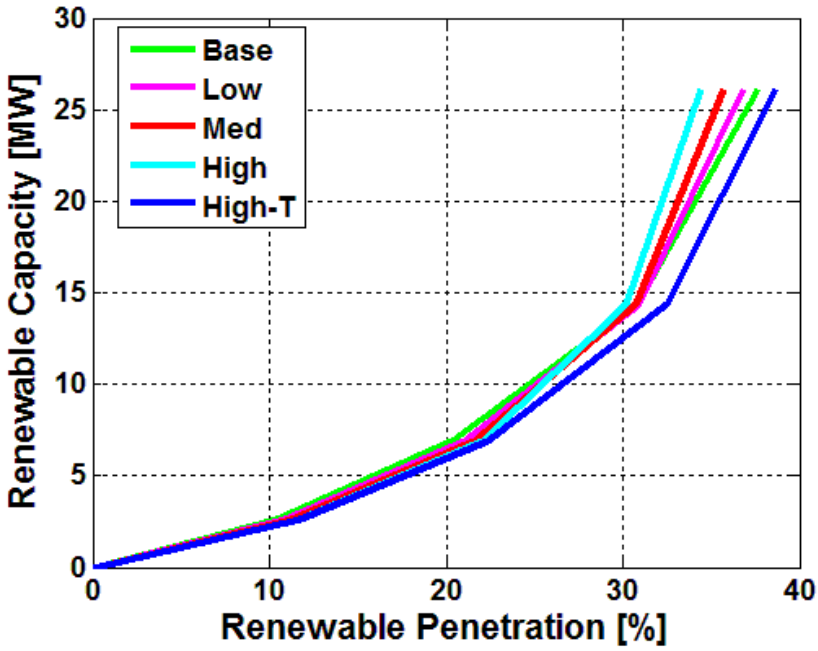

Similar to the trends displayed in the spanning and chiller dispatch cases (Task 3.4.3 and Task 7.2.1), the total renewable capacity increases in an exponential manner with renewable penetration. Curtailment of renewable power causes the required capacity to reach a given renewable penetration level to accelerate at higher renewable penetration levels. Also similar to the trend shown in the chiller dispatch sensitivity analysis, none of the cases reach the targeted renewable penetration level dictated by the installed renewable capacity. This occurs for the same reasons as discussed in the chiller dispatch sensitivity analysis.

The effect of demand response on the renewable capacity required to reach a given renewable penetration level depends on two factors:

1. **Reduction in the total load demand.** Since demand response reduces the total energy of the load demand, a given amount of energy obtained from renewable resources is able to account for serving a larger fraction of the load. This serves to increase the renewable penetration level for a given renewable capacity.

56. **Reduction in the portion of load available to be served by renewable resources.** The UCI campus has an on-site gas turbine that has a minimum power level. Therefore, the gas turbine has a minimum contribution to the load demand. Only the remaining load demand is available to be served by renewable resources. Since demand response reduces the total load but the minimum contribution of the gas turbine towards serving

the load is constant, the portion of the load available to be served by renewable resources decreases. This serves to decrease the renewable penetration level for a given renewable capacity.

The net effect of these factors on the renewable capacity required to reach a given renewable penetration level depends on whether curtailment is occurring or not for a large portion of the hours of the year. For a given hour, the first factor dominates if curtailment is not occurring and the second factor dominates if curtailment is occurring. A demonstration of these effects for a single example hour without curtailment is shown in Figure 458:

Figure 458: Effect of DR on Renewable Contribution to Load with No Curtailment

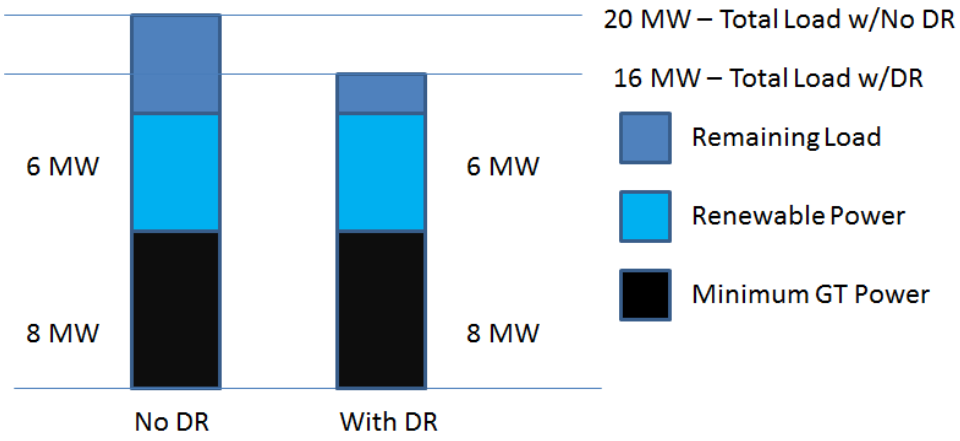

In the case without curtailment, the remaining load after the minimum gas turbine contribution is larger than the available power from renewable resources and all of the renewable power can be used to serve the load. The remaining load is met by a combination of the gas turbine operating above its minimum power level and imports from the utility grid. When demand response measures are implemented in this case, reductions in total load translate to reductions in gas turbine or import power. With a lower total load but a constant contribution from renewable power, the fraction of the load served by renewable power is increased. In this example, demand response increases the renewable contribution for this hour from 30.0% to 42.8%.

A demonstration of the case with curtailment for an example single hour is presented in Figure 459:

Figure 459: Effect of DR on Renewable Contribution to Load with Curtailment

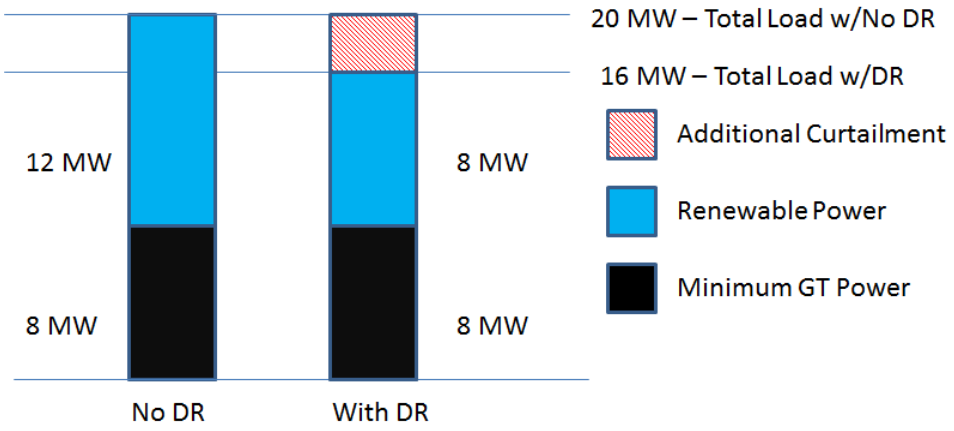

However, when curtailment is occurring due to high renewable power generation causing the balance to drop below the minimum power level of the gas turbine, the effect of demand response is different. Since renewable power generation is excessive in this case, renewable power serves the entirety of the remaining load and has additional generation that is not used to serve the load. When demand response measures are implemented in this case, the reduction in total load translates to a reduction in the amount of load that can be served by renewable resources. At the same time, however, the contribution of the gas turbine towards serving the load remains constant. Therefore, the fraction of the total load that renewable resources are able to serve is decreased and renewable curtailment is increased. In this particular example, demand response reduces the renewable contribution for this hour from 60.0% to 50.0%. This occurs for any system with an uninterruptible base load capacity.

The overall effect on the renewable penetration level depends on the number of hours out of the year that are affected by both active demand response measures and curtailment. An increased number of these hours cause demand response to reduce the overall renewable penetration level for a given capacity. At lower renewable penetration levels, all of the demand response cases reduce the renewable capacity required to reach a given renewable penetration level. The higher impact cases show the largest reductions, and below the 23% renewable penetration level, the high impact case and the modified high impact case show negligible differences. At higher renewable penetration levels, however, the trend reverses and all of the standard demand response cases require more renewable capacity to reach a given renewable penetration level compared to the base case. The higher impact cases reduce the achievable renewable penetration more than the lower impact cases.

The exception to this trend is the modified high impact case, which takes into consideration the tripping of the gas turbine. In this application, demand response does not reduce the load during periods of very high renewable power generation, which mostly correspond to the periods when gas turbine trips would become an issue. Therefore, the fraction of the load that can be served by renewable power is not reduced during periods of high renewable generation. Additionally, the case still benefits from the reduction in total load during hours affected by

demand response without curtailment. These effects allow the modified high impact case to garner increases in renewable penetration level compared to the base case for a given renewable capacity across all renewable penetration levels considered.

Overall, this indicates that from the perspective of increasing renewable penetration level, the most beneficial application of demand response will change at higher renewable penetration levels. Reductions in load must be coordinated with renewable power generation to gain the most benefit.

7.3.3.2.2.2. Effect on Surplus Renewable Generation

The progression of the surplus renewable fraction with renewable penetration level for the different demand response cases is presented in Figure 460:

Figure 460: Surplus Renewable Fraction vs. Renewable Penetration Level

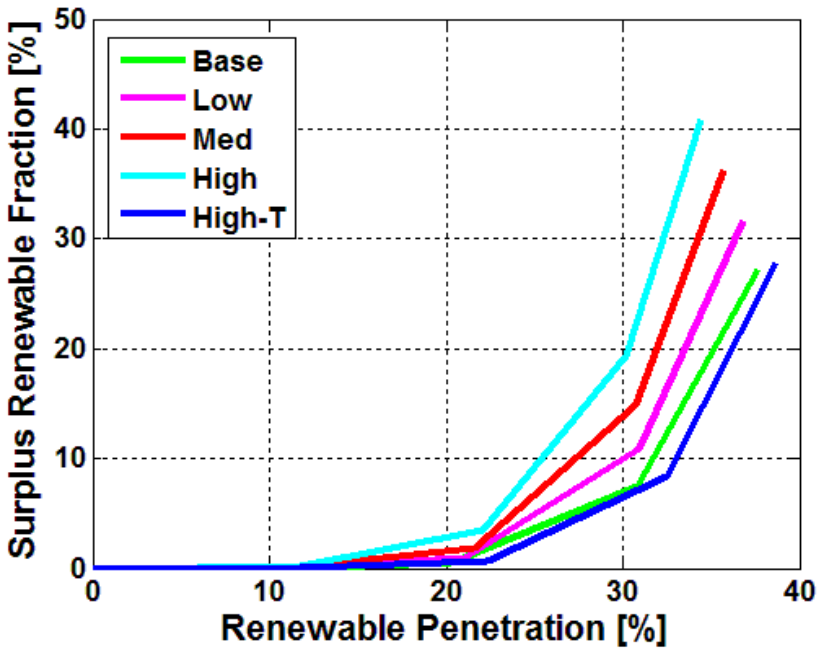

Before discussing these results, it is important to note that demand response alone does not cause curtailment for the UCI campus. In the case without any renewable power, even the high impact demand response case does not reduce the load at any point in the year below the minimum gas turbine power level plus the import margin. Therefore only renewable power is curtailed in this analysis.

As implied by the qualitative shape of the renewable capacity curves, the curtailed renewable fraction increases exponentially with renewable penetration level. This general shape is similar to that displayed in the chiller dispatch sensitivity and renewable spanning cases (Task 3.4.3 and Task 7.2.1). This trend occurs for the same reasons of wind and solar power being peak-dominated resources which require high capacities to contribute a given amount of energy to the load. Therefore, to increase the renewable penetration level, increased capacity allows off-

peak generation to contribute to serving the load, but also causes the peak renewable generation capacity to exceed the available load.

The differences between the demand response and base cases are implied by the previous discussion of the required renewable capacity. The higher impact cases exhibit increased curtailment even at a low renewable penetration level compared to the lower impact and base cases. While the magnitude of curtailed power is larger for the higher impact cases even at low renewable penetration levels, the number of hours affected by both demand response measures and curtailment is low. This causes the point at which the higher impact cases begin to require more renewable capacity to reach a given renewable penetration level to occur at higher renewable penetration levels than that implied by the curtailment curve.

Similar to the previous discussion, the high impact case considering gas turbine trips is the only case that is able to reduce the magnitude of curtailment compared to the base case at all renewable penetration levels. Since this case only reduces the total load when it will not cause the gas turbine to trip, it allows the campus to make more use of the available renewable power during hours when curtailment is occurring.

These results further highlight how the application of demand response will need to change at higher renewable penetration levels to contribute a benefit to a community at increased renewable penetration levels.

7.3.3.2.2.3. Effect on the Gas Turbine Capacity Factor

The progression of the gas turbine capacity factor with renewable penetration level for the different demand response cases is presented in Figure 461:

Figure 461: GT Capacity Factor vs. Renewable Penetration Level

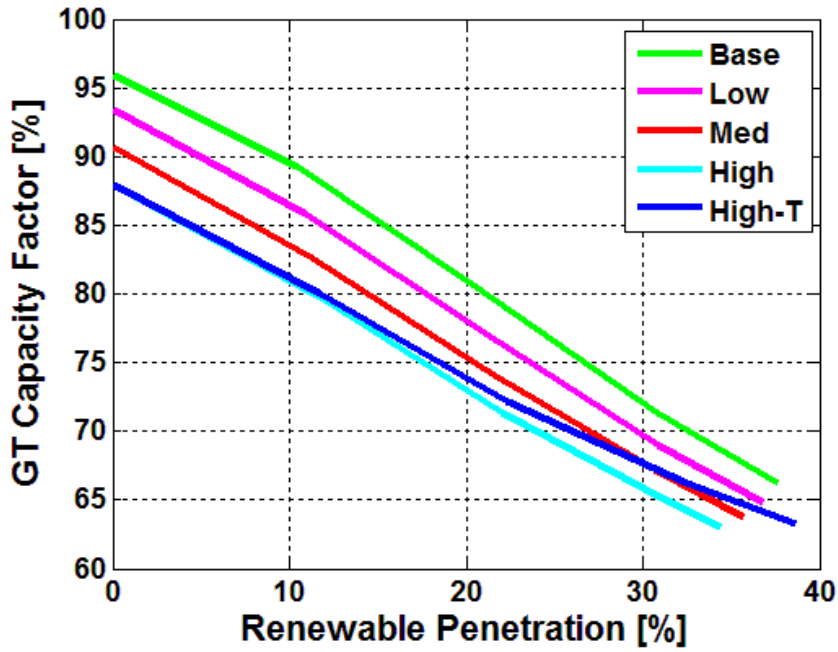

The gas turbine capacity factor decreases linearly with renewable penetration level, similar to the spanning scenario with the gas turbine not allowed to shut down (Task 7.2.1). Since the gas turbine is forced to stay online, an increase in renewable utilization causes only turndowns in the gas turbine. Therefore, gas turbine capacity factor levels are tied to renewable penetration level and are similar overall to that displayed in the spanning and chiller dispatch cases (Task 3.4.3 and Task 7.2.1).

At all renewable penetration levels considered in this analysis, all of the demand response cases show decreased gas turbine capacity factors compared to the base case. The higher impact cases exhibit larger decreases in gas turbine capacity factor compared to the lower impact cases. This trend occurs due to the use of demand response measures reducing the total load demand during hours without curtailment. As discussed previously, this causes the remaining load which is met by the gas turbine and a small amount of imports to be decreased, decreasing the energy contribution of the gas turbine towards serving the load. A larger decrease in the total load demand translates into the gas turbine operating at or near minimum power for these hours while its peak capacity remains the same, therefore resulting in decreased gas turbine capacity factors.

The modified high impact case initially follows the behavior of the standard high impact case, however as the renewable penetration level (and therefore curtailment) increases, the modified case begins to show higher gas turbine capacity factors compared to the standard high impact case. This effect occurs due to the manner in which the chillers respond to the different cases. The chiller and thermal energy storage system will respond to prevent potential gas turbine trips. The chillers focus the cooling load during periods where the balance power is expected to

drop below the minimum power level of the gas turbine combined with the import margin, attempting to raise the balance to prevent curtailment of gas turbine power. In the standard high impact case, the indiscriminate occurrence of load reduction during times of high renewable power generation causes more potential gas turbine trips to occur. The chillers then respond by focusing the cooling load during these times, which has the effect of removing load from other hours of the year when trips are not an issue. However, depending on how low the balance has been decreased during a given hour, the chillers may not necessarily be successful in preventing a potential trip alone if the balance is too low and renewable power is curtailed to prevent the gas turbine from shutting down anyway. Therefore, a decrease in gas turbine power due to load removal from one time period is not necessarily compensated for by an increase in gas turbine power above the minimum level at the time when the cooling load is focused. The net effect is to decrease the gas turbine capacity factor.

In the modified high impact case, the number of potential gas turbine trips is decreased, since the demand response measures will not be fully utilized if doing so will potentially cause a gas turbine trip. Therefore, the chillers are able to distribute the cooling load more evenly throughout other hours of the year. This decreases the occurrence of the effect described for the standard high impact case and allows the gas turbine capacity factor to be slightly increased compared to the standard high impact case. The difference between the modified and standard high impact cases increases as the renewable penetration level increases.

This trend is also reflected in the contribution of the HRSG to serving the campus heating demand, presented for the different cases at higher renewable penetration levels in Figure 462:

Figure 462: HRSG Contribution vs. Renewable Penetration Level

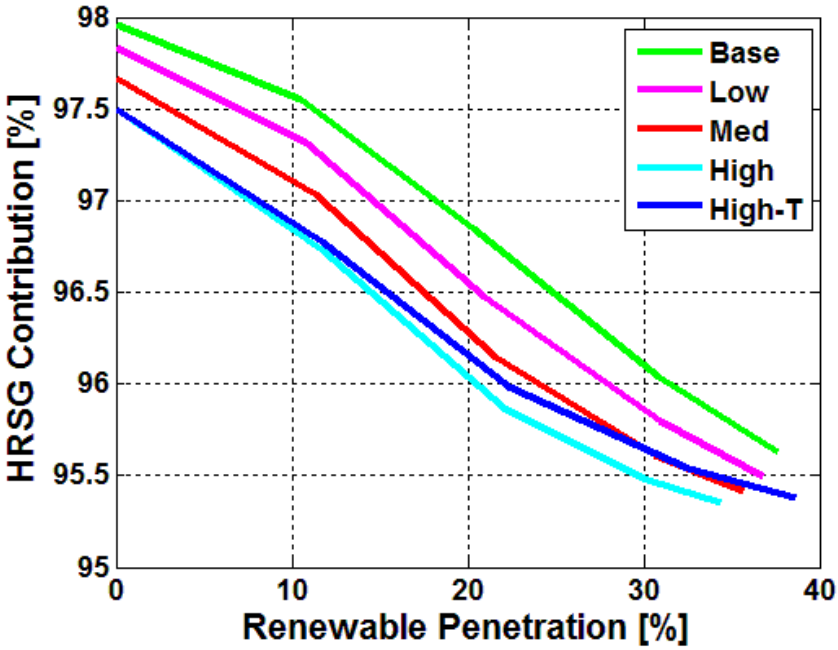

The contribution of the HRSG towards meeting the campus heating demand follows the behavior of the gas turbine capacity factor, since the heat input to the HRSG is sourced from the

gas turbine exhaust. Since the different cases apply demand response primarily at the same hours of the day, lower gas turbine power levels correspond with lower HRSG heat inputs and a lower contribution towards serving the campus heating demand.

7.3.3.2.2.4. Effect on the Import Power Signal

By modifying the balance signal, the use of demand response also modifies the properties of the import power profile to the campus. The properties of the import power profile indicate how the campus interacts with the utility grid when attaining higher renewable penetration levels. The distribution of import power levels for the different demand response cases is displayed in Figure 463 for a low renewable penetration level (10.47% target penetration) and in Figure 464 for a high renewable penetration level (50.79% target penetration):

Figure 463: Import Power Distribution: 10.47% Target Penetration

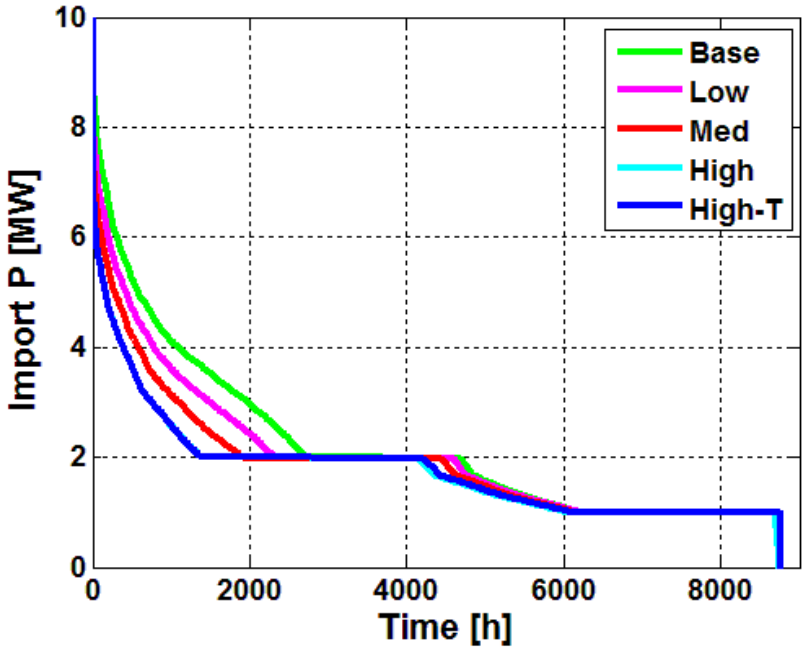

Figure 464: Import Power Distribution: 50.79% Target Penetration

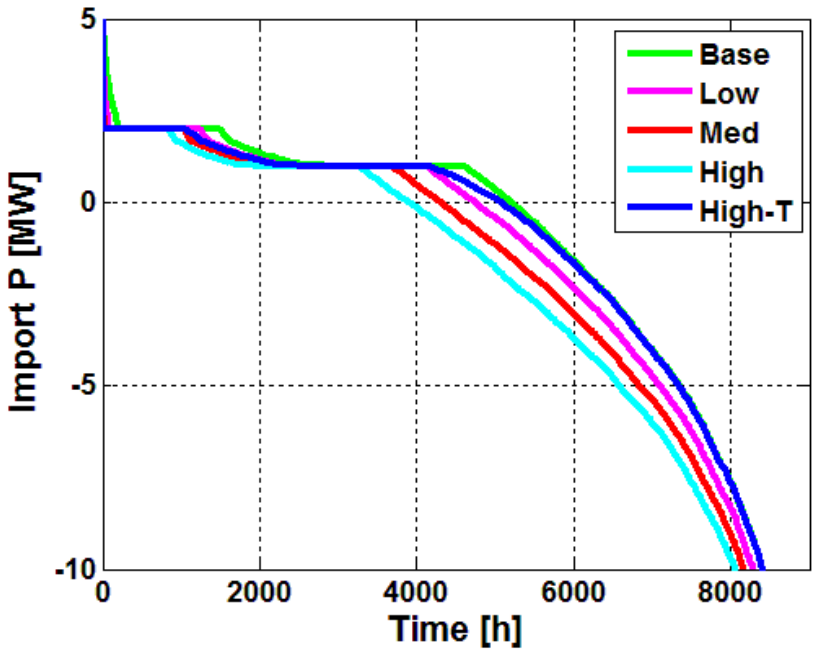

For a target renewable penetration of 10.47%, the import power restriction for the campus is only violated for a few hours out of the year. The higher impact cases exhibit slightly more import restriction violations compared to the lower impact cases due to larger load demand reductions. As expected, the use of demand response measures causes reductions in import power levels for the campus. This is expected since the demand response reduces the load demand, allowing the campus to depend more on available renewable or gas turbine power to meet the load demand. Since renewable power capacities are low at this penetration level, the gas turbine is able to operate above its minimum power level. The reduction in import power levels typically occurs during the daytime and early evening hours, corresponding to periods when buildings are occupied and corresponding loads are high, indicating that demand response is effective at slightly leveling high load periods.

For a target renewable penetration level of 50.79%, the import power restriction for the campus is violated for many hours out of the year. The base case violates the import power restriction on the campus for 4136 out of the years. This increases to 4626 hours, 5061 hours, and 5473 hours out of the year for the standard low, medium, and high impact demand response cases. The higher impact cases exhibit more hours of import violation due to larger reductions in the load demand during periods of high renewable power generation. This indicates that for at least half of the year, the campus will have to curtail large amounts of power generation to prevent from exporting to the utility grid. Even if the utility grid allowed the campus to export, it would have to be capable of managing very high export power levels on a regular basis. The exception to this trend is the modified high impact case, which exhibits import power violations for 4558 hours out of the year, lower than all of the standard demand response cases but still higher than the base case.

Since demand response addresses periods of high load, it affects the maximum import power, as displayed for the different cases with renewable penetration level in Figure 465. The maximum import power is tied to the demand charge that the utility charges the campus.

Figure 465: Maximum Import Power vs. Renewable Penetration Level

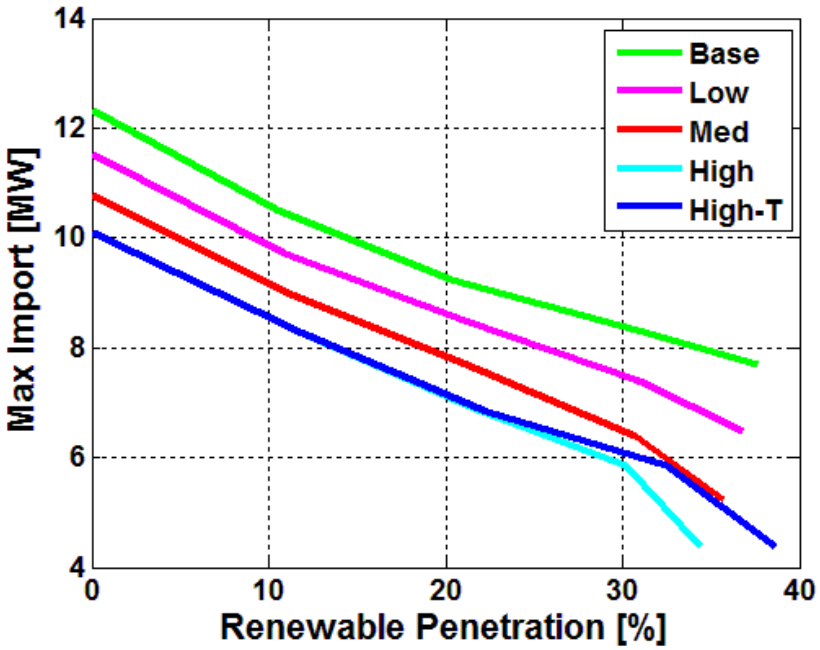

As implied from the import power distribution curves, the use of demand response reduces the maximum import power compared to the base case. Higher impact cases reduce the maximum import power to a larger extent than the lower impact cases. Demand response measures impart reductions in the load demand when the load demand is already high; therefore these measures are well suited toward reducing the maximum load and therefore the maximum import power. The modified high impact case starts to become less effective than the standard high impact case at reducing the maximum import power level at very high renewable penetration levels. This is caused by the same reason that allows the gas turbine capacity factor of the modified high impact case to be higher than the standard high impact case. This reduces the demand charge to the campus.

7.3.3.2.2.5. Effect on the Cost of Electricity

The behavior of the levelized cost of electricity with renewable penetration level for the different demand response cases compared to the base case is displayed in Figure 466. The base case is the same as that used in the chiller dispatch sensitivity analysis (Task 3.4.3).

Figure 466: Change in LCOE of Different Demand Response Cases Compared to Base Case

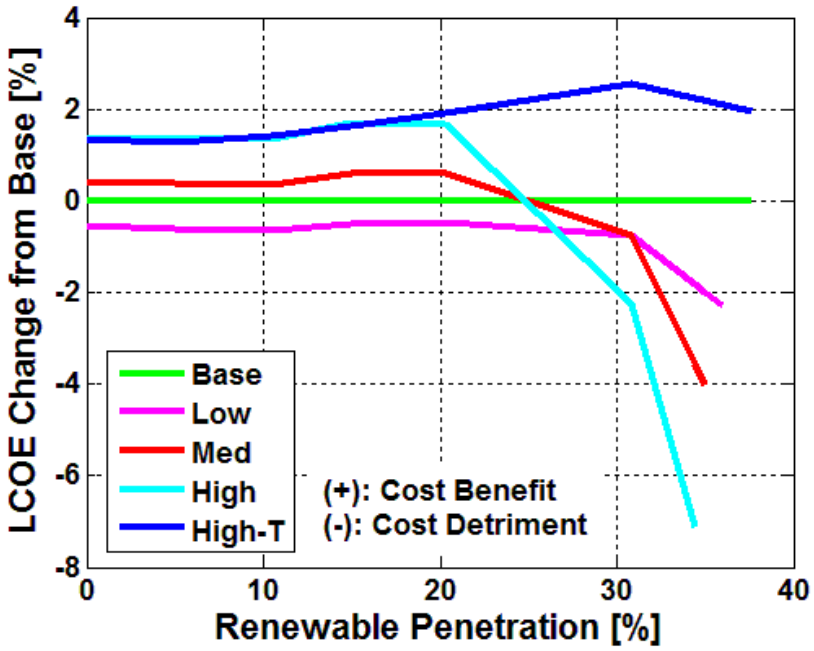

When interpreting the percentage difference from base, note that a positive difference indicates a cost benefit or decrease in the levelized cost of electricity compared to the base case and a negative value indicates a cost detriment or increase in the levelized cost of electricity.

Similar to the chiller dispatch sensitivity analysis, the cost model used in this analysis does not take into account the cost benefit of peak shaving, which demand response is suited for. This was deemed appropriate when assuming connection to a utility grid with increased renewable penetration levels, since the times when the balance power on the utility grid as a whole is high will become unpredictable with increased renewable penetration levels.

The low-impact case is shown to not be cost competitive at any renewable penetration, while the standard medium and high impact cases are initially cost competitive, but become a cost detriment as the renewable penetration level increases.

The difference in cost-competitiveness between the standard low-, medium-, and high-impact cases is due to the differences in equipment utilization. In this case, increasing the extent of the impact of demand response measures did not necessarily entail the installation of additional equipment. Different equipment is required to implement each demand response measure, however, once the equipment is in place, the impact is determined by the extent to which it is used and limited by occupant preferences. In this analysis, the installed equipment, and therefore, the capital investment is the same across all of the demand response cases considered here. For example, the low-impact case and the high-impact case exhibit the same amount of equipment installed, the key difference is the extent to which that equipment is utilized. This was deemed appropriate considering the hardware required to implement these measures. The measures considered in this analysis, fan turndown and lighting reduction, require control and communications equipment as well as variable speed fan motors and adjustable lighting

ballasts. Once this equipment is in place, however, it can be used to impart any level of fan turndown or lighting reduction. For example, reducing the fan speed by 40% does not require any additional equipment over what is needed to reduce the fan speed by 10%. Therefore, the capital investment is fixed across all demand response cases.

The economic effect of using this equipment to different extents varies across cases, however, and is an artifact of a number of competing factors. Demand response reduces costs by reducing the amount of imported electricity purchased and reduces fuel usage in the gas turbine. At low renewable penetration levels, these savings must offset the capital cost of installing demand response measures and costs due to reductions in the gas turbine capacity factor. Higher utilization of this equipment in the high-impact cases allows these cost savings to be garnered to a larger extent for the same amount of capital investment compared to the low-impact cases. Therefore, the high impact cases will tend to be more cost competitive at lower renewable penetration levels.

As the renewable penetration level increases, however, this trend reverses due to the effects of curtailment. For the standard cases, the higher impact cases exhibit larger cost detriments (cost increases) compared to the lower impact cases. This occurs since indiscriminate reductions in the load demand does not complement renewable power behavior and increases curtailment in an exponential manner at the high penetration levels compared to the base case, as discussed previously. This increases the renewable capacity required to reach a given renewable penetration level, increasing costs in an exponential manner.

The exception to this trend is the modified high impact case, which withholds from reducing the load demand during periods when high renewable power would cause the gas turbine to trip offline. This behavior reduces curtailment compared to the base case as discussed previously, but still allows the campus to take advantage of cost savings due to load reductions during periods of low renewable power generation. This allows the benefits of the standard high-impact case to be maintained at high renewable penetration levels, decreasing the levelized cost of electricity compared to the base case across all of the renewable penetration levels considered here.

For the beneficial cases, however, the magnitude of the change in the levelized cost of electricity compared to the base case is relatively small. The cost benefit of the modified high impact case was limited to a maximum of 2.3%.This indicates that the factors which contribute to cost increases are non-trivial and can somewhat limit realization of the economic benefits of demand response. A primary factor is the reduction in the gas turbine capacity factor, which can be extensive as discussed previously since the on-campus gas turbine has a fixed capacity and was not sized to accommodate renewable power or demand response. This highlights the realization that in order to achieve the full economic benefits of demand response, independent of utility programs, distributed energy resources need to be sized appropriately to optimally accommodate the reduction in load due to demand response. Additionally, this also indicates the importance of appropriate demand response programs for the magnitude of economic benefits to become significant.

Overall, these results further emphasize the importance of using demand response in a smart, targeted manner as opposed to unrestrained operation in order to complement the behavior of renewable power generation and aid the campus in reaching higher renewable penetration levels. Operation that takes into account and coordinates with the behavior of other system resources garners technical benefits which, in the case of demand response, translate directly into economic benefits.

7.3.3.2.3. Conclusions

This analysis examined the effect of utilizing demand response measures to different extents of occupant impact and operating strategies on the ability of a community such as the UCI campus to accommodate increased renewable penetration levels. The key insights of this analysis are presented here.

- **The use of demand response measures must coordinate with other system resources to provide benefits for integrating variable renewable power from both technical and economic standpoints.** The cases where demand response measures were used to reduce the load demand as much as possible only increased the renewable penetration level compared to the base case and reduced curtailment for a given renewable capacity at low renewable penetration levels. At high renewable penetration levels, using demand response in this manner caused more curtailment and required more renewable capacity at a given renewable penetration level compared to the base case. This occurs since load reductions in these scenarios reduce the fraction of the load that can be served by renewable resources, decreasing contribution of renewable resources towards serving the load since there exists a minimum non-renewable contribution (base load). The case which took this behavior into account was able to provide technical benefits across all renewable penetration levels compared to the base case.
- **Reductions in imported energy and reliance on the utility can be garnered by using demand response measures.** Demand response measures are able to reduce the energy imported from the utility as well as the maximum import power. This can reduce the demand charge on the campus and decrease reliance of the campus on the utility grid.
- **Distributed energy resources need to be appropriately sized to accommodate the reduction in load demand due to demand response measures to realize the full economic benefit of demand response.** For the UCI campus, the on-site gas turbine was sized to accommodate certain load levels. Demand response measures decrease load levels and therefore decrease the capacity factor of on-campus resources by a significant amount. This decrease results in cost of electricity increases that limited the cost benefit of implementing demand response on campus for the cases that could have been cost-competitive.

Overall, demand response could potentially provide many benefits for a community such as the UCI campus in reaching increased renewable penetration levels. However, there are many considerations that need to be addressed to ensure that use of these measures is effective from a technical and financial perspective for the campus.

7.3.3.3. California Results

7.3.3.3.1. Description of Cases

There are many ways that DR can be dispatched. Two distinct sets of dispatch strategies are considered herein. The first set of strategies consider the maximum technical capability of DR to reduce both energy and spinning reserve requirements. The purpose is to develop a sense of scale for the potential impacts of DR and how they can support the integration of renewables. The second set explores the ability of DR programs to reduce demand, subject to more practical constraints based on the historical behavior of three DR programs administered by Southern California Edison (SCE).

7.3.3.3.2. Results

7.3.3.3.2.1. Bounding Strategies

The three major strategies explored in this section include an "all energy" strategy where all available DR is utilized for reducing the demand, an "all spinning reserve" strategy where all available DR is maintained for spinning reserve purposes and does not reduce the demand and lastly a "peaker only" strategy, where all available DR reductions are used to displace power that would otherwise have to be generated by peakers.

Figure 467 and Figure 468 show the DR signal with 100% DR penetration into commercial buildings in California (using CEUS end-use data), and the maximum occupant impact for both lighting and fan management to achieve the desired reductions. There are three strategies employed as the boundaries of DR operation including:

1. All Energy (AllE): involves using all DR capacity available, all the time for reducing the demand. This behavior is similar to a baseload reduction.

57. Peaker Only (PKonly): Information about the operation of the grid is inputted into the DR model and the peaker signal is minimized. In other words, PKonly operates all the hours that the peakers are operating above their minimum set point and can provide as much DR capacity as is available but will not exceed the energy of the peaker signal.

58. All Spinning Reserve (AllSP): The DR capacity for each hour of the day is directed toward meeting spinning reserve. In this way, the DR never reduces the demand, but by reducing the spinning reserve it removes the burden from other dispatchable generation to provide spinning reserve.

For all three strategies the most energy is available in the afternoon when temperatures are highest so the fans are, on average, at their highest set point (Figure 467). The "All Energy" and "Peaker Only" lines represent a reduction in the grid energy requirement, while the "All SP" line represents the spinning reserve capacity that is provided by demand response.

Figure 467: Daily Average Profiles for Demand Response Bounding Strategies Affecting Commercial Buildings in California in 2005

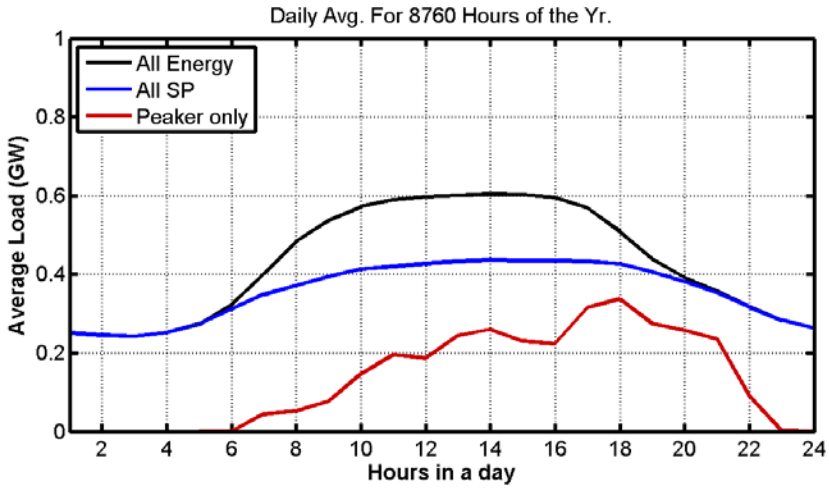

The potential capacity for demand response separated by season is shown in Figure 468. The behavior for AllE, AllSP are predictable, as they are related to the capacity of demand response, while the PKonly is less predictable because of the dependence on the peaker signal and how it compares to the availability of DR for that hour.

Figure 468: Daily Average Profiles by Season for Demand Response Bounding Strategies Affecting Commercial Buildings in California in 2005

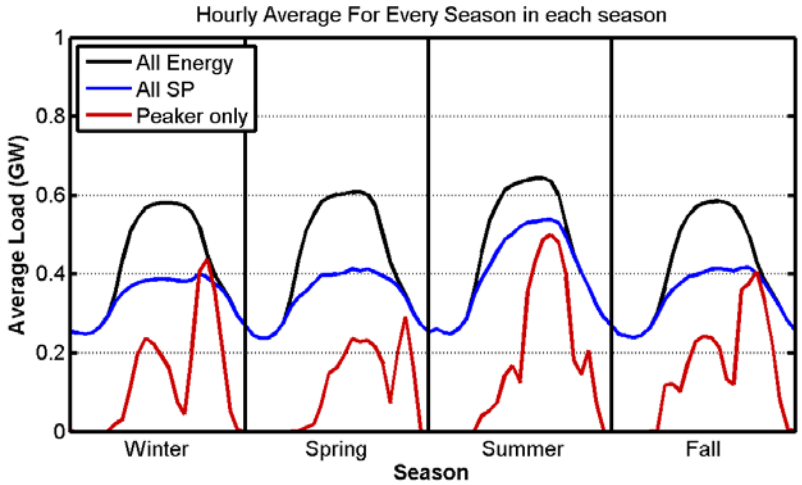

7.3.3.3.2.2. System-wide Effects

Demand response affects demand by reducing it at the point of demand. Additionally, DR can provide this reduction without the use of fuel. That means that demand response can increase the grid fuel to electrical efficiency conversion beyond the amount that adding renewables already can provide. Figure 469 shows the overall effect on grid efficiency for each bounding strategy with the 50/50 wind and solar case while Figure 470 shows the same information as a difference from the wind and solar case without any demand response. Both the energy and peaker support increase the efficiency because of their displacement of fueled generation.

While none of the DR strategies improves the efficiency more than 1.4%, the last strategy, all spinning reserve, provides the least effect on the efficiency, which is not a surprising result since meeting spinning reserve does not actually provide any generation thus will not reduce the fuel consumption directly. The efficiency improvement is caused by two reasons 1) greater uptake of renewables since less balance generation is required to operate and 2) removing the spinning reserve requirements from balance generation increases the overall efficiency of the load-following fleet in particular.

Figure 469: Effects of Demand Response Bounding Strategies on Overall Grid Efficiency for 50/50 Mixture of Wind and Solar

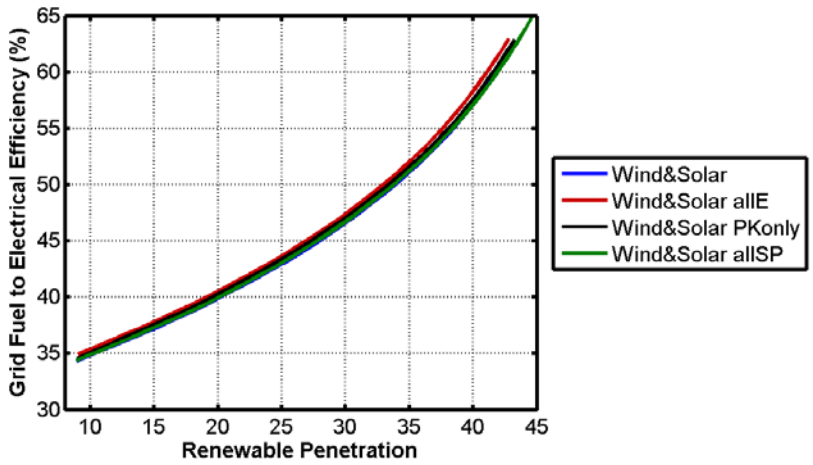

Figure 470: Effects of Demand Response Bounding Strategies on Grid Efficiency as difference from Base Case for 50/50 Mixture of Wind and Solar

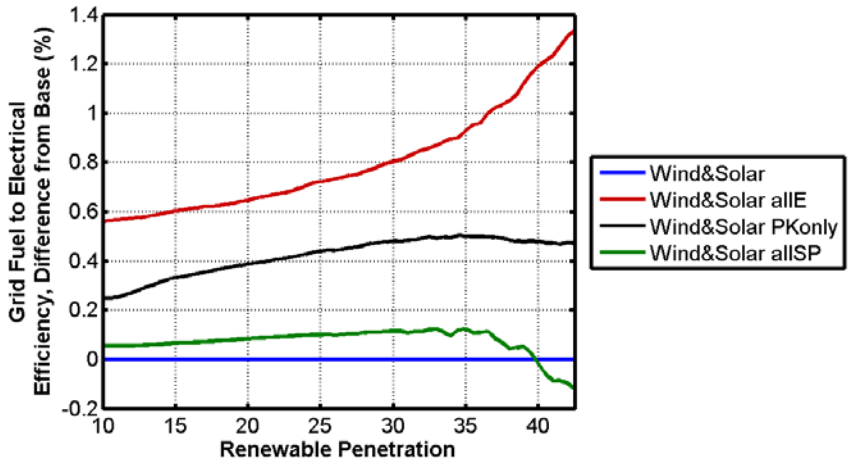

Use of demand response affects the system in other ways as well. When installing renewables, the capacity factor will steadily drop as has been shown, but the effect from demand response depends on the bounding strategy employed. By focusing the strategy on all energy, the

capacity factor will not improve because the profile effectively behaves as a baseload technology as shown in Figure 471. As the renewable penetration increases the baseload profile actually precludes the uptake of additional renewables, so there is reducing value of using the "allE" strategy because it does not intelligently affect the balance profile. Reducing peaking capacity has a positive effect on the capacity factor with a slight increase for the majority of renewable penetrations. This is because the demand response is focused on reducing the number of peakers and in so doing increases their capacity factor which increases the system-wide capacity factor. As the renewable penetration increases the value of controlling peakers is less effective. This is because with higher renewables the excess generation increases and provides some firming of the renewables thereby lowering the need for peakers.

Figure 471: Effects of Demand Response Bounding Strategies on System Capacity Factor as difference from Base Case

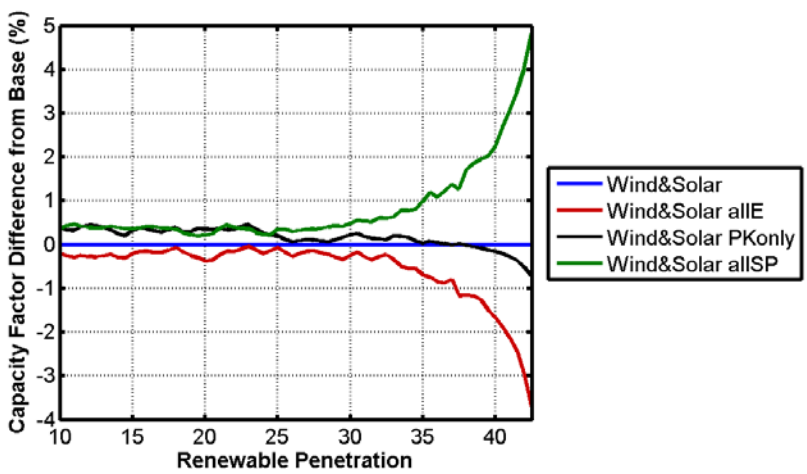

In addition to improving grid efficiency and capacity factor, demand response has the ability to further reduce the carbon dioxide emissions beyond what renewables alone can achieve. Figure 472 presents the resulting CO_2 reductions from all three bounding scenarios as compared to the base case without DR. The all energy case reduces the most CO_2 because it reduces the most energy. The peaker support case also reduces emissions between 0.5% and 1% more than the base case. Lastly, the all spinning reserve case reduces emissions by improving the load-following fleet efficiency and further enabling the uptake of renewables but is limited in its effectiveness because it does not actually reduce generation.

Figure 472: Effects of Demand Response on CO_2 Emissions as a Percentage Change

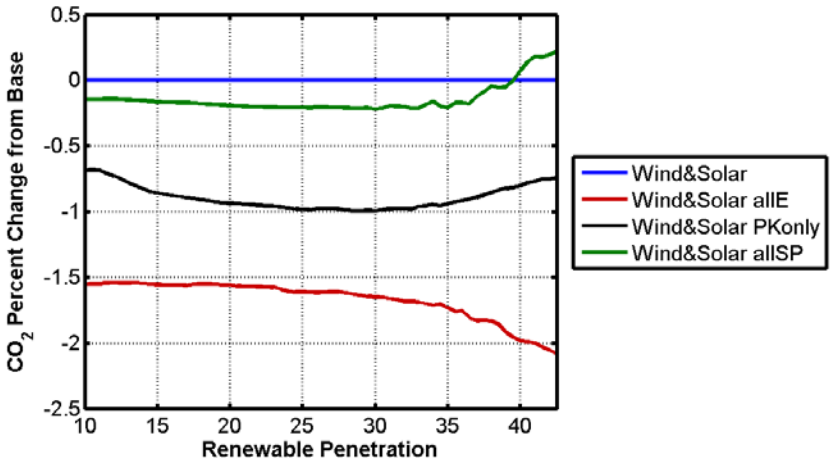

The levelized cost of electricity for each strategy is presented in Figure 473 as a percentage change from the baseline case without demand response. Initially, all DR strategies are more cost competitive than the base case. The all energy case crosses around 33% penetration and peaker support crosses around 39.5% penetration. This crossing point signifies, particularly for the all energy case, when the near base load behavior actually reduces the potential renewable penetration. DR should behave differently at different renewable penetrations to maximize its economic benefit. Because the grid system can initially support greater baseload capacity and can benefit from lower generation requirements the all energy case is the most competitive; however as the grid's ability to support additional baseload while implementing renewables decreases so does the value of the all energy case. The peaker support value rises once additions of solar and wind power intensify the need for peakers and is able to maintain value much longer and only turns down because of the firming effect from the curtailment of excess generation. The DR strategy providing spinning reserve starts with a lower value than the other resources because of the relative abundance of generation that can be turned down to provide spinning reserve and regulation. As the penetration increases and the availability of dispatchable generation decreases the value of DR providing spinning reserve increases significantly.

Figure 473: Effects of Demand Response on Levelized Cost of Electricity. Positive Values: Cost Benefit (cheaper), Negative Values: Cost Detriment (more expensive).

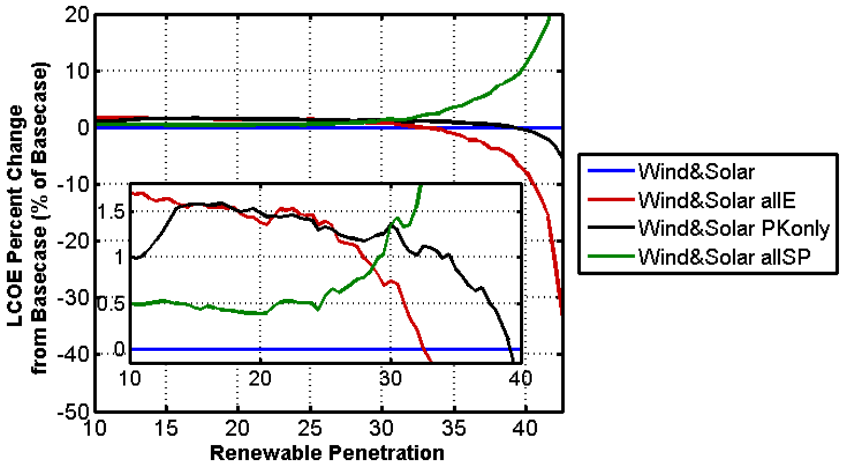

Renewable penetration is calculated based on the sum of the renewable power generated divided by the retail sales of electricity. Since demand response does not contribute to the retail sales of electricity, but rather reduces the demand, the renewable penetration will increase with the inclusion of demand response technologies.

This following set of figures show the value of DR that could be paid to the customer in a per energy fee ($/MWh) or a capacity-based fee ($/MW) (Figure 474 and Figure 475). DR Programs can include capacity payments, or energy payments so these figures present the value of integrating DR. Just as in the previous figure the value of DR tapers off at sufficiently high penetrations, where significant curtailment occurs; however, it is interesting to note that the $/MWh for PKonly is more than the allE despite the fact that allE provides more significant advantage (as shown in the previous figure). AllSP for the top figure is included with levelization coming from the energy provided for SP (though it may not be called on). The bottom figure uses the installed lighting and fan capacity as its denominator.

Figure 474: Value of DR Distributed Over Energy Provided

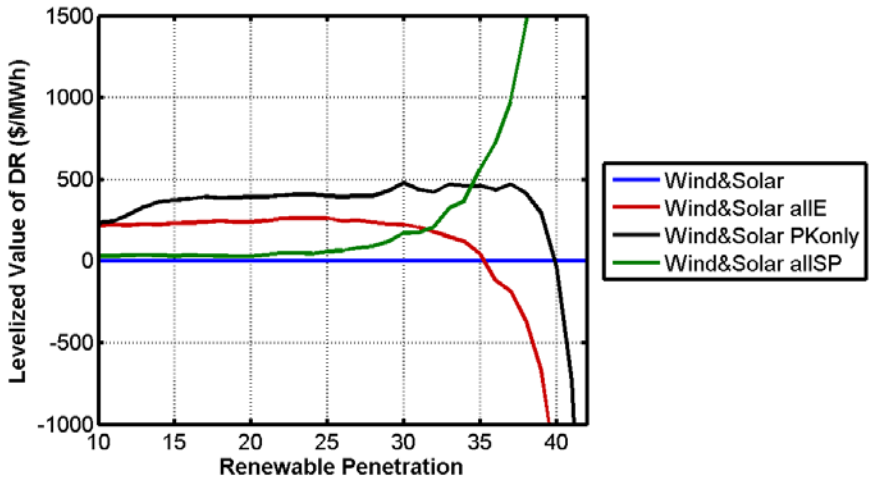

Figure 475: Value of DR Distributed Over Installed Power Capacity

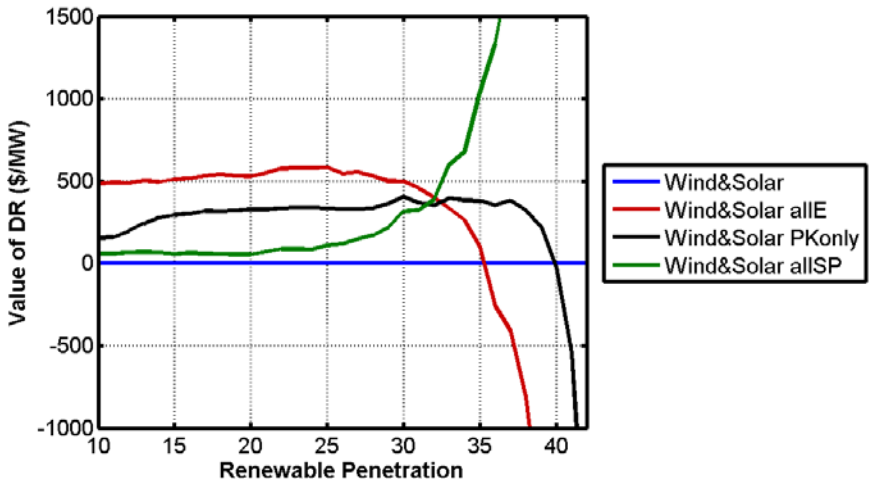

Interestingly, the peaker support value for Figure 474 is greater than all energy and spinning reserve, while the value for all energy is the highest for the capacity payment in Figure 475. This means that the value of providing energy for peaker support is greater than that of all energy; however, all energy provides more energy and is more valuable from a capacity point of view. For both figures, the value of spinning reserve starts below that of the other scenarios and picks up as the renewable penetration increases. This does not signify that spinning reserve is less valuable than providing energy but that the value of demand response to provide spinning reserve is initially less valuable than demand response to provide energy. Using demand response to reduce the load on the system also removes the fuel cost and variable operation and maintenance cost of the generation that is displaced. Investments for generation capacity, once made, are available for use the entire year, so while reducing the load on a given generator will reduce its economic competitiveness, it will also reduce the system-wide LCOE thus resulting in the benefit seen above.

7.3.3.3.2.2.1. Conclusions

- Different operating strategies should be employed for DR as the renewable penetration changes to maximize economic value.
    - At low renewable penetrations, DR should focus on reducing as much energy as possible
    - At medium renewable penetrations, DR to support peaker operation becomes the most cost competitive strategy (briefly)
    - At high renewable penetrations, DR should focus on providing spinning reserve
- Demand response can increase the apparent renewable penetration by enabling greater renewable generation while lowering the retail sales of electricity since it reduces the demand on-site.
- A unique technique to determine the value of DR based on its impact on the grid is presented (results are shown based on installed DR capacity ($/MW) and energy provided ($/MWh))

7.3.3.3.2.3. Demand Response Programs

Practically, DR will not be used all the time. Restrictions include time of the year, time of the day and weekend/weekday. There are many details that differ for each program and one of the major differences is with the compensation structure. Three types of programs offered by SCE are explored including the capacity bidding, critical peak pricing and demand bidding programs.

7.3.3.3.2.3.1. Capacity Bidding Program (CBP)

The CBP is a program that operates from May to October for between 1-8 hours a day. The event is triggered when the heat rate of thermal resources is at or over 15,000 Btu/kWh. This criterion may be caused by any one of the following as described in SCE's tariff sheet:

- High temperatures
- Resource limitations
- A generating unit outage
- Transmission constraints
- CAISO Alert
- SCE system emergency

Compensation is provided in two steps. The first is a capacity credit paid per kW committed per month. Participants can apply for one of two capacity credit schedules; either day-ahead or the day-of. The second part of compensation provided to participants occurs when an event is

called. Participants are paid the SCE city gas price times the heat rate factor of 15,000 Btu/kWh. More details can be found on Southern California Edison's website.

7.3.3.3.2.3.2. Critical Peak Pricing (CPP)

The CPP is a program that offers discounts during non-critical peak periods in an effort to reduce or shift customer's use of electricity from peak periods to non-peak periods. This program operates between June 1 and October 1 to accommodate for the summer peak demand period. More details can be found on Southern California Edison's website.

7.3.3.3.2.3.3. Demand Bidding Program (DBP)

The DBP is a program that operates year round. Participants are given day-ahead notice and can respond if they desire but are not penalized for not responding. DBP can be triggered at SCE's discretion based on factors such as:

- CAISO emergencies, defined as a stage 1 event or higher
- Day-Ahead load and/or price forecasts
- Extreme or unusual temperature conditions impacting system demand; and/or
- SCE procurement needs

Compensation is provided on a per MWh basis and is 50 cents per kWh but depending on your affiliation it could be lower. The participant's compensation will be administered as a credit on their bill. More details can be found on Southern California Edison's website.

7.3.3.3.2.4. Current Program Usage

Over the past three years (2009-2011) SCE has called 214 events averaging 71 events per year. More details can be found on Southern California Edison's website. Most events are CBP at 49.3 events/year, followed by CPP at 12 events/year and lastly DBP at 10 events/year (see Figure 476 and Table 88).

Figure 476: Average Usage of Demand Response Programs by SCE for 2009-2011

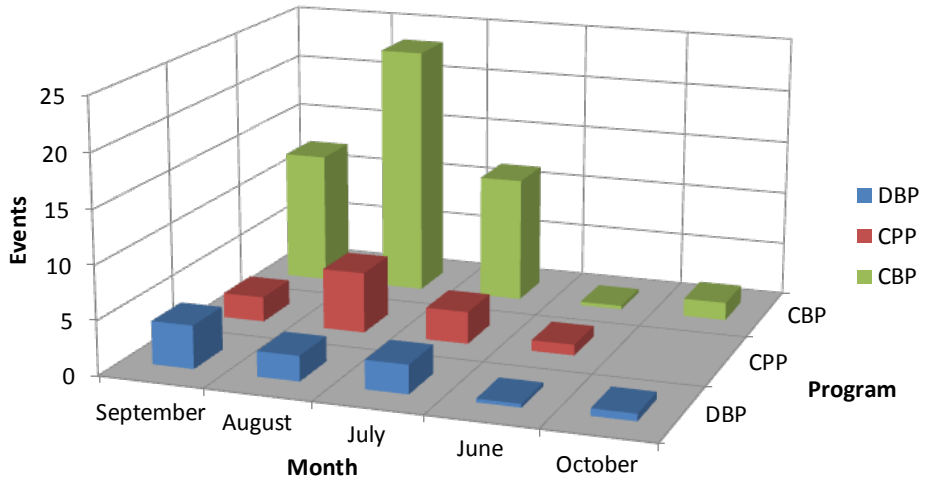

The same information presented graphically in Figure 476 is presented in Table 88.

Table 88: Average Event Count for Three SCE DR Programs from 2009-2011

Program / Month	DBP	CPP	CBP	Total
September	4.000	2.333	12.333	18.667
August	2.333	5.667	23.333	31.333
July	2.667	3.000	11.667	17.333
June	0.333	1.000	0.333	1.667
October	0.667		1.667	2.333
Total	10.000	12.000	49.333	71.333

7.3.3.3.2.5. DR Control Schemes Subject to Current Program Usage

Demand response programs require participants to submit a bid for the capacity that they pledge to reduce in the case that an event occurs. Depending on when these events occur can have an impact on the efficacy of DR.

In addition to being constrained by the occupant impact, technology penetration, weekday/weekend usage and time-of-day usage, each program can come with additional constraints on the events per day, events per month and events per year. Based on the current program usage the following constraints were also added to the system.

Table 89: Event Restrictions Placed on Modeled DR Programs base on SCE's 2009-2011 Event History

SCE	Events per	Events per	Events per

Program	Day	Month	Year
CBP	1	13	50
CPP	1	7	12
DBP	1	6	15

Three control schemes for DR are considered including “maximum reduction”, “grid smoothing” and “peaker support”. These are particularly important to explore because there are a limited number of events each year and deciding when these events occur and how participating DR should respond is important for DR program development. DR programs in California are currently structured by the utility and most often exhibit the grid support control scheme, where the value to the grid is made the most important.

The “maximum reduction” scheme isolates the time of day that yields the highest potential capacity bid for a given event duration, thereby maximizing the profits for an owner, while “grid smoothing” evokes events at the times of highest demand to relieve the generation requirement. Lastly, the “peaker support” scheme places available events at times that peakers are on, in an effort to reduce the required output of peakers.

Figure 477 shows how the average daily operation for the three DR control schemes differs with no wind or solar installed on the system (i.e., 9% renewable penetration from geothermal, small-hydro, biomass and biogas). Notice the focus of demand reduction for the grid smoothing and peaker support are similar in both magnitude and occurrence. This is a result of the coincidence of highest demand to operation of peaker plants. The max reduction scheme provides the most demand reduction with an average daily reduction of 812MWh, while the grid smoothing reduces 459MWh and the peaker support, 734MWh for the minimal renewable scenario.

Figure 477: Daily Average Profiles with DR Control Schemes using Current Program Limitations for Commercial Buildings in California at 9% Renewable Penetration

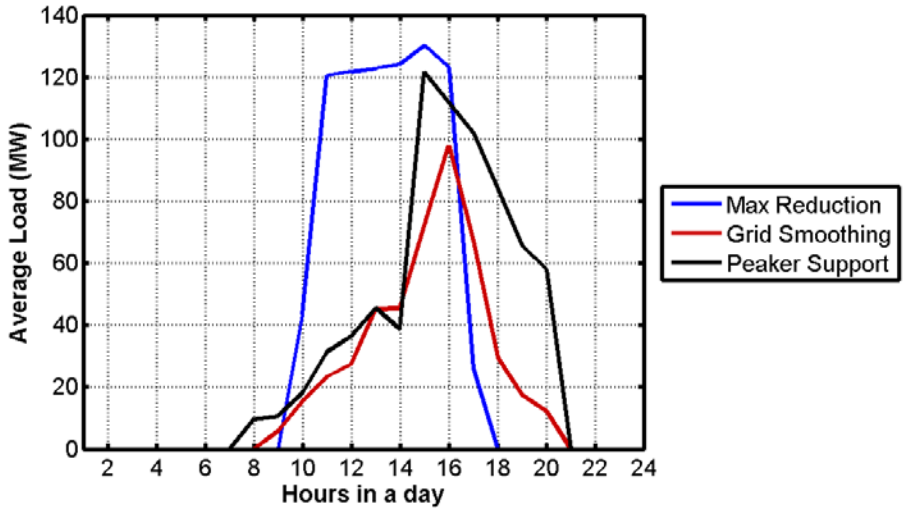

Seasonally, the focus is on the summer with some DR in spring. The peaker support is off more because peakers operate at many different times throughout the year, while grid smoothing has the most value in the summer. The max reduction is consistently at the same times of day, because those times represent occasions when the most DR is available and are associated with high temperatures increasing the potential turndown of fans for cooling.

Figure 478: Daily Average Profiles by Season with DR Control Schemes using Current Program Limitations for Commercial Buildings in California at 9% Renewable Penetration

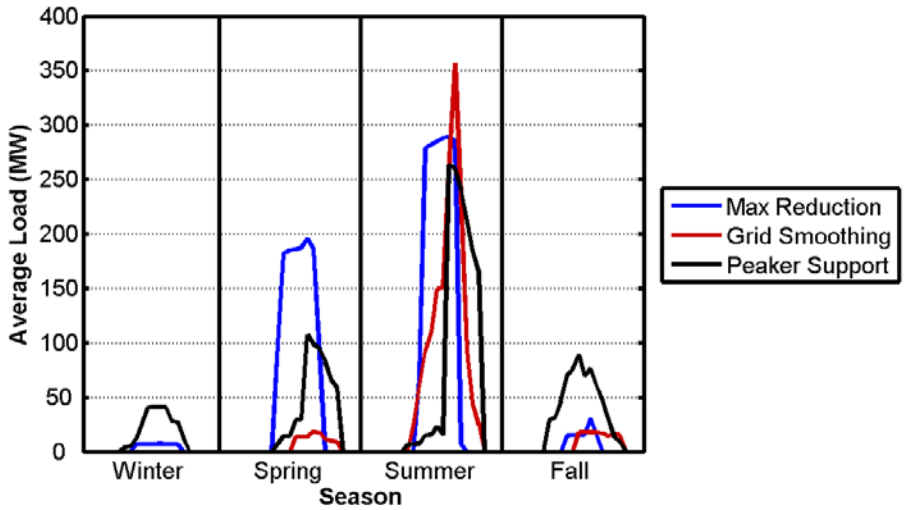

The shape of the optimal DR reduction potential changes as the renewable penetration changes for both grid smoothing and peaker support strategies. Max reduction will not change with increasing renewable penetration because it is based on the available DR signal and not on what is best for the operation of the grid. The peaker support signal has changed its focus from 3PM

with 8.9% penetration to 11AM at 33% renewable penetration as shown in Figure 479. Similarly the grid smoothing transitions form a peak at 4PM with 8.9% penetration to noon at 33%.

Figure 479: Daily Average Profiles with DR Control Schemes using Current Program Limitations for Commercial Buildings in California at 33% Renewable Penetration

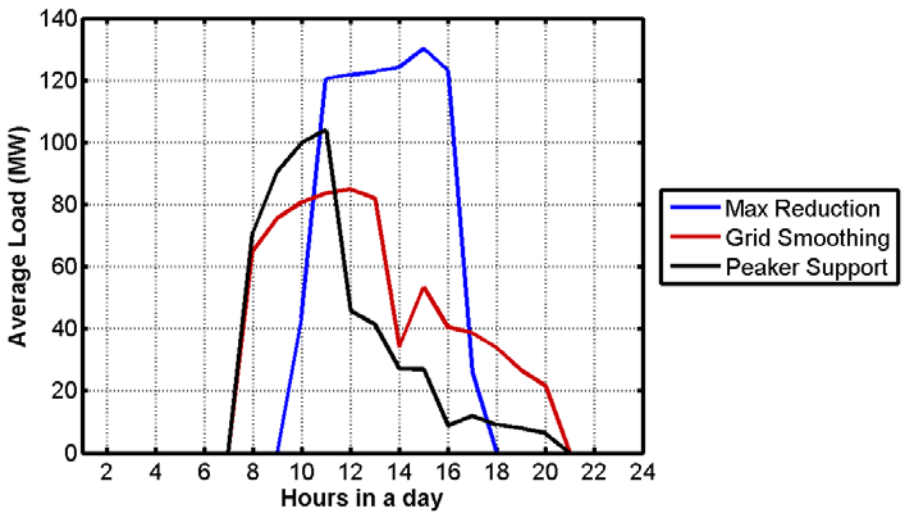

The distribution of DR events changes with increasing renewable penetration and the seasonal distribution of DR changes as well. Max reduction remains constant because it is based only on the available DR signal while grid smoothing and peaker support become more important in the fall rather than in the summer (Figure 480). This is because excess generation from solar, which predominantly occurs in the summer when the solar generation is highest, removes the need for DR to reduce the demand between 8AM and 8PM in the summer. Progression to this point is incremental with increasing renewable penetration meaning that as the renewable penetration increases DR events will transition from summer and spring to times in the fall.

Figure 480: Daily Average Profiles by Season with DR Control Schemes using Current Program Limitations for Commercial Buildings in California at 33% Renewable Penetration

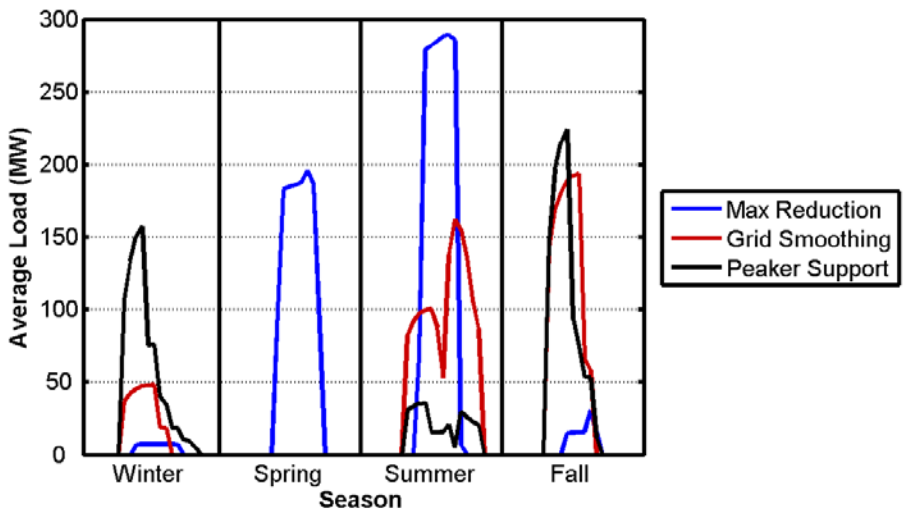

7.3.3.3.2.5.1. Conclusions

- When developing DR programs, the selected control scheme can have significant impacts on the resulting operation
- A participant receives the maximum compensation by selecting DR events when they can pledge the maximum amount of potential; however, this will not support operation of the grid.
- DR reductions should occur predominantly in the summer, which is corroborated by the historical operation.
- Increased renewables change the optimal times for DR events
    - Daily: Maximum DR reductions shift from late afternoon to late morning (based on 50/50 Wind and solar mixture)
    - Seasonally: Maximum DR reductions shift from summer to fall (based on 50/50 Wind and solar mixture)

Task 7.3.4. Electric transportation

Integrating electric transportation into the grid will bring together the electrical and transportation sectors. Just as with aggregation on the electrical grid, increased efficiency from combining these sectors has the potential to benefit both sectors for efficiency and GHG emissions.

7.3.4.1.1. Introduction

This analysis looks at the three of the thirteen vehicle categories. The three categories include light-duty automobiles, light-duty trucks 1 and 2. In California, these categories represent 21.1 million vehicles that travel an average 758 million miles per day during 2005. Additionally, 38.3 million gallons of gasoline and diesel are consumed each day resulting in a fleet efficiency of 19.81 miles per gallon. Using 33.8 kWh/gallon of gasoline and 37.7 kWh/gallon of diesel the resulting thermal efficiency per mile is 0.585 Miles/kWh$_{th}$.

In 2005, the efficiency of the California grid is calculated at 34.3% (thermal to electrical conversion). Using the assumption that electric vehicles can travel 2.94 miles with 1 kWh of electricity, hybrid electric vehicles' thermal efficiency per mile is 1.01 Miles/kWh$_{th}$. The difference between conventional vehicles and hybrid electric vehicles represents the potential improvement from implementation of hybrid electric vehicles (i.e., 1.01 – 0.585 = 0.425 Miles/kWh$_{th}$). As the efficiency of the conventional fleet rises the disparity between the two will lessen; however, as the efficiency of the grid increases hybrid electric vehicles will become more beneficial.

An increase in electric vehicles will increase the demand for electricity. Figure 481 shows the absolute increase and the relative increase with respect to the total energy required to support electrical demand without electric vehicles and the numerical values are shown in Table 90. The relation is shown for increasing percentages of vehicle miles traveled (VMT) provided by hybrid electric vehicles.

To perform the analysis for the UCI community the values in Figure 481 are scaled down to represent the population of students, faculty and staff.

Figure 481: Energy Consumed by PHEV Charging for All Vehicle Penetrations for California

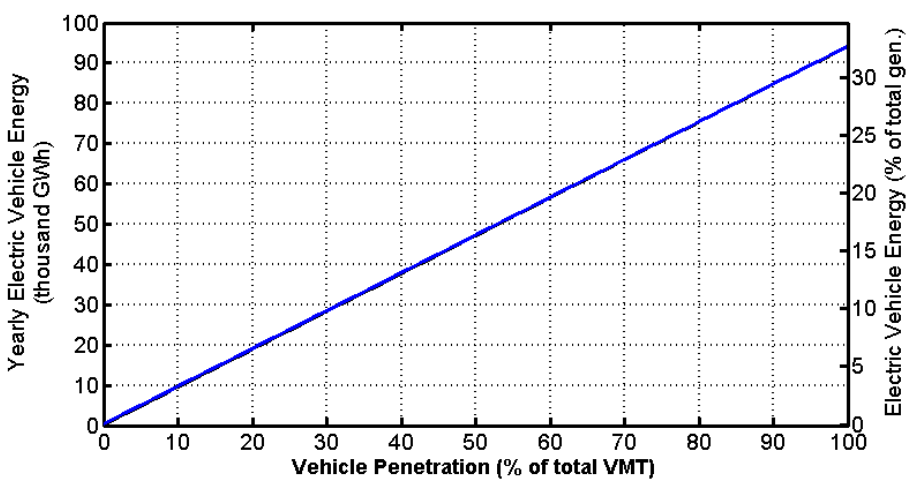

Table 90: Relation between PHEV VMT and Charging Energy

Percentage	Daily VMT	Total Electrical	Generation	Generation

of Total VMT	served by PHEVs in CA for 2005 [million VMT]	Demand for CA [GWh] (excluding electric trans)	required for charging [GWh]	required for charging [% of Total Demand]
0%	0	287,445	0	0%
5%	37.9	287,445	4,704	1.64%
25%	189.5	287,445	23,521	8.18%
50%	379.1	287,445	47,041	16.37%
100%	758.1	287,445	94,083	32.73%

This work isolates the effect that increasing plug-in hybrid electric vehicles on the grid will have on the operation, GHG emissions and cost. The focus is on the system-wide effects. While there are certainly strong implications for the distribution of electricity, particularly how transformers and other distribution systems will be affected, this work considers the effect on balance generation of integrating electric vehicles into a grid with increasing renewable generation.

7.3.4.2. Approach

Electric vehicle energy usage is modeled using a tool that accounts for the electricity and fuel use associated with plug-in hybrid electric vehicles (PHEV). The two part model determines how vehicles are operating and charging. Inputs include: vehicle type, miles per gallon, energy consumption per mile, battery depth of discharge, vehicle range, charging power, charging location, and charging strategy. The model interfaces with National Household Travel Survey (NHTS) data to provide realistic trip information. Using the inputs and trip data, electrical and fuel consumption profiles can be determined.

Figure 482: PHEV Operating and Charging Model

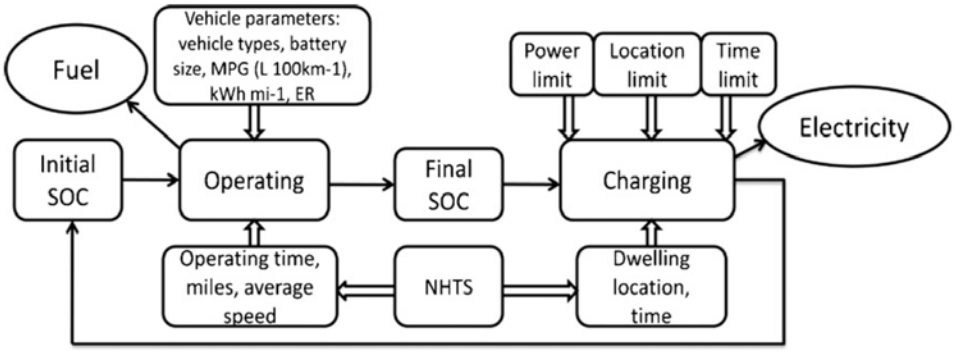

Source: Zhang, 2011

There are occasions where driving distances or durations require that the vehicles are operated using the gasoline engine. The model ensures that all trips can be made either on electricity or gasoline and attempts to maximize the portion of miles driven using electricity.

7.3.4.3. UCI Campus Results

7.3.4.3.1. Description of Cases

The electric transportation model used to analyze the effects of implementing electric vehicles on the UCI campus is the same as that used to analyze grid-wide effects, but applied at the scale of the UCI campus.

In order to use this model, however, the effects of electric transportation had to be appropriately scaled to the UCI campus. Examining the effects of integrating electric transportation on the UCI campus is quite different than doing so on the grid-wide scale. On the grid-wide scale, the entire state of California can be treated as a single isolated system since the vast majority of the vehicles that travel within the state will charge from an outlet within the state. The entirety of the additional load demand due to charging is placed onto the California electric grid.

On the scale of a community such as the UCI campus, however, this may not be the case. Many people who attend or work at UCI live off-campus, therefore the home-charging portion of the electric load due to charging would not be added to the campus load profile while the daytime work portion would be. There are also many people who live on the UCI campus but work elsewhere, placing the home-charging portion of the electric charging load on the UCI campus but not the work-related portion. These influxes and out-fluxes of vehicles from the campus is very difficult to determine and would require driving data for all of the tens of thousands of students, staff, and faculty that regularly interact with the campus.

To address this issue in this analysis, the entirety of the electric load demand due to electric vehicle charging is assumed to be added to the UCI campus system, but the effective number of vehicles is scaled down using the ratio of vehicle-miles-traveled (VMT) to GWh of original electric load exhibited by the state of California. This ensures that the amount of additional load placed on the UCI campus is a reasonable fraction of the stationary electric load demand. In terms of the charging profile, both work and home portions are included. Finally, the electric vehicle types used in this analysis are assumed to be plug-in hybrid vehicles (PHEVs) with an all-electric range of 35 miles.

This section will describe the cases examined to determine the effect of energy storage from the PEVs on the behavior of the UCI campus at increased renewable penetration levels. These cases consist of a base case and cases utilizing different electric vehicle charging strategies.

7.3.4.3.1.1. Base Case without Energy Storage

To examine the effect of electric transportation on the UCI campus, a base case is first established to determine the performance of campus resources without any electric vehicles present at a given renewable penetration level. The base case used in this analysis is the same as the 'Free Chiller Dispatch Case' described in the chiller dispatch sensitivity analysis (Task 3.4.3). The reasons for selecting this dispatch strategy as opposed to the base chiller dispatch strategy used in the other sensitivity analyses are explained later in this section.

7.3.4.3.1.2. Immediate Vehicle Charging

This case involves consumers charging their vehicles as soon as they arrive at home or work. This equates to high charging loads during the late afternoon and early evening hours when drivers arrive at their residences, and a slightly smaller charging load during the daytime while consumers charge their vehicles at work. The work-related charging load is smaller than the residential charging load, since not all vehicles are driven to work every day, while all vehicles eventually return to residences typically in the evening. More details on this behavior are included in the description of the electric transportation module for the grid-wide case. The residential charging peak typically occurs between 7-8 pm, dropping afterwards as EV batteries reach full charge and a lower amount of vehicles arrive home during the late night hours. The daytime charging load typically begins between 7-8 am and lasts throughout the workday. This period has some overlap with the residential charging load due to variability in work schedules.

7.3.4.3.1.3. Delayed Vehicle Charging

This case involves delaying the charging of vehicles to a later time period after the vehicle has been plugged in at a residence or workplace. Utilizing this strategy requires that the charger be given information about how long the vehicle will dwell at a particular location and the state of charge of the vehicle battery upon arrival. Charging of the vehicle will then be delayed until as late as possible, under the constraint that the vehicle will be fully charged by the end of the dwelling period. For example, consider a vehicle that arrives at a workplace, will be at that location for 8 hours, and will require 3 hours to fully charge the battery. Charging will then take place during the last 3 hours of the dwelling period.

In terms of charging profile, this strategy typically moves the residential charging peak past midnight and towards the early morning hours. The work-related charging peak is slightly shifted towards the late afternoon hours, however, the shape of this peak is similar to the immediate charging case since the average dwelling time at the workplace is relatively short.

7.3.4.3.1.4. Smart Vehicle Charging

This case involves using the charging of electric vehicles as a dispatchable load that acts to smooth out the balance profile to the extent possible with the constraint that the vehicle battery will be fully charged by the end of the vehicle's dwelling period. Utilizing this strategy requires that the charger be given information about the forecast of the balance (including load demand and renewable power profiles) for the entire dwelling period. The charger will then plan its charging profile to maximize charging during periods of low balance levels (high renewable power) and minimize charging during periods of high balance levels.

The ability of this strategy to complement renewable power is limited by the amount of vehicles plugged into the campus, which varies with the time of day.

An example of the charging profiles for the three different charging strategies for a single day is presented in Figure 483:

Figure 483: Sample Daily Charging Profiles for Immediate, Delayed, and Smart Charging Strategies

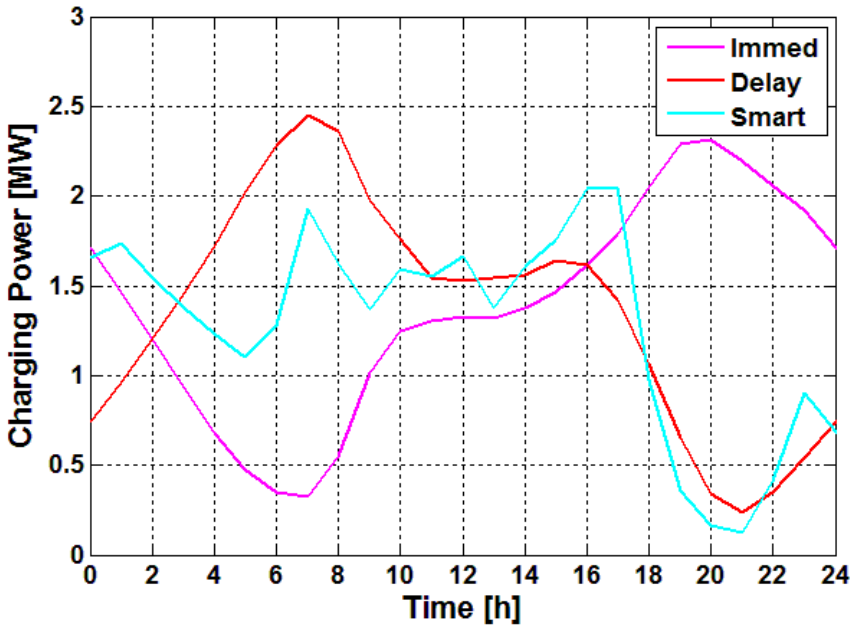

A PHEV vehicle penetration of 30% will be used to compare the effects of the different charging strategies. This indicates that 30% of the VMT demand will be met by electric-drive in each case. Each individual vehicle charger is assumed to only be capable of Level 1 charging, corresponding to a maximum charging power of 1.44 kW per charger.

7.3.4.3.1.5. Renewable Mix

The effect of complementary technologies such as chiller dispatch in this case will be carried out with the gas turbine not being allowed to trip offline. Since this scenario represents a more practical operating scheme under current standards, the ability of complementary technologies to mitigate potential issues can be more clearly examined.

Additionally, the renewable mix used for different renewable penetration levels parallels that used by the CPUC rollout strategy for attaining the 33% renewable penetration level, scaled down to the community level. The effective renewable capacities used are as follows:

Table 91: Renewable Mix used for Complementary Technologies

Targeted Renewable Penetration	Regional Wind Capacity [MW]	Local Fixed PV Capacity [MW]	Regional 1-Axis PV Capacity [MW]	Base Load Renewable Capacity [MW]	Local Wind Capacity [MW]
0	0	0	0	0	0
10.47 %	0.8655	0.0559	0.1134	1.6245	0
20.40 %	3.7644	0.3179	0.6455	2.2477	0
33.36 %	8.0111	1.3049	2.6493	2.4387	0

50.79 %	17.1297	2.2842	4.6376	2.4387	0

The base load renewables include geothermal, biomass and small hydroelectric. The 50.79% targeted penetration uses an extension of the 33% mix by energy. The targeted renewable penetration level represents the penetration level achieved with the corresponding capacity mix if all of the energy obtained from renewables is used to serve the load demand (i.e. no curtailment).

7.3.4.3.1.6. Coordinated vs. Uncoordinated Operation

The sensitivity analyses for the other complementary technologies hinted at the importance of coordinating the operation of dispatchable technologies with each other in order to ensure the realization of benefits for the campus from using these technologies. For the UCI campus in particular, this refers to the coordination of these technologies with the operation of the chiller/TES system. Otherwise, unintended consequences due to interference between these technologies may result. This was not very prevalent in the case of demand response, since the occurrence of demand response events did not overlap with the chiller activation window. With energy storage, this effect caused an unusual result for the maximum annual import power but only occurred for a few hours out of the year and did not interfere regularly with the operation of the energy storage system and realization of benefits.

With electric transportation, however, the use of the base chiller dispatch strategy (uncoordinated) caused the operation of the chiller/TES system to regularly interfere with the operation of electric vehicle chargers. Therefore, instead of using the base chiller dispatch strategy for analyzing the effect of electric transportation on the UCI campus, the free chiller dispatch strategy is used. With this strategy, the chillers actively respond to the effect of electric vehicle charging and prevent interference.

An example of the difference between coordinated and uncoordinated operation is displayed for the effect on the gas turbine capacity factor at low renewable penetration as displayed in Figure 484:

Figure 484: Comparison of Uncoordinated and Coordinated Operation at Low Renewable Penetration Levels

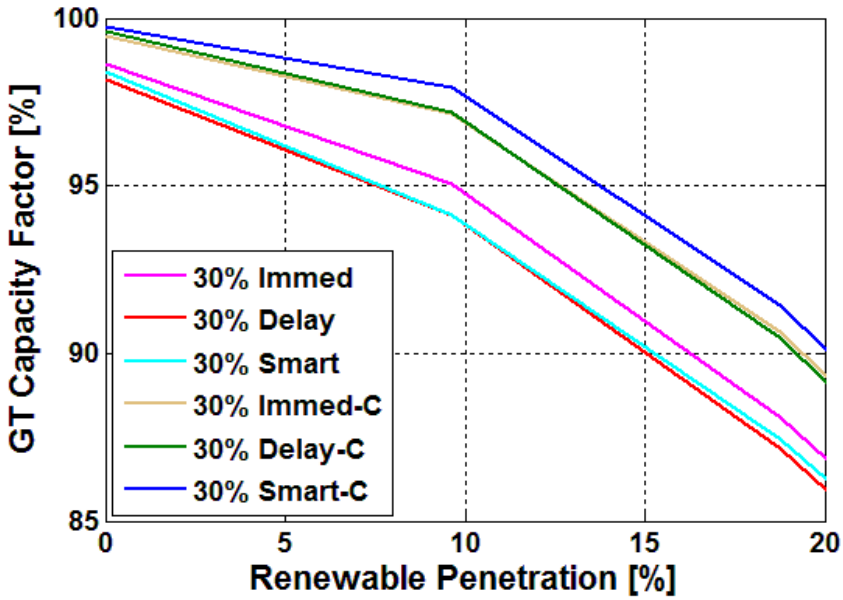

The fact that the coordinated charging cases exhibit higher gas turbine capacity factors is expected. The primary differences between the two lie in the differences of the effects of the different charging strategies. In the uncoordinated cases which use the base chiller dispatch, the immediate charging strategy outperforms the smart charging strategy. This occurs because the immediate charging case tends to introduce its peak charging load between 7-8 pm, before the activation of the chillers at 10 pm in the base case and during a typical wind ramp up. Therefore, the immediate charging case accidentally mitigates the associated balance profile drop (and gas turbine turndown) during this time. The smart charging strategy, on the other hand, will introduce charging load to mitigate a drop in the balance profile which would have been mitigated anyway by the latter addition of the cooling load. The cooling load is large enough that it would have put the gas turbine at full capacity during the chiller activation window and additional load would not increase the gas turbine capacity factor. If the smart charger was coordinated with the chiller operation, it would have placed the charging load elsewhere where it is needed instead of double-stacking on top of the cooling load.

To avoid these types of interference and accurately determine the effects of electric transportation on the UCI campus, the free chiller dispatch without electric transportation is used as the base case for comparison. In the coordinated cases, the smart charging strategy outperforms the other two since its operation is not interfered with by the base chiller operation. This once again highlights the importance of coordination between dispatchable loads and load-shifting technologies.

7.3.4.3.2. Analysis

7.3.4.3.2.1. Effect on Renewable Capacity Requirements

The progression of the required renewable capacity with renewable penetration level for the different demand response cases is displayed in Figure 485:

Figure 485: Renewable Capacity vs. Renewable Penetration

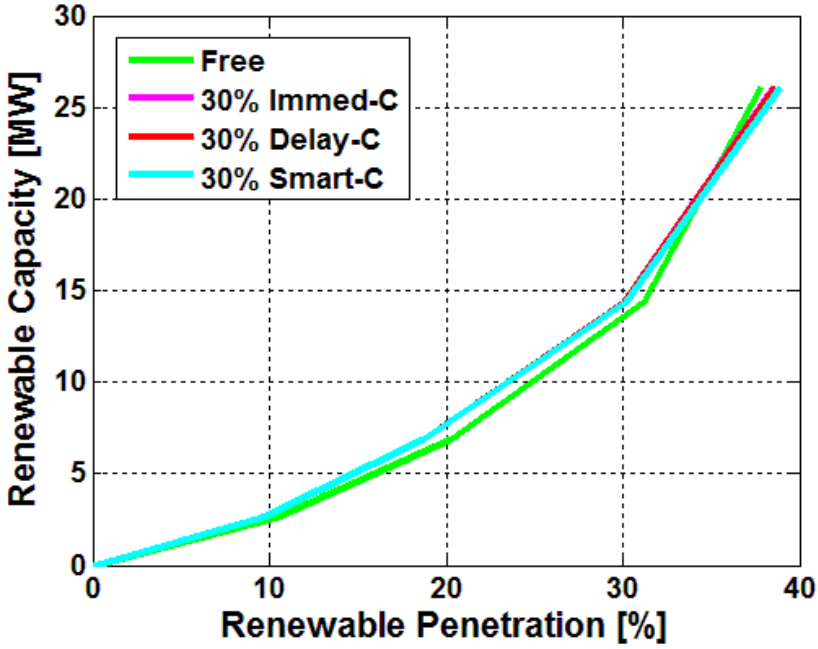

Similar to the results presented for the other complementary technologies, the renewable capacity required to reach a given renewable penetration level increases exponentially with renewable penetration level due to curtailment. Additionally, none of the cases reached the targeted renewable penetration level.

The implementation of electric transportation onto the UCI campus introduces additional electric load onto the campus, increasing the total electric load demand. For the UCI campus, a 30% PHEV penetration increases the annual energy of the load demand by about 8.6%. In order for renewable energy to contribute to serving a given percentage of this increased load demand, additional renewable generation is required, resulting in increased renewable capacities. The renewables required to reach a given renewable penetration level is higher for all of the cases with electric transportation for most of the renewable penetration range up to about 33% in this analysis . For the most part, this is regardless of charging strategy for low renewable penetration levels.

As the renewable penetration level increases above about 33%, this trend reverses and the cases with electric transportation start to require lower renewable capacities to reach the same renewable penetration levels. The additional load due to electric charging is able to reduce the amount of curtailment in these cases in the opposite manner that demand response was shown to increase the amount of curtailment. Differences between the charging strategies begin to emerge in this renewable penetration range. The smart charging strategy requires the least renewable capacity whereas the immediate charging strategy requires the most renewable

capacity. This result is expected since a smart charging strategy is able to dispatch the PHEV charging load to make the most effective use of renewable power generation.

Since the PHEV charging load is a relatively small fraction of the total load demand, however, the differences between the charging strategies is fairly small. Additionally, each case adds the same amount of load to the system but simply dispatches it differently. Even with the smart charging strategy, the ability of the charger to dispatch the PHEV charging load is limited by the fact that the fraction of vehicles plugged in to the campus varies throughout the day. Overall, the integration of electric transportation onto the campus can aid the system in terms of reducing the required renewable capacity, but the effect is somewhat small due to vehicle constraints.

7.3.4.3.2.2. Effect on Surplus Renewable Generation

The progression of the surplus renewable fraction with renewable penetration level for the different electric transportation cases is presented in Figure 486:

Figure 486: Surplus Renewable Fraction vs. Renewable Penetration Level

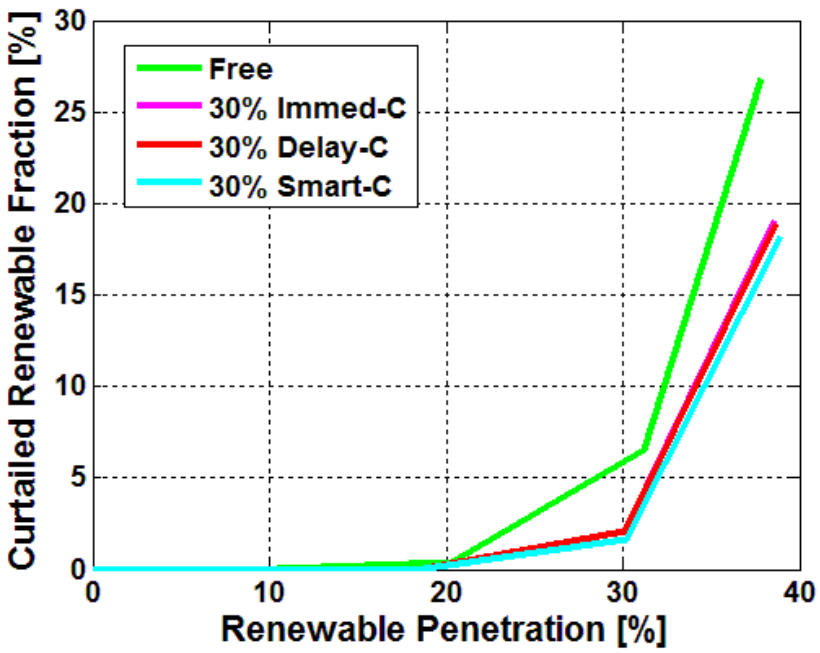

The implementation of electric transportation on the UCI campus reduces the amount of surplus renewable energy. This occurs by virtue of increasing the portion of the load demand that can be met by renewable power since the minimum gas turbine power does not change. The concept behind this behavior is discussed in more detail in the demand response sensitivity analysis (Task 7.3.3). As the renewable penetration level increases, the amount of curtailment increases exponentially as the electric transportation strategies are unable to sufficiently adapt to extreme renewable capacities.

While the difference between the electric transportation cases and the base case is significant, the differences between the three charging strategies are relatively small. The immediate and

delayed charging cases exhibited nearly identical curtailment until very high renewable penetration levels, where the immediate charging case begins to exhibit more curtailment than the delayed case. This is similar to the effect displayed for the grid-wide case (7.3.4.4). The charging load of the immediate charging case tends to peak in the early evening hours. The charging load of the delayed charging case tends to peak in the mid-morning hours. Wind power in this region tends to be relatively low during both of these time periods, however, the load demand is higher during the early evening hours which reduces curtailment relative to the mid-morning hours. Since the delayed case is unable to shape its charging profile to complement wind power from day to day, however, it is not as effective as the smart charging case.

The smart charging case exhibits lower curtailment amounts compared to the other charging strategies, as expected. The smart charging profile is shaped to smooth the balance profile, adding load when possible during periods of high renewable generation and minimizing load during periods of low renewable generation. The advantage of the smart charging strategy, however, is limited by the availability of vehicles plugged into the grid with remaining capacity to be charged. This varies throughout the day, therefore the extent to which the EV charging load can smooth the balance profile varies throughout the day. More availability is present during the night hours, however, this is also the time that the chiller load is absorbing most of the wind power. Additionally, the constraints of limited charging power and the need to have vehicle batteries fully charged by the end of the work and home dwelling periods limit the dispatchability of the EV charging load. Therefore, the advantage of the smart charging strategy is noticeable but not significant in this case.

7.3.4.3.2.3. Effect on the Gas Turbine Capacity Factor

The progression of the gas turbine capacity factor with renewable penetration level is presented in Figure 487:

Figure 487: GT Capacity Factor vs. Renewable Penetration Level

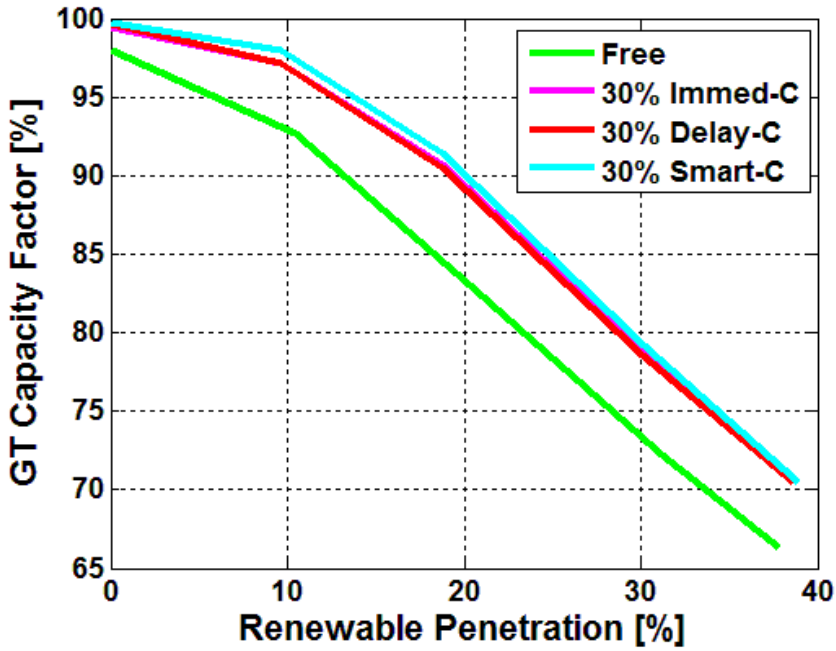

The progression of the gas turbine capacity factor also shows a significant difference between the cases with electric transportation compared to the base case, but only small differences between the different charging strategies. The increase in gas turbine capacity factor from the base case is due to the increased energy of the load demand due to electric transportation. Since the gas turbine has a fixed capacity, the gas turbine is able to operate at full or near-full capacity for more hours out of the year.

Between the three charging strategies, the smart charging strategy shows the largest increase in gas turbine capacity factors for all renewable penetration levels. This is expected since with smart charging, the charging load is placed to mitigate drops in the balance profile which often correspond to periods when the gas turbine would need to turn down. When coordinated with the chillers, this strategy is able to allow the gas turbine to operate at higher power levels for more hours out of the year. This advantage decreases with increased renewable penetration levels since with very high renewable capacities in the system, the charging load is simply not large enough to restore the gas turbine to operate above its minimum power level in many cases.

The immediate and delayed charging cases exhibit nearly identical effects on the gas turbine capacity factor. Very small differences between the cases arise at different renewable penetration levels due to changes in the renewable mix causing the profile of renewable power to complement one strategy more than the other at different penetration levels. These differences decrease at high renewable penetration levels due to overwhelming renewable capacities in the system.

Contrary to the results displayed in the other sensitivity analyses, these trends are not exactly reflected in the behavior of the HRSG contribution towards serving the heating demand as

presented for the different electric transportation cases at different renewable penetration levels in Figure 488:

Figure 488: HRSG Contribution vs. Renewable Penetration Level

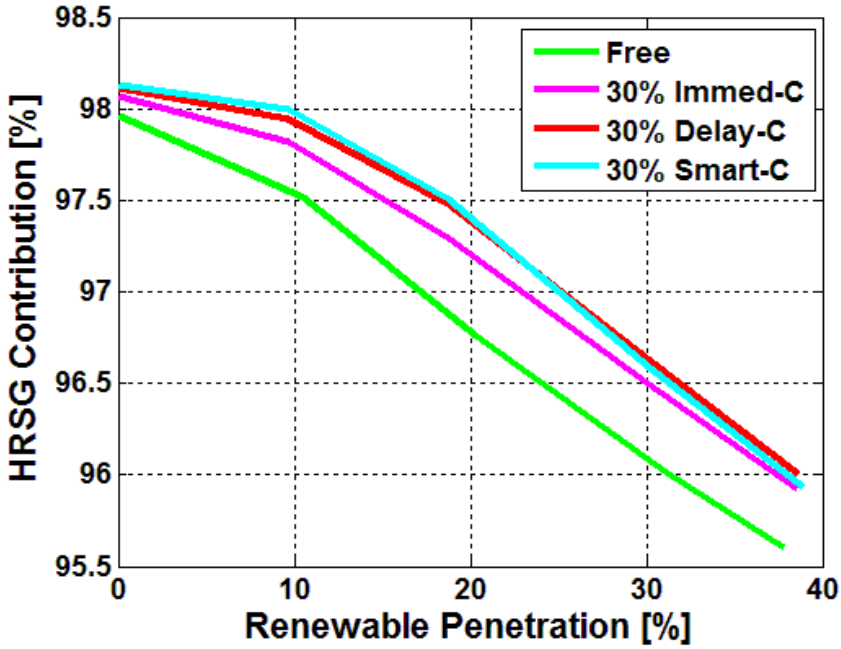

The increased load due to electric transportation allows the gas turbine to run at higher power levels, allowing more total exhaust enthalpy to be available for use by the HRSG to serve the campus heating demand during hours when excess heat is not yet available. This allows the HRSG contribution for the electric transportation cases to be increased compared to that of the base case.

In this result, however, there are larger differences between the cases with the different charging strategies but are still small on the absolute scale. The immediate charging case displays the lowest HRSG contributions, since the periods when it allows the gas turbine to operate at higher power levels tend to correspond with times when the heating demand for campus is low in the early evening hours and excess thermal energy is produced. The delayed charging case allows the gas turbine to operate at higher power levels during the mid-morning hours when the heating load is ramping up in preparation for activities on campus. The smart charging strategy initially exhibits the highest HRSG contribution, but drops below that of the delayed charging strategy at high renewable penetration levels. This occurs since the times when the smart charging strategy places the EV charging load at times that do not necessarily correspond to periods of high heating demand.

7.3.4.3.2.4. Effect on the Import Power Signal

The use of electric transportation also modifies the properties of the import power signal to the campus and therefore influences how the campus affects the utility grid when attaining higher renewable penetration levels. The distribution of the import power signal for the different demand response cases is displayed in Figure 489 for a low renewable penetration level (10.47%

targeted penetration) and in Figure 490 for a high renewable penetration level (50.79% targeted penetration):

Figure 489: Import Power Distribution: 10.47% Target Penetration

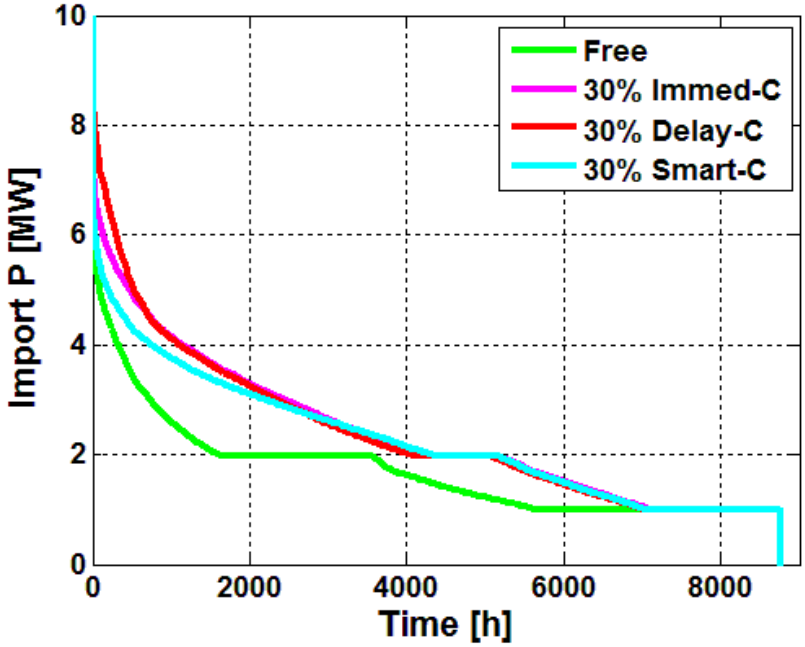

Figure 490: Import Power Distribution: 50.79% Target Penetration

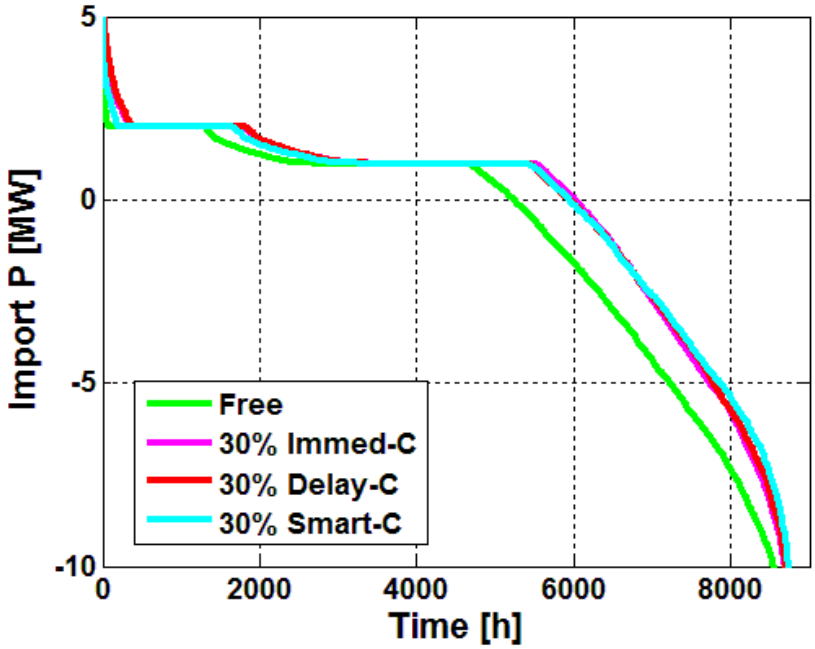

As implied from previous results, import power levels are generally higher for the cases with electric transportation at all renewable penetration levels. This is expected due to the increase in

the load demand associated with the implementation of electric transportation onto the UCI campus.

At low renewable penetration levels, the import restriction for the campus is not violated for any of the cases considered. This is expected since the free chiller dispatch case did not exhibit any import restriction violations and the implementation of electric transportation increases the load demand and reduces the likelihood of import violations. At low renewable penetration levels, the smart charging strategy is able to reduce import levels by the largest amount out of the three charging strategies. This is expected since this case will produce a charging profile aimed at smoothing the balance profile as much as possible, minimizing the load added during high balance periods. The immediate and delayed charging cases exhibit nearly identical reductions in import power levels over the year. The differences in the import power distribution between the delayed and immediate charging cases are due to the different times of the day when the electric vehicle charging load is not present.

At high renewable penetration levels, the cases with electric transportation exhibit a lower amount of import violations compared to the base case as expected due to the increased load. However, only relatively small differences exist between the different charging strategies in this context, with a strange result being that the smart charging case actually exhibits the highest number of import violations in this case. The immediate, delayed, and smart charging strategies exhibit 3223, 3310, and 3323 hours of import violation throughout the year. This occurs since at this renewable penetration level, the renewable capacity is so high that very severe drops in the balance profile occur. The smart charging strategy will focus the EV charging load to mitigate the most severe drops, however the charging load is typically insufficient to restore the balance to meet the import power restriction of the campus. The total energy of the electric charging load is fixed, however. Therefore, by placing most of the load during severe balance drops but being unable to restore compliance with the minimum import restriction, the remaining load available to mitigate less severe drops in the balance which could actually be brought into compliance is diminished. Essentially, the smart charging strategy minimizes curtailment/export power magnitudes at the expense of allowing slightly more hours of curtailment or export. The immediate case happens to place the charging load during times of high raw load demand and relatively low renewable power, addressing small drops in the balance profile which can be brought into compliance. The delayed case has an effect between the smart and immediate charging strategy.

The implementation of electric transportation also has effects on the maximum import power, as displayed for the different cases with renewable penetration level in Figure 491:

Figure 491: Maximum Import Power vs. Renewable Penetration Level

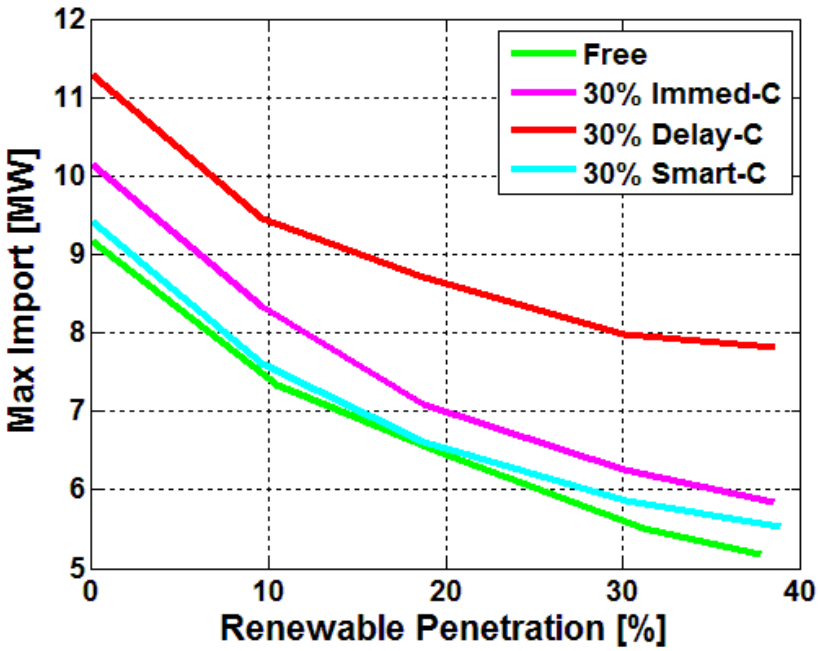

In general, the implementation of electric transportation increases the maximum import power level of the campus compared to the case without electric transportation by virtue of increasing the load demand. This may increase the demand charge on the campus. Depending on charging strategy, however, the increase in the maximum import power can be minimized or exacerbated.

The smart charging strategy is able to maintain maximum import power levels near that of the case without electric transportation. This behavior is expected since this strategy would prevent the EV charging load from being placed during hours of high balance power to the extent possible, therefore minimizing the extent to which the magnitude of the balance is increased. Small increases in the maximum annual import power still occur because the smart charging strategy operates with the constraint of ensuring that the electric vehicle batteries are charged to full capacity by the end of the dwelling period at home or work. Therefore, the smart charging strategy cannot completely prevent the placement of charging load during these hours at least once throughout the year, but it can minimize its magnitude. Recall that only one hour of high balance power levels are required to increase the maximum annual import power.

The delayed charging strategy increases the maximum import power by the largest magnitude at all renewable penetration levels. The maximum import levels for the delayed and immediate charging cases tend to occur in the fall season, where wind power in this region becomes more variable and is not typically consistent in occurrence from day to day. The maximum import level for the immediate charging case occurs during hours when the electric vehicle charging load is placed during periods of high load and low renewable power. The maximum import level for the delayed charging case occurs over a series of hours where the electric vehicle charging load is placed during a period when both wind and solar power are non-existent.

While the load demand is not particularly high during the hours when the electric vehicle charging load is placed, the lack of any wind or solar power is enough to cause the balance to reach slightly higher levels than the immediate case. Since the hours of high load for the immediate case have non-zero renewable power generation present, increasing the renewable penetration levels increases the difference between the two cases.

7.3.4.3.2.5. Effect on the Cost of Electricity

The behavior of the levelized cost of electricity with renewable penetration level for the different demand response cases compared to the case without electric transportation is displayed in Figure 492:

Figure 492: Change in LCOE of Different Demand Response Cases Compared to Base Case

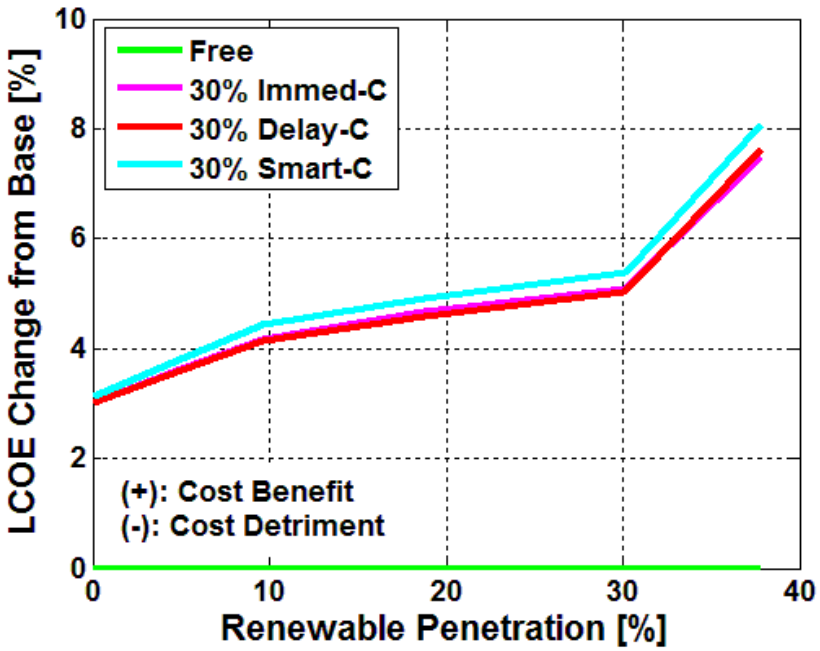

When interpreting the percentage difference from base, note that a positive difference indicates a cost benefit or decrease in the levelized cost of electricity compared to the base case and a negative value indicates a cost detriment or increase in the levelized cost of electricity.

Before discussing these results, it is important to note that the cost model used in this analysis does not take into account the cost of the charging and communications infrastructure required to support the requisite amount of electric vehicles on campus. The cost of the chargers themselves, capacity upgrades to the distribution infrastructure, and the communications equipment for smart grid operations are not included. Assigning costs for these different components is difficult in terms of magnitude and which entity different costs should be assigned. For example, should the cost of the chargers be included with the vehicle price and therefore burdened by automakers, or is the campus responsible for funding the installation of these units? Should the cost of changes to the distribution system in terms of capacity and management be assigned to the utility or the campus? At the current time, sound answers to these questions are not readily available. Therefore, in this analysis, these factors are not

included and represents somewhat of a 'best-case' cost scenario where the infrastructure required to support the requisite amount of electric vehicles and the corresponding charging strategies has already been installed and paid for. These cost numbers then reflect the change in the cost of electricity compared to the case without electric transportation due to alterations in the operation of on-campus resources. Additionally, as described in the sensitivity analyses for the other complementary technologies, the effect of time-of-use rate structures on the levelized cost of electricity is not taken into account since an appropriate structure would be difficult to determine with increased variable renewable capacities in the system.

Without taking infrastructure costs into account, the implementation of electric transportation changes the operation of on-campus resources in a manner that decreases the levelized cost of electricity for the UCI campus. This reduction ranges from 3% to 8% depending on renewable penetration and charging strategy. This reduction in cost is increased with higher renewable penetration levels, due to increasing reductions in renewable curtailment and therefore required renewable capacity. The steep increase in economic benefit at the higher renewable penetration levels is due to decreased curtailment. The smart charging strategy garners the largest reductions in cost compared to the case without electric transportation since it introduces these benefits to a much larger extent than the other strategies. The immediate and delayed charging strategies exhibit virtually identical cost reductions from the case without electric transportation, due to similar extents of gas turbine capacity factor increases and curtailment reductions.

Overall, however, these cost savings will have to be weighed against the cost of the requisite infrastructure to support these vehicles on campus. Depending on the extent of these costs and which cost elements are assigned to the campus, these costs may significantly outweigh the cost savings displayed here or may only reduce them to a small extent.

7.3.4.3.3. Conclusions

This analysis examined the effect of implementing electric transportation on the ability of a community such as the UCI campus to accommodate increased renewable penetration levels. The key insights of this analysis are presented here.

- **Realizing the benefits of smart charging strategies require coordination with and smart dispatch of other dispatchable load or energy shifting technologies on campus.** Without coordinating electric vehicle charging with dispatchable loads such as the cooling load, the benefits of intelligent dispatch of electric vehicle charging can be completely negated. Lack of coordination can inadvertently cause intelligent charging dispatch to be less favorable than immediate charging.
- **Electric vehicle charging reduces renewable curtailment and increases the gas turbine capacity factor by virtue of increasing the fraction of the load that can be met by renewable power.** By increasing the load demand but not increasing the minimum power level of the gas turbine (base load generation), a larger fraction of the load demand is available for renewable power to serve. This reduces renewable curtailment and makes more effective use of renewable power. Additionally, the increased load

allowed the fixed-capacity gas turbine to run at higher power levels, increasing the gas turbine capacity factor.

- **Smart charging offers increased benefits for the operation of energy resources on the UCI campus compared to immediate and delayed charging, which had essentially similar effects.** Immediate and delayed charging exhibited essentially similar effects on the operation of the UCI campus in the context of the metrics used, with the exception of the maximum import power. Smart charging in coordination with a freely-dispatchable cooling load exhibited reduced renewable curtailment, increased gas turbine capacity factors, and lower costs compared to the other charging strategies.
- **The implementation of electric transportation can reduce the levelized costs of electricity for the campus from a resource operation standpoint, but these benefits need to be weighed against the cost of the requisite charging and communications infrastructure.** The implementation of electric transportation allowed the levelized cost of electricity to be reduced from the case without electric transportation by altering the operation of on-campus resources. These cost figures, however, do not take into account the offsetting of costs for installing the infrastructure required to support electric vehicles for each strategy. Infrastructure costs may possibly reduce or negate the operational cost benefits depending on the assignment of cost elements to different entities and the magnitude of these costs.

Overall, the implementation of electric transportation onto the UCI campus can increase utilization of on-campus energy resources. However, uncertainty regarding infrastructure costs and the fact that the electric vehicle charging load is relatively small compared to the scale of the total load demand can limit realization of these benefits.

7.3.4.4. California Results

7.3.4.4.1. Description of Cases

Two charging locations are considered, which include, home-only and both home and work. This assumes that the opportunity exists for a vehicle owner to charge the vehicle at either home or home and work, respectively.

Additionally, three charge strategies are explored. 1) Immediate charging, also known as ASAP, is when vehicle owners plug their car in immediately when they arrive to their destination and begin charging at maximum power until the vehicle is completely charged. 2) Delayed charging is when vehicle owners do not immediately charge their vehicles when they arrive to a destination but rather charge their vehicle at the latest possible time such that they receive a full charge before they leave. 3) Smart charging is when vehicle owners rely on a control signal to determine when the vehicle will charge. The control signal can take a variety of forms including a utility rate structure (i.e., $/MWh), the Automatic Generation Control (AGC) signal from the grid (i.e., signal used to control regulation resources) or any other signal that can establish priority for charging at different times.

Values selected for the analysis are contained in Table 92.

Table 92: Selected Values for PHEV Model

Property	Value
Vehicle Penetration	0, 5, 25, 50 and 75 (% of total Vehicle Miles Traveled (VMT))
Charger Power	1.44kW
Vehicle Range	35 miles/charge
Energy Consumption	0.34 kWh/mile
Charging Location	Home Home and Work
Charging Strategy	Immediate (ASAP) Delayed Smart

The electric vehicle model is added into the HiGRID model to look at the effect of electric vehicle penetration, charge location and charge strategies on the grid. The following section presents the results from this work, including an assessment of the ideal charging strategies to support raising the renewable penetration for different mixtures of wind and solar power as well as the most advantageous charging locations and charging strategies for varying vehicle penetrations.

7.3.4.4.2. Results

Use of electric vehicles will cause the grid demand to increase and ideally, the selected charging strategy and location will allow for electric vehicles to charge at times when the increase in demand can support grid operation. The selected cost function for dispatching vehicle charging relies on the total demand less renewable generation signal. By subtracting the time-resolved renewable generation from time-resolved demand creates a signal that preferentially selects low load and high renewable times to charge vehicles if they are available. To complement renewables while minimizing demand, the available demand, wind, and solar profiles are provided in Figure 493.

Figure 493: Daily Average Profiles for California Demand and 30GW of Wind and Solar

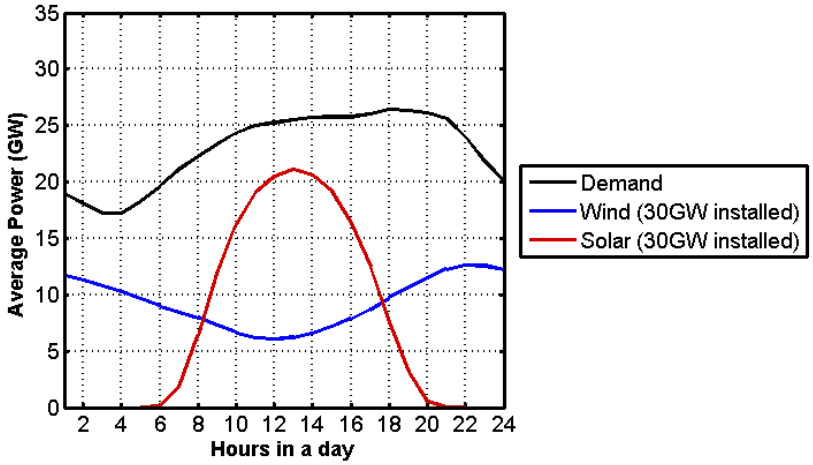

7.3.4.4.2.1. Ideal Charging Profiles

Depending on the mixture of renewables, the ideal charging time will change. The next three figures show the ideal charging strategy to maximize implementation of renewables for three different renewable mixtures (i.e., wind, solar, and wind&solar). Notice that for Figure 494 all three profiles are the same since 9% represents the initial amount of non-wind/solar renewables. The 20% penetration profiles shows both wind and wind&solar as similar, while solar only, is shifted to the afternoon to compensate for the afternoon solar peak.

Figure 496 further accentuates the 20% profiles. "Solar only" no longer has a morning peak and the afternoon peak for wind&solar is more pronounced.

Figure 494: Ideal Daily Average Charging Profile with 5% of VMT served by PHEVs for different Renewable Mixtures with 9% Penetration

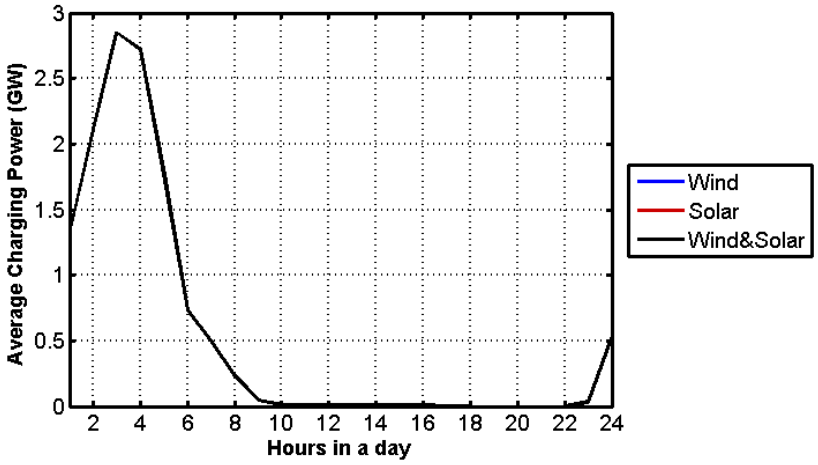

Figure 495: Ideal Daily Average Charging Profile with 5% of VMT served by PHEVs for different Renewable Mixtures with 20% Penetration

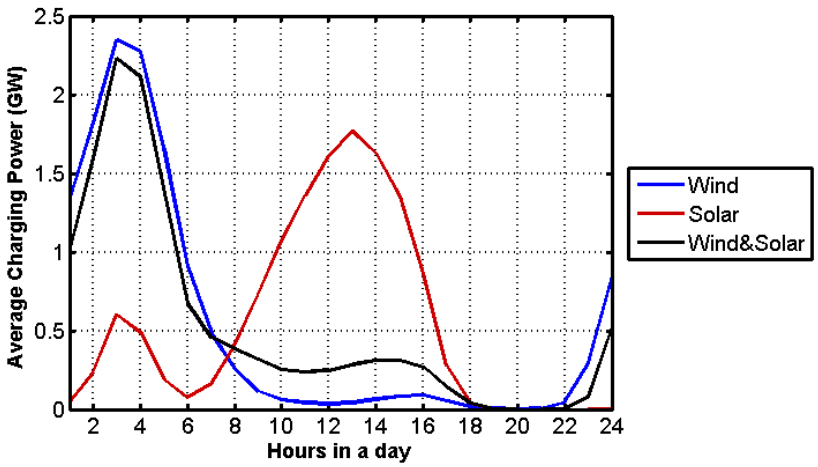

Figure 496: Ideal Daily Average Charging Profile with 5% of VMT served by PHEVs for different Renewable Mixtures with 33% Penetration

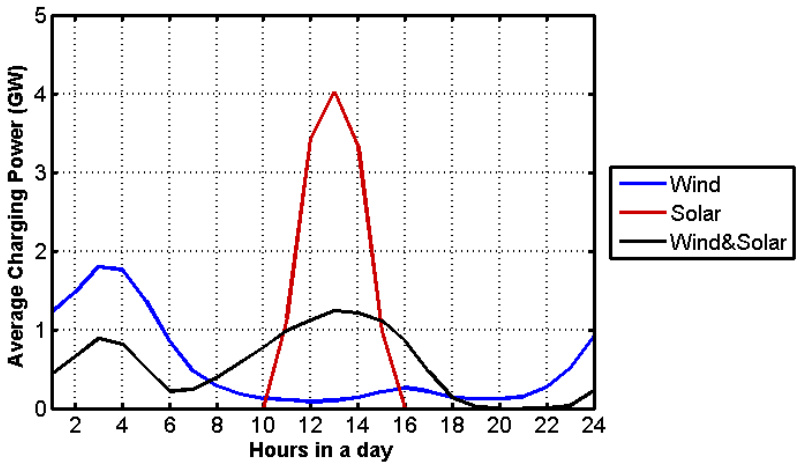

Different renewable penetrations have a significant effect on the charging profile. Initially, the charging is focused on smoothing the demand by increasing the nighttime minimum load. With more renewables, particularly solar, the charging profile focuses more on smoothing the renewable profile than the demand, as evidenced by the progression from a 3AM maximum at 9% penetration to a 1PM maximum at 33% penetration. While 5% VMT penetration was selected for this analysis, larger VMT penetrations increase the scale of the ideal profiles but do not change the relative shape.

7.3.4.4.2.1.1. Conclusions

- Ideal electric vehicle charging profiles are strongly affected by the renewable mixture and renewable penetration

- Vehicle charging transitions from smoothing the demand at low renewable penetrations to smoothing the supply at high renewable penetrations

7.3.4.4.2.2. Charging Locations

Practically, vehicle owners are not always at a location with a charger but the goal is selecting charging locations to meet the needs of the vehicle owners, and maximize the use of that equipment to minimize the number and costs of installation.

By determining the dwelling time for vehicles at different locations it is possible to see if the ideal strategies are plausible. In a paper released in 2011 entitled "Fuel reduction and electricity consumption impact of different charging scenarios for plug-in hybrid electric vehicles", Zhang, et.al., break down the dwelling time at a variety of locations across the country. This information is presented in Table 93.

Table 93: Distribution of Dwelling Times by Activity (Zhang, 2011)

Location	Portion of Dwelling Time	Average Dwelling Time (hours)
Home	75%	10.5
Work	14%	6.0
School	1%	4.2
Medical/Dental Services	0%	1.2
Shopping and Service	2%	0.8
Gym/Exercise/Sports	1%	0.9
Pick Up and Drop Off	1%	0.2
Get/Eat Meal	1%	1.0
Others	5%	2.3

The two most important categories are "Home" and "Work". The average dwelling time while at "Home" is the largest followed by "Work." Typically, vehicle owners that work are at work during the day and return to home at night and vehicle owners that do not work can be at home during the day and night. While other locations can support charging and potentially provide benefit to both vehicle user and the grid, they do not have sufficient dwelling times to completely support the vehicle owners.

Comparing the dwelling times and locations with the ideal profiles above, all penetrations for "wind" are well aligned with the time-of-day (e.g., 11PM to 7AM) and duration (i.e., 8 hours) that vehicle owners are at home. When installing large amounts of "solar" the ideal charging location is at work with the time-of-day alignment for solar between 10AM and 4PM (6 hour duration). While this aligns well the average dwell time for electric vehicles at work two complications exist. 1) Not all vehicle owners work so those without chargers at their home will not have access to charging equipment and 2) charging a battery in a shorter time takes a higher

power charger, which will potentially come with additional costs and safety requirements. Lastly, the "wind&solar" due to the combination of both wind and solar could initially benefit from mostly home chargers then for moderate renewable penetrations (20%-30%) both home and work would be required to achieve the ideal profile and for high amounts of solar the shape begins to favor the installation of work chargers since the solar peak is the first to bring curtailment.

7.3.4.4.2.2.1. Conclusions

- Ideal charger selection is dependent on aligning vehicle owner needs with grid needs.
- Home charging well aligns with the time-of-day and duration requirements to charge vehicles and support the grid for high wind and low solar capacity.
- Work charging well aligns with the time-of-day requirements and to a lesser extent duration requirements to charge vehicles and support the grid for high solar and low wind capacity.
- Other locations do not offer the necessary dwelling time to support all charging needs but could provide additional benefit for vehicle owners and the grid.
- Work charging has an additional challenge because not all vehicle owners work.

7.3.4.4.2.3. Charging Strategies Compared to Ideal

In addition to varying the charging location, different charging strategies have the ability to greatly impact the shape of the resulting charging profile. Three charging profiles are explored herein: 1) immediate, 2) delayed and 3) smart charging. The behavior of these strategies was described in the previous section. To compare the three different strategies all home charging will be used.

Four profiles are presented in Figure 497, Figure 498, and Figure 499 to show how the charging strategies affect the resulting charge profiles. Immediate charging is representative of the business-as-usual case since charging vehicles at the earliest time provides them the most flexibility in the event that the vehicle is needed before the prescribed time. The profile does not change with the mixture of renewables or the renewable penetration. Delayed charging profiles, like immediate charging profiles, are not affected by changes in renewable mixture or penetration. The delayed charging strategy nearly inverts the immediate charging strategy profile. Smart charging has the ability to respond to needs in the electrical system while meeting the charging needs of vehicle owners. Smart control is dependent on both the renewable mixture and renewable penetration.

Figure 497: Daily Average Charging Profiles at 9% Penetration with different Charging Strategies for a 50/50 Mixture of Wind and Solar

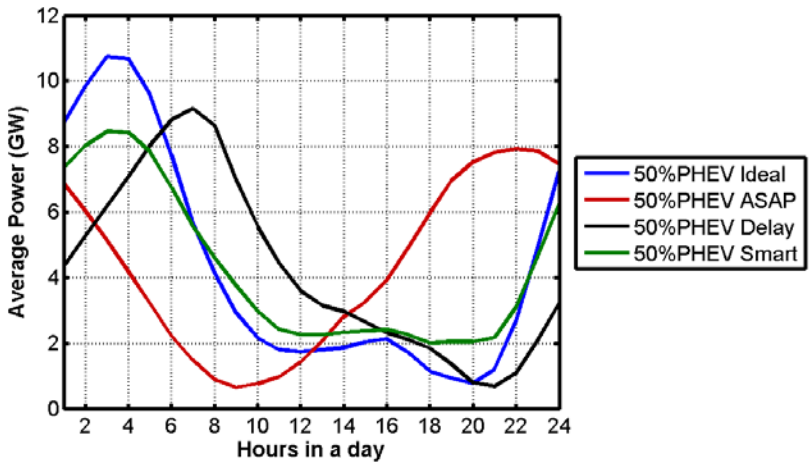

Figure 498: Daily Average Charging Profiles at 20% Penetration with different Charging Strategies for a 50/50 Mixture of Wind and Solar

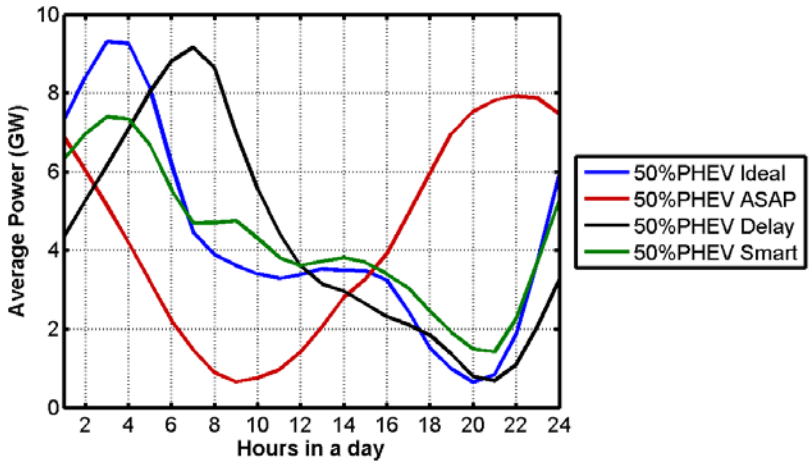

Figure 499: Daily Average Charging Profiles at 33% Penetration with different Charging Strategies for a 50/50 Mixture of Wind and Solar

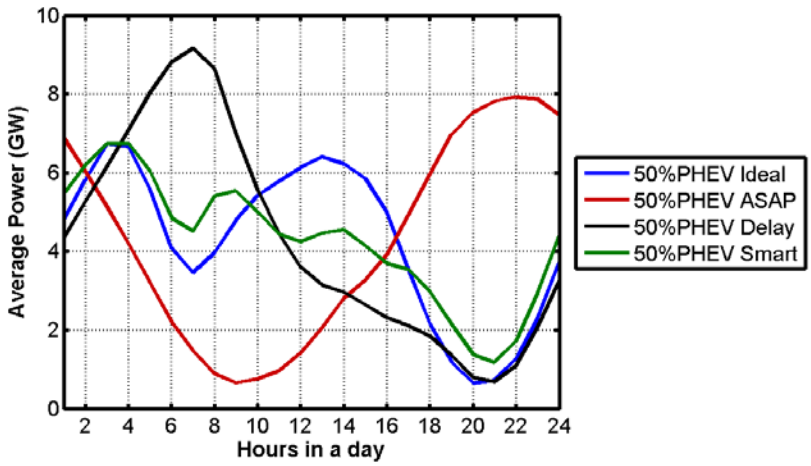

A measure of the difference between each charging strategy's profile and the ideal charging profile are presented in Table 94. The values are calculated by taking the sum of the absolute value of the difference between each signal and the ideal signal, then taking a percentage of the sum of the ideal signal. In this way both positive and negative differences are penalized. Smart charging is the most similar to the ideal strategy, followed by delayed charging and lastly by immediate charging.

Table 94: Charging Strategy Percentage Difference from Ideal Daily Average Charging Signal

Percentage Difference from Ideal Signal	Renewable Penetration		
	9%	20%	33%
Ideal	0%	0%	0%
Immediate	78.8%	76.6%	84.4%
Delay	51.4%	38.7%	40.3%
Smart	20.9%	17.6%	20.2%

In addition to multiple charging strategies, there are also multiple charging power levels. While this is not explored in this research, increasing or reducing the selected power level can change the ability of each strategy to provide service to the grid, while meeting the requirements of the vehicle owner. The lifetime of the battery is affected by how it is charged. Vehicle chargers with the ability to regulate the power provided to the battery in addition to the time present, can provide additional benefit to the grid and if the electricity rates are structured appropriately, some of this benefit can be passed to electric vehicle users. The effects on lifetime of the battery must be compared with the benefits garnered from grid supporting operation.

Each control strategy has different resulting behavior and different information requirements to implement. Immediate charging requires no information about the user or from the grid, since

charging begins right when the plug is engaged. Delayed charging requires information from the user in the form of a desired departure time. Smart charging requires information from the user for departure time and information from the grid to know when to charge. For low renewable penetrations, a control signal from the grid is very simple as the demand and generation are predictable. As intermittent renewable generation increases it becomes more challenging to determine exactly when the grid will need to add or shed load from charging systems. Battery systems have very high power density and can rapidly ramp up or down, which can be very beneficial for supplementing or replacing ramping capacity from conventional rotating machinery.

Comparing each charging location and strategy to the ideal provides one measure of the effectiveness of each option; however, there are other important measures to explore. The next section examines the effect on different measures including: capacity factor, grid efficiency, curtailment, ramp rates and cost.

7.3.4.4.2.3.1. Conclusions

- Smart charging represents the most similar shape to that of the ideal profile while considering each vehicle's location and charging needs throughout the day.
- Delayed charging is the second best followed by immediate charging
- Immediate and delayed charging profiles are nearly inverse being offset by 10 hours
- Immediate charging requires no information about the user or the grid, delayed charging requires information from the user and smart charging requires information from the grid and from the user

7.3.4.4.2.4. System-wide Effects From Different Charging Strategies

Increasing the energy generation requirement with electric transportation can have beneficial or detrimental impacts on the operation of the other generators and will change as the renewable penetration increases. An increase in demand must be met by some generation. This generation initially comes from additional load-following and peaking plants since no new coal plants can be installed in the state and there is a moratorium on nuclear plants. This is important to note and will be revisited throughout the document, since differences in the generation mix can change the system results.

One example of this can be seen with the capacity factor. Figure 500 shows how the system-wide capacity factor will change with PHEVs and increasing renewable penetration. As suggested earlier, the smart charging provides the greatest increase in capacity factor followed by the delayed charging and lastly by immediate charging. Since baseload generation will not change appreciably for any of these changes, that means the inclusion of PHEVs can reduce the dynamics experienced by balance generation or reduce the required installed balance generation to meet the same demand. Notice the last "W&S+5%VMTdemand" line signifying the base case with the electricity demand linearly scaled to the total yearly demand as the electric transportation cases. Comparison with this case removes the effect of different

generation mixtures and focuses on the benefits of being able to shape the demand as opposed to a linear increase. Both the base case and base case with additional demand are important to review as they tell different stories.

Figure 500: Grid-wide Capacity Factor Difference for Home-Charging Strategies with a 50/50 Mixture of Wind and Solar

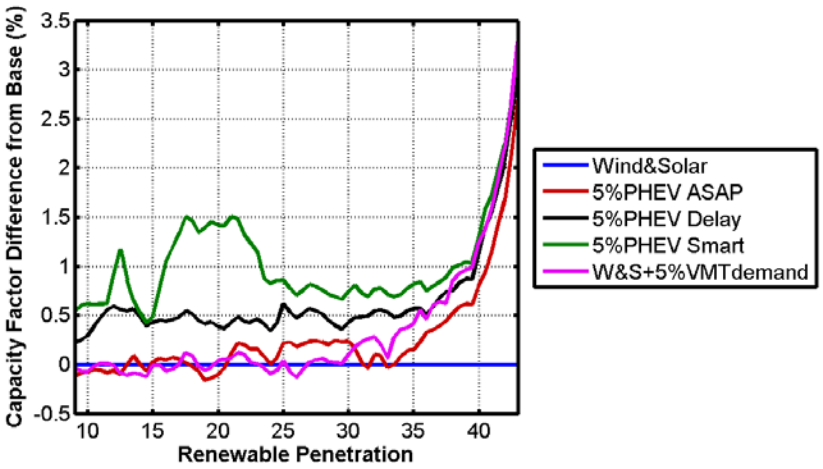

The importance of comparing both base cases is evident from Figure 501 where the grid efficiency with electric transportation is almost always lower than the wind and solar base case but when compared to the case with additional demand the efficiency increases in all cases. This is because with additional generation balance generation must be installed, but the fleet efficiency for load-followers and peakers is lower than that of the coal and nuclear, resulting in an apparent decrease in efficiency. However, when the electric transportation cases are compared to the base case with additional demand, additional control over when the generation occurs, even in the immediate case, results in a higher grid efficiency.

Figure 501: Grid Efficiency Difference for Home-Charging Strategies with a 50/50 Mixture of Wind and Solar

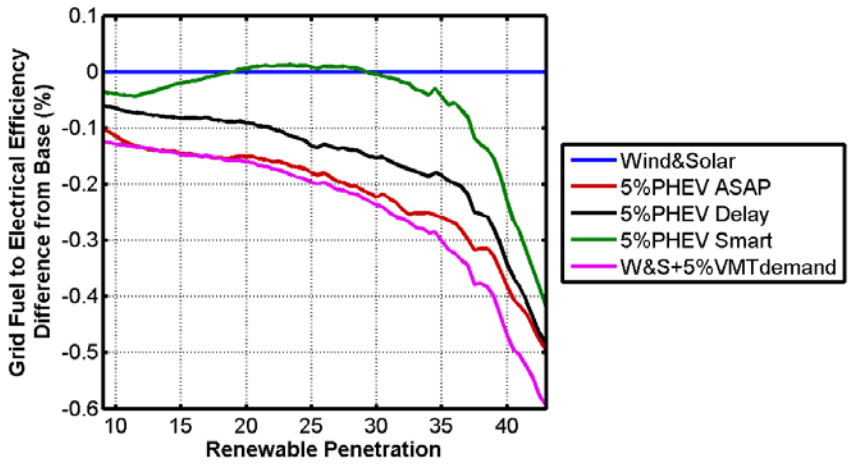

Inclusion of PHEVs at any VMT penetration initially increases the amount of renewables needed to achieve the same renewable penetration, as shown in Figure 502 and Figure 503. This is because increasing the required electricity demand when the renewable penetration is low means that electricity will come from non-renewable generation and the renewable penetration will actually decrease. As renewable capacity is added; the transportation cases eventually reach a crossover point, signifying that the integration of electric transportation will increase the renewable penetration with the same capacity of renewables as the base case. This crossover occurs first for smart charging, then delayed and lastly immediate (29.4, 31.9, and 35.9%, respectively). The crossover point for smart and delayed charging is more favorable when compared using the base case with additional demand (22.6 and 29.0, respectively), while the immediate charging never improves the renewable penetration. This is because the base case+demand, like the electric transportation cases, delays the exponential rise of curtailment a few extra percentages of renewable penetration (i.e., very visible at the high penetrations in Figure 502), which in-turn appears more dramatic when compared to the base case in Figure 503.

Figure 502: Renewable Penetration versus Installed Capacity for Home-Charging Strategies with a 50/50 Mixture of Wind and Solar

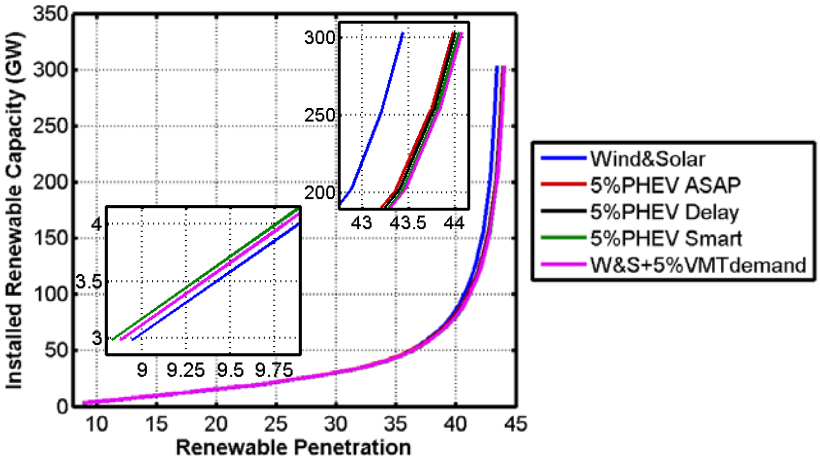

Figure 503: Renewable Capacity Difference for Home-Charging Strategies with a 50/50 Mixture of Wind and Solar

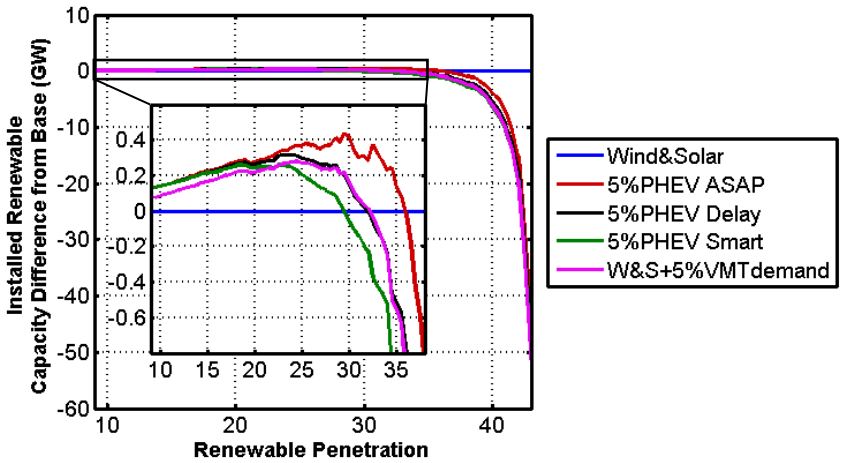

Comparing the fleet ramp rate up, ramp rate down, and average starts provides an indication of the effect that electric transportation could have on the grid if operated according to the defined strategies (Figure 504, Figure 505 and Figure 506). Immediate charging increases the required balance fleet ramp rate up and down for almost every renewable penetration and its effect on generator starts is negligible. Delayed charging is mostly negligible for ramp rate up since its profile is nearly the same as the base case and slightly improved for the base case plus demand. There is a slight improvement for ramp rate down and starts up to 20% renewable penetration but its effect is negligible after that. Smart charging provides a significant reduction in balance fleet ramp rate up, ramp rate down, and average starts up to 40% renewable penetration. After 40% penetration, excess generation causes significant reductions in the required ramp rates and starts, as load-follower and peakers are removed and replaced with large installations of

renewables. This can be seen in Figure 502 for penetrations above 40% the required renewable capacity increases rapidly with little increase in penetration.

Figure 504: Average Balance Fleet Ramp Rate Up for Home-Charging Strategies with a 50/50 Mixture of Wind and Solar

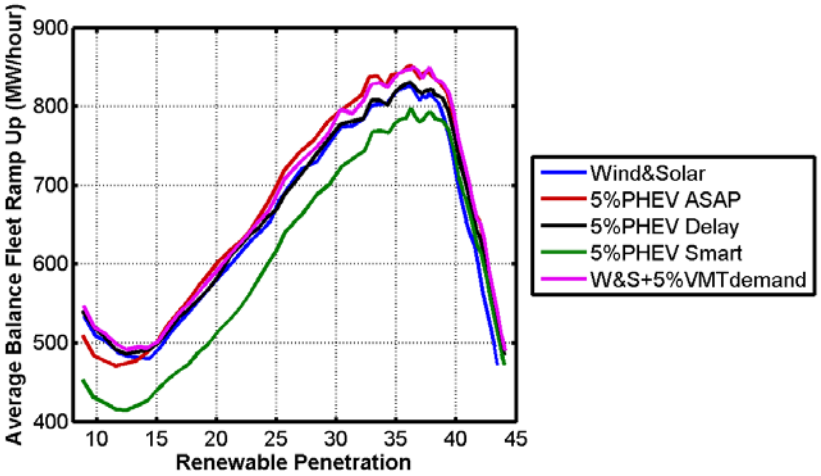

Figure 505: Average Balance Fleet Ramp Rate Down for Home-Charging Strategies with a 50/50 Mixture of Wind and Solar

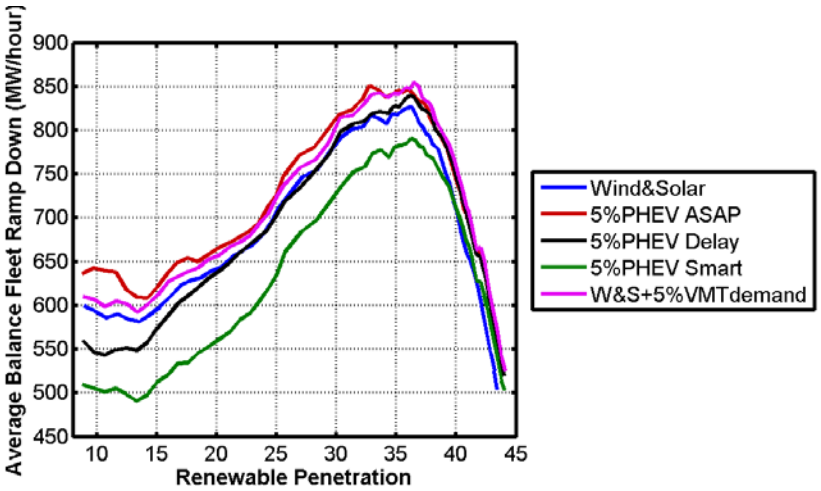

Figure 506: Yearly Average Balance Fleet Starts for Home-Charging Strategies with a 50/50 Mixture of Wind and Solar

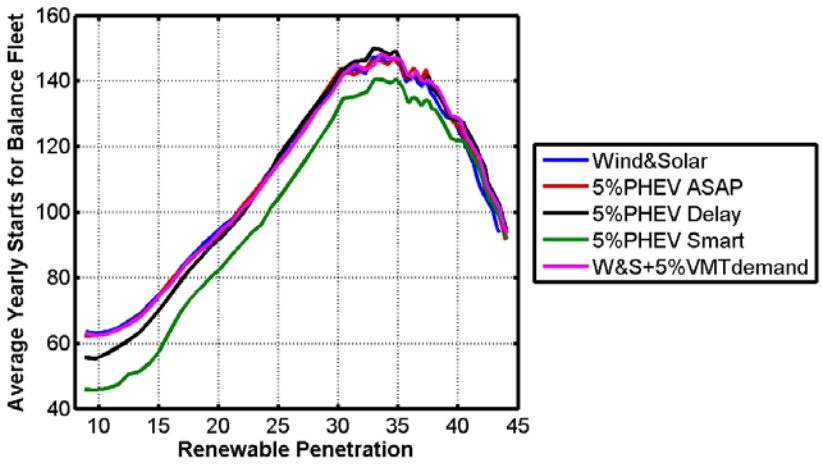

Calculating carbon dioxide emissions from PHEVs requires knowledge of both the electric sector and the transportation sector. Emissions that would normally be attributed to the transportation sector are attributed to the electric sector because of the required additional generation. By exploring the combined emissions from both sectors it is possible to determine any tradeoffs that exist and isolate the strategy with the greatest emissions reduction.

The overall CO_2 reduction is presented in Figure 507 and the percentage difference from the base case (i.e., wind and solar spanning scenario) is presented in Figure 508. Both figures contain CO_2 emissions from the electric sector as well as the CO_2 contribution from all passenger vehicles, and light duty trucks in 2005. Conventional vehicles are assumed to have an efficiency of 19.81 miles/gallon and emit 437 grams of CO_2 per mile.

All three charging strategies result in a reduction from the base case. Two main factors contribute to this. The most prominent reduction is from more efficient use of energy for transportation. As noted earlier the mile per thermal energy equivalent for electric transportation is much greater than the conventional fleet in 2005. Any improvements in the conventional fleet will reduce the benefit; however, improvements in the fuel to electrical efficiency of the grid from renewables will improve the value of using electric transportation. Lastly, while the CO_2 emissions increase in the electric sector due to increased generation requirements, they increase at a reduced rate because of the dispatchability of electric transportation. This is best shown in Figure 508 by the increase in CO_2 reduction compared to the base case with increasing renewable penetration from 0.8% to 1.4%.

Figure 507: CO_2 Percentage Reduction for Electricity and Transportation Sectors using Home-Charging Strategies with a 50/50 Mixture of Wind

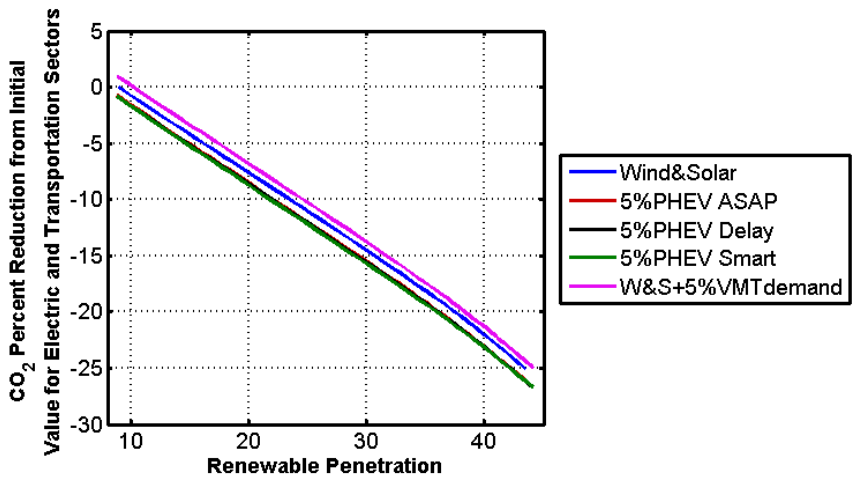

Figure 508: CO_2 Emissions Percentage Difference for Electricity and Transportation Sectors using Home-Charging Strategies with a 50/50 Mixture of Wind and Solar

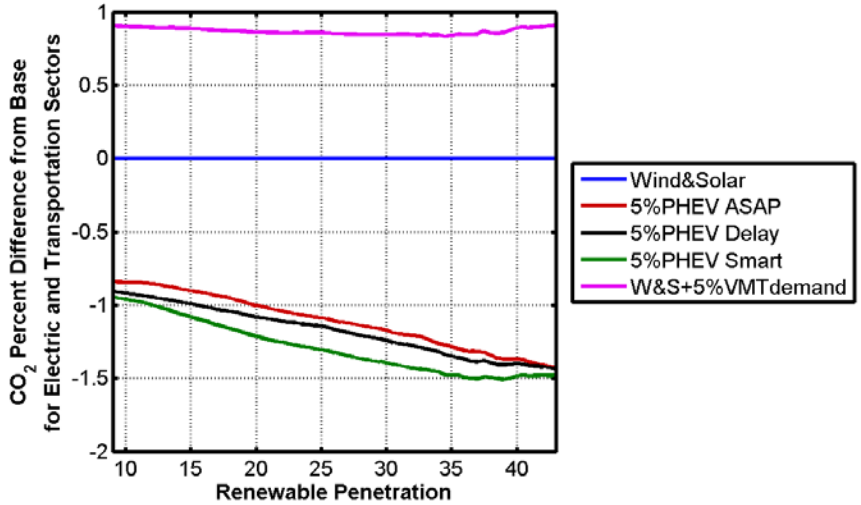

Changes in the operation of balance generation and renewable generation fleets will result in a change in the cost of generation. For this analysis, the purchase of equipment to charge vehicles and the need for upgrades to electrical distribution equipment to support increased demand and purchase of transportation fuel are not considered.

The portfolio levelized cost difference between each charging strategy and the base case is shown in Figure 509. The use of smart charging is cost competitive even with the lowest renewable penetrations and reduces cost an average of 1.1% up to 30% penetration and increases even more so as excess generation increases at higher penetrations. Delayed charging stays near the cost competitive mark but before 30% dips below several times with an average

increase in LCOE of 0.11%. After 30% penetration, delayed charging becomes cost competitive and rapidly increases its value with increasing excess generation. Lastly, immediate charging does not become cost competitive until 34.7% penetration and increases quickly as a result of excess generation.

Figure 509: Levelized Cost of Electricity for Home-Charging Strategies with a 50/50 Mixture of Wind and Solar. Positive Values: Cost Benefit (cheaper), Negative Values: Cost Detriment (more expensive).

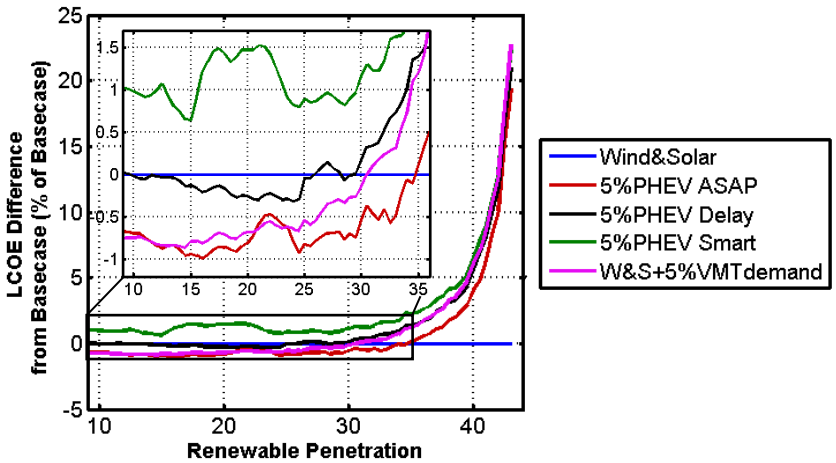

7.3.4.4.2.4.1. Conclusions

- Electric transportation can improve grid operations or aggravate both current balancing challenges and future challenges with intermittent generation.
    - Electric transportation expands the amount dispatchable demand.
    - Smart charging causes a reduction in grid efficiency with respect to the base case at the same renewable penetration but improves capacity factor, balance fleet ramping requirements and starts, and can reduce the system-wide LCOE for all renewable penetrations.
    - Delayed charging slightly improves grid capacity factor, reduces grid efficiency, has a negligible effect on balance fleet ramp rates and starts and is generally not cost competitive until high renewable penetrations.
    - Immediate charging lowers capacity factor and efficiency, increases LCOE and provides negligible effect on balance fleet ramp up, ramp down and yearly starts.
- Electric transportation can enable higher renewable penetrations.
    - Additional demand will require greater installed renewable capacity to achieve the same penetration in the case without electric transportation until sufficient excess generation becomes available to contribute to the penetration.
    - By increasing demand the amount of renewable energy that can be supported by the grid before the minimum load is reached is also increased

7.3.4.4.2.5. Effects From Varying Electric Transportation Penetration

It is also important to understand the effects of increasing the vehicle penetration. Smart charging provides the most benefit of the three selected charging strategies so this section will explore the resulting effects of varying the VMT penetration for electric transportation in California. The three values selected are 5%, 25%, 50% and 75%, additional information is provided in Table 90 for selected VMT penetrations.

As the VMT penetration is increased the charging energy increases. Figure 510 and Figure 511 show the resulting daily average profile and load duration curves for the four different VMT penetrations.

Figure 510: Daily Average Charging Profile for different VMT Penetrations of Smart Home-Charging at 9% Renewable Penetration with a 50/50 Mixture of Wind and Solar

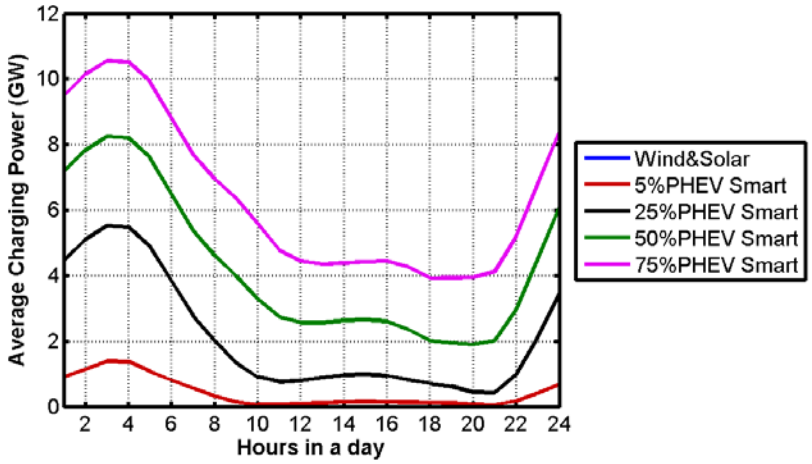

Figure 511: Load Duration Curve of Charging Profile for different VMT Penetrations of Smart Home-Charging at 9% Renewable Penetration with a 50/50 Mixture of Wind and Solar

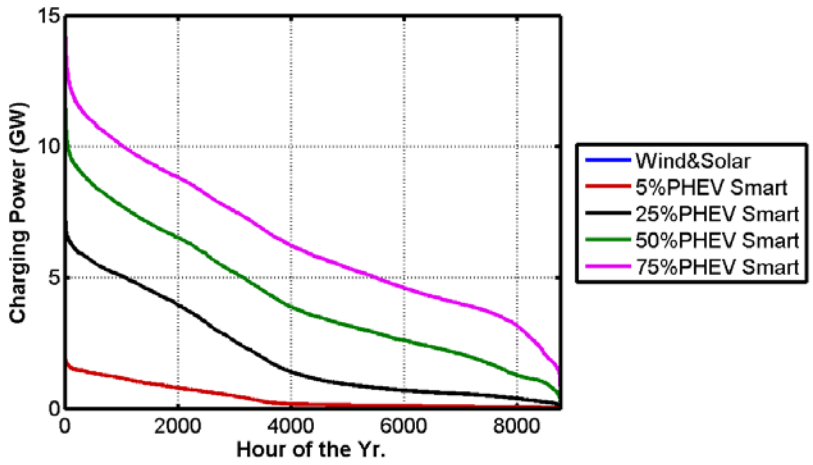

The system-wide capacity factor increases with increasing VMT penetration; however, as the VMT penetration increases the capacity factor does not uniformly follow. At low renewable penetrations the capacity factor increases near uniformly for each VMT penetration in comparison to the base case but around 20% renewable penetration the difference between the capacity factor for 75% and 50% VMT is negligible and at 30% the capacity factor for 75%, 50% and 25% VMT are nearly the same. Following 30% renewable penetration excess generation increases rapidly allowing electric transportation to become more effective at improving system capacity factor than for the base case, hence the capacity factor difference from the base case rises for high renewable penetrations.

Figure 512: Grid-wide Capacity Factor Difference for different VMT Penetrations of Smart Home-Charging with a 50/50 Mixture of Wind and Solar

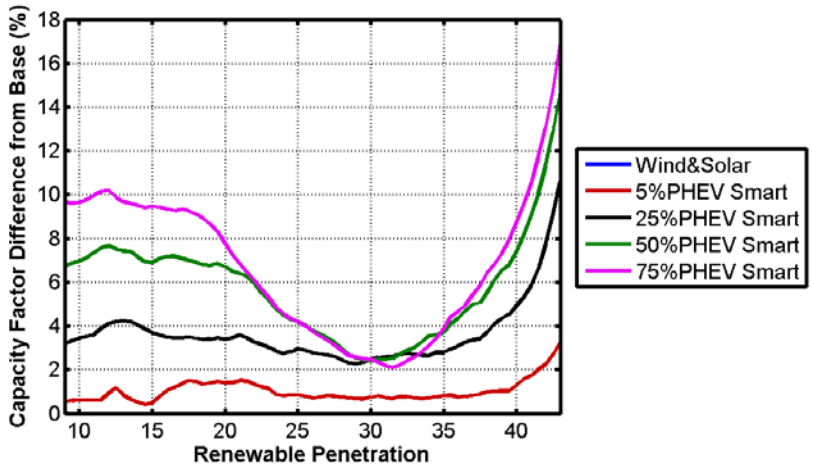

Increasing VMT penetration will reduce grid efficiency because additional generation comes from conventional load-following and peaking units. These units, when considering their age

and operation, are lower efficiency than coal and nuclear technologies. As the VMT penetration increases, the contribution of lower efficiency generation is increased as shown in Figure 513.

Figure 513: Grid Efficiency Difference for different VMT Penetrations of Smart Home-Charging with a 50/50 Mixture of Wind and Solar

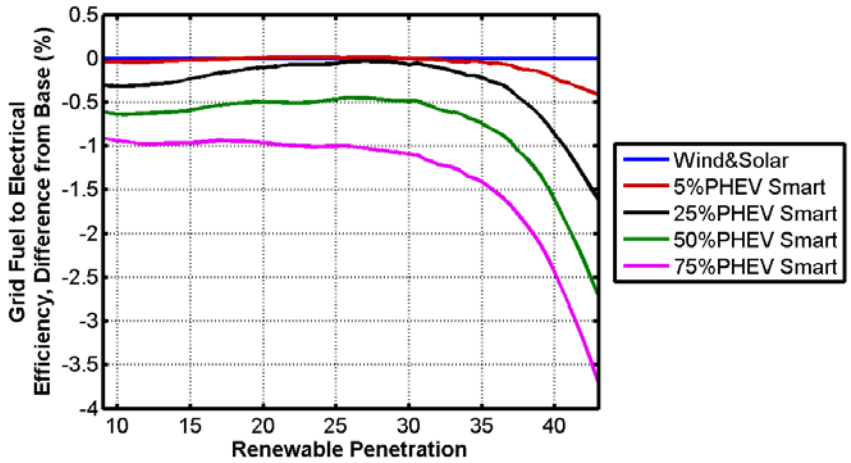

Electric vehicles can significantly increase the renewable penetration compared to the cases without electric transportation at high renewable penetration as shown in Figure 514. This can be attributed to two factors 1) large increases in dispatchable demand and 2) increases in demand are met with load-following plants and will reduce the fraction that baseload supplies, which in-turn increases the amount of renewable energy that can be supported by the grid before the minimum load is reached (i.e., baseload plus generation to meet spinning reserves and regulation). For low renewable penetrations the addition of electric transportation increases the required renewable capacity to achieve the same penetration as the case without transportation. It is not until 29.5% renewable penetration that the 5% VMT case begins to reduce the required renewable capacity. For the other VMT penetrations, this crossover occurs at 32.5%, 34.4% and 35.6% renewable penetration for 25%, 50% and 75% VMT, respectively.

Figure 514: Installed Renewable Capacity for different VMT Penetrations of Smart Home-Charging with a 50/50 Mixture of Wind and Solar

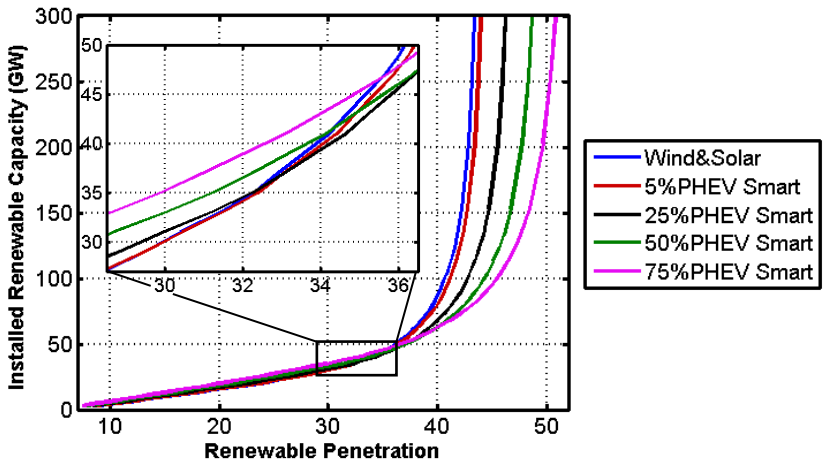

The balance generation fleet ramp rates and starts are generally reduced with increasing VMT penetration (Figure 515, Figure 516 and Figure 517). As with grid capacity factor, expanding VMT penetration beyond 50% provides only a limited reduction for average ramp rates and starts.

Figure 515: Average Balance Fleet Ramp Rate Up for different VMT Penetrations of Smart Home-Charging with a 50/50 Mixture of Wind and Solar

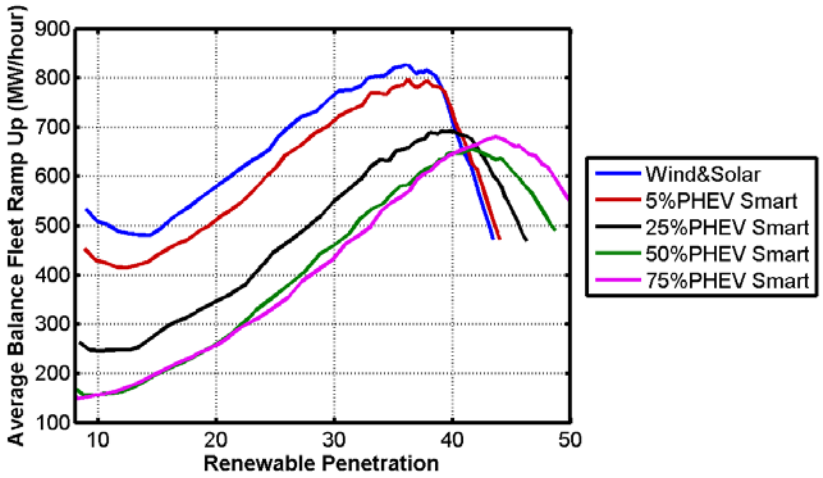

Figure 516: Average Balance Fleet Ramp Rate Down for different VMT Penetrations of Smart Home-Charging with a 50/50 Mixture of Wind and Solar

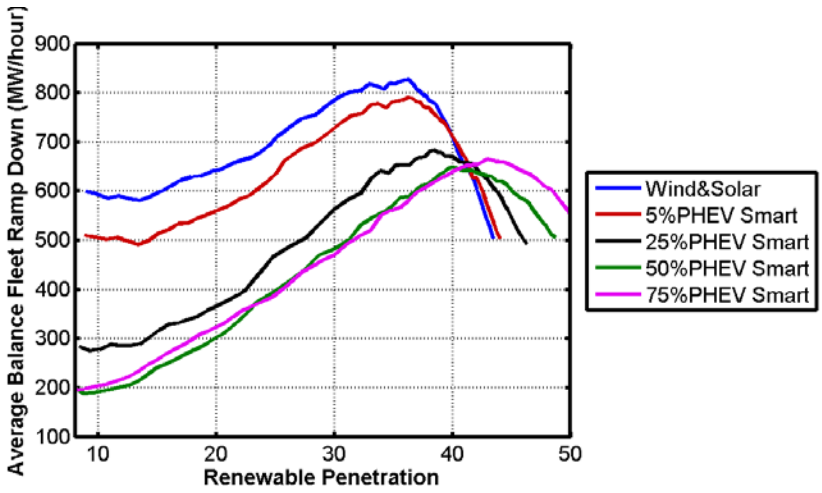

Figure 517: Yearly Average Balance Fleet Starts for different VMT Penetrations of Smart Home-Charging with a 50/50 Mixture of Wind and Solar

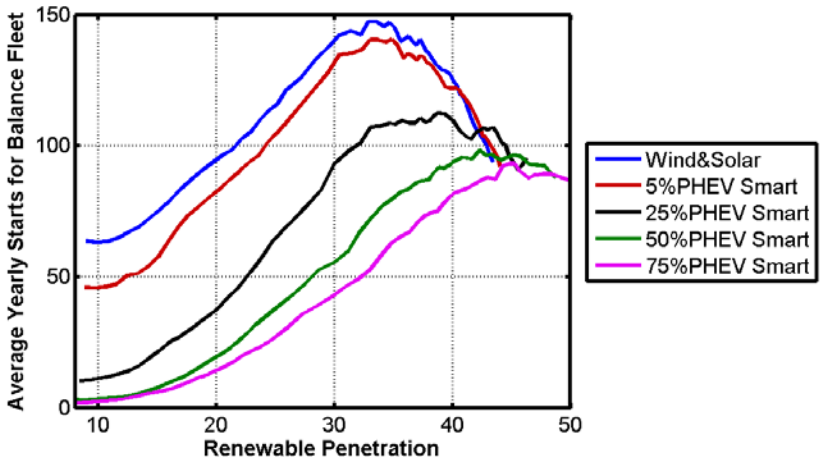

Similar to the 5% VMT penetration cases when comparing each charging strategy, the combined electric and transportation sectors CO_2 emissions are reduced because of the lower carbon intensity of using generation from the electric sector when compared with conventional vehicles in 2005. Additionally, the added dispatchability allows the reduction in CO_2 with respect to the base case (i.e., 50/50 wind and solar mixture) to improve as the renewable penetration increases.

Figure 518: CO_2 Emissions Percentage Difference for Electricity and Transportation Sectors for different VMT Penetrations of Smart Home-Charging with a 50/50 Mixture of Wind and Solar

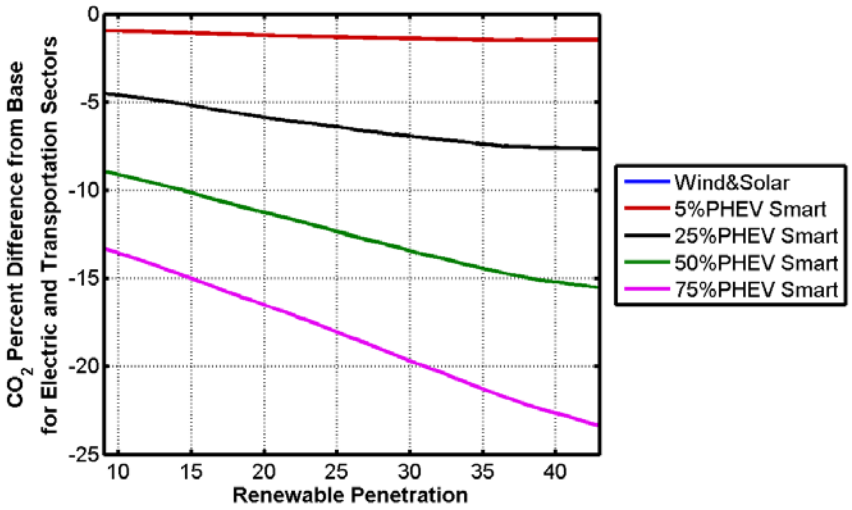

By comparing the LCOE of each VMT penetration case to the base case (i.e., wind and solar spanning case), Figure 519 shows that as the renewable penetration grows the cost competitiveness of all VMT penetrations increase. Both 5% and 25% VMT penetrations remain competitive for all renewable penetrations, while 50% and 75% do not become competitive until 29.6% and 32.2% renewable penetration. The 25% VMT penetration case provides the highest average value of all cases. The ideal VMT% penetration is determined by a variety of things including the mixture and capacity of resources in the system as well as the ancillary service requirements.

Figure 519: Levelized Cost of Electricity for different VMT Penetrations of Smart Home-Charging with a 50/50 Mixture of Wind and Solar

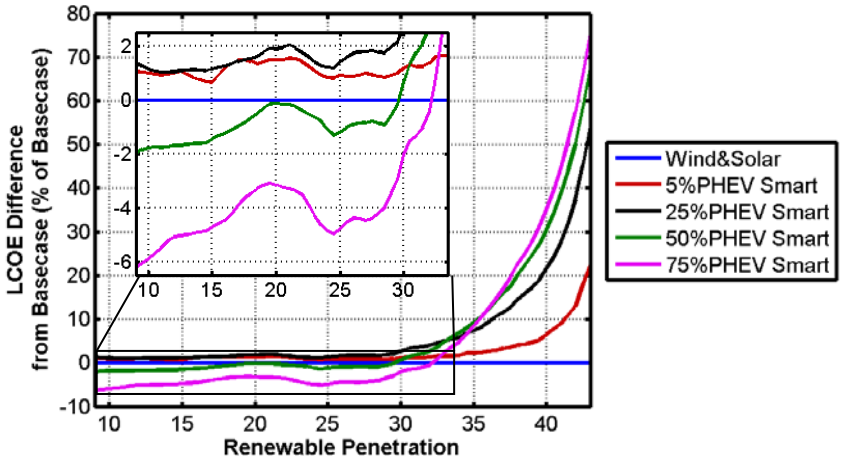

7.3.4.4.2.5.1. Conclusions

- Raising the vehicle penetration will increase demand for electricity, capacity factor and achievable renewable penetration when compared to the base renewable mixture without electric transportation.
- Greater VMT penetration will lower CO_2 emissions and in most cases lower the required balance fleet ramp rate and startups.
- Value of Electric Transportation for grid operations can become saturated for high VMT penetrations.
    - LCOE and capacity factor exhibit this behavior for select renewable penetrations.
    - Balance fleet ramp rate and starts exhibit this behavior for all renewable penetrations.

Task 7.3.5. References

Electricity Energy Storage Technology Options: A White Paper Primer on Applications, Costs, and Benefits. EPRI. Palo Alto, CA. 2010. 1020676.

Ibrahim H, Ilinca A, Perron J. Energy storage systems – Characteristics and comparisons. Renewable and Sustainable Energy Reviews. 2008;12(5):1221-50.

Klein, Joel. (2010). Cost of Generation Model User's Guide Version 2. California Energy Commission. CEC-200-2010-002.

Zhang L, Brown T, Samuelsen GS. Fuel reduction and electricity consumption impact of different charging scenarios for plug-in hybrid electric vehicles. Journal of Power Sources. 2011;196(15):6559-66.

Task 7.4. Solar Heating in RESCO

Solar water heating applications include low to medium temperature (i.e., 40-90 C) applications such as domestic hot water production, pool heating, space heating, etc. Applications can also include high temperature applications such as the production of high temperature water or steam generation for industrial purposes. The application of interest here is the production of hot water for domestic hot water and space heating needs of the UC Irvine campus. There are several types of solar collectors available for solar water heating in low to medium temperature applications: unglazed flat plate, glazed flat plate, evacuated tube, and compound parabolic. These are stationary collectors. Sun tracking collectors, which are more appropriate for providing high temperature water or steam generation given their cost and operating temperatures, could be integrated with the campus' district heating loop of high temperature water (350 F/350 psig).

The appropriate solar collector system for an application depends on the temperature, capacity, cost, and space requirements of the application. The collector efficiency and how it varies as a function of temperature will be an important parameter for selection of a solar collector. Collector efficiency, capacity supplied per unit area, and cost are related. Achieving higher concentration ratios typically increases costs, yet it also results in higher operating temperatures and greater efficiency. The concentration ratio is the area of the aperture space collecting or reflecting solar radiation divided by the area of the receiver. In all solar thermal technologies, thermal efficiency increases as irradiation levels increase. Similarly, efficiency decreases due to heat loss as the temperature difference between the collector inlet and ambient air increases. Lower concentration ratios have greater heat loss and lower thermal efficiency because larger proportions of receiver area to aperture area provide more area for heat transfer to the ambient air. Table 95 lists the concentration ratio, operating temperature, and relative cost of prominent collector technologies.

Table 95: Technology comparison of solar energy collectors

Solar Technology	Motion	Concentration ratio	Operating temperature (C)	Relative cost
Flat-plate collector	Stationary	1	30 – 80	Lowest
Evacuated tube collector	Stationary	1	50 – 200	Low
Compound parabolic collector	Stationary	1 – 5	60 – 240	Low
Linear Fresnel reflector	Single-axis tracking	10 – 40	60 – 250	Medium
Parabolic trough collector	Single-axis tracking	10 – 85	60 – 400	Medium
Parabolic dish reflector	Two-axis tracking	600 – 2000	100 - 1500	High
Heliostat field collector	Two-axis tracking	300 – 1500	150 - 2000	Highest

Source: Kalogirou, 2009

When selecting the appropriate solar collector technology to evaluate the use of solar water heating at UCI, the initial step includes identifying: temperature requirements, major practical issues (e.g., space constraints), solar collector market penetration in the United States such that the results will be applicable to other communities, and solar collector system cost. Major

practical issues were identified with the use of a sun axis tracking system that is integrated with the UCI district heating loop (i.e., campus shutdowns would be required for the installation; major infrastructure modifications would be needed; and land requirements would be a problem because these tracking systems are not suited for rooftop installation). A sun tracking system was not selected given the severity of these issues. Stationary compound parabolic collectors were not selected given the cost (See Table 95) and small market penetration (this technology is not shown in Figure 521).

Figure 520 illustrates the typical efficiency variation versus the temperature difference between the collector inlet and the ambient for flat plat collector and evacuated tube technologies. This figure shows that, for solar water heating at UCI, unglazed flat plate collectors are unsuitable because of their very low efficiencies at the temperature of interest. It is also clear that, for this application, the evacuated tube will provide higher efficiencies at the temperature of interest.

Figure 520: Collector efficiency versus solar parameter for various flat plate and evacuated tube collectors

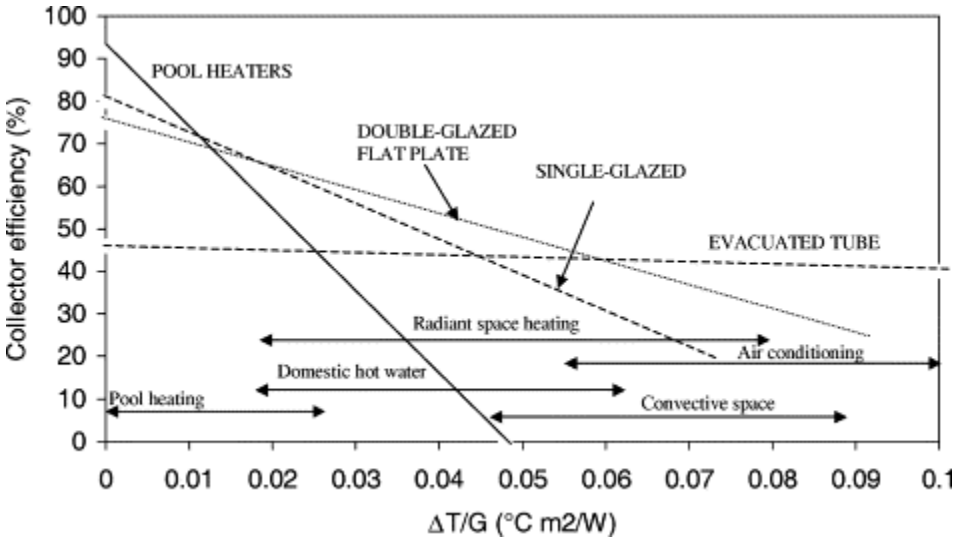

Source: Kalogirou, 2004

However, the market representation of glazed flat plate collectors in the United States is much higher than evacuated tube technologies. Figure 521 shows the installed capacity for three types of solar thermal heating collectors in various nations across the world. The evacuated tube collectors have the largest installed capacity in the world, which is driven by China's focus on this technology. The rest of the world continues to most frequently use flat plate collectors, although this may change in the future as a result of China's focus on evacuated tube collectors. The United States has a large amount of unglazed collectors installed that are typically used for low temperature applications, such as heating pools, where the temperature difference between the water to be heated and the ambient temperature is low. The rest of the installed capacity in the US is accounted for by flat plate collectors.

Figure 521: Installed capacity [MWth] of solar thermal heating collectors in various countries

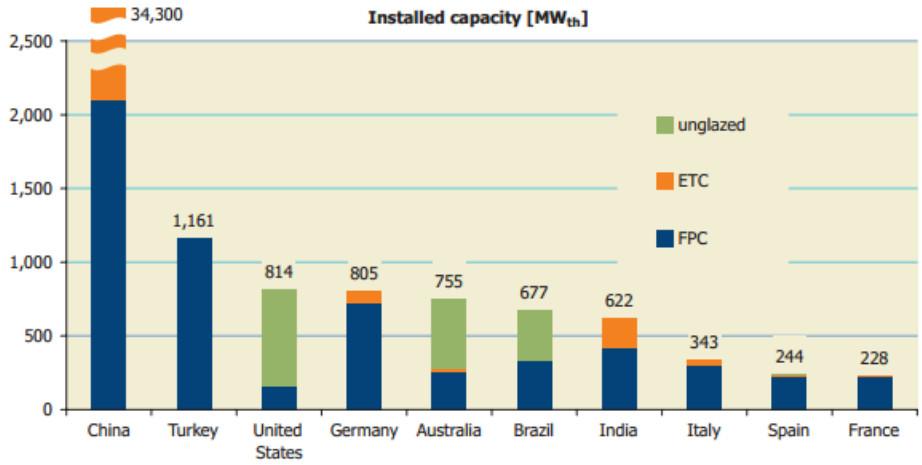

Source: Weiss, 2012

Given that glazed flat plate collectors are more commonly adopted in the United States and that their efficiencies are acceptable at the temperatures of interest, they were chosen for use in the development of the residential and central/commercial solar water heater models. This exemplifies economies of scale influencing technology adoption. It is also interesting to note that worldwide applications that include domestic hot water production in addition to space heating are not widely adopted as shown in Figure 522.

Figure 522: Distribution of solar water heating applications for various regions

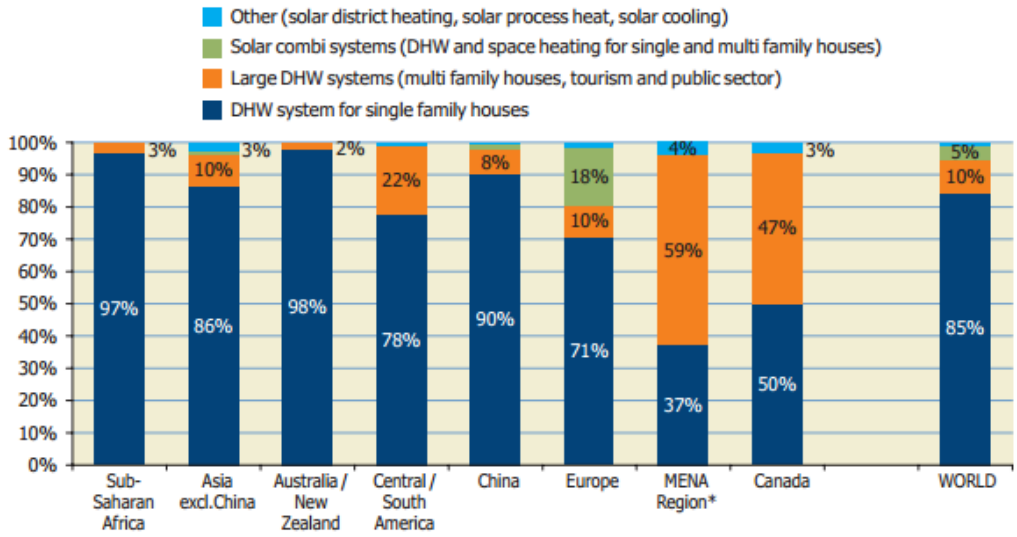

Source: Weiss, 2012

Task 7.4.1. Model of Residential Water Solar Heater

The model of the residential solar water heater is the same as the central solar water heating system since in each application the same collector technology (flat plate collector) is employed (see next section for details).

Task 7.4.2. Model Central Solar Heating System

The central solar heating system consists of multiple glazed flat plate collector systems situated on building rooftops, over parking lots, and over the top floors of parking structures. Simplifying assumptions are made to reduce computational intensity and model build time. Initial analyses show that a more complex model is not needed to evaluate the potential to meet 90% of the campus heating needs using a solar water heating system with storage (See Task 7.4.3). The major simplifying assumptions are:

1. Pipe friction losses and the associated pumping power requirements are not modeled.
59. Other parasitic electrical requirements are not included.
60. No heat loss occurs in the storage tank or pipes.
61. Heat exchangers are 100% effective.
62. Storage tank is perfectly mixed.

The parasitic losses are not included in the analysis due to extensive additional effort required to model the friction loss associated with the configurations at each of the different collector array locations across the UCI campus. Friction loss typically accounts for 10% of the total energy collected (Morehouse, 1993; Smith, 1993). Given the assumptions above, heat collected by the collectors can be simulated as if occurring in one location with one large tank at that location. This resulting assumption of a central collector/tank system is reasonable for the feasibility studies of the next section (Task 7.4.3) where the overall system's ability to meet 90% of the campus heating load is evaluated. A schematic of the system model is shown in Figure 523. The schematic does not include heat exchangers because heat exchange is 100% effective. Consequently, this model is essentially a thermal model with the ability to capture the temperature change of the storage from resulting heat inputs/outputs.

Figure 523: Solar water heater model schematic

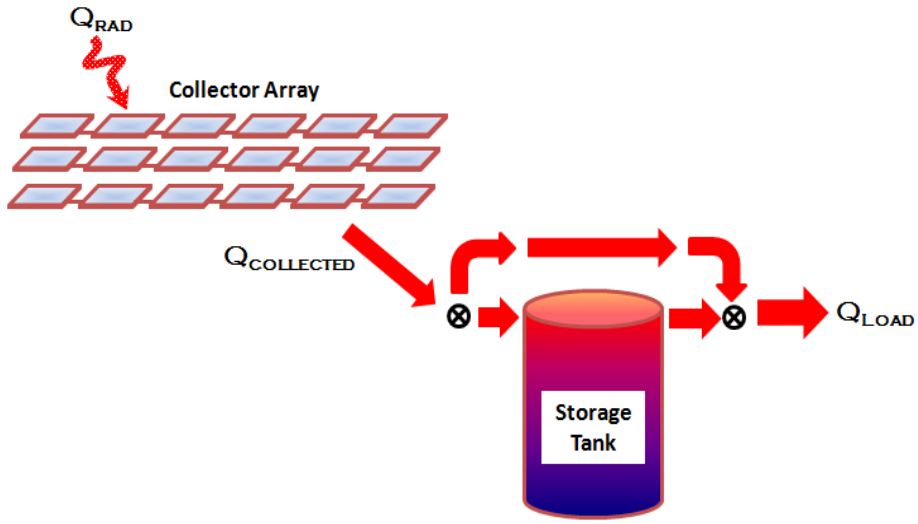

The area available for the installation of these flat plate collector systems was determined using Geographic Information Systems (GIS) (See Task 4.1.4). However, the total area available on these rooftops and in these parking lots is not fully utilizable given spacing constraints as well as irregular roof spaces. It was determined in Task 4.1.4 that only 20% of the total area available could be used by the PV panels. This same number is used in this application given that the geometry of the flat plate collectors is very similar to PV panels. Table 96 shows the calculated areas for the different spaces available for placement of flat plate collectors.

Table 96: Utilizable area for installation of flat plate collectors on UCI campus

Location	Area [Acres]
Building Rooftops	9.1
Parking Lots	7.1
Parking Structures	6.6
Total	22.7

Total incident radiation (beam, diffuse, and reflected) is calculated using the equations as discussed in Section 7.1.3.2.

Flat plate collectors are modeled using the standard flat plate collector efficiency equation as used by the Solar Rating & Certification Program (SRCC). This standard efficiency equation is:

$$\eta = a_0 K_{\tau\alpha} - a_1 \frac{T_{in} - T_a}{G} \tag{99}$$

where

$$K_{\tau\alpha} = 1 - b_0\left(\frac{1}{\cos\theta} - 1\right) \quad (100)$$

The constants a_0, a_1, and b_0 are defined experimentally. The SRCC publishes these constants for various types of collectors. The particular constants used in this study are for an advanced flat plate collector as discussed by (Kalogirou, 2003). The definition of each term in the above equations and the values of the constants are shown in Table 97. The collected heat per square meter is calculated by multiplying the total incident radiation by the efficiency defined above. This is then multiplied by the area to obtain the heat collected.

Table 97: Parameter definitions for the flat plate solar collector model

a_0	Intercept Efficiency	0.8	-
a_1	Slope Coefficient for Efficiency	4.78	W/m^2-K
b_0	Incidence Angle Modifier Constant	0.1	-
B	Tilt Angle	25	Deg
T_{in}	Collector inlet temperature		K
T_a	Ambient Temperature		K
$K_{\tau\alpha}$	Incidence Angle Modifier		-
Θ	Incidence Angle		Deg
G	Incident Radiation		W/m^2

The collector inlet temperature (T_i) has been determined from building data and the UCI central plant design constraints. The UCI central plant provides hot water to the campus using a high temperature water (HTW) loop (450 F/350 psig) that exchanges heat with building hot water (BHW) that is then used in the building HVAC equipment. Limited building data suggests that the BHW supply temperature to the HVAC equipment operates at 120 to 150 F. The BHW system is designed for a maximum temperature of 275 F and at times may provide supply temperatures of 180 F. For the purposes of the hot water storage evaluation, the diurnal variation in the BHW temperatures shown in Figure 524 will be assumed since annual building hot water temperature data has not been collected. These BHW temperatures were assumed based on the limited building data collected. The BHW return temperature is used as the collector inlet temperature in the collector efficiency equation.

Figure 524: Diurnal variation of building hot water return and supply temperatures

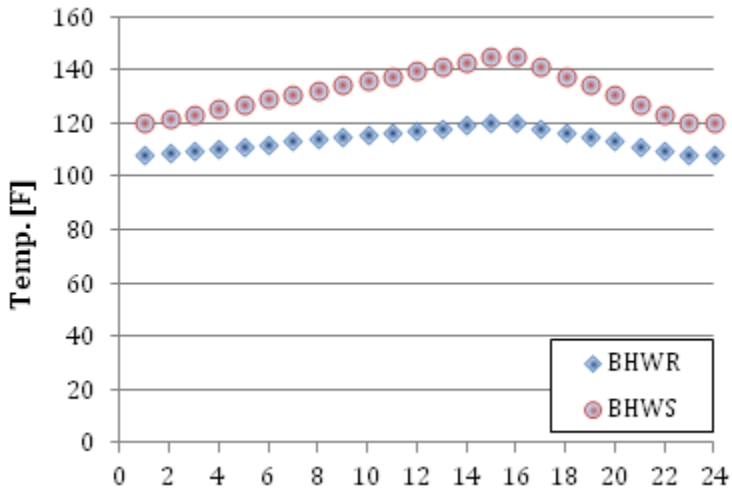

In order to calculate the temperature, the storage tank is modeled as if perfect mixing occurred within the tank. The temperature of the tank is calculated using the following equation, where $Q_{net,in}$ is the heat entering the tank less the heat exiting the tank at a given time.

$$T_{tank} = \frac{Q_{net,in}}{\rho V_{tank} c_p} \quad (101)$$

Modeling the tank assuming perfect mixing produces a low value of the maximum tank temperature achievable, which is good for a feasibility study since a stratified tank would allow higher supply temperatures from the tank (Beckman, 1993). The volume of the tank has been determined based on the design guidelines for seasonal storage as set forth by Lund (1989). This author performed calculations for a system of similar characteristics as in this case and showed that a storage volume to collector area ratio of 7.4 m^3/m^2 is required to reach a solar fraction of 90%. This ratio was used to determine the storage tank size. However, other rules of thumb have been suggested for storage tank sizes, a common one being: 1.5 to 3 gallons (Morehouse, 1993), but this storage tank size recommendation is likely not for seasonal storage.

The tank is filled when the collected heat is greater than the campus heat demand. If the collected heat is not greater than the campus demand, the collected heat is supplied directly to the campus demand without entering the tank. When the collected heat is insufficient to supply the campus heating demand, the tank will be emptied to supplement the supply until there is not enough left to supply the heating needs for the next hour.

Task 7.4.3. Evaluate Hot Water Storage

The use of hot water storage to supply 90% of the UCI campus heating load will be evaluated using the UCI campus heating load from September 2009 to August 2010. As a first step to determine the ability of solar water heating, with hot water storage to satisfy 90% of the UCI campus heating load, it is acceptable as a best case scenario to assume that the tank can be as large as needed. This much storage allows seasonal shifting, enabling all the solar energy collected to be used (since no heat loss is assumed) despite the solar energy and the heating

loads not coinciding. Table 98 shows the results from several different annual simulations with different areas of installations. The most important result in Table 98 is the result for an installation of 22.7 acres because it shows that, even with utilizing the maximum amount of area for solar water heating and using as much storage as is needed, only 77.1% of the UCI campus heating load is delivered. This suggests that meeting 90% of the campus heating load will be very difficult given the land area constraints and the ideal assumptions made for the 77.1% result.

Table 98: Solar water heating model results for full year simulation with infinite storage

	Collector Area [Acres]	Annual Campus Heat [MWhr]	Annual Solar Heating Delivered to Campus [MWhr]	Annual Solar Heat Collected [MWhr]	Annual Incident Solar Radiation [MWhr]	Campus Heating Load Served [%]
Building Rooftops	9.1	112,149	34,672	34,672	66,104	30.9
Parking Lots	7.1	112,149	27,051	27,051	51,575	24.1
Parking Structures	6.6	112,149	25,146	25,146	47,943	22.4
Total	22.7	112,149	86,488	86,488	164,896	77.1

The amount of storage needed to meet 77.1% of campus heating demand can be seen in Figure 525. The storage capacity is so large that it dwarfs the solar energy collected and campus heating loads. This large storage capacity allows for seasonal shifting of the solar energy used to serve the campus heating load. Figure 526 shows the same plot for the case of the 9.1 acre installation where 30.9% of the campus heating load can be served but with much smaller storage capacity (i.e., ten times smaller storage capacity decreases load served by little more than half, 57%). These results suggest that there are diminishing returns with larger storage capacity in terms of how much more load can be served (Morehouse, 1993).

Figure 525: Daily average in each season for the annual simulation for the case of a 22.7 acre installation

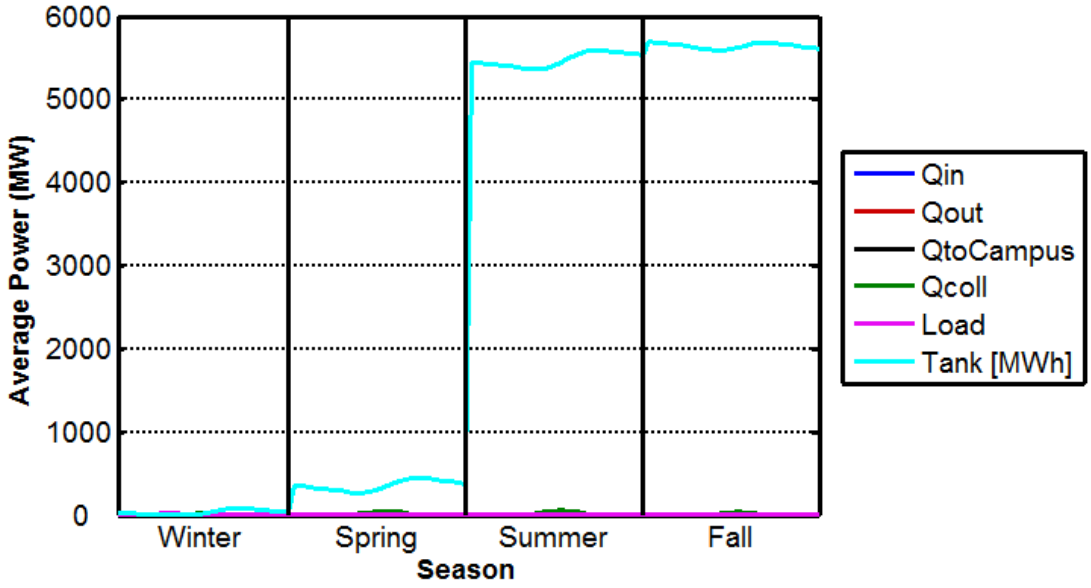

Figure 526: Daily average in each season for the annual simulation for the case of a 9.1 acre installation

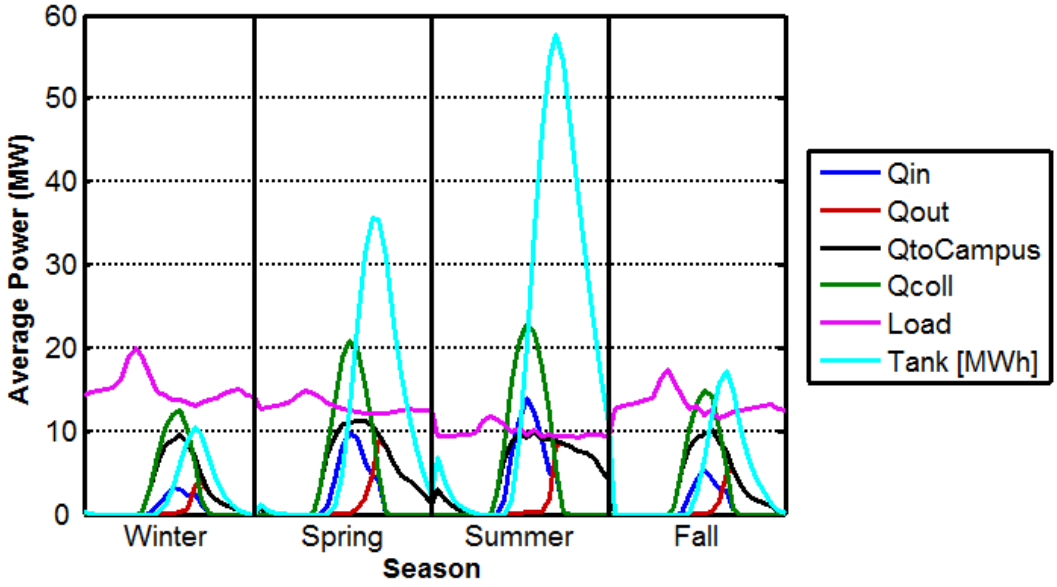

The heating load profile plays a large role in assessing how much storage there will need to be in order to satisfy a certain percentage of the heating needs. In this case, the UCI campus heating load is rather flat with the exception of seasonal variation and a peak that occurs in the early morning due to the Biological Sciences department animal cages cleaning processes. These

features can be seen in Figure 526. UCI's heating load profile further supports the conclusion that a large amount of storage will be needed in order to supply 90% of the campus heating needs. In fact, given the design guidelines given by Lund (1989) (7.4 m^3 of storage per m^2 of collector area), for a collector area of 22.7 acres, the required storage tank size is 179.6 million gallons. Figure 527 shows the temperature of the storage tank for the year with a tank size of 179.6 million gallons. These temperatures will be acceptable for integration with the building hot water systems as seen in Figure 524. However, this tank size is massive and would likely be prohibited by cost and space constraints, but if high solar fractions are to be achieved, seasonal storage is required and for the case of UCI the tank will be very large as shown here.

For comparison, some demonstration projects in Germany that have utilized seasonal storage tanks in district solar heating plants have tank sizes on the order of several million gallons for an annual heating need on the order of 1,000 MWh (Bauer, 2010). The annual heating energy need for UCI is 100,000 MWh hence requiring a much larger tank. Additionally, it should be noted that the design solar fractions for those demonstration projects did not exceed 62%, and the actual solar fraction achieved was lower than design due to many unexpected factors such as higher than expected hot water return temperatures which lead to increased heat losses (Bauer, 2010).

Figure 527: Storage tank temperature for a collector installation area of 22.7 acres and a storage tank size of 179.6 million gallons

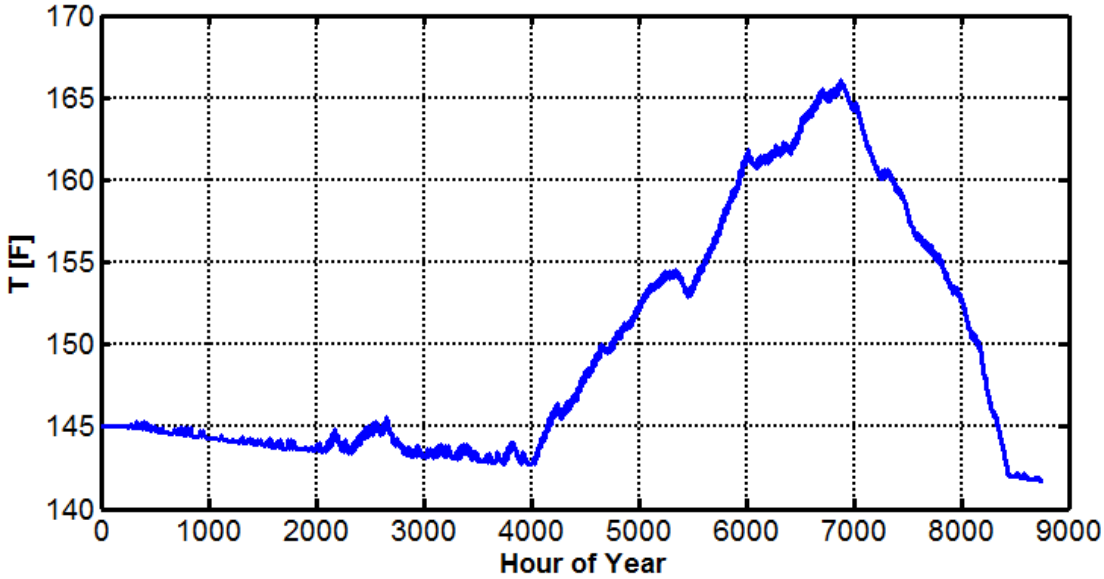

To conclude, supplying 90% of the UCI campus heating load with solar water heating using hot water storage is difficult given the space constraints on campus and the storage size required. Using the maximum amount of available space for the installation of collectors and allowing as much storage as may be needed, while also assuming no heat loss, serves 77.1% of the campus heating needs.

Task 7.4.4. Comparison of combined heat and power and centralized solar heating

A combined heat and power (CHP) system currently serves the UCI campus heating needs. The system consists of a gas turbine and heat recovery steam generator with a duct burner to provide additional heat if necessary. The system also includes a steam turbine that can utilize excess heat in the case of low heat loads. Although this system has resulted in increased overall campus efficiencies, it still relies on natural gas, a non-renewable fuel. In addition, this system creates various issues when higher levels of campus electric renewables are achieved (See Task 7.2). It is therefore worthwhile to consider implementing a centralized solar thermal heating system for UCI heating needs.

In order to achieve high solar fractions that approach 90%, seasonal storage will be required. However, locations where the periods of high solar irradiation are in phase with the periods of high heating loads may not require seasonal storage to achieve high solar fractions (i.e. locations at low latitudes). The need for seasonal storage results in increased costs and space requirements. Several centralized solar thermal systems with seasonal storage demonstrations exist in Germany (Bauer, 2010). Some of these systems have been operational for over 10 years and most have been operational for more than 5 years. These systems have demonstrated the technical feasibility of seasonal storage, however, the actual system performance has been lower than design. In addition, costs of these systems still remain high precluding market adoption.

Currently, solar thermal systems with seasonal storage (seasonal storage is required to reach high solar fractions) are not cost competitive with current boiler systems (Fuller, 2007; Lozano, Anastasia, 2010; Rudston, 2011). These systems were estimated by Lozano et al. (2010) to provide heat at a cost of $40-150/MMBtu, whereas boiler systems can provide heat at a cost of $19/MMBtu in places where natural gas prices of $15/MMBtu were used. Therefore, a lower natural gas price will decrease that $19/MMBtu value much lower, making it even harder for these solar thermal systems with seasonal storage to compete. It should be noted here that in locations where natural gas and electricity are very expensive (as in Hawaii: $30-50/MMbtu) these systems are cost competitive. In fact, Hawaii has experienced increased solar thermal installations. The need for seasonal storage is also reduced in Hawaii since the heating loads will remain nearly constant throughout the year due to small ambient temperature changes, which will decrease overall system costs by eliminating large storage tanks (see paragraph below for estimates on storage tank costs).

To compare with CHP systems, the value of heat recovered in CHP systems comes from the resulting avoided costs associated with a conventional boiler system and the necessary natural gas purchases. It can be estimated that the value of the heat associated with CHP systems is similar to those values discussed in the preceding paragraph. The same conclusion can also be made with respect to the cost effectiveness of a solar thermal system with seasonal storage. It is also useful to estimate the upfront costs of the systems discussed in Task 7.4.3. The values used to estimate the upfront costs are $28/ft^2 of collector area installed and $96/m^3 of installed storage volume. The price for solar collectors was obtained from data available from the Energy Information Administration's Annual Energy Review 2011 (EIA, 2012), and the price for the

seasonal storage was obtained from Lozano et al. (2010). Using these prices, the total upfront costs can be examined as shown in Table 99. These prices would likely be prohibitive.

Table 99: Solar thermal heating with seasonal storage upfront costs

	Collector Area [m^2]	Tank Volume [m^3]	Tank price [million $]	Collector Price [million $]
Building Rooftops	36,826	272,516	26.16	10.82
Parking Lots	28,733	212,622	20.41	8.443
Parking Structures	26,709	197,649	18.97	7.849
Total	91,864	679,792	65.26	26.99

Task 7.4.5. Conclusions

Solar thermal heating with seasonal storage is technically feasible but cost and space requirements hinder them. Conventional fossil fuel heating systems are still much cheaper in most locations (an exception being Hawaii). Current natural gas price trends suggest that they will likely not increase to levels where solar thermal heating systems with seasonal storage could compete unless dramatic price decreases are achieved with regard to collectors and seasonal storage tanks. Combined heat and power systems can also provide high percentages of the heating needs of a campus at a lower cost and smaller footprint. However, the CHP system requires fossil fuel and will emit carbon (which will be regulated in California under the California Air Resources Board cap and trade program in 2013). Additionally, the CHP system will affect the UCI campus' ability to increase the renewable penetration on campus as discussed in Task 7.2.

- **Achieving a high fraction of UCI's campus heating load served by solar water heaters is challenging but possible.**
    - 77.1% of the campus heating load can be served by solar water heaters assuming that all building rooftops, parking structure rooftops and open parking lot area is covered with glazed flat plate collectors (22.7 acres) and that the storage system experiences no heat losses.
    - Covering only building rooftops with as much solar water heating capacity as possible (9.1 acres) yields a 30.9% solar fraction
    - **A tank capable of seasonal storage is required for UCI to achieve a high fraction of campus heating load provided by solar water heaters.** To support a 77.1% solar fraction a 180 million gallon tank with seasonal storage capability is required.

- **Current solar water heating and storage systems are not cost competitive with conventional fossil fuel heating systems, to date.**

Task 7.4.6. References

Bauer, D., R. Marx, et al. (2010). "German central solar heating plants with seasonal heat storage." Solar Energy 84(4): 612-623.

Beckman, W. (1993). Detailed Simulation Methods and Validation. Active Solar Systems. G. Lof. Cambridge, MIT Press.

Bialobrzeski, R. (2007). Optimization of SEGS Solar Field for Cost Effective Power Output. Mechanical Engineering, Georgia Institute of Technology. Master of Science.

Energy Information Administration (2012). Annual Energy Review 2011.

Fuller, R. a. A., Lu (2007). Seasonal storage for solar thermal systems in Australia? . Australian and New Zealand Solar Energy Society 45th Annual Conference, Alice Springs, Australia.

Kalogirou, S.A. (2003). "The potential of solar industrial process heat applications." Applied Energy 76(4): 337-361.

Kalogirou, S.A. (2004). "Solar thermal collectors and applications." Progress in Energy and Combustion Science 30(3): 231-295.

Kalogirou, S.A. (2009). Solar Energy Engineering: Processes and Systems. London, Elsevier.

Lozano, M., A. Anastasia, et al. (2010). Thermoeconomic Cost Analysis of Central Solar Heating Plants Combined with Seasonal Storage. ASME International Mechanical Engineering Congress & Exposition Vancouver, Canada ASME.

Lund, P. D. (1989). "A general design methodology for seasonal storage solar systems." Solar Energy 42(3): 235-251.

Morehouse, J. (1993). Optimum Design Techniques. Active Solar Systems. G. Lof. Cambridge, MIT Press.

NSRDB (2005). National Solar Radiation Database 2005, National Renewable Energy Laboratory.

Rudston, J. (2011). Techno-Economic Analysis of Sustainable Energy Systems for Meeting the Energy Demand of a Greenhouse in South Australia. School of Energy Resources, Australia, University College London. MSc.

Smith, C. (1993). System Performance. Active Solar Systems. G. Lof. Cambridge, MIT Press.

Weiss, W., Mauthner, F. (2012). Solar Heat Worldwide: Markets and Contribution to the Energy Supply 2010, International Energy Agency.

Task 7.5. UCI Campus Roadmap Toward RESCO Vision

Roadmap information for the UCI community is located in Chapter 3 and begins on page 20.

Task 7.6. Generic Community Roadmap Toward RESCO Vision

Roadmap information for generic communities is located in Chapter 4 and begins on page 29.

Appendix G:Task 8:
Public Outreach, Education and Technology Transfer

TABLE OF CONTENTS

Task 8.1. Issues for Policy Makers and Industry Leaders G-2

Task 8.2. Public Website G-2

Task 8.3. Public Acceptance G-4

Task 8.3.1. Technology G-4

Task 8.3.2. Cost-of-Electricity G-5

Task 8.3.3. Conservation G-5

Task 8.4. Technology Transfer G-6

Task 8.4.1. Dissemination of Information to the City of Irvine and the OC Great Park G-6

Task 8.4.2. Conferences and Technical Publications G-7

Task 8.4.3. Interaction with Industry G-9

Task 8.4.4. Public Outreach (RESCO Website & Social Media) G-10

Task 8.4.5. Conclusion G-10

Dissemination of the findings to policy makers, industry leaders and the public represents a key component of the RESCO program. The information gathered in this report can help many communities reach renewable goals and help the state make decisions to reach its energy goals. However, it is only through effective outreach that these entities can receive this information.

Task 8.1. Issues for Policy Makers and Industry Leaders

Policy findings are located in chapter 4 and begins on page 38.

Task 8.2. Public Website

An APEP – RESCO website will be a "one-stop-shop" for anyone looking to learn about the RESCO project and distributed energy resources. As mentioned earlier, the RESCO website is accessible at http://resco.apep.uci.edu. Its design is two-fold in that it will present the findings in an interactive, user friendly way, with minimal text and engineering jargon so that a non-technical audience can comprehend the concepts behind the renewable technologies presented. However, a more technical audience will still find immense value in visiting the site as it will also house research results, plots, and data. A screenshot of the website is shown in Figure 528.

Figure 528: Screenshot of the APEP – RESCO website in its development stage

Upon first entering the site, visitors will be able to view a short video on the RESCO project as well asget an introduction to the research conducted by APEP. An especially powerful and

thought-provoking feature is the interactive "Living Laboratory" tour where visitors will be able to visit all of the Pilot Projects that make up the RESCO project such as, but not limited to:

- University of California, Irvine
    - Central Plant
    - Rooftop Solar
    - Amonix Concentrated Solar Photovoltaic
    - 300 kW On-Site Fuel Cell
- UCI Hydrogen Refueling Station
- Orange County Sanitation District Tri-Generation Fuel Cell System
- Orange County Great Park
- Zev-NET Program
- Irvine Smart Grid Demonstration Project
- Alternative Transportation Vehicle Fleet
    - Fuel Cell Vehicles
    - Electric Vehicles
    - Bio-diesel Buses

The website will also take advantage and build off of the experience of APEP's Outreach Team which has held outreach activities for students and teachers from all educational levels:

- Elementary Schools
    - Viejo Elementary, Mission Viejo, CA
    - Our Lady of Peace Elementary, North Hills, CA
- Junior Colleges
    - Saddleback College, Mission Viejo, CA
- International Universities
    - Shibaura Institute of Technology, Japan
    - Sichuan University, China

For instance, during the visit by Our Lady of Peace Elementary, a "Fuel Cell" game involving tennis balls and sidewalk chalk was used to teach the kids the principles behind how a fuel cell operates. These games can be made available on the RESCO website in a presentation format that educators anywhere can utilize. The website will also include:

- A complete list of relevant publications as well as links to other resources and the aforementioned APEP partners.
- Answers to frequently asked questions surrounding distributed energy resources at the community level as well as detail the benefits of a RESCO.
- In addition to having a link to the APEP group website, the RESCO site integrates common social media outlets as a method to increase public recognition of the findings.

Task 8.3. Public Acceptance

Increasing the renewable penetration safely, reliably and at the lowest cost of electricity becomes more and more challenging as the penetration rises. California has a significant potential capacity of renewables predominantly from intermittent wind and solar. It has been shown that through correct selection and placement of intermittent renewables, their variability can be reduced. It was also shown that there are complementary technologies that can support the implementation of renewables and further advancements to conventional technologies by increasing flexibility and efficiency can also support the implementation of renewables.

Public awareness and desire to pursue clean and sustainable technologies is continually growing. Based on the findings there are many things that the public can do to support implementation of renewables. Along with conservation, many technology advances can help. The following sections explore opportunities for the public.

Task 8.3.1. Technology

New technologies are continually being developed in the energy field that are more efficient and more flexible. The importance of continuity in research and development is important. The public, though oftentimes not directly involved in the research, can support technology development by actively pursuing environmentally friendly alternatives.

This research finds that regional renewables should be installed, and a large portion should be wind. It has been shown that installing local resources plays a role; however, if the opportunity exists, purchasing regional resource generation is one step that the public can take otherwise advocacy for regional resources is another step the public could take. Educating the public on the most viable renewable options plays a pivotal role in establishing public acceptance for renewables.

Electric transportation is not a new technology but it has been slow to acceptance on a large scale. Results from this work show that where and when vehicle charging occurs can either can improve system performance or reduce it. Scientists, engineers and policy makers can develop an ideal strategy for implementing electric transportation but unless the public is willing to switch to the new technology it will not work.

Currently, most residents in California pay for electricity based on monthly usage. By changing to a real-time pricing structure, where the cost of electricity varies based on the time it is consumed.. Using this rate structure, utilities can incentivize the use of electricity at specific times and disincentivize electricity consumption at others. Many communities in California have already installed "smart" meters. These meters can aid in a transition to real-time pricing because they track the time-resolved use of electricity. Public acceptance of smart meters and new pricing structures is pivotal for the full value of electric transportation to be realized.

Task 8.3.2. Cost-of-Electricity

Currently, many of the available renewable technologies are more expensive than their conventional counterparts. Also, as has been described in detail in Task 7.2, increasing renewables does not necessarily replace any generation because of the intermittency and will yield additional costs for other generation to mitigate fluctuations arising from the renewables. None of the cases explored during the course of this research resulted in a reduction to the cost-of-electricity. As the technology continues to advance and manufacturing volumes increase, the cost of renewables will fall; however, in the meantime, without incentives, the cost of installing renewables will result in a rise in the cost-of-electricity. This is likely unacceptable to the public but right now it is the reality of the situation.

The cost-of-electricity does not reflect long-term depletion of resources or long-term environmental impacts, which if considered might change the competitiveness of renewable resources. However, as the state of California tries to reach its goal of 20% renewable penetration by 2013 and 33% by 2020, other technologies can help lower the cost-of-electricity.

Task 8.3.3. Conservation

Conservation continues to be a valuable technique to reduce a community's cost-of-electricity. Conservation can be pursued for many areas including transportation, water and electricity.

High efficiency and alternative fuel vehicles offer an opportunity to reduce CO_2 emissions but oftentimes living close to the workplace, human powered transport, carpooling and public transportation present just as much or greater value but require an adjustment to behavior or longer travel times.

Conservation of electricity through both energy efficiency and demand response measures present valuable opportunities to reduce the cost-of-electricity and increase the uptake of renewable generation. Continued implementation through regulation and outreach to further the use of energy efficient technologies and building designs will require continued support from the public.

Task 8.4. Technology Transfer

In an effort to maximize the impact of findings garnered from the RESCO project, the results must be vetted with the public and disseminated to interested groups. The Technology Transfer strategy pursued during this project can be grouped into 5 areas:

- Dissemination of information to the City of Irvine and the Orange County Great Park
- Conferences and technical publications
- Interaction with Policy makers and Industry
- Public Outreach

A representation of the affiliations that APEP will involve in the technology transfer for the RESCO program are depicted in Figure 529.

Figure 529: APEP's Technology Transfer will involve affecting local communities, industry, as well as hosting conferences to present to a broader audience.

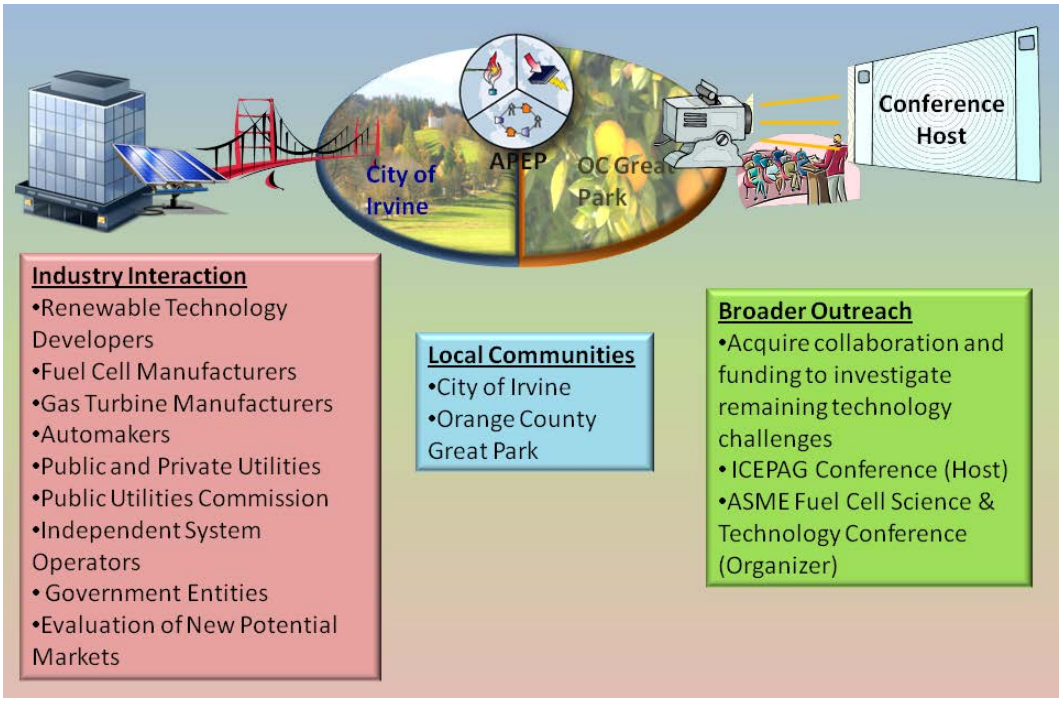

Task 8.4.1. Dissemination of Information to the City of Irvine and the OC Great Park

Research findings will be disseminated to the local area via presentations to community leaders and key community figures. Once completed, final reports and all documentation will be collected and made available to other communities through the APEP – RESCO website (http://resco.apep.uci.edu).

APEP has been working closely with the City of Irvine and the Orange County Great Park on a number of projects. RESCO research continues to develop that relationship while providing those organizations with valuable information regarding RESCO philosophies and measures that the communities can pursue.

Additional transfer of technology will occur through Cadmus (formerly CTG Energetics), a partner on the project and a local sustainable design and building operations consulting firm that regularly works with both the City of Irvine and the OC Great Park. Example projects that Cadmus has supported are pictured in Figure 530.

Figure 530: Examples of Past Cadmus Projects

Task 8.4.2. Conferences and Technical Publications

APEP was able to disseminate the findings from RESCO through hosting, organizing and attending conferences. Additionally, the publishing of material in technical journals provides another venue by which results from the RESCO project are distributed to the community.

By hosting the annual International Colloquium for Environmental Preferred Advanced Power Generation (ICEPAG) conference and helping organize the ASME Fuel Cell Science and Technology Conference, APEP brings together industry leaders, policy makers, and research scientists from all over the world.

RESCO methodology and results were presented to the community at each of the three ICEPAG conferences that occurred during the course of the RESCO program from 2010-2012. The following RESCO material was presented:

- 2010: Assessing Grid Instability Associated with a Large Penetration of Solar and Wind Resources

- 2010: Renewable Energy Secure Communities
- 2011: Assessment of Utility-Scale Energy Management with High Penetration of Renewable Power
- 2011: Transient Generation Challenges with Increased Intermittent Renewable Power
- 2011: Implications of the Spatial Diversification of Intermittent Renewable Power Installations
- 2011: A Study on the Dispatch Potential of Electrical Building Loads
- 2012: Increasing Renewable Generation: The Journey vs. The Destination
- 2012: Evaluation of Differing Photovoltaic Technologies in Parallel Platforms
- 2012: Grid Ramifications: The Future of Plug-In Vehicles (Plenary lecture)

Apart from ICEPAG, RESCO material was presented in several conferences both in the United States and internationally.

- International Workshop of Energy Conversion (IWEC) at the Kyo-tanabe Campus, Doshisha University, Kyoto, Japan (Invited speaker: Joshua Eichman)
- USAEE/IAEE conference in Washington D.C. 2011: Technical and Cost Impacts of Integrating Renewables: A Case Study for California (presented by Lori Schell)
- IAEE conference in Perth Australia 2012: Increased Renewables in California: Impact on Fossil Fuel Generation, Levelized Costs, and Grid CO2 Emissions (presented by Lori Schell)

During the course of this research, findings were published in academic journals. The following four papers were written and accepted during the course of this work.

1. Tarroja B, Mueller F, Eichman JD, Brouwer J, Samuelsen S. Spatial and temporal analysis of electric wind generation intermittency and dynamics. Renewable Energy. 2011;36(12):3424-32.

63. Tarroja B, Mueller F, Eichman JD, Samuelsen S. Metrics for evaluating the impacts of intermittent renewable generation on utility load-balancing. Energy. 2011;42(1):546-62.

64. Tarroja B, Mueller F, Samuelsen S. Solar power variability and spatial diversification: implications from an electric grid load balancing perspective. International Journal of Energy Research. 2012. DOI: 10.1002/er.2903

65. Eichman JD, Mueller F, Tarroja B, Schell LS and Samuelsen S, Exploration of the Integration of Renewable Resources into California's Electric System Using the HiGRID Tool. Energy. 2012. (Accepted for publication)

Task 8.4.3. Interaction with Industry

The Advanced Power and Energy Program, which encompasses the National Fuel Cell Research Center (NFCRC) and the UCI Combustion Laboratory (UCICL), has formed partnerships with leaders in the automotive, power generation, and aerospace industry. In doing so, **synergistic relationships have been formed** where 1) the time span in which APEP's research findings are translated to practical applications is minimized and 2) APEP benefits from the marketing and product design experience that only comes from industry entities. Extending beyond industry, APEP's partnerships include government agencies as well as other domestic and foreign academic institutions. The non-exhaustive list of strategic alliances include:

Table 100: List of APEP Relationships

INDUSTRY	GOVERNMENT	ACADEMIA
General Electric	NTSEL	Doshisha U.
Siemens	DOE - RAC	UC Berkeley
Parker Hannifin	DOE - CaSFCC	UC Davis
Boeing	DoD - Base Camp	Tsinghua U.
General Motors	DoD - CaSFCC	Hamburg U.
Toyota	EPA	Llieda U.
Honda	ARB	U. of Tokyo
Nissan	CEC	KAIST
Hyundai/Kia	CPUC	U. of Genoa
Mercedes-Benz	F&A	Seoul National U.
Mitsubishi	DGS	U. of Birmingham
ZipCar	CAISO	Imperial College
Sempra	AQMD	Georgia Tech
PG&E	BAAQMD	U. of Washington
Edison	SJVAPCD	CSU San Francisco
Shell	City of Irvine	CSU San Diego
Chevron		CSU Los Angeles
Air Products		
Linde		
Rolls-Royce		
Solar Turbines		
Pratt & Whitney		

Throughout the course of this program APEP provided presentations and discussions involving RESCO material to support the academia/industry/government collaborations. Some of those presentations are as follows:

- Southern California Edison, Smart Grid Research Symposium: "Electric Vehicle and Grid Interactions" (2010)
- CARE Foundation, San Onofre Nuclear Generating Station: "The Need and Options for Renewable Power" (2011)
- California Clean Energy Roundtable: "The Future of Transportation" (2011)
- California Energy Commission PIER Workshop, Research Breakthroughs: What's Needed to Accelerate Path to Market and Achieve California's 2020 Renewable Energy Goals?: "Demonstrating an Integrated Renewable Energy System (RESCO)" (2012)
- ETAP workshop: "The Breadth of the Smart Grid" (2012)
- University Turbine Systems Research Workshop: "Grid Ramifications: The Future of Plug-In Vehicles" (2012)

Task 8.4.4. Public Outreach (RESCO Website & Social Media)

As part of this work a website (http://resco.apep.uci.edu) has been developed to provide information to the public, as well as industry, government and academia. The APEP- RESCO website is the culmination of this experience in that it will have a means to present information to individuals with different backgrounds. Development of the website is further described in Task 8.2.

Task 8.4.5. Conclusion

APEP serves as a central hub for the interaction and coordinated activity of industry, academia, and government as shown in Figure 531. As such, dissemination of results for the RESCO program have benefitted from the unique delivery engine provided by APEP at UC Irvine. From conference participation, technical papers, industry and government partnerships and public outreach the results from the RESCO program have and will continue to receive wide exposure.

Figure 531: APEP serving as a central hub for the coordinated interaction and collaboration of industry, government, and academia to expedite the release of novel renewable technologies in local communities

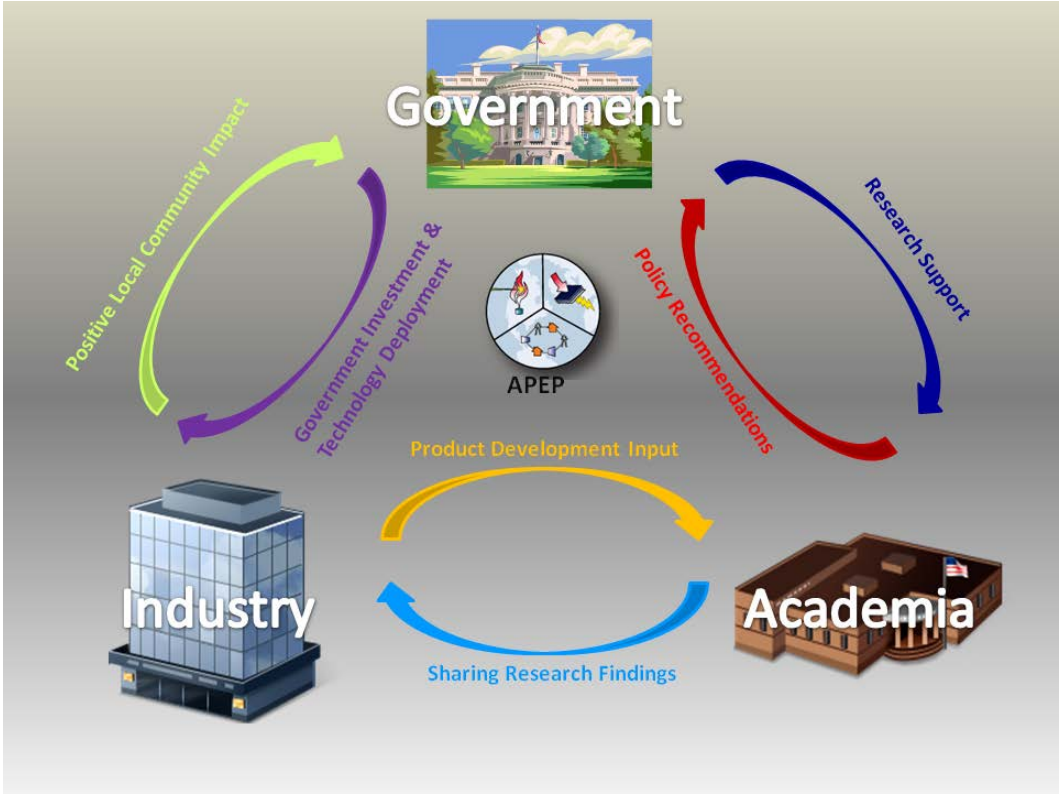

Appendix H:Task 9:
Production Readiness Plan

The University of California, Irvine is a unique location for exploring the feasibility and readiness of energy technologies. The backbone of the UCI micro-grid is made of several 12kV circuits fed from a 66kV substation. Heating and cooling on campus is provided by hot and cold water loops circulating around the ring-shaped campus. The heating and cooling is provided from the on-campus central plant, which is home to a 13.5 MW gas turbine and 5.5 MW steam turbine co-generation facility. Heating is provided from a heat recovery steam generator connected to the gas turbine and cooling is provided by electric chillers. The chilled water can be stored using the thermal energy storage tank on-campus.

Supplementing the electrical generation from the central plant is nearly 900kW of rooftop solar PV panels and two Amonix HCPV panels totaling 113 kW. Though not on the UCI campus, electricity and hydrogen are generated from biogas at the tri-generation facility at Orange County Sanitation District, which consists of a fuel cell and an anaerobic digester.

Some of the technologies serving UCI are proven, mature technologies, while others are still emerging.

The thermal energy storage tank is a mature technology and provides significant performance and cost savings to the campus. During the summer, the cold storage tank on campus saves $30,000 in energy cost and $79,000 in demand costs per month if fully used each day. During the winter, the tank can save $16,200 per month if fully used each day. This makes the cold storage tank a cost competitive technology.

The campus co-generation facility was installed in 2007 and is a mature technology. The facility operates year-round, apart from outages, providing heating and power to the campus. The calculated combined heat and power efficiency (HHV) for the plant is 63% in 2010 and 58% in 2009. This product is cost competitive for the campus; however, as more renewables are installed on campus, operation of this plant will become more and more challenging if export is not allowed as shown in Task 7.2.1. Thus, the plant is still cost competitive but consideration must be given to the amount of renewables that can be installed on campus while preserving operation of the co-generation plant and preventing the curtailment of excess renewable generation.

The fixed solar PV panels are installed with a power purchase agreement between UCI and SunEdison. They have operated on campus very reliably. Fixed panel solar is a maturing technology; however, to be cost competitive its installation must be incentivized.

The Amonix high concentrated PV arrays on campus have been installed and operating for nearly one year. HCPV is an emerging technology but very promising for its high efficiency. The university is working toward installing additional panels on-campus. Installing additional panels for evaluation will increase the amount of experience with the technology and can accelerate its deployment.

The tri-generation facility at the OCSD is recognized as the world's first hydrogen co-production system installed at a customer site. While the components that make up the tri-generation facility are not emerging, this concept is new and several challenges were overcome with its installation, as evidenced in Task 4.3. There can be many configurations for this product and the control strategies determining how the plant operates can be different depending on the location in which it is installed. As this product moves toward commercialization better integration will alleviate many of the challenges experienced at OCSD.

In addition to the products supporting UCI, to enable the highest penetration of renewables at the least cost, other renewables must be further developed, particularly wind power and complementary technologies. While specific energy efficiency measures and demand response programs are cost competitive at present, greater performance at a lower cost for other complementary technologies can further enable them to become cost competitive sooner.